Canadian Special Publication of Fisheries and Aquatic Sciences 108

EFFECTS OF OCEAN VARIABILITY ON RECRUITMENT AND AN EVALUATION OF PARAMETERS USED IN STOCK ASSESSMENT MODELS

Edited by
R.J. Beamish
and G.A. McFarlane

Fisheries
and Oceans

Pêches
et Océans

Canadä

Canadian Special Publication of Fisheries and Aquatic Sciences 108

Effects of Ocean Variability on Recruitment and an Evaluation of Parameters Used in Stock Assessment Models

(Proceedings of the International Symposium held at Vancouver, British Columbia, October 26–29, 1987)

Edited by

R. J. Beamish and G. A. McFarlane

Department of Fisheries and Oceans
Biological Sciences Branch
Pacific Biological Station
Nanaimo, British Columbia V9R 5K6

Scientific Excellence
Resource Protection & Conservation
Benefits for Canadians

Sponsored by

International Recruitment Investigations in the Subarctic (IRIS)
and
International North Pacific Fisheries Commission (INPFC)

DEPARTMENT OF FISHERIES AND OCEANS
OTTAWA 1989

90-02496/

Published by
Fisheries and Oceans
Communications Directorate

Publié par
Pêches et Océans
Direction générale des communications

© Minister of Supply and Services Canada 1989

Available from authorized bookstore agents, other bookstores
or you may send your prepaid order to the
Canadian Government Publishing Centre
Supply and Services Canada, Ottawa, Ont. K1A 0S9

Make cheques or money orders payable in Canadian funds to the Receiver General for Canada.

A deposit copy of this publication is also available
for reference in public libraries across Canada.

Cat. No. Fs 41-31/108E
ISBN 0-660-13360-1
ISSN 0706-6481
DFO/4220

Communications Directorate

Director General: Nicole Deschênes
Director: John Camp
Editorial and Publishing Services: Gerald J. Neville

Correct citation for this publication:

BEAMISH, R. J., AND G. A. MCFARLANE. 1989. Effects of ocean variability on recruitment and an evaluation of parameters used in stock assessment models. Can. Spec. Publ. Fish. Aquat. Sci. 108: 379 p.

Also published as Bulletin Number 49 of the International North Pacific Fisheries Commission (In Japanese).

Contents

Abstract/Résumé v
Sponsors, Steering Committee, Organizing Committee vi–viii
List of Contributors ix–x
Acknowledgements xi
Introduction. *R. J. Beamish, G. A. McFarlane, and W. S. Wooster* 1–3
Introductory Address – Before and After Ricker (1954) and Beverton Holt (1957). *P. A. Larkin* 5–9

TOPIC 1. An Evaluation of the Accuracy of Parameters Used in Stock Assessment

An experimental strategy for groundfish management in the face of large uncertainty about stock size and production. *C. J. Walters and J. S. Collie.* 13–25
Implications of age determination errors to yield estimates. *A. V. Tyler, R. J. Beamish, and G. A. McFarlane.* 27–35
Influence of errors in parameter estimates on stock assessment. *S. Tanaka.* 37–42
Errors in the stock assessment of the Japanese sardine (*Sardinops melanosticta*) using the line-transect method. *I. Hara* 43–50
Importance of environmental fluctuations in the management of Pacific hake (*Merluccius productus*). *R. C. Francis, S. A. Adlerstein, and A. Hollowed.* 51–56
Variability in estimating catch-in-numbers-at-age and its impact on cohort analysis. *D. K. Kimura.* 57–66
Time series analysis: Quantifying variability and correlation in SE Alaska salmon catches and environmental data. *J. T. Quinn II and R. P. Marshall.* 67–80
Distribution, size composition, and abundance of the Pacific hake (*Merluccius productus*) along the Pacific coast of North America in 1985. *M. A. Stepanenko* 81–86
Incorrect parameter values used in virtual population analysis (VPA) generate spurious time trends in reconstructed abundances. *M. J. Bradford and R. M. Peterman.* 87–99
The influence of statistical error in stock assessments: illustrations from Schaefer's model. *J. Schnute.* 101–109
Internal regulation of reproduction in Japanese anchovy (*Engraulis japonica*) as related to population fluctuation. *Y. Tsuruta and K. Hirose.* 111–119
The dynamic pool model and consequences of its approximations to fisheries management. *X. Li.* 121–126
Further aspects of catch-age analysis with auxiliary information. *R. B. Deriso, P. R. Neal, and T. J. Quinn II* 127–135
Scale patterns of commercial stocks of Asian sockeye salmon, *Oncorhynchus nerka. V. F. Bugaev* 137–150

TOPIC 2. The Effects of Ocean Variability on Recruitment

Recruitment of marine fishes revisited. *W. S. Wooster and K. M. Bailey.* 153–159
Forecasts of runs of West Kamchatka pink salmon (*Oncorhynchus gorbuscha*) based on analysis of the downstream migration and inshore feeding of the juveniles. *N. A. Chebanov.* 161–168
Buoyancy of walleye pollock (*Theragra chalcogramma*) eggs in relation to water properties and movement in Shelikof Strait, Gulf of Alaska. *A. W. Kendall, Jr. and S. Kim* 169–180
Characteristics of development of atmospheric circulation in the northern Pacific Ocean and their role in determining long-term changes in the abundance of certain fishes. *I. V. Davydov.* 181–194
Ecological studies of the pomfret (*Brama japonica*) in the North Pacific Ocean. *K. Shimizaki.* 195–205
New perspectives on the relationship between recruitment of Pacific hake (*Merluccius productus*) and the ocean environment. *A. B. Hollowed and K. M. Bailey* 207–220
Influence of oceanographic and meteorological processes on the recruitment of Pacific halibut, *Hippoglossus stenolepis*, in the Gulf of Alaska. *K. S. Parker.* 221–237
Estimation of the effects of flow on dispersion of larval pollock, *Theragra chalcogramma*, in Shelikof Strait, Alaska. *R. K. Reed, L. S. Incze, and J. D. Schumacher* 239–246
A numerical model for the variability of the northeast Pacific Ocean. *W. W. Hsieh and W. G. Lee.* 247–254
Comparisons of time scales for biomass transfer up the marine food web and coastal transport processes. *K. L. Denman, H. J. Freeland, and D. L. Mackas.* 255–264

The Vancouver Island coastal current: fisheries barrier and conduit. *R. E. Thomson, B. M. Hickey, and P. H. LeBlond*. 265–296

Transportation of eggs and larvae of mackerel, *Scomber japonicus (Houttuyn)*, by the Kuroshio Current. *A. Tomosada*. 297–303

Effects of ocean variability on the abundance of Dungeness crab (*Cancer magister*) megalopae. *G. S. Jamieson, A. C. Phillips, and W. S. Huggett*. 305–325

Effects of temperature and stock size on year-class production for rock sole (*Lepidopsetta bilineata*) in northern Hecate Strait, British Columbia. *J. Fargo and S. McKinnell*. 327–333

A family of Ricker SRR curves of the prawn (*Penaeus orientalis*) under different environmental conditions and its enhancement potential in the Bohai Sea. *Q. Tang, J. Deng, and J. Zhu*. 335–339

Contributions of Ozernaya River sockeye salmon (*Oncorhynchus nerka*) to ocean catches with special reference to their distribution in time and space. *M. M. Selifonov*. 341–352

The role of environmental factors in fluctuations of stocks of walleye pollock (*Theragra chalcogramma*) in the eastern Bering Sea. *O. A. Bulatov*. 353–357

Fisheries production domains in the northeast Pacific Ocean. *D. M. Ware and G. A. McFarlane*. 359–379

Abstract

BEAMISH, R. J., AND G. A. MCFARLANE [ED.]. 1989. Effects of ocean variability on recruitment and an evaluation of parameters used in stock assessment models. Can. Spec. Publ. Fish. Aquat. Sci. 108: 379 p.

Invited speakers from Canada, The People's Republic of China, Japan, the United States of America, and the Union of Soviet Socialist Republics met in Vancouver, British Columbia, Canada, to discuss the effects of ocean variability on recruitment and to evaluate the accuracy of parameters used in stock assessment models. In addition to providing new information on two important topics, the symposium attempted to stimulate communication among fisheries and oceans scientists and to encourage interdisciplinary research. The symposium also provided an example of the potential benefits of a proposed new North Pacific fisheries and oceans science organization.

Résumé

BEAMISH, R. J., AND G. A. MCFARLANE [ED.]. 1989. Effects of ocean variability on recruitment and an evaluation of parameters used in stock assessment models. Can. Spec. Publ. Fish. Aquat. Sci. 108: 379 p.

Des conférenciers invités du Canada, de la République de Chine, du Japon, des États-Unis et de l'Union des républiques socialistes soviétiques se sont réunis à Vancouver en Colombie-Britannique (Canada) afin d'étudier les effets de la variabilité des océans sur le recrutement et d'évaluer la précision des paramètres utilisés pour les modèles d'évaluation du stock. En plus de fournir de nouvelles données sur deux sujets importants, le colloque visait à stimuler la communication entre les halieutes et les océanologues et à favoriser les recherches interdisciplinaires. Le colloque a aussi fourni un exemple des avantages potentiels relativement à une nouvelle organisation scientifique des pêches et des océans dans le Pacifique nord.

Sponsors

International Pacific Halibut Commission
University of Alaska
University of British Columbia
National Marine Fisheries Service
Canada Department of Fisheries and Oceans
International North Pacific Fisheries Commission (INPFC)
International Recruitment Investigations in the Subarctic (IRIS)

Steering Committee

Canada

Dr. R. J. Beamish (Chairman)	Director Department of Fisheries and Oceans Biological Sciences Branch Pacific Biological Station Nanaimo, B.C. V9R 5K6
Dr. C. Mann	Director-General Institute of Ocean Sciences Sidney, B.C. (Retired) 9751 Ardmore Drive R.R. No. 2 Sidney, B.C. V8L 3S1
Dr. N. J. Wilimovsky	Professor Institute of Animal Resource Ecology University of British Columbia Vancouver, B.C. V6T 1W5

China

Mr. Jia Jiansan	Director Division of Foreign Economics and Techniques Bureau of Aquatic Products 31 Minfeng Lane, Xidan Beijing China

Japan

Dr. Sigeiti Hayasi	Director Far Seas Fisheries Research Laboratory Japan Fisheries Agency 7-1, Orido 5 Chome Shimizu 424, Japan

USSR

Dr. S. A. Studenetsky	Director Research Institute of Marine Fisheries and Oceanography 17, V. Krasnoselskaya Moscow, B-140, 107140 USSR

INPFC

Mr. Bernard E. Skud
Executive Director
International North Pacific
Fisheries Commission
6640 Northwest Marine Drive
Vancouver, B.C.
V6T 1X2

USA

Dr. Vera Alexander
Director and Professor
Institute of Marine Science
University of Alaska — Fairbanks
Fairbanks, Alaska 99701
USA

Dr. William Aron
Director
Northwest and Alaska Fisheries Center
2725 Montlake Boulevard East
Seattle, Washington 98112
USA

Mr. Andrew Bakun
Director
Pacific Fisheries Environmental Group
Southwest Fisheries Center
P.O. Box 831
Monterey, California 93942
USA

Dr. Karl Banse
Professor
School of Oceanography WB-10
University of Washington
Seattle, Washington 98195
USA

Dr. Donald E. Bevan
Director
College of Ocean and Fishery Sciences
University of Washington
Mail Stop HA-40
Seattle, Washington 98195
USA

Dr. Eddie Bernard
Director
Pacific Marine Environmental Laboratory
7600 Sand Point Way N.E.
BIN C15700
Seattle, Washington 98115
USA

Dr. Loh-Lee Low
Deputy Director
Resource Ecology and Fisheries
Management Division
Northwest and Alaska Fisheries Center
7600 Sand Point Way Northeast
BIN C15700, Bldg. 4
Seattle, Washington 98115-0070
USA

Dr. Donald A. McCaughran
Director
International Pacific Halibut Commission
P.O. Box 95009
University Station
Seattle, Washington 98145-2009
USA

Dr. Ole A. Mathisen
Dean
School of Fisheries
University of Alaska
11120 Glacier Highway
Juneau, Alaska 99801
USA

Dr. William G. Pearcy
Professor
College of Oceanography
Oregon State University
Corvallis, Oregon 97331
USA

Dr. Gary Stauffer
Division Director
Resource Assessment Conservation Engineering
Northwest and Alaska Fisheries Center
7600 Sand Point Way N.E.
Seattle, Washington 98115-0070
USA

Dr. Robert R. Stickney
Director
School of Fisheries, WH-10
University of Washington
Seattle, Washington 98195
USA

Dr. Warren S. Wooster
Professor
Institute for Marine Studies, HF-05
University of Washington
3707 Brooklyn Avenue N.E.
Seattle, Washington 98195
USA

Organizing Committee

(Department of Fisheries and Oceans, Pacific Region, Biological Sciences Branch, Pacific Biological Station, Nanaimo, B.C.)

Ms. M. Arbanas

Dr. R. Beamish (Chairman)

Mr. J. Corriveau

Mrs. K. Francis

Dr. G. Jamieson

Mr. G. A. McFarlane

Dr. Z. Kabata

Mrs. W. Mitton

Mrs. A. Steele

Mr. J. A. Thomson

Mrs. A. Thompson (Secretary)

Dr. D. Welch

List of Contributors

Adlerstein, S., Fisheries Research Institute, University of Washington, Seattle, Washington, 98195, USA

Bailey, K. M., National Marine Fisheries Service, Northwest and Alaska Fisheries Center, 7600 Sand Point Way N.E., Seattle, Washington, 98115, USA

Beamish, R. J., Department of Fisheries and Oceans, Biological Sciences Branch, Pacific Biological Station, Nanaimo, B.C. V9R 5K6

Bledsoe, L. J., Center for Quantitative Science in Forestry, Fisheries and Wildlife, University of Washington, Seattle, Washington, 98195, USA

Bradford, M. J., Natural Resource Management Program, Simon Fraser University, Burnaby, B.C. V5A 1S6

Bugaev, V. F., Pacific Research Institute of Fisheries and Oceanography (TINRO), Kamchatka Branch, Petropavlovsk-Kamchatsky, USSR

Bulatov, O. A., Pacific Research Institute of Fisheries and Oceanography (TINRO), Vladivostok, 690600, USSR

Chebanov, N. A., Pacific Research Institute of Fisheries and Oceanography (TINRO), Yuzhno-Sakhalinsk, USSR

Collie, J. S., Resource Management Science, University of British Columbia, Vancouver, B.C. V6T 1W5

Davydov, I. V., Pacific Research Institute for Fisheries and Oceanography (TINRO), Kamchatka Branch, Petropavlovsk-Kamchatsky, USSR

Deng, J., Marine Fisheries Research Division, Yellow Sea Fisheries Research Institute, 19, Laiyang Road, Qingdao, Shandong, 266003, The People's Republic of China

Denman, K. L., Department of Fisheries and Oceans, Biological Sciences Branch, Institute of Ocean Sciences, P.O. Box 6000, Sidney, B.C. V8L 4B2

Deriso, R. B., International Pacific Halibut Commission, P.O. Box 95009, Seattle, Washington, 98145-2009, USA

Fargo, J., Department of Fisheries and Oceans, Biological Sciences Branch, Pacific Biological Station, Nanaimo, B.C. V9R 5K6

Fisher, J. P., Oregon State University, School of Oceanography, Corvallis, Oregon, 97331, USA

Francis, R. C., Fisheries Research Institute, University of Washington, Seattle, Washington, 98195, USA

Freeland, H. J., Department of Fisheries and Oceans, Ocean Physics Branch, Institute of Ocean Sciences, P.O. Box 6000, Sidney, B.C. V8L 4B2

Hara, I., Tokai Regional Fisheries Research Laboratory, 5-5-1, Kachidoki, Chuo-ku, Tokyo 104, Japan

Hickey, B. M., School of Oceanography, University of Washington, Seattle, Washington, 98195, USA

Hirose, K., National Research Institute of Aquaculture, 422-1 Nakatsuhamaura, Nansei-cho, Mie-ken 516-01, Japan

Hollowed, A. B., National Marine Fisheries Service, Northwest and Alaska Fisheries Center, 7600 Sand Point Way N.E., Seattle, Washington, 98115, USA

Hsieh, W. W., Department of Oceanography, University of British Columbia, Vancouver, B.C. V6T 1W5

Huggett, W. S., Department of Fisheries and Oceans, Canadian Hydrographic Service, Institute of Ocean Sciences, Sidney, B.C. V8L 4B2

Incze, L. S., Pacific Marine Environmental Laboratory, NOAA, 7600 Sand Point Way N.E., Seattle, Washington, 98115, USA

Jamieson, G. S., Department of Fisheries and Oceans, Biological Sciences Branch, Pacific Biological Station, Nanaimo, B.C. V9R 5K6

Kendall Jr., A. W., Northwest and Alaska Fisheries Center, 7600 Sand Point Way N.E., Seattle, Washington, 98195, USA

Kim, S., Kodiak Facility, Northwest and Alaska Fisheries Center, P.O. Box 1638, Kodiak, Alaska, 99615, USA

Kimura, D. K., Northwest and Alaska Fisheries Center, National Marine Fisheries Service, Bldg. 4, BIN C15700, 7600 Sand Point Way N.E., Seattle, Washington, 98115-6349, USA

Le Blond, P. H., Department of Oceanography, University of British Columbia, 6270 University Boulevard, Vancouver, B.C. V6T 1W5

Lee, W. G., Department of Oceanography, University of British Columbia, Vancouver, B.C. V6T 1W5

Li, X., Department of Marine Fisheries, Zhanjiang Fisheries Institute, Guangdong, The People's Republic of China

McFarlane, G.A., Department of Fisheries and Oceans, Biological Sciences Branch, Pacific Biological Station, Nanaimo, B.C. V9R 5K6

McKinnell, S., Department of Fisheries and Oceans, Biological Sciences Branch, Pacific Biological Station, Nanaimo, B.C. V9R 5K6

Mackas, D. L., Department of Fisheries and Oceans, Biological Sciences Branch, Institute of Ocean Sciences, P.O. Box 6000, Sidney, B.C. V8L 4B2

Marshall, R. P., School of Fisheries and Science, University of Alaska — Juneau, Juneau, Alaska, 99801, USA

Neal, P. R., International Pacific Halibut Commission, P.O. Box 95009, Seattle, Washington, 98145-2009, USA
Parker, K. S. International Pacific Halibut Commission and College of Ocean and Fishery Sciences, University of Washington, Seattle, Washington 98195, USA
Pearcy, W. G., Oregon State University, School of Oceanography, Corvallis, Oregon, 97331, USA
Peterman, R. M., Natural Resource Management Program, Simon Fraser University, Burnaby, B.C. V5A 1S6
Phillips, A. C., Department of Fisheries and Oceans, Biological Sciences Branch, Pacific Biological Station, Nanaimo, B.C. V9R 5K6
Pikitch, E. K., Assistant Professor, Fisheries Research Institute, WH-10, University of Washington, Seattle, Washington, 98195, USA
Quinn II, T. J., School of Fisheries and Science, University of Alaska — Juneau, Juneau, Alaska, 99801, USA
Reed, R. K., Pacific Marine Environmental Laboratory, NOAA, 7600 Sand Point Way N.E., Seattle, Washington, 98115, USA
Schnute, J., Department of Fisheries and Oceans, Biological Sciences Branch, Pacific Biological Station, Nanaimo, B.C. V9R 5K6
Schumacher, J. D., Pacific Marine Environmental Laboratory, NOAA, 7600 Sand Point Way N.E., Seattle, Washington, 98115, USA
Selifonov, M. M., Pacific Research Institute of Fisheries and Oceanography (TINRO), Kamchatka Branch, Petropavlovsk-Kamchatsky, USSR
Shimazaki, K., Faculty of Fisheries, Hokkaido University, 3-3-1, Minatomachi, Hakodate 040, Japan
Stepanenko, M. A., Pacific Fisheries Research Station (TINRO), Vladivostok, 6900600, USSR
Tanaka, S., Tokyo University of Fisheries, Konan 4-5-7, Minato-Ku, Tokyo 108, Japan
Tang, Q., Marine Fisheries Research Division, Yellow Sea Fisheries Research Institute, 19, Laiyang Road, Qingdao, Shandong, 266003, The People's Republic of China
Thomson, R. E., Department of Fisheries and Oceans, Ocean Physics Division, Institute of Ocean Sciences, 9860 West Saanich Road, Sidney, B.C. V8L 4B2
Tomosada, A., Tokai Regional Fisheries Research Laboratory, 5-5-1 Kachidoki, Chuo-ku, Tokyo 104, Japan
Tsuruta, Y., Tokai Regional Fisheries Research Laboratory, 5-5-1 Kachidoki, Chuo-ku, Tokyo 104, Japan
Tyler, A. V., Department of Fisheries and Oceans, Biological Sciences Branch, Pacific Biological Station, Nanaimo, B.C. V9R 5K6
Walters, C.J., Resource Management Science, University of British Columbia, Vancouver, B.C. V6T 1W5
Ware, D. M., Department of Fisheries and Oceans, Biological Sciences Branch, Pacific Biological Station, Nanaimo, B.C. V9R 5K6
Wooster, W. S., Institute for Marine Studies HF-05, University of Washington, Seattle, Washington, 98195, USA
Zhu, J., Marine Fisheries Research Division, Yellow Sea Fisheries Research Institute, 19, Laiyang Road, Qingdao, Shandong, 266003, The People's Republic of China

List of Contributors — Poster Session

Ziemann, D., Association of Primary Production and Recruitment in a Subarctic Ecosystem (APPRISE), Oceanic Institute, Makapuu Point, Waimanalo, Hawaii, 96795, USA
Hyatt, K. D., Barkley Sound Sockeye, Department of Fisheries and Oceans, Biological Sciences Branch, Pacific Biological Station, Nanaimo, B.C. V9R 5K6
Kendall, A. W., Fisheries-Oceanography Coordinated Investigations (FOCI), Northwest and Alaska Fisheries Center, 7600 Sand Point Way N.E., Seattle, Washington, 98195-0070, USA
Schumacker, J., Fisheries-Oceanography Coordinated Investigations (FOCI), Pacific Marine Environmental Laboratory, R/E/TM, 7600 Sand Point Way N.E., Seattle, Washington, 98115-0070, USA
Tyler, A. V., Hecate Strait Project, Department of Fisheries and Oceans, Biological Sciences Branch, Pacific Biological Station, Nanaimo, B.C. V9R 5K6
Crawford, W. R., Hecate Strait Project, Department of Fisheries and Oceans, Canadian Hydrographic Service, Institute of Ocean Sciences, 860 West Saanich Road, P.O. Box 6000, Sidney, B.C. V8L 4B2
Ware, D. M., La Perouse Project, Department of Fisheries and Oceans, Biological Sciences Branch, Pacific Biological Station, Nanaimo, B.C. V9R 5K6
Thomson, R. E., La Perouse Project, Department of Fisheries and Oceans, Biological Sciences Branch, Institute of Ocean Sciences, 9860 West Saanich Road, P.O. Box 6000, Sidney, B.C. V8L 4B2
Healey, M. C., Marine Survival of Salmon Program (MASS), Department of Fisheries and Oceans, Biological Sciences Branch, Pacific Biological Station, Nanaimo, B.C. V9R 5K6
Theilacker, G., Sardine - Anchovy Recruitment Project (SARP), National Marine Fisheries Commission, P.O. Box 271, La Jolla, California, 92038, USA

Acknowledgements

This symposium required the support and cooperation of a large number of people. Financial assistance was provided by the Department of Fisheries and Oceans, University of Alaska, University of British Columbia, International Pacific Halibut Commission, and the National Marine Fisheries Service, Seattle, USA. Support for a reception was kindly provided by the Fisheries Council of British Columbia.

We appreciate the support of the organizing committee members in each of the participating countries for coordinating the selection of speakers. In particular, we appreciated the efforts of Dr. S. Hayasi from Japan, Mr. Jia Jiansan from China, and Dr. S. A. Studenetsky from USSR. During the 3 years it took to plan the symposium, a large number of people contributed to its organization. It is difficult to list everyone that assisted, but we do want to acknowledge the sound advice provided by Dr. N. Wilimovsky from the University of British Columbia. Introductory presentations were given by Dr. Bill Evans, Assistant Administrator for Fisheries, National Marine Fisheries Service, Washington, D.C., and Dr. P. A. Larkin, Vice President, Research, The University of British Columbia, Vancouver, B.C., and summary remarks were provided by Dr. G. Stauffer and Dr. C. Mann.

Closing remarks were provided by Mr. P. S. Chamut, Director-General, Pacific Region, Department of Fisheries and Oceans, Vancouver, B.C. All participants were grateful for the efforts of Kelly Francis, Annette Steele, and Ann Thompson for the local arrangements, and to Dr. G. Stauffer for coordinating the Poster Session. We also thank Dr. D. McCaughran, Dr. R. R. Stickney, Dr. D. Bevan, Dr. V. Alexander, Dr. N. J. Wilimovsky, and Dr. J. C. Davis for chairing the respective Sessions.

Papers in these proceedings were reviewed by at least two referees. Referees for North American authors were selected by the local coordinating committee members and for other authors by the editors. The reviewing, revising, and editing of manuscripts on a timely basis required the cooperation and the immediate attention of reviewers and authors. As editors, we were impressed with the professionalism of the reviewers and the authors. Papers originally written in a language other than English were edited to improve the original English translation. Again, it is difficult to list everyone that assisted. However, we want to acknowledge the assistance of Dr. W. E. Ricker, Dr. K. S. Ketchen, and Mr. J. Westrheim. We sincerely appreciate the editorial assistance of Ann Thompson. Ray Scarsbrook and Barbara Thomson verified references and redrew some figures. For logistic reasons the reviews of the Soviet papers were primarily for style and format.

Introduction

The Need for Interdisciplinary Research in Fisheries and Oceans Sciences

R. J. Beamish, G. A. McFarlane, and W. S. Wooster

Attempts to manage marine fish populations on a scientific basis are very recent. It was really not until the 1960's that scientists and managers developed and applied theories of population dynamics to management of exploited marine fish populations. To put this in perspective, consider the length of time and the number of doctors that have studied just one species — humans. Despite this enormous effort, numerous problems affecting the well-being of our species continue to elude attempts to solve them. Accepting that fisheries science is in its infancy, what direction should fisheries research take to give us an understanding of the factors that control the abundance, distribution and behaviour of fishes?

The organizers of this symposium believed that a better understanding of the population dynamics process required more interdisciplinary research among fisheries scientists and oceanographers. Many in the scientific community now believe this cooperation is not only essential, but there are limits on the time we have to understand the relationship between ocean conditions and fish abundance.

Fisheries scientists spend little time studying environmental effects and relatively few oceanographers seem interested in how their findings might relate to fishery problems. The sponsorship of this symposium was intended to stimulate research in this area. Sponsors hope that the results of this symposium will encourage scientists as well as the many patrons of fisheries and oceans science to recognize the need to understand the relationship among oceans, climate and fish populations.

The North Pacific Ocean and Bering Sea have some of the largest fisheries in the world. Walleye pollock (*Theragra chalcogramma*) have been exploited since the turn of the century, however, it was not until the late 1960's and early 1970's that the resource was fully utilized by the fleets of Japan, the USSR, and North and South Korea. Catches ranged from 5.7 to 6.0 million t in 1973–76 but declined slightly after this period as a result of fishery restrictions imposed by the U.S. and USSR, reflecting concern over reduced abundance of pollock. However, even with these restrictions, the walleye pollock fishery in the North Pacific Ocean has been the largest fishery in the world. Since the mid-1980's pollock catches have increased dramatically and averaged between 10 and 11 million tons annually. More recently, the expansion of this fishery into international waters of the Bering Sea has caused international concern that overfishing may be occurring.

The flying squid (*Ommastrephes bartrami*) fishery is the second largest fishery in the North Pacific Ocean. Squid are captured using surface gillnets that are set throughout the central North Pacific. This fishery has expanded dramatically since its inception in 1978. By 1986, Japan alone accounted for approximately 150 thousand tonnes; and it has been estimated that Korean and Taiwanese vessels catch a similar amount. Japanese, Korean, and Taiwanese vessels set an estimated 30 000 km of driftnet each night. This amount of net would stretch back and forth from Vancouver to Tokyo approximately four times each night. Clearly, this is a massive fishery that impacts not only on squid but also inadvertently on other species such as salmon, other fishes, and marine mammals.

The area is also the feeding grounds for steelhead (*Salmo gardneri*) and 6 species of salmon that originate from the U.S.A., Canada, Japan, and the USSR. Estimates of the size of salmon stocks in the North Pacific are generally unavailable. However, recent work indicates that the salmon biomass in the Gulf of Alaska alone (E 170° W) was 2 million t in the early 1980's (Ware and McFarlane, this volume), supporting an average catch of over 200 thousand t by North American fisheries annually. The landed value of North American salmon fisheries (in 1987 U.S. dollars) would be in excess of 3 billion dollars. Other major fisheries include Pacific hake (*Merluccius productus*), Pacific halibut (*Hippoglossus stenolepis*), sablefish (*Anopolopoma fimbria*), rockfishes, Pacific herring (*Clupea harengus pallasi*), Japanese sardine (*Sardinops melanosticta*). In addition, there is a large biomass of pomfret (*Brama japonica*), Pacific saury (*Cololabis saira*) and tuna which utilize the area intermittently.

It is obvious that the health of these and other fisheries is very important to the countries that surround the North Pacific Ocean. Because of the complexity of the fish-ocean interactions, there is a need to study the region as an integrated unit. This can be accomplished most effectively through a program that promotes interdisciplinary and multinational scientific collaboration.

IRIS (International Recruitment Investigations in the Subarctic) was formed to encourage research on ocean-fish interactions to understand better the affects of ocean variability on the abundance and distribution of fish stocks. IRIS was initiated in 1982 as a collaborative effort among university and government oceanographic and fishery institutions on the west coast of North America in British Columbia, Alaska, Oregon and Washington. This organization encouraged cooperative research among fisheries scientists and oceanographers by providing a communication network among senior scientists and administrators.

In support of these goals, IRIS jointly sponsored this symposium and has endorsed a proposal to establish a new international scientific organization in the northern North Pacific Ocean.

This proposed new organization is supported by IRIS because oceanic and atmospheric processes span the entire width of the North Pacific, and even the ecosystems usually extend over regions much larger than those containing the commercial fisheries. To be successful the study of such large regions and systems requires widely distributed research, monitoring and effective international cooperation. The information needs go well beyond the usual fisheries data, requiring the contributions of ocean and atmospheric scientists in addition to those of fisheries scientists.

The needs and benefits of a broader scientific forum for the North Pacific have been recognized by some scientists over the past 15 years. The need for this forum is particularly urgent now that biologists and oceanographers are aware of the importance of ocean conditions in determining global climate and local oceanographic conditions. A new North Pacific fisheries and oceans scientific organization would promote the systematic collection and exchange of scientific information, encourage multinational programs of benefit to the countries bordering the North Pacific Ocean, and generally promote a regular and timely exchange of ideas. IRIS proposed to co-host this symposium with the International North Pacific Fisheries Commission (INPFC) so that countries considering formation of a new North Pacific organization could meet in a manner similar in format and content to that proposed. INPFC was interested in co-hosting the symposium because it had previously sponsored international symposia on non-anadromous fisheries in the North Pacific, and its commissioners were interested in the establishment of a new organization that would accept INPFC's responsibility for non-anadromous species.

One of the topics of this symposium proposed by IRIS, the effects of ocean variability on recruitment, is timely in view of the advances that have been made in oceanography in recent years. There are well developed techniques for describing current regimes and upwelling events and for monitoring salinity, temperature, and production. Fisheries biologists stress the importance of conducting oceanographic studies on the continental shelves. The studies that have been carried out demonstrate the complex nature of the current systems. Despite this complexity, there are now sufficient oceanographic data to design studies to test hypotheses relating to the variability of recruitment. Papers of the symposium have paid particular attention to variations in ocean circulation as measured directly or suggested by surrogates such as sea surface temperature and related year-class strengths. Not content with just describing the relationships, most authors have sought possible explanatory mechanisms.

The INPFC was established in 1952 to ensure that fisheries of joint interest to Canada, United States, and Japan were maintained and conserved. The INPFC promotes and coordinates scientific studies necessary to determine conservation measures that need to be taken by the contracting parties. A major function of the Commission has been to regulate the catch of salmon of North American origin on the high seas. The convention was amended in 1978 when it was agreed that the contracting parties would work towards the establishment of an international organization with broader membership that would deal with species other than salmonids. It was also agreed that it would be useful to have scientific symposia that dealt with the biology and stock assessment issues of non-anadromous fishes. In an attempt to implement both of these initiatives, the INPFC commissioners agreed to hold a joint symposium with IRIS on the condition that topics be restricted to non-anadromous species. Thus, studies on salmon were not emphasized at this symposium. The topic suggested by INPFC members was the evaluation of the accuracy of parameters used in stock assessment of non-anadromous species.

The importance of error is commonly evaluated in most sciences. However, in fisheries science, in general, and in stock assessment models, in particular, there are very few practical evaluations of the consequences of errors in parameters. Errors can result from incorrect assumptions such as constant natural mortality, or from measurement errors in the accuracy of parameters such as incorrect age determinations or biases in sampling. Many models assume parameter values are constant, yet we know that variability is inherent in biological processes. When models are tested with each other, those that best reduce variance are usually accepted as representative of the particular data set. The agreement with data sets in such cases is given more emphasis than the accuracy of parameters used. Some models in fisheries science minimize the number of parameters used because of their uncertainty. For example, the original stock production model was developed because there was no method for ageing tuna (Schaefer 1954). Thus there was no doubt that uncertainty exists in the parameters, and assessing the accuracy of these parameters was an important topic.

Several papers indicated that the assumption of constant parameters, in particular that environmental conditions are invariant, restricts our ability to develop theories to explain the fundamental principles, especially in terms of the scales of climate change. In fisheries management, we know that in extreme cases a fishery can have major effects on the abundance of fish stocks. However, the development of good predictive models has proven difficult. Models predicting the abundance of fish populations are often based on catch information. Unfortunately, the various processes controlling abundance simply cannot be determined by the study of catch. Fisheries experimentation by intentionally altering catch is important but does not preclude the necessity to study other factors that control abundance. Undoubtedly better quality data, longer time series, and improved analytical techniques will help. But there also is no doubt that an understanding of the underlying relationships between the environment and the life history strategies of the important species is needed.

The vastness of the ocean, the difficulty of sampling large areas in sufficient time, combined with the need for extensive information on fish and fisheries present major obstacles to the understanding of the principles that govern stock size. In spite of these difficulties we should not avoid the challenge of unravelling the population dynamics process. We are certain that this barrier of complexity separates us from something fundamentally simple. Eventually we will uncover some underlying principles that govern the choice of life history types, migratory behaviour, reproductive strategy, longevity, and perhaps speciation. We will understand the importance of species interactions throughout the life of fishes and we will use this knowledge to regulate harvest to ensure future productivity of marine animals. Interdisciplinary research, particularly between fisheries and oceans scientists, is the key to establishing the framework to develop this understanding.

We expect in the future to be able to predict stock size or, in the case of salmon, run timing and migration routes. There are other benefits, in the longer term, potentially very useful for the resource-based economies of countries around the North Pacific Ocean. For example, we believe that significant changes in climate will occur in the next few decades. Many scientists are taking the predictions of global warming seriously. The effects on fisheries are relatively unstudied but observations for some fisheries show a strong relationship between temperature and commercial landings (Cushing 1982). We are also aware that the presence and absence of currents or upwelling can result in the production of strong or weak year-classes. Thus many scientists believe that global warming will change the nature of our fisheries. The time in which these changes could occur appears to be quite short. In fact, we may already be receiving signals indicating that important changes are occurring. Those of us who organized this symposium believe that we must move forward quickly. IRIS members expect to have another symposium in 1991 that will address the issue of climate change and its effect on the distribution and abundance of fishes in the North Pacific and North Atlantic. We hope that by this time a new North Pacific Science organization will be in place, and that countries will be more actively investigating the problem of understanding the relationships between ocean variability and recruitment.

Some participants felt that the topics and the format that combined papers on population dynamics, on physical and chemical oceanography, and on some old-fashioned biology, would not encourage interdisciplinary communication. Participants came to this symposium with labels such as biologist, oceanographer, physicist, or chemist. But during the conference there was a marriage of these interests. At the end of the 3 days, people thought a little differently about issues in their own field. A unity was developing between disciplines and the scientists of the participating countries. There was not indifference or frustration but rather acceptance of the need for fish-ocean science and of the problems and complexities of one another's fields. This change in attitude was surprising. The interest, even enthusiasm, indicates that under the right circumstance, an interdisciplinary approach in fisheries and oceans science can be made to work.

As scientists we know there are limits to production, to distribution, and to survival. We know that the oceans and marine animals can be overexploited. We have seen minor and major examples in the last few decades of man's ability to alter processes that regulate population size in fishes. It concerns many of us that our lack of understanding may mean that present and future exploitation of the oceans and marine animals may adversely affect our general quality of life. The role of science in preserving our quality of life is recognized but is more or less taken for granted. Unfortunately, there is a tendency to provide new resources and direction only when extreme examples of environmental damage occur. Despite the difficulty in obtaining resources, it is important that we not wait for a major crisis to occur before we improve our understanding of the factors regulating marine populations. We require innovative thinking, new approaches in our research, and some risk taking if we are to ensure that irrepairable changes do not occur as a consequence of world population increases.

The next decade will be a most exciting and stimulating period for fisheries biologists and oceanographers. It is possible that biology and oceanography will be more important in the planning and development of national economies. To meet these challenges in our science we must coordinate and integrate our understanding of fisheries and oceanography in the North Pacific. It is our hope that this symposium was a step toward the achievement of this aim and that it will be followed by many more, similar steps.

References

CUSHING, D. H. 1982. Climate and fisheries. Academic Press, New York, NY. 373 p.

SCHAEFER, M. B. 1954. Some aspects of the dynamics of populations important to the management of the commercial marine fisheries. Bull. Inter-Am. Trop. Tuna Comm. 1(2): 27–56.

WARE, D. M., AND G. A. MCFARLANE. 1989. Fisheries production domains in the northeastern Pacific Ocean, p. 359–379. *In* R. J. Beamish and G. A. McFarlane [ed.] Effects of ocean variability on recruitment and an evaluation of parameters used in stock assessment models. Can. Spec. Publ. Fish. Aquat. Sci. 108.

Before and After
Ricker (1954) and Beverton and Holt (1957)

P. A. Larkin
Resource Ecology, The University of British Columbia, Vancouver, B.C. V6T 1W5

I confess to some difficulty in preparing my remarks for this occasion, and it was only after considerable reflection that I decided to entitle what I had to say as, "Before and After Ricker (1954) and Beverton and Holt (1957)". For me, those were pivotal contributions and determined much of the research that many of us subsequently attempted. What I have to say, then, is something of a personal memoir which confirms what I understand is called Felson's Law, which states,

"If you steal the ideas of one person, it is called plagiarism; if you steal the ideas of several people, it is called research."

Before

Stock recruitment relations expressed in the form of mathematical models came into vogue in fisheries biology in the mid-1950's with the publications of Ricker (1954) and Beverton and Holt (1957). Both models were derived from notions of density dependent predation, Ricker's with mortality dependent on initial abundance, and that of Beverton and Holt on densities over a sequence of stages. Both arose in part from the literature of fisheries biology, and in part from a much broader literature concerned with the regulation of abundance of natural populations, a subject on which controversy had been brewing for many years.

After several decades of study by such now forgotten great names as Uvarov (1931), Chapman (1933), Bodenheimer (1938), and Thompson (1939), much if not most of the work on insect populations, there were two schools of thought on the subject of population regulation. Some argued that only density dependent biological factors such as cannibalism, diseases, parasites and predation, could regulate abundance. Their champion came to be Nicholson, who in 1933 submitted to Charles Elton, then editor of the *Journal of Animal Ecology*, a paper which deduced 76 conclusions from some simple propositions concerning the balancing of populations through processes of competition. The referees who reviewed the paper didn't think it should be published because it contained no data and was just speculation, but the editor, exercising his prerogative, published the paper (C. Elton, pers. comm.). Battle was soon joined by those who believed that density independent factors of the physical environment, such as temperature and humidity, were the major determinants of animal (i.e., insect) distribution and abundance (Andrewartha and Birch 1954). Because Nicholson, Andrewartha and Birch were all Australians, the debate was vociferous and conducted with Australian rugby rules.

The essence of Nicholson's argument was this: that factors which acted independently of density, such as climate, were inherently incapable of regulating abundance. You couldn't rely on a cold summer to come along and kill, say, grasshoppers when they were abundant. By contrast, predators, parasites, and diseases could be counted on to respond to the density of their victims and, together with famine, could therefore regulate population size. Supporting Nicholson's hypothesis was the elegant demonstration of Holdaway (1932) working with cultures of the stored products beetle *Tribolium confusum*. Holdaway observed that by changing the relative humidity, he could change the equilibrium population level of *Tribolium* in culture. But at any given relative humidity the regulation of population was accomplished through cannibalism. Thus, physical and chemical factors of the environment, acting independently of population density, set the stage on which density dependent factors regulated population size — at least in laboratory populations. The famous study by Errington (1943) supported the Holdaway conception, dry years rendering muskrats much more vulnerable to predation.

The essence of the opposition argument was that given favorable climatic conditions, the grasshoppers would explode into abundance and the density dependent horsemen of the apocalypse were just out for a pleasant ride that was quite incapable of regulating the population before climate changed to being unfavorable, freezing, frying, soaking or drying any that couldn't run away or find a place to hide. The debate between the two schools of thought continued for a decade or two, and finally degenerated into semantics. Solomon (1949) pretty well wrapped up the debate.

Subsequently, there were a few new wrinkles on some old ideas. Lack (1954) contributed the important distinction between the factor which predisposed an animal to die (starvation) and what actually killed it (a predator). Ferris Neave (1952) made a significant contribution in suggesting that when populations reached low levels, they might be preyed upon proportionately more heavily (depensatory or inversely density dependent mortality). This happens to pink salmon in circumstances where predators tend to take a fixed number of prey, regardless of prey abundance. This was a variation on a theme of Allee (1938) that emphasized that the social life of animals gave safety in numbers. A similar idea was contained in the work of Morris and his colleagues (Morris 1963a) on the causes of population fluctuation of the spruce budworm, who also focussed attention on the "key stage" of the life history when density dependent regulation might occur (Morris 1963b).

As time went by, there was an accumulation of studies of population regulation on various species of organisms. The comprehensive analysis of Tanner (1966) made clear that the higher vertebrates were more likely to be regulated by density dependent factors while insects were much more likely to temporarily escape density dependent controls when climatic factors were favourable. Naturally occurring fish populations fell somewhere in between, the abundance of year-classes being determined early in life, but thereafter the effects of density or oceanographic conditions being reflected in growth rate rather than in survival (Larkin 1978).

The literature of fisheries biology and management was not in the mainstream of this controversy, which was unfortunate because it had much to contribute. Our scientific grandparents of the early part of this century had quickly identified recruitment as a central issue and had speculated that year-class size was determined at an early age (Hjort 1914; Thomasson 1981). Subsequent studies suggested that after the egg yolk was exhausted, fish larvae face a critical period in which starvation influences survival (Sette 1943). Additionally, the time of metamorphosis seems to be a critical period for flatfish (Beverton and Holt 1957). The notion that density dependent factors regulated year-class size was thus well entrenched in the thinking of fisheries biologists when Ricker and Beverton and Holt presented their models.

But it was also realized that oceanographic conditions set the stage on which the density dependent action takes place (see Harding 1974 for a brief review). It was known, for example, that oceanographic conditions influenced the quantity and species composition of prospective food for larvae. It was also clear that vagaries in ocean currents could carry the larvae away from the regions of most abundant food.

To summarize, at the time that Beverton and Holt and Ricker devised their models, there was (1) widespread controversy about the factors that regulate animal abundance, most of the argument based on studies of insects, small mammals and birds, and (2) a good body of evidence to support the notion that for fish populations, year-class size is determined early in life, and as for Holdaway's beetles, physical and chemical factors set a stage on which density dependent factors act to regulate numbers.

After

Since the days when Ricker and Beverton and Holt produced their models, stock and recruitment research has taken two major directions. First has been the development of their models and other models, and the techniques of estimating their parameters. This line of activity was appealing to those oriented to fisheries management because it provided a quantitative means by which to make day-to-day decisions. The second direction of research was toward better understanding of just what does happen to determine year-class size during the early life history of fish.

On the modelling side, it didn't take Ricker very long to ask the obvious question: "What happens if, on models of stock and recruitment, you superimpose simulated effects of environmental variability?" (Ricker 1958). The advent of computers made life a lot easier for those who wished to ask these kinds of questions, exploring the theoretical consequences of making various assumptions. In 1964, I did an extensive computer confirmation of Ricker's 1958 study of the implications of environmental variability on harvesting strategies. When I told Ricker that my results confirmed his, he remarked that that only proved I had written a good program.

The ICES symposium on Fish Stocks and Recruitment in 1973, held in Aarhus, Denmark, was a landmark (Parrish 1973). By that time, a number of alternative models had been developed. It was becoming obvious that with the advent of computers, theoretical variations were only really limited by the imagination of the investigator (Larkin 1973). The data certainly didn't impose many constraints, and if it weren't for the certainty that zero stock would produce zero recruits, almost anything could be fitted. I vividly recall a meeting of the Pacific Fisheries Biologists at which one young biologist said that the best fit to his stock-recruit data was a star.

Because the data are so typically indicative of a lack of a stock-recruit relationship, it has often been suggested that one might as well fit them with a polynomial, the only problem arising when you wish to extrapolate beyond the range of the observations. A more recent statistical approach has been time series analysis, which has the merit of taking into account the additional information of the sequence of the data points, but I can tell you from bitter experience that it is almost as perilous to predict next year from a time series analysis as by any other means.

Alternatively, one can take an empirical approach of accepting the mean values of recruitment associated with each level of stock and examining their recursive properties. (Chapman (1973) and Larkin (1973) give examples of this approach.) Going a step further, one can use the observed probabilities of getting various sized recruitments from a given level of stock as has been suggested by Rothschild and Mullen (1985) and Evans and Rice (1988). The trouble with this sort of model is that it takes a long time to get enough data to have any confidence in predictions. But maybe that's the way it is.

Since the Aarhus symposium, a number of workers, most notably Carl Walters, Ray Hilborn and Don Ludwig (Walters and Hilborn 1976; Walters and Hilborn 1978; Walters and Ludwig 1981; Ludwig and Walters 1981; Smith and Walters 1981; Ludwig and Walters 1982), have examined a wide range of theoretical stock-recruit questions and have suggested strategies of adaptive management to guide decisions on how much to harvest. Acknowledging that the information available is subject to sampling errors and that there is a large amount of variability, much of which is associated with oceanographic conditions, which cannot be controlled, they ask, "What is the best way to gain information about the systems while achieving over the long term the greatest yield consistent with a stated risk?"

It is my personal feeling that this sort of thing has gone about as far as it will go with the data available. Essentially, it attempts to depict highly complex processes with simplified two-dimensional models that are reasonably tractable for good mathematicians, and capable of generating broad brush advice to managers. It almost certainly pays *always* to harvest less than the stock-recruit relationship suggests as the maximum sustainable yield. But further progress will depend on better understanding of the mechanisms of population regulation and bold steps in experimental management.

Another line of modelling research has been the mixed stocks problem, which was first addressed (as usual) by Ricker (1958). When two or more stocks of Pacific salmon of differing productivity are harvested jointly, a rate of harvesting that is a compromise may fish one stock at less than an optimal rate, but another at greater than an optimal rate. Paulik et al. (1967) developed a quantitative model for any number of jointly harvested salmon stocks, and Hilborn (1985) has recently pointed out that the history of exploitation strongly influences the estimates of stock productivity and may lead to techniques of management that will maintain over-exploitation of unproductive stocks. McDonald (1981) and Healey (1982) give excellent reviews of the background to the problem of mixed stocks of several species of Pacific salmon all harvested jointly.

The mixed stock-mixed species problem of Pacific salmon is, as the saying goes, "just the tip of the iceberg" of the more general problem of multispecies interactions in aquatic communities. For these highly complex systems, stock-recruit relationships may be an important component of large scale simulation models, which can best be described as expressions of religious conviction. Having spent many hours on these sorts of exercises, I can say in retrospect that they were remarkably stimulating, generated many insights as well as ideas for research, but didn't do much to advance the state of knowledge. Suffice to say that some who have built large simulation models have come to believe that their results are more reliable than those that can be obtained from fishing. That's faith.

In recent years, the second field of research, that was directed to better understanding of what happens in nature, was in large part pursued by investigators with little or no direct involvement in stock assessment or management. It included biological oceanographers and oceanographical biologists, and a few hybrids, who also developed models of stock and recruitment. Perhaps the most eclectic of these hybrids was David Cushing, who stimulated a great deal of interest in the broad questions of the relative roles of density dependent and physical environmental factors on year-class abundance (for example, Cushing and Walsh 1976), and conceived the concept of various degrees of "matching" of plankton production and larval feeding. The most prophetic of the hybrids was Derek Iles, who boldly drew attention in 1973 to correlations in abundance of whitefish in Alberta lakes, and sardines in California which he said reflected global patterns in environmental conditions (Iles 1973). I was asked to review an earlier version of Iles' paper, and blush to admit I recommended that it not be published! But the theme was subsequently picked up by Cushing in 1978 who correlated Swedish, Norwegian and two Japanese fisheries on herring, also suggesting the effect of global climatic variations. Since then, all sorts of people have got in on the act of correlating biological and oceanographic events on a global scale.

Cushing's (1978) paper appeared in another ICES symposium that was a milestone in the documentation of understanding of why stock-recruit relations are as they are. Held in Edinburgh in 1976, the symposium dealt with Marine Ecosystems and Fisheries Oceanography (Parsons et al. 1978). The timing couldn't have been better. The North Sea stocks of fisheries were showing changes in species composition with the increasing rate of fishing, an El Niño event had occurred off Peru in 1972/73 and had suggested changes in the phytoplankton species composition of possible significance to survival of anchoveta (*Engraulis ringens*). Lasker's superb study of the relation between oceanographic conditions and larval anchovy food in the California current told a similiar story in rich detail (Lasker 1978). The timing of the onset and the duration of upwelling are crucial determinants for survival of northern anchovy (*Engraulis mordax*).

A whole section of the symposium was devoted to the theme of biological effects of ocean variability, elaborating on the significance of various temporal and spatial scales. For example, Paul Smith emphasized that present sampling practices are biassed in the direction of convenience to investigators rather than to the scales of important oceanographic events (Smith 1978). It reminded me that many years ago Monte Lloyd had defined an animal population as the number of animals in an area that a researcher found it convenient to study. Most importantly, the symposium made abundantly clear that studies of larval ecology were bringing new understanding to the old problem of stock and recruitment.

It was nevertheless apparent that there was and still is a long way to go. Large to medium scale surveys have been greatly facilitated by satellite surveillance, but give only some of the characteristics of the surface layer and only partially substitute for data from vessel surveys or automated buoys. *In situ* experiments of sufficient size to be meaningful are expensive and time consuming. The sheer volume of work in identifying and counting organisms can be daunting to even the most intrepid investigator.

It is also apparent that we are still a long way away from understanding multispecies interactions. The Dahlem Conference in Berlin in 1982 (May 1982) is a comprehensive but discouraging account of present knowledge of multispecies fisheries. There was an abundance of evidence that heavy rates of exploitation can lead to dramatic changes in species composition and presumably stock-recruitment relations are involved. Skud (1982) has drawn attention to some curious relationships between Atlantic herring and mackerel that sound strangely like the anchovy/sardine relation of the Pacific. But the mechanisms involved in even these two species dependencies are not yet clear. In general, for situations involving three or more species, speculation runs far ahead of understanding.

Geographically speaking, it is useful to remind ourselves that a major part of the relevant work in the past has been done in the North Sea or off the Atlantic coast of North America. Comparatively speaking, much less has been done in other parts of the world, particularly for tropical near-shore fisheries. The Cronulla workshop on tropical multispecies fisheries (Pauly and Murphy 1981) brought many of the problems into focus and stressed the need for a "long-term multidisciplinary research program to improve understanding of the ways in which species interact." A particular need is for studies of recruitment directed at larval ecology and interrelations of species in nursery areas.

The North Pacific is less well studied than the North Atlantic. While this shortcoming has been redressed in some measure in recent years, it is nevertheless important to keep it in mind. For example, the USSR Bering Sea expedition begun in 1958 had, by 1963, (Moiseev 1963), completed the first comprehensive surveillance of the fisheries and marine biota of the Eastern Bering Sea, a surveillance that provided the sort of basic benchmark that was available for the North Sea in, say, the 1930's. The Japanese literature is rich in examples of the significance of oceanographic conditions in influencing concentrations of catchable fish, but has not focussed particularly on factors influencing year-class strength. The North American literature has been dominated by contributions to fish population dynamics and concern with Pacific salmon, which pose rather atypical problems of stock and recruitment (who but a salmon biologist would worry about the impact of railway construction on recruitment!). For the other major commercial species, there is an abundance of catch statistics and age determinations on which stock assessments are based, but comparatively little literature that goes beyond a sketch of the early life history ecology.

This symposium is thus very timely. It brings together researchers from both sides of the Pacific to address questions of recruitment over a wide range of species. It brings together the numerical witch doctors who pretend to know all of the answers now and the larval ecologists who promise to know all of the answers someday. It addresses matters of methodology and provides some new theories. It reports on a variety of aspects of early life history biology of fishes and provides new material on oceanography related to fisheries. The only thing it doesn't have is Ricker, and Beverton and Holt, but then you can't have everything!

References

Allee, W. C. 1938. The social life of animals. Norton, New York, NY. 293 p.

Andrewartha, H. E. and L. C. Birch. 1954. The distribution and abundance of animals. University of Chicago Press, Chicago, Ill. 782 p.

Beverton, R. J. H., and S. J. Holt. 1957. On the dynamics of exploited fish populations. Fish. Invest., Ser. 2, 19: 533 p.

Bodenheimer, F. S. 1938. Problems of animal ecology. Oxford University Press, London. 183 p.

Chapman, D. G. 1973. Spawner-recruit models and estimation of the level of maximum sustainable catch. Rapp. P.-v. Reun. Cons. int. Explor. Mer 164: 325-332.

Chapman, R. N. 1933. The cause of fluctuations of populations of insects. Proc. Hawaii Entom. Soc. 8: 279-297.

Cushing, D. H. 1978. Biological effects of climatic change. Rapp. P.-v. Reun. Cons. int. Explor. Mer 1973: 107-116.

Cushing, D. H., and J. J. Walsh. [ed.] 1976. The ecology of the seas. 467 p. W. B. Saunders, Toronto, Ont. 467 p.

Errington, P. L. 1943. An analysis of mink predation upon muskrats in north central United States. Iowa State College, Agric. Exp. Stn., Res. Bull. 320: 797-924.

Evans, G. T., and J. C. Rice. 1988. Predicting recruitment from stock size without the mediation of a functional relation. J. Cons. int. Explor. Mer. 44. 111-122.

Harding, D. 1974. The biology of fish larvae with particular reference to the plaice (*Pleuronectes platessa* Linn.) p: 55-66. *In* F.R Harden-Jones [ed.] Sea fisheries research, Halstead Press, New York, NY.

Healey, M. C. 1982. Multispecies, multistock management problems in the management of Pacific salmon. *In* M. C. Mercer [ed.]. Multispecies approaches to fisheries management advice. Can. Spec. Publ. Fish. Aquat. Sci. 59: 119-126.

Hilborn, R. 1985. Apparent stock recruitment relationships in mixed stock fisheries. Can. J. Fish. Aquat. Sci. 42: 718-723.

Hjort, J. 1914. Fluctuations in the great fisheries of northern Europe viewed in the light of biological research. Rapp. P.-v. Reun. Cons. perm. int. Explor. Mer, 20: 1-228.

Holdaway, F.G. 1932. An experimental study of the growth of populations of the "flour beetle" *Tribolium confusum* Duval, as affected by atmospheric moisture. Ecol. Monogr. 2: 261-304.

Iles, T. D. 1973. The interaction of environment and parent stock size in determining recruitment in the Pacific sardine, as revealed by analysis of density-dependent O-group growth. Rapp. P.-v. Reun. Cons. int. Explor. Mer 164: 228-240.

Lack, D. 1954. The natural regulation of animal numbers. Clarendon Press, Oxford. 343 p.

Larkin, P. A. 1973. Some observations on models of stock and recruitment relationship for fishes. Rapp. P.-v. Reun. Cons. int. Explor. Mer 164: 316-324.

1978. Fisheries management-an essay for ecologists. Ann. Rev. Syst. Ecol. 9: 57-73.

Larkin, P. A., and W. E. Ricker. 1964. Further information on sustained yields from fluctuating environments. J. Fish. Res. Board Can. 21: 1-7.

Lasker, R. 1978. The relation between oceanographic conditions and larval anchovy food in the California current: identification of factors contributing to recruitment failure. Rapp. P.-v. Reun. Cons. int. Explor. Mer 173: 212-230.

Ludwig, D., and C. J. Walters. 1981. Measurement errors and uncertainty in parameter estimates for stock and recruitment. Can. J. Fish. Aquat. Sci. 38: 711-720.

1982. Optimal harvesting with imprecise parameter estimates. Ecol. Model. 14: 273-292.

May, R. M. 1982. Exploitation of marine communities. Dahlem Konferenzen, Life Science Research Report 32. Springer-Verlag., Berlin. 366 p.

McDonald, J. 1981. The stock concept and its application to British Columbia fisheries. Can. J. Fish. Aquat. Sci. 38: 1657-1664.

Moiseev, P. A. [ed]. 1963. Soviet fisheries investigation in the northeast Pacific, Part 1. VNIRO Trudy 48: 315 p. [English Translation] Israel Prog. Sci. Trans., Jerusalem, 1968.]

Morris, R. F. [ed.]. 1963a. The dynamics of epidemic spruce budworm populations. Mem. Entomol. Soc. Can. 31: 332 p.

1963b. Predictive population equations based on key factors. Mem. Entomol. Soc. Can. 32: 16-21.

NEAVE, F. 1952. Even-year and odd-year pink salmon populations. Trans. R. Soc. Can. Ser. 3, 46 (v): 55–70.

NICHOLSON, A. J. 1933. The balance of animal populations. J. Anim. Ecol. 2: 132–178.

PARRISH, B. C. [ED.]. 1973. Fish stocks and recruitment. Rapp. P.-v. Reun. Cons. int. Explor. Mer 164: 372 p.

PARSONS, T. R., B.-O. JANSSON, A. R. LONGHURST, AND G. SAETERSDAHL [ED.]. 1978. Marine ecosystems and fisheries oceanography. Rapp. P.-v. Reun. Cons. int. Explor. Mer 173: 240 p.

PAULIK, G. J., A. S. HOURSTON, AND P. A. LARKIN. 1967. Exploitation of multiple stocks by a common fishery. J. Fish. Res. Board Can. 11(5): 559–623.

PAULY, D., AND G. I. MURPHY. 1981. Theory and management of tropical fisheries. Proc. ICLARM/CSIRO Workshop at Cronulla. ICLARM Cont. 105: 360 p.

RICKER, W. E. 1954. Stock and recruitment. J. Fish. Res. Board Can. 11: 559–623.

1958. Maximum sustained yields from fluctuating environments and mixed stocks. J. Fish. Res Board Can 15: 991-1006.

ROTHSCHILD, B. J., AND A. J. MULLEN. 1985. The information content of stock-and-recruitment data and its nonparametric classification. J. Cons. int. Explor. Mer 42: 116–124.

SETTE, O. E. 1943. Biology of the Atlantic mackerel of North America. Part I. Early life history, including the growth, drift and mortality of egg and larval populations. U.S. Fish Wild. Serv., Fish. Bull. 50: 149–234.

SKUD, B. E. 1982. Dominance in fishes: the relation between environment and abundance. Science 216: 114-149.

SMITH, A. D. M., AND C. J. WALTERS. 1981. Adaptive management of stock-recruitment systems. Can. J. Fish. Aquat. Sci. 38: 690–703.

SMITH, P. E. 1978. Biological effects of ocean variability: time and space scales of biological response. Rapp. P.-v. Reun. Cons. int. Explor. Mer 173: 117–127.

SOLOMON, M. E. 1949. The natural control of animal populations. J. Anim. Ecol. 18: 1-35.

TANNER, J. T. 1966. Effects of population density on growth rates of animal populations. Ecology 47: 733–745.

THOMASSON, E. M. [ED.]. 1981. Study of the Sea: the development of marine research under the auspices of the International Council for the Exploration of the Sea. Fishing News Books, Farnham, UK. 256 p.

THOMPSON, W. R. 1939. Biological control and the theories of the interactions of populations. Parasitology 31: 299–388.

UVAROV, B. P. 1931. Insects and climate. Trans Entomol. Soc. London 79: 1–247.

WALTERS, C. J., AND R. HILBORN. 1976. Adaptive control of fishing systems. J. Fish. Res. Board Can. 33: 145–159.

1978. Ecological optimization and adaptive management. Ann. Rev. Ecol. Syst. 9: 157–188.

WALTERS, C. J., AND D. LUDWIG. 1981. Effects of measurement errors on the assessment of stock-recruitment relationships. Can. J. Fish. Aquat. Sci. 38: 704–710.

Topic 1

An Evaluation of the Accuracy of Parameters Used in Stock Assessment

An Experimental Strategy for Groundfish Management in the Face of Large Uncertainty about Stock Size and Production

Carl J. Walters and Jeremy S. Collie

Resource Ecology/Resource Management Science,
University of British Columbia, Vancouver, B.C. V6T 1W5

Abstract

WALTERS, C.J., AND J.S. COLLIE. 1989. An experimental strategy for groundfish management in the face of large uncertainty about stock size and production, p. 13–25. *In* R.J. Beamish and G.A. McFarlane [ed.] Effects of ocean variability on recruitment and an evaluation of parameters used in stock assessment models. Can. Spec. Publ. Fish. Aquat. Sci. 108.

Estimates of stock size and yield for some major demersal stocks, such as Pacific ocean perch off the B.C. coast, vary by as much as a factor of six depending on how historical catch, CPUE, and survey data are interpreted. There is further uncertainty about how low such stocks can be pushed before severe recruitment overfishing occurs. The mathematical and statistical tools of stock assessment cannot eliminate such uncertainty; these tools point instead to the importance of collecting survey abundance data independently of commercial fishing, and of directly measuring stock responses to more extreme disturbances. For species occurring as several more-or-less spatially distinct substocks within a region, we recommend an experimental management strategy involving (1) designating substocks for unregulated harvest, quota management, and complete closure to fishing (to permit direct comparisons of stock performance under these alternative harvest regimes), (2) development of cooperative survey schemes in which the commercial fishermen spend part of their time surveying all substocks, and (3) development of contingency plans that are agreeable to both fishermen and government for detecting and responding to potential collapse of the unregulated substocks. Such an adaptive strategy would meet several conflicting objectives of parties involved in the fishery: fishermen would have improved access to some areas, managers would have the safety of closed and quota areas, and scientists would gain valuable information about stock sizes and recruitment variation by comparing the areas. A difficulty in implementing the strategy for B.C. slope rockfish is the issue of who should pay for the abundance surveys; the fishermen are unwilling to bear this burden, and it is not clear that the public (government) should take risks with some substocks and also pay the direct cost of taking these risks.

Résumé

WALTERS, C.J., AND J.S. COLLIE. 1989. An experimental strategy for groundfish management in the face of large uncertainty about stock size and production, p. 13–25. *In* R.J. Beamish and G.A. McFarlane [ed.] Effects of ocean variability on recruitment and an evaluation of parameters used in stock assessment models. Can. Spec. Publ. Fish. Aquat. Sci. 108.

Les estimations de la taille des stocks et du rendement de certains stocks importants de poissons démersaux, comme le sébaste à longue mâchoire fréquentant les eaux au large de la côte de la Colombie-Britannique, varient jusqu'à un facteur de 6 selon l'interprétation des données antérieures sur les prises, la CPUE et les données obtenues lors de campagnes d'étude. Jusqu'à quel point on peut abaisser ces stocks avant que la surpêche affecte le recrutement constitue une autre source d'inquiétude. Les outils mathématiques et statistiques d'évaluation du stock ne peuvent pas éliminer une telle source d'inquiétude; ces outils montrent plutôt l'importance de recueillir des données sur l'abondance indépendamment de la pêche commerciale, et de mesurer directement la réaction des stocks à des perturbations plus grandes. Dans le cas d'espèces pour lesquelles il existe plusieurs sous-stocks plus ou moins différents sur le plan spatial dans une région, nous recommandons une stratégie expérimentale de gestion comprenant (1) le choix de sous-stocks en vue d'une capture non réglementée, d'une gestion par contingent et d'une fermeture complète de la pêche (afin de permettre des comparaisons directes du rendement des stocks dans ces autres régimes de capture), (2) l'élaboration de plans coopératifs de campagnes d'étude dans le cadre desquels les pêcheurs commerciaux passent une partie de leur temps à surveiller tous les sous-stocks, et (3) l'élaboration de plans de contingentement qui soient acceptables pour les pêcheurs et le gouvernement en vue de déceler un effondrement possible des sous-stocks non réglementés et d'y remédier le cas échéant. Ce type de stratégie d'adaptation répondrait à plusieurs objectifs contradictoires des parties participant à la pêche : les pêcheurs pourraient avoir un plus grand accès à certaines zones, les gestionnaires bénéficieraient de la sécurité des zones fermées et contingentées, et les scientifiques pourraient obtenir des données valables sur la taille des stocks et la variation du recrutement en comparant les zones. Dans le cas des sébastes du talus de la Colombie-Britannique, une des difficultés d'application de la stratégie est de savoir qui devrait payer pour les études d'abondance; les pêcheurs ne sont pas disposés à assumer cette charge, et il n'est pas évident que le public (gouvernement) devrait prendre des risques relativement à certains sous-stocks et assumer aussi le coût direct de ces risques.

Introduction

Fisheries management often takes place in a twilight zone of uncertainty about stock sizes and surplus production. For example, estimates of current stock size for Pacific Ocean perch (POP, *Sebastes alutus*) in Goose Island Gully, Queen Charlotte Sound, B.C., range from a conservative 10 000 tonnes (metric tons) based on the lower error limits of biomass surveys up to an optimistic 60 000 t based on historical catches and changes in commercial catch per unit effort (CPUE). Alternative estimates of stock size imply widely varying estimates of maximum sustainable yield (MSY) as well: conservative estimates of MSY for this stock range from 800 to 3500 t yr^{-1}. Because of this uncertainty, stock assessment biologists have been rightly loath to provide single best estimates and policy choices, and have tended instead to present relatively conservative estimates and to recommend cautious (low) harvesting policies. Particularly for long-lived species such as POP, there has been a tendency to emphasize the risk of extinction or long recovery times that would result from severe recruitment overfishing. Government biologists, recognizing the uncertainty associated with these yield estimates, instituted a program of experimental fishery harvest areas to provide the information with which to reduce this uncertainty. This program included open-fishing and pulsed-fishing areas as well as traditional quota-management areas.

Since 1980 there has been explosive development of improved mathematical and statistical models for stock assessment, particularly for situations in which age composition data are available (Collie and Sissenwine 1983; Fournier and Archibald 1982; Deriso et al. 1985; Gudmundsson 1986). This development led many of us to hope for much improved analysis of historical data, and hence better understanding of fish population dynamics. In a few instances that hope appears to have been justified, but in many others the modern methodology has simply demonstrated more forcefully how hopelessly inadequate the data are — no matter how thoroughly they are analyzed. Methods such as Virtual Population Analysis (VPA) may give a good fix on historical stock trends, but prove dangerously inadequate when used to estimate current stock size and make short-term forecasts (Rivard and Foy 1987; Bradford and Peterman 1989). Two weaknesses surface repeatedly in fisheries data: (1) commercial catch-and-effort data seldom provide a good indication of stock trends, since catchability/age selectivity patterns can change rapidly over time, and (2) in conservatively managed fisheries, there has been a lack of informative contrasts in stock sizes and fishing patterns over time. The latter weakness is particularly important in stock-recruitment assessments, for which the typical shotgun scatter of observations may simply represent statistical errors-in-variables and time-series effects (Walters and Ludwig 1981; Walters 1985). We might eventually find better reporting and statistical techniques for extracting more information about stock size and trend from commercial fishing data, but there are no magical recruitment models that can reliably extrapolate beyond empirical experience to predict how low stocks can be pushed before effects on recruitment become evident.

The prospects for stock assessment and management are bleak, unless we can take at least two key steps: (1) work cooperatively with commercial fishermen to harness the ability of fishing fleets to systematically sample fish densities and distributions, and (2) execute planned, large-scale experiments that deliberately induce substantial changes in fish stock sizes to provide information on the risk of recruitment failure. It is particularly important to incorporate these steps in the development of new fisheries before traditions and expectations make cooperation from fishermen more difficult to establish. Neither of these steps will be of much value without the other; it is of little value to gather ever more precise data under relatively stable conditions where informative changes are prevented (if possible), and it is obviously foolish to make big changes without having the means to promptly measure what their effect has been. Development of cooperative survey and experimental programs will require: (1) incentives for commercial fishermen, (2) careful economic analysis of short-term versus long-term benefits and costs, with objective weighing of risks and opportunities, and (3) contingency plans and spatial arrangement of experimental areas that will guarantee acceptably low levels of biological risk.

This paper proposes an experimental management plan that is currently under review for British Columbia slope rockfishes such as POP. This plan was developed cooperatively by the Department of Fisheries and Oceans (DFO) and the Deep Sea Trawlers Association of B.C. It is an extension of experimental programs initiated for B.C. slope rockfishes in the early 1980's (Leaman and Stanley 1985). We hope it will provide a prototype for cooperative, experimental management of other groundfisheries. Slope rockfish were selected as a prototype because of their growing economic value to the trawlers, because the extreme uncertainty about stock size is a point of considerable conflict with DFO, and because of the high risk involved in managing long-lived species with apparently low but highly variable recruitment rates. Firstly we describe the general plan that evolved from several meetings during 1987 between DFO and trawlers. Then we review methods used to evaluate various options for monitoring surveys, predicting how soon any stock collapses would be detected, and contingency plans for responding to collapses. Finally we discuss methodological and institutional problems that will have to be resolved before the plan is implemented.

An Experimental Management Plan for B.C. Slope Rockfish

Modest domestic fisheries existed for slope rockfish (mainly *Sebates alutus* but also *S. reedi* and *S. aleutianus*) prior to the mid-1960's. Then a few very large catches were taken by Japanese and Russian trawlers, and the domestic fishery has been low or declining ever since. It appears from CPUE and survey data that the foreign fleets depleted the major stocks by at least 50%, and CPUE data for the domestic fleet after 1970 do not clearly indicate either further decline or recovery (Leaman and Stanley 1985). However, the CPUE data probably do not reflect abundance trends at all, due to non-random (schooling) behavior of the fish and to effective search by the fleet. Uncertainty about the initial extent of depletion and about recent trends is the reason the current range of stock size estimates is so large. Regular trawl surveys in one area, Goose Island Gully (Nagtegaal et al. 1986) have not resolved the uncertainty because the effective area swept by the survey gear is unknown.

Some experienced fishermen have fuelled a debate with DFO about the status and productivity of the stocks, claiming that they can now find fish in all areas where they were historically abundant; a few fishermen even claim that the stocks are as abundant as they ever were. Increasing prices over the last few years have made the fishery much more attractive, leading to a clamor for more liberal total allowable catches (TAC) even among fishermen who are suspicious about claims that the stocks are fully recovered. In this atmosphere of growing mistrust, DFO has responded by implementing some economically inefficient regulatory tactics such as seasonal quotas and trip limits, while generally recommending low TACs. If the current situation persists, the fishery will continue to produce low catches, poor information about stock size and productivity, and a continued deterioration in relations between DFO and the trawlers: in short, all parties to management will lose. There will still be a growing risk of losing the stocks due either to continued declines that the existing monitoring system has failed to detect, or to a political decision to allow the fishermen higher catches despite DFO recommendations. Though the current management strategy appears superficially to be biologically conservative and safe, it may in fact be the riskiest long-term strategy.

We feel that a break from the current, unstable state of affairs should involve three elements: (1) an improved, coastwide survey for monitoring abundance trends, (2) a reasonably safe experimental demonstration of the impacts of liberalized regulations, with enough experimental replication to determine whether the results are applicable to the coast as a whole, and (3) contingency plans for discontinuing the experiment and allowing stock recovery in the event of catastrophic declines. The following subsections describe the current proposal for how to deal with each of these elements.

A Coastwide Experimental Design

After considerable discussion between DFO and the trawlers, about the identification of distinct substocks and how large experimental areas need be in order to permit economical enforcement of disparate regulations among areas, we recommended the arrangement of fishing areas shown in Fig. 1. This plan involves three "free-fishing" areas where catch regulations would be either omitted or made very liberal (TACs at least 3 times as large as at present), two adjacent to the U.S. borders and one at Goose Island Gully where there has been a long-term survey to detect abundance trends. For comparison with the free-fishing areas, there would be three "quota" areas where existing TACs and regulatory tactics (season quotas, trip limits, etc.) would be maintained. Finally, there would be one permanently closed area at Moresby Gully, where only survey fishing would be permitted, which would generate exploitation rates of less than 1% per year. The intent of this closed area is not to "control" for effects of fishing in the other areas, but rather to act as a safe refuge against the risk of biological extinction in the other areas. The closed areas would provide controls for the effect of continued low quota fishing as well as heavy fishing, but the primary management interest is in comparing conservative to heavy fishing.

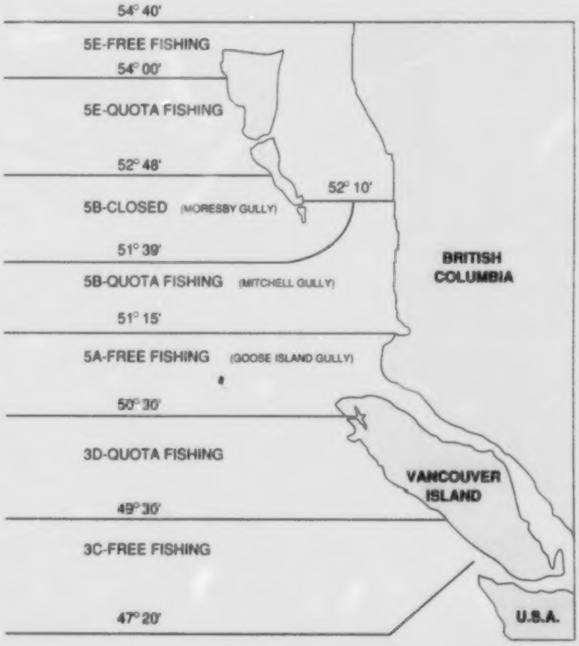

FIG. 1. Proposed arrangement of closed, free-fishing, and quota management areas for a slope rockfish experimental management program off the B.C. coast. Area 5E(N) is already (1985–87) designated an experimental free-fishing area.

An alternative to initiating free fishing on three areas simultaneously would be to sequentially open the areas to "pulse" fishing, in a "staircase" experimental design (Walters et al. 1988). A sequential design would provide somewhat lower but more stable catches over the first decade of the experiment, and it would permit estimation of differential responses to environmental trends by treated (free-fishing) as opposed to control (quota) populations ("time-treatment interactions"). However, it would take much longer under a sequential design to learn how similar the areas are to one another in their response to free fishing, and there might be uneconomical crowding of vessels into the one or two areas that would be open each year. There may in effect be a sequential application of high fishing rates even if the simpler block design is used, since at least one of the free-fishing areas (3C) is not yet attractive to the fishermen. On balance, we feel that it is not necessary to implement a more complex sequential design.

The selection of areas for free fishing, quota management, and closure was obviously not random as might be preferred in a scientific experiment. The northern border area is already open to experimental free fishing; the southern border area has not attracted much fishing in the past, and may not be much affected by the experiment. The Goose Island Gully free fishing area is one of the most attractive areas on the coast for POP, and has been intensively studied. Quota areas on both sides of the Moresby Gully closed area are intended at least partly to provide a "buffer" zone around the Moresby stock and to simplify enforcement of the closure. Luckily, these various concerns that led to the proposed experimental arrangement also lead to a good "interspersion" (Hurlburt 1984) of treatment (free fishing) and control (quota) units along any latitudinal gradients that may exist in productivity and stock size, and will permit pairwise comparisons between adjacent quota and free-fishing areas.

Survey Fishing By Commercial Fishermen

We recommend that a systematic trawl survey be conducted in each of the seven areas every year. Considering variability in past survey data from the region, we expect that relative abundance (mean CPUE over the entire area) can be measured with a standard error of around 20% of the mean by conducting about 120 survey trawls in each area, taken in three seasonal trawl grids of 40 tows. Each trawl grid would comprise five onshore-offshore transects, each with 8 tows beginning well inshore and ending well offshore of the known POP depth distribution. These expectations are based on variability measured in past POP surveys (Nagtegaal et al. 1986).

The target standard error of 20% of mean survey CPUE was selected on the basis of Monte Carlo simulations of future learning about stock size in free-fishing areas, assuming that the method of analysis (see Appendix A) should be able to detect whether the stocks were initially low within 5 years of heavy fishing. Under this "worst-case" scenario, stocks in the free-fishing area would be depleted by about 40% from their 1987 levels before it would become clear, in 2 to 3 years, that remedial action were necessary. Under more optimistic stock size scenarios or lower exploitation rates, it would probably take considerably longer to obtain an accurate fix on stock sizes (Fig. 2) but in such cases there would be much lower risk of dangerous depletion. Estimation performance depends on both survey precision and the exploitation rate (Fig. 2); increasing the survey sample size has a much smaller effect on performance than does increasing the experimental exploitation rate. Estimation performance does not depend on how variable the recruitment rates are because the methods treat each year-class size as an independent statistical parameter to be estimated.

A systematic grid survey was considered preferable to random or index site trawls because of fears that fishermen might some day raise a "black hole" argument: they might rationalize that declining abundance in index sites was due simply to the fish moving off- or on-shore from these sites, in response to various oceanographic factors. They argue that such movements have in fact occurred in recent years, perhaps in response to warm water associated with the most recent ENSO event.

The total of 840 survey trawls required annually by this survey design would require about 200 working days (because of tidal and diurnal effects on trawl success for POP), which would occupy one trawler essentially full time. Considering that this trawler would probably achieve only about one-third its normal catch, the net cost (or bid to do the survey for DFO) would be around $700,000 (roughly two-thirds of a "normal" one million dollar annual gross income). Obviously no single fisherman will volunteer to do the survey, and it would require a substantial financial commitment from each of the 20 or so vessels that would benefit from the free-fishing areas to either hire one of their number to do the survey or to each accept a share of the work without direct compensation. To remove intervessel variability from the data and to allow cheaper observer and sampling programs, it would be better to have a single vessel do the entire survey.

We are currently at an impasse about how to implement the survey program. The fishermen are unwilling to do it for free, and DFO is unwilling to both engage in a risky experiment and pay for monitoring its results. All parties would prefer to see a single (or pair) of vessels do the work. A less desirable option would be to close the "free-fishing" areas entirely, then issue fishing permits in pairs: one permit would be to do a survey trawl grid (40 tows in an area), and the second would be to take a guaranteed catch or make one unrestricted fishing trip in the closed areas. The legality of this option is questionable, and it might provide very erratic data. Assuming that the coastwide catch of POP increases by around 3000 t immediately after the free-fishing areas are opened, and that two-thirds of the survey vessel's normal catch also becomes available to the rest of the fleet, then the landed value of catches should increase by about $2.5 million; perhaps it will be necessary to directly "tax" this increase to pay for the survey, which would be equivalent to having the fishermen sell the extra catch at the lower prices prevalent a decade ago.

The trawlers have suggested two survey options worth considering: (1) have 21 vessels survey simultaneously

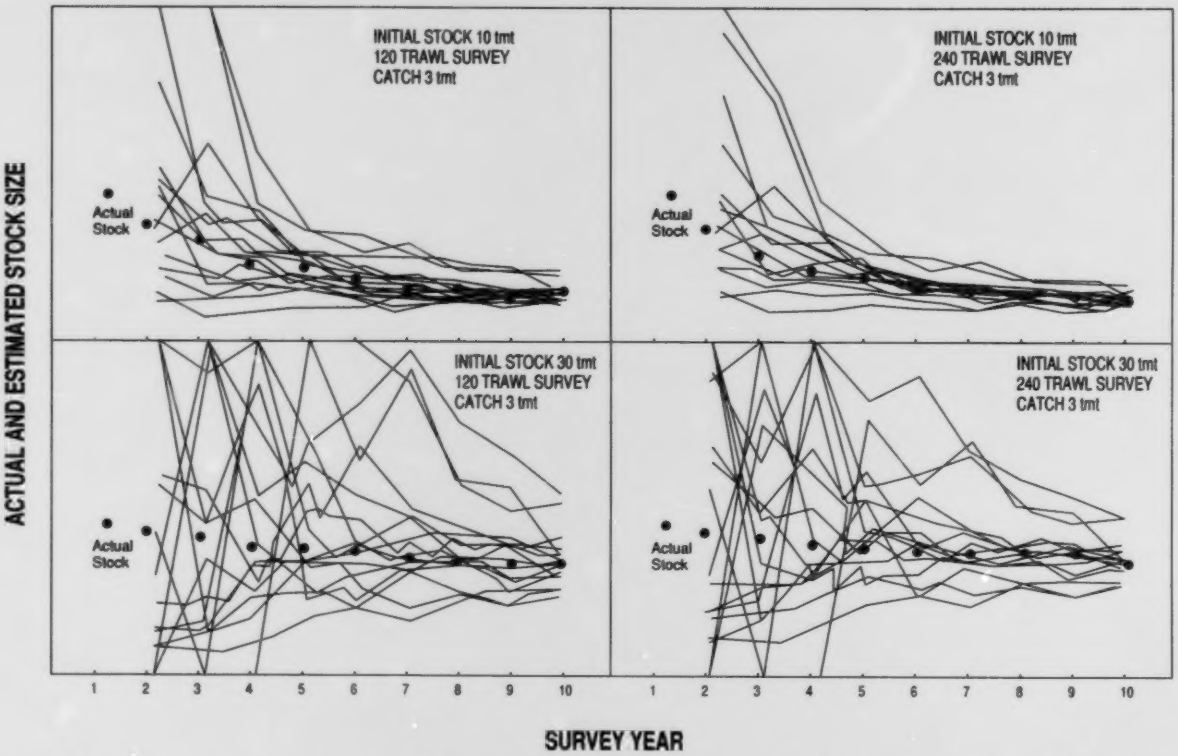

FIG. 2. Monte Carlo simulations showing the effect of initial stock size and annual survey size on the expected performance of a population estimation procedure based on age-structured survey and commercial catch data (depletion estimation of Appendix A). Variance among trawls is assumed to be three times the mean CPUE of each survey, and samples of 500 fish annually, from the survey and commercial catch, are assumed to be aged (ages 10–30).

during 2- to 3-day periods at least twice a year, and (2) assign an existing research vessel, such as the W.E. Ricker, exclusively to the trawlers and let them do the surveys with it using rotating crews from the commercial vessels, with DFO perhaps paying part of the operating costs. The trawlers favor the first of these options, providing the data can be properly standardized among vessels.

Contingency Plans For Stock Depletion

Unexpectedly high catches or low initial stock sizes in the free fishing areas could lead to rapid stock declines, which could not be detected with confidence until several years into the experiment. It is therefore important to specify in advance precisely what pattern of observations (or estimates based on observations) will be taken as clear evidence that a severe decline has occurred, and what remedial actions will be taken.

We expect that the best approach to detecting declines will be to analyze age-composition data from the survey and the commercial fishery, to provide recursively updated estimates of stock size and recruitment (see Appendix A and Fig. 2). This expectation comes from simulating estimation performance using various stock assessment models ranging from VPA to Schnute's (1985) age-aggregated model of biomass dynamics. The simpler, age-aggregated models perform poorly due to uncertainty about future recruitment; VPA and its relatives require dangerous assumptions about the commercial exploitation rate. It appears best to use a method that is age-disaggregated, makes simple assumptions about recruitment and catchability, and uses the survey data to measure changes in relative abundance over time. With such a method (see Appendix), it should be possible to detect a severe decline within 5 years (Fig. 2); otherwise detection within 5 years would require a massively larger annual survey, in the order of 1000 trawls per area each year.

Given that a severe decline is detected, there are three extreme responses: (1) move immediately to a long-term MSY policy, which would involve shutting down the fishery entirely until the stock has recovered to an optimum level of around one-half the unfished stock size, (2) move to a sustained yield policy for the depleted stock, without allowing it to recover, or (3) "write-off" the stock by imposing no regulations, and allow it to reach a "bionomic equilibrium" at whatever stock level the fishermen would no longer find it economically attractive to continue fishing. Options (2) and (3) are obviously not attractive from a resource husbandry viewpoint; option (3) might result in economic extinction, while option (2) would result in very low annual yields. Option (1) would result in a long recovery period, assuming that there would still be an exploitation rate of around 1% per year due to survey fishing and that recruitment rates would remain below average (proportional to stock size) until the stock recovers to one-half its unfished equilibrium level (Fig. 3). Considering the sporadic character of rockfish recruitment (Leaman and Stanley 1985; and pers. comm.), recovery times under option (1) could vary from less than half to about four times the averages shown in Fig. 3.

There are various compromises between the extremes of complete closure and sustained yield at low stock levels, representing reduced exploitation rates that would allow eventual stock recovery but would allow some catch over the recovery period. However, such policies could greatly delay recovery, while not contributing significantly to the economic well-being of the trawl fleet. In short, they are bad compromises, as indeed is the current policy for areas such as Goose Island Gully if in fact the stocks have already been depleted to below the levels that will produce MSY. We recommend the complete closure, minimum recovery time option as the best contingency plan for the long-term future of the resource.

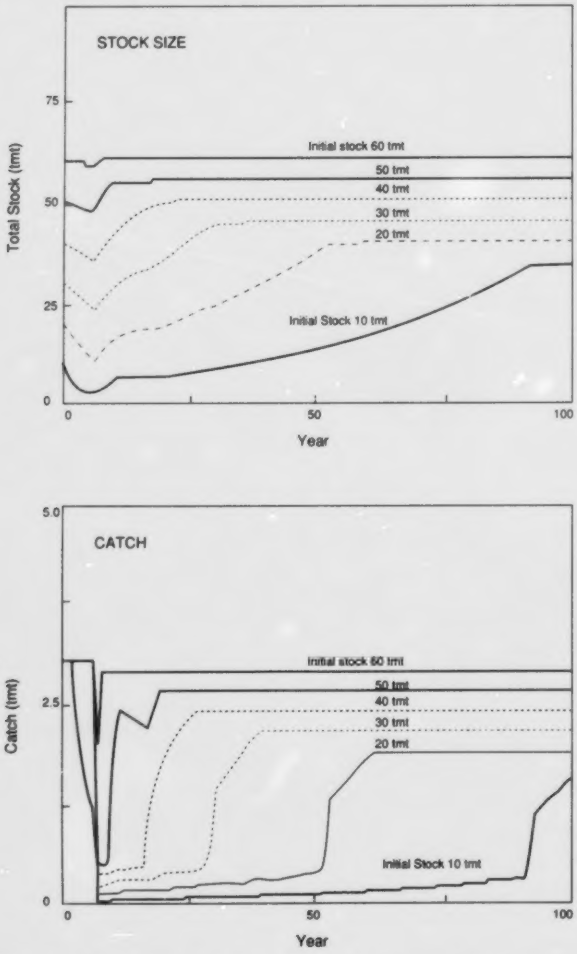

FIG. 3. Mean trends in simulated stock size and catch, averaged with respect to recruitment variation, for different initial stock sizes of Pacific ocean perch in Goose Island Gully. Harvest for first 5 yr is 3 TMT up to a maximum of 40% of the stock size; harvest after 5 yr is calculated as biomass minus 1/2 the unfished stock size subject to 1% minimum and 3 TMT maximum (long-term MSY policy).

Suppose that stocks collapse in the free-fishing areas, and that these areas are closed except to survey fishing. Should the trawl fleet be provided an economic "cushion" against this sudden drop in catches, by allowing at least a few years of more liberal catches in the quota and/or closed areas? Note that evidence of low initial stock sizes in the free-fishing areas would also be a good indication that stock sizes in the quota areas are also likely to be below optimum for MSY, so any increase in catches would invite a longer recovery period for the coast as a whole. The "price" of avoiding some short-term economic hardship might well be a considerable economic loss in the long term. Therefore, we would not recommend that the fishermen be compensated by increased catches in the quota areas, unless the survey data for those areas indicate substantially higher stock sizes than is now anticipated.

Suppose that there is not an immediate stock collapse during the initial 5-year evaluation period of the free-fishing areas. Should more liberal quotas or free fishing then be allowed in the initial quota areas? Here our response is that 5 years is simply not long enough to fully evaluate the impacts of the free fishing; species such as POP do not recruit until ages 8–12, so that possible recruitment effects of the free fishery will not become evident for at least 10 years (and more likely 20–30 years considering recruitment variability in these species). We recommend that changes in quota area regulations be delayed for at least 15 yr even if all data from these and from the free-fishing areas indicate large stock sizes.

Formal Evaluation of Experimental Policy Options

The experimental plan for B.C. rockfish management described in the previous section was developed through an informal "brainstorming" process, where trawlers and DFO personnel met several times to identify various options, then tried to reach consensus on each element of the plan by intuitively balancing various cost, benefit, and risk considerations. This process worked well for the identification of experimental units, where it was clear to all concerned that the areas needed to be large enough to have some biological integrity and to facilitate enforcement, yet small enough to permit reasonable replication and safety in the event of stock collapses. The process was much less effective in looking carefully at the various trade-offs and risks involved in survey design and contingency planning. Here we need to have more formal models to examine possible future trajectories of data, stock sizes, and management responses, and to weigh the potential economic benefits and costs as well as biological risks. This section reviews our current attempts to develop formal evaluations of the B.C. rockfish case, using a framework for decision analysis suggested by Walters (1977).

Steps in Formal Decision Analysis

Five steps are required to develop and compare alternative plans: (1) identify a range of alternative hypotheses or models about the status of the stocks and their possible future responses to harvesting, (2) develop a model of how future data will be gathered and used to discriminate among the alternative hypotheses, (3) identify a range of feedback policy options for responding to future data, (4) define performance measures, such the discounted sum of future catches, for ranking each possible hypothesis/option combination in relation to the others, and (5) using Monte Carlo simulations of future data gathering errors and recruitment variations, calculate the statistical expected value of the performance measures for each hypothesis/option combination.

The result of step (5) is a decision table showing the expected performance of each policy option across the set of alternative biological hypotheses that have been identified. Some options, such as continued low catches in all areas, may provide essentially the same outcome under all alternative hypotheses; such policies are "robust" to uncertainty about the stocks. Other options may provide very good performance if an optimistic hypothesis (e.g., large initial stock size) proves correct, but very poor performance if a pessimistic hypothesis proves correct. Generally the "risky" options, with a wide spread of outcomes across the alternative hypotheses, will also be the most informative as to which model is correct. Once the decision table has been constructed, the outcomes across hypotheses for each policy option can be weighted or averaged in various ways to provide expected overall performance measures for each option. In weighting the outcomes, the issue is whether to behave in a "risk averse" manner (weigh the bad outcomes or risks heavily relative to the good ones or opportunities), and here it is not clear that biologists (who are generally very risk averse) will provide judgements that reflect the public's interest in the resource.

In the rockfish case, it is relatively easy to construct a range of alternative hypotheses about stock response given the range of current stock size estimates. Given any current stock size in the range, we backcalculate, using variations on Kimura's (1982, 1984) methods of stock reduction analysis, how large the average unfished stock size must have been, and then use annual survival rate estimates (e.g., 0.95 for POP) to estimate mean recruitment rates for the unfished stock. We then estimate a conservative mean stock-recruitment relationship by assuming that recruitment will be independent of stock size unless the stock size drops to less than one-half its unfished level, and will be proportional to stock size for still smaller stocks. Each estimate of initial stock size thus implies a distinct hypothesis about the relationship between stock size and surplus production. The range of hypotheses can be further broadened by including alternative assumptions about the mean stock-recruitment relation, but the effect of including these would be modest compared to the large differences in predictions based on alternative estimates of initial stock size.

Models of future learning in the rockfish case were discussed in the previous section. The simulations of future performance need to (1) generate trawl survey CPUE with reasonable levels of random error, (2) simulate the multinomial sampling of age compositions from the survey and commercial catch, and (3) apply assessment models to the simulated data to obtain simulated stock size estimates over time. The simulated learning effects will be greatest in the first 5 to 10 years (Fig. 2), except for policies involving very low exploitation rates; for such policies the simulations should recognize a substantial long-term risk of greatly under- or overestimating the stock size, and hence of not responding soon enough to either the need to reduce catches or opportunities to take larger catches.

Policy options in the rockfish case involve differences in the exploitation rate attained in the first few years in free fishing areas, the number of years of free fishing permitted before switching to a "certainty equivalent" policy based on the stock size estimate at the end of the period, and the policy used after the experimental period. Also, we could consider options involving switching from experimental to sustained yield management based on various "information state" measures (Walters 1986) such as the mean and variance of the stock size estimate; options might involve switching when the variance of the stock size estimate drops below different percentages of the estimate (switching when the variance is still high would correspond to using a short experimental period). On a longer time scale, there are various options for deciding whether and when to liberalize regulations on quota areas in the event that high stock sizes are found in the experimental areas.

Two questions arise in identifying performance measures for comparing alternative hypotheses and policy options: (1) how should annual net benefits from the fishery be measured (catch, landed value, landed value less operating and monitoring costs, etc.), and (2) how much should long-term net benefits be discounted relative to the present value of the stock? In the present rockfish analyses we have used total annual catch to compare alternative outcomes, since the experimental fishing plan will not cause large changes in commercial fishing operating costs or fish prices, and the experimental monitoring costs are similar under all options (except maintaining a status quo quota management policy). However, we are finding it necessary to be much more careful about discounting and simulation time horizons, as expected from bioeconomic theory (Clark 1976; Mangel 1985). For short time horizons (50 yr or less) or high discount rates (>4–5% per annum), the best economic policy for long-lived, unproductive species such as POP is to deplete the stocks as rapidly as possible, without regard to learning or long-term rehabilitation. Positive values of learning and rehabilitation are predicted in 100-yr simulations without discounting, but here we must wonder whether the results are socially or economically meaningful. If a long enough time horizon is used then any experiment can be justified because even unlikely optimistic outcomes will translate into a large cumulative benefit, while any transient losses under pessimistic outcomes will appear small compared to the total benefits.

Experimental Options for Goose Island Gully

Expected 100-yr catches or POP from the Goose Island Gully experimental area for a range of hypotheses about initial stock size and for several policy options are shown in Table 1. Each entry in the table is an average of 50 Monte Carlo simulations with randomly varying survey CPUE, age-composition samples, and recruitments log-normally distributed around the mean recruitment curve. Comparing the baseline (continued low quotas) option to the various experimental options, it is clear that the benefits of experimentation may be large even if the results from the Goose Island area are not applicable later to other areas.

Under the lowest stock-size hypothesis (10 000 t), even the current catch of 800 t per year is not sustainable, and the stock would eventually crash after 20 to 40 years. The improved performance of all experimental options relative to the quota baseline is mainly due to implementation of the survey abundance, which would permit a "feedback" policy to adjust catches over time in response to changing stock size (Clark and Kirkwood 1986; Kirkwood 1987).

Policies 1 and 3 in Table 1, although impractical to implement, provide useful standards against which to compare experimental options. In the "perfect knowledge" row, yields were calculated by assuming that a massive biomass survey is conducted in the first year, eliminating all uncertainty about the current stock size (and hence about the mean stock-recruit relation and the optimum stock size for producing long-term MSY). For all but the highest stock-size hypothesis, the optimum policy, given perfect knowledge, would be to immediately shut down the fishery until recovery to the optimum is achieved (see Fig. 3). The third row of Table 1 shows what might be achieved if exact stock-size estimates were available after 1987 and if the stock were managed in perpetuity as though the lowest stock-production hypothesis were correct; this would involve shutting down the fishery for many years under the first two hypotheses, and holding a suboptimally low stock size for all years under all but the first hypothesis. Still, it would be a robust policy in giving near optimum yields under all but the most optimistic hypotheses.

The last two rows of Table 1 list expected yields for two experimental options, differing only in the duration of free fishing permitted before management is switched to the estimated optimum regime for long-term catch. Under both policies the expected performance, given high initial stock sizes (30+ thousands of metric tons [TMT]), is poor compared to the perfect knowledge baseline; this is due to a relatively high risk of underestimating the initial stock size as of the end of the experiment, then having the underestimates persist into the future when management switches over to lower (and relatively uninformative) catches. The risk of underestimation is lessened in the 10-yr experiment option (e.g., expected catch of 218 versus 205 for the 60 TMT hypothesis), but it remains high due to persistently poor estimation performance under the high initial stock hypotheses (see Fig. 2). On the other hand, the 10-yr experiment would give substantially lower performance (34 TMT v. 51 TMT) if the lowest stock hypothesis proves correct, since it would allow stock depletion to continue for twice as long.

The results of experimental options (Table 1) suggest that an "open-loop", adaptive rule should be used in contingency planning. After an initial 5-year experimental period, the experiment should be discontinued only if the data clearly favor a very low initial stock hypothesis. Otherwise, a second 5-year experiment should be initiated, perhaps encouraging the industry to take even higher catches from the free-fishing areas. If there is still considerable uncertainty after 10 years, then extend the experiment for another 5 years, etc.

Table 1 appears to present a simple decision problem: the experimental policies are clearly preferable to the baseline no matter which hypothesis is correct, so the choice is really only about how long and how harsh to make the experiments. However, there is a hidden assumption in the calculations, that survey fishing will continue even after closures at the end of experiments, to provide information about when to reopen the fishery after any recovery period that might appear to be optimal. A more conservative assumption would be that the fishery is permanently lost under the most conservative hypotheses = (10-to-20-TMT initial stock), so that the appropriate 100-yr yields to enter in the first two columns of the decision table would be only the 6 to 15 TMT that would probably be taken in the first few years of the experiment. Under that assumption the decision problem becomes much more difficult: is it worth risking a low 6-to-15-TMT outcome against the "sure" option of at least 35 TMT under the baseline, to test for the possibility

TABLE 1. Expected 100-yr yields of Pacific ocean perch from Goose Island Gully (PMFC minor statistical area 5A), estimated as means of 50 Monte Carlo simulations under a range of policy choices and for six alternative hypotheses about the 1987 stock size. Yields and stock sizes in thousands of metric tons (TMT). Policies 2, 4, and 5 assume that the annual catch cannot exceed 40% of the stock.

	Hypothesized 1987 stock size					
Policy	10	20	30	40	50	60
1. Perfect knowledge after 1988 (massive survey)	82	169	178	229	255	292
2. Baseline quota (0.8 TMT yr^{-1})	35	80	80	80	80	80
3. Assuming 1987 biomass is 10 TMT, perfect stock data	82	166	165	200	214	237
4. 5-yr experiment with 3 TMT annual catch	51	102	131	163	187	205
5. 10-yr experiment with 3 TMT annual catch	34	88	125	169	201	218

of obtaining much higher yields (125 to 218 TMT) under the more optimistic hypotheses? Here we believe that most decision makers would still opt for the experiment, even if the most optimistic outcome were the 125-to-130-TMT catches associated with the 30-TMT initial stock hypothesis.

The yields in Table 1 were calculated with very conservative assumptions about the stock sizes needed to avoid recruitment overfishing (one-half the unfished stock size). Substantially more optimistic results, more strongly favoring an experimental program, would be obtained by assuming average recruitment to be independent of stock size over a wider range of stock sizes. This more optimistic assumption would imply more rapid recoveries after depletion and higher annual sustainable yields after recovery. We did not consider it worthwhile to pursue such calculations further, since the basic risks and opportunities are apparent from the more conservative calculations.

At 1987 prices, 1 TMT of POP have a landed value of around $0.8 million. Assuming an annual survey cost of around $0.7 million, or around $70 million over a 100-yr planning horizon, it appears that the expected catch gains from Goose Island Gully POP alone (average catch across rows of Table 1, multiply by price, and subtract baseline value) would be sufficient to pay for the direct costs of the coastwide experiment. Since there would be other beneficiaries from the survey investment besides trawl fishermen (processors, marketers, etc.), who should presumably bear part of the burden for survey costs, the indirect benefits of experimentation may be substantially greater than the expected increases in yield (Table 1).

Coastwide Experimental Options

Though much less data are available for other POP stocks, we have attempted a coastwide version of the Goose Island Gully analysis. Ranges of stock-size hypotheses for the other areas (Table 2) were abstracted from data in Leaman and Stanley (1985), and alternative estimates of the unfished stock sizes and recruitment rates were obtained by stock reduction analysis. For all alternatives we assumed that recruitment is proportional to stock size for stock size below one-half the unfished level, and independent of stock size for higher stocks. Annual survival rates of 0.95 were assumed for all areas, and effects of body growth on yield were ignored.

The coastwide analysis raises two issues that are not evident when single areas are examined in isolation: (1) how many treatment (free-fishing) and control (quota) areas there should be, and (2) how valuable information from the treatment areas will be in deciding long-term policy for the control areas. This analysis focusses mainly on the first of these issues; until more comparative data become available on variation in abundance among areas, we can only speculate qualitatively about how directly applicable the initial free-fishing area results will be to the other areas.

Consider an experiment in which M areas are treated (free fishing) for T years, while the remaining $N-M$ areas are subject to conservative quota regulation ($N=6$ in the rockfish case if area 5B is permanently closed). The expected total long-term value of catches from this experiment can be expressed as

$$(1) \qquad V = M(v_e + V_e) + (N-M)(v_q + V_q - L_{M,q})$$

where: v_e = average value of catches per treated area over the T year treatment period,

V_e = average long-term (time T forward) value of catches per treated area,

v_q = average value of catches per quota area over the T year treatment period,

V_q = average long-term (time T forward) value of catches per quota area, assuming that perfect knowledge about how to manage each quota area results from the experiment,

$L_{M,q}$ = expected average loss in long-term (time T forward) value per quota area due to imperfect information at the end of the experiment (risk of over- or underharvesting the quota areas by incorrectly applying experimental results to them).

Note the trade-off among the v and V value components of Eq. (1): high short-term catches v_e will imply reduced long-term catches V_e from the experimental areas, while lower short-term catches v_q in the quota areas will imply higher long-term values V_q in these areas; Eq. (1) is a dynamic programming relationship. The average loss $L_{M,q}$ should be a decreasing function of the number of experimental areas M and of the treatment duration T, with the maximum loss $L_{0,q}$ being associated with a nonexperimental policy where there would not even be a survey to provide information on stock trends in response to the quota management regime. In general we expect

TABLE 2. Range of estimates of current stock sizes, unfished stock sizes and current recommended quotas of the main POP stocks in British Columbia, ordered geographically from south to north (see Fig. 1). Estimates in TMT.

Area	Stock size in 1980	Unfished stock size	Current quota
3C	10–20	50–100	0.3
3D	2–10	2–10	0.1
5B(s)	10–60	60–120	0.8
5B(n)	3–12	20–40	0.2
5C	35–135	35–135	2.0
5E(s)	11–25	20–50	0.6[a]
5E(n)	20–60	70–120	0.1[a]

[a]5E areas are currently experimental areas, with free fishing in 5E(n).

lower yields in the free-fishing areas than would result from a quota policy followed by perfect management after year T ($v_e + V_e < v_q + V_q$), if it were magically possible to obtain perfect information for management from the experiment.

The qualitative behavior of Eq. (1) in relation to M is shown in Fig. 4. The total value V is bounded by triangle ABC, the apices of which can be computed from the coastwide simulation results in Table 3. Point A represents the expected value (averaged across the stock-size hypotheses in Table 3) of continuing a quota policy on all areas, without the benefit of a feedback policy based on survey information. Point B represents the expected value (across stock size hypotheses) of following a quota policy for T years ($T = 5$ in the Table 3 example) on all areas, then magically switching to an optimum feedback policy for maximizing long-term catch. Point C represents the expected value of following a free-fishing policy (30% annual exploitation rate up to maximum annual catch of 5 TMT per area) in every area for T years, then magically switching to an optimum feedback policy for maximizing long-term catch. Attainable coastwide catch increases sharply from point A even for $M = 1$, due to implementation of a survey system as part of the experiment. For higher values of M, the attainable value approaches the upper bound defined by the line BC, as information from the experimental areas is used to reduce the long-term losses $L_{M,q}$ from the initial quota areas. The attainable value reaches a local optimum at some intermediate value, $M < N$, provided the experimental areas are quite informative about how to manage the quota areas in the long term (i.e., losses relative to the line BC fall quickly as M increases). However, the attainable value is maximal at $M = N$ if the experimental results are not informative about how to manage quota areas, and if the average long-term value from an experimentally managed area is higher than the long-term value of managing that area by a quota policy without feedback (point C higher than point A, see Tables 1 and 3).

For the rockfish experiment, we cannot yet predict where the attainable value curve will be in relation to the bounds defined by triangle ABC in Fig. 4. In assuming that the best value of M is around 3, we are in effect being optimistic about the applicability of the free-fishing area results to the rest of the coast. Were we not optimistic, it appears that the best policy would be to allow free fishing in all areas; even substantial long-term losses (low values of V_e) would be preferable to the low short- and long-term values associated with perpetuating the existing quota system indefinitely.

Perhaps we have been too pessimistic about quotas changing in response to long-term learning under the present management regime, and too optimistic about the impacts of experimental free fishing. The effect in Fig. 4 of being more optimistic about management would be to move point A upward, and the effect of greater damage due to experimentation would be to move point C downward. However, we would have to change these assessments substantially (>30%) before we could conclude that an experimental regime is not warranted at all (no peak in the attainable-catch curve at nonzero M).

The results in Table 3 and Fig. 4 can be used to infer the value of having a coastwide survey that would permit implementation of feedback policies for MSY. Over the next 100 years, the total survey cost would be in the order of $100 million. Over this period we expect that continued quota management would result in a total POP catch of around 200 TMT while an experimental regime coupled with surveys should permit an expected catch in the order of 580 TMT. At the current landed value of about $0.8 million per TMT, the gain in landed value would be 0.8 (580-200) = $304 million. In short, the expected gain in landed value is about $3 per dollar spent on surveys, averaged over the next 100 years.

Is Experimentation Necessary At All?

High simulated values for the experimental policies (Tables 1 and 3) are largely due to changing from quota management to feedback catch regulation in which the total allowable catch each year (C_t) is set to $C_t = B_t - B_0/2$, subject to the survey and capacity constraints $0.01B_t < C_t < 5$ TMT. B_t is the estimated stock size in year t, simulated with an error of magnitude predicted from the depletion estimation procedure of Appendix A. B_0 is the estimated unfished equilibrium stock size,

TABLE 3. Expected 100-yr yields of POP from the entire B.C. coast, estimated as means of 20 Monte Carlo simulations under various policy options. Initial stock-size hypotheses (1)-(6) are taken from the ranges in Table 2: (1) is low end of range for all areas, (6) is high end, etc. Yields in TMT. Mean across hypotheses of first row shown as point A in Fig. 4; mean of second row shown as point B, and mean of third row as point C.

	Initial stock size hypothesis					
Policy	(1)	(2)	(3)	(4)	(5)	(6)
1. Continued quota management in all areas	125	198	210	211	212	212
2. 5-yr quota mgmt in all areas, followed by MSY mgmt based on perfect information	396	550	639	757	868	940
3. 5-yr free fishing in all areas, with 30% expl. rate up to max of 5 TMT per area, followed by MSY management based on estimates at the end of year 5	266	427	538	659	739	863
4. 5-yr free fishing in 3C, 5A, 5E, followed by MSY mgmt based on estimates at end of year 5	261	426	528	650	728	844

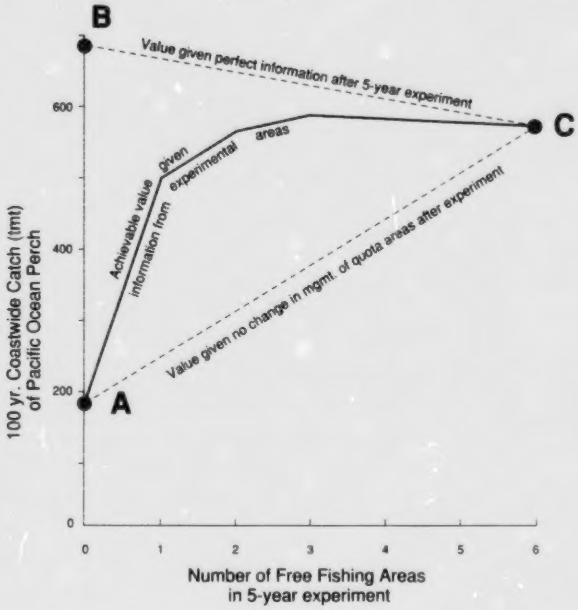

FIG. 4. Effect of the number of experimental areas (*M*) on the expected performance of a program involving 5 yr of free fishing in the experimental areas followed by MSY management based on unfished stock size estimates at the end of the experiment. Points A, B, and C are the averages of values in rows 1 to 3, respectively, of Table 3. A — base value of continued quota management in all areas; B — value of 5 yr quota followed by MSY management based on perfect information; C — value of experimenting on all areas together, assuming MSY management based on estimates at the end of year 5.

calculated from B_t, the stock-size estimate at the end of the experimental period. As noted above in connection with Table 1, the long-term yield is insensitive to the choice of B_0 because such feedback policies produce near long-term MSY even if B_0 is taken to be the unfished stock size for the most conservative initial stock-size hypothesis. Thus it might seem that the best policy would be to implement a survey then act as though the most conservative hypothesis were correct, without allowing any free-fishing areas. There are three immediate problems with that approach, considering that the best initial catch for most areas would be very low ($0.01B_t$): (1) the fishermen would have no incentive to cooperate in surveys and enforcement of closures, (2) the surveys would be difficult to justify by short-term measures of economic performance, and (3) only very poor or misleading stock size estimates (B_t) would be obtained (see Fig. 1, Appendix A).

If recruitment does indeed switch from being independent of stock size to being proportional to stock size for stocks below one-half the unfished level, as assumed in our simulations, it would also be unwise to implement a survey and then try to maintain the existing approach of setting quotas equal to the optimum long-term fishing rate, *F*, times the estimated stock size. This policy would keep short-term yields higher (at about present levels) and would be slightly more informative than closures, but it would permit almost no recovery at all toward the optimum stock size (less than 1% annual population growth assuming $F = 0.05$).

Discussion

Thus far, we have concentrated our formal decision analysis of rockfish experimental options on the POP stock in Goose Island Gully. Our estimates of long-term yields span the range of previous assessments of this stock (Archibald et al. 1983; Leaman and Stanley 1985). However, had we considered only the more conservative figures presented by Leaman and Stanley (1985), we would have reached a radically different conclusion: under even their most optimistic hypothesis, the stock is currently so overfished that the fishery should be either shut down to build toward an MSY stock level or else opened completely and allowed to decline to economic extinction, depending on what discount rate is used in value calculations. Leaman and Stanley evaluated only fixed exploitation rate strategies for stock rehabilitation, which would produce a dribble of yields over time but substantially delay stock recovery; we do not consider such a compromise to be either biologically or economically optimal.

The results of the proposed experiment could obviously be confounded by movement of POP among areas. Lacking direct measurements of larval transport, we can only infer from the duration of the larval stage (Carlson and Haight 1976) that larvae may potentially be transported the length of the B.C. coast by ocean currents. Larval transport seems to prevent any genetic differentiation among stocks (Seeb and Gunderson 1988). Adult migrations are largely confined to seasonal onshore-offshore shifts in depth; adult populations in the different areas have different growth rates, ages at maturity, fecundities and parasite species (Gunderson et al. 1977). Thus we expect substantial transport of pelagic larvae, but little movement of adult POP among experimental areas.

The proposed experiment was designed primarily to determine exploitable stock size, not the stock-production relationship. As POP recruit to the fishery at about age 10, results of the first 10 years of the experiment would not be affected by larval transport among areas. After 10 years, larval transport could confound the estimates of the stock-production relationship in the free-fishing areas. Independent estimates of larval transport are desirable regardless of which management strategy is pursued.

The stumbling block to implementing the rockfish plan is who should pay for the surveys and additional management costs, which may total $1.2 to $1.5 million per year. The trawl fishermen are currently unwilling or unable to make this investment themselves, possibly because they hope provincial and federal agencies will pay as an investment in economic development. Unfortunately, the immediate benefits of the plan are likely to be modest, with the main benefits accruing after 15 years or more. At discount rates currently used in public investment planning in Canada, for programs such as Salmonid Enhancement, the long-term benefits receive almost no weight. Also, there is no standard procedure for calculating expected benefits across a wide range of possible outcomes (across rows of Table 1, for example), and the absence of such a standard encourages public planners and decision makers to employ personal, usually quite risk-averse calculations. In short, our plan will probably fail unless the trawl fishermen bear a substantial share of the costs.

At least 20 trawl fishermen are now willing to volunteer enough time to do parallel surveys with their own vessels, or to man a survey vessel on a rotating schedule among crews. Such a voluntary scheme could set an important precedent for cooperative management of many fisheries. Thus we believe it is worth trying despite uncertainties about the standardization of data and about how to insure a continuing supply of volunteers over many years.

The same approach could be applied at relatively low marginal cost to some other B.C. fish stocks, for which there is also substantial uncertainty about stock sizes and potential yields. Groundfish, such as Pacific cod (*Gadus macrocephalus*) and rock sole (*Lepidopsetta bilineata*), also appear to have considerable substock structure such that comparisons of high and low exploitation rates can be made without severe confounding due to dispersal of fish between areas. Experimental survey and high exploitation plans would be worth considering in the Pacific herring (*Clupea pallasii*) fishery. Indeed, these more productive species may be better candidates for this approach because they would recover much more quickly if overfishing occurred. Several experimental plans have been suggested for B.C. salmon (Walters and Hilborn 1976; Collie and Walters 1987), though in these cases the problems of decision analysis and obtaining cooperation from fishermen are more difficult because the best options appear to involve immediate reductions in fishing pressure to test for the possibility of improved recruitment at higher stock sizes.

Our experimental approach to management conflicts with two widely held precepts of fisheries management in North America: (1) biologically conservative policies should be recommended when uncertainty is high, and (2) fishermen are competitors or adversaries, but never collaborators, in the management process. We see little social or economic justification for either of these precepts, and more importantly, they severely hinder the development of a better scientific understanding of the behavior of exploited populations.

References

ARCHIBALD, C. P., D. FOURNIER, AND B. M. LEAMAN. 1983. Reconstruction of stock history and development of rehabilitation strategies for Pacific ocean perch in Queen Charlotte Sound, Canada. N. Am. J. Fish. Manage. 3: 283–294.

BRADFORD, M. J., AND R. M. PETERMAN. 1989. Inaccurate parameter estimates, generation of artificial time trends in fish abundance, and management decisions, p. 87–99. *In* R. J. Beamish and G. A. McFarlane [ed.] Effects of ocean variability on recruitment and an evaluation of parameters used in stock assessment models. Can. Spec. Publ. Fish. Aquat. Sci. 108.

CARLSON, H. R., AND R. E. HAIGHT. 1976. Juvenile life of Pacific ocean perch, *Sebastes alutus*, in coastal fjords of southeastern Alaska: their environment, growth, food habits, and schooling behavior. Trans. Am. Fish. Soc. 105: 191–201.

CLARK, C. W. 1976. Mathematical bioeconomics. Wiley, New York, NY. 347 p.

CLARK, C. W., AND G. P. KIRKWOOD. 1986. On uncertain renewable resource stocks: optimal harvest policies and the value of stock surveys. J. Environ. Econ. Manage. 13: 235–244.

COLLIE, J. S., AND M. P. SISSENWINE. 1983. Estimating population size from relative abundance data measured with error. Can. J. Fish. Aquat. Sci. 40: 1871–1879.

COLLIE, J. S., AND C. J. WALTERS. 1987. Alternative recruitment models of Adams River sockeye salmon, *Oncorhynchus nerka*. Can. J. Fish. Aquat. Sci. 44: 1551–1561.

DERISO, R. B., T. J. QUINN, AND P. R. NEAL. 1985. Catch-at-age analysis with auxiliary information. Can. J. Fish. Aquat. Sci. 42: 815–824.

FOURNIER, D., AND C. P. ARCHIBALD. 1982. A general theory for analysing catch-at-age data. Can. J. Fish. Aquat. Sci. 39: 1195–1207.

GUDMUNDSSON, G. 1986. Statistical considerations in the analysis of catch-at-age observations. J. Cons. Cons. int. Explor. Mer 43: 83–90.

GUNDERSON, D. R., S. J. WESTRHEIM, R. L. DEMORY, AND M. E. FRAIDENBURG. 1977. The status of the Pacific ocean perch (*Sebastes alutus*) stocks off British Columbia, Washington and Oregon in 1974. Fish. Mar. Serv. Tech. Rep. 690: 63 p.

HURLBURT, S. H. 1984. Pseudoreplication and the design of ecological field experiments. Ecol. Monogr. 54: 187–211.

KIMURA, D. K., AND J. V. TAGART. 1982. Stock reduction analysis, another solution to the catch equation. Can. J. Fish. Aquat. Sci. 39: 1467–1472.

KIMURA, D. K., J. W. BALSINGER, AND D. H. ITO. 1984. Generalized stock reduction analysis. Can. J. Fish. Aquat. Sci. 41: 1325–1333.

KIRKWOOD, G. P. 1987. Optimal harvest policies for fisheries with uncertain stock sizes, p. 43–53. *In* T. L. Vincent, Y. Cohen, W. J. Grantham, G. P. Kirkwood, and J. M. Skowrownski [ed.] Modelling and management of resources under uncertainty. Springer-Verlag Lecture Notes in Biomathematics, 72.

LEAMAN, B. M., AND R. D. STANLEY. 1985. Shelf and slope rockfishes, p. 247–307. *In* A. V. Tyler and G. A. McFarlane [ed.] Groundfish stock assessments for the west coast of Canada in 1984 and recommended yield options for 1985. Can. MS Rep. Fish. Aquat. Sci. 1813.

LESLIE, P. H., AND D. H. S. DAVIS. 1939. An attempt to determine the absolute number of rats on a given area. J. Anim. Ecol. 8: 94–113.

MANGEL, M. 1985. Decision and control in uncertain resource systems. Academic Press Series on Mathematics in Science and Engineering 172: 255 p.

NAGTEGAAL, D. A., B. M. LEAMAN, AND R. D. STANLEY. 1986. Catches and trawl locations of R/V G. B. REED and M/V EASTWARD HO during the Pacific ocean perch assessment cruise to Queen Charlotte Sound, August–September 1984. Can. Data Rep. Fish. Aquat. Sci. 611:109 p.

PALOHEIMO, J. E. 1980. Estimation of mortality rates in fish populations. Trans. Am. Fish. Soc. 109: 378–386.

RICKER, W. E. 1975. Computation and interpretation of biological statistics of fish populations. Bull. Fish. Res. Board Can. 191: 382 p.

RIVARD, D., AND M. G. FOY. 1987. An analysis of errors in catch projections for Canadian Atlantic fish stocks. Can. J. Fish. Aquat. Sci. 44: 967–981.

SCHNUTE, J. 1985. A general theory for analysis of catch and effort data. Can. J. Fish. Aquat. Sci. 42: 414–429.

SEEB, L. W., AND D. R. GUNDERSON. 1988. Genetic variation and population structure of Pacific ocean perch (*Sebastes alutus*). Can. J. Fish. Aquat. Sci. 45: 78–88.

WALTERS, C. J. 1977. Management under uncertainty, p. 262–297. *In* D. V. Ellis [ed.] Pacific Salmon: management for people. Univ. Victoria Press, West. Geog. Ser. 13.

1985. Bias in the estimation of functional relationships from time series data. Can. J. Fish. Aquat. Sci. 42: 147–149.

1986. Adaptive management of renewable resources. Macmillan Pub. Co., New York, NY. 374 p.

WALTERS, C. J., J. S. COLLIE, AND T. WEBB. 1988. Experimental designs for estimating transient responses to management disturbances. Can. J. Fish. Aquat. Sci. 45: 530–538.

WALTERS, C. J., AND R. HILBORN. 1976. Adaptive control of fishing systems. J. Fish. Res. Board Can. 33: 145–159.

WALTERS, C. J., AND D. LUDWIG. 1981. Effects of measurement errors on the assessment of stock-recruitment relationships. Can. J. Fish. Aquat. Sci. 38: 704–710.

Appendix A.

A depletion estimator for recruitments and stock size using survey and commercial catch-at-age composition

For Monte Carlo simulation studies of future learning about stock sizes using survey and commercial catch data, it is important to have a computationally efficient model of how the data will be used. The actual analysis will presumably be based on a statistically efficient but computationally cumbersome algorithm such as CAGEAN (Deriso et al. 1985). In this appendix we review a regression procedure that is statistically inefficient (estimates have higher variance) compared to CAGEAN, but is very quick to compute. Due to its statistical inefficiency, this procedure provides conservative estimates of how long it will take to learn about stock depletion. Details of the procedure will be published by B. Johnson (U. Wisconsin, manuscript in prep.).

Suppose that when the survey begins, the stock consists of a set $N_{i,t}$. . .$N_{k,t}$, where $N_{i,t}$ is the number of fish in cohort i in year t. These cohorts span an arbitrary range of absolute ages (e.g., 8 to 30 in the POP case) that can be assumed equally vulnerable (equal catchability) to the survey gear. The dynamics of each cohort is given by

$$N_{i,t+1} = S\,(N_{i,t} - C_{i,t}) \tag{A1}$$

where the annual survival rate S is assumed known in advance (as in Virtual Population Analysis) and $C(i,t)$ is the commercial catch from the cohort in year t. Looking n years forward in time, Eq. (A1) can be written as a difference between the initial stock size $N_{i,t}$ and a weighted sum of catches over time:

$$N_{i,t+n} = S^{n-1}N_{i,t} - K_{i,n} \tag{A2}$$

where $K_{i,n}$ is a sum of catches weighted by survival: $K_{i,n} = SC_{i,t+n-1} + S^2C_{i,t+n-2} + \ldots + S^{n-1}C_{i,t}$. $K_{i,n}$ can be computed recursively from the relationship $K_{i,n} = S\,(K_{i,n-1} + C_{i,n-1})$; this calculation is analogous to a recursive VPA back-calculation of $N_{i,t}$ from the catches, $C_{i,t+1}, \ldots, C_{i,t+n}$, except that it proceeds forward in time and does not use the inverse survival rate.

Assuming that all cohorts are equally vulnerable to the survey gear and that the survey is designed to give a standardized abundance index that is an unknown proportion, q, of the total stock size, the observed abundance for the cohort i in year t, $y_{i,t}$, is

$$Y_{i,t+n} = qN_{i,t+n} + \text{survey and aging error.} \tag{A3}$$

Substituting the state dynamics Eq. (A2) into the observation Eq. (A3), and collecting terms involving the parameters $N_{i,t}$ and q, gives the regression relationship

$$Y_{i,t+n} = b_iS^{n-1} - qK_{i,n} + \text{errors} \tag{A4}$$

where the regression parameters are $b_i = qN_{i,t}$ and q, and the regression independent variables associated with $Y(i,t+n)$ are S^{n-1} and $K_{i,n}$. Setting $S = 1$ in Eq. (A4) results in the familiar "Leslie depletion estimator" (Leslie and Davis 1939, see Ricker 1975 sect. 6.2). The regression model Eq. (A4) is also similar to Paloheimo's (1980) method for estimating initial cohort sizes and q, except that (A4) makes no assumptions about the relationship between commercial catches $C_{i,t+n}$ and $N_{i,t+n}$; the catches can follow a completely arbitrary pattern over time, as can the recruitments, $N_{i,t}$.

This method of estimating population size is the same as the method of Collie and Sissenwine (1983) except in the assumptions made about the errors. Collie and Sissenwine admitted process errors in the state dynamics Eq. (A1), which required nonlinear regression to solve the resultant mixed-errors problem. Ignoring the process errors in the present formulation allows the state dynamics to be written as Eq. (A2) and the parameters of Eq. (4) to be estimated by simple linear regression. The regression model (A4) increases in size by one parameter each year, as a new cohort R_i begins to be observed in the survey data. The estimates of all $N_{i,t}$ and R_i then improve over time as further $Y_{i,t+n}$ data are gathered on each cohort and as the estimate of q improves. The estimation of the survey q does not depend on any prior assessment of the effective area swept by the survey gear relative to the total survey area. In the extreme case that there is no catch ($K_{i,n} = 0$ for all i,n), only the combined parameters $b = qN$ can be estimated, and the absolute total stock size cannot be estimated at all.

The ratio estimates $N_{i,t} = b_i/q$ are biased upward, with an approximate bias $[N_{i,t}\,\mathrm{var}(q) - \mathrm{cov}(b_i,q)]/q^2$. This bias decreases rapidly over time as catches accumulate from each cohort and var(q) decreases, provided the exploitation rate is high (Fig. 2). For analyses of rockfish management performance using survey data, we first simulated regression performance to estimate the bias and variance of the $N_{i,t}$ estimates and of the total stock size (sum of Eq. (A2) estimates across cohorts). We then applied the resulting estimates of average bias in the overall management simulations such that the overall simulations had realistically varying but unbiased stock size estimates.

Monte Carlo simulations of POP in Goose Island Gully revealed a useful approximation for the standard error of the stock-size estimate in relation to the annual exploitation rate (U) and the number of years (n) of survey data available. The standard error divided by the actual stock size is approximately equal to $k/(Un)$, where $0.3 < k < 0.5$ for the survey and age sampling variances expected in that case. This approximation only holds for $0.05 < U < 0.4$ and $n < 15$, but this is the exploitation rate and time frame of greatest interest in experimental policy evaluation. The approximation shows clearly that higher exploitation rates and/or longer experimental times both help to reduce uncertainty about the stock size.

Implications of Age Determination Errors to Yield Estimates

A. V. Tyler, R. J. Beamish, and G. A. McFarlane

Department of Fisheries and Oceans, Biological Sciences Branch,
Pacific Biological Station, Nanaimo, B.C. V9R 5K6

Abstract

TYLER, A. V., R. J. BEAMISH, AND G. A. MCFARLANE. 1989. Implications of age determination errors to yield estimates, p. 27-35. *In* R. J. Beamish and G. A. McFarlane [ed.] Effects of ocean variability on recruitment and an evaluation of parameters used in stock assessment models. Can. Spec. Publ. Fish. Aquat. Sci. 108.

Recently there has been a realization that significant errors occur in estimating ages of many fish. This development has brought about a need for mathematically based models for examining and assessing the consequences of errors in age estimates. We addressed the subject by applying known errors in age-determination to hypothetical fish species with contrasting differences in life expectancy. One species completed its life in 10 years; the other in 100 years. We also modelled sablefish on the west coast of Canada as an example of a species with a life span of about one half century. We incorporated growth, and mortality rates into a stock simulation along with age-determination errors to explore the potential effects on yield estimation using dynamic pool models. Yield-per-recruit expectations increased over the true levels by as much as 19% if the only errors were from mean size-at-age. The analysis was sensitive to the behavior of the ageing error after the age of maturity. Management recommendations based on ageing methods that fail at the age of maturity can cause serious overfishing. However, the possible yield errors included overestimates as well as underestimates depending on when the age-determination method was modelled to fail.

Résumé

TYLER, A. V., R. J. BEAMISH, AND G. A. MCFARLANE. 1989. Implications of age determination errors to yield estimates, p. 27-35. *In* R. J. Beamish and G. A. McFarlane [ed.] Effects of ocean variability on recruitment and an evaluation of parameters used in stock assessment models. Can. Spec. Publ. Fish. Aquat. Sci. 108.

On s'est rendu compte dernièrement qu'il se produit des erreurs importantes au niveau de l'évaluation de l'âge de nombreux poissons. Cette constatation a soulevé la nécessité de modèles mathématiques pour étudier et évaluer les conséquences des erreurs d'estimation de l'âge. Le sujet a été traité de la façon suivante : des erreurs connues de détermination de l'âge ont été appliquées à des espèces hypothétiques de poisson dont l'espérance de vie présentait des différences marquées. Une espèce avait un cycle de vie de 10 ans; l'autre, de 100 ans. Nous avons également utilisé comme modèle la morue charbonnière de la côte ouest du Canada comme exemple d'une espèce dont l'espérance de vie est d'environ 50 ans. Nous avons introduit le taux de croissance et de mortalité dans la simulation d'un stock et les erreurs de détermination de l'âge afin d'étudier les effets possibles sur l'estimation du rendement au moyen de modèles de la dynamique en bassin. Les prévisions du rendement par recrue étaient jusqu'à 19 % plus élevées par rapport au niveau réel si les seules erreurs se situaient au niveau de la taille moyenne selon l'âge. L'analyse était sensible au comportement de l'erreur de vieillissement lorsque l'âge de la maturité était dépassé. Les recommandations de gestion qui reposent sur des méthodes de détermination de l'âge qui donnent un âge à la maturité inexact peuvent être à l'origine d'une importante surpêche. Cependant, les erreurs de rendement peuvent autant être la cause de surestimations que de sous-estimations tout dépendant du moment où la modélisation de la détermination de l'âge prévoit que celle-ci n'est plus valable.

Introduction

Age is one of the most important variables used in fisheries science. For many fishes, estimating age is difficult. However, because investigators are not aware of this difficulty, the error associated with age-determination estimates has seldom been considered in stock assessments. Beamish and McFarlane (1983) showed that in an unselected sample of 75 stock assessment papers published between 1965 and 1980 in five major journals, not one author used validated ages in the analysis. In other sciences it is fundamental to estimate error for each parameter in a calculation and to provide an estimate of how these accumulated errors affect the final result.

Some investigators believe the problem of error in age determination is unimportant because they think the error is small. This belief, of course, is paradoxical because the magnitude of the error is unknown. However a belief that errors are small appears to be the reason most investigators have ignored incorporating age-determination errors in their stock assessment models. The subject of age-determination errors in stock assessment requires an assessment of the accuracy of past and present age-determination techniques, and if important errors are present, then the consequences of these errors in determining yields and understanding biology need to be examined.

Accuracy of Age Determination

In this report we briefly review the accuracy of age-determination methods to show that errors exist. We then examine the consequences of these errors on yield from models of three populations that represent a range of life history types found in fish populations.

The accuracy of age-determination methods was re-examined by Beamish and McFarlane (1983). The standard methods that use scales or surface examinations of otoliths probably provide accurate estimates of age over the range of more rapid growth. The problem with these methods, however, is that they assume an isometric relationship between the length of the fish and the growth of the scale or otolith surface area. When growth stops or is reduced, there will be a change in the growth pattern of these structures that will result in a change in annulus development. Examples of the importance of the ageing error that resulted from the use of the scale method were provided by Beamish and McFarlane (1987) for 16 species of common freshwater and saltwater fishes. In all cases, fish were found to be much older than previously thought. Examples of fish being older than previously thought continue to appear indicating that traditional interpretations have, in some cases, produced age estimates that seriously underestimate the true age of fish in a population. The use of new age-determination methods, such as sectioning otoliths, breaking and burning otoliths, or the use of opercula and fin rays, have produced some major changes in the understanding of fish growth and production. For example, on the west coast of Canada, most of the commercially important species are now believed to be much older than previously thought (Beamish and McFarlane 1987). Nine percent of the species now are believed to have maximum ages less than 20 yr, 48% range from 21 to 49 yr and 43% range from 50 to 100 yr (Chilton and Beamish 1982; Beamish and McFarlane 1987). Even small errors are important when the maximum age of the fish is only a few years. We believe that the example of the change in understanding of the age composition of West Coast groundfishes, the increasing accounts of ageing error and the general lack of age validation studies, indicate the errors in the accuracy and precision of age estimates are more common than previously thought. Unquestionably, ageing errors exist and the consequences of such errors need to be examined.

Methods

We developed our model with two hypothetical species of fish; one that completed its lifespan in ten years, that we called the "decadefish;" and one that completed its lifespan in 100 years, that we called the "centuryfish". The decadefish matured at 3 years of age, and recruited to the fishery at the same age. The centuryfish matured and recruited to the fishery at 15 years. We also developed a model of a half-centuryfish from published parameters of the sablefish *(Anoplopoma fimbria)*. This species had its age of 50% maturity at 5 years, was formerly and erroneously aged by using scales, but is at present aged with otoliths using the break and burn method (McFarlane and Beamish 1983). In our model we looked at the implications to potential yield of using each of the age-determination methods.

We arranged the models of the decadefish and centuryfish so that we first sampled the population prior to exploitation by the fishery. This meant that the estimation of the total instantaneous mortality rate from our sample was an estimate of the instantaneous natural mortality rate, M ($Z=M$). The fish of this sample were put into our age-determination simulator to induce the kind of error that historically has been made for species similar to the decadefish and centuryfish. It is this induced error that we investigated.

To incorporate age-determination error into the model, we developed an *a priori* schedule of percentage errors that an age reader might make using erroneous age-determination techniques such as scale reading. The kind of errors that could occur were similar to the known ageing errors for species that have a range of longevities (white suckers, lake trout, lake whitefish, rockfish). The percentages were set up as a matrix of coefficients giving the probability of a fish of a given age being assigned to any age including its true age (Tables 1 and 2). In addition to the published studies, our experience leads us to think that these errors are representative of errors that are being made by age readers.

For the decadefish, the simulated age reader did not recognize fish older than age 7. Fish were assigned either to the true age, or to the adjacent ages. The reader became progressively less accurage with older fish (Table 1). The chance of an age-1 or age-2 fish being called correctly

TABLE 1. Transfer coefficients of the decadefish as probabilities of reassignment by the age reader from the fish's true age to any age.

		Age transferred TO									
		1	2	3	4	5	6	7	8	9	10
Age transferred	1	0.95	0.05	0.00	0.0	0.0	0.0	0.0	0	0	0
FROM	2	0	0.90	0.10	0.0	0.0	0.0	0.0	0	0	0
	3	0	0.03	0.85	0.09	0.03	0.0	0.0	0	0	0
	4	0	0.0	0.10	0.80	0.10	0.0	0.0	0	0	0
	5	0	0.0	0.0	0.70	0.30	0.0	0.0	0	0	0
	6	0	0.0	0.0	0.30	0.40	0.30	0.0	0	0	0
	7	0	0.0	0.0	0.20	0.40	0.30	0.10	0	0	0
	8	0	0.0	0.0	0.0	0.42	0.56	0.02	0	0	0
	9	0	0.0	0.0	0.0	0.42	0.56	0.02	0	0	0
	10	0	0.0	0.0	0.0	0.42	0.56	0.02	0	0	0

TABLE 2. Transfer coefficients of the centuryfish as probabilities of reassignment by the age reader from the fish's true age to any age. To simplify this presentation ages are given by the 10-yr interval as mean probabilities for the intervals. Year-interval probabilities were actually used in the calculations, with smoothed transitions from one 10-yr interval to the next.

	Age interval transferred TO				
	1–10	11–20	21–30	31–40	41–100
Age interval transferred					
FROM					
01–10	90	10	0	0	0
11–20	6	82	12	0	0
21–30	8	20	64	8	0
31–40	0	25	30	45	0
41–50	0	25	30	45	0
51–60	0	25	30	45	0
61–70	0	20	30	50	0
71–80	0	10	30	60	0
81–90	0	0	35	65	0
91–100	0	0	10	90	0

was 95 and 90%, respectively. Age-4 and age-5 individuals had a chance of 80 to 30%, respectively. As can be seen from these percentages, the age-determination method largely failed after age 4.

For the centuryfish, the simulated age reader did not recognize fish older than age-40. Individuals in the first decade of life (age 1–10) had a 90% mean chance of being aged correctly. In their second decade, the chance was 82%; in the third decade, 64%; and in the fourth decade 45%. The method of age determination first failed in the third decade (ages 21–30). In fact, after age-28 there was only a 50% chance of correct age assignment. For the most part, the errors in age determination were spread over a 3-decade age span. For example, fish whose true age was between 31–40 had a mean chance of 25% of being mis-assigned to the age range of 11–20; 30% into ages 21–30; and 45% into the range 31–40 (Table 2). Fish whose true age was 41–60 were mis-assigned to the age 11–40 range. Individuals older than 60 had a progressively increasing chance of being assigned to the 31–40 range rather than to the younger ages.

The depletion curves of number-at-age with induced error were fitted with a log-linear, least-squares regression to determine the apparent value of M. This estimated M, along with mean size-at-age with induced error, was used directly in dynamic-pool (yield-per-recruit) model calculation (Gulland 1983, p. 147) of potential yield.

For the half-centuryfish the "reference" data that corresponded to the error-free case were the published production parameters of the sablefish determined by the break and burn method, including an estimate of the instantaneous mortality rate (M) (McFarlane et al. 1985), and von Bertalanffy parameters (McFarlane and Beamish 1983). The values, applying to fish in the Queen Charlotte Sound on the west coast of Canada, are as follows: $M=0.10$, $K=0.243$, $W_\infty=6500$ and $t_0=0.86$, where K is the Brody growth coefficient, W_∞ is the ultimate weight, and t_0 is the age correction-factor. The numbers-at-age data "with error" were reconstructed from the older estimate of $M=0.22$ from scale readings (Low et al. 1976). To derive the comparable von Bertalanffy parameters we used the same values of W_∞ and t_0 but adjusted K so that the fish in the age range of 5-10 years were a maximum of 0.5 kg heavier than the later estimates. This approximated the difference between weight-at-age curves determined by break and burn methods and by scale reading (Lai 1985).

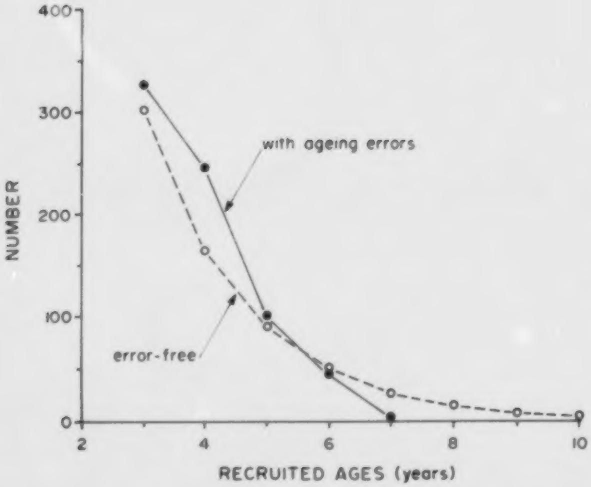

FIG. 1. Decadefish. Number-at-age for fishery-recruited ages, showing error-free data and the same sample with simulated age-determination error. The biologist would normally be aware of only the curve with induced error.

Results

Number-at-Age

For the decadefish the simulated induction of ageing errors shifted many individuals forward in the age distribution. There were more fish at age four than at any other single age (Fig. 1). Age-4 was the oldest age for which there was reasonable accuracy in age determination. At older ages less than half of the fish were correctly classified to the correct age. Fish accumulated at age-4 because few individuals were shifted out of this age, but many were assigned into the age from the older ages. There was a tendency to underage the fish. Because of the mis-assignments, the slope of the number-at-age line appeared to be steeper than the slope for the true curve.

For centuryfish, there were more fish in the 11–40 age range in the erroneous number-at-age curve than there were in the true distribution (Fig. 2, top panel). All fish

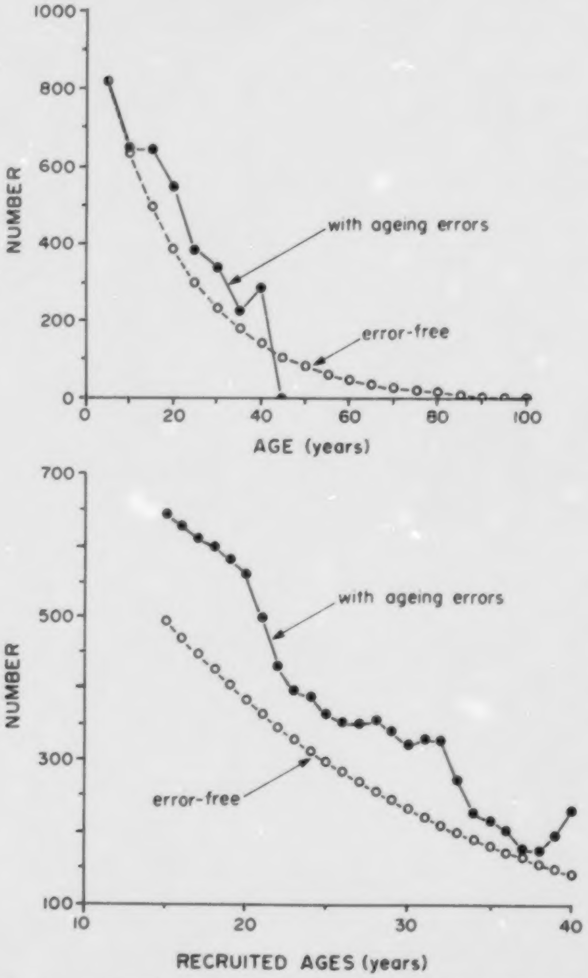

FIG. 2. Centuryfish. Top panel: Number-at-age plotted at 5-yr intervals for the total stock, showing the sample with error-free data and simulated age-determination error. Bottom panel: number-at-age at 1-yr intervals for the recruited ages. The youngest, fully recruited age (knife-edge) was 15, and the oldest, 40. Fish older than 40 were not recognized as such, and were assigned to younger ages.

over 40 were shifted to younger ages. At ages 10 and younger, the erroneous and true number-at-age curves are about the same. The greatest discrepancy between the erroneous curve and the true curve occurred in the 15–20 age group (Fig. 2, bottom panel). As with the decadefish, the accumulation of true-aged fish and mis-aged fish was greatest prior to the age at which the age-determination method fails. Errors occurred over most of the fishery-recruited ages. As a consequence, the slope of the depletion curve increased only a little, and appeared higher than, and almost parallel to, the true curve.

For the half-centuryfish (sablefish) most individuals were younger than age 40 (98%) for the more accurate or "reference" population reconstruction. The oldest age in the sample of 3400 fish was 56. On the other hand, for the erroneous population reconstruction most of the fish were younger than age 10 (97%) (Fig. 5).

Our models of decadefish and centuryfish were set up so that the calculated slope of the depletion curve was an estimate of *M*. The induced errors caused *M* to shift from its true value of 0.60 to 1.05 for the decadefish, and from 0.050 to 0.056 for the centuryfish. A biologist unaware of the age-determination error might conclude that the age-specific mortality rate of the centuryfish in the last five years of life was actually very high, higher than the average rate of the younger portion of the stock, in order to account for the disappearance of the fish and the truncation of the number-at-age curve.

Weight-at-Age

When older fish were assigned to younger ages, their body weights were averaged in with those of the younger fish when mean weight at age was calculated. This process caused an increase in the mean weight-at-age for the hypothetical species (Fig. 3). Most of the oldest decadefish were assigned to age-6. Though there were only a few old fish, they were heavier than age-6 fish, and their weight increased the mean weight-at-age (Fig. 3).

Similarly, the weight-at-age curve for the centuryfish was shifted upward, particularly for fish in the 10–20 age bracket. These were the ages with the greatest increases on number-at-age due to older fish being reassigned to younger ages, and so the weight increase here was not surprising. However, there was only a small increase in weight of the oldest fish, where one might expect a greater rise because of the increase in numbers at ages 39 and 40 due to reassignment. There was little increase in mean weight, however, because fish older than age 30 had grown very little.

For the half-centuryfish the maximum difference in weight-at-age between the erroneous and reference data occured at age 7. There was very little difference at age 20 (Fig. 5).

Potential Yield

The levels of error in estimates of potential yield from biased and unbiased data were examined in two stages with the dynamic pool model: (1) the addition of error solely from the biases in weight-at-age relationships, (2) the addition of error due to biases in the natural mortality rate . Natural mortality rate and age-specific weights are the two factors that play off against one another in the calculation of yield-per-recruit as a function of fishing mortality rate (*F*) in the dynamic pool model.

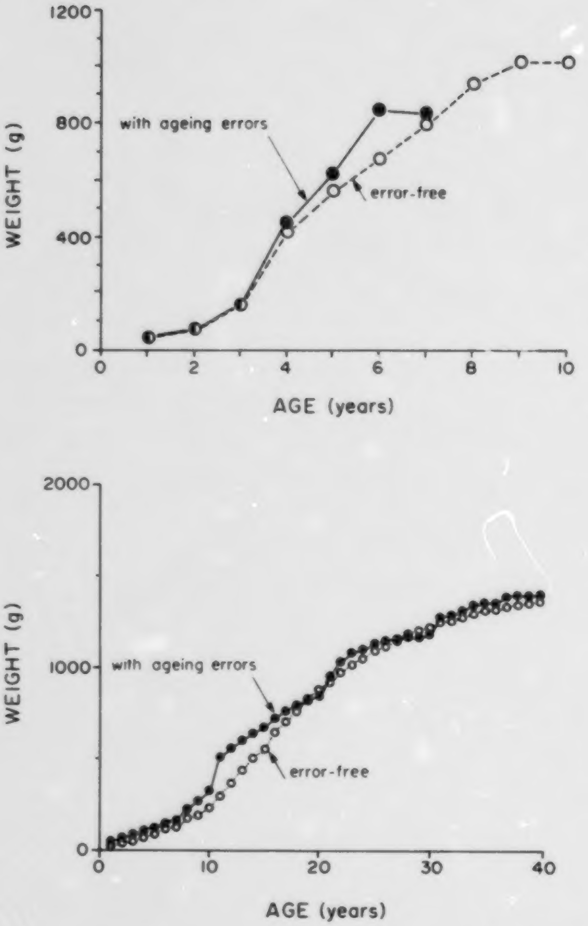

FIG. 3. Weight-at-age. Top panel: decadefish plot for all ages, showing the same sample with error-free data and data with induced error. Bottom panel: centuryfish plot for all ages showing the same sample with error-free data and data with induced error.

As expected, yield-per-recruit increased with increase in *F*, rapidly at first, and then very slowly (Fig. 4). The curves for the centuryfish showed maxima, then decreasing yields, whereas the curves for the decadefish increased asymptotically. The yield-per-recruit curves were compared by examining the differences between them at a selected level of *F*. By making the comparison at an intermediate value of *F* ($F = 1.0$), it was easy to see that the use of biased weight data and the true value of *M* increased the expected yield-per-recruit for both species — up to 91% for the decadefish and 16% for the centuryfish. So if there were only weight biases, yields would be overestimated.

The biased values of *M* were higher than the true values. With an increase in *M*, more individuals would die due to natural causes, and there would be fewer fish available to the fishery. Potential yield would be less for

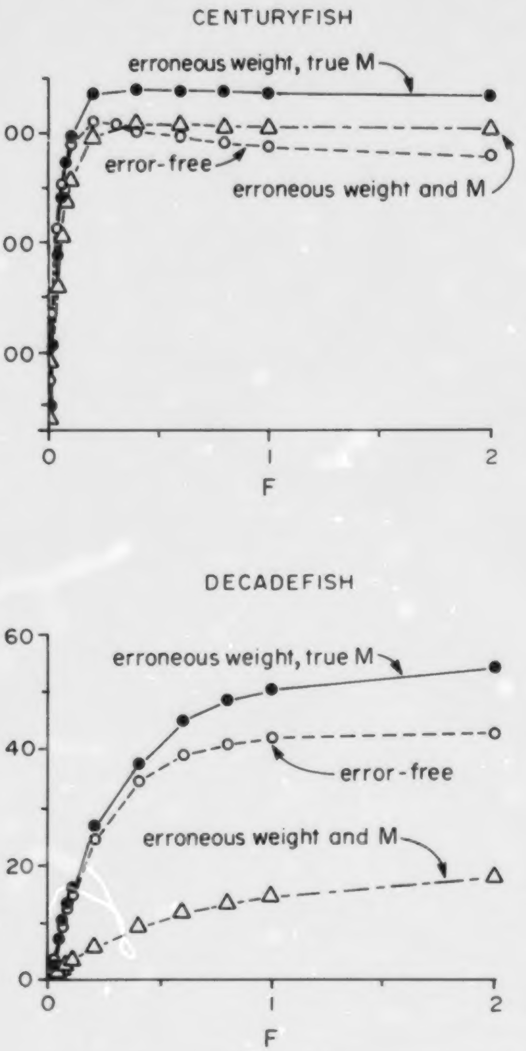

FIG. 4. Yield curves from dynamic pool models for the decadefish (top panel) and centuryfish (bottom panel), giving yield potentials (*t*) versus instantaneous fishing mortality rate (*F*). The three curves shown in each panel are (1) open circles, potential yields without bias due to age determination error; (2) solid circles, potential yields without bias in the instantaneous mortality rate (*M*), but with bias in weight-at-age due to age-determination error; (3) open triangles, potential yields with biased natural mortality rates (*M*) and weight-at-age.

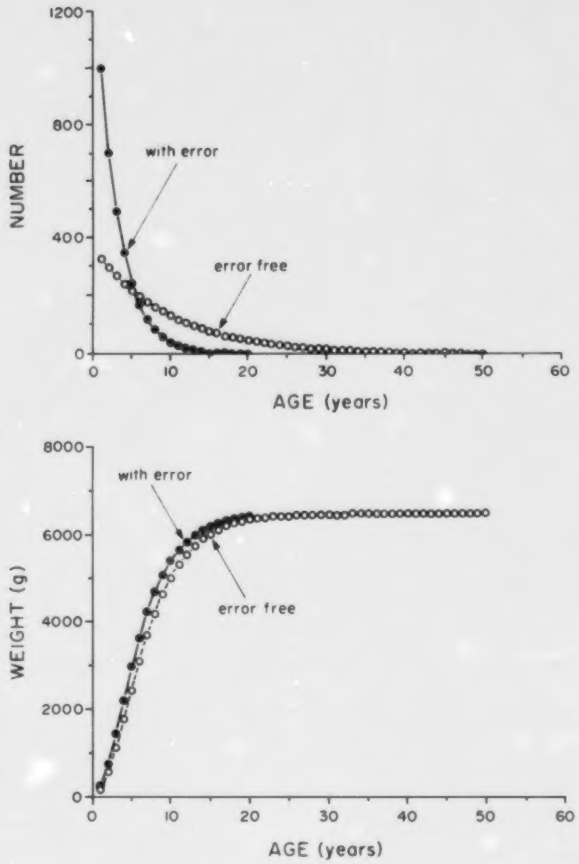

FIG. 5. Half-century fish. Top panel: number-at-age with induced error, solid points. Error-free (= reference) data, open points; Bottom panel: weight-at-age data for error-free (= reference) and data with error.

a given level of fishing effort. Consequently, the yield-per-recruit curves using biased *M* as well as biased weights were lower at $F = 1.0$ than were the curves with biased weight alone. For the centuryfish, the lowering of the curve made the estimate of yield only 6% higher than the true estimate. In effect, the mean weight and mortality rate biases tended to cancel one another. The greater bias (increase) in *M* in the decadefish caused a greater reduction in yield-per-recruit, so much so that the potential yield was underestimated by 65% at $F = 1.0$.

For the centuryfish and decadefish there was little change in the age of the cohort biomass maximum with the erroneous and error-free data. For the erroneous data of the centuryfish the age was 19, and 21 for the error-free case. For the decadefish, the biomass maximum occurred at age-4 in both cases. For the half-centuryfish, the differences in the parameter values caused cohort biomass to maximize at age-8 for the error-free data, and age-4 for the erroneous data, i.e., at half the age (Fig. 6). The change in the biomass maximum in the half-centuryfish means that the optimum age at first capture, as well as *F*, would influence the potential yield, and so we follow the standard practice of using yield isopleths to analyze the influence of both factors acting simultaneously. For the reference data of the half-centuryfish, the yield-per-recruit maximized when fish were first taken at age-8 with an *F* value of 0.90 or greater (Fig. 7, top panel). However, for the erroneous data, yield-per-recruit maximized when fish were exploited as young as age-5 with an *F* value of 0.70 or greater (Fig. 7, bottom panel). Further, the maximum yield per recruit expected from the erroneous data was 900 g, whereas the correct value was 2500 g (Fig. 7).

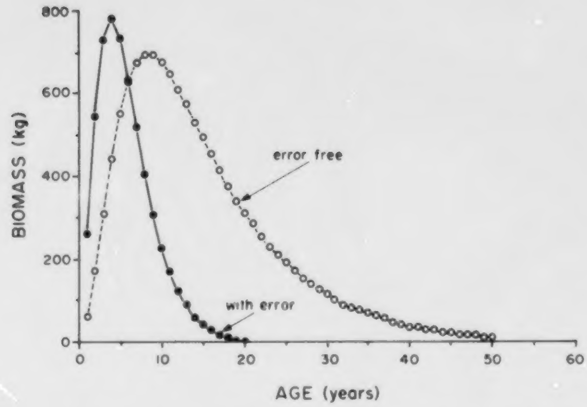

FIG. 6. Half-century fish. Biomass-at-age. Open points indicate error-free (= reference) data. Solid points indicate data with age-determination error.

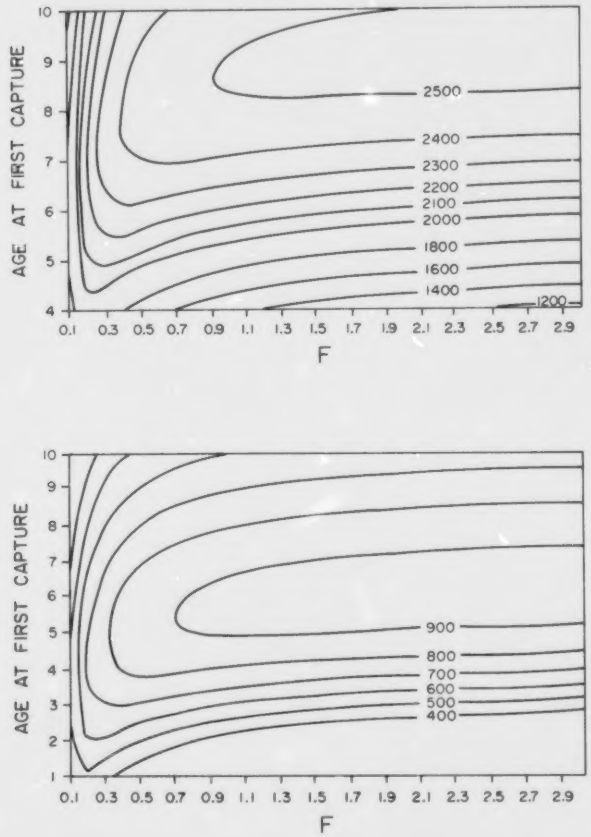

FIG. 7. Half-century fish, yield-per-recruit isopleths. Top panel: Error-free data. Bottom panel: data with age determination error.

Discussion

A wide range of errors in yield estimation was caused by incorrect age determination. The possible yield-per-recruit errors demonstrated here included modest overestimates, ranging through small and large underestimates. For a given *F*, overestimation resulted when there were biases in weight-at-age but not in mortality rate, because the biased mean weight-at-age was usually greater than the true weight values. Ageing errors caused a false increase in natural mortality rate estimates that resulted in an underestimate of yield-per-recruit. However, the true estimate of natural mortality rate would indicate a larger yield per-recruit. This does not mean that more fish can be harvested. The paradoxical situation occurs because the true lower *M* also indicates lower production. If the tactic of setting $F = M$ (Alverson and Pereyra 1969) were adopted using the erroneously high *M*, overfishing would result. The importance of maintaining larger standing stocks for older, slow growing fishes is well known for species such as rockfish.

In a recently published analysis of walleye pollock (Lai and Gunderson 1987), it was shown that under-ageing could cause overestimation of yield-per-recruit. The overestimation was due to the bias in weight-at-age being far stronger than the bias in the mortality rate. We showed that under-ageing could lead to both overestimation and underestimation of the yield per recruit, depending on the relative strengths of bias in mortality rate and weight-at-age. The degree of bias associated with either weight-at-age or mortality rate depended on the patterns of error in assigning individual fish to specific ages. The failure of the age-determination method at a relatively young age caused a substantial upward bias in the estimation of *M*. This bias was produced by an accumulation of fish at the age range where the age-determination method failed (< 50% correct age-classification). Also, when decadefish were misassigned into a narrow portion of the true age range through under-ageing, mortality rates determined from the age distribution were strongly biased, and the yield-per-recruit error was large. In contrast, when the age-determination method broke down gradually over a large range of ages (centuryfish), the estimate of the mortality rate was only slightly biased upward, and yield-per-recruit error from this source was small.

Weight biases were substantial except when the fish being mis-read were approaching W_∞, e.g., if individuals at sizes close to ultimate weight were reassigned to younger ages that were also close to the ultimate weight, little weight bias occurred. When biases in both weight and *M* were in the model, errors in estimated yield-per-recruit were somewhat reduced because the effects of the biases on yield tended to cancel each other.

The half-centuryfish was modelled with sablefish data. As with the hypothetical species, age-determination error led to a large overestimate in *M*. The erroneous estimate of *M* was 0.22, and the true estimate was 0.10. However, there were only small errors in weight-at-age because older fish in general increased very little in weight. At age-7, where weight-at-age error maximized, the erroneous weight was only 14% (0.5 kg) higher than the true weight, and the erroneous *K* was only 13% higher than the more accurate *K*. As with the decadefish, yield-per-recruit was underestimated due to the bias in mortality rate. If the erroneous *M* was used to decide *F*, there would be overfishing.

The ageing error that contributes to the decrease in yield-per-recruit estimates is associated with the higher estimate of M. The effect on F of overestimating M was considered by Bradford and Peterman (this volume) by examining the relationship between mortality and yield. In addition the erroneous yield-per-recruit diagrams suggest that the age at first capture should be age-5, though only half of the fish at this age are mature. Since the erroneously recommended value of F would be 0.70, the corresponding survival rate would be only 40% per year ($S=e^{-(F+M)}$, where $F+M = 0.92$). The fishing rate would reduce the spawning stock and recruitment overfishing would be likely.

Because there is no F_{opt} for the decadefish, one might use the conservative tactic of setting F at a value equal to M (Alverson and Pereyra 1969). There are theoretical reasons that this policy would sometimes prevent recruitment overfishing (Shepherd 1982). Due to age-determination errors this F value would be erroneously high because M was estimated as too high (erroneous M estimate level = 1.05; true level = 0.60). If management control were made on the basis of fishing effort, say allowing 1.75 times as such effort as at present (by the ratio 1.05/.60), then the result would be an overfished stock because of the high effort that was recommended.

In the case that an estimate of recruitment is made with a catch-at-age analysis technique such as virtual population analysis, use of erroneous percentage age compositions, and a much inflated M value in the equations would lead to a gross overestimation of recruitment levels. More specifically, VPA would use the erroneously high M value iteratively (Gulland 1965, 1983) to produce a multiplicative error in the estimation of starting year-class sizes. With an erroneously high M, the method would calculate that the number of fish dying due to natural causes was greater than actually occured. These deaths would be incorporated as part of the starting year-class size (before natural mortality). The error would be compounded by the age-determination error incorporated in the percentage age-composition figures. These percentages would determine the age composition of the catch that is used by the VPA equations. The bias in these percentages will inflate the estimation of starting cohort size. The resulting quota would be higher than the quota using a true value of recruitment. In this case an *a priori* estimate of the resulting error is not possible. Since the Y/R curve is erroneously low, re-scaling with an erroneously high estimate of recruitment could be higher or lower than the true potential yield.

The effect of biased M and weight-at-age depends to some extent on the particular yield model being used. We have chosen the example of the dynamic pool model because it is so widely used in fish stock assessments. In addition, the principles of yield estimation utilized in this type of model are incorporated into other age-structure models, and so the effects of the biases discussed here would be similar. Nevertheless, we would expect that other stock assessment workers might find it useful to test the most appropriate model for their situation with the kind of age-determination error presented in this paper.

We examined three life history types to study the effect that a management strategy based on erroneous age determinations would have on stocks. The decadefish represented a relatively short-lived species typical of species such as Pacific cod, walleye pollock and Pacific hake. A second life history type was represented by sablefish. This life history type has a relatively long life. In the past it was thought that only a few fishes had this type of life history, however, the use of new methods of age determination has shown that a number of commercially important fishes, such as rockfish, lake trout and lake whitefish are considerably older than previously thought. The third hypothetical life history type is a species that is aged by a method that does not break down until well after the age of maturity, producing inaccurate ages for the oldest fish in the population. We are not aware of many situations, other than spiny dogfish, where the ageing method breaks down well after the age of maturity. However, it is possible that more examples will be found as age-determination techniques are validated. Rockfish have the live expectancy of the centuryfish, but the ageing error breaks down more like the decadefish.

Other life history types could be examined, however, we believe we have demonstrated the importance of considering ageing error in stock assessment models.

This symposium was about errors in stock assessment models and the implications for yield estimation. We found age determination errors can cause serious biases in vital parameters and subsequent yield estimations. The errors have reduced effect when the method of age determination fails gradually over a broad range of ages in the middle of the lifespan. The errors are critical when the method fails in the age-range prior to the age at which cohort biomass is maximized and it is this case that is the most common type of age determination error.

Acknowledgements

We thank Mark Saunders for making computer calculations for sablefish, and Han Lin Lai for suggestions made in his review of our paper.

References

ALVERSON, D. L., AND W. T. PEREYRA. 1969. Demersal fish explorations in the northeastern Pacific ocean — an evaluation of exploratory fishing methods and analytical approaches to stock size and yield forecasts. J. Fish. Res. Board Can. 26: 1985–2001.

BEAMISH, R. J., AND G. A. MCFARLANE. 1983. The forgotten requirement for age validation in fisheries biology. Trans. Am. Fish. Soc. 112(6): 735-743.

1987. Current trends in age determination methodology, p. 15–42. *In* R. C. Summerfelt and G. E. Hall [ed.] Age and growth of fish. Iowa State University Press, Ames, IA.

CHILTON, D. E., AND R. J. BEAMISH. 1982. Age determination methods for fishes studied by the Groundfish Program at the Pacific Biological Station. Can. Spec. Publ. Fish. Aquat. Sci. 60: 102 p.

Cushing, D. H. 1975. Marine ecology and fisheries. Cambridge University Press. 278 p.

Gulland, J. A. 1965. Estimation of mortality rates. Annex to Arctic Fisheries Working Group Report (Hamburg). ICES. C.M. 1965. Doc. No. 3 (mimeo).

1983. Fish stock assessment. A manual of basic methods. John Wiley and Sons, New York, NY. 223 p.

Lai, H. L. 1985. Evaluation and validation of age determination for sablefish, pollock, Pacific cod, and yellowfin sole; optimum sampling design using age-length key; and implications of ageing variability in pollock. Ph.D. thesis, University of Washington, Seattle, WA. 426 p.

Lai, H. L., and D. R. Gunderson. 1987. Effects of ageing errors on estimates of growth, mortality and yield per recruit for walleye pollock (*Theragra chalcogramma*). Fish. Res. 5: 287–302.

Low, L. L., G. K. Tanonaka, and H. H. Shippen. 1976. Sablefish of the Northeastern Pacific Ocean and Bering Sea. Northwest and Alaska Fisheries Center. Processed Report. October 1976.

McFarlane, G. A., and R. J. Beamish. 1983. Biology of adult sablefish (*Anoplopoma fimbria*) in waters off western Canada. *In* B. Melteff [ed.] Proceedings of the International Sablefish Symposium. Lowell Wakefield Series. Alaska Sea Grant Rep. 83-8: 59–93.

McFarlane, G. A., W. Shaw, and A. V. Tyler. 1985. Sablefish. *In* Tyler, A. V. and G. A. McFarlane [ed.] Groundfish stock assessments for the west coast of Canada in 1984 and recommended yield options for 1985. Can. MS Rep. Fish. Aquat. Sci. 1813: 163–186.

Shepherd, J. G. 1982. A family of general production curves for exploited populations. Math. Biosci. 59: 77–93.

Influence of Errors in Parameter Estimates on Stock Assessment

Syoiti Tanaka

Tokyo University of Fisheries, Minatoku, Tokyo, Japan 108

Abstract

TANAKA, S. 1989. Influence of errors in parameter estimates on stock assessment, p. 37–42. *In* R. J. Beamish and G. A. McFarlane [ed.] Effects of ocean variability on recruitment and an evaluation of parameters used in stock assessment models. Can. Spec. Publ. Fish. Aquat. Sci. 108.

Problems in estimating recruitment N_0, the catchability coefficient q and the natural mortality coefficient M using data on fishing effort X and catch C of a year-class are considered by examining the shape of the response surface of the goodness-of-fit to the observed data. The response surface for the three unknown parameters shows an extremely elongated ellipsoidal contour, and high correlations among estimates of the three parameters are indicated. The correlation is derived from the dynamic model. For instance, $(q \times N_0)$ is related to the observed catch per unit effort and estimate of $\hat{q}$ tends to be inversely correlated with $\hat{N}_0$. When $\hat{M}$ or $\hat{N}_0$ value is available a priori they can be used to improve the estimates of other parameters. The effect of observation error in $\hat{M}$ on the estimate of $\hat{N}_0$ is amplified but that of $\hat{N}_0$ on $\hat{M}$ is reduced. Natural mortality which increases with age leads to biases if estimations are conducted on the basis of a constant value. Both $\hat{N}_0$ and $\hat{M}$ are overestimated when fishing effort increases with time and a decreasing fishing effort causes biases in the opposite direction.

Résumé

TANAKA, S. 1989. Influence of errors in parameter estimates on stock assessment, p. 37–42. *In* R. J. Beamish and G. A. McFarlane [ed.] Effects of ocean variability on recruitment and an evaluation of parameters used in stock assessment models. Can. Spec. Publ. Fish. Aquat. Sci. 108.

La forme de la surface de réponse de la qualité de l'ajustement aux données observées a servi à étudier les problèmes d'évaluation du recrutement N_0, du potentiel de capture q et du coefficient de mortalité naturelle M au moyen des données sur l'effort de pêche X et les prises C d'une classe annuelle. La surface de réponse des trois paramètres inconnus présente un contour ellipsöidal allongé, et de fortes corrélations entre les évaluations des trois paramètres sont indiquées. La corrélation est dérivée du modèle dynamique. Par exemple, $(q \times N_0)$ est lié à la capture par unité d'effort observée et l'évaluation de $\hat{q}$ a tendance à être inversement relié à $\hat{N}_0$. Lorsque les valeurs $\hat{M}$ ou $\hat{N}_0$ sont accessibles a priori, elles peuvent être utilisées pour mieux évaluer d'autres paramètres. L'effet de l'erreur d'observation de $\hat{M}$ sur l'évaluation de $\hat{N}_0$ est accentué mais celui de $\hat{N}_0$ sur $\hat{M}$ est réduit. La mortalité naturelle qui augmente avec l'âge entraîne des biais si les évaluations sont effectuées en fonction d'une valeur constante. Les valeurs $\hat{N}_0$ et $\hat{M}$ sont surestimées lorsque l'effort de pêche augmente avec le temps et un effort de pêche décroissant produit des biais dans le sens opposé.

Introduction

Recent improvement in computer techniques has enabled us to deal with complicated computations quite quickly. Thus, the nonlinear least squares problem, which used to be very difficult mathematically, can now be handled easily. Simultaneous estimation has become a reality for models with sufficient numbers of parameters to be both realistic and detailed. Shirakihara and Tanaka (1983, 1984, 1985) and Tanaka (1983) estimated stock abundance of sperm whales in the Northwest Pacific Ocean by analysing length-frequency data for the catch. From this calculation, yearly fishing rates and length-specific selectivities were estimated. Sakuramoto and Tanaka (1985, 1986) applied the technique of cohort analysis to catch-at-age data for Southern Hemisphere minke whales. They calculated yearly fishing rates, age-specific selectivities, and year-class strengths. The number of parameters estimated by this analysis involved 11 years, 35 age-classes, and 45 year-classes, and computation required a few hours with a large general purpose computer.

In these estimation methods, some biological parameters such as the natural mortality coefficient were treated as known values. Sakuramoto and Tanaka obtained results for Southern Hemisphere minke whales which suggested that yearly recruitment increased at a rate of a few percent per year from about 1940 to 1965. Many arguments were presented in the meeting of the Scientific Committee of the International Whaling Commission as to whether or not this increasing trend was real (IWC 1985). It had been shown by Monte Carlo simulation that if the true natural mortality coefficient (M) is relatively high, say 0.126/yr as opposed to the commonly used value of 0.086/yr, an annual rate of increase of 4% would be obtained even when recruitment is actually constant throughout the period (Sakuramoto and Tanaka 1985).

Often sensitivity tests are conducted to find the relation between input value and the estimate obtained. However, sometimes such relation is not anticipated and we may be trapped in a false conclusion. To avoid this kind of difficulty it may be important to predict possible relations in advance.

Estimated values are not only affected by input parameter values, but also are usually correlated with each other. It is extremely difficult, however, to predict or to interpret such interrelations intuitively if the model is realistically complicated.

The purpose of this paper is to study, with a simple model, the behaviour of such estimates obtained from complicated models by the nonlinear least squares technique, and to examine the mechanism of their linkage.

Model and Estimation Method

Following a procedure commonly used for whale populations, the basic model for the dynamics of a year-class is set as follows:

$$N_{t+1} = (N_t - C_t)e^{-M} \qquad (1)$$
$$C_t = q\, X_t\, N_t$$

where:

t: year or age. $t = 0$ when this year-class is recruited.
N_t: initial population size in numbers in year t.
C_t: catch in year t.
X_t: fishing effort in year t.
M: natural mortality coefficient, so the annual survival rate is $s = e^{-M}$ in the absence of fishing mortality.
q: catchability coefficient.

Both M and q are assumed to be constant in the basic model. Putting recruitment $N_0 = 1000$, $s = 0.80$, and $q = 1.0$ and then applying the X_t values arbitrarily given in Table 1, allows values for N_t and C_t to be calculated by (1) (Table 1).

Suppose that C_t and X_t are all known or observed values, so that the unknown parameters are N_0, q, and $s = e^{-M}$. For least squares estimation, the residual sum of squares is calculated as

$$\text{SS} = \sum_{t=0}^{7} (C_t - \hat{q}X_t\hat{N}_t)^2 \qquad (2)$$

where $\hat{N}_t$ values are those calculated for N_t by (1) starting from a specified value for $\hat{N}_0$, and $\hat{q}$ is an estimate of q. Generally C_t and X_t are subject to observation errors from various sources, and the SS would never be zero.

By definition, the least squares estimates of N_0, q, and s are those values which minimize the SS value. Various computer programs have been developed to search for a set of parameter values corresponding to the minimum SS. In this paper, however, the dependence of the sum of squares response surface on various sets of values of $\hat{N}_0$, $\hat{q}$, and $\hat{s}$ will be examined in detail. To simplify the development, all C_t and X_t values are assumed to be error free. That is, if the true N_0, q, and s values are applied, the SS would be reduced to zero except for rounding errors. In the following sections, discussions are first presented with special reference to the cases where either $\hat{s}$ or $\hat{N}_0$ is known a priori.

Response Surface of SS

Natural Mortality Known

Taking $\hat{N}_0$ and $\hat{q}$ on the abscissa and ordinate, respectively, and assuming the true value of $s = 0.8$ is known, contour lines of SS are obtained as shown in Fig. 1. As all observed values are error free, the center of the contour lines is at $\hat{N}_0 = 1000$ and $\hat{q} = 1.0$ and the SS is 0. These contours describe elongated ellipses, with both the parameter pairs $\hat{q} = 0.967$, $\hat{N}_0 = 1028$ and $\hat{q} = 1.032$, $\hat{N}_0 = 974$ giving an SS value of only 5.0. This SS value is a sum of 8 terms and hence the mean residue is only $\sqrt{5.0/8} = 0.79$, very small relative to the mean C_t of 67.9 (Table 1). These two sets of values therefore give a fit essentially as good as that of the true values. Minor observational errors would in practice produce much higher SS values than this and variability of $\hat{q}$ or $\hat{N}_0$ would be far larger than this example. Thus the substantial difficulty in separately estimating both q and N_0 with high precision is indicated.

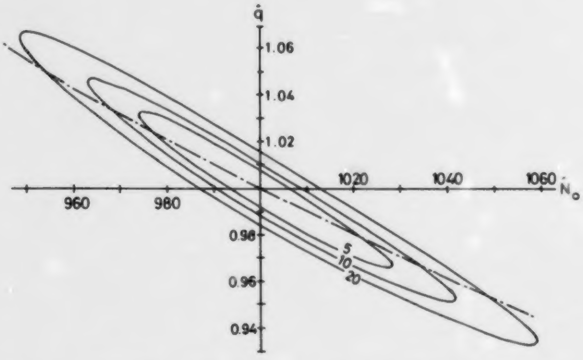

FIG. 1. Response surface of goodness of fit SS on $N_0 - q$ plane. Data in Table 1 are applied. Figures on contour lines; SS values. SS = 0 at the true values of $N_0 = 1000$, $q = 1.0$. Chain line; $qN_0 = 1000$.

TABLE 1. Data for calculation of dynamics of a year-class for response surface. $e^{-M} = 0.8$, $q = 1.0$.

Year t	0	1	2	3	4	5	6	7	Mean
X_t	0.2	0.3	0.2	0.1	0.1	0.1	0.2	0.2	
N_t	1000	640	358.4	229.38	165.15	118.91	85.61	54.79	
C_t	200	192	71.68	22.94	16.52	11.89	17.12	10.96	67.9

It should be noted that for the two sets of parameter values given above, ($\hat{q} \times \hat{N}_0$) is very close to 1000. Thus, estimation by this model would provide fairly precise estimates of (qN_0), but separation of this value into the individual parameters would be difficult. The response surface in Fig. 1 is a trough roughly oriented along the line $\hat{q} = 1000/\hat{N}_0$, shown by a broken line in the figure. The reason for this orientation is the original assumption in (1) that $C_t = qX_tN_t$. As C_t and X_t are observed values, $\hat{q}$ and $\hat{N}_t$ must jointly take values which satisfy $\hat{q}\hat{N}_t = C_t/X_t$ as closely as possible. This means that doubling $\hat{q}$ while halving $\hat{N}_t$ will produce no change in the goodness of fit. Because the level of $\hat{N}_t$ is determined by $\hat{N}_0$, the goodness of fit tends to be constant as long as the product ($\hat{q}\hat{N}_0$) remain fixed.

If $\hat{N}_t$ is proportional to $\hat{N}_0$, ($\hat{q}\hat{N}_t$) is also proportional to ($\hat{q}\hat{N}_0$) and ($\hat{q}\hat{N}_0$) = 1000. The trough of the response surface shows a slight deviation from the curve of $\hat{q} = 1000/\hat{N}_0$. This is caused by an effect of fishing which makes $\hat{N}_t$ not proportional to $\hat{N}_0$. For instance, halving of $\hat{N}_0$ causes a decrease of $\hat{N}_t$ to less than a half because C_t is kept invariable. When fishing intensity is high in comparison with natural mortality, the cumulative catch approaches N_0 and separation of N_0 and q becomes possible. The geometric reflection of this fact is that the response ellipse tends to become rounder when fishing intensity increases, reflecting the enhanced ability to separately estimate N_0 and q.

Unknown Natural Mortality

So far, N_0 and q have been estimated under the condition that the true survivorship is known. We now consider the general case where all three of the parameters are unknown. From (1) it is evident that knowledge of X_t and $\hat{q}$ are not needed to calculate $\hat{N}_t$, and that estimates of s and N_0 only are required. Values of X_t and $\hat{q}$ are, however, required when C_t is calculated from $\hat{N}_t$. Thus, when $\hat{N}_0$ and $\hat{s}$ are given, $\hat{q}$ for the minimum SS of (2) is obtained by the ordinary least squares technique. Putting

$$-\frac{1}{2}\frac{\partial SS}{\partial q} = \Sigma\,(C_t - \hat{q}X_t\hat{N}_t)X_t\hat{N}_t = 0$$

then

$$\hat{q} = \Sigma\, C_tX_t\hat{N}_t / \Sigma\,(X_t\hat{N}_t)^2 \tag{3}$$

Substituting this $\hat{q}$ into (2)

$$SS = \Sigma\, C_t^2 - (\Sigma\, C_tX_t\hat{N}_t)^2/\Sigma\,(X_t\hat{N}_t)^2 \tag{4}$$

In drawing the response surface, it should be noted that among the three unknown parameters, independent parameters are only $\hat{N}_0$ and $\hat{s}$ and hence two-dimensional illustration is possible. Contour lines of SS are drawn with $\hat{s}$ on the abscissa and $\hat{N}_0$ on the ordinate (Fig. 2). The contour for SS = 5.0 shows an elongated but slightly bent ellipse, and the value of $\hat{q}$ has the relation $\hat{q}\hat{N}_0 = 1000$ on the broken line in the figure. The contour surface in three dimensional space of $\hat{N}_0$, $\hat{q}$, and $\hat{s}$ is an ellipsoid. The section through the ellipsoid cut at $\hat{s} = 0.80$ (the true value) corresponds to Fig. 1.

An elongated ellipsoidal contour indicates difficulty in estimating N_0 (or q) and s separately, since a large $\hat{s}$ with a small $\hat{N}_0$, (or conversely), will give similar SS values. This is also evident from model (1). From (1)

$$N_{t+1}/N_t = (1 - qX_t)s$$

As N_t is proportional to catch per unit effort

$$(C_{t+1}/X_{t+1})/(C_t/X_t) = (1 - qX_t)s \tag{5}$$

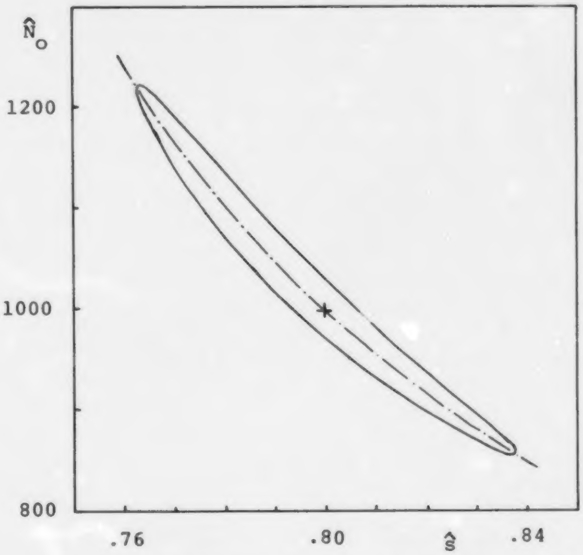

FIG. 2. Contour line of SS = 5.0 of response surface on $\hat{s} - \hat{N}_0$ plane. On chain line, $\hat{q}\hat{N}_0 = 1000$.

The left-hand side of (5) is an observed value, with which estimated values of q and s should be consistent. This implies that the goodness of fit would change very little if a high fishing mortality associated with a high value of $\hat{q}$ is coupled with a low natural mortality (i.e., a high $\hat{s}$ value). As a result the estimated total survival rate remains essentially constant. For example, in Fig. 2 the SS value is only 5.0 when $\hat{s} = 0.73$ and $\hat{N} = 1215$ ($\hat{q} = 0.824$), or when $\hat{s} = 0.837$ and $\hat{N}_0 = 860$ ($\hat{q} = 1.162$). In comparison with Fig. 1, where $\hat{s}$ is known, the ellipse becomes further elongated and the range of plausible $\hat{N}_0$ or $\hat{q}$ values is extended.

Figure 2 also provides some information on the effect of error in an observed value of $\hat{s}$. When the true value of $s = 0.8$ is given exactly, the minimum is obtained at $\hat{N}_0 = 1000$ and $\hat{q} = 1.0$, the correct values. A 1% smaller value of $\hat{s}$ (0.792) will give $\hat{N}_0 = 1040$ or about a 4% overestimation. Conversely, a 1% larger $\hat{s}$ value ($\hat{s} = 0.808$) will result in $\hat{N}_0 = 965$ or about a 3.5% underestimation. Thus any error in specifying $\hat{s}$ will be amplified several fold in estimating N_0 or q. This clearly indicates the need for a high degree of accuracy in estimating the natural mortality rate, a task usually difficult to achieve.

Recruitment $\hat{N}_0$ known

From the above arguments it is to be expected that error in initially specifying a value for $\hat{N}_0$ would have relatively little subsequent influence on the estimation of s. In Fig. 2, $\hat{N}_0 = 1010$ corresponds with $\hat{s} = 0.798$ and $\hat{N}_0 = 990$ corresponds with $\hat{s} = 0.802$. That is, an error of 1% in $\hat{N}_0$ would introduce an error of only 0.25% in $\hat{s}$.

A section through the three dimensional ellipsoid parallel to the $\hat{s}$-$\hat{q}$ plane and centered at $\hat{N}_0 = 1000$ is shown in Fig. 3, along with the contour $SS = 5.0$. The contour is elliptical because as $\hat{s}$ becomes larger more fish survive from a given $\hat{N}_0$ level, and thus a smaller $\hat{q}$ is required to achieve a given level of catch. However, the relative change in the total number of survivors $\hat{N}$, due to the change in $\hat{s}$ is different depending on the age being larger in higher age-groups. The linkage of $\hat{s}$ and $\hat{q}$ is therefore weaker than that of $\hat{q}$ and $\hat{N}_0$ (Fig. 1), and the ellipse is rounder.

Separate estimation of q and s under the condition of known $\hat{N}_0$ value will therefore generally be easier than the separate estimation of N_0 and q when $\hat{s}$ is known. That is, in estimating population parameters, estimating $\hat{N}_0$ first and then calculating $\hat{s}$ may provide better results than the reverse. Similar arguments can be applied to the case where $\hat{q}$, instead of $\hat{N}_0$, is known. If a good estimate of q is available, it is possible to estimate N_0 and s with corresponding accuracy. In this case, however, estimation of q independent of estimates of the population level, for instance from studies on the catchability of a particular gear type, is usually very difficult.

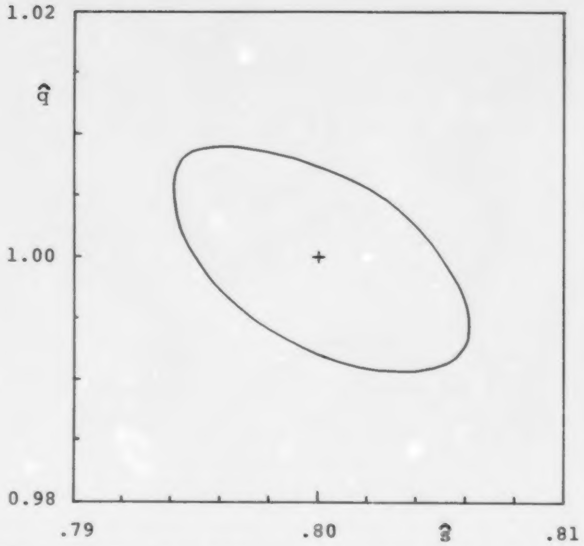

FIG. 3. Contour line of SS = 5.0 of response surface on $\hat{s} - \hat{q}$ plane. SS = 0 at $\hat{s} = 0.8$, $\hat{q} = 1.0$. $\hat{N}_0 = 1000$.

Considerations of Some Effects of Age-Dependent Natural Mortality

For many kinds of animals it is known that natural mortality is age-dependent, being highest in the young and old stages. Among fishes, the high mortality during larval and juvenile stages is well known (e.g., May 1974) but evidence of high mortality due to senescence is scarce (Ricker 1975). Nevertheless, it is quite possible that natural mortality increases as an animal ages. For modeling purposes natural mortality is usually assumed to be age-independent. Possible biases due to the assumption of constant natural mortality will be considered here.

A schedule of age-dependent survival rates (s_t), where natural mortality alone is operating, and the natural mortality coefficient M_t is arbitrarily assumed to increase approximately exponentially from age 1 to age 7 is provided in Table 2. For this series the average survival rate according to Heincke's formula (Ricker 1975) is

$$\sum_{t=1}^{7} N_t \;/\; \sum_{t=0}^{7} N_t = 0.754$$

and would provide somewhat comparable survival pattern with Table 1. For annual changes of fishing effort, X_t, two patterns are considered: decreasing effort (Table 2A) and increasing effort (Table 2B). For each case the

TABLE 2. Data for calculation of response surface for dynamics of a year-class with age-dependent natural mortality.

Year t	0	1	2	3	4	5	6	7
s_t	0.85	0.85	0.81	0.75	0.68	0.59	0.49	0.37
(A) decreasing fishing effort								
X_t	0.3	0.3	0.3	0.2	0.2	0.1	0.1	0.1
N_t	1000	595	354.03	200.73	120.44	65.52	34.79	15.34
C_t	300	178.5	106.21	40.15	24.09	6.55	3.48	1.53
(B) increasing fishing effort								
X_t	0.1	0.1	0.1	0.2	0.2	0.3	0.3	0.3
N_t	1000	765	585.23	426.63	255.98	139.25	57.51	19.73
C_t	100	76.5	58.52	85.33	51.20	41.78	17.25	5.92

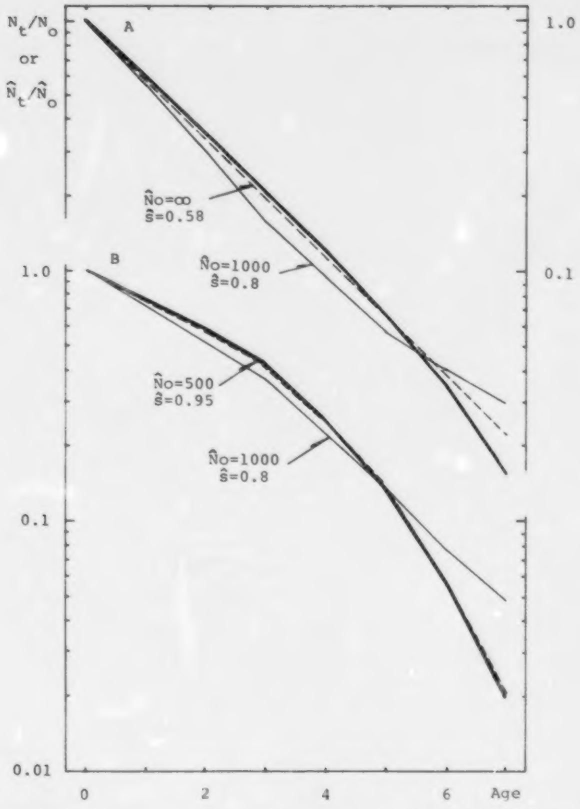

FIG. 4. Decreasing trend of N_t/N_0 with age. (A) decreasing fishing effort, (B) increasing fishing effort. Thick lines; from data in Table 2. Note logarithmic scale.

corresponding N_t and C_t values are also provided. Catchability is simply set to $q = 1.0$.

In Fig. 4 values of N_t/N_0 corresponding to the survivorships in Table 2 are illustrated with thick lines. A and B in the figure correspond to data sets A and B in Table 2. Both thick lines are convex-upward. This trend is accentuated in Fig. 4B where effort increases with time, because the effect on survivorship of increasing both natural mortality and fishing mortality is additive. In Fig. 4A the effects of increasing the natural mortality rate with age and the effect of decreasing the fishing mortality with time are cancelling each other and in this example the curve is only slightly convex. Values of $\hat{N}_t/\hat{N}_0$ for $\hat{N}_0 = 1000$ and $\hat{s} = 0.8$ are shown with thin lines. As $\hat{s}$ is constant regardless of age, the shape of this curve depends on the pattern of fishing effort, being concave-up when fishing effort decreases with time, and concave-down when fishing effort increases.

When fishing effort is decreasing (Fig. 4A), curves with constant $\hat{s}$ are concave, and the SS gets smaller as the degree of concavity decreases. The curve becomes a straight line when $\hat{N}_0$ increases infinitely and the effect of fishing disappears. In such a case the SS value decreases monotonously with increase of $\hat{N}_0$ and estimation of N_0 is not possible. Even when it is possible, the estimate of N_0 may be biased upward, and the estimate of s, downward. A curve of $\hat{N}_t/\hat{N}_0$, where the parameters are chosen as $\hat{N}_0 = \infty$ ($\hat{q} = 0$) and $\hat{s} = 0.58$ is shown by the broken line in Fig. 4A. The curve fits the data from Table 2A quite closely.

In order to trace the age-dependent trend in the data when fishing effort is increasing (Fig. 4B), the effect of increasing fishing is given more emphasis in the minimizing process than natural mortality, which is assumed to be constant. The bias is downward for N_0 and upward for s in this case. The broken line in Fig. 4B illustrates $\hat{N}_t/\hat{N}_0$ for $\hat{N}_0 = 500$ and $\hat{s} = 0.95$. Again, the line fits the data very well. It should be noted that bias is dependent upon the pattern of yearly changes in fishing effort.

In this example, only natural mortality is assumed to be age-dependent and q is assumed constant after recruitment. It is possible, however, that the value of q or selectivity also depends upon age, possibly owing to factors such as a change in availability with age. In such cases the separate estimation of age-dependent natural mortality and selectivity is impossible with data for a single cohort.

Usually one can expect to partition year effects, age effects, and year-class effects by the technique of multicohort analysis if catch-at-age data are available for a fairly long period and for a fairly large number of age-classes. Satisfactory results can be obtained, particularly when fluctuations in fishing effort and year-class strength are large and occur rather randomly. However, separation of age-dependent natural mortality and selectivity is not possible because both are functions of age. In such a case it may be better to conduct calculations on the basis of either constant natural mortality or constant selectivity, regardless of age. Effects of these false assumptions on estimations of year effect and year-class effect would not usually be serious, but it should be noted that in such situations individual estimates of natural mortality and/or selectivity will have little meaning.

Discussion and Conclusion

Problems in estimating recruitment, N_0, the catchability coefficient, q, and the natural mortality coefficient, M (or equivalently, the survival rate $s = e^{-M}$) using data on fishing effort X_t and catch C_t of a year-class are considered by examining the shape of the goodness of fit response surface. Numerical examples are also presented using a simple model.

A close linkage between estimates of N_0 (or q) and s is observed. Also $\hat{N}_0$ and $\hat{q}$ show a high correlation. These correlations originate from the population model. For instance correlation between $\hat{N}_0$ and $\hat{q}$ is introduced by the model $C_t/X_t = qN_t$ where C_t/X_t or the catch per unit effort is an observed value.

The linkage between $\hat{N}_0$ (or $\hat{q}$) and $\hat{s}$ does not disturb estimation of total mortality Z because e^{-z} is obtained directly from the ratio of the catches per unit effort for two consecutive years. On the contrary, assessment by yield per recruit curve on whether a population is overfished or not would be seriously affected. If both $\hat{q}$ and $\hat{s}$ are overestimated, the fishing coefficient which provides MSY is underestimated and the population condition tends to be judged as overfishing. Small $\hat{q}$ and $\hat{s}$ values, on the other hand, tend to give an optimistic conclusion.

A similar argument could be applied to a problem in which the logistic model or similar model is fitted to a time series data of the catch per unit effort of a stock. Population abundance, fishing intensity and productivity of the stock may be considered to correspond to $\hat{N}$, $\hat{q}$, and $\hat{s}$ in this paper, respectively. The estimate of population level for MSY may be unreliable in absolute value whereas the estimate of sustainable yield at present population level may be quite robust.

One interesting feature suggested by this analysis is that any misspecification error in the input value of $\hat{s}$ is amplified several fold in the estimation of N_0, but that of $\hat{N}_0$ is reduced considerably in the estimate of s. Any information on the population abundance from sources other than the catch and effort data would enhance the reliability of the estimate of s.

If the population model assumed for the estimation is different from the actual situation, serious error may be introduced into the estimates of population parameters. One example is given for a case where natural mortality is age-dependent but is assumed to be constant. Assuming a natural mortality rate which increases with age leads to biases that depend upon the way in which fishing effort changes with time. $\hat{N}_0$ is overestimated (and $\hat{s}$ underestimated) when fishing effort increases with time. A decreasing fishing effort causes biases in the opposite direction. Often the catchability coefficient q is assumed to be constant. However it is quite possible that q is actually variable according to, say, age or population abundance. Separate estimation of age-dependent selectivity and natural mortality is not possible in practice. In order to estimate the age-dependent natural mortality, elimination of age-dependent selectivity or practicing of random sampling would be necessary.

Conclusions obtained from the model used in this paper seem to be features common in various other models. Therefore they are expected to provide useful suggestions in estimations of population parameters. However, examples studied here are very specific and any generalization of the conclusions needs to be assessed for the particular situation.

References

INTERNATIONAL WHALING COMMISSION. 1985. Report of the sub-committee on Southern Hemisphere minke whales. Rep. Int. Whaling Comm. 35: 75–89.

MAY, R. C. 1974. Larval mortality in marine fishes and the critical period concept, p.3–19. *In* J. H. S. Blaxter [ed.] The early life history of fish.

RICKER, W. E. 1975. Computation and interpretation of biological statistics of fish populations. Bull. Fish. Res. Board Can. 191: 382 p.

SAKURAMOTO, K., AND S. TANAKA. 1985. A new multi-cohort method for estimating Southern Hemisphere minke whale populations. Rep. Int. Whaling Comm. 35: 261–271.

1986. Further development on an assessment technique for Southern Hemisphere minke whale populations using a multi-cohort method. Rep. Int. Whaling Comm. 36: 207–212.

SHIRAKIHARA, K., AND S. TANAKA. 1983. An alternative length-specific model and population assessment for the western North Pacific sperm whales. Rep. Int. Whaling Comm. 33: 287–294.

1984. Simulation studies on length-specific population assessment techniques for western North Pacific sperm whales. Rep. Int. Whaling Comm. 34: 259–264.

1985. Further simulation studies on length-specific population assessment techniques for western North Pacific sperm whales. Rep. Int. Whaling Comm. 35: 199–203.

TANAKA, S. 1983. Dynamics model of male sperm whales for generalised selectivity. Rep. Int. Whaling Comm. 33: 723–724.

Errors in the Stock Assessment of the Japanese Sardine *(Sardinops melanosticta)* Using the Line-Transect Method

Ichiro Hara

Tokai Regional Fisheries Research Laboratory,
Kachidoki, Chuo-ku, Tokyo, 104 Japan

Abstract

HARA, I. 1989. Errors in the stock assessment of the Japanese sardine *(Sardinops melanosticta)* using the line-transect method, p. 43–50. *In* R. J. Beamish and G. A. McFarlane [ed.] Effects of ocean variability on recruitment and an evaluation of parameters used in stock assessment models. Can. Spec. Publ. Fish. Aquat. Sci. 108.

The author developed a line transect method to assess stock size of Japanese sardine, *Sardinops melanosticta*, in the southeastern waters off Hokkaido. Estimates by the method are compared with the outputs from acoustic surveys which provide two parameters including number of fish schools transected by ships and length across the horizontal dimension of the schools in the cruise plane. The length of a school indicates the density on area per square mile, or percentage of area covered by fish schools. This technique is called a line intercept method, one of the line transect methods.

In the surveyed area, sardine schools can be sighted and counted easily, making the direct counting very advantageous. Thus a strip transect method was applied to estimate density of schools. Biases due to unsatisfied assumptions are discussed together with random errors. A comparison of density estimated by duplicating the same transect line showed differences in the behavior of the fish such as movement of schools.

Résumé

HARA, I. 1989. Errors in the stock assessment of the Japanese sardine *(Sardinops melanosticta)* using the line-transect method, p. 43–50. *In* R. J. Beamish and G. A. McFarlane [ed.] Effects of ocean variability on recruitment and an evaluation of parameters used in stock assessment models. Can. Spec. Publ. Fish. Aquat. Sci. 108.

L'auteur a élaboré une méthode de transect linéaire afin d'évaluer la taille du stock de sardine du Japon, *Sardinops melanosticta*, dans les eaux du sud-est au large d'Hokkaido. Les estimations obtenues par la méthode sont comparées aux résultats des prospections acoustiques qui fournissent deux paramètres dont le nombre de bancs de poissons qui sont coupés par la route des navires et la longueur à l'horizontale des bancs vue de l'avion. La longueur d'un banc est une indication de la densité en surface par mille carré, ou le pourcentage de la superficie couverte par des bancs de poisson. Cette technique est désignée sous le nom de méthode d'interception linéaire, une des méthodes de transect linéaire.

Dans la zone étudiée, les bancs de sardine peuvent être observés et dénombrés facilement, ce qui rend le dénombrement direct très avantageux. On a donc utilisé une méthode de transect par bande pour évaluer la densité des bancs. Les erreurs attribuables à des hypothèses non satisfaisantes sont étudiées avec les erreurs aléatoires. Une comparaison de la densité évaluée par reproduction de la même ligne de déplacement a montré des différences de comportement du poisson comme le déplacement des bancs.

Introduction

Development of a rapid and direct method for assessing stock abundance is one of the most important subjects of fish population studies. There are many kinds of methods to assess stock abundance in the sea, and they can be classified into three types: (1) count all the fish of a particular species over an entire area, (2) count passage of fish through a given area per unit time, and (3) estimate abundance over an entire area from the density in a portion of that area. I developed acoustic and aerial methods for rapid assessment of stock abundance of the Japanese sardine, *Sardinops melanosticta*, off the southeast coast of Hokkaido (Fig. 1). I discuss the results

---

[1] Present address: Seikai Regional Fisheries Research Laboratory, 49 Kokubu-machi, Nagasaki, 850 Japan.

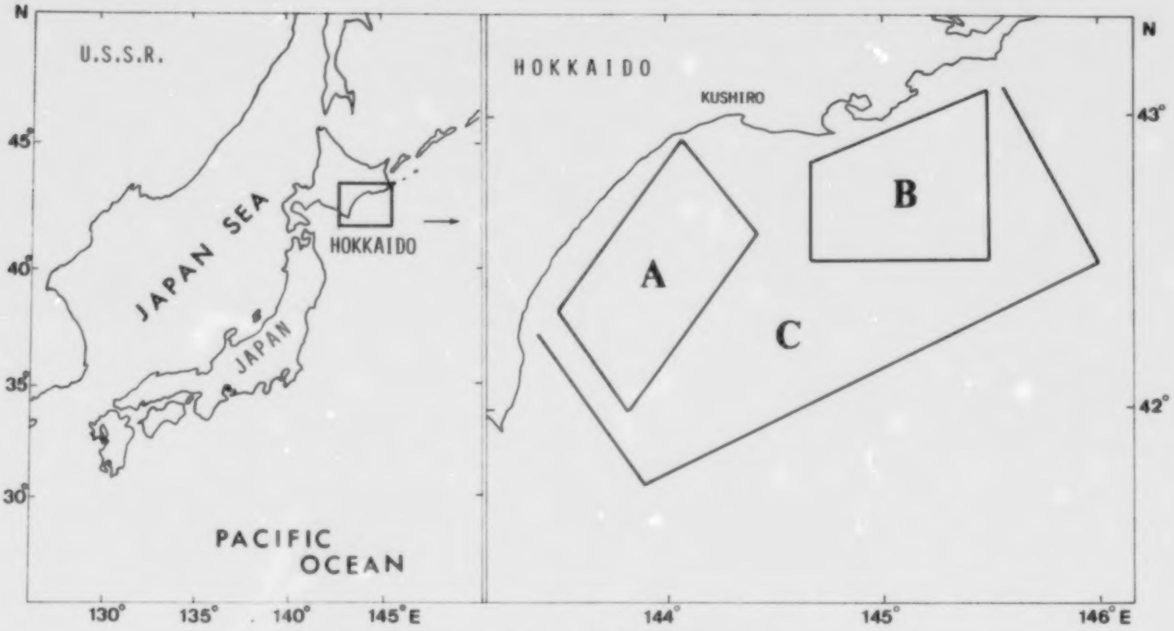

FIG. 1. Locations of the areas which were surveyed.

of these methods and the errors of estimating parameters and densities. I then compare the results of surveying the same transect line at different times of day, and on different days.

The landings of sardines around Japan, which fluctuate with a period of 50–100 years, have remained at approximately 4 million tonnes (t) since 1984 (Fig. 2). Four localized sardine stocks around Japan have been identified, based on unique distributional and migratory patterns. These are the Pacific, Ashizuri, Kyushu, and Japan Sea stocks (Ito 1961). In recent years, landings from the Pacific stock have comprised 60–85% of the total landings in Japan, and reached 3 million t in 1983, a level persisting through 1986. The sardine catch in the area off the southeastern coast of Hokkaido, which is of concern in this paper, exceeded 1 million t in 1983 during the July–October fishery, and comprised about 25% of the total landings from the Pacific stock.

During periods of high stock abundance, sardines expand their range by making a large scale, north–south migration. This migration to the northern waters is not observed by the fishery when abundance is low. Sardines migrate to northern waters off southeastern Hokkaido in summer, during the feeding migration (Kondo 1980). Sardine schools swim in the shallow layer above the thermocline at this time (Hara 1984) and can be sighted and counted easily from the air. They are mostly elongate in horizontal shape and their cruising speeds are 0.4–1.5 knots (Hara 1987). The dimensions of almost all the schools are 100–150 m long and about 15 m wide (Hara 1985a, b).

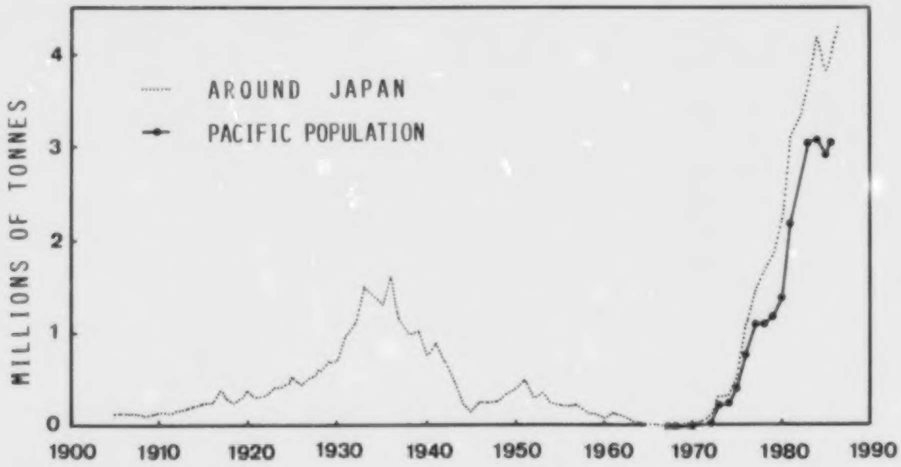

FIG. 2. Annual catch (t) of sardine off Japan, 1905–86.

Survey Methods

Line-Transect Methods

The line-transect method involves an observer moving a distance L, and either counting the number of schools sighted (n) or measuring the size of each school intercepted (l_i). Many methods have been proposed for estimating stock density from the above data. Eberhardt (1978) and Gates (1979) summarized these methods, and classified the line-transect methods into several categories. The methods of estimating sardine school density in this study included two acoustic surveys (step-count and line-intercept) and one acoustic/aerial survey (strip-transect). These survey areas are shown in Fig. 1 and listed in Table 1.

Step-Count Method

There are several shortcomings to the use of an echo-sounder, such as the difficulty of identifying the species, and limitation of data to the area immediately below the ship. In spite of handicaps, an echo-sounder survey is one of the more advantageous methods. We can easily count the number of schools per transect line from an echo-trace, in the case of sardine schools. Then, the relative density index is estimated as follows,

$$I = n/L,$$

where I = relative density index; n = numbers of schools sighted; and L = length of the transect line. I is expressed as numbers of schools per nautical mile. This method only yields relative values, since no information is available on the horizontal extent of the schools. The method is useful as a preliminary survey where data precision is not essential, because it is quick and easy.

Line-Intercept Method

The line-intercept has been used by plant ecologists for many years. This method is applicable to locating objects intercepted along a transect line (Eberhardt 1978). Sardines, which form large schools (Hara 1985a), satisfy these conditions. An observer moves along a distance L, and measures the size (l_i) of schools intercepted (Fig. 3). In cases where the shape of schools is arbitrarily determined, we obtain the unbiased estimate (Lucas and Seber 1977; Gates 1979),

$$P = \sum_i l_i / L,$$

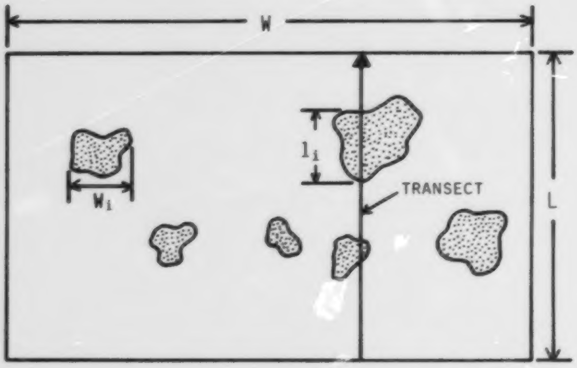

Eberhardt(1978)

FIG. 3. Hypothetical set-up used in line-intercept method. (Shaded areas represent fish schools.)

TABLE 1. List of areas surveyed. A, B, and C indicate the areas shown in Fig. 1.

Time	Echo-sounder	Sonar	Aircraft	Remarks
1984				
29 July–3 Aug.	C			Fig. 8
7–14 Aug.	C			Fig. 8
19 Sept.			C	
20 Sept.			part	bad weather
21 Sept.			part	experiment
22 Sept.			C	
23 Sept.			C	
1985				
21–26 July		C		
29 July–1 Aug.		A		
4–7 Aug.		C		
28 Sept.			A & B	
29 Sept.			A & B	
4 Oct.			C	
6 Oct.			C	
9 Oct.			part	experiment
1986				
15–18 July	C			
20–21 July	B	B		
22–23 July	B	B		
26–27 July	A	A		
18–20 Aug.	A	A		
26–27 Aug.	B	B		

where P = the proportion of the area covered by schools, or is expressed as the area of the schools per square nautical mile. P is estimated from the information on l_i taken from the school images on the echograms. Thus we can estimate the two-dimensional measure of P using the measurement of a one-dimensional quantity (l_i). This density estimate indicates the schools/area per square mile, or percentage of area covered by schools. Thus it can be used for assessment of horizontally distributed stocks.

Strip-Transect Method

For the strip-transect method, an observer moves a distance L, and counts the number of schools sighted (n). For all schools sighted within a given distance from the observer, school density is estimated (Eberhardt 1978 and Gates 1979), as follows,

$$D = n/2LW,$$

where D = number of schools per square nautical mile; n = number of schools sighted; L = length (miles) of the transect line; and W = the average distance under observation to the right or left of the transect line, (half of the swath). Generally, the probability of sighting a school is expressed as a function of the distance between the observer and the target, because visibility of the target varies inversely with distance from the observer. Both horizontal-scanning sonar and light aircraft were used for counting schools on the condition that the probability of sighting within W is unity. In this analysis, the horizontal dimensions of all schools were fixed at 100–150 m × 15 m. Thus the estimate of school density (D) is expressed as number of schools per square mile. Furthermore, we can estimate the standing crop from the school density, school size, and school weight.

Results

Echo-Sounder Surveys

Results of the 1986 step-count and line-intercept methods are shown in Table 2. The echo-sounder surveys were taken at ship's speed of 10 knots. Densities are expressed as number of schools per nautical mile in the step-count, and percent of area covered in the line-intercept method. Densities ranged from 1.2 to 3.5 schools/mile for the step-counts and 2.7–5.7% for the line intercepts. Both methods exhibited small variation in estimates.

TABLE 2. Estimates of density by echo-sounder.

Time	No. of schools	Distance (miles)	Density: Step-count (No./mile)	Density: Line-intercept (% of cove)
1986				
15-18 July	1413	478	3.0	4.8
20–21 July	383	193	2.0	5.7
22–23 July	231	193	1.2	2.7
26–27 July	856	242	3.5	5.4
18–20 Aug.	293	242	1.2	3.5
26–27 Aug.	394	215	1.8	3.4

Scanning Sonar Surveys

Table 3 shows the 1985 and 1986 results of the strip-transect surveys, which employed scanning sonar at a speed of 10 knots. Counts on the sonar image were taken at a range of 400 m and an angle of depression between 0 to 5 degrees. Stock densities ranged from 6.3 to 36.4 schools/square mile, a sixfold variation with respect to survey time and area. In 1986, the sonar survey was conducted concurrently with the echo-sounder surveys shown in Table 2.

TABLE 3. Estimates of density by sonar.

Time	No. of schools	Distance (miles)	Density (schools/mile^2)
1985			
21–26 July	1541	242	14.7
29 July–1 Aug.	3517	364	22.4
4–7 Aug.	1231	319	8.9
1986			
20–21 July	2027	193	24.3
22–23 July	939	193	11.3
26–27 July	3807	242	36.4
18–20 Aug.	659	242	6.3
26–27 Aug.	1494	215	16.1

Aerial Surveys

The 1984 and 1985 aerial surveys were performed, during daylight hours, at the altitude of 500 m, a speed of 103–113 knots, and during calm sea conditions. Participants were two spotter-pilots and the author. In this survey, the strip-transect method was employed. Estimated width of the counting strips was 839 m, on each side of the aircraft. Results are shown in Table 4. The low estimate (0.3 schools/square mile) on 20 September 1984 was caused by bad weather, encountered mid-way in the survey, which made the sea rough and dark. As a result, visibility of schools was substantially reduced. Otherwise, density estimates ranged from 3.4 to 16.4 schools/square mile. These estimates were substantially less than those obtained by the scanning-sonar method (6.3–36.4

TABLE 4. Density estimates by aircraft.

Time	No. of schools	Distance (miles)	Density (schools/mile^2)
1984			
19 Sept.	2174	477	5.0
20 Sept.	89	290	0.3
22 Sept.	2811	450	6.9
23 Sept.	1388	445	3.4
1985			
28 Sept.	1267	167	8.4
29 Sept.	1538	270	6.3
4 Oct.	4186	357	12.9
6 Oct.	3452	232	16.4

schools/square mile). However, the two surveys were not conducted concurrently, and such differences in estimates might be due to the timing of surveys and/or location of the transect lines. During the aerial observations, schools could not be sighted when they were in deep water. Sonar may be better than an aerial survey, because of the focusing of the sound wave, which gives a 3-dimensional effect to aid in counting. However, there are several handicaps to sonar counting, such as overlooking schools due to eye strain from prolonged observations, and distinguishing schools from "noise". This will be discussed later when echo-sounder and sonar are compared.

Duplicating Surveys

To measure counting errors, surveys were conducted on the same transect line by ship or aircraft. The time required for a round trip was several hours by the aircraft, and several days by the ship. A large difference in results between ship and aircraft is recognized. Figure 4 shows the transect lines of the aircraft. During the survey conducted along line *C*, fishing vessels were concentrated inshore off Kushiro, and remained there for 3 wk. Line *C* was one of the transect lines over the fishing ground. The aircraft flew from north to south in the morning, and from south to north in the afternoon.

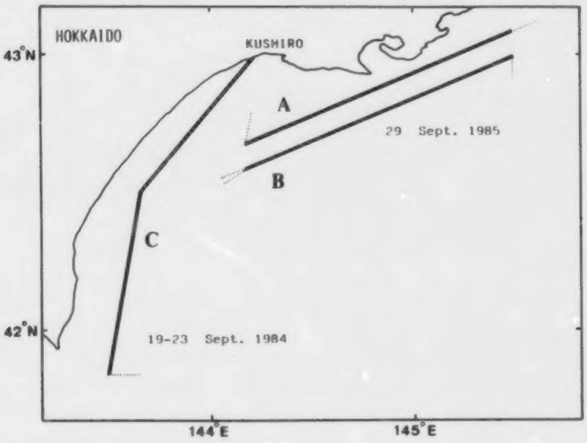

FIG. 4. Transect lines of the aerial surveys.

Results of the daily observations for 19–23 September 1984 are shown in Table 5. The sea was rough on 21 September, and therefore school-counting was inhibited. Density estimates differed between morning and afternoon on 2 successive days. Hara (1985a) offered two explanations. First, the morning schools were stagnant and small, while the afternoon schools were numerous and actively moving north. Second, the reason why the large number of schools were observed is that the schools were continuously recruited along the coast from the southern part of the area to the fishing ground during September, the season of northward feeding migration. There are no data on 21 September and only one set of morning and afternoon observations for the same day. Hence, we cannot conclude that behavior of schools was different at different times. In any case, the density estimates fluctuate with time of day. This may become a serious problem when estimating stock size from aircraft.

TABLE 5. Density estimates by aircraft and sonar (part of the surveys).

Time	No. of schools	Distance (miles)	Density (schools/mile^2)
Aircraft			
1984			
19 Sept. PM	1844	68	29.9
20 Sept. AM	20	68	0.3
22 Sept. PM	1960	67	32.3
23 Sept. AM	958	67	15.8
Sonar			
1986			
20–21 July	2027	193	24.3
22–23 July	939	193	11.3

Results of sonar surveys of 20–21 and 22–23 July 1986 are shown in Fig. 5 and Table 5. It took two days to complete each transit of the transect line, because the ship's speed was slow compared with that of the aircraft. The black dots show the positions occupied by sardine purse seiners during the survey. The fishing grounds were formed in the water mass with temperatures between 13 and 14°C. The grounds expanded towards southeastward, following the same extension of the 14-degree isotherm. As shown in Table 5, the density estimate on the first transit shows a value twice that on the second transit. During 20–21 July, purse seine catches totaled 28 780 t from 112 sets. During 22–23 July, the catch was 25 520 t from 154 sets. CPUE decreased from 257 t/set to 166 t/set. These results suggest that changes in number and density of schools were caused by changes of water mass and affected fishing success.

In order to observe changes over a short time period, two adjacent transect lines (*A* and *B*) were traversed by aircraft on the same day (Fig. 4; Table 6). It took 39–40 min to traverse Line *A* and *B* from west to east, and 33 min from east to west. A strong east wind was blowing during the survey. Observations indicated that sardine schools were moving eastward along the transect line. On the Line *A*, the difference between density values of eastward and westward transits is nearly fourfold. On the

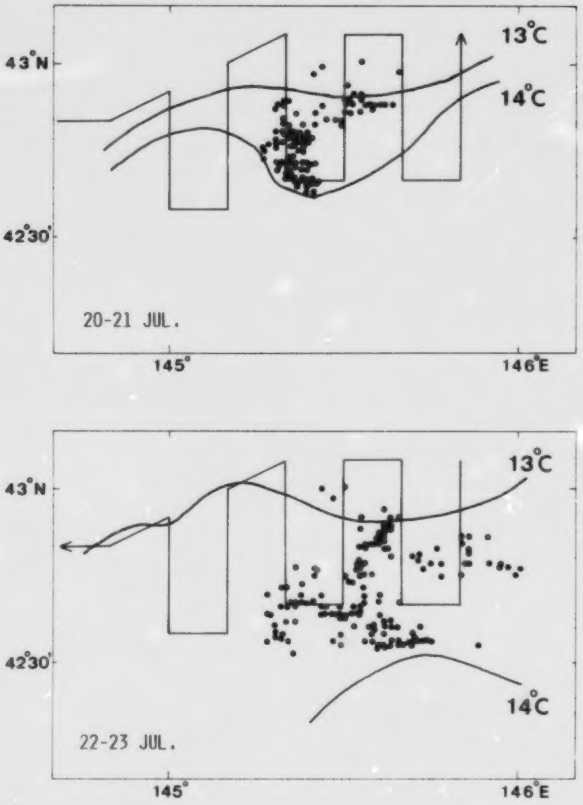

FIG. 5. Transect lines of the sonar surveys completed during July 20–21 and 22–23, 1986. (Dots show the fishing positions by purse seiners.)

Line *B*, the corresponding difference is small. The large difference on the Line *A* was caused by the eastward emigration from the survey area. The small difference on the Line *B* was caused by moving eastward without eastward emigration from the survey area. This is merely a shifting of schools eastward (Hara 1987).

TABLE 6. Results of traversing the same line by aircraft.

Time	No. of schools	Distance (miles)	Density (schools/mile^2)
29 Sept. 1985			
(A) 09:21–10:00	41	71	0.6
12:48–13:21	147	71	2.3
(B) 10:40–11:13	542	71	8.4
12:05–12:45	469	71	7.3

Lines (A) and (B) are parallel to each other and 5 miles apart.

Comparison of Different Methods

Tables 2 and 3 show the simultaneous results of the echo-sounder and sonar observations in 1986. Sonar observations were not undertaken during 15–18 July 1986.

The relationship between the density estimates by the step-count/strip-transect and line-intercept/strip-transect methods is shown in Fig. 6. The coefficient of correlation (*r*) is 0.82, not significant at the 5% level in case of the line-intercept/strip-transect method. The echo-sounder trace might not accurately show the school size, because of mechanical weak points or sound-wave characteristics.

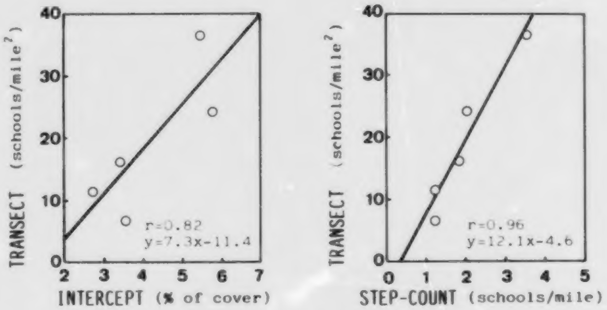

FIG. 6. The relationships among three kinds of methods.

For the comparison of the strip-transect with step-count, $r = 0.96$, significant at the 1% level. The regression slope, estimated from the least squares, is nearly 12. These results suggest that the step-count estimate is satisfactory in this survey area, with respect to relative density.

Errors Affecting Estimates

Four parameters (n, l_i, W, and L) are employed to estimate densities. L can be measured accurately with the modern navigation systems available. With respect to the line surveys, such as step-count and line-intercept methods, the parameters n and l_i are affected by variations in school images on the echo-traces due to variable response to the high- and low-frequency outputs. Occasionally with the echo-sounder, due to difference in frequency, school images do not appear on the echo-trace.

For strip-transects, W is one of the most important parameters. However, underwater range reported by the sonar implies the sound wave is straight horizontally. Unfortunately, this is not always true, and it is difficult to measure the error induced by non-linear sound waves. During aerial surveys, the width of observer's sampling strip depends on the altitude. Figure 7 shows a schematic diagram. The width is measured as follows.

$$W = A\ [\cot(d) - \tan(25)],$$

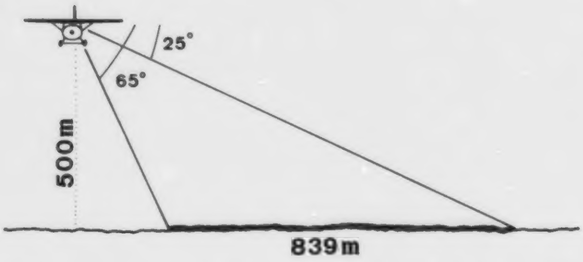

FIG. 7. The effect of flying altitude above sea level on the effective width of sample strip.

where, W = width (swath); A = altitude; and d = angle of depression for sighting the most distant school. W is proportional to A, if d is constant, or proportional to cot (d), if A is constant. Assuming little error in the altimeter, the change of A is small, due to the vertically stable flight over the sea. Thus, W is mostly dependent on d. Table 7 contains examples of the relationship between altitude and angle of depression. For the present surveys, altitude was maintained at 500 m, and the swath (W) at 839 m, since the angle of depression was measured 65-25°.

TABLE 7. Effect of changing altitude above sea level and angle of depression on the strip width (m).

Altitude (m)	Strip width (m) 65-25°	Strip width (m) 65-20°
600	1007	1369
550	923	1255
500	839	1141
450	755	1027
400	671	912

The number of school sightings, n, is related to the detection ability of the observer and/or the echo-sounder or sonar. For direct counting by sonar, or aircraft sightings, there are no automatic recording systems as with the echo-sounder. Thus, observer fatigue may lead to errors in counting or recording the number of schools. Furthermore, not only are schools not always detected on the echo-sounder or sonar, ship wake or other "noise" can produce an "image" on the echo-sounder or sonar screen which might be misinterpreted as a school.

The probability of oversight may increase with the speed of observer's "platform" (Clarke 1986). This may not be as important aboard a ship traveling at 10 knots, as from an aircraft traveling at 100 knots. However, from a relatively high altitude in an aircraft, fish schools appear to be moving slowly, are large, and hence easily detected. School detection from an aircraft is also a function of the distance from the observer, but this function has not been determined yet. A formation flight would probably provide insight.

Probability of Detection

With the line-transect method, the most likely error is oversight, which results in an underestimate of the number of schools. With sonar counting, the angle of depression is set at 0-5 degrees, the same angle used by the commercial purse-seine vessels. Probability of school detection is related to the angle of depression and the draft of the vessel. However, neither factor is important. Figure 8 indicates that the sonar range almost covers the distribution of the sardine schools, and the draft of the 45-t survey vessel was too small to affect school detection, and school interception. I observed from the air that one school did not avoid the approaching small ship. School detection, and counting, on the Braun tube of the sonar is related to the distance from observer to school. At maximum sonar range, a school is merely a point on the screen. Optimum sonar range is probably 50-100 smaller than maximum. Similarly, for aerial surveys, the angle of depression should not be set at the maximum (25° in Fig. 7). These modifications would reduce the probability of overestimating the number of schools caused by counting schools outside the swath or on a boundary.

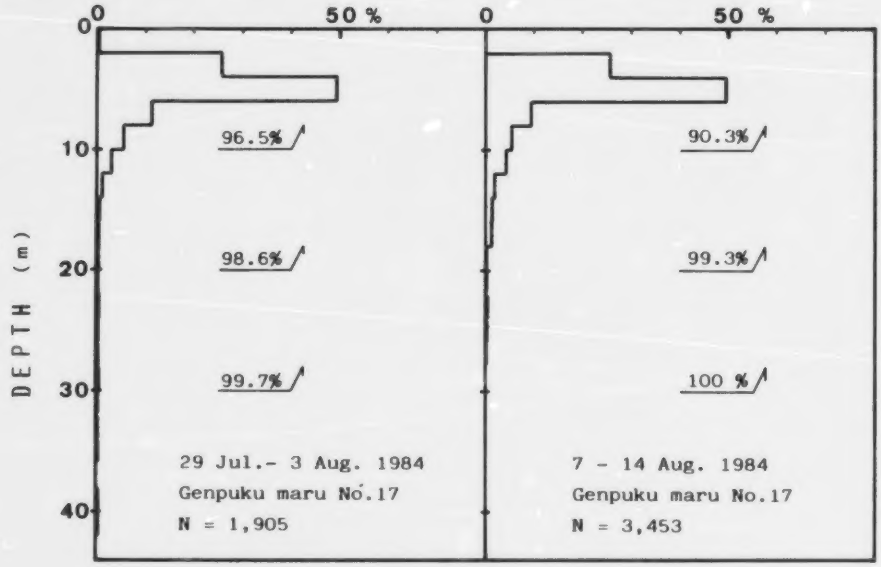

FIG. 8. Frequency distribution of the depth of sardine schools.

With aerial surveys, important factors to be considered are: depth of school, water transparency, and brightness of daylight. Under conditions of good brightness, surveys should be conducted during midday to minimize reflection from the sea surface. More than 90% of sardine schools swim at 0–10 m (Fig. 8), and exhibit little variation among seasons. Of course, this results in an underestimation of numbers of schools, since aerial detection of schools in deeper layers is less effective. No data are available as to the depth limit of school detection from an aircraft. However, we could use aerial surveys as effectual methods, making the depth limit clear.

Discussion

The sardine-school densities estimated by three types of the line-transect method have been described. The results from the step-count, which estimate relative density, are in approximate agreement with the results of the sonar counts. This means that the step-count method, using an echo-sounder, is effective for a relative assessment of the sardine stock. To estimate absolute stock size, several assumptions must be accepted. The line-intercept method demonstrates that two-dimensional measures can be estimated from measurements of one-dimensional data. A two-dimensional density estimate was only shown here, but using three-dimensional line-intercept data, we could assess the density without the data on weight and thickness of schools. In this case, an area of a school transected by ship must be measured precisely, instead of l_i. This method can easily be expressed in mathematical terms, but it is hardly applicable to other cases. Error due to these methods are not well defined, but the methods are useful to measure l_i.

The strip-transect method using aircraft has a tendency to underestimate school density, but it can be used for rapid monitoring. It is difficult to estimate the errors quantitatively without more information about schools.

The sonar survey may be more efficient than the aircraft survey in counting schools, but the aerial survey provides a description of the shape and size of individual schools, as well as their patterns of movement and distribution. Ship surveys have the disadvantage of prolonged duration due to the slow speed of vessel, but provide more diverse information.

It is clear from the replicated surveys that the densities fluctuated with the change of factors, such as immigration, distribution, sea condition and catch. These factors are also important for determining the density of fish in addition to the parameters which are used in the line-transect methods. In order to assess the abundance more accurately, information is required on the behavior of schools in addition to improvements of the accuracy of parameter estimation. Moreover, a stratification of a survey area, which can be made with any combination of environmental or ecological characteristics, may play an important role in stock assessments. It is essential to note that the objective is to obtain more precise estimates for maximizing the variations within each transect line and minimizing the variations between them. It can be said that duplicating acoustic and visual observations is both important and effective in direct stock assessment.

In this study I discussed the results from independent surveys. It is necessary to establish a synchronized system of air and ship-borne observations, or another system to obtain more precise information and to solve the problems described above. It is possible to use the line-transect method for non-pelagic fishes, using a flashing probability as used in whale assessments (Doi 1970, 1971). In the same manner, fish can be assessed using an acoustic method.

References

Clarke, R. 1986. The handbook of ecological monitoring. Clarendon Press, Oxford. 298 p.

Doi, T. 1970. Re-evaluation of population studies by sighting observation of whale. Bull. Tokai Reg. Fish. Res. Lab. No. 63: 1–10.

1971. Further development of sighting theory on whale. Bull. Tokai Reg. Fish. Res. Lab. No. 68: 1–22.

Eberhardt, L. L. 1978. Transect methods for population studies. J. Wildl. Manage. 42: 1–31.

Gates, C. E. 1979. Line transect and related issues. *In* Sampling biological populations. Statistical Ecology Vol. 5 Int. Co-op. Publ. House.

Hara, I. 1984. Distribution and school size of Japanese sardine in the waters off the southeastern coast of Hokkaido on the basis of echo sounder surveys. Bull. Tokai Reg. Fish. Res. Lab. No. 113: 63–74.

1985a. Shape and size of Japanese sardine schools in the waters off southeastern Hokkaido on the basis of acoustic and aerial surveys. Bull. Japan. Soc. Sci. Fish. 51: 41–46.

1985b. Moving direction of Japanese sardine school on the basis of aerial surveys. Bull. Japan. Soc. Sci. Fish. 51: 1939–1945.

1987. Swimming speed of sardine schools on the basis of aerial survey. Bull. Japan. Soc. Sci. Fish. 53: 223–227.

Ito, S. 1961. Fishery biology of the sardine, *Sardinops melanosticta* (T. & S.), in the waters around Japan. Bull. Japan Sea Reg. Fish. Res. Lab. No. 9: 1–227.

Kondo, K. 1980. The recovery of the Japanese sardine — The biological basis of stock-size fluctuations. Rapp. P.-v Réun. Cons. int. Explor. Mer 177: 332–354.

Lucas, H. A., and G. A. F. Seber. 1977. Estimating coverage and particle density using the line intercept method. Biometrika 64: 618–622.

Importance of Environmental Fluctuations in the Management of Pacific Hake *(Merluccius productus)*

R. C. Francis, S. A. Adlerstein[1], and A. Hollowed

Fisheries Research Institute, University of Washington, Seattle, WA 98195, USA

Abstract

FRANCIS, R. C., S. A. ADLERSTEIN, AND A. HOLLOWED. 1989. Importance of environmental fluctuations in the management of Pacific hake (*Merluccius productus*), p. 51–56. *In* R. J. Beamish and G. A. McFarlane [ed.] Effects of ocean variability on recruitment and an evaluation of parameters used in stock assessment models. Can. Spec. Spec. Publ. Fish. Aquat. Sci. 108.

This paper presents Pacific hake (*Merluccius productus*) as a case study to illustrate the importance in fisheries management of incorporating linkages between environment and stock production. Over ranges of stock biomass observed to date, hake recruitment appears to be independent of spawning stock size and strongly correlated with environmental conditions occurring during early life history. These features have been incorporated in a fishery model that is currently used to develop long- and short-term hake management policy.

The analysis of this paper applies a particular form of the model to show how estimates of fishery production vary when alternative representations of the recruitment process and the manner in which it is driven are used. The inclusion of both short- and long-term variability in the recruitment process can have significant impact on the estimation of potential fishery production. Biases can enter the estimation process in all cases. We speculate that the dynamics of many fish resources of the north Pacific are strongly related to large-scale climate/ocean processes that appear to exhibit periodic fluctuations.

Résumé

FRANCIS, R. C., S. A. ADLERSTEIN, AND A. HOLLOWED. 1989. Importance of environmental fluctuations in the management of Pacific hake (*Merluccius productus*), p. 51–56. *In* R. J. Beamish and G. A. McFarlane [ed.] Effects of ocean variability on recruitment and an evaluation of parameters used in stock assessment models. Can. Spec. Publ. Fish. Aquat. Sci. 108.

Le présent document présente le merlu du Pacifique (*Merluccius productus*) comme une étude de cas pour illustrer l'importance au niveau de la gestion des pêches de l'introduction de liens entre l'environnement et la production du stock. En ce qui concerne les plages de biomasse du stock étudiées jusqu'à maintenant, le recrutement du merlu semble être indépendant de la taille du stock de géniteurs et présenter une forte corrélation avec les conditions du milieu au début de son cycle vital. Ces caractéristiques ont été introduites dans un modèle de pêcherie couramment utilisé pour l'élaboration d'une politique de gestion du merlu à long et à court terme.

L'analyse effectuée dans le présent document applique une forme particulière du modèle pour montrer comment des estimations de la production d'une pêche varient lorsque l'on utilise d'autres représentations du processus de recrutement et de la façon dont il est effectué. L'inclusion de la variabilité à court et à long terme dans le processus de recrutement peut avoir des répercussions importantes sur l'estimation de la production potentielle de la pêche. Dans tous les cas, des erreurs peuvent se glisser dans le processus d'estimation. Nous émettons l'hypothèse selon laquelle la dynamique de plusieurs ressources halieutiques du Pacifique nord sont fortement liées à des processus climatiques et océaniques de grande envergure qui semblent présenter des variations périodiques.

Introduction

One of the major goals of both the Pacific Fishery Management Council and the North Pacific Fisheries Management Council is to maximize the long-term biological yield from marine fish stocks. In several cases, estimates of long-term yield are based on deterministic equilibrium models (Major and Wilderbuer 1987; Bakkala 1987; Anon. 1987). However, many of these stocks exhibit a high degree of short- and long-term variations that strongly violate steady-state assumptions.

Long-term variability in fish stocks has recently been linked with variation in environmental conditions (Cushing 1982; Sharp 1977; Schuntov and Vasil'kov 1982;

---

[1] Present address: Resource Ecology and Fisheries Management Division, Northwest and Alaska Fisheries Center, NOAA, 7600 Sand Point Way NE, Bldg. 4, Seattle, WA 98115-0070, USA.

Schuntov 1986). Unfortunately, establishing reliable linkages between fish production and environmental variables has been inhibited by the short extent of available time series of recruitment data, lack of testing of a priori hypotheses, and possible measurement errors in the recruitment data (Bakun 1985; Walters and Ludwig 1981; Walters 1985). Because of these problems, environmental mechanisms have rarely been included as factors that influence marine fish production. In this paper, we will explore the consequences of ignoring and misinterpreting the relationship between the environment and fish production when such relationships exist.

One example of a highly variable stock to which environmental factors appear to be the major cause of short- and long-term variability is Pacific hake (*Merluccius productus*).

The offshore stock of Pacific hake supports one of the largest single-species fisheries on the west coast of North America. Since 1966, this stock has been the target of a large fishery off the coasts of both the United States and Canada. The fishery, which runs from April to October, is managed separately in U.S. and Canadian waters. In recent years, the stock appears to have been significantly underexploited in U.S. waters because of a lack of North American markets and the exclusion of Soviet and Polish national fleets. Even under these conditions, the Pacific hake fishery is of interest to both the United States and Canada because of opportunities for joint ventures for domestic fishermen. The stock insures a revenue when other groundfish (e.g., rockfish, flatfish) stocks are depleted or quotas are met.

Over the past 20 years, the fishery has been highly variable, with estimated annual catches ranging 91 000 to 236 000 t. Not only does the fishery fluctuate, but the resource itself exhibits extreme variations in abundance and age composition as a result of variation in year-class strength. This translates into a stock dominated by a small number of strong year-classes, illustrated by the fact that for the past 25 years the fishery has been dominated by just six strong year-classes (Fig. 1).

As is the case with other gadoids, the fluctuation in Pacific hake year-class strength is not closely coupled to the spawning stock size, at least not over the range of stock sizes observed (Fig. 2). Also, like other gadoid species, hake are highly fecund; consequently, small changes in early life-stage survival rates could generate the large variations observed in recruitment. In support of this hypothesis, Bailey et al. (1985) showed post-larval abundance to be related to recruitment to the fishery 3 years later (Fig. 3). Current research points toward conditions in the physical environment around the time of spawning as the major driving variable for hake recruitment (Hollowed and Bailey 1989). Bailey (1981) found recruitment to be inversely correlated to wind driven Ekman transport on the spawning grounds and positively correlated with sea surface temperature (Fig. 4). Years of "cold" water temperatures on the spawning ground are assumed to be years of high offshore transport and low larval survival, and years of "warm" temperatures on the spawning ground are assumed to be years of low offshore transport and higher, although more variable, larval survival.

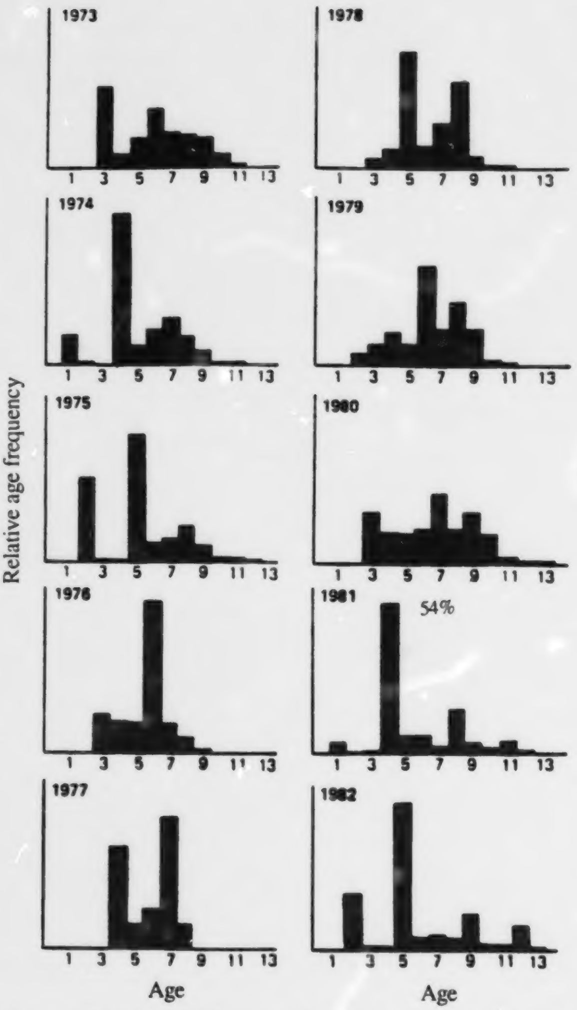

FIG. 1. Relative age-frequency of Pacific hake in U.S. waters, 1973–82.

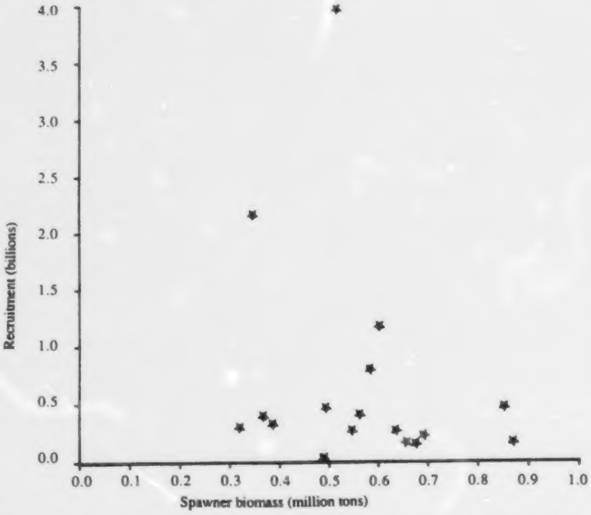

FIG. 2. Recruitment vs. spawner biomass of Pacific hake, 1967–83.

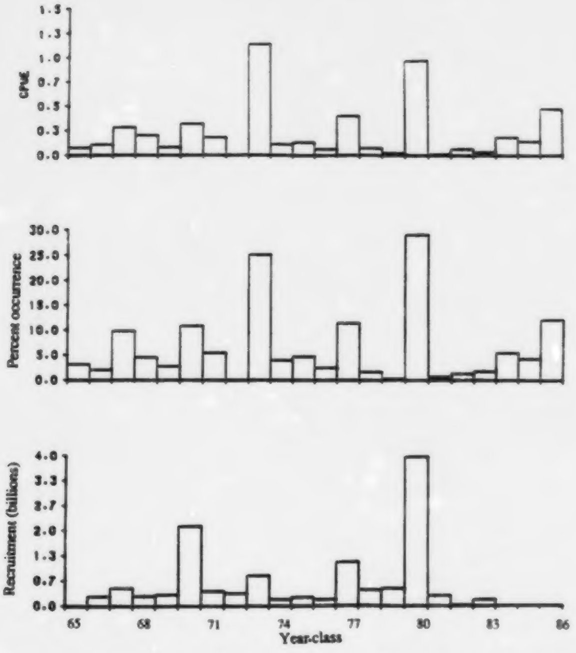

FIG. 3. Indices of 0-age hake abundance (top and middle) and recruitment 3 years later.

Francis (1985) incorporated the above hypothesis about the hake recruitment process, along with other population dynamics aspects, into an age-structured simulation model of the form described by Walters (1969). The model calculates production as a function of recruitment, growth and mortality. This model has been used as a basis for management of both the U.S. and Canadian components of the offshore hake fishery since 1985. It is run under deterministic and stochastic modes for various fishing scenarios and management options to derive long- and short-term potential yields. Long-term production is projected under constant and variable effort options and short-term projections for management options include constant and variable effort, and constant catch.

In the most recent management scenario (Hollowed et al. 1988), an optimal yield algorithm was developed based on projections of long-term average yield with recruitment being driven by a cyclic time series of average sea surface temperature at the time of spawning. Because the observed levels of spawning biomass are restricted to abundance over 0.319 million, and facing the impossibility of predicting the recruitment response at lower population levels, the management policy was developed with the constraint of a minimum allowable spawning biomass. Namely, the spawner biomass was not allowed to drop below the lowest observed value more than 10% of the time for long-term production calculations. Projections of MSY from the hake stock under constant effort were then made by searching the effort that maximizes yield within the constraint on the number of years that the spawner biomass fell below the critical level.

Allowable Biological Catch for any given year was set based upon application of the optimal yield algorithm to short-term (<5 years) stock production projections with

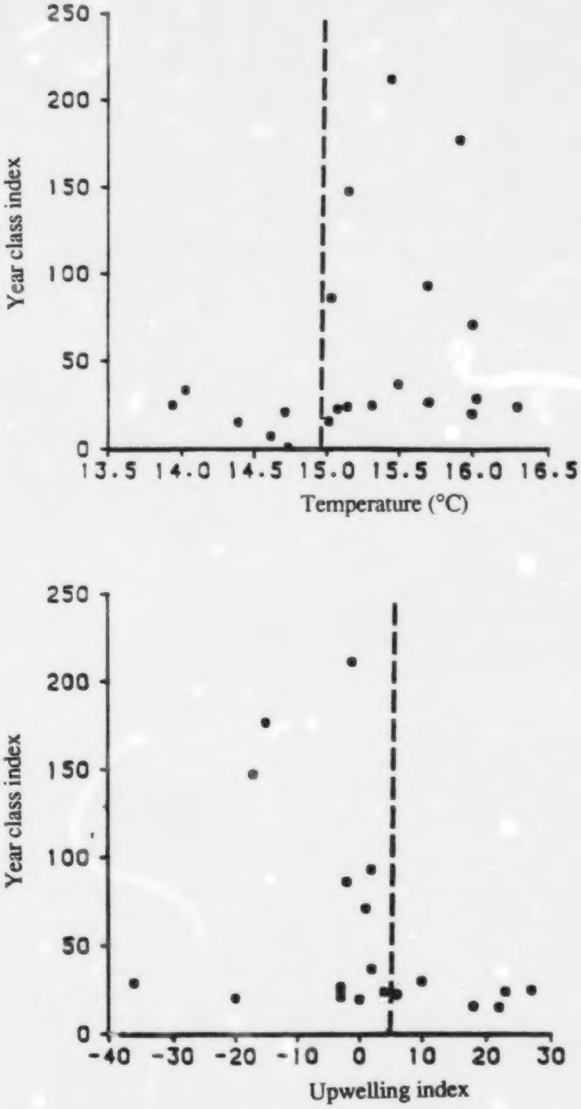

FIG. 4. Year-class index of hake (1960–82) in relationship with upwelling and temperature in the spawning grounds.

recruitment estimated from California Department of Fish and Game 0-age juvenile surveys and National Marine Fisheries Service pre-recruit and adult surveys.

Methods

In this analysis, we used the age-structured simulation model to explore the effect of ignoring or misinterpreting the influence of environmental variability on recruitment and, further, in long-term fishery production projections. In order to illustrate the major points of this paper, which have to do with relative rather than absolute fisheries production, a constant effort management option was employed. The derivation of these parameters is described in Hollowed et al. (1988). Simulation runs were made using both the stochastic and the deterministic versions of the model. For the stochastic option, recruitment at age 3 was incorporated into the model as a log-normal random variable, with mean and coefficient of variation at age 3 under temperature conditions at the time of spawning 3 years earlier. The algorithm for generating log-normal variates of given mean and variances is given by Naylor et al. (1966). For the deterministic option, the coefficients of variation were set to zero.

Three different scenarios were explored in this analysis:

I. *Unexploited population biomass under environmentally driven recruitment*

Recruitment in the simulation model is assumed to be solely a function of temperature at the time of spawning. The model was run under a stochastic and a deterministic recruitment option. Recruitment means under warm and cold conditions were respectively 0.971 billion, CV(R) = 117.9% and 0.206 billion, CV(R) = 76.8%. Recruitment is driven by a time series of average temperatures for the January–March sea surface in the Los Angeles Bight, the approximate center of hake spawning range (Fig. 5).

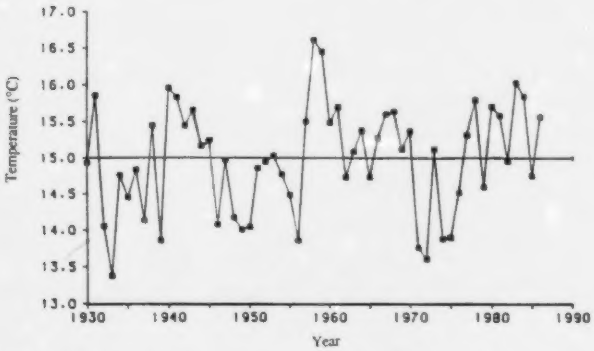

FIG. 5. Sea surface temperature times series from Los Angeles Bight (Mean January–March, 1931–85).

II. *Fisheries production under environmentally driven recruitment*

(a) Recruitment driven by a long temperature time series (1943–82):

Deterministic and stochastic runs of the model were performed under the management policy of constant effort which maximizes long-term catch subject to the constraint that the spawner biomass is allowed to drop below the lowest observed level only 10% of the time. Recruitment is incorporated as in the previous analysis.

(b) Recruitment driven by a short temperature time series dominated by warm temperatures:

Deterministic and stochastic runs were performed, with recruitment being driven by cycling the 1977–86 temperature times series.

(c) Recruitment driven by a short temperature time series dominated by cold temperatures:

One-thousand-year runs were performed, with recruitment being driven by a temperature time series corresponding to a mirror image of the 1977–86 series (i.e., all of the warm years transformed to cold years and vice versa).

III. *Fishery production under constant (environmentally independent) recruitment*

We applied the same management policy of constant effort as that used in the previous analysis. Recruitment was both density and environmentally independent and set at the overall average recruitment from 1960 to 1983 (R = 0.684 billion, CV = 142.1%).

Results and Discussion

Figure 6 shows the results of the two 40-yr simulations of unexploited hake stock biomass, where the temperature time series (also shown) is driving the recruitment process. The first biomass time series is deterministically driven and the second is stochastically driven by the environment. We present this comparison to illustrate the difference in biomass estimates when different types of variability are incorporated in this system. In the first case, the system is driven by what appear to be fairly regular, long-term fluctuations in the environment. In the second case, long-term and short-term variability are confounded. We know that this short-term variability is in the system, but it can only be characterized by its overall magnitude (what Hilborn (1987) refers to as "noise"). The short-term variability seems to amplify the long-term environmentally driven fluctuations.

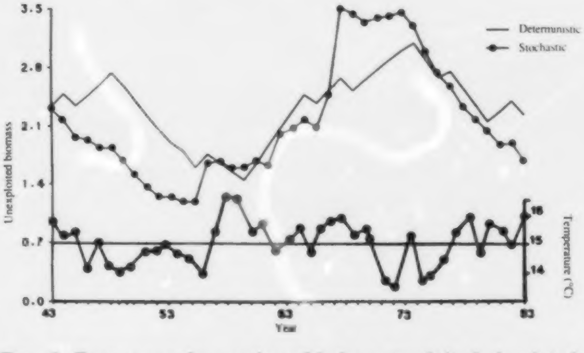

FIG. 6. Forty-year time series of hake unexploited simulated biomass, under a variable recruitment scenario.

Estimates of fisheries production obtained from the various recruitment and environmental scenarios are presented in Table 1. We believe that the variable recruitment scenario, in which the temperature time series from 1943 to 1982 is used under the stochastic option of the model, optimally represents the long-term population dynamics of Pacific hake. This, in fact, is the form of the model presently used to make long-term management decisions. Overestimates and underestimates of long-term average production of the stock can be obtained when the environmental role is considered, but the tempera-

TABLE 1. Summary of the results from the 1000-year runs of the model under a constant effort management policy.

Scenario	Run	$\bar{Y}$ (CV) 1000 t	Effort (F) 1000 days	$\bar{B}$ (CV) 1000 t (i)
Constant recruitment	Det.	254 (0)	35.0	0.575 (0)
	Stoch.	210 (44)	6.7	1.149 (48)
Variable recruitment 1943–82 environmental time series	Det.	185 (29)	6.3	1.048 (31)
	Stoch.	165 (51)	3.9	1.263 (53)
Warm environmental time series	Det.	302 (14)	31.0	0.729 (16)
	Stoch.	272 (45)	10.0	1.193 (51)
Cold environmental time series	Det.	97 (14)	4.0	0.726 (17)
	Stoch.	64 (40)	1.6	0.943 (42)

ture data used to represent environmental fluctuations is incomplete and this is due to the fact that 1960–83 years are used. Overestimates in production are obtained when the link between recruitment and the environment is ignored and recruitment is considered as constant.

To us, the most striking aspect of this analysis is the recognition that a failure to take into account the role of the physical environment in the recruitment process, and incorporate this into long-term fisheries production estimates, can provide results that are misleading to the fishery manager.

We feel that it is of particular importance to note that the large-scale temporal pattern in the environment, hypothesized to drive hake production, is not unique to the California Current or eastern boundary current systems in general. Francis et al. (1987) summarized results linking production dynamics of several important fisheries (walleye pollock, king crab, sockeye salmon) of the Eastern Bering Sea with large-scale environmental dynamics. Figure 7 shows the case of the Bristol Bay sockeye salmon. Hollowed et al. (1987) observed synchrony of extreme year-classes of fish stocks across the entire region of the Northeast Pacific (California Current to Bering Sea), as well as inverse relationships in recruitment between subregions of the Northeast Pacific (e.g., North Pacific groundfish vs. California Current pelagics). Figure 8 presents the environmental time series that are closely related to hake production in the California Current and sockeye salmon production in Bristol Bay. The linkages are quite obvious. The implication is that the major dynamics of many fish resources are strongly related to oceanographic and ecological processes that are large-scale (regional or global), apparently periodic, and climate-driven, and these processes are rarely, if ever, in equilibrium. The hake example presented above demonstrates potential problems associated with stock assessments that fail to incorporate these phenomena when they in fact exist. The challenge is to begin the formidable task of monitoring the climate and the oceans, developing an understanding of their linkages to the production processes of commercially important fish stocks, and using that information to resolve the management problems associated with major changes in food production.

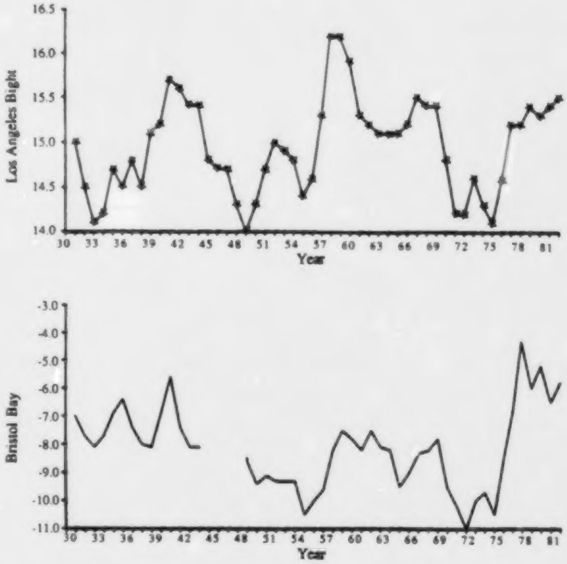

FIG. 7. Ten-year running mean Bristol Bay Nov.–Mar. air temperature and sockeye salmon catches.

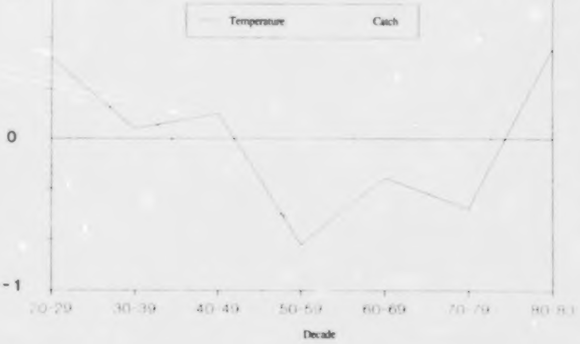

FIG. 8. Three-year running mean Bristol Bay air temperatures and Los Angeles Bight sea surface temperatures during the winter.

References

Anonymous. 1987. Status of the Pacific coast groundfish fishery through 1987 and recommended acceptable biological catches for 1986. Pacific Fisheries Management Council, Metro Center, Suite 420, 2000 SW. First Avenue, Portland, OR 97201.

Bailey, K. M. 1981. Larval transport and recruitment of Pacific hake, *Merluccius productus*. Mar. Ecol. Prog. Ser. 6: 1–9.

Bailey, K. M., R. C. Francis, and K. F. Moss. 1985. Evaluating incidental catches of 0-age Pacific hake to forecast recruitment. CalCOFI Rep. 27: 109–112.

Bakkala, R. G. 1987. Condition of Groundfish Resources of the Eastern Bering Sea and Aleutian Islands Region in 1987. Unpubl. rep., 187 p. Northwest and Alaska Fish. Cent., Natl. Mar. Fish. Serv., NOAA, 7600 Sand Point Way NE, Seattle, WA 98115. (Submitted to the International North Pacific Fisheries Commission in October 1987.)

Bakun, A. 1985. Comparative studies and the recruitment problem: searching for generalizations. Calif. Coop. Oceanic Fish. Invest. Rep. 26: 30–40.

Cushing, D. H. 1982. Climate and fisheries. Academic Press, London. 373 p.

Francis, R. C. 1985. Status of the Pacific hake resource and recommendations for management in 1986. In PFMC, Status of the Pacific Coast Groundfish Fishery and Recommendations for Management in 1986.

Francis, R. C., S. Adlerstein, and R. Brodeur. 1988. Biological basis for management of commercial fishery resources of the eastern Bering Sea, p. 187–209. *In* W. S. Wooster [ed.] Fishery science and management. Lecture notes on coastal and estuarine studies. Vol. 28. Springer-Verlag, New York, NY.

Hilborn, R. 1987. Living with uncertainty in resource management. North Am. J. Fish. Manage. 7: 1–5.

Hollowed, A. B., S. Adlerstein, R. C. Francis, M. Saunders, N. Williamson, and T. Dark. 1988. Status of the Pacific whiting resource in 1987 and recommendations for management in 1988. NOAA Tech. Memo. F/NWC, 50 p.

Hollowed, A. B., and K. M. Bailey. 1989. New perspectives on the relationship between recruitment of Pacific hake (*Merluccius productus*) in the ocean environment, p. 207–220. *In* R. J. Beamish, and G. A. McFarlane [ed.]. 1989. Effects of ocean variability on recruitment and an evaluation of parameters used in stock assessment models. Can. Spec. Publ. Fish. Aquat. Sci. 108.

Hollowed, A. B., K. M. Bailey, and W. S. Wooster. 1987. Patterns in recruitment of marine fishes in the North East Pacific Ocean. Biol. Ocean. 5: 99–131.

Hollowed, A. B., and R. C. Francis. 1986. Status of the Pacific whiting resource and recommendations for management in 1987. NOAA Tech. Memo., NMFS F/NWC-118. 29 p.

Major, R. L., and T. K. Wilderbuer. 1987. Condition of Groundfish Resources of the Gulf of Alaska Region as Assessed in 1987. Document submitted to the annual meeting of the International North Pacific Fisheries Commission, Vancouver, B.C., October 1987. U.S. Dept. Comm., Natl. Mar. Fish. Ser., Northwest and Alaska Fisheries Center, 7600 Sand Point Way NE, BIN C15700, Bldg. 4, Seattle, WA 98115. 228 p.

Naylor, T. H., J. L. Balintly, D. S. Burdik, and K. Chu 1966. Computer simulation techniques. John Wiley & Sons, Inc., New York, NY. 352 p.

Sharp, G. D. 1977. Climate and fisheries: Causes and effect of managing the long and short of it all. S. Afr. J. Mar. Sci. 5: 811–838.

Schuntov, V. P. 1986. The present state of knowledge on long-term cyclical fluctuations in the abundance of fish in seas of the Far East. (Translated from Biologiya Marya 3: 3–14.)

Schuntov, V. P., and V. P. Vasil'kov. 1982. Long-term population fluctuations of north Pacific sardines. II. Epochs of atmospheric circulation and cyclic nature of the population dynamics of the Pacific and California sardines. J. Ichthyol. 22.

Walters, C. J. 1969. A generalized computer simulation model for fish population studies. Trans. Am. Fish. Soc. 98(3): 505–512.

1985. Bias in the estimation of functional relationships from time series data. Can. J. Fish. Aquat. Sci. 42: 147–149.

Walters, C. J., and D. Ludwig. 1981. Effects of measurement errors on the assessment of stock-recruitment relationships. Can. J. Fish. Aquat. Sci. 38: 704–710.

Variability in Estimating Catch-in-Numbers-at-Age and Its Impact on Cohort Analysis

Daniel K. Kimura

Northwest and Alaska Fisheries Center, National Marine Fisheries Service
Bldg. 4. BIN C15700, 7600 Sand Point Way N.E., Seattle, WA 98115-6349, USA

Abstract

KIMURA, D. K. 1989. Variability in estimating catch-in-numbers-at-age and its impact on cohort analysis, p.57–66. *In* R.J. Beamish and G. A. McFarlane [ed.]. Effects of ocean variability on recruitment and an evaluation of parameters used in stock assessment models. Can. Spec. Publ. Fish. Aquat. Sci. 108.

Formulas are derived for estimating catch-in-numbers-at age for complex, multi-area, multi-nation, multi-gear fisheries. Assuming catch-in-weight is known for each substratum, the method involves applying randomly sampled length frequencies from these substrata to age-length and weight-length keys sampled from broader strata. Variance estimates are derived using standard statistical calculations and the delta method. This variance is the variance due to the biological sampling of age, length, and weight. The impact of this sampling variance component on Cohort Analysis is compared with the impact of possible errors in estimating the substratum catch-in-weight, the natural mortality rate, and the terminal fishing exploitation rate. The resulting formulas are applied to data collected from the 1983 fishery for walleye pollock (*Theragra chalcogramma*) in the central portion of the Gulf of Alaska.

Résumé

KIMURA, D. K. 1989. Variability in estimating catch-in-numbers-at-age and its impact on cohort analysis p.57–66. *In* R. J. Beamish and G. A. McFarlane [ed.]. Effects of ocean variability on recruitment and an evaluation of parameters used in stock assessment models. Can. Spec. Publ. Fish. Aquat. Sci. 108.

Des formules sont élaborées afin d'évaluer l'effectif des classes d'âge dans les captures pour des pêches complexes, dans plusieurs zones, intéressant plusieurs pays et à engins multiples. En supposant que l'on connaisse le poids des captures pour chaque sous-strate, la méthode applique des fréquences de longueur obtenues par échantillonnage au hasard de ces sous-strates à des clés âge-longueur et poids-longueur échantillonnées à partir de strates plus vastes. Des estimations de la variance sont dérivées au moyen de calculs statistiques ordinaires et de la méthode du delta. Cette variance est la variance attribuable à un échantillonnage biologique selon l'âge, la longueur et le poids. Les répercussions de cette composante de la variance aléatoire sur l'analyse de cohorte sont comparées aux répercussions des erreurs possibles d'estimation du poids des captures de la sous-strate, du taux de mortalité naturelle et du taux d'exploitation de la pêche de la dernière année étudiée. Les formules résultantes sont appliquées aux données recueillies lors de la pêche à goberge de l'Alaska (*Theragra chalcogramma*) en 1983 dans la partie centrale du golfe de l'Alaska.

Introduction

This paper provides formulas for converting catch-in-weight to catch-in-numbers-at-age. Variance estimates of catch-in-numbers-at-age are derived from classical random sampling formulas and extensive use of the delta method (Seber 1973, section 1.3.3).

The main sampling unit is a time-area stratum in which weight-at-length and age-at-length data can be pooled. For most fisheries, these data are the most expensive to collect, and so pooling will generally be necessary. Next, substrata are defined for which the catch-in-weight is known. These substrata may be defined by various criteria: for example, vessel-class, time, and area. It is assumed that each substratum has been randomly sampled for length frequencies.

For each substratum, the average weight of fish and proportion-at-age are calculated by applying the substratum length frequencies to the weight-at-length and age-at-length data. Numbers-at-age are calculated by dividing the catch-in-weight by the average weight of fish, and multiplying the resulting number by proportion-at-age.

Pope's (1972) Cohort Analysis is used to obtain some perspective on how sampling variability of catch-at-age data can affect modeling results. This was done by simply applying the delta method for estimating variance to Pope's formula.

In the final section the estimation formulas derived in this paper are applied to catches from the walleye pollock (*Theragra chalcogramma*) fishery in the central portion of the Gulf of Alaska. Estimates of catch-in-numbers-at-age and its coefficient of variation are provided for actual and hypothetical sampling levels. The variance formula derived from Pope's Cohort Analysis is used to gain further perspective concerning the appropriate levels of sampling.

Estimating Catch-in-numbers-at-age

Because the estimation of catch-in-numbers-at-age and its variance require fairly extensive calculations, a great deal of notation will have to be developed. However, the calculations are straightforward, and nothing more complicated than the delta method will be used.

Indices and Subscripts

The following indices and subscripts will be used throughout this paper:

i = 1, . . . , I is the length group index
j = 1, . . . , J is the age group index
k = 1, . . . , K is the substratum index
ℓ = a subscript referring to length frequencies
m = a subscript referring to males
f = a subscript referring to females
q = a subscript referring to the age-length key
ω = a subscript referring to fish weight.

Variables Sampled Directly from the Fishery

The following, fundamental quantities are statistics calculated directly from sampled data, assuming these data were randomly selected:

c_{kt} = the total catch-in-weight taken from substratum k. This quantity is initially assumed to be known without error.

n_{km}, n_{kf} = the number of males and females in a random sample of $n_k = n_{km} + n_{kf}$ fish taken from the catch in substratum k.

ℓ_{ikm}, ℓ_{ikf} = the length distribution for males and females, based on sample sizes of n_{km} and n_{kf} fish, respectively. The distributions have been normalized so that $\Sigma_i \ell_{ikm} = 1$, and $\Sigma_i \ell_{ikf} = 1$.

ω_{im}, ω_{if} = the average weight of length i males and females, respectively.

$\sigma^2_{\omega im}$, $\sigma^2_{\omega if}$ = the variance of the weight of a randomly selected male or female fish, of length i.

$n_{\omega im}$, $n_{\omega if}$ = the sample sizes used to estimate $\hat{\omega}_{im}$ and $\hat{\omega}_{if}$.

q_{ijm}, q_{ijf} = the age–length keys for male and female fish. The distributions are normalized so that $\Sigma_j q_{ijm} = 1$, and $\Sigma_j q_{ijf} = 1$.

n_{qim}, n_{qif} = the sample sizes in length category i for the age–length keys.

Formulas for Converting Catch-in-Weight to Catch-in-numbers

$r_k = n_{kf} / n_{km}$
= the ratio of females to males in the random sample taken from substratum k.

$\omega_{km} = \Sigma_i \ell_{ikm} \omega_{im}$
= the average weight of males sampled from substratum k.

$\omega_{kf} = \Sigma_i \ell_{ikf} \omega_{if}$
= the average weight of females sampled from substratum k.

$c_{km} = c_{kt} n_{km} / (n_{km} \omega_{km} + n_{kf} \omega_{kf})$
$= c_{kt} / (\omega_{km} + r_k \omega_{kf})$
= the number of males caught in substratum k.

$c_{kf} = c_{kt} n_{kf} / (n_{km} \omega_{km} + n_{kf} \omega_{kf})$
$= c_{kt} / (\omega_{km} / r_k + \omega_{kf})$
= the number of females caught in substratum k.

Formulas for Converting Catch-in-numbers to Catch-in-numbers-at-age

$p_{jkm} = \Sigma_i \ell_{ikm} q_{ijm}$
= the proportion of c_{km} that are j-yr-olds.

$p_{jkf} = \Sigma_i \ell_{ikf} q_{ijf}$
= the proportion of c_{kf} that are j-yr-olds.

$X_{jm} = \Sigma_k c_{km} p_{jkm}$
= the total number of j-yr-old male fish caught.

$X_{jf} = \Sigma_k c_{kf} p_{jkf}$
= the total number of j-yr-old female fish caught.

$X_j = X_{jm} + X_{jf}$
= the total number of j-yr-old fish caught.

Variance of Catch-in-numbers-at-age

This section develops variance formulas for the estimated catch-in-numbers-at-age. Since

$$\hat{X}_{jm} = \Sigma_k \hat{c}_{km} \hat{p}_{jkm},$$

$$\hat{X}_{jf} = \Sigma_k \hat{c}_{kf} \hat{p}_{jkf}, \text{ and}$$

$$(1) \quad \hat{X}_j = \hat{X}_{jm} + \hat{X}_{jf},$$

it follows that

$$V(\hat{X}_j) = V(\hat{X}_{jm}) + V(\hat{X}_{jf}) + 2\mathrm{COV}\,(\hat{X}_{jm}, \hat{X}_{jf}).$$

The quantities $V(\hat{X}_{jm})$, $V(\hat{X}_{jf})$, and COV $(\hat{X}_{jm}, \hat{X}_{jf})$ can be approximated by a combination of classical statistical calculations and the delta method.

Estimating $V(\hat{X}_{jm})$ and $V(\hat{X}_{jf})$ using the delta method requires estimation of the covariance matrix

$$\Sigma_{jm} = \begin{pmatrix} \Sigma_{pjm} & \Sigma_{pcjm} \\ \Sigma_{pcjm} & \Sigma_{cm} \end{pmatrix},$$

and a similarly defined Σ_{jf}. In this $2K \times 2K$ matrix, all submatrices are $K \times K$.

Σ_{pjm} = the $K \times K$ covariance matrix of $\hat{p}_{jkm}$, $k=1, \ldots, K$.

Σ_{cm} = the $K \times K$ covariance matrix of $\hat{c}_{km}$, $k=1, \ldots, K$.

Σ_{pcjm} = the $K \times K$ diagonal matrix whose $k,k-$th entry is COV $(\hat{p}_{jkm}, \hat{c}_{km})$.

Similar matrices can be defined for Σ_{pjf}, Σ_{cf}, and Σ_{pcjf}.

The matrix Σ_{cmf}, required to estimate $V(\hat{X}_j)$, is defined to be

Σ_{cmf} = the $K \times K$ matrix whose k,k' – th entry is COV $(\hat{c}_{km}, \hat{c}_{k'f})$.

Also define

$$C'_m = (c_{1m}, \ldots, c_{Km}),$$

$$P'_{jm} = (p_{j1m}, \ldots, p_{jKm}), \text{ and}$$

$$Y'_{jm} = (C'_m, P'_{jm}),$$

with similar quantities defined for C_f, P_{jf}, and Y_{jf}.

Then, by application of the delta method,

$$V(\hat{X}_{jm}) = Y'_{jm} \Sigma_{jm} Y_{jm}, \text{ and}$$

$$V(\hat{X}_{jf}) = Y'_{jf} \Sigma_{jf} Y_{jf}.$$

From the definition of covariance,

$$\text{COV}(\hat{X}_{jm}, \hat{X}_{jf}) = P'_{jm} \Sigma_{cmf} P_{jf}.$$

Hence,

$$(2)\quad V(\hat{X}_j) = Y'_{jm}\Sigma_{jm}Y_{jm} + Y'_{jf}\Sigma_{jf}Y_{jf} + 2P'_{jm}\Sigma_{cmf}P_{jf}.$$

Appendices A–D describe how Σ_{pjm}, Σ_{cm}, and Σ_{pcjm}, similar quantities for females, and Σ_{cmf} can be estimated.

Impact of Variability on Cohort Analysis

From one point of view all we need to determine appropriate sampling levels is the estimate and variance of catch-in-numbers-at-age. Then we would simply choose a sampling level that gave a desired coefficient of variation for a particular age or combination of ages. However, this approach fails to consider how the catch-at-age data will be used, and how sampling errors compare with other sources of error. Pope's (1972) Cohort Analysis provides a vehicle in which both of these additional considerations can be made.

Using Cohort Analysis, the population-numbers-at-age is:

$$(3)\quad N_i = \sum_{j=0}^{[t-i-1]} [C_{i+j}\exp((0.5+j)M)] + C_t\exp((t-i)M)/U_t.$$

Estimating the variance of N_i using the delta method:

$$V(N_i) = \left\{ \sum_{j=0}^{[t-i-1]} [V(C_{i+j}) \exp((1+2j)M)] + V(C_t) \exp(2(t-i)M) / U_t^2 \right\}$$

$$(4)\quad + \left\{ \sum_{j=0}^{[t-i-1]} [C_{i+j}\, (0.5+j)\exp((0.5+j)M)] + [(C_t / U_t)(t-i)\exp((t-i)M)] \right\}^2 V(M)$$

$$+ [C_t \exp((t-i)M) / U_t^2]^2 V(U_t).$$

As usual the delta method provides an additive decomposition of total variance. In this formula the first term is due to variance in the estimate of catch-at-age, the second term is due to variance in the estimate of the natural mortality rate, M, and the final term is due to variance in the estimate of the terminal exploitation rate, U_t. If we have estimates of the variances of these parameters it would be possible to estimate the total variance of population-numbers-at-age, and attribute proportions of this variance to specific parameters.

The variance due to estimating catch-at-age is composed of two components. First there is the sampling component described in equation 2 as $V(\hat{X}_j)$. And second there is a component due to uncertainty in estimating substrata catches. These variances can be added to provide a total variance estimate for catch-at-age:

$$V(C_j) = V(\hat{X}_j) + \Sigma_k X_{jk}^2 \text{ cv}(c_{kt})^2.$$

In this formula X_{jk} is the total number of j-yr-olds estimated in the catch of substratum k, and cv(c_{kt}) is the coefficient of variation for the catch-in-weight in substratum k.

Application

Introduction

Equations 1 and 2 for estimating catch-in-numbers-at-age and its variance were applied to data from the 1983 walleye pollock (*Theragra chalcogramma*) fishery in the central portion of the Gulf of Alaska. Stratum sampling levels for weight-at-length and age-at-length data were evaluated by varying sample sizes in the variance formulas. It was assumed that the same numbers of fish were weighed and aged. The hypothetical numbers sampled from each length category were proportional to actual sampling. For each hypothetical sampling level, the coefficient of variation (cv) of catch-in-numbers-at-age was graphed.

As a further indicator of the effect of stratum sample sizes, Pope's Cohort Analysis formulas were used. Estimates of population-numbers-at-age were obtained from equation 3, along with associated variance estimates from equation 4. These variances were of two types. The first assumes only the sampling variance given by equation 2. The second begins with this sampling variance, but in addition includes variability associated with uncertainty in catch-in-weight estimates, natural mortality, and terminal exploitation rate. Since it is difficult to give variance estimates for these final three quantities, I assume that they are known with the same degree of relative accuracy (i.e., that they have the same coefficient of variation). High, medium, and low accuracy in these parameter estimates are described by cv (parameters) = 0.1, 0.2, and 0.3, respectively.

Stratum and Substratum Definitions

The principal strata were 4-month time periods in which age-at-length and weight-at-length samples could be pooled. In the case of pollock, these were length stratified samples in which samplers attempted to collect

5 otoliths/cm/sex. Substrata were defined as a combination of area/nation/vessel-class, within the principal time stratum. In the analysis provided here United States joint venture fisheries are treated as a nation/vessel-class. So that most substrata would be sampled for length frequencies, the Chirikoff and Kodiak International North Pacific Fisheries Commission regions were combined.

Catch-in-weight for these substrata, with Chirikoff and Kodiak catches separated, are given in Table 1. For example, in the May–August time stratum a typical substratum would be Chirikoff–Kodiak/Japan/surimi-large-trawler, with a catch of 2 810 t. In Table 1, the underlined catches were not sampled for length frequencies, and were therefore not included in the estimated catch-in-numbers-at-age. Because these unsampled catches represent 1.5% of the total catches, the estimated catch-in-numbers-at-age were adjusted upward by this factor.

Estimates and Variability of Catch-in-numbers-at-age

The estimated catch-in-numbers-at-age and coefficient of variation, using the preceding estimation formulas, are shown in Table 2. Also in Table 2 are the "old" estimates used in the "status of stocks" document. Although the

TABLE 1. Catches (t) of pollock from the central portion of the Gulf of Alaska by time, nation, vessel-class, and area, in 1983. Underlined catches were not sampled for length frequencies.

Time	Nation (vessel-class)	International North Pacific Fisheries Commission Region: Shumagin	Chirikoff	Kodiak
Jan.–Apr.	U.S. joint venture	4	124 493	6 897
	Japan (surimi large trawler)	9	40	0
	R.O.K. (large freezer trawler)	126	19	0
May–Aug.	U.S. joint venture	305	12	272
	Japan (small trawler)	2 965	104	1 423
	Japan (surimi large trawler)	6 284	45	2 765
	Japan (large freezer trawler)	1 014	67	641
	R.O.K. (small trawler)	792	16	0
	R.O.K. (large freezer trawler)	7 134	392	0
Sept.–Dec.	U.S. joint venture	189	35	1 926
	Japan (small trawler)	2 161	3 138	773
	Japan (surimi large trawler)	4 685	17 590	0
	Japan (large freezer trawler)	167	2 410	982
	R.O.K. (small trawler)	1 530	1 716	0
	R.O.K. (large freezer trawler)	12 244	9 663	0
Total		39 609	159 740	15 679

TABLE 2. Comparison of new and old methods of estimating catch-in-numbers-at-age. Estimated catches in thousands of pollock from the central portion of the Gulf of Alaska.

Age (years)	New Way (Catch)	(CV)	Old Way (Catch)
2	3 824	0.042	4 707
3	19 583	0.072	22 438
4	110 706	0.035	127 293
5	137 654	0.032	123 189
6	69 698	0.050	57 617
7	40 335	0.070	44 822
8	7 063	0.149	11 529
9	989	0.234	1 141

new formulas give nearly the same estimates of total numbers of fish caught (within 1%), the estimated catch-in-numbers-at-age are seen to be different. This is especially true for the most abundant age groups, ages 4 and 5 yr. These differences are most probably attributable to the way the sampled length frequencies were weighted by the total days' catch under the old method. Also of interest are the small cv's for the most abundant age groups, and generally for ages 7 yr and under. It can be noted that small proportions of young fish are much easier to estimate than small proportions of old fish. This is attributable to the overlapping age–length relationships which become severe in older age-groups. This is probably due to the allocation of more ages to the first time stratum when most of the catch occurred, and also the larger weight–length sample sizes in the actual sampling (Table 3).

Estimates From Cohort Analysis

Another way to look at sample size is to see what effects sampling levels have on the variability of abundance estimates derived from Cohort Analysis. To do so from only one year's data requires the unrealistic assumption that the estimated catch-in-numbers-at-age and estimated variance are from a single cohort sampled in different years. Although this assumption is obviously wrong, it can be interpreted in a manner that appears more realistic. That is, if a fishery is sampled every year, and each year's sampling results are the same, then the analysis given here would be valid.

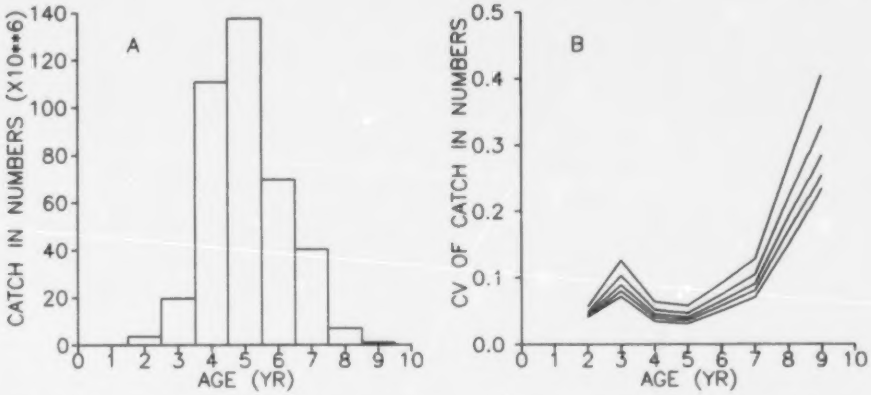

FIG. 1. (A) Estimated catch-at-age of pollock from the central portion of the Gulf of Alaska in 1983; (B) Coefficient of variation of catch-at-age assuming catch-in-weight is known without error. Curves from top to bottom are for hypothetical sampling levels of 200, 300, 400, and 500 fish/sex/stratum. The actual sampling level (Table 3) is represented by the bottom line.

TABLE 3. Sampled numbers of pollock from the central portion of the Gulf of Alaska in 1983.

Time	Sex	Weight samples	Age samples
Jan.–Apr.	males	1 086	717
	females	921	627
May–Aug.	males	558	321
	females	814	487
Sept.–Dec.	males	579	460
	females	668	509
Total	males	2 223	1 498
	females	2 403	1 623
Average per stratum	males	741	499
	females	801	541

The new estimates of catch and their cv's are shown in Fig. 1A, 1B, along with the cv's projected under different hypothetical sampling levels. The sample sizes shown are for a sex/stratum combination. Therefore, a stratum sample size of 500 fish means that 3 000 fish are weighed and aged. These sampling levels can be compared with the actual sampling levels shown in Table 3. Since the actual sampling level is approximately 500 per sex/stratum, it is interesting to note that current sampling outperforms the 500 per sex/stratum sampling level (Fig. 1B).

Figure 2 shows the estimated population-numbers-at-age from Cohort Analysis. We used $M = 0.3$, and starting U_t values of 0.01, 0.02, 0.05, 0.1, and 0.5. If U_t is between 0.02 and 0.5, this hypothetical cohort would be expected to have a population of between 1.2 and 1.6 billion fish at age 2 yr.

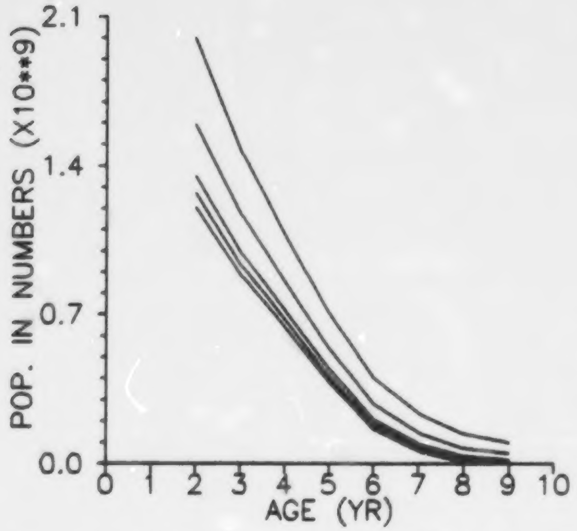

FIG. 2. Estimated population numbers of pollock at each age for a hypothetical cohort assuming $M = 0.3$. Curves from top to bottom assume $U_t = 0.01, 0.02, 0.05, 0.1$, and 0.5.

Figure 3A shows for $U_t = 0.1$, the cv's of the estimated population-numbers-at-age at the actual sampling level, and at hypothetical sampling levels. This figure includes only sampling error. It should be noted that the estimated cv (N_i) depend strongly on the value of U_t, but for $U_t = 0.1$, they very much approximate cv ($\hat{X}_j$). As with the case of estimating $\hat{X}_j$, the N_i appear to be accurately estimated under 7 yr of age, regardless of sampling levels.

Figures 3B–3D are similar to Fig. 3A, but also include uncertainties in parameters. This was done by using equation 4, and assuming the same coefficient of variation for catch-in-weight, natural mortality rate, and initial exploitation rate. Low, medium, and high parameter uncertainty were described by cv's of 0.1, 0.2, and 0.3. Comparing Fig. 3A with Fig. 3B–3D shows that the uncertainty in estimating population-numbers-at-age from Cohort Analysis is probably dominated by these other sources of error. This is especially true for the middle and younger ages.

An interesting way to examine how uncertainty in parameters affects Cohort Analysis is to make stacked histograms of the proportion of the total variance-at-age that is attributable to a source [illegible]ation. Such histograms will always sum to one which represents the total variance-at-age. In viewing such histograms it is important to realize that total variability varies greatly with age, sampling level, and degree of parameter uncertainty, and is not represented on these graphs.

Figures 4A–4D are stacked histograms which assume $M = 0.3$, and $U_t = 0.1$. Figures 4A–4C are at actual sampling levels (Table 3), and assume low (Fig. 4A, cv = 0.1), medium (Fig. 4B, cv = 0.2), and high (Fig. 4C, cv = 0.3) uncertainty in parameters. Figure 4D is the same as Fig. 4B, but assumes a reduced sampling level of 300 fish/sex/stratum.

Although the total variance, and portions of total variance attributable to sources of uncertainty vary greatly, the portion of total variance dependent on a specific source of uncertainty follows a definite pattern with age. For older age groups sampling error, and uncertainty in U_t are important. For middle age-groups, uncertainty in catch-in-weight has its greatest influence; and for youngest age-groups uncertainty in the natural mortality rate dominates. Figure 4D is the same as Fig. 4B, but with sampling at 300 fish/sex/stratum, compared with around 500 fish/sex/stratum at actual sampling levels. Figure 4D shows that sampling error becomes important in middle age-groups at lower sampling levels.

Discussion

The principal sampling problems I wish to discuss are whether biological age and weight samples should be proportional or stratified with respect to the length category, and what the absolute level of sampling should be. These problems have been "solved" again and again by statisticians, and yet the problem appears to remain. Two reasons for this are probably the complexity of the problem across different fisheries and circumstances, and our inability to choose a universally acceptable measure of error. For example, in this paper we use both the coefficient of variation of catch-in-numbers-at-age and estimated population-numbers-at-age from Cohort Analysis as measures of error.

First, let me discuss the question of whether the age subsample should be proportional or stratified. That is, whether the same number of fish should be selected from each length category for ageing, or whether the number selected for ageing should be proportional to the random length frequency. Ketchen (1949) thought samples should be stratified. Southward (1976) and Kimura (1977) concluded that subsamples should be proportional.

I concluded that subsamples should be proportional solely on the behavior of vartot = Σ var ($\hat{p}_j$). Vartot appears to be a reasonable measure of how well the overall distribution is measured, so I still feel that aged subsamples should be proportional to the random length frequency.

However, in making such a recommendation it is important to distinguish between a sampling objective, and a sampling plan. My opinion is that the sampling objective should be proportional subsampling of age structures. A sampling plan that is built around proportional subsampling may have problems of a different sort. A sampler attempting to collect proportional samples could easily collect all of his samples from the center of the length frequency so that the tails of the distribution are undersampled. On the other hand, a sampling plan designed to collect stratified samples may actually collect proportional samples due to the availability of fish. In our example (Fig. 5), the sampling results are seen to be proportional although the sampling plan was stratified.

The next question I would like to consider is what the absolute sampling level should be? Again, the problem becomes what measure of error should be used? Catch-at-age for middle and lower ages are well estimated even at low sampling levels (Fig. 1B). The coefficient of variation for older ages would remain large even at higher sampling levels.

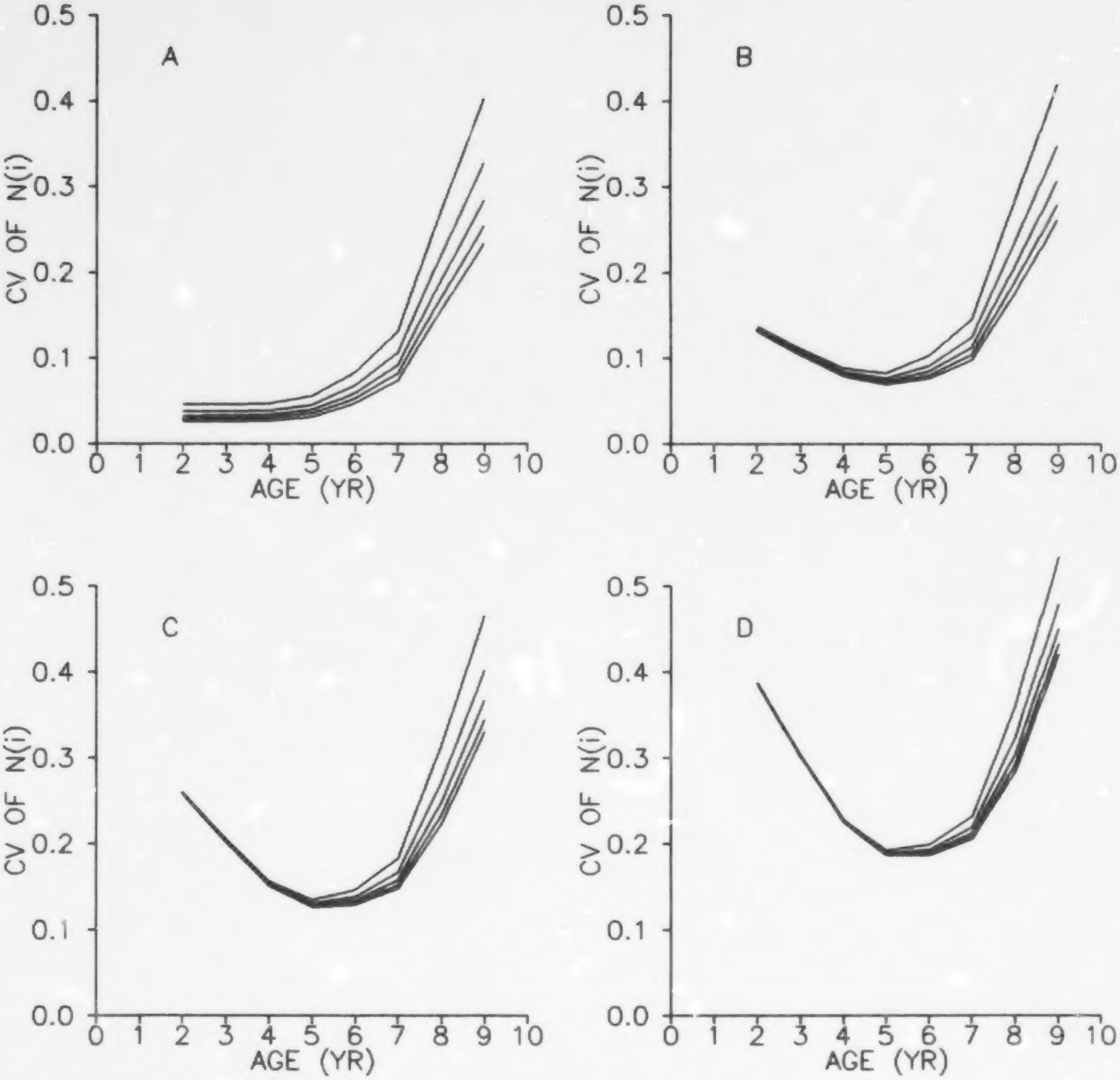

FIG. 3. (A) The coefficient of variation at each age for a hypothetical cohort of pollock (from Fig. 2, $M = 0.3$, $U_t = 0.1$). Curves from top to bottom are for hypothetical sampling levels of 200, 300, 400, and 500 fish/sex/stratum. The bottom line represents actual sampling levels; (B) Same as Fig. 3A but assuming additional sources of error due to substratum catch-in-weight estimates, natural mortality rate estimates, and initial exploitation rate estimates. These three parameters are assumed to have a coefficient of variation of 0.1; (C) Same as Fig. 3B, but assuming a coefficient of variation for parameter errors of 0.2; (D) Same as Fig. 3B and 3C, but assuming a coefficient of variation for parameter errors of 0.3.

If the primary usage of the data will be in Cohort Analysis, Fig. 3A indicates satisfactory results even at low sampling levels. This assumes that the representativeness of the samples can be maintained at low sampling levels. One way this can be done is to collect large stratified samples of structures, and later subsample structures that will be aged using some proportional, random selection method.

From a broader perspective, Fig. 3, 4 indicate that sampling error represents a relatively minor source of error in Cohort Analysis. Except for the older ages, the results from Cohort Analysis are probably dominated by other sources of error. Particularly of note is the uncertainty in the numbers of young fish caused by uncertainty in the natural mortality rate. Considering the magnitude of these other uncontrolled sources of error, it appears futile to try to reduce sampling error with excessively large samples.

There are two major sources of bias for the method of estimating catch-in-numbers-at-age described here. First, sampling of length frequency data may not be completely random. And second, applying the same age-length key to different length frequency data will inevitably give some biased results (Kimura 1977). I have assumed these biases are within tolerable limits.

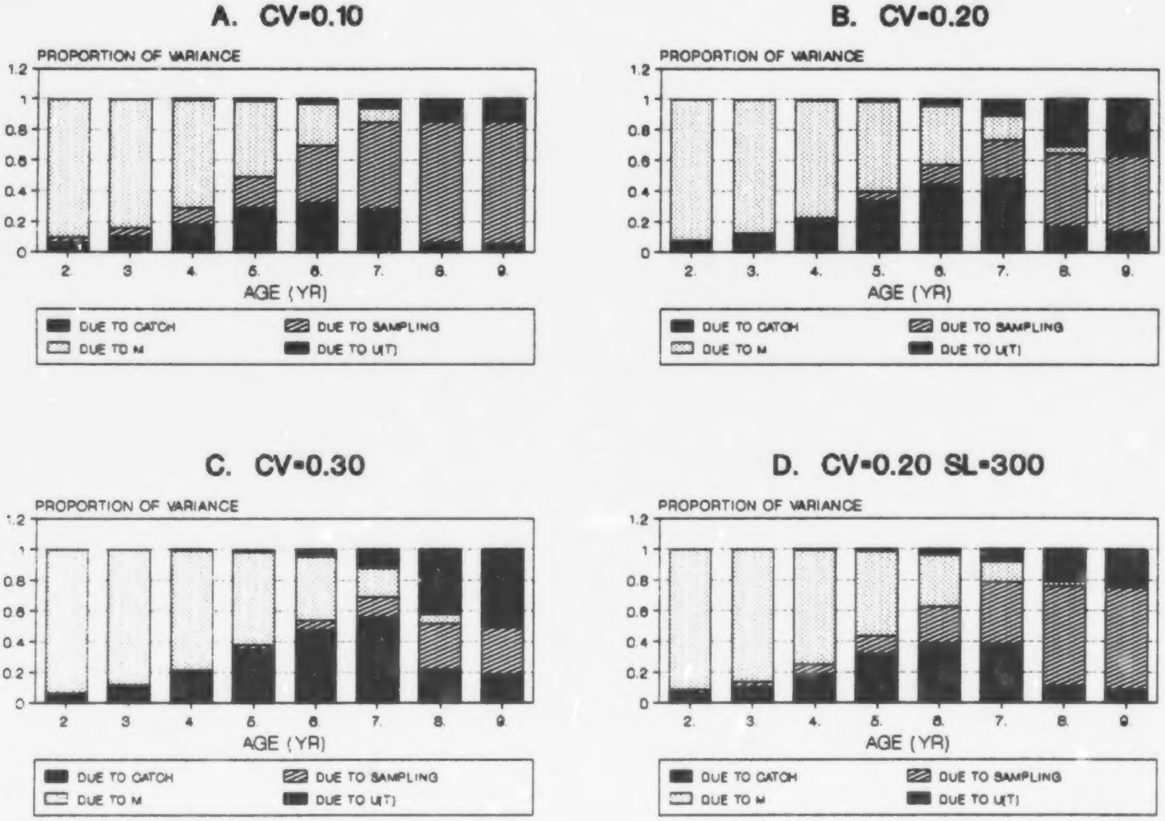

FIG. 4. (A) Stacked histograms of the proportion of total variance of N_i estimated at each age, attributable to uncertainty in substratum catch-in weight, sampling, natural mortality rate, and initial exploitation rate. That is, the first band in the histogram represents the proportion of total variance attributable to uncertainty in substratum estimates of catch-in-weight; the second band represents the proportion of total variance attributable to sampling error, and so forth. This histogram assumes actual sampling levels and the low parameter uncertainty of cv = 0.1; (B) Same as Fig. 4A, but assuming the medium parameter uncertainty of cv = 0.2; (C) Same as Fig. 4A and 4B, but assuming a high parameter uncertainty of cv = 0.3; (D) Same as Fig. 4B, but assuming a decreased sampling level of 300 fish/sex/stratum.

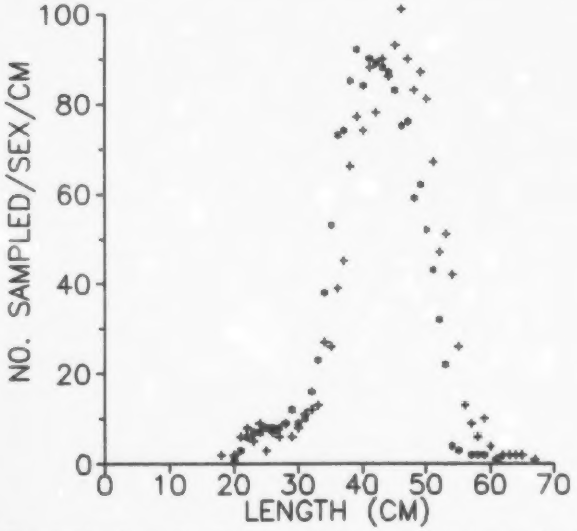

FIG. 5. Numbers of pollock sampled for age data (per sex/cm) in the central portion of the Gulf of Alaska in 1983 (males (*), females (+)).

References

COCHRAN, W. G. 1963. Sampling techniques. Second edition. J. Wiley & Sons, New York, 413 p.

KETCHEN, K. S. 1949. Stratified subsamples for determining age distribution. Trans. Am. Fish. Soc. 79: 205–212.

KIMURA, D. K. 1977. Statistical assessment of the age-length key. J. Fish. Res. Board Can. 34: 317–324.

POPE, J. G. 1972. An investigation of the accuracy of virtual population analysis using cohort analysis. Res. Bull. Int. Comm. Northwest Atl. Fish. 9: 65–74.

SEBER, G. A. F. 1973. The estimation of animal abundance. Hafner Press, New York, 506 p.

SOUTHWARD, G. M. 1976. Sampling landings of halibut for age composition. Int. Pac. Halibut Commission, Sci. Rep. 58: 31 p.

Appendix A: Estimating Σ_{pjm}

Since Σ_{pjm} is the $K \times K$ covariance matrix of $(\hat{p}_{j1m}, ..., \hat{p}_{jKm})$, the diagonal elements of Σ_{pjm} are the $\hat{V}(\hat{p}_{jkm})$. These diagonal elements can be estimated using variance formulas derived for the standard age-length key

(Cochran 1963, section 12.2; Kimura 1977). The off-diagonal elements, COV $(\hat{p}_{jkm}, \hat{p}_{jk'm})$ can be derived using methods similar to Kimura (1977).

By definition,

$$\text{COV}\,(\hat{p}_{jkm}, \hat{p}_{jk'm}) = E\,(\hat{p}_{jkm}\,\hat{p}_{jk'm}) - p_{jkm}\,p_{jk'm},$$

where $\hat{p}_{jkm} = \Sigma_i\,\hat{\ell}_{ikm}\,\hat{q}_{ijm}$. It follows that

$$\begin{aligned} E\,(\hat{p}_{jkm}\hat{p}_{jk'm}) &= E[(\Sigma_i\hat{\ell}_{ikm}\hat{q}_{ijm})\,(\Sigma_{i'}\hat{\ell}_{i'k'm}\hat{q}_{i'jm})] \\ &= E[\Sigma\Sigma_{ii'}\hat{\ell}_{ikm}\hat{\ell}_{i'k'm}\hat{q}_{ijm}\hat{q}_{i'jm}]. \end{aligned}$$

For $i = i'$,

$$E\,(\hat{\ell}_{ikm}\,\hat{\ell}_{ik'm}\,\hat{q}^2_{ijm}) = \ell_{ikm}\,\ell_{ik'm}\,[q_{ijm}\,(1. - q_{ijm})/n_{qim} + q^2_{ijm}].$$

For $i \neq i'$,

$$E\,(\hat{\ell}_{ikm}\,\hat{\ell}_{i'k'm}\,\hat{q}_{ijm}\,\hat{q}_{i'jm}) = \ell_{ikm}\,\ell_{i'k'm}\,q_{ijm}\,q_{i'jm}.$$

Therefore,

$$\text{COV}\,(\hat{p}_{jkm}, \hat{p}_{jk'm}) = \Sigma_i\,\ell_{ikm}\,\ell_{ik'm}\,q_{ijm}(1. - q_{ijm})/n_{qim}.$$

Appendix B: Estimating Σ_{cm}

Σ_{cm} is the $K \times K$ covariance matrix of $(\hat{c}_{1m}, \ldots, \hat{c}_{Km})$. Estimating Σ_{cm} directly is difficult, so we resort to the delta method. Define

$$\Sigma^*_{ck} = \begin{bmatrix} V(\hat{\omega}_{km}) & 0 & 0 \\ 0 & V(\hat{\omega}_{kf}) & 0 \\ 0 & 0 & V(\hat{r}_k) \end{bmatrix}$$

Let $\delta'_{km} = (\partial c_{km}/\partial\omega_{km}, \partial c_{km}/\partial\omega_{kf}, \partial c_{km}/\partial r_k)$,

where $\partial c_{km}/\partial\omega_{km} = -c_{kt}/(\omega_{km} + r_k\omega_{kf})^2$,

$\partial c_{km}/\partial\omega_{kf} = -c_{kt}r_k/(\omega_{km} + r_k\omega_{kf})^2$, and

$\partial c_{km}/\partial r_k = -\,c_{kt}\omega_{kf}/(\omega_{km} + r_k\omega_{kf})^2$.

Then by the delta method, the diagonal elements of Σ_{cm} can be approximated by $V(\hat{c}_{km}) = \delta'_{km}\,\Sigma^*_{ck}\,\delta_{km}$.

The off-diagonal elements of Σ_{cm}, $\text{COV}(\hat{c}_{km}, \hat{c}_{k'm})$, can also be approximated by the delta method. To do so, define

$$\Sigma^*_{ckk'} = \begin{bmatrix} \Sigma^*_{ck} & \text{T}_{ckk'} \\ \text{T}_{ckk'} & \Sigma^*_{ck'} \end{bmatrix}$$

where

$$T_{ckk'} = \begin{bmatrix} \text{COV}(\hat{\omega}_{km}, \hat{\omega}_{k'm}) & 0 & 0 \\ 0 & \text{COV}(\hat{\omega}_{kf}, \hat{\omega}_{k'f}) & 0 \\ 0 & 0 & 0 \end{bmatrix}$$

Let $\bar{0}' = (0, 0, 0)$. Then by the delta method,

$$\begin{aligned} \text{COV}(\hat{c}_{km}, \hat{c}_{k'm}) &= (\delta'_{km}, \bar{0}')\,\Sigma^*_{ckk'}\begin{bmatrix} \bar{0} \\ \delta_{k'm} \end{bmatrix} \\ &= \delta'_{km}\text{T}_{ckk'}\,\delta_{k'm}. \end{aligned}$$

The corresponding formulas for estimating Σ_{cf} are constructed by replacing δ_{km} with

$$\delta'_{kf} = (\partial c_{kf}/\partial\omega_{km}, \partial c_{kf}/\partial\omega_{kf}, \partial c_{kf}/\partial r_k),$$

where $\partial c_{kf}/\partial\omega_{km} = -\,(c_{kt}/r_k)/(\omega_{km}/r_k + \omega_{kf})^2$,

$\partial c_{kf}/\partial\omega_{kf} = -\,c_{kt}/(\omega_{km}/r_k + \omega_{kf})^2$, and

$\partial c_{kf}/\partial r_k = (c_{kt}\,\omega_{km}/r_k^2)\,(\omega_{km}/r_k + \omega_{kf})^2$.

Derivations of $V(\hat{\omega}_{km})$, $\text{COV}(\hat{\omega}_{km}, \hat{\omega}_{k'm})$, and $V(\hat{r}_k)$ can be found in Appendices E, F, and G, respectively.

Appendix C: Estimating Σ_{pcjm}

The k, k' – th entry of Σ_{pcjm} is $\text{COV}(\hat{p}_{jkm}, \hat{c}_{k'm})$. Only the diagonal elements of Σ_{pcjm} are non-zero. Recall that

$\hat{p}_{jkm} = \Sigma_i\hat{\ell}_{ikm}\,\hat{q}_{ijm}$, and

$\hat{c}_{km} = \hat{c}_{kt}/(\hat{\omega}_{km} + \hat{r}_k\,\hat{\omega}_{kf})$.

Therefore, $\partial c_{km}/\partial\omega_{km} = -c_{kt}/(\omega_{km} + r_k\,\omega_{kf})^2$, and by the delta method,

$$\text{COV}(\hat{p}_{jkm}, \hat{c}_{km}) = -\left\{c_{kt}/(\omega_{km} + r_k\,\omega_{kf})^2\right\}\,\text{COV}(\hat{p}_{jkm}, \hat{\omega}_{km}).$$

Similarly,

$$\text{COV}(\hat{p}_{jkf}, \hat{c}_{kf}) = -\left\{c_{kt}/(\omega_{km}/r_k + \omega_{kf})^2\right\}\,\text{COV}(\hat{p}_{jkf}, \hat{\omega}_{kf}).$$

A derivation of COV $(\hat{p}_{jkm}, \hat{\omega}_{km})$ is provided in Appendix H.

Appendix D: Estimating Σ_{cmf}

The k, k' – th entry of Σ_{cmf} is $\text{COV}(\hat{c}_{km}, \hat{c}_{k'f})$. These convariances can be estimated using the delta method, much as in the calculation of Σ_{cm}. Using the same notation used to calculate Σ_{cm}.

$$\text{COV}(\hat{c}_{km}, \hat{c}_{kf}) = \delta'_{km}\,\Sigma^*_{ck}\,\delta_{kf}, \text{ and}$$

$$\begin{aligned} \text{COV}(\hat{c}_{km}, \hat{c}_{k'f}) &= (\delta'_{km}, \bar{0}')\,\Sigma^*_{ckk'}\begin{bmatrix} \bar{0} \\ \delta_{k'f} \end{bmatrix} \\ &= \delta'_{km}\,T_{ckk'}\,\delta_{k'f}. \end{aligned}$$

Appendix E: Derivation of $V(\hat{\omega}_{km})$

By definition,

$$V(\hat{\omega}_{km}) = E(\hat{\omega}^2_{km}) - \omega^2_{km},$$

where $\hat{\omega}_{km} = \Sigma_i\hat{\ell}_{ikm}\hat{\omega}_{im}$. It follows that

$$\begin{aligned} E\,(\hat{\omega}^2_{km}) &= E\,[(\Sigma_i\hat{\ell}_{ikm}\hat{\omega}_{im})\,(\Sigma_{i'}\hat{\ell}_{i'km}\hat{\omega}_{i'm})] \\ &= E\,[\Sigma\Sigma_{ii'}\hat{\ell}_{ikm}\hat{\ell}_{i'km}\hat{\omega}_{im}\hat{\omega}_{i'm}] \end{aligned}$$

For $i = i'$,

$$E(\hat{\ell}^2_{ikm}\hat{\omega}^2_{im}) = \left\{\ell_{ikm}(1. - \ell_{ikm})/n_{km} + \ell^2_{ikm}\right\}\left\{\sigma^2_{\omega im}/n_{\omega im} + \omega^2_{im}\right\}$$

For $i \neq i'$,

$$E\,[\hat{\ell}_{ikm}\hat{\ell}_{i'km}\hat{\omega}_{im}\hat{\omega}_{i'm}] = \left\{-\,\ell_{ikm}\ell_{i'km}/n_{km} + \ell_{ikm}\ell_{i'km}\right\}\omega_{im}\omega_{i'm}.$$

Let $\Sigma_{\ell km}$ = the covariance matrix of $\hat{\ell}_{ikm}$, $i = 1,\ldots,I$,

$\sigma^2_{i\ell km}$ = the i – th diagonal element of $\Sigma_{\ell km}$, and

$W'_m = (\omega_{1m},\ldots,\omega_{Im})$.

Then,

$$V(\hat{\omega}_{km}) = W'_m\,\Sigma_{\ell km}\,W_m + \Sigma_i\left\{(\sigma^2_{i\ell km} + \ell^2_{ikm})\,\sigma^2_{\omega im}/n_{\omega im}\right\}.$$

Appendix F: Derivation of $\mathrm{COV}(\hat{\omega}_{km},\hat{\omega}_{k'm})$

By definition,

$$\mathrm{COV}(\hat{\omega}_{km},\hat{\omega}_{k'm}) = \mathrm{E}(\hat{\omega}_{km}\,\hat{\omega}_{k'm}) - \omega_{km}\,\omega_{k'm},$$

where $\hat{\omega}_{km} = \Sigma_i \hat{\ell}_{ikm}\,\hat{\omega}_{im}$. It follows that

$$E(\hat{\omega}_{km}\,\hat{\omega}_{k'm}) = E[(\Sigma_i \hat{\ell}_{ikm}\,\hat{\omega}_{im})\ (\Sigma_{i'} \hat{\ell}_{i'k'm}\,\hat{\omega}_{i'm})]$$
$$= E[\Sigma\Sigma_{ii'} \hat{\ell}_{ikm}\hat{\ell}_{i'k'm}\,\hat{\omega}_{im}\,\hat{\omega}_{i'm}].$$

For $i = i'$,

$$E(\hat{\ell}_{ikm}\hat{\ell}_{ik'm}\,\hat{\omega}^2_{im}) = \ell_{ikm}\ell_{ik'm}(\sigma^2_{\omega im}/n_{\omega im} + \omega^2_{im}).$$

For $i \neq i'$,

$$E(\hat{\ell}_{ikm}\hat{\ell}_{i'k'm}\,\hat{\omega}_{im}\,\hat{\omega}_{i'm}) = \ell_{ikm}\ell_{i'k'm}\,\omega_{im}\,\omega_{i'm}.$$

Therefore,

$$\mathrm{COV}(\hat{\omega}_{km},\hat{\omega}_{k'm}) = \Sigma_i \ell_{ikm}\ell_{ik'm}\,\sigma^2_{\omega im}/n_{\omega im}.$$

Appendix G: Derivation of $V(\hat{r}_k)$

By definition, $r_k = n_{kf}/n_{km}$.

Let $n_k = n_{km} + n_{kf}$, $s_{km} = n_{km}/n_k$, and

$$t_{km} = 1. - s_{km}$$
$$= n_{kf}/n_k.$$

Then $r_k = t_{km}/s_{km}$,

$$= (1. - s_{km})/s_{km}, \text{ and}$$
$$\partial r_k/\ \partial s_{km} = -1./s^2_{km}.$$

Therefore, by the delta method,

$$V(\hat{r}_k) = (1./s^4_{km})\ (s_{km}t_{km}/n_k)$$
$$= t_{km}/(n_k s^3_{km}).$$

Appendix H: Derivation of $\mathrm{COV}(\hat{p}_{jkm},\hat{\omega}_{km})$

By definition,

$$\mathrm{COV}(\hat{p}_{jkm},\hat{\omega}_{km}) = E(\hat{p}_{jkm}\,\hat{\omega}_{km}) - p_{jkm}\,\omega_{km}$$

where $\hat{p}_{jkm} = \Sigma_i \hat{\ell}_{ikm}\,\hat{q}_{ijm}$, and

$$\hat{\omega}_{km} = \Sigma_i \hat{\ell}_{ikm}\,\hat{\omega}_{im}.$$

It follows that

$$E(\hat{p}_{jkm}\,\hat{\omega}_{km}) = E[(\Sigma_i \hat{\ell}_{ikm}\,\hat{q}_{ijm})\ (\Sigma_{i'} \hat{\ell}_{i'km}\,\hat{\omega}_{i'm})]$$
$$= E[\Sigma\Sigma_{ii'} \hat{\ell}_{ikm}\hat{\ell}_{i'km}\,\hat{q}_{ijm}\,\hat{\omega}_{i'm}].$$

For $i = i'$,

$$E(\hat{\ell}^2_{ikm}\,\hat{q}_{ijm}\,\hat{\omega}_{im}) = q_{ijm}\,\omega_{im}\left\{ \ell_{ikm}(1. - \ell_{ikm})/n_{km} + \ell^2_{ikm} \right\}.$$

For $i \neq i'$,

$$E(\hat{\ell}_{ikm}\hat{\ell}_{i'km}\,\hat{q}_{ijm}\,\hat{\omega}_{i'm} = q_{ijm}\,\omega_{i'm}\left\{ -\ell_{ikm}\ell_{i'km}/n_{km} + \ell_{ikm}\ell_{i'km} \right\}.$$

Therefore, if we define

$Q'_{jm} = (q_{1jm}, \ldots, q_{Ijm})$,

$\Sigma_{\ell km} =$ the covariance matrix of $\hat{\ell}_{ikm}$, $i = 1, \ldots, I$, and

$W'_m = (\omega_{1m}, \ldots, \omega_{Im})$,

then,

$$\mathrm{COV}(\hat{p}_{jkm},\hat{\omega}_{km}) = Q'_{jm}\,\Sigma_{\ell km}\,W_m.$$

Time Series Analysis: Quantifying Variability and Correlation in SE Alaska Salmon Catches and Environmental Data

Terrance J. Quinn II and Robert P. Marshall

Juneau Center for Fisheries and Ocean Sciences
University of Alaska Fairbanks, 11120 Glacier Highway, Juneau, AK 99801, USA

Abstract

QUINN, T. J., II, AND R. P. MARSHALL. 1989. Time series analysis: quantifying variability and correlation in SE Alaska salmon catches and environmental data, p. 67–80. *In* R. J. Beamish and G. A. McFarlane [ed.] Effects of ocean variability on recruitment and an evaluation of parameters used in stock assessment models. Can. Spec. Publ. Fish. Aquat. Sci. 108.

We applied univariate and multivariate time series analysis to SE Alaska salmon catches. Model identification, estimation, and forecasting are illustrated with pink and chum salmon series. Univariate models generally contained an autoregressive parameter at lag one and parameters at lags corresponding to the generation length of the species. Models using salmon catch in weight contained the same time series structure as catch in numbers. Accuracy of one-step-ahead forecasts varied dramatically, and mean and median absolute percent forecast errors were generally high. Multivariate transfer function models using air temperature, sea surface temperature and freshwater discharge information improved the fit and prediction of salmon catch to a limited degree. We compared our forecasts with those made by the Alaska Department of Fish and Game, which use shorter time series, multiple regression analysis, and additional variables. Neither approach had a consistently lower relative forecast error. Graphical techniques suggested that despite high variability, large-scale factors affect salmon catches similarly over time.

Résumé

QUINN, T. J., II, AND R. P. MARSHALL. 1989. Time series analysis: quantifying variability and correlation in SE Alaska salmon catches and environmental data, p. 67–80. *In* R. J. Beamish and G. A. McFarlane [ed.] Effects of ocean variability on recruitment and an evaluation of parameters used in stock assessment models. Can. Spec. Publ. Fish. Aquat. Sci. 108.

L'analyse de séries chronologiques à une variable et à plusieurs variables a été appliquée aux prises de saumon dans le sud-est de l'Alaska. L'identification du modèle, l'estimation et les prévisions sont illustrées à l'aide des séries concernant le saumon rose et le saumon kéta. Les modèles à une variable comportaient en général un paramètre autorégressif à décalage un et des paramètres à décalages correspondant à la durée de génération de l'espèce. Les modèles faisant appel au poids des captures de saumon comportaient la même structure de série chronologique que l'effectif des classes d'âge. La précision des prévisions de l'étape suivante variait énormément, et les erreurs de prévension moyennes et médianes en pourcentage absolu étaient en général élevées. Les modèles à plusieurs variables de la fonction de transfert utilisant des données sur la température ambiante, la température à la surface de l'océan et les réjets d'eau douce ont amélioré de façon limitée l'ajustement et les prévisions des prises de saumon. Nous avons comparé nos prévisions à celles du Department of Fish and Game de l'Alaska, qui utilise des séries chronologiques plus courtes, une analyse de régression multiple et des variables additionnelles. Aucune des approches ne présentait une erreur de prévision relative uniformément plus faible. D'après des techniques graphiques, malgré une grande variabilité, des facteurs intervenant à grande échelle modifient de la même façon les prises de saumon au cours des années.

Introduction

Commercial catches of Pacific salmon (*Oncorhynchus* spp.) in Alaska have been recorded for over 100 years. In addition to large yearly variations and a controversial history of declining harvests (Cooley 1961), recent annual catches of over 100 million salmon mark a level not realized since 1941. Forecasts of catches in Alaska salmon fisheries, needed by the fishing industry and scientists, have not been accurate due to the short-term variation and long-term changes in catch levels. Catch information remains the major source used for forecasting most salmon fisheries, because total returns are determined for only a few stocks, such as Bristol Bay sockeye salmon (Eggers et al. 1984; Fried and Yuen 1986). Environmental phenomena are thought to be important components of salmon catch and dynamics (several papers in Pearcy 1984). Variables such as stream flow, air and sea temperature, upwelling, and sea level have been identified as correlates with salmon catch, abundance, and growth.

In this paper, we use time series analysis to quantify variability in SE Alaska pink (*O. gorbuscha*), chum (*O. keta*), coho (*O. kisutch*), and sockeye (*O. nerka*) salmon catch series and to determine correlation patterns within each series. Chinook salmon catches were not used, because quotas determine the annual catch in most fisheries. For pink and chum salmon, we also determine correlation between the series and auxiliary environmental information. We evaluate time series models in terms of adequacy of fit and significance of parameters, whether model assumptions appear to be met, whether model parameters are related to salmon generation length and other life history characteristics, and the accuracy of one-step-ahead forecasts.

Pink and chum salmon were selected to explore the effect of differences in the complexity of life history on the analyses. Pink salmon recruit to the fishery at 2 years of age. Because of this life history cycle, even-yr and odd-yr pink salmon catches can be considered to be from different populations (Alexandersdottir and Mathisen 1983). Like pink salmon, chum salmon fry migrate to the marine environment during their first year of life. However the most common age of a chum salmon in recent Alaska catches is probably 4 years, while chum aged at 3 and 5 years are common (Clark et al. 1986).

The time series approach has been used successfully for modeling the catch process of species other than salmon (Mendelssohn 1981; Saila et al. 1980; Jensen 1985; Mendelssohn and Cury 1987; Cohen and Stone 1987). In four of the five papers, the success is enhanced by using fortnightly or monthly breakdowns of the data, which increases sample size and hence reduces parameter variability. The other analysis (Jensen 1985) uses annual data, resulting in high variability for forecasts. Mendelssohn (1981) found transfer function models useful for modeling catches of skipjack tuna but had little success improving forecasts when environmental information was included. Mendelssohn and Cury (1987) were able to improve forecasts by incorporating environmental data into the model by using multiple time series analysis and flexible nonlinear transformations. Cohen and Stone (1987) used multivariate time series analysis to determine species interactions and to obtain reasonable short-term forecasts on a logarithmic scale.

Time Series Methods

A set of time-sequenced observations is a time series. The time series considered here are discrete; observations are from evenly spaced intervals in time. The analysis of a time series can be formulated in the time domain or in the frequency domain. The theory and practices for the time domain, summarized in the classic text by Box and Jenkins (1976), describe the philosophy adopted for this study. In these stochastic forecasting models, the value of a series $Z(t)$ at time t can be expressed by a mean and a linear combination of random shocks $\{a(t)\}$,

$$(1) \quad Z(t) = \mu + a(t) + \psi_1 a(t-1) + \psi_2 a(t-2) + \ldots ,$$

where the shocks $\{a(t)\}$ are a sequence of uncorrelated normally distributed random variables with mean 0 and variance σ^2 and the sequence of ψ's are called the psi weights. The time series $Z(1)$, $Z(2)$, ..., $Z(n)$ is regarded as a sample realization from an infinite number of series that could have been generated by the stochastic process of interest. The generating process and the coefficients are unknown and an empirical methodology is used to construct a model which characterizes the behavior of the observations.

Two important representations of the stationary time series model (1) are the autoregressive (AR) and moving average (MA) forms. The p^{th} order autoregressive model, AR(p), is written

$$(1 - \phi_1 B - \phi_2 B^2 - \ldots - \phi_p B^p)\, z(t) = a(t),$$

where $z(t) = Z(t) - \mu$, μ is the mean of the series, and a linear operator B is defined such that $B^k z(t) = z(t-k)$. AR models express the current value of the series as a function of past values. The q^{th} order moving average model, MA(q), is written

$$z(t) = (1 - \theta_1 B - \theta_2 B^2 - \ldots - \theta_q B^q)\, a(t).$$

MA models express the current value of the series as a function of past shocks rather than the past values of a series.

Variance heterogeneity is a form of nonstationarity which can be remedied by applying a variance-stabilizing power transformation (Vandaele 1983, p. 18–20, Quinn 1985). Homogeneous nonstationary occurs when the mean of the series exhibits a changing level or trend over time. Many homogeneous nonstationary series can be made stationary by taking successive differences of the series $\nabla Z(t)$, $\nabla^2 Z(t)$, ..., where $\nabla = (1 - B)$ (Box and Jenkins 1976). When differencing is performed, $Z(t)$ is reconstructed from the sum of previous differences, or "integrated". The number of differences required to impose stationarity is called d.

Combining an AR(p), MA(q), and differencing d into a single autoregressive, integrated, moving average model, ARIMA(p,d,q), results in the form

$$(1 - \phi_1 B - \phi_2 B^2 - \ldots - \phi_p B^p)\, \nabla^d Z(t) =$$
$$(1 - \theta_1 B - \theta_2 B^2 - \ldots - \theta_q B^q)\, a(t).$$

By convention, $\nabla^0 Z(t) = z(t)$. Terms of order less than p or q which are not included in a polynomial factor are noted ϕ_k or $\theta_k = 0$ following the (p,d,q) notation. The model (2,1,4) $\theta_{2,3} = 0$ thus signifies an AR(2), MA(4) model for a series that has been differenced once for stationarity and with 0 coefficients for the lag 2 and 3 moving average parameters.

When seasonal data are available (e.g., daily, monthly), multiplicative models are introduced, as in $(p,d,q)\,(P,D,Q)_s$, where s denotes the season length, P and Q denote numbers of seasonal autoregressive and moving average terms, and D denotes the number of the seasonal differences of the series. Terms of order less than P or Q are generally not considered present. Additional multiplicative terms can be introduced for additional seasonal effects. Although seasonal models are used mainly with seasonal data, they can be used for periodicities in annual data as well, as will be observed in application below.

Examination of the sample autocorrelation function (SACF) and sample partial autocorrelation function (SPACF) leads to identification of a time series model. Autocorrelation at lag k is the correlation of a series with itself at a lag of k time units. The SACF is a plot of the sample values of autocorrelations at different lags with confidence intervals. Partial autocorrelation at lag k measures the excess correlation not accounted for by a lag k-1 autoregression (Vandaele 1983, p. 87). The SPACF is a plot of sample values of partial autocorrelations with confidence intervals. Autoregressive models are usually identified by an exponential or oscillatory decay in the SACF and spikes in the SPACF at appropriate lags, while the opposite occurs for moving average models (Abraham and Ledolter 1983, p. 250). A mixed ARIMA $(p,0,q)$ model is usually identified by a SACF which tails off after q–p lags or a SPACF which tails off after $p-q$ lags. In practice, determining these patterns can be difficult. Further details on identification, estimation, and forecasting of univariate time series may be found in Box and Jenkins (1976), McCleary and Hay (1980), Vandaele (1983), Pankratz (1983), and Abraham and Ledolter (1983).

Additional methods help to identify the appropriate model (Akaike 1974; Bequin et al. 1980; Tsay and Tiao 1984). The Extended Sample Autocorrelation Function (ESACF), based on iterative autoregressions (Tsay and Tiao 1984), is particularly useful for identification of mixed autoregressive and moving average models for both stationary and nonstationary series. Examples are found below in application and in Tsay and Tiao (1984) and Schnute (1987).

Multivariate time series models are appropriate when several series are analyzed (Kendall et al. 1983). Different approaches to such modeling depend on whether feedback is allowed between the series (Box and Jenkins 1976, Tiao and Box 1981). Multiple time series analysis is defined as the use of independent variables with a single dependent variable (series) (Vandaele 1983, p. 8). Independent variables can be considered as time series or variables measured without error.

The most common multivariate approach is transfer function modeling, which allows feedback only from the independent variables to the dependent variable. The general form of the transfer function for a series $Z(t)$ and a single independent variable $X(t)$ is

$$(2) \quad \nabla^{d} Z(t) = \delta^{-1}(B)\,\omega(B)\,B^{b}X(t) + \phi^{-1}(B)\,\theta(B)\,a(t),$$

where the notation $\delta(B)$ denotes a polynomial in B with coefficients $\{\delta_i\}$. The 0th order term of each polynomial is 1 with the exception of $\omega(B)$, where it is ω_0. The former term in (2) is the relationship between the dependent variable and lag terms of the independent variable; other independent variables are added analogously. The latter term in (2) is the noise process which is modeled as an ARIMA $(p,0,q)$ process.

Identification, estimation, and forecasting of multivariate time series are similar to univariate time series. In analogy to the SACF and SPACF, the cross-correlation function (CCF) between the dependent variable $Z(t)$ and lags of the independent variable $X(t)$ is used in identification of the multivariate time series. If $X(t)$ is itself a time series, then a process known as prewhitening may enhance identification (Box and Jenkins 1976; Liu and Hanssens 1984). Both the dependent and independent variable are fitted with the time series model of the independent variable, and the residuals from the model fits are called the prewhitened series. The impulse response function, related to the cross-correlation of both prewhitened series, aids in identification of the transfer function (Abraham and Ledolter 1983, p. 337–342). Forecasting with transfer function models requires forecasting of each independent variable. The mean of the series is used for forecasting independent variables, when the errors are found to be white noise. Further details on multivariate time series analysis are found in Box and Jenkins (1976), McCleary and Hay (1980), Vandaele (1983), and Kendall et al. (1983).

Data

We used commercial salmon catch data in numbers of fish from SE Alaska and its subareas, southern SE, northern SE, and Yakutat (Alaska Dep. of Fish and Game (ADF&G) 1985a; Eggers 1986). Further details of the preparation of these data are found in Marshall and Quinn (1987). The catch of salmon in weight between 1911 and 1957 was estimated from conversions of product weight information (Marshall and Quinn 1988). The catch of salmon in weight between 1958 and 1985 was estimated from catch sampling by the U.S. Fish and Wildlife Service and ADF&G (Marshall and Quinn 1988).

Environmental data were from a variety of sources. For long-term analyses (since 1911), we located Juneau air temperature data, which was analysed in Juday (1984). For short-term analyses (since 1948), we used "Namias" sea surface temperature (SST), freshwater discharge, and Juneau air temperature. "Namias" sea surface temperature data consisted of monthly means from 27 stations on a 5° grid in the Northeast Pacific Ocean at 60°W, 145°W and eastward from 170°W at 45°N, 50°N, and 55°N (Chelton 1984; Royer 1986). We averaged data over stations. Monthly discharge estimates for SE Alaska were based on a model of Royer (1982) using air temperature and precipitation data between approximately 130°W to 140°W. Monthly estimates of environmental data were averaged into quarterly means for use as independent variables.

Application

Univariate models were constructed for pink, chum, coho, and sockeye salmon series. Results from pink and chum salmon illustrate the time series model-building process. A summary of univariate models is given for all species and subareas in SE Alaska. Multivariate transfer function models were constructed for combined pink and chum salmon series.

All series needed variance-stabilizing transformation of some kind, as deduced from visual inspection of the series and from estimation results. The square-root transformation was most appropriate for even-yr pink, chum, and sockeye salmon series. A logarithmic transformation was most appropriate for odd-yr pink, combined pink, and coho salmon series.

Tentative models for each univariate series were deduced from the SACF, SPACF, and ESACF tables of variance-stabilized series. Acceptable models were determined using a variety of computer software (e.g., BMDP Statistical Software. 1985. 1964 Westwood Blvd., Suite 202, Los Angeles, CA.; AUTOBOX. Automatic Forecasting Systems, Inc. 1984. P.O. Box 563, Hatsboro, PA. 19040). A model was deemed adequate if all parameters were significantly different from zero at a significance level α of at least 0.20 and no significant residual correlations were found in the SACF and SPACF. The Portmanteau test was used to simultaneously test residual series for autocorrelation. After an adequate model was identified and estimated, several alternate models were fitted to the series for diagnostic checking. Model fit was evaluated graphically and with the residual mean square error (RMS), an estimate of the unexplained variability σ^2 not accounted for by the model.

Identification of multivariate transfer function models was based primarily on the cross-correlation and impulse response functions. We discarded significant environmental correlates which appeared to be spurious. For example, a correlation of an environmental variable with pink salmon catch at a lag greater than 2 years, the generation length, is probably meaningless.

Accuracy of model forecasts was evaluated with a reverse-withholding procedure. The five most recent data values were deleted in succession. After each deletion, model parameters were re-estimated, and a one-step-ahead forecast was compared with the deleted data value. Summary statistics were computed from the five one-step-ahead forecast errors.

Univariate Model Results

The sample autocorrelations in the SACF for the odd-yr and even-yr pink salmon series decay rapidly (Fig. 1). This decay, combined with the spiked partial autocorrelation at lag 1 in the SPACF (Fig. 1), suggests an autoregressive (1,0,0) model. For these series, catch in a year is linearly related to the previous catch, which occurred 2 years before, corresponding to the generation length of pink salmon. For combined pink salmon data, the decay in the SACF and the presence of spikes at lags 1 and 2 in the SPACF are evidence for identifying an (2,0,0) model, relating catch in a year to that of two years before. Significant correlations at lag 5 in the SACF and SPACF are considered spurious, being over two generations before the catch.

For even-yr pink salmon, the ESACF table (Fig. 2) indicates an (1,0,0) model from the pointer at position $p=1$, $q=0$. Fitting the (1,0,0) model (Table 1) resulted in residuals that were not significantly autocorrelated. Overfitting an (1,0,1) model resulted in highly correlated parameter estimates and hence a less parsimonious model. Hence, the (1,0,0) model was considered most appropriate.

For odd-yr pink salmon, the ESACF table indicates either a (1,0,0) or a moving average (0,0,1) model (Fig. 2). A (1,0,0) model was fitted to the series (Table 1) with the result that no significant correlations remained in the residuals. Diagnostic procedures indicated that the (1,0,0) model was most appropriate.

For combined pink salmon, the ESACF table (Fig. 2) cannot be interpreted without ambiguity. Either a (2,0,0) or (1,0,1) model are candidates, but an (2,0,0) is the most reasonable biological model. Using the (2,0,0) model, the ϕ_1 estimate of 0.29 was smaller than the ϕ_2 estimate of 0.43, showing the greater relative strength of the two-year generation cycle. Diagnostic procedures showed no problems with this model.

Model fits for the three pink salmon data sets were compared after transformation back to the original catches. The square roots of RMS for the original catches are 9.9, 13.7, and 11.4 for even-yr, odd-yr, and combined data, respectively. These values are high compared to the range of data (3 to 51 million), showing the large amount of variability in pink salmon catches after fitting a model. Nevertheless, the fit of the univariate model for the combined data is not unreasonable (Fig. 3).

Forecasts for pink salmon were made using even- and odd-yr models in succession and by using the combined model. Mean and median absolute percent forecast error and standard deviation over the last 5 years for the combined model are nearly identical to those using even- and odd-yr models (Table 2), suggesting that either approach could be used. Median forecast error is large (33–34%), but the forecasts may still be useful, because the range of data is large as well. Both approaches underforecasted catch in all 5 years, suggesting that a change in the catch process may have occurred, since there is only 1 chance in 2^5 or 32 that this could have occurred at random.

The slow decay of the SACF for the chum series (Fig. 1) may indicate nonstationarity. The high correlations (to around lag 6) in the SACF can also indicate moving average components. Significant correlations at lags 1, 2, 4, and 6 in the SPACF suggest autoregressive terms. Several autoregressive and/or moving average time series models can be considered for chum salmon, generally with terms at lags of 1, 4, and 6. Lag 4 corresponds to the dominant generation length for some stocks of chum salmon. It was impossible to conclusively decide whether the process is stationary. The ESACF table suggests a (1,0,3) model after example 4 in Tsay and Tiao (1984) for a series with a seasonal moving average (Fig. 2). Estimation of this model leads to the conclusions that differencing once is necessary, because the estimate of ϕ_1 was near 1, and that $\theta_2 = 0$; this nonstationary model is (0,1,3) $\theta_2 = 0$.

We found an alternative stationary model by trial and error that had a lower RMS than the previous model: a multiplicative seasonal model $(1,0,0)\ (1,0,0)_4\ (1,0,0)_6$ (Table 1). The fit of the model is acceptable (Fig. 4). The signs of the forecast errors are not the same in all years, in contrast to pink salmon. The distribution of relative errors from the five one-step-ahead forecasts is skewed due to very poor forecasts for 1981 catch. Median absolute percent forecast error is 20% (Table 3).

To determine if common time series structures persisted, we identified time series models for even-yr and odd-

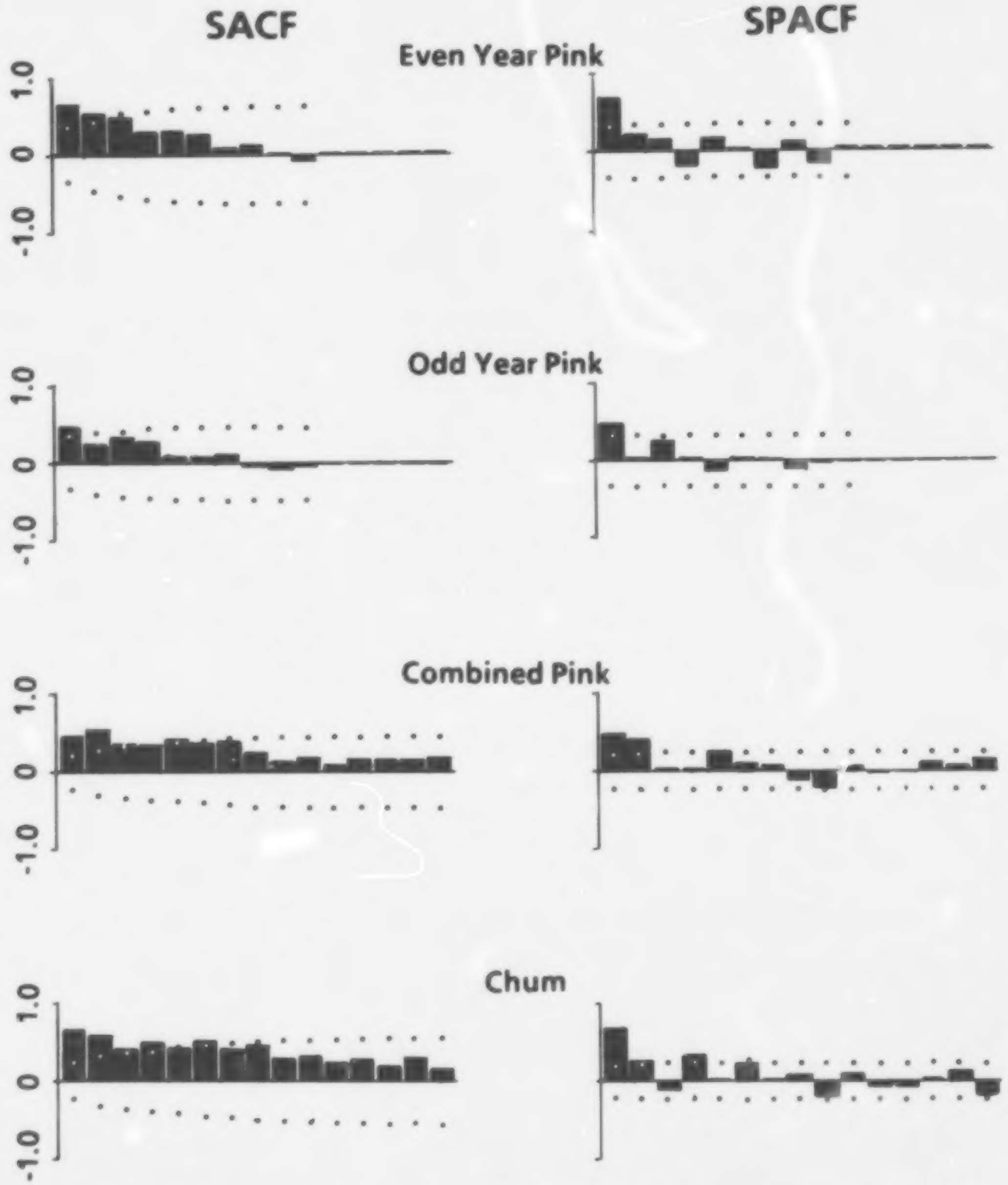

FIG. 1. Sample autocorrelation function (SACF) and sample partial autocorrelation function (SPACF) for transformed long-term even-yr, odd-yr, and combined pink, and chum salmon catch series in SE Alaska with 95% confidence bands.

yr pink, chum, coho, and sockeye salmon series for SE Alaska and its subareas (Table 4). For pink salmon, the (1,0,0) model was identified consistently for all series. For chum salmon, models for the two subareas with catch data had a similar structure to the whole area. Lag 4 appeared in all three chum series. For coho salmon, models were quite different. Only the Yakutat series model contained a lag corresponding with generation length. For sockeye salmon, the most consistent feature found in the models was nonstationarity, as evidenced by the difference term. All sockeye models contained a lag two term, either autoregressive or moving average. Overall, the most common feature in the models was the presence of a lag 1 term, usually autoregressive but sometimes a moving average term. Models were more consistent among areas for a species than among species within an area.

Analysis of catch in weight data produced results almost identical to those for numbers (for details, see Marshall and Quinn 1987). A single notable difference occurs for the even-yr pink salmon series. For even-yr pink salmon, the coefficient of the (1,0,0) term is 0.77 as opposed to 0.67 for the catch in numbers data. This difference may result from the decreasing average weight

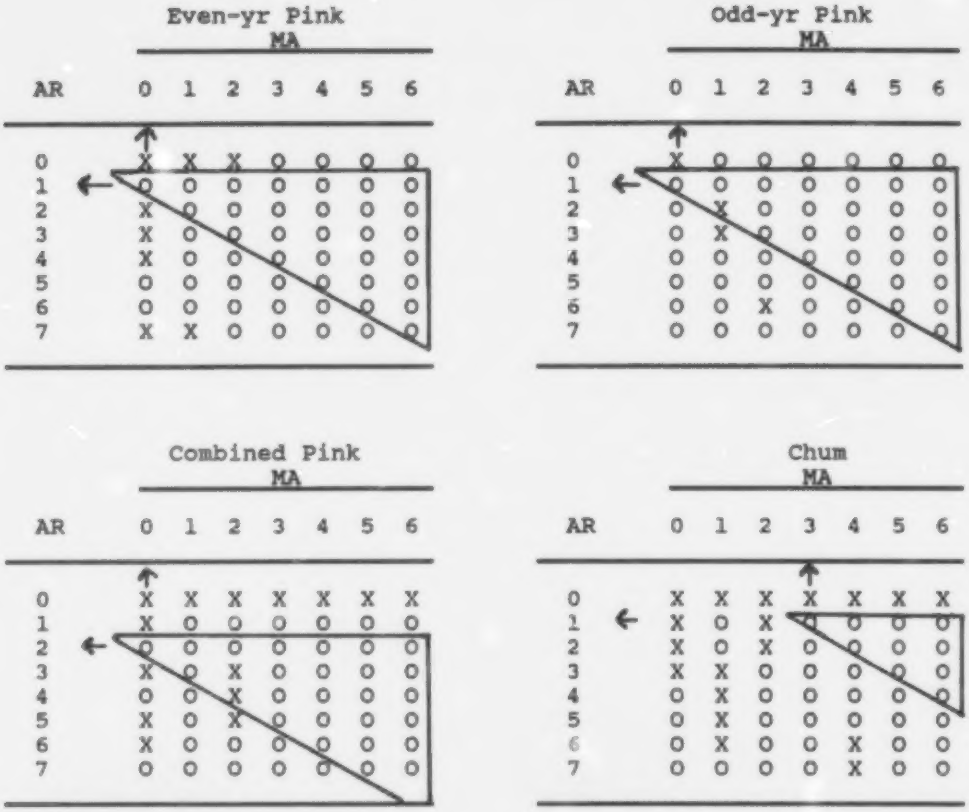

Even-yr Pink

AR \ MA	0	1	2	3	4	5	6
0	X	X	X	O	O	O	O
1	O	O	O	O	O	O	O
2	X	O	O	O	O	O	O
3	X	O	O	O	O	O	O
4	X	O	O	O	O	O	O
5	O	O	O	O	O	O	O
6	O	O	O	O	O	O	O
7	X	X	O	O	O	O	O

Odd-yr Pink

AR \ MA	0	1	2	3	4	5	6
0	X	O	O	O	O	O	O
1	O	O	O	O	O	O	O
2	O	X	O	O	O	O	O
3	O	X	O	O	O	O	O
4	O	O	O	O	O	O	O
5	O	O	O	O	O	O	O
6	O	O	X	O	O	O	O
7	O	O	O	O	O	O	O

Combined Pink

AR \ MA	0	1	2	3	4	5	6
0	X	X	X	X	X	X	X
1	X	O	O	O	O	O	O
2	O	O	O	O	O	O	O
3	X	O	X	O	O	O	O
4	O	O	X	O	O	O	O
5	X	O	X	O	O	O	O
6	X	O	O	O	O	O	O
7	O	O	O	O	O	O	O

Chum

AR \ MA	0	1	2	3	4	5	6
0	X	X	X	X	X	X	X
1	X	O	X	O	O	O	O
2	X	O	X	O	O	O	O
3	X	X	O	O	O	O	O
4	O	X	O	O	O	O	O
5	O	X	O	O	O	O	O
6	O	X	O	O	X	O	O
7	O	O	O	O	X	O	O

FIG. 2. Extended autocorrelation function (ESACF) tables for transformed long-term even-yr, odd-yr, and combined pink, and chum salmon catch series in SE Alaska. X's and O's denote significant and nonsignificant extended autocorrelations, respectively. The right-triangular area mapped is the interpreted extended autocorrelation pattern. The upper left point of the triangle indicates the values of *p* and *q* in an ARIMA (*p,d,q*) model from the row and column, respectively. (See text for details of interpretation.)

of pink salmon in recent years (Marshall and Quinn 1988). The pattern of signs in the forecast errors is the same as the catch in numbers but the absolute error is smaller in every year. As a result the weight series would seem to be more predictable in recent years than the number series. Because catch in weight offered little improvement in forecast accuracy for most series, we used only catch in numbers in multivariate models.

Multivariate Model Results

Long-Term Series

Prewhitening models for Juneau air temperature were either white noise or autoregressive with a lag of 3. For the combined pink salmon series, examination of the CCF (Fig. 5 A,B) and the impulse response function revealed the following potential environmental correlates: Jan.–Mar. temperature at lags of 0, 1, and 2 yr; Apr.–June temperature at lags 6 and 7; July–Sept. temperature at lags 2, 3, and 4; Oct.–Dec. temperature at lag 0. The lag 1 crosscorrelation with Jan.–Mar. temperature is not significant, but it became significant when examining residuals during estimation. Oct.–Dec. temperature at lag 0 is unreasonable since it occurs after the catch that year, and lags greater than 2 probably are spurious. A multivariate model with the remaining variables was fitted to the data and nonsignificant estimates were deleted, producing a final model with Jan.–Mar. temperature at lags 0 and 1 and July–Sept. temperature at lag 2 and a noise model of $(0,0,1)_2$ (Table 1). Not all potential variables appear in the final model, because the significant correlation is explained by a subset of variables, just as in multiple regression. The RMS was similar to the univariate model (Table 1). Diagnostic tests revealed no major problems. The fit of the multivariate model (Fig. 3) was as good as the univariate model and slightly better in recent years. Substantial discrepancies occur among the two models, and many of the actual data points are far away from both fitted models. Forecast errors for the last five years are of the same large magnitude as for the univariate models (Table 2). Therefore, no significant improvement in forecasting pink salmon catch occurred, even though significant environmental factors were found.

For the chum salmon series, examination of the CCF (Fig. 5C) and impulse response function revealed only two potential environmental correlates: July–Sept. temperature at lags 4 and 6. The lag 6 variable shows the strongest relationship but is longer than the usual generation

TABLE 1. Summary of time series models for pink and chum salmon with long-term and short-term data series (T_1: Jan.–Mar. Juneau temperature, T_3: July–Sept. Juneau temperature, T_4: Oct.–Dec. Juneau temperature, D_1: Dec.–Feb. freshwater discharge, S_3: July–Sept. sea surface temperature). All variables are expressed as deviations from the series mean.

Pink Salmon

Long-term Series

Even-yr data, square root transformation, $n = 35$, RMS = 0.111
Univariate Model (1,0,0): $(1 - 0.65B)\ z(t) = a(t)$
t-statistic: (4.8)

Odd-yr data, logarithmic transformation, $n = 36$, RMS = 0.457
Univariate Model (1,0,0): $(1 - 0.53B)\ z(t) = a(t)$
t-statistic: (3.5)

Combined data, logarithmic transformation, $n = 71$, RMS = 0.332
Univariate Model (2,0,0): $(1 - 0.29B - 0.43B^2)\ z(t) = a(t)$
t-statistic: (2.6) (3.9)

Combined data, logarithmic transformation, $n = 71$, RMS = 0.341
Multivariate Model $z(t) = (1 - 0.85B)^{-1}\ 0.047T_1 - 0.057B^2T_3 + (1 + 0.57B^2)\ a(t)$
t-statistic: (6.2) (2.9) (1.4) (5.7)

Short-term Series

Combined data, logarithmic transformation, $n = 38$, RMS = 0.377
Univariate Model $(1,0,0)_2$: $(1 - 0.56B^2)\ z(t) = a(t)$
t-statistic: (3.8)

Combined data, logarithmic transformation, $n = 38$, RMS = 0.363
Multivariate Model $z(t) = 0.027BD_1 + (1 - 0.60B^2)^{-1}\ a(t)$
t-statistic: (1.8) (4.0)

Chum Salmon

Long-term Series

Square root transformation, $n = 74$, RMS = 0.149,
Univariate Model $(1,0,0)\ (1,0,0)_4\ (1,0,0)_6$:
$(1 - 0.56B)\ (1 - 0.25B^4)\ (1 - 0.35B^6)\ z(t) = a(t)$
t-statistic (5.6) (2.2) (3.3)

Square root transformation, $n = 74$, RMS = 0.130,
Multivariate Model:
$z(t) = (-0.028 - 0.056B^2)\ B^4T_3 + [(1 - 0.57B)\ (1 - 0.41B^4)\ (1 - 0.31B^6)]^{-1}\ a(t)$
t-statistic: (1.2) (2.5) (5.6) (3.5) (2.6)

Short-term Series

Square root transformation, $n = 38$, RMS = 0.097
Univariate Model $(1,0,0)\ (1,0,0)_4$: $(1 - 0.50B)\ (1 - 0.55B^4)\ z(t) = a(t)$
t-statistic: (3.3) (3.7)

Square root transformation, $n = 38$, RMS = 0.051
Multivariate Model: $z(t) = 0.38B^5S_3 + 0.038B^4T_4 + (1 - 0.55B^4)^{-1}\ a(t)$
t-statistics: (5.8) (3.2) (5.8)

length of chum salmon; however it is included in the model to represent potential brood effects. A multivariate model was fitted to the data and nonsignificant estimates were deleted, producing a final model with July–Sept. temperature at lags 4 and 6 and a noise model of $(1,0,0)\ (1,0,0)_4\ (1,0,0)_6$ (table 1). The RMS was slightly lower than for the univariate model (Table 1). Diagnostic tests revealed no major problems. The fit of the multivariate model was as good as the univariate model and slightly better in recent time (Fig. 4). No substantial discrepancies occur among the two models, but many of the actual data points are far away from both fitted models. Forecast errors for the last 5 years are of the same large magnitude as for the univariate models (Table 3), but the SD of the relative error is lower. The median and mean relative errors for chum are lower than for pink salmon.

Short-Term Series

Using a time range from 1948 to 1985 allowed us to use three environmental series, but the sample size of 38 may be only marginally adequate for multivariate time series methods. No significant correlations were found in the SACF or SPACF of quarterly discharge or Juneau

TABLE 2. One-step-ahead forecasts of pink salmon using univariate and multivariate time series analyses, and ADF&G forecasts. APE denotes absolute percent error.

Pink univariate (Even/odd long-term)

yr	Forecast	Actual	% Error	APE
81	13.0	19.0	−31.6	31.6
82	16.1	24.3	−33.7	33.7
83	17.2	37.5	−54.1	54.1
84	22.8	25.8	−11.6	11.6
85	24.6	51.0	−51.8	51.8
		median	−33.7	33.7
		mean	−36.6	36.6
		s.d.	17.3	17.3

Pink univariate (combined long-term)

yr	Forecast	Actual	% Error	APE
81	13.3	19.0	−30.0	30.0
82	16.2	24.3	−33.3	33.3
83	19.6	37.5	−47.7	47.7
84	24.9	25.8	−3.5	3.5
85	27.4	51.0	−46.3	46.3
		median	−33.3	33.3
		mean	−32.2	32.2
		s.d.	17.8	17.8

Pink multivariate (long-term)

yr	Forecast	Actual	% Error	APE
81	11.7	19.0	−38.4	38.4
82	19.6	24.3	−19.3	19.3
83	16.3	37.5	−56.5	56.5
84	27.5	25.8	6.6	6.6
85	34.0	51.0	−33.3	33.3
		median	−33.3	33.3
		mean	−28.2	30.8
		s.d.	23.6	19.0

Pink univariate (short-term)

yr	Forecast	Actual	% Error	APE
81	10.6	19.0	−44.2	44.2
82	12.0	24.3	−50.6	50.6
83	13.8	37.5	−63.2	63.2
84	16.3	25.8	−36.8	36.8
85	20.9	51.0	−59.0	59.0
		median	−50.6	50.6
		mean	−50.8	50.8
		s.d.	10.7	10.7

Pink multivariate (short-term)

yr	Forecast	Actual	% Error	APE
81	10.8	19.0	−43.2	43.2
82	13.5	24.3	−44.4	44.4
83	12.3	37.5	−67.2	67.2
84	19.4	25.8	−24.8	24.8
85	26.0	51.0	−49.0	49.0
		median	−44.4	44.4
		mean	−45.7	45.7
		s.d.	15.1	15.1

Pink by ADF&G

yr	Forecast	Actual	% Error	APE
81	10.6	19.0	−44.2	44.2
82	25.5	24.3	4.9	4.9
83	13.5	37.5	−64.0	64.0
84	29.6	25.8	14.7	14.7
85	32.1	51.0	−37.1	37.1
		median	−37.1	37.1
		mean	−25.1	33.0
		s.d.	33.6	23.6

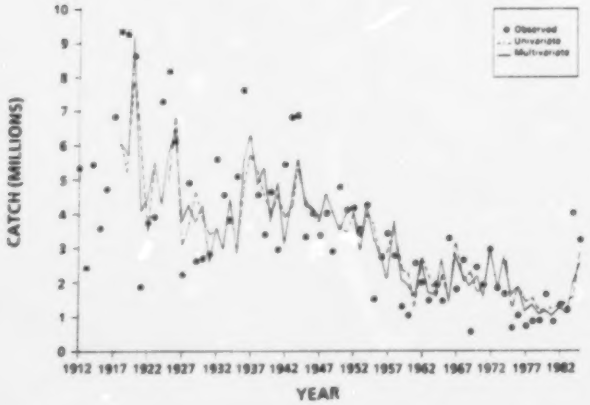

FIG. 3. Observed catch and fitted values from univariate and multivariate time series models for the long-term series for pink salmon.

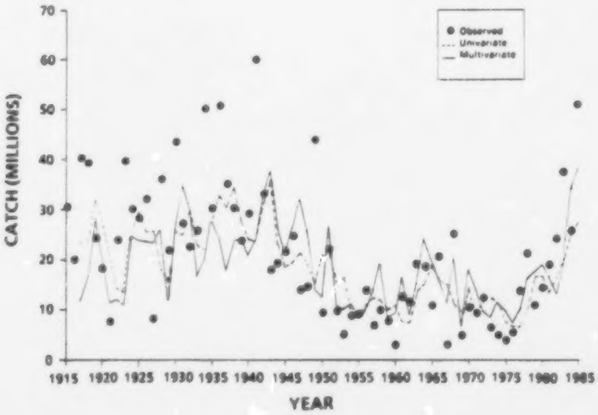

FIG. 4. Observed catch and fitted values from univariate and multivariate time series models for the long-term series for chum salmon.

TABLE 3. One-step-ahead forecasts of chum salmon using univariate and multivariate time series analyses, and ADF&G projections. APE denotes absolute percent error.

Chum univariate (long-term)

Yr	Forecast	Actual	% Error	APE
81	1.36	0.85	60.0	60.0
82	1.24	1.36	−8.8	8.8
83	1.44	1.20	20.0	20.0
84	1.65	4.05	−59.3	59.3
85	2.89	3.27	−11.6	11.6
		median	−8.8	20.0
		mean	0.1	31.9
		s.d.	43.9	25.6

Chum multivariate (long-term)

Yr	Forecast	Actual	% Error	APE
81	1.04	0.85	22.4	22.4
82	1.24	1.36	−8.8	8.8
83	1.08	1.20	−10.0	10.0
84	1.96	4.05	−51.6	51.6
85	2.51	3.27	−23.2	23.2
		median	−10.0	22.4
		mean	−14.3	23.2
		s.d.	26.8	17.2

Chum univariate (short-term)

Yr	Forecast	Actual	% Error	APE
81	1.28	0.85	50.6	50.6
82	1.07	1.36	−21.3	21.3
83	1.29	1.20	7.5	7.5
84	1.70	4.05	−58.0	58.0
85	1.98	3.27	−39.4	39.4
		median	−21.3	39.4
		mean	−12.1	35.4
		s.d.	42.6	20.8

Chum multivariate (short-term)

Yr	Forecast	Actual	% Error	APE
81	0.29	0.85	−65.9	65.9
82	1.56	1.36	14.7	14.7
83	1.04	1.20	−13.3	13.3
84	2.61	4.05	−35.6	35.6
85	2.49	3.27	−23.9	23.9
		median	−23.9	23.9
		mean	−24.8	30.7
		s.d.	29.6	21.6

Chum by ADF&G

Yr	Projection	Actual	% Error	APE
81	0.90	0.85	5.9	5.9
82	1.30	1.36	−4.4	4.4
83	1.00	1.20	−16.7	16.7
84	1.30	4.05	−67.9	67.9
85	2.20	3.27	−32.7	32.7
		median	−16.7	16.7
		mean	−23.2	25.5
		s.d.	28.9	26.3

TABLE 4. Time series models identified for SE Alaska salmon catches for even-yr and odd-yr pink, chum, coho, and sockeye salmon. See text for model notation. "—" indicates lack of data.

Area[a]	Even-yr Pink	Odd-yr Pink	Chum	Coho	Sockeye
SE	(1,0,0)	(1,0,0)	$(1,0,0)(1,0,0)_4(1,0,0)_6$	$(1,0,0)(0,0,1)_6$	$(0,1,0)(1,0,0)_6(0,0,1)_2$
SSE	(1,0,0)	(1,0,0)	$(1,0,0)(1,0,0)_4(1,0,0)_5$	(0,1,1)	$(0,1,0)(0,0,1)_2$
NSE	(1,0,0)	(1,0,0)	$(1,0,0)(1,0,0)_4(1,0,0)_5$	$(0,0,1)_7$	(0,1,2)
YAK	—	—	—	$(1,0,0)(0,0,1)_4$	(2,1,0)

[a] Area abbreviations: SE: SE Alaska, SSE: Southern SE Alaska, NSE: Northern SE Alaska, YAK: Yakutat.

air temperature. Significant correlations at lag 1 in the Apr.–June SST and at lag 2 in the Oct.–Dec. SST were found. Nevertheless, we forecast each environmental series by its mean for consistency and simplicity.

Univariate analysis of the short-term pink and chum salmon series produced models similar to, but not the same as, the models found for the long-term series (Table 1). Pink salmon were modeled with the seasonal model $(1,0,0)_2$ for consistency with the long-term series. The best chum salmon model found was a multiplicative autoregressive model with lags at one and four, $(1,0,0)(1,0,0)_4$. The 6-year cyclic pattern found in the long-term chum series is not significant in the short-term series.

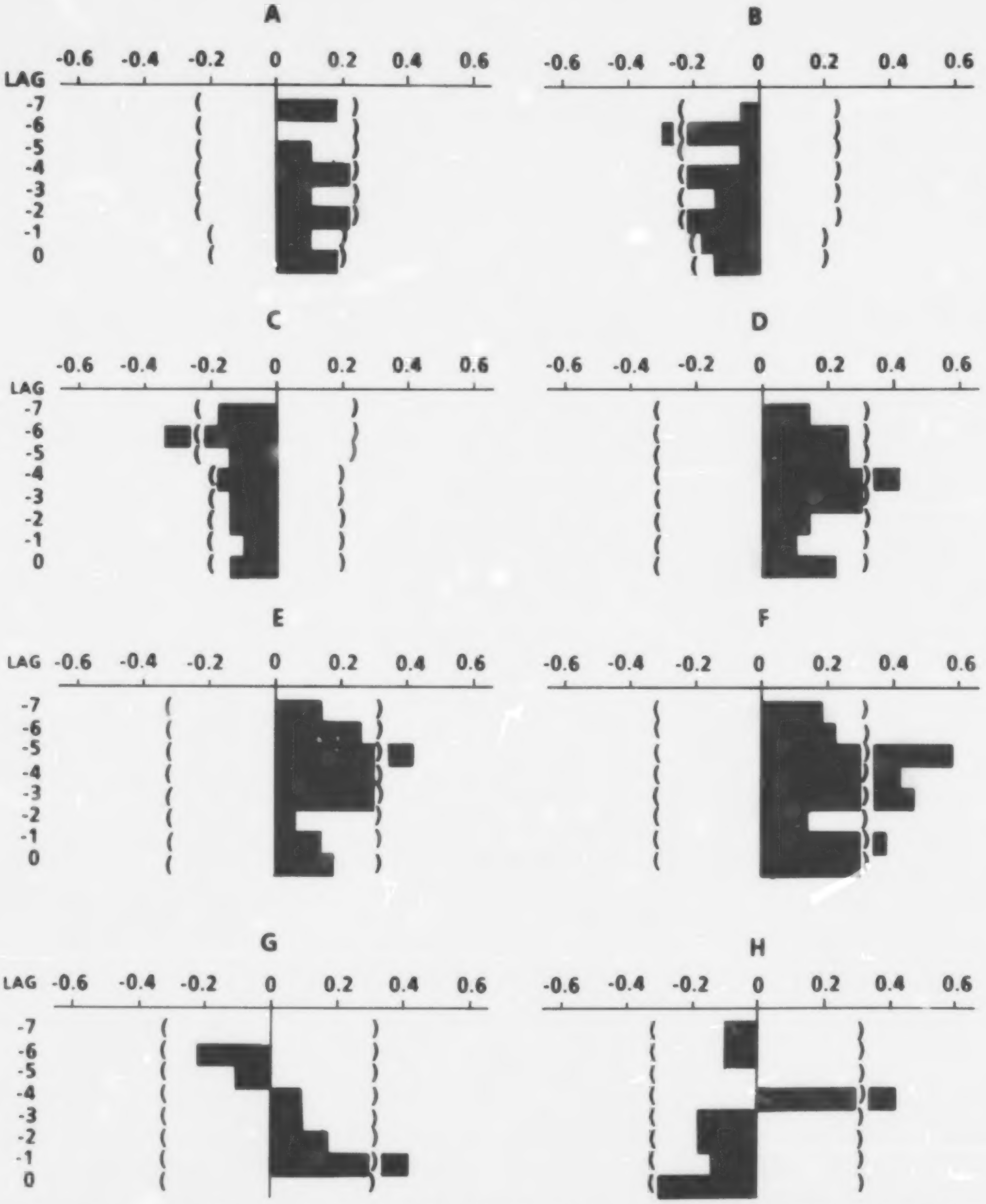

FIG. 5. Cross-correlation function (CCF) of transformed pink and chum salmon catch data with selected environmental variables with 95% confidence bands. A: long-term pink salmon catch with Jan.–Mar. air temperature, B: long-term pink with July–Sept. air temperature, C: long-term chum with July–Sept. air temperature, D: short-term chum with Jan.–Mar. SST, E: short-term chum with Apr.–June SST, F: short-term chum with July–Sept. SST, G: residuals from first short-term pink multivariate model with Dec.–Feb. freshwater discharge, H: residuals from first short-term chum multivariate model with Oct.–Dec. air temperature.

Significant cross-correlations between the environmental series and the pink series were not found without prewhitening. Prewhitening the pink series revealed a significant correlation with Jan.–Mar. temperatures lagged one year and a stronger correlation with Dec.–Feb. discharge lagged one year (Fig. 5G). A transfer function between the Dec.–Feb. discharge and pink catches was then estimated (Table 1) with a $(1,0,0)_2$ noise model, resulting in a significant discharge parameter estimate. The fit of the multivariate model was about the same as for the univariate (Fig. 6). The multivariate model produced only 4% reduction in the RMS and marginal improvement in average forecast error (Table 2).

For chum salmon, catch is significantly correlated with Jan.–Mar. SST at lag 4, Apr.–June SST at lag 5, and July–Sept. SST at lags 1, 3, 4, and 5 (Fig. 5 D,E,F); all are plausible given the 3, 4 and 5 year age of returns in SE Alaska. We first constructed a transfer function model

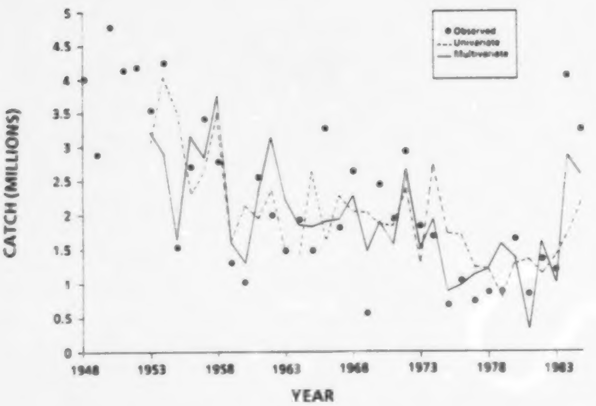

FIG. 6. Observed catch and fitted values from univariate and multivariate time series analyses for the short-term series for pink salmon.

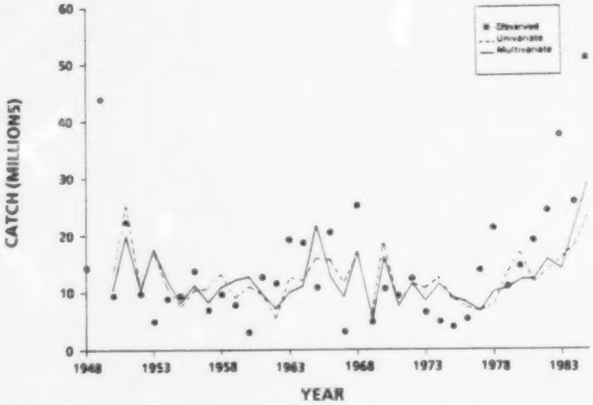

FIG. 7. Observed catch and fitted values from univariate and multivariate time series analyses for the short-term series for chum salmon.

having an $(1,0,0)_4$ noise model with July–Sept. SST at lag 5, which had an RMS of 0.066. We then found that July–Sept. SST at lag four could also be included with improved fit (RMS of 0.055). Residuals from the former model were significantly cross-correlated with Oct–Dec. Juneau air temperature at lag 4 (Fig. 5H). A model with July–Sept. SST at lag 5 and Oct.–Dec. air temperature at lag 4 had the lowest RMS of the three models (RMS = 0.051, Table 1). The RMS is much lower than for the univariate model (0.097), and its fit was better than the univariate model (Fig. 7). This model also provides better forecasts than the univariate model (Table 3).

Preliminary forecasts of the commercial pink salmon harvest in SE Alaska and preliminary projections of commercial harvests of chum salmon in SE Alaska are published yearly by the Alaska Department of Fish and Game (ADF&G 1985b). Preliminary forecasts of pink salmon harvests are made by a variety of methods including multiple linear regressions with pre-emergent fry indices and temperature indicators as predictor variables. ADF&G forecasts of pink salmon harvests error are, on average, similar to the time series models (Table 2). The signs of all odd-yr pink salmon forecast errors are the same between the ADF&G and (1,0,0) models. However, a similar correspondence between the signs of the forecast errors for even-yr catches from the two methods is not present.

Preliminary ADF&G projections of chum salmon harvests are averages of recent harvests subjectively modified by qualitative information. The ADF&G projection error, on average, is similar to time series models (Table 3). The presence of the autoregressive component at lag 1 in the time series models produces a forecast that is based strongly on the previous year's catch. The ADF&G projection is based on a similar philosophy.

Graphical Analysis

As before, a square root or logarithmic transformation was applied to stabilize the variance of each series. The Lowess scatterplot smoother (Cleveland 1979) in the *S* data analysis and graphics program was then used to extract a smoothed series from each variance stabilized series. The smoothing window used was 0.3 times the width of the series. The Lowess algorithm provides a robust fit to the central portion of the time series and a less robust fit at the ends. The values for each smoothed series were transformed back to the original scale and then normalized to a range between 0 and 1 so that the trends could be easily compared.

The smoothed commercial catch trends of even-and odd-yr pink, chum, coho, and sockeye salmon in SE Alaska (Fig. 8) show a similar U-shaped pattern: a pronounced decline between roughly 1940 and 1955, a low level period between 1955 and 1970, followed by a rapid increase to 1985. One exception is chum salmon, which has not increased in recent times. Similarities in trend in even-yr pink salmon catches in SE Alaska, Prince William Sound, Cook Inlet, and Kodiak (Fig. 9) include one U-shaped pattern between roughly 1940 and 1960 followed by a second U-shaped pattern between 1960 and 1980. Although differences in trend are also present for some time periods, similarities in trend much of the time suggest that large-scale phenomena affect salmon catches.

Discussion

This study is the first attempt to model Alaska salmon catches with univariate and multivariate time series analysis. Time series analysis provided reasonable models to explain salmon catch series in terms of model fit and meeting model assumptions. Data transformations were generally needed to stabilize the variance of the time series process, which is consistent with other models of catch data (e.g., Quinn 1985). Most models contained an autoregressive term at lag one, suggesting that catch in a given year is related to the catch that occurred in the previous year (or 2 years before for pink salmon). Generation length of a species was sometimes absent from a time series model (Table 4), indicating that a spawner-recruit relationship is not evident in those series. Some series appeared to be well represented by a stationary

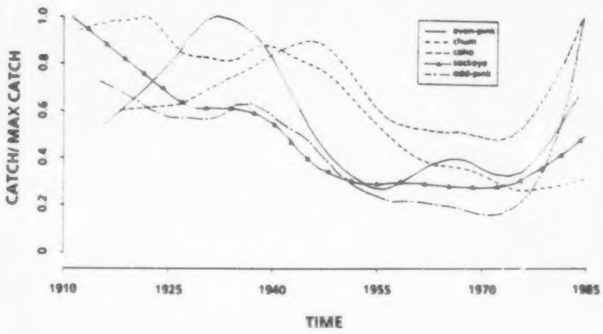

FIG. 8. Trends in salmon catches in SE Alaska for even- and odd-yr pink, chum, coho, and sockeye salmon. Data were smoothed by Lowess algorithm with a window of 0.3 and scaled by maximum smoothed catch.

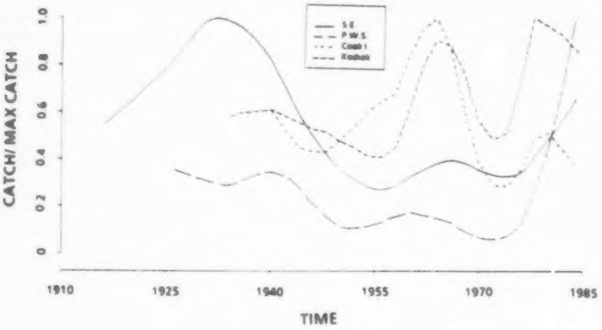

FIG. 9. Trends in even-yr salmon catches in SE Alaska, Prince William Sound, Cook Inlet, and Kodiak. Data were smoothed by Lowess algorithm with a window of 0.3 and scaled by maximum smoothed catch.

model, while others were not. Lack of stationarity implies that the process generating the catches changed over the time period, which complicates the understanding of long-term phenomena affecting the series.

Univariate models for pink salmon, the species with the shortest generation length, were simple autoregressive models. Although the AR models fit the series acceptably, the median absolute percent forecast errors are the highest from any species (Marshall and Quinn 1987). Because similar errors occur with the ADF&G model, univariate models are benchmarks for establishing unexplained variability.

Univariate models for chum salmon were more complicated. Both stationary and nonstationary series were entertained based on the identification process. Chum series models contained lags of 1, 4, 5, or 6 years. Median forecast error was slightly smaller than for pink salmon, suggesting that age structure may mediate variability in the system.

In general, the large forecast errors from univariate models indicate that catch data alone cannot give accurate forecasts. Furthermore, recent forecasts have usually underestimated the actual catch, due to the unprecedented rise in catch in recent years. Using short data series with multiple regression analysis (used by ADF&G for pink salmon) does not improve forecast accuracy. Using catch in biomass rather than numbers offers no substantial improvement. The use of short-term data generally increased forecast error over that obtained using long-term data in our time series modeling. Using data over a longer time period increases the chances of encountering the varying conditions faced by the species over time. The use of seasonal data has proved beneficial for increasing sample size in time series modeling with short-term data, but there is the risk of obtaining significant relationships that would not persist over a longer period.

The use of environmental data in multivariate models may be the best approach for improving forecast accuracy. Explaining salmon catch based on correlation patterns with environmental data is speculative. However, such patterns may suggest useful mechanisms for further examination. For long-term pink salmon data, the multivariate time series model included winter temperature in the year of catch as a positive effect, possibly related to ocean survival, and summer temperature two years before as a negative effect, which would have involved the parents of the returning generation. The short-term series included winter freshwater discharge in the previous year as the only significant correlate, suggesting an effect on eggs or emerging fry. Spawning effects may be indicated in the noise component of the two models as a lag 2 term.

For long-term chum salmon data, the multivariate model included autumn air temperature 4 and 6 years before as negative effects, which would have involved the parents of the returning generation. For the short-term series, the model included a positive winter temperature effect 4 years before, which would have involved eggs, and a positive effect of autumn sea surface temperature 5 years before. The lag 4 terms in the noise component of both data sets suggest spawning effects corresponding to the major age of return. Mechanisms by which sea surface temperature lagged 5 years might affect catch presumably relate to parental factors affecting survival of progeny. Such mechanisms were proposed to explain a strong correlation between sea surface temperature lagged 2 years and odd-yr pink salmon survival in Prince William Sound (Willette 1985).

Multivariate models for pink salmon had about the same forecast error as univariate models, but multivariate models for chum salmon had lower forecast errors than univariate models. It appears that the longer generation length and age structure of chum salmon makes forecasting for chum salmon more successful than for short-lived pink salmon, although models are more complicated.

The transfer function models we constructed did not exploit the total range of available environmental data or transformations of the data that might explain salmon catches. Using data from smaller areas, shorter time periods, different groupings or statistics from the data, or other auxiliary information on returns, enhancement, and environment could perhaps improve the models. Further work is also needed to determine if reasonable mechanisms can be found to explain the terms in the transfer function models. Multivariate models allowing for feedback (Cohen and Stone 1987) may also prove to be useful.

Graphical analysis of the salmon time series showed similar time trends among species in SE Alaska and pink salmon across all Alaskan areas. If series were independent realizations of time series processes, then such similar trends could not result. Such consistency suggests that there may exist underlying biological, environmental, or economic variables that drive salmon catch dynamics. In contrast, the lack of consistency in time series models across areas for some species (Table 4) suggests that localized phenomena affect the series as well.

Factors affecting salmon catches include biological factors related to stock and recruitment, fishery factors related to management considerations, and environmental factors, which can influence each of the former factors. Univariate time series analysis subsumes these factors into time series parameters which generally cannot be identified with regard to these underlying processes. One exception is the generation length of each salmon species, which is often present in the time series model. Multivariate models with environmental data offer limited improvement. As a result of the influence of multiple competing processes, the system contains substantial variability which precludes precise projections of the future of this system and masks correlative processes. The difficulty of determining stationarity of the time series of salmon catches could easily be a result of changes in the underlying processes over time. To resolve this conundrum, better auxiliary information on underlying processes is needed; otherwise the status quo forecast error of 20–40% or more can be expected.

Acknowledgments

This work is the result of research funded by the Alaska Sea Grant College Program supported by NOAA, Office of Sea Grant and Extramural Programs under grant NA86AA-D-SG041 projects R/06-26 and A/75-01, and by the University of Alaska Fairbanks with funds appropriated by the state. Phil Mundy originated this research topic and discussed results with us. Amir Aczel (University of Alaska Juneau) helped us with his perspectives on time series problems and obtained the ESACF program from Ruey Tsay (Carnegie-Mellon University). Discussions with Scott Marshall, Leon Shawl, John E. Clark, Douglas Eggers, and Samuel Sharr (ADF&G), and Paul Tukey (Bell Labs) contributed to the analysis. Hal Geiger and Doug Jones of ADF&G provided the Juneau air temperature data. Tom Royer (University of Alaska Fairbanks) was instrumental in providing access to and interpretation of environmental data series. We thank an anonymous referee for helpful comments.

References

ABRAHAM, B., AND J. LEDOLTER. 1983. Statistical methods for forecasting. John Wiley & Sons, New York, NY 445 p.

ALASKA DEPARTMENT OF FISH AND GAME (ADF&G). 1985a. Alaska commercial salmon catches, 1878-1984. Div. Commercial Fish, Juneau, AK. 54 p.

1985b. Preliminary forecasts and projections for 1985 Alaska salmon fisheries. Info. Leafl. 224: 53 p.

AKAIKE, H. 1974. A new look at the statistical model identification. IEEE Trans. Automat. Contr. AC-19: 716–723.

ALEXANDERSDOTTIR, M., AND O. A. MATHISEN. 1983. Life history of pink salmon (*Oncorhynchus gorbuscha*) and implications for management. Univ. Wash., Fish. Res. Inst., Seattle, WA, FRI-UW 8313: 72 p.

BEQUIN, J. M., C. GOURIEROUX, AND A. MONFORT. 1980. Identification of a mixed autoregressive moving average process: the corner method, p.423–435. *In* O.D. Anderson [ed.] Time Series. North-Holland, Amsterdam.

BOX, G. E. P., AND G. M. JENKINS. 1976. Time series analysis: forecasting and control, 2nd ed. Holden-Day, San Francisco, CA. 575 p.

CHELTON, D. 1984. Commentary: short term climatic variability in the northeast Pacific Ocean, p. 87-89. *In* W. Pearcy [ed.] The Influence of Ocean Conditions on the Production of Salmonids in the North Pacific. Oregon State University, Sea Grant College Program, Corvallis, OR, ORESU-W-83-001.

CLARK, J. E., M. S. PRITCHETT, AND J. L. WELLER. 1986. Age, sex, and size of chum salmon (*Oncorhynchus keta* Walbaum) catches and escapements in southeastern Alaska, 1985. Alaska Dep. Fish & Game, Tech. Data Rep. 169: 46 p.

COHEN, Y., AND J. N. STONE. 1987. Multivariate time series analysis of the Canadian fisheries system in Lake Superior. Can. J. Fish. Aquat. Sci. 44 (Suppl. 2): 171–181.

COOLEY, R. A. 1961. Decline of the Alaska salmon: a case study in resource conservation policy. Ph.D. thesis, Univ. Michigan, Ann Arbor, MI. 350 p.

CLEVELAND, W. S. 1979. Robust locally weighted regression and smoothing scatterplots. J. Am. Stat. Assoc. 74: 829–836.

EGGERS, D. M. 1986. Preliminary forecasts and projections for 1986 Alaska salmon fisheries. Alaska Dep. Fish & Game, Inform. Leafl. 253: 55 p.

EGGERS, D. M., C. P. MEACHUM, AND D. C. HUTTUNEN. 1984. Population dynamics of Bristol Bay sockeye salmon, p. 200–225. *In* W. Pearcy [ed.] The Influence of Ocean Conditions on the Production of Salmonids in the North Pacific. Oregon State University, Sea Grant College Program, Corvallis, OR, ORESU-W-83-001.

FRIED, S. M., AND H.Y. YUEN. 1986. A synopsis and critique of forecasts of sockeye salmon (*Oncorhynchus nerka*) returning to Bristol Bay in 1986. Alaska Dep. Fish & Game, Inform. Leafl. 255: 37 p.

JENSEN, A. L. 1985. Time series analysis and the forecasting of menhaden catch and CPUE. N. Am. J. Fish. Manage. 5: 78–85.

JUDAY, G. P. 1984. Temperature trends in the Alaska climate record: problems, update, and prospects, p. 76–91. *In* J.H. Barth [ed.] The Potential Effects of Carbon Dioxide-induced Climatic Changes in Alaska. School of Agriculture and Land Resource Management, Univ. of Alaska Fairbanks, Fairbanks, AK.

KENDALL, M., A. STUART, AND J. K. ORD. 1983. The Advanced Theory of Statistics, Vol. 3: Design and Analysis, and Time-series, 4th ed. Griffin, London. 780 p.

LIU, LON-MU, AND D. M. HANSSENS. 1984. Identification of multiple-input transfer function models via least squares. BMDP Tech. Rep. 68: 25 p.

MARSHALL, R. P., AND T. J. QUINN II. 1987. Univariate time series analysis of commercial catches of pink, chum, coho, and sockeye salmon in Alaska fisheries. Juneau Center for Fisheries and Ocean Sciences, University of Alaska, Juneau AK, Report UAJ SFS-8717: 140 p.

1988. Estimation of average weight and biomass of pink, chum, sockeye, and coho salmon in Southeastern Alaska commercial harvests. Alaska Dep. Fish. & Game, Comm. Fish. Div., Fishery Research Bull. 88-07: 52 p.

McCleary, R., and R. A. Hay, Jr. 1980. Applied time series analysis for the social sciences. Sage, Beverly Hills, CA. 331 p.

Mendelssohn, R. 1981. Using Box-Jenkins models to forecast fishery dynamics: identification, estimation, and checking. U.S. Fish. Bull. 78: 887–896.

Mendelssohn, R., and P. Cury. 1987. Fluctuations of a fortnightly abundance index of the Ivoirian coastal pelagic species and associated environmental conditions. Can. J. Fish. Aquat. Sci. 44: 408–421.

Pankratz, A. 1983. Forecasting with univariate Box–Jenkins models: concepts and cases. John Wiley & Sons, New York, NY. 562 p.

Pearcy, W. [ed.] 1984. The Influence of Ocean Conditions on the Production of Salmonids in the North Pacific. Oregon State University, Sea Grant College Program, Corvallis, OR, ORESU-W-83-001: 327 p.

Quinn, T. J. II. 1985. Catch-per-unit-effort: A statistical model for Pacific halibut. Can. J. Fish. Aquat. Sci. 42: 1423–1429.

Royer, T. C. 1982. Coastal fresh water discharge in the northeast Pacific. J. Geophys. Res. 87: 2017–2021.

1986. Temperature fluctuations in the northeast Pacific from 1954 to 1985 in response to El Nino/southern oscillations and longer period forcing. Int. North Pac. Fish. Comm. Bull. 47: 203–208.

Saila, S. B., M. Wigbout, and R. J. Lermit. 1980. Comparison of some time series models for the analysis of fisheries data. J. Cons. Cons. int. Explor. Mer 39: 44–52.

Schnute, J. 1987. Data uncertainty, model ambiguity, and model identification. Natural Resource Modeling 2: 159–212.

Tiao, G. C., and G. E. P. Box. 1981. Modeling multiple time series with applications. J. Am. Stat. Assoc. 76: 802–816.

Tsay, R. S., and G. C. Tiao. 1984. Consistent estimates of autoregressive parameters and extended sample autocorrelation function for stationary and nonstationary ARMA models. J. Am. Stat. Assoc. 79: 84–96.

Vandaele, W. 1983. Applied time series analysis and Box–Jenkins models. Academic Press, Orlando, FL. 417 p.

Willette, T. M. 1985. The effects of ocean temperatures on the survival of the odd- and even-year pink salmon (*Oncorhynchus gorbuscha*) populations originating from Prince William Sound, Alaska. M.S. thesis, Univ. of Alaska, Fairbanks, AK. 115 p.

Distribution, Size Composition, and Abundance of the Pacific Hake *(Merluccius productus)* Along the Pacific Coast of North America in 1985

M. A. Stepanenko

Pacific Research Institute for Fisheries and Oceanography (TINRO), Vladivostok, USSR

Abstract

STEPANENKO, M. A. 1989. Distribution, size composition, and abundance of the Pacific hake (*Merluccius productus*) along the Pacific coast of North America in 1985, p. 81–86. *In* R. J. Beamish and G. A. McFarlane [ed.] Effects of ocean variability on recruitment and an evaluation of parameters used in stock assessment models. Can. Spec. Publ. Fish. Aquat. Sci. 108.

The condition of the Pacific hake (*Merluccius productus*) stock off the west coast of North America was evaluated. Estimated abundance from ichthyoplankton catches and trawl and acoustic data, shows that during the early 1980's the biomass of the population was at a level close to the historical maximum. The trawl and acoustic data make it possible to evaluate the population in the post-spawning period. The distribution and catch per unit effort of 1-year-olds can be used to estimate the strength of a year-class and to predict the potential catch 3–5 years later.

Résumé

STEPANENKO, M. A. 1989. Distribution, size composition, and abundance of the Pacific hake (*Merluccius productus*) along the Pacific coast of North America in 1985, p. 81–86. *In* R. J. Beamish and G. A. McFarlane [ed.] Effects of ocean variability on recruitment and an evaluation of parameters used in stock assessment models. Can. Spec. Publ. Fish. Aquat. Sci. 108.

L'état du stock de merlu du Pacifique (*Merluccius productus*) dans les eaux au large de la côte ouest de l'Amérique du Nord a été évalué. L'abondance estimée à partir des prises d'ichtyoplancton et des données de chalutage et des données acoustiques, montre qu'au début des années 1980 la biomasse de la population s'approchait du niveau maximal antérieur. Les données de chalutage et les données acoustiques ont permis d'évaluer la population pendant la période qui suit la fraye. La répartition et les captures par unité d'effort des poissons âgés d'un an peuvent être utilisées pour évaluer l'effectif d'une classe annuelle et prévoir le prises possibles de 3 à 5 ans plus tard.

Introduction

Pacific hake (*Merluccius productus*) is the most abundant commercially important species off the west coast of Canada and the southern United States. The offshore stock has been fished commercially since the mid-1960's and catches in the last few years have reached the quotas imposed by Canada and the United States. In this paper I present the results of studies conducted in 1985 on the distribution, abundance and biology of hake off the Pacific coast of North America.

Materials and Methods

Information on the distribution of the 1984 year-class was obtained from test trawls performed during the first ichthyoplankton survey made off northern California at the end of March and beginning of April, 1985.

Standard trawl and acoustic surveys were conducted in the region 37°160′N to 48°20′N during May 12–28, 1985 to evaluate the condition of the hake stock, study its behavior, and to collect biostatistical information.

Trawl and acoustic survey transects were run at intervals of 10 nm. The transects extended seaward from the 3-mile territorial waters to the extreme of the hake distribution or to the 600-m isobath (when no stocks were observed). The survey was carried out during daylight hours. Regular trawl hauls were conducted to verify echogram targets and to obtain catch per unit effort estimates of fish density. The pelagic trawl hauls were carried out using a 58/370-m trawl with a 30-m vertical by 40-m horizontal opening. The average trawling speed was 3.5 knots.

Estimation of the hake pelagic stock biomass was made using the equation:

$$Q = \sum_{1}^{n} \frac{Y \cdot A \cdot H}{a \cdot h} \cdot K, \text{ where}$$

Q — hake stock biomass in tons;
Y — catch per unit effort in tons (an average catch for the equilibrium catch zone);
A — zone (stock) area, sq km;
a — control trawling area (0.259 sq km);
H — average height of schools in a stock, m;
h — vertical trawl opening;
K — catchability coefficient;
n — number of trawl hauls.

Estimation of the hake spawning population biomass in 1985 was made on the basis of larvae sampled during the ichthyoplankton survey off California from March 15 to April 5, 1985 in cooperation with the Southwest Fisheries Center (National Marine Fisheries Service). A double CalCOFI bongo net with a 0.707-m diameter opening was used for the icthyoplankton sampling.

When estimating the hake spawning population biomass (S), the following equation was used:

$$S = K_1 K_2 \sum_{i=1}^{n} a_i d_i t \,(fbcr)^{-1}, \text{ where}$$

a_i — number of 10 sq m areas in the survey region;
d_i — number of the larvae per 10 sq m (average number in the equilibrium catch zone);
t — survey duration;
f — fecundity (per unit of female biomass);
b — spawning fraction (ratio of spawning female biomass to the total mature female biomass);
c — sex composition (ratio of female biomass to the total biomass of the mature population);
r — duration of the eggs incubation at a certain temperature;
K_1— coefficient defined as: $K_I = \frac{E}{L}$, where
E — total quantity of registered eggs in the spawning area;
L — quantity of eggs without anomaly in development;
K_2— percentage of hake spawning at the survey period during an average statistical year.

Preliminary data on the distribution of post-spawning aggregations of hake were obtained during the hydroacoustic survey over the shelf and upper part of the continental slope off California and Oregon on April 13-16.

Test trawling on the pelagic concentrations of hake was conducted using a 57/350-m trawl, while northern catches were made using a 43-m trawl. The duration of pelagic hauls was controlled using a cable control apparatus (type MTOK-M), and was limited to 15-30 min. Bottom trawl hauls of up to 1 hour in duration were performed when the seabed surface was suitable.

Results and Discussion

Rates of catch per unit effort increased steadily off of California, Oregon and Washington throughout the spring months. Results of the test trawling are shown in Table 1. Maximum catches were obtained off Oregon in May and June, and catch per unit effort was practically identical in northern California and Oregon.

Large concentrations of young hake were encountered in the coastal shelf zone between Cape Conception and Monterey Bay (34°10′N-36°30′N). In the Monterey Bay region, large aggregations of 1-year-olds were located over great depths outside the shelf zone. These fish were scarcely feeding at all, and the aggregations were moving in a northerly direction.

The northerly migration of hake along the coast was unusually slow in comparison with earlier years. In the previous 5 years, large accumulations in mid-April were observed as far north as the boundary of Canadian waters. In April 1985 schools were not found further north than Cape Blanco (southern Oregon, 42°50′N).

TABLE 1. Results of test trawling using pelagic and bottom trawls on the aggregations of Pacific hake in March-June, 1985 (catch per hour of trawling).

		Northern California				Washington-Oregon			
Month	Gear used	No. of hauls	Total catch	Mean catch /h	Max. haul	No. of hauls	Total catch	Mean catch /h	Max. haul
March	57/350	1	2.5	2.50	2.50	—	—	—	—
	43	3	1.7	0.56	1.40	—	—	—	—
April	57/350	4	17.3	3.96	11.84	1	9.9	11.99	11.99
	43	2	0.9	0.40	0.51	4	1.4	0.35	1.4
May	57/350	13	89.2	13.30	48.0	32	18.42	13.37	72.9
	43	10	12.9	2.02	8.69	29	11.9	0.6	3.34
June	57/350	—	—	—	—	14	35.8	16.09	75.0
	43	—	—	—	—	17	1.8	0.21	2.38

Later studies investigated this unusual slowness and the delayed appearance of hake to the north, especially of the abundant 1980 year-class (Fig. 1). Because the peak of hake spawning took place at the end of winter and early spring, the late migration cannot be explained by delayed spawning, but rather by their feeding behavior in the part of the region where they forage. Test trawling, conducted at the time of the standard ichthyoplankton hauls during April and May support this hypothesis. In all of the collections, the most northern of which were made near the central part of Oregon at the end of April, the intensity of hake feeding was very weak (Table 2). Plankton samples indicated that the abundance of food, in particular euphausiids, was low.

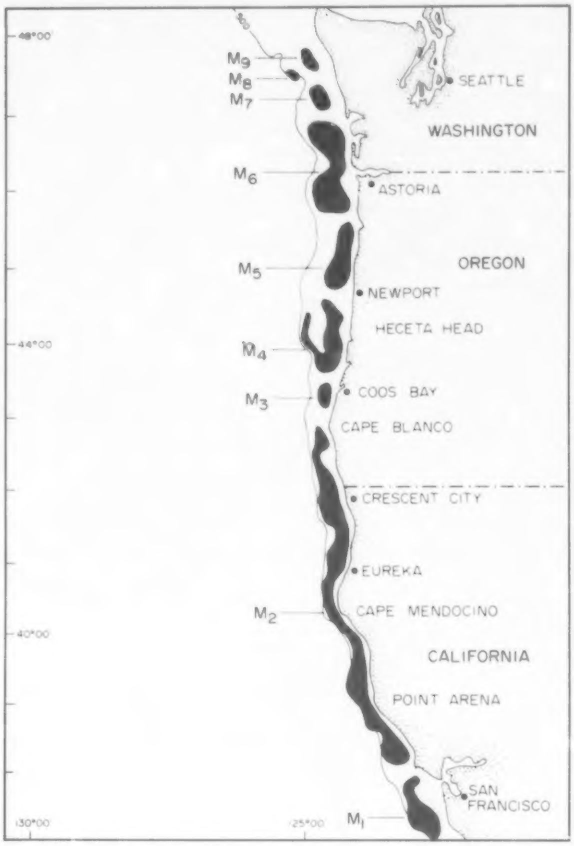

FIG. 1. Distribution of Pacific hake in May, 1985 (May 12–May 28, 1985).

In May, hake were unevenly distributed along the coast, forming aggregations from northern California to central Washington (Fig. 2). Information characterizing individual aggregations, including biomass, is presented in Table 3.

A total estimate of 2.82 million tons of hake was obtained, from standard trawl and acoustic data. This figure is close to the estimate of the biomass of the spawning portion of the population (3.6 million tons) presented earlier. The trawl and acoustic samples do not include hake that are in accumulations near the bottom, hence these estimates are considered low. Experience has shown that although the main body of hake are found in pelagic schools during their foraging period, a certain part live near the bottom and are always present in the catches of bottom trawls.

The most southerly aggregation of hake (M_1) was comprised mainly of hake 40–42 cm long, belonging to the strong 1980 year-class. In the southernmost part of the aggregation, there were young fish 18–22 cm long belonging to the 1984 year-class (Fig. 1). In March and April of 1985, large aggregations of this year-class developed in the region of Cape Conception and Monterey Bay. At the end of May, they were discovered northward along the northern part of Oregon, where test catches per hour of trawling were 7.0–13.0 tons. One year-olds are only found in significant numbers this far north when the year-class is very strong. One year-olds of weak and medium year-classes do not migrate in large numbers further north than northern California.

The largest aggregation (M_2) in terms of biomass and area occurred in the waters off of northern California.

TABLE 2. Feeding intensity of Pacific hake in March–May, 1985.

		Fullness of stomach						
Region	Month	0	1	2	3	4	No.	Mean
California	March	97.0	10.0	39.0	38.0	16.0	200	1.33
		48.5	5.0	19.5	18.0	8.0	100	
	April	217.0	75.0	49.0	24.0	4.0	360	0.71
		58.8	20.3	13.3	6.5	1.1	100	
	May	153.0	10.0	54.0	43.0	29.0	289	1.26
		52.9	3.5	18.7	14.9	10.0	100	
Washington	April	51.0	1.0	20.0	13.0	9.0	94	1.33
		54.2	1.1	21.3	13.8	9.6	100	
Oregon	May	108.0	46.0	120.0	128.0	56.0	458	1.35
		23.6	10.0	26.2	28.0	12.2	100	

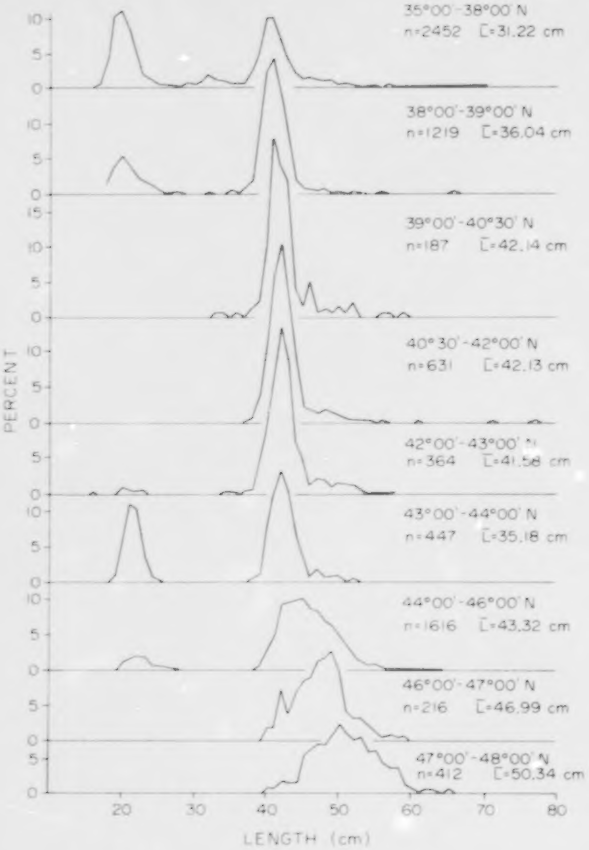

FIG. 2. Length composition of Pacific hake off northern California, Oregon and Washington in April–May, 1985. (n = sample size, $\bar{L}$ = mean length in cm).

This aggregation consisted almost entirely of hake of the strong 1980 year-class. Here hake were found, for the most part, over the lower part of the shelf (which in this region is very narrow) and the continental slope, in the 140–180-m stratum. Near Point Arena and Cape Mendocino, hake were found to depths of over 1000-m. In the northern part of this aggregation, the largest concentration of hake was observed in waters over the boundary between the shelf and the slope in the 150–180-m stratum. Test catches with the pelagic trawl averaged 48 tons/h.

The biomass of aggregation M_3 was small. Most hake were present near the lower part of the shelf, over depths of 50–200 m with smaller concentrations over 100–150 m. The hake in the shallower zone were predominantly small fish 20–33 cm long belonging to the 1984 year-class.

Aggregation M_4 was one of the densest. Test catches averaged 72 tons/h. This aggregation was distributed over Heceta Head and the adjacent shelf zone. As a rule, hake were not observed right on the bank. There were young hake inhabiting the coastal zone, with aggregations near the bottom at depths of 80–110 m. At greater depths, from 150 m out, concentrations of hake of the 1980 year-class predominated. This aggregation was the northernmost one in which hake of the 1980 year-class were abundant. The northernmost part of Heceta Head had the largest concentration of hake observed up to the end of May.

The M_5 aggregation had almost the same distribution as the M_4 aggregation, but immature fish were less abundant. Catches in the test trawl hauls were up to 26 tons/h. A significant portion of the aggregation, especially in its northern part, consisted of older hake 46–48 cm long.

TABLE 3. Biomass and characteristics of the schools of Pacific hake in May, 1985 (May 12–28).

School numbers	Position	Area, km²	Mean depth of the schools, m	Catch per hour of trawling, tons	Biomass of the schools, tons
1	2	3	4	5	6
M_1	37°10'-37°50'N	1699	29.0	12.0	190235.50
M_2	38°10'-42°50'N	7787	29.4	21.12	1555710.8
M_3	43°10'-43°20'N	292	15.0	9.0	12683.37
M_4	43°40'-44°50'N	2716	25.0	33.5	588557.73
M_5	44°50'-45°30'N	2224	23.0	14.0	237666.65
M_6	45°50'-46°50'N	3067	13.5	17.0	226473.48
M_7	47°10'-47°20'N	320	15.0	3.65	15032.17
M_8	47°35'-47°38'N	42	40.0	3.0	465.40
M_9	47°40'-47°50'N	171	10.0	0.5	275.37
M_1-M_9	37°10'-47°50'N				2824844.7

Samples of these hake were aged by scales and otoliths and were found to be comprised of fish of year-classes from the late 1970's. These year-classes were not as large as the dominant ones, and had not developed schools of large biomass in previous years. The main bulk of the hake in this aggregation was found in the shelf zone, including the near-bottom layers at moderate depths, right up to the coastal 3-mile zone.

The M_6 aggregation consisted mainly of fish 47–50 cm long, with a lower proportion of the hake being of the 1980 year-class. The concentrations of fish in this aggregation were of uneven size, probably as a result of influence by the fresh water from the Columbia River estuary. Catch per unit effort in the test trawlings varied from 3 to 24 tons/h. The densest hake concentrations were observed in the shelf zone, both in the 100–150-m pelagic layer and near the bottom. The density of fish in this aggregation decreased gradually toward its northern boundary.

Aggregation M_7 was small and the hake were mainly of the 1977–79 year-classes. In this region, large concentrations of euphasiids were observed with the hake.

Aggregation M_8 was small. It consisted of older migrating fish. Hake were found over depths of 350–400-m and were feeding lightly.

Aggregation M_9 occurred in almost the same region as M_8, but closer to shore. Farther north of this region hake did not form concentrations. By the end of May, this was the limit of the range of post-spawning hake.

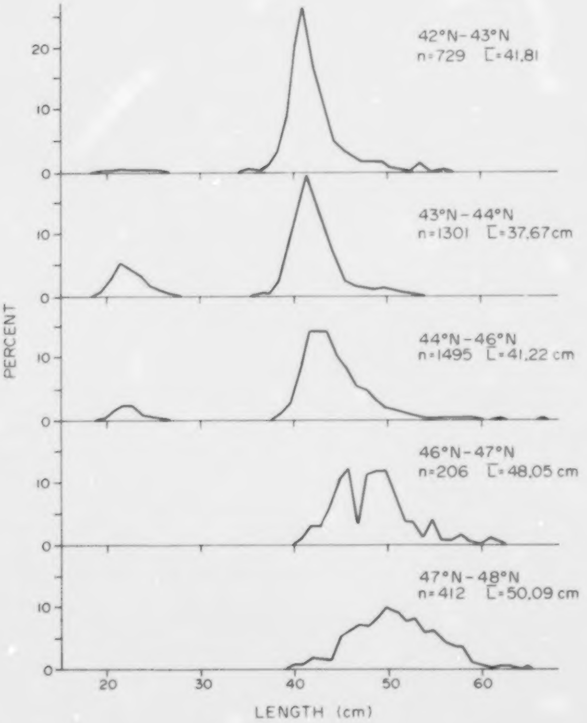

FIG. 3. Length composition of Pacific hake off the coast of Washington and Oregon in June, 1985. (n = sample size, $\bar{L}$ = mean length in cm).

At the end of the first week of June, the pattern of the distribution of size groups described above was essentially unchanged (Fig. 3). However, the schools of the oldest and largest hake had moved farther north, off the Strait of Juan de Fuca.

In summer, for the series of years starting in 1982, data on the size composition of hake are well illustrated by individual year-classes (Fig. 4). In 1982 the population consisted of two abundant year-classes, that of 1977 and 1980. By 1983, the abundant 1977 year-class had practically disappeared, and the productive part of the population consisted almost wholly of the single abundant year-class of 1980. The year-classes appearing between 1977 and 1980 were either small or only of average size.

Data on the size composition of the population in 1985 support the conclusion obtained earlier from ichthyoplankton catches — that the 1984 year-class would be strong. Great abundance of this year-class was indicated off central California as early as March and April of 1985 (Fig. 5), and later off northern California (Fig. 6), Oregon and Washington (Fig. 7).

Comparative data over a period of a year illustrates very clearly that the abundant 1980 year-class was retarded in its increase in length as compared with other year-classes (Fig. 4). A significant retardation was observed as early as 1983 (at 4–5 cm), and continued throughout the 4th or 5th year of their life. Apparently, the growth of this generation of hake was slowed down by a shortage of food, especially in the spawning and post-spawning period, when very concentrated schools were observed off California. In these schools the intensity of feeding gradually declined to a very low level (Table 2). A particularly low level of feeding by the schools of hake was observed in April off California.

In the spring of 1985, feeding intensity was low. Because of this, development of productive processes was late compared to earlier years, in both California and

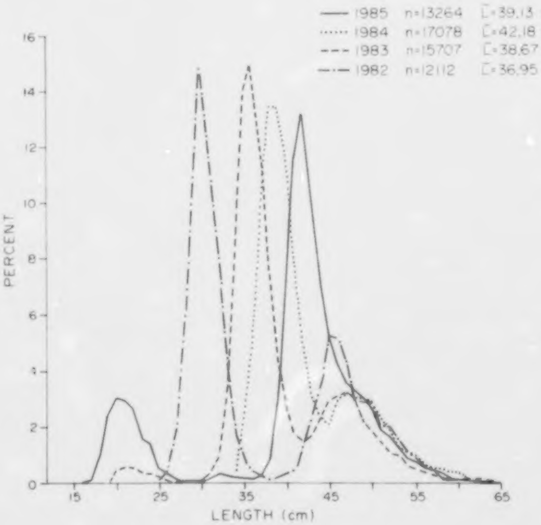

FIG. 4. Length composition of Pacific hake off the Pacific coast of North America in 1982–85. (n = sample size, $\bar{L}$ = mean length in cm).

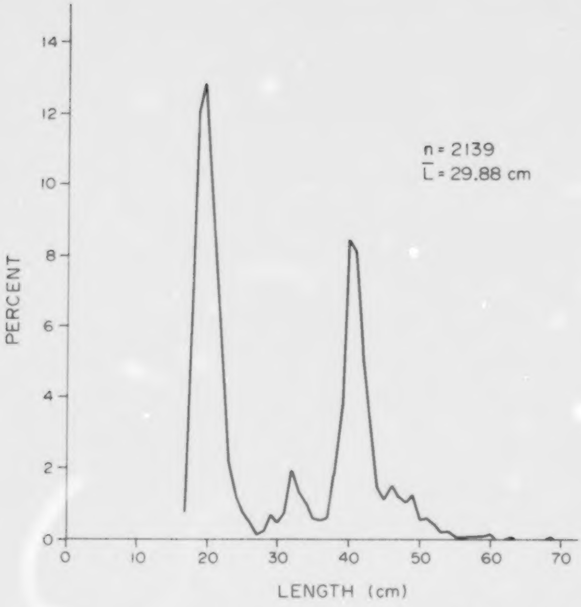

FIG. 5. Length composition of Pacific hake off the coast of central California in March–April, 1985. (*n* = sample size, L̄ = mean length in cm).

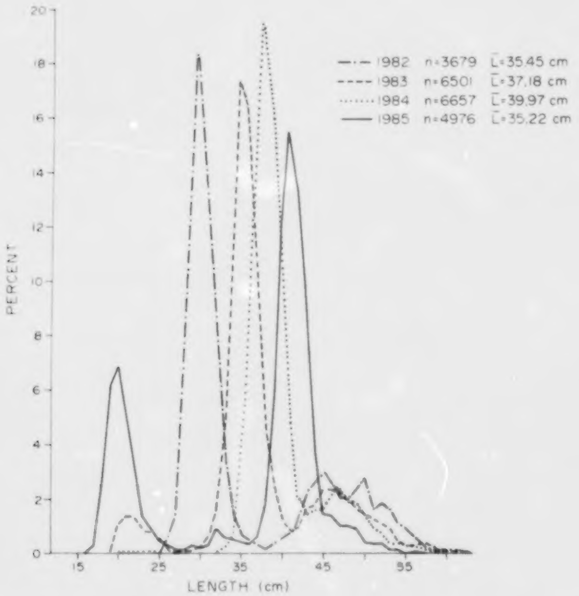

FIG. 6. Length composition of Pacific hake off the coast of California from March to May, 1985. (*n* = sample size, L̄ = mean length in cm).

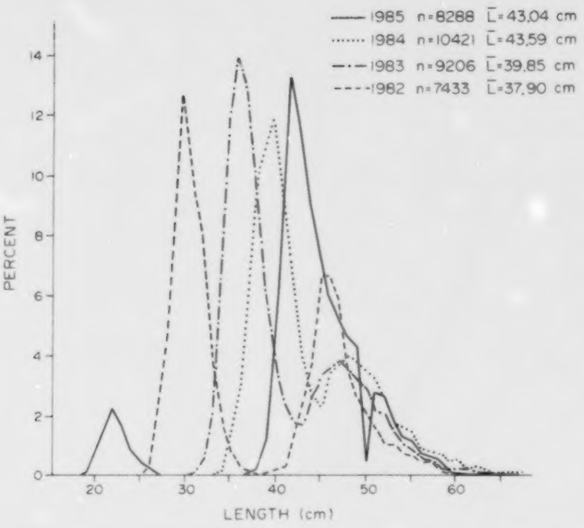

FIG. 7. Length composition of Pacific hake off the coast of Washington and Oregon in 1982–85. (*n* = sample size, L̄ = mean length in cm).

regions farther north. For this reason, the rate of migration of hake was relatively slow. In the second half of May, a very large concentration of euphausiids was observed off the coast of Washington, however, there were few hake there.

In all regions of the Pacific coast euphausiids are the principal food of hake. However, off Washington and Oregon there was a significant proportion of fish found in the diet of hake, especially in April when the euphausiid biomass was low.

Euphausiids are one of the primary prey items of hake, and their abundance largely determines hake behavior and the rate of northward migration by hake in the post-spawning period. The lower the development of euphausiid production, the broader the spectrum of other kinds of food eaten by hake (such as various species of fish, shrimps and squids). This, in turn, depends equally on the abundance of the year-class and of the whole population of hake.

References

ANON. 1984. Status of Pacific coast groundfish fishery. Document submitted to the 1985 USSR–U.S. bilateral meeting in Bellingham, WA. 45 p.

1985. Report of the 1985 USSR–U.S. bilateral meetings on assessment of commercial fish stocks in the North Pacific. Document submitted to the 1985 USSR–U.S. bilateral meeting in Bellingham, WA. 14 p.

Incorrect Parameter Values Used in Virtual Population Analysis (VPA) Generate Spurious Time Trends in Reconstructed Abundances

Michael J. Bradford[1] and Randall M. Peterman[2]

Natural Resource Management Program, Simon Fraser University, Burnaby, B.C. V5A 1S6

Abstract

Bradford, M. J. and R. M. Peterman, 1989. Incorrect parameter values used in virtual population analysis (VPA) generate spurious time trends in reconstructed abundances, p. 87–99. *In* R. J. Beamish and G. A. McFarlane [ed.]. Effects of ocean variability on recruitment and an evaluation of parameters used in stock assessment models. Can. Spec. Publ. Fish. Aquat. Sci. 108.

Virtual population analysis (VPA) and related methods are commonly used to reconstruct annual fish abundances from age-specific catch and auxiliary data. In typical data sets on medium- to long-lived fishes, a substantial portion of cohorts may be incomplete, i.e., many cohorts or year-classes will not have reached the terminal age by the last year of the catch data. Nonetheless, management agencies are often forced to use such incomplete data sets. Spurious time trends in abundance of recruits and stock biomass can arise from incomplete cohorts if VPA uses erroneous values of the natural mortality rate (*M*) or fishing mortality rate (*F*) on the oldest age-class. Spurious trends from this source occur only when VPA is used in a non-iterative mode, that is, when the partial recruitment vector is not estimated by iteratively applying VPA and calculating its values from each resulting *F* matrix. Using data from ten stocks, we show that the severity of these spurious trends is inversely related to the ratio of fishing to natural mortality. Results from a stochastic simulation model illustrate that a manager's ability to correctly identify the true trend in the population can be substantially reduced if incorrect values of *M* are used in VPA. We caution users of VPA that apparent trends (or the lack of them) in reconstructed abundances may be artifacts, and extensive sensitivity analysis must therefore be done on the parameters *M* and *F* input to VPA.

Résumé

Bradford, M. J., and R. M. Peterman. 1989. Incorrect parameter values used in virtual population analysis (VPA) generate spurious time trends in reconstructed abundances, p. 87–89. *In* R. J. Beamish and G. A. McFarlane [ed.]. Effects of ocean variability on recruitment and an evaluation of parameters used in stock assessment models. Can. Spec. Publ. Fish. Aquat. Sci. 108.

L'analyse des populations virtuelles et des méthodes connexes sont couramment utilisées pour reconstruire l'abondance annuelle des poissons à partir de données sur les prises à un âge donné et de données auxiliaires. Dans le cas d'ensembles de données caractéristiques sur les poissons qui ont une durée de vie de moyenne à longue, une partie importante des cohortes peuvent être incomplètes, c'est-à-dire que plusieurs cohortes ou classes annuelles ne feront pas partie du dernier groupe d'âge dans les données sur les prises que nous possédons. Néanmoins, les organismes de gestion sont souvent obligés d'utiliser ces ensembles de données incomplètes. Des tendances chronologiques fausses au niveau de l'abondance des recrues et de la biomasse du stock peuvent provenir de cohortes incomplètes si l'analyse des populations virtuelles fait appel à des valeurs erronées du taux de mortalité naturelle (*M*) ou du taux de mortalité par pêche (*F*) pour la classe la plus âgée. Cette source peut fournir des tendances fausses seulement lorsque l'analyse des populations virtuelles est utilisée selon un mode non itératif, c'est-à-dire lorsque le vecteur de recrutement partiel n'est pas évalué par l'application itérative de l'analyse des populations virtuelles et ses valeurs calculées à partir de chacune des matrice *F* résultante. À l'aide de données provenant de dix stocks, nous montrons que la gravité de ces fausse tendances est inversement liée au rapport entre la mortalité par pêche et la mortalité naturelle. Les résultants d'un modèle de simulation stochastique montrent que la capacité d'un gestionnaire à identifier correctement la tendance vraie de la population peut être considérablement réduite si des valeurs *M* incorrectes sont utilisées pour l'analyse des populations virtuelles. Nous

---

[1] Current address: Department of Biology, McGill University, 1205 Ave. Dr. Penfield, Montreal, Quebec H3A 1B1.

[2] Person to whom correspondence should be addressed.

informons les utilisateurs de l'analyse des populations virtuelles que des tendances apparentes (ou l'absence de celles-ci) dans les abondances reconstituées peuvent être des artéfacts, et l'analyse exhaustive de sensibilité doit donc porter sur les paramètres M et F avant leur introduction dans l'analyse des populations virtuelles.

Introduction

Virtual population analysis (VPA) is a commonly used method of reconstructing abundances of fish from age-structured catch data (Gulland 1983). The abundances of each age-group within a cohort are estimated sequentially, starting with the oldest age-group for that cohort in the catch-at-age matrix, and working backwards to the youngest age-class (Fig. 1). To initiate VPA, users provide an estimate of the instantaneous annual fishing mortality rate (F^{VPA}) for the oldest age-group for each cohort and an estimate of the instantaneous annual natural mortality rate (M^{VPA}). The exact equations for doing VPA are not readily soluble, so approximations of them are popular, although they incur a slight loss in accuracy (Pope 1972; MacCall 1986). Pope's (1972) method is frequently referred to as "cohort analysis."

An inaccurate value of F^{VPA} or M^{VPA}, compared with the true value in nature, will further affect the accuracy of reconstructed abundances. For cohorts in which all age-groups are present in the catch matrix ("complete cohorts," solid diagonals of Fig. 1), Pope (1972) demonstrated that errors in estimated abundances due to an erroneous choice of F^{VPA} for the oldest age-class diminish as the reconstruction goes backwards to the younger ages, unless the stock is very lightly fished. However, in the recent years of any set of catch data there are many year-classes or cohorts for which one or more age-classes are not yet present in the catches, simply because not enough time has elapsed since the cohort was first caught ("incomplete cohorts," dashed diagonals of Fig. 1). In such incomplete cohorts, the convergence property with accumulating F has less chance to take effect and estimates of abundance of these cohorts are more sensitive to the input F^{VPA} values. This problem is often exacerbated by a different phenomenon, partial recruitment, in which enough time *has* elapsed to have all ages appear in the catch, but the youngest ages are not fully vulnerable to the fishing gear. This further reduces the accumulated F on a cohort.

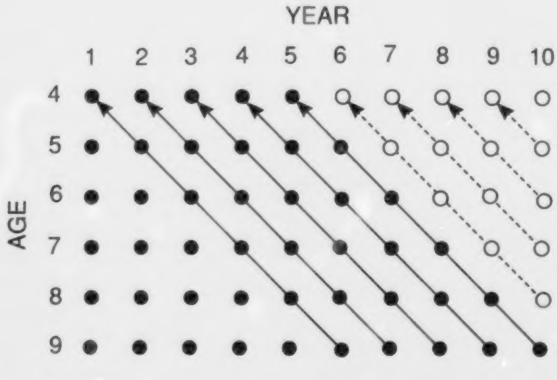

FIG. 1. Idealized catch-at-age matrix for a stock with 6 fished ages, beginning at age 4. Each cell would contain the number of fish caught by age and by year. Diagonal arrows indicate the path taken by VPA to reconstruct cohorts. Open circles and dashed diagonals are incomplete cohorts for which VPA begins on an age less than the oldest age; solid diagonals are complete cohorts. Age 4 recruitments indicated by open circles are estimated from incomplete cohorts.

An incorrect value of M^{VPA} (input to VPA) has been found to produce the opposite effect of an incorrect F^{VPA}; the errors in reconstructed abundances at each age increase as VPA goes backwards through a cohort when M^{VPA} is wrong (Agger et al. 1973; Ulltang 1977; Sims 1984). In this case, estimated abundances of the youngest age-classes will be the least accurate. Because of a lack of data, most researchers assume that natural mortality is constant across all years and ages in VPA, and the M^{VPA} will be in error to the extent that this assumption is violated.

In spite of these and many other known limitations of VPA (e.g., Pope 1972; Fournier and Archibald 1982; Deriso et al. 1985), VPA and its related sequential reconstruction techniques are still widely used and attract considerable attention from researchers (e.g., Winters et al. 1985; Pope and Shepherd 1985; MacCall 1986; Sampson 1987; Prager and MacCall 1988).

In this paper we quantify the extent to which errors in M^{VPA} and F^{VPA} create spurious time trends in recent abundances of estimated recruits (defined here to mean the youngest fished age) and estimated total stock biomass (summed over all fished ages). The existence of such spurious time trends from VPA has been suggested by Rivard (1983) but to our knowledge, no one has documented them. To quantify such trends, we first used a simple deterministic model to demonstrate how these trends are generated. For clarity of interpretation, we initially assumed that recruitment and fishing mortalities are constant, but our conclusions are not contingent on these assumptions and we relax them later. We then generalize our results over a variety of stocks with different life histories and exploitation patterns. Finally, using a stochastic simulation model, we show how incorrect input parameters can affect the probability that fishery managers will correctly interpret estimated time trends in recruitment or stock biomass when random variability is included in a realistic manner.

We emphasize that the spurious trends identified here occur only with the "non-iterative" approach to VPA (described below). They do not occur when the iterative VPA procedure is used (M.F. Lapointe and R.M. Peterman, unpublished data). The non-iterative and iterative uses of VPA differ as follows. In both approaches, users specify a fishing mortality rate for the oldest age of the complete cohorts, F_L (along the bottom row of Fig. 1), and a partial recruitment vector for the oldest available age of each incomplete cohort (along the right edge of

Fig. 1). The partial recruitment vector of age-specific fishing mortalities F_i, is usually defined as, $F_i = s_i F_L$, where s_i values are age-specific selection coefficients. In the first, or non-iterative aproach to VPA, the s_i values are estimated empirically (e.g. Gulland 1983; Roff 1981; Wakabayashi 1984), VPA is run, and the analysis stops after producing the first matrix of F_i and of numbers at age by year. In the second, or iterative approach to VPA, selectivity coefficients are estimated iteratively (Rivard 1983). From an initial VPA run, s_i values are calculated from the resulting F_i values averaged over time for each age and these s_i values are used as the input partial recruitment vector in a second VPA. The selectivity coefficients are again recalculated from the new F_i matrix and this procedure is repeated until the s_i values stabilize. Assumptions about the number of fully recruited ages and smoothing methods may be used to reduce random variation in the s_i values in this iterative procedure (Rivard 1983).

Many authors do not explicitly state whether they used iterative or non-iterative VPA. However, at a minimum, non-interative VPA is normally applied (e.g., Winters et al. 1985) in situations in which age-specific selectivities of fishing gear have changed through time, either gradually due to changing size at age or rapidly due to changes in regulations on fishing gear. Because such situations are common, we explore the creation of spurious time trends by non-iterative VPA.

Methods

To evaluate any method of estimating abundance of marine fish stocks, one must create an experimental arena in which true abundances are known and in which the method being tested can generate estimates. The true and estimated values can then be compared. We used computer simulation to create such an experimental situation, as have many other authors (e.g. Pope and Shepherd 1985; Tyler et al. 1985; Deriso et al. 1989).

Deterministic Analysis

Using a simple deterministic model, we quantified the magnitude of spurious time trends in abundance caused by errors in parameters input to VPA. We did this by comparing the trend in a simulated "true" population with the trend in abundances estimated by non-iterative VPA, which used the simulated "true" catch-at-age data as input. We thus assumed that catches were known exactly. To clearly illustrate these trends we assumed that the true population had a constant annual recruitment of one million fish to the youngest fished age group (this assumption is relaxed in the stochastic section below). We also assumed that the true age-specific fishing mortalities, F_i, were constant over time and that the true M was constant over age and time. Throughout the rest of this paper, these "true" parameter values used in the forward simulation are identified by the lack of a VPA superscript, whereas the values of those parameters used as input to VPA have that superscript.

In the forward simulation of the true population, the abundance of each age-group in a cohort was depleted each year using the standard equation,

$$(1) \qquad N_{i+1} = N_i \exp(-Z_i),$$

where N_i = number of fish at the start of age i, and $Z_i = M + F_i$. The true population thus had a stable age distribution and no time trend in the abundance of recruits or stock biomass. M and F_i values were drawn from the literature on 10 stocks representing marine fishes with a range of longevities and exploitation patterns (Tables 1 and 2). Mean F_i values were taken directly from

TABLE 1. Sources of data used to generalize effects of input errors to VPA across stocks.

Species	Location	Abbreviation	Source
Atlantic menhaden	East coast, U.S.	Men	Hightower and Grossman (1985) Schaaf (1980)
Herring	Fortune Bay, Nfld	FBH	Winters et al. (1985)
Herring	ICES area 6a	NSH	Saville and Bailey (1980)
Atlantic mackerel	ICNAF areas 3-6	Mac	Anderson and Paciorkowski (1980)
Pacific cod	Hecate Strait, B.C.	Cod	Fournier (1983)
Pacific ocean perch	Queen Charlotte Sound, B.C.	Pop	Hightower and Grossman (1985) Archibald et al. (1983)
English sole	Oregon	Eng	Hayman et al. (1980), Peterman and Bradford (1987)
Dover sole	Oregon	Dov	Hayman et al. (1980)
Yellowfin sole	Eastern Bering Sea	Yel	Wakabayashi (1984)
Pacific halibut	Area 2	Hal	Hoag and McNaughton (1978)

TABLE 2. Parameter values used for 10 different marine fish stocks in the general analysis of biased input parameters to VPA. Abbreviations of stock names in the top row are defined in Table 1, where literature sources are also given. M and F_L are the instantaneous annual natural mortality rate and fishing mortality rate on the oldest age-class, respectively. F_L/M is a measure of relative exploitation intensity used in Fig. 7 and 8. Coefficients of partial recruitment to the fishery are given for each fished age, scaled so that the coefficient for the last fished age-class is 1.0 in all cases. Unfished ages are shown by a hyphen.

	Stock									
	Men	FBH	NSH	Mac	Cod	Pop	Eng	Dov	Yel	Hal
M	0.25	0.20	0.10	0.30	0.65	0.05	0.29	0.20	0.25	0.20
F_L	1.47	0.43	0.50	0.35	0.60	0.19	0.26	0.19	0.12	0.19
F_L/M	5.88	2.15	5.00	1.17	0.92	3.80	0.90	0.95	0.48	0.95
Age	Partial recruitment coefficients									
0	0.34	—	0.22	—	—	—	—	—	—	—
1	1.06	—	0.33	0.12	—	—	—	—	—	—
2	0.93	0.14	0.61	0.37	0.14	—	—	—	—	—
3	0.91	0.52	0.82	0.63	0.48	—	—	—	—	—
4	0.84	0.86	0.81	0.78	0.76	—	0.56	—	—	—
5	1.07	1.09	0.81	0.80	0.92	—	0.99	—	0.04	—
6	1.00	1.08	0.85	0.77	1.00	0.05	1.19	0.48	0.17	—
7	1.00	1.07	0.95	0.92	1.00	0.11	1.16	0.61	0.33	—
8	—	1.07	0.98	0.97	1.00	0.21	0.95	0.67	0.56	0.63
9	—	1.03	1.00	1.00	1.00	0.36	1.00	0.81	0.73	0.79
10	—	1.02	—	—	—	0.58	—	0.89	0.88	0.84
11	—	1.00	—	—	—	0.85	—	0.95	0.97	0.90
12	—	—	—	—	—	1.14	—	1.08	1.00	0.95
13	—	—	—	—	—	1.40	—	1.00	1.00	1.00
14	—	—	—	—	—	1.56	—	—	1.00	1.00
15	—	—	—	—	—	1.60	—	—	1.00	1.00
16	—	—	—	—	—	1.50	—	—	1.00	1.00
17	—	—	—	—	—	1.28	—	—	1.00	1.00
18	—	—	—	—	—	1.00	—	—	—	1.00
19	—	—	—	—	—	1.00	—	—	—	1.00
20	—	—	—	—	—	1.00	—	—	—	1.00
21	—	—	—	—	—	1.00	—	—	—	—
22	—	—	—	—	—	1.00	—	—	—	—
23	—	—	—	—	—	1.00	—	—	—	—
24	—	—	—	—	—	1.00	—	—	—	—
25	—	—	—	—	—	1.00	—	—	—	—
26	—	—	—	—	—	1.00	—	—	—	—
27	—	—	—	—	—	1.00	—	—	—	—
28	—	—	—	—	—	1.00	—	—	—	—
29	—	—	—	—	—	1.00	—	—	—	—

those literature sources, where available, or were averaged from published F-matrices; weight-at-age vectors also came from these sources.

Next, we generated a simulated catch-at-age matrix for this true case using the Baranov catch equation (Ricker 1975):

$$C_i = \frac{N_i\, F_i\, (1-\exp(-Z_i))}{Z_i}, \tag{2}$$

where C_i is the number of fish in the catch at age i. Note that the recruitments of the last $k-1$ years were from incomplete cohorts (Fig. 1), where k is the number of fished age-classes of the catch. Thus, this forward simulation used the same assumptions as VPA.

Non-iterative VPA was then performed on this deterministic catch-at-age matrix to reconstruct abundances, which we later compared with those generated in the forward simulation by the above equations. For this VPA we either used the approximation equations of Pope (1972) or MacCall (1986). First, the standard rearrangement of the Baranov equation was used to estimate the abundances of the oldest age-class of each cohort in the catch matrix,

$$(3) \qquad N_i = \frac{C_i Z_i^{\mathrm{VPA}}}{F_i^{VPA}\,(1-\exp(-Z_i^{VPA}))}.$$

The abundances of younger ages for each cohort were calculated from either Pope's (1972) equation,

$$(4a) \quad N_i = N_{i+1}\exp(M^{\mathrm{VPA}}) + C_i \exp(M^{\mathrm{VPA}}/2)$$

or MacCall's (1986) recent modification:

$$(4b) \quad N_i = N_{i+1}\exp(M^{\mathrm{VPA}}) + C_i M^{\mathrm{VPA}}/(1-\exp(-M^{\mathrm{VPA}})).$$

We assumed that the age-specific partial recruitment coefficients (s_i) used in the VPA were estimated accurately; i.e., they were the same as the s_i used in the forward simulations. We calculated the s_i for the forward simulation by dividing the F_i values from the literature by F_L, the fishing mortality for the oldest age group (Table 2). This scaled the partial recruitments so that the coefficient for the oldest age group was 1.0. The age-specific F_i values used in equation 3 to calculate abundances in the last year (along right side of Fig. 1) were $= s_i F_L^{\mathrm{VPA}}$.

We focused on the extent of artificial time trends in abundance created by using incorrect values of M^{VPA} and F_L^{VPA}. Unless mentioned otherwise, all results presented below were from Pope's (1972) approximation (equation 4a) to VPA. In all cases, results from Pope's and MacCall's methods closely approximated those from exact VPA. In terms of the % spurious change in abundance described in the following paragraph, all of our results were within 2% of the spurious time trend change that exact VPA would have calculated. Our results showing spurious tends are applicable to the generic set of sequential reconstruction techniques, of which VPA is the most widely used. Hence, to simplify our terminology, we refer to VPA throughout this paper, instead of cohort analysis.

Time trends were examined in the abundance of recruits and stock biomass that were calculated from the reconstructed numbers-at-age matrix and weight-at-age vector. We quantified these time trends by calculating the precentage change in abundance from the last year in which recruits were estimated from a complete cohort (year 5 of example in Fig. 1) to the most recent year of catch data, when only the youngest age-class was recruited to the fishery (year 10 of Fig. 1). As we explain below, no time trend occurs in the years prior to year 5 because (1) all of the cohorts are complete, (2) the bias was therefore the same for all of them, and (3) recruitment was constant in our simulated population. Our index of the change in abundance of recruits or in stock biomass over time was thus,

$$(5) \qquad \rho(N) = \frac{N_t - N_{t-k+1}}{N_{t-k+1}} \bullet 100,$$

where N_t is the most recent abundance, N_{t-k+1} is the abundance in the year of the most recent complete cohort, and k is the number of fished ages.

Stochastic Example

We also used a more realistic stochastic simulation model to demonstrate how incorrect inputs to VPA can affect estimated time trends in abundance when there is interannual variability in the true M and F values, as well as in the biological components. Here we focused mainly on the effects of using incorrect M^{VPA} because this parameter is more difficult to estimate and may be prone to larger errors than F^{VPA}, which is frequently "tuned" with ancillary data (Rivard and Foy 1987).

For this stochastic analysis, we used a simulation model of the flatfish, English sole (*Parophrys vetulus*), which inhabit coastal waters of Oregon and Washington, USA (Peterman and Bradford 1987). The empirically based components of this sole model are described in detail elsewhere (Peterman et al. 1987), but briefly they include size-specific maturity and fecundity, stochastic temperature-dependent spawning and egg hatching rates, larval and juvenile mortality, and temperature-dependent body growth of ages 1 through 13. Instantaneous natural and fishing mortality rates were also stochastic, drawn from normal distributions as in Peterman and Bradford (1987). Natural and fishing mortality losses were removed using the standard Baranov catch equation (2). Coefficients of partial recruitment to the fishable population were zero for ages ≤ 3, 0.5 for age 4, and 1.0 for ages ≥ 5. There were 10 fished ages (4–13) in the model, rather than the 6 used for English sole in Hayman et al. (1980) and in the first part of this paper. The resulting stochastic model dynamically calculated interannual variability in year-class strength of the incoming recruits and growth and survival of older fish. Forward simulations with this model thus generated the "true" fish abundance each year, measured by numbers of fish at each age and total stock biomass.

As in Peterman and Bradford (1987), the model also generated annual "estimated" abundance of recruits and stock biomass by performing a VPA (Pope's 1972 cohort analysis) on the simulated catch-at-age matrix, using constant M^{VPA} and F_L^{VPA} parameters. However, in Peterman and Bradford (1987), these constant parameter values were imprecise but *unbiased* estimates of the "true" values (i.e., equal to the mean of the distribution of M and F_L values used in the forward simulations). Here we added the assumption of *biased* parameter estimates to the assumption of imprecision because in reality, the M^{VPA} value put into a given VPA analysis will likely be higher or lower than the long-term mean true value. Again, the non-iterative VPA procedure was used, and we assumed that the input partial recruitment vector, s_i, was accurate.

We determined how well VPA with biased and imprecise input parameters would reflect true trends in abundance over time by comparing trends in our simulated "true" and estimated abundance data over 10 years. We first took natural logs of annual abundances, fit a regression line on time for each of the true and estimated abundances, and then tested the significance of the fitted lines.

The lines were categorized in one of three ways, (1) significantly increasing abundance over time, (2) significantly decreasing, or (3) trend not significantly different from zero. We said that VPA correctly reflected the true trend when the estimated and true trends in abundance were both in the same one of these three categories.

This process of comparing estimated and true trends was repeated 1000 times to derive the probability that biased and imprecise VPA will correctly reflect true trends in abundance. At the end of each 10-yr simulation, after the VPA was done and estimated and true trend lines were categorized, the population was reset to its original condition (Peterman and Bradford 1987) and another 10-yr run was done with a different sequence of random numbers. The proportion of these 1000 runs in which the estimated trend was in the same category of significance as the true trend was our main measure of the adequacy of VPA. This procedure was repeated for different true mean values of fishing mortality, ranging from $F_L = 0.1$ to 1.0 to reflect lightly to heavily fished situations. The model used a mean true adult natural mortality rate (M) of 0.29 (Hayman et al. 1980), with a $\sigma = 0.05$, while we simulated biased VPA by using $M^{\mathrm{VPA}} = \pm 25\%$ or $\pm 50\%$ of the mean.

Results

Deterministic Analysis

Single species examples

Erroneous parameters input to VPA caused spurious time trends in the estimated abundances of recruits in the simple deterministic model because of the incomplete cohorts. In our English sole example (*Parophrys vetulus*; parameters in Table 2), when M^{VPA} was 50% higher than the true value of M used in the forward simulation (M), recruitment showed a distinct decreasing time trend (Fig. 2, top curve), even though the true abundance was constant. An apparent increasing trend in reconstructed abundance of recruits resulted when M^{VPA} was 50% below M (Fig. 2, bottom curve). A F_L^{VPA} 50% $> F_L$ led to an artificial trend of decreasing recruitment, whereas a F_L^{VPA} value less than F_L generated an increasing time trend in recruitment (Fig. 3). The main difference between the effects of errors in M^{VPA} and F_L^{VPA} was that, going back in time (from right to left in Fig. 2 and 3), error in M^{VPA} resulted in reconstructed recruitments that diverged from the true value, while incorrect F_L^{VPA} values gave recruitments that tended to converge toward the true value. There was a -36% and $+43\%$ change in estimated recruitment over the last 6 yr of the time series when M^{VPA} was greater or less than M, respectively, even though true recruitment was constant. A -25% and $+54\%$ change in estimated recruits occurred when F_L^{VPA} was greater or less than F_L, respectively.

Estimates of stock biomass calculated from VPA with incorrect inputs also showed false trends in abundance similar to the trends in recruitment (open circles of Fig. 2, 3). The biomass of age 4 recruits was only 30% of the total biomass of this stock, so the time trends in biomass resulted from the effects of incorrect input parameters on older ages as well as on recruitment.

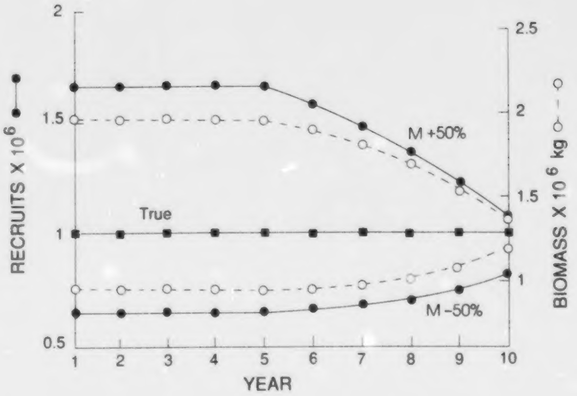

FIG. 2. Time series of English sole age 4 recruits (solid circles) and stock biomass (open circles) estimated by VPA runs which used different values of M^{VPA} (the parameter value input to VPA). Note that our simulated English sole had 6 ages in the simulated fishery, from age 4 to 9 years. True recruitment was constant at 1×10^6 fish, which gave a contant true stock biomass of 1.3×10^6 kg. Upper 2 curves are recruits (•) and biomass (○) when M^{VPA} was 50% greater than the true natural mortality rate, M; lower curves are for M^{VPA} 50% less than M. Abundances for years 6–10 were estimated from incomplete cohorts.

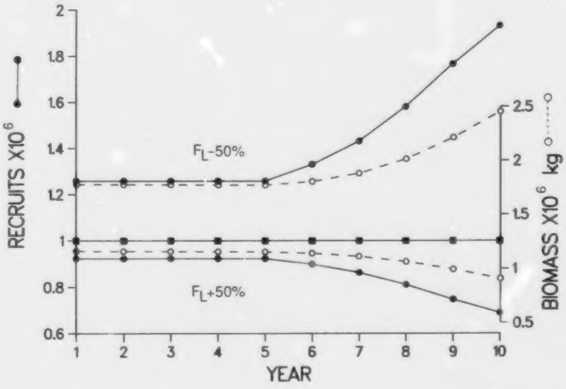

FIG. 3. Recruitment (•) and stock biomass (○) time series for simulated English sole as in Fig. 2, except that the upper two curves are for F_L^{VPA} 50% less than the true F_L, and the lower curves are for F_L^{VPA} 50% greater than F_L.

The artificial time trends of recruitment can be explained by examining the equations used in VPA. For incorrect values of F_L^{VPA} (Fig. 3) the bias in recruitment abundances diminished as each successive cohort became more complete (moving to the left in Fig. 1) because the erroneous F_L^{VPA} value was used only in equation 3 for calculation of abundance of the last fished age (Pope 1972). Because catches were assumed to be accurate, as more of each cohort was caught, the error in the estimate of the relatively rare oldest age-class became less important. Thus, as one goes back from the most recent year in Fig. 3, the recruitment estimates are based on more complete cohorts and the estimates converge towards the true value (Pope 1972). No time trend occurs in the reconstruction of age 4 recruits from years 1-5 because these were estimated from a series of complete cohorts, and hence the cumulative F and its effect on bias were constant for each of the cohorts.

Spurious trends in abundance also result from incorrect M^{VPA} (Fig. 2), but in contrast to the case in which $F_L{}^{VPA}$ is in error, the biases in recruitment estimates are largest for the complete cohorts. M^{VPA} is used in the calculation of abundance of every age-class in succession (equations 4a and 4b) and the error compounds as more age-classes are used in the analysis (Sims 1984). If M is too large, abundance will be overestimated and spurious trends in the time series of abundance (Fig. 2) will result because the VPA equations are applied an unequal number of times to different cohorts, depending on how complete they are. This causes the estimated abundance of the age 4 fish in Fig. 1, for example, to be least biased in year 10, and progressively more biased going back in time to year 5. The bias is constant for years 1-5 because age 4 fish in those years are reconstructed from complete cohorts, which all had the same amount of accumulated bias due to the error in M^{VPA}.

Figures 4 and 5 show, for our English sole example, the spurious change (from equation 5) in estimated abundance of recruits or stock biomass over the time series of incomplete cohorts for various values of M^{VPA} and $F_L{}^{VPA}$. These changes in estimated abundances were spurious because true recruitment and stock biomass were constant. Incorrect M^{VPA} and $F_L{}^{VPA}$ values caused smaller spurious changes in stock biomass than in recruitment (cf. open circles with solid circles for English sole case in Fig. 4 and 5) because the age-classes differed in the degree of bias. Biomass includes both younger ages, which have time trends due to incorrect inputs, (e.g., Fig. 2 and 3) and older ages, which have little or no time trends, because the VPA equations are applied only once or a few times. Thus, when we calculated annual stock biomass by doing a weighted sum across ages, the strong spurious trend in recruits was diluted by the weak (or no) trends in older ages. Hence, stock biomass generated smaller spurious trends than recruits alone.

Time trends in recruitment and biomass produced by incorrect parameters input to VPA for a long-lived species, Pacific ocean perch (*Sebastes alutus*; Tables 1 and 2) were similar to those for English sole (Fig. 4, 5, dashed lines). High M^{VPA} gave rise to strong decreasing trends in biomass and recruitment (Fig. 4). Higher M values have been estimated in other analyses of this stock (Gunderson 1977), and if included in VPA, they could give rise to overly pessimistic trends in abundance if the true M value is lower.

Pope (1972) and Sims (1984) provide formulas to calculate the bias in abundance estimates caused by incorrect inputs to VPA. Pope's (1972, eqtn 2.3) exact formula for errors due to incorrect $F_L{}^{VPA}$ gave identical results to ours, but he did not explicitly point out that this bias would lead to spurious time trends in recent cohorts. We found that the formula given by Sims (1984, eqtn 8) for approximate errors in abundance due to errors in M^{VPA} substantially overestimated the error when M^{VPA} was too small relative to the correct value, and it underestimated the errors in abundance when M^{VPA} was too high relative to M (Fig. 6). Sim's approximation is thus only useful for small errors in M^{VPA}.

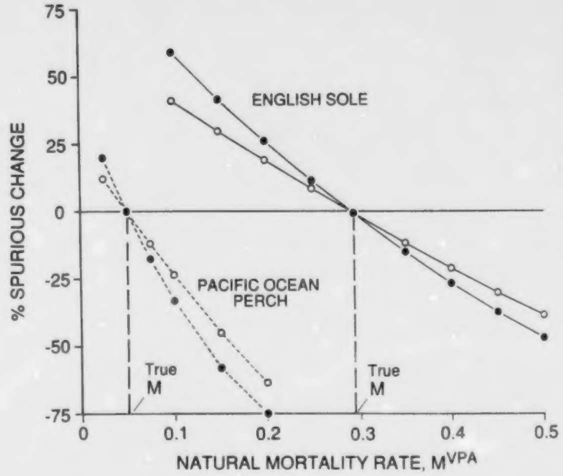

FIG. 4. Spurious change (% increase or decrease) in the abundance of recruits (●) and stock biomass (○) over the incomplete cohorts of English sole (solid lines) and Pacific ocean perch (dashed lines) resulting from using different values of M^{VPA}. True M values were 0.29 for English sole, and 0.05 for perch. The last 6 years of abundances, for English sole, and 24 years for Pacific ocean perch were used to calculate the time trends, according to equation (5).

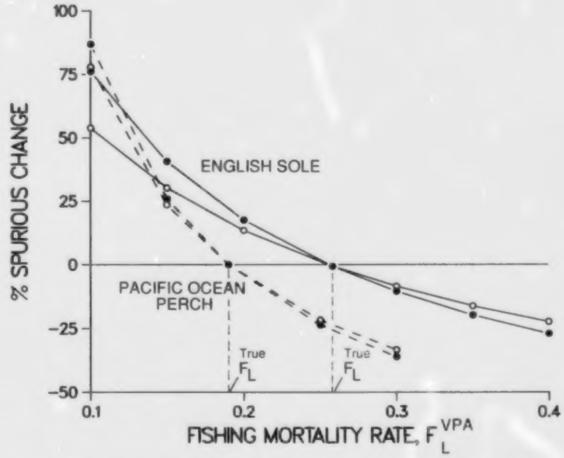

FIG. 5. Spurious change (% increase or decrease) in the abundance of recruits (●) and stock biomass (○) over the incomplete cohorts of English sole (solid lines) and Pacific ocean perch (dashed lines) resulting from biased $F_L{}^{VPA}$. True values of F_L were 0.26 for English sole and 0.19 for perch.

MacCall's (1986) equations for VPA gave results that were very similar to those from Pope's (1972) equations. For the English sole example, the difference between the two methods was less than 1% for the time trends in recruitment in Fig. 4 and 5. Pope's equations gave slightly smaller increasing artificial time-trends, whereas MacCall's equations gave smaller decreasing trends.

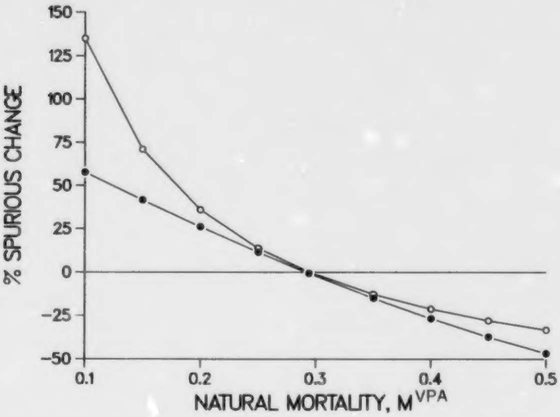

FIG. 6. Spurious change in time trends of recruits as calculated from Sims' (1984, p. 151) equation for the approximate errors in abundance estimates from VPA due to incorrect values of M^{VPA} (○) and the actual trends from VPA (●) for various values of M^{VPA}, for English sole. True M was 0.29.

Comparison across species

To explore the generality of our results, we examined stocks with a range of "true" F and M values, and a number of exploited age-classes ranging from 6 to 24 years. To ensure realistic combination of these parameters, we used data for 10 different stocks (Tables 1 and 2). We calculated the percent change in recruitment over the time series of incomplete cohorts from equation 5 when the error in M^{VPA} was ±25 or ±50% of the true value. These error rates in natural mortality were roughly the ones generated by ±1 or 2 SD around the empirical relationship between M, growth parameters, and temperature derived by Pauly (1980). Empirical relationships such as this are sometimes used to estimate M^{VPA} (e.g., Winters et al. 1985), in the absence of other data. We found that the severity of the artificial time trend in recruitment caused by errors in M^{VPA} was not related to the true F_L or M separately, but was inversely related to the ratio of the true fishing to natural mortalities (F_L/M), (Fig. 7). This ratio is a relative measure of the intensity of exploitation. For moderately fished stocks ($F \approx M$), the change in recruitment over the incomplete cohorts was very roughly equal to the relative error in M^{VPA}, though opposite in sign. For example, at $F_L/M = 1$, a M^{VPA} 25% above M resulted in about a 25% decrease in estimated recruitment. As stocks were more heavily exploited, the bias due to inaccuracies in M^{VPA} decreased because more of the stock was dying due to fishing and errors in M^{VPA} became relatively unimportant (Fig. 7).

There was little evidence of a relation between the magnitude of time trends produced by errors in $F_L{}^{VPA}$ and the ratio F_L/M (Fig. 8). For a given relative error in $F_L{}^{VPA}$, the magnitude of the spurious time trend was confined to a fairly narrow range, independent of the exploitation patterns of the 10 stocks. Although from Fig. 7 one might expect for a given M^{VPA} that time trends would be less severe when a stock is heavily fished (i.e., $F_L/M > 1.0$), this was offset by the tendency of VPA to produce steeper time trends at high F than at low F. These steeper trends resulted because as VPA worked backwards through each cohort, abundance estimates converged toward their true values more quickly when the cohort was heavily fished (Pope 1972).

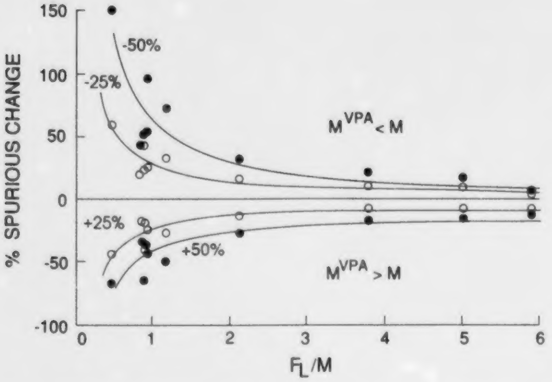

FIG. 7. Percentage change in recruitment due to spurious time trends resulting from ±25% (○) and ±50% (●) errors in M^{VPA} for the 10 stocks in Table 1, as a function of F_L/M, a relative measure of exploitation. Increasing spurious time trends resulted when M^{VPA} was less than the true value, M, by −25% or −50%; negative time trends occurred when M^{VPA} was greater than M by +25% or +50%. Curves were fit by linear regression, with inverse transformation of the independent variate.

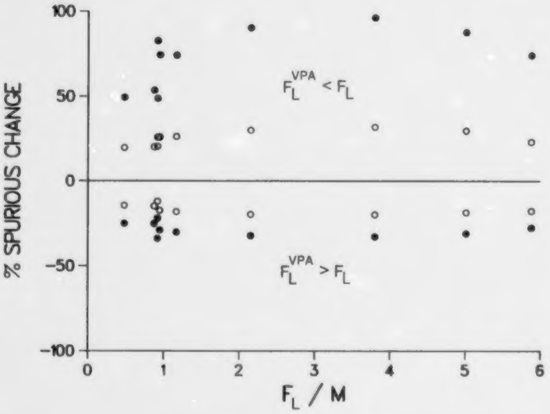

FIG. 8. Percentage change in recruitment due to spurious time trends resulting from ±25% (○) and ±50% (●) errors in $F_L{}^{VPA}$ for the 10 stocks in Table 1. Increasing spurious time trends resulted when $F_L{}^{VPA}$ was less than the true value, F_L; negative time trends occurred when $F_L{}^{VPA}$ was greater than F_L.

Stochastic Example

Recruitment

A biased M^{VPA} in the stochastic model that included realistic amounts of variation reduced the probability that VPA on the simulated catch would correctly identify the true population time trend, relative to the case where

M^{VPA} was unbiased. Note that in addition to variability in M and F, the assumption of a constant trend in recruitment was relaxed in the stochastic model. Recruitment trends varied with fishing intensity; the equilibrium occurred with $F \approx 0.3$.

The probability of correctly detecting a time trend in 10 years of recruitment data on age 4 English sole was related to the fishing mortality rate, F_L, and the amount of bias in M^{VPA} (Fig. 9). When M^{VPA} was unbiased (Fig. 9 squares) the rate of correct detection was about 90–95%. This unbiased case was not perfect because of the effects of stochastic variation in the true F and M on the catch-at-age data. The probability of correct detection was high (>0.8) when F_L was high (>0.4) because when the stock was heavily fished, errors in M^{VPA} have less effect (Sims 1984; Pope 1972). When F was small (0.1), the chance of drawing a correct conclusion about the true trend in abundance was $<65\%$ for the case where M^{VPA} was 25% larger than the true M, and $<50\%$ for M^{VPA} 50% $>M$ (Fig. 9A and B, closed circles). The latter occurred because a lightly fished population is more likely to have an increasing time trend in "true" abundance, but as documented in the first section of this paper, M^{VPA} that is greater than M tends to create a spurious decreasing time trend (Fig. 2). This bias led to a lower probability that the true and estimated trends in recruitment had the same sign and category of significance. Probabilities of obtaining correct trends when M^{VPA} was less than M were not affected as much or in the same way at low F (Fig. 9 open circles) because this direction of bias in M^{VPA} tended to generate spurious increasing trends in abundance, the same direction as the majority of the 1000 true trends at low F. Some incorrect cases occurred at low F because some true trends that were not significantly diferent from zero gave significant increasing trends in the estimated abundances when the value of M^{VPA} was less than M.

Stock Biomass

Similar to the situation with recruits, the probabilities of correctly identifying time trends in stock biomass in the stochastic model were generally $>75\%$ for $F>0.5$, and the probabilities increased with increasing F in that region (Fig. 10). However, using a M^{VPA} too high relative to M led to lower probabilities of correct detection (35–65%) in estimated trends at $F<0.5$ (Fig. 10). The probability of correct detection was lower for trends in biomass than in recruitment because biomass has lower interannual variability than recruitment; thus, more statistically significant increasing time trends in true biomass were produced at low F. A high value of M^{VPA} led to some of these trends being estimated as non-significant; this gave rise to lower probabilities than were found for recuitment (Fig. 10B).

The general pattern of lower probability of correct detection at intermediate F values occurred because in that region, the simulated population was near equilibrium and many true trends in biomass were non-significant. However, because of errors in M^{VPA}, some of these gave rise to significant trends in abundances estimated by VPA. At either high or low F, stronger decreasing or increasing trends were generated which were less easily masked by random noise.

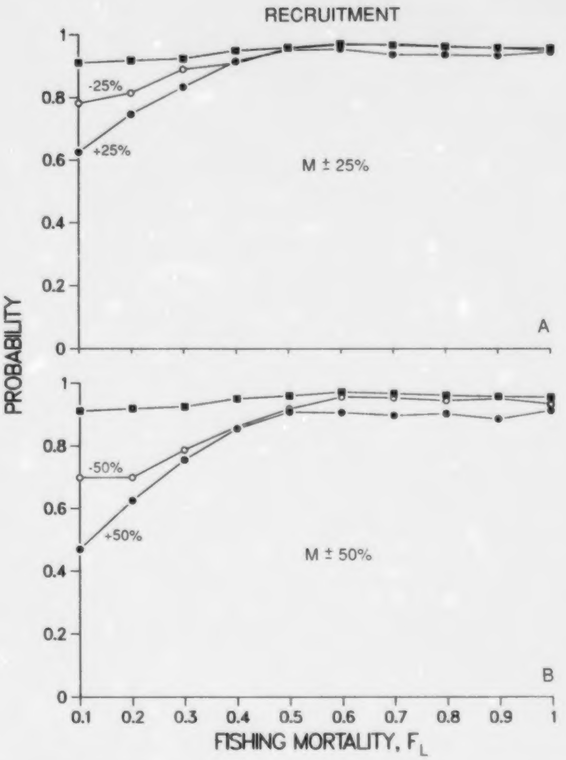

FIG. 9. Probability that the true time trend in age 4 recruitment was correctly identified by estimates from VPA for 10-yr runs of the English sole model. Here and in Fig. 10, F_L was the fishing mortality in the fully recruited ages (≥ 5 yr old). Results shown are for when M^{VPA} was unbiased (■), and greater than the true M (•) or less than the true M (○) by, (A) 25%, or (B) 50%.

When the length of the time series was extended to 20 yr from 10, the probability that the true trend was correctly identified by VPA when M^{VPA} was incorrect generally increased due to larger sample sizes. One exception was for trends in recruitment at low F, where there was a very low rate of successfully identifying the true trend over 20 yr when M^{VPA} was 50% $>M$. A larger number of significant increasing trends in true recruitment were produced with the 20-yr than the 10-yr runs, and the large error in M^{VPA} was sufficient to make many of the estimated trends non-significant, resulting in an incorrect classification.

Discussion

Deterministic Analysis

We have shown that spurious time trends in the most recent estimates of recruitment or stock biomass can be generated by incorrect inputs to non-iterative virtual population analysis. While this problem could be avoided by omitting incomplete cohorts from the VPA, managers

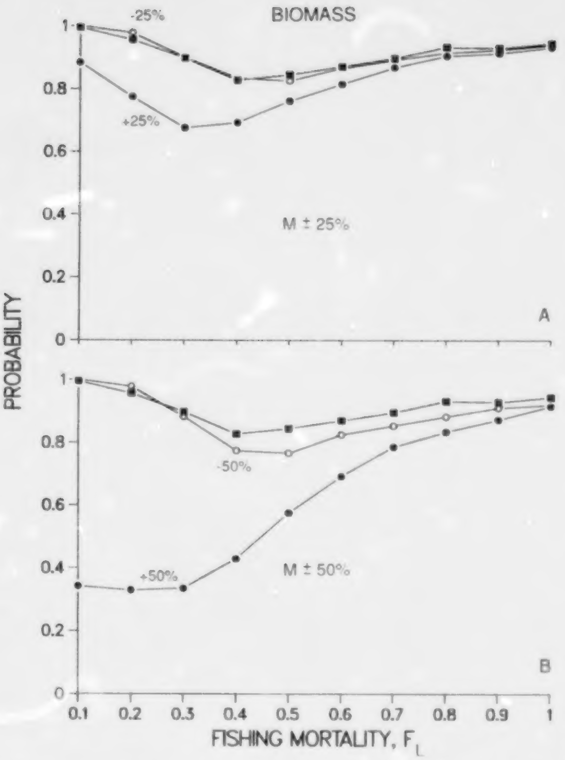

FIG. 10. Probability of correctly detecting a trend in stock biomass. Results are for when M^{VPA} was unbiased (■), and greater than the true M (•) or less than the true M (○) by, (A) 25%, or (B) 50%.

often face situations in which data sets are too short to do this. For example, in long-lived species such as Pacific ocean perch, which may live 30 or more years, the number of years of catch data (n) may be in the same range as the number of ages (k) caught in the fishery. Since there are $n-k+1$ complete cohorts, even an unusually long 30-yr set of catch data composed of 25 ages would have only 6 complete cohorts. Since spurious trends caused by incorrect $F_L{}^{VPA}$ and M^{VPA} are a result of incomplete cohorts, the high proportion of such cohorts in a data set on long-lived species would potentially lead to spurious trends. The magnitude of such trends would depend on the ratio of the true F_L/M and the extent of errors in $F_L{}^{VPA}$ and M^{VPA}. Note that even if an analysis were limited just to complete cohorts in order to eliminate spurious time trends, abundance estimates would still be biased if M^{VPA} and $F_L{}^{VPA}$ were incorrect. This is clearly illustrated in Fig. 2 and 3 by the horizontal portions of the estimated time series, which were derived from complete cohorts. These estimates were higher or lower than the true values, depending on the error in M^{VPA} or $F_L{}^{VPA}$, as noted by Pope (1972).

Errors in reconstructed abundances that result from inaccurate F^{VPA} for the oldest age have long been recognized as a limitation of VPA in making timely estimates of recent stock abundances and projecting future yields (Pope 1972; Rivard 1983). Auxiliary information, such as effort, is therefore frequently used to "tune" the analysis to attempt to reduce uncertainty about the $F_L{}^{VPA}$ values (e.g., Mohn 1983; Pope and Shepherd 1985). To the extent that these methods are successful, they should help to reduce the time trends in abundance that may result from the use of incorrect $F_L{}^{VPA}$ values. In any case, Pope's (1972) equation for bias in abundance estimates for VPA can be used to assess the effects of errors in $F_L{}^{VPA}$.

In contrast, errors in the input M^{VPA} cannot be reduced by tuning methods. Although methods to estimate M^{VPA} in exploited populations have been developed (Ricker 1975; Paloheimo 1980; Fournier and Archibald 1982), they often give poor estimates (Fournier and Archibald 1982). Frequently, M^{VPA} is chosen by historical precedent or by using correlations that have been observed between mortality and other measurable life history traits (Beverton and Holt 1959; Pauly 1980; Myers and Doyle 1983; Roff 1984). The choice of M^{VPA} is most important for lightly fished stocks, because M constitutes a large portion of total mortality ($F+M$). An error in M^{VPA} thus may result in steep spurious trends in the incomplete cohorts. Luckily, for heavily fished stocks in which accurate estimates of abundance are critical, errors in M^{VPA} result in much weaker spurious time trends (Fig. 7). Also, the most recent years' estimates of biomass are the least affected by errors in M^{VPA}, allowing for more accurate projections of future yield (Rivard and Foy 1987), assuming, of course, that the partial recruitment coefficients are accurate.

When methods for estimating M^{VPA} and $F_L{}^{VPA}$ are used that cause one parameter to be overestimated and the other underestimated (as in some tuning methods), the spurious trends that we have documented for each of these biases will be in opposite directions. Thus, for example, an increasing spurious trend caused by M^{VPA} being too low will be offset to some extent by the decreasing time trends caused by the overestimate of $F_L{}^{VPA}$. However, these trends will probably not compensate exactly for one another, and there will still be a spurious net time trend, albeit smaller than documented above.

The spurious time trends that we describe only occur if non-iterative procedures are used to estimate the partial recruitment coefficients. A separate analysis for all 10 stocks in Table 2 shows that when iterative procedures are used, the estimated partial recruitments, s_i, converge on values that mainly reflect the complete cohorts, and which virtually eliminate the spurious time trends (M.F. Lapointe and R.M. Peterman, unpublished data). However, there will still be errors in absolute abundances when erroneous $F_L{}^{VPA}$ and M^{VPA} are used in iterative VPA (Rivard and Foy 1987).

Although the iterative procedure has the desirable property of eliminating spurious time trends, its use is based on the assumption that the age-specific selectivities have remained constant over the entire data series. There are a number of reasons why these selectivities may change over time, such as changing fish size-at-age, new regulations on gear type, and changing fleet composition and behavior. For example, Winters et al. (1985) note that as abundance declines over time in an overexploited stock, fishing effort focuses on the younger age-groups, as the older ages become scarce. If historical partial recruitment patterns are used in a stock reconstruction, selection coefficients for the young ages in recent years will be underestimated which will result in dangerous overestimates of abundance (Winters et al. 1985). Rivard and Foy (1987) also note that inaccurate partial recruitment coefficients are a major source of error in making catch projections. These examples illustrate the potential dangers of using iteratively determined partial recruitment coefficients in VPA. Thus, this iterative use of VPA may not always be a reasonable alternative to non-iterative VPA.

Stochastic Example

Fish stock assessments based upon VPA will likely be biased as well as imprecise because the estimate of natural mortality rate used in the VPA will probably be different from the true mean value of M over time. Our stochastic simulation results showed that the probability of drawing a correct conclusion about the time trend in abundance depended upon the extent and direction of bias in M^{VPA} and the intensity of fishing.

If a stock is lightly fished, there is a moderately high chance of drawing an incorrect conclusion about trends in abundance. The consequences of being incorrect depend on the specific management situation. A potentially dangerous example is the case where $M^{\mathrm{VPA}} < M$, resulting in an estimated time trend that is too positive compared to the true trend. The impact of fishing on the stock abundance would be underestimated, which could result in dangerous conclusions about the stock's ability to withstand future increases in exploitation. Conversely, a tendency for M^{VPA} to be greater than the true M would lead to a bias toward spurious decreasing trends in abundance. These might result in unwarranted, overly conservative fishing regulations that could create unnecessary economic problems in the fishing industry.

The extent to which these spurious trends appear in regressions fitted to reconstructed abundances will depend in part on the number of years in the catch-at-age data relative to the number of age-classes that are fished. The proportion of incomplete cohorts will be higher in short data sets for a given fish species. In this situation, the effects of incorrect inputs to VPA on time trends in abundance will tend to diminish with longer time series as more complete cohorts become available.

Estimated time trends in abundance of fish are only one component of the information upon which fishery managers base decisions. Nevertheless, to the extent that those trends affect decisions, the biases noted above will be important, and managers should therefore recognize the biases inherent in VPA.

General conclusions

We suspect that spurious time trends may he embedded in many time series of fish abundances that were reconstructed in the past using non-iterative VPA, because M^{VPA} or $F_L{}^{\mathrm{VPA}}$ were unlikely to have equalled their true values. Such trends may not be obvious when partially masked by stochastic variation, but they may potentially have influenced interpretations of past dynamics of fish populations in response to management regulations or hypothesized biological or physical oceanographic mechanisms.

Recently, a number of non-sequential, statistically fitted catch-at-age models have been developed to overcome problems of poor estimates of recent abundances resulting from VPA (Doubleday 1976; Fournier and Archibald 1982; Pope and Shepherd 1982; Collie and Sissenwine 1983; Deriso et al. 1985; Gudmundsson 1986; Methot 1989). Although the methods usually require independent estimates of natural mortality, to our knowledge they will not generate spurious time trends in the most recent abundances, even if incorrect M values are used. However, these methods make a number of assumptions to reduce the number of unknown parameters and may require extra structure, such as a relationship between effort and fishing mortality (Deriso et al. 1985). Therefore, because of the potential for hidden biases of the sort we have demonstrated for VPA, we strongly urge that the performance of these newer models be tested extensively via the simulation approach used here and elsewhere (e.g., Deriso et al. 1988). Using simulation, the accuracy of estimates of abundance from these models should be determined under realistic conditions, including those in which input parameters are incorrect or in which assumptions are violated.

These recent models for stock reconstruction have an important advantage over standard VPA; they incorporate auxiliary information such as effort, abundance surveys, etc. (e.g., Deriso et al. 1985; Methot 1989) in the estimation procedure. Better estimates of abundance will likely result if a larger number of independent and reliable sets of information are included in an analysis. A bias in any one type of input information is more likely to be offset by an opposite bias in another set than in VPA, which uses relatively few types of information.

Regardless of the methods used to estimate fish stock abundance, our results further illustrate the need to support abundance estimates, predictions and advice given to managers with sensitivity analyses. In this way managers can assess how incorrect parameter estimates and errors in assumptions may combine with peculiarities of the analytical model to give rise to misleading results. This was highlighted in the results we present here, where erroneous input parameters to VPA gave either positive or negative spurious trends. One way to quantify the effects of errors in the stock assessment method is to calculate the probability that the method will correctly assess a stock's status, as was done here and for whale abundances by Allen and Kirkwood (1976) and de la Mare (1984). Such probability or statistical power analyses could provide important additional insights to complement the wider array of information on which fishery managers base decisions.

Acknowledgments

We are extremely grateful to Alec MacCall, Jeremy Collie, Darren Gillis, Michael F. Lapointe, and two anonymous reviewers whose comments greatly improved the draft manuscript. Funding was provided by the Natural Sciences and Engineering Research Council of Canada.

References

Agger, P., I. Boetius, and M. Lassen. 1973. Error in the virtual population analysis: the effect of uncertainties in the natural mortality coefficient. J. Cons. Cons. int. Explor. Mer 35: 93.

Allen, K. R., and G. P. Kirkwood. 1976. Is experimental management of whale stocks practicable. Comment on ACMRR/MM/SC/57,61,82. FAO Scientific Consultations on Marine Mammals, Bergen, Norway. 10 pp. MS. (summarized in Allen, K.R. 1980. Conservation and Management of Whales. Univ. of Washington Press).

Anderson, E. D., and A. J. Paciorkowski. 1980. A review of the northwest Atlantic mackerel fishery. Rapp. P.-v. Reun. Cons. int. Explor. Mer 177: 175-211.

Archibald, C. P., D. Fournier, and B. M. Leaman. 1983. Reconstruction of stock history and development of rehabilitation strategies for Pacific ocean perch in Queen Charlotte Sound, Canada. N. Am. J. Fish. Manage. 3: 283-294.

Beverton, R. J. M., and S. J. Holt. 1959. A review of the lifespans and mortality rates of fish in nature, and their relation to growth and other physiological characteristics. Ciba Found. Colloq. Aging 5: 142-180.

Collie, J. S., and M. P. Sissenwine. 1983. Estimating population size from relative abundance data measured with error. Can. J. Fish. Aquat. Sci. 40: 1871-1879.

de la Mare, W. K. 1984. On the power of catch per unit effort series to detect declines in whale stocks. Rep. Int. Whaling Comm. 34: 655-662.

Deriso, R. B., T. J. Quinn II, and P. R. Neal. 1985. Catch-age analysis with auxiliary information. Can. J. Fish. Aquat. Sci. 42: 815-824.

Deriso, R. B., P. R. Neal, and T. J. Quinn II. 1989. Further aspects of catch-age analysis with auxiliary information, p. 127-135. *In* R. J. Beamish and G. A. McFarlane [ed.] Effects of ocean variability on recruitment and an evaluation of parameters used in stock assessment models. Can. Spec. Publ. Fish. Aquat. Sci. 108.

Doubleday, W. G. 1976. A least squares approach to analyzing catch at age data. Int. Comm. Northwest Atl. Fish. Res. Bull. 12: 69-81.

Fournier, D. A. 1983. An analysis of the Hecate Strait Pacific cod fishery using an age-structured model incorporating density-dependent effects. Can. J. Fish. Aquat. Sci. 40: 1233-1243.

Fournier, D. A., and C. P. Archibald. 1982. A general theory for analyzing catch at age data. Can. J. Fish. Aquat. Sci. 39: 1195-1207.

Gulland, J. A. 1983. Fish stock assessment. Wiley-Interscience. Chichester, U.K. 223 p.

Gudmundsson, G. 1986. Statistical considerations in the analysis of catch-at-age observations. J. Cons. Cons. int. Explor. Mer 43: 83-90.

Gunderson, D. R. 1977. Population biology of Pacific ocean perch (*Sebastes alutus*) stocks in the Washington-Queen Charlotte Sound region, and their response to fishing. Fish. Bull. (U.S.) 75: 369-403.

Hayman, R. A., A. V. Tyler, and R. L. Demory. 1980. A comparison of cohort analysis and catch per unit effort for Dover sole and English sole. Trans. Am. Fish. Soc. 109: 35-53.

Hightower, J. E., and G. D. Grossman. 1985. Comparison of constant effort harvest policies for fish stocks with variable recruitment. Can. J. Fish. Aquat. Sci. 42: 982-988.

Hoag, S. H., and R. S. McNaughton. 1978. Abundance and fishing mortality of Pacific halibut, cohort analysis, 1935-1976. Int. Pac. Halibut Comm. Sci. Rep. 65: 45 p.

MacCall, A. D. 1986. Virtual population analysis (VPA) equations for nonhomogeneous populations, and a family of approximations including improvements on Pope's cohort analysis. Can. J. Fish. Aquat. Sci. 43: 2406-2409.

Methot, R. D. 1989. Synthetic estimates of historical abundance and mortality for northern anchovy, *Engraulis mordax*. *In* E.F. Edwards and B.A. Megrey [ed.] Mathematical analysis of fish stock dynamics: review and current applications. Am. Fish. Soc. Symp. Ser. 6.

Mohn, R. K. 1983. Effects of error in catch and effort data on tuning cohort analysis, with a postscript on logistic production models, p. 141-150. *In* W.G. Doubleday and D. Rivard [ed.] Sampling commercial catches of marine fish and invertebrates. Can. Spec. Publ. Fish. Aquat. Sci. 66.

Myers, R. A. and R. W. Doyle. 1983. Predicting natural mortality rates and reproduction-mortality trade-offs from life history data. Can. J. Fish. Aquat. Sci. 40: 612-620.

Paloheimo, J. E. 1980. Estimation of mortality rates in fish populations. Trans. Am. Fish. Soc. 109: 378-386.

Pauly, D. 1980. On the interrelationships between natural mortality, growth parameters and mean environmental temperature in 175 fish stocks. J. Cons. Cons. int. Explor. Mer 39: 175-192.

Peterman, R. M., and M. J. Bradford. 1987. Statistical power of trends in fish abundance. Can. J. Fish. Aquat. Sci. 44: 1879-1889.

Peterman, R. M., M. J. Bradford, and G. H. Kruse. 1987. Simulation model of English sole (*Parophrys vetulus*) population dynamics in Washington and Oregon coastal waters. Can. J. Fish. Aquat. Sci. 44: 1870-1878.

Pope, J. G. 1972. An investigation of the accuracy of virtual population analysis using cohort analysis. Int. Comm. Northwest Atl. Fish. Res. Bull. 9: 65-74.

Pope, J. G., and J. G. Shepherd. 1982. A simple method for the consistent interpretation of catch-at-age data. J. Cons. Cons. int. Explor. Mer 40: 176-184.

1985. A comparison of the performance of various methods for tuning VPAs using effort data. J. Cons. Cons. int. Explor. Mer 42: 129-151.

Prager, M. H., and A. D. MacCall, 1988. Sensitivities and variances of virtual population analysis as applied to the mackerel, *Scomber japonicus*. Can. J. Fish. Aquat. Sci. 45: 539-547.

Ricker, W. E. 1975. Computation and interpretation of biological statistics of fish populations. Bull. Fish. Res. Board Can. 191: 382 p.

Rivard, D. 1983. Effects of systematic, analytical, and sampling errors on catch estimates: a sensitivity analysis, p. 114-129. *In* W. G. Doubleday and D. Rivard [ed.], Sampling commercial catches of marine fish and invertebrates. Can. Spec. Publ. Fish. Aquat. Sci. 66.

Rivard, D., and M. G. Foy. 1987. An analysis of errors in catch projections for Canadian Atlantic fish stocks. Can. J. Fish. Aquat. Sci. 44: 967-981.

Roff, D. A. 1981. On estimating partial recruitment in virtual population analysis. Can. J. Fish. Aquat. Sci. 38: 1003-1005.

1984. The evolution of life history parameters in teleosts. Can. J. Fish. Aquat. Sci. 41: 989-1000.

Sampson, D. B. 1987. Variance estimators for virtual population analysis. J. Cons. Cons. int. Explor. Mer 43: 149-158.

SAVILLE, A., AND R. S. BAILEY. 1980. The assessment and management of the herring stocks in the North Sea and to the west of Scotland. Rapp. P.-v. Reun. Cons. int. Explor. Mer 177: 112–142.

SCHAAF, W. E. 1980. An analysis of the dynamic population response of Atlantic menhaden, ***Brevoortia tyrannus***, to an intensive fishery. Rapp. P.-v. Reun. Cons. int. Explor. Mer 177: 243–251.

SIMS, S. E. 1984. An analysis of the effect of errors in the natural mortality rate on stock-size estimates using virtual population analysis (cohort analysis). J. Cons. Cons. int. Explor. Mer 41: 149–153.

TYLER, A. V., L. L. SEBRING, M. C. MURPHY, AND L. F. MURPHY. 1985. A sensitivity analysis of Deriso's delay-difference equation using simulation. Can. J. Fish. Aquat. Sci. 42: 836–841.

ULLTANG, O. 1977. Sources of errors in and limitations of virtual population analysis (cohort analysis). J. Cons. Cons. int. Explor. Mer 37: 249–260.

WAKABAYASHI, K. 1984. Estimations of biomass and yield for yellowfin sole in the eastern Bering Sea. Int. North Pac. Fish. Comm. Bull. 42: 65–72.

WINTERS, G. M., E. L. DALLEY, AND J. A. MOORES. 1985. Fortuity disguised as fisheries management: the case history of Fortune Bay herring. Can. J. Fish. Aquat. Sci. 42 (Suppl. 1): 263–274.

The Influence of Statistical Error on Stock Assessment: Illustrations from Schaefer's Model

Jon Schnute

Department of Fisheries and Oceans, Biological Sciences Branch,
Pacific Biological Station, Nanaimo, B.C. V9R 5K6

Abstract

SCHNUTE, J. 1989. The influence of statistical error on stock assessment: illustrations from Schaefer's model, p. 101–109. *In* R. J. Beamish and G. A. McFarlane [ed.] Effects of ocean variability on recruitment and an evaluation of parameters used in stock assessment models. Can. Spec. Publ. Fish. Aquat. Sci. 108.

Data available for fish stock assessment almost never lead to unambiguous conclusions. One method of dealing with this problem is to use the data to determine confidence intervals, rather than mere estimates, of the parameters of interest. For example, a confidence interval for the total allowable catch (TAC) may be more useful than a single estimate. In this paper I show that confidence intervals depend crucially, not only on the choice of model (such as the Schaefer model), but also on assumptions related to statistical error. To illustrate the importance of this point, I examine the consequences of various error assumptions in Schaefer's original analysis and demonstrate that different statistical models can lead to radically different conclusions.

Résumé

SCHNUTE, J. 1989. The influence of statistical error on stock assessment: illustrations from Schaefer's model, p. 101–109. *In* R. J. Beamish and G. A. McFarlane [ed.] Effects of ocean variability on recruitment and an evaluation of parameters used in stock assessment models. Can Spec. Publ. Fish. Aquat. Sci. 108.

Il est très rare que les données concernant l'évaluation des stocks de poissons aboutissent à des conclusions non ambiguës. Une façon de remédier à cette situation est d'employer les données pour établir des intervalles de confiance, plutôt que de simples estimations, à l'égard des paramètres à l'étude. Par exemple, il peut être plus utile d'établir un intervalle de confiance en ce qui concerne le total des prises admissibles (TPA) que de procéder à une seule estimation. Dans cet article, l'auteur démontre que les intervalles de confiance dépendent, de façon cruciale, non seulement du choix du modèle (comme le modèle Schaefer), mais également des hypothèses formulées quant à l'erreur statistique. Afin de souligner l'importance de ce point, il examine les conséquences de diverses hypothèses relatives à l'erreur statistique dans l'analyse originale de Schaefer et démontre que divers modèles statistiques peuvent aboutir à des conclusions tout à fait différentes.

Introduction

This IRIS-INPFC International Symposium is being held in a curiously auspicious year: 1987 is the thirtieth anniversary of the publication of Schaefer's (1957) dynamic model for the yellowfin tuna fishery in the eastern tropical Pacific Ocean. As a personal note, I might add that this is also the tenth anniversary of my own first publication in fishery literature (Schnute 1977), which happened to address the problem of estimating parameters in the Schaefer model.

Many changes have taken place in fishery research during the 30 years since Schaefer published his ideas. Statistical theory in general has advanced on many fronts. Furthermore, computing technology has improved dramatically, making it possible to explore statistical models that would have been prohibitively difficult to implement technically in 1957. Today we can readily compare the results of several competing models to discover which seems to provide the most reasonable description of a fishery.

Consider a fundamental question: what is a model and what use can we make of it in stock assessment? Above all, it must provide a tool for making rational management decisions. For example, given all the data from the fishery, it should be able to suggest values (or ranges of values) for key parameters such as the total allowable catch (TAC) or the maximum sustainable yield (MSY). A model, then, is a *filter* for the data: lots of numbers are fed into it and only a few come out.

Our daily life involves the use of filters that we hardly think twice about. For example, a radio selects one signal from a vast spectrum of electromagnetic radiation. In fact, the interesting thing about a radio is that the user can tune it to define the signal. This is done essentially by eliminating all other signals. Noise by one definition is signal by another. No doubt we have all experienced the problem of a "ghost" station that creeps into the broadcast we're really trying to hear.

Can "ghosts" creep into fishery models? In this paper I'm going to demonstrate that the answer is emphatically *yes*. As with a radio, the signal passed by the filter (i.e., the parameters suggested by the model) can depend crucially on the choice of filter (model). For example, one might reach the statistically rigorous conclusion that an estimate of MSY is 192 million lb and that, with 95% confidence, the true MSY lies somewhere between 163 and 247 million lb. Yet, with a different model and equal statistical rigor, it may turn out that the estimate is 138 million lb, far outside the confidence interval suggested by the first model. *This example is not merely academic.* I will demonstrate that both these conclusions follow from data on the yellowfin tuna fishery up to the year 1957, when Schaefer published his dynamic model.

The plan of the paper is this. In section 2 I will formulate six versions of a Schaefer model, all of which boil down to special ways of writing a single general equation. In section 3 I will discuss two ways of introducing statistical error into each of the six models, thus giving a total of 12 statistical models. I will also provide a simple example to show convincingly why different models can give fundamentally different results. Finally, in section 4 I will apply the 12 models to the tuna data up to 1967, as published by Pella and Tomlinson (1969). This time series extends by a decade the data available to Schaefer in 1957.

I want to stress that the examples worked here are not intended to constitute an analysis of the eastern tropical Pacific tuna fishery. I have chosen that fishery merely for convenience, because of the high quality of available data and because of the fishery's historical relationship to Schaefer's research. A broad conclusion of the paper is that results from a model depend dramatically on model choice. This means that the modeler must work closely with people knowledgeable about the fishery. I have no such intimate knowledge of the tuna fishery and seek only to explore the range of outcomes possible based on a variety of model choices.

The Schaefer Model

Schaefer's model can be expressed in several ways. More precisely, one can think of a family of models oriented to three time series: the total catch C_t, the fishing effort E_t, and the catch per unit effort (CPUE) U_t in year t. These three data sets are, of course, dependent because

$$(2.1) \qquad C_t = E_t U_t .$$

The key idea underlying all forms of the model is this: *in the long run, higher effort levels E lead to lower levels of catch per unit effort U*. The simplest version of the model assumes a linear relationship between E and U,

$$(2.2) \qquad U_t = \alpha - \beta E_t ,$$

with nonnegative parameters α and β independent of t.

Figure 1 illustrates the line (2.2) against the background of curves on which the catch (2.1) is constant. Notice that one particular catch contour is tangent to the line. This corresponds to the maximum possible catch C^*, that is, the maximum value of (2.1) subject to the constraint (2.2). The point (E^*, U^*) where this maximum is achieved turns out to be

$$(2.3a) \qquad E^* = \alpha/(2\beta)$$

$$(2.3b) \qquad U^* = \alpha/2.$$

Furthermore, it follows from (2.1) and (2.3) that

$$(2.4) \qquad C^* = \alpha^2/(4\beta).$$

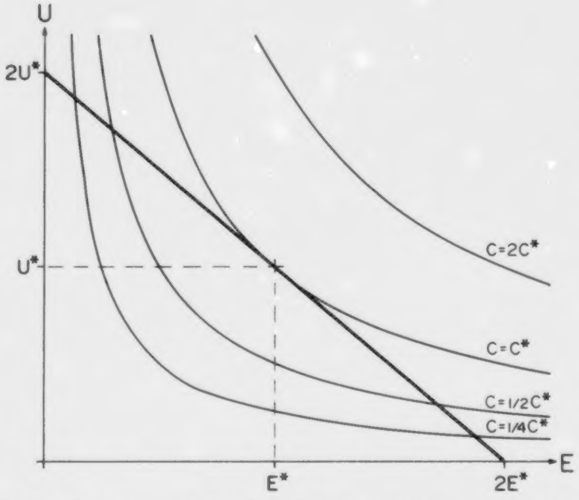

FIG. 1. The linear relationship (heavy line) between E and U defined by Schaefer's equilibrium model (2.2). Four contours (light curves) of the surface $C = EU$ are also shown. The highest value of C along the line occurs at (E^*, U^*), where $C = C^*$.

Thus, the parameters α and β define the maximum long-term catch C^* for the fishery.

For the sake of argument in this paper, I interpret C^* as the maximum sustainable yield (MSY). Since (2.2) is a model for the data series E_t and U_t, it can be used to estimate α and β. These estimates, in turn, give the estimate (2.4) for C^*. Thus, in the language of the introduction, (2.2) can serve as a filter for deriving one key quantity (the MSY) from the available fishery data. I will focus primarily here on the estimate and confidence interval for C^*, although other quantities may also be of interest to the manager. For example, E^* in (2.3a) might be interpreted as an acceptable long term level of fishing effort.

In (2.2) U_t is treated as the predicted quantity. The following equivalent relationship describes E_t as a function of U_t:

$$(2.5) \qquad E_t = (\alpha - U_t)/\beta.$$

Furthermore, combining (2.1) and (2.2) gives the quadratic expression

$$(2.6) \qquad C_t = (\alpha - \beta E_t)\, E_t$$

for C_t. Figure 2 illustrates the parabola (2.6) against a background of lines along which U_t is constant. In this case, the high point of the parabola evidently corresponds to the point (E^*, C^*), whose coordinates are given by (2.3a) and (2.4), respectively. Notice that each of the three relationships (2.2), (2.5), and (2.6) could be used to define regressions on the basis of which α and β (and thus C^*) could be estimated. I'll return to this point in the next section.

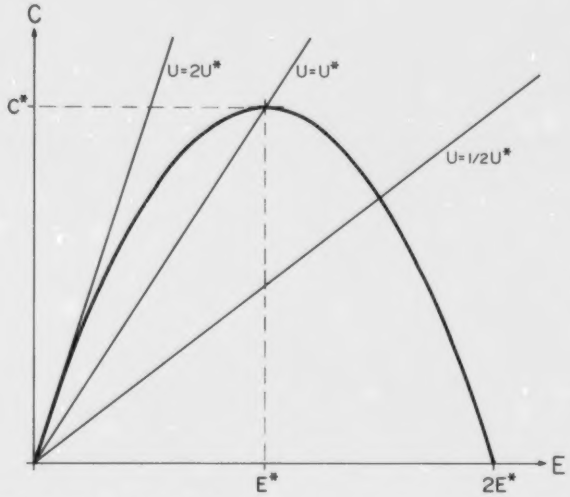

FIG. 2. The parabolic relationship (heavy curve) between E and C defined by Schaefer's equilibrium model (2.6). Three contours (light lines) of the surface $U = C/E$ are also shown. As in Fig. 1, the highest value of C, i.e., C^*, occurs where $E = E^*$ and $U = U^*$.

The models described so far are all *equilibrium* models, in that they are oriented toward long-term effects. For example, (2.6) would make no sense at all if it were intended to describe a single year. After all, how could the catch decline with increasing effort, as predicted on the descending limb of the parabola in Fig. 2? The model seems to suggest that fishermen will start throwing live fish overboard after they have invested the effort E^*! Obviously, (2.6) attempts only to describe the effects of high effort levels in the long run: overfishing results in a declining population and a reduced catch.

A simple way to render (2.2) *dynamic* is to assume that U_t depends both on E_t and on U_{t-1}:

$$(2.7) \qquad U_t = \alpha - \beta E_t + \gamma U_t - 1,$$

where

$$(2.8) \qquad |\gamma| < 1.$$

The idea underlying (2.7) is that the CPUE in year t depends not only on the effort that year but on a residual effect left from the previous year. Typically one would expect a positive γ, but negative values of γ need not be ruled out. In any case the condition (2.8) guarantees that U_t remains bounded.

If E_t is held at the fixed level E for many years, then U_t in (2.7) converges to the limiting value

$$U = (\alpha - \beta E)/(1-\gamma).$$

Thus, (2.7) is consistent with the equilibrium model (2.2), except that α and β must be replaced by $\alpha/(1-\gamma)$ and $\beta/(1-\gamma)$, respectively. In particular, it follows from (2.7) – (2.8) that the maximum sustainable catch

$$(2.9) \qquad C^* = \alpha^2/[4\beta(1-\gamma)]$$

is achieved at the constant effort level

$$(2.10) \qquad E^* = \alpha/(2\beta).$$

A fishery operating at this level will maintain the CPUE

$$(2.11) \qquad U^* = \alpha/[2(1-\gamma)].$$

Notice the correspondence between equations for equilibrium and dynamic models shown below:

Equilibrium Model	Dynamic Model
(2.2)	(2.7)
(2.3a)	(2.10)
(2.3b)	(2.11)
(2.4)	(2.9)

Each equilibrium equation can be obtained from its dynamic counterpart by setting $\gamma = 0$.

Using (2.9) – (2.10), one can eliminate the parameters α and β in (2.7) in favor of C^* and E^* to obtain

$$(2.12) \qquad U_t = (1-\gamma)\frac{C^*}{E^*}\left(2 - \frac{E_t}{E^*}\right) + \gamma U_{t-1}.$$

This equation clarifies the significance of (2.7), since it represents U_t as the weighted sum of two terms: (1) last year's CPUE U_{t-1} with weight γ and (2) an equilibrium correction with weight $1-\gamma$. The equilibrium correction serves to bring the dynamic model into line with the equilibrium model. When $\gamma = 0$, only this correction is operative, and (2.12) reduces to an equilibrium model. When $\gamma = 1$, there is no equilibrium correction, and the model reduces to constant CPUE: $U_t = U_{t-1}$.

I showed earlier that the equilibrium model has three equivalent versions (2.2), (2.5), and (2.6), which predict U_t, E_t, and C_t, respectively. Similarly, the dynamic model can be written in three equivalent ways that focus on U_t, E_t, or C_t. The first of these is given by (2.12). Thus, (2.12) can serve as the starting point for a general class of models for which there are three possible dependent variables (U_t, E_t, C_t) and two possible predictive modes (equilibrium with $\gamma = 0$ or dynamic with $\gamma \neq 0$). This gives $3 \times 2 = 6$ possible combinations. Table 1 lists the model equation for each case.

The equations in Table 1 involve three parameters (C^*, E^*, γ) with simple interpretations. As discussed earlier, C^* and E^* represent, respectively, MSY and the appropriate long-term effort for achieving MSY. The parameter γ relates to the fishery's tendency to approach

TABLE 1. Model equations for six possible models obtained from the general equation (2.12). There are three possible dependent variables (U_t, E_t, C_t) and two possible predictive modes (equilibrium or dynamic).

Variable	Mode	Equation
U_t	Equilibrium	$U_t = \frac{C^*}{E^*}\left(2 - \frac{E_t}{E^*}\right)$
U_t	Dynamic	$U_t = (1-\gamma)\frac{C^*}{E^*}\left(2 - \frac{E_t}{E^*}\right) + \gamma U_{t-1}$
E_t	Equilibrium	$E_t = E^*\left(2 - \frac{E^*}{C^*}U_t\right)$
E_t	Dynamic	$E_t = E^*\left[\left(2 - \frac{E^*}{C^*}U_t\right) - \frac{\gamma}{1-\gamma}\frac{E^*}{C^*}(U_t - U_{t-1})\right]$
C_t	Equilibrium	$C_t = C^*\frac{E_t}{E^*}\left(2 - \frac{E_t}{E^*}\right)$
C_t	Dynamic	$C_t = (1-\gamma)C^*\frac{E_t}{E^*}\left(2 - \frac{E_t}{E^*}\right) + \gamma E_t U_{t-1}$

equilibrium. If γ is near 1, the approach is slow and steady. If γ is near -1, the approach is again slow, but oscillatory around equilibrium conditions. If γ is near 0, the fishery approaches equilibrium rapidly. When $\gamma = 0$, dynamic effects are absent, and the model reduces to pure equilibrium.

Statistical Error

To apply any of the models in Table 1, it is necessary to render them statistical. At first glance, this might seem to be a minor matter. One could, for example, simply add a normal error term to each model. It turns out, however, that the choice of error structure can have a profound influence on the outcome of the analysis. A simple example illustrates this point dramatically.

Consider the problem of finding a regression line though the four points (1, 1), (1, 3), (3, 1), and (3, 3). These form the corners of a square, as illustrated by the solid dots in Fig. 3. Suppose first that the x-coordinate of each point is known exactly and that the error is in y. Then at both $x = 1$ and $x = 3$ there are two observed values of y: $y = 1$ and $y = 3$. Consequently, the mean value of y is 2 at both $x = 1$ and $x = 3$. Joining these two means, i.e., the points (1, 2) and (3, 2), I obtain the horizontal (broken) line shown in Fig. 3. Alternatively, suppose that the error is in x. Then the above argument must be altered by reversing the roles of x and y: at both $y = 1$ and $y = 3$, there are two x-measurements with mean value 2. Joining these means gives the vertical (dashed) line in Fig. 3.

The two possibilities, horizontal or vertical, represent extremes for the slope of a line (0 or ∞). Consequently, the conclusion to be drawn from the four data points *depends entirely on the description of error*. It is not that the data are complete nonsense; rather, the issue is one of experimental design. The data suggest either that y is independent of x or that x is independent of y. The correct conclusion hinges on which variable (x or y, respectively) is measured without error.

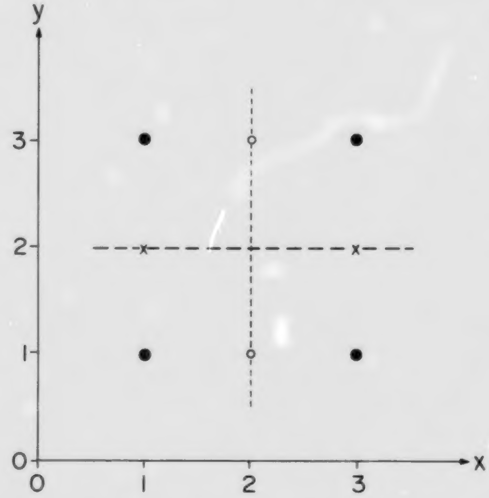

FIG. 3. The problem of finding a regression line through four points (solid dots) that comprise the vertices of a square. If the error is in y, then two mean values of y (labelled with crosses) determine a horizontal line. If the error is in x, then two mean values of x (labelled with open circles) determine a vertical line.

Compare equations (2.2) and (2.5) in the light of this example. These are apparently equivalent ways of writing the Schaefer equilibrium model. Suppose, however, that they are treated as regression equations in which the error is either in U_t or E_t, respectively. If four data points (E_t, U_t) happened to lie on a square, as in Fig. 3, then the regression estimates for β from (2.2) and (2.5) would be 0 and ∞, respectively. Since real data (E_t, U_t) typically define a highly disperse scatter plot, it appears that an analysis from a Schaefer model (and hence an estimate of MSY) may depend crucially on the choice of error structure.

In this paper I consider two possible forms for the error: normal and lognormal. Each type of error can be incorporated into each of the six models in Table 1. This gives the $6 \times 2 = 12$ possible statistical models listed in Table 2, where (for convenience throughout the rest of the paper) I assign a number to each model. For example, model 2 is an equilibrium model for U_t with lognormal error, that is,

$$(3.1) \quad \log(U_t) = \log \left[\frac{C^*}{E^*} \left(2 - \frac{E_t}{E^*} \right) \right] + \sigma \epsilon_t,$$

where (i) $\sigma > 0$ represents a standard deviation, (ii) ε_t is normal with mean 0 and variance 1, and (iii) ε_s and ε_t are independent for $s \neq t$.

Although 12 models are listed in Table 2, there are really only 10 distinct models here. It turns out that models 2 and 10 are identical, as are models 4 and 12. This is true because from (2.1)

$$\log(C_t) = \log(U_t) + \log(E_t).$$

TABLE 2. Model numbers for 12 possible statistical models based on three dependent variables (U_t, E_t, C_t), two predictive modes (equilibrium or dynamic), and two predictive error structures (normal or lognormal). It turns out that models 2 and 10 are equivalent, as are models 4 and 12.

Model Number	Variable	Mode	Error
1	U_t	Equilibrium	Normal
2	U_t	Equilibrium	Lognormal
3	U_t	Dynamic	Normal
4	U_t	Dynamic	Lognormal
5	E_t	Equilibrium	Normal
6	E_t	Equilibrium	Lognormal
7	E_t	Dynamic	Normal
8	E_t	Dynamic	Lognormal
9	C_t	Equilibrium	Normal
10	C_t	Equilibrium	Lognormal
11	C_t	Dynamic	Normal
12	C_t	Dynamic	Lognormal

Thus, for example, model 10 can be obtained directly from model 2 by adding $\log(E_t)$ to both sides of (3.1). This constant cancels in computing the sum of squares of residuals, which is the main component of the likelihood function. Similar remarks apply to models 4 and 12.

To discuss estimates and confidence intervals for a parameter (such as C^*), I need to give a brief description of underlying statistical theory. Let y_t denote the observed value of a normal variable, such as U_t in model 1 or $\log(U_t)$ in model 2. Let $z_t(\Theta)$ denote the predicted value of y_t, where $\Theta = (\theta_1, \ldots, \theta_m)$ is a parameter vector. For example, in model 2: $m = 2$, $\Theta = (C^*, E^*)$, and $z_t(\Theta)$ is the expression $\log[(C^*/E^*)(2 - (E_t/E^*))]$ in (3.1) above. Then the model for y_t takes the form

$$(3.2) \quad y_t = z_t(\Theta) + \varepsilon_t,$$

where $\sigma > 0$ and ε_t have the meanings described in connection with (3.1).

Suppose that y_t is observed at times $t = 1, \ldots, N$. Then, for a given parameter vector Θ, the maximum likelihood estimate for σ^2 is

$$(3.3) \quad \hat{\sigma}^2(\Theta) = \frac{1}{N} \sum_{t=1}^{N} [y_t - z_t(\Theta)]^2.$$

Furthermore, it turns out that twice the negative log likelihood for the model (3.2), evaluated at the estimate (3.3), is given by

$$(3.4) \quad \ell(\Theta) = N \log \left(\left[\sum_{t=1}^{N} [y_t - z_t(\Theta)]^2 \right) \right.,$$

except for a constant independent of Θ. Thus, the maximum likelihood estimate $\hat{\Theta}$ for Θ can be obtained by minimizing $\ell(\Theta)$. Let $\tilde{\ell}$ denote the minimum value of ℓ, that is,

$$\tilde{\ell} = \min_{\Theta} \ell(\Theta) = \ell(\hat{\Theta}).$$

Suppose it is desired to find a confidence interval for one parameter, say, θ_1. This can be done by considering the function

$$(3.5) \quad L(\theta_1) = \min_{\theta_2, \ldots, \theta_m} \ell(\theta_1, \theta_2, \ldots, \theta_m).$$

The equation

$$(3.6) \quad L(\theta_1) = \tilde{\ell}$$

has the solution $\theta_1 = \tilde{\theta}_1$ (the first component of $\hat{\Theta}$), since the minimum of L (a function of one parameter) occurs at the overall minimum for ℓ (a function of m parameters). A confidence interval for θ_1 is determined by allowing $L(\theta_1)$ to be larger than $\tilde{\ell}$ by a specified amount, as in the equation

$$(3.7) \quad L(\theta_1) = \tilde{\ell} + N \log \left[1 + \frac{1}{N-m} F_p(1, N-m) \right],$$

where $F_p(1, N-m)$ refers to the upper cutoff point at probability p for the F-distribution with 1 and $N-m$ df. Just as (3.6) typically has one solution $\tilde{\theta}_1$, corresponding to the minimum of L, so (3.7) typically has two solutions $\bar{\theta}_1$ and $\bar{\bar{\theta}}_1$ with

$$\bar{\theta}_1 < \tilde{\theta}_1 < \bar{\bar{\theta}}_1.$$

The interval

$$(3.8) \quad I_p = (\bar{\theta}_1, \bar{\bar{\theta}}_1)$$

defined by the solutions of (3.7) is a p-level confidence interval for θ_1.

The idea leading to the confidence interval I_p is that a probability level p (such as 95%) is specified and then (3.7) is solved to give the end points of I_p. This concept can be turned around by supposing that p is to be determined from θ_1. It follows from (3.7) that

$$(3.9) \quad F_p(1, N-m) = (N-m) \left[e^{[L(\theta_1) - \tilde{\ell}]/N} - 1 \right].$$

In (3.9), θ_1 determines an F-value from which p can be calculated. Use this to define the function

$$(3.10) \quad P(\theta_1) = p.$$

As I illustrate in the next section, $P(\theta_1)$ is essentially a scaled version of $L(\theta_1)$, where units of log likelihood are converted to units of probability.

In closing this section, I should stress that (3.7) is an exact equation for determining the interval (3.8) only if the regression is linear. For nonlinear models (such as most of those here), (3.7) is only approximate (Draper and Smith 1966, p. 273–274). Furthermore, when the number of observations N in (3.2) is large, it can be shown that

$$N \log \left[1 + \frac{1}{N-m} F_p \ (1, N-m) \right] = \chi_p^2 (1),$$

where $\chi_p^2(1)$ is the upper cutoff point of probability p for the χ^2 distribution with 1 df. Thus, for large N, (3.7) is asymptotically equivalent to

$$(3.11) \quad L(\theta_1) = \hat{\ell} + \chi_p^2 (1).$$

This expresses changes in likelihood in terms of a χ^2 statistic, as in the generalized likelihood ratio test.

Depending on the choice of approximation, then, either (3.7) or (3.11) could be used as the basis for statistical analysis. Both methods define a confidence interval with reference to values of the likelihood function. In this paper I use the method based on (3.7), because it takes account of the degrees of freedom associated with the number of observations N. A more refined theory along these lines would, at most, reveal a better choice for the term to be added to $\hat{\ell}$ on the right side of (3.7) or 3.11).

Example from the Tuna Fishery

To illustrate the ideas discussed above, I use data (C_t, U_t, E_t) for the yellowfin tuna fishery in the eastern tropical Pacific Ocean, compiled by Pella and Tomlinson (1969) for the period 1934–67. These data include the series for 1934–55 analyzed by Schaefer (1957), although the Pella and Tomlinson series includes minor adjustments and corrections discovered after Schaefer's paper was published. Figure 4 shows a scatter plot of data points (E_t, U_t). These certainly suggest a linear trend, as in the theoretical Fig. 1, and Fig. 4 illustrates the trend lines estimated from models 1 and 5. As a guide for considering the value of additional data points, the figure distinguishes the series from 1934–57 from that during the subsequent decade 1957–67. As part of my analysis, I investigate the improvement (if any) in parameter estimates that accrues from longer data series.

Figure 5 shows a similar scatter plot of data points (C_t, E_t), which can be compared with the theory in Fig. 2. Again, there is a suggestion of a parabolic trend, although the descending limb of the parabola does not appear to be particularly evident in the data. This suggests that an upper limit for sustainable catch (C^*) may be better defined than the sustained effort level (E^*) required to achieve it. Figure 5 also includes the estimated parabolas from models 1 and 5 that correspond to estimated trend lines shown in Fig. 4.

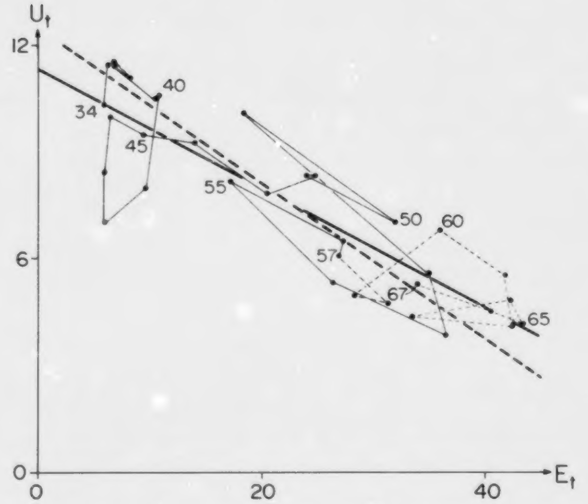

FIG. 4. The yellowfin tuna data series (E_t, U_t) for the period 1934-67. Estimated linear relationships (2.2) from model 1 (solid line) and model 5 (broken line) are also shown. See Table 2 for model descriptions.

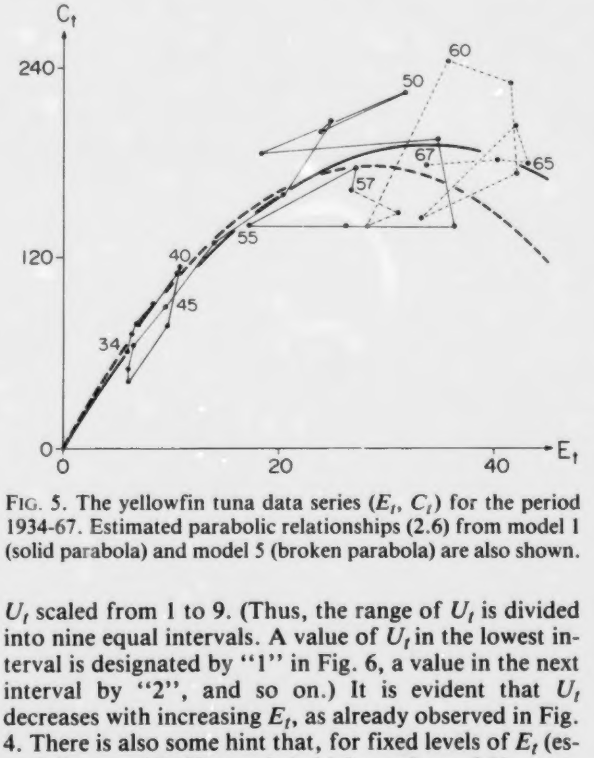

FIG. 5. The yellowfin tuna data series (E_t, C_t) for the period 1934-67. Estimated parabolic relationships (2.6) from model 1 (solid parabola) and model 5 (broken parabola) are also shown.

Figure 6 examines the data from the point of view of dynamic model (2.12), in which U_t depends on both E_t and U_{t-1}. For each point (E_t, U_{t-1}), the figure shows U_t scaled from 1 to 9. (Thus, the range of U_t is divided into nine equal intervals. A value of U_t in the lowest interval is designated by "1" in Fig. 6, a value in the next interval by "2", and so on.) It is evident that U_t decreases with increasing E_t, as already observed in Fig. 4. There is also some hint that, for fixed levels of E_t (especially near 10 effort units), higher values of U_t correlate with higher values of U_{t-1}. The evidence is not compelling, however, and the usefulness of a dynamic model appears marginal on the basis of exploratory data analysis.

As indicated earlier in Section 2, I intend to focus my analysis on the parameter C^*. Each model leads to an estimate of this parameter. Furthermore, a new estimate $\hat{C}_t^*$ is available in each year t, based on the data from

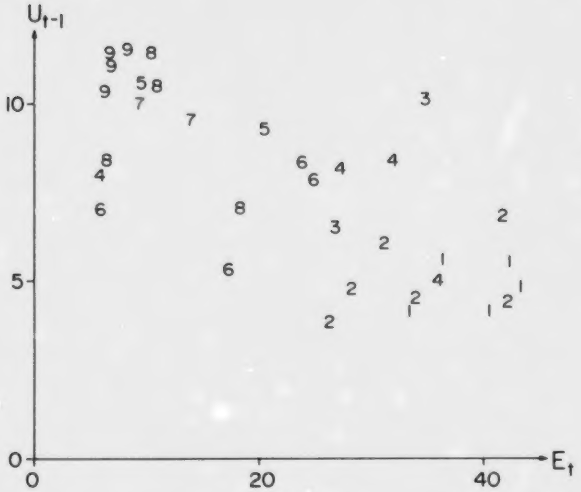

FIG. 6. A representation of U_t as a function of both E_t AND U_{t-1} for the yellowfin tuna data, with t = 1935 to 1967. For each t, the value of U_t (scaled from 1 to 9) is plotted at the point (E_t, U_{t-1}).

the first available year (1934) up to year t. Figure 7 illustrates the series $\hat{C}_t^*$ (t = 1952, . . . , 1967) obtained from each of the 10 distinct models in Table 2. The models give a highly disperse set of estimates when the analysis is confined to the limited data series up to 1952. As more data are included, however, the estimates tend to converge.

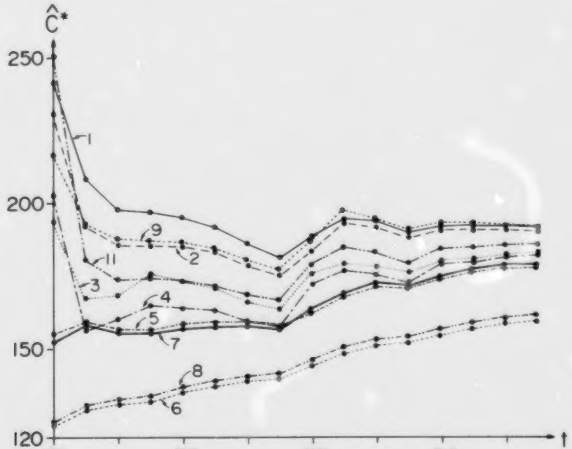

FIG. 7. Estimates $\hat{C}_t^*$, based on yellowfin tuna data up to and including year t. The figure shows the series of estimates $\hat{C}_t^*$, for each model listed in Table 2. Since models 2 and 10 are identical, as are 4 and 12, ten distinct series are shown here.

Visually, the 10 curves in Fig. 7 seem to suggest four groups of models:

(A) 1, 2, 9, and 10, where 2 and 10 are identical;
(B) 3, 4, 11, and 12, where 4 and 12 are identical;
(C) 5 and 7;
(D) 6 and 8.

The groups are arranged in order of decreasing size of estimates for C^*; that is, estimates $\hat{C}_t^*$ from group A are generally higher than comparable estimates in group B, and so on. Notice that the groups can be characterized as follows:

(A) equilibrium models for U_t or C_t with normal or lognormal error;
(B) dynamic models for U_t or C_t with normal or lognormal error;
(C) equilibrium or dynamic models for E_t with normal error;
(D) equilibrium or dynamic models for E_t with lognormal error.

In general, the estimate $\hat{C}_t^*$ is larger for an equilibrium model than for its dynamic counterpart. Similarly, $\hat{C}_t^*$ is larger if the error is normal, rather than lognormal. When the model predicts U_t or C_t, the mode (equilibrium vs. dynamic) is more important than the error (normal vs. lognormal). By contrast, when the model predicts E_t, the error is more important than the mode. In fact, when a model for E_t is allowed to be dynamic, the estimated value of γ typically is very small. This explains why the estimated curves for models 4 and 6 (and, similarly for models 5 and 7) are so close to each other in Figure 7.

The next step in the analysis involves finding confidence limits for C^*. Figure 8 illustrates how this process works. The solid curve in the figure represents the function L (C^*) defined by (3.5) for model 1, based on data from 1934 to 1957. To be precise, $L(C^*)$ is computed from

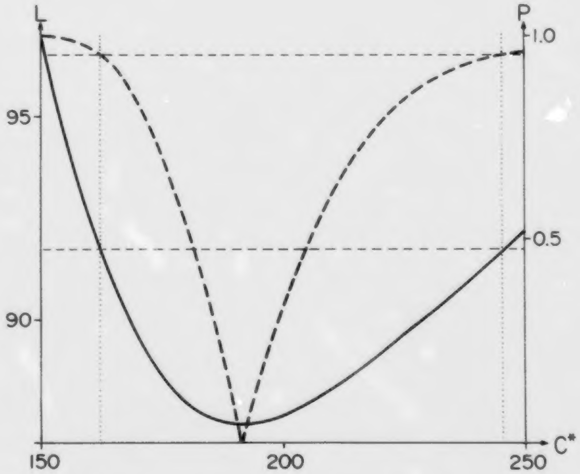

FIG. 8. The functions $L(C^*)$ (solid curve) and $P(C^*)$ (broken curve) for model 1, based on yellowfin tuna data from 1934 –57. General definitions of L and P are given by (3.5) and (3.10), respectively, and the particular calculation of L here is described in (4.1) - (4.2). The intersection of the solid curve with the line at $L = 91.70$ defines the confidence interval (4.6), as does the intersection of the broken curve with the line at $P = 0.95$.

(4.1)

$$\ell(C^*,E^*) = 24 \log \left\{ \sum_{t=1934}^{1957} \left[U_t - \frac{C^*}{E^*} (2 - \frac{E_t}{E^*}) \right]^2 \right\}$$

by calculating the minimum

(4.2) $$L(C^*) = \min_{E^*} \ell(C^*, E^*).$$

Thus, $\ell(C^*, E^*)$ is essentially the log of the sum of squares of residuals, and $L(C^*)$ is the lowest possible value of ℓ for the given parameter C^*. If the model were dynamic, ℓ would be a function of three variables, $\ell(C^*, E^*, \gamma)$, and the minimum in (4.2) would be over both E^* and γ.

As in equation (3.6), the low point on the curve $L(C^*)$ gives the estimate

(4.3) $$\hat{C}^* = 192 \times 10^6 \text{ lb},$$

where the minimum value of L is

(4.4) $$\hat{\ell} = 87.42.$$

According to (3.7), a 95% confidence interval for C^* can be obtained by solving the equation

(4.5)
$$L(C^*) = \hat{\ell} + 24\log\left[1 + \frac{1}{24-2}F_{0.95}(1, 24-2)\right] = 91.70,$$

where the term involving the F-statistic in (4.5) is 4.28. Thus, the horizontal line at $L = 91.70$ in Fig. 8 lies 4.28 units above the minimum $\hat{\ell}$, and the intersection of this line with the curve $L(C^*)$ corresponds to the two solutions of (4.5). These give the 95% confidence interval.

(4.6) $$163 \times 10^6 \text{ lb} < C^* < 247 \times 10^6 \text{ lb}.$$

The above example shows that a given p-level defines an allowable increase in L above the minimum $\hat{\ell}$. Thus, when $p = 0.95$, L can be 4.28 units above $\hat{\ell}$. From a reverse point of view, one can assign a p-level to each value of L above $\hat{\ell}$. This calculation, summarized in (3.9) - (3.10), leads to the broken curve $P(C^*)$ shown in Fig. 8. The equation

(4.7) $$P(C^*) = 0.95$$

has the same solutions as (4.5), that is, it also defines the confidence interval (4.6), as illustrated in Fig. 8. The advantage of the curve $P(C^*)$ over $L(C^*)$ is that the units have a direct interpretation. The significance of a change in L is unclear, while P relates directly to probabilities.

The shape of the curve $P(C^*)$ in Fig. 8 is typical: a "V" that flares out at the top. The wider the angle of the "V", the broader the confidence interval. Figure 9 shows $P(C^*)$ for models 1, 4, 6, and 9, again based on data from 1934 to 1957. The figure implies the following estimates and 95% confidence intervals for C^*, where the units are 10^6 lb:

Model	Estimate	Confidence Interval
1	192	(163,247)
4	163	(138,196)
6	138	(108,177)
9	184	(171,202)

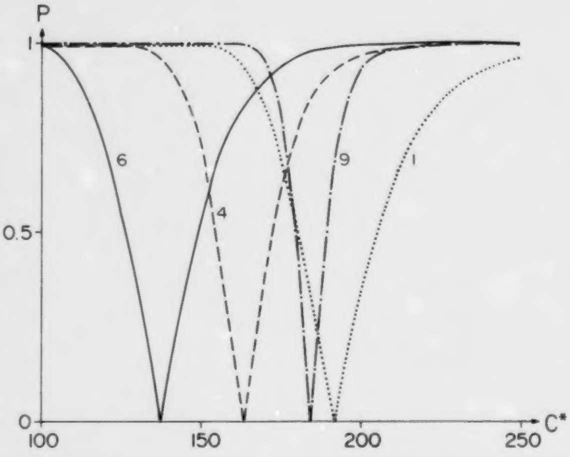

FIG. 9. The function $P(C^*)$ for models 1, 4, 6, and 9, based on yellowfin tuna data from 1934–54.

The first line of this table agrees with (4.3) and (4.6) above. Notice that model 4 is the dynamic, lognormal counterpart of model 1, and, as suggested in the discussion earlier, it leads to a lower estimate of C^* than model 1. Furthermore, a confidence interval at any p-level is narrower for model 4 than model 1 because the "V"-curve for this model is somewhat narrower. The lowest estimate here (138×10^6 lb) is obtained with model 6, and the comparison between models 1 and 6 is cited in the introduction to this paper to illustrate the degree to which different models can suggest different results.

Of the four "V"-curves in Fig. 9, the narrowest corresponds to model 9, an equilibrium model for C_t with normal error. If models were assessment biologists, one could say that model 9 is most sure of itself. Figure 10 compares the results from models 6 and 9 for the period 1952–67. The confidence interval for model 6 narrows as more data become available, and the estimate increases

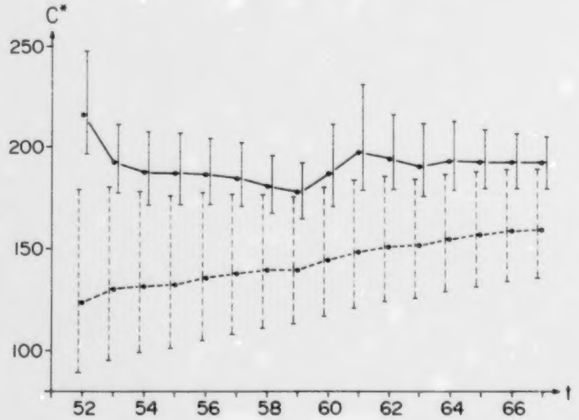

FIG. 10. Estimates $\hat{C}_t^*$, based on yellowfin tuna data up to and including year t, for model 6 (broken curve) and model 9 (solid curve). Upper and lower 95% confidence bounds for each estimate are indicated also.

steadily. By contrast, both the estimate and confidence interval from model 9 are fairly stable over the period.

Figure 11 summarizes the results from all 12 models for three time periods: 1934–54 (left legends, broken), 1934–57 (middle legends, solid), and 1934–67 (right legends, dotted). In each case, the legend indicates the estimate (an interior dot) and the confidence interval (the bounding line) for C^*. It is generally true that confidence intervals narrow as more data become available. Also, models for U_t (1, 2, 3, and 4) tend to give the broadest confidence intervals, while models for C_t (9, 10, 11, and 12) give the narrowest. Models for E_t (5, 6, 7, and 8) give intervals of intermediate size, and they also give the lowest estimates for C^*. In general an equilibrium model (1, 2, 5, 6, 9, or 10) gives a narrower interval than its dynamic counterpart (with model number increased by 2).

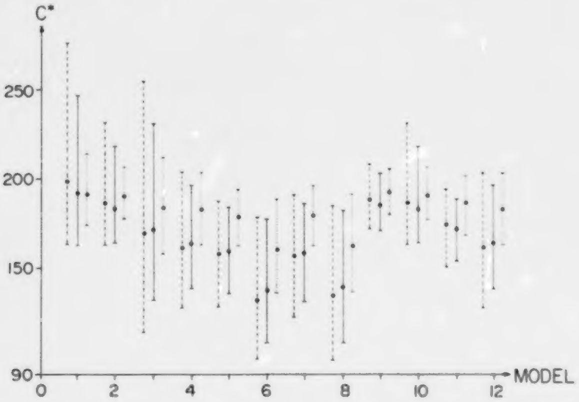

FIG. 11. Estimates and confidence intervals for C^* derived from each of the 12 models listed in Table 2. For each model, three time periods of yellowfin tuna data are used: 1934 - 54 (broken interval, left), 1934 - 57 (solid interval, center), and 1934 - 67 (dotted interval, right).

I cannot resolve here the contradictions suggested by these different analyses. Indeed, as the example of Fig. 3 illustrates, resolution depends on knowing more about the data. Schaefer (1957) used a statistical model different from any discussed here, because it allowed for error in more than one variable. The key purpose of this paper is only to demonstrate, as I have done with the tuna data, that the choice of statistical model is crucial to management decisions. I see this as a central issue for the emerging science of fishery management.

Epilogue

Since this paper was written, I have collaborated with L. Richards and A. Cass to devise models for catch and effort data that exploit techniques of modern time series analysis. As a result of this research, it appears that a scientific method for determining the appropriate error structure may be possible in some cases. For further information, see Schnute et al. (1989a, 1989b).

References

DRAPER, N. R., AND H. SMITH. 1966. Applied regression analysis. John Wiley & Sons, Inc. New York, NY. ix + 407 p.

PELLA, J. J., AND P. K. TOMLINSON. 1969. A generalized stock production model. Inter-Am. Trop. Tuna Comm. Bull. 13: 421–496.

SCHAEFER, M. B. 1954. Some aspects of the dynamics of populations important to the management of commercial marine fisheries. Inter-Am. Trop. Tuna Comm. Bull. 1: 25–56.

1957. A study of the dynamics of the fishery for yellowfin tuna in the eastern tropical Pacific Ocean. Inter-Am. Trop. Tuna Comm. Bull. 2: 245–285.

SCHNUTE, J. 1977. Improved estimates from the Schaefer production model: theoretical considerations. J. Fish. Res. Board Can. 34: 583–603.

1987. Data uncertainty, model ambiguity, and model identification. Natural Resource Modeling 2: 1–55.

SCHNUTE, J. T., L. J. RICHARDS, A. J. CASS. 1989a. Fish growth: investigations based on a size = structured model. Can. J. Fish. Aquat. Sci. 46: 730–742.

1989b. Fish survival and recruitment: investigations based on a size = structured model. Can. J. Fish. Aquat. Sci. 46: 743–769.

Internal Regulation of Reproduction in the Japanese Anchovy (*Engraulis japonica*) as Related to Population Fluctuation

Yoshinari Tsuruta

Tohoku Regional Fisheries Research Laboratory,
Japan Fisheries Agency, Shinhama-cho, Shiogama 985, Japan

and Keiji Hirose

National Research Institute of Aquaculture,
Japan Fisheries Agency, Nansei, Mie 516-01, Japan

Abstract

TSURUTA, Y., AND K. HIROSE. 1989. Internal regulation of reproduction in the Japanese anchovy *(Engraulis japonica)* as related to population fluctuation, p. 111–119. *In* R. J. Beamish and G. A. McFarlane [ed.] Effects of ocean variability on recruitment and an evaluation of parameters used in stock assessment models. Can. Spec. Publ. Fish. Aquat. Sci. 108.

Field surveys and laboratory experiments on the Japanese anchovy, *Engraulis japonica*, were conducted in order to identify mechanisms which promote stock size stability. Field surveys confirmed the relatively long spawning season and short time interval between spawning episodes (interspawning interval); for example, April through October and 1.4 to 4.3 days, 1984 in the study area, Sagami Bay. In laboratory experiments, a reduction in food resulted in, first, a prolongation of interspawning interval, second, a reduction in batch fecundity and third, a change in egg size when the food ration was below the level required for body maintenance. The number of eggs spawned per female was reduced at high density even when food was held constant. On the other hand, the growth was better than that at low density. Sea water taken from high density tank and discharged into the low density tank, reduced the number of eggs spawned per female in a low-density tank. However, this did not apply for sea water from a low-density tank. Therefore, some unknown organic substance may control gonad maturation.

Résumé

TSURUTA, Y., AND K. HIROSE. 1989. Internal regulation of reproduction in the Japanese anchovy *(Engraulis japonica)* as related to population fluctuation, p. 111–119. *In* R. J. Beamish and G. A. McFarlane [ed.] Effects of ocean variability on recruitment and an evaluation of parameters used in stock assessment models. Can. Spec. Publ. Fish. Aquat. Sci. 108.

Des études sur le terrain et des expériences en laboratoire avec l'anchois japonais (*Engraulis japonica*) ont été réalisées afin de déterminer quels sont les mécanismes favorisant la stabilité des effectifs d'un stock. Les études sur le terrain ont confirmé que la saison de la fraye était relativement longue et que les périodes s'écoulant entre les pontes étaient courtes; par exemple, en 1984, dans la baie Sagami, la fraye a duré d'avril jusqu'en octobre et l'intervalle entre les pontes variait de 1,4 à 4,3 jours. Pendant les expériences menées en laboratoire, une réduction des rations de nourriture ont eu les répercussions suivantes : premièrement, une prolongation de la période s'écoulant entre les pontes; deuxièmement, une diminution de la fécondité des lots de poissons; et, troisièmement, un changement de la taille des œufs lorsque les rations n'étaient pas suffisantes pour assurer un état biologique normal. À de fortes densités, on a observé une réduction du nombre d'œufs pondus par femelle, même lorsque les rations de nourriture étaient constantes. Toutefois, le taux de croissance était plus élevé dans ces conditions qu'à de plus faibles densités. Le fait de verser de l'eau de mer provenant d'un réservoir à densité élevée dans un réservoir à faible densité a entraîné une diminution du nombre d'œufs pondus par femelle dans celui-ci. Cependant, le même phénomène n'a pas été observé lorsqu'on a utilisé de l'eau de mer provenant d'un réservoir à faible densité. Par conséquence, une substance organique inconnue influe peut-être sur la maturation des gonades.

Introduction

Since Hjort (1914) suggested the critical period theory, there has been controversy centered around the survival of early life stages. However, egg production has rarely been discussed except that Nikolskii (1969), Bagenal (1973) and Ware (1980) have discussed how variations in egg production can regulate population size in fishes, even though it must be one of the major elements of recruitment. Recent advanced histological techniques, using the incidence of postovulatory follicles, have revealed that in multiple spawners the number of eggs laid annually is much higher than the fecundity multiplied by the number of modes of oocyte (Hunter and Goldberg 1980, Hunter and Macewicz 1980). Cushing (1975, 1982) suggested that the match or mismatch between the timing of peak spawning and the production cycle of plankton used by larvae as food determines the size of recruitment of fish inhabiting middle and higher latitudes. He concluded that a longer spawning season in mid-latitudes may mitigate the effects of a highly variable production cycle. Cushing's match-mismatch hypothesis and recent works on egg production imply that a number of variables related to fecundity play a very important role in recruitment fluctuations.

The Japanese anchovy, *Engraulis japonica*, undergoes only moderate change of abundance, compared to the Japanese sardine and other ecologically related neritic-pelagic species (Table 1). The case of this stability has not yet been identified, but the traits described below indicate that fecundity may play some part as a density-dependent population control mechanism. Japanese anchovy spawn over a much longer period of the year, reach first maturity at a younger age and shorter length, and have a much shorter life-span than other neritic-pelagic species. Moreover, the total number of eggs laid annually by the anchovy population is relatively high and stable compared with that of two ecologically related species, the sardine *Sardinops melanostictus* and the Japanese mackerel, *Scomber japonicus* (Tsuruta 1987).

The present paper aims to identify the mechanism which maintains the stock size of anchovy at a relatively stable level. The reproductive features are studied by examination of specimens collected from the field surveys and from fish studied experimentally using captive individuals reared at differenct levels of food supply and population density.

Materials and Methods

Field Surveys

Adult anchovy were sampled from 0500 to 0700 h from commercial set-net catches in Sagami Bay from 1984 through 1986. The numbers of samples were 14 in 1984, 8 in 1985 and 9 in 1986. The number of fish per sample was approximately from 30 to 70 according to the extent of body length. All the fish were measured for body length, body weight and gonad weight. All the gonads were fixed in Bouin's fluid for histological analysis, sectioned at 8 μm and stained with hematoxylin/eosin. Occurrence of postovulatory follicles on each ovary was examined under a microscope for estimating the interspawning interval from the fraction of mature female spawning per day. The postovulatory follicles degenerated within 24 h after spawning occurred between approximately 2000 and 2200 h at 23°C under experiment (Tsuruta and Hirose 1985). Therefore, the interspawning interval is defined as the total number of captured females divided by the number of females with postovulatory follicles. This ratio should approximate the time interval (in days) between spawning episodes. A portion (about 0.1 to 0.3 g) of the ovaries were also preserved in 10% formalin for count of batch fecundity. Oocytes in the ovaries were completely separated with a forefinger and two needles, then the longest diameter of the oocytes was measured to the nearest 0.02 mm at 50× magnification under Nikon Profile Projector. Number of oocytes measured per ovary was from 200 to 400. Batch fecundity, that is, the number of oocytes in the most advanced mode, was determined by means of probability paper (Cassie 1954).

Laboratory Experiments

Adult Japanese anchovy, caught by commercial bait-fishermen in the spring of 1984 to 1986 in Sagami Bay, were transported to the Arasaki Marine Station of the Tokai Regional Fisheries Research Laboratory in Yokosuka City. They were kept in two 4-m diameter

TABLE 1. The amounts of catch and coefficients of variation in the major neritic-pelagic species in Japanese water area, 1956–85.

	Amount of catch (tonnes)			
Species	Maximum (× 1000)	Minimum (× 1000)	Mean (× 1000)	Coefficient of variation
Japanese sardine *Sardinops melanostictus*	4.179	9	959	142.2
Jack mackerel *Trachurus japonicus*	552	54	259	62.6
Japanese mackerel[a] *Scomber japonicus*	1.629	266	846	48.6
Japanese anchovy *Engraulis japonica*	430	135	300	29.9

[a] Includes a small part of catch from spotted mackerel, *Scomber australasicus*.

tanks with a depth of 1 m and allowed to acclimate for about 3 wk. Five separate experiments were conducted from 1984 to 1986 to investigate the reproductive traits, and the effects of food supply and density on egg production.

Experiment 1

Experiment 1 was carried out from May 8, 1984 to January 11, 1985 to investigate the seasonal change in the size of spawned eggs, fecundity and developmental stage of gonads. About 700 anchovy (SL 12.0 cm, 16.9 g) were placed in a 12 000-L circular tank (diameter 4 m) supplied with fresh sea water at about 80 L/min. The pen was provided with "Ayu-dry" pellets, normally used for feeding ayu fish (*Plecoglossus alitivelis*), at a rate of about 3% of body weight per day. About 30 fish were sampled and the body and gonad weighed at approximately monthly intervals, and all the ovaries were used for histological analysis and batch fecundity count as described in the field surveys. Spawned eggs were collected from the overflow water with a GG54 nylon net, which was set from about 1700 to 0900 h during the experiment. Collected eggs were preserved in 10% formalin diluted with sea water. Those were divided from one-half to one-sixty-fourths by the plankton divider in proportion to the amount and counted with naked eye or under a magnifying glass. In the approximately 5-day intervals, the major and minor axis of 50 to 100 eggs were measured to the nearest 0.02 mm at 50× magnification under Nikon Profile Projector after preserving for 1 month. The water temperature was measured at 1000 hours every day.

Experiment 2

Experiment 2 was carried out from July 4 to August 3, 1986 to investigate the effect of food supply on egg production. Groups of 150 anchovy (SL 9.5 cm, BW 8.9 g) were placed in each of three separate 4000-L tanks (3 × 1.5 × 1 m depth) with fresh sea water overflowing at approximately 1620% exchange/day. Each pen was provided with "Ayu-dry" pellets at one of three rations of 1, 1.5 and 2% of body weight per day, respectively. Twenty fish from each pen were subsampled and the body and gonad weighed at about 10-day intervals on July 15 and 25, and the rations recalculated. On August 3, 36 fish were taken from each pen. Batch fecundity was determined as described in the field survey. Spawned eggs were collected, counted and measured as described in experiment 1. As the number of eggs collected was over 2000, the major and minor axis of sixty eggs were measured. The number of ovaries sampled was 12, 13 and 13 for the 1-, 1.5- and 2% ration tanks, respectively. Interspawning interval was determined as the number of eggs spawned per female during the experiment divided by the mean batch fecundity in the fish with hydrated ovaries which were sampled at the end of the experiment. The total number of females and males was checked from the samples during and at the end of the experiment. The water temperature in each tank was measured at 1000 h every day.

Experiment 3

Experiment 3 was carried out from July 9 to 22, 1984 to determine the effect of fish density on egg production. Anchovy were placed at densities of 30, 50 and 116 fish in three 4000-L tanks with fresh sea water overflowing at approximately 1620% exchange/day. "Ayu-dry" pellets were supplied to each tank at a rate of about 3% of body weight per day. At the end of the experiment, all ovaries were checked histologically to determine whether there were new postovulatory follicles or not. Spawned eggs were collected, counted and measured as described in experiment 1. The specimens for which egg size was measured were collected from July 17 to 21, and the numbers were about 3 from each tank.

Experiment 4

Experiment 4 was carried out from July 24 to August 31, 1985 to determine if there was an effect of density on egg production. Anchovy were placed in two 4000-L tanks at densities of 50 and 160 fish. Each stocking density was replicated in two additional tanks, and all were supplied with fresh sea water at about 40 L/min (1440% exchange/day). One of each pair of tanks was kept as a control, and water overflowing (10 L/min) from the control tank was transferred into the tank containing the fish of different density in the course of the experiment. The amount of food supplied per fish was the same in all the tanks. Spawned eggs were collected and counted as described above.

Experiment 5

Experiment 5 was carried out from August 6 to 25, 1986 to determine the effect of density on the shift of food energy to the somatic growth or gonosomatic growth. Anchovy were placed in three 4000-L tanks at densities of 50, 100 and 150 fish each. "Ayu-dry" pellets were supplied to each tank at a ration of about 3% of body weight per day. The percentage change in fresh body weight per day was determined by dividing the change in weight during the interval by the middle weight during the interval multiplied by 100. Spawned eggs were collected as described above.

Results

General Reproductive Traits

(a) Duration of spawning season and interspawning interval

The approximate duration of the 1984 spawning season is shown in Fig. 1 as the time of elevated gonosomatic indices of specimens collected in the field survey. The interspawning interval is defined as the total number of captured females divided by the number of females with postovulatory follicles. This ratio should approximate the time interval (in days) between spawning episodes. The anchovy spawned over a period of seven months from

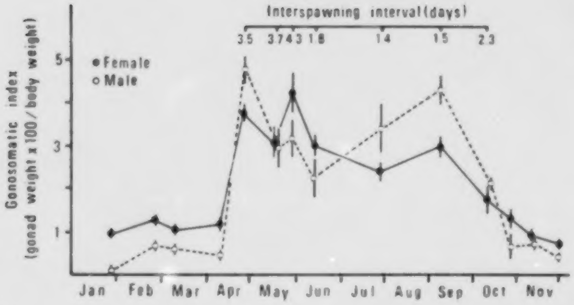

FIG. 1. Seasonal change in gonosomatic index in anchovy collected during 1984 field survey. The interspawning interval is defined as the total number of females divided by the number with postovulatory follicles. Each point represents the mean (± SD) gonosomatic index.

late April to mid-October, 1984. Their interspawning interval in 1984 varied seasonally from 4.3 days in spring, at the beginning of spawning, to 1.4 days in summer. The interspawning interval changed annually as well as seasonally (Fig. 2). For example, in June 1985, it was 3.5-5.7 days or two to three times longer than in the same month of 1984 and 1986 (1.4-2.0 days).

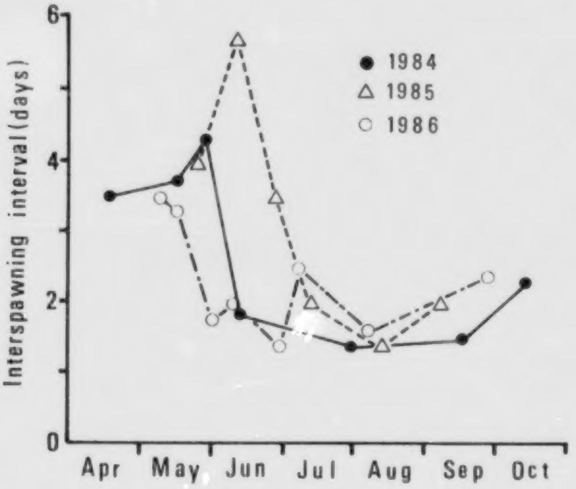

FIG. 2. Seasonal change in interspawning interval, 1984-86.

(b) Fecundity and size of eggs

The fecundity data of April and May were from the 1984 field survey and those of July to October were from experiment 1, because in July to October the fish sampled in the field surveys did not have plump ovaries. Batch fecundity (BF; the number of eggs in the most advanced mode of oocyte length) and relative batch fecundity (RBF; BF/total body weight) varied seasonally from 3834 (BF) and 194 (RBF) in spring to 10 548 (BF) and 611 (RBF) in summer (Table 2). Mean diameters of eggs spawned by reared anchovy (in experiment 1) varied from about 0.9 mm in July to September to over 1.0 after November (Fig. 3). Egg size varied inversely with batch fecundity. The relationship between water temperature, egg diameter and batch fecundity is shown in Fig. 4. Egg diameter was inversely related to water temperature below 24°C and almost stable above that point. On the other hand, batch fecundity tended to increase linearly through the full range of temperatures.

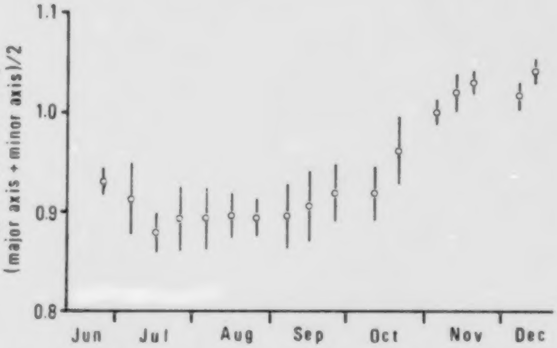

FIG. 3. Seasonal change in mean diameter of eggs laid by reared anchovy. Each point represents the mean (± SD) egg diameter. The number of eggs measured is 50 each point.

TABLE 2. Seasonal change in fecundity of the Japanese anchovy collected in 1984.

		Apr. 18	May 26	July 18	Sept. 19	Oct. 11
No. of fish		4	4	7	4	5
Body length (cm)	Mean	12.5	12.0	12.0	12.0	11.8
	SD	0.33	0.85	0.73	0.66	0.33
Body weight (g)	Mean	19.7	16.0	17.6	17.2	15.6
	SD	1.27	2.59	3.53	2.31	2.01
Batch fecundity[a]	Mean	3834	5410	10548	6784	5993
	SD	1248	2849	3042	1722	1537
Relative batch fecundity[b]	Mean	195	330	611	392	384
	SD	63	152	239	74	82

[a] Number of eggs in the most advanced oocyte mode in ovary.
[b] Batch fecundity/body weight in grams.

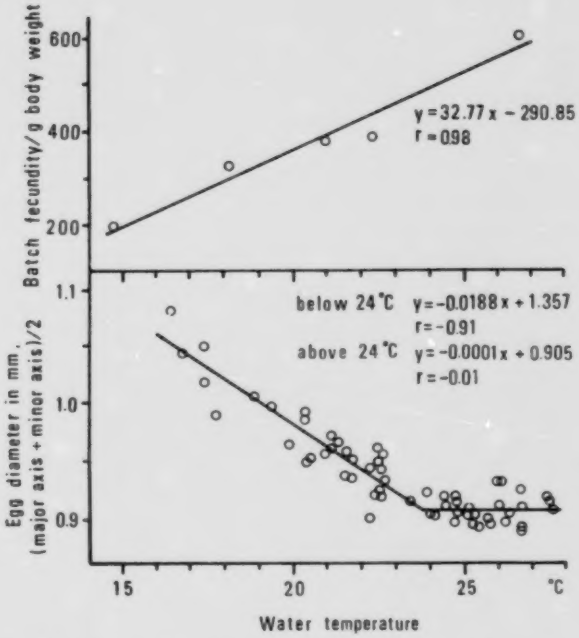

FIG. 4. Relationship between water temperature and two egg-production variables: batch fecundity and egg size.

Effect of Food Supply on Egg Production

(i) *Experiment 2.* There were substantial daily changes in number of eggs spawned daily by anchovy fed the three different levels of food rations (Fig. 5). Anchovy in all the tanks began to spawn about one week after commencement of the experiment. They continued to spawn, except for some interruption in the low- and middle-ration tanks at over 23°C and all had their greatest spawning peak on about 27th to 29th day at which time water temperature had risen to 26°C.

The effect of food ration was detected in the number of eggs spawned between 11–21 days after the ration changed, and the response was very pronounced after 22nd to 30th. This result was also applied for the mean diameter of eggs spawned from each tank (Table 3, Table 4). Table 4 shows the results of Student '*t*' tests between the number of eggs spawned (and egg size) among the three tanks. All the egg sizes between July 25 to August 3 grew smaller with increased water temperature.

TABLE 3. The numbers of eggs spawned per female per day and sizes of eggs spawned in three food level tanks during experiment.

	July 4–15	July 15–25	July 25–Aug. 3
No. of eggs spawned per female per day			
1% tank	11	49	164
1.5%	6	79	461
2%	4	233	735
Size of eggs spawned			
1% tank	0.906(2)[a]	0.907(4)	0.888(6)
1.5%	0.934(1)	0.931(7)	0.916(6)
2%	0.935(1)	0.929(6)	0.914(6)

[a]Number in parentheses indicates number of specimens.

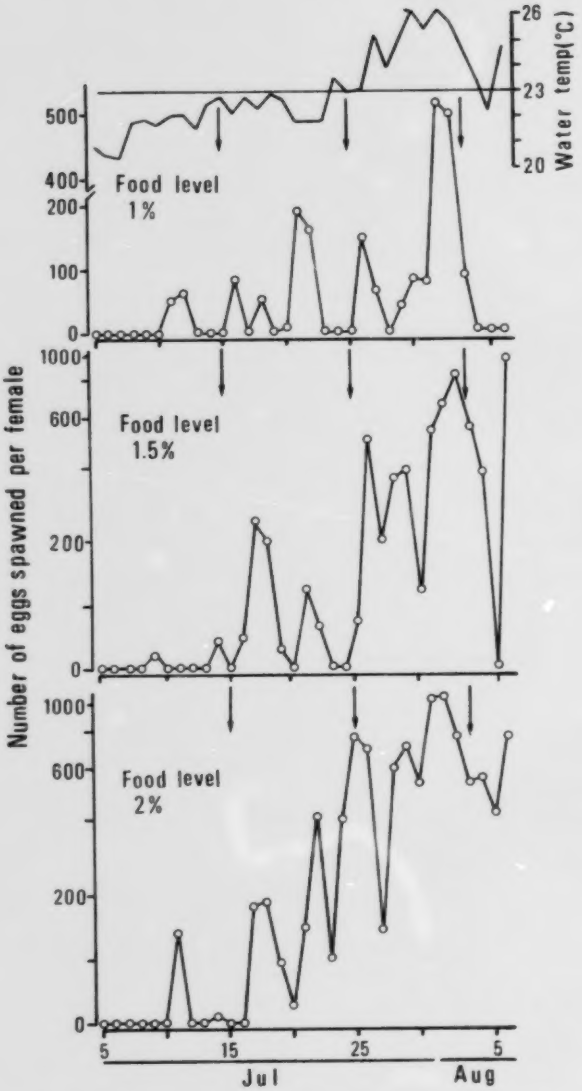

FIG. 5. Daily change in numbers of eggs spawned at three food levels in 1986. The arrows indicate dates on which the sampling of fish took place.

Table 5 shows the details of body length, weight, condition factor, and number of fish sampled during experiment. Mean body weight was almost constant in the 1%-ration tank and increased in the 1.5- and 2.0%-ration tanks during the first 20 days. Subsequently, body weights in all the tanks decreased markedly. The decrease during peak spawning was the greatest in the highest ration tank, and amounted to 1.77% per day between July 25 and August 3 (Table 6). Average daily growth rates throughout the experiment were −0.21% in the 1% ration, −0.03% in the 1.5% ration and +0.12% in the 2% ration. It seems that the marked

TABLE 4. The significance of the differences in number of eggs spawned and size of eggs among three tanks.

	July 4–15	July 15–25	July 25–Aug. 3
No. of eggs spawned			
1% tank and 1.5% tank	N.S.[a]	N.S.	*
1% tank and 2% tank	N.S.	*	**
1.5% tank and 2% tank	N.S.	*	*
Size of eggs			
1% tank and 1.5% tank	N.S.	*	*
1% tank and 2% tank	N.S.	*	*
1.5% tank and 2% tank	N.S.	N.S.	N.S.

[a] N.S. indicates not significant, * indicates significant at 5% probability level and ** indicates significant at 1%.

TABLE 5. Body lengths. weights and condition factors of sample anchovy from three food level tanks during experiment.

	July 4	July 15	July 25	Aug. 3
1% tank				
Mean length (cm)	9.50	9.64	9.66	9.56
Mean weight (g)	8.94	9.13	9.14	8.39
Condition factor[a]	10.05	10.10	10.07	9.55
Number of fish	31	21	20	36
1.5% tank				
Mean length (cm)	9.50	9.61	9.88	9.62
Mean weight (g)	8.94	9.27	9.73	8.87
Condition factor	10.05	10.36	9.91	9.86
Number of fish	31	20	23	36
2% tank				
Mean length (cm)	9.50	9.85	9.95	9.58
Mean weight (g)	8.94	9.76	10.87	9.27
Condition factor	10.05	10.11	10.73	10.36
Number of fish	31	20	21	36

[a] 1000 × body weight/(body length)^3.

TABLE 6. The food rations (% of body weight) and daily growth rates in three food level tanks during experiment.

	July 4–15	July 15–25	July 25–Aug. 3
Food ration			
1% tank	0.99	0.92	0.88
1.5%	1.48	1.58	1.89
2%	2.00	1.99	2.16
Daily growth rate			
1% tank	0.19	0.01	−0.95
1.5%	0.33	0.48	−1.03
2%	0.80	1.08	−1.77

weight loss between July 25 to August 3 resulted from high spawning rate and the increase of body maintenance energy because of a high water temperature (over 23°C). This resulted in a decrease in the condition factors of the anchovy from the three ration tanks. However, there may be substantial sampling error from the small samples of 20 fish, for the mean length of August 3 from each tank was smaller than that of July 25.

Table 7 summarizes the details of egg production: batch fecundity, interspawning interval and mean diameter of eggs spawned during the spawning peak of July 25 to August 3. Results from the 1%-ration tank, which was below the level of body maintenance, are clearly distinguishable from those of the other ration tanks; namely, batch fecundity in the 1%-ration tank was 43% to 51% lower than in the other tanks, and the spawning interval was two to three times longer. Moreover, egg size was smaller.

Effect of Population Size on Reproduction

Experiments indicated the effects of population size on egg production and the change in partitioning of food energy between growth and reproduction.

(i) *Experiment 3*. Table 8 shows the effect of three population sizes on the variables related to egg production: interspawning interval, number of eggs per spawning and egg diameter. The interspawning interval, determined by histological analysis at the end of the experiment and the number of eggs produced per female, was lowest in the dense population; specifically, the interspawning interval in 116-density tank was 7.0 days for about 3.0 day in the lower tanks, and number of eggs per spawning female, batch fecundity, was lower by about 20% than in the other tanks. There was no significant difference in egg size among the three densities at 5% probability level.

(ii) *Experiment 4*. Water discharged from the dense tanks into low density tanks reduced the number of eggs produced per female in the lower density tanks (Fig. 6A). In contrast, water from the lower density tank did not reduce or increase the number of eggs spawned in the higher density tank (Fig. 6B). Analyses of covariance were carried out on the logarithms of the numbers of eggs spawned in the two same density tanks by each period before and after the exhaust water from the other different density tank was transferred. There were no significant differences in the regression coefficients of log number of eggs spawned in the high density tanks. In the lower density tanks, the regression coefficients were not significantly different between two tanks before water transferral but were significantly different after water transferral. Moreover, there was a significant difference between the mean number of eggs spawned at the 1% level.

(iii) *Experiment 5*. Table 9 shows the effect of population size on somatic growth and egg production where the food ration per individual was held more or less cons-

TABLE 7. Effect of three food levels on egg production during the period of peak spawning from July 25 to August 3.

Food level	No. of eggs spawned/ female/day	Batch fecundity[a]	Interspawning interval (days)[b]	Size of eggs spawned (mm)[c]
1%	164 ± 186[d]	5580 ± 1529[d]	34	0.888 ± 0.024[d]
1.5%	461 ± 228	7955 ± 4669	17.5	0.916 ± 0.016
2%	731 ± 372	8405 ± 1603	11.5	0.914 ± 0.023

[a] Number of hydrated eggs in ovary.
[b] Batch fecundity/number of eggs spawned per female per day.
[c] (Major axis + minor axis)/2.
[d] Mean (± SD).

TABLE 8. Difference in egg production among three population sizes.

No. of fish	Food ration (% of body weight)	No. of eggs spawned/ female/day	No. of eggs collected on final day of experiment	No. of females with postovulatory follicles on final day of experiment	No. of eggs/ spawning female[a]	Interspawning interval (days)[b]	Size of eggs (mm)[c]
30	2.66	2045 ± 922[d]	18 624	3	6208	3.0	0.914 ± 0.009[d]
50	3.00	1942 ± 1295	28 736	5	5747	2.5	0.901 ± 0.010
116	2.88	660 ± 438	48 432	10.5	4651	7.0	0.904 ± 0.007

[a] Number of eggs collected on final day of experiment/number of females with postovulatory follicles on final day of experiment.
[b] Number of eggs per spawning female/number of eggs spawned per female per day.
[c] (Major axis + minor axis)/2.
[d] Mean (± SD) value.

tant. At the higher population densities fewer eggs were spawned but their daily growth rates were greater than those at the lowest density.

Discussion

Most neritic–pelagic species in mid-latitudes are multiple spawners but their spawning seasons are very brief. Further, most are subject to large variations in abundance. The anchovy is an exception; it has a prolonged spawning period and a relatively stable abundance. The length of time between the main feeding season and spawning season may be a factor in population fluctuations. For example, the time lag in the Japanese sardine is over 6 months (Kondo et al. 1976). Failure of this species to accumulate the required nutrition in summer results in unsuccessful spawning in the next spring (Tsuruta 1987). The anchovy, on the other hand as suggested by the present study, has a prolonged spawning season and is capable of making short-term (within-season) adjustments to changes in food supply. The result of experiment 2 indicates that food intake affects egg production about 2 wk later (Table 4). Moreover, all the condition factors and mean body weights decreased in spite of the food supply increases except in the 1%-ration tank during peak spawning. It appears that the accumulated body energy is converted very quickly into gonad growth. These characteristics allow Japanese anchovy to spawn rapidly and repeatedly when feeding conditions become suitable.

The seasonal change in egg size, which is large in the local winter and small in the local summer, appears to be a common pattern among clupeoid fishes (Blaxter and Hunter 1982). A similar change was reported by Asami (1953) for the wild Japanese anchovy. He found a good correlation between temperature and egg diameter. Our work reconfirmed a similar seasonal change in egg size for reared fish, and found that fecundity is correlated with temperature. Ware (1977) reported for Atlantic mackerel that the mean egg diameter is conversely proportional to surface temperature. Moreover he found that the mean diameter of mackerel eggs synchronizes with the mean length of the plankton which is inversely correlated with water temperature. The change in the egg size and number of eggs produced per spawning of

TABLE 9. Effect of population size on the body growth and egg production.

No. of fish	Daily feeding rate (%)	Daily growth rate (%)	No. of eggs spawned/ female/day
50	2.66	0.48	978 ± 723[a]
100	2.57	0.72	457 ± 284
150	2.54	0.78	337 ± 129

[a] Mean (± SD) value.

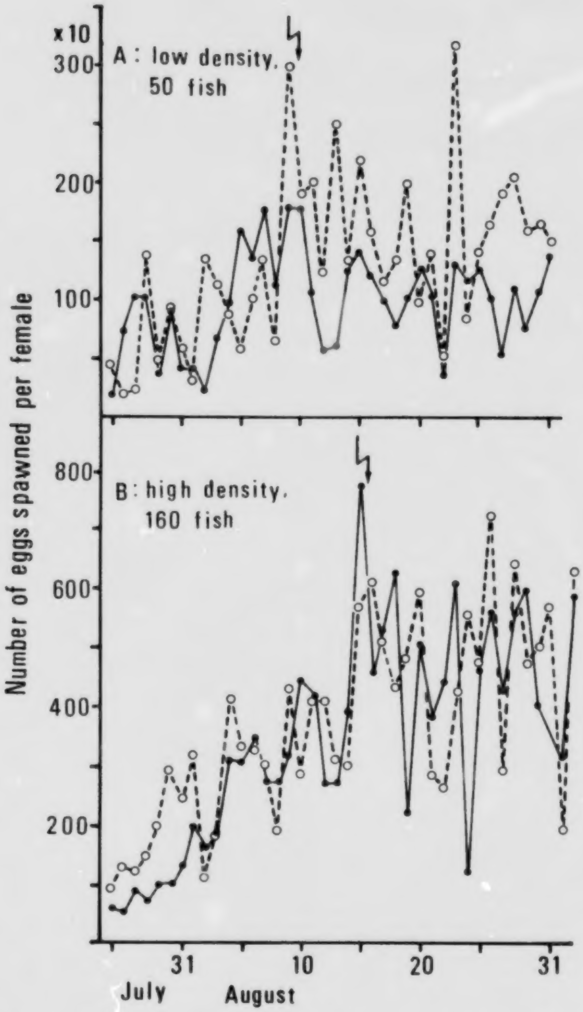

FIG. 6. Effect of water from the high-density (A) and low-density (B) rearing tanks on the number of eggs spawned in the other tanks of different density. The dashed lines show control tank results, and the solid lines show results in the tank to which the water from the tank of different density was transferred. The broken arrows indicate the start of water transferral.

Japanese anchovy may also well coincide with the food supply correlated to water temperature, which must result in the high survival of larvae.

The interspawning interval of the Japanese anchovy varies from 1.4 to 5.7 days. It is much shorter than those of the northern and Peruvian anchovy which are reported as lasting about 6–10 days (Hunter and Goldberg 1980; Hunter and Macewicz 1980; Alheit et al. 1984). Thus, within-year spawning of the Japanese anchovy can be expected to be much more frequent than the figure of 20 times noted for the northern anchovy (Hunter and Leong 1981). On the contrary, the interspawning interval (11.5-34 days) in the food experiment anchovy was much longer than in the wild anchovy. It seems to have resulted from two factors; namely, lower food supply (2.16% in the high ration tank) and high density (about 100 fish during the peak spawning). Thus, it is quite obvious that food supply is most important. However, the results of density experiments imply that fish density also affects the interspawning interval.

The present findings on the effect of food upon egg production agree with those of Hislop et al. (1978) in respect to haddock that spawned more than once in a season. But the present experiment did not confirm an observation reported by Bagenal (1969) for brown trout; i.e., that low-fed females produce heavier eggs.

In the case of Japanese anchovy, a reduction in food resulted in, first, a prolongation of spawning intervals; second, a reduction in batch fecundity, and third, a change in egg size when a small ration below the level of body maintenance was given. However, the females were fed so little as to cause a change in egg size and continued spawning throughout the experiment, although the body weight fell rapidly. It appears that the shift of food energy, as much as possible into gonad growth, may be important for the existence of the short-lived anchovy.

Tsukayama and Alverez (1980) found that the population size of Peruvian anchovy affected egg production. They concluded that their results can be explained by a density-dependence factor which is related to availability of food. The present experiment showed that fewer eggs were spawned and better growth was observed for the higher density even if food ration per individual was exactly the same. This suggests that the shift of food energy to somatic growth or gonosomatic growth is density-dependent. The density-dependent shift of food energy in favour of egg production when density decreases may be the major reproductive strategy to keep the population of Japanese anchovy stable. Two factors, independent of food supply, can be considered for the cause of the density dependence: a mutual interference (behavioural interaction) and a biological conditioning of the environment. The effect of the latter was demonstrated by the present experiment. Therefore, it appears that some unknown organic substance may control gonad maturation.

Acknowledgments

We thank the numerous people who allowed us to work at the Arasaki Marine Station of Tokai Regional Fisheries Research Laboratory, especially Sukekata Ito, Taisuke Watanabe, Kazunori Kuroda, Shigeru Odate and Keiichiro Mori. We also thank the staffs of The Arasaki Marine Station, particularly Yoshihiro Satomi, Sekio Kimura and the late Motoyoshi Yokote for making valuable suggestions, and Yoko Takahasi and Tadashi Endo for assisting in rearing the Japanese anchovy.

References

ASAMI, T. 1953. Studies on the spawned eggs of anchovy, *Engraulis japonicus* T. et S. Contribution Nankai Reg. Fish. Res. Lab. 1: 1–7.

ALHEIT, J., V. H. ALARCON, AND B. J. MACEWICZ. 1984. Spawning frequency and sex ratio in the Peruvian anchovy, *Engraulis ringens*. Calif. Coop. Oceanic. Fish. Invest. Rep. 25: 43–52.

Bagenal, T. B. 1969. The relationship between food supply and fecundity in brown trout *Salmo trutta* L. J. Fish Biol. 1: 167–182.

1973. Fish fecundity and its relations with stock and recruitment. Rapp. P.-V. Réun. Cons. int. Explor. Mer 164: 186–198.

Blaxter, J.H.S., and J. R. Hunter. 1982. The biology of the clupeoid fishes. Adv. Mar. Biol. 20: 1–223.

Cassie, R. M. 1954. Some use of probability paper in the analysis of size frequency distributions. Aust. J. Mar. Freshwater Res. 5: 513–522.

Cushing, D. H. 1975. Marine ecology and fisheries. Cambridge Univ. Press, Cambridge. 278 p.

1982. Climate and fisheries. Academic Press, London. 373 p.

Hislop, J. R. G., A. P. Robb, and J. A. Gauld. 1978. Observations on effects of feeding level on growth and reproduction in haddock, *Meranogrammus aeglefinus* (L.) in captivity. J. Fish Biol. 13: 85–98.

Hjort, J. 1914. Fluctuations in the great fisheries of northern Europe reviewed in the light of biological research. Rapp. P.-V. Réun. Cons. int. Explor. Mer 20: 1–228.

Hunter, J. R., and S.P. Goldberg. 1980. Spawning incidence and batch fecundity in northern anchovy, *Engraulis mordax*. Fish. Bull., U.S. 77: 641–652.

Hunter, J. R., and B. J. Macewicz. 1980. Sexual maturity, batch fecundity, spawning frequency, and temporal pattern spawning for the northern anchovy, *Engraulis mordax*, during the 1979 spawning season. Calif. Coop. Oceanic. Fish. Invest. Rep. 21: 139–149.

Hunter, J. R., and R. Leong. 1981. The spawning energetics of female northern anchovy, *Engraulis mordax*. Fish. Bull., U.S. 79: 215–230.

Kondo, K., Y. Hori, and K. Hiramoto. 1976. Life pattern of the Japanese sardine, *Sardinops melanosticta* (Temminck et Schlegel), and its practical procedure of marine researches of the stock (2nd edition). Suisankenkyusosho 30: 1–68.

Nikolskii, G. V. 1969. Theory of fish population dynamics. Oliver and Boyd, Edinburgh, 323 p.

Tsukayama, I., and M. A. Alvarez. 1980. Fluctuaciones en el stock de anchovetas desovantes durante los ciclos reproductivos de primaversa 1964–1978. *In* "Workshop on the effects of environmental variation on the survival of larval pelagic fishes". Intergovernmental Oceanographic Commission Report 28: 223–240. Unesco, Paris.

Tsuruta, Y. 1987. Notes on the reproduction of the Japanese sardine and anchovy as related to population fluctuation. Bull. Japan. Soc. Fish. Oceanogr. 51: 51–54.

Tsuruta, Y., and K. Hirose. 1985. The sexual maturation and spawning of the Japanese anchovy, *Engraulis japonica*. Annual report on the distributions of fish eggs and larvae in Tokai regional fisheries water area. 5: 76–78.

Ware, D. M. 1977. Spawning time and egg size of Atlantic mackerel, *Scomber scombrus*, in relation to the plankton. J. Fish. Res. Board Can. 34: 2308–2315.

1980. Bioenergetics of stock and recruitment. Can. J. Fish. Aquat. Sci. 37: 1012–1024.

The Dynamic Pool Model and Consequences of its Approximations to Fisheries Management

Xuanhai Li

Department of Marine Fisheries, Zhanjiang Fisheries Institute,
Guandong, The People's Republic of China

Abstract

Li, X. 1989. The dynamic pool model and consequences of its approximations to fisheries management, p. 121–126. *In* R. J. Beamish and G. A. McFarlane [ed.] Effects of ocean variability on recruitment and an evaluation of parameters used in stock assessment models. Can. Spec. Publ. Fish. Aquat. Sci. 108.

Three simplifications of the dynamic pool model are tested on data based on *Gymnocypris przewalskii*, a long-lived fish and *Decapterus maruadsi*, a short-lived species. All approximations tested resulted in error in yield per recruit estimations. Utilization of $T_\lambda = \infty$ instead of the true T_λ is practical only for species with a life span in excess of 15 years, subjected to high rates of instantaneous fishing. Substantial errors are likely in short-lived species.

Résumé

Li, X. 1989. The dynamic pool model and consequences of its approximations to fisheries management, p. 121–126. *In* R. J. Beamish and G. A. McFarlane [ed.] Effects of ocean variability on recruitment and an evaluation of parameters used in stock assessment models. Can. Spec. Publ. Fish. Aquat. Sci. 108.

Trois versions simplifiées du modèle de la dynamique en bassin ont été mises à l'épreuve avec *Gymnocypris przewalskii*, un poisson dont la durée de vie est longue, et *Decapterus maruadsi*, une espèce dont la durée de vie est courte. Toutes les approximations utilisées ont abouti à des erreurs d'estimation du rendement par recrue. L'emploi de $T_\lambda = \infty$ plutôt que le T_λ réel ne peut servir que pour les espèces vivant plus de quinze ans et qui sont soumises à des taux instantanés élevés de pêche. Des erreurs importantes sont susceptibles de se produire avec les espèces dont la durée de vie est courte.

Introduction

Because many mathematical models are available for stock assessment, investigators must be concerned about the adequacy of these models for fitting data sets. The accuracy of an assessment can have significant impact on fishery management strategies.

The tendency of using approximations of models has been noted by workers in the field of stock assessment with limited computer resources. There remains a significant gap between developed and other countries as far as computer resources are concerned. It may be practical to utilize approximations under certain circumstances when the accuracy is satisfactory. In this paper, three different modifications or simplifications of the dynamic pool model are tested on two species of fish caught by bottom trawl in the South China Sea to detect the errors produced; and figures drawn by computer are analyzed. Suggestions are made for overcoming deficiencies of the simplified expressions.

Model Background

With development of advanced computer techniques, it is now possible to perform many analyses not possible previously. The advent of various useful mathematical models for stock assessment has played an important role in fishery management strategies. In European and American countries, fishery scientists, biologists and computer experts work together to enhance the accuracy of stock assessment and forecast. Thanks to the help of various types of models, it is now possible to obtain estimates of the abundance of fish in the sea, but confidence in these estimates may be severely limited. Inconsistencies in using different models to draw conclusions regarding the status of fish stocks and efforts to forecast the trend in potential catch have created an awareness that errors in stock assessment models or their simplified variants may lead to faulty fishery management strategies and thereby cause serious damage to stocks of commercial species. For example, severe lessons have been learned from the Norwegian herring and Peruvian anchovy fisheries. Consequently, caution is required when collecting data and using mathematical models to determine catch quotas for various fisheries.

Mathematical models for fish stock assessment have been available in China since the 1950's. Since that time they have not been used as widely as in other countries. The main reasons for this are the inadequacy of basic data which are fundamental to the application of the models, and difficulties with computer resources. Among existing models, three of them are most commonly used in China: the so-called dynamic pool model, surplus production model and stock-recruitment model. This paper deals only with the dynamic pool model to show the possibility of using approximations of the model and how errors produced by using different forms of it would affect fishery management strategies.

Review of the Model

The well-known dynamic pool model leads to the following expression for yield per recruit:

$$(1)\quad \frac{Y}{R} = FW_\infty e^{-M(T_c - T_r)} \sum_{n=0}^{3} \frac{\Omega_n e^{-nK(T_c - T_0)}}{F+M+nK} \left[1 - e^{-(F+M+nK)\,(T_\lambda - T_c)}\right]$$

where (i) Y is the biomass yield and R the number of recruits, (ii) F and M are the instantaneous fishing and natural mortalities, (iii) W_∞, K, and T_0 are von Bertalanffy parameters associated with weight growth, (iv) T_r, T_c, and T_λ are the ages of recruitment, first capture, and ultimate mortality, respectively, and (v) Ω_n is the binomial coefficient $\binom{3}{n}$. Equation (1) is derived by Beverton and Holt (1957, p. 35-36), based on a theory summarized in the following diagram:

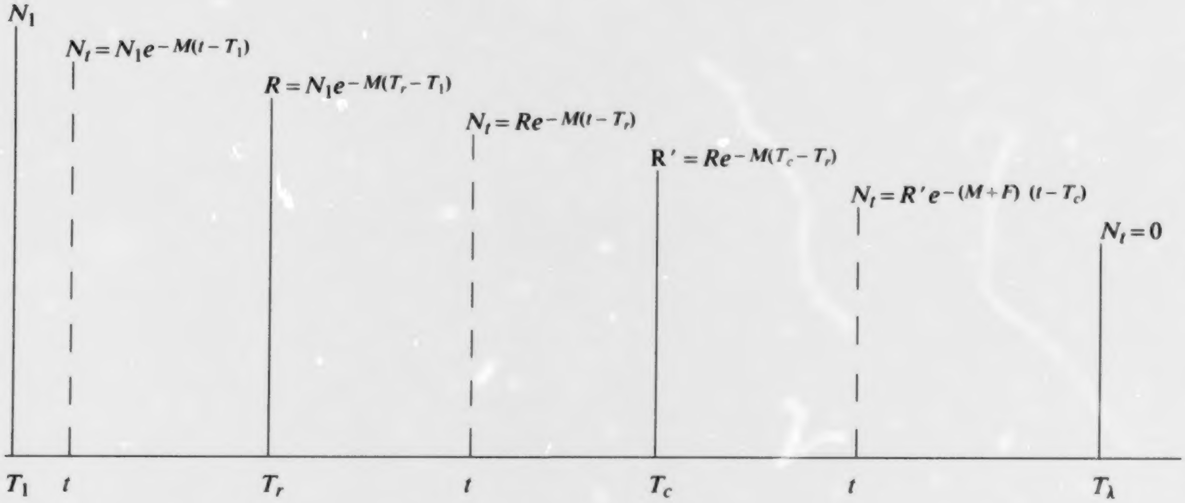
N_1
$N_t = N_1 e^{-M(t-T_1)}$
$R = N_1 e^{-M(T_r - T_1)}$
$N_t = Re^{-M(t-T_r)}$
$R' = Re^{-M(T_c - T_r)}$
$N_t = R' e^{-(M+F)\,(t-T_c)}$
$N_t = 0$
T_1
t
T_r
t
T_c
t
T_λ

This represents the fish population size (N_t) and recruitment (R or R') at various ages, starting at an arbitrary age T_1. In particular, the population is recruited (i.e., first susceptible to the gear) at age T_r, when the recruitment is R. Perhaps due to regulation, the actual age of first capture may be T_c ($\geq T_r$), when the recruitment is R'.

The Beverton-Holt model that leads to (1) is based on three assumptions, which must be considered before applying this result to a management situation. First, recruitment is presumed constant from year to year. Second, individual fish within a brood all follow the same growth law

$$w = W_\infty[1 - e^{-K(T-T_0)}]^3,$$

where w is the weight of a fish at age T. Third, the instantaneous rates of fishing and natural morality are assumed constant, independent of age or year.

Expression (1) is somewhat difficult to calculate without computer assistance. If fishing commences right after recruitment, i.e. $T_c = T_r$, then (1) can be converted to:

$$(2)\quad \frac{Y}{R'} = FW_\infty \sum_{n=0}^{3} \frac{\Omega_n e^{-nK(T_c - T_0)}}{F+M+nK} \left[1 - e^{-(F+M+nK)\,(T_\lambda - T_c)}\right]$$

Some works (Ricker 1975; Wilimovsky and Wicklund 1963) have suggested that the Beverton-Holt model can be simplified by omitting terms containing $e^{-(F+M+nK)\,(T_\lambda - T_c)}$, corresponding to the assumption that $T_\lambda = \infty$. This gives

$$(3)\quad \frac{Y}{R} = FW_\infty e^{-M(T_c - T_r)} \sum_{n=0}^{3} \frac{\Omega_n e^{-nK(T_c - T_0)}}{F+M+nK}$$

or, assuming also that $T_c = T_r$ (as in (3)),

$$(4)\quad \frac{Y}{R'} = FW_\infty \sum_{n=0}^{3} \frac{\Omega_n e^{-nK(T_c - T_0)}}{F+M+nK}$$

Expressions (2) - (4) are modifications of the original result (1) and differ from it by the absence of terms

$$e^{-M(T_c-T_r)};\ e^{-(F+M+nK)\,(T_\lambda-T_c)};\ e^{-M(T_c-T_r)} \text{ and}$$

$$e^{-(F+M+nK)\,(T_\lambda-T_c)},$$

respectively.

Presumably, the calculation of four expressions will give different yields per recruit (Y/R, Y/R'). How large are the differences, and what impact would they have on fishery management strategies? In order to address these questions, data from two species of fish (Table 1) were fitted to each expression and graphs were drawn by "Apple II plus" computer to show the extent of the discrepancy. To compare the errors produced by using different expressions, the estimated value of the parameters in Table 1 are assumed to be desirable.

TABLE 1. Parameters of the marine fish *Gymnocypris przewalskii* and *Decapterus maruadsi*.

	Gymnocypris przewalskii	*Decapterus maruadsi*
T_r	2 year	1 year
T_c	4 year	2.7 year
T_0	0.14 year	− 1.7 year
T_λ	21 year	4 year
K	0.07	0.29
W_∞	2700 g	333.2 g
F	0.446	0.38
M	0.14	0.32

Results and Discussion

Influence of the Instantaneous Rate of Fishing (F)

For the species *Decapterus maruadsi* which has a short life span, the difference between Y/R and Y/R' is positive (Fig. 1). Presence or absence of the term $e^{-(F+M+nK)\,(T_\lambda-T_c)}$ causes the difference in yield per recruit to be greatest at low fishing rate (ca. $F=0.2$ to 0.3) but after that decreases, finally getting very close when $F=1.5$. Note that the error A in Fig. 1 is produced by the term $e^{-M(T_c-T_r)}$ and the error B is created by the term $e^{-(F+M+nK)\,(T_\lambda-T_c)}$. Both errors increase with an increase in T_c. (See solid vs. broken lines in Fig. 1.)

Figure 2 is computed using data for *Gymnocypris przewalskii*. Apparently, both errors A and B reach their maximum magnitude at $F=0.1$; error A vanishes at $F=0.3$ while error B decreases gradually with increasing F. Comparing solid and broken curves in Fig. 3 shows that the difference between Y/R and Y/R' increases when T_c becomes larger.

Influence of the Age at First Capture

In Fig. 3, the difference between Y/R and Y/R' is caused by both terms $e^{-M(T_c-T_r)}$ and $e^{-(F+M+nK)\,(T_\lambda-T_c)}$. The error tends to expand increasing T_c. The term $e^{-M(T_c-T_r)}$ does not make any difference to Y/R and Y/R' before T_c reaches 1.75 when $F=2$ (broken lines in Fig. 3), but after that point, becomes increasingly apparent. At the point where $T_c=4$, the yields computed from (1) and (2) drop to zero owing to the function of term $T_\lambda-T_c=0$, but the yields from (3) and (4) continue their increasing trends.

For the species *Gymnocypris przewalskii* which has a long life span, different patterns of curves can be observed. This becomes more obvious as rate of fishing increases. The broken line in Fig. 4 shows that (1) can be replaced by (3) when T_c is less than 19, which means that term $e^{-(F+M+nK)\,(T_\lambda-T_c)}$ is not so important in cases involving long lived fish, if T_c is small.

Yield per Recruit Contour Diagrams

Yield per recruit contour diagrams in Fig. 5 are computed for *Gymnocypris przewalskii* by expression (1) (solid lines) and expression (3) (broken lines). A slight difference can be seen when F is very small (ranging from 0.02 to 0.2) and that it increases gradually with increasing T_c. Results computed by expression (2) (solid lines) and (4) (broken lines) in Fig. 6 are similar. However, if we compare Fig. 5 with Fig. 6, 7, 8, the inconsistency in estimates of maximum yield per recruit becomes readily apparent. The former is 120 g per fish, while the latter rises by a factor of 5 to 600 g per fish.

Figures 9 to 12 show the variation in yield per recruit with factors T_c and F, computed by expressions (1), (2), (3) and (4) for *Decapterus maruadsi*. If expression (1) is computed, maximum yield per recruit appears between $F=1.2$ and 3.0 and T_c from 2.0 to 3.3 years in Fig. 9 (solid lines), but this maximum yield is reached between $F=2$ and 2.7, and $T_c=2.2$ to 2.8 computed by expression (3) (broken lines). If F and T_c are set at the same value, different yields per recruit are evident in Fig. 9, 10 and 11. There is a large difference between the solid lines (computed by expression (1)) and the broken lines (computed by expression (4)) in Fig. 12, which results from omitting terms $e^{-M(T_c-T_r)}$ and $e^{-(F+M+nK)\,(T_\lambda-T_c)}$. Thus for fisheries for species having a short life span, choice of yield equation becomes very critical.

Summary and Conclusions

The above calculations and figures lead to three general conclusions. First, all three approximations (2), (3), (4) cause errors, in varying degrees, to the estimated yield per recruit and thus reduce the accuracy of stock assessment and forecasts compared with (1), which is considered to be the most accurate expression among the four. As a general rule, (1) should be used under any circumstances. Second, expressions (2) and (4) exaggerate yield per recruit to a great extent if we use them to assess the status of a fish stock or forecast the potential catch for a fishery. Therefore, they are not suitable for developing fishery management strategies. Finally, the substitution of $T_\lambda=\infty$ for the true value of T_λ seems practical only when the instantaneous rate of fishing is high and the species has a minimum life span of 15 years. The chance of substantial error becomes high in applications to short lived species, especially when F is low.

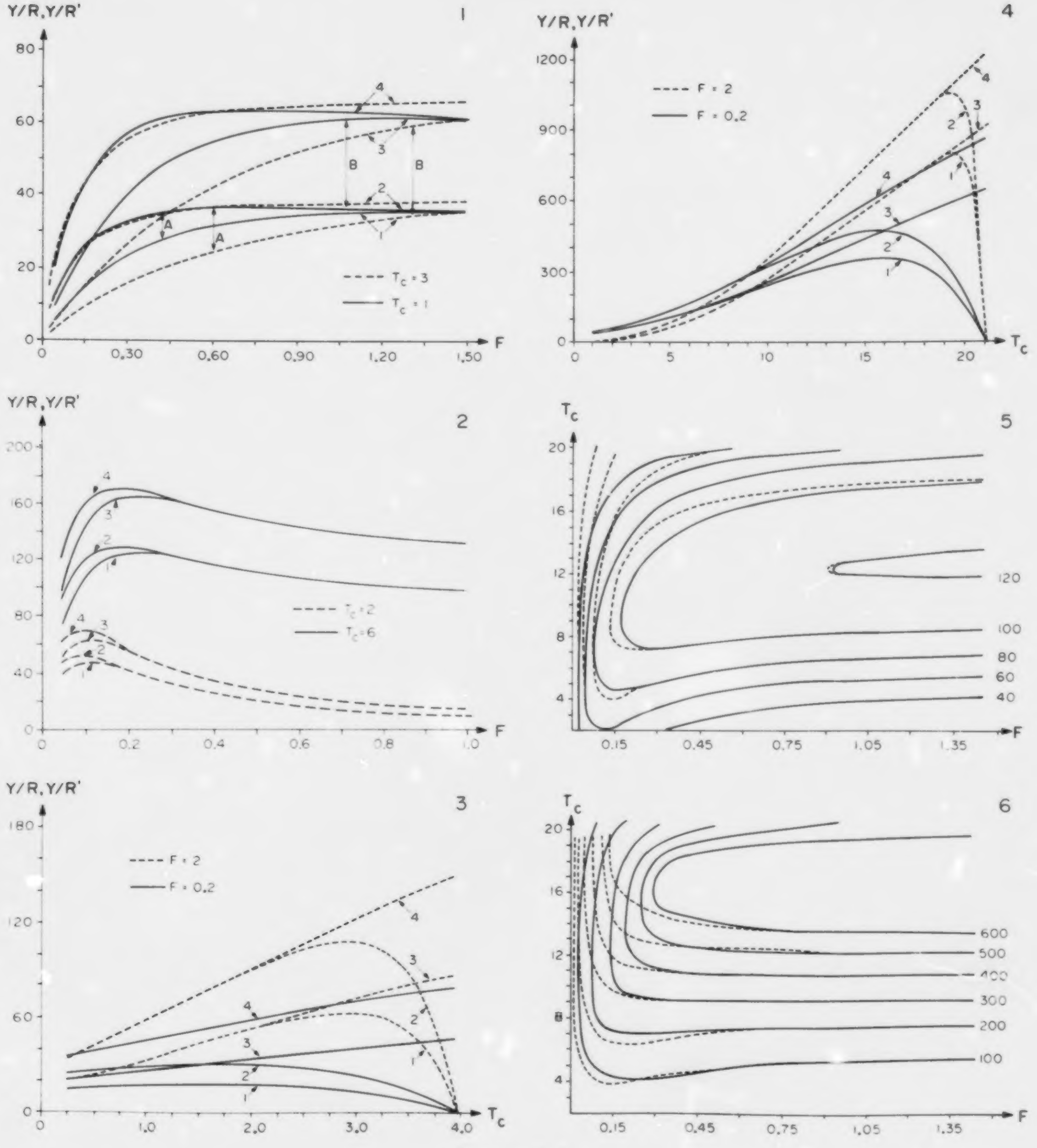

FIGURES 1–6

FIG. 1. Yield per recruit (Y/R, Y/R') vs. instantaneous fishing mortality (F), based on *Decapterus maruadsi* data. Numbers in the figure refer to equation numbers in the text. Solid curves are based on the value $T_c = 1$ yr (i.e., $T_c = T_r$), while broken curves assume that $T_c = 3$ yr. Errors A indicate discrepancies between equations (1) and (2); similarly, errors B indicate differences between (1) and (3).

FIG. 2. Yield per recruit (Y/R, Y/R') vs. instantaneous fishing mortality (F), based on *Gymnocypris przewalskii* data. Again, numbers in the figure refer to equation numbers, and solid and broken curves correspond to the indicated values of T_c.

FIG. 3. Yield per recruit (Y/R, Y/R') vs. age at first capture T_c, based on *Decapterus maruadsi* data. Numbers refer to equation numbers, and solid and broken curves correspond to the indicated values of F.

FIG. 4. Yield per recruit (Y/R, Y/R') vs. age at first capture T_c, based on *Gymnocypris przewalskii* data. Numbers refer to equation numbers, and solid and broken curves correspond to the indicated values of F.

FIG. 5. Comparative yield contour diagrams for *Gymnocypris przewalskii*. Yields shown are in grams per fish. The solid lines are computed by expression (1) and the broken lines are computed by expression (3), using the data listed in Table 1.

FIG. 6. Comparative yield contour diagrams for *Gymnocypris przewalskii*. Yields shown are in grams per fish. The solid lines are computed by expression (2) and the broken lines are computed by expression (4), using the data listed in Table 1.

7

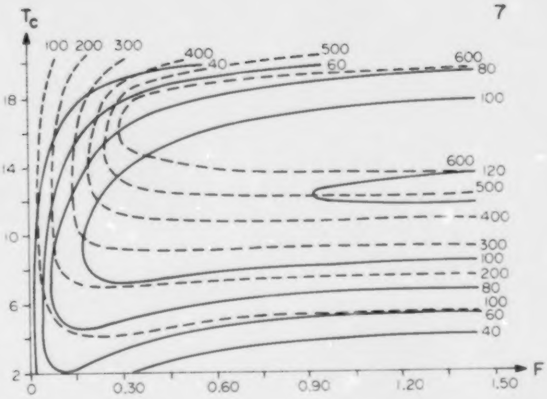

8

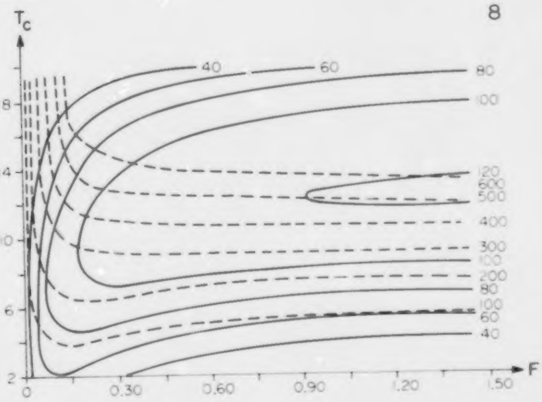

9

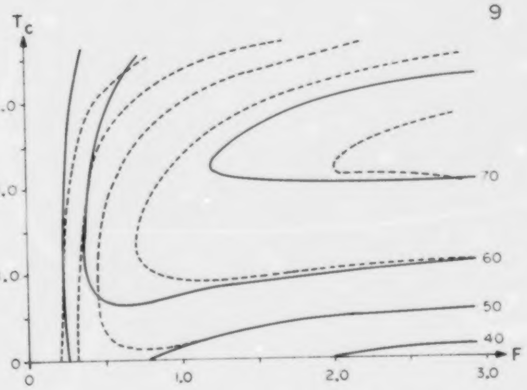

10

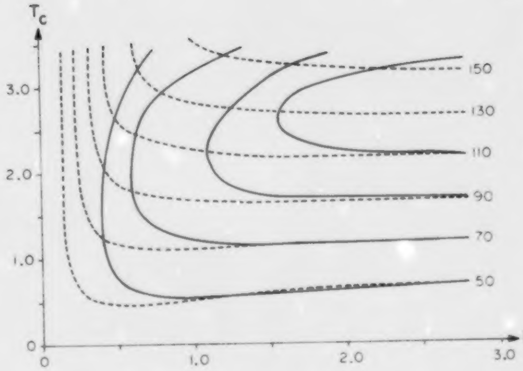

11

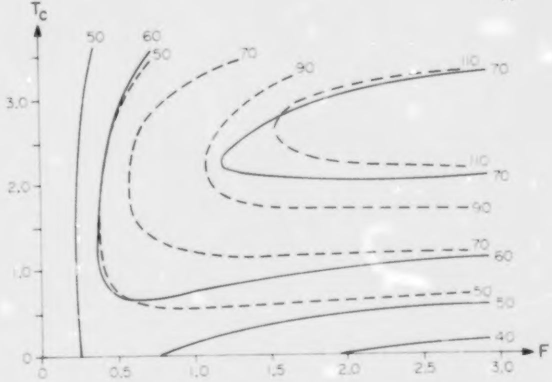

12

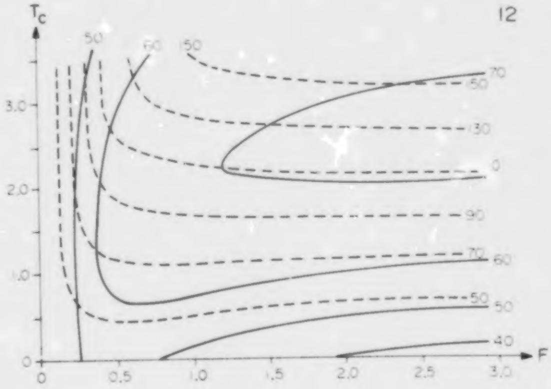

FIGURES 7–12

FIG. 7. Comparative yield contour diagrams for *Gymnocypris przewalskii*. Yields shown are in grams per fish. The solid lines are computed by expression (1) and the broken lines are computed by expression (2), using the data listed in Table 1.

FIG. 8. Comparative yield contour diagrams for *Gymnocypris przewalskii*. Yields shown are in grams per fish. The solid lines are computed by expression (1) and the broken lines are computed by expression (4), using the data listed in Table 1.

FIG. 9. Comparative yield contour diagrams for *Decapterus maruadsi*. Yields shown are in grams per fish. The solid lines are computed by expression (1) and the broken lines are computed by expression (3), using the data listed in Table 1.

FIG. 10. Comparative yield contour diagrams for *Decapterus maruadsi*. Yields shown are in grams per fish. The solid lines are computed by expression (2) and the broken lines are computed by expression (4), using the data listed in Table 1.

FIG. 11. Comparative yield contour diagrams for *Decapterus maruadsi*. Yields shown are in grams per fish. The solid lines are computed by expression (1) and the broken lines are computed by expression (2), using the data listed in Table 1.

FIG. 12. Comparative yield contour diagrams for *Decapterus maruadsi*. Yields shown are in grams per fish. The solid lines are computed by expression (1) and the broken lines are computed by expression (4), using the data listed in Table 1.

Acknowledgements

I thank Mr. Lin De-Yin for assistance in running the computer programs.

References

BEVERTON, R. J. H., AND S.S. HOLT. 1957. On the dynamics of exhibited fish populations. Fish. Invest. Ser. II Mar. Fish. G.B. Minist. Agric. Fish. Food 11: 533 p.

RICKER, W. E. 1975. Computation and interpretation of biological statistics of fish populations. Bull. Fish. Res. Board Can. 191: 382 p.

WILIMOVSKY, N. J., AND E. C. WICKLUND. 1963. Tables of the incomplete beta function, for the calculation of fish population yield. Inst. Fish., Univ. British Columbia, 291 p.

Further Aspects of Catch-Age Analysis with Auxiliary Information

Richard B. Deriso[1], Phillip R. Neal

International Pacific Halibut Commission, P.O. Box 95009,
Seattle, WA 98145-2009, USA

and Terrance J. Quinn II

Juneau Centre for Fisheries and Ocean Sciences, University of Alaska at Juneau,
11120 Glacier Hwy., Juneau, AK 99801, USA

Abstract

DERISO, R. B., P. R. NEAL, AND T. J. QUINN II. 1989. Further aspects of catch-age analysis with auxiliary information, p. 127–135. *In* R. J. Beamish and G. A. McFarlane [ed.] Effects of ocean variability on recruitment and an evaluation of parameters used in stock assessment models. Can. Spec. Publ. Fish. Aquat. Sci. 108.

We describe several generalizations of our published catch-age models, including methods for incorporating multi-gear catch information, survey abundance estimates, and aggregated catch-at-age data. We show that auxiliary information is needed to define a unique solution to the relative year-class model described in a previous paper. We evaluate the use of survey catch-at-age and effort data on Pacific halibut of the Gulf of Alaska and reject this data in favor of assessments based solely on commercial catch-at-age and effort data. We show results of a Monte Carlo study for Pacific halibut supporting the aggregation of catch-at-age data on older aged fish.

Résumé

DESIRO, R. B., P. R. NEAL, AND T. J. QUINN II. 1989. Further aspects of catch-age analysis with auxiliary information, p. 127–135. *In* R. J. Beamish and G. A. McFarlane [ed.] Effects of ocean variability on recruitment and an evaluation of parameters used in stock assessment models. Can. Spec. Publ. Fish. Aquat. Sci. 108.

Les auteurs procèdent à plusieurs généralisations en ce qui concerne les modèles de la composition des captures en fonction de l'âge qu'ils ont publiés, dont des méthodes permettant l'intégration de données relatives aux captures réalisées à l'aide de divers engins, des estimations de l'abondance à partir des études et des données regroupées au sujet des captures en fonction de l'âge. Ils démontrent que des données complémentaires sont nécessaires afin de pouvoir utiliser le modèle de classe d'âge décrit antérieurement. Ils évaluent l'utilisation des données scientifiques concernant la composition des captures en fonction de l'âge et l'effort pour le flétan du Pacifique du golfe de l'Alaska; ils estiment qu'il est préférable d'avoir recours aux données fournies par la pêche commerciale sur les mêmes aspects. Ils donnent les résultats d'une étude réalisée à Monte Carlo avec le flétan du Pacifique qui appuient l'emploi des données regroupées au sujet des captures en fonction de l'âge pour les poissons plus âgés.

Introduction

The catch-age models in Deriso et al. (1985) can be extended in a variety of ways. In this paper, we describe some generalizations with emphasis placed on those extensions that are useful for analyzing multi-gear data, survey data, and catch-at-age data aggregated over several ages. Such data are common in many types of fisheries and they can be easily accommodated with minor changes in our previous paper.

Results were presented in Alton and Deriso (1983) on catch-age analysis of a multi-gear fishery, although the method was not derived in that paper or in the subsequent Deriso et al. (1985) paper. We present a derivation of multi-gear catch-age analysis with auxiliary information. Survey catch-at-age and fishing effort data can be regarded as data from a particular gear type and, thus, the multi-gear model can be used to incorporate survey data into stock assessment. We analyze Pacific halibut data collected from both survey fishing and commercial fishing in the Gulf of Alaska.

The principal reason for aggregating age-specific catch data over several ages is that errors are present in estimates of the age composition of catch. Some errors in estimates of Pacific halibut age composition arise because of the need to sub-sample commercial catch landings, as discussed in Quinn et al. (1983). In addition, there are ageing errors: age is estimated for a given halibut by visually counting the annual rings on the ear otolith, which are sometimes difficult to see. Fournier and Archibald (1982) apply a version of the model in Deriso (1980) to aggregate catch data for fish of a given age and older. Their aggregation scheme assumes equal vulnerability of all those fish to exploitation. In this paper, we develop a method which allows for age-specific selectivity of fishing mortality, yet it can be applied to aggregate data. We then examine the precision of estimates obtained by aggegating catch-at-age data with a Monte Carlo simulation study.

---

[1] Present address: Inter-American Tropical Tuna Commission c/o Scripps Institute of Oceanography, La Jolla, CA 92093, USA.

An auxiliary sum of squares term is useful for including types of information other than just fishing effort, as in equations 9, 10 and 11 of Deriso et al. (1985). On the other hand, there are practical difficulties in writing reliable computer programs to handle such information. One alternative presented in this paper is to use our existing catch-at-age computer program CAGEAN © by adapting new information to an existing mathematical model. We show how survey abundance estimates and specified fishing mortalities can be incorporated in our existing model.

Theory of Stratified Catch-Age Analysis

A key assumption in catch-age analysis is that fishing mortality is separable into a product of an age-specific selectivity coefficient, $s(a)$, and a full-recruitment fishing mortality, $f(t)$; thus, fishing mortality in year t for individuals age a years old is given as

$$F(t,a) = s(a)f(t)$$

as discussed in detail in Deriso et al. (1985). When several types of gear with differing selectivity properties are used on a given fish species then the separability assumption can be grossly violated. For example, a shift in the mix of gear-types over time would induce systematic shifts in the overall age-selectivity of fishing mortality.

In Beverton and Holt (1957, page 82), yield theory is developed for the effects of simultaneous use of gear with different selectivity properties. The catch equations for each gear g are extensions to the usual Baranov catch equation:

$$\text{(1)} \quad C(t,a,g) = \mu(t,a,g)N(t,a)$$

$$\mu(t,a,g) = \frac{F(t,a,g)}{Z(t,a)}\,[1 - e^{-Z(t,a)}]$$

$$N(t+1,a+1) = N(t,a)e^{-Z(t,a)}$$

$$Z(t,a) = M(t,a) + \sum_g F(t,a,g)$$

$$F(t,a,g) = s(a,g)f(t,g)$$

where

$C(t,a,g)$ = predicted catch in year t for a year-olds by gear g,

$N(t,a)$ = population abundance of a year-olds at the beginning of year t,

$F(t,a,g)$ = fishing mortality rate in year t for a year-olds by gear g,

$s(a,g)$ = age-specific selectivity factor for gear g,

$f(t,a)$ = full recruitment fishing mortality rate for gear g in year t,

$M(t,a)$ = natural mortality rate.

In our model, observed catch-at-age data $C'(t,a,g)$ are assumed to differ from predictions in (1) by a log-normal random variable, which has a variance that is dependent upon gear-type. Thus,

$$\epsilon(t,a,g) = \log C'(t,a,g) - \log C(t,a,g),$$

where $\epsilon(t,a,g)$ is a normal $(0,\sigma^2_{cg})$ random variable and σ^2_{cg} denotes the variance of logarithm catch for a particular gear-type. The symbol "log" denotes natural logarithm. Nonlinear least-squares can be applied to

$$\text{(2)} \quad \text{minimize } SSQ(\text{catch}) = \sum_g \lambda_{cg} \sum_{t,a} \epsilon(t,a,g)^2,$$

a weighted sum of squared residuals of all catch data. The λ_{cg} coefficients are weighting terms that adjust the amount of influence of catch data for each g gear-type; for at least one gear, say [$g = 1$, we set $\lambda_{c1} = 1$] in order for (2) to be well defined. Maximum likelihood of the catch data is achieved when (2) is minimized while λ_{cg} is set equal to the ratio of variances (σ^2_{c1} divided by σ^2_{cg}), for all gear-types. The lambda coefficients cannot be estimated in (2), as discussed in our previous paper, and so they must be provided external to the analysis.

These are the generalizations needed for catch equations given in our previous paper. Separability is assumed for each gear-type and accordingly we estimate separate selectivity parameters, $s(a,g)$, and full-recruitment fishing mortalities, $f(t,g)$, for each gear. To implement the stratified method in CAGEAN ©, catch data are partitioned by year, age, and gear, and natural mortality is constant over age and year. Applications of this method are given in Alton and Deriso (1983) and Rami (1984).

In order to stabilize parameter estimates, Deriso et al. (1985) found it necessary to add an auxiliary sum of squares term to our minimization criterion (2). We assume that gear-specific fishing mortality and fishing effort are proportional up to a multiplicative log-normal random variable. We can write the random variables as differences between logarithms of fishing mortality and the product of a catchability coefficient and fishing effort:

$$\epsilon_e(t,g,) = \log\,[f(t,g)] - \log[q_g E(t,g)]$$

where $\epsilon_e(t,g)$ is a normal $(0,\sigma^2_{eg})$ random variable, q_g is a catchability coefficient, and $E(t,g)$ is fishing effort for gear-type g in year t. Our nonlinear least-squares criterion is now to

$$\text{(3)} \qquad \text{minimize } SSQ(\text{catch}) + SSQ(\text{effort})$$

where the auxiliary effort term is given by:

$$\text{(4)} \qquad SSQ(\text{effort}) = \sum_g \lambda_{eg} \sum_t \epsilon_e(t,g)^2.$$

The λ_{eg} coefficients are weighting terms that adjust the amount of influence of fishing effort data for each gear-type g. Maximum likelihood estimation calls for setting the lambda coefficient λ_{eg} equal to the ratio of variances (σ^2_{eg} divided by σ^2_{c1}), where catch gear-type 1 is the standard for which we have chosen $\lambda_{c1} = 1$. As in the catch *SSQ* term, the effort lambda coefficients must be supplied external to the analysis. In practice, some guidance can be provided from the data on the proper size of the lambda coefficients, as discussed in the later section on application of our model to survey data.

Flexibility of the *SSQ* (Effort) Term

The auxiliary effort term (4) can be used for a number of purposes other than for including fishing effort information. Indeed, any information about fishing mortality can stabilize mortality estimates in catch-age analysis. We consider the case for a single gear type; the stratified model is developed in an analogous fashion. Let us generalize the definition of $E(t)$ to be any specified data which is proportional, up to a log normal random variable, to full-recruitment fishing mortality, $f(t)$, in year t.

Independent estimates of fishing mortality can be incorporated in the catch-age analysis simply by replacing the $E(t)$ data with the mortality estimates and fixing $q = 1.0$. Merely to influence the trend in catch-at-age estimates of fishing mortality, we can allow q to be an additional parameter estimated by the complete analysis. Two types of applications are discussed below:

A. Full- recruitment fishing mortality is specified for the most recent year. This approach has been applied in one type of catch-age analysis by Pope and Shepherd (1982). Here we have only one piece of $E(t)$ data, the one for specified fishing mortality during the most recent year; the previous years of $E(t)$ data are treated as missing data. Setting λ_e to a large number (e.g., 1000000) and fixing q at the value of 1.0 will effectively tie down the last $f(t)$ fishing mortality at the specified $E(t)$ value. Lower values of λ_e can be used to influence the last $f(t)$ value without insisting that it be set precisely to $E(t)$.

B. Estimates are available of fully recruited adult abundance (say, $\hat{N}(t)$) from a survey experiment (or mark-recapture, acoustics, etc.). Given estimates of $N(t)$ for any year (or years), we first calculate the full-recruitment exploitation fraction, $\mu(t)$, as

$$\mu(t) = \frac{C(t)}{\hat{N}(t)}$$

the ratio of total catch $C(t)$ from fully recruited age-classes to abundance. Given a value for natural mortality rate, M, we then implicitly solve for $F(t)$ from

$$\mu(t) = \frac{F(t)}{F(t) + M}\left[1 - e^{-(F(t)+M)}\right].$$

Each solution $F(t)$ is used as the auxiliary $E(t)$ data point. This approach has been applied to the Bering Sea walleye pollock population where acoustic-bottom trawl survey estimates are available to estimate $N(t)$ for three out of the 11 years of data used in the analysis (personal communication, V. Wespestad, NWAFC, Seattle, Wa.). Again, we can either fix $q = 1.0$ to use directly the independent estimates of fishing mortality rate or we can allow q to be an additional parameter in the estimation procedure to merely influence the trend in $f(t)$ estimates. The size of λ_e controls the amount of influence the auxiliary data exerts on the $f(t)$ estimates.

In both of the above examples, it is uncertain whether the assumption, that $\epsilon_e(t)$ is a normal random variable, is satisfied. This may not matter much since, by analogy, linear regression theory supports least-squares parameter estimates as long as the random deviates are homogeneous, irrespective of their underlying distribution (Chatterjee and Price 1977). Furthermore, three catch-age models, each with a different assumption about error structure, performed similarly in our comparative study (Deriso et al. 1985).

The requirement that q is a single parameter for the entire time series of data can be relaxed. We have extensively applied the obvious extension of our model where the time series of data is blocked into two consecutive groups of years, each with its own q parameter. This is particularly useful when the fishery (or the survey design) undergoes some major change during the years for which data are analyzed. We find this generalization useful for estimating Pacific halibut parameters in long time series since an increase in the minimum size limit in 1973 shifted the fishery away from some important fishing grounds where mainly smaller halibut were caught (Deriso and Quinn 1983).

Aggregate Catch-at-Age Data

Fournier and Archibald (1982) discuss the application of a simple difference equation for modelling catch aggregated over age categories. This approach is applicable when fish of a given age, say A^+, and older are fully vulnerable to fishing mortality (that is, $s(a) = 1.0$). Abundance of the A^+ aggregate is the combination of survivors of the aggregate plus new entrants into the aggregate from the previous age $(A^+) - 1$. The dynamics of abundance of fish in the aggregated age categories, $N(t,A+)$, can be written as

$$\text{(5)} \qquad N(t+1,A^+) = N(t,A^+)e^{-Z(t,A^+)} + N(t,(A^+)-1)e^{-Z(t,(A^+)-1)}$$

where total mortality rate of the aggregate age category is $Z(t,A^+) = f(t) + M$, assuming that those fish are fully vulnerable to fishing mortality. For other ages, the standard population equations (1) apply. Natural mortality is assumed to equal a constant M, independent of age and year, in this paper; although, in theory M can vary by year for the aggregate. Predicted catch of the aggregate is obtained by multiplying the full-recruitment exploitation fraction by abundance in (5).

More generally, equation (5) can be used to model fish of any given age A^+ and older, even if they are not fully vulnerable to fishing, as long as both the age selectivity of fishing mortality and the age structure of fish in the aggregate remains stable; here $f(t)$ would be set equal to fishing mortality averaged across the aggregated ages. In practice, fish populations seldom maintain a stable age distribution, and so application of (5) is at best an approximation. We investigate below, with Monte Carlo simulations, the consequences of applying (5) to arbitrarily chosen age groupings.

We can derive an aggregate catch equation with the same underlying survival and exploitation structure as given in (1) by simulating the full age-structure of a population and then summing across age categories:

$$C(t,A^+,g) = \sum_{a=A^+}^{A_{max}} \mu(t,a,g)N(t,a). \tag{6}$$

Equation (6) explicitly accommodates age and gear specific, separable, fishing mortality for arbitrary age distributions.

Restrictions on Relative Abundance Analysis

One modification of catch-age analysis is based on a method where total catch is not even used. In Deriso et al. (1985), we describe such a method for estimating year-class strength. The method uses data on observed proportion of catch by age (within year) which is fitted to the predicted proportion, $p(t,a)$, of catch by age a and year t, as given by

$$p(t,a) = \frac{a^{\alpha}e^{-\beta^* a}n(t-a+1,1)}{\sum_{j=1}^{A_{max}} j^{\alpha}e^{-\beta^* j}n(t-j+1,1)} \tag{7}$$

where $\beta^* = \beta + Z$; α and β are parameters of a gamma age selectivity function, and $n(t,1)$ is relative year-class abundance in year t of reference age 1 fish.

Our method of fitting equation (7) in our previous paper relied exclusively on observed catch data. The problem with that procedure, as pointed out by Dr. Justin Cooke (UBC, Vancouver, B.C., personal communication), is that the estimates of the $n(t,1)$ parameters can be changed by an exponential time trend to generate a new set of parameter estimates which has the same value of the log-likelihood function. To see this let us suppose $(\hat{n}(t,1),\hat{\beta}^*,\hat{\alpha})$ are solutions that minimize the log-likelihood equation (6) of our previous paper. Let r be any arbitrary number. Then a set of parameters with the same value of $p(t,a)$ in (7) and the same value of the objective function is given by $\tilde{n}(t,1) = \hat{n}(t,1)exp(-rt)$, $\tilde{\beta} = \hat{\beta}^* + r$, and $\tilde{\alpha} = \hat{\alpha}$. This property is similar to the characteristic of stable age distributions where age composition remains constant over time although population abundance increases (or decreases) exponentially. Therefore, information auxiliary to relative catch is needed to identify a unique set of parameter estimates in equation (7). An independent estimate of β^* will suffice. Alternatively, information about the $n(t,1)$ parameters can be used; for example, we can fix two of the $n(t,1)$ parameters at specified relative levels rather than the one $n(t,1)$ parameter fixed in our previous paper.

An independent estimate of β^* was made for Pacific halibut. From cohort analysis estimates of abundance, we estimate average total mortality, Z, across ages (8–20 years of age) and years (1935–70) as $\hat{Z} = 0.39$. Those abundance estimates were also used to estimate age selectivity by age and year, which were then fitted to the gamma selectivity function used in equation (7) to get $\hat{\alpha} = 0.88$ and $\hat{\beta} = 0.09$. Therefore, $\hat{\beta}^* = 0.48$, which is fortuitously close to the $\beta^* = 0.45$ estimate found by our minimization software for the example reported on page 823 in our previous paper. This similarity of estimates probably explains why we obtained such a close correspondence between the relative year-class estimates and cohort estimates from VPA (as shown in Fig. 5 of our previous paper). We arbitrarily fixed β^* at the value of 0.80, ran our minimization software for the problem again, and obtained essentially the same value for the objective function as before; but relative year-class estimates changed considerably. Thus relative abundance can be estimated with relative catch data, only if auxiliary information is available.

Analysis of Survey and Commercial Catch Data for Pacific Halibut

Research survey fishing has been conducted over a fixed grid of sampling locations in the Gulf of Alaska since 1977. Hoag et al. (1980) describe the survey design and discuss the desire to obtain assessment data on halibut, independent of the commercial fishery. Overall, the survey in the Gulf of Alaska provides confirmation of trends depicted in our stock assessment results; for the 1977 to 1986 time period an $R = 0.83$ exists between the survey CPUE (legal-sized biomass of catch per unit skate of fishing effort) and our "best estimates" of exploitable biomass in the Gulf of Alaska. However, the survey data shows a much more erratic time series than the rather smooth increase in abundance shown in either the commercial CPUE data or in our estimates of exploitable biomass.

We applied the stratified catch-age model (1) to both commercial and survey catch and fishing effort data on Pacific halibut in the Gulf of Alaska. Our main interest was to see whether or not the inclusion of survey catch and effort data would reduce variance in current estimates of exploitable biomass and annual surplus production. Exploitable biomass is defined as

$$B(t) = \sum_{a=8}^{\infty} s^*(a)w(t,a)N(t,a) \tag{8}$$

where the selectivity factors $s^*(a)$ are fixed numbers chosen to represent a year 1984 standard — this helps maintain comparability of estimates. The weight-at-age estimates $w(t,a)$ are estimated separately from the catch-age analysis. Annual surplus production (ASP) for year t is calculated for the exploitable biomass in the usual manner, $ASP(t) = B(t+1) - B(t) + Y(t)$ where $Y(t)$ is total catch in biomass (yield).

Lambda coefficients are needed to include survey data in our catch-age analysis, as specified in equations (2) and (4). Although in theory the lambda coefficients cannot be estimated simultaneously in the analysis, in practice much can be learned by a preliminary analysis of the data. We first analyzed only the commercial data (gear-type c) using our "standard" age categories (8 to 20$^+$ years of age) for years of data 1977–86. Results of this baseline analysis appear in Table 1 beside the rows titled "Scenario 1". The λ_{ec} coefficient for fishing effort in the commercial data was set at a value of 0.5, following results given in our previous paper. The λ_{cc} coefficient for commercial catch data is set to 1.0 and natural mortality rate is fixed at $M = 0.2$ for all ages, as in our previous paper.

We obtained rough estimates of the lambda coefficients in the survey data (gear-type s). We applied catch-age analysis only to survey data, but fixed parameter values for abundance, commercial fishing mortality and catchability, and commercial age selectivity at those obtained in the baseline estimates; thus, only survey fishing mortality, catchability, and selectivity coefficients were estimated. The average squared residual in the logarithm survey catch is 0.0786, while the average squared residual in the logarithm commercial catch in the baseline analysis is 0.0299; thus, an estimate of $\lambda_{cs} = 0.38 = 0.299/0.0786$ is an estimate of the lambda coefficient in the survey catch data. In a similar fashion, we obtain $\lambda_{es} = 0.19$ as an estimate of the lambda coefficient in the survey effort data. Results from this configuration of lambda coefficients are reported in Table 1 beside the rows titled "Scenario 3". We did not want to overemphasize the survey data in our catch-age analysis so we also tested performance of the procedure with $\lambda_{cs} = 0.14$ and $\lambda_{es} = 0.10$. Results from this configuration of lambda coefficients are reported in Table 1 beside the rows titled "Scenario 2".

A bootstrap Monte Carlo procedure was applied to results obtained from estimation of 1977–86 halibut data for each of the three scenarios listed above. As described in Deriso et al. (1985), "The essence of the bootstrap technique is to randomly sample with replacement the residuals from the nonlinear catch-age analysis and to sequentially add the sampled residuals to the [predicted] catch-age and effort data. This process creates a new data set with the same statistical properties as the original data set...". One hundred bootstrap data sets were generated for each of the three scenarios. Maintenance of two features of possible heterogeneity in the distribution of residuals was provided: we constrained the assignment of residuals in the bootstrap so that residuals were assigned only to predicted quantities within the same gear-type; we assigned catch residuals only to predicted catches and effort residuals to predicted efforts.

In Table 1, we list the average and standard deviation of some of the quantities estimated by nonlinear catch-age analysis of the bootstrap data. The bootstrap means are very similiar to original estimates within each scenario, which indicates bias is small. The main difference in estimates and in the means is between scenarios, with a general tendency toward higher biomass and production as the amount of weighting given survey data is increased. However, the biomass estimates all lie within ± two standard deviations of each other (as computed in any of the three scenarios). There is little pattern in the standard deviation estimates and including survey data can either increase or decrease variances, depending on the size of the lambda coefficient and the quantity under consideration.

We lowered the value of the lambda coefficients to 0.0001 for both survey catch and effort data and repeated a catch-age analysis on the 1977–86 halibut data sets. The resultant parameter estimates were ridiculous. Exploitable biomass, for example, was three times the estimates obtained in Table 1 for 1986. The model might be expected to show pathological behavior in such a scenario since the survey fishing mortality parameters are virtually unconstrained by the survey data; they can take on whatever value is beneficial in altering the total mortality rate $Z(t,a)$ in (1) so as to help commercial catch data fit predicted catch. This happened in our analysis; the commercial catch residual sum of squares decreased from 2.99 to 1.68 by including survey data with the small weights listed above.

In summary, there was little improvement in parameter estimates when survey catch and effort data were included in catch-age analysis of Pacific halibut of the Gulf of Alaska.

TABLE 1. Comparison of mean and standard deviation estimates from 100 Bootstrap simulations of commercial and survey catch-age and effort data. Parameter estimates listed as 'original estimate' correspond to those obtained by catch-age analysis of 1977–86 Gulf of Alaska halibut data. Three scenarios are listed: 1. Results when only commercial catch and effort data is used; 2. Results when both commercial and survey data are used where the weighting coefficient for survey catch is $\lambda_{cs} = 0.14$ and the weighting coefficient for survey fishing effort is $\lambda_{es} = 0.1$; 3. Results when both commercial and survey data are used and here $\lambda_{cs} = 0.38$ and $\lambda_{es} = 0.19$. The weighting coefficient for commercial fishing effort is $\lambda_{ec} = 0.5$ in all scenarios. All quantities are in units of tonnes.

Scenario	Parameter	Original estimate	Bootstrap mean	Standard deviation
1	1977	27 700	27 964	1 555
2	Exploitable	28 074	28 374	1 650
3	Biomass	29 185	29 381	1 703
1	1986	62 447	62 657	9 467
2	Exploitable	68 572	69 511	8 275
3	Biomass	78 181	78 575	9 373
1	1985 Annual	14 643	14 542	2 116
2	Surplus	15 401	15 654	1 850
3	Production	16 297	16 462	1 993

Monte Carlo Experiment on Aggregate Catch Data

Data and Methods

Our Monte Carlo study starts with the construction of a set of "true" hypothetical catch and effort data. We generated these values by first analyzing Pacific halibut commercial catch and effort data for the years 1974–86 from the Gulf of Alaska (International Pacific Halibut Commission (IPHC) regulatory area 3A) with the catch-age model (1). "True" catch and effort values were defined to be the predicted catch and effort calculated from the age-specific analysis of 8–19 year-olds, with aggregation, as in equation (5), for the 20^+ year-old fish. In the context of our Monte Carlo study, these "true" values are in fact hypothetical values generated by a catch-age model with assumed parameters.

The assumption behind the Monte Carlo technique is that all data sets used must be sampled from the same distribution defined by the "true" estimates. In order to follow this assumption, the catch and effort data sets that were used for each Monte Carlo experiment were generated by randomly choosing a residual from a fixed set of residuals and adding it to a "true" catch or "true" effort estimate. This assignment of a random residual was done for each catch and effort estimate from the "baseline" analysis. The set of residuals used in our Monte Carlo study were those obtained from the baseline analysis. In equation form, the randomization process can be written:

$$y'(i) = y(i) + \epsilon(k)$$

where k is a random index chosen with replacement from $k(1,\ldots,k)$, the index i from $(1,\ldots n)$, n is the total number of catch and effort observations, $y'(i)$ is a hypothetical "observed" data point, and $y(i)$ is a "true" data point.

Another test of robustness of the estimates from aggregated catch-age analysis was performed. Each baseline residual was "doubled" before being randomly assigned to a baseline estimate. In equation form, this variation can be written:

$$y'(i) = y(i) + 2\epsilon(k)$$

where all variables and indices are the same as in the above equation.

The randomized age 8 to 20^+ data sets were then pooled at a given age of aggregation. The given age corresponds to the particular scenario under consideration. The aggregation process can be written:

$$C'(t,A^+) = \sum_{a=A+}^{20+} C'(t,a)$$

for any given A^+ age of aggregation. The range of age of aggregation in our study was from A^+ equal to age 10 years to age 20 years. Thus, there were 1100 (100 bootstraps by 11 ages of aggregation) data sets in total generated for this study, each of which was analyzed using the nonlinear least-squares criterion (3) and aggregation model (5).

At IPHC, we use a fixed set of age-specific selectivity coefficients for calculation of certain output quantities, as seen in the definition of exploitable biomass in (8). In this study, we allowed selectivity to be estimated in each experiment, but set estimates to the "fixed values" for calculating exploitable biomass and exploitable annual surplus production. The selectivity coefficients were fixed in the following manner: for any age greater than or equal to 15 (the usual age of full selectivity for halibut) the selectivity coefficient was set to 1.0; if the age of aggregation was less than 15, then full selectivity was set at the age of aggregation.

Simulation experiments with model (6) were limited to a single parameterization with aggregation of ages 10^+. Further restrictions on this particular scenario are the following: age selectivity coefficients are fixed at the "true" values for ages 10–15 [initial 1974 abundance was fixed at the "true" values for ages 11 and older]. These restrictions were made so that model (6) and model (5) scenarios for the age 10^+ aggregation have the same number of unknown parameters, which we believe makes those results comparable. Also, we have good estimates of abundance of the 1974 population, as well as selectivity for older fish, so that the above restrictions are reasonable for analysis of Pacific halibut.

Results

The goal of this exercise was to investigate the robustness of catch-age analysis to the aggregation of catch data. The impact of aggregating catch data was examined for both parameter estimates and abundance estimates. The model (5) method of aggregation is used in all figures and tables unless noted otherwise.

In Fig. 1, Monte Carlo mean 1986 estimates of exploitable biomass and numerical abundance are shown for different ages of aggregation. Exploitable biomass estimates vary from 48 600 to 52 500 t around the "true" value of 51 500 t. This represents a maximum difference of less than 6% for any age of aggregation. Numerical

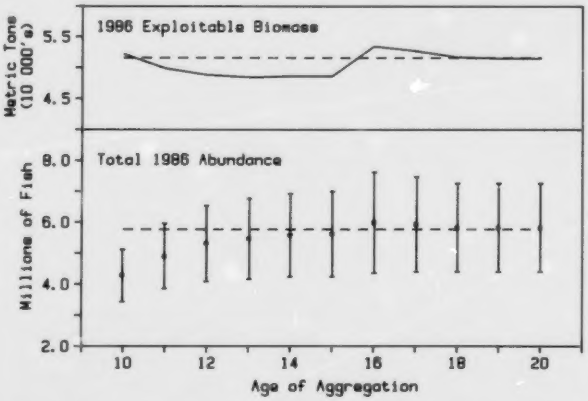

FIG. 1. Comparison of estimates of exploitable biomass and total abundance from Monte Carlo simulations of catch-age and effort data. Simulated catch data were aggregated for ages above the listed age. (---- indicates the "true" value). Bars represent a distance of 1 standard deviation from the estimate.

abundance estimates vary from 4.27 million fish at a minimum, to 5.99 million fish at a maximum around the "true" value of 5.77 million fish. The maximum difference is found at age 10 aggregation and the difference converges to the true by about age 15 aggregation.

The goodness of fit for the solution using baseline data aggregated to the appropriate age is shown in Fig. 2. The mean square error of the fit increases with the age of aggregation because the variance of a pooled catch is smaller than the sum of the variances of individual catches. The standard deviation of the estimates of 1985 exploitable annual surplus production and exploitable biomass are also shown in Fig. 2. The standard deviation of the exploitable annual surplus production ranges from 2 650 to 4 324 t. This estimate holds steady after age 15 aggregation. The standard deviation of exploitable biomass ranges from 9 100 to 14 000 t. This estimate is fairly consistent across all ages of aggregation past age 10.

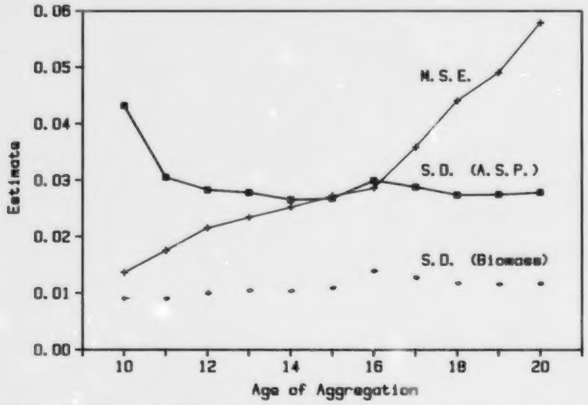

FIG. 2. Variance estimators for Monte Carlo simulations of catch-age and effort data. Simulated catch data were aggregated for ages above the listed age. (M.S.E. — Mean square error of solution using aggregated baseline data, S.D. (A.S.P.) — Standard deviation of 1985 Exploitable annual surplus production × 100 000 t, S.D. (Biomass) — Standard deviation of 1986 Exploitable Biomass × 1 000 000 t)

Another estimate of the health of the stock that was examined during this analysis was recruitment. In Fig. 3 recruitment estimates are shown for runs made with the original residuals and with residuals multiplied by a factor of two, which we refer to as simple residuals and double residuals, respectively. For aggregation ages 15 and 20 there is little difference in estimates of recruitment. Aggregate age 10 results, although lower, still are much the same. This shows the robustness of the methodology to higher variance in the estimates of the catch. The standard deviation of the Ln (recruitment) estimates was also examined. In Fig. 4, the standard deviations using simple residuals were a factor of about two times lower than standard deviations using doubled residuals for all aggregation ages, as expected. Aggregation does not affect standard deviation estimates for aggregation ages 15 or 20. In all cases the estimates increase as time increases. This is because catch-age analysis estimates are based on fewer observations of a year-class in later years as it moves forward in time.

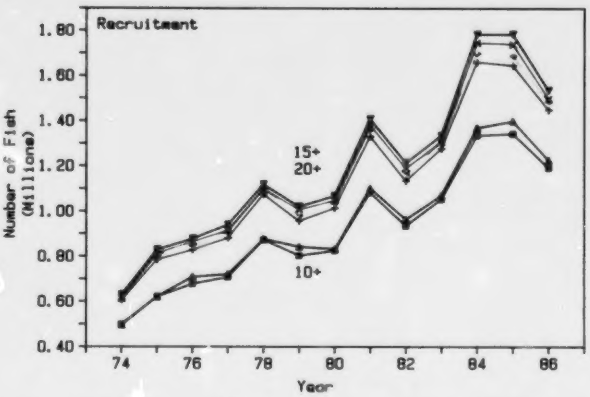

FIG. 3. Comparison of estimates of recruitment from Monte Carlo simulations of catch-age and effort data. (■ — age 10 simple residuals, △ — age 10 double residuals, + — age 15 simple residuals, × — age 15 double residuals, ◇ — age 20 simple residuals, ▽ — age 20 double residuals)

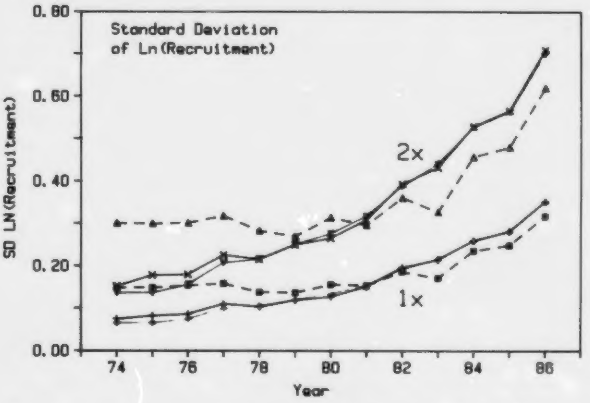

FIG. 4. Comparisons of estimates of the standard deviation of Ln (recruitment) from Monte Carlo simulations of catch-age and effort data. (■ — age 10 standard residuals, △ — age 10 double residuals, + — age 15 standard residuals, × — age 15 double residuals, ◇ — age 20 standard residuals, ▽ — age 20 double residuals)

Another important parameter, fishing mortality, is shown in Fig. 5. Aggregate ages 10 and 15 form an envelope around the "true" values and track the "true" values fairly well. Fishing mortality estimates for the aggregate age 16 through aggregate age 19 scenarios move incrementally towards the aggregate age 20 results from the age 15 results. Also included in Fig. 5 are fishing mortality estimates computed for aggregation age 10 data using model (6) that correctly calculates selectivity for ages of fish in the aggregate; these estimates of fishing mortality are very close to estimates for the full age 8 to 20 data. The favorable results given in Fig. 5 for model (6) with age 10+ aggregation show that substantial pooling of age-specific data can result in nearly unbiased estimates, if the selectivities are handled properly in the model.

Estimates of the standard deviation of Ln (fishing mortality) are shown in Fig. 6. The aggregate age 10 estimates using model (6) are uniformly higher than the aggregate age 20 results. In all cases the estimates increase dramatically in later years. Again, this is because catch-age analysis has less data to compute estimates as it moves forward in time.

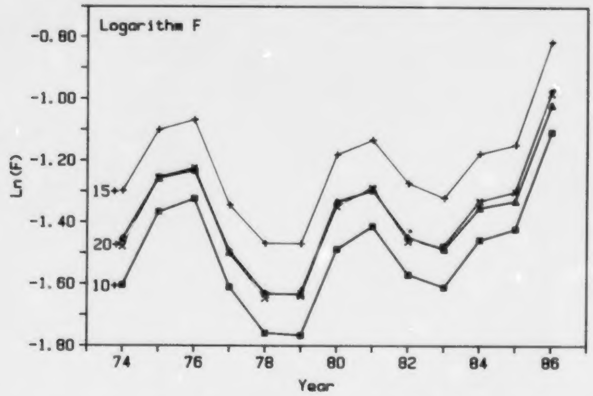

FIG. 5. Comparison of estimates of Ln (fishing mortality) from Monte Carlo simulations of catch-age and effort data. (■ — age 10, + — age 15, ◇ — age 20, △ — age 20 baseline, × — age 10 wih model (6))

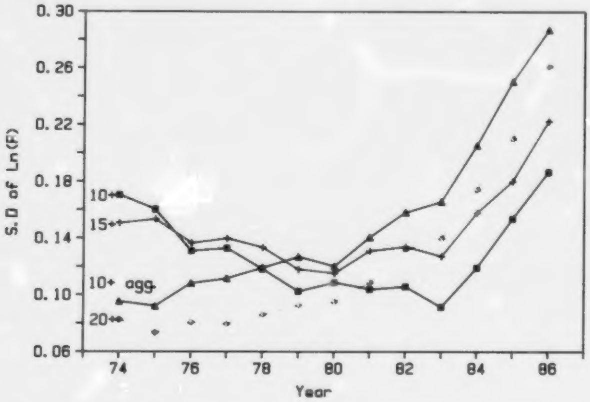

FIG. 6. Comparison of estimates of the standard deviation of Ln (fishing mortality) from Monte Carlo simulations of catch-age and effort data. (■ — age 10, + — age 15, ◇ — age 20, △ — age 10 with model (6)).

Estimates of abundance, biomass, and recruitment are shown in Table 2. Results from model (6) with age 10+ aggregation compare well with the baseline case and the aggregate 20+ model. The standard deviations from model (6) are generally larger than those in the aggregate 20+ model, except for 1974 exploitable biomass. The 1974 standard deviation results reflect the fact that abundance and age selectivity of age 11+ fish in 1974 were assumed to be known in the Monte Carlo experiments.

Results of our Monte Carlo study show that aggregation of catch-at-age data produces estimates comparable to those in our standard "8–20+" data. We suspect that the aggregated model performs so well because of the structure of the underlying "true" values used in our study. Those true values are based on Pacific halibut and reflect a rather modest amount of stochasticity in the relationship between fishing effort and fishing mortality rate; trends in $f(t)$ are well represented by trends in the fishing effort data. Therefore, catch-at-age data is not needed to establish trends in fishing mortality. Recruitment in the "true" data, as shown in Fig. 3, displays a smooth time trend and so it is not surprising that only a couple of age-specific catch values (ages 8,9) are needed to identify recruitment.

Acknowledgments

We are grateful to J. Cooke for his insightful remarks on our relative abundance method. We appreciate the reviews given by two anonymous reviewers. We thank R. Price for technical assistance with figures in the paper.

References

ALTON, M. S., AND R. B. DERISO. 1983. Pollock, p. 1–62. *In* D. H. Ito and J. Balsiger [ed.] Condition of groundfish resources of the Gulf of Alaska in 1982. NOAA Tech. Memo. NMFS F/NWC-52.

BEVERTON, R. J. H., AND S. J. HOLT. 1957. On the dynamics of exploited fish populations. U.K. Minist. Agric. Fish. Food, Fish. Invest. Ser. 2, 19: 533 p.

TABLE 2. Comparison of estimates from 100 Monte Carlo simulations of catch-age and effort data. Results are listed for the aggregate age 10+ model with correct selectivity (model 6) and the aggregate 20+ model. Biomass values are given in units of tonnes and abundance is given both in number and logarithm of number of fish.

	Parameter	True value	Estimate 10^+	Estimate 20^+
1974	Exploitable Biomass	21 358	21 381	21 435
	Standard Deviation		231	757
1986	Exploitable Biomass	51 513	52 055	51 364
	Standard Deviation		12 910	11 750
1986	Total abundance	5 778 920	5 879 809	5 817 735
	Standard Deviation		1 565 869	1 432 685
1974	Log (Recruitment)	13.363	13.353	13.348
	Standard Deviation		0.126	0.065
1984	Log (Recruitment)	14.367	14.334	14.346
	Standard Deviation		0.298	0.258

CHATTERJEE, S., AND B. PRICE. 1977. Regression analysis by example. John Wiley and Sons, Inc., New York N.Y. 228 p.

DERISO, R. B. 1980. Harvesting strategies and parameter estimation for an age-structured model. Can. J. Fish. Aquat. Sci. 37: 268–282.

DERISO, R. B., AND T. J. QUINN II. 1983. The Pacific halibut resource and fishery in regulatory area 2. II. Estimates of biomass, surplus production, and reproductive value. Int. Pac. Halibut Comm. Sci. Rep. No. 67: 55–89.

DERISO, R. B., T. J. QUINN II, AND P. R. NEAL. 1985. Catch-age analysis with auxiliary information. Can. J. Fish. Aquat. Sci. 42: 815–824.

FOURNIER, D., AND C. P. ARCHIBALD. 1982. A general theory for analyzing catch-at-age data. Can. J. Fish. Aquat. Sci. 39: 1195–1207.

HOAG, S. H., G. H. WILLIAMS, R. J. MYHRE, AND I. R. MCGREGOR. 1980. Halibut assessment data: Setline surveys in the North Pacific Ocean, 1963–1966 and 1976–1979. Int. Pac. Halibut Comm., Tech. Rep. 18: 42 p.

POPE, J. G., AND J. G. SHEPHERD, 1982. A simple method for the consistent interpretation of catch-at-age data. J. Cons. Cons. Int. Explor. Mer 40: 176–184.

QUINN, T. J. II, E. A. BEST, L. BIJSTERVELD, AND I. R. MCGREGOR. 1983. Sampling Pacific halibut (*Hippoglossus stenolepis*) landings for age composition: history, evaluation, and estimation. Int. Pac. Halibut Comm. Sci. Rep. 68: 56 p.

RAMI, M. 1984. A non-linear catch-at-age analysis of the central sub-population of the Atlantic Moroccan sardine (*Sardina pilchardus* Walbaum). M.S. thesis, Fisheries Department, University of Washington, Seattle, WA. 87 p.

Scale Patterns of Commercial Stocks of Asian Sockeye Salmon, *Oncorhynchus nerka*

Victor F. Bugaev

Pacific Research Institute of Fisheries and Oceanography (TINRO),
Kamchatka Branch, Petropavlovsk-Kamchatsky, USSR

Abstract

BUGAEV, V. F. 1989. Scale patterns of commercial stocks of Asian sockeye salmon (*Oncorhynchus nerka*), p. 137–150. *In* R. J. Beamish and G. A. McFarlane [ed.] Effects of ocean variability on recruitment and an evaluation of parameters used in stock assessment models. Can. Spec. Publ. Fish. Aquat. Sci. 108.

Highly specific growth conditions exist for juvenile Asian sockeye in each of the bodies of water studied. In addition there are year-to-year variations that complicate the identification of stocks. Because sockeye from the Ozernaya and Kamchatka rivers comprise 90–95% of the total Far Eastern sockeye catch, the problem of identification of Asian sockeye may be reduced by developing methods to distinguish these two stocks. Two zones of closely situated circuli in the scale centrum are characteristic of stocks of both the Ozernaya and Kamchatka rivers. Salmon with scales that have one closely spaced zone of circuli were considered to be from the Kamchatka River. Individuals with three or four closely spaced zones were identified as those of the Ozernaya River, as such individuals are more rare in the Kamchatka River basin. Estimates of age composition of Asian stocks have been included in this report.

Résumé

BUGAEV, V. F. 1989. Scale patterns of commercial stocks of Asian sockeye salmon (*Oncorhynchus nerka*), p. 137–150. *In* R. J. Beamish and G. A. McFarlane [ed.] Effects of ocean variability on recruitment and an evaluation of parameters used in stock assessment models. Can. Spec. Publ. Fish. Aquat. Sci. 108.

Les conditions de croissance des saumons rouges juvéniles étaient très spécifiques dans chacun des plans d'eau étudiés en Asie. En outre, ces conditions varient d'une année à l'autre, ce qui complique l'identification des stocks. Étant donné que les saumons rouges des rivières Ozernaya et Kamchatka représentent entre 90 et 95% des captures totales de cette espèce en Extrême-Orient, on pourrait faciliter l'identification des saumons rouges d'Asie en mettant au point des méthodes qui permettraient d'établir une distinction entre les stocks des deux cours d'eau. Deux zones d'anneaux de croissance fortement rapprochées au centre des écailles sont caractéristiques des stocks des rivières Ozernaya et Kamchatka. On a déterminé que les saumons dont les écailles comportaient une zone d'anneaux de croissance très rapprochées provenaient de la rivière Kamchatka et que ceux qui en avaient trois ou quatre appartenaient aux stocks de la rivière Ozernaya, étant donné que ces spécimens étaient plus rares dans le réseau de la rivière Kamchatka. L'auteur présente des estimations de la composition en fonction de l'âge des stocks d'Asie.

Introduction

Scale analysis based on the counts and spacing of circuli is used to identify stocks caught at sea as well as to indicate age (Krogius 1958; Anas and Murai 1969; Mosher 1972; Messinger and Bilton 1974; Krasnowski and Bethe 1978; Cook and Zord 1978; Cook 1982). A number of workers have used scale patterns for the identification of Asian stocks of sockeye (Krogius 1958; Mathisen 1966; Konovalov 1971; Mosher 1972). Krogius (1967) used the results of her studies to identify Ozernaya River sockeye in Japanese ocean catches, but there was probably significant bias in some years due to the lack of information on year-to-year variations in scale pattern. More reliable results are obtained when both scales and parasites are used for identification. The complex scale-parasite technique proposed by Konovalov (1971) has not been widely used in the USSR, because the Japanese only submit scale samples from ocean catches.

The identification of Asian sockeye is difficult because the scales of sockeye exhibit year-to-year variations in growth, as well as variations from one site to another. Sockeye from the Ozernaya and Kamchatka rivers formerly comprised up to 90% of the total catch in Asia (Krogius and Krokhin 1956), and recently about 95%. Thus as concluded by Selifonov (1975), the problem of identification of sockeye salmon is primarily the recognition of these two stocks.

Investigation of the scale structure of the smaller Asian sockeye stocks is of interest as scale pattern is often related to environmental conditions, and is useful for local management such as: identification in inshore areas, growth pattern and age composition studies for the purpose of developing techniques of abundance forecasts, recommendations for lake fertilization and the recognition of these salmon in Japanese catches. The present report is the first to treat the data on scale patterns of most of the Asian stocks of sockeye with a uniform procedure, and it deals with the year-to-year variability in the scales of the two largest stocks, those of the Ozernaya River and the Kamchatka River.

Materials and Methods

Data on scale patterns of 26 stocks of Asian sockeye (Fig. 1) sampled in commercial catches were used in the study, as were data on file at the Kamchatka Branch of TINRO, at the Institute of Biology of Sea of the Far Eastern Scientific Centre of the USSR Academy of Sciences, and in the personal collections of the author. In most cases scales were sampled from the dorsal fin area using Pravdin's technique (Pravdin 1966). All scale samples of the stocks of the Ozernaya River and in some years of Lake Azabachye (Kamchatka River) were taken between the dorsal and adipose fins using the technique of Clutter and Whitesel (1956). In an earlier paper we investigated the effect of sampling position on scale characteristics (Bugaev 1983a). If scales are taken using both sampling techniques, circuli must be counted in the first growth zone. The regression is:

$$Y = 0.956X - 0.406$$

where X is the number of circuli in the first growth zone (1st year) according to Clutter and Whitesel, and Y is the number of circuli in the first growth zone (1st year) according to Pravdin's technique.

The distance between lacustrine circuli and marine circuli is, on the average, larger by 11% if the scales are taken using the technique of Clutter and Whitesel (1956) as compared with the technique of Pravdin (1966) when the scales are taken below the dorsal fin above the lateral line.

Scales from 8800 individual fish were examined under 100× magnification. Numbers of broad and narrow circuli were counted in growth zones of the central (fresh or brackfish water) part of the scale (the centrum), and the zone of the first marine growth. In addition, the lengths of these zones were measured.

Until now, no extensive comparison of the scale patterns of Ozernaya and Kamchatka sockeye had been made. Unbiased comparisons of the scales of the Ozernaya and Kamchatka river stocks became possible as a result of a recent project carried out in the basin of the Kamchatka River (Bugaev 1983b, 1986). The following stocks and group of stocks could be identified by

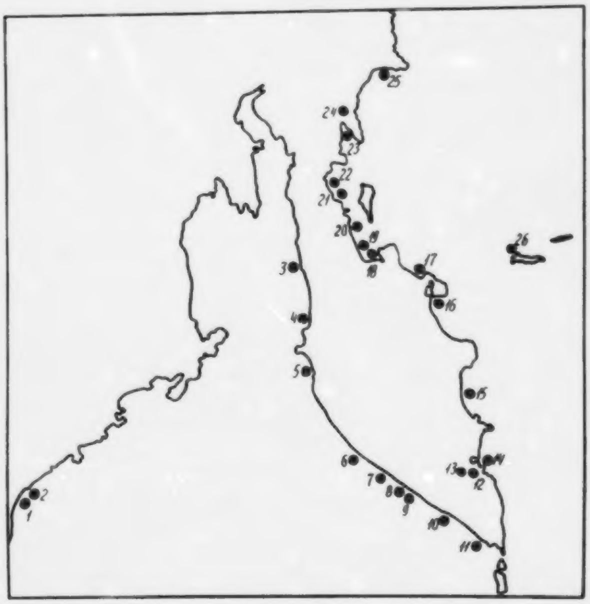

FIG. 1. Areas of scale sampling: 1 — Okhota River, 2 — Kukhtui River, 3 — Palana River, 4 — Tigil River, 5 — Khairyuzova River, 6 — Krutugorova River, 7 — Vorovskaya River, 8 — Kikhchik River, 9 — Utka River, 10 — Bolshaya River, 11 — Ozernaya River, 12 — Lake Dalneye, 13 — Lake Blizhneye, 14 — Lake Listvennichnoye, 15 — Tikhaya River, 16 — Kamchatka River, 17 — Stolbovaya River, 18 — Malamvayam River, 19 — Khailula River, 20 — Ivashka River, 21 — Tymlat River, 22 — Kichiga River, 23 — Avyavayam River, 24 — Kultushnaya River, 25 — Apuka River, 26 — Lake Sarannoye.

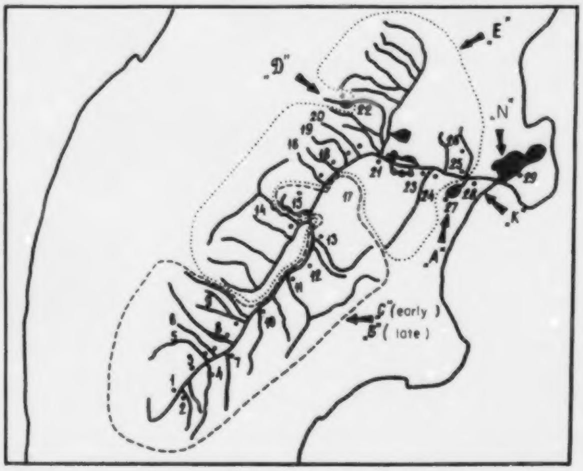

FIG. 2. Local stocks and groups of stocks of sockeye identified in the basin of the Kamchatka River.
1 — Kamchatka River near Pushchino village, 2 — Kashkan River, 3 — Kamchatka River near Sharoma village, 4 — Kavycha River, 5 — Andrianovka River, 6 — Zhupanka River, 7 — Vakhvina (Valagin) River, 8 — Kirganik River, 9 — Kimitina River, 10 — Kitilgina River, 11 — Shchapina River, 12 — stream fed by underground springs (rheocrene) "Nikolka", 13 — Tolbachik River, 14 — Bystraya-Kozyrevka, 15 — Shehlun, 16 — Kreruk River, 17 — Lake fed by underground springs (limnocrene) "Lake Ushkovskoye", 18 — Kryuki River, 19 — Polovinnaya River, 20 — Belaya River, 21 — Yelovka River, 22 — Lake Dvukhyurtochnoye, 23 — Bolshayan Khapitsa River, 24 — Khapitsa River, 25 — Raduga River, 26 — Lake Nizovtsevo, 17 — Lake Azabachye, 28 — Lake Kursin, 29 — Soldatskaya River (basin of Lake Nerpichye).

using scale structure and infestation levels of the parasite *Diphyllobothrium* sp. (Fig. 2): a group of local stocks of early-running sockeye in the tributaries of the upper and middle Kamchatka River which go to sea in the year of hatching (group C) (the sockeye of Lake Ushkovskoye are exceptional in being late-running); a group of local stocks of late-running sockeye of the middle and upper Kamchatka River which spend their first year on the spawning grounds and go to sea in the next year (group B) (on the whole, their spawning area coincides with that of group C); a group of local stocks of the tributaries of the lower and, in part, the middle Kamchatka River, which migrate into Lake Azabachye in the year of hatching and go to sea in the next year (group E); a local stock of Lake Azabachye which feeds together with group E as juveniles and usually spends two years in the lake (group A); the local stock of Lake Dvukhyurtochnoye, which mainly spends two years in the lake as juveniles (group D); the local stock of brackish Lake Nerpichye, and a group of local stocks of tributaries of the lower Kamchatka River which migrate as young to feed in Lake Nerpichye (no identification of the constituent stocks is possible in catches), with the juveniles spending one winter in the lake (group N); the local stock of Lake Kursin, which as a rule spends one year in the lake (group K). The E group is the most numerous, the next largest being C and then A. During 1957–83 the representation by spawners of group C varied from 5.3 to 57.7% (25.9% on the average); of E, 9.3–65.0% (40.6%); of B, 1.7–32.5% (9.1%); of N, 1.1–7.5% (4.8%); of A, 3.7–43.1% (16.2%); of D, 0.5–14.6% (3.5%); and of K, less than 0.1–0.6% (0.1%) (Bugaev and Ostroumov 1986).

Our study included ageing the spawners of the stocks in question. Duration of the freshwater period was estimated from a sample of fish of unknown age (Mina 1976; Bugaev 1983a). The number of circuli in the second growth zone was taken as the basis for estimating the length of the freshwater period in sockeye spawners having two zones of closely-spaced circuli (ZCC) in the scale centrum. I then determined which ZCC was an accessory one and which was an annulus using the relationship between the number of circuli in the first and second growth zones, the proposed length of the annuli formation period, the growth rate of circuli, and the pattern of ZCC. The scale pattern of spawning salmon indicated that some fry migrate in the river basins between lakes of different types where they feed and rear before going to sea in the next year. The scale patterns with both distinct and indistinct ZCCs indicate that there are accessory rings in the scale. A similar method of ageing was also used for individuals with more than two ZCC in the scale centrum. In this case I selected the ZCC growth zone (excepting the first one) that contained the largest number of circuli.

ZCC may be formed annually ("annuli") or at other times ("accessory"). The presence or absence and number of circuli in these ZCC often differs among stocks (Bugaev 1978). For example, in the Kamchatka River, a "river-type" ZCC can be distinguished from a typical "lake-type" ZCC since the former comprises fewer circuli (0–2 compared with 3–8). Following Bugaev (1978), indistinct ZCC were recorded as having "zero circuli".

As was found previously (Bugaev 1981), the onset of seasonal growth in sockeye of the Kamchatka River varies from early February (in bodies of water fed by springs) to early July (in lakes). It is related to the type of water body, its site, and to weather conditions. In cold spring-fed bodies of water a circulus is formed on the average of 20.7 days, while in warmer lakes and bayous (former river channels) it is only 12.3 days (Bugaev 1981). Recently, Bugaev (1984) reported that juveniles with two ZCC feeding in Lake Azabachye may form circuli every 6.3 days in the marginal zone of the scale during the final freshwater year. This results in broader intercircular distances, which are visible to the naked eye. In cases where the juvenile growth data at our disposal were limited to a small amount of material on the Khailula River and Kuril Lake, ageing was done on the basis of whether the stock was predominantly of the "lake" or "river" type. Lake stocks were considered to be those from rivers having lakes in their basins large enough to provide adequate food for the juveniles up to the time of their downstream migration (Lakes Palanskoye, Kuril, Listvennichnoye, Ilir-Gytkhyn, Dalneye, Azabachye and Sarannoye), while all the rest were classified as river stocks.

Ages of sockeye of the Kamchatka River in our study are based on catches of ocean trap nets, that were separated into early catches (up to June 30) and late catches (July 1 and later). Individuals were first identified as belonging to one of the stocks or group of stocks of the Kamchatka River, using the method developed earlier (Bugaev 1986); and were then aged, taking into account these identifications.

Results and Discussion

Geographical Variability of Scale Patterns

Table 1 shows the number of zones of closely-spaced circuli (ZCC) in the central part of the scale from the different stocks (Fig. 1). It should be borne in mind that the number of ZCC in the center does not necessarily correspond to a freshwater (brackish water) period of life, because it is a characteristic of most Asian sockeye stocks that an accessory ZCC is formed during this period. Analysis of Table 1 shows that individuals with two central ZCC predominate in rivers of the Okhotsk coast, and those with one or three ZCC are rare. Individuals with one or two ZCC are found in approximately equal numbers in rivers of West Kamchatka, except for Ozernaya River. Individuals with two ZCC comprise about 55.1% of the Ozernaya stock, and those with three ZCC, 39.3%. A trend toward a larger number of ZCC is observed in rivers of East Kamchatka (except the Kamchatka River), although individuals with one or two ZCC predominate. Individuals of the Kamchatka River with one ZCC definitely predominate on the spawning grounds of group C (Fig. 2), while individuals with two ZCC predominate on those of group E, and also groups A and D. Individuals with one or two ZCC are most common in group B where they occur in about equal numbers. Sockeye of Bering Island mostly have three or four ZCC. A. S. Agapov (pers. comm.) reports that individuals with one ZCC predominate in the stock of the Seutakan River (East Chukotka).

TABLE 1. Number of ZCCs in the scale centra of Asian sockeye spawners.

River or lake	Year	Number of ZCC					Sample size
		None	One	Two	Three	Four	
Continental Okhotsk							
Okhota River	1983		8.2	66.3	24.5	1.0	98
Kukhtui River	1983		14.4	68.1	17.5		97
West Kamchatka							
Palana River	1983			100.0			100
Tigil River	1981	2.8	41.7	47.2	8.3		36
Khairyuzova River	1984	2.1	51.5	42.3	4.1		97
Krutogorova River	1971	1.1	39.1	45.7	11.9	2.2	92
Vorovskaya River	1965		39.3	49.5	11.2		89
Kikhchik River	1931	4.6	56.3	34.5	4.6		87
Utka River	1965	7.6	49.4	38.0	3.8	1.2	79
Bolshaya River	1957–71	1.3	48.9	38.2	10.6	1.0	479
West Kamchatka Rivers (without Ozernaya River)	1931–84	1.9	42.3	46.0	8.1	0.8	1059
Ozernaya River	1965–84		0.7	55.1	39.3	4.9	883
East Kamchatka							
Paratunka River:							
Lake Dalneye	1943		2.2	72.8	21.7	3.3	92
" "	1962		1.0	35.9	42.7	18.4[a]	103
Lake Blizhneye	1949			33.0	56.4	10.6	94
Lake Listvennichnoye	1980			30.4	58.7	10.9	46
Tikhaya River	1981	4.9	48.8	46.3			41
Stolbovaya River	1984		34.7	49.0	15.3	1.0	98
Malamvayam River	1983		8.5	74.4	17.1		82
Khailula River	1977–83	2.2	31.9	56.3	8.9	0.7	542
Ivashka River	1966	4.7	64.7	27.1	3.5		85
Tymlat River	1973		54.2	38.6	7.2		83
Kichiga River	1981	1.0	31.4	55.9	11.7		102
Avyavayam River (Korf cannery)	1962		50.0	42.9	7.1		56
Avyavayam River	1985		73.2	25.8	1.0		97
Kultushnaya River (Lake Ilir-Gytkhyn)	1983		5.9	92.1	2.0		51
Apuka River	1985	1.0	58.8	39.2	1.0		102
East Kamchatka rivers (without Kamchatka River)	1943–86	1.2	31.7	49.6	14.9	2.4[b]	1674
Kamchatka River							
Group C	1963–78	5.6	75.2	17.6	1.5	0.1	1866
B	1958–78		41.1	44.5	13.3	1.1	263
E	1976–79	0.4	15.1	72.5	11.5	0.5	1406
A	1963–78		14.8	71.2	13.4	0.6	1257
D	1975–78		7.2	92.2	0.6		166
Bering Island							
Lake Sarannoye	1985			9.1	50.0	31.8[c]	22
East Chukotka							
Seutaken River[d]	1985	1.9	69.2	25.0	3.9		104

[a] 1.0% 5 ZCC, 1.0% 6 ZCC.

[b] 0.1% 5 ZCC, 0.1% 6 ZCC.

[c] 9.1% 5 ZCC.

[d] Data kindly submitted by A.S. Agapov.

Comparison of the numbers of ZCC (Table 1), and numbers of circuli (Tables 2–4), failed to reveal any trends in the pattern of variation in the structure of the centrum by longitude or latitude, or between the stocks of East and West Kamchatka. In addition, local stocks of the Kamchatka River vary in respect to the number of circuli in the growth zones (Tables 2–4). Individuals of groups E and A that have one ZCC have a greater number of circuli than groups C and B. Group B, which is a late run group, is characterized by a greater number of circuli in the margin of the scale. Among individuals with two ZCC in the centrum (Table 3), there are more circuli in the first and second zones in groups E and A. For individuals with three ZCC in the scale center, group A spawners have more circuli in the first, second and third zones than do those of group E (Table 4). However, the group E spawners have more marginal circuli than do those of group A.

On the whole, among the Kamchatka River sockeye that migrate to sea in the year they hatch (except for group C), there is a relation between the number of circuli in the marginal zone and the previous increment

TABLE 2. Number of circuli in growth zones in the scale centra of Asian sockeye spawners having one ZCC.

Water body (River)	Year	First growth zone		Marginal growth zone		Sample size
		Range	$\overline{X}$	Range	$\overline{X}$	
Continental Okhotsk						
Okhota River	1983	9–14	11.13 ± 0.61	1–5	3.13 ± 0.48	8
Kukhtui River	1983	7–14	10.86 ± 0.56	1–8	3.79 ± 0.49	14
West Kamchatka						
Tigil River	1981	5–8	6.53 ± 0.27	2–8	4.40 ± 0.39	15
Khairyuzova River	1984	4–11	7.30 ± 0.22	1–8	4.50 ± 0.20	50
Krutogorova River	1971	4–13	8.08 ± 0.31	0–7	3.03 ± 0.26	36
Vorovskaya River	1965	2–12	6.46 ± 0.35	1–7	3.66 ± 0.28	35
Kikhchik River	1931	3–11	6.33 ± 0.26	0–7	3.33 ± 0.24	49
Utka River	1965	2–12	7.41 ± 0.32	0–8	3.97 ± 0.22	39
Bolshaya River	1957–71	2–12	6.24 ± 0.12	0–8	3.50 ± 0.11	234
East Kamchatka						
Tikhaya River	1981	4–14	10.20 ± 0.86	0–13	4.90 ± 0.69	20
Kamchatka River						
Group C	1976–78	2–14	6.11 ± 0.06	0–10	2.61 ± 0.04	884
B	1958–78	2–11	5.95 ± 0.18	2–11	5.44 ± 0.16	108
E	1976–78	2–14	7.67 ± 0.17	0–11	4.46 ± 0.15	152
A	1976–78	4–14	8.74 ± 0.19	0–11	3.98 ± 0.18	70
Stolbovaya River	1984	3–15	6.82 ± 0.44	0–9	4.32 ± 0.37	34
Malamvayam River	1983	3–8	6.71 ± 0.75	2–5	3.71 ± 0.42	7
Khailula River	1977–83	2–13	7.07 ± 0.16	0–10	3.32 ± 0.14	173
Ivashka River	1966	3–9	5.45 ± 0.25	0–9	3.85 ± 0.22	55
Tymlat River	1973	3–13	6.13 ± 0.27	0–8	3.44 ± 0.26	45
Kichiga River	1981	3–13	7.66 ± 0.42	0–6	2.28 ± 0.26	32
Avyavayam River (Korf cannery)	1962	5–11	7.36 ± 0.29	0–6	3.00 ± 0.31	28
Avyavayam River	1985	3–12	7.59 ± 0.21	0–8	2.42 ± 0.23	71
Apuka River	1985	5–14	9.33 ± 0.31	0–6	2.27 ± 0.23	60
East Chukotka						
Seutakan River[a]	1985	4–13	8.36 ± 0.28	0–14	5.25 ± 0.43	72

[a] Data kindly submitted by A. S. Agapov.

($r = 0.947$, $p < 0.01$, $n = 9$), as is seen in Tables 2–4. The more circuli there are in growth zones before the year of going to sea, the more are found in the marginal zone ($Y = -0.249X + 6.15$, where X is the number of circuli previous to the downstream migration and Y is the number of circuli in the year of downstream migration). That is, on the basis of the very good relationship between body size and number of circuli in juvenile sockeye (Clutter and Whitesel 1956), it appears that larger smolts in the Kamchatka River basin go to sea earlier than smaller ones. Variations in the number of circuli in early-running spawning sockeye of the tributaries of the Kamchatka River, support the preceding conclusions (Tables 2 and 3) and illustrate certain peculiarities of the variation in the number of circuli (Fig. 3 and 4). Because of the scarcity of late-running sockeye in tributaries in the region of spawning area E, I have not provided illustrative material on the individual spawning streams of group B, as no complete comparative procedure has been done for the whole river basin.

Scales with one ZCC in the centrum had a significant increase in the number of circuli in the first growth zone (Fig. 3). Those sockeye from the lower (downriver) Kamchatka tributaries also had an increase in the circuli in the marginal zone although the pattern was less clear. Among sockeye with two ZCC in the centrum (Fig. 4), a greater number of circuli in the first and second growth zones (and fewer in the marginal zone) was characteristic of Lake Dvuchyurtochnoye. In general, the average number of circuli in the two growth zones was somewhat greater in lower tributaries (which was best seen in the second zone) and, the number of circuli in the marginal zone was not related to the distance from the river's mouth (Fig. 4). Detailed studies were not carried out on fish with three central ZCC because only a few were found.

As is seen from Table 5, the distinctness of the ZCC varies significantly among stocks and groups of stocks of Asian sockeye. Among sockeye with one ZCC in the center, the clearest "lake" ZCC are in the stocks of the continental Okhotsk coast, the Kamchatka River groups A and D, and the Seutakan River stock of East Kamchatka; while the vaguest "river" ZCC occur in sockeye of Kamchatka River groups C, B, and E (particularly C). The first and second ZCCs are clear only in the A and D groups of the Kamchatka basin. In the Okhotsk Sea stocks and in some stocks of the Kamchatka River (group E), the second ZCC is on the average, more distinct than the first one. Among the sockeye with three ZCC in the scale center, the first and the third ZCCs are particularly

TABLE 3. Number of circuli in growth zones of the scale centra of Asian sockeye spawners having two ZCC.

River or lake	Year	First growth zone		Second growth zone		Marginal growth		Sample size
		Range	$\overline{X}$	Range	$\overline{X}$	Range	$\overline{X}$	
Continental Okhotsk								
Okhota River	1983	2–11	6.52 ± 0.26	3–13	7.11 ± 0.29	0–8	2.85 ± 0.17	65
Kukhtui River	1983	3–13	6.81 ± 0.26	4–12	7.38 ± 0.23	0–5	2.48 ± 0.17	66
West Kamchatka								
Palana River	1983	2–8	4.59 ± 0.11	5–10	6.94 ± 0.13	0–4	0.91 ± 0.08	100
Tigil River	1981	3–7	5.00 ± 0.28	3–8	5.12 ± 0.33	0–6	2.35 ± 0.40	17
Khairyuzova River	1984	3–9	5.68 ± 0.25	2–11	4.37 ± 0.31	0–6	3.29 ± 0.28	41
Krutogorova River	1971	2–9	5.12 ± 0.28	3–13	5.71 ± 0.38	0–6	2.26 ± 0.26	42
Vorovskaya River	1965	2–11	5.32 ± 0.31	2–11	5.68 ± 0.34	0–6	2.30 ± 0.23	44
Kikhchik River	1931	3–9	5.47 ± 0.28	3–16	5.73 ± 0.62	0–6	2.53 ± 0.32	30
Utka River	1965	2–9	4.90 ± 0.36	2–9	5.07 ± 0.26	0–6	2.57 ± 0.29	30
Bolshaya River	1957–71	1–9	4.84 ± 0.12	2–13	5.36 ± 0.18	0–9	2.10 ± 0.12	183
Ozernaya River								
(5_2+)	1965–84	3–11	6.84 ± 0.09	4–16	10.73 ± 0.12	0–9	2.69 ± 0.08	210
(4_2+)	" "	3–11	6.30 ± 0.12	4–14	11.35 ± 0.15	0–6	2.93 ± 0.09	143
East Kamchatka								
Paratunka River:								
Lake Dalneye	1943	3–17	8.51 ± 0.31	4–18	9.55 ± 0.37	0–6	2.15 ± 0.17	67
" "	1962	4–17	9.76 ± 0.59	6–21	13.03 ± 0.75	0–7	2.46 ± 0.32	37
Lake Blizhneye	1949	2–18	4.16 ± 0.26	3–11	6.65 ± 0.32	1–7	4.13 ± 0.26	31
L. Listvennichnoye	1980	5–9	6.93 ± 0.36	6–11	8.71 ± 0.40	0–4	1.07 ± 0.36	14
Tikhaya River	1981	3–11	8.16 ± 0.57	3–15	6.74 ± 0.73	0–11	2.63 ± 0.65	19
Kamchatka River:								
Group C	1976–78	2–11	5.01 ± 0.09	2–13	5.66 ± 0.12	0–10	2.40 ± 0.08	321
B	1958–78	2–8	4.98 ± 0.11	2–10	5.20 ± 0.14	0–8	3.40 ± 0.14	116
E	1976–78	2–14	6.07 ± 0.06	2–14	7.62 ± 0.07	0–10	2.24 ± 0.04	862
A	1976–78	2–12	6.95 ± 0.13	3–15	9.42 ± 0.15	0–11	1.23 ± 0.12	187
D	1975–78	8–15	11.41 ± 0.16	9–16	12.26 ± 0.14	0–3	0.55 ± 0.09	106
Stolbovaya River	1984	2–11	6.19 ± 0.34	3–13	6.75 ± 0.37	0–9	2.92 ± 0.35	48
Malamvayam River	1983	3–9	5.69 ± 0.20	2–12	7.00 ± 0.31	0–6	2.39 ± 0.20	61
Hailula River	1977–83	2–13	5.42 ± 0.10	2–16	4.91 ± 0.13	0–8	2.68 ± 0.09	305
Ivashka River	1966	3–7	5.09 ± 0.33	2–11	5.52 ± 0.52	0–7	2.00 ± 0.37	23
Tymlat River	1973	2–8	4.50 ± 0.29	2–8	4.97 ± 0.35	0–6	2.44 ± 0.35	32
Kichiga River	1981	2–9	4.84 ± 0.19	2–12	5.37 ± 0.24	0–6	2.63 ± 0.19	57
Avyavayam River								
Korf cannery	1962	2–10	5.08 ± 0.28	2–12	6.33 ± 0.29	0–6	2.17 ± 0.30	24
Avyavayam River	1985	2–8	4.44 ± 0.32	3–8	5.88 ± 0.29	0–4	1.44 ± 0.22	25
Kultushnaya River								
Lake Ilir-Gytkhyn	1983	4–11	6.32 ± 0.21	5–11	8.42 ± 0.21	0–3	0.64 ± 0.11	47
Apuka River	1985	2–10	5.75 ± 0.34	2–11	5.80 ± 0.31	0–5	1.20 ± 0.20	40
East Chukotka								
Seutakan River[a]	1985	2–8	4.88 ± 0.41	4–14	8.42 ± 0.53	0–11	3.31 ± 0.59	26

[a] Data kindly submitted by A. S. Agapov.

clear in group A, the second ZCC is clear in the Okhotsk stocks and the Bering Island stock, while the first ZCC is vague in the Bering stock and the group E stocks of the Kamchatka River.

Comparison of the numbers of circuli in the first sea year suggests that they are similar in all stocks except those of the Kamchatka River, Bering Island and the Seutakan River, which are somewhat less (Table 6). There is great similarity among all the sockeye stocks on the Kamchatka peninsula (except that of the Ozernaya River) in the mean width of the zone of six initial sea circuli (Fig. 5) and the mean distance between circuli in the first sea year (Fig. 6). Part of the dissimilarity of Ozernaya sockeye may be attributed to the sampling technique, as sampling was done according to Clutter and Whitesel (1956). The mean width of the zone of six initial sea circuli in Okhotsk coast sockeye is 26.70 ± 0.25 mm ($n = 195$), in Bering Island sockeye 30.45 ± 0.82 mm ($n = 22$), and in Seutakan River sockeye 27.06 ± 0.42 mm ($n = 104$). These values are on the whole larger than those of Kamchatka sockeye (except the Ozernaya), though the scales were sampled using Pravdin's (1966) technique (except for the Seutakan stock). The mean distance between circuli in the first sea year in Okhotsk coast sockeye is 4.54 ± 0.04 mm ($n = 195$), in Bering Island sockeye 4.58 ± 0.10 mm ($n = 22$), and in Seutakan sockeye 4.49 ± 0.04 ($n = 104$) which is somewhat less than in Kamchatka sockeye.

TABLE 4. Number of circuli in the growth zones of the scale centra of Asian sockeye spawners having three ZCC.

River or lake	Year	First zone		Second zone		Third zone		Marginal zone		Sample size
		Range	$\overline{X}$	Range	$\overline{X}$	Range	$\overline{X}$	Range	$\overline{X}$	
Continental Okhotsk										
Kukhtui River	1983	3–9	5.53 ± 0.51	4–10	5.82 ± 0.44	2–14	5.41 ± 0.69	0–7	2.82 ± 0.46	17
Okhota River	1983	3–11	5.50 ± 0.46	3–9	5.88 ± 0.35	3–9	4.92 ± 0.28	0–7	2.04 ± 0.33	24
West Kamchatka										
West Kamchatka rivers (without Ozernaya River)		2–9	4.01 ± 0.15	2–8	4.42 ± 0.18	2–11	4.99 ± 0.21	0–6	1.62 ± 0.16	86
Ozernaya River	1965–84	2–9	4.78 ± 0.08	2–13	6.78 ± 0.09	2–14	6.99 ± 0.10	0–7	1.76 ± 0.08	347
East Kamchatka										
Paratunka River:										
Lake Dalneye	1943	3–13	6.05 ± 0.55	5–15	9.05 ± 0.63	5–15	9.85 ± 0.82	0–4	1.25 ± 0.26	20
" "	1962	4–16	8.59 ± 0.53	4–14	8.91 ± 0.34	5–19	11.56 ± 0.59	0–7	1.68 ± 0.18	44
Lake Blizhneye	1949	2–6	3.36 ± 0.15	3–9	5.36 ± 0.18	2–9	5.77 ± 0.26	0–5	2.96 ± 0.16	53
L. Listvennichnoye	1980	4–11	6.26 ± 0.29	3–11	6.48 ± 0.33	4–10	6.63 ± 0.32	0–5	1.15 ± 0.27	27
Kamchatka River:										
Group E	1976–78	2–10	5.55 ± 0.19	2–11	5.18 ± 0.20	2–12	5.78 ± 0.24	0–9	2.62 ± 0.24	82
A	1972–76	2–11	6.36 ± 0.17	2–9	5.69 ± 0.14	2–12	6.35 ± 0.18	0–7	1.70 ± 0.13	117
Other rivers of East Kamchatka		2–10	4.56 ± 0.17	2–8	4.26 ± 0.15	2–9	4.41 ± 0.17	0–6	1.73 ± 0.17	102
Bering Island										
Lake Sarannoye	1985	3–11	5.64 ± 0.86	3–14	7.09 ± 1.01	4–12	8.54 ± 0.80	1–6	2.82 ± 0.48	11

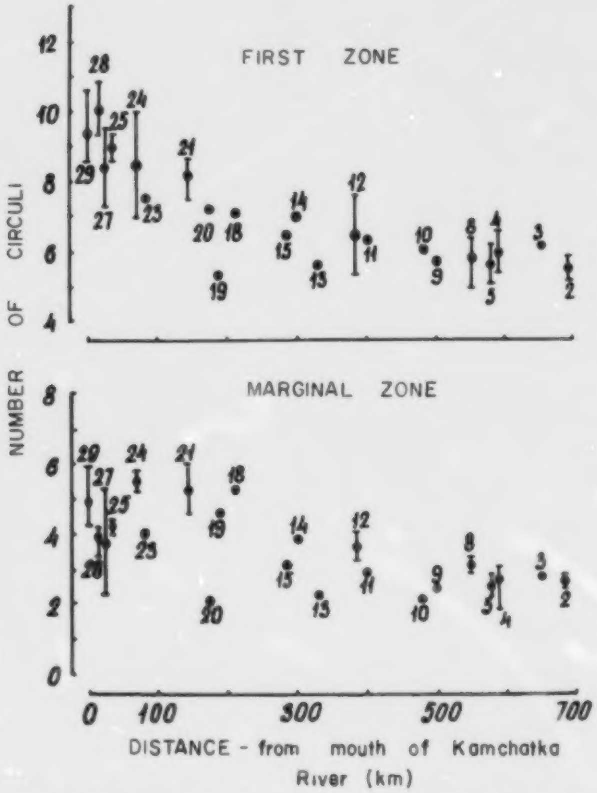

FIG. 3. Mean number of circuli in spawners of early-running sockeye having one zone of closely-spaced circuli (ZCC) in the centrum (freshwater part) of their scales, in river and lake stocks of the Kamchatka River basin (1976–78). Mean values are shown as dots; the lines indicate the range of variation of the means of different years; numbers refer to the stocks shown in Fig. 2.

Year-To-Year Variability of Scale Patterns of Sockeye of the Ozernaya and Kamchatka Rivers

Individuals with two ZCC in the centrum (Table 1) are the most common type in the Ozernaya and Kamchatka rivers. At present an adequate series of data is available only for the Lake Azabachye stock, which includes about 16% of all spawners in the Kamchatka River basin (Bugaev and Ostroumov 1986). Our studies have shown that about 70–80% of Azabachye spawners are of age 5_2+. Figure 7 shows variations in the mean number of circuli in growth zones of Ozernaya sockeye of age 5_2, and of the early Azabachye sockeye (mainly age 5_2+) in the same years of spawning. The early Azabachye race comprises about 80% of the total stock (Ostroumov 1972), and year-to-year variations in the scale patterns of the early and late sockeye are similar (Bugaev 1983a). The mean number of circuli in the growth zones of sockeye of both stocks vary, but may be similar in certain years (Fig. 7). Analysis of variations of mean number of circuli in the centrum in Ozernaya sockeye of 1964–86 indicates that the mean number of circuli in growth zones of age 4_2+ and 5_2+ of the same year-class is usually similar, although in certain years there are significant differences whose causes are unknown. As an example, Fig. 8 shows the similarity of the total number of circuli during the first two growth years in Ozernaya sockeye of ages 4_2+ and 5_2+.

I noticed that as the number of circuli in the two initial growth zones increased, those in the marginal zone decreased in Azabachye sockeye (the larger juveniles go to sea earlier). The correlation coefficient is $r = 0.446$ ($n = 22$, $P < 0.05$); the regression is:

$$Y = -0.164X + 4.35$$

where X is the total number of circuli in the two initial

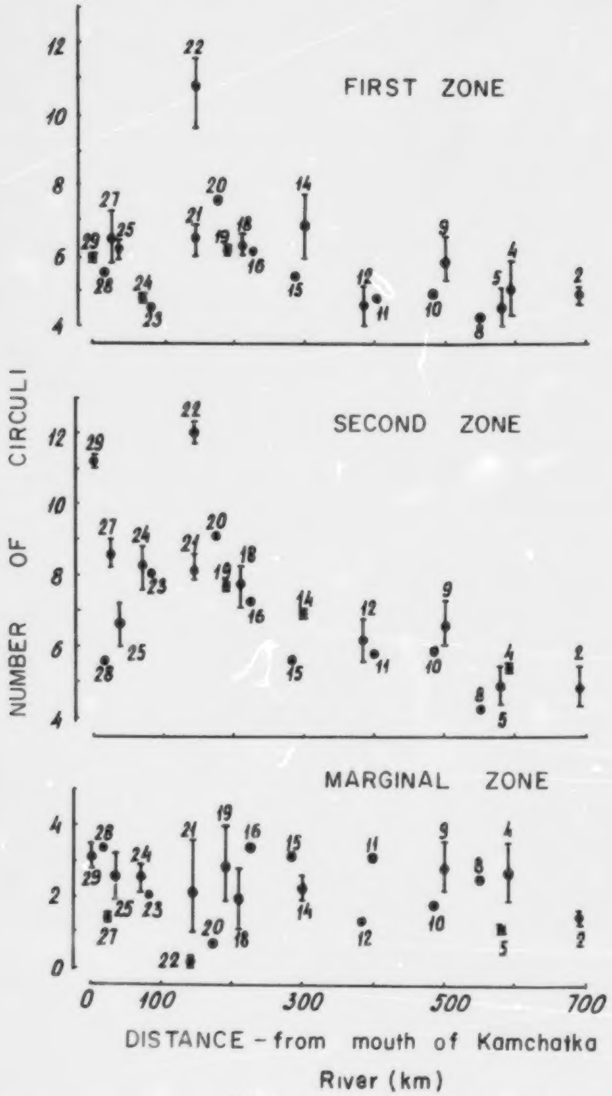

FIG. 4. Mean number of circuli in spawners of early-running sockeye with two ZCC in the scale centrum, in river and lake stocks of the Kamchatka River basin (1976–78). Symbols as in Fig. 3.

growth zones, and *Y* is the number of circuli in the marginal zone of the scale center. No such relationship was found for Ozernaya sockeye: for age 5_2+, $r=0.025$ ($n=22$, $P>0.05$); for age 4_2+, $r=0.002$ ($n=22$, $P>0.05$).

A relationship between the growth rate of juvenile sockeye and environmental conditions is well known (Krogius 1961; Ward and Larkin 1964; Johnson 1965; Burgner et al. 1969; Goodlad et al. 1974; Rogers 1980; Rogers et al. 1982; Bugaev 1983a; Dubynin 1986). Dubynin showed that body size of Ozernaya seaward migrants (age 2+ and 3+) decreased as abundance of their parents increased. Our study (in cooperation with V. A. Dubynin) of the variability of the patterns in the scale centrum of Kurilskoye sockeye showed a very close relationship between the number of circuli in sockeye of age 4_2+ and 5_2+ during the first 2 years of life and the abundance of *Cyclops scutifer* Sars in the lake in August–October ($r=0.549$–0.881, $0.01<P<0.05$). This suggests that juvenile growth occurs mainly during this period. Figure 9 shows a high correlation between the number of circuli in the scale centrum of Ozernaya spawners and the abundance of *Cyclops*. The relationship between circuli number and water temperature is much less marked. Unfortunately, no similar analysis can be done for Lake Azabachye as there is little information on plankton abundance.

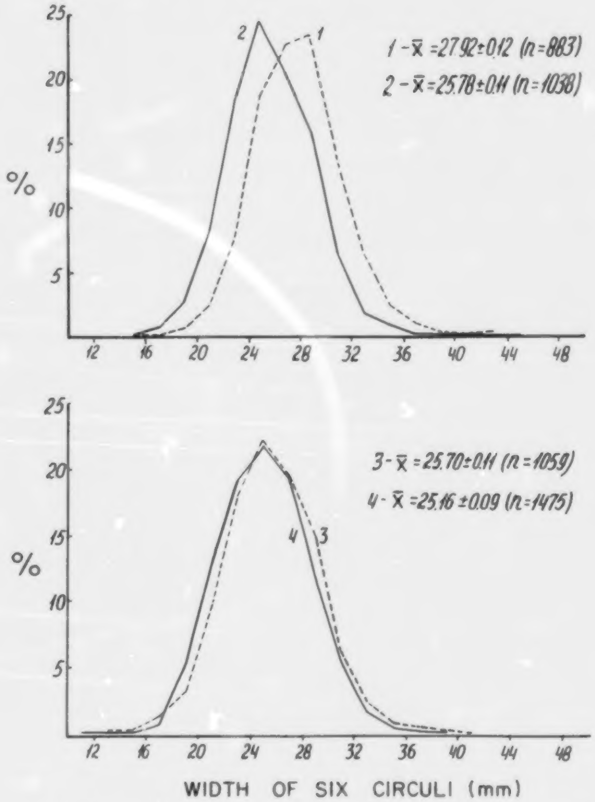

FIG. 5. Width of the first 6 ocean sclerites among Kamchatka sockeye: 1 — Ozernaya River; 2 — Kamchatka River; 3 — rivers of western Kamchatka; 4 — rivers of eastern Kamchatka.

It was shown previously, using data of 1963–79 (Bugaev 1983a) that with an increase in abundance of spawners in Lake Azabachye (group A), in the tributaries of the lower Kamchatka River (groups A and E) and in the basin of Kamchatka River as a whole, there is a decrease in the number of circuli in the first and second growth zones (mainly the first and second years of growth). It is known that juveniles from tributaries of the lower Kamchatka River feed with juveniles of the Lake Azabachye stock (Bugaev 1983a, 1986). While we have not yet analyzed the variations in the pattern of the scale centrum for group E, there are indications that variations in the growth rate of the scales of spawners in the Azabachye basin and the lower tributaries of the Kam-

TABLE 5. Percent occurrence of "lake" ZCCs in the scale centra of Asian sockeye spawners.

River or lake	One ZCC		Two ZCC			Three ZCC			
	First %	Sample size	First %	Second %	Sample size	First %	Second %	Third %	Sample size
Continental Okhotsk									
Kukhtui and Okhota rivers	86.4	22	17.6	51.1	131	14.6	43.9	14.6	41
West Kamchatka									
All water bodies (except Ozernaya River)	39.3	458	22.2	21.1	487	30.2	31.4	34.9	86
Ozernaya River	—	—	24.6	25.3	487	29.1	13.8	17.3	347
East Kamchatka									
All water bodies (except Kamchatka River)	46.3	400	24.8	36.2	765	29.6	21.9	32.4	247
Kamchatka River:									
Group C	4.6	1251	11.0	9.6	218	—	—	—	—
B	25.9	108	20.0	3.8	105	—	—	—	—
E	29.0	327	10.7	47.3	1047	9.8	20.7	28.0	82
A	91.2	205	75.1	68.2	973	66.7	34.2	64.1	117
D	100.0	12	85.0	81.0	153	—	—	—	—
Bering Island									
Lake Sarannoye	—	—	—	—	—	9.1	27.3	63.6	11
East Chukotka									
Seutakan River[a]	70.8	72	30.8	46.2	26	—	—	—	—

NOTE: According to Bugaev (1978) a "river" ZCC has 0–2 close (narrow) circuli; a "lake" ZCC has 3–8. The percent occurrence of "river" ZCCs = 100% – percent occurrence of "lake" ZCCs.

[a] Data kindly submitted by A. S. Agapov.

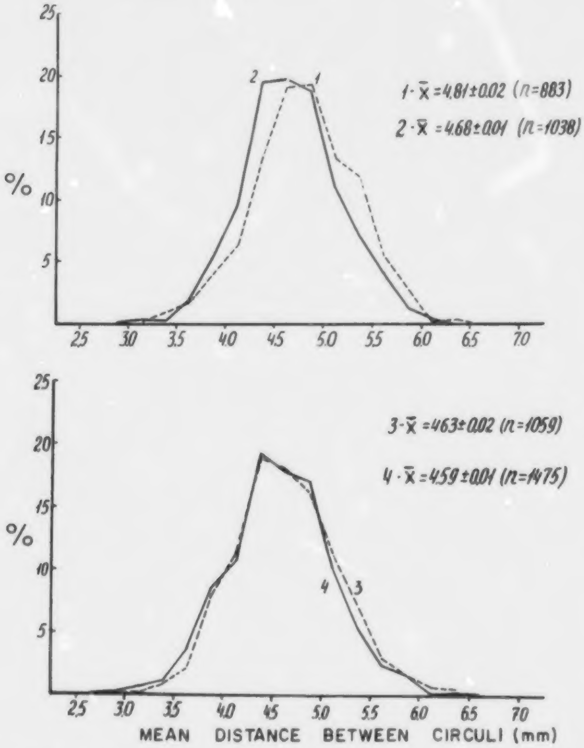

FIG. 6. Mean distance between circuli during the first ocean year in Kamchatka sockeye. Symbols as in Fig. 5.

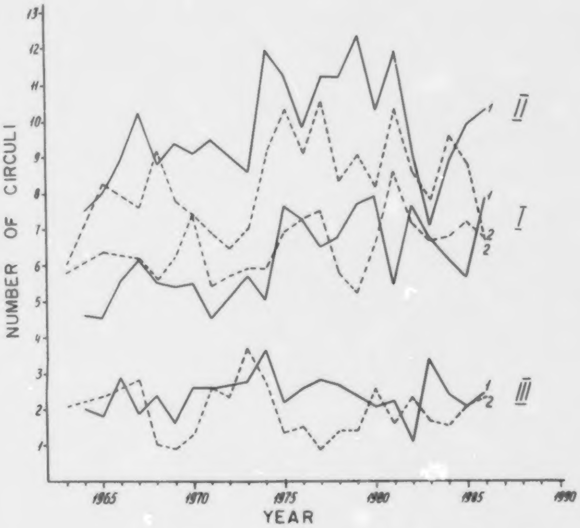

FIG. 7. Year-to-year variations in mean number of circuli in the scale centrum of age 5_2+ sockeye spawners of Lake Azabachye and the Ozernaya River: 1 — Ozernaya River (sampling technique of Clutter and Whitesel 1956); 2 — Azabachye River (characteristics of the first year adjusted using Pravdin's technique (1966)). I — first year of growth, II — second year of growth, III — increment in the year of downstream migration.

TABLE 6. Number of circuli in the first sea year on the scales of Asian sockeye spawners.

River system or water body	One ZCC			Two ZCC			Three ZCC		
	Range	$\overline{X}$	Sample size	Range	$\overline{X}$	Sample size	Range	$\overline{X}$	Sample size
Continental Okhotsk									
Kukhtui and Okhota rivers	20–27	24.68 ± 0.39	22	16–31	24.01 ± 0.25	131	16–28	23.49 ± 0.40	41
West Kamchatka									
All water bodies (except Ozernaya River)	12–34	24.85 ± 0.15	458	11–33	23.74 ± 0.15	487	15–33	24.27 ± 0.31	86
Ozernaya River				14–31	23.81 ± 0.12	487	14–29	23.48 ± 0.13	347
East Kamchatka									
All water bodies (except Kamchatka River)	15–34	24.34 ± 0.15	400	12–32	23.42 ± 0.11	765	12–30	22.57 ± 0.20	247
Kamchatka River									
Group C	11–30	21.55 ± 0.09	763						
B	14–30	22.81 ± 0.29	81	18–30	21.91 ± 0.39	47			
E	12–27	20.94 ± 0.28	108	12–29	20.86 ± 0.10	636	14–24	20.39 ± 0.22	119
A	15–29	21.47 ± 0.36	78	13–32	22.17 ± 0.14	339	17–26	22.00 ± 0.25	65
D	15–27	20.94 ± 0.85	16	12–26	20.78 ± 0.18	150			
East Chukotka									
Seutakan River[a]	14–28	21.63 ± 0.46	72	13–28	21.04 ± 0.68	26			

The number of circuli in the first sea year in sockeye of Lake Sarannoye (Bering Island) varied from 17 to 22 (mean 19.00 ± 0.29). Calculations are based on 22 specimens, which were not divided up on the basis of the number of central ZCC.

[a] Data kindly submitted by A. S. Agapov.

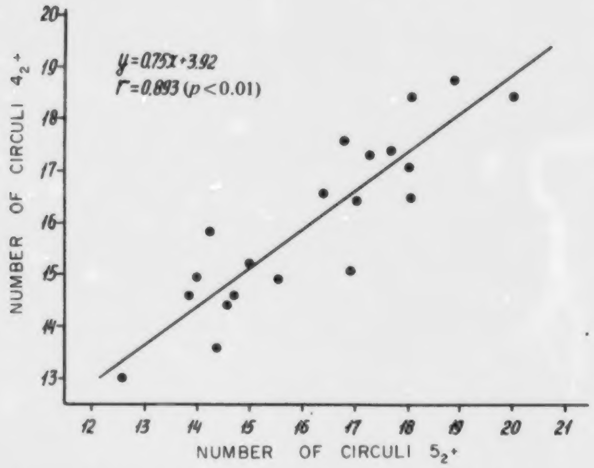

FIG. 8. Comparison of ages 4_2+ and 5_2+ of the same year-class, in respect to the number of circuli during the first 2 years of growth on scales of sockeye spawners of the Ozernaya River.

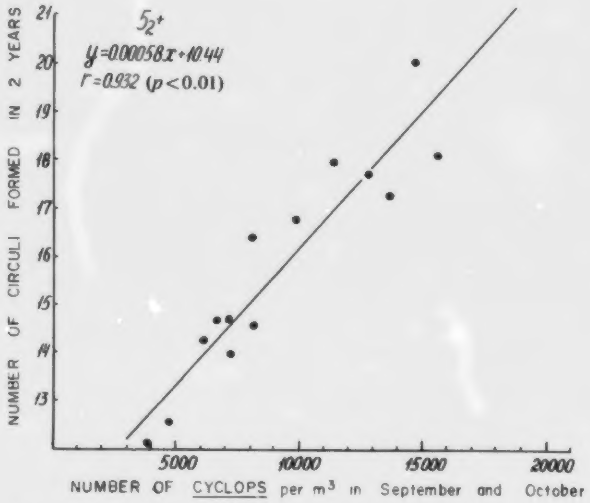

FIG. 9. Relationship between the total number of circuli during the first 2 years of growth in Ozernaya River sockeye spawners of age 5_2+, and the mean density of *Cyclops* in September–October in Lake Kuril.

chatka are related to spawner abundance, just as in group A. However, no definite conclusions are possible as to the actual pattern of variation without special studies. We can only postulate that there is a negative relationship between scale increments and numbers of spawners in group E. Such a suggestion is supported by 1979–87 data from groups A and E on the size of smolts migrating as a mixed group from Lake Azabachye to the sea. Table 7 shows that recently there has been both decreases and increases in smolt size for groups A and E. Our present state of knowledge suggests that growth rate is related to the abundance of spawners in more than 50% of the

TABLE 7. Size of smolts migrating from Lake Azabachye.

Year	Group A			Group E		
	Range (mm)	$\bar{X}$ (mm)	Sample size	Range (mm)	$\bar{X}$ (mm)	Sample size
1979	81–125	102.6 ± 0.60	149	72–120	97.7 ± 0.70	197
1980	77–117	95.3 ± 1.30	57	60–112	89.3 ± 0.70	130
1984	70–104	88.9 ± 0.70	88	68–104	83.2 ± 0.90	69
1985	67–95	78.4 ± 0.60	91	63–92	77.6 ± 0.50	129
1986	64–89	76.6 ± 2.30	11	54–88	74.2 ± 1.00	54
1987	68–99	82.09 ± 0.69	68	56–97	77.6 ± 0.51	172

NOTE: The method of identifying juveniles of Groups A & E is described by Bugaev and Bazarkin (1987).

Kamchatka River sockeye, because the percentage of groups A and E among spawned-out carcasses was about 56.8% in 1957–83 (Bugaev and Ostroumov 1986). Also, available data indicate that in 1978–83 fishing mortality was 58.3% for group A, 53.3% for group E and 53.2% for the whole river. A study of year-to-year variability of scale structure of identifiable local stocks and groups of stocks of the Kamchatka basin is planned for the near future, using USSR coastal and river catches from 1978 to the present. The preliminary assignment of fish to the various stocks will be according to the "differential method" of Bugaev (1986).

Age Structure of Sockeye Spawners

As indicated in the scale centra of certain stocks of Asian sockeye, it is common to encounter supplementary ZCC which do not correspond to the resumption of growth after an interruption during autumn and winter, and hence are not annual rings. Table 8 shows the major age-groups, scarce age-groups are not included. Comparing the duration of the freshwater period (Table 8) with the number of ZCC in the centrum (Table 1) shows that the actual duration of the freshwater period in Asian sockeye is often less than the number of ZCC. Age 4_1+ is predominant in sockeye of the Okhotsk coast and West Kamchatka, except at the Ozernaya River where age 5_2+ prevails among abundant year-classes (1940–44) and 4_2+ among weak ones (1970–75) (Selifonov 1982), and the Palana River where spawners of 5_2+ are a large majority. I used age determinations of Ozernaya sockeye from Selifonov (1982), because a new ageing of Ozernaya spawners using the same materials gave practically the same results as Selifonov's.

On the whole, East Kamchatka sockeye have somewhat more variable age composition than sockeye of West Kamchatka, but age 4_1+ more often prevails in river stocks. The Avyavayam River is of particular interest where the proportion of 5_1+ (with four ocean years) was large in 1962, but was rare in 1985–86. A high occurrence of age 5_1+ was also observed in certain years in the Khailula and Bolshaya rivers. It is too soon to report on the factors that influence the duration of the ocean period of life; however, the abundant dominant year-classes of pink salmon in western and northeastern Kamchatka may well be one such factor. The same may be true for the Kikhchik stock in 1931, when pinks were abundant in West Kamchatka.

Ages 3_1+, 4_1+, and 4_2+ prevail in sockeye of Lake Dalneye during years of high abundance (1935–47), while ages 3_1+, 4_2+, and 5_3+ were commonest when abundance was low (1948–63). That is, as the abundance of spawners decreased, their age increased because of a longer period of freshwater life (Krogius et al. 1969).

Of interest are variations in age composition of the stock of Lake Listvennichnoye (Table 8). The representation of fish with three freshwater years decreased in 1984, as compared with 1980. This fact may be related to the fertilization of this lake, which improved conditions for juvenile growth (Kurenkov 1985) and resulted in a shorter freshwater period.

Ages 4_2+ and 5_2+ (Table 8) were the commonest ones in streams of Iturup Island (Kuril Islands) and Bering Island in the 1960's. Age 6_3+ predominated among spawners of Lake Sarannoye (Bering Island) in 1985; that is, mean age had increased compared to previous years. Quite possibly this is related to the increase of the Sarannoye stock. The limitations imposed on the Japanese fishery, starting in 1977–78, have been followed by a marked increase in the abundance of Asian stocks of sockeye.

In East Chukotka ages 4_1+ and 5_2+ prevail in Lake Achchen, and 5_2+ and 3_1+ in Lake Seutakan (Table 8).

The above analysis indicates that various factors may influence age structure of Asian sockeye (abundance, food availability, type of water body, etc.), but further long-term and many-faceted observations will be needed to establish general principles and make a classification.

Conclusions

1. Data on the great geographical variation in the structure of the scale centra from 26 stocks of Asian sockeye from the main spawning areas, collected with a uniform subjective error, indicate highly specific conditions for juvenile growth in each of the bodies of water in question, with year-to-year variations that complicate the situation.

2. Comparison of the occurrence of zones of closely situated circuli (ZCC), and of the number of circuli in the scale centrum, failed to reveal any regular trends within the investigated area either in the north-south or the east-west directions.

3. Comparison of the number of circuli in the first sea year showed a general uniformity, except for the stocks of the Kamchatka River and Bering Island where the number of circuli was somewhat smaller.

TABLE 8. Percent occurrence of major age-groups of spawners among Asian sockeye.

River or lake	Year	Percent occurrence								Total sample size	Notes
		3_0+	3_1+	4_1+	4_2+	5_1+	5_2+	5_3+	6_3+		
Continental Okhotsk											
Okhota River (Uegin lakes)	1968			40.9			34.5			not cited	Nikulin (1975)
Okhota River	1983			65.7			16.2			99	Our data
Kukhtui River	1983			68.0			15.0			100	" "
West Kamchatka											
Palana River	1983						96.2			299	" "
Tigil River	1981			78.9						38	" "
Khairyuzova River	1984			93.0						298	" "
Icha River	1986			94.1						51	" "
Krutogorova River	1971			84.9						93	" "
Vorovskaya River	1965			77.8						99	" "
Kikhchik River	1931			51.7		22.5				89	" "
Utka River	1965	26.8		65.9						82	" "
Bolshaya River	1957–71			57.2		17.8				484	" "
Ozernaya River	1940–44				25.8		74.2			not cited	Selifonov (1982)
" "	1970–75				48.8		33.9			" "	" "
East Kamchatka											
Paratunka River:											
Lake Dalneye	1935–47		37.0	25.0	32.0					not cited	Krogius et al. (1969)
" "	1948–63		33.0	10.0	32.0			14.0			" "
Lake Listvennichnoye	1980				21.3		19.1		34.0	47	Our data
" "	1984						83.7			50	" "
Tikhaya River	1981	22.5	22.5	45.0						40	" "
Kamchatka River (early run)	1978–83	6.9		54.9			19.6			1697	" "
Kamchatka River (late run)	1978–83	10.7		56.9			17.0			1166	" "
Stolbovaya River	1984			66.1			13.9			115	" "
Malamvayam River	1983			43.0			44.2			86	" "
Khailula River	1977–83	7.3		52.3		28.4				587	" "
Ivashka River	1966	36.3		45.1						91	" "
Tymlat River	1973			76.5						85	" "
Kichiga River	1981			81.4						102	" "
Avyavayam River (Korf cannery)	1962			31.6		42.1				57	" "
Avyavayam River	1985–86		11.9	81.3						395	" "
Kultushnaya River (Lake Ilir-Gytkhyn)	1983						72.0			50	" "
Apuka River	1985			77.5						102	" "
Bering Island											
Lake Sarannoye	1960–65				34.8		23.0	14.8	12.2	230	Kurenkov (1970)
" "	1985				13.6		18.2		40.9	22	Our data
East Chukotka											
Lake Achchen	1975			41.0	24.6		32.8			61	Chereshnev (1981)
Seutakan River (Lake Seutakan)	1976		45.6	52.6						57	" "
Iturup Island											
Lake Krasivoye	1964–67				48.3		20.5			345	Ivankov (1984)

4. Taking into account that sockeye of the Ozernaya and Kamchatka River, both in the past and at present, have comprised up to 90–95% of the total Far Eastern sockeye catch, the problem of identification of Asian sockeye may in practice be reduced to the necessity of developing methods to distinguish these two stocks.

5. Investigations (in cooperation with V. A. Dubynin) of variability of circulus patterns in the centrum of scales of ages 4_2+ and 5_2+ showed that a significant relationship existed between the number of circuli during the first and second years of life, and the abundance of *Cyclops scutifer* Sars in the lake in August–October. Any rela-

tionship of water temperature in the lake and the number of circuli is secondary.

6. Given the present state of knowledge, there is good evidence that about 50% of the sockeye of the Kamchatka River (the stock of Lake Azabachye and a group of stocks of the lower river) exhibit a negative relationship between scale growth and abundance of spawners.

7. Two zones of closely situated circuli in the scale centrum are characteristic of stocks of both the Ozernaya and Kamchatka rivers. Taking into account year-to-year variability in the number of circuli in the centrum of such scales, sampling should be done annually, and regressions of scale characteristics be developed (for individual local stocks or groups in the case of the Kamchatka).

8. In ocean catches of individuals of Asian origin, those with one ZCC may provisionally be considered to be from the Kamchatka River, taking into account relative numbers of the Ozernaya and Kamchatka river stocks. Individuals with three or four ZCC should be identified as those of the Ozernaya River, as such individuals are more rare in the Kamchatka River basin.

9. When juvenile growth data was unavailable, the age composition of the Asian stocks was determined by taking into consideration information on the growth patterns of juvenile sockeye in the Kamchatka River basin, and information published on other water bodies.

References

Anas, R. E., and S. Murai. 1969. Use of scale characters and a discriminant function for classifying sockeye salmon (*Oncorhynchus nerka*) by continent of origin. Int. North Pac. Fish. Comm. Bull. 26: 157–192.

Bugaev, V. F. 1978. Using the structure of zone narrow-situated sclerites in the scale as a criterium for distinguishing between the different local groups of sockeye *Oncorhynchus nerka* (Walbaum) in the Kamchatka River basin. Vopr. Ikhtiol. 18(5): 826–836. (In Russian)

1981. On the time of the first annual ring formation on the scale of young sockeye salmon *Oncorhynchus nerka* (Walbaum) from the Kamchatka River basin. Vopr. Ikhtiol. 21(2): 284–292. (In Russian)

1983a. On scale formation in the sockeye salmon *Oncorhynchus nerka* (Walbaum) (Salmonidae) from Lake Azabachye (Kamchatka) during the freshwater period of life. Vopr. Ikhtiol. 23(3): 412–418. (In Russian)

1983b. Spatial structure of the sockeye salmon *Oncorhynchus nerka* (Walbaum) populations in the Kamchatka basin. Avtoref. dis. kand. biolog. Nauk, Moskovskii Gosudarstvennyi Universitet, Moskva. 22 p. (In Russian)

1984. On the sclerite formation rate and growth pattern in young sockeye salmon from the Kamchatka River basin in the year of seaward migration. Vopr. Ikhtiol. 24(6): 991–1002. (In Russian)

1986. Methods for identification in coastal and river catches of individuals from major local populations and groups of the sockeye salmon *Oncorhynchus nerka* (Walbaum) of the Kamchatka River basin. Vopr. Ikhtiol. 26(4): 600–609. (In Russian)

Bugaev, V. F , and V. N. Bazarkin. 1987. On the scale structure and growth of young sockeye salmon *Oncorhynchus nerka* (Walbaum) from Lake Azabachye (Kamchatka). Vopr. Ikhtiol. 27(1): 59–71. (In Russian)

Bugaev, V. F., and A. G. Ostroumov. 1986. Relative abundance of local stocks and subgroups of sockeye *Onchorhynchus nerka* (Walbaum) in the basin of the Kamchatka River, p. 47–52. *In* Dinamika chislennosti promyslovykh zhivotnykh Dal'nevostvchnykh morei. TINRO, Vladivostok. (In Russian)

Burgner, R. L., C. I. Dicostanzo, R. I. Ellis, C. J. Harry, W. L. Hartman, O. E. Kerns, O. A. Mathisen, and W. F. Royce. 1969. Biological studies and estimates of optimum escapements of sockeye salmon in the major river systems in southwestern Alaska. Fish. Bull. (U.S.) 67(2): 405–459.

Chereshnev, I. A. 1981. Contribution to biology of migratory salmonids of Eastern Chukotka, p. 116–146. *In* Ryby v ekosistemakh lososevykh rek Dal'nego vostoka. Akademiia Nauk SSR, Dal'nevostochnyi Nauchnyi Tseutr, Vladivostok. (In Russian)

Clutter, R. I., and L. E. Whitesel. 1956. Collection and interpretation of sockeye salmon scales. Int. Pac. Salmon Fish. Comm. Bull. 9: 159 p.

Cook, R. C. 1982. Stock identification of sockeye salmon (*Oncorhynchus nerka*) with scale pattern recognition. Can. J. Fish. Aquat. Sci. 39(4): 661–617.

Cook, R. C., and G. E. Zord. 1978. Identification of stocks of Bristol Bay sockeye salmon, *Oncorhynchus nerka*, by evaluating scale patterns with a polynominal discriminant method. Fish. Bull. (U.S.) 76(2): 415–423.

Dubynin, V. A. 1986. Relationship between size-weight indices of downstream migrants and the year-class strength and numbers of spawners in the sockeye salmon *Oncorhynchus nerka* (Walbaum) from Lake Kurilskoye (Kamchatka). Vopr. Ikhtiol. 26(6): 1023–1026. (In Russian)

Goodlad, J. C., T. W. Gjernes, and E. L. Brannon. 1974. Factors affecting sockeye salmon (*Oncorhynchus nerka*) growth in four lakes of the Fraser River system. J. Fish. Res. Board Can. 31(5): 871–892.

Ivankov, V. N. 1984. Migratory and landlocked forms of sockeye, *Oncorhynchus nerka* (Walbaum) of Lake Iturup (Kuril Islands), p. 65–73. *In* Biologiya prokhodnykh ryb Dal'nego Vostoka. Far-Eastern State University Press, Vladivostok. (In Russian)

Johnson, W. E. 1965. On mechanisms of self-regulation of population abundance in *Oncorhynchus nerka*, p. 66–87. *In* Symposium: Factors that regulate the size of natural populations in fresh water. Mitt. Int. Ver. Theor. Angew. Limnol. 13.

Konovalov, S. M. 1971. Differentiation of local populations of sockeye salmon. Izd. Nauka, Leningrad. 229 p. (In Russian)

Krasnowski, P. V., and M. L. Bethe. 1978. Stock separation studies of Alaska salmon based on scale pattern analysis. Alaska Dep. Fish Game Inf. Bull. 175: 37 p.

Krogius, F. V. 1958. On the scale pattern of Kamchatka sockeye of different local populations, p. 52–63. *In* Materiali po biologii morskogo perioda zhizni Dalnevostochnykh lososei. VNIRO Press, Moscow. (In Russian) (Fish. Res. Board Can. Transl. Ser. 181.)

1961. On the relation between rate of growth and population density in sockeye salmon, p. 132–146. *In* Trudy Soveshchaniya po dinamike chislennosti ryb. (In Russian) (Fish. Res. Board Can. Trans. Ser. 441).

1967. Methods of determining abundance of sockeye, p. 71–77. *In* T. F. Dement'eva and K. A. Zemskoi [ed.] Metodi Otsenki zapasov i prognozipovaniia ulovov ryb. Tr. VNIRO 62. (In Russian)

Krogius, F. V., and E. M. Krokhin. 1956. Results of a study of the biology of sockeye salmon, the conditions of the stocks and fluctuations in numbers in Kamchatka waters. Vopr. Ikhtiol. 7: 3–20. (In Russian) (Fish. Res. Board Can. Transl. Ser. 176.)

KROGIUS, F. V., E. M. KROKHIN, AND V. V. MENSHUTKIN. 1969. The Lake Dalneye pelagic fish community. Izd. Nauka, Leningrad. 88 p. (In Russian)

KURENKOV, I. I. 1985. An experiment at fertilizing a salmon lake. Rybn. Khoz. 1985(8): 31-32. (In Russian)

KURENKOV, S. I. 1970. *Oncorhynchus nerka* (Walbaum) in Lake Sarannoye (Komandor Islands). Izv. TINRO 78: 49-60. (In Russian)

MATHISEN, O. A. 1966. Some scale characters of the Ozernaya sockeye salmon. J. Fish. Res. Board Can. 23: 459-462.

MESSINGER, H. B., AND H. T. BILTON. 1974. Factor analysis in discriminating the racial origin of sockeye salmon (*Oncorhynchus nerka*). J. Fish. Res. Board Can. 31: 1-10.

MINA, M. V. 1976. On the method of determining age of fish in conducting population studies, p. 31-37. *In* Tipoviye metodiki issledovaniya produktivnosti vidov ryb v predelakh ikh arealov. Mokslas, Vilnius. (In Russian)

MOSHER, K. H. 1972. Scale features of sockeye salmon from Asian and North American coastal regions. Fish. Bull. (U.S.) 70(1): 141-183.

NIKULIN, O. A. 1975. Reproduction of sockeye salmon (*Oncorhynchus nerka* Walbaum) in the Okhota River basin. *In* Lososevye Dal'nego Vostoka. Tr. VNIRO 106: 97-105. (In Russian)

OSTROUMOV, A. G. 1972. Spawning success of sockeye salmon (*Oncorhynchus nerka* Walbaum) in the springs of Lake Azabachye. Izv. TINRO 82: 135-142. (In Russian)

PRAVDIN, I. F. 1966. Handbook of the study of fishes (particularly freshwater fishes). Pishchevaya prom Press, Moskva. 373 p. (In Russian)

ROGERS, D. E. 1980. Density dependent growth of Bristol Bay sockeye salmon, p. 267-283. *In* W. J. McNeil and D. C. Himsworth [ed.] Salmon ecosystems of the North Pacific. Oregon State Univ. Press. Corvallis, USA.

ROGERS, D. E., B. J. ROGERS, AND F. J. HARDY. 1982. Effects of fertilization of Little Togiak Lake on the food supply and growth of the sockeye salmon, p. 125-141. *In* B. R. Melteff and R. A. Neve [ed.] Proceedings of the North Pacific Aquaculture Symposium. Alaska Sea Grant Rep. 82-2.

SELIFONOV, M. M. 1975. The fisheries and sockeye reproduction in the basin of the Ozernaya River. Avtoref. dis. kand. biolog. Nauk. TINRO, Vladivostok. 23 p. (In Russian)

1982. Fluctuations in abundance of sockeye salmon of the Ozernaya River stock, p. 93-96. *In* B. R. Melteff and R. A. Nevé [ed.] Proceedings of the North Pacific Aquaculture Symposium. Alaska Sea Grant Rep. 82-2.

WARD, F. J., AND P. A. LARKIN. 1964. Cyclic dominance in Adams River sockeye salmon. Int. Pac. Salmon Fish. Comm. Bull. 11: 116 p.

Topic 2
The Effects of Ocean Variability on Recruitment

Recruitment of Marine Fishes Revisited

Warren S. Wooster

Institute for Marine Studies, University of Washington, Seattle, WA 98105, USA

and Kevin M. Bailey

*Northwest and Alaska Fisheries Center, 7600 Sandpoint Way NE,
Seattle, WA 98115, USA*

Abstract

WOOSTER, W. S., AND K. M. BAILEY. 1989. Recruitment of marine fishes revisited, p. 153–159. *In* R. J. Beamish and G. A. McFarlane [ed.] Effects of ocean variability on recruitment and an evaluation of parameters used in stock assessment models. Can. Spec. Publ. Fish. Aquat. Sci. 108.

Present hypotheses and recent research on recruitment in marine fish populations are reviewed in order to identify impediments to development of a general framework of recruitment theory. Difficulties arise from complexity of the interactions between multiple abiotic forcing functions and biotic responses as well as from limitations on the availability and accuracy of measures of both the relevant environmental variability and the biotic response. Although some generalizations are emerging, prediction of year-class strength in a form useful to fishery managers may initially only deal with response to extreme environmental conditions. A next step will be to relate regime changes in fish stocks to longer term trends in the environment.

Résumé

WOOSTER, W. S., AND K. M. BAILEY. 1989. Recruitment of marine fishes revisited, p. 153–159. *In* R. J. Beamish and G. A. McFarlane [ed.] Effects of ocean variability on recruitment and an evaluation of parameters used in stock assessment models. Can. Spec. Publ. Fish. Aquat. Sci. 108.

Les auteurs examinent les hypothèses actuelles et les recherches réalisées récemment au sujet du recrutement dans les populations de poissons marins afin de déterminer ce qui entrave l'établissement d'une théorie générale en la matière. Les difficultés sont dues à la complexité des interactions entre les divers facteurs de forçage abiotiques et les réactions biotiques, ainsi qu'aux mesures limitées et peu exactes tant de la variabilité des facteurs écologiques pertinents que des réactions biotiques. Bien qu'on ait fait certaines généralisations, initialement, les prévisions quant à l'effectif des classes d'âge sous une forme utile aux gestionnaires des pêches ne traiteront peut-être que des réactions aux conditions environnementales extrêmes. Il faudra ensuite établir un rapport entre les changements des régimes des stocks et les tendances à plus long terme des paramètres de l'environnement.

Introduction

Understanding what controls success of recruitment, i.e., year-class size in marine fish populations, is important not only to managing for conservation, but also to more efficient harvesting through improved predictions of abundance. While the "recruitment problem" has become a major target of fishery investigations, it has a much broader significance, being central to the regulation of animal populations. The contribution to the dynamics of populations and communities of the influx of new members has recently been called "supply-side ecology" by Roughgarden (Lewin 1986). Both exploitation and environmental change have been credited with controlling recruitment; in harvested marine fish populations, the effects are particularly difficult to disentangle.

Several reviews of the recruitment problem have been published in the last few years (see, for example, Bakun et al. 1982; Shepherd et al. 1984; Leggett 1986). Despite this attention, we think it useful to present the views of scientists from different backgrounds and perspectives. While we briefly review existing hypotheses and update pertinent research, our principal interest is to see what impediments there are to development of a general framework of recruitment theory and to consider what sort of predictive capability might eventually emerge.

Spawner-Recruit Models and Density Dependence

Spawner-recruit models attempt to account for the mortality of fish between spawning and recruitment (Rothschild 1986). The most common models are those of Ricker (1954) and Beverton and Holt (1957); they are compared by Ricker (1975) and discussed, along with several other models, by Cushing (1973) and Rothschild (1986). Briefly, both models have density-independent and density-dependent terms. The density-dependent term has the effect of reducing the rate of recruitment with increasing stock size via compensatory mortality. Density dependence is stronger in the Ricker model, resulting in a dome-shaped spawner-recruit curve, whereas in the Beverton–Holt model the relationship is asymptotic. In both models compensatory mortality acts on new recruits, and Ricker attributes it to several possible factors including aggregation of predators, cannibalism and in some cases competition. Beverton and Holt account for compensatory mortality by assuming that the number of eggs and thus of pre-recruits increases with increasing spawner abundance while the amount of food per individual fish declines. This results in slower growth, and therefore higher mortality. Shepherd and Cushing (1980) elaborated on these assumptions in a model of density-dependent larval fish growth and recruitment in which predation is responsible for increased mortality on slower growing fish.

Although many studies still attempt to apply spawner-recruit models to fisheries data, their success has been limited. A workshop organized to evaluate the relationship between environmental change and fish stock abundance (Sharp 1980), concluded that spawner-recruit relationships that ignore other factors are fruitless. More recently, Jones and Henderson (1985) concluded that there is little convincing evidence for a significant relationship between spawners and recruits for fish species in general. Koslow et al. (1987) found few data to support the fact that year-class strength of Atlantic cod or haddock in the Northwest Atlantic was a function of stock reproductive effort, although they did find that other biological and environmental factors were influential.

With regard to the ideas of Beverton and Holt, numerous studies have cast doubt on the concept of density-dependent growth in the larval phase (Murphy 1961; Laurence 1982; Cushing 1983). However, Bollens (in press) has calculated that high densities of larval fishes can affect prey density. Density-dependent growth in the juvenile phase seems probable (Peterman and Bradford 1987).

Density-dependent mortality of juvenile fishes has been noted in some studies. Lockwood (1980) attributed density-dependent mortality in O-group plaice to migrant predators such as older flatfishes and gadoids. Van der Veer and Bergman (1987) found density-dependent predation by shrimp on newly settled juveniles that could account for most of their mortality.

Intuitively, there should be some relationship between the number of eggs produced and the number of recruits. However, variability in early mortality caused by many confounding influences obscures the form of the stock-recruit relationship. For example, in the case of northern anchovy recruitment, MacCall (1980) concluded that while there is probably a strong density-dependent effect due to cannibalism, which would lead to a Ricker-type relationship, this process is overwhelmed by density-independent effects. Similarly, Welch (1986) could demonstrate density-dependent mortality in a number of fish stocks only after the obfuscating density-independent terms were statistically filtered out. Hollowed and Bailey (1989) also found an underlying spawner-recruit relationship after filtering out interannual variability.

Causes of Interannual Variability in Recruitment

Whatever the relationship between spawning stock and subsequent recruitment, the large interannual variations characteristic of many stocks cannot be attributed to concomitant fluctuations in parent stock which are generally of a different magnitude and frequency. But variability of comparable scale is apparent in the ocean environment (Mysak et al. 1982), and this, along with an intuitive appeal, has led to a search for mechanisms linking recruitment fluctuations with those in the environment.

The abundance of fish stocks varies not only from year to year but also changes markedly over longer periods. Environmental conditions also vary through a spectrum that in addition to higher frequencies, includes trends of years to decades (Dickson et al. 1988). Although the same linkages between environment and year-class presumably operate at high and low frequencies, their relative importance may differ and there may be additional mechanisms that play a role at lower frequencies.

Features of the abiotic environment that could affect recruitment include the distributions in space and time of heat, salt, light, and motion. Features of the biotic environment include distributions of food, competitors, and predators. Variations in the abiotic environment may directly affect survival of pre-recruits or may work indirectly by altering the biotic environment or relationship of the eggs and larvae to it.

Many studies of recruitment variations can be traced back to Hjort (1914) who considered that year-class strength was determined in the early stages of larval development and who proposed two processes whereby this occurred, starvation and expatriation (transport). Both processes could respond strongly to inter-annual changes in the physical environment, either, as in the first case, working through the food web or acting directly on the larvae. A third process, predation, is presumably a major cause of mortality in the early life of marine fishes, but its dependence on environmental variability has been more difficult to demonstrate. Some of the studies of these processes are reviewed in the following sections.

It should be observed that there is not universal agreement on the stage of development when year-class strength is established. While many agree with Hjort that this occurs in the early days of larval development, others suggest that it may occur at a later larval or juvenile phase (Sissenwine 1984; Peterman et al. 1988). There is no reason, of course, to assume that the "critical stage" is the same for all species. It is our perception that most of those who consider that year-class strength is determined early in life by density-independent processes are field or experimental biologists and oceanographers whereas those who favor density-dependent control at the juvenile stage work primarily in population dynamics and fishery data analysis. In our opinion, this dichotomy is associated with the lack of an interdisciplinary approach which has been a major impediment to progress on the "recruitment problem".

Starvation

Hjort's (1914) starvation hypothesis has been the basis of most field and laboratory work on larval survival. The hypothesis has been extended to include the influence of variability in the physical environment on larval food availability. For example, Cushing (1975) proposed that larval mortality is determined by the match/mismatch in the seasonal availability of food and the feeding readiness of fish larvae. He postulated that seasonal availability of food is controlled by the timing of the spring phytoplankton bloom, which is influenced by the depth of the wind-mixed layer and light penetration. In turn, the spring phytoplankton bloom gives rise to production of copepod nauplii, a primary larval food. This hypothesis has intuitive appeal, but it still lacks support from field data (Sinclair and Tremblay 1984; Leggett 1986; Sinclair 1988).

In Lasker's (1975) view, fish larvae need dense concentrations of proper-sized food, including dinoflagellates for larval anchovy. These concentrations are attained when the ocean is calm and there is a stable mixed layer. He tested this concept in the field by estimating larval anchovy feeding success before and after a wind mixing event. Peterman and Bradford (1987) also found that calm periods are related to good larval survival, although in a later paper (Peterman et al. 1988), they note that abundances of early life stages of northern anchovy are not correlated with subsequent recruitment. Also, in Methot's (1983) study of birthdate distributions of anchovy that survived to be sampled as juveniles, markedly good survival was not always associated with calm ocean conditions.

Until recently, starvation in the sea has been difficult to demonstrate because of methodological limitations. New technological developments now enable investigators to detect sub-optimal growth in the sea. These methods include RNA/DNA analyses (Buckley and Lough 1987), lipid profiles (Fraser et al. 1987), histological condition (Theilacker 1986) and assays of hormones using antibody probes (Brown et al. 1987).

Transport

Hjort (1914) also hypothesized a relationship between recruitment variability and transport of eggs and larvae away from favorable nursery areas. The net movement of eggs and larvae by currents has been demonstrated in a number of studies (e.g., Fortier and Leggett 1985; Shelton and Hutchings 1982; Kendall et al. 1987; see also review by Norcross and Shaw 1984). Several studies go further and show the linkage between environmental conditions and transport (Talbot 1977; Ellertsen et al. 1981), and Power (1986) modeled the effect of wind on drift and subsequent distribution of larval anchovy. Although environmental conditions associated with transport and recruitment have been correlated (Nelson et al. 1977; Bailey 1981; Sinclair et al. 1985), accompanying field work carried through to the pre-recruit stages has been rare. In particular, few studies have demonstrated unequivocally that transport of larvae into unfavorable areas is detrimental.

Several hypotheses link temporal and spatial aspects of transport to adaptations of spawning populations. Parrish et al. (1981) hypothesized that spawning by fishes in the upwelling zone of the California Current is adapted to the adverse effects of offshore transport of eggs and larvae. They cite numerous examples of species that spawn in locations or at times when offshore transport is minimal.

The Parrish model was more extensively developed for the case of northern anchovy by MacCall (1984) who proposed that in the most suitable habitats for northern anchovy, expatriation is minimal. When adult density becomes high in these areas, the loss of eggs from cannibalism is heavy, and anchovy expand their habitat to spawn in areas that from the transport point of view are less favorable.

Iles and Sinclair (1982) hypothesized that the richness of stocks of Atlantic herring is determined by the number of areas that are suitable for retaining larvae, and further that the abundance of a stock is determined by the size of its larval retention area. Sinclair (1988) extended this hypothesis to include other species, and was less equivocal in his assertion that fishes spawn in certain areas as an adaptation to retention, in contrast to the traditional Harden-Jones larval drift hypothesis (Cushing 1975).

Predation

Predation on early life stages of marine fishes has been among the most difficult areas to study. While Hjort did not list predation among the factors affecting recruitment strength, variable levels of predation clearly can be important (Hunter 1981, 1984). However, the possibility that this could cause variable levels of recruitment is difficult to test in the field. Several recent reviews document instances of predation and discuss the problems in this area (Hunter 1981, 1984; Purcell 1985; Bailey and Houde 1989).

There is evidence that predation can be important to specific populations under certain circumstances. Two studies that have attempted to partition larval mortality into predation and starvation have concluded that predation is the major source of larval mortality (Hewitt et al. 1985; Leak and Houde 1987). However, they have not shown a direct connection between predation pressure on eggs and larvae and recruitment of later stages.

Johannes (1978) postulated that transport and predation are linked in some tropical fishes. He noted that tropical species often have protracted spawning seasons in which eggs are spawned offshore, or they spawn in regions where they will be transported offshore. This can be seen as a strategy whereby the intense predation pressure occurring in nearshore regions is avoided. At a later stage, the larvae will be brought inshore by favorable circulation.

In a similar vein, Frank and Leggett (1985) have suggested that patterns of spawning are adaptive responses, at least in part, to historical patterns of predation. They pointed out that capelin and other nearshore spawners in eastern Canada spawn at times and in locations whereby their larvae occupy different water masses from major concentrations of predators. This has been termed the "safe-site hypothesis".

Houde (1987) proposed that predation and its interaction with growth rate may be a major regulatory mechanism that commonly operates in the sea. Unfavorable growth conditions can lead to prolonged stage durations and thereby increase the time of vulnerability of pre-recruit fish to predators. By comparing the sensitivity of different species to reasonable variations in growth (possibly caused by variations in food levels or temperature), he concluded that for many species large fluctuations in year-class strength could result from small variations in larval growth.

Some Impediments to Development of Recruitment Models

A simple deterministic model that accurately predicts recruitment from observed local environmental changes is unlikely. A basic problem is that variability in the abiotic ocean environment is usually a non-linear response to multiple forcing functions that vary over a wide range of space and time scales. Coupling between abiotic and biotic environments has similar characteristics. The difficulties of non-linearity are compounded by limitations in accuracy of measures of both the relevant environmental variability and the biotic response.

While some environmental measures are commonly available (e.g., sea surface temperature, SST, and sea level at a coastal station, or SST averaged over a large area), more diagnostic indices (e.g., wind stress along a coastal stretch or thickness and velocity of the surface layer) are difficult to obtain. Sampling in space and time is usually inadequate and time series of reasonable length are rare. There are few places in the world where marine plankton and nekton are regularly sampled. The sizes of incoming year-classes of commercial stocks are usually estimated from adult catch data rather than being directly measured.

Sampling larvae for determination of mortality rates is one of the most difficult problems encountered in field studies. Larval vulnerability to sampling gear changes as larvae develop, and few studies attempt to standardize for catchability of different sampling devices. Small larvae are extruded through the mesh of commonly used gear; for example, up to 90% of yolk-sac anchovy larvae are lost through 0.5-mm mesh plankton netting (Lo 1983). Where corrections for extrusions are made, the coefficients are assumed to be constant from year to year, even though larval depth and therefore the length of time they are in the net may vary significantly. Some studies repetitively sample stations representing small areas through time and assume that diffusion or transport is negligible. Other studies, such as the CalCOFI program, sample wide areas, but in most locations sampling is infrequent so that the same cohort may never be sampled twice. As Leggett (1986) has pointed out, sampling for accurate determination of meaningful larval mortality rates must be accomplished on time and space scales that are relevant to the processes and the life history of the organism involved.

Another complication arises in the case of low frequency variability, where the biotic system may have more than one equilibrium state, with response to variable environmental conditions differing for each state. For example, in some cases there is evidence for shifts in biological communities, suggesting jumps between alternate equilibrium states of ecological systems. Skud (1982) suggested that animals may respond differently to environmental change depending on whether the species is dominant or subordinate; the position of dominance may change with time. Steele and Henderson (1984; also Steele 1985) described a model driven by realistic environmental variability, in which a population has two alternate equilibrium states, one essentially resource-limited, the other predator-limited. Transitions from one level to the other, taking place every 50 years or so, might be set off by relatively small environmental changes.

Discussion

There is no simple, unifying hypothesis to explain recruitment variations for all species in all circumstances. Clearly, individual populations respond to their local environments in different ways. Yet perhaps some generalizations can be formulated that take into account life histories in relation to individual environments; these can be the basis of hypotheses that can be subjected to carefully designed field tests. As examples, we propose the following strawman hypotheses:

1. Transport is particularly important (a) where nurseries are in localized areas (e.g., estuaries for menhaden (Nelson et al. 1977), embayments for English sole (Boehlert and Mundy 1987), marshes, etc.); (b) where the continental shelf is narrow and juveniles are associated with the bottom (e.g., flatfishes, cod; Parrish et al. 1981).
2. Stocks at the poleward (cold) end of their species range are influenced favorably by oceanic warming, unfavorably by cooling; stocks at the equatorward limit of their range have the opposite response (Bailey and Incze 1985).
3. Some tropical and subtropical fish species may be "prey sensitive" because metabolic rates are high and the time to starvation is short (Houde 1987).
4. In the subtropics and upwelling regions where pelagic fishes are abundant, cannibalism or predation by filter-feeding fishes can be important (Hunter and Kimbrell 1980; Alheit 1987).
5. Recruitment of some pelagic forage fish (e.g., anchovy, capelin) could be controlled by predation on late larvae or juveniles (Peterman et al. 1988). These fishes generally are exposed to the same complex of predators throughout their post-larval lifetime, as they do not undergo marked size or habitat changes during this developmental phase.

Support of these generalizations would mark progress in understanding but would be difficult to apply directly to fishery decisions. Decision makers would like firm predictions of year-class strength, but a more realistic goal might be a crude recruitment prediction scheme in which, depending on whether environmental conditions had been extreme during the "critical period" for the stock in question, a credible statement could be made on the probability that its recruitment would be unusually large or small.

For characterizing environmental conditions, either an index variable or an appropriate suite of conditions could be used. However, methodology for characterizing environmental conditions on the basis of time series of diverse variables remains to be established. It is unlikely that a single environmental measure would be adequate, and patterns of the variability would have to be identified to permit characterizing conditions as extreme.

Similarly, the recruitment levels over time of various stocks must be determined. Such analyses of patterns of recruitment have been made by Koslow (1984) in the North Atlantic and Hollowed at al. (1987) in the eastern North Pacific. In both studies, groups of stocks with similar life histories showed similar responses.

Little work has yet been done on comparing environmental and recruitment variability at this level of generality. The relation of extreme year-classes and extreme environmental conditions (e.g., El Niño) in the several eastern boundary current upwelling ecosystems would be useful to establish for a start. Hollowed et al. (1987) showed that conditions favorable for one set of stocks, such as California pelagics, could be unfavorable for others such as subarctic demersal stocks.

While this scheme has been discussed in terms of interannual variability in year-class strength, longer term trends in environmental conditions should also be associated with predictable trends in the success of recruitment. One should look to the possibility of using large scale changes in environmental conditions to predict major regime changes in fish stocks such as those associated with the Russell cycle (Southward 1980), the North Sea gadoid outburst (Cushing 1984), and the explosions and collapses of Pacific sardine populations (Kawasaki 1983).

At our present levels of understanding, detailed forecasts of recruitment success from either the level of parent stock biomass or environmental conditions are unlikely. However, generalizations can be tested and rough predictions should be possible on interannual and longer time scales. Perhaps with continued interdisciplinary attention to the recruitment problem, results with greater utility for fishery management will be forthcoming in the next decade.

References

Alheit, J. 1987. Egg cannibalism versus egg predation: their significance in anchovies. S. Afr. J. Mar. Sci. 5: 467–470.

Bailey, K. M. 1981. Larval transport and recruitment of Pacific hake *Merluccius productus*. Mar. Ecol. Prog. Ser. 6: 1–9.

Bailey, K. M., and E. D. Houde. 1989. Predation on eggs and larvae of marine fishes and the recruitment problem. Adv. Mar. Biol. (In press)

Bailey, K. M., and L. S. Incze. 1985. El Niño and the early life history and recruitment of fishes in temperate marine waters, p. 143–165. *In* W. S. Wooster and D. L. Fluharty [ed.] El Niño north. Washington Sea Grant Program, Seattle, WA, USA.

Bakun, A., J. Beyer, D. Pauly, J. G. Pope, and G. D. Sharp. 1982. Ocean sciences in relation to living resources. Can. J. Fish. Aquat. Sci. 39: 1059–1070.

Beverton, R. J. H., and S. J. Holt. 1957. On the dynamics of exploited fish populations. U. K. Ministry of Agriculture and Fisheries. Fish. Invest. (Series 2), 533 p.

Boehlert, G. W., and B. C. Mundy. 1987. Recruitment dynamics of metamorphosing English sole *Parophrys vetulus*, to Yaquina Bay, Oregon. Estuarine Coast. Shelf Sci. 25: 261–281.

Bollens, S. M. 1989. A model of the predatory impact of larval marine fish on the population dynamics of their zooplankton prey. J. Plankton Res. (In press)

Brown, C. L., C. V. Sullivan, H. A. Bern, and W. W. Dickoff. 1987. Occurrence of thyroid hormones in early development stages of teleost fish. Am. Fish. Soc. Symp. 2: 144–150.

Buckley, L. J., and R. G. Lough. 1987. Recent growth, biochemical composition, and prey field of larval haddock (*Melanogrammus aeglefinus*) and Atlantic cod (*Gadus morhua*) on Georges Bank. Can. J. Fish. Aquat. Sci. 44: 14–25.

Cushing, D. H. 1973. Recruitment and parent stock in fishes. Washington Sea Grant Publ. WSG 73-1, Seattle, WA, 197 p.

1975. Marine ecology and fisheries. Cambridge Univ. Press, Cambridge. 278 p.

1983. Are fish larvae too dilute to affect the density of their food organisms? J. Plankton Res. 5: 847–854.

1984. The gadoid outburst in the North Sea. J. Cons. Cons. Int. Explor. Mer 41: 159–166.

Dickson, R. R., P. M. Kelly, J. M. Colebrook, W. S. Wooster, and D. H. Cushing. 1988. North winds and production in the eastern North Atlantic. J. Plankton Res. 10: 151–169.

Ellertsen, B., P. Solemdal, T. Stromme, S. Sundby, S. Tilseth, T. Westgard, and V. Oiestad. 1981. Spawning period, transport and dispersal of eggs from the spawning area of arcto-Norwegian cod (*Gadus morhua* L.). Rapp. P.-v. Reun. Cons. Int. Explor. Mer 178: 260–267.

Fortier, L., and W. C. Leggett. 1985. A drift study of larval fish survival. Mar. Ecol. Prog. Ser. 25: 245–257.

Frank, K. T., and W. C. Leggett. 1985. Reciprocal oscillations in densities of larval fish and potential predators: a reflection of present or past predation? Can. J. Fish. Aquat. Sci. 42: 1841–1849.

Fraser, A. J., J. R. Sargent, J. C. Gamble, and P. MacLachlan. 1987. Lipid class and fatty acid composition as indicators of the nutritional condition of larval Atlantic herring. Am. Fish. Soc. Symp. 2: 129–143.

Hewitt, R. P., G. H. Theilacker, and N. Lo. 1985. Causes of mortality in young jack mackerel. Mar. Ecol. Prog. Ser. 26: 1–10.

Hjort, J. 1914. Fluctuations in the great fisheries of northern Europe. Rapp. P.-v. Reun. Cons. Int. Explor. Mer 20: 1–228.

Hollowed, A. B., and K. M. Bailey. 1989. New perspectives on the relationship between recruitment of Pacific hake (*Merluccius productus*) and the ocean environment, p. 207–220. *In* R. J. Beamish and G. A. McFarlane [ed.] Effects of ocean variability on recruitment and an evaluation of parameters used in stock assessment. Can. Spec. Publ. Fish. Aquat. Sci. 108.

Hollowed, A. B., K. M. Bailey, and W. S. Wooster. 1987. Patterns in recruitment of marine fishes in the northeast Pacific Ocean. Biol. Oceanogr. 5: 99–131.

Houde, E. D. 1987. Fish early life dynamics and recruitment variability. Am. Fish. Soc. Symp. 2: 17–29.

Hunter, J. R., and C. A. Kimbrell. 1980. Egg cannibalism in the northern anchovy, *Engraulis mordax*. Fish. Bull. U.S. 78: 811–816.

Hunter, J. R. 1981. Feeding ecology and predation of marine fish larvae, p. 33–77. *In* R. Lasker [ed.] Marine fish larvae: morphology, ecology and relation to fisheries. Washington Sea Grant Program, Seattle, WA.

1984. Inferences regarding predation on the early life stages of cod and other fishes, p. 533–562. *In* E. Dahl, D. Danielssen, E. Moksness and P. Solemdal [ed.] The propagation of cod. Flodevigen Rapp. 1.

Iles, T. D., and M. Sinclair. 1982. Atlantic herring: stock discreteness and abundance. Science 215: 627–633.

Johannes, R. E. 1978. Reproductive strategies of coastal marine fishes in the tropics. Environ. Biol. Fishes 3: 65–84.

Jones, R., and E. W. Henderson. 1985. Population regulation and implications for the recruitment process in fish. Int. Council Explor. Sea. Demersal Fish Comm. CM 1985/G:21.

Kawasaki, T. 1983. Why do some pelagic fishes have wide fluctuations in their numbers? Biological basis of fluctuation from the viewpoint of evolutionary ecology. FAO Fish. Rep. No. 291, 3: 1065–1080.

Kendall, A. W., M. E. Clarke, M. Yoklavitch, and G. Boehlert. 1987. Distribution, feeding and growth of larval walleye pollock, *Theragra chalcogramma*, from Shelikof Strait, Gulf of Alaska. Fish. Bull. U.S. 85: 499–521.

Koslow, J. A. 1984. Recruitment patterns in northwest Atlantic fish stocks. Can. J. Fish. Aquat. Sci. 41: 1722–1729.

Koslow, J. A., K. R. Thompson, and W. Silvert. 1987. Recruitment to northwest Atlantic cod (*Gadus morhua*) and haddock (*Melanogrammus aeglefinus*) stocks: influence of stock size and climate. Can. J. Fish. Aquat. Sci. 44: 26–39.

Lasker, R. 1975. Field criteria for survival of anchovy larvae: the relation between inshore chlorophyll maximum layers and successful first feeding. Fish. Bull. U.S. 73: 453–462.

Laurence, G. C. 1982. Nutrition and trophodynamics of larval fish-review, concepts, strategic recommendations and opinions, p. 123–171. *In* B. Rothschild and C. Rooth [ed.] Fish ecology III. CIMAS, Univ. of Miami, FL.

Leak, J. C. and E. D. Houde. 1987. Cohort growth and survival of bay anchovy *Anchoa mitchilli* larvae in Biscayne Bay, Florida. Mar. Ecol. Prog. Ser. 37: 109–122.

Leggett, W. C. 1986. The dependence of fish larval survival on food and predator densities, p. 117–137. *In* S. Skreslet [ed.] The role of freshwater outflows in coastal marine ecosystems. Springer-Verlag, Berlin.

Lewin, R. 1986. Supply-side ecology. Science 234: 25–27.

Lo, N. 1983. Re-estimation of three parameters associated with anchovy egg and larval abundance: temperature dependent incubation time, yolk-sac growth rate and egg and larval retention in mesh nets. NOAA Tech. Memo. NMFS/SWFC-31: 33 p.

Lockwood, S. J. 1980. Density-dependent mortality in 0-group plaice (*Pleuronectes platessa* L.) populations. J. Cons. Cons. Int. Explor. Mer 39: 148–153.

MacCall, A. D. 1980. The consequences of cannibalism in the stock-recruitment relationship of planktivorous pelagic fishes such as Engraulis. FAO, IOC Workshop Rep. 28: 201–220.

1984. Population models of habitat selection with application to the northern anchovy. Southwest Fisheries Center Admin. Rep. LJ 8401: 98 p.

Methot, R. D. 1983. Seasonal variation in survival of larval *Engraulis mordax* estimated from the age distribution of juveniles. Fish. Bull. U.S. 81: 741–750.

Murphy, G. I. 1961. Oceanography and variations in the Pacific sardine population. California Cooperative Fisheries Investigation Reports 8: 55–64.

Mysak, L. A., W. W. Hsieh, and T. R. Parsons. 1982. On the relationship between interannual baroclinic waves and fish populations in the northeast Pacific. Biol. Oceanogr. 2: 63–103.

Nelson, W. R., M. C. Ingham, and W. E. Schaaf. 1977. Larval transport and year-class strength of Atlantic menhaden, *Brevoortia tyrannus*. Fish. Bull. U.S. 75: 23–41.

Norcross, B.L., and R. F. Shaw. 1984. Oceanic and estuarine transport of fish eggs and larvae: a review. Trans. Am. Fish. Soc. 113: 153–165.

Parrish, R. H., C. S. Nelson, and A. Bakun. 1981. Transport mechanisms and reproductive success of fishes in the California Current. Biol. Oceanogr. 1: 175–203.

Peterman, R. M. and M. J. Bradford. 1987. Wind speed and mortality rate of a marine fish, the northern anchovy (*Engraulis mordax*). Science 235: 354–356.

Peterman, R. M., M. J. Bradford, N. Lo, and R. Methot. 1988. Contribution of early life stages to interannual variability in recruitment of northern anchovy (*Engraulis mordax*). Can. J. Fish. Aquat. Sci. 45: 8–16.

Power, J. H. 1986. A model of the drift of northern anchovy, *Engraulis mordax*, larvae in the California Current. Fish. Bull. U.S. 84: 585–603.

Purcell, J. E. 1985. Predation on fish eggs and larvae by pelagic cnidarians and ctenophores. Bull. Mar. Sci. 37: 739–755.

Ricker, W. E. 1954. Stock and recruitment. J. Fish. Res. Board Can. 11: 559–623.

1975. Computation and interpretation of biological statistics of fish populations. Bull. Fish. Res. Board Can. 191: 382 p.

Rothschild, B. J. 1986. Dynamics of marine fish populations. Harvard University Press, Cambridge, Ma. 277 p.

Sharp, G. 1980. Workshop on the effects of environmental variation on the survival of larval pelagic fishes. Intergovernmental Oceanographic Commission Workshop Rep. No. 28, FAO, Rome. 323 p.

Shelton, P. A. and L. Hutchings. 1982. Transport of anchovy, *Engraulis capensis* Gilchrist, eggs and early larvae by a frontal jet current. J. Cons. Cons. Int. Explor. Mer 40: 185–198.

Shepherd, J. G. and D. H. Cushing. 1980. A mechanism for density-dependent survival of larval fish as the basis of a stock-recruitment relationship. J. Cons. Cons. Int. Explor. Mer 39: 160–167.

Shepherd, J. G., J. G. Pope, and R. D. Cousens. 1984. Variations in fish stocks and hypotheses concerning their links with climate. Rapp. P.-v. Reun. Cons. Int. Explor. Mer. 185: 255–267.

Sinclair, M. 1988. Marine populations: an essay on population regulation and speciation. Wash. Sea Grant Program, Seattle, WA. 252 p.

Sinclair, M., and M. J. Tremblay. 1984. Timing of spawning of Atlantic herring (*Clupea harengus harengus*) populations and the match-mismatch theory. Can. J. Fish. Aquat. Sci. 41: 1055–1065.

Sinclair, M., M. J. Tremblay, and P. Bernal. 1985. El Niño events and variability in a Pacific mackerel

(*Scomber japonicus*) survival index: support for Hjort's second hypothesis. Can. J. Fish. Aquat. Sci. 42: 602–608.

SISSENWINE, M. P. 1984. Why do fish populations vary?, p. 59–94. *In* R. May [ed.] Exploitation of marine communities. Springer-Verlag, Berlin.

SKUD, B. E. 1982. Dominance in fishes: the relation between environment and abundance. Science 216: 144–149.

SOUTHWARD, A. J. 1980. The western English Channel — an inconstant ecosystem? Nature 285: 361–366.

STEELE, J. H. 1985. A comparison of terrestrial and marine ecological systems. Nature 313: 355–358.

STEELE, J. H., AND E. W. HENDERSON. 1984. Modeling long-term fluctuations in fish stocks. Science 224: 985–987.

TALBOT, J. W. 1977. The dispersal of plaice eggs and larvae in the southern bight of the North Sea. J. Cons. Cons. Int. Explor. Mer 37: 221–248.

THEILACKER, G. H. 1986. Starvation-induced mortality of young sea-caught jack mackerel, *Trachurus symmetricus*, determined with histological and morphological methods. Fish. Bull. 84: 1–17.

VAN DER VEER, H. W., AND M. J. N. BERGMAN. 1987. Predation by crustaceans on a newly settled 0-group plaice *Pleuronectes platessa* population in the western Wadden Sea. Mar. Ecol. Prog. Ser. 35: 203–215.

WELCH, D. W. 1986. Identifying the stock-recruitment relationship for age-structured populations using time-invariant matched linear filters. Can. J. Fish. Aquat. Sci. 43: 108–123.

Forecasts of Runs of West Kamchatka Pink Salmon (*Oncorhynchus gorbuscha*) Based on Analysis of the Downstream Migration and Inshore Feeding of the Juveniles

N. A. Chebanov

Pacific Research Institute of Fisheries and Oceanography (TINRO)
Petropavlovsk-Kamchatsky, USSR

Abstract

CHEBANOV, N. A. 1989. Forecasts of runs of West Kamchatka pink salmon (*Oncorhynchus gorbuscha*) based on analysis of the downstream migration and inshore feeding of the juveniles, p. 161–168. *In* R. J. Beamish and G. A. McFarlane [ed.] Effects of ocean variability on recruitment and an evaluation of parameters used in stock assessment models. Can. Spec. Publ. Fish. Aquat. Sci. 108.

Archival records were used to analyze the effect of environmental conditions on pink salmon abundance during downstream migration and in inshore areas of the Sea of Okhotsk in the region of West Kamchatka where young pink salmon feed. I have used (1) the mean water temperature in the inshore zone in May and June and the summer average temperature, (2) difference between the temperature of river and sea water in June, and (3) the volume of river flow in June. Abundance was also taken into consideration, i.e. the number of spawners on the spawning grounds and the absolute and relative (per pair of spawners) number of downstream young. The reproductive levels in the populations were estimated, by area, by the rate of return which is the ratio of the abundance of the daughter generation (catch by USSR and Japan plus the number on the spawning grounds) to the abundance of the parental generation on its spawning grounds.

This report includes characteristics of the hydrometeorological conditions in certain inshore areas. These conditions have been different for the odd-year and the even-year reproductive lines. The nature of the impact of each factor on success of reproduction is discussed. For each region of the coast, individual correlation coefficients are computed for each factor, and the multiple coefficient for them together. In some cases, correlations for limited time periods are also computed. An example of a forecast of the rate of return of West Kamchatka pink salmon is given, based on environmental conditions during downstream migration and the feeding of the young in the coastal region.

Résumé

CHEBANOV, N. A. 1989. Forecasts of runs of West Kamchatka pink salmon (*Oncorhynchus gorbuscha*) based on analysis of the downstream migration and inshore feeding of the juveniles, p. 161–168. *In* R. J. Beamish and G. A. McFarlane [ed.] Effects of ocean variability on recruitment and an evaluation of parameters used in stock assessment models. Can. Spec. Publ. Fish. Aquat. Sci. 108.

L'auteur s'est servi des archives afin d'analyser les effets des conditions écologiques sur l'abondance des saumons roses au cours de la migration d'avalaison ainsi que dans les zones littorales de la mer d'Okhotsk dans la région de la Kamchatka ouest où les jeunes saumons de cette espèce s'alimentent. Il a eu recours à (1) la température moyenne de l'eau dans la zone littorale au cours des mois de mai et de juin et à la température moyenne de l'eau en été, (2) l'écart de température entre l'eau de la rivière et de la mer en juin et (3) le débit du cours d'eau en juin. Il a également tenu compte de l'abondance des poissons, c'est-à-dire du nombre de géniteurs fréquentant les frayères et des nombres absolu et relatif de jeunes poissons en aval (par couple de géniteurs). Il a estimé le taux de reproduction des populations par zone, et par le taux de retour qui est le rapport entre l'abondance de la progéniture (captures par l'URSS et le Japon plus le nombre de spécimens dénombrés dans les frayères) et l'abondance des géniteurs dans les frayères.

Cet article présente des caractéristiques des conditions hydrométéorologiques dans certaines zones littorales. Ces conditions différaient pour les poissons se reproduisant au cours des années impaires et paires. L'auteur aborde la nature des effets de chacun des facteurs sur le succès de reproduction. Dans chacune des régions de la côte, il a établi des coefficients de corrélation pour chaque facteur et des coefficients multiples pour la totalité d'entre eux. Dans certains cas, il a également établi des corrélations pour des périodes limitées. Il donne un exemple d'une prévision du taux de retour des saumons roses dans la Kamchatka ouest, reposant sur les conditions écologiques au cours de la migration d'avalaison et l'alimentation des jeunes dans la zone côtière.

Introduction

Planning the catch of any fish in the USSR requires scientific forecasts of abundance about 2 years ahead. The pink salmon, *Oncorhynchus gorbuscha* Walbaum, is the species of Pacific salmon that has the shortest life history and only a brief freshwater period. In forecasting abundance 2 years ahead, scientists have mainly used a relationship between abundance and progeny known as "Ricker's reproduction curve"; for example, Karpenko (1982) applied it to the pink salmon of Karagin Bay. However, this relationship completely ignores the impact of environmental factors, with the result that there have been significant errors in the forecasts. Considering this circumstance, it is desirable to make forecasts of pink salmon after their downstream migration and early inshore feeding period.

All specialists now treat the period of downstream migration and inshore feeding as an extremely important one for determining year-class strength. The role of the environment is extremely great at this time; its influence is exerted mainly by way of the growth rate of the young, the availability of food, and predation (Karpenko 1982; Chupakhin and Kaev 1982; Ivankov 1984). Studies of the factors affecting survival and abundance of young pink salmon in rivers and in inshore areas must contribute importantly to the development of forecasting techniques. This has been shown convincingly for the pink salmon stock of Karagin Bay (Karpenko 1982). However, such studies are fragmentary or do not exist for other important stocks, due to the lack of data or insufficient series of observations.

This report uses available archival records of hydrological conditions in West Kamchatka during the period of downstream migration and coastal feeding of pink salmon, to clarify the impact of these conditions on year-class abundance.

Materials and Methods

Data from weather stations situated in the main fishing areas of western Kamchatka were used in the analysis. Estimates of the Japanese catch of pink salmon for six fishing areas of western Kamchatka were made using stock identification data from Japanese catches in the sea. The ratio of total return (catch by USSR and Japan plus abundance on the spawning grounds) to abundance of parent generation (L. E. Grachev, personal communication) was used as the main index of reproductive success of pink salmon, and is called here the rate of return. This index, to our mind, is the most appropriate one for the analysis of the effect of environmental factors on year-class abundance. For the best comparability of results we have used the classification of fishing areas of western Kamchatka developed by L. E. Grachev. Six areas have been delimited: (1) extreme Northwest (from Lesnaya R. to Utkholok R.); (2) Khairyuzovsky (from Kovran R. to Sopochnaya R.); (3) Krutogorovsky (from Kisun R. to Kolpakova R.); (4) Kirovsky (from Bryumka R. to Pymta R.); (5) Oktyabrsky (from Kikhchik R. to Udoshk R.); (6) Ozernovsky (from Opala R. to Kambalna R.). Basic estimates were made for the four areas for which the best series of weather observations were available. These are from the stations at Ptichii Island, at the Icha River, and at the settlements of Oktyabrsky and Ozernovsky. In addition, for the Oktyabrsky region, I have used information on the downstream migration of young pink salmon in the Utka River. Most of the estimates from these indices were made for 1957–85, because it was in 1957 that aerial surveys of salmon in Kamchatka began.

Results and Discussion

Temperature Regime of Coastal Waters in West Kamchatka During Downstream Migration and Inshore Feeding of Young Pink Salmon

Downstream migration of pink salmon in rivers of West Kamchatka usually begins about May 10, reaches its peak in mid-June, and ends in late June or early July.

The action of the temperature regime in the coastal region of the sea upon the abundance of year-classes is as follows: in May it affects the character and intensity of development of the zooplankton that pink salmon feed on; in June and throughout the summer it also affects the rate of growth of the young directly, and consequently the rate at which they escape from the attacks of predators (Karpenko 1982). It is evident also that survival of the young can be affected, in some cases, by the temperature gradient between river and sea water at the time of migration. The nature of the impact is obscure (possibly the high temperature gradient results in thermal shock).

The highest mean sea water temperature in May occurs in the Oktyabrsky area, while the other inshore areas had lower and similar temperatures (Table 1). Water temperatures in June and the summer were highest off Ptichii Island, somewhat lower in the Oktyabrsky area, and lowest in the Ozernovsky area. It is interesting that during the first half of summer the young pink salmon that have gone to sea are carried with a system of currents and tidal movements of the water masses that becomes altered precisely in the region of Ptichii Island, where they remain throughout the second half of the summer (L. E. Grachev and G. E. Karmanov, personal communication). Possibly, the temperature gradient between the regions in question plays some role in this change.

Analysis of data for many years revealed differences in temperatuare between odd and even years in the inshore zone of western Kamchatka during the time that young pink salmon are feeding there. During 1959–85 the average May and June seawater temperatures in the inshore zone were somewhat higher in even years than in odd ones. That is, the young of odd-numbered year-classes had better feeding conditions. No such trend was evident for summer average temperatures in northern coastal areas, and the trend was reversed in southern areas (Table 1).

On the other hand, in 1959–85 year-to-year variations in average May and June temperatures in the inshore zone (except for the Krutogorovsky and Khairyuzovsky regions in May) were significantly greater during even years than

TABLE 1. Long-term average temperatures of sea water in different regions of the western coast of Kamchatka during the time of pink salmon migration to the sea and their feeding in coastal waters (°C).

	May				June				June–August			
	1959–85		Observed period		1959–85		Observed period		1959–85		Observed period	
Region	$\overline{X} \pm m_{\bar{x}}$	σ	$\overline{X} \pm m_{\bar{x}}$	σ	$\overline{X} \pm m_{\bar{x}}$	σ	$\overline{X} \pm m_{\bar{x}}$	σ	$\overline{X} \pm m_{\bar{x}}$	σ	$\overline{X} \pm m_{\bar{x}}$	σ
Ozernovsky	2.63 ± 0.13	0.48	2.98 ± 0.14	0.68	4.93 ± 0.14	0.49	5.28 ± 0.14	0.66	7.43 ± 0.15	0.53	7.63 ± 0.11	0.53
	2.89 ± 0.20	0.71	3.10 ± 0.17	0.76	5.20 ± 0.23	0.82	5.39 ± 0.16	0.76	7.06 ± 0.14	0.45	7.41 ± 0.13	0.60
Oktyabrsky	3.22 ± 0.09	0.30	3.30 ± 0.11	0.51	6.62 ± 0.19	0.67	6.56 ± 0.16	0.73	9.24 ± 0.16	0.57	9.16 ± 0.16	0.75
	3.43 ± 0.20	0.73	3.32 ± 0.17	0.77	6.68 ± 0.28	0.97	6.57 ± 0.21	0.94	8.80 ± 0.16	0.53	8.96 ± 0.15	0.64
Krutogorovsky	2.39 ± 0.18	0.65	2.39 ± 0.15	0.67	5.47 ± 0.22	0.78	5.57 ± 0.24	1.07	8.73 ± 0.23	0.81	8.88 ± 0.24	1.03
	2.52 ± 0.16	0.55	2.40 ± 0.18	0.79	5.88 ± 0.31	1.03	5.88 ± 0.23	0.98	8.67 ± 0.17	0.57	8.63 ± 0.23	1.01
Ptichii Island	2.26 ± 0.32	1.14	2.36 ± 0.25	1.05	6.69 ± 0.21	0.75	6.66 ± 0.16	0.65	9.61 ± 0.19	0.70	9.59 ± 0.16	0.67
	2.67 ± 0.25	0.82	2.62 ± 0.20	0.73	6.90 ± 0.31	0.98	6.69 ± 0.27	1.01	9.72 ± 0.18	0.56	9.61 ± 0.17	0.65

NOTE: Data for odd years in the numerator, and data for even years in denominator.
($\overline{X}$ = mean. $m_{\bar{x}}$ = standard error of the mean. σ = standard deviation of the observations.

during odd years. Thus, young pink salmon of odd year-classes appeared to be more susceptible to the impact of temperature than those of even year-classes. The opposite exists in the summer average temperatures, but their variations are not as important to pink salmon as are the variations in the average temperatures for May and June.

The Effects of Hydrometeorological Conditions in Rivers and Inshore Areas on their Rate of Return of Pink Salmon

Pink salmon of odd and even years differ significantly in abundance. The two lines are essentially isolated from each other, so they will be treated separately below.

For odd-year generations during years of low pink salmon abundance, there is quite a clear relationship between the rate of return and either the water temperatures in May and June or the summer average temperature. During the period of high abundance that began in 1975 and 1977, stock density became more important and dominated the effects of hydrological factors. Thus, during this period there is a marked inverse relationship between the rate of return and abundance of parental spawners. The direct relationship between rate of return and abundance of downstream migrating young (both absolute and per pair of spawners) is also significant for Utka River in the Oktyabrsky area.

In the southern regions, the pattern of water level during downstream migration did not significantly influence the rate of return during either odd or even years. The difference between the temperatures of river and sea water is significant only for the lowest temperatures. In the southern regions the relation of rate of return to the monthly mean temperatures in the coastal zone near the Icha River and Ptichii Island was less pronounced than it was to the summer average temperatures in the regions of downstream migration.

Thus, analysis of the situation in the two southern areas (Ozernovsky and Oktyabrsky) already suggests that a complex of factors can influence young pink salmon in the rivers and coastal areas, any one of them being of possible importance in limiting abundance when its magnitude is critically low. Therefore, while these factors may equally influence abundance of year-classes, one of them dominates under actual ecological conditions. So in this situation, as noted by Dekhnik et al. (1985), it is not possible to select a factor that would determine the abundance of all year-classes.

In order to evaluate the individual impact of each of the factors in question, and of their sum, simple and multiple coefficients of correlation were estimated for each area and, in some cases, for certain time periods; the latter were concluded to evaluate the role of each factor during periods of its greatest importance to the population (Table 2). Inclusion of a greater number of indices in the estimate was usually accompanied by a shortening of the time period, both because of shortage of data and also the necessity of considering the possibility of unequal impact of factors on the population under different conditions. In spite of the decrease in the number of degrees of freedom, this procedure always resulted in a marked increase in the magnitude, and in some cases, of the significance, of the multiple correlation coefficient. Thus, the multiple correlation coefficients for odd generations of pink salmon of southwestern Kamchatka (Ozernovsky and Oktyabrsky areas) were increased to 0.747 and 0.980, respectively (Table 2).

The odd-year pink salmon year-classes in the Krutogorovsky and Khairyuzovsky regions were less affected by the temperature regime in the rivers and coastal zone than were those farther south. In the Krutogorovsky and Khairyuzovsky regions a significant role was played by the volume of flow of the rivers in June, as well as by the abundance of the parent spawners. (This factor is of importance only when population abundance is high, so that simple correlation coefficients, computed over long time spans that include periods of low abundance, have low values; that is, its effect is leveled out in these cases.) Addition of the June river levels increased the multiple correlation coefficients for the Krutogorovsky area to 0.833, and for the Khairyuzovsky area to 0.401 (Table 2).

TABLE 2. Simple (r) and multiple (R) correlation coefficients of the rate of return of pink salmon in different regions of the west coast of Kamchatka with hydrometeorological factors (in rivers and coastal waters at time of downstream migration and inshore feeding) and with abundance of spawners.

Region	Odd year-classes				Even year-classes			
	Years	Factors	r	R	Years	Factors	r	R
Ozernovsky	1959–83 (n = 13)	X_1	0.168		1960–84 (n = 13)	X_2	0.346	
		X_2	0.150			X_3	0.425	
		X_3	0.057			X_4	0.492	
		X_4	0.061	0.238		X_7	0.130	0.601*
	1967–81 (n = 8)	X_1	0.559					
		X_2	0.247					
		X_3	0.443					
		X_4	0.654					
		X_5	0.377	0.747				
Oktyabrsky	1959–77 (n = 10)	X_1	0.390		1960–84 (n = 13)	X_2	0.260	
		X_2	0.087			X_4	0.388	
		X_3	0.627	0.742*		X_7	0.258	0.474
	1975–85 (n = 6)	X_1	0.794		1972–84 (n = 7)	X_2	0.936	
		X_2	0.033			X_4	0.930	
		X_3	0.224			X_6	0.957	
		X_4	0.898	0.898		X_7	0.930	
	1971, 1973 and 1977–85 (n = 7)	X_1	0.959			X_8	0.944	
		X_2	0.508			X_9	0.969	0.993
		X_3	0.771					
		X_4	0.571					
		X_8	0.967					
		X_9	0.881	0.980				
Krutogorovsky	1959–85 (n = 14)	X_1	0.269		1960–84 (n = 13)	X_2	0.199	
		X_2	0.028			X_3	0.473	
		X_3	0.025			X_4	0.446	0.553
		X_4	0.455	0.577*				
	1967–81 (n = 8)	X_1	0.259		1966–82 (n = 9)	X_2	0.335	
		X_2	0.520			X_3	0.384	
		X_3	0.646			X_4	0.289	
		X_4	0.039			X_5	0.583	
		X_5	0.603	0.833		X_6	0.475	0.842*
Khairyuzovsky	1959–69, 1973, 1977–83 (n = 11)	X_1	0.494		1960–84 (n = 13)	X_1	0.198	
		X_2	0.327			X_2	0.103	
		X_3	0.259			X_3	0.228	
		X_4	0.064	0.069		X_4	0.341	0.496
	1967–81 (n = 8)	X_4	0.033		1966–82 (n = 9)	X_1	0.007	
		X_5	0.334	0.401		X_2	0.145	
						X_3	0.225	
						X_4	0.069	
						X_5	0.114	
						X_6	0.175	0.596

NOTE: Sea water temperature: X_1 in May, X_2 in June, X_3 average for summer; X_4 is numbers of spawners on spawning grounds; X_5 is yield of river water in June; X_6 is the difference in temperature between river and sea water; X_7 is the average summer temperature in the area of Icha River-Ptichii Island; X_8 is absolute numbers of downstream juveniles in Utka River; X_9 is average of downstream juveniles in Utka River per pair of spawners.

*R is statistically significant at the P = 0.05 level.

Temperature regime was not as important for even-year generations, even in southern areas. This is especially true for May, and to some extent, June temperatures, which, as was mentioned above, were quite uniform between years. In the northern areas also, only extreme negative anomalies could be a major and undeniable cause of reproduction decrease, as happened in May 1969 in the Khairyuzovsky area.

Abundance factors were basic in determining the strength of even-year generations. In addition to the abundance of the parental generation on the spawning grounds, one such factor was the abundance, both relative and absolute, of the young migrating downstream (in the Utka River in our case), in the Oktyabrsky area. The multiple correlation coefficient for this area, estimated using all the factors in question, appeared to be very high, 0.993 (Table 1). In addition to the abundance factors, the factor of river water flow in June in northern areas was important in even-year generations, just as in odd ones. It increased the multiple correlation coefficient to 0.842 for the Krutogorovsky area and to 0.596 for the Khairyuzovsky area.

On the whole, in spite of usually large and sometimes extremely large, simple and multiple correlation coefficients, estimates of their significance rarely permitted rejection of the null hypothesis. However, as Lakin (1973) has emphasized, this does not mean that there is no correlation between the characters. This fact may indicate too small a sample and not necessarily an absence of correlation.

Forecasting the 1987 Rate of Return of Pink Salmon in Regions of Western Kamchatka

Regressions of rate of return on each hydrometeorological and abundance factor were obtained for the purpose of forecasting this rate of return to the various Kamchatka areas in 1987. Such curves were estimated for a number of odd-year generations of pink salmon for each of four areas (Fig. 1–4). Values of the factors that are expected to influence the run of 1987 are marked by vertical broken lines. Their intersection with the curves indicates the rate of return in 1987, as predicted from the influence of a single factor only. It is too bad that such a significant factor as water level in June could not be used, owing to the lack of appropriate information.

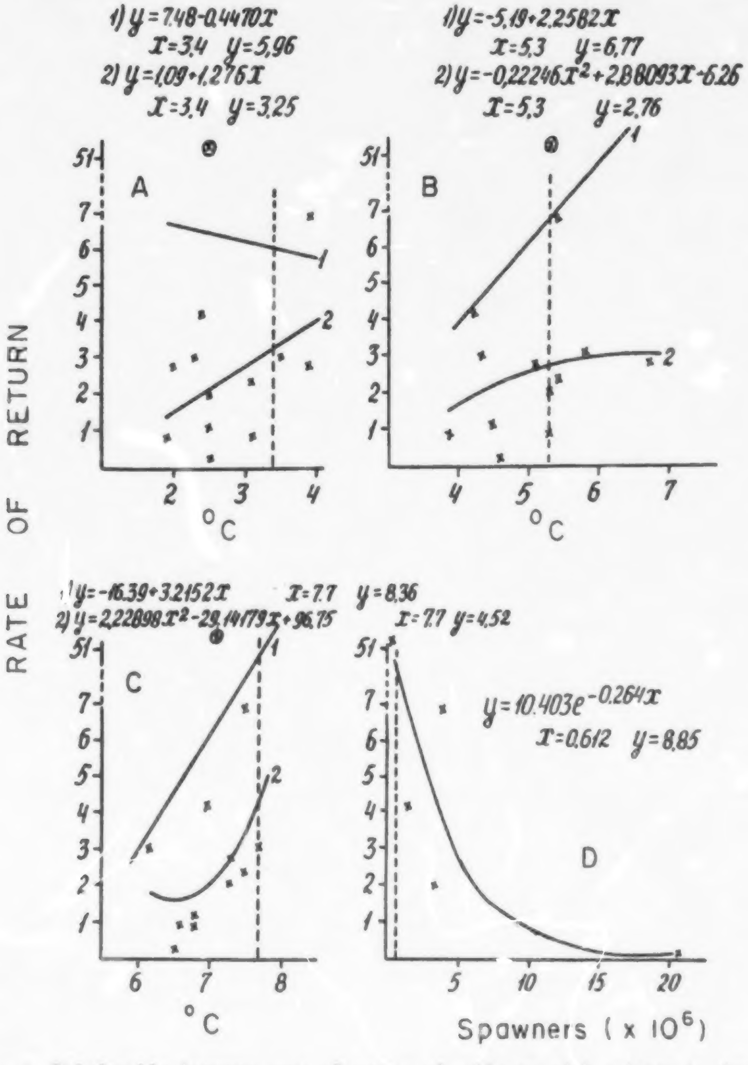

FIG. 1. Relationship between rate of return of odd-year pink salmon in the Ozernovsky region and mean temperature in the coastal region: (A) in May; (B) in June; (C) in the entire year. Panel (D) relates rate of return to the abundance of parental spawners. Vertical broken lines indicate the 1987 temperature values used for forecasts. Return rate for 1987 is indicated for each regression. The 1975 rate of return was 51, greatly exceeding all other years. Consequently two different regressions were computed: 1. using 1975; and 2. without 1975.

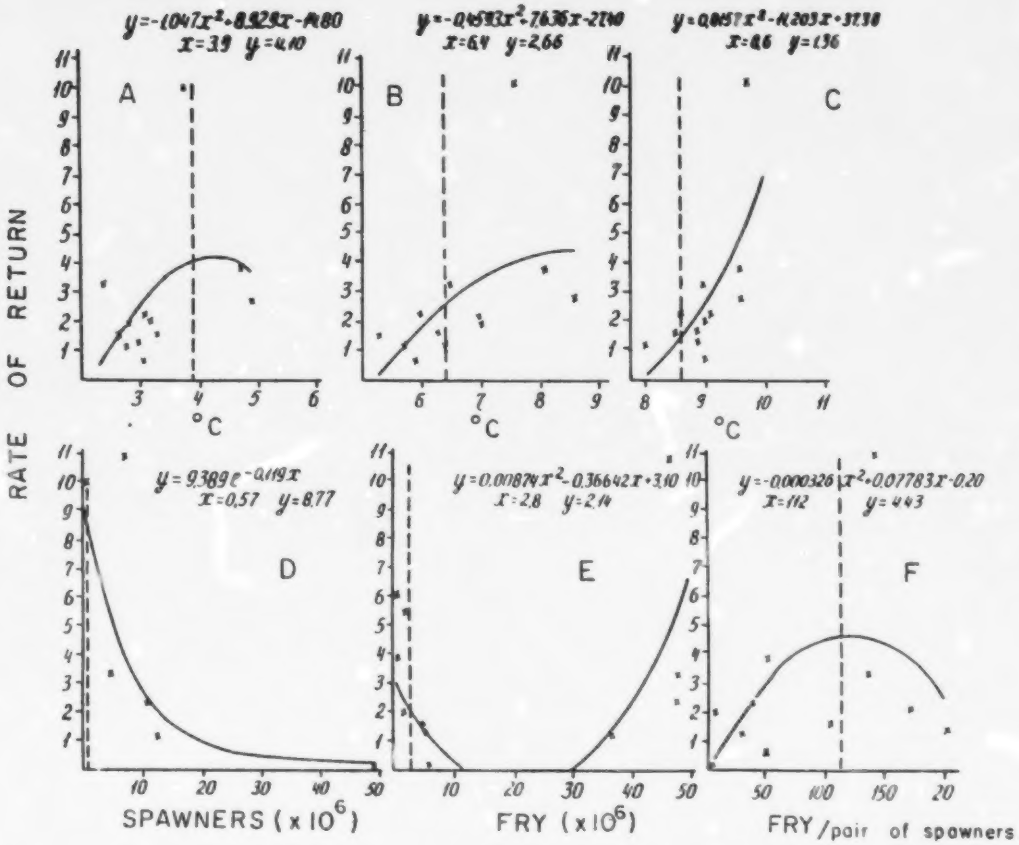

FIG. 2. Relationship between rate of return of odd-year pink salmon in the Oktyabrsky region and mean temperature in the coastal region: (A) in May; (B) in June; (C) in the entire year. Panel (D) relates rate of return to the abundance of parental spawners. Panel (E) is the relationship of rate of return to the absolute number of downstream migrants in the Utka River; and panel (F) is the number of Utka migrants per pair of parental spawners.

Sets of necessary factors (Table 1) were chosen for the time period which, to our mind, was most representative of modern conditions and which have large enough simple and multiple correlation coefficients. The second set was chosen for the Ozernovsky region; the third for the Oktyabrsky region; and the fourth for the Krutogorovsky and Khairyuzovsky regions (Table 2). For the sets chosen I computed, for each factor, the magnitude of its simple correlation coefficient with the rate of return, and then the percentage that each coefficient was of the total. This approach makes it possible, from the estimate of the rate of return obtained from the regression line, to compute the relative influence of each factor on the resulting rate of return in 1987 for each region (Table 3). These estimates suggest that in the Ozernovsky region 5.41 times as many pink salmon will return in 1987 as were present in the parent generation. The other figures are: Oktyabrsky, 3.72; Krutogorovsky, 2.50; and Khairyuzovsky, 3.67 (Table 3).

Because no adequate data were available to make analyses for the extreme northwestern and Kirovsky regions, estimates for Khairyuzovsky and Krutogorovsky were used, respectively, because the patterns of population dynamics appeared to be similar in the corresponding regions.

To sum up, knowing the number of spawners on spawning grounds of pink salmon in western Kamchatka in 1985, it was not difficult to estimate the runs expected in 1987, for individual areas as well as for the whole region.

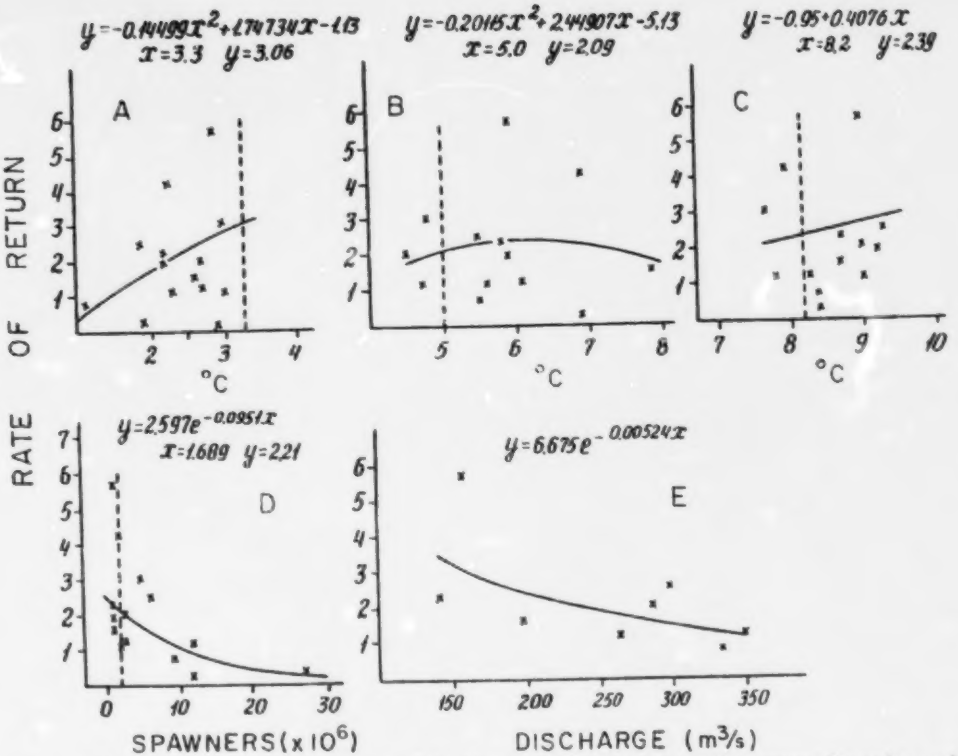

FIG. 3. Relationship between rate of return of odd-year pink salmon in the Krutogorovsky region and mean temperature in the coastal region: (A) in May; (B) in June; (C) in the entire year. Panel (D) relates rate of return to the abundance of parental spawners. Panel (E) is the relation of rate of return to the mean discharge of the rivers in June.

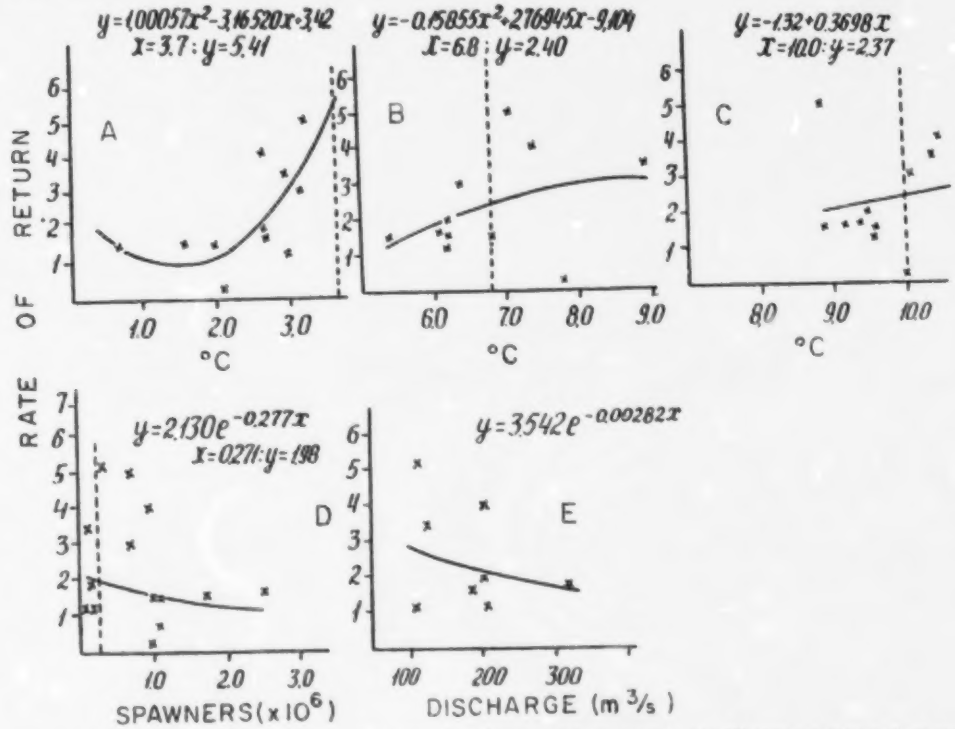

FIG. 4. Relationship between rate of return of odd-year pink salmon in the Khairyuzovsky region and mean temperature in the coastal region: (A) in May; (B) in June; (C) in the entire year. Panel (D) relates rate of return to the abundance of parental spawners. Panel (E) is the relation of rate of return to river discharge in June.

TABLE 3. Computation of predicted rates of return of pink salmon spawners in different regions of West Kamchatka in 1987.

Region	Spawning year-classes used in computations	Factors	Simple correlation coefficient (*r*)	Percentage of their total	Estimated rate of return from regression	Contribution of each factor to total rate of return	Total predicted rate of return
Khairyuzovsky							
	1959–69,	X_1	0.494	43.18	5.41	2.336	
	1973,	X_2	0.327	28.58	2.40	0.686	
	1977–83	X_3	0.259	22.64	2.37	0.537	
		X_4	0.064	5.60	1.98	0.111	3.67
		$\Sigma =$	1.144	100.00			
Krutogorovsky							
	1959–85	X_1	0.269	34.49	3.06	1.055	
		X_2	0.028	3.59	2.09	0.075	
		X_3	0.025	3.20	2.39	0.076	
		X_4	0.458	58.72	2.25	1.298	2.50
		$\Sigma =$	0.780	100.00			
Oktyabrsky							
	1971, 1973,	X_1	0.959	20.59	4.10	0.844	
	1977–85	X_2	0.508	10.91	2.66	0.290	
		X_3	0.771	16.56	1.36	0.225	
		X_4	0.571	12.26	8.77	1.075	
		X_8	0.967	20.76	2.14	0.444	
		X_9	0.881	18.92	4.43	0.838	3.72
		$\Sigma =$	4.657	100.00			
Ozernovsky							
	1967–81	X_1	0.559	29.37	3.25	0.955	
		X_2	0.247	12.98	2.76	0.358	
		X_3	0.443	23.28	4.52	1.052	
		X_4	0.654	34.37	8.85	3.042	5.41
		$\Sigma =$	1.903	100.00			

References

CHUPAKHIN, V. M., AND A. M. KAEV. 1982. The problem of how year-class abundance of pink and chum salmon is determined in the coastal waters of the Island of Iturup, p. 331–332. *In* Vsesoyuzn. konf. po teorii formirovaniya chislennosti i ratsionalnogo ispolzovaniya stad promyslovykh ryb (tez. dokl., Moskva, Oktyabr 1982), Moskva. (In Russian)

DEKHNIK, T. V., V. P. SEREBRYAKOV, AND S. G. SOIN. 1985. The importance of early stages of development in determining the abundance of year-classes of fish, p. 56–72. *In* Teoriya formirovaniya chislennosti i ratsionalnogo ispolzovaniya stad promyslovykh ryb. Nauka, Moskva. (In Russian)

IVANKOV, V. N. 1984. Causes of periodic and yearly fluctuations in the abundance, and changes in the biological signs of pink salmon (*Oncorhynchus gorbuscha* Walbaum — Salmonidae) of the southern Kuril Islands. Vopr. Ikhtiol. 24(6): 895–906. (In Russian)

KARPENKO, V. I. 1982. Factors that determine the survival and abundance of young Pacific salmon in the coastal waters of eastern Kamchatka, p. 158–159. *In* Vsesoyuzn. konf. po teorii formirovaniya chislennosti i ratsionalnogo ispolzovaniya stad promyslovykh ryb (tez. dokl., Moskva, Oktyabr 1982), Moskva. (In Russian)

LAKIN, G. F. 1973. Biometry. Vysshaya shkola, Moskva. 343 p. (In Russian)

Buoyancy of Walleye Pollock (*Theragra chalcogramma*) Eggs in Relation to Water Properties and Movement in Shelikof Strait, Gulf of Alaska

Arthur W. Kendall, Jr.

Northwest and Alaska Fisheries Center, Resource Assessment and Conservation Engineering Division,
7600 Sand Point Way Northeast, BIN C15700, Building 4, Seattle, WA 98115-0070, USA

and Suam Kim

School of Fisheries, University of Washington, Seattle, WA 98195, USA

Abstract

Kendall, A. W., Jr., and S. Kim. 1989. Buoyancy of walleye pollock (*Theragra chalcogramma*) eggs in relation to water properties and movement in Shelikof Strait, Gulf of Alaska, p. 169–180. *In* R. J. Beamish and G. A. McFarlane [ed.] Effects of ocean variability on recruitment and an evaluation of parameters used in stock assessment models. Can. Spec. Publ. Fish. Aquat. Sci. 108.

Specific gravity measurements of developing walleye pollock (*Theragra chalcogramma*) eggs show that during their 2-wk incubation period they become heavier during middle stages of development, while they are lighter just after spawning and just before hatching. Comparisons of specific gravity of the eggs and of water at depth in Shelikof Strait indicate the levels of neutral buoyancy at various stages of development. Young and old stages of eggs balance with the water in the deep layer of the water column, while middle-stage eggs balance with that of mid-depth. Discrete depth plankton sampling confirms the stage-depth distribution predicted from specific gravity considerations. This has allowed us to develop a model of the depth distribution of eggs and to infer how horizontal water movements at various depths affect egg dispersal from the spawning area. Generally, the egg mass has a relatively low advection rate (e.g., 2.5 km d^{-1} in April 1985) due to its deep location. Interannual differences in water properties, the specific gravity of the eggs, and the current system largely determine the area of hatching and may influence subsequent larval abundance, transport, and feeding regime.

Résumé

Kendall, A. W., Jr., and S. Kim. 1989. Buoyancy of walleye pollock (*Theragra chalcogramma*) eggs in relation to water properties and movement in Shelikof Strait, Gulf of Alaska, p. 169–180. *In* R. J. Beamish and G. A. McFarlane [ed.] Effects of ocean variability on recruitment and an evaluation of parameters used in stock assessment models. Can. Spec. Publ. Fish. Aquat. Sci. 108.

Les mesures de la densité des oeufs de la goberge de l'Alaska (*Theragra chalcogramma*) révèlent que durant la deuxième semaine de la période d'incubation, ils sont plus lourds au cours des stades intermédiaires de développement, tandis qu'ils sont plus légers juste après la ponte et juste avant l'éclosion. En comparant la densité des oeufs et celle des eaux profondes dans le détroit de Shelikof, les auteurs ont déterminé les degrés de flottabilité au cours des diverses étapes du développement. Au début et à la fin de la croissance, les oeufs demeurent en suspension dans l'eau dans la couche profonde de la colonne, tandis qu'au cours des stades intermédiaires de leur développement, c'est au milieu de la colonne d'eau qu'ils se maintiennent en équilibre. Les échantillons de planctons prélevés en discontinu confirment les données sur la distribution obtenues d'après la densité. À l'aide de ces données, les auteurs ont pu élaborer un modèle de la distribution des oeufs en fonction de la profondeur et déterminer par inférence comment les mouvements horizontaux de l'eau à diverses profondeurs influent sur la dispersion des oeufs dans la zone de fraye. En règle générale, la masse des oeufs présente un taux d'advection relativement faible (par exemple, 2,5 km j^{-1} en avril 1985) en raison de la profondeur de l'eau. Les différences observées d'une année à l'autre quant aux propriétés de l'eau, à la densité des oeufs et aux systèmes de courants déterminent, dans une large mesure, la zone d'éclosion et peuvent ultérieurement influer sur l'abondance des larves, leur transport et leur régime alimentaire.

Introduction

Many marine teleosts spawn a large number of eggs every year; however, most of these die as planktonic eggs and larvae due to starvation, predation, transport to unfavorable nursery areas, or intrinsic physiological weakness. Mass mortality during the planktonic stage has been reported frequently (Smith 1973; Lasker 1975; Koslow et al. 1985). Knowledge of the distribution and advection patterns of fish eggs and larvae near the spawning or nursery ground provides the context for studying the mechanisms of survival and the recruitment process (Nakatani and Maeda 1981, 1983). The distribution and abundance of eggs and larvae depend on biological characteristics (e.g., spawning intensities with time and place, developmental periods, buoyancy of eggs and larvae, existence of predators and food organisms) as well as interactions with environmental variables (e.g., current velocities and directions, water temperatures, and water densities).

Limited investigations on the buoyancy of pelagic fish eggs have been conducted. The main force for positive buoyancy of pelagic fish eggs is not lipid content, but instead the large quantities of dilute aqueous fluid, which originates from maternal body fluid (Craik and Harvey 1987). Sundnes et al. (1965) found that changes in hydrostatic pressure did not affect the flotation of Atlantic cod (*Gadus morhua*) eggs, and that egg density steadily increased with development. Such a density increase of fish eggs during ontogeny has been reported by several investigations, e.g., Haug et al. (1986) for Atlantic halibut (*Hippoglossus hippoglossus*) eggs in Norway, Coombs et al. (1985) for sprat (*Sprattus sprattus*) and pilchard (*Sardina pilchardus*) eggs off Plymouth, U.K., and Nakatani and Maeda (1984) for walleye pollock (*Theragra chalcogramma*) eggs in Japan. These studies are based on averages of point estimates of specific gravity of individual eggs at various stages of development. From field observations in the Bering Sea, Nishiyama et al. (1986) hypothesized that young walleye pollock eggs were abundant in the upper layer but older eggs sank and aggregated in the 20- to 30-m layer.

Planktonic fish eggs will meet with continuously changing environmental situations once they are spawned, because currents and turbulence in the ocean will transport and disperse them. Advection (or nontidal drift) is one of the ways water movements may affect pelagic early life stages. Frequently in the distribution of fish eggs and larvae, transport by major currents is more important than other effects such as diffusion and periodic tidal motion (Fujimoto and Hirano 1972).

Since the discovery in 1980 of a large spawning population of walleye pollock in the Shelikof Strait, Gulf of Alaska, extensive research has been conducted on the life history of this population (e.g., Kendall et al. 1987; Reed et al. 1989). Walleye pollock in Shelikof Strait have a relatively short spawning period (March–May) and a relatively long incubation period (around 2 wk at 5°C) (Bates 1987). In contrast to the shallow (mostly 0–50 m) vertical distribution of this species in the Bering Sea (Serobaba 1974) and near Funka Bay, Japan (Nakatani and Maeda 1981), walleye pollock eggs in Shelikof Strait are spawned and develop at depth (100–300 m) and the larvae reside in the upper layers (20–50 m) (Kendall et al. 1987). As we show in this paper, during incubation the eggs exhibit vertical movement within the water column due to changes in egg specific gravity during development and differences in water density with depth. Concurrently, the eggs meet various current velocity fields corresponding to their depth in the water column, and are advected from the site of spawning. After hatching, the larvae are found in the upper layer and have a long period of drift (ca. 2 mo) before transforming into juveniles. Because of the relatively long duration (at least 3 mo) of the planktonic egg and larval period together, environmental conditions may severely affect recruitment.

In this paper, the vertical distribution of walleye pollock eggs, their changes in specific gravity during ontogeny, and advection, diffusion, and aggregation of the egg mass will be examined, focusing on environmental effects on egg dispersal.

Methods and Data

Plankton Collections

Data used to describe the distribution patterns of eggs were collected in Shelikof Strait aboard the NOAA ship *Miller Freeman* during April 1985 and April 1986.

During the egg survey in April 1985, 98 bongo samples were collected to investigate horizontal distribution, and 20 Tucker trawl samples were taken at five stations in the region of peak spawning to investigate vertical distribution. The nets used were a 20-cm diameter MARMAP bongo sampler and a 1-m^2 mechanically operated Tucker trawl, both with 0.505 mm mesh. At the bongo stations, the sampler was lowered to near-bottom at a rate of 50 m of wire out per min, allowed to stabilize for around 30 sec, and then retrieved at a wire speed of 20 m/min. Flowmeters mounted in the center of net mouths and a bathykymograph (BKG) attached to the sampler were used to calculate the amount of water filtered and to determine maximum tow depth and to evaluate tow profile during sampling. The Tucker trawl was deployed to sample four depth intervals (average depth intervals from the five stations were 40–94 m, 93–157 m, 158–223 m, and 218–251 m). Separate tows were made in quick succession for each depth interval. The Tucker trawl was lowered to the predetermined lower limit of the sampling interval, and the net mouth was opened with a messenger. The trawl was then towed with constant wire angle for about 5–6 min as the wire was retrieved at a rate of between 10 and 50 m/min. When the sampler reached the upper limit of the sampling depth interval determined by wire-out, a second messenger closed the net mouth, and the net was brought to the surface. Flowmeters and bathykymographs were used as with the bongo tows.

In April 1986, Clarke-Bumpus plankton nets with 0.505 mm mesh were used at 16 stations located in or near the peak spawning area in order to study the vertical distribution of eggs. Five nets were used simultaneously on the same towing wire with each net sampling a specified depth interval. Two 25.0-cm diameter samplers were used for the upper two layers of the water column (0–54 m and 54–108 m) and three 12.5-cm diameter samplers were used for the lower three layers (108–162 m, 162–216 m, and 216–277 m). The samplers were deployed in a closed configuration, to be opened by a messenger trip after the string of samplers had obtained the desired depths and the ship had reached towing speed. They were then towed for about 20 min, closed by messenger, and retrieved. Flowmeters were used in each sampler and a bathykymograph was attached to the towing wire near the deepest sampler.

Adult Walleye Pollock Collections

If ambient light were insufficient to stimulate adult feeding on eggs at depth, fish might swallow eggs accidentally, so that each walleye pollock caught could be regarded as a sampling device. Under the assumption that the adults swallow eggs inadvertently, the numbers of eggs in their stomachs provided information on the distribution of the eggs where the adults were collected. For these investigations adult walleye pollock were collected by trawling in the main spawning area with a Diamond 1000 midwater trawl having a mouth height of 12–20 m, as used by the Northwest and Alaska Fisheries Center (NWAFC) hydroacoustic assessment task (E. Nunnallee, NWAFC, pers. comm.). During April 1986, four tows at different depths were made, two during the night, (97 m and 205 m) and two during the day (152 m and 229 m) to distinguish day–night and depth differences in egg predation. The trawl was towed for 15–40 min (around 1.6–3.6 km). Approximately 100 walleye pollock were randomly selected from each catch, standard length and sex were recorded, and stomachs were preserved in 10% formalin. Eggs found in each stomach were counted later in the laboratory.

Sorting, Counting, and Staging of Eggs

Ichthyoplankton samples from bongo nets were sorted and counted at the Polish Plankton Sorting Center, Szczecin, Poland, and samples from Tucker trawl and Clarke-Bumpus samplers were sorted and counted at the NWAFC, Seattle, Washington. The eggs in adult stomachs were counted at the NWAFC. The embryonic development of the eggs was originally divided into 21 stages (Fig. 1), but the eggs were regrouped into the following categories assuming 5°C seawater temperature throughout development:

Group 1: Stage 1 to 6 (cell stage; less than 1 day old)
Group 2: Stage 7 to 8 (early germ ring stage; 2–3 days old)
Group 3: Stage 9 to 12 (germ ring stage; 4–5 days old)
Group 4: Stage 13 to 15 (middle stage; 6–7 days old)
Group 5: Stage 16 to 18 (early late stage; 8–10 days old)
Group 6: Stage 19 to 21 (late late stage; 11–14 days old)

The catches of eggs of each age-group from each sample were standardized to number per 10 m² or number per 1 000 m³ using the procedures described by Smith and Richardson (1977).

Specific Gravity Measurements

To measure specific gravity of walleye pollock eggs continuously from fertilization to hatching, we performed two kinds of experiments using an Egg Density Gradient Apparatus (EDGAR; Coombs 1981). Long-term experiments occurred when the specific gravities of eggs were continuously observed during embryonic development. Instantaneous specific gravity measurements for various stages of eggs collected from the sea were regarded as short-term experiments.

In April 1985, eggs collected from Shelikof Strait were kept in insulated water bottles and transported by air to Seattle for specific gravity measurements. Only middle and late stage eggs were then available for experiments. A total of 45 eggs was used for short-term experiments, while 10 eggs were used for long-term experiments (a maximum of 145 h from introduction until hatching in the gradient water columns at a water temperature of around 5°C).

In April 1986, the EDGAR was used aboard the NOAA ship *Miller Freeman* to include very young eggs in the experiments. Twelve eggs were obtained by artificial fertilization and used in a long-term experiment. Their specific gravities were noted at time intervals of 0.5 to 3.0 h until the end of the cruise (a total of 180 h). Also, 37 eggs were collected from the sea, and their instantaneous specific gravities were measured. All eggs were preserved after the experiments in 3–5% formalin and identified by developmental stage later in the laboratory.

Analytical Methods

The vertical velocity of eggs within the water column was estimated by applying Stokes law to the results from the specific gravity experiments as in Alderdice and Forrester (1971) and Sundby (1983). When the Reynolds number (the ratio of inertial to viscous forces) is less than about 0.5 (Sundby 1983), the terminal velocity (w) of a particle in a fluid is a function of its size, the density difference between the particle and the medium, and the molecular viscosity of the fluid. For the case of fish eggs in water,

$$w = \frac{1}{18} g d^2 (p(e) - p(w)) v^{-1}$$

where w is the terminal velocity in cm/s, g is the gravitational acceleration (cm•s^{-2}), d is egg diameter (cm), $p(e)$ and $p(w)$ are the densities of egg and water, and v is the molecular viscosity of water.

Advection and diffusion of eggs based on the 1985 bongo net survey were examined by calculating the location of the distributional centroid and the variance of the distribution, respectively (Koslow et al. 1985). When the egg mass is defined in terms of number of eggs sampled at station i and their distance from an arbitrarily fixed point (here, 59°N and 153°W is used), the centroid is identical to the weighted mean distance:

$$\overline{X}(j) = \frac{\sum_{i=1}^{n} N(j,i) X(i)}{\sum_{i=1}^{n} N(j,i)}$$

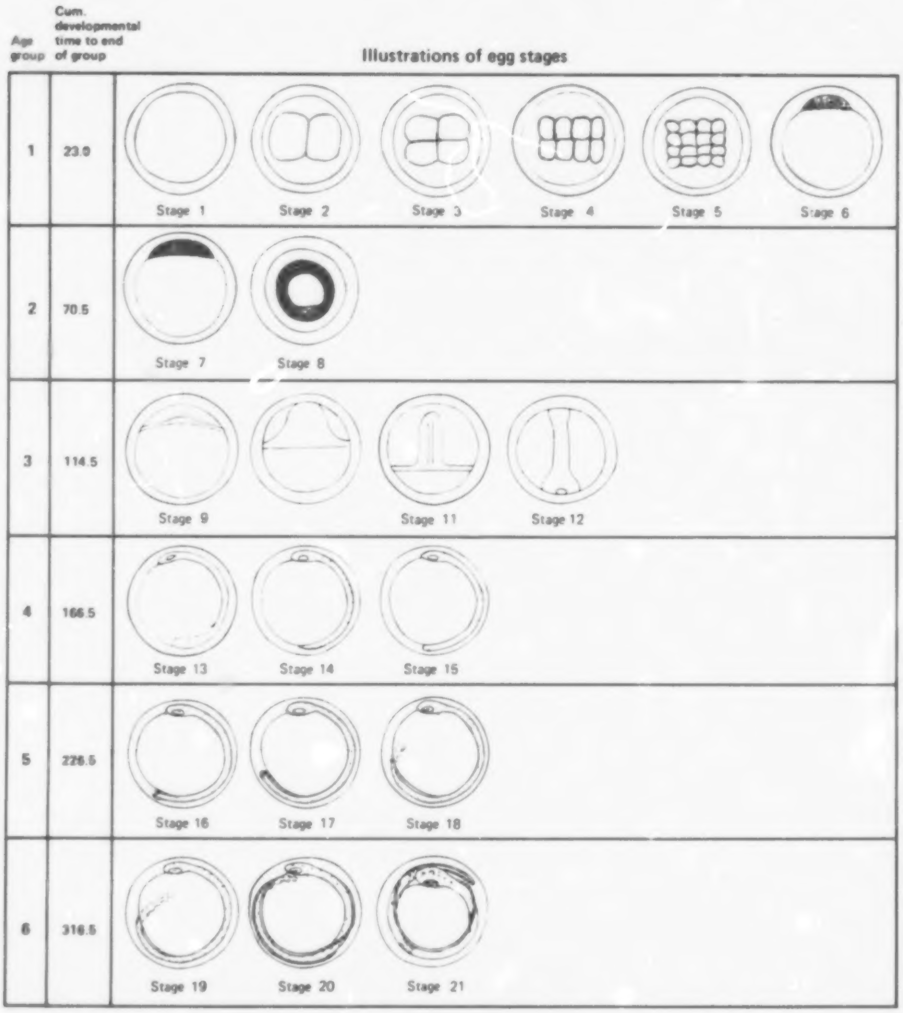
Age group
Cum. developmental time to end of group
Illustrations of egg stages
1
23.0
Stage 1
Stage 2
Stage 3
Stage 4
Stage 5
Stage 6
2
70.5
Stage 7
Stage 8
3
114.5
Stage 9
Stage 11
Stage 12
4
166.5
Stage 13
Stage 14
Stage 15
5
226.5
Stage 16
Stage 17
Stage 18
6
316.5
Stage 19
Stage 20
Stage 21

FIG. 1. Walleye pollock egg stages and age-groups based on constant (5°C) water temperatures. Egg stages from A. C. Matarese, NWAFC, pers. comm.

$$\overline{Y}(j) = \frac{\sum_{i=1}^{n} N(j,i)\,Y(i)}{\sum_{i=1}^{n} N(j,i)}$$

where $X(i)$ and $Y(i)$ are distances of along- and cross-strait components from origin point to station i, $N(j,i)$ is the number of age-group j eggs sampled at station i, and $\overline{X}(j)$ and $\overline{Y}(j)$ are the centers of along- and cross-strait components. The standard deviation of the particle distribution can be regarded as the diffusion width at that time (Okubo 1980), and the variance from the centroid is expressed as:

$$S^2(x,j) = \frac{\sum_{i=1}^{n} N(j,i)(X(i)-\overline{X}(j))^2}{\sum_{i=1}^{n} N(j,i)}$$

$$S^2(y,j) = \frac{\sum_{i=1}^{n} N(j,i)(Y(i)-\overline{Y}(j))^2}{\sum_{i=1}^{n} N(j,i)}$$

$$S^2(x,y) = 2((S^2(x,j))(S^2(y,j)))^{0.5}$$

where $S^2(x,j)$ and $S^2(y,j)$ are variances of along- and cross-strait coordinates of age-group j, respectively, and $S^2(x,y)$ is the variance of distribution of egg group j.

To describe the aggregation of the distribution based on the stomach content data, Lloyd's (1967) Patchiness Index (LPI), the ratio of "mean crowding" to the mean density, was used because it is unaffected by population density (Hewitt 1982). The LPI estimation by moments leads to:

$$\text{LPI} = \frac{\overset{*}{X}}{\overline{X}}$$

$$= \frac{\overline{X} + ((S^2/\overline{X} - 1)\,(1 + S^2/(q\,\overline{X}^{\,2})))}{\overline{X}}$$

$$\text{Var (LPI)} = ((S^2/\overline{X}^2)^2)\,(2\overset{*}{X}/q\overline{X})$$

where $\overline{X}$, S, q, and $\overset{*}{X}$ are the mean egg number, standard deviation of sample, sample size, and mean crowding, respectively.

In addition to LPI, the binomial statistical test was used to evaluate the patchiness of stomach content data. As the mean number of individuals per sampling unit becomes smaller, the binomial distribution tends to a Poisson distribution. Therefore, by comparing the sample mean (m) with the variance (s^2), distributions can be distinguished as random (i.e., $s^2/m = 1$), uniform (i.e., $s^2/m < 1$), or clumped (i.e., $s^2/m > 1$) (Okubo 1980; Zar 1974).

Results and Discussion

Vertical Distribution of Eggs

For 1985 and 1986 the vertical distribution of eggs showed similar patterns (Table 1). All sampling in 1985 was successful, whereas in 1986 we achieved good vertical samples at only eight (50%) of the Clarke-Bumpus stations due to mechanical problems with the samplers. Furthermore, because two of these stations were not in the area of the concentrated egg mass, data for 1986 are based on only six stations.

In April 1985, the number of eggs increased with depth (Table 1a). Over 70% of all eggs were found in the deepest layer (218–251 m), 27% in the middle layer (158–223 m), and only 2.5% from surface to 157 m. Greater than 80%

TABLE 1. Standardized average number of eggs per 1000 m^3 at different depth intervals in the primary spawning area taken at (a) five Tucker Trawl stations, April 1985 and (b) six Clarke-Bumpus sampling stations, April 1986. Standard deviations are shown in parentheses.

Depth interval (m)	No. eggs sampled	Egg age-groups (age in days)					
		1 (1)	2 (2–3)	3 (4–5)	4 (6–7)	5 (8–10)	6 (11–14)
(a) Tucker Trawl							
40–94	752	31 (26)	189 (170)	232 (93)	142 (56)	139 (67)	20 (15)
93–157	4 338	267 (89)	579 (478)	809 (617)	965 (173)	1 385 (944)	332 (389)
158–223	55 035	26 620 (27 786)	1 707 (1 322)	4 322 (2 532)	7 236 (4 582)	8 776 (4 592)	6 375 (3 293)
[illegible]3–251	147 186	108 146 (64 065)	3 082 (3 104)	5 163 (3 248)	9 099 (7 222)	14 527 (6 740)	7 167 (3 840)
Total	207 311	135 065	5 557	10 525	17 442	24 827	13 894
(b) Clarke-Bumpus							
0–54	516	33 (71)	76 (87)	163 (183)	162 (205)	70 (59)	12 (13)
54–108	566	7 (11)	84 (103)	236 (212)	157 (120)	56 (43)	26 (44)
108–162	6 402	253 (427)	4 029 (4 907)	1 204 (1 845)	549 (293)	267 (209)	100 (94)
162–216	29 784	2 777 (4 975)	18 732 (29 944)	5 356 (4 938)	1 584 (1 457)	825 (665)	510 (397)
216–277	36 923	14 716 (26 354)	5 403 (6 815)	5 642 (4 694)	3 149 (2 359)	5 333 (2 556)	2 680 (1 061)
Total	74 231	17 753	28 324	12 601	5 601	6 551	3 328

of 1-d-old eggs (Group 1) were collected in the deepest layer, which indicated that the major spawning depth was below 200 m. For each age-group, over 50% of the eggs were in the deepest layer and approximately 90% were below 150 m. Approximately 99% of eggs that were 1 d old (Group 1) and 11–14 d old (Group 6) were found in the two lower layers, but for the middle age-groups, this tendency was decreased to around 90%. This difference in depth distribution of eggs as a function of age was substantiated by our specific gravity experiments.

Because young eggs are positively buoyant at the depth where they are spawned, they move toward the surface until their specific gravity is in balance with seawater density. Thereafter the eggs sink corresponding to an increase in density with development (see next section for details). Evidence for this can be seen by looking at the age composition from the upper layer samples. The largest component in the upper layer (40–94 m) samples was 4- to 5-d-old eggs (Group 3), with very small fractions of 1-d-old eggs (Group 1) and 11- to 14-d-old eggs (Group 6).

In April 1986, most eggs (90%) were in the lower layers (162–277 m), but when compared to 1985, a slightly larger fraction (10%) of the eggs was found in the surface layers (0–162 m). This might be caused by differences in upper layer water densities between 1985 and 1986. In April 1985 the average sigma-*t* values near Cape Kekurnoi, Alaska, at 50 m, 100 m, and 150 m were 25.34, 25.47, and 25.64, respectively, while those in 1986 were 25.56, 25.62, and 25.69 at layers of 0–54 m, 54–108 m, and 108–162 m, respectively. If the eggs had almost the same specific gravities in both years, the larger density difference between newly spawned eggs and the ambient sea water in 1986 would have increased the positive buoyancy of the eggs. Consequently, a larger proportion of the eggs would have floated to the upper layer in 1986. (This interannual difference in vertical distribution will be modelled later in this paper.) Another similarity in the vertical distribution patterns is that most 1-d-old eggs (Group 1) and 11- to 14-d-old eggs (Group 6) (96–99% of each stage total) were in the lower layers (162–277 m), and the percentage of middle age groups (2- to 7-d-old eggs; Groups 2–4) was greater in the upper (0–162 m) layer.

Clear evidence of vertical movements of eggs during development is seen when we examine the percentage of eggs occurring in each depth interval for each age group of eggs collected in 1986 (Fig. 2). The sum of proportions in each layer is 100% for each age-group of eggs. For example, among the 1-d-old eggs, 83% were found in the deep layer, 16% were in the middle layer, and only 1% was found in the upper layer. However, for 2- to 3-d-old eggs, 19% of total were in the deep layer and 66% were found in the middle layer. The dramatic decrease of 2- to 3-d-old eggs (Group 2) in the deep layer (216–277 m) and the corresponding increase of 2- to 3-d-old eggs in the middle layer (162–216 m) indicates rapid upward movement of eggs after spawning. As the eggs developed, an increasing fraction of old eggs was found in the deep layer, suggesting that the older eggs sink. Note that in the surface layer samples the largest component was 4- to 7-d-old eggs (Groups 2–4).

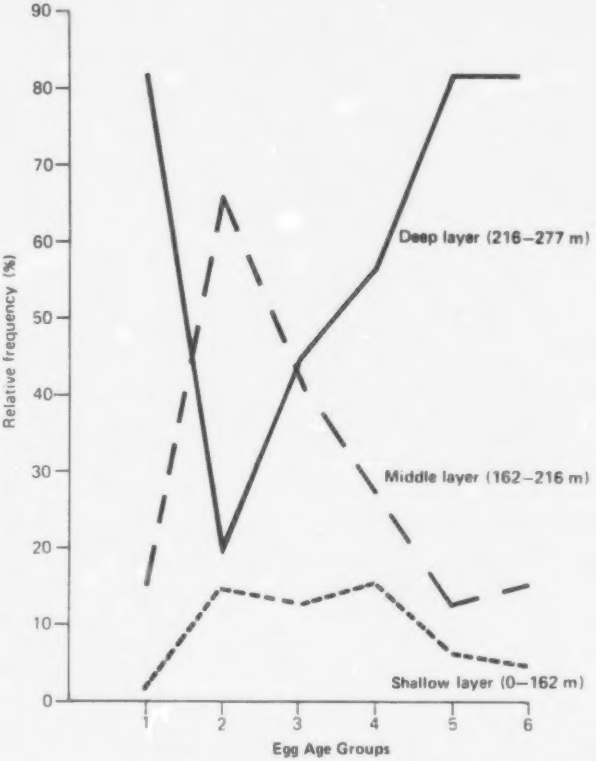

FIG. 2. Relative abundance of egg age-groups by depth.

At one location in the primary spawning area on 9 April 1986, where echo sounders indicated that walleye pollock schools were at around 100 m, and 150 m, and below 200 m, vertical Clarke-Bumpus samplings, 4 trawl hauls, and conductivity/temperature/depth (CTD) casts were made. The average numbers of eggs per stomach were small (<5) in the two trawl hauls at 97 m and 152 m, but those from the two deeper hauls (205 m and 229 m) were relatively high (>20) (Fig. 3). Comparison of samples from the shallow and deep trawls indicated no significant day-night difference in abundance of eggs in the fish stomachs (Mann-Whitney test, $P>0.6$ and $P>0.05$ at shallow and deep layers, respectively). Therefore, the data from each depth were combined for analysis and significant differences in egg abundance in the stomachs were found between trawling depths ($P<0.001$).

For comparison, the numbers of eggs sampled by the Clarke-Bumpus samplers at the trawl stations were superimposed on the same graph (Fig. 3). The middepth of each sampling interval coincided with the depth of a trawl tow, and the vertical pattern of egg density within the water column agreed with that from the fish stomachs. The pycnocline that was formed at the upper layer (97 m) might have prevented the eggs from moving toward the surface, so that eggs may have aggregated at this depth where the highest LPI is shown. The reason why the deepest Clarke-Bumpus sample does not show the greatest concentration of eggs might be explained by the egg ages at this station. The number of 1-d-old eggs

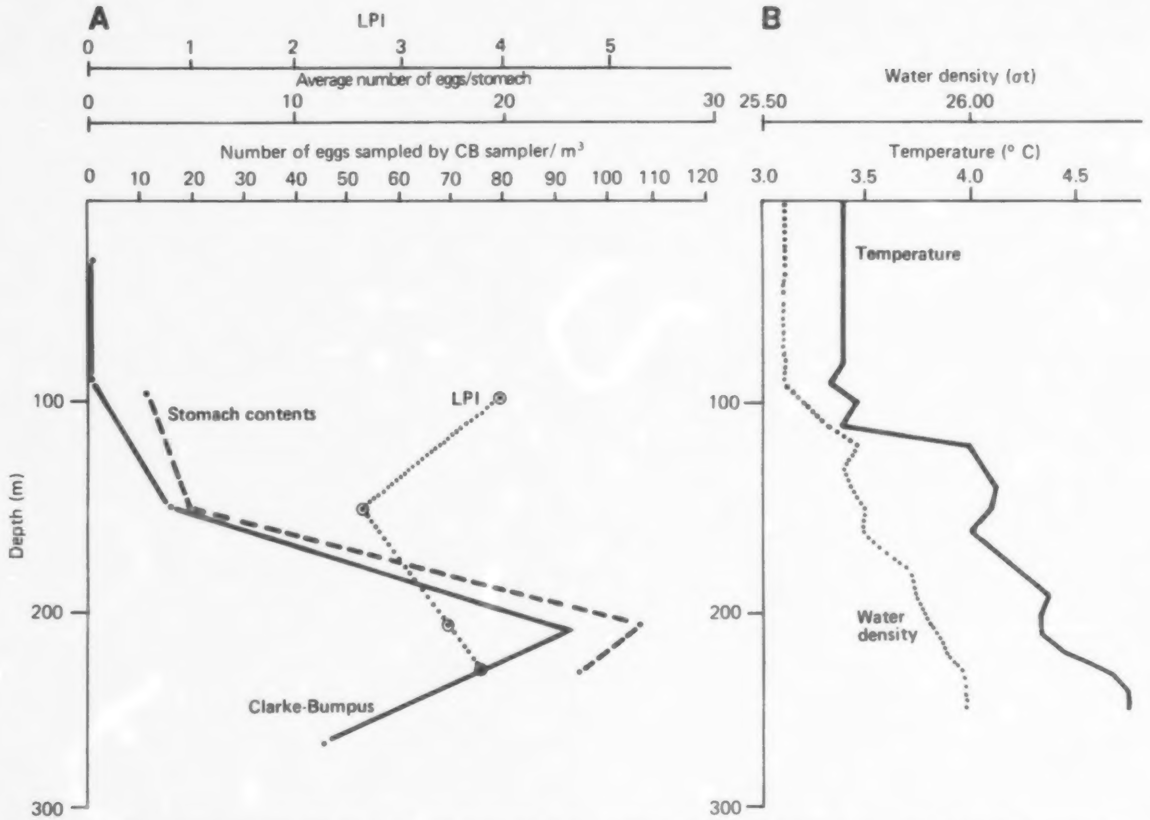

FIG. 3. Depth distribution of walleye pollock eggs from adult stomachs and Clarke-Bumpus samples (A) and of water density and temperature (B) near Cape Kekurnoi in 1986.

(Group 1) was only 5% that of 2- to 3-d-old eggs (Group 2) (data not shown). These data suggest that at this location spawning within 24 h prior to sampling was very limited. Eggs spawned more than 24 h before sampling had already moved up to around 200 m.

Changes in Specific Gravity and Vertical Velocity of Eggs

The 1985 and 1986 experiments demonstrated that the specific gravity of walleye pollock eggs varies with developmental state (Fig. 4). Specific gravity gradually increased during early development from fertilization through the end of Group 3 (4- to 5-d-old eggs), showed no change or a slight decrease in density during middle development (6- to 7-d-old eggs; Group 4), then increased abruptly during late development (8- to 14-d-old eggs; Groups 5 and 6) until about 10 to 30 h before hatching. At this point specific gravity decreased very quickly as hatching approached.

Eggs fertilized at depth may have positive buoyancy, because specific gravity just after fertilization ranged from 1.0243 to 1.0253 while the mean seawater density at 250 m near Cape Kekurnoi was 1.0259 in early April 1986. The eggs would have moved upward in the water column to float at the level of neutral buoyancy. Concurrently, the rising eggs would encounter different current velocities which, along with spawning location, should be the major controlling factors for egg distribution in Shelikof Strait. Because eggs increased in density

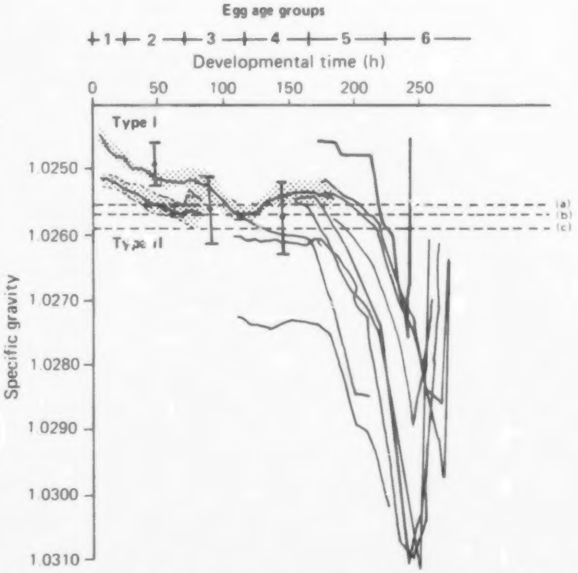

FIG. 4. Changes in walleye pollock egg specific gravity during development. The shading over the young stages of eggs represents one standard deviation around the mean ($n = 12$) in 1986, and lines for the older stages indicate changes in specific gravity of individual eggs with time in 1985. The circles and vertical bars indicate the mean and one standard deviation from each short-term experiment in 1986. (a), (b), and (c) represent the water densities in the shallow, middle, and bottom layer at the main spawning area in 1985.

continuously after equilibrating with surrounding seawater, they would sink until they reached their maximum specify gravity 10–30 h before hatching. Since egg density declines as hatching approaches, the eggs would move upward again when their density becomes less than the specific gravity of the surrounding water, and hatch at some mid-depth in the water column.

As shown previously, the major egg concentrations regardless of age group were found below 200 m. Therefore, eggs located above 200 m may have had abnormally low specific gravities. The eggs used for the short-term experiments (1985 and 1986) and the long-term experiment (1985) were collected from above 200 m. Accordingly, these eggs may have had lower specific gravities than the artificially fertilized eggs used in the other experiments.

The vertical velocity of eggs varies with developmental status of the eggs and water density. Because the development rate of eggs is a function of ambient seawater temperature, and because water temperature and water density vary interannually in Shelikof Strait, the vertical velocity and distribution of eggs should also differ interannually. Changes in the specific gravity of eggs during development are much larger (1.0243–1.0310) than the range of water density through the water column (e.g., 1.0256–1.0259 $g \cdot cm^{-3}$ in 1985). In particular, the specific gravity of the eggs during their early development is distinctly less than the water density at the depth where they are spawned. Thus, the vertical distribution of egg abundance and age composition through the water column was primarily the result of the positive buoyancy of the relatively long-lasting early stage.

Model of Changes in Vertical Distribution of Eggs

Based on field and experimental data on seawater temperature, seawater density, and egg specific gravity, we developed a schematic that describes the vertical distribution and velocity of eggs in the spawning area for 1986 (Fig. 5). The following assumptions and data were used to develop this representation:

1) Specific gravity of the eggs is the same every year. However, 1986 specific gravity measurements showed two different values for the early stages, while the 1985 experiments demonstrated large variations in specific gravity among older stage eggs. Therefore, we created two data sets (Type I and Type II eggs) for specific gravity of eggs at different stages of development with different initial values for Group 1 to Group 4, and the same values for Group 5 and 6 because of large variation (Table 2).
2) The average egg diameter is assumed to be 1.4 mm.
3) Spawning depth is assumed to be 290 m where the highest abundance of spawners was found during the hydroacoustic surveys (Kim 1987).

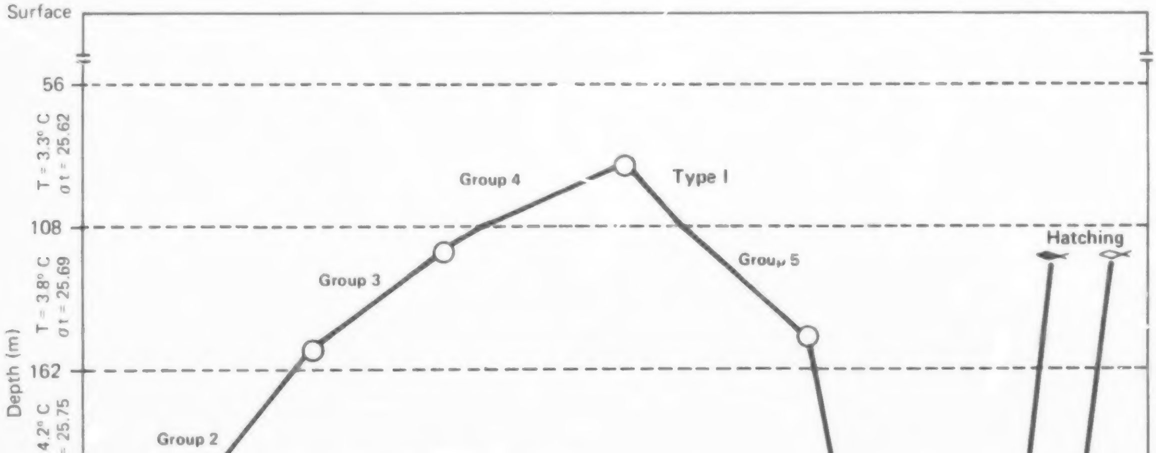

FIG. 5. Model of vertical distribution of Type I (open symbols) and Type II (closed symbols) walleye pollock eggs during development in 1986.

TABLE 2. Specific gravity of each egg age-group based on 2 yr of experiments.

	Egg age-groups (age in days)					
	1 (1)	2 (2–3)	3 (4–5)	4 (6–7)	5 (8–10)	6 (11–14)
Type I	1.02470	1.02515	1.02535	1.02542	1.02608	1.02780
Type II	1.02515	1.02550	1.02570	1.02577	1.02608	1.02780

4) The water column is divided into five intervals, which are identical to the depth intervals of the Clarke-Bumpus sampling.
5) The temperature/water density in each layer was averaged from four CTD casts conducted at the Clarke-Bumpus sampling stations in 1986.
6) Egg development rate at specific temperatures is taken from Bates (1987). One modification was made by careful examination of the data set used in his model; the time duration of stage 21 in his model was reduced by 60%.
7) The mean specific gravity of newly hatched embryos is the same as that of 3–4 mm larvae (i.e., 1.02567 (Kim 1987)).
8) Stokes law is applicable for the vertical velocity of these eggs (see Sundby 1983).

This schematic illustrates that the lighter eggs (Type I eggs) are distributed throughout the water column, and that their upward and sinking velocities are high relative to the heavier (Type II) eggs. Type II eggs are confined to the bottom layers (below 200 m). It is inferred that most eggs have specific gravities similar to Type II because heavy concentrations of all age groups are always found in the bottom layer. The eggs found in the upper layers could be Type I eggs. If some eggs follow the Type I model, the early (Group 1) and late (Group 6) stages of eggs should be located in the deepest layer in the water column and Groups 3, 4, and 5 should be above 150 m. This figure is in good agreement with the results of the Clarke-Bumpus net sampling, as shown in Table 1b. The youngest and the oldest eggs are mostly in the bottom layer, and intermediate egg age-groups are relatively more abundant in the middle and upper layers.

Using this model, a difference in egg development duration is implied. Because the Type II eggs are located in the deeper layers where warm water occurs, their embryonic period is estimated to be around 1 d shorter than that of Type I eggs which spend more time at lower temperatures.

According to this model, late stage eggs (Group 6) should be on the bottom for some time because of their very high specific gravity compared to the surrounding water. Also, if hatching occurred at the depth where the egg's specific gravity balances with that of surrounding seawater, the hatching depth in 1986 would be around 120 m.

Advection and Diffusion of Eggs

Generally the mass center of young eggs (Group 1) was found in the deepest trough area of the northeastern strait, and the egg mass centers moved from the northeast to the southwest as eggs developed (Fig. 6). The advection rate can be estimated from the displacements of the mass centers with time (Fig. 7). The least-squares regressions indicate egg advection rates of 2.9 $cm \cdot s^{-1}$ (or 2.5 $km \cdot d^{-1}$) during early April 1985. This advection rate, however, might be high compared to advection in the rest of the strait, because the spawning area was in the northeastern strait where the current generally is higher than that in the southwestern strait (Kim 1987). In addition, baroclinic estimates of current strength in 1985 were much greater than in other years (Reed et al. 1986).

Diffusive processes increase the area occupied by dispersing particles and are irreversible, while advective processes could be reversed so that the center of a patch might return to its original position if current directions and velocities completely reversed. From the results of the surveys conducted in 1985, the diffusion processes for eggs, as measured by the variance of displacement of the centroids, were clearly shown (Fig. 6). The variance of each egg group increased as a function of developmental stage (time from spawning) from 590 km^2 for 1-d-old eggs (Group 1) to 1 330 km^2 for 11- to 14-d-old eggs (Group 6) (Fig. 7).

Egg Patchiness

Stomach examinations showed that eggs were clumped in the water column, and this clumping tendency was stronger in the deep layer than in the middle layer. Based on the chi-square goodness of fit test to the Poisson distribution of numbers of eggs per stomach, the null hypothesis, that the eggs are distributed randomly, was rejected ($P<0.05$). Also, s^2/m values were relatively high for samples from both the deep layer (around 70) and middle layer (around 10), again suggesting that the eggs were distributed in distinct patches at all depth levels. Evidence for patchiness also can be shown by LPI calculated from the same data sets. The LPI was high in deep water (205 m and 229 m), and comparatively low at 152 m (Fig. 3). Due to the presence of a pycnocline around 100 m, the eggs aggregated there, producing a high LPI.

Consequences of Interannual Variation in Water Properties

If it is assumed that there are no interannual changes in egg specific gravity (Type II) and egg size, and if the vertical movement of eggs follows Stokes law, interannual differences in vertical distribution and development time can be modelled based on the water temperatures and water density in the main spawning area during spring

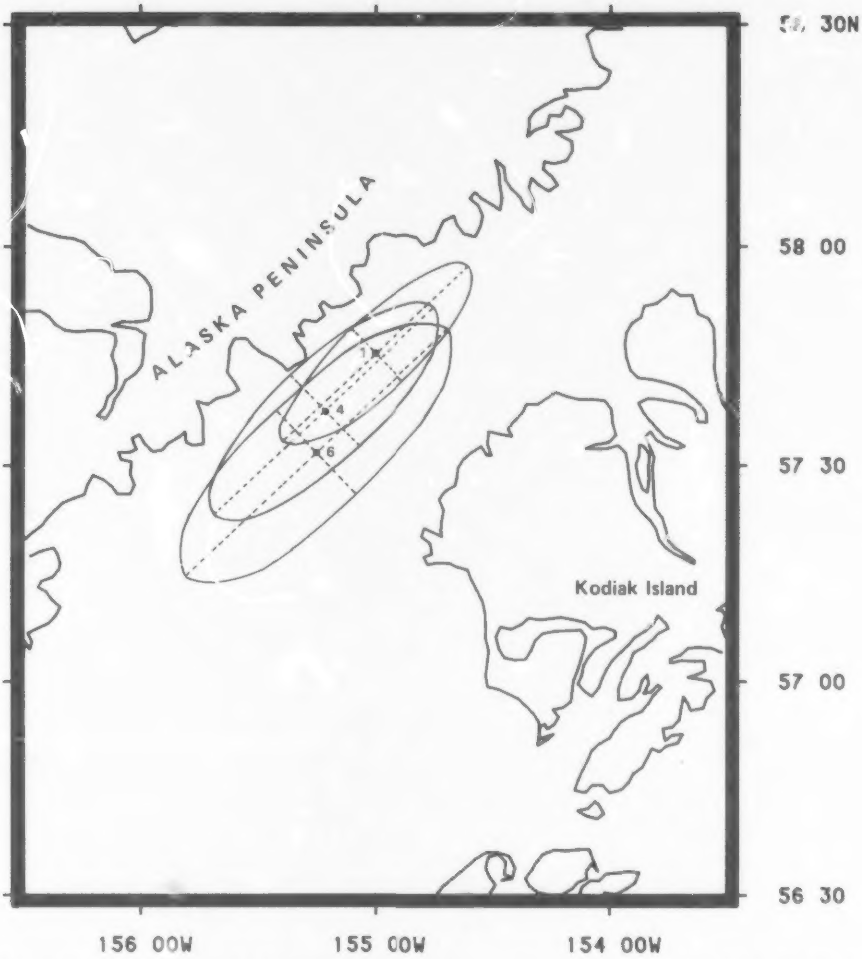

FIG. 6. Centroids of distribution of walleye pollock eggs in age-groups 1, 4, and 6 in Shelikof Strait, April 1985. The mass centers of the centroids are indicated by the age-group numbers. One standard deviation of displacement in the along- and cross-strait directions is shown by dashed lines, and an ellipse encloses the area of one standard deviation around the mass centers.

(Fig. 8). According to this schematic the eggs are usually located below 150–200 m throughout the embryonic period, and do not rise to a depth shallower than 150 m. Generally the time requirement from fertilization to hatching is 12–15 d, depending on the ambient temperature. Cold water conditions during the 1986 spawning season delayed egg development for 2 d compared to 1977 and 1985. The strong year-classes in 1977 and 1985 (Nelson and Nunnallee 1987) could have been due in part to shorter total embryonic periods and a reduced period for egg mortality. For walleye pollock eggs, the instantaneous rate of daily mortality ranged from 0.1–0.4 in 1981 (Kim and Gunderson 1989). If an instantaneous daily mortality rate of 0.3 was applied, it would reduce the population size by half within a 2 d period.

Aside from developmental duration, the vertical distribution of eggs might also influence the spatial distribution of eggs and larvae. Varying vertical distribution of eggs also enhances variation in horizontal distribution. If eggs were aggregated at only one depth, dispersion due to vertical shear of horizontal currents would have limited effect. However, if the eggs are distributed throughout the water column, they will experience maximum dispersion. Therefore, walleye pollock eggs will be displaced from the spawning area differently each year, depending on the temperature and density properties of the water column.

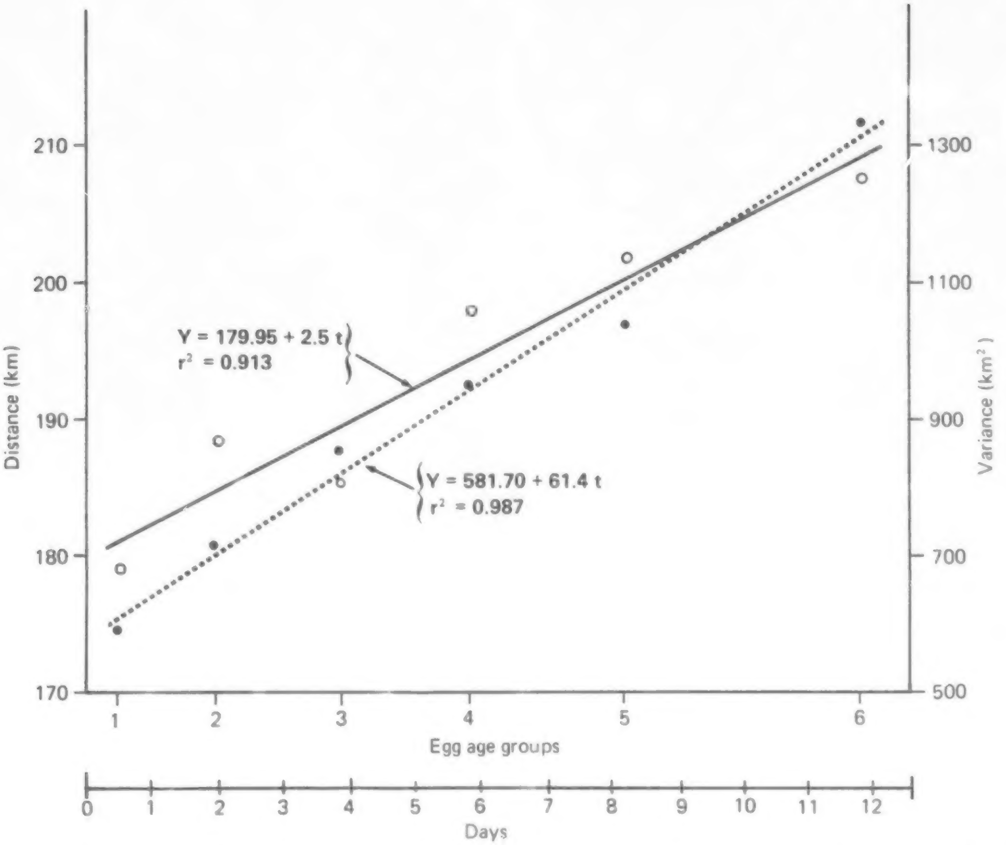

FIG. 7. Advection (open circles) and diffusion (closed circles) rates of walleye pollock eggs in Shelikof Strait, April 1985, based on displacement and variance of centroids of six age-groups of eggs.

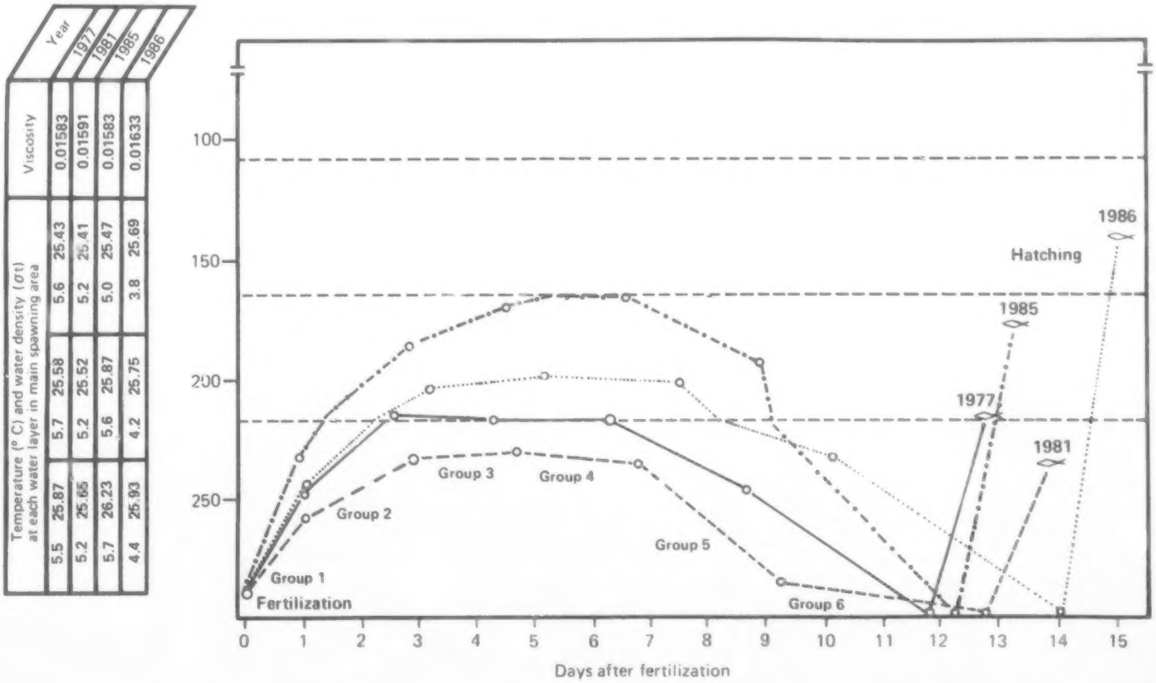

Year	Viscosity	Temperature (° C) and water density (σt) at each water layer in main spawning area					
1977	0.01583	5.6	25.43	5.7	25.58	5.5	25.87
1981	0.01591	5.2	25.41	5.2	25.52	5.2	25.65
1985	0.01583	5.0	25.47	5.6	25.87	5.7	26.23
1986	0.01633	3.8	25.69	4.2	25.75	4.4	25.93

FIG. 8. Comparison of modelled vertical distribution of walleye pollock eggs during development in 1977, 1981, 1985, and 1986.

References

Alderdice, D. F., and C. R. Forrester. 1971. Effects of salinity and temperature on embryonic development of the Petrale sole (*Eopsetta jordani*). J. Fish. Res. Board Can. 28: 727–744.

Bates, R. D. 1987. Estimation of egg production, spawner biomass and egg mortality for walleye pollock, *Theragra chalcogramma*, in Shelikof Strait from ichthyoplankton surveys during the 1981 spawning season. M.S. thesis, University of Washington, Seattle, WA. 132 p.

Coombs, S. H. 1981. A density-gradient column for determining the specific gravity of fish eggs, with particular reference to eggs of the mackerel, *Scomber scombrus*. Mar. Biol. 63: 101–106.

Coombs, S. H., C. A. Fosh, and M. A. Keen. 1985. The buoyancy and vertical distribution of eggs of sprat (*Sprattus sprattus*) and pilchard (*Sardina pilchardus*). J. Mar. Biol. Assoc. U.K. 65: 461–474.

Craik, J. C. A., and S. M. Harvey. 1987. The causes of buoyancy in eggs of marine teleosts. J. Mar. Biol. Assoc. U.K. 67: 169–182.

Fujimoto, M., and T. Hirano. 1972. Study of Kuroshio functioning as a means of transportation and diffusion of fish egg and larvae. I. The results of drift bottle experiments. Bull. Tokai Reg. Fish. Res. Lab. 71: 51–68. (In Japanese with English abstract.)

Haug, T., E. Kjosvik, and P. Solemdal. 1986. Influence of some physical and biological factors on the density and vertical distribution of Atlantic halibut, *Hippoglossus hippoglossus*, eggs. Mar. Ecol. Prog. Ser. 33: 207–216.

Hewitt, R. P. 1982. Spatial pattern and survival of anchovy larvae: Implications of adult reproductive strategy. Ph.D. dissertation, University of California, San Diego, CA. 187 p.

Kendall, A. W. Jr., M. E. Clarke, M. M. Yoklavich, and G. W. Boehlert. 1987. Distribution, feeding, and growth of larval walleye pollock, *Theragra chalcogramma*, from Shelikof Strait, Gulf of Alaska. Fish. Bull., U.S. 85: 499–521.

Kim, S. 1987. Spawning behavior and early life history of walleye pollock, *Theragra calcogramma*, in Shelikof Strait, Gulf of Alaska, in relation to oceanographic factors. Ph.D. dissertation, University of Washington, Seattle, WA. 220 p.

Kim, S., and D. R. Gunderson. 1989. Cohort dynamics of walleye pollock (*Theragra chalcogramma*) in Shelikof Strait, Gulf of Alaska, during the egg and larval period in 1981. Trans. Am. Fish. Soc. (In press)

Koslow, J. A., S. Brault, J. Dugas, and F. Page. 1985. Anatomy of an apparent year-class failure: The early life history of the 1983 Browns Bank haddock, *Melanogrammus aeglefinus*. Trans. Am. Fish. Soc. 114: 478–489.

Lasker, R. 1975. Field criteria for survival of anchovy larvae: The relation between inshore chlorophyll maximum layers and successful first feeding. Fish. Bull., U.S. 73: 453–462.

Lloyd, M. 1967. Mean crowding. J. Anim. Ecol. 36: 1–30.

Nakatani, T., and T. Maeda. 1981. Transport process of the Alaska pollock eggs in the Funka Bay and the adjacent waters, Hokkaido. Bull. Jap. Soc. Sci. Fish. 47: 1115–1118.

1983. Distribution of walleye pollock larvae and their food supply in Funka Bay and the adjacent waters, Hokkaido. Bull. Jap. Soc. Sci. Fish. 49: 183–187.

1984. Thermal effect on the development of walleye pollock eggs and their upward speed to the surface. Bull. Jap. Soc. Sci. Fish. 50: 937–942.

Nelson, M. O., and E. P. Nunnallee. 1987. Condition of the walleye pollock resource of the Gulf of Alaska as estimated in 1986, p. 15–38. *In* R. L. Major [ed.] Condition of groundfish resources of the Gulf of Alaska region as assessed in 1986. U.S. Dep. Commer., NOAA Tech. Memo. NMFS F/NWC-119.

Nishiyama, T., K. Hirano, and T. Haryu. 1986. The early life history and feeding habits of larval walleye pollock in the southeast Bering Sea. Int. North Pac. Fish. Comm. Bull. 45: 177–277.

Okubo, A. 1980. Diffusion and ecological problems: Mathematical models. Biomathematics, Vol. 10. Springer-Verlag, Berlin, 254 p.

Reed, R. K., L. S. Incze, and J. D. Schumacher. 1989. Estimation of the effects of flow on dispersion of larval pollock, *Theragra chalcogramma*, in Shelikof Strait, Alaska, p. 239–246. *In* R. J. Beamish and G. A. McFarlane [ed.] Effects of ocean variability on recruitment and an evaluation of parameters used in stock assessment models. Can. Spec. Publ. Fish. Aquat. Sci. 108.

Reed, R. K., J. D. Schumacher, and L. S. Incze. 1986. Water properties and circulation in Shelikof Strait, Alaska, during 1985. U.S. Dep. Commer., NOAA Tech. Memo. ERL PMEL-68: 35 p.

Serobaba, I. I. 1974. Spawning ecology of the walleye pollock, *Theragra chalcogramma*, in the Bering Sea. J. Ichthyol. 14: 544–552.

Smith, P. E. 1973. The mortality and dispersal of sardine eggs and larvae. Rapp. P.-V. Reun. Cons. Int. Explor. Mer 164: 282–292.

Smith, P. E., and S. L. Richardson. 1977. Standard techniques for pelagic fish egg and larval surveys. FAO Fish. Tech. Paper 175: 99 p.

Sundby, S. 1983. A one-dimensional model for the vertical distribution of pelagic fish eggs in the mixed layer. Deep Sea Res. 30(6A): 645–661.

Sundnes, G., H. Leivestad, and O. Iversen. 1965. Buoyancy determination of eggs from the cod (*Gadus morhua* L.). J. Cons., Cons. Int. Explor. Mer 29: 245–252.

Zar, J. H. 1974. Biostatistical analysis. Prentice-Hall, NJ, 620 p.

Characteristics of Development of Atmospheric Circulation in the Northern Pacific Ocean and Their Role in Determining Long-Term Changes in the Abundance of Certain Fishes

I. V. Davydov

Pacific Research Institute for Fisheries and Oceanography (TINRO), Kamchatka Branch, Petropavlosk-Kamchatsky, USSR

Abstract

DAVYDOV, I. V. 1989. Characteristics of development of atmospheric circulation in the northern Pacific Ocean and their role in determining long-term changes in the abundance of certain fishes, p. 181–194. *In* R. J. Beamish and G.A. McFarlane [ed.] Effects of ocean variability on recruitment and an evaluation of parameters used in stock assessment models. Can. Spec. Publ. Fish. Aquat. Sci. 108.

The two contrasting types of atmospheric pressure and circulation patterns that determine the type of water regime in various far-eastern seas develop due to the geographical position and intensity of high-altitude pressure ridges and troughs in the northwestern Pacific. This sea area may be treated as a single environmental system with interrelated development of hydrometeorological conditions and biological processes.

The trends in the occurrence of specific types of pressure and circulation conditions, and related trends in fish abundance, change both in 10–11-yr periods and also over longer intervals. The former may be related to the 22-yr cycle of solar activity, while the latter may depend on the "geoeffectiveness" of the times of transition of solar activity (Wolf numbers) through their long-term average level in the "centennial" cycle (approximately 100-yr), and on the maximum of the "centennial" cycle of frequency of sun spots, which usually occurs in the 11-yr cycle following the "centennial" minimum of solar activity. As a result, natural processes may develop cycles of 40–60 yr (depending on the length of a particular "centennial" cycle of solar activity).

Résumé

DAVYDOV, I. V. 1989. Characteristics of development of atmospheric circulation in the northern Pacific Ocean and their role in determining long-term changes in the abundance of certain fishes, p. 181–194. *In* R. J. Beamish and G. A. McFarlane [ed.] Effects of ocean variability on recruitment and an evaluation of parameters used in stock assessment models. Can. Spec. Publ. Fish. Aquat. Sci. 108

Les deux types de tendance quant à la pression et la circulation atmosphériques à l'origine du type de régime hydrologique observé dans diverses mers de l'Extrême-Orient sont dus à la situation géographique et à l'intensité des crêtes de pression et des dépressions à de hautes altitudes dans le nord-ouest du Pacifique. Cette zone marine peut être considérée comme un système en soit, où les conditions hydrométéorologiques et les processus biologiques sont liés entre eux.

Les tendances quant à la présence de conditions précises de pression et de circulation ainsi que les tendances quant à l'abondance de poissons qui y sont liés changent durant des périodes se répétant tous les 10 à 11 ans et au cours de périodes plus longues. Les tendances relatives à la pression et la circulation atmosphériques peuvent être liées au cycle de 22 ans de l'activité solaire tandis que les tendances en matière d'abondance peuvent dépendre de la «géoefficacité» des périodes de transition de l'activité solaire (nombres de Wolf) via leur moyenne à long terme dans le cycle «séculaire» (environ 100 ans) et du maximum de l'activité solaire dans le cycle «séculaire», lequel survient généralement dans le cycle de 11 ans qui suit le minimum. En conséquence, les processus naturels peuvent développer des cycles de 40 à 60 ans (selon la longueur d'un cycle «séculaire» donné de l'activité solaire).

Introduction

The basis for rational management of a fishery is an up-to-date forecast of changes in the abundance of the exploited population. It permits selection of optimal strategy and tactics and the reduction of any undesirable consequences. The studies on the problems presented by the long-term fishery predictions, at present still insufficiently developed, are, therefore, of great importance. To solve the problem, one must work on the patterns of long-term changes in the abundance of exploited populations; factors causing these changes must be clarified. Many investigators postulate at present that climatic cycles are the basic cause of periodic changes in fish abundance, because these cycles are responsible for marked changes in environmental conditions (Izhevsky 1961; Dement'eva 1976; Cushing 1975). Seen in this way, long-term forecasts of changes in fish abundance must be founded on an inter-system approach. This approach is based on the assumption that the behaviour of a system at any given time used as a prognosticator (e.g. hydrometeorological conditions during the spawning season) determines the future behaviour of the system, the prognosis for which is being sought (e.g. trends in the abundance of fish).

Inasmuch as the abundance of any fish population is a result of the action of a complex multi-layered bioecological system, long-term forecasts, in the present state of our knowledge, must be based on extrapolation of trends that have been formulated mainly at the qualitative (descriptive) level. The reliability of such prognoses depends on the care taken in selecting limits of extrapolation (times of change in direction of developmental trends of the predicted phenomena), as well as the choice of an index that would reflect the conditions of the basic links in the bioecological system with sufficient accuracy.

For the far-eastern seas (Bering, Ohkotsk and Japan) such an index can be provided by the anomalies of minimum water temperature in the cold intermediate layer (the temperature of the "nucleus" of this layer) near the southeastern coast of Kamchatka (referred to as CILSEK hereafter) (Davydov and Kutsykh 1967; Davydov 1984).

The cold intermediate layer (CILSEK) is present during the period of the year, when it constitutes a characteristic feature of the vertical structure of subarctic water masses. Its minimum temperature depends on the rate of winter cooling of the water and on the influx of heat in a particular region. Therefore, its anomalies reflect the characteristics of the water regime developing in connection with these processes ("water regime" in this case is defined as inter-related inorganic and organic processes).

Materials and Methods

Minimum temperature of CILSEK scarcely changes at all throughout the warm season. This fact permits us to use data from a standard hydrological transect in Avacha Bay (southeastern Kamchatka), which is done once a year, to estimate its anomalies. The calculation was done using the average value for the years 1957–81.

Statistical comparison of the year-class abundance with anomalies of minimum temperature was done using the index of closeness of qualitative relationship proposed by Bershtein (1946):

$$P = \frac{x_1y_2 - y_1x_2}{x_1y_2 + y_1x_2} \quad \text{, where}$$

x_1 is the number of cases when the abundance of herring year-classes hatched in years of negative anomalies, or the abundance of pollock year-classes hatched in years of positive anomalies, exceeded the long-term average;

y_1 is the number of cases when herring year-classes exceeding the long-term average were not observed in years of positive anomalies of minimum temperature, or of pollock in years of negative anomalies;

x_2 is the number of cases when year-classes exceeding the long-term average were hatched in years of positive anomalies for herring, or of negative anomalies for pollock;

y_2 is the number of cases when year-classes below the long-term average were hatched in years of positive anomalies for herring, or of negative anomalies of pollock.

Results and Discussion

Figure 1 compares the year-class abundance of certain fish populations inhabiting far-eastern seas with year-to-year variation in the anomaly of the CILSEK. The more abundant year-classes appeared in the Okhotsk and Korfo-Karagin herring populations mainly during a negative anomaly of minimum temperature, while in the population of pollock of the northeastern Sea of Japan they appear during positive anomalies of the minimum temperature.

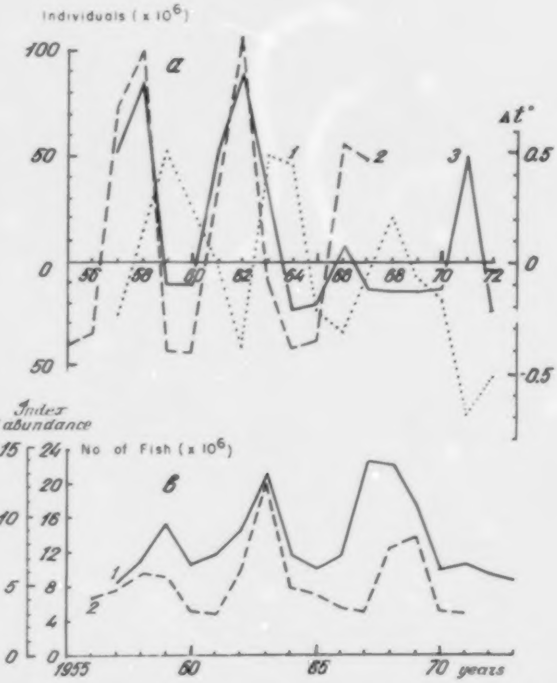

FIG. 1. Year-to-year changes. *Upper panel*. 1. Anomalies of minimum temperature of CILSEK–the cold intermediate layer off the southwestern coast of Kamchatka. 2. Anomalies of abundance of year-classes of Okhotsk herring in millions (from Tyurin 1967). 3. Abundance of year-classes of Korfo-Karagin herring (from Kachina 1981). *Lower panel:* 1. Abundance of year-classes of east-Okhotsk walleye pollock (from Kachina and Sergeyeva 1981). 2. Abundance of year-classes of walleye pollock of the northeastern part of the Sea of Japan (from Zverkova 1981).

TABLE 1. Values of coefficients of qualitative relationship.

Populations	Coefficients
Okhotsk herring	0.96
Korfo-Karagin herring	0.78
Northeastern Sea of Japan pollock	0.93
Eastern Okhotsk Sea pollock	0.60

Coefficients of qualitative relationship shown in Table 1 show that anomalies in minimum water temperature of CILSEK reflect not just hydrometeorological conditions but also the state of the biocenoses in far-eastern seas insofar as is indicated by the abundance of fish populations.

Mechanism of Forming Index of Oceanic Conditions

Let us consider the basic processes that create the anomalies of minimum temperature in CILSEK, and the associated characteristics of development of hydrometeorological conditions in far-eastern seas.

Of special interest for our investigation is the work of Girs (1960), who classified the microprocesses in the atmosphere of the Pacific sector of the northern hemisphere into three types: a zonal type (*Z*), and two meridional types (M_1 and M_2). The latter both reflect the meridional state of the atmosphere, but they have opposite geographic positions for the high-altitude ridges and troughs (Fig. 2). Development of meridional patterns of atmospheric circulation in the troposphere is characterized by long waves of great amplitude, with a stable positioning of ridges and troughs over the North Pacific.

The M_1 pattern of atmospheric circulations is characterized by the presence of the eastern part of a high altitude ridge (western part of a trough) over the eastern region of the ocean, whereas the western part of the ridge (eastern part of the trough) is located over the western regions.

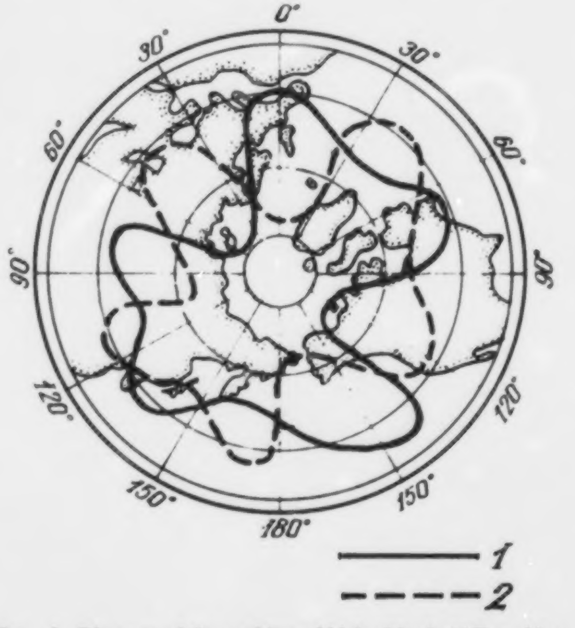

FIG. 2. Diagram of the position of high-altitude (AT_{500} ridges and troughs for macroprocess M_1(1) and M_2 (2). (After Girs 1974.)

The M_2 meridional pattern of circulation is characterized by the western part of a ridge (eastern part of a trough) being over the eastern areas, and the eastern part of the ridge (western part of the trough) being over the western areas.

In the troposphere cold advection occurs along the eastern part of ridges (western part of troughs), while heat advection prevails along their western part (eastern part of troughs).

Using monthly mean anomalies of the magnitudes of the repeated basic forms of atmospheric circulation presented in the work of Girs (1971), we computed their average values separately for years of positive and negative temperature anomalies in CILSEK (Table 2).

TABLE 2. Long-term average values of anomalies of frequency of the three basic forms of atmospheric circulation in the North Pacific, for years with positive and negative anomalies of the minimum temperature.

	Years	
Circulation patterns	Positive anomalies	Negative anomalies
Zonal (*Z*)	-4.6	3.7
Meridional (M_1)	-3.6	11.6
Meridional (M_2)	-8.8	-15.2

A higher frequency of the M_2 meridional circulation pattern is observed with positive anomalies, and of M_1 and zonal processes with negative anomalies.

It is known that temperature anomalies in the ocean may be caused by the dynamic action of an abnormal wind system, causing movement of the mass of surface waters (Sorkina 1974).

Taking this into account, the following scheme of hydrometeorological development over the North Pacific may be postulated, given the above picture of developments of the main patterns of atmospheric circulation, and using the position of high-altitude ridges and troughs typical for these patterns.

When meridional circulation pattern M_2 prevails during winter, and the frequency of M_1 and zonal patterns of circulation is below the long-term average, a temperature increase is observed over the eastern part of the North Pacific due to internal advection from southern areas and the impact of warmer south winds. This effect is intensified by a decrease in frequency of zonal processes that acts to distribute warm water from southern areas.

Warming in the extensive region washed by the Alaska Current results in increased internal heat transport to the eastern Bering Sea, which of course influences the heat content of the cold intermediate layer during subsequent seasons; hence, positive anomalies of temperature are formed in the CILSEK.

Northeast winds in the western part of the ocean hinder intrusion of warmer waters from the south, and increase the cold influx from the Okhotsk and Bering seas; which, in its turn, must result in lower water temperatures off the Pacific coast of Japan.

In winters when the frequency of M_1 and zonal processes increase, northeast and west winds must prevail in the northeastern Pacific. The northeasterlies hinder heat transport to middle latitudes, while the westerlies increase this effect. As a result, water temperature drops in the region of the Alaska current, and consequently internal heat transport to the eastern Bering Sea decreases, resulting in negative temperature anomalies in CILSEK.

In the western part of the North Pacific during the same years, temperatures must increase, because prevalence of winds from the southern quarter decreases the flow from the Okhotsk and Bering seas.

For each of the circulation patterns in question there is a characteristic position and condition of the main centers of atmospheric activity in the Pacific sector of the northern hemisphere (Girs 1974).

Figure 3 shows, for the groups of years in question, the average picture of surface atmospheric pressure in winter. Two pressure configurations are evident: the Aleutian depression and the Siberian anticyclone.

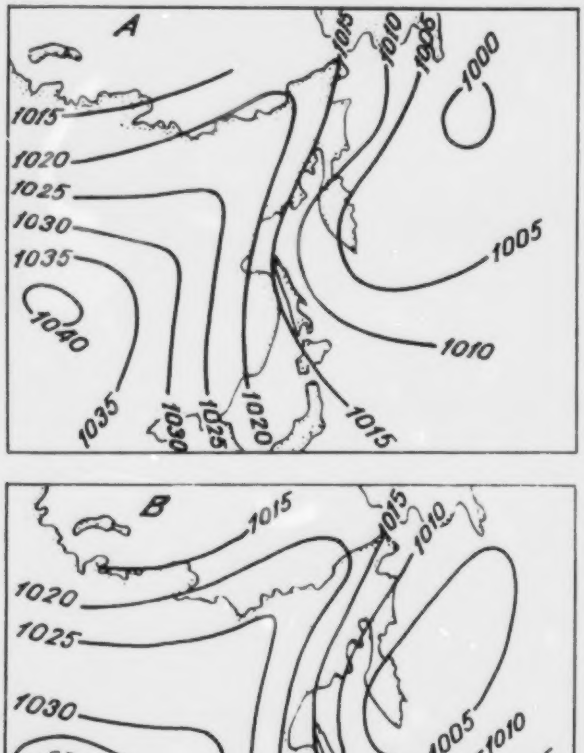

FIG. 3. Average surface atmospheric pressure in winter for two types of years. *Upper panel*: Years with positive anomalies of minimum temperature in CILSEK. *Lower panel*: Years with negative anomalies in CILSEK.

In years with a predominant development of the M_2 meridional circulation (positive anomalies of the temperature minimum) the center of the Aleutian depression is characteristically situated off southeastern Kamchatka. During years with predominant development of the M_1 pattern it shifts to the region of the Gulf of Alaska.

In the M_2 situation, the intensity of both the Aleutian depression and the Siberian anticyclone increases; their position being related to positive and negative anomalies of atmospheric pressure, respectively (Fig. 4). In the M_1 situation, the intensity of these centers of atmospheric activity is lower.

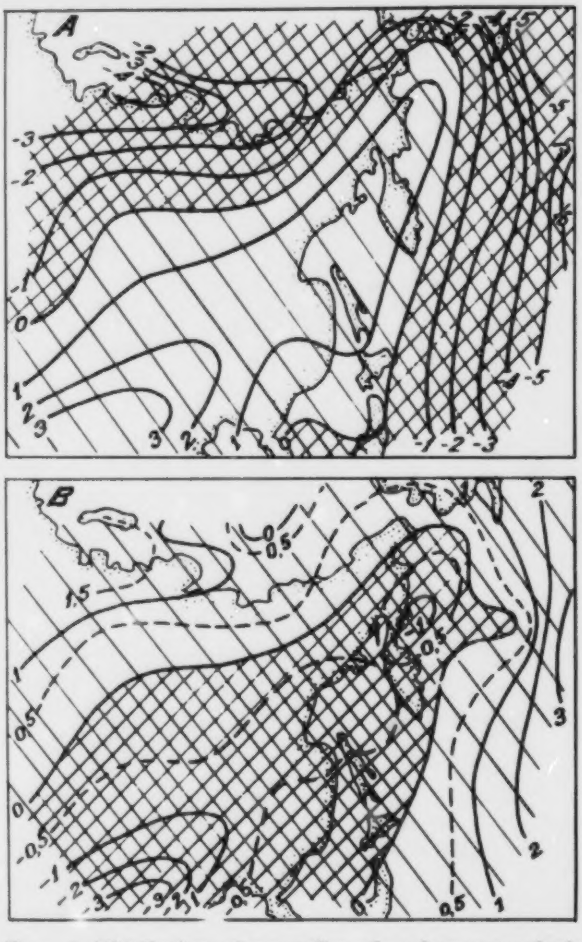

FIG. 4. Distribution of anomalies of surface atmospheric pressure in winter. *Upper panel*: Years with positive anomalies of minimum temperature in CILSEK. *Lower panel*: Years with negative anomalies in CILSEK.

Uda (1963) reviewed the main characteristics of the mechanism of redistribution of intensity in the system of currents comprising the Subarctic circulation, basing his review on variations in the gradients of pressure between centers of atmospheric activity. He showed, for example, that the difference in atmospheric pressure between the Siberian maximum and the Aleutian depression determines hydrometeorological conditions in the western regions of the North Pacific, while the difference in pressure between the Canadian maximum and the Aleutian depression determines it in the eastern regions. An increase in the difference between these atmospheric pressure configurations promotes warming in the East due to the intrusion of warmer water into the area, and to cooling in the West due to the increase of cold water transport from the Okhotsk and Bering seas. This is accompanied by retardation of the northern extension of warm Kuroshio waters, which are deflected eastward off the coast of Japan.

Comparison of average values of the difference in atmospheric pressure for the year groups in question (data from Sorkina 1972), support the validity of the above scheme, describing formation of the sign of the anomalies of minimum temperature in CILSEK (Table 3).

TABLE 3. Values of the difference of atmospheric pressure (in millibars), in winter, between centers of atmospheric activity in the North Pacific. Averages are shown separately for series of years with positive and years with negative anomalies of the temperature minimum (winter).

	Difference in atmospheric pressure	
Center of atmospheric activity	For positive anomalies	For negative anomalies
Siberian maximum Aleutian depression	34.4	29.5
Canadian maximum Aleutian depression	25.5	13.4

In years with positive anomalies of the temperature minimum, the difference in atmospheric pressure between the pressure structures in question was greater, that is, in the eastern regions of the northern part of the Pacific Ocean there was a warming trend, and in the western part a cooling trend.

Thus, a specific geographical situation and intensity of ridges and anticyclones, troughs and cyclones, in the North Pacific in winter corresponds to a specific sign of the anomalies of temperature of CILSEK in summer.

The pressure and circulation formed over the northwestern Pacific in spring, when the reproduction of many fish species takes place, will now be treated in more detail.

It is known that the general atmospheric circulation retains its characteristic features during the transition from winter to summer (Belinskii 1957). High-altitude ridges and troughs are observed within the same intervals of longitude in winter and in summer (Sazonov 1964).

The geographic position of the main pressure structures persists during the transition from winter to spring in the northwestern Pacific (Fig. 5). However, in years when negative anomalies of temperature form in CILSEK, there is a more pronounced spring breakdown of the seasonal Siberian anticyclone, and of the quasi-stationary Aleutian depression (their ranges correspond, respectively, to negative and positive air pressure anomalies) (Fig. 6).

Therefore during the transition from winter to the following seasons the distribution of intensity in the system of currents comprising the Subarctic circulation persists. This is supported by a comparison of anomalies of August water temperature in the region of the northwestern branch of the polar oceanological front (data from Kryndin 1966) with anomalies of temperature in CILSEK (Table 4).

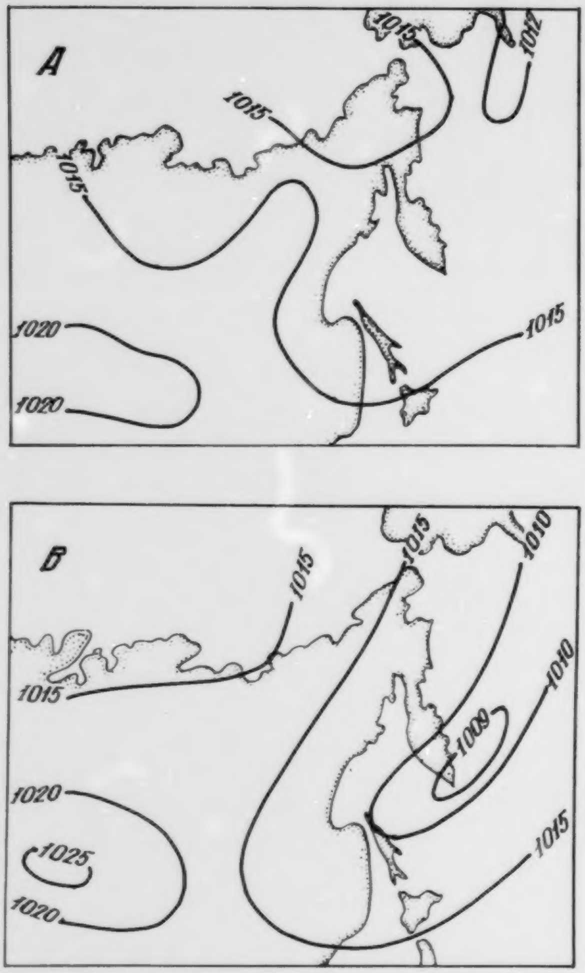

FIG. 5. Mean fields of surface atmospheric pressure in spring. *Upper panel*: Years with positive anomalies of minimum temperature in CILSEK. *Lower panel*: Years with negative anomalies in CILSEK.

TABLE 4. The sign of anomalies of surface water temperature in the region of the polar oceanographic front, and the sign of anomalies of temperature in CILSEK.

Years	1957	1958	1959	1960	1961	1962	1963	1964
CILSEK	-	-	+	+	-	-	+	+
Polar Front	-	-	+	+	-	-	-	+

Only in 1963 do the signs of these anomalies fail to correspond. We are inclined to attribute this to an error in estimating the average surface water temperature in the frontal zone, because in that year there was a drastic decrease in temperatures recorded off of Japan, related to a southward retreat of the Kuroshio (Kajura 1963).

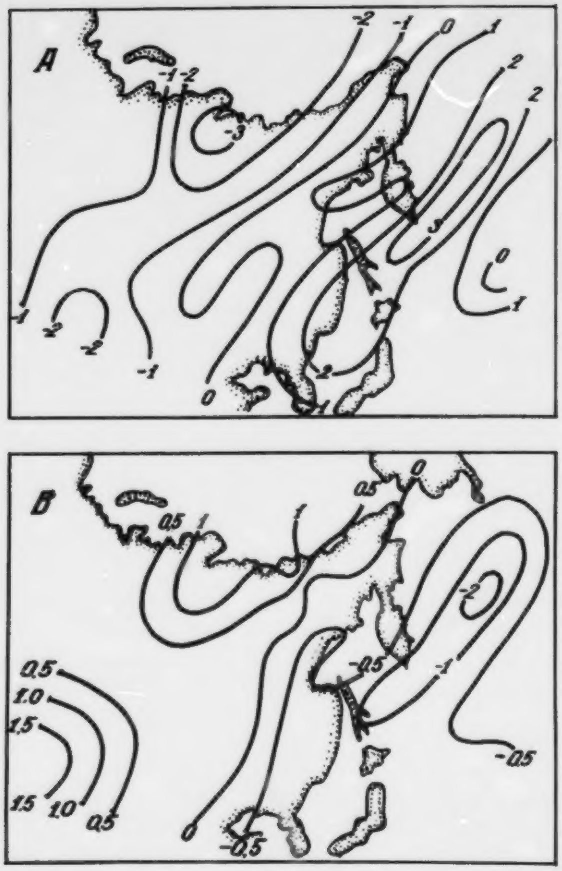

FIG. 6. Distribution of magnitudes of the anomalies of surface atmospheric pressure in spring. *Upper panel*: Years with positive anomalies of minimum temperature in CILSEK. *Lower panel*: Years with negative anomalies in CILSEK.

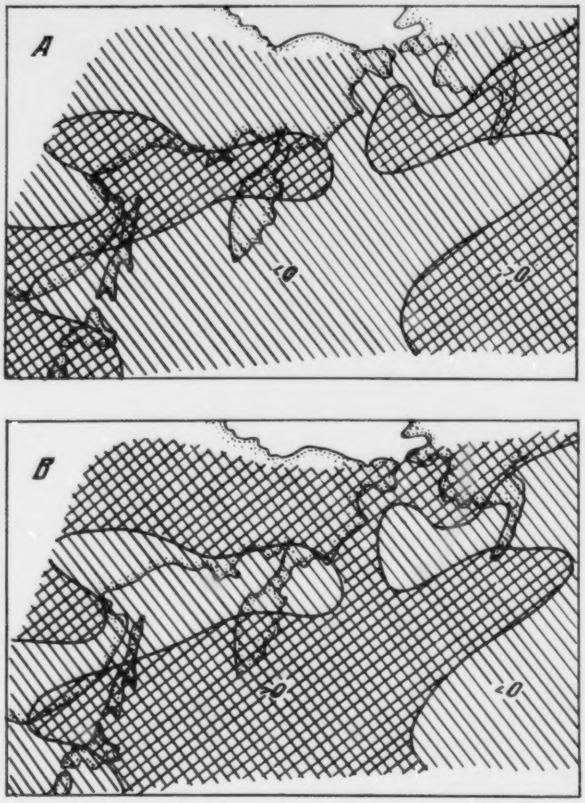

FIG. 7. Distribution of the sign (+ or −) of the "density" of centers of atmospheric cyclones in spring. *Upper panel*: Years with positive anomalies of minimum temperature in CILSEK. Lower panel: Years with negative anomalies in CILSEK.

It is known (Il'insky and Egorova 1962; Kryndin 1966) that the relative position of high-altitude ridges and troughs, as well as the thermal condition of the underlying surface of the North Pacific, determine the features of cyclonic activity.

Figure 7 shows the spring distribution of the sign of anomalies of "density" of centers of atmospheric cyclones in the northwestern Pacific (anomalies of averages for the series of years concerned). Density was determined by a simple count of centers of cyclones in 1° squares, using daily maps of weather. Anomalies were calculated from the long-term averages obtained for the same series of years as those used for the long-term average of minimum temperatures in CILSEK.

For years with predominant development of the M_2 meridional form of atmospheric circulation, the number of atmospheric cyclones coming to the Sea of Japan, the northern Okhotsk Sea and the Gulf of Alaska in spring tends to be large.

Predominant arrival of southern cyclones on the coast of North America during such years is due to a northeasterly shift of the North Pacific high-altitude ridge. In accordance with the direction of their main course, the cyclones shift to the Gulf of Alaska where they become stationary. This process is assisted by the increased background temperature of the underlying surface which is characteristic of such years. A greater cyclonic circulation over the Sea of Japan and the northern Okhotsk Sea takes place when there are more frequent arrivals of continental atmospheric cyclones over the far-eastern seas, following the spring break-up of the Siberian anticyclone.

During years with predominant development of the M_1 pattern of meridional atmospheric circulation in spring, diametrically opposite pressure and circulation conditions are formed over the northwestern Pacific. The trajectories of the southern cyclones in such years have an almost meridional direction associated with the circulation of the western part of the high-altitude ridge, which extends towards the Aleutian Islands. Stationary positions of the cyclones occur mainly off southeastern Kamchatka.

A well-developed spring Siberian anticyclone hinders formation of continental atmospheric cyclones and their extension to the far-eastern seas, resulting in a weakening of the cyclonic circulation over the Sea of Japan and the northern Okhotsk Sea.

The observed characteristics of the development of pressure and circulation conditions over the northwestern Pacific affect the development of temperature conditions in the different regions of the far-eastern seas.

In years when positive anomalies of minimum water temperature are observed in CILSEK, water temperature in the eastern part of the Okhotsk Sea also increases, due to greater internal heat transport through the channels between the northern Kuril Islands, caused by the great cyclonic circulation over the northern Okhotsk Sea (Davydov 1984).

Internal heat advection also plays a predominant role in the formation of the temperature regime of the Sea of Japan. Distribution of water temperature and development of its anomalies are related to variations in the intensity of currents, which in turn are related to atmospheric processes (Glagoleva and Skriptunova 1979). Therefore, in years when the M_2 meridional pattern of atmospheric circulation prevails (positive anomalies of the temperature minimum), the Tsushima Current is enhanced as a result of greater cyclonic circulation over the Sea of Japan, and consequently, water temperature increases in the eastern and northern sectors of this sea.

The reality of the above mechanism of interrelated development of temperature conditions in various far-eastern seas is indicated by comparison of year-to-year temperature variations off southeastern Kamchatka, in the eastern Okhotsk Sea and northern Sea of Japan (Fig. 8).

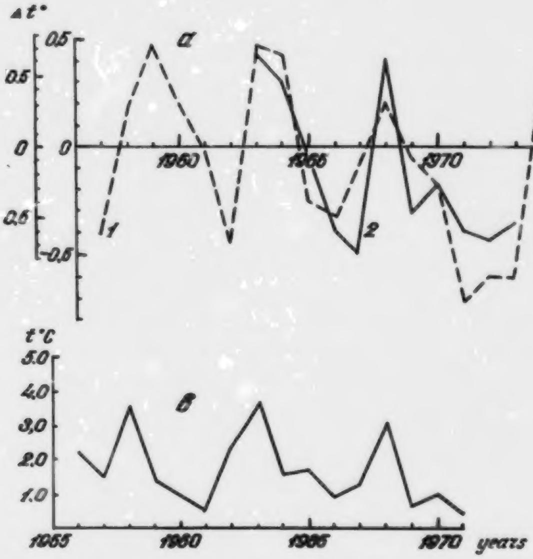

FIG. 8. *Upper panel*: 1. Year-to-year changes in the temperature of CILSEK. 2. the same, on the west-Kamchatka shelf. (Deviations from a long-term mean.) *Lower panel*: Water temperature in the 0–200-m stratum off southwestern Sakhalin in March (after Zverkva 1981).

Oceanic Conditions and Fish Reproduction

The two opposed patterns of pressure and circulation condition over the northwestern Pacific, which create specific hydrometeorological conditions in the areas in which fish spawn, influence their reproductive success. Davydov (1972) showed previously that surface currents in spawning areas are important in the formation of year-classes of Korfo-Karagin herring. Abundant year-classes are produced when the deep water transport occurs mainly from offshore areas to shallow inlets (negative anomalies in CILSEK). On the other hand, when the direction of the currents is reversed, from the shallow inlets out to the oceanic part of the region, weak year-classes are produced (for such years positive temperature anomalies are usual in CILSEK).

In the first of the above scenarios the direction of the flow of water is caused by the predominance, in the northeastern part of the peninsula, of winds from northern quarters, which develop as a result of the increase in frequency of atmospheric cyclones along the southeastern coast of Kamchatka. Deep waters rich in nutrients penetrate into shallow areas and increase the level of primary production and, consequently, the biomass of food (by several hundred percent) (Davydov 1972). Herring larvae drift into areas favorable for survival. All this results in an increase in the abundance in the herring year-classes hatched during these years.

In the second scenario the breakdown in spring of the Aleutian depression (the strengthening of the anticyclone generation process along the southeastern coast of Kamchatka), leads to a predominance of winds from the southern quarters in the northeastern part of the peninsula, and consequently to a change in the direction of the entire movement of water in the region where herring reproduce. The biomass of food organisms is sharply reduced in the inlets. Herring larvae are transported into areas unfavorable for their development, which in turn leads to a decrease in the size of the year-classes.

In some years ice blocking spawning grounds becomes a decisive factor for the Okhotsk herring population (Zavernin 1972). Thus, when the frequency of atmospheric cyclones is high in the spring off the northeastern coast of Kamchatka, it produces conditions favorable for reproduction of the local herring population; similarly, in the northern Sea of Okhotsk the prevalence of winds from northern quarters (from land to sea) results in the early removal of ice from the herring spawning grounds. Unfavorable conditions occur in years when the intensity of cyclonic circulation is high over the northern part of the Sea of Okhotsk. In this case a preponderance of winds from the southern quarters results in blocking of the herring spawning grounds by ice and a decrease in the abundance of year-classes hatched in those years.

These years are also characterized by an increase in the strength of the West Kamchatka current. Its flow is well developed due to increased frequency of southerly winds, which prevail over the whole West Kamchatka shelf (Davydov 1975) where the pollock population of the eastern Sea of Okhotsk spawns. When that happens, fish eggs and larvae are transported into the northern part of the Sea of Okhotsk, which is more productive than other parts (Chernyavsky et al. 1981). This circumstance, and decreased competition from weak year-classes of Okhotsk herring, make for abundant year-classes of east Okhotsk pollock.

When the frequency of spring cyclones off southeastern Kamchatka increases, the predominance of north winds in the eastern part of the Sea of Okhotsk weakens the West Kamchatka Current. Its stream becomes divided into several well-developed gyres (Davydov 1975). Pollock eggs and larvae remain for a long time in local spawning areas, which can increase food competition significantly and result in low abundance of the year-classes.

Zverkova (1981) has shown that years when waters of the warm Tsushima Current penetrate the spawning grounds of pollock in the Tatar Strait are favorable for reproduction of pollock in the northeastern part of the Sea of Japan. In these cases, the bulk of the eggs develop on the spawning grounds or in the northern parts of the strait. When there is only a weak intrusion of water from the south there is a large-scale transport of eggs out of the strait and away from the spawning grounds, which has a bad effect on year-class strength. Therefore, abundant year-classes of Sea of Japan pollock emerge in years of greater cyclonic circulation which increase the intensity of the Tsushima Current.

The arguments and data presented above permit us to classify the water regimes of far-eastern seas as "warm" or "cold". The origin of these two types is related to characteristics of the development of the atmospheric circulations in the Pacific sector of the Northern Hemisphere which determine the nature of the thermal and dynamic processes in the northwestern part of the Pacific Ocean, as well as determining the associated development of hydrometeorological conditions in various other regions of the far-eastern seas. Thus, the anomalies of temperature in CILSEK constitute an index which adequately reflects hydrometeorological conditions in the northwestern Pacific, as well as their biotropic effect.

The 22-Year Solar Cycle and Climatic Fluctuations

It is known that the system of macroprocesses included in the atmospheric circulation varies considerably on year-to-year and long-term scales (Girs 1971). At the present time there is no single point of view concerning the causes that underlie the rhythmic changes in natural processes. However, many investigators are of the opinion that climatic cycles may be related to variations of solar activity of similar duration. However, there are few convincing data on statistical relationships between natural processes and cycles of solar activity. The difficulty is that in many cases short series of observations on the dynamics of natural processes do not provide the sufficient data for comparison with the long-term (more that 11 yr) variations in solar activity. Moreover, solar activity is a complex phenomenon, and Wolf sunspot numbers, which are usually used in the analysis of solar-terrestrial relationships, are only one of several indices of solar activity and characterize only part of a complex situation. A suggestion may also be put forward that the physical agent influencing the lower troposphere is related not only to the number of spots on the sun's disc but also to qualitative variations in solar activity. As an example, we may consider the effect of the 22-yr or Hale cycle of solar activity on terrestrial processes. This cycle is believed to be one of the qualitative characteristics of high solar activity. It is evident both in the change of the polarity of the magnetic field in the bipolar groups of sun spots, but also in the general magnetic field of the sun during transition from the even 11-year solar cycle to the odd one (Vitinskii et al. 1976.) In other words, the difference between odd and even 11-yr cycles of solar activity (using the Zurich numbering of cycles in which the 11-yr cycle with its maximum in 1750 is considered to be No. 0) is more qualitative than quantitative in character.

Change of polarity of the general magnetic field of the sun occurs during the time of maximum 11-yr solar cycles (Vitinskii et al. 1976). This phenomenon is reflected in variations in the disturbance of the earth's magnetic field; the abrupt change in the curve in the course of the 22-yr fluctuation of the geomagnetic perturbation index is observed during maxima of the 11-yr cycles of solar activity (Davydov 1981). Thus a minimum of disturbance corresponds to the maximum of the even 11-yr cycles (No. 14 in 1905; No. 16 in 1927; No. 18 in 1947), while maxima of the odd-numbered cycles (No. 15 in 1917; No. 17 in 1937; No. 19 in 1959) correspond to maximum disturbance of the earth's magnetic field. There is a whole series of studies pointing to a relationship between that field's variations and weather processes (Poloskin 1974). Manifestations of the 22-yr cycle of solar activity in terrestrial processes have now been demonstrated. They are planetary in scope (Karklin 1973) and their amplitude is greater than the manifestations of the 11-yr solar cycle (Vitinskii et al. 1976).

Change in the nature of the relationship of atmospheric processes to solar activity occurs not only in 22-yr cycles but also during change of phases of the "centennial" cycle (Sazonov and Loginov 1969). It appears that qualitative variations in solar activity are more important than quantitative ones, which hampers statistical evaluation of solar-atmospheric relationships. Many studies on the subject are based on the analysis of coincidences between crucial events in both quantitative and qualitative characteristics of solar activity, and those in atmospheric patterns.

Possible causes of long-term (22-yr and more) variations of hydrometeorological conditions in different regions of the North Pacific are considered below because this problem is most interesting from the point of view of very long-term forecasts of trends in the abundance of fish.

Figure 9 shows variations in long-term average values of spring surface air pressure off southeastern Kamchatka (data from the weather station on Bering Island) compared with 22-yr variations in the index of disturbance of the earth's magnetic field (Davydov 1981).

There is a reciprocal relationship in the long-term course of the curves analysed; surface atmospheric pressure off southeastern Kamchatka decreases as disturbance of the earth's magnetic field increases, and becomes greater as the field calms down. As shown above, in the former case, the processes characteristic of "cold" years should predominantly develop in the far-eastern seas, and in the latter case, those characteristic of "warm" years.

Manifestation of the 22-yr cycle of solar activity in development of atmospheric processes results in a 10–11-yr duration of the periods of unidirectional development of pressure and circulation conditions in the northwestern Pacific. Predominant development of the pressure of

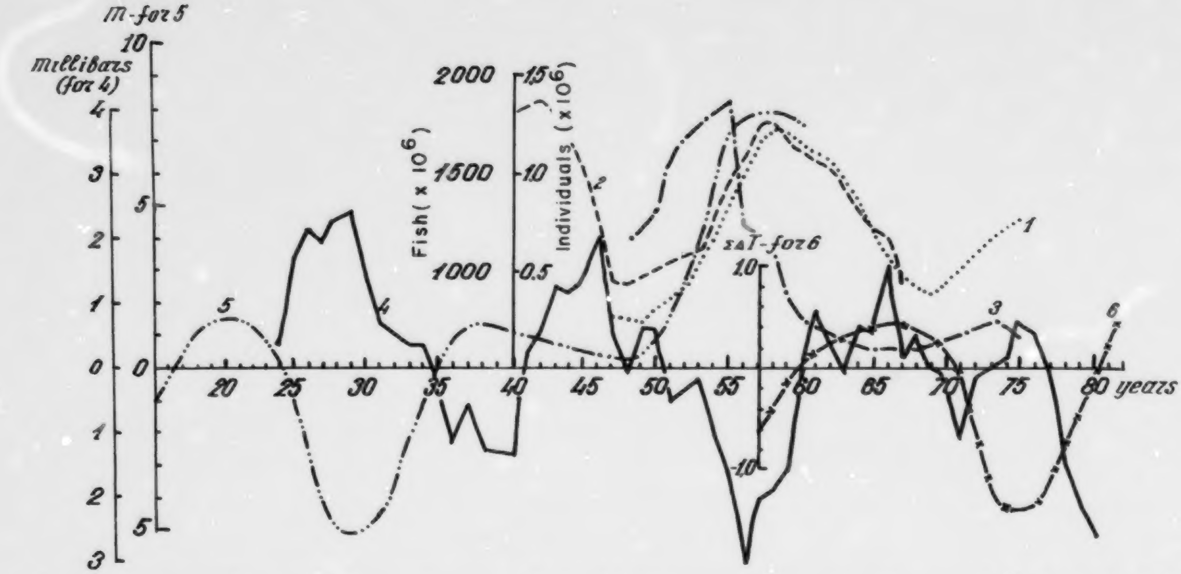

FIG. 9. Long-term changes in the spawning stock of several herring populations, and environmental conditions for their reproduction. 1. Eastern Bering Sea. 2. Okhotsk. 3. Korfo-Karagin. (Curves are shifted 5 years to the left, this being the interval from hatching to first maturity.) 4. Mean value of surface atmospheric pressure in spring along the southeastern coast of Kamchatka (all curves are smoothed by a 5-yr running average). 5. Twenty-two-year changes in the index of disturbance of the geomagnetic field (Davydov 1981). 6. Integrated curve of minimum temperature in CILSEK (smoothed by fives).

circulation conditions of "cold" years occurs in years from the maximum of the even 11-yr solar cycles to the maximum of the odd ones (periods of increased disturbance of the earth's magnetic field), whereas those characteristic of "warm" years occur in years between the maximum of the odd 11-yr cycle and the maximum of the even cycle (periods of a calm in earth's magnetic field).

The most recent 22-yr cycle began in 1964 (the minimum of 11-year cycle No. 20) and was over in 1986 (the minimum of the 11-yr cycle No. 21). Therefore conditions characteristic of "warm" years should have been developing between the maximum of the odd 11-yr cycle No. 19 (1959) and the maximum of the following even cycle (1970), and those characteristic of "cold" years between 1970 and 1981 (the maximum of the 11-yr cycle No. 21).

The integrated relationship of anomalies of minimum temperature of CILSEK, averaged by 5-yr periods, indicates that actually positive anomalies of the temperature minimum prevailed in 1960–70, and negative anomalies in 1970–81 (Fig. 9).

Thus, the discussion above gives some reason for believing that periods of lengthy (10–11 yr) prevalence of processes characteristic of one or the other type of pressure and circulation condition are related to the influence of the 22-yr cycle of solar activity. Acting through the oceanological conditions in individual regions of reproduction, and through the ecological specificity of some species of fish, the cycle is reflected in the dynamics of their abundance.

Figure 9 shows the long-term dynamics of the spawning stock of the Okhotsk (Tyurnin 1980), the Korfo-Karagin (Kachina 1981), and the eastern Bering Sea herring populations (the curves are displaced to the left by 5 yr, the interval from hatching to recruitment as spawners).

Comparing the long-term dynamics of the spawning stocks of these herring populations with 22-yr variations of surface atmospheric pressure off southeastern Kamchatka, and with anomalies of minimum temperature of CILSEK, suggests that the trends of long-term decrease in abundance coincide with pressure and circulation conditions characteristic of "warm" years, whereas increasing trends coincide with "cold" years. Some deviation is observed in the case of the Korfo-Karagin herring. The trend of increasing abundance lasted only until 1954, not to 1960 as in other herring populations. However, in subsequent years abundance variations of these populations corresponded fully to the above pattern. In my opinion the drastic decrease in abundance of the Korfo-Karagin herring after 1954 is related to the fact that in 1959–65 the spawning stock of this population did not reflect the actual abundance of the spawning recruitment. This is related to a trawl fishery for herring that developed in the late 50s. Moreover, the Japanese fleet began fishing Korfo-Karagin herring in 1961 and in that year 50% of the commercial stock was taken (Kachina 1981).

Unfortunately, at present there is no series of observations long enough to analyze long-term variations of abundance of year-classes of the pollock of the eastern Bering Sea or of the northeastern Sea of Japan. However, from the shapes of the smoothed integrated curves of the indices of relative abundance of the year-classes it is possible to make a few observations on the problem (Fig. 10). Indices of relative abundance of year-classes of the eastern Okhotsk Sea pollock are from Kachina and Sergeyeva (1981), and those of the northeastern Sea of Japan are from Zverkova (1981).

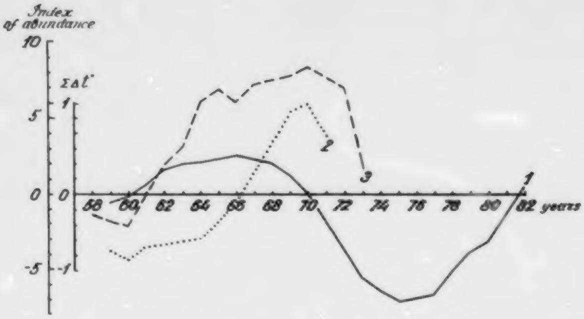

FIG. 10. Integrated curves. 1. Minimum temperature of CILSEK. 2. Relative abundance of year-classes of walleye pollock in the northeastern part of the Sea of Japan. 3. Relative abundance of year-classes of pollock in the eastern Sea of Okhotsk. (All the curves are smoothed by 5-yr averages.)

Starting in 1961, when pressure and circulation conditions characteristic of "warm" years began to appear over the northwestern Pacific the pollock year-classes hatched were more abundant than the long-term average. In 1971, when "cold" year conditions returned, year-classes of less than average abundance are indicated by the integrated curve.

The relationship between the minimum temperature of CILSEK and long-term average values of plankton biomass off southwestern Sakhalin also indicate an interrelated development of ocean conditions in different regions of the far-eastern seas (Fedotova 1984) (Fig. 11).

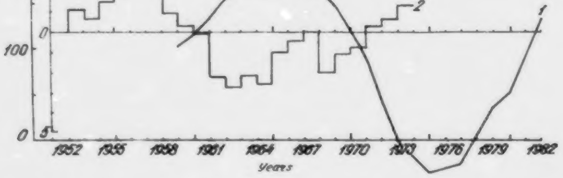

FIG. 11. Integrated curves. 1. Minimum temperature of CILSEK (smoothed by a 5-yr running average). 2. Long-term changes in the biomass of zooplankton of southwestern Sakhalin (after Fedotova 1984).

In years of high frequency of the "cold" type of hydrometeorological processes, maximum productivity of the waters off southwestern Sakhalin was observed. On the other hand, the 12-month mean biomass of zooplankton was less that the long-term average during "warm" year conditions.

We conclude that, for certain fish populations of far-eastern seas, it is usual for a change in abundance to occur when the pressure and circulation system over the North Pacific changes from one type to the other; this in turn is related to the 22-yr cycle of solar activity.

The "Half-Centennial" Cycle in Relation to World Fisheries

In the history of world fisheries there are instances of cycles of abundance longer than 22 yr. Examples include the collapse of the fisheries for California and Japanese sardines, the Atlantic herring, and the pink salmon of western Kamchatka (Dement'eva 1976; Cushing 1975; Davydov 1981; and Shuntov and Vasilkov 1982). However, in many cases the change in long-term abundance occurred concurrently in widely separated geographical regions. This suggests the possible existence of a common cause for the changes in abundance for many species of fish.

At the present time a majority of investigators are of the opinion that the cause may be changes in the earth's climate which, acting through the ecological specificity of fishes, become reflected in their abundance (Dement'eva 1976; Cushing 1975). Especially numerous are studies of the ecological consequences of the period of warming that was observed in the northern hemisphere from the start of this century up to the 1930s, and the subsequent period of cooling (Vinnikov et al. 1980).

The warming was accompanied by an increase in the frequency of strong year-classes of Barents Sea cod and Atlanto-Scandian herring (Dement'eva 1976). During this period there was a significant increase in the abundance of Japanese and Californian sardines (Cushing 1975), and of western Kamchatka pink salmon of the even year-classes (Davydov 1981). Starting in the 1940's and up to the end of the 1960's (the period of cooling), these species decreased again.

Such changes are not exceptional but recur throughout the history of the climate of the Northern Hemisphere (Polozova 1975). Hence to work out the ecological bases of very long-term fishery forecasts (with a duration of several decades), it is extremely important to understand the causes of the formation of long-term fluctuations (within the limits of a century) in climate. As a rule investigators have explained these changes as fluctuations in intensity of the general circulation of the atmosphere caused by changes in solar activity (Girs 1971; Le Roi Ladyuri 1971; Vitinskii et al. 1976). However, the question of whether the "centennial" cycle of solar activity affects the earth's climate is still controversial. Doubts arise, most of all, from the fact that the overwhelming majority of cycles in the development of meteorological processes appear to be shorter than the "centennial" (Drozdov 1975).

The reason for the differences in views on links between climatic processes, on the one hand, and the "centennial" cycle of solar activity on the other, might be due to the differences in the manner in which the cycles become manifested in different geographical regions. Thus Polozova (1970) believes that the "centennial" solar cycle is best manifested in high and subtropical latitudes. In temperate latitudes, according to Vitinskii et al. (1976) climate becomes milder when there is an intermediate number of sun spots, before and after the "centennial" maximum of solar activity. A series of studies have indicated that the sign of the relationship between solar activity and atmospheric processes is different during the ascending and the descending phases of the "centennial" solar cycle (Vitel's 1948; Willet 1951).

Thus the cycles of 30 yr or more, which are characteristic of hydrometeorological processes in many parts of the world, may be formed as a result of the change in the sign of the relationship between solar activity and terrestrial processes, during transition from one phase of development of the "centennial" cycle to another. Sherstyukov and Loginov (1986) believe that the change in sign and of the closeness of the relationship of the frequency of the forms of atmospheric circulation is related to asymmetry of the spotting of the solar hemisphere, which influences the conditions for injection of solar particles into the earth's magnetosphere in a specific manner. It is known (Vitinskii et al. 1976) that solar activity develops simultaneously in the two solar hemispheres when it has reached its average level. Therefore, we may postulate that the sign of the relationship between solar activity and weather processes must change during its transitions through the average level of the "centennial" cycle.

To test this hypothesis we analyzed the "geoeffectiveness" of different phases of the "centennial" sun spot cycle on atmospheric processes in the North Pacific. As indices we used the mean annual quantity of rain at Seoul, and the thickness of annual rings on Japanese cypress from central Japan (Arakawa 1954) (Fig. 12).

In the analysis we used the series of years having reliable estimates of Wolf numbers (1744–1985). Anomalies of Wolf numbers were estimated using the average for a given "centennial" cycle (limits of the "centennial" cycles for the last 200 years are taken from Vitinskii 1973) (Fig. 13).

Available information allows us to analyse the "geoeffectiveness" of the different phases of two "centennial" cycles of solar activity. Phases of the cycles were determined as follows:

1. Periods when solar activity in "centennial" cycles was below the long-term average, including the epoch of the great sun spot minimum (1744–1765; 1798–1822; 1878–1912).
2. Periods with negative anomalies of Wolf numbers, after the epochs of "centennial" minima of solar activity (1823–1842; 1913-1932).
3. Periods with positive anomalies of Wolf numbers, including the epochs of "centennial" maxima of solar activity (1784–1797; 1867–1877).
4. Periods with positive anomalies of Wolf numbers after the "centennial" maxima of solar activity (1784–1797; 1867–1877).

Average values of the climatic indices in question were obtained for the same periods. Breaks in their long-term course occurred during transition of Wolf numbers through long-term average levels and after epochs of maxima of the "centennial" cycle (Fig. 13). No such breaks were observed during epochs of "centennial" maxima of solar activity.

Change of direction in the development trends of climatic processes observed after times of "centennial" minima of solar activity is supported by Zaushinskaya's (1975) study, who showed that during the "centennial" minimum of solar activity the maximum of the 80-yr cycle of sun-spot frequency could be geoeffective. In the present "centennial" cycle this is evident in 11-yr solar cycle No. 15 (1913–23), i.e., in the 11-yr cycle following the minimum of the "centennial" cycle. A similar relationship between phases of the "centennial" minimum of relative number of sun spots (Wolf numbers) and the

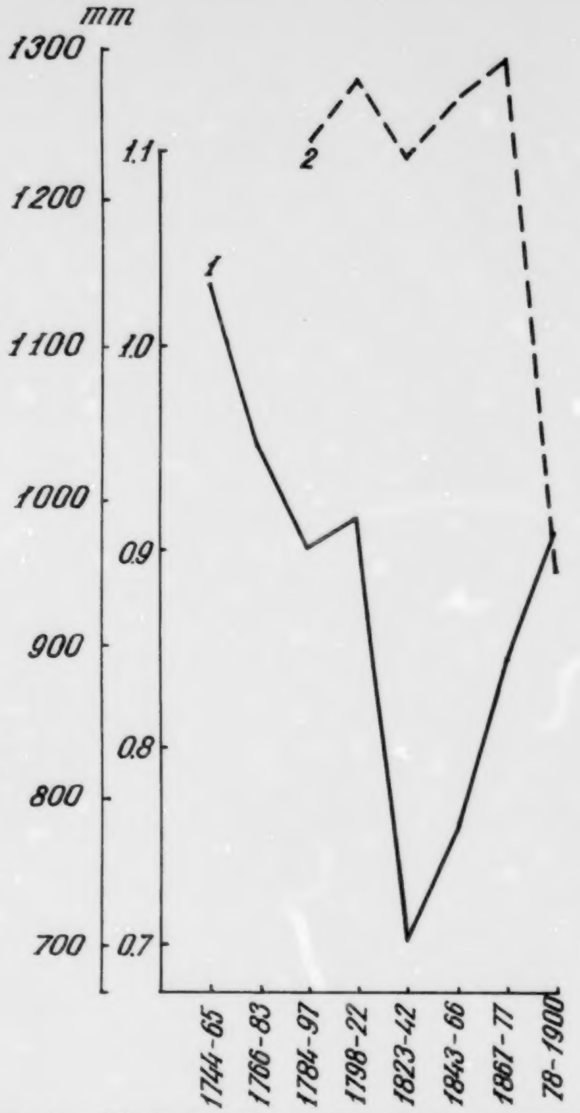

FIG. 12. 1. Distribution of mean values of thickness of annual rings on Japanese cypress. 2. Quantity of rainfall at Seoul, Korea. Both indices are divided according to the phases of the "centennial" cycle of solar activity.

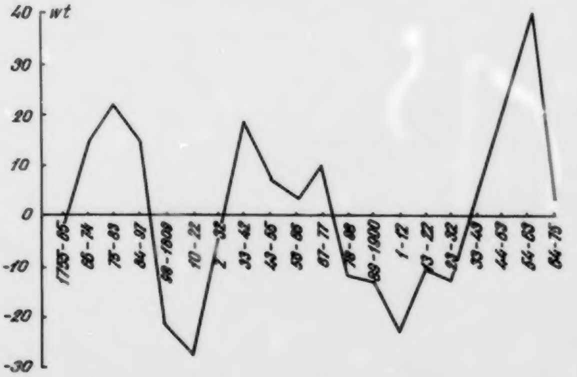

FIG. 13. The course of solar activity throughout its "centennial" cycles in terms of the mean anomaly of the Wolf numbers for each 11-yr cycle.

maximum sun-spot frequency was evident in the two previous "centennial" cycles.

Taking into account the similarity of development of hydrometeorological conditions in the different areas of the North Pacific, we may postulate that long-term variations of selected local climatic indices adequately represent variations of climate in other parts of the region, and are a consequence of variations in the frequency of large-scale processes of similar duration that affect atmospheric circulation in the North Pacific. Bearing in mind that in "warm" years over the Sea of Japan the frequency of cyclones increases, and in "cold" years they decrease (with precipitation increasing or decreasing respectively), processes characteristic of the M_1 meridional circulation pattern may be thought to have prevailed in the North Pacific during periods of decreased precipitation in Seoul (1744–1797, 1823–1842, 1878–1922), while the M_2 pattern prevailed during rainy periods (1798–1822, 1843–1877).

Within the present "centennial" cycle of solar activity the sun spot minimum period occurred during 11-yr cycle No. 14 (1901–1913), the next reversal in the course of climatic variations should have occurred in 11-yr solar cycle No. 15 (1913–1923). Hence, starting from that time, the frequency of the M_2 meridional form of circulation should increase. Durations of the period when it prevailed was limited by the effect of the next transition of solar activity (Wolf numbers) through the long-term average level within the "centennial" cycle (11-yr cycle No. 17: 1933–1943).

In fact Figure 14, showing the long-term variations in 18-month averages of M_1 in the North Pacific (the result of progressive running averages of 5 and 21 items) from the beginning of this century until the middle 1930's, indicates that there was an increasing frequency first of M_2, and then of M_1. In other words, recurrent shifts in the development of atmospheric circulation in the North Pacific have occurred as expected, after the "centennial" minimum of solar activity and at the time of its transition through the long-term average level of the "centennial" cycle.

Unfortunately, the lack of adequate series of observations makes it impossible to follow the pattern of long-term variations of any parameter of oceanological conditions in the regions under discussion. Nevertheless, analysis of trends of abundance of certain commercial species in the North Pacific can to some extent shed light on the problem.

A positive relationship exists between the year-class strength of California sardines and water temperature in their spawning areas. An increase in abundance of Japanese sardines is observed when water temperatures are decreasing off the Pacific coast of Japan and are increasing in the Sea of Japan (Watanabe 1981). Anchovies of California prefer cooler water than do sardines, while Japanese sardines prefer cooler water than do the anchovies of the coast of Japan (Shuntov and Vasilkov 1982).

Success of the Pacific squid fishery depends greatly on water temperatures off Japan. The catch decreases when temperatures decline, and increases when the temperatures rise (Pavlychev and Shevtsov 1977).

Summing up, water temperatures were increasing in the northeast Pacific, and decreasing off the Pacific coast of Japan, from the early 1920's to the middle 1930's when the abundance of California and Japanese sardines were increasing while catches of Pacific squid were far below the long-term average (Fig. 14-15). The trend in abundance of these species was reversed in the middle 1930's suggesting a change in the direction of development of temperature conditions in the eastern and western regions of the North Pacific Ocean.

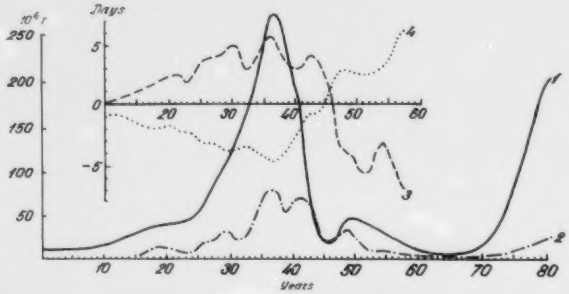

FIG. 14. Long-term changes in the catches of (1) Japanese sardines, and (2) California sardines (from Shuntov and Vasilkov 1982), as compared with (3) long-term changes in the frequency of occurrence of the M_2 type of atmosphere macroprocess, and (4) the same for the M_1 type.

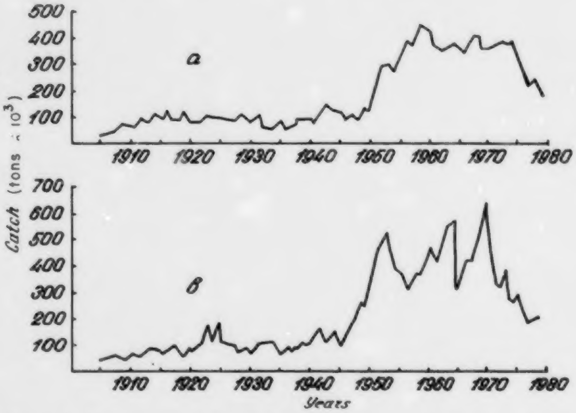

FIG. 15. *Upper panel*: Total Japanese catch of anchovy. *Lower panel*: Total Japanese catch of squid.

Thus, times of reversal in the development of temperature conditions correspond to times of change in the prevailing form of atmosphere circulation from M_1 to M_2. The recurrence of the increases in abundance of California and Japanese sardines, which began in the early 1970's coincided with the passage of solar activity through its long-term average level of the "centennial" cycle (11-yr cycle No. 21: 1976–86), which once again supports the hypothesis proposed here.

The above data provide some basis for believing that climatic cycles of 40–60 yr in length may appear in the North Pacific as a result of the geoeffectiveness of the transition of solar activity through its long-term average level in the "centennial" cycle, and of the maximum of sun spots. The duration of climatic cycles is related to the length of the "centennial" cycle of solar activity.

These cycles have an effect upon the dynamics of the variations in abundance of several species of fish, through the intermediation of their characteristic ecological features.

Conclusions

As a result of a specific interaction of high-altitude ridges and troughs in the northwestern part of the Pacific Ocean, two diametrically opposite types of pressure and circulation patterns in the atmosphere are formed which in turn are responsible for the formation of specific types of water regime in different regions of the far-eastern seas. These seas may be viewed as a single natural system, with interrelated hydrometeorological and biological processes.

As an index of the type of pressure and circulatory conditions, and consequently of the particular type of water regime, we can use the anomalies of minimum temperature of "CILSEK" (the cold intermediate layer of a standard hydrological section in the Avacha Bay of the southeastern coast of Kamchatka). The relationship established between anomalies of the temperature minimum and the pattern of atmospheric pressure and circulation and of oceanological processes allows the water regimes of far-eastern seas to be classified as a "warm" type (positive anomalies of water temperature) or a "cold" type (negative anomalies of the same).

Changes of direction from one to the other of these types occur at 10–11-yr intervals, and also over longer periods. The former may be related to the 22-yr cycle of solar activity, while the latter depends on the "geoeffectiveness" of the passage of solar activity in (Wolf numbers) through the long-term average level of the "centennial" cycle, and on the maximum of the "centennial" cycle of sun spot frequency which is usually observed in the 11-yr cycle following the "centennial" minimum of solar activity.

Considering this, one may postulate that the predominant development of "warm" year processes which began in 1982 last to about 1990–91 (until the return of the maximum of the 11-yr solar cycle. This trend in hydrometeorological conditions will be reflected in the abundance of several fishes. Thus, the next decade will be favourable for reproduction of pollock of the eastern Okhotsk Sea and the northeastern Sea of Japan, while it will be unfavorable for the herring populations of the Okhotsk and Bering seas.

The most recent of the periodic reversals of climatic trends in the North Pacific determined by the time when solar activity crossed its long-term average level, occurred in the early 1970's. Climatic warming began at this time in the northeastern Pacific and the Sea of Japan and, as a result, the abundance of Japanese and California sardines will increase, while that of Pacific squids and Japanese anchovies will decrease. The duration of this period will be limited by the arrival of the "centennial" maximum of solar activity (maximum frequency of sun spots).

According to forecasts of certain authors (Maksimov 1970; Zaushinskaya 1975) solar activity will be at its minimum at the end of the 1980's and early 1990's. Therefore cyclical change of climatic trends should occur in the North Pacific in the late 1900's (the "centennial" maximum of sun spot frequency). Corresponding changes will occur in the trends of abundance of several fish species.

The average duration of intervals having similar anomalies of Wolf numbers during two "centennial" cycles of solar activity was about 40 yr. Taking this into account, the next cyclical change of trends in climatic conditions related to the passage of the solar activity curve through its long-term average level of the "centennial" cycle is to be expected late in the second decade of the next century.

References

ARAKAWA, H. 1954. Climate and climate variation. Sekisetsu shirizu 5. 84 p. (In Japanese)

BERSHTEIN, S. P. 1946. Probability theory. Gidrometeoizdat, Moskva. 103 p. (In Russian)

BELINSKII, N. A. 1957. The use of certain peculiarities of atmospheric processes for long-term forecasting. Gidrometeoizdat, Moskva. 306 p. (In Russian)

CHERNYAVSKY, V. I., V. A. BOBROV, AND N. N. AFANASYEV. 1981. Major productive zones of the Okhotsk Sea. Izv. TINRO 105: 20–25. (In Russian)

CUSHING, D. H. 1975. Marine ecology and fisheries. Cambridge University Press, New York, N.Y. 278 p.

DAVYDOV, I. V. 1972. On the problem of the oceanological background of the determination of abundance of year-classes of herring in the western part of the Bering Sea. Izv. TINRO 82: 281–307. (In Russian)

1975. The water regime of the West Kamchatka shelf and certain features of the behaviour and reproduction of commercial fishes. Izv. TINRO 97: 63–81. (In Russian)

1981. Certain peculiarities of the dynamics of abundance of pink salmon (with reference to the West Kamchatka stock). Izv. TINRO 105: 3–6. (In Russian)

1984. Concerning the consequences of oceanological conditions in the main fishing areas of far-eastern seas. Izv. TINRO 109: 3–16. (In Russian)

DAVYDOV, I. V., AND A. G. KUTSYKH. 1967. Water temperature of the cold intermediate layer as a prognostic index of the thermal condition of the waters off Kamchatka. Izv. TINRO 61: 301–308. (In Russian)

DEMENT'EVA, T. F. 1976. The biological basis of commercial fishery forecasts. Pishchevaya Promyshlennost, Moskva. 239 p. (In Russian)

DROZDOV, O. A. 1975. Cyclic variations of precipitation and temperature used in very long-term forecasting, and the possible role of polar activity in their formation. Tr. Gl. Geof. Obs. 354: 3–13. (In Russian)

FEDOTOVA, N. A. 1984. On cyclic variations in the biomass of zooplankton off southwestern Sakhalin. Izv. TINRO 109: 20–25. (In Russian)

GIRS, A. A. 1960. Basic principles of long-term weather forecasting. Gidrometeoizdat, Leningrad. 559 p. (In Russian)

1971. Fluctuations in atmospheric circulation over many years, and long-term forecast of the weather. Gidrometeoizdat, Moskva. 280 p. (In Russian)

1974. The macrocirculation method of making long-term hydrometeorological forecasts. Gidrometeoizdat, Leningrad. 435 p. (In Russian)

GLAGOLEVA, M. G., AND L. I. SKRIPTUNOVA. 1979. Forecasting the temperature of water in the ocean. Gidrometeoizdat, Leningrad. 168 p. (In Russian)

Izhevsky, G. K. 1961. Oceanological basis of the development of commercial productivity in the sea. Pishchevaya Promyshlennost, Moskva. 206 p. (In Russian)

Il'insky, O. K., and N. V. Egorova. 1962. Cyclonic activity over the Okhotsk Sea during the cold half of the year. Trudy DVNIGMI 1962(14): 34–83. (In Russian)

Kachina, T. F. 1981. Herring of the western part of the Bering Sea. Pishchevaya Promyshlennost, Moskva. 120 p. (In Russian)

Kachina, T. F., and N. P. Sergeyeva. 1981. Dynamics of abundance of pollock of the eastern Sea of Okhotsk. *In* Ekologiia, zapasy i promysel'mintaya. TINRO, Vladivostock. 1981: 19–27. (In Russian)

Kajura, K. 1986. Physical processes associated with the Kuroshio. Proceedings of the Symposium on the Kuroshio, Tokyo.

Karklin, V. N. 1973. 22-year fluctuations in the field of atmospheric pressure at moderate and high latitudes during winter. Tr. Arktich i Antarktich Nauchno-issled. Inst. 307: 133–141 (In Russian)

Kryndin, A. M. 1966. The role of the oceanic temperature field in the formation of anomalies of atmospheric circulation and of anomalies of severity of winters at sea (with reference to the northwestern part of the Pacific). Tr. NNIIA 2966. No. 36. (In Russian)

Le roi ladyuri, E. 1971. The history of climate from the year 1000. Gidrometeoizdat, Leningrad. 279 p. (Translated into Russian)

Maksimov, I. V. 1970. Geophysical forces and ocean waters. Gidrometeoizdat, Leningrad, 279 p. (In Russian)

Pavlychev, V. P., and G. A. Shevtsov. 1977. The influence of hydrological conditions on the squid fishery in the northwestern Pacific. Izv. TINRO 101: 13–17. (In Russian)

Poloskin, G. E. 1974. Change in kinetic energy of the atmosphere in relation to the earth's entering a particle stream, p. 121–127. *In* E. R. Mustel' [ed.] Solnechnoatmosfernyue svyazi v teorii klimata i prognoza pogody. Gidrometeoizdat, Leningrad. (In Russian)

Polozova, L. G. 1970. An analysis of cyclical fluctuations of the mean monthly air temperaure in the northern hemisphere. Tr. Gl. Geof. Obs. 269: 36–73. (In Russian)

1975. On the century-long course of temperature in the Northern Hemisphere. Tr. Gl. Geof. Obs. 355: 95–101. (In Russian)

Sazonov, B. I. 1964. High altitude pressure formations and solar activity. Gidrometeoizdat, Leningrad. 132 p. (In Russian)

Sazonov, B. I., and V. F. Loginov . 1969. Solar-tropospheric relationships. Gidrometeoizdat, Leningrad. 115 p. (In Russian)

Sherstyukov, B. G., and V. F. Loginov. 1986. Short-period cyclic variations in the lower atmosphere and heliophysical processes. Gidrometeoizdat, Moskva. 87 p. (In Russian)

Shuntov, V. P., and V. P. Vasilkov. 1982. Long-period variations of an abundance of North Pacific sardines. Report No. 2. Atmospheric circulation epochs and cyclic population dynamics of the far eastern and Californian sardines. Vopr. Ikhtiol. 22(8): 187–199. (In Russian)

Sorkina, A. I. 1972. Long-term variations in mean monthly values of the position and intensity of centres of atmospheric activity in the northern hemisphere. Sinopticheskii Bulletin 1972, Appendix 2, 20 p. (In Russian)

1974. The role of large-scale atmospheric circulation in the formation of temperature anomalies of surface waters, with special reference to the northwestern Pacific, p. 15–18. *In* A. A. Dmitriev [ed.] Fizika morya i atmosfery. Nauka, Moskva. (In Russian)

Tyurnin, B.V. 1980. On the causes of the reduction of the stocks of Okhotsk herring, and measures for increasing them. Biologiya morya, 1980(2): 64–74. (In Russian)

Uda, M. 1963. Oceanography of the Subarctic Pacific Ocean. J. Fish. Res. Board Can. 20: 119–179.

Vinnikov K. Ya., G. V. Gruza, V. F. Zakharov, A. A Kirillov, N. P. Kovyneva, and E. Ya. Rankova. 1980. Current changes in climate of the northern hemisphere. Meterologiya i Gidrologiya 1980(6): 5–7. (In Russian)

Vitel's, L. A. 1948. Long-term changes in the pressure and circulation regime, and their effects on climatic fluctuations. Tr. IIO 1948(8): 51–109. (In Russian)

Vitinskii, Yu. I. 1973. Cyclicity and the forecasting of solar activity. Nauka, Leningrad. 255 p. (In Russian)

Vitinskii, Yu. I., A.I. Oi', and B. I. Sazonov. 1976. The sun and the earth's atmosphere. Gidrometeoizdat, Leningrad. 350 p. (In Russian)

Watanabe, T. 1981. Survival of Japanese sardines in their early stages of life. Izv. TINRO 105: 92–107. (In Russian)

Willet, H. C. 1951. Extrapolations of sunspot-climate relationships. J. Meteorol. 8: 1–6.

Zaushinskaya, T. M. 1975. Manifestation and forecasting of the 80-year cycle in indices of climate and solar activity. Tr. Gl. Geof. Obs. 355: 104–125. (In Russian)

Zavernin, Yu. P. 1972. Effect of hydrometeorological conditions on the time that Okhotsk herring approach their spawning area, and on the strength of their year-classes. Izv. TINRO 81: 44–51. (In Russian)

Zverkova, L. M. 1981. Effects of natural factors and the fishery on the abundance of the Alaska pollock of the northeastern part of the Sea of Japan, p. 28–40. *In* Ekologiya zapasy i promysel mintaya. TINRO, Vladivostok. (In Russian)

Ecological Studies of the Pomfret *(Brama japonica)* in the North Pacific Ocean

Kenji Shimazaki

Research Institute of North Pacific Fisheries,
Faculty of Fisheries, Hokkaido University,
Hakodate, Japan

Abstract

SHIMAZAKI, K. 1989. Ecological studies of the pomfret (*Brama japonica*) in the North Pacific Ocean, p. 195–205. *In* R. J. Beamish and G. A. McFarlane [ed.] Effects of ocean variability on recruitment and an evaluation of parameters used in stock assessment models. Can. Spec. Publ. Fish. Aquat. Sci. 108.

The pomfret (*Brama japonica* Hilgendorf) is widely distributed throughout the North Pacific Ocean. The region is separated into Subarctic waters and Subtropic waters in accordance with different ecological parameters. These ecological differences, together with results from observations of the seasonal changes in condition factor, stomach contents, and ovarian maturation indicate that the immature and spent group migrates from the Subtropic region toward the Subarctic region from April to May. This is a feeding group. Around October and November, the feeding group begins to scatter over an extensive area in the Subtropic region and now becomes a spawning group.

Ovarian maturation among pomfret has been presumed segregated and pelagic based on asynchronistic oocyte development. It is now suggested, however, that the pomfret engages in multiple spawnings over a protracted period. In summer, when the fish move northward beyond the Subarctic Boundary, maturity is in the yolk vesicle stage or in the oil drop stage. In fall, when the fish migrate southward, the accumulation of yolk becomes gradually active. During the period from winter to early summer, the pomfret spawns in the Subtropic region, especially in waters adjacent to the Subarctic Boundary in early summer.

The transitional seasons of ecological stages are thought to be rather short periods around spring and fall, and that large scale migration occurs between the ocean current systems in these seasons.

Résumé

SHIMAZAKI, K. 1989. Ecological studies of the pomfret (*Brama japonica*) in the North Pacific Ocean, p. 195–205. *In* R. J. Beamish and G. A. McFarlane [ed.] Effects of ocean variability on recruitment and an evaluation of parameters used in stock assessment models. Can. Spec. Publ. Fish. Aquat. Sci. 108.

La castagnole (*Brama japonica* Hilgendorf) est répartie dans l'ensemble du nord de l'océan Pacifique. Cette région est subdivisée en eaux subarctiques et subtropicales en fonction de divers paramètres écologiques. Ces différences écologiques ainsi que les observations des changements saisonniers du coefficient de condition, du contenu stomacal et du degré de maturation des ovaires, révèlent que les groupes de poissons n'ayant pas atteint la maturité et des poissons guais migrent depuis la région subtropicale vers la région subarctique d'avril à mai. Ce groupe est en phase d'alimentation. Vers les mois d'octobre et novembre, il commence à se disperser dans la vaste région subtropicale. Il est alors en phase de reproduction.

On a présumé que le développement des ovaires se fait de façon distincte et dans les zones pélagiques d'après le développement asynchrone des oocytes, et l'on présume actuellement que la castagnole a plusieurs pontes pendant une assez longue période de fraye. En été, lorsque ces poissons se dirigent vers le nord et pénètrent les eaux subarctiques, les femelles se trouvent au stade de vésicule vétilline ou au stade de vitellus à goutte d'huile. En automne, quand les poissons migrent vers le sud, l'accumulation de vitellus entre progressivement dans une phase active. Pendant la période qui s'étend depuis l'hiver jusqu'au début de l'été, la castagnole fraie dans la région subtropicale, particulièrement, au début de l'été, dans les eaux adjacentes à la limite subarctique.

L'on croit que les saisons de transition des étapes écologiques sont plutôt courtes aux alentours du printemps et de l'automne, et que des migrations massives s'effectuent entre les systèmes de courants pendant ces saisons.

Introduction

Six genera and seven species of Bramidae are currently recognized (Mead 1972) and all occur in the North Pacific Ocean. The pomfret (*Brama japonica* Hilgendorf) comprises the largest proportion of the biomass of all these species (Larken 1964). The pomfret is widely distributed and migrates seasonally from feeding grounds in the Subarctic region to spawning grounds in the Subtropic region adjacent to the Subarctic boundary (Machidori and Nakamura 1971; Shimazaki 1979; Yoon and Shimazaki 1981; Shimazaki and Nakamura 1981). As the pomfret comprises a significant biomass, this species plays an important ecological role in both regions. Little information is available on the ecological importance of the pomfret although it has received much attention as an unutilized resource. This report summarizes information currently available, and discusses results of recent ecological studies.

Seasonal Distribution and Ecological Features

Seasonal Changes in Distribution

In the northeastern Pacific, the northern limit to the pomfret during May and June occurs at approximately 50°N latitude. It extends to approximately 55°N in July, reaching the deep part of the Gulf of Alaska from August to September (Neave and Hanavan 1960). In the northwestern Pacific (west of 180°), the northernmost limit of distribution coincides with the Subarctic boundary from March to April. It extends northward from this boundary during May and June and reaches the Kurile and Aleutian islands in August and September (Machidori and Nakamura 1971; Shimazaki and Nakamura 1981).

Seasonal changes in the north–south distribution of pomfret correspond closely with a rise in surface water temperature above 9–10°C. Surface water temperatures within the northern portion of the area to the west of 180° exceed those of the eastern area (Dodimead et al. 1963; Favorite et al. 1976). Water temperature around the northern limit of pomfret distribution is 9–10°C (Neave and Hanavan 1960; Machidori and Nakamura 1971). The vertical distribution of pomfret is also limited to waters in which temperatures exceed 9–10°C within the upper thermocline layers that develop in shallow layers during the summer (Machidori and Nakamura 1971; Kikuchi and Tsujita 1977).

Seasonal changes in CPUE by region result from vertical and horizontal changes in water temperature. According to Dodimead et al. (1963) and Favorite et al. (1976), the Subarctic boundary, which separates the Subarctic and Subtropic regions, lies at approximately 41°N latitude (Fig. 1). Additionally, the boundary between the transitional domain and the Subarctic domain lies at approximately 44°N. The structure of the seas, however, is complicated and indistinct. Where observations have been conducted, CPUE of pomfret is high in the transitional domain, and declines sharply to the south and north of that area. The range of distribution from north to south advances northward with the rise in surface water temperature and is associated with a decline in CPUE in the south (Shimazaki and Nakamura 1981). Pomfret are distributed widely from east to west in the Subarctic region during the summer and migrate quickly southward with the onset of fall to become widely distributed in the Subtropic region during

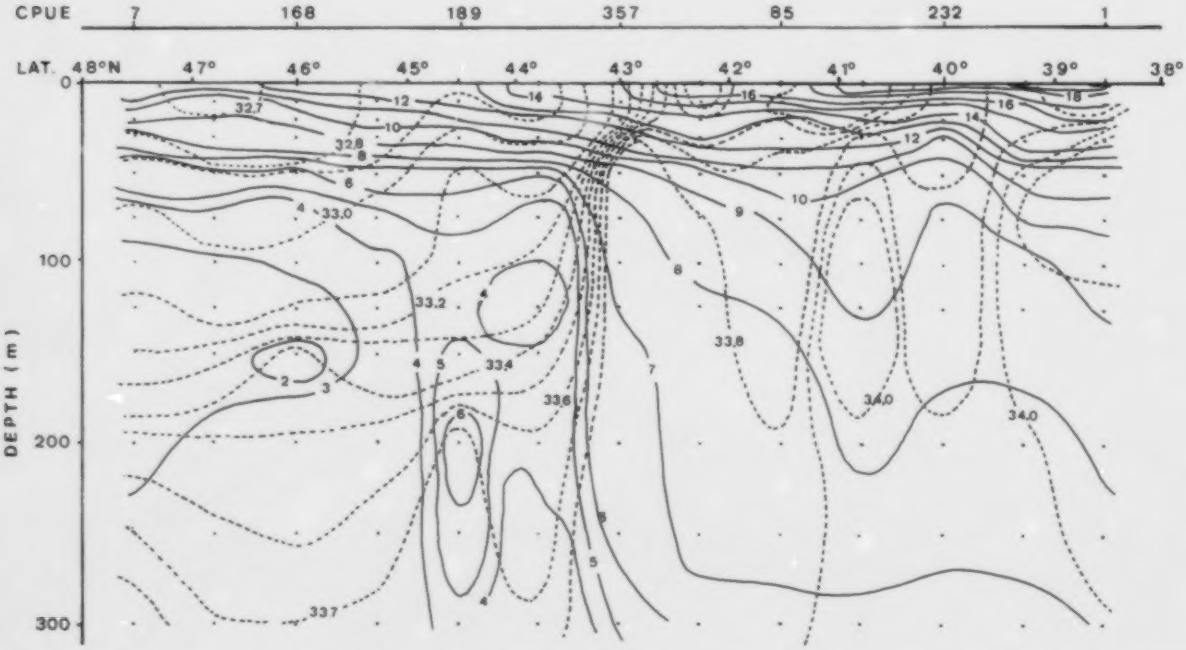

FIG. 1. Vertical distribution of temperature (solid) and salinity (broken) along longitude 175°30′E in late July, 1986, and associated CPUE of pomfret catches.

winter. Except in localized areas, CPUE is lower in winter than in summer (Fig. 2). The wide distribution of pomfret within the Subtropic region contrasts with the concentrated distribution within the Subarctic region. Mead (1972) found the southern-most limit of distribution to be north of 20°N where surface water temperatures exceed 21°C. That latitude is considered to approximate the Subtropical convergence.

In summary, migration of the pomfret northward across the Subarctic boundary in spring coincides with the rise of water temperatures above 9-10°C. While in the Subarctic region and until fall, the species distribution is relatively concentrated. As water temperatures decline in the fall, pomfret migrate rapidly southward and become widely distributed within the neighboring Subtropic region in winter.

Latitudinal Differences in Fork Length

A consistent difference in the north-south distributions of fork lengths is found in early summer observations along longitude 170°E and 175°30′E within the range of 38° - 48°N (Fig. 3). Pomfret of relatively short fork length are distributed to the south of the Subarctic boundary, while only larger fish are to be found to the north of that boundary. Fish of mixed size composition occur in the transitional domain which separates the Subarctic and Subtropic regions. This indicates a tendency for shoals (schools) of large-sized pomfret to migrate northward first consistently from spring to fall.

Age Determination by Scale and Otolith

No conclusion as to whether large pomfret are older than small ones is possible because no method of age determination has been established. Recent studies by Mugiya and Shimazaki (unpub. data) suggest that, of nine possible body parts, scales and otoliths provide the most promise of yielding estimates of age.

Scales were removed from each of 15 areas (Fig. 4) and examined for age-related characteristics in circuli patterns. Scales removed from these areas varied widely in configuration (Fig. 5). A close correlation was found between what appear to be annuli (areas of relatively compact circuli patterns) on scales taken from the caudal peduncle, and fork length (Fig. 6), indicating the possibility of their usefulness in age determination.

Designation of ages based on these scales was established as follows: (A) 0.5 where no annuli were found, (B) 1.0 if an annuli was found on the edge of the scale with no subsequent circuli, (C) 1.5 where scales had one annulus and subsequent circuli, (D) 2.0 where two annuli were found, and (E) 2.5 where two annuli plus subsequent circuli were found, and (F) 3.0 where three annuli were found and no subsequent circuli (Fig. 7). Clear distinctions were found between the ranges for fork lengths among pomfret designated as age 0.5, and those exceeding 1.5 (Fig. 8) indicating that this technique may be valid for establishing age. It is possible, however, that larger pomfret are comprised of more age-classes than are evidenced by circuli patterns.

By observing the outer edges of otoliths with transmitted or reflected light, an opaque zone is seen in large-sized pomfret that is not present in smaller fish (Fig. 9). Otoliths were sectioned along the long axis and polished. The polished surfaces were etched with acid and observed under a scanning electron microscope for minute growth increments. As a result, small-sized pomfret were found to have less than 160 growth increments and larger

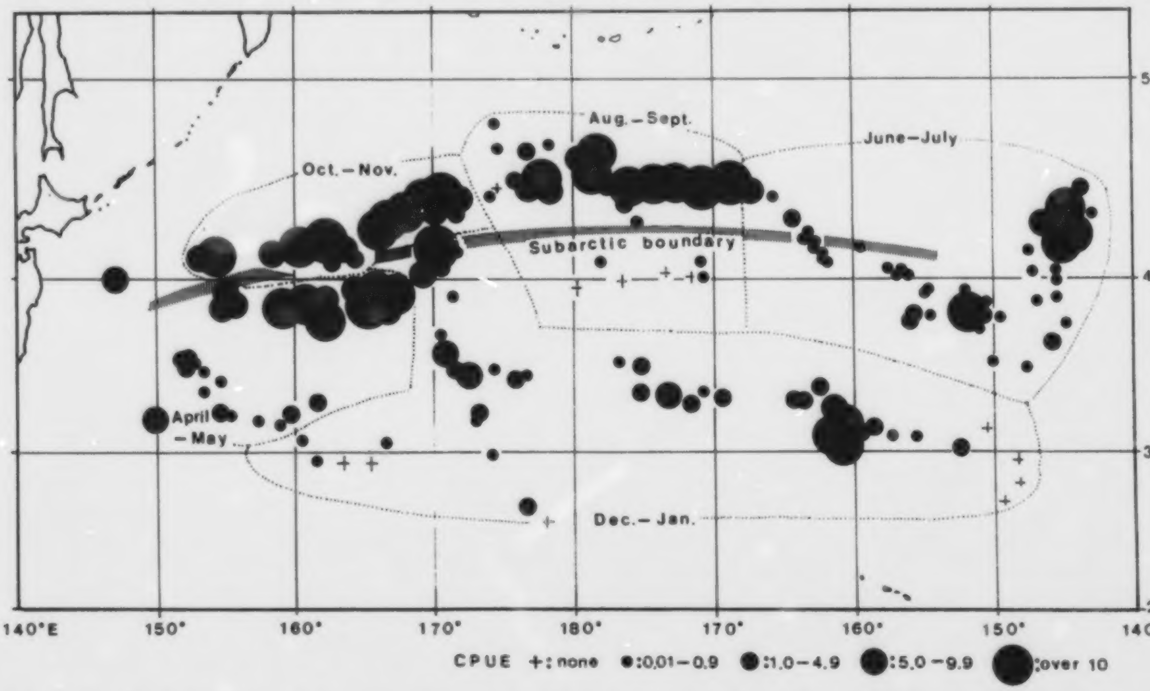

FIG. 2. The relative abundance of large pomfret caught by the R/V *Shinyo Maru* in 1979 (after Shimazaki and Nakamura 1981).

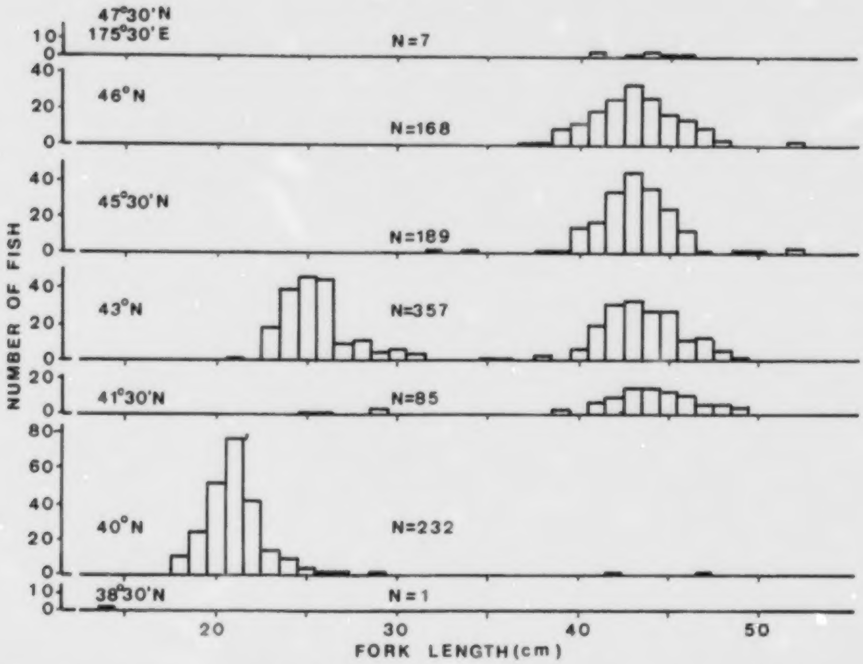

FIG. 3. Latitudinal changes in fork length of pomfret caught by non-selective gill nets along longitude 175° 30′E in late July, 1986.

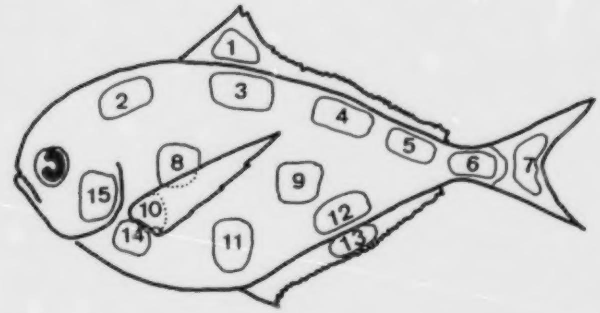

FIG. 4. Areas where scales were collected from pomfret for the purpose of age determination (Mugiya and Shimazaki Unpubl. data).

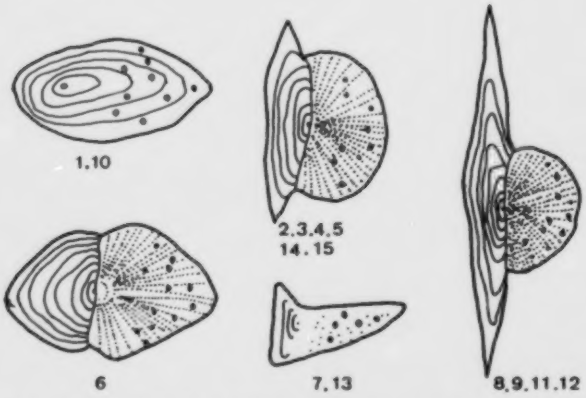

FIG. 5. Representative sample of various scale configurations on pomfret. Numerals correspond with areas where scales were removed (See Fig. 4).

(≥40 cm) pomfret had from 360 to 720 increments (Fig. 10).

The use of circuli density found on scales taken from the caudal peduncle, or minute growth increments from otoliths is more reliable for age determination of younger fish than of older fish. Growth patterns of pomfret older than 1 yr are varied and a relationship between scale annuli numbers and fork length is not distinct. Additionally, it is not known whether the period wherein one annulus is formed is indeed 1 yr, or whether the time required for the formation of the opaque zone found in the otoliths of larger pomfret applies to a similar period. These subjects require further investigation before the age of pomfret can be accurately determined. What are assumed to be minute growth increments in otoliths, however, indicate that small-sized pomfret are approximately 5 mo old. Subtracting this from the date of capture indicates that these fish were hatched in approximately February. In this same manner, larger sized pomfret are 14–20 mo old and the estimated hatching time is from November to May. These back-calculated hatching times correspond with the reproduction period found by Yoon and Shimazaki (1981).

Seasonal Change of Condition Factor

The most striking characteristic of pomfret distribution is the seasonal migration between regions. During this migration, a change in condition factor (body weight per unit of fork length) reflects the energy dynamics of both an individual and the population. Shimazaki and Nakamura (1981) calculated the condition factor of large-sized pomfret in the years 1978 and 1979 (Fig. 11). The

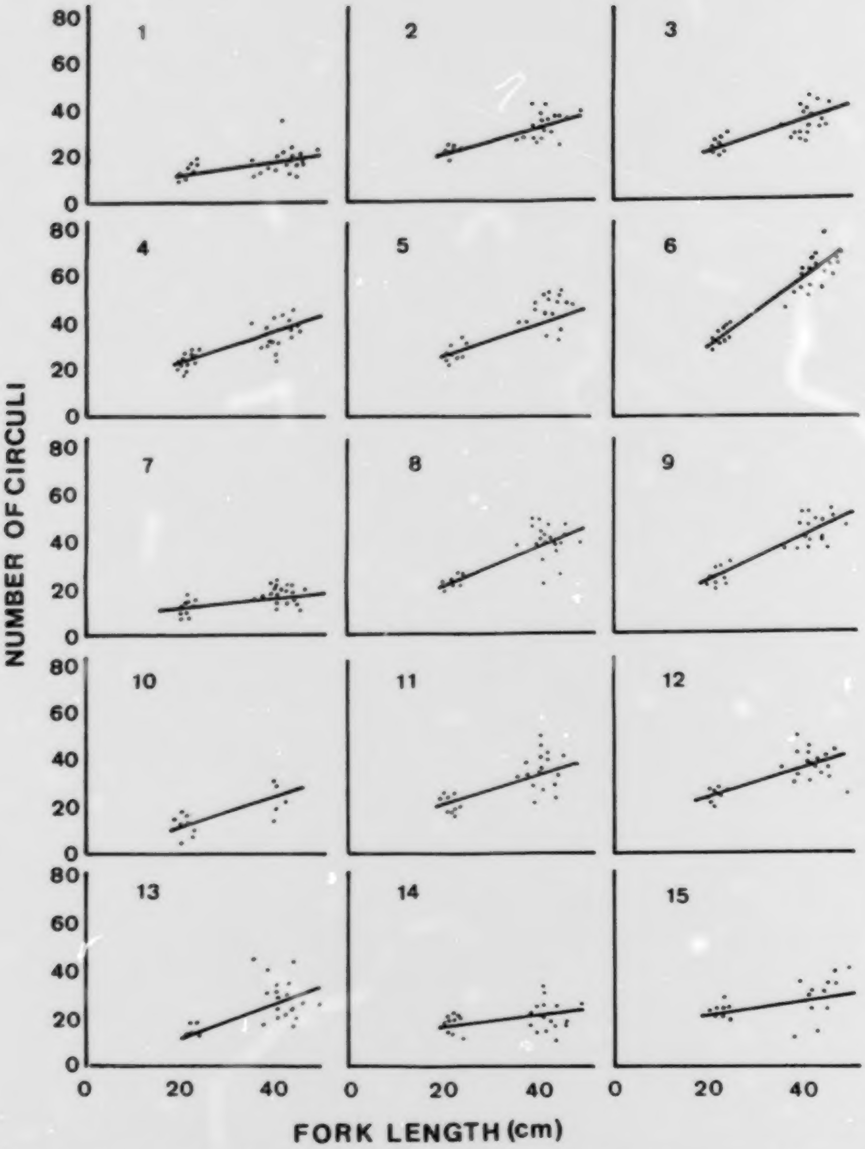

FIG. 6. Relation between fork length and the number of circuli on scales removed from 15 body areas of pomfret. Numerals with each graph indicate the body area (See Fig. 4).

condition factor of both sexes was low during the winter months and increased from spring to summer, peaking from September to October. Recalling the seasonal distribution of this species, the pomfret stores energy actively in the Subarctic region from spring to fall, and then discharges that energy for reproduction in the Subtropic region from winter to spring.

Seasonal and Regional Changes in Stomach Content

Feeding habits of the pomfret have been studied only within a limited ocean area and for a limited period (Pinckard 1957; Machidori and Nakamura 1971; Kikuchi and Tsujita (1977). Shimazaki and Nakamura (1981) observed the stomach contents of 1 099 large pomfret collected during the period from April to the following January. Squids and fishes comprised the most frequent food item during that entire period, indicating these are important sources of food. Many pomfret prey upon crustacea, especially euphausiids in spring and when other prey items are less abundant. Squids and fishes were found in the stomachs of pomfret sampled in the Subarctic domain from September to October and the volume of stomach content was larger where CPUE was high (Fig. 12). The types of fish eaten by pomfret include migratory fishes from the south such as the Subarctic and Pacific saury, sardine, and the Atka mackerel.

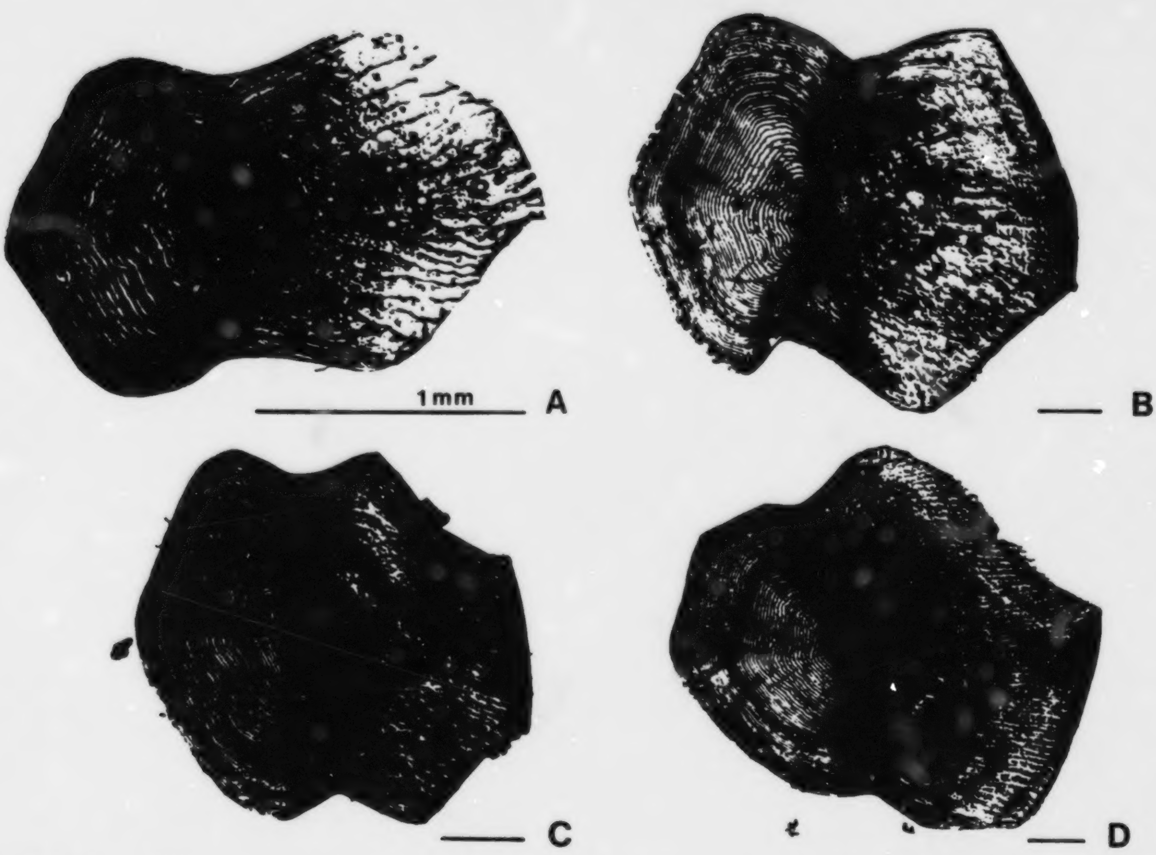

FIG. 7. Scales which were removed from the caudal peduncle and are representative of four age classifications of the pomfret. Scale line = 1 mm. Age designation is based on the number of annuli, or what appear as areas of closely compacted circuli (arrows) A:0.5; no annuli; male, F.L. = 231 mm, B.W. = 190 g. B:2.0; male, F.L. = 416 mm, B.W. = 1377 g. C: 2.5; male, F.L. = 404 mm, B.W. = 1407 g. D: 3.0 female, F.L. = 400 mm, B.W. = 1469 g.

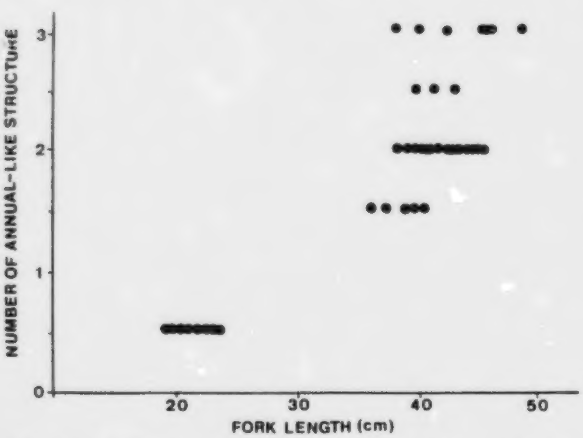

FIG. 8. Relation between fork length and the number of annuli found on scales removed from the caudal peduncle of pomfret.

Ovarian Maturation

Yoon and Shimazaki (1981) made histological and cytological observations of pomfret ovaries to describe the characteristics of oogenesis and the mechanism of reproduction. Based on those findings, ovarian development in the pomfret was found to be of the asynchronous oocyte type. This type of development is in contrast to the synchronous oocyte development found in rainbow trout (Yamamoto et al. 1965) and the walleye pollock (Yoon 1981). In the latter type of development, the ovaries develop uniformly, the period of spawning is relatively short, and the increase or decrease in ovary weight and GSI (gonadosomatic index, gonad weight per body weight) directly reflect the process of maturation and spawning. The relationship between ovarian development and GSI in the pomfret must be established before conclusions on sexual maturation based on these indices is possible.

The relation between ovary and body weight, and between GSI and body weight has been examined at the oil drop stage. It was determined that GSI is an appropriate maturity index for female pomfret. The relation between GSI and the stage of maturity was calculated, presuming the period of oogenesis is the histological stage of maturity. GSI values were 0.8 or less at the yolk vesicle stage, 0.6 to 1.5 at the oil drop stage and thereafter increased gradually with the progress of the yolk stage. All fish examined during spawning were at the nucleus migration or mature stages and GSI values

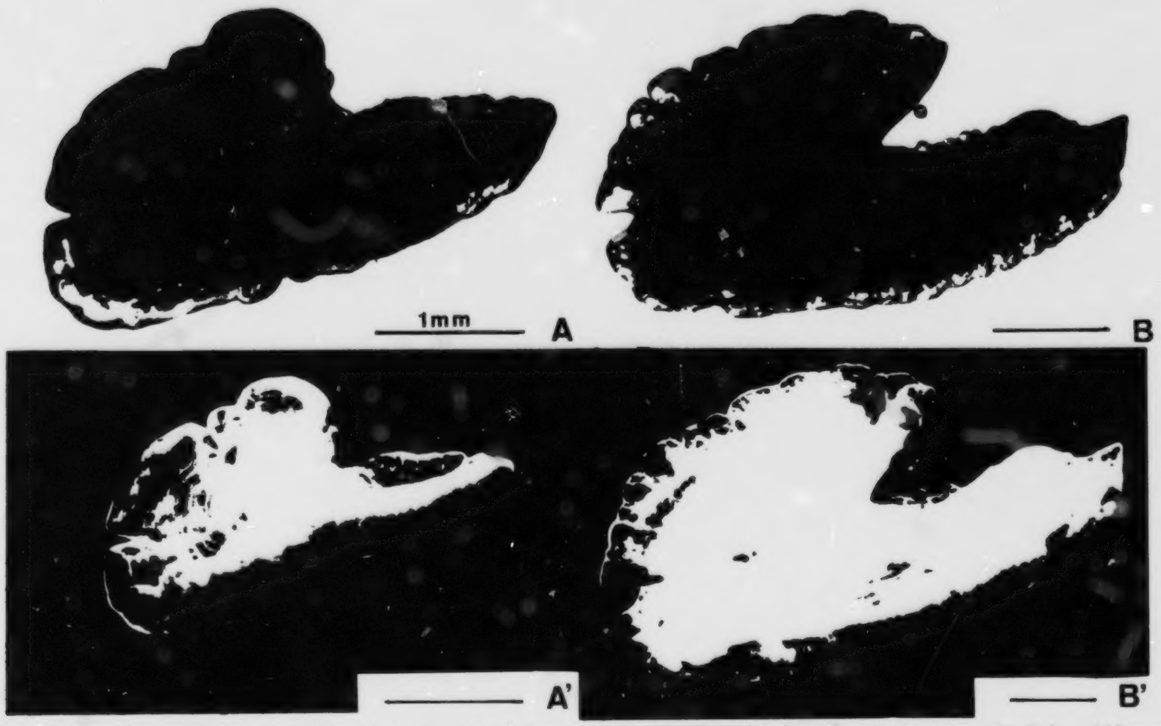

FIG. 9. Pomfret otolith as seen through transmitted light (upper) and reflected light (lower). A, A′: male, F.L. = 213 mm, B.W. = 164 g. B, B′: female, F.L. = 426 mm, B.W. = 1570 g.

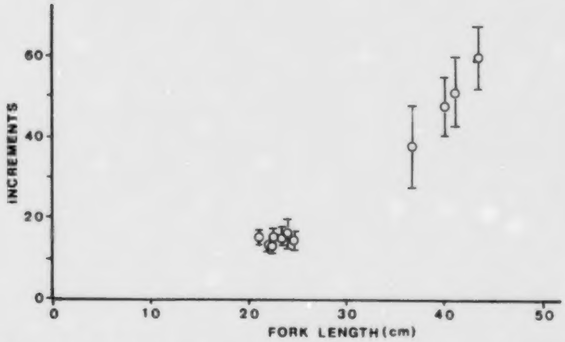

FIG. 10. Relation between the fork length and minute otolith growth increments of the pomfret (observations represent the average of several counts ± SD).

exceeded 3.0. This reflects the fact that yolk formation continues even after the initiation of spawning. Having finished spawning, pomfret maintain ovarian maturity until reaching the oil drop stage. The GSI of the pomfret is higher during this time than during the oil drop stage or younger. Accordingly, it is possible to explain the maturational stage of female pomfret by the GSI. GSI values of 1.5 to 3.0 indicate the yolk stage and marks the activation of maturity. The nucleus or matured stages are found where GSI values exceed 3.0 which indicates that the fish is either in spawning condition or will spawn in the near future.

Using GSI as a criterion, the annual cycle of ovarian development can be plotted (Fig. 13). No fish were found with a GSI value above 1.5 during August, and few during September to November. Fish maintained the oil drop stage from September to October, with a few in the yolk stage. It can be concluded that pomfret distributed north of the Subarctic boundary during September are sexually immature. Not all fish among those migrating north possessed closed follicles generated by ovarian regression following spawning. This indicates that pomfret migrating in a northerly direction include those that will be spawning for the first time and those having spawned in the past. With the increase in number of individuals having a GSI value of 1.5 to 3.0, namely at the yolk stage beginning in late November, some individuals are to be found with GSI values in excess of 3.0, indicating fish which will spawn in the very near future. On the basis of GSI values, it is evident that spawning occurs from December through April, and from early June to early July. Though no specimens have been collected in February or March, this period is considered part of the spawning season in view of GSI values in the preceding and subsequent months.

The period of spawning is protracted through the winter months. This may be because each individual has a long spawning period and may spawn more than once. That different shoals of pomfret spawn at different periods is also conceivable. Pomfret taken from ocean waters around western longitudes of the Subarctic boundary were found to have high GSI values in June and July, declining to less than 1.5, marking the end of the spawning period in late July. On the other hand, in eastern longitudes, the GSI values declined to less than

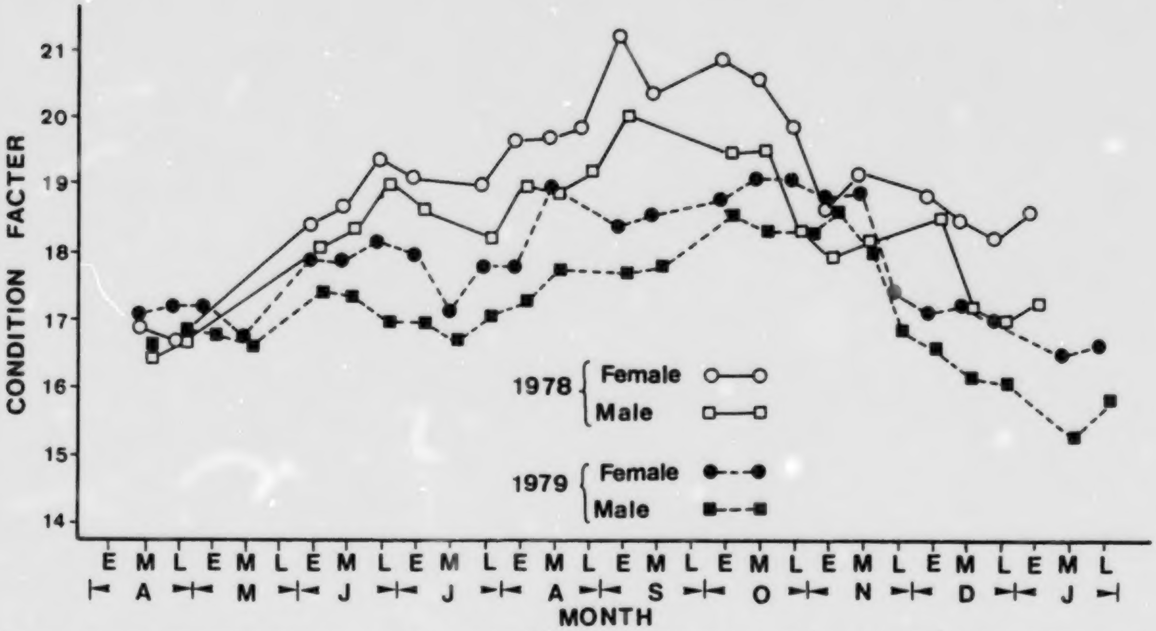

FIG. 11. Seasonal changes of the mean condition factor {(body weight(g)/fork length^3(cm)) × 10^3} of large pomfret (from Shimazaki and Nakamura 1981).

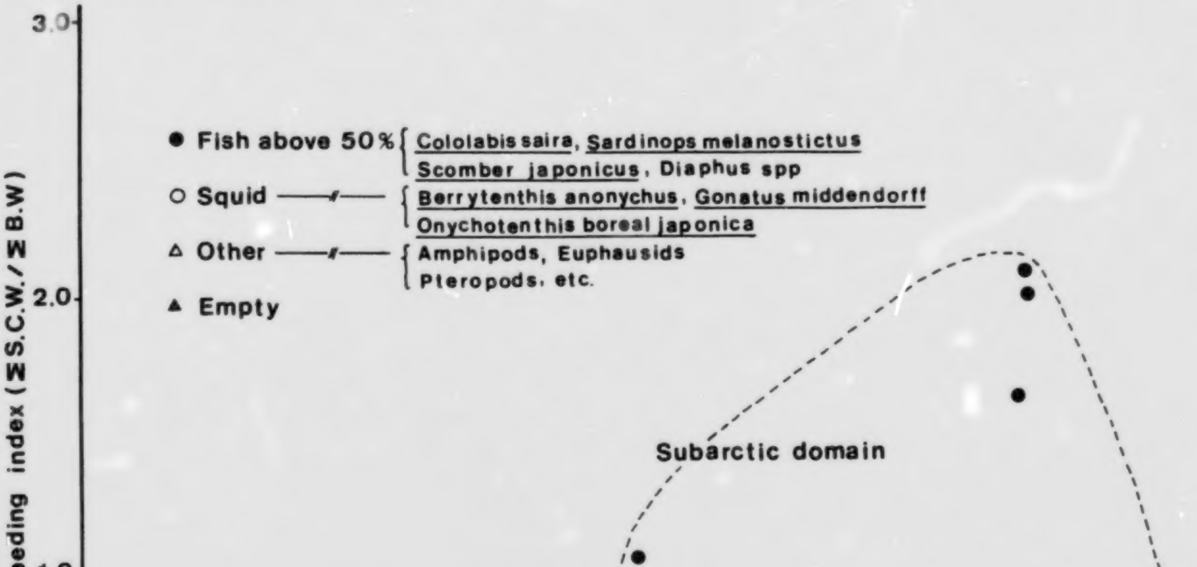

FIG. 12. Relation between CPUE of pomfret and average feeding indices at several sampling stations from September to October (from Shimazaki 1981).

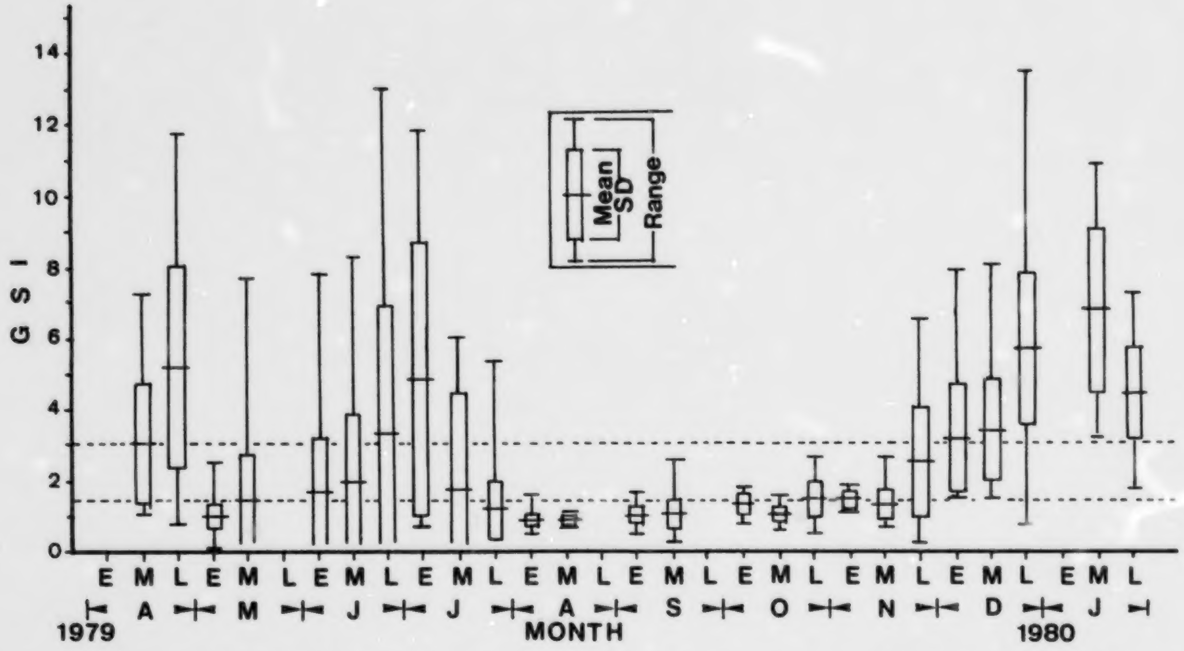

FIG. 13. Seasonal change of GSI in female pomfret in the North Pacific Ocean during the early(E), middle(M), and late(L) parts of each month from April, 1979, to January, 1980. Dotted lines indicate where GSI values are 1.5–3.0 at yolk formation stage and more than 3.0 before spawning or at the spawning stage (from Yoon and Shimazaki 1981).

1.5 around May. More detailed observation is required to describe the protracted spawning season of the pomfret.

Male testis weight is 10 g or less throughout the year and does not change as does female ovary weight. This aspect should be examined in the future considering the possibility that mature pomfret are distributed in the surface or deeper layers.

Discussion

The tunas are found in the Tropic region and in the immediately adjacent part of Subtropic region (Nakamura and Yamanaka 1959). The geographic distribution of these species as it is related to feeding period, spawning, growth and age, has been studied intensively (Otsu and Uchida 1961; Suda and Shiohama 1962; Suda 1962; and others). In marked contrast, there is little information available on the ecology of the pomfret in spite of the fact that this species is considered important in terms of biomass.

The pomfret is widely distributed from the Subtropic region to the Subarctic region of the Pacific Ocean and migrates between these regions seasonally. Migration northward is initiated in spring and is coincident with the rise of surface water temperatures over 9°C. The pomfret feeds intensively in northern waters until fall, increasing body weight by 30% over that of the winter. Migration southward is somewhat sudden and the pomfret become distributed throughout the Subtropic region until the following spring. Based on ovarian development, the spawning period is protracted from fall to spring.

Food consists of a variety of fishes, squids, and zooplankton. In the eastern longitudes some very important food items are immature sardine, Atka mackerel and Pacific saury which are consumed during the northward migration in summer (Shimazaki and Nakamura 1981; Kohno 1983; Shimazaki 1986). Differences in stomach contents of pomfret collected from different ocean regions is related to regional productivity. The pomfret feed extensively in the Subarctic region during the period of high productivity in summer. Following the migration south to the Subtropic region, they spawn during periods of low productivity (Fig. 14).

Though a reliable method of age determination has not been established, scales or otoliths are considered the most likely prospect for providing these data. Studies are required to determine the deposition period of what appear to be annuli found on scales taken from near the caudal peduncle. A clearly established method of age determination will allow identification of groups of pomfret by reproductive age, which segregate by fork length during the northward migration. This information is vital for resource management.

Little information is available concerning the ova, larvae, and juvenile stages of pomfret and other Bramidae (Hotta 1964; Mead 1972). Furthermore, the possibility that there are pomfret groups which are separated by spawning period has been hypothesized but not studied. Further research is needed in the Subtropic region to confirm local populations, to collect mature pomfret at the spawning stage in the surface layer or below, and to collect eggs and larvae.

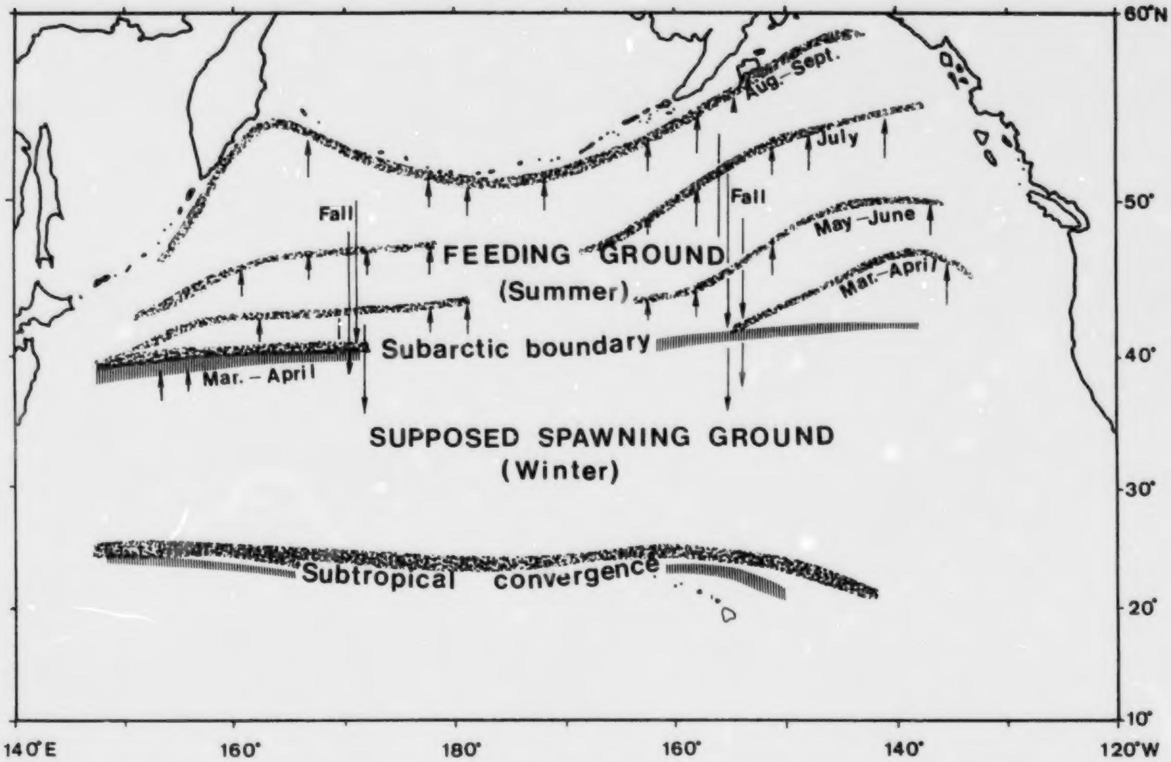

FIG. 14. Proposed schematic representation of pomfret annual migrations (from Shimazaki and Nakamura 1987).

Acknowledgments

The author expresses his sincere gratitude to Captain Shoichi Yamamoto and his crew of the T/S *Hokusei Maru* for their support and aid in sampling. Thanks are also due to Mr. Brian Bigler and the staff of the Research Institute of North Pacific Fisheries, Hokkaido University, for their cooperation.

References

DODIMEAD, A. J., F. FAVORITE, AND T. HIRANO. 1963. Salmon of the North Pacific Ocean-Part II. Review of oceanography of the Subarctic Pacific region. Bull. Int. North Pac. Fish. Comm. 13: 195 p.

FAVORITE, F., A. J. DODIMEAD, AND K. NASU. 1976. Oceanography of the Subarctic Pacific region. 1960–71. Bull. Int. North Pac. Fish. Comm. 33: 187 p.

HOTTA, H. 1964. Diagnostic study of fishes in stomachs of piscivorous fish (II). Bramiformes; Lepidotidae (Bramidae) and Pteraclidae. Bull. Tohoku Reg. Fish. Res. Lab. 24: 81–87.

KIKUCHI, T., AND T. TSUJITA. 1977. Some relations between spacing of pelagic fishes in economic importance and the oceanographic structure in the Northwestern North Pacific Ocean. Res. Inst. North Pac. Fish., Hokkaido Univ. Spec. Vol.: 397–438.

KOHNO, N. 1983. Distributional patterns and prey organisms of pelagic fishes occurring in the Subarctic Pacific region in summer. M. S. thesis, Hokkaido Univ. Grad. School. 142 p.

LARKINS, H. A. 1964. Some epipelagic fish of the North Pacific Ocean, Bering Sea and Gulf of Alaska. Trans. Am. Fish. Soc. 93: 286–290.

MACHIDORI, S., AND S. NAKAMURA. 1971. Distribution and some biological information of pomfret (*Brama raii*) in the northwestern North Pacific Ocean. Bull. Far Seas Fish. Res. Lab. 5: 131–145.

MEAD, G. W. 1972. Bramidae. Dana Rep. 81: 49–55.

NAKAMURA, H., AND H. YAMANAKA. 1959. Relation between the distribution of tunas and the ocean structure. J. Ocean. Soc. Japan 15: 143–149.

NEAVE, F., AND M. G. HANAVAN. 1960. Seasonal distribution of some epipelagic fishes in the Gulf of Alaska region. J. Fish. Res. Board Can. 17: 221–233.

OTSU, T., AND R. N. UCHIDA. 1959. Sexual maturity and spawning of albacore in the Pacific Ocean. Fish. Wildl. Ser. Bull. 59: 287–305.

PINCKARD, W. F. 1957. Pomfret off the British Columbia coast. Progress Rep. Pac. Coast Sta., Fish Res. Board Can. 109: 6–8.

SHIMAZAKI, K. 1979. Distributions and biological features of the pomfret. Bull. Jap. Soc. Fish. Oceangr. 35: 69–71.

1986. Distribution of the pelagic fish community around the Subarctic boundary in the North Pacific Ocean. Bull. Int. North Pac. Fish. Comm. 47: 247–264.

SHIMAZAKI, K., AND S. NAKAMURA. 1981. Ecological studies of the pomfret (*Brama japonica* Hilgendorf). I. The seasonal distributional pattern and ecological considerations. Res. Inst. North Pac. Fish., Hokkaido Univ. Spec. Vol: 9–103.

SUDA, A. 1962. Studies on the albacore. III. Ecological considerations on the movement of big sized albacore from distributing ground of immature group (North Pacific current area) to supposed spawning ground (North Equatorial current area). Bull. Nankai Reg. Fish. Res. Lab. 16: 127–134.

SUDA, A., AND T. SHIOHAMA. 1962. Some consideration on the relationship between distribution of albacore and the surface water temperature in the long-line fishing ground of the North West Pacific. Bull. Nankai Reg. Fish. Res. Lab. 15: 39–68.

YAMAMOTO, K., I. OOTA, K. TAKANO, AND T. ISHIKAWA. 1965. Studies on the maturing process of the rainbow trout (*Salmo gairdnerii irideus*) — I. Maturation of the ovary of a one-year old fish. Bull. Japan. Soc. Sci. Fish. 31: 123–132.

YOON, T. 1981. Reproductive cycle of female walleye pollock, *Theragra chalcogramma* (Pallas), in the adjacent waters of Funka Bay, Hokkaido. Bull. Fac. Fish. Hokkaido Univ. 32: 22–38.

YOON, T., AND K. SHIMAZAKI. 1981. Ovarian maturation of the Pacific pomfret, *Brama japonica* Hilgendorf, in the North Pacific Ocean. Res. Inst. North Pac. Fish., Hokkaido Univ., Spec. Vol: 79–90.

New Perspectives on the Relationship Between Recruitment of Pacific Hake *Merluccius productus* and the Ocean Environment

Anne Babcock Hollowed and Kevin M. Bailey

Northwest and Alaska Fisheries Center, 7600 Sand Point Way NE,
Seattle, WA 98115, USA

Abstract

HOLLOWED, A. B., AND K. M. BAILEY. 1989. New perspectives on the relationship between recruitment of Pacific hake (*Merluccius productus*) and the ocean environment, p. 207–220. *In* R. J. Beamish and G. A. McFarlane [ed.] Effects of ocean variability on recruitment and an evaluation of parameters used in stock assessment models. Can. Spec. Publ. Fish. Aquat. Sci. 108.

This paper describes an analysis of factors underlying fluctuations in year-class strength of Pacific hake (*Merluccius productus*). We attempt to identify the period of the early life history within which the relative magnitude of year-classes of Pacific hake is determined. Comparison of the relative abundance of young-of-year juveniles and late-stage larvae (11.5–15.75 mm) with estimates of recruitment to the fishery at age 3 indicated that the relative magnitude of year-class strength is detectable within the first 1–3 mo after spawning. We examine the relationship between recruitment of Pacific hake and environmental conditions in waters off the coast of California. The results show that larval survival is favored by periods of weak offshore transport during early winter (January and February) followed by periods of increased upwelling in March. Linear and second order quadratic regression models using these two environmental variables accounted for 60 and 70% of the variance in recruitment, respectively.

Résumé

HOLLOWED, A. B., AND K. M. BAILEY. 1989. New perspectives on the relationship between recruitment of Pacific hake (*Merluccius productus*) and the ocean environment, p. 207–220. *In* R. J. Beamish and G. A. McFarlane [ed.] Effects of ocean variability on recruitment and an evaluation of parameters used in stock assessment models. Can. Spec. Publ. Fish. Aquat. Sci. 108.

Cet article présente une analyse des facteurs à l'origine des fluctuations de l'effectif des classes d'âge du merlu du Pacifique (*Merluccius productus*). Les auteurs tentent de déterminer à quel moment du début du cycle vital se précise la taille relative des classes d'âge du merlu du Pacifique. La comparaison entre, d'une part, l'abondance relative des jeunes de l'année, des juvéniles et des larves au cours de leur dernier stade de développement (11,5–15,75 mm) et, d'autre part, les estimations du recrutement dans la zone de pêche à l'âge 3 a révélé que l'importance relative des classes d'âge peut être déterminée au cours des trois premiers mois suivant la ponte. Les auteurs examinent les rapports entre le recrutement des merlus du Pacifique et les conditions écologiques dans les eaux au large de la côte de la Californie. D'après les résultats obtenus, la survie des larves est favorisée par des périodes de faible mouvement de l'eau vers le large au début de l'hiver (janvier et février) suivies de périodes de remontée accrue en mars. Ces deux variables écologiques ont été utilisées dans modèles linéaires et de régression quadratique de second ordre pour expliquer respectivement 60 et 70% de la variance du recrutement.

Introduction

Research on the causes of variations in recruitment of marine fishes often begins with the assumption that mortality during the early life history is critical in determination of year-class strength. Then, statistical linkages between environmental conditions during larval life and recruitment are identified. Defining which environmental variables and life stages are most important often depends on the approach of the investigators and the indices available for analysis. One problem with this approach is that actual mechanisms that cause the variability in magnitude of recruitment may not always be limited to events in larval life. For example, Sissenwine (1984) and Peterman et al. (1988) contend that late-larval or juvenile mortality may be critical in determining the relative size of year-classes of marine fishes.

The coastal stock of the Pacific hake (also known as Pacific whiting) (*Merluccius productus*) exhibits large variations in year-class strength. The coefficient of variation in recruitment of Pacific hake is 1.29, and adjacent year-classes may vary tenfold to thirtyfold in abundance. In contrast, northern anchovy (*Engraulis mordax*), which spawns in roughly the same season and geographic location as Pacific hake, has a coefficient of variation in recruitment of only 0.61, and adjacent year-classes may vary threefold in abundance (calculated from data in Peterman et al. 1988).

The early life history stages of Pacific hake are spent in waters off the coast of California, where the oceanic environment is dynamic. In this region, the interannual physical variability results in a strong biological response (Chelton et al. 1982). Therefore, the strong signals in recruitment variability of Pacific hake make it an ideal candidate to study the stock's response to interannual variations in ocean conditions off the coast of California.

Because of its abundance, Pacific hake is commercially and ecologically one of the most important fish species on the west coast of North America. Pacific hake support a large foreign fishery with historical yields of between 90 000 and 238 000 t (Francis and Hollowed 1985).

Pacific hake are most abundant over the continental shelf and slope within the California Current system from roughly 25 to 50°N. During the summer months, adult Pacific hake undergo an extensive migration to the northern end of their distribution to feed. In the autumn months the adults migrate southward to spawn off the coasts of central, southern, and Baja California. Based on indices of larval abundance, most of the spawning activity occurs between January and March. The eggs are usually spawned in deep waters (100–500 m) and the eggs and larvae are distributed below the mixed layer (Bailey 1982).

The purpose of this analysis was to attempt to identify environmental conditions that may be related to relative year-class success or failure of Pacific hake. This goal is similar to many prior recruitment studies; however, the availability of a long time-series of larval and juvenile abundance data provided a unique opportunity to identify the months during which relative recruitment levels were established.

Methods

Time series data on larval, juvenile, and adult stages of Pacific hake were used to define the period when the relative success of a year-class was first recognized. Once the critical time period was identified, we explored the relationship between biological and environmental variables with recruitment success in an attempt to develop hypotheses to explain variability in recruitment of Pacific hake.

Our analysis was conducted in the following steps. We began by distinguishing between the density dependent and density independent variability in recruitment. This step revealed that much of the variability in the recruitment of Pacific hake appeared to be attributed to density independent variability. Therefore, the relationship between recruitment and several key environmental variables was explored. A matrix of correlation coefficients was constructed to identify collinearity between variables. Then scatter plots of the remaining key environmental variables were examined for linear or curvilinear relationships. Discriminant analysis was applied to determine the combinations of environmental variables that most effectively classified the year-classes of Pacific hake. Strong and weak year-classes were defined as those that fell into the upper or lower quartiles respectively, and all others were defined as average year-classes. Stepwise multiple linear regression was applied as a second approach to identifying key environmental variables. Finally, second-order (quadratic) curvilinear fitting was performed using a modified form of response surface analysis (RSA). This method is described in Schnute and McKinnell (1984).

Biological Data Sources

The time series of larval data was collected from California Cooperative Oceanic and Fisheries Investigation (CalCOFI) surveys. These surveys were conducted along a fixed sampling grid on a monthly basis from 1950 to 1960. From 1961 to 1969 surveys were conducted every third month, and from 1969 to 1984 complete sampling of the grid pattern was conducted every third year (i.e. 1972, 1975, 1978, 1981, and 1984). Since 1985 surveys have been conducted on a quarterly basis over a reduced portion of the sampling grid.

Several notable improvements in the design of the plankton sampling procedures took place. In 1969 the net material was changed from 0.550 mm mesh silk to 0.505 mm mesh nylon (Lo 1985) and the depth of tow was extended from 140 m to 210 m (Richard Charter, Southwest Fisheries Center, La Jolla, CA, Pers. Comm.). Larval Pacific hake were sampled by oblique tows with a 1-m ring net from 1951 to 1976, and with bongo nets after 1976 (Richard Charter, Southwest Fisheries Center, La Jolla, CA, pers. comm.). The new net configuration decreased net avoidance by larger larvae (Hewitt 1980).

The number of fish larvae captured was standardized to the number per 10 m^2 of sea surface area on the basis of the depth and duration of each tow. An estimate of the total number of larval Pacific hake observed at a station between the months of January and June was available for all years from 1951 to 1986 with the exception of the following years: 1970, 1971, 1973, 1974, and 1976. Information on the size distribution of larval Pacific hake is available for 1961, 1963–69, 1972, 1975, 1977, and 1978–86. Only larvae greater than 10 mm were sorted and enumerated from surveys in 1961 and 1977. An index of the number of late-stage larvae was developed based on the number of larvae per tow observed in March and April. Late-stage larvae were defined as larvae between 11.5 and 15.75 mm in length.

Indices of juvenile abundance were obtained from pelagic fish surveys of the California Department of Fish and Game (CDF&G) (Bailey et al. 1986). Juvenile survey data were available from 1965 to 1987. In general, hydroacoustic surveys were conducted during the day and midwater trawl samples were collected at night along the same tracklines. A midwater trawl with a 4.6 or 5.6 m^2 opening and 1.3 cm mesh size at the codend was deployed for 20 min in the upper 15 fathoms of the water column.

Bailey et al. (1986) described the relationship between incidental catches of age-0 Pacific hake in CDF&G surveys and relative year-class strength. The authors defined a standardized survey subarea of 30–35°N and developed two indices of juvenile abundance based on either the percent occurrence or CPUE of juvenile Pacific hake observed between April and March of the following year.

Estimates of the number of fish recruited to the fishery at age 3 were derived from: (1) an index of year-class strength based on annual research trawl surveys and U.S. and Canadian commercial fishery data, and (2) cohort analysis using commercial catch statistics. The year-class index (YCI) was calculated by summing the percent contribution to the total annual age composition determined at age 4, 5, and 6. The YCI provides an index of year-class strength back to 1960 (Table 1).

An estimate of the number of fish recruited to the fishery at age 3 was also available from cohort analysis based on commercial catch data from 1973 to 1986 (Hollowed et al. 1987). The cohort analysis method used was developed by Francis (1983) and applies the analytic formulation of Pope (1972) and Tomlinson (1970). The analysis was performed in such a way to minimize the sum of squares differences between the estimated numbers-at-age from the cohort analysis and the numbers-at-age derived from the 1977, 1980, 1983, and 1986 Northwest and Alaska Fisheries Center (NWAFC) triennial trawl-hydroacoustic surveys.

The time series of year-class indices and recruitment levels are shown in Table 1. The first column gives the YCI estimated by Bailey (1981). This index was developed from Northwest and Alaska Fisheries Center survey data collected during the 1960's and from U.S. observer data in more recent years. The second column gives an analog of Bailey's YCI based on commercial catch data only. The YCI for the 1967–82 year-classes was calculated from estimates of catch-at-age data from the commercial fishery. The YCI for the 1960–66 year-classes was derived

TABLE 1. Estimates of year-class index, recruitment at age 3, and spawner biomass for Pacific hake 1960–86.

Year-class	YCI[1a] Bailey	YCI[1b] Catch	Recruitment[2ab] at age 3 (billions)	Egg[3] numbers (trillions)
1960	54	(71.6)	(0.887)	—
1961	130	(183.3)	(2.378)	—
1962	14	(12.8)	(0.123)	—
1963	19	(20.1)	(0.201)	—
1964	20	(21.6)	(0.217)	—
1965	8	(4.0)	(0.030)	—
1966	20	(21.6)	(0.217)	—
1967	34	56.1	(0.680)	—
1968	28	32.0	(0.328)	—
1969	29	17.3	(0.171)	—
1970	78	140.5	1.887	—
1971	18	21.0	0.316	—
1972	14	21.7	0.208	—
1973	86	94.0	0.857	91.373
1974	16	21.0	0.167	100.286
1975	30	24.0	0.176	102.935
1976	—	16.4	0.153	101.282
1977	—	126.1	1.764	89.842
1978	—	9.1	0.099	84.518
1979	—	12.1	0.100	74.288
1980	—	184.6	3.123	86.150
1981	—	19.0	0.234	85.200
1982	—	5.6	0.029	84.561
1983	—	—	0.161	125.840
1984	—	—	—	145.909
1985	—	—	—	153.594
1986	—	—	—	143.865

*Values in parenthesis are estimated from linear regression.

[1] YCI = Year-Class Index as percent contribution of 4-, 5-, and 6-yr-old fish. a, From Bailey et al. (1981); b, From commercial catch statistics 1973–1986.

[2] $R3$ = recruitment at age 3 to the commercial fishery.

a, Regression based on all years used for estimation of $R3$ when YCI above 50:
$R3 = -68.901 + 13.3505 * \text{YCI}$ ($R^2 = .962$)

b, Regression based on all years when YCI < 50, used for estimation of R3 when YCI less than 50:
$R3 = -12.73 + 10.640 * \text{YCI}$ ($R^2 = .589$)

[3] $$\# \text{ Eggs} = \sum_{i=1}^{n} N_i C_i \, 1.8934 \times 10^5 \, W^{1.25}$$

W = average weight of females at age,
C = Proportion mature at age.

from Bailey's index to represent the percent contribution from commercial fishery data (Francis et al. 1984).

The third column gives estimates of recruitment at age 3 (R3). Recruitment was estimated from the cohort analysis for the 1970–83 year-classes and predicted from a linear regression of YCI in column 2 on R3 (using the 1970–82 year-classes) for the 1960–69 year-classes. Close examination of the regression between the YCI and recruitment showed the large year-classes were highly influential in the regression. Inclusion of the large year-classes resulted in an underestimation of recruitment from years with a low YCI. Therefore, a second regression was performed excluding the large year-classes. The second linear equation was used to estimate recruitment when the YCI was less than 50%.

The fourth column shows the estimates of the number of eggs produced in a given year. The number of eggs in a given year (E) was estimated from the fecundity-weight relationship derived for the Strait of Georgia hake stock (McFarlane and Beamish 1983):

$$E = \sum_{i=1}^{n} N_i * O_i * 189{,}340 * W_i^{1.25}$$

Where N_i is the number of females in the population in year i, O_i is the fraction of an age-class that is sexually mature, and W_i is the mean weight-at-age of females at age i. The value of N_i was determined from cohort analysis of fisheries data from 1973 to 1986. The mean weight-at-age was estimated from the 1975–87 data collected from the U.S. commercial fishery. Maturity-at-age was set equal to the values in Francis et al. (1984). Age at 50% maturity was 3 years.

Environmental Data Sources

An extensive time series of oceanographic data was available for the California Current region. In this analysis five primary indices were examined: sea level, sea surface temperature, the depth of the 14°C isotherm (D14), upwelling intensity, and temperature at 100 m depth.

Monthly estimates of sea level were available from coastal stations along the western coast of North America. Sea level data corrected for barometric pressure from coastal stations at La Jolla and San Francisco, California were obtained from the Pacific Marine Environmental Laboratory (PMEL), Seattle, Washington. Chelton et al. (1982) demonstrated that time-series of sea level height was negatively correlated with southward transport. Roesler and Chelton (1987) found that three months after the initiation of a positive (negative) sea level anomaly, low (high) equatorward advection was observed in the California Current system. In addition, sea level generally is inversely related to upwelling (Chelton et al. 1982).

Monthly mean sea surface temperature was obtained from the Pacific Fishery Environmental Group (PFEG), Monterey, California. Sea surface temperature was calculated from the second quadrant of Marsden square-120 (off the southern California coast). Each of the monthly sea surface temperature records represents a compilation of all ship observations taken within the square during a monthly time period. Changes in sea surface temperature are indicative of several physical processes including southward advection and upwelling intensity. In addition, the temperature index represents a large scale measure of extended periods of sea surface warming or cooling.

The D14 indices were provided by Doug McLain, PEG. Monthly means were recorded from Scripps Pier, La Jolla, California from 1950 to 1983. The depth of the 14°C isotherm generally occurs near the top of the thermocline. Therefore, the D14 indices may provide a rough indication of the depth of the upper mixed layer.

Monthly measures of upwelling intensity and mean monthly temperature at 100 m were calculated from compilations of data collected from 3° Marsden squares. Records from three stations (33°N 119°W, 36°N 122°W and 39°N 125°W) were examined. Upwelling was estimated using Bakun's upwelling index (Bakun 1973; Mason and Bakun 1986). Monthly means were calculated from indices of the intensity of wind-induced coastal upwelling along the west coast of North America. Examination of the magnitude of upwelling is important due to its role in the advection of nutrients to the surface and in the relative degree of offshore transport of eggs and larvae.

Estimates of the mean monthly temperature at 100 m were calculated by the PFEG. In general, Pacific hake larvae are found in deeper waters; therefore, the temperature at the 100 m depth would be a useful index for developing hypotheses concerning the physiological influence of temperature on survival.

An additional environmental variable was considered in this analysis. This variable was the minimum value of the January and February upwelling indices (MJFU) (Bailey 1981). The rationale for using this variable was that the peak spawning period of Pacific hake generally occurs in January or February. If upwelling was low in January and high in February, then eggs spawned in January might still be retained in favorable nursery areas while eggs spawned in February would be lost. Conversely, if upwelling was high in January and low in February, then eggs spawned in February might be retained in favorable nursery areas while eggs spawned in January would be lost. Since hake have a high fecundity, the eggs retained in favorable nursery areas during a given month could potentially produce strong year-classes. If an average of upwelling in January and February was calculated this information would be lost.

Results

Exploration of Density Dependent Factors

In an analysis like this, it is important to distinguish the effects of density independent and density dependent factors on recruitment. Welch (1986, 1987) noted that in some stocks the relationship between density dependent factors and recruitment can be masked by the confounding influence of density independent factors. Welch (1986) observed that in iteroparous populations such as Pacific hake, short term fluctuations in stock size are usually smaller than the variability in year-class strength since the spawning stock is composed of more than one age-class. Therefore, Welch (1986) suggested that the influence of density independent variability should be removed from the time series prior to analyzing the density dependent relationships.

Welch (1987) provided one method of filtering density independent variability in recruitment from a recruitment time series. He noted that the Fournier transform can be used to describe the ratio of density-dependent signal to noise as a function of frequency. The transform describes the proportion of the variability at each frequency which could possibly contain information about density-dependent processes and shows that proportion as a function of the age-structure.

Application of Welch's (1987) method is based on the following assumptions. First, pre-recruit survival is assumed to be dependent on the density of the 0-age fish, and other density dependent factors such as cannibalism are assumed to be of minor importance. Second, the average age-specific distribution of reproductive effort is assumed to be applicable to the entire history of the fishery.

Welch (1986) defined the reproductive effort distribution ($k(i)$) as :

$$k(i) = C(i) * O(i) * \gamma(i)$$

Where $C(i)$ is the fecundity at age i, $O(i)$ is the fraction of female cohort that is sexually mature at age i, and $\gamma(i)$ is the survival to age i. In this study, $C(i)$ and $O(i)$ were estimated as described earlier. Estimates of $\gamma(i)$ were calculated from the decay of cohorts between survey periods (Hollowed et al. 1987). The resulting reproductive effort distribution calculated from the values described above is shown in Fig. 1.

Comparison of the time series of unfiltered and filtered recruitment suggested that the majority of the interannual variability in recruitment of Pacific hake could be attributed to density independent variability (Fig. 2). The filtered recruitment time series was remarkably stable over the entire time period. Therefore, the effects of density dependence were not removed from the time series. Plots of unfiltered and filtered recruitment against the estimated number of eggs from 1973–82 are shown in Fig. 3a and b.

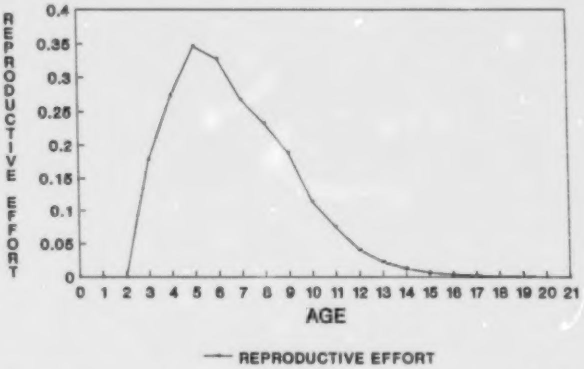

FIG. 1. Estimated reproductive effort distribution for Pacific hake.

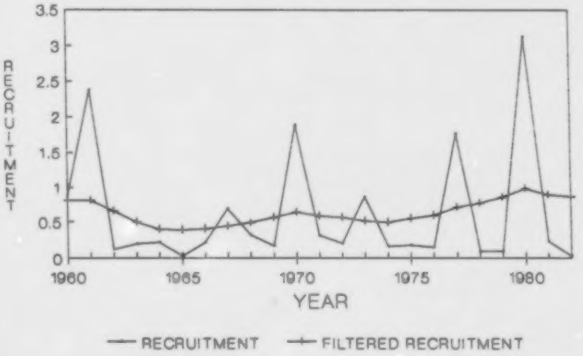

FIG. 2. Historical time series of estimated recruitment and filtered recruitment 1960–82.

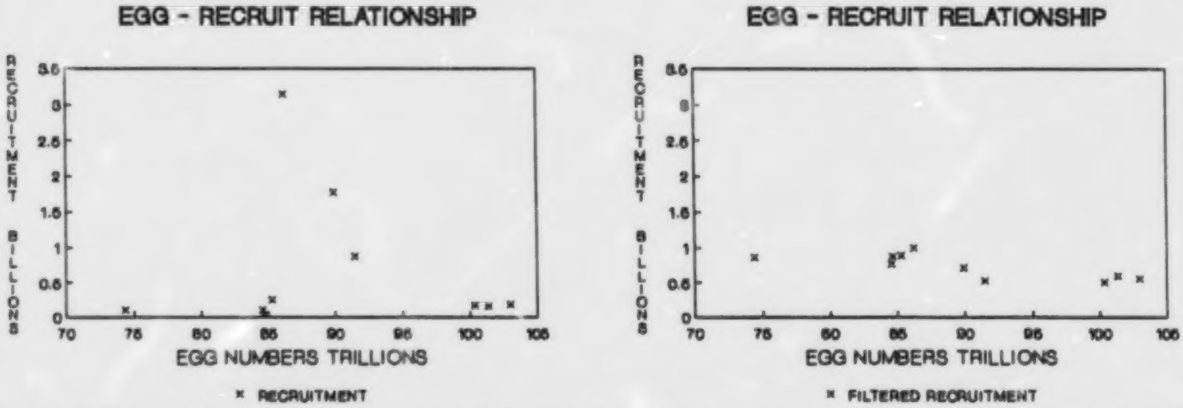

FIG. 3. Relationship between the number of eggs spawned and recruitment three years later for unfiltered (left) and filtered (right) recruitment data.

Recruitment Data Transformations

Based on the data described above, we assumed that density independent factors accounted for the majority of the interannual variability in recruitment of Pacific hake at the current levels of stock abundance. Therefore, the possible relationships between recruitment and environmental variability were explored.

The distribution of recruitment indices was highly skewed (Fig. 3). The high degree of skewness in the recruitment data represented a serious statistical problem because several statistics that required an assumption of normality were applied in the analysis of linear relationships between density independent variables and recruitment. Therefore, an attempt was made to normalize the data prior to the analysis. After a logarithmic transformation was applied to the data, the goodness-of-fit of the recruitment data to the normal distribution was examined using the Kolmogorov–Smirnov (KS) test as described in Hennemuth et al. (1982). Test results indicated that the distribution of the log-transformed indices was not significantly different from the normal. Therefore, log-transformed indices were used in the analysis of linear relationships between environmental variables and recruitment.

Identification of Critical Period

Figure 4 illustrates the time series of indices of age-0 juvenile abundance and recruitment to the fishery at age 3. From this comparison it is clear that the strong year-classes that historically supported the fishery (1967, 1970, 1973, 1977, 1980) were also present in the age-0 data.

Our comparison of the index of late-stage larvae (11.5–15.75 mm) to recruitment was broken into two intervals corresponding to periods when the meter net and bongo nets were used (Fig. 5). This division is necessary because the catchability of the two net configurations cannot be considered equivalent (Lo 1985). In all cases, the index of larval abundance was high in years that produced strong year-classes (1961, 1977 and 1980). This relationship is most apparent from samples taken using a bongo net (Fig. 5), possibly because the bongo net is a more efficient sampler of large larvae.

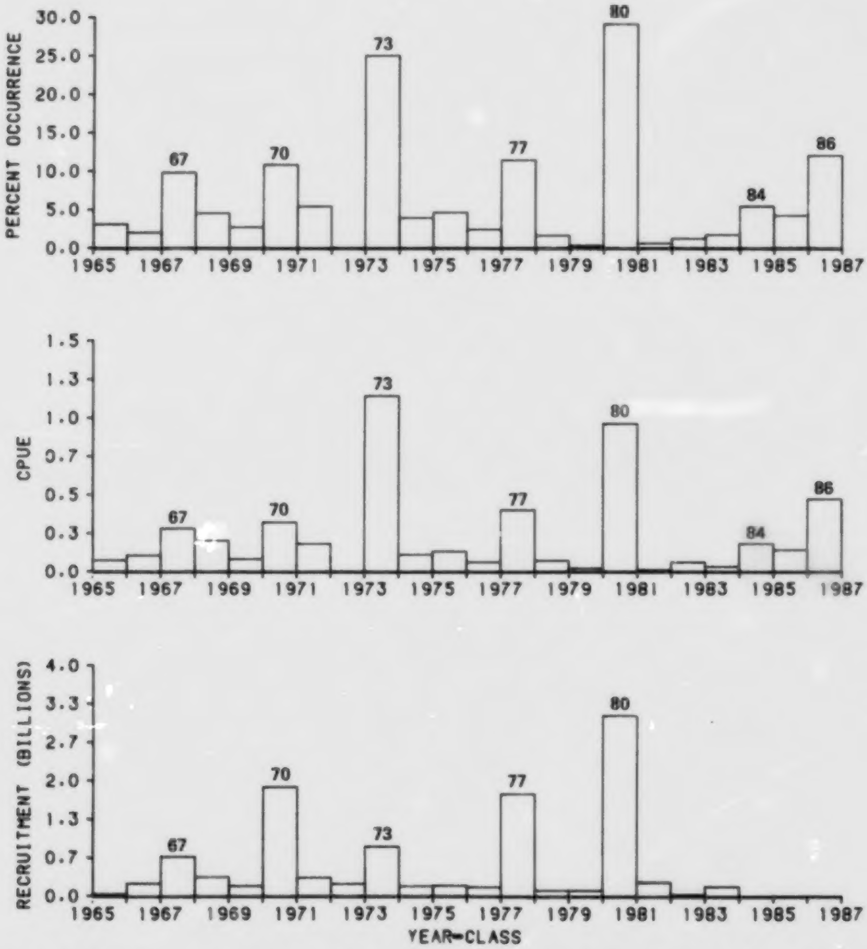

FIG. 4. Percent occurrence (*top*) and catch per unit effort (CPUE) (*middle*) of 0-age hake in midwater trawl surveys compared with year-class strength determined by cohort analysis (*bottom*).

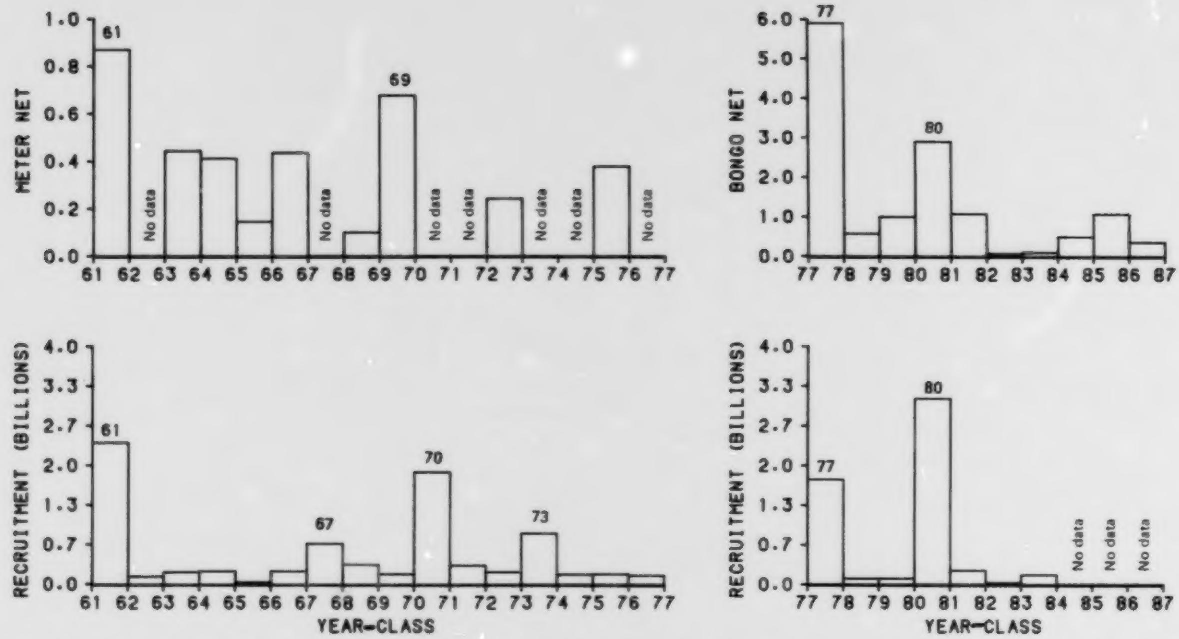

FIG. 5. Number of large larvae (11.5–15.75 mm) per 10 m^2 per tow in CalCOFI cruises compared with year-class strength determined by cohort analysis.

Exploration of Density Independent Variables

The results discussed above indicated that the relative magnitude of Pacific hake year-class strength was determined during the first few months of life and that some indication of relative year-class strength was apparent as early as March or April. Therefore, we restricted analysis of monthly environmental variables to January, February, and March (the peak period of spawning).

Comparison of monthly data on upwelling, temperature at 100 m, and sea level revealed that data from different stations during the same month were highly correlated. Therefore, monthly data on upwelling and temperature at 100 m depth recorded at 36°N latitude 122°W longitude, and sea level data from a coastal station near San Francisco were selected.

Comparison of the environmental variables at a given station revealed that the monthly values of D14, sea surface temperature, temperature at 100 m depth and sea level were all highly correlated. However, the monthly upwelling indices were not highly correlated. Therefore, monthly upwelling indices were used and a composite 3-mo index was used for D14, sea surface temperature, temperature at 100 m depth, and sea level.

Prior to examining the collinearity between the remaining environmental variables, an analysis of the distribution of the five variables was conducted. Analysis of the distribution of each of the environmental variables revealed that the upwelling indices and the sea surface temperature data were normally distributed. However, the El Niño year (1983) produced an extreme value for the temperature at 100 m depth, and sea level data. These extreme values were highly influential in the correlations between variables. With the removal of the El Niño year from these three indices, the data exhibited nearly normal distributions.

Correlations between the remaining environmental variables revealed that the indices of January upwelling, February upwelling, minimum level of upwelling in January or February (MJFU), average sea level, and average sea surface temperature data were all highly correlated ($P < 0.01$) (Table 2). Upwelling in January was negatively correlated with sea surface temperature, and sea level.

TABLE 2. Comparison of correlations between environmental variables.

	1	2	3	4	5	6	7	8
1. Average depth 14°		−.00	−.03	.48	−.16	.49	.54	.11
2. January upwelling	ns		.31	.30	.89	−.62	−.29	−.54
3. February upwelling	ns	ns		.31	.53	−.23	−.50	−.59
4. March upwelling	*	ns	ns		.21	.01	.20	−.37
5. MJFU	ns	***	**	ns		−.56	−.49	−.66
6. Average SST	*	***	ns	ns	***		.39	.40
7. Average temp. 100 m	*	ns	*	ns	*	?		.27
8. Average sea level	ns	**	***	?	***	?	ns	

Symbol codes: ? $P < 0.1$; * $P < 0.05$; ** $P < 0.01$; *** $P < 0.005$.

Scatter plots of recruitment vs. biological and environmental variables appear in Fig. 6a–h. The scatter plots revealed the following patterns between recruitment and environmental variables:

1) Recruitment was generally higher when the 14°C isotherm was deep (Fig. 6a).
2) All of the strong year-classes occurred when sea surface temperatures were higher than 15°C (Fig. 6d).

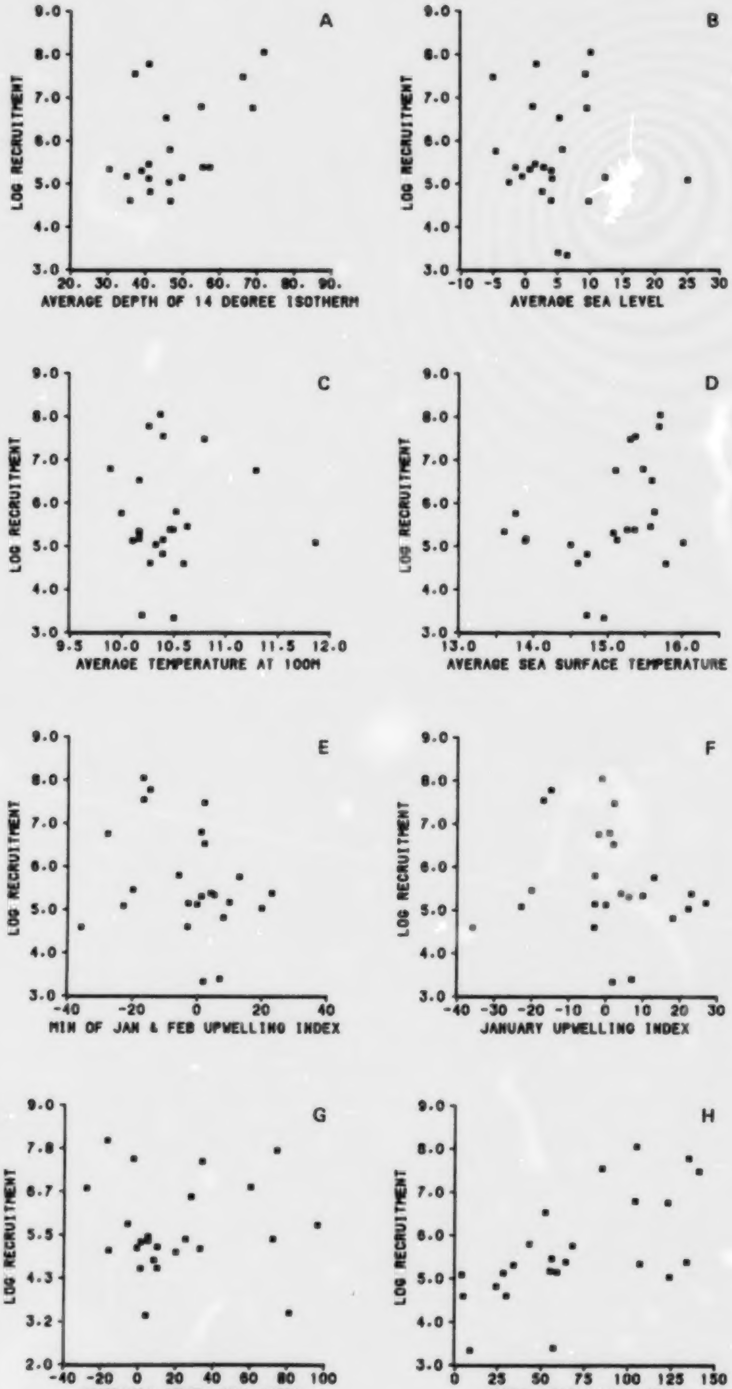

FIG. 6. Scatter plots of log transformed recruitment indices with average depth of the 14°C isotherm (a), average sea level (b), average temperature at 100 m (c), average sea surface temperature (d), minimum of January and February upwelling (e), monthly upwelling indices (f, g, h).

3) None of the strong year-classes occurred during years when high upwelling occurred in January (Fig. 6f).
4) There appeared to be a positive linear relationship between the log transformed recruitment indices and the magnitude of upwelling in March (Fig. 6h).

The relationship between recruitment and the remaining variables was not apparent from the scatter plots.

Discriminant Analysis

The results from the discriminant analysis indicated that strong year-classes could be correctly classified 100% of the time based on two environmental variables: upwelling in March (MU) and the minimum level of upwelling in January or February (MJFU). This classification is illustrated in Fig. 7. Although the two upwelling indices were useful in classifying strong year-classes, the weak and average year-classes were not clearly defined.

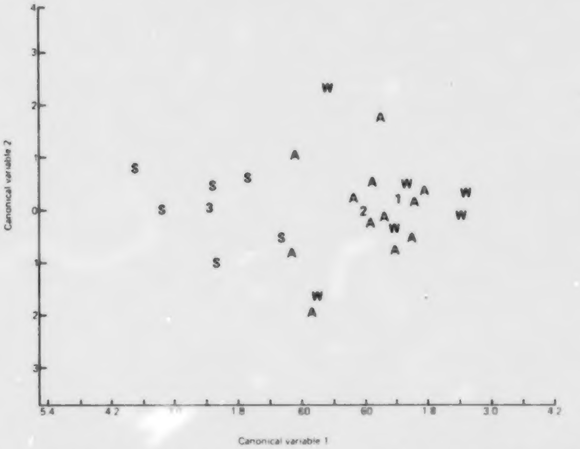

FIG. 7. Plot of group means (numbers) and points (letters) showing the classification of strong (S), average (A), and weak (W) year-classes based on discriminant analysis. Canonical variables derived from selected environmental variables MJFU and MU as environmental variables. The center of strong, average, and weak year-classes is illustrated by the numbers 1, 2, and 3, respectively.

Stepwise Linear Regression

The two variables selected using stepwise linear regression of environmental variables against the log transformed recruitment indices were also MJFU and MU (Table 3). This result differs from a similar study by Bailey (1981). Bailey (1981) compared the relationship between environmental variables and the YCI from 1960 to 1975. Bailey found that average sea surface temperature (SST) and the MJFU accounted for 68% of the variability in the log transformed YCI. In order to compare our results with those of Bailey (1981) we regressed the updated recruitment data on MJFU and SST (Table 3). This regression was not significant ($P > 0.05$) and only accounted for 14% of the variance. In contrast, regression of the updated recruitment indices against the MJFU and MU accounted for 60% of the variance and the regression was significant ($P < 0.0005$) (Table 3).

Nonlinear Regression

Response surface analysis was used to explore the nonlinear response of recruitment to environmental variation. The model fits a quadratic equation of the form:

$$R_3{}^{\gamma} = a + \sum_{i=1}^{m} \left[b_i x_i^{\alpha_i} + \sum_{j=i}^{m} c_{ij} x_i^{\alpha_i} x_j^{\alpha_j}\right]$$

where m is the number of factors (2), and the x's correspond to the environmental variables. Schnute and McKinnell (1984) defined new parameters for the response surface that limited the search for the optimal solution to a window of values found within reasonable numerical ranges for the data. The minimum (u_i) and maximum (U_i) values for the factors and the minimum (v_i) and maximum (V_i) values for the response were set equal to the minimum and maximum high values for the factors x_i and the recruitment response ($R3$). The parameters p, q_i, and r_{ij} are defined as the constant, linear, and quadratic coefficients, respectively. The constant coefficient provides information about the response in the midrange of factor values. The linear trends in $R3$ associated with the variable x_i are measured by the linear coefficient q_i.

TABLE 3. Comparison of linear recruitment models.

---

1. Best model based on stepwise multiple linear regression and discriminant analysis for 1960–83 data.

Log Transformed Recruitment (LTR) vs Minimum of January and February Upwelling (MJFU), and March Upwelling (MU):

$LTR = 4.1037 + 0.020958 * MU - 0.03726 * MJFU$

R squared = .600
F statistic = 15.720, df = (2,21), $P < 0.0005$
T statistic for MU = 5.20, $P < 0.0005$
T statistic for MJFU = −3.13, $P < 0.005$

---

2. Bailey model for 1960–83 data.

LTR vs MJFU and Sea Surface Temperature (SST).

$LTR = -1.985 - 0.01098 * MJFU + 0.5056 * SST$

R squared = .138
F statistic = 1.674, df = (2, 21), not significant
T statistic for SST = −0.53, not significant
T statistic for MJFU = 1.15, not significant

The quadratic coefficients r_{ij} describe departures from linear responses inside the window of interest.

Due to the large number of parameters used in RSA, we restricted our analysis to models with no more than 2 independent variables. Even with this restriction, models that contained 2 independent variables had 13 parameters. Since only 24 recruitment data points were available, there were approximately 2 data points per parameter for a 2 variable model. Based on this low degree of determination, the linear model is superior to the non-linear model.

The relationship between recruitment and variation in environmental variables was explored in the following models.

1) R vs March upwelling and average sea level.
2) R vs March upwelling and January upwelling.
3) R vs March upwelling and average sea surface temperature.
4) R vs March upwelling and MJFU.
5) R vs January upwelling and average sea level.
6) R vs average sea surface temperature and average sea level.
7) R vs January upwelling and average sea surface temperature.

Models were successfully fitted for the first four cases. There was little difference between the models that included March upwelling (models 2–4, Table 4). The close correspondence between models 2–4 was expected because January upwelling, MJFU, and average sea surface temperature are all highly correlated (Table 2). For purposes of comparison with the linear model, only model 4 was considered further. The solution to the quadratic equation for model 4 is shown in Table 4.

Parameter estimates for the non-linear fit of model 4 are presented in Table 5. The relatively low value of the constant coefficient ($P = -0.094$) shows that the response is relatively small near the window center. The negative value of q_1 (-0.4304) and positive value of q_2 (0.6267) indicate that recruitment is negatively correlated with MJFU and positively correlated with MU. The value of r_{12} shows there is some interaction between MJFU and MU. The large negative value of r_{11} indicates there is downward curvature corresponding to a maximum possible response in MJFU. The more moderate positive value r_{22} indicates that there is an upward curvature to the response of recruitment to MU but this curvature is more flat than the dome-shaped response in MJFU. These features are illustrated in the response surface of recruitment to MJFU and MU (Fig. 8). This figure shows that the highest level of recruitment is found when upwelling in March is high and the MJFU is slightly negative.

TABLE 4. Comparison of non-linear recruitment models derived from response surface analysis.

Model	X_1	X_2	P value	R^2
1	March Upwelling	Average sea level	0.0500	.500
2	January Upwelling	March Upwelling	0.0025	.693
3	March Upwelling	Average SST	0.0020	.714
4	March Upwelling	MJFU	0.0020	.709

Model 4.

Recruitment at age 3 (billions) vs March upwelling and MJFU

$$R^{0.035} = 1.7271 - 1.595 * MU^{0.097} + 0.2078\,(50 + MJFU)^{0.417} + 0.5705 * MU^{0.193} - 0.0364 * (50 + MJFU)^{0.835} + 0.06569 * MU^{0.097} * (50 + MJFU)^{0.417}$$

Note: negative values are not permitted in this model, therefore, a constant of 50 was added to MJFU.

F statistic = 8.792, df = (13,10), $P < 0.002$.

TABLE 5. Comparison of constant, linear, and quadratic coefficients from response surface analysis. The upper section shows the bounds on MJFU, March upwelling (MU) and recruitment used in this analysis.

x_i	u_i	U_i	α_i	v	V	γ
MJFU	14	73	0.4174	28	3122	0.0353
MU	4	143	0.0965			

x_i	p	q_i	r_{1i}	r_{2i}
MJFU	−0.0939	−0.4304	−0.7952	
MU		0.6267	0.2255	0.3078

NOTE: This form of RSA requires that the input variables are all positive, therefore, a constant of 50 was added to MJFU.

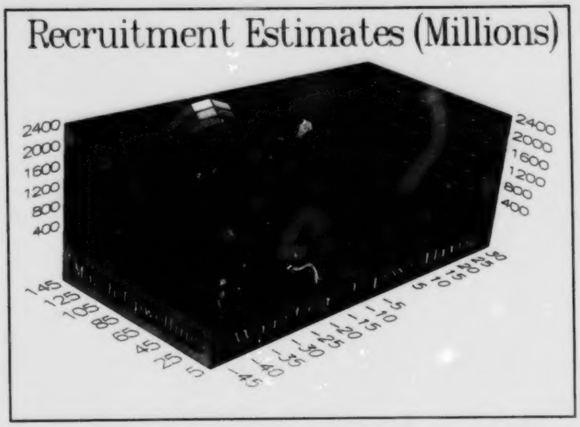

FIG. 8. Contours of recruitment responses of Pacific hake to varying conditions of early winter and March upwelling.

Discussion

The results of this study show that relative year-class strength is determined in the larval and early juvenile stages of Pacific hake. Strong year-classes are characterized by high abundances of large larvae and high abundances of young-of-the-year juveniles, and weak year-classes occurred when the indices of large larvae or young-of-the-year juvenile abundance were low. An exception to this relationship was observed in 1969 when relatively high larval numbers were observed but recruitment was low. Indices of juvenile abundance from this study and from Bailey and Francis (1985) covering the April to June period indicated that the 1969 year-class was weak. The large number of larvae and low number of 0-age hake observed in 1969 may be a result of either inadequate larval sampling as noted below, the change in the depth of the icthyoplankton tows from 140 to 210 m in 1969, or the potential for some regulation of year-class strength between April and June. However, taking into account all of the years of the comparison, we conclude that the relative magnitude of year-class strength in Pacific hake is usually established by March or April, within the first 1–3 mo after spawning.

Several sampling problems associated with the icthyoplankton surveys used in this study should be noted. First, the nets used in the CalCOFI sampling program are inefficient for larvae greater than 10 mm. Second, the surveys were not designed to sample Pacific hake larvae. Third, Lo (1983) estimated that 92% of anchovy eggs and 80% of small larvae are extruded from the 505–555 μm mesh netting which is used most often in these surveys. Although hake larvae have a larger head than anchovy larvae, the structure of the head is soft during the early stages of development, therefore, similar extrusion rates might be expected for Pacific hake.

In addition, the distribution of hake larvae can be patchy, and sampling at selected points in the water column each month cannot be expected to reflect the true dynamics of larval birth and death rates. Therefore, we did not attempt to compare larval mortality rates to recruitment, as has been done for anchovy (Peterman et al. 1988).

Despite the problems described above, we conclude that since the relative abundance of larvae is usually reflected in year-class strength, the larval signal of Pacific hake must be very great, particularly in years of high abundance.

Problems also exist in interpreting the results from the midwater trawl juvenile surveys. The midwater surveys were not designed to sample juvenile Pacific hake and they were only captured incidentally. The mesh size of the net, depth of tow, and geographic distribution of sampling were not optimal for sampling Pacific hake juveniles. Since the midwater sampling data generally reflects relative year-class strength, this further indicates that the signal of variations in abundance of young-of-the-year Pacific hake is strong.

In addition to the sampling problems described above, three shortcomings of the stepwise regression method used in this study should also be noted. First, predictors unrelated to the process of recruitment may appear significant (Weisberg 1985). Second, when two (or more) variables are highly collinear, one (or more) of the variables may be excluded from model. Since the recruitment process is comprised of events occurring through several developmental stages, the selection process may eliminate variables linked to intermediate processes that are important. For example, average sea surface temperature was significantly negatively correlated with MJFU ($P < 0.001$) and was excluded from our model. However, the effect of temperature and upwelling on survival may be different. Low upwelling in January or February may be related to transport processes, while warm temperatures may be related to how quickly the larvae develop to a stage where they actively avoid predation.

The final problem associated with applications of stepwise regression methods is that recruitment time series are typically short and the number of variables that contribute a significant amount to the regression is limited by the degrees of freedom. However, the recruitment process is probably a function of several highly variable processes occurring throughout the first year of life (Sissenwine 1984). In this case, it may be unreasonable to assume that a few environmental processes could yield significant nonspurious correlations with a complex ecological process (Bakun 1985).

The problems associated with the stepwise regression method described above must be considered. However, the results of our study show that insight into factors that influence the recruitment process can be detected by utilizing the stepwise regression approach as an exploratory method.

The exploratory approach taken here differs from that of other studies in that we attempt to establish the critical period controlling the relative magnitude of the year-class before selecting environmental variables used for comparison to recruitment. The environmental variables used in this study were selected because they were indicators of key processes that could influence survival of 0-age Pacific hake. The result of this approach was the identification of a suite of environmental variables that are strongly related to year-class strength. However, the functional significance of these variables to recruitment remains speculative, because it is possible that these variables are correlated with other variables that are more directly related to survival and that have not yet been identified.

Successful year-classes of Pacific hake apparently occur after periods of low upwelling during early winter (either January or February) followed by a period of intense upwelling in March. Interpretation of this result requires an understanding of the linkages between variations in upwelling and other physical processes occurring in the California Current system.

Interannual variability in the flow of the California Countercurrent has been associated with variations in winter upwelling. McLain and Thomas (1983) explain that the relaxation of equatorward winds (or persistent southerly winds) is associated with downwelling, onshore transport and increased poleward flow. The processes of downwelling and onshore transport result in depressed isotherms and elevated coastal sea level. McLain and Thomas found that high onshore Ekman transport and/or depressed isotherms existed during the winters of 1957-58, 1960-61, 1969-70, 1972-73, 1976-77, 1977-78 and 1979-80. Several of these winters also produced strong year-classes of Pacific hake (1961, 1970, 1973, 1977 and 1980).

Large scale atmospheric forcing may also influence the expression of anomalous temperature, and upwelling conditions in waters off the coast of California. Emery and Hamilton (1985) investigated the relationship between interannual variability in oceanic conditions in the northeast Pacific and atmospheric pressure. They developed an index of the relative strength of atmospheric circulation in the northeast Pacific, (the Northeast Pacific Atmospheric Pressure Index, NEPI). This index was defined as the difference between the seasonal mean pressure at 40°N 120°W and 50°N 170°W. The winters of 1960-61, 1969-70, and 1976-77 coincided with periods when the winter (Dec.-Feb.) NEPI was high. Specifically, Emery and Hamilton (1985) noted that atmospheric circulation was anomalously strong during the winters of 1960-61 and 1976-77. Both of these winters were characterized by a strong Aleutian low, and orientation of the isobars was such that the gradient winds would drive surface water onshore and northward.

Our study showed that strong March upwelling is positively correlated with recruitment of Pacific hake. McLain and Thomas (1983) found that sharp transitions from northward to southward flow generally follow winters of above normal sea level, and depressed isotherms. This "spring transition" results from the shift in wind speed and direction. The signature of this transition may be observed in the onset of intense upwelling in March. McLain and Thomas (1983) found a sharp drop in sea level occurred in early 1970 and 1973. This drop provides evidence of a sharp transition from northward to southward flow.

Strub et al. (1987) studied the physical processes occurring during the spring transition in 9 different years (1971-75, 1980-83). The authors observed that the spring transition tended to occur abruptly over a period of 3-10 days sometime between mid-March and mid-April. They noted that the transition was characterized by a sharp drop in sea level in waters north of 37°N. In waters south of 37°N, the transition was characterized by an intensification of southward wind stress and a gradual drop in sea level during the month preceding the transition event. However, the timing of the actual transition in regions south of 37°N was coincident with the spring transition in the north. Strub et al. (1987) observed that the weakening, splitting and northward displacement of the Aleutian low pressure center and the northward movement of the North Pacific high pressure system generally coincided with the dates of the spring transition.

It is possible that the increase in upwelling in March, which was positively correlated with strong year-classes of hake, is associated with events preceding the spring transition. It is interesting to note that the estimated date of the spring transition occurred in March in 1973, 1975, 1980 and 1981. Of these years, the 1973 and 1980 year-classes were strong. Upwelling was strong during the winters of 1975 and 1981 which may explain the absence of strong recruitment in these years. Emery and Hamilton (1985) also contrasted the progression of the spring transition during El Niño years 1972-73 and 1982-83. The 1973 transition was large scale and low sea level persisted throughout the summer, whereas, the 1983 transition was weak and low sea levels persisted for only a short time.

Several hypotheses have been presented that explain possible mechanisms through which low upwelling during January and February could be linked to successful year-classes of Pacific hake. Bailey (1981) showed that the offshore distribution of larvae was positively correlated to offshore Ekman transport (strong upwelling). Bailey (1981) hypothesized that since the juvenile nursery areas of Pacific hake are inshore over the continental shelf, the seaward advection of larvae may result in poor survival.

Bailey and Francis (1985) compared the year-class strength (measured by levels of recruitment to the fishery at age 3) with time series of sea-surface temperature data. This comparison showed that cold years consistently produce weak year-classes and warm years may produce strong year-classes. They noted that cold years are characterized by equatorward flow, upwelling events, isotherms oriented parallel to the coast, and cold nearshore water. In contrast, isotherms are generally oriented normal to the coast during warm years and the nearshore water is warm. Bailey and Francis (1985) submitted the following possible explanations for the observed relationship between temperature and survival:

1) Since cold temperatures are typically associated with periods of strong upwelling, cold years may be associated with higher advection of eggs and larvae offshore. Survival may be inhibited in the offshore environment due to reduced growth resulting from reduced prey abundance.
2) Since cold temperatures are typically associated with increased southward flow, spawning may occur further south or eggs and larvae may be advected to the south. These processes may be detrimental to survival of Pacific hake due to reduced zooplankton abundance in the southern nursery areas or reduced juvenile habitat due to the narrowing of the shelf there.
3) Cold temperatures may result in slower growth rates which may extend the period when larvae are most vulnerable to predation.

The results of this study suggest that strong upwelling in March is favorable to recruitment of Pacific hake. This result seems contradictory with the concept of strong upwelling and increased offshore transport. However, it is important to consider the sequence of events. The results of this study suggest that low upwelling periods must be followed by a period of intense upwelling. Considering this sequence it is reasonable to assume that periods of low upwelling in January or February allow the larvae to reach favorable nursery areas in the near shore environment. Parrish et al. (1981) and Bakun (1985) found waters within the California Bight were protected from strong offshore transport later in the year. If larval hake are entrained in the nearshore waters of the California Bight then the larvae may benefit from enhanced productivity associated with the onset of the upwelling season.

Bakun (1985) noted that it is important to consider the velocity of offshore transport when considering the influence of offshore transport in survival of larval fish. As an index of the velocity of offshore transport (Ekman velocity), Bakun (1985) divided estimates of wind driven surface Ekman transport by the depth of the upper mixed layer. Using this index he shows that the peak period of offshore Ekman transport precedes the peak period of Ekman velocity by 2-4 mo. Bakun (1985) shows the period of minimum Ekman velocity in the southern California Bight and southern Baja California occurs during January and February when upwelling is at a minimum. Whereas, although maximum upwelling occurs in the spring, the Ekman velocity is only intermediate. Bakun interpreted this finding as an indication the volume of water transported offshore is greatest in the spring (March–April) in the California Bight, however, the larvae would be transported offshore more quickly during the summer (July–August).

The onset of upwelling in March may also be related with processes that occur later in the year. Roesler and Chelton (1987) studied the relationship between zooplankton abundance and environmental variability in the California Current system. These authors also found a significant relationship between high zooplankton biomass and southward advection of northern zooplankton and nutrient-rich water. The authors noted that sea level could be used as an index of the magnitude of equatorward transport. In the northern areas off the coast of California, increased equatorward flow, indicated by low sea level resulted in increased zooplankton abundance within a period of 2 mo. In the southern areas a lag of 5 mo was observed between periods of low sea level and outbursts of zooplankton biomass. The authors concluded that in the northern areas the zooplankton biomass increase results from the introduction of zooplankton species from the north, whereas, in the southern areas the zooplankton outburst results from the introduction of nutrient-rich waters from the north. If this hypothesis is correct, then the onset of increased equatorward flow in March may result in increased zooplankton populations later in the year. This process may be important in determining the availability of prey for juvenile hake.

One feature of the time series of recruitment indices which has not been addressed in the discussion above is its notable periodicity. Since 1967 a strong year-class has occurred every 3–4 yr (Fig. 2). This time period coincides with the age of maturity in hake (age 3-5). The length of the time series of recruitment data for Pacific hake is insufficient to adequately explore the possibility of cycling using time-series analysis methods. However, it was possible to explore the autocorrelations in the time series. None of the autocorrelations were significant. Furthermore, although the relative contribution of 3- and 4-yr-old hake can be large (Fig. 1), the influence of incoming strong year-classes on the number of eggs spawned does not appear to account for the observed periodicity (Fig. 2). Based on the apparent relationship between recruitment and the environment illustrated in this study a more reasonable hypothesis is that the success or failure of a given year-class is influenced by sequences of environmental events, which may themselves be periodic, during the first 1-3 months of life.

In conclusion, our study showed that although some of the relationships described in Bailey and Francis (1985) hold true (i.e., strong upwelling in January or February and cold winter temperatures produce poor recruitment), their model failed to characterize recruitment variability observed after 1978. The models described in this paper may suffer from a similar fate as additional years of data are added to the time-series. It is possible that models based on variables that are not directly related to recruitment may never completely define variability in recruitment of Pacific hake. Furthermore, this model utilized indices of large-scale physical factors that may not fully represent intricate features of the California Current such as eddies and coastal jets which may have a profound impact on the survival of Pacific hake larvae. We hope continuing efforts will lead to the development of models which provide a more accurate simulation of year-class variability and stochastic environmental processes.

Acknowledgements

We thank Jim Ingraham, Doug McClain, Patricia Pullen, and Richard Charter for providing the environmental and biological data used in this study. We also thank Jim Schumacher and Sandy McFarlane who allowed us to access VAX computers at the Pacific Marine Environmental Laboratory and the Pacific Biological Station which enabled us to run the response surface analyses used in this paper. We also appreciate the helpful comments and suggestions provided by Sara Adlerstein, Richard Methot, David Welch, Warren Wooster, and two anonymous reviewers.

References

BAILEY, K. M. 1981. Larval transport and recruitment of Pacific hake *Merluccius productus*. Mar. Eco. Prog. Ser. 6: 1-9.

1982. The early life history of the Pacific hake, *Merluccius productus*. Fish. Bull. U.S. 80: 589–598.

BAILEY, K. M., AND R. C. FRANCIS. 1985. Recruitment of Pacific whiting, *Merluccius productus*, and the ocean environment. Mar. Fish. Rev. 47(2): 8-15.

BAILEY, K. M., R. C. FRANCIS, AND K. F. MAIS. 1986. Evaluating incidental catches of 0-age Pacific hake to forecast recruitment. CalCOFI 27: 109–112.

Bakun, A. 1973. Coastal upwelling indices, west coast of North America 1946–71. U.S. Dep. Commer., NOAA Tech. Rep. NMFS SSRF-671. 103 p.

1985. Comparative studies and the recruitment problem: searching for generalizations. CalCOFI Rep. 26: 30–40.

Chelton, D. B., P. A. Bernal, and J. A. McGowan. 1982. Large-scale interannual physical and biological interaction in the California current. J. Mar. Res. 40(4): 1095–1125.

Emery, W. and K. Hamilton. 1985. Atmospheric forcing of interannual variability in the northeast Pacific ocean: connections with El Nino. J. Geophysical Res. 90(C1): 857–868.

Francis, R. C. 1983. Population and trophic dynamics of Pacific hake (*Merluccius productus*). Can. J. Fish. Aquat. Sci. 40: 1925–1943.

Francis, R. C., and A. B. Hollowed. 1985. History and management of the coastal fishery for Pacific whiting, *Merluccius productus*. Mar. Fish. Rev. 47(2): 95–98.

Francis, R. C., G. A. McFarlane, A. B. Hollowed, G. L. Swartzman, and W. M. Getz. 1984. Status and management of the Pacific hake (*Merluccius productus*) resource and fishery off the west coast of the United States. NWAFC Proc. Rep. 84-18, Northwest and Alaska Fish. Cent., 7600 Sand Point Way NE, Seattle, WA 98115. 73 p.

Hennemuth, R. E., J. E. Palmer, and B. E. Brown. 1982. A statistical description of recruitment in eighteen selected fish stocks. J. Northwest. Atl. Fish. Sci. 1: 101–111.

Hewitt, R. 1980. Distributional atlas of fish larvae in the California Current region: northern anchovy, *Engraulis mordax* Girard 1966 through 1979. CalCOFI Atlas 28. 101 p.

Hollowed, A. B., S. Adlerstein, R. C. Francis, and M. Saunders. 1987. Status of the Pacific whiting resource in 1987 and recommendations for management in 1988. Document submitted to the Pacific Marine Fisheries Council, Metro Center Suite 420, 2000 S.W. First Avenue, Portland, OR.

Lo, N.C.H. 1983. Re-estimation of three parameters associated with anchovy egg and larval abundance: temperature, dependent incubation time, yolk-sac growth rate and egg and larval retention in mesh nets. NOAA Tech. Memo., NMFS-SWFC-31: 33 p.

1985. Egg production of the central stock of northern anchovy 1951–83. Fish. Bull. U.S. 83: 137–150.

Mason, J. E., and A. Bakun. 1986. Upwelling index update U.S. west coast 33N–48N latitude. NOAA Tech. Memo. NOAA-TM-NMFS-SWFC-67: 81 p.

McFarlane, G. A., and R. J. Beamish. 1986. Biology and fishery of Pacific hake (*Merluccius productus*) in the Strait of Georgia. Int. North Pac. Fish. Bull. 45: 365–392.

McLain, D. R., and D. H. Thomas. 1983. Year-to-year fluctuations of the California countercurrent and effects on marine organisms. CalCOFI Rep. 24: 165–181.

Parrish, R. H., C. S. Nelson, and A. Bakun. 1981. Transport mechanisms and reproductive success of fishes in the California Current. Bio. Ocean. 1(2): 175–203.

Peterman, R. M., M. J. Bradford, N. C. H. Lo, and R. D. Methot. 1988. Contribution of early life stages to interannual variability in recruitment of northern anchovy, *Engraulis mordax*. Can. J. Fish. Aquat. Sci. 45(1): 8–16.

Pope, J. A. 1972. An investigation of the accuracy of virtual population analysis using cohort analysis. Int. Comm. Northwest Atl. Fish. Res. Bull. 9: 65–74.

Roesler, C. S., and D. B. Chelton. 1987. Zooplankton variability in the California Current, 1951–1982. CalCOFI Rep. 28: 59–96.

Schnute, J., and S. McKinnell. 1984. A biologically meaningful approach to response surface analysis. Can. J. Fish. Aquat. Sci. 41: 936–953.

Sissenwine, M. P. 1984. Why do fish populations vary? p. 54–94. *In* R. M. May [ed.] Exploitation of marine communities. Life Sciences Research Report 32. Springer-Verlag, New York, NY.

Skud, B. E. 1982. Dominance in fishes: the relation between environment and abundance. Science 216(9): 144–149.

Smith, R. L. 1983. Physical features of coastal upwelling systems. Wash. Sea Grant Tech. Rep. WSG-83-2: 34 p.

Strub, P. T., J. S. Allen, A. Huyer, R. L. Smith, and R. C. Beardsley. 1987. Seasonal cycles of currents, temperatures, winds and sea level over the northeast Pacific continental shelf: 35°N to 48°N. J. Geophys. Res. 92(C2): 1507–1526.

Tomlinson, P. K. 1970. A generalization of the Murphy catch equation. J. Fish. Res. Board. Can. 27: 821–825.

Weisberg, S. 1985. Applied linear regression, second edition. John Wiley and Sons, New York, NY. 324 p.

Welch, D. W. 1986. Identifying the stock-recruitment relationship for age-structured populations using time-invariant matched linear filters. Can. J. Fish. Aquat. Sci. 43: 108–123.

1987. Frequency domain filtering of age-structured population data. Can. J. Fish. Aquat. Sci. 44(3): 605–618.

Influence of Oceanographic and Meteorological Processes on the Recruitment of Pacific Halibut, *Hippoglossus stenolepis*, in the Gulf of Alaska

Kenneth S. Parker

International Pacific Halibut Commission and College of Ocean and Fishery Sciences,
University of Washington, Seattle, WA 98195, USA

Abstract

PARKER, K. S. 1989. Influence of oceanographic and meteorological processes on the recruitment of Pacific halibut, *Hippoglossus stenolepis*, in the Gulf of Alaska, p. 221–237. *In* R. J. Beamish and G. A. McFarlane [ed.] Effects of ocean variability on recruitment and an evaluation of parameters used in stock assessment models. Can. Spec. Publ. Fish. Aquat. Sci. 108.

Environmental conditions during the winter spawning season for Pacific halibut are critical to the success of their reproductive products. Specifically, the transport of larvae along the continental shelf is dependent upon wind-forced and buoyancy-driven coastal circulation. It is argued that fluctuations in transport of the Alaska Coastal Current system influence cross-shelf flux of slope water onto the shelf by associated mechanisms. Onshore transport then affects survival as larvae rise to the surface layers from deep offshore slope waters to subsequent deposition in shallow shelf nursery areas. It is hypothesized *a priori* that year-class strength is enhanced or depressed by transport rates integrated over the 6-month pelagic phase.

Time series of oceanographic and meteorological conditions developed for this study include: geotriptic surface gradient wind speeds and stress; sea surface slope (pressure-corrected sea level); atmospheric surface pressure; and freshwater discharge. Two recruitment series from 1935 to 1977 are estimated from existing CPUE, cohort, and (migratory) catch-age analyses of 60 yr of commercial fishery data. Using existing estimates of spawning biomass, a clear density-dependent relation is revealed with a robust locally-weighted regression (LOWESS). The extent to which this relation is driven by environmental change is investigated.

In two oceanographically contrasted regimes represented by the northeast and northwest Gulf of Alaska continental shelf, multivariate regression models that index mean coastal transport intensity and duration explained up to 66% of recruitment variability not accounted for by the effects of spawning stock size and density dependence. In particular, strong winter-averaged wind conditions favored the production of large year-classes.

Substantial interannual variations exist in these parameters of the regional physical environment. The analyses suggest alongshore and cross-shelf wind-generated horizontal and vertical transport processes that are related to variations in Pacific halibut recruitment success. Principal mechanisms involved include Ekman convergence and upper layer wind-wave drift, onshore shelf-slope flux (continuity and bathymetric steering), and turbulent wind-mixing.

Résumé

PARKER, K. S. 1989. Influence of oceanographic and meteorological processes on the recruitment of Pacific halibut, *Hippoglossus stenolepis*, in the Gulf of Alaska, p. 221–237. *In* R. J. Beamish and G. A. McFarlane [ed.] Effects of ocean variability on recruitment and an evaluation of parameters used in stock assessment models. Can. Spec. Publ. Fish. Aquat. Sci. 108.

Les conditions environnementales qui prévalent pendant la période hivernale de fraye du flétan du Pacifique sont cruciales pour le recrutement fructueux des géniteurs de cette espèce. Tout particulièrement, le transport des larves le long de la plate-forme continentale dépend de la circulation littorale invoquée par le vent et les écarts de flottabilité. On émet l'hypothèse que les variations observées dans le transport du système de courants côtiers de l'Alaska influent sur l'écoulement à en travers de la plate-forme de l'eau de la pente continentale sur celle-ci par des mécanismes connexes. Le transport côtier influe alors sur la survie étant donné les larves se rendent dans les couches superficielles venant des eaux profondes de la pente continentale au large pour se déposer ultérieurement dans des aires de croissance peu profondes de la plate-forme.

On émet l'hypothèse a priori que le taux de classes annuelles s'accroit ou diminue selon les taux de transport intégrés au cours de la phase pélagique de 6 mois.

Les séries chronologiques des conditions météorologiques et océanographiques établies pour cette étude comprennent : la vitesse et la force d'entraînement des vents géostrophiques liés au gradient en surface; la pente de la ligne d'eau marine (niveau de la mer corrigé à la pression atmosphérique);

la pression atmosphérique en surface; et le débit d'eau douce. Deux séries de modèles de recrutement de 1935 à 1977 sont estimées à partir des analyses existantes des PPUE, des analyses par cohorte ainsi que des analyses des prises par âge (en période de migration) sur 60 ans de données de pêche commerciale. En se servant des estimations actuelles de la biomasse de reproducteurs, l'auteur fait apparaître une relation claire dépendante de la densité qui a une solide régression pondéré localement (LOWESS). On cherche à savoir dans quelle mesure cette relation est due à l'altération de l'environnement.

Dans deux régimes dissemblables du point de vue océanographique, représentés par les parties nord-est et nord-ouest de la plate-forme du golfe d'Alaska, des modèles de régression à plusieurs variables qui font ressortir l'intensité et la durée moyennes du transport côtier expliquaient jusqu'à 66% des variations observées dans le recrutement non attribuables aux effets de la taille des stocks reproducteurs ni à la densité. En particulier, un régime de vents en moyenne forts au cours de l'hiver a favorisé la production de classes annuelles importantes.

Ces paramètres du milieu physique de la région connaissent des variations interannuelles importantes. Les analyses portent à croire qu'il existe des phénomènes de transport vertical et horizontal engendrés par les vents le long de la côte et en travers de la plate-forme qui sont liés aux variations observées dans le succès de recrutement de flétans du Pacifique. Les principaux mécanismes en cause sont la convergence d'Ekman et la dérive des vagues de vent dans la couche supérieure, la circulation côtière entre la plate-forme et la pente continentale (continuité et guidage bathymétrique) et le mélange turbulent dû au vent.

Introduction

The long and vigorous controversy between proponents of natural (climatic, oceanographic) and fishery-induced mortalities in Pacific halibut stocks ("Thompson–Burkenroad Debate") was reviewed by Skud (1975) who concluded that observed abundance variations were not necessarily due to fishing levels alone. Burkenroad (1948, 1953) Huntsman (1953), Ketchen (1956) and others argued that favorable environmental conditions during the early life history were also responsible for stock increases, but generally with an emphasis on long-term climatic trends and changes in juvenile survival.

This paper addresses the controls of the physical environmental on biological recruitment, i.e., upon winter spawning success via larval survival through the critical early spring with juvenile settlement. Thompson (1950, 1952) and others (e.g., Bell 1970; Bell and Pruter 1958) repeatedly discounted this argument to the level of short-term influences considered secondary to fishery effects. Other authors (e.g., Ricker 1948; Holt 1951; Dickie 1973a, b; Skud 1975) conceded the combined importance of both and remained undecided, while stressing the need to consider each effect with an integrated management approach.

The reproductive strategy of the migratory Pacific halibut (*Hippoglossus stenolepis*) displays a pattern highly dependent upon major features of onshelf flux and coastal transport. Pelagic larvae originating well offshore in winter must be carried by prevailing coastal circulation to complete their development in shallow nursery areas during the critical spring productivity period. Mechanisms controlling shelf-slope exchange are thus important. These include wind-driven Ekman convergence, onshore flux (continuity and bathymetric steering), and turbulent wind-mixing. In this report I examine the hypothesis *a priori* that recruitment success as measured by year-class strength is largely influenced by interannual variations in the intensity and consistency of these on- and alongshore transport processes, with a comparison between two geographically distinct study areas.

The Pacific halibut fishery has historically ranked as one of the five most valuable luxury food resources in North America, with a current value exceeding $100 million per year. The present level of the halibut stocks is healthy and increasing, approaching historical highs (above maximum sustained yield (MSY)) in the northeast, central, and western Gulf of Alaska. Long-term regional abundance trends were reviewed by Quinn et al. (1985). A complete review of life history dynamics and the relevance of environmental forcing upon them is presented by Parker (1988, 1989).

Widespread batch spawning proceeds from late November through January in deep waters just beyond the continental shelf break from 200–500 m, with localized egg concentrations that appear consistent interannually (St-Pierre 1984). Hatching occurs within 2–3 wk (temperature-dependent) and early yolk-sac larvae begin to ascend the water column as they acquire positive buoyancy. Based on 1928–34 data throughout the Gulf of Alaska, Thompson and Van Cleve (1936) described a highly protracted winter larval phase with its remarkable metamorphic transitions, as well as horizontal and vertical distributions from extensive egg (c.f., Van Cleve and Seymour 1953) and larval surveys throughout the Gulf of Alaska. By 3–5 months all larvae were taken in the upper 100 m. Even at times of peak abundance the halibut larvae are exceedingly rare in the plankton. Extremely high rates of filtration are therefore required for their collection, and considerable variation exists by month and development stage (Thompson and Van Cleve 1936; Parker 1988).

The deep larvae rising offshore drift with a prevailing cyclonic *oceanic* circulation. The recently described Haida Current off northwestern British Columbia and southeast Alaska (Thomson and Emery 1986) flows as a narrow jet over the continental slope predominantly from November through February (with a January peak), and may provide an important transport mechanism for offshore larvae down to 500 m. Upward movement of larvae then continues at an as yet unknown and temperature-dependent rate through intermediate depths to an upper layer drift that eventually deposits them in shallow bays.

Ultimately, halibut larvae may traverse 1000 km of ocean while experiencing a wide spectrum of depth-dependent current velocities, until the extensive pelagic phase from slope to shore is completed within 5–7 months after hatching. It is the more vigorous *coastal* circulation that transports postlarvae alongshore and onshelf with a cyclonic downwelling pattern. Thompson and Van Cleve (1936) also suggested the drift of some larvae from the Gulf into the Bering Sea where a potentially important source of recruitment is indicated by the apparent presence of such circulation (Schumacher et al. 1982; Nof and Im 1985; Schumacher and Reed 1986).

Schmitt (1985) found 30 yr of juvenile abundance estimates to be unreliable measures of relative year-class strength for predicting recruitment to the fishery. For the purposes of interannual comparison, recruitment success is assumed to be set largely at the larval stage with survival levels remaining relatively intact through the 7–8 yr preceding entry into the commercial fishery.

The Environment — The Gulf of Alaska is a region of strong atmospheric cyclogenesis (Winston 1955) that represents one of the most environmentally energetic regions in the world. The Aleutian Low atmospheric pressure system dominates weather influences over a highly variable annual cycle with essentially two seasons: summer, from May–September, and winter, from October–April (Brower et al. 1977; Overland and Heister 1980). The maximum winter intensity (lowest pressure) is reached in the western and central Gulf where winds reaching 80 knots are generated by repeated storms (Danielson et al. 1957; Wilson and Overland 1986).

Greatly compressed surface pressure gradients are maintained against a high mountainous coastline. The large-scale cyclonic easterlies drive divergent ocean surface flows with associated Ekman transport piling up water against the coast ("set-up"), as reflected in progressive sea level maxima around the Gulf (Reed and Schumacher 1981). Resulting barotropic pressure gradients (normal to the coast) force the convergent coastal currents that larval drift is dependent upon.

The Alaska Current System dominates the offshore oceanic circulation in the Gulf of Alaska beginning with the broad Alaska Current in the east that narrows and intensifies into the swifter (>100 cm/s), deep (300 m) Alaskan Stream, a permanent western boundary current impinging upon the continental slope and characterized by relatively warmer and more saline waters than those found over the shelf (Fig. 1; Thomson 1972; Reed 1980, 1984, 1987; Reed et al. 1981; Royer 1981a; Niebauer et al. 1981; Reed and Schumacher 1984).

Buoyancy-driven coastal flows around the Gulf (with a winter minimum) are typical of the subarctic region, where salinity rather than temperature differences give rise to density gradients. Though the continental drainage pattern is less coherent in the east and south, a vast line source of precipitation and accumulated runoff extending westward of the Copper River region generates an important coastal current system (Royer 1979, 1982). While slower and more diffuse to the east, the Alaska Coastal Current (ACC; formerly "Kenai Current") is distinct in the north and western Gulf (corresponding to study area 3A) and has been the subject of active investigation for its remarkable characteristics as a coastal jet with speeds often exceeding 100 cm/s during peak fall runoff (Fig. 1 and 3; Schumacher et al. 1978; Schumacher and Reed 1980, 1986; Royer 1981a, b, 1982, 1983). In the northeast (corresponding to study area 2C), prevailing flow is generally alongshore throughout the water column and considerably greater in winter (Fig. 1 and 3; Hayes and Schumacher 1976; Hayes 1979; Lagerloef et al. 1981; Reed et al. 1981). Strong barotropic flow components (the

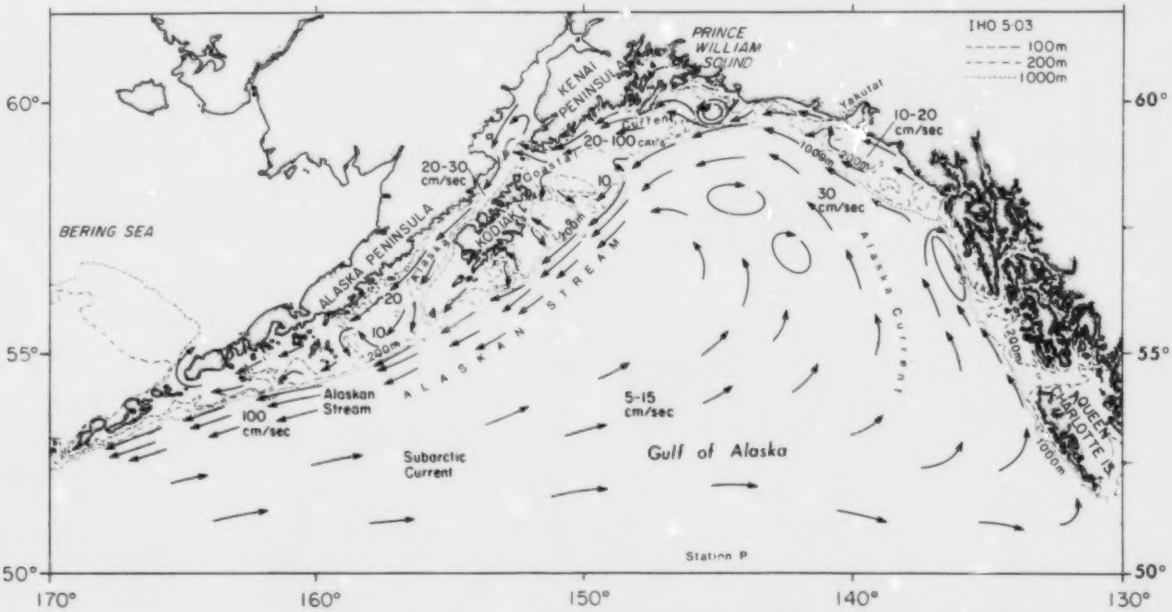

FIG. 1. Schematic representation of the major current speeds and directions in the Gulf of Alaska. Depth contours are from International Hydrographic Office Chart 5.03. (Modified from Reed and Schumacher 1986).

dominant mode) have been linked with local winter wind forcing (Lagerloef et al. 1981; Reed and Schumacher 1981).

The prevailing winter wind stress represents the key forcing mechanism of concern here for onshore transport and downwelling conditions constraining a narrowing westward-flowing coastal stream tightly against an arcing coastal boundary (Schumacher and Reed 1980; Royer 1982). A weaker wind-driven coastal convergence is produced along the eastern margin (Brower et al. 1977), where associated flow is less concentrated. Though negligible in summer, the barotropic gradient may be approximately equal in winter to the baroclinic — which is far less variable at that time — and therefore significantly augments the ACC.

Methods and Data

Of the three principal theories generally considered to affect critical early life history stages — transport, starvation, and predation — the first was selected *a priori* for this investigation. A specific mechanistic approach was then applied to the problem of ocean variability affecting recruitment, with consideration for the extent to which abundance variations may also be density-dependent.

The analysis focuses on the potential influence of coastal winds and associated transport processes in the year of birth upon eventual recruitment to the commercial fishery. A preliminary test within the Kodiak region indicated a statistically significant relation (parametric and nonparametric tests) between indices of year-class strength and alongshore wind through a pairing of strong or weak years (Fig. 2; Parker and Schumacher 1984; Parker 1989). To further explore this relationship, a specific suite of environmental parameters was identified to collectively index the relevant transport dynamics. More refined and accurately adjusted year-class strength estimation procedures were adapted for comparison with the best physical oceanographic and meteorological time series available for the region.

Halibut Recruitment Estimates

Maximum Pacific halibut recruitment variability has been approximately seven-fold (numbers-based) over the 60-yr history of the managed fishery, with a pattern that includes occasional extreme year-classes and longer term trends. Probable causes include changes in spawning biomass and the variable survival of pre-recruits in response to environmental change. Several historical methods of recruitment estimation for halibut exist (e.g., Fukuda 1962; Hoag and McNaughton 1978; Schmitt and Skud 1978), while more recent procedures were reviewed by Quinn et al. (1985) and incorporated into this study. The two general methods presently utilized to estimate abundance and productivity continue to provide relatively similar estimates spanning the last 50 yr: (1) catch-age analysis with CPUE partitioning, and (2) cohort analysis, with migratory catch-age analysis.

Stock assessment procedures follow the four major International Pacific Halibut Commission (IPHC) regulatory management areas along the coast from California to the Aleutian Islands and the Bering Sea, with divisions into two or more subareas each (Myhre et al. 1977; IPHC Pacific Halibut Fishery Regulations). From completed analyses comparing all four subareas ("Areas" herein) encompassing the Gulf of Alaska, this paper addresses interactions in the northernmost two: Areas 2C and 3A (Fig. 3; see Parker 1989 for more complete methodology).

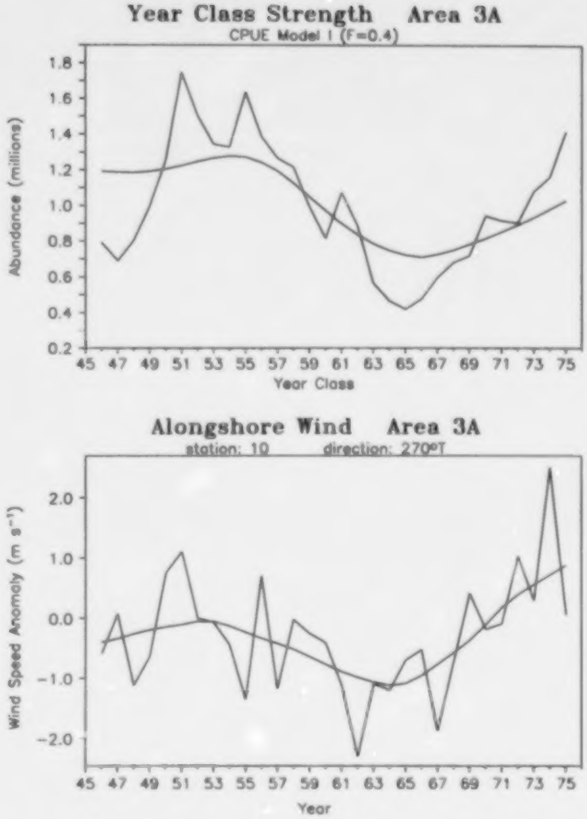

FIG. 2. Comparison between LOWESS-smoothed (f = 0.4) and unsmoothed Area 3A Model I year-class strength estimates, and the alongshore component of derived geotriptic winter mean (November–April) winds at coincident wind station 10. (Refer to Fig. 3 for station locations.)

Model I: Catch-Age Analysis with CPUE Partitioning — This method utilizes catch-per-unit effort (CPUE) as an index of population density in numbers of fish per unit area. Considering age 8 as the first age-class yielding reasonable abundance estimates, a moving average of the 8, 9 and 10 age-classes was calculated to provide the basis for each year-class estimate. Because catchability varies each year by age-class, this procedure serves to improve reliability in estimating each year-class by sampling its representation over 3 successive years. This required that the final series be lagged 10 yr back to the year of birth (year-class).

Various adjustments were applied to the CPUE values for each age-class. Values since 1978 were reduced by 10% to correct for an estimate of average weight (catch

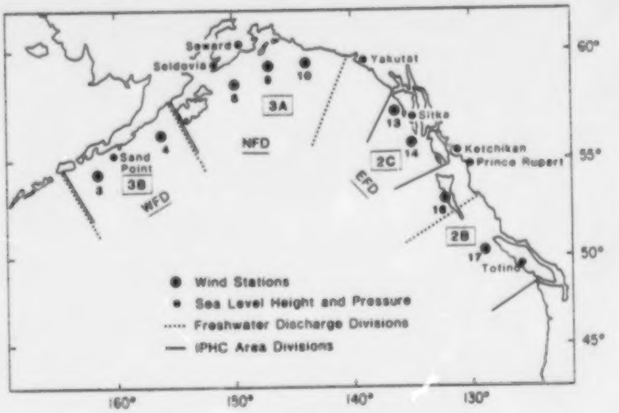

FIG. 3. Geotriptic gradient wind analyses loci, coastal stations of sea level height and atmospheric pressure, freshwater discharge (*FD*) divisions (Eastern, Northern and Western), and current IPHC regulatory areas for the Pacific halibut fishery.

biomass adjustment; Deriso, IPHC, pers. comm.). From 1983 to 1985, actual commercial catch data in numbers by Area were divided by effort values that accounted for a new shift in circle-hook use over the more traditional fixed-hook effort (Quinn et al. 1985; Williams and McCaughran 1985).

Regional differences in setline catchability (the ratio of fishing mortality to effort) were also adjusted to account for the varying degree of change in historic CPUE between Areas, based on trawl-setline experiments between Area 2B and other Areas (Hoag et al. 1984). CPUE Adjustment III was selected (Quinn et al. 1985), which increased CPUE in Area 2B by 25% while decreasing it by 25% in Areas 2C, 3A and 3B since 1981 (Fig. 3).

Gear selectivity indices were incorporated to remove the effects of differential vulnerability to the fishing gear by age, assuming full vulnerability for all fish aged 15 and over. The procedure followed cohort analysis to provide estimates of abundance by age and year, with terminal values taken from catch-age analysis (Deriso et al. 1985). Thus, CPUE values were divided by corresponding yearly age-specific gear selectivity values.

Fishing mortality and selectivity estimates by age and year were incorporated with relative CPUE variations by adjusting for halibut habitat size between Areas (Deriso and Quinn 1983). Quinn et al. (1985) describe the procedure for deriving absolute abundance values from these relative variations, thereby attempting to remove catchability effects between Areas (q = CPUE/abundance). The final series was obtained by multiplying the habitat-adjusted moving averages by the corresponding yearly age-eight estimates taken from cohort analysis for all Areas combined.

Model II: Cohort Analysis, with Migratory Catch-Age Analysis and Incidental Catch Adjustment — Deriso and Quinn (1983) reconsidered the data sources used in an earlier analysis (Hoag and McNaughton 1978) and reapplied cohort analysis without using the incidental catch data, as these were considered to be of poor quality and biased toward overestimation. Only ages 8–20 were used (incidental losses are mainly among juveniles), and an updated analysis for the most recent years was obtained using fishing mortality values from a previous catch-age analysis (Quinn et al. 1985).

A more powerful catch-at-age methodology (Deriso et al. 1985) was then used to estimate absolute year-class abundance from relationships between commercial catch and population parameters by age and year, producing fishing mortality starting values for the cohort analysis used here. Pre-1970 estimates were from Hoag and McNaughton (1978); new catch-age estimates after 1970 were obtained from Quinn et al. (1983). Auxiliary CPUE information was incorporated in the catch-age analysis only to stabilize the updated area estimates (Deriso et al. 1985; Quinn et al. 1985).

Migratory catch-age analysis, a new method developed at IPHC to provide biomass estimates independent of CPUE-partitioning (Quinn et al. 1985), also provided the basis for year-class values in which the Area 4 (Bering Sea) contribution was factored out. Though each assessment Area was separately considered, they are linked to each other with information on migration rates and population abundance.

Closed-subarea (no migration) cohort analysis results were applied in year-class estimation from 1935 to 1973. From 1974 to 1985, results from the open-area (migratory) catch-age analysis were included. All values were of age-eight abundances; therefore each estimate in the final series was lagged 8 yr back to the year-class, and the Area 4 component was eliminated as in Model I.

Additionally, a correction for incidental catch estimates was made with a moving average of incidental catch estimates (in weights) taken from 1960 to 1984 for ages 2–4, when losses are believed to have the greatest impact (Deriso, IPHC, pers. comm.). A 5-yr lag was therefore required from the age-eight abundance stock assessment standard (at the time of entry to the fishery) back to age 3. These values were then corrected to 8-yr-old biomass by adjusting for growth loss between the ages of incidental catch and fishery recruitment (multiplied by a factor of 1.58, after Quinn et al. 1985). Deriso (1985) presented biomass estimates for 8-yr-olds vs. mature adults.

The average weight of 8-yr-olds was required next to convert to the age-eight abundance standard in numbers. These data were derived by combining two Area-specific IPHC data files, the first from 1935 to 1973 (ages 1–24) and the second for 1974–85 (ages 8–20). Finally, the lagged and averaged incidental catch indices were added to the corresponding Area- and year-specific age-eight abundance estimates since 1959 from the new cohort and migratory catch-age analysis (with the 6.5% correction to eliminate Area 4).

Spawning Biomass Index — An index of spawning biomass was taken from existing estimates of exploitable biomass (see Discussion) by Area from 1935 to 1977 as derived from the cohort analysis with CPUE partitioning (adjustment III CPUE estimates in Quinn et al. (1985), since 1974), and fixed-age selectivity from catch-age analysis. Quinn et al. (1985) discussed the use of fixed-age selectivity (ages 8–20) to reduce the tendency of exploitable biomass estimates to be highly variable over time, when based on smoothed annual age selectivity estimates from cohort analysis (due to changes in halibut availability, minimum size limits and gear modifications). Finally, no adjustment for incidental catch losses was made, as an estimate was desired of fish actually surviving to spawn a given year-class.

Time Series of Oceanographic and Meteorological Variables

Alongshore and Cross-Shelf Winds (W, WC) — Geostrophically-derived surface-gradient wind estimates (*geotriptic:* from 1946 to 1982) were derived from the 6-hourly 3° synoptic northern hemisphere atmospheric surface pressure grid at the U.S. Navy Fleet Numerical Oceanography Center (Bakun 1973, 1975). Of seventeen stations analyzed around the entire Gulf of Alaska continental shelf margin, two were selected for each study Area considered here (Fig. 3–5).

Derived monthly mean values of wind speed and direction were resolved from the zonal and meridional vector components. Alongshore and cross-shelf wind magnitudes were then resolved for each station along major axes tangent and orthogonal to the adjacent section of arcing coast through methodology discussed elsewhere (Parker 1989).

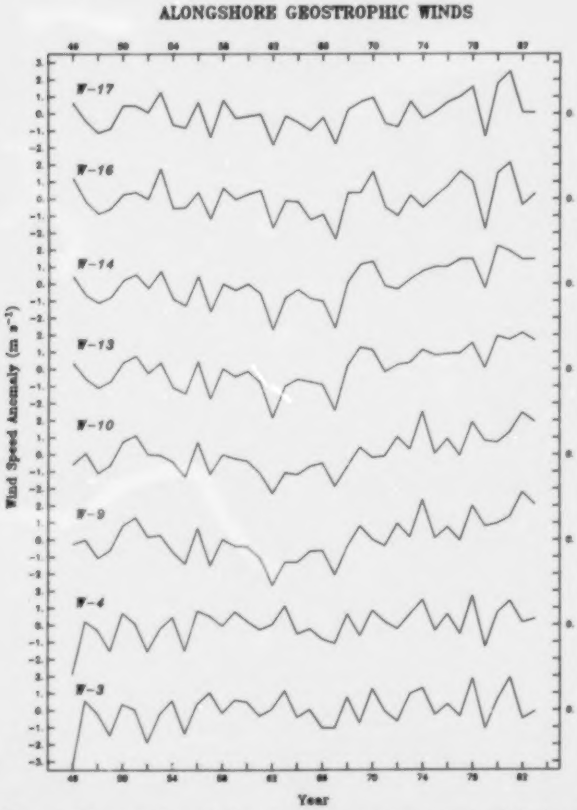

FIG. 4. Time series of the alongshore component of derived geotriptic winter mean (November–April) winds around the Gulf of Alaska shelf. Values shown are deviations from the long-term mean for the period 1946–82. (Refer to Fig. 3 for station locations.)

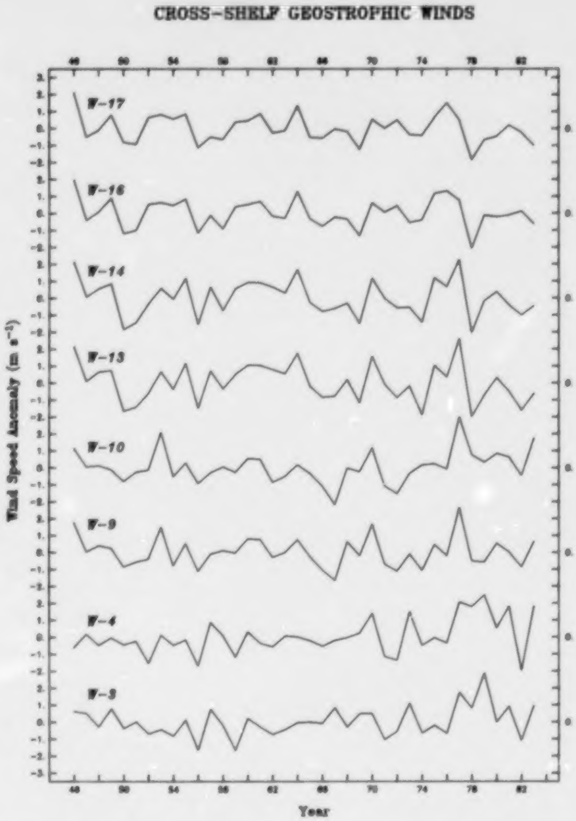

FIG. 5. Time series of the cross-shelf component of derived geotriptic winter mean (November–April) winds around the Gulf of Alaska shelf. Values shown are deviations from the long-term mean for the period 1946–82. (Refer to Fig. 3 for station locations.)

Adjusted Coastal Sea Level (ASL) — Four coastal sea level data series ranging from 1919 to 1981 (with gaps) were selected from available tide gauge stations around the Gulf (National Ocean Service Tides and Water Levels Branch) on the basis of data quality, record length, and proximity to the regional analysis scheme: Ketchikan, Sitka, Yakutat and Seward (Fig. 3 and 6). Monthly mean adjusted sea level height series were produced with atmospheric surface pressure corrections from the same locations (see SLP series below) to remove the inverse barometer effect (Beegle 1986).

The phenomenon of isostatic rebound, a long-term linear depression in sea level caused by the rising of previously glacier-depressed land, can be particularly significant along the seismically active Alaskan coastal boundary with its continuing glacial retreats (Hicks and Shofnos 1965; Hicks 1972). Based on the weight-dependent equilibrium of the lithosphere's geopotential height, such changes occur on the order of cm/yr. Each series was detrended by linear least squares regression to remove this long-term secular datum shift (Beegle 1986). In addition, a corrected data series for Seward was used to adjust for seismic activity which can cause dramatic vertical land shifts on the order of cm to m (e.g., the 1964 Anchorage earthquake) (Hicks 1972; Beegle 1986).

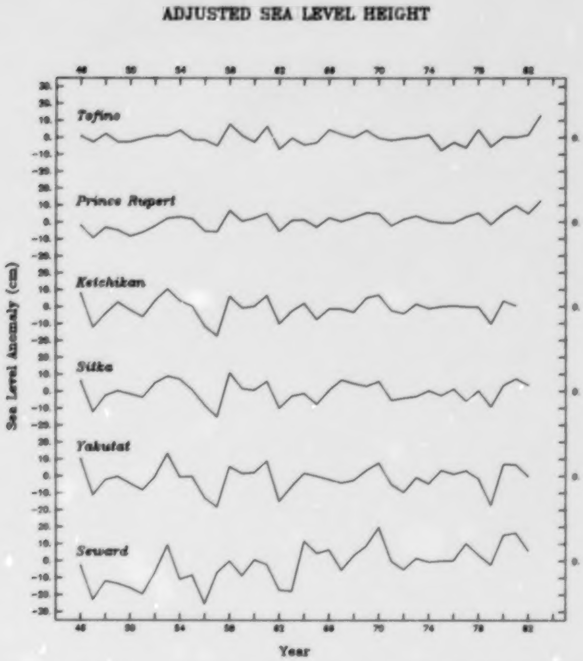

FIG. 6. Time series of winter mean (November–April) coastal sea level heights around the Gulf of Alaska shelf, adjusted for inverse barometer (from the same locations) and isostatic rebound effects. Values shown are deviations from the long-term mean for the period 1946–82. (Refer to Fig. 3 for station locations.)

Sea Level Atmospheric Pressure (SLP) — Data sources for monthly mean sea level data for Ketchikan, Sitka, Yakutat and Seward included: Climate Research Group, Scripps Institution of Oceanography, North Pacific grids (5° × 5°, Jan. 1919 to Mar. 1954; or 3° × 3°, Apr. 1954 to July 1982); older weather bureaus of the U.S. Departments of Agriculture (1919–40) and Commerce (1941–47) for nearby stations; National Weather Service (gap-filling when possible) (Fig. 3 and 7). Station pressures reduced to SLP were used, according to the pressure reduction ratios for each location (Beegle 1986).

Freshwater Discharge (FD) — Royer (1982) provided estimates of coastal freshwater discharge into the northeast Pacific for two divisions (Southeast and Southcoast) for 1931–84 from monthly mean U.S. Weather Service precipitation and air temperature data, together with drainage estimates that allowed for the interannual ablation of glacial fields in the coastal mountains. Estimates for a third drainage area ('Westcoast', west of approximately 155°W) were then produced here to index the relative baroclinic influence beyond Seward, incorporating river drainage data ranging from 1947 to 1985 (U.S. Geological Survey Water Resources Division, Alaska; see Parker 1989) (Fig. 3 and 8).

Two of the areal discharge series calculated from these data were used here to correspond with Areas 2C and 3A, with adjustment for phase shifts due to the transit times between Areas:

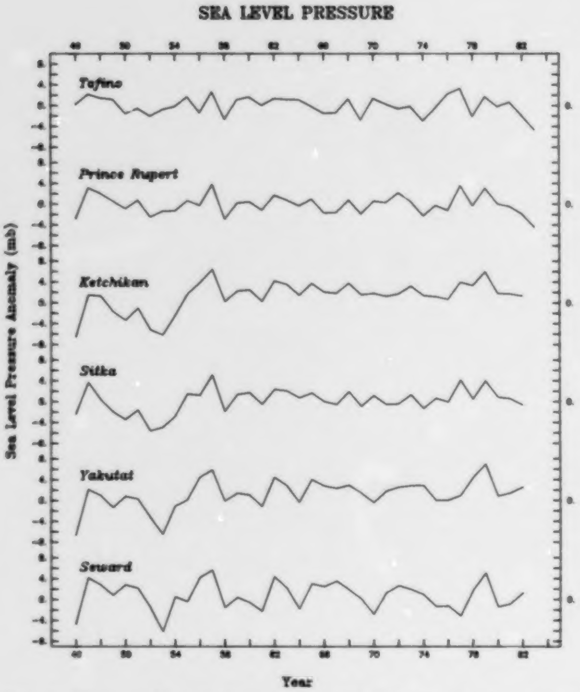

FIG. 7. Time series of winter mean (November–April) coastal sea surface atmospheric pressure around the Gulf of Alaska shelf. Values shown are deviations from the long-term mean for the period 1946–82. (Station pressures reduced to SLP according to pressure reduction ratios for each location; see text). (Refer to Fig. 3 for station locations.)

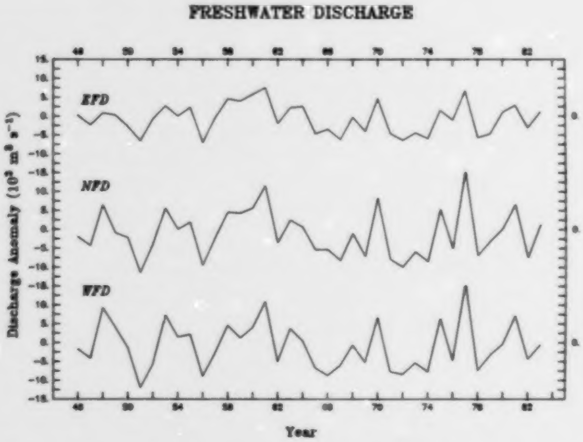

FIG. 8. Time series of winter mean (November–April) estimates of coastal freshwater discharge (*FD*) into Eastern, Northern and Western areal divisions, with one- and two-month lags cumulatively around the Gulf of Alaska coast (see text). Values shown are deviations from the long-term mean for the period 1946–82. (Refer to Fig. 3 for station locations.)

Eastern (EFD): Southeast only
Northern (NFD): Southeast + (Southeast − 1 month)
Western (WFD): Westcoast + (Southcoast − 1 month)
+ (Southeast − 2 months)

Note that the Alaska Coastal Current flowing beyond the Northern division thus encompasses input from all three divisions.

Northeast Pacific Pressure Index (NEPPI) — After Emery and Hamilton (1985), the strength of the atmospheric circulation over the Gulf of Alaska is represented by the seasonal zonal mean surface pressure difference between 40°N 120°W and 50°N 170°W (see Discussion).

All environmental series were de-meaned to remove annual signals by subtracting each long-term calendar month mean from its respective monthly value for each year. The resulting anomalies at each station were used in the regression analyses that follow (Fig. 4–8).

Adjustment for Density Dependence

An attempt was made next to control for the effect of variability in adult spawner abundance upon year-class strength. The strategy was to first determine whether there was a significant density-dependent relationship, and then to examine how the regression model designed to index the coastal transport process could account for the remaining recruitment variance.

An adjusted value of year-class strength was thus developed in terms of adult biomass. The exploitable biomass series described above (produced by the catch-age analysis) had already been partitioned by Areas (Quinn et al. 1985). Conforming to this series entailed a regrettable reduction in time series length from setting the first year of the following regression analyses at 1935 (rather than 1927) for both recruitment model series, as 8 yr of data are needed prior to the representation of the first year-class in the commercial fishery.

Smoothed series of both recruitment models were first generated using the robust locally-weighted LOWESS methodology (smoothing factor $f = 0.4$; Cleveland 1979). The adjusted dependent variable was then computed from the residuals of the regression of year-class strength (YC) on spawning biomass (SB). Smoothed and unsmoothed residual series (RYC) were thus produced for the final regression analyses (Fig. 9, for Model II).

Ricker (1975) noted that unit changes in environmental factors probably act in a multiplicative (proportionate) rather than additive manner in changing the number of recruits and recommended the use of log-transformed dependent variables in linear regression analyses. Natural logarithms of all abundance series were therefore incorporated into the regressions.

Multivariate Regression Models

Each environmental series of monthly means needed to be consolidated to a single seasonal mean per year. From the perspective of environmental controls, the seasonality of the early life stages is important. Because spawning extends from November through January and larval development then continues from each batch into early spring, a 6-month winter period spanning

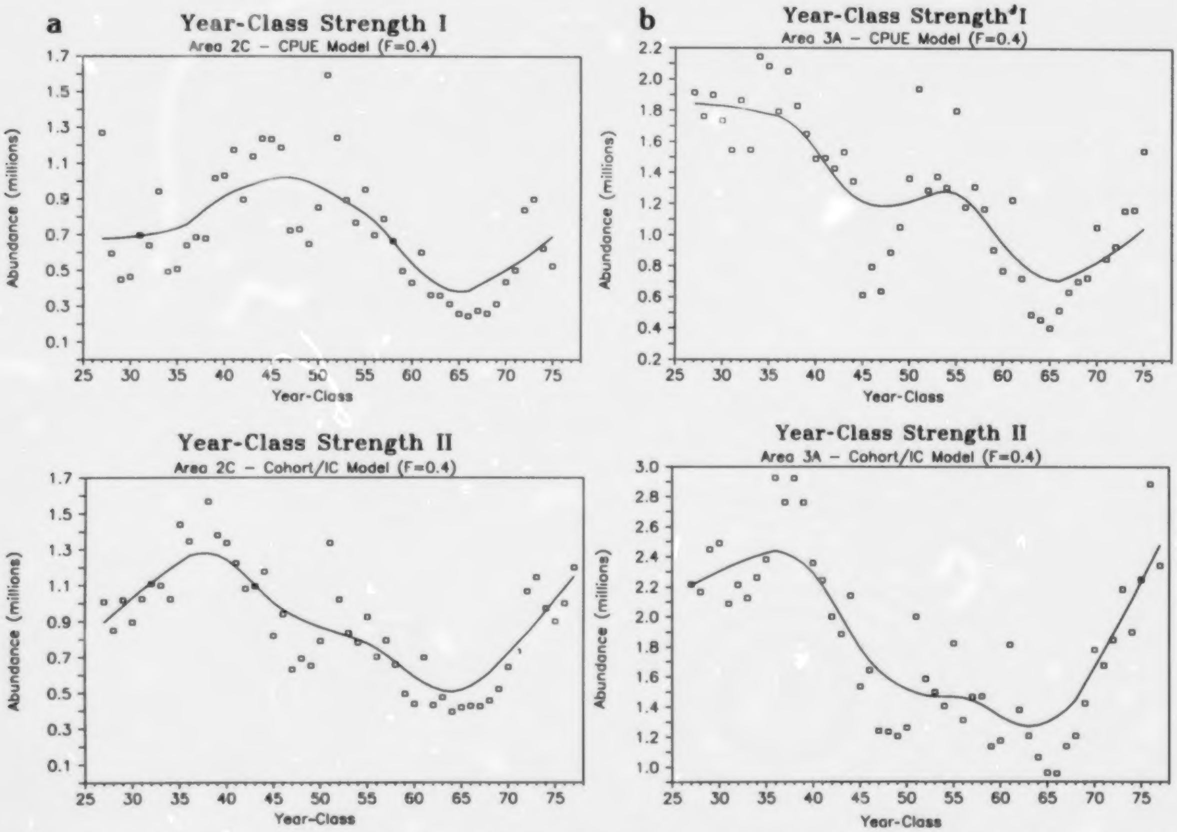

FIG. 9. Time series of LOWESS-smoothed ($f = 0.4$) and unsmoothed year-class strength estimates for (a) Area 2C and (b) Area 3A. Values shown are abundance in numbers for the period 1927–75 (Model I) and 1927–77 (Model II).

November–April was defined to cover the full pelagic phase in which the environment is the principal determinant of critical drift trajectories (assuming larvae are essentially passive drifters).

Surface wind maxima extend from December through March in the Gulf of Alaska, decrease through spring, and exhibit a large standard deviation in all months (Fig. 10; Brower et al. 1977; Gilhousen et al. 1983). Schumacher and Reed (1980) found wind forcing to impose maximum barotropic set-up from December through February, and associated coastal transport falls off markedly into late spring and summer. Therefore, averaging beyond April could attenuate the seasonal pulse of the physical indices and thereby weaken the interannual signal.

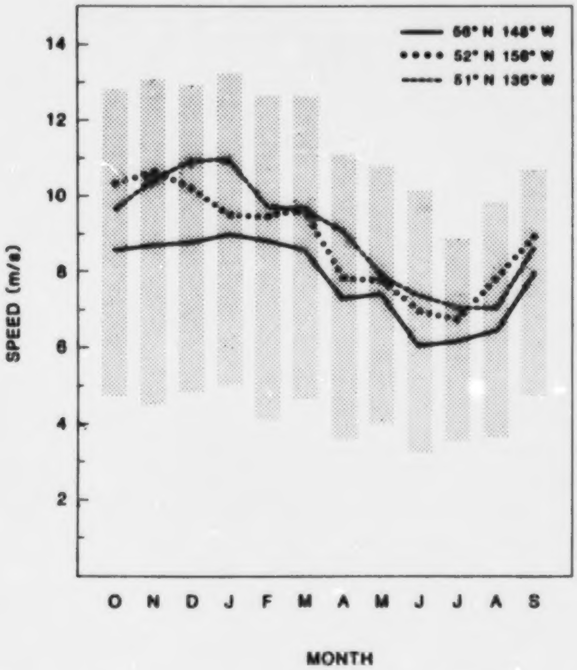

FIG. 10. Monthly-mean surface wind speeds at three Gulf of Alaska offshore NDBO wind buoys for the period 1972 to 1981. Vertical bars represent monthly standard deviations at 56°N 148°W and have similar magnitudes at the other two stations. (Adapted from Gilhousen et al. 1983).

A 30-yr period from 1946 to 1975 was finally selected for the regression analyses. While many of the environmental data series used here do extend back to the 1935 start of the adjusted recruitment series, the surface gradient wind analyses are not presently available before 1946. Wind was considered essential for testing the transport hypothesis in view of its central role in driving relevant shelf processes during the winter. The period ends in 1975 as does the Model I year-class series.

Multivariate regression analyses were run between the two residual recruitment series (RYC1, RYC2) and six independent variables for the physical environment: W, WC, ASL, FD, SLP and NEPPI. Because comparative effects between the two stations for each variable within an Area were also of interest, a linear combination was sought of a subset having the best predictive power and "fidelity" to the data. Model-fitting followed the general strategy described by Miller (1984). As a final precaution against selecting poor models, an additional random noise variable was added. When the procedure selected a "best" model including this variable, the next smallest order was referred to.

Model selection involved all possible regressions of each order (32 possible combinations) computed with the "Leaps and Bounds" procedure (Furnival and Wilson 1974), based on the Akaike Information Criterion (AIC; Akaike 1974). These facilities were available with the SAS/STAT package for personal computers (SAS Institute 1985). Its powerful "RSQUARE" procedure performs all regressions for all possible combinations within each subset of explanatory variables ("all possible subsets" selection), and in decreasing order of R^2 within each subset size (one-variable, two-variable, three-variable, and so forth) to assure determination of the highest R^2 models.

The AIC statistic is an asymptotically unbiased estimate of the expected negative entropy, i.e., a system's unexplained disorder that is reduced by a model. Decreasing AIC values (negative increase in Tables 1 and 2) are associated with models that reduce this disorder, while representing the statistically significant inclusion of additional variables (c.f., F-test); hence minimum values indicate the most explanatory or preferred models. Traditional methods of model selection (e.g., forward and backward stepwise selection) are justified by *ad hoc* criteria based on residual variances and proportionality, and are comparatively weaker (P. Smith, IPHC, pers. comm.).

Results

Marked interannual variability is revealed in the seasonally-averaged series for each physical parameter of the regional environment, along with limited evidence of lower frequency long-term secular trends (Fig. 4–8). Both stations selected within each study Area (Fig. 3) are included for comparison.

The plots of LOWESS-smoothed recruitment (Fig. 9) illustrate the roughness of the original series, attributable partly to the sampling error inherent in commercial catch statistics, as well as to the estimation error associated with stock assessment procedures. Smoothing these estimates serves to reduce these effects by revealing a less noisy behavior over time.

The results of regressing both YC series (LOWESS-smoothed, $f = 0.4$) on the SB index in Areas 2C and 3A yielded maximum R^2 values in Areas 2C and 3A of 0.36 ($p = 0.0005$) and 0.49 ($p = 0.0001$) with smoothed YC, and 0.26 ($p = 0.01$) and 0.28 ($p = 0.002$) with unsmoothed YC, respectively, and are presented in more detail elsewhere (Parker 1989). This analysis indicates that spawning biomass has varied sufficiently to significantly influence recruitment. The plot with LOWESS-smoothed YC clarifies an interesting trend between the two, revealing the long-term influence of compensatory density dependence in the halibut population history (Fig. 11).

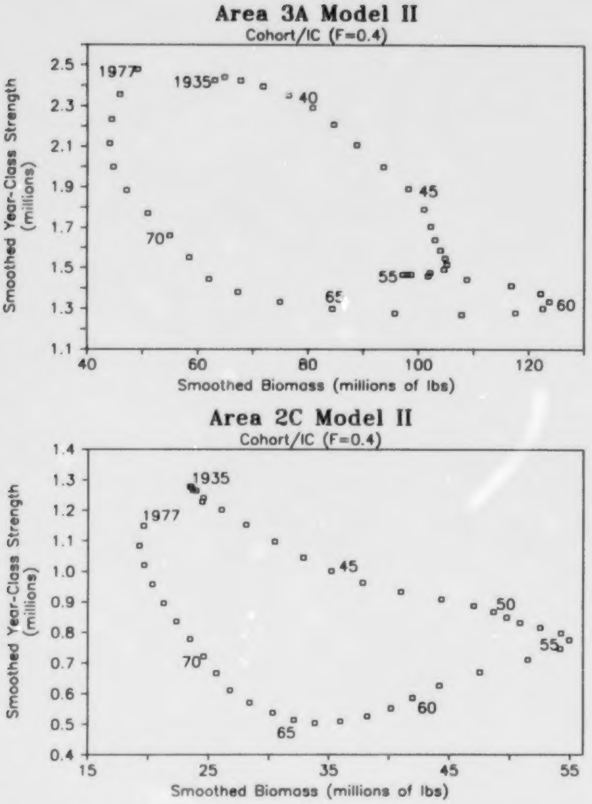

Area 3A Model II
Cohort/IC (F=0.4)

FIG. 11. Time series of LOWESS-smoothed ($f = 0.4$) estimates of year-class strength against spawning biomass at the year of birth. Values shown are abundance in numbers (year-class) and abundance in weights (biomass) for the period 1935–77 (Model II in Areas 2C and 3A).

Note the values proceed consecutively from 1935 to 1977 in a clockwise pattern — particularly in the Area 2C case where the time series actually "closes the circle". Two levels of recruitment success are associated with a given spawning abundance, perhaps in synchrony with different ecological regimes (see Discussion). The effects of SB variability must exist in concert with environmental fluctuations, and this study therefore attempts to control for this relation while examining the response to the physical dynamics.

It is important to point out that the analyses with either smoothed or unsmoothed year-class estimates produced results that were quite similar, quantitatively and qualitatively, in both study Areas. More detailed results from both methodologies are reported elsewhere (Parker 1989); what follows are R^2 values taken from runs using smoothed values because they can be regarded as representative. The best one, two, three and four variable models from each were essentially identical, and their coefficients were only slightly higher with the smoothed series (though not even in all cases).

Area 2C — The "best model" runs for both year-class series involved only three variables, which in all cases determined the model: alongshore wind | sea level pressure | adjusted sea level (Table 1). Fifty-six percent of the recruitment variance was explained, with the strongest relation exhibited for the recruitment model II series. Freshwater discharge and the Northeast Pacific Pressure Index (NEPPI) were not represented in any of the 'best' regressions.

Either alongshore wind or sea level pressure represented the best single-variable model among all 32 possible models, alone explaining 20 and 26% of the variance, respectively, in the model II series. Wind effects were therefore most strongly related to recruitment variability. Figure 12 is representative of the improvement gained with the best environmental model over this single variable in fitting the predicted to observed recruitment values.

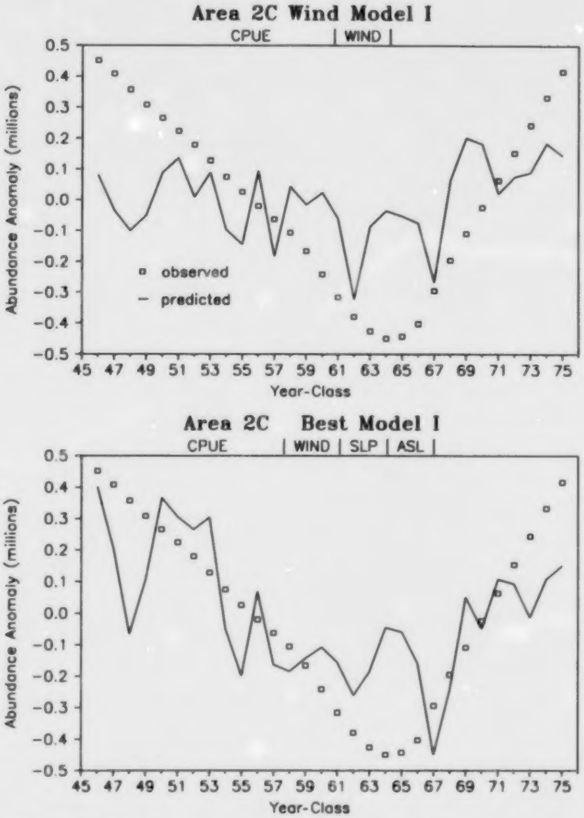

Area 2C Wind Model I
CPUE | WIND |

FIG. 12. Results of multivariate regressions, Area 2C: adjusted recruitment Model II series (observed values, LOWESS-smoothed, $f = 0.4$), compared to *wind-only* and *best* regression models (predicted values). Environmental parameters are winter means from previous figures. Values shown are deviations from the long-term mean for the period of analysis, 1946–75.

The next most consistently important variable was adjusted sea level, which with sea level pressure could account for 41% of the recruitment variance (RYC1). This was consistently the best two-variable model (17 of 32), followed closely by the alongshore wind | sea level pressure model (14 of 32). Finally, the inclusion of only one additional variable (beyond the two-variable models) yielded minimum AIC values for selecting the best model with remarkable consistency and a substantial improvement in the R^2 value (Table 1).

TABLE 1. Results of representative multivariate regression best models ($p = .01$), Area 2C: adjusted halibut recruitment series (LOWESS-smoothed, $f = 0.4$) and selected winter season environmental parameters (year-class strength Model I and Model II). Key refers to station locations (Fig. 3).

Best Models (variables)	R^2	- AIC
Model I (RYC1)		
SLP1	0.256	81.35
W2	0.189	78.75
SLP1/ASL2	0.410	86.32
W2/SLP2	0.228	78.26
W2/SLP1/ASL2	0.528	90.99
W2/SLP1/ASL1	0.514	90.15
Model II (RYC2)		
SLP1	0.317	92.93
W2	0.200	95.06
SLP1/ASL1	0.506	100.65
W2/SLP1	0.332	98.46
W1/SLP1/ASL1	0.565	102.48
W2/SLP1/ASL1	0.559	102.05

W: alongshore geotriptic wind
1: station 14 2: station 13

SLP: sea level pressure **ASL:** adjusted sea level
1: Sitka 2: Ketchikan

Area 3A — This region produced the strongest regression models with a closer fit to observed trends than in Area 2C, indicating that a higher proportion of recruitment variance was explained by the combined indices of wind-driven coastal transport (Fig. 13; c.f., Fig. 12). Tables 2 and 3 compare correlation and regression coefficients for a representative model from the Area 3A analysis with that in Area 2C. Again, freshwater discharge and NEPPI were poorly represented.

The best models usually included four variables, accounting for 66% of the variance in both recruitment series. This value was associated with two models that included wind station 10 located directly at the head of the northern Gulf. The variables included in the equation were consistently identical: alongshore wind | sea level pressure | adjusted sea level | freshwater discharge. Wind and sea level appeared in all 32 best model equations, with a wind parameter constituting the best single-variable model in all but four. It was the most predictive for both year-class series, alone accounting for 22% of the variance, as well as dominating the best two-variable models which accounted for 52% (note similarity with ASL | SLP model in Area 2C).

As in the previous Area, the importance of both wind forcing and coastal sea level dynamics was reflected by these results. Surface pressure again figured prominently here (third behind alongshore wind and sea level) to complete the only four best single-variable models not consisting of either alongshore or cross-shelf wind. It was then replaced by a wind variable in the best two-variable equations, with 40% of recruitment model II variance explained. In all, 23 of 32 two-variable models consisted of either the alongshore/cross-shelf wind | sea level or the surface pressure | sea level subsets.

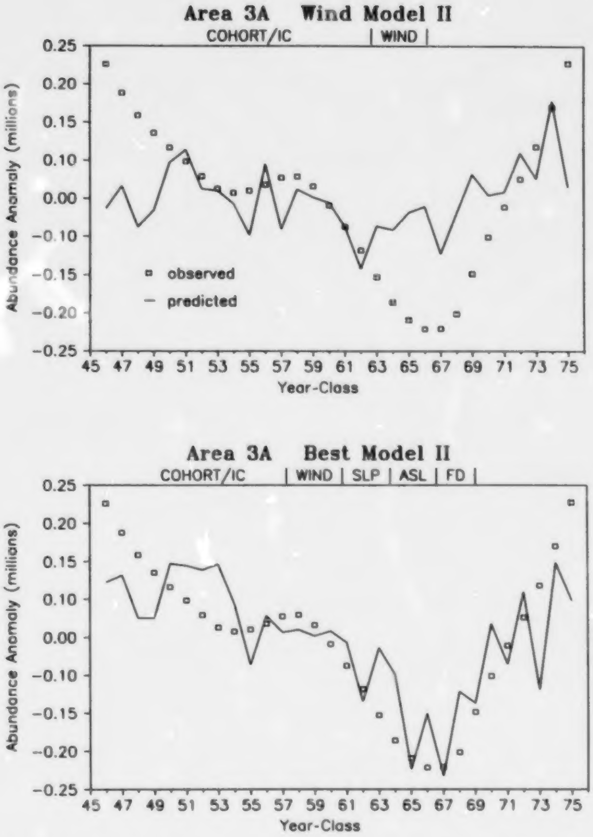

FIG. 13. Results of multivariate regressions, Area 3A: adjusted recruitment Model II series (observed values, LOWESS-smoothed, $f = 0.4$), compared to *wind-only* and *best* regression models (predicted values). Environmental parameters are the winter means from previous figures. Values shown are deviations from the long-term mean for the period of analysis, 1946–75.

Discussion

The essential element in this examination is a *mechanistic* approach involving preselected environmental parameters to index the onshore flux dynamics that exchange waters along the deeper continental slope with those on the shelf — and eventually along shallow coastal embayments. In two oceanographically contrasted regimes represented by the northeast and northwest Gulf of Alaska shelf, multivariate regression models with three or four of these parameters could explain substantial amounts of recruitment variability not accounted for by the effects of spawning stock size and density dependence. In particular, strong winter-averaged wind conditions favored the production of large year-classes.

TABLE 2. Results of representative multivariate regression best models (p = .01), Area 3A: adjusted halibut recruitment series (LOWESS-smoothed, $f = 0.4$) and selected winter season environmental parameters (year-class strength Model I and Model II). Key refers to station locations (Fig. 3).

Best Models (variables)	R^2	- AIC
Model I (RYC1)		
W1	0.215	103.02
W2	0.212	102.90
W2/ASL2	0.356	106.94
WC1/ASL2	0.345	106.45
W1/SLP1/ASL2	0.547	115.52
W2/SLP1/ASL2	0.530	114.40
W1/SLP1/ASL1/FD	0.610	117.97
W2/SLP1/ASL1/FD	0.597	116.99
Model II (RYC2)		
W1	0.179	142.34
W2	0.169	141.97
WC1/ASL2	0.520	154.37
SLP2/ASL2	0.465	151.08
W1/WC1/ASL2	0.608	158.45
W2/WC2/ASL2	0.595	157.42
W1/SLP1/ASL2/FD	0.658	160.50
W1/SLP1/ASL1/FD	0.643	159.26

W: alongshore geotriptic wind **WC:** cross-shelf geotriptic wind
1: station 10 2: station 9

SLP: sea level pressure **ASL:** adjusted sea level
1: Yakutat 2: Seward

FD: freshwater discharge (NFD — Northern)

Spawning Biomass and Density Dependence

The relation of recruitment to parent stock size in Pacific halibut has been considered by others (Thompson and Van Cleve 1936; Van Cleve and Seymour 1953; Fukuda 1962; Skud 1975). Cushing (1971) suggested that historical catches of halibut and other flatfishes have exhibited relatively low variability due to the stabilizing tendency of recruitment with respect to the parent stock, i.e., as density dependence increases so does stability. This influence has also been treated quantitatively by Cushing and Harris (1973) and Ricker (1975) in discussions of recruitment variability and compensatory density-dependent response.

Using a recent Ricker-type spawner-recruit analysis, Deriso (1985) also argued that density-dependent mechanisms appear to have affected recruitment variability. Higher levels of recruitment associate with low mature stock sizes, as indicated by both the age-structured and CPUE analyses (Fig. 11). If this relation holds, management goals to maximize yields might require lowering stock size (Deriso et al. 1985). Aside from the few particularly large recruitment year-classes (1951, 1955, 1961, 1970, 1972, 1973 and 1975), the increase in the recently rebuilt halibut stock tends to accompany a mildly decreasing recruitment trend (Deriso 1985).

The use of an exploitable biomass index here as a relative interannual estimator of actual spawning biomass is based confidently on earlier research (e.g., Schmitt and Skud 1978; Quinn 1981). Yet while both fecundity and selectivity have been found to increase with age, identification of a weight-specific selectivity relation is still needed. The questions of actual sex ratios and long-term changes in age at sexual maturity (i.e., growth rate trends) also need clarification to reduce the error in using this index of spawning biomass.

Schmitt and Skud (1978) also used biomass to relate fecundity to recruitment. The results here corroborate their evidence for density-dependent recruitment, though neither Ricker nor asymptotic curves could adequately describe the relation from 1935 to 1971. The relative influence of environmental change versus density-related factors in controlling recruitment remained undetermined.

While high population density itself may serve to increase or reduce spawning *level*, spawning *success* must also be controlled by several processes critical to larval survival. These in turn might be tracked by a particular suite of physical variables, indicating how physical controls can modify or even determine the direction and intensity of density dependence. The rotating plots depicted here probably reveal a simplified two-dimensional projection of these biotic effects (Fig. 11). There is likely to be at least one identifiable third dimension hidden in these patterns — that of environmental change.

Larval Transport

It is difficult to ascertain precisely which mechanisms are responsible for entraining drifting Pacific halibut larvae into the several cross-shelf and alongshore transport processes peculiar to the varied shelf regions of the Gulf of Alaska. It can however be argued, from physical oceanography theory and considerable empirical evidence, that increases in winter coastal wind energy will improve the efficiency of larval transport through an enhanced circulation from the continental slope to the nearshore shelf environment (e.g. Ekman 1905; Munk 1950; Winant 1980; Huthnance 1981; Lagerloef 1983; Petrie 1983).

Wind Forcing — There was clearly an overwhelming recurrence of the wind variables — particularly the alongshore component — in the best multiple regression models for both analysis areas. This was followed closely by the index of an associated sea level set-up condition that augments the prevailing buoyancy-driven flow. The importance of a vigorously sustained wind-driven coastal transport in winter is therefore strongly indicated, supporting the hypothesis that larval success and eventual recruitment into the halibut population are enhanced by onshore flux processes.

As strong wind stress constrains and intensifies the ACC against the coast, a more favorable vehicle for the larvae should develop. While the density-driven baroclinic

TABLE 3. Correlation coefficients (*r*) from two representative best model multivariate regressions, Areas 3A (upper values) and 2C (lower values): final adjusted halibut recruitment series for year-class strength Model I and Model II (RYC1 and RYC2, see text; LOWESS-smoothed, $f = 0.4$) and selected winter season environmental parameters. A single asterisk denotes significance at the 0.05 level; two denote the 0.01 level. (See Table 1 and 2 for station keys.)

	RYC2	W1	WC1	SLP1	ASL1	FD	NEPPI
W1	0.423** 0.448**						
WC1	0.336* -0.129	0.059 -0.251					
SLP1	-0.361* -0.476**	-0.017 -0.286	-0.644** -0.046				
ASL1	0.051 -0.028	-0.019 0.243	0.662** 0.098	-0.794** -0.580**			
FD	0.124 -0.130	-0.394** -0.057	0.662** 0.790**	-0.442** -0.245	0.615** 0.456**		
NEPPI	0.129 -0.027	-0.130 0.204	0.829** 0.672**	-0.509** -0.239	0.633** 0.423**	0.798** 0.849**	
RYC1	0.839** 0.991**	0.464** 0.434**	0.298 -0.089	-0.353** -0.506**	0.001 -0.027	0.008 -0.095	0.055 0.018

W: alongshore geotriptic wind; **WC:** cross-shelf geotriptic wind; **SLP:** sea level atmospheric pressure; **ASL:** adjusted sea level height; **FD:** freshwater discharge; **NEPPI:** Northeast Pacific Pressure Index.

flow would otherwise tend to spread seaward from the coast, a strong barotropic component generated by consistent winds converging on the coast will tighten the geopotential topography (Schumacher and Reed 1980) and effectively retain the larvae-rich surface waters close to shore. Because the interannual variation in ACC transport that is related to wind is likely to be concommitant with the greater Ekman transport cross-shelf, the mechanism driving onshore drift is principally the wind. Hence we find that wind independently accounts for at least one quarter of the recruitment variance in the northwest Gulf of Alaska.

Wind parameters correspond closely with observed onshore transport along the entire continental shelf in the Ekman layer, where response to transferred wind momentum extends to approximately 50 m. Schumacher and Reed (1980) found high coherence (95% level) between fluctuations in alongshore winds and downstream current velocity across several frequency bands. Recent current meter records in Shelikof Strait (J. Schumacher, National Oceanic and Atmospheric Administration (NOAA)/Pacific Fisheries Environmental Group (PMEL), pers. comm.) revealed vigorous transport fluctuations in essentially geostrophic flows, with about one third of their energy accounted for by the alongshore wind component (computed similarly to this study).

Schumacher (pers. comm.) also found derived geotriptic winds to account for approximately half of the variance in ACC transport over large scales from simultaneous current meter records on the Kodiak shelf. Using the same data, several new correlations were computed for present purposes (with P. Stabeno, NOAA/PMEL, pers. comm.), with inclusion of a sea level slope series between Seldovia on the Kenai Peninsula and Sand Point on the Alaska Peninsula (Fig. 3). A substantial relation resulted between sea slope and total transport through Shelikof Strait for the period January-March 1985 ($r = 0.62$, $p = .01$). Moreover, a regression using both the slope and derived wind series yielded a stronger relation with the measured transport over the same period ($r = 0.75$). This represents an important verification of the physical forcing mechanism being considered here from the perspective of empirical current velocities corresponding with winds in the Area 3A vicinity, and during the winter season.

Increased wind energy also deepens the effect of vertical mixing and turbulence, which in turn may improve larval distribution by enhancing their upward transport into a swifter, high-productivity surface layer. Periods with greater mixed layer depths (MLD) therefore reflect a wind-related process that might increase larval survival.

Lastly, wind-forced propogating wave fields generated over the shelf results in an additional surface-layer mechanism. This wave drift can combine with the Ekman wind drift to produce net onshore transport components with appreciable speeds in the upper 20-50 m, providing late postlarvae with locally accelerated trajectories toward stable shallow feeding areas.

Shelf-Slope Exchange — Flow field dynamics at the shelf break would be particularly instrumental in carrying larvae up from the offshore spawning depths through an onshelf flux of slope waters. Although the ACC is not dynamically coupled to the Alaskan Stream, the frequent intrusion of slope waters (lower salinity, higher temperature signal) from the Stream's inshore edge into the coastal environment would increase with stronger sustained onshore winds (Hayes and Schumacher 1976; Schumacher et al. 1978; Schumacher and Reed 1980). Hydrographic sections and satellite imagery often show intermediate and deep waters being "drawn up" periods of vigorous ACC transport, particularly along the various trough features cut into the shelf (Poole and Hufford 1982; Schumacher and Reed 1980).

Topographically controlled flow represents a mechanism that modulates this process, as described by Lagerloef (1983) in the vicinity of Kodiak Island. In effect, accelerated ACC transport would be expected to induce offshore waters up the troughs by entrainment, and from the upper layers by continuity. Observational evidence from Amatuli Trough northeast of Kodiak Island, for example (Schumacher and Reed 1980) suggests this as a key avenue for directing larvae in the northwest Gulf toward nearby food-rich shallow waters. Bathymetric steering may thus be providing special viaducts for the cross-shelf migration of developing larvae, and the potential in this process should not be underestimated. Other important mechanisms by which offshore waters communicate with the inshore shelf environment include midshelf and shelf break upwelling and other sources of upward vertical motion (e.g., Hill and Johnson 1974; Hsueh and Ou 1975; Galt 1980; Huthnance 1981; Petrie 1983; Werner 1984).

Atmospheric Pressure — The intimate relation between wind and sea level pressure (winds as derived from the geostrophic resolution of gradients in SLP) is apparent in the results — although correlations do not indicate consistent patterns of collinearity (Table 3). However, *regional* pressure influences are distinguishable from more *local* event-scale fluctuations, with remote forcing being an important factor in the time-averaged conditions over large sections of coast. Along the eastern Gulf margin for example, poleward surges of southern (warmer) water are often induced by southeasterly local wind events generated by teleconnective atmospheric forcing (Horel and Wallace 1981; Wallace and Gutzler 1981; Emery and Hamilton 1985). Since such winds associate with the intensification of the Aleutian Low, the NEPPI index of large-scale regional pressure patterns has been included in this study (though without substantial improvement in recruitment predictability). Propogating features, which are non-local, also involve wind and surface pressure effects that are separable on the basis of spatial extent.

Ocean-atmosphere exchange mechanisms, such as differential heating of the upper water layer density structure, can also affect shelf dynamics independently of the wind. Periods of extended insolation during winter (high pressure blocking ridges) can decrease MLD and induce stronger water density gradients. Stratification with a shallower Ekman layer in turn resists wind mixing, reducing the depth to which convergent Ekman transport will extend. In view of the hypothesis under consideration, halibut larvae below this level would then be restricted from a more timely emergence into critical surface layers.

Blocking high pressure ridges in the large-scale atmospheric pressure field are largely responsible for the interannual variability in storm tracks (Wilson and Overland 1986). While discrepancies in their precise identification exist, these ridges are almost exclusively a midwinter phenomenon and can resist the passage of low pressure systems into the area for up to two months. Preliminary comparisons between several blocking-high climatology summaries and halibut year-class strength indicated reasonable but inconsistent correlations; e.g., White and Clark 1975; Egger 1978; Treidl et al. 1981; Lejenas and Okland 1983; Quiroz 1986. Deflected either to the north, west or south, the loss of storm energy input to the Gulf system can have important consequences with regard to the strength and character of coastal transport processes. Related weather processes have also been shown to significantly affect wind stress and sea level differences between the eastern and western Gulf (Emery and Hamilton 1985).

Sea Level — As an important indicator of the strength of coastal transport (in terms of the set-up relation described earlier), sea level height was expected to feature prominently in the analyses. The best results in Area 2C emerged from models that included data from Sitka, whose seaward position on an open coast appears to reduce the biasing associated with the more protected inland waters at Ketchikan. While Sitka may therefore be more representative of actual flow conditions, there was no apparent difference in Area 3A between Seward or Yakutat which both lie inside relatively exposed embayments.

Buoyancy Flux — Freshwater discharge represents a more integrated parameter in time and space than the previous physical indices, with a signal that becomes less distinct geographically — particularly during the minimal winter contribution to the coastal circulation. Moreover, while winds can effectively increase ACC speeds by redistributing mass, total alongshore baroclinic transport does not increase in the process (Schumacher and Reed 1980). Thus this variable was not expected to be a major factor accounting for recruitment variability, and indeed the correlations were weak or inconsistent. Only in Area 3A, where total input accumulating around the Gulf constitutes the highest forcing from buoyancy flux, does this effect surface — but with a decidedly secondary importance to the wind.

The proposed causal relationship tested here is after all an imperfect though *identifiable* one, with regard to both the high-frequency interannual signal (unsmoothed regressions) and the low-frequency (smoothed) long-term trends. As a final caveat, it should be realized that the approach pursued here ultimately involves inadequate and uncertain linear approximations of the behavior of a vigorous and highly complex system, based upon an approximate knowledge of its parameters and possible interactions. It is therefore not surprising to find recruitment response to be nonperiodic and irregular, without a strictly proportionate (linear) correspondence to environmental fluctuations. As the emerging study of dynamical systems (chaos theory) has revealed, small perturbations can have large consequences where nonlinearities, feedback, and a sensitive dependence on initial conditions prevail. Conventional linear regression analysis eliminates the possibility of discerning richer yet nonrandom patterns, and until these aspects are addressed such inherent determinism (in apparent disorder) will likely remain hidden.

Acknowledgements

The author wishes to thank W. Wooster and J. Wallace of the University of Washington, D. McCaughran of the International Pacific Halibut Commission, J. Schumacher of the NOAA Pacific Marine Environmental Laboratory, and T. Royer of the University of Alaska for their helpful reviews and discussions. K. Foote, T. Henchman and R. Price of the IPHC computing staff provided indispensable assistance with data processing, and R. Deriso and P. Smith guided aspects of the analyses. C. Beegle (UW) furnished important elements in the data assembly, A. Bakun (NOAA/PFEG) provided the wind time series, and K. Exelby (IPHC) and P. Stabeno (NOAA/PMEL) supplied graphics support. Funding for this research was generously provided by the IPHC.

References

Akaike, H. 1974. A new look at the statistical model identification. IEEE Trans. Automatic Control 19: 716–723.

Bakun, A. 1973. Coastal upwelling indices, west coast of North America, 1946–1971. U.S. Dep. Commer. NOAA Tech. Rep. NMFS-SSRF 671: 103 p.

1975. Daily and weekly upwelling indices, west coast of North America, 1967-1973. U.S. Dep. Commer. NOAA Tech. Rep. NMFS-SSRF 693: 114 p.

Beegle, C. 1986. Time and space scales of some oceanic and atmospheric parameters in the Gulf of Alaska. M.S. thesis, Univ. Alaska, Fairbanks. 99 p.

Bell, F. H. 1970. Management of Pacific halibut. *In* A century of fisheries in North America. Am. Fish. Soc. Spec. Publ. 7: 330 p.

Bell, F. H., and A. T. Pruter. 1958. Climatic temperature changes and commercial yields of some marine fisheries. J. Fish. Res. B Can. 15: 625–683.

Brower, W. A., Jr., H. F. Diaz, A. S. Prechtel, H. W. Searby, and J. L. Wise. 1977. Climatic atlas of the outer continental shelf waters and coastal regions of Alaska. Volume 1, Gulf of Alaska. NOAA/OCSEAP, Final Rep. RU-347: 439 p.

Burkenroad, M. D. 1948. Fluctuations in abundance of Pacific halibut. Bull. Bingham Oceanogr. Collect. Yale Univ. 11: 81–129.

1953. Theory and practice of marine fishery management. Rapp. P.-v. Reun. Cons. Inter. Explor. Mer 18(3): 300–310.

Cleveland, W. S. 1979. Robust locally-weighted regression and smoothing scatterplots. J. Am. Stat. Assoc. 74: 829–836.

Cushing, D. H. 1971. The dependence of recruitment on parent stock in different groups of fishes. Rapp. P.-v. Reun. Cons. Inter. Explor. Mer 33: 340–362.

Cushing, D. H., and J. G. K. Harris. 1973. Stock and recruitment and the problem of density-dependence. Rapp. P.-v. Reun. Cons. Inter. Explor. Mer 164: 142–155.

Danielson, E. F., W. V. Burt, and M. Rattray, Jr. 1957. Intensity and frequency of severe storms in the Gulf of Alaska. Trans. Am. Geophys. Union 38: 44–49.

Deriso, R. B. 1985. Management of the North Pacific halibut fishery, II. Stock assessment and new evidence of density dependence, p. 49–60. Washington Sea Grant Tech. Rep. WSG-85-1. Univ. Wash., Seattle, WA.

Deriso, R. B., and T. J. Quinn II. 1983. The Pacific halibut resource and fishery in Regulatory Area 2. Part II: Biomass, surplus production, and reproductive value. IPHC Sci. Rep. 67: 55–89.

Deriso, R. B., T. J. Quinn II, and P. R. Neal. 1985. Catchage analysis with auxiliary information. Can. J. Fish. Aquat. Sci. 42: 815–824.

Dickie, L. M. 1973a. Interaction between fishery management and environmental protection. J. Fish. Res. Bd. Can. 30: 2496–2506.

1973b. Management of fisheries: ecological subsystems. Trans. Am. Fish. Soc. 102: 470–480.

Egger, J. 1978. Dynamics of blocking highs. J. Atmos. Sci. 35: 1788–1801.

Ekman, V. W. 1905. On the influence of the earth's rotation on ocean currents. Ark. f. Math. Astron. och. Fysik 2: 1–53.

Emery, W. J., and K. Hamilton. 1985. Atmospheric forcing of interannual variability in the northeast Pacific Ocean: connections with El Niño. J. Geophys. Res. 90: 857–868.

Fukuda, Y. 1962. On the stocks of halibut and their fisheries in the Northeastern Pacific. INPFC Bull. 7: 39–50.

Furnival, G. M., and R. W. Wilson. 1974. Regression by leaps and bounds. Technometrics 16: 499–511.

Galt, J. A. 1980. A finite element solution procedure for the interpolation of current data in complex regions. J. Phys. Oceanogr. 10: 1984–1997.

Gilhousen, D. B., R. G. Quayle, R. G. Baldwin, T. R. Karl, and R. O. Brines. 1983. Climatic summaries for NOAA data buoys. Nat. Clim. Data Ctr., NWS, NOAA Data Buoy Center, NSTL Station, MS. 214 p.

Hayes, S. P. 1979. Variability of current and bottom pressure across the continental shelf in the northeast Gulf of Alaska. J. Phys. Oceanogr. 9: 88–103.

Hayes, S. P., and J. D. Schumacher. 1976. Description of wind, current and bottom pressure variations on the continental shelf in the northeast Gulf of Alaska from February to May 1975. J. Geophys. Res. 81: 6411–6419.

Hicks, S. D. 1972. Vertical crustal movements from sea level measurements along the east coast of the United States. J. Geophys. Res. 77: 5930–5934.

Hicks, S. D., and W. Shofnos. 1965. The determination of land emergence from sea level observations in southeast Alaska. J. Geophys. Res. 70: 3315–3320.

Hill, R. B., and J. A. Johnson. 1974. A theory of upwelling over the shelf break. J. Phys. Oceanogr. 4: 19–26.

Hoag, S. H., and R. J. McNaughton. 1978. Abundance and fishing mortality of Pacific halibut, cohort analysis, 1935-1976. IPHC Sci. Rep. 65: 45 p.

Hoag, S. H., R. B. Deriso, and G. St-Pierre. 1984. Recent changes in halibut CPUE: Studies on area differences in setline catchability. IPHC Sci. Rep. 71: 44 p.

Holt, S. J. 1951. Review of: W. F. Thompson (1950) and Anon., "Regulation and Investigation of the Pacific halibut fishery in 1947 and 1948". Rapp. P.-v. Reun. Cons. Inter. Explor. Mer 17: 320–322.

Horel, J. D., and J. M. Wallace. 1981. Planetary-scale atmospheric phenomena associated with the Southern Oscillation. Mon. Weather Rev. 109: 813–829.

Hsueh, Y., and H. W. Ou. 1975. On the possibilities of coastal, midshelf, and shelf break upwelling. J. Phys. Oceanogr. 5: 670–682.

Huntsman, A. G. 1953. Fishery management and research. Rapp. P.-v. Reun. Cons. Inter. Explor. Mer 19: 44–55.

Huthnance, J. M. 1981. Waves and currents near the continental shelf edge. Prog. Oceanogr. 10: 193–226.

Ketchen, K. S. 1956. Climatic trends and fluctuations in yield of marine fisheries of the northeast Pacific. J. Fish. Res. Bd. Can. 13: 357–374.

Lagerloef, G. 1983. Topographically controlled flow around a deep trough transecting the shelf off Kodiak Island, Alaska. J. Phys. Oceanogr. 13: 39–146.

Lagerloef, G., R. D. Muench, and J. D. Schumacher. 1981. Low frequency variations in currents near the shelf break: northeast Gulf of Alaska. J. Phys. Oceanogr. 11: 627–638.

Lejenas, H., and H. Okland. 1983. Characteristics of northern hemisphere blocking as determined from a long time series of observational data. Tellus 35A: 350–362.

Miller, A. J. 1984. Selection of subsets of regression variables. J. Royal Stat. Soc., Series A, 147: 389–425.

Munk, W. H. 1950. On the wind-driven ocean circulation. J. Meteor. 7: 79–83.

Myhre, R. J., G. J. Peltonen, G. St-Pierre, B. E. Skud, and R. E. Walden. 1977. The Pacific halibut fishery: Catch, effort and CPUE, 1929–1975. IPHC Tech. Rep. 14: 94 p.

Niebauer, H. J., J. Roberts, and T. C. Royer. 1981. Shelf break circulation in the northern Gulf of Alaska. J. Geophys. Res. 86C: 4231–4242.

Nof, D., and S. H. Im. 1985. Suction through broad oceanic gaps. J. Phys. Oceanogr. 15: 1721–1732.

Overland, J. E., and T. R. Heister. 1980. Development of a synoptic climatology for the northeast Gulf of Alaska. J. Appl. Meteor. 19: 1–14.

Parker, K. S. 1989. Pacific halibut, *Hippoglossus stenolepis*, in the Gulf of Alaska, p. 94–111. *In* N. J. Wilimovsky, L. S. Incze, and S. J. Westrheim [ed.] Species synopses: Life histories of selected fish and shellfish of the Northeast Pacific and Bering Sea. Washington Sea Grant Publ. 88-2, Fish. Res. Inst., Univ. Wash., Seattle, WA. 111 p.

1989. Influence of oceanographic and meteorological processes on the recruitment of Pacific halibut, *Hippoglossus stenolepis*, in the Gulf of Alaska. Ph.D. dissertation, Univ. Washington, Seattle, WA. 154 p.

Parker, K. S., and J. D. Schumacher. 1984. Interannual variations in Pacific halibut abundance and the Kenai Current in the Gulf of Alaska. Trans. Am. Geophys. Union 64: 1080.

Petrie, B. D. 1983. Current response at the shelf break in transient wind forcing. J. Geophys. Res. 88: 9567–9578.

Poole, F. W., and G. L. Hufford. 1982. Meteorological and oceanographic factors affecting sea ice in Cook Inlet. J. Geophys. Res. 87C: 2061–2070.

Quinn, T. J., II. 1981. The use of Leslie-type matrix models for the Pacific halibut population, p. 217–242. *In* D. G. Chapman and V. F. Gallucci [ed.] Quantitative population dynamics. Int. Coop. Publ. House, Fairland, MD.

Quinn, T. J., II, R. B. Deriso, and S. H. Hoag. 1985. Methods of population assessment of Pacific halibut. IPHC Sci. Rep. 72: 52 p.

Quinn, T. J., II, E. A. Best, L. Bijsterveld, and I. R. McGregor. 1983. Sampling Pacific halibut landings for age composition: History, evaluation, and estimation. IPHC, Sci. Rep. 68: 56 p.

Quiroz, R. S. 1986. The association of stratospheric warmings with tropospheric blocking. J. Geophys. Res. 91D: 5277–5285.

Reed, R. K. 1980. Direct measurement of recirculation in the Alaskan Stream. J. Phys. Oceanogr 10: 976–978.

1984. Flow of the Alaskan Stream and its variations. Deep-Sea Res. 31: 369–386.

1987. Salinity characteristics and flow of the Alaska Coastal Current. Cont. Shelf Res. 7: 573–576.

Reed, R. K., and J. D. Schumacher. 1981. Sea level variations in relation to coastal flow around the Gulf of Alaska. J. Geophys. Res. 836: 6543–6546.

1984. Additional current measurements in the Alaskan Stream near Kodiak Island. J. Phys. Oceanogr. 14: 1239–1246.

1986. Physical oceanography, p. 57–75. *In* D. W. Hood and S. T. Zimmerman [ed.] The Gulf of Alaska: Physical Environment and Biological Resources. U.S. Dept. Int., Mineral Management Service, OCS study, MMS 86-0095. 655 p.

Reed, R. K., J. D. Schumacher, and C. Wright. 1981. On coastal flow in the northeast Gulf of Alaska near Yakutat. Atmos.-Ocean 19: 47–53.

Ricker, W. E. 1948. Methods of estimating vital statistics of fish populations. Indiana Univ. Publ. Sci. Ser. 15: 101 p.

1975. Computation and interpretation of biological statistics of fish populations. Bull. Fish. Res. Bd. Can. 191. 382 p.

Royer, T. C. 1979. On the effect of precipitation and runoff on coastal circulation in the Gulf of Alaska. J. Phys. Oceanogr. 9: 555–563.

1981a. Baroclinic transport in the Gulf of Alaska. Part I. Seasonal variations of the Alaska Current. J. Mar. Res. 39: 239–250.

1981b. Baroclinic transport in the Gulf of Alaska. Part II. A fresh water driven coastal current. J. Mar. Res. 39: 251–266.

1982. Coastal fresh water discharge in the northeast Pacific. J. Geophys. Res. 87C: 2017–2021.

1983. Observations of the Alaska Coastal Current, p. 9–30. *In* H. G. Gade, A. Edwards, and H. Svendsen [ed.] Coastal oceanography. Plenum Press, New York, NY.

SAS Institute, Inc. 1985. SAS/STAT Guide for Personal Computers, Version 6 Edition. Cary, NC.

Schmitt, C. C. 1985. Review of a trawl survey program for juvenile Pacific halibut. M. S. thesis, Univ. Wash., Seattle, WA. 182 p.

Schmitt, C. C., and B. E. Skud. 1978. Relation of fecundity to long-term changes in growth abundance and recruitment. IPHC Sci. Rep. 66: 31 p.

Schumacher, J. D., and R. K. Reed. 1980. Coastal flow in the northwest Gulf of Alaska: The Kenai Current. J. Geophys. Res. 85: 6680–6688.

1986. On the Alaska Coastal Current in the western Gulf of Alaska. J. Geophys. Res. 91: 9655–9661.

Schumacher, J. D., C. A. Pearson, and J. E. Overland. 1982. On the exchange of water between the Gulf of Alaska and the Bering Sea through Unimak Pass. J. Geophys. Res. 87: 5785–5795.

Schumacher, J. D., R. Sillcox, D. Dreves, and R. D. Muench. 1978. Winter circulation and hydrography over the continental shelf of the northwest Gulf of Alaska. NOAA Tech. Rep. ERL-404 PMEL-31: 16 p.

Skud, B. E. 1975. Revised estimates of halibut abundance and the Thompson-Burkenroad Debate. IPHC Sci. Rep. 56: 36 p.

St-Pierre, G. 1984. Spawning locations and season for Pacific halibut. IPHC Sci. Rep. 70: 46 p.

Thompson, W. F. 1950. The effects of fishing on stocks of halibut in the Pacific. Fish. Res. Inst., Univ. Wash., Seattle, WA. 60 p.

1952. Condition of stocks of halibut in the Pacific. Rapp. P.-v. Reun. Cons. Inter. Explor. Mer 18: 141–166.

THOMPSON, W. F., AND R. VAN CLEVE. 1936. Life history of the Pacific halibut (2): Distribution and early life history. Int. Fish. Comm. Rep. 9: 184 p.

THOMSON, R. E. 1972. On the Alaskan Stream. J. Phys. Oceanogr. 2: 363–371.

THOMSON, R. E., AND W. J. EMERY. 1986. The Haida Current. J. Geophys. Res. 91: 845–861.

TREIDL, R. A., E. C. BIRCH, AND P. SAJECKI. 1981. Blocking action in the Northern Hemisphere: a climatological study. Atmos.-Ocean 19: 1–23.

VAN CLEVE, R., AND A. H. SEYMOUR. 1953. The production of halibut eggs on the Cape St. James spawning bank off the coast of British Columbia 1935–1946. IFC Rep. 19: 44 p.

WALLACE, J. M., AND D. S. GUTZLER. 1981. Teleconnections in the geopotential height field during the Northern Hemisphere winter. Mon. Weather Rev. 109: 784–812.

WERNER, F. E. 1984. Finite element computations of spin-up and wind-driven coastal ocean circulation. Ph.D. dissertation, Univ. Wash., Seattle, WA. 130 p.

WHITE, W. B., AND N. E. CLARK. 1975. On the development of blocking ridge activity over the central North Pacific. J. Atmos. Sci. 32: 489–502.

WILLIAMS, G. H., AND D. A. MCCAUGHRAN. 1984. Results of comparative fishing of J hooks and circle hooks. 1985 IPHC Stock Assessment Document II: Research Results, 1984, p. 34–49.

WILSON, J. G., AND J. E. OVERLAND. 1986. Meteorology, p. 31–54. *In* D. W. Hood and S.T. Zimmerman [ed.] The Gulf of Alaska: Physical Environment and Biological Resources. U.S. Dep. Int. Mineral Management Service, OCS study MMS 86-0095. 655 p.

WINANT, C. D. 1980. Coastal circulation and wind-induced currents. Ann. Rev. Fluid Mech. 12: 271–301.

WINSTON, J. S. 1955. Physical aspects of rapid cyclogenesis in the Gulf of Alaska. Tellus 7: 481–500.

Estimation of the Effects of Flow on Dispersion of Larval Pollock, *Theragra chalcogramma*, in Shelikof Strait, Alaska[1]

R. K. Reed, L. S. Incze[2], and J. D. Schumacher

Pacific Marine Environmental Laboratory, National Oceanic and Atmospheric Administration,
7600 Sand Point Way NE, Seattle, WA 98115-0070, USA

Abstract

REED, R. K., L. S. INCZE, AND J. D. SCHUMACHER. 1989. Estimation of the effects of flow on dispersion of larval pollock, *Theragra chalcogramma*, in Shelikof Strait, Alaska, p. 239–246. *In* R. J. Beamish and G. A. McFarlane [ed.] Effects of ocean variability on recruitment and an evaluation of parameters used in stock assessment models. Can. Spec. Publ. Fish. Aquat. Sci. 108.

The focus of this work is to examine the effects of oceanic motions on the larvae of walleye pollock, *Theragra chalcogramma*, in Shelikof Strait, Alaska. A baroclinic coastal current flows southwestward through Shelikof Strait with typical peak speeds of 20 cm s^{-1}. Data from current moorings were used to derive eddy diffusivities and horizontal divergence (typical estimates were 5×10^6 cm^2 s^{-1} and -1.5×10^{-6} s^{-1}, respectively). The effects of horizontal advection, divergence, and turbulent diffusion on changing concentration of larvae with time were estimated. The estimates suggest that all factors may be important. Finally, changes which could result from physical effects were compared with observed changes in abundance and distribution to estimate larval mortality.

Résumé

REED, R. K., L. S. INCZE, AND J. D. SCHUMACHER. 1989. Estimation of the effects of flow on dispersion of larval pollock, *Theragra chalcogramma*, in Shelikof Strait, Alaska, p. 239–246. *In* R. J. Beamish and G. A. McFarlane [ed.] Effects of ocean variability on recruitment and an evaluation of parameters used in stock assessment models. Can. Spec. Publ. Fish. Aquat. Sci. 108.

Le but de cette recherche est d'étudier les effets du mouvement des eaux océaniques sur les larves de la morue du Pacifique occidental, *Theragra chalcogramma*, dans le détroit de Shelikof en Alaska. Ce détroit est traversé par un courant côtier barocline qui circule vers le sud-ouest et dont la vitesse maximale est habituellement de 20 cm s^{-1}. Des données recueillies à l'aide de mouillages ont permis de calculer les diffusivités tourbillonnaires et la divergence horizontale (typiquement, les estimations étaient de 5×10^6 cm^2s^{-1} et de $-1.5 \times 10^{-6}s^{-1}$ respectivement). Les effets de l'advection horizontale, de la divergence et de la diffusion turbulente sur la concentration des larves en fonction du temps ont été estimés. Les estimations portent à croire que tous ces facteurs peuvent être importants. Finalement, on a comparé les variations qui auraient pu être causées par des facteurs physiques avec les variations observées relatives à l'abondance et à la distribution des larves dans le but d'estimer la mortalité des larves.

---

[1] Contribution No. 972 from NOAA/Pacific Marine Environmental Laboratory.

[2] Current address: Bigelow Laboratory for Ocean Sciences, West Boothbay Harbor, ME 04575, USA.

Introduction

A goal of many fisheries recruitment studies is to ascertain the effects of the flow field and its variations on the movement and dispersion of larvae. Movement, or transport, is most often considered in instances where larvae are transported measurable distances from a spawning area to other locations. Such transport may be advantageous or deleterious to the organism, depending on its requirements and the characteristics of its new environment (Bailey 1981; Parrish et al. 1981; Norcross and Shaw 1984). Studies of circulation, larval transport, and life history phenomena, including post-larval requirements, can indicate some of the consequences that transport variations may have on fisheries recruitment. In this paper we examine characteristics of water motion in Shelikof Strait, Alaska as they affect the transport and dispersal of larval walleye pollock, *Theragra chalcogramma*.

Shelikof Strait is a long, narrow fjord-like feature, a submarine valley, between the Kodiak Island plateau and the Alaska Peninsula (Fig. 1). Maximum depths of about 300 m occur in the main channel from the Semidi Islands northward to central Kodiak Island; the sill depth west of Chirikof Island is about 200 m, and maximum depths in the northernmost part of the Strait are typically 150 m. The upper waters in the Strait are affected by the Alaska Coastal Current (ACC; Royer 1981), which enters the Strait after flowing along the Kenai Peninsula. The ACC flows westward down the Strait; near the Semidi Islands the flow sometimes bifurcates, with one branch continuing along the Alaska Peninsula and the other moving seaward (Schumacher and Reed 1986). The ACC exists in the Strait throughout the year, but maximum speeds occur in autumn as a result of a maximum in freshwater discharge.

Large concentrations of walleye pollock spawn in Shelikof Strait each spring. The most concentrated spawning occurs in late March–early April on the northern side of the Strait from Cape Kekurnoi (Fig. 1) northeastward about 50 km (Nelson and Nunnallee 1986;

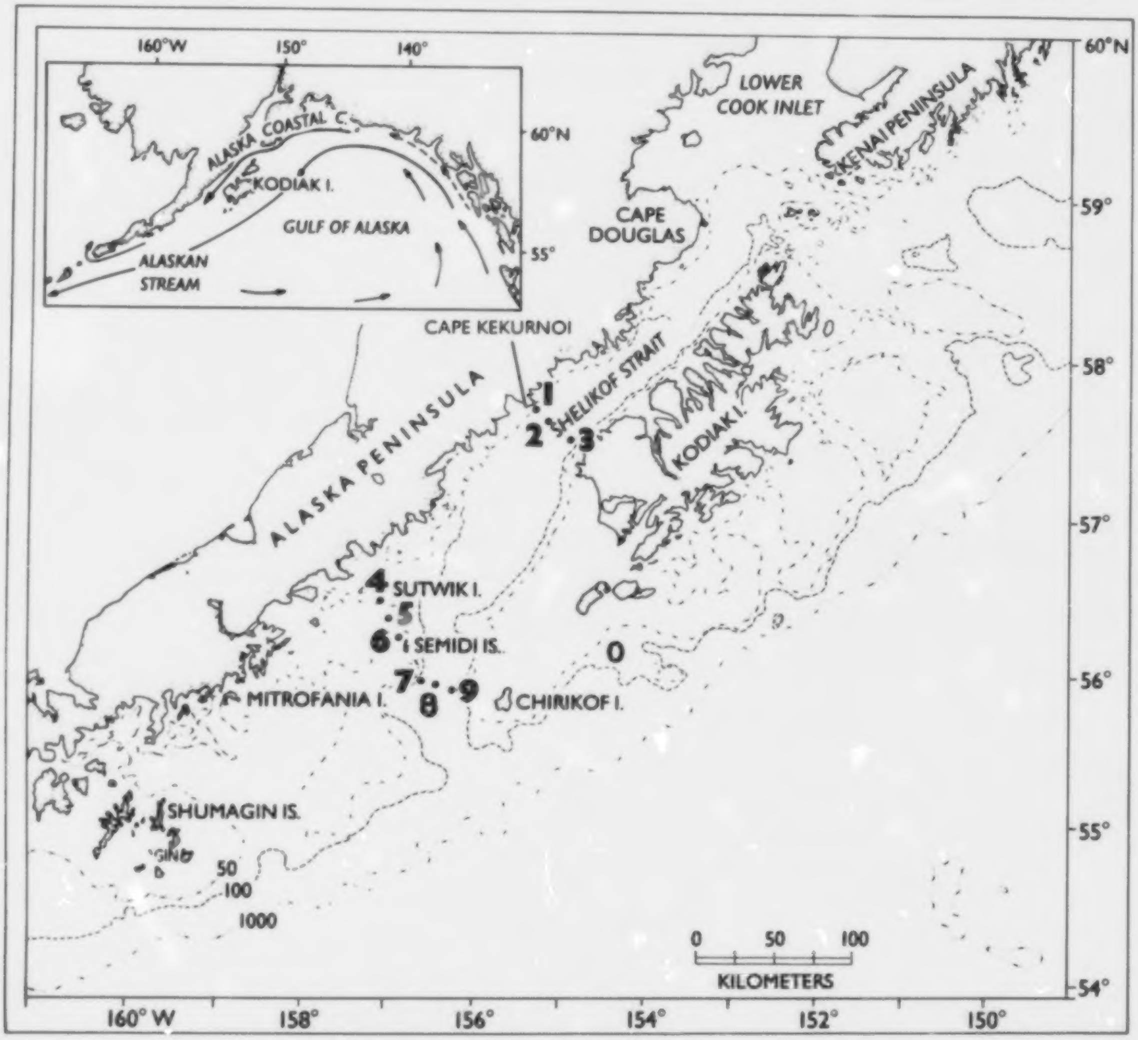
160°W
150°
140°
60°N
55°
ALASKA COASTAL C.
KODIAK I.
GULF OF ALASKA
ALASKAN STREAM
LOWER COOK INLET
KENAI PENINSULA
CAPE DOUGLAS
CAPE KEKURNOI
SHELIKOF STRAIT
ALASKA PENINSULA
KODIAK I.
1
2
3
4
SUTWIK I.
5
6
SEMIDI IS.
7
8
9
0
MITROFANIA I.
CHIRIKOF I.
SHUMAGIN IS.
50
100
1000
0
50
100
KILOMETERS
60°N
59°
58°
57°
56°
55°
54°
160° W
158°
156°
154°
152°
150°

FIG. 1. Shelikof Strait region with depth contours in fathoms (1 fm = 1.83 m). The typical upper-ocean circulation is shown in the insert. Locations of current moorings are shown by the numbered dots.

Kim 1987). Dense concentrations of eggs and larvae result. Eggs remain mostly below 150 m (Kim 1987), but the larvae form a "patch" of relatively high abundance in the upper layer and are transported southwestward as they develop (Kendall et al. 1987; Incze et al. 1989). Larvae hatch approximately 2 weeks after eggs are spawned and require 6–8 weeks to grow to the juvenile stage (Haryu 1980). Data referred to in this paper represent larvae less than 15 mm in length.

Larval survey data from 3 years — 1981, 1983, and 1985 — suggest different fates of larval patches from the main spawning event. Data from 1981 indicate relatively simple transport along the Peninsula. Data from 1983 indicate distortion of the larval patch by water movements, and data from 1985 suggest rapid removal of most larvae from the Strait. Here we consider features of the flow field that might affect larval patches in the region.

Data and Methods

Various physical data sets were obtained. CTD (conductivity/temperature/depth) casts were made with Grundy or Seabird systems, and the data were recorded on tape or disk. Extensive surveys, with dense station spacing, were conducted in March and October 1985. Various routines eliminated spurious scans and derived 1-m averages from which density and geopotential anomaly were computed. These data are only used here to describe general features of circulation.

Current meter moorings were maintained at nine sites as shown in Fig. 1. The moorings were deployed in August 1984; moorings 1–3 were retrieved in January 1985, and the others were recovered in July 1985. The moorings were all taut-wire systems with the subsurface float at about 25 m. The instruments used were Aanderaa RCM4 meters, which also contained thermistors and conductivity sensors. Similar systems with flotation at 18 m were found by Pearson et al. (1981) to have no significant contamination from mooring motion. The data records were checked for errors, and the time series (with sampling interval of 1 h) were passed through a 35-h filter, which passed 99% of the amplitude at periods >55 h, 50% at 35 h, and <0.5% at periods <25 h. Daily net vectors were derived and are used below to obtain estimates of eddy coefficients and velocity divergence but are not used to determine advection.

Larval pollock were enumerated from plankton samples collected with double-oblique tows of 60 cm bongo samplers (Posgay and Marak 1980) equipped with 500 μm (1981) or 333 μm (1983) mesh nets. Tows were taken to 200 m (as depth permitted), and samples were preserved in 3% buffered formalin: sea water.

Oceanic Motions

Horizontally uniform currents will advect larval patches by uniform translation. In general though, there is velocity shear in Shelikof Strait which can generate relative vorticity, divergence, and deformation. These parameters can result in distortion of fluid parcels and, in some instances, an increase or decrease in the area occupied by the parcel. Finally, patches will tend to spread out through the effects of *turbulent diffusion* because it is a random, irreversible process (in a probabilistic sense; Okubo 1980). The combined effects of advection and diffusion are here termed dispersion.

Flow (Advection)

Larvae are obviously subjected to movement by the coastal current or ACC. The larvae are mainly found between 20 and 50 m (Kendall et al. 1987); this should be below the level of significant wave drift (Stokes drift; James 1966), and major wind drift (Ekman drift) effects this deep are likely to be transitory and rare.

Numerous computations of baroclinic (geostrophic) velocity have been made (Reed et al. 1987a). The Strait is wide enough (about 40 km versus 10–15 km for the internal deformation radius) that Coriolis effects are important. An appropriate reference level is difficult to select because a level surface may slope across the Strait. Reed et al. (1987a), however, obtained plausible results for both the upper and deeper waters using a depth of 150 m. This was based on property distributions, the depth of inflowing waters, and current measurements at moorings 7, 8, and 9 (Fig. 1). The results may be generalized as follows. During most of the year, peak speeds near the surface are about 20 cm s^{-1}, but in autumn maximum flows increase to about 40 cm s^{-1} as a result of increased fresh water discharge which intensifies the baroclinic slopes. The southwestward flow normally does not span the entire main channel. The region of appreciable flow is frequently only about 20 km wide and may be anywhere in the channel; elsewhere flow is weak or even reversed. This spatial (and temporal) variability means that the flow may remove large parts of larval patches or leave them relatively undisturbed.

Previous current records in Shelikof Strait suggest the existence of appreciable barotropic or depth-independent flows (Schumacher and Reed 1980), in addition to the baroclinic flows discussed above. Figure 2 shows vector plots of daily-averaged currents at station 8; numerous events in this record suggest barotropic pulses that are superimposed on the background flow. These and other current measurements were used to infer that barotropic flows of ~15 cm s^{-1} and a few days' duration are typical.

Data from our current measurements in 1984–85 have been used to derive estimates of eddy fluxes and horizontal divergence of velocity. We then consider how these properties of the flow field may have influenced larval patterns seen in earlier (1981 and 1983) surveys, which lack comparable physical data sets. This is not an optimal approach, but it provides insight into flow processes which may be important in early phases of recruitment.

Eddy Fluxes

An effort is now made to estimate effects of turbulent diffusion. The eddy momentum flux can be related to the horizontal velocity gradient by:

$$(1) \qquad -\overline{u'v'} = A_h \frac{\partial v}{\partial x}$$

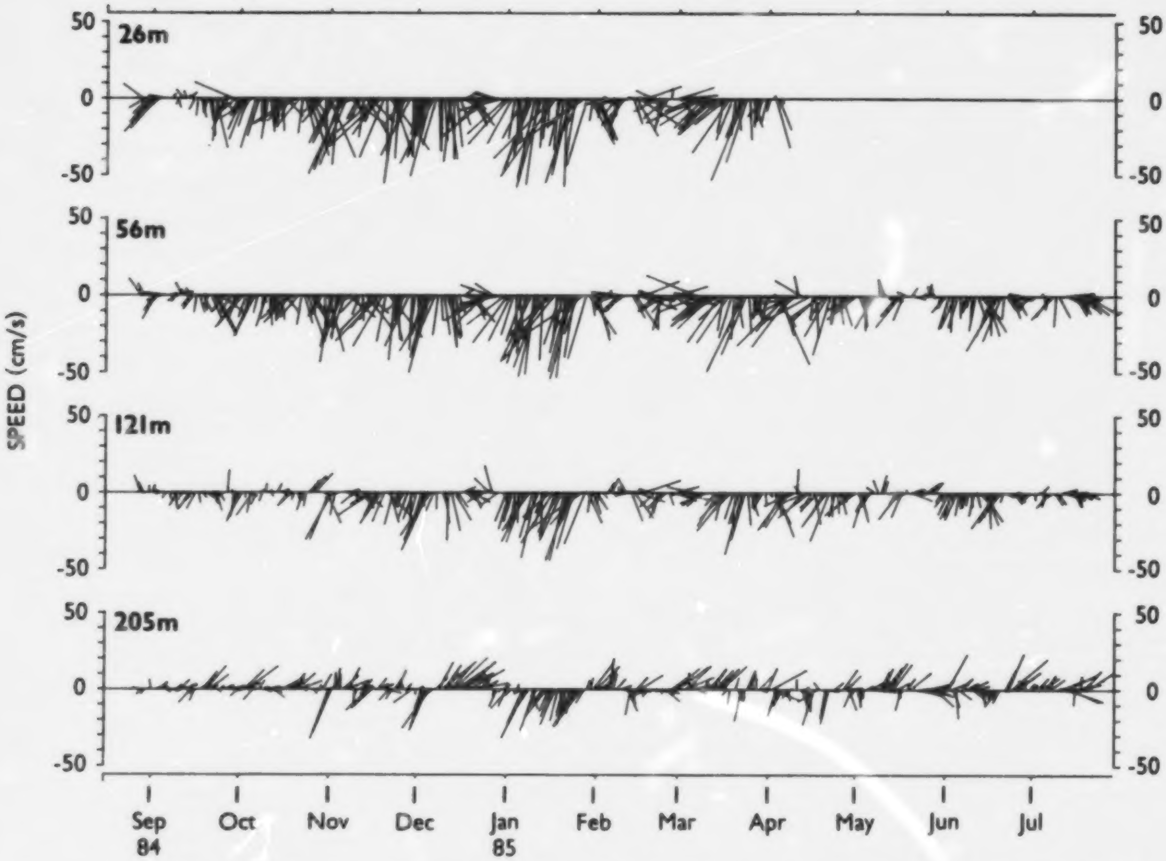

FIG. 2. Daily vector plots of measured currents at station 8, August 1984–July 1985. North is up on these plots.

where $\overline{u'v'}$ is the velocity covariance or mean eddy momentum flux, $\partial v/\partial x$ is the cross-channel velocity gradient, and A_h is the eddy viscosity. This relation is strictly true only for two-dimensional turbulence, where buoyancy effects are negligible, but has been used widely (Lukas 1987). In general, covariance can be computed from the data at current moorings and the transfer coefficients derived if the cross-stream gradients are large enough to exceed likely errors and are well behaved (velocity, for example, changes in a regular manner, preferably linearly, without reversals). Estimates on the current mooring sections were derived where quantities appeared to exceed likely errors and the cross-channel changes had no significant reversals; results are listed in Table 1.

The results in Table 1 give mean magnitudes of the eddy coefficients of 6×10^6 cm^{2}s^{-1} for section 1-3 and 5×10^6 cm^{2}s^{-1} for both sections 7-9 and 4-6. The values are plausible but correspond to length scales (Okubo 1980) of about 200-300 km, which seems large for this semi-enclosed region. Officer (1977), however, gave values for estuaries, especially during high river discharge, that are comparable to those here. The most striking feature of the results is the sign of the values. For section 1-3 the three values are negative, on section 7-9 all but one are positive, and at section 4-6 half are positive and half are negative. The negative results imply that small-scale, eddy-like features help intensify the mean flow as on the inshore edge of the Gulf Stream (Webster 1965). The positive values indicate the mean flow tends to spin down into smaller scales. More data are needed to establish if a regional difference in sign consistently exists. With adequate data on the spatial concentration of larvae, those eddy coefficients can be used to estimate the change in concentration with time as a result of turbulent diffusion.

Divergence of Flow

Larval pollock remain in the upper water column (Kendall et al. 1987) and probably are little affected by weak vertical velocities. When dealing with concentration equations for physical or chemical properties, the divergence of velocity is not a factor because it is zero for the approximately incompressible ocean. We assume that the mobility of larval pollock effectively cancels the vertical component of divergence (e.g., Olson and Backus 1985) and that horizontal divergence (which is generally nonzero) can spread or shrink the patches and should be considered.

In theory one could use data from the moorings and a vorticity equation (Hess 1959) to estimate horizontal divergence. Some of the assumptions needed to integrate the equation are not well justified, however, and there

TABLE 1. Determination of eddy viscosities from the covariances and the cross-channel velocity gradients at current moorings. The standard errors of $\overline{u'v'}$, computed from the record variances and integral time scales, are also given.

Section	Depth (m)	$\overline{u'v'}$ ($cm^2\ s^{-2}$)	$\partial v/\partial x$ ($10^{-6}\ s^{-1}$)	A_h ($10^7\ cm^2\ s^{-1}$)
*1-3	56	41.7 ± 32.2	6.4	−0.7
	106	30.1 ± 19.5	4.3	−0.7
	165	8.9 ± 7.9	3.3	−0.3
*7-9	121	22.2 ± 10.9	2.1	−1.0
*8-9	26	−30.9 ± 12.5	11.5	+0.3
	56	−24.0 ± 11.9	12.0	+0.2
	168	−9.0 ± 4.5	4.4	+0.2
7-9	56	27.2 ± 27.0	−2.5	+1.1
8-9	168	−3.1 ± 2.3	5.4	+0.1
*4-5	56	6.2 ± 2.2	0.9	−0.7
*5-6	26	−31.5 ± 31.0	3.7	+0.9
	56	−16.5 ± 11.1	5.0	+0.3
	75	−11.1 ± 6.8	4.1	+0.3
4-6	26	21.2 ± 10.1	5.3	−0.4
	56	11.6 ± 4.2	4.0	−0.3

* Data for Aug. 84–Jan. 85. Unmarked entries are for Jan. 85–July 85.

is considerable velocity shear across the Strait in places. Instead, we make estimates from the net velocity vectors at adjacent moorings and the effect they should have in altering an arbitrary area, using the relation:

$$D = \frac{1}{A}\frac{dA}{dt} \tag{2}$$

where D is horizontal divergence, A is area, and t is time. The following criteria were used: (1) net speeds at adjacent sites did not differ by more than 2 cm s^{-1}; (2) net speeds had to exceed their standard error; (3) the difference in flow direction between the sites had to be approximately 10° or more.

Only two estimates which met all of these criteria are available. The vectors are shown in Fig 3; the dashed squares are arbitrary areas, and the dashed vectors extending from the vertices are translations of the flow vectors from mooring 2. It is apparent that these flow fields would produce negative divergence (convergence), and values were obtained from the effect of the normal components of flow in shrinking the area. The estimates were both approximately $-1.5 \times 10^{-6}\ s^{-1}$. (Varying the areas and time intervals by plausible amounts gave values no different than $0.2 \times 10^{-6}\ s^{-1}$ from that above.) This value is an order of magnitude less than some direct measurements in swift boundary currents (Molinari and Kirwan 1975) but is comparable to values in a Gulf Stream ring given by Olson and Backus (1985). The fact that the estimates are negative is supported by the existence of negative wind-sress curl on the right side of the Strait looking downstream near section 1–3 (Reed et al. 1987a). Bathymetric steering might also be a factor for this tendency.

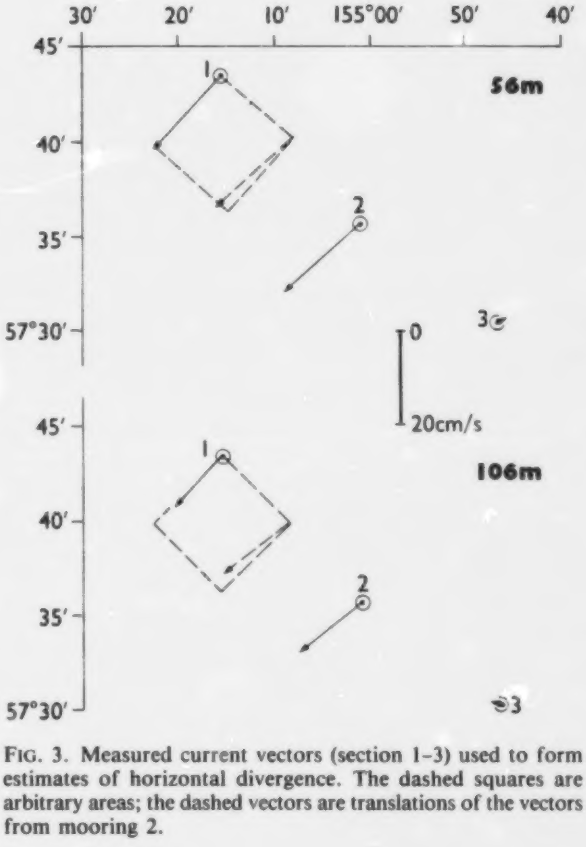

FIG. 3. Measured current vectors (section 1–3) used to form estimates of horizontal divergence. The dashed squares are arbitrary areas; the dashed vectors are translations of the vectors from mooring 2.

Effects of Motion on Larvae

Larval patches from 1981 and 1983 are shown in Fig. 4. The total survey pattern is not shown here but is illustrated by Kendall et al. (1987). The abundance of larvae within the patches in each case is distinctly different from general background abundances and can be related to the intense spawning of pollock in the region between the two shaded capes. Still, defining the patch "boundaries" is difficult. Here, we have chosen to draw the boundaries at larval concentration (number per 10 m^2) isopleths which are one fourth of the maximum observed value in each case. This criterion works well in defining coherent patches; only a few scattered stations outside these patches had values within the range of values in the patches, and none were nearby. Furthermore, there is no clear gradient of larval concentrations outside the areas we have defined. An area-weighted mean concentration of larvae was calculated for each patch. These data are given with estimated patch size (as defined above) and estimated total number of larvae in Table 2.

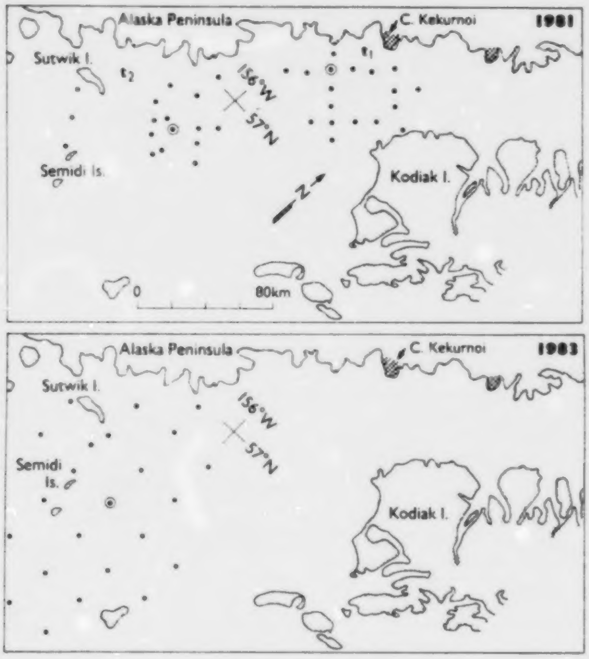

FIG. 4. Patches of larval walleye pollock defined by patterns of abundance in 1981 and 1983. The most abundant station in each patch is circled. The densest grey area covers the region in which estimated larval concentration (number per 10 m^2) is ≥ one-half of the most abundant station; the patch boundary is defined by one-fourth the maximum. Sampling stations within the patches and the nearest neighboring stations are shown. Details of the patches and sampling periods are given in Table 2.

The concentration of organisms will change with time at a fixed point (Eulerian perspective) as a result of advection of concentration gradients, horizontal divergence of flow, and turbulent diffusion. Symbolically,

$$\frac{\partial C}{\partial t} = -v\frac{\partial C}{\partial y} - CD + K_h\frac{\partial^2 C}{\partial y^2} \tag{3}$$

where C is concentration of larvae, t is time, v is along-stream (y-directed) velocity, D is horizontal divergence, and K_h is horizontal eddy diffusivity. We attempt to determine the magnitude of these terms and their relative importance. An effort is also made to assess the impact of physical processes in relation to estimating larval abundance and mortality.

Eulerian Changes

Based on the net movement of the larval patch over 25 days in 1981 (Fig. 4), an along-stream velocity (v) of 5 cm s^{-1} is indicated. This velocity is small compared to typical flows in the ACC, which emphasizes that circulation can vary considerably in space and time. It is supported, however, by small transport estimates at section 1-3 in spring 1981 (Reed et al. 1987b). It is conceivable that the patch was not in the core of the ACC during part or all of the 25-d period shown. A horizontal divergence (D) of -1.5×10^{-6} s^{-1} was used as estimated above from data in 1984-85. An area-weighted concentration (C) of 4.9×10^4 (10 m^2)$^{-1}$ was taken from Table 2. A K_h of 5×10^6 cm^2 s^{-1} was used. From data for Fig. 4 we estimated $\partial C/\partial y$ to be -4.4×10^{-2} cm^{-1} (10 m^2)$^{-1}$ and $\partial^2 C/\partial y^2$ to be -4.9×10^{-8} cm^{-2} (10 m^2)$^{-1}$.

Replacing the symbols on the right-hand side of eq. (3) with numbers, one obtains:

$$\frac{\partial C}{\partial t} = 0.22\ \mathrm{s}^{-1}\ (10\ \mathrm{m}^2)^{-1} + 0.07\ \mathrm{s}^{-1}\ (10\ \mathrm{m}^2)^{-1} - 0.24\ \mathrm{s}^{-1}\ (10\ \mathrm{m}^2)^{-1}$$

$$= 0.05\ \mathrm{s}^{-1}\ (10\ \mathrm{m}^2)^{-1}$$

This is the change in concentration per unit time that should occur at a point (that is, the local rate of change) downstream from the initial patch. These changes result

TABLE 2. Data for larval patches shown in Fig. 4. Patches are identified by year and by period of sampling. $\overline{C}_w$ = area-weighted mean concentration; $\hat{N}$ = estimated total number of larvae in patch; SE = standard error of $\hat{N}$.

Patch	Dates of sampling	$\overline{C}_w$ (No. larvae/10 m^2)	Area (km^2)	$\hat{N}$	SE
1981 - t_1	28-30 Apr.	4.9×10^4	442	2.2×10^{12}	1.4×10^{11}
1981 - t_2	24-25 May	9.7×10^3	378	3.6×10^{11}	2.6×10^{10}
1983	23-24 May	1.2×10^3	1 417	1.7×10^{11}	1.4×10^{10}

only from physical processes and do not consider potentially large biological changes. Furthermore, the balance would change rapidly as the patch is swept past the fixed point. It is apparent from the values above that all terms are important to the Eulerian changes in concentration. If v were as large as 20 cm s^{-1}, which would not appear to be unusual, advection of gradients would be the dominant term. The estimated size and shape of a patch and the mean concentration of larvae within it could be significantly affected by the time required to sample the area through which the patch transited.

The estimates of D and K_h are of course not synoptic with the larval data. If they are too large by a factor of three, for example, these two terms are reduced to 0.02 and -0.08 or a $\frac{\partial C}{\partial t}$ of 0.16 s^{-1} (10 m^2)$^{-1}$. The discussion in the next section certainly suggests that divergence and diffusion are not insignificant even if their magnitude is not firmly established.

Lagrangian Changes

For some purposes it is useful to view changes within the patch as it is advected. This moving system requires use of the total derivative $dC/dt = \partial C/\partial t + v\ \partial C/\partial y$, which here is $0.05 - 0.22 = 0.17$ s^{-1} (10 m^2)$^{-1}$. This change results from combined effects of the divergence and diffusion terms. The total derivative seems likely to be more conservative than the local derivative because of rapidly changing advective effects; this perspective is used in the following section.

Mortality Estimates

Numerous processes obey a relation of the form

$$C = C_0 e^{kt} \tag{4}$$

where C_0 and C are here taken as area weighted concentrations of larvae per 10 m^2 at times (t) 1 and 2 and k is a coefficient of change. Solving for k gives

$$k = \frac{\ln C - \ln C_0}{t}$$

and

$$e^k - 1 = \text{average change of } C \text{ per day.}$$

Using larval data from 1981 and the patches as defined above, we get $k = -6.48 \times 10^{-2}$ d^{-1} and $e^k - 1 = 6\%$ decrease per day. The cumulative decrease over the 25-day period was 80%, a number in agreement with some other studies (see Taggart and Leggett 1987). Approximately these same values are obtained using a variety of criteria to define the patches; thus the estimate appears robust despite uncertainty in defining patch "boundaries." However, these calculations describe only observed change and do not distinguish between contributions from physical processes and mortality. The decrease in concentration would serve as an estimate of mortality if we could assume no significant physical change.

To estimate the effect of turbulent diffusion on the larvae after 25 days, we used the relation from Bowden (1983; eq. 8.22)

$$C = \frac{C_0}{4\pi K_h t} \exp \frac{-r^2}{4K_h t} \tag{5}$$

where r is a patch radius or scale length. The formula predicts that concentration would decrease from 4.9×10^4 to 1.5×10^3 larvae (10 m^2)$^{-1}$. This change is much greater than actually observed (Table 2). Even when a very conservative value of K_h is used (1×10^6 instead of 5×10^6 cm^2 s^{-1}), the predicted larval concentration (4.9×10^3/10 m^2) at t_2 is still less than that observed. A K_h less than 1×10^6 cm^2 s^{-1} seems unlikely for a region like Shelikof Strait; since some mortality must be taking place, there must be some process compensating for turbulent diffusion. We suggest that this process may be the convergence (negative divergence) we noted earlier.

The dominant meteorological conditions of the region during spring suggest that nearshore convergence is common (Schumacher and Reed 1986), but its magnitude probably varies spatially and temporally. If we use the value of D obtained from 1984–85 (-0.13 d^{-1}) in the relation

$$C = C_0 e^{-Dt}, \tag{6}$$

we calculate that the effect of turbulent diffusion on larval concentration would be negated and that there would be an increase of 14% d^{-1} (effected by larvae counteracting downwelling). When this predicted increase from convergence is combined with the 6% d^{-1} decrease actually observed, it would require either that larvae experienced an average mortality rate of 20% d^{-1} (99.6% over the 25 d period) or that part of the original patch was removed by water movements. We feel, however, that the average larval mortality rate in 1981 probably was closer to the lower estimate (6% d^{-1}) and that average convergence was less than the value used above. The lower rate (6% d^{-1}) is closer to the observed decline in average larval concentration from the rest of the study area (~3% d^{-1}), but we caution that dispersion may differ inside and outside the patch. Several investigators have reported mortality rates below 10% d^{-1}, especially for temperate species (Dahlberg 1979; McGurk 1986; Houde 1987). The time over which the rates are averaged must be considered, however, since they involve larvae in various states of development which may experience different mortality rates.

Clearly, estimates of mortality are very sensitive to physical dispersion or concentration and our ability to measure these processes. Even where the physical rates are well measured, other problems can arise. When dispersive forces dominate it may be difficult to define patch boundaries. In years of very strong convergence it may be unreasonable to estimate mortality over 25 d periods because the patch at time 2 may consist of larvae not associated with the patch at time 1. In the future, other characteristics of larvae within patches may become known which might aid in elucidating patch dynamics and their role in recruitment variability.

In 1983 the mean concentration of larvae in the patch was $1.2 \times 10^3 (10\ m^2)^{-1}$, nearly an order of magnitude less than in 1981 at virtually the same time (t_2, see Table 2). Decrease in spawning stock size by 37% from 1981 to 1983 (Nelson and Nunnallee 1986) and the apparent increase in patch size account for 84% of the difference. The remainder is less than 1% on an average daily basis. Thus the mortality rate would appear to have been similar between 1981 and 1983 despite apparently significant differences in larval size attained by late May (Kendall et al. 1987, Table 6). Again, the importance of dispersion to larval mortality estimates is clear. Dispersion may also affect larval and early juvenile ecology, and these topics deserve further investigation.

In this paper, we have used estimates of divergence and eddy coefficients which were reasonable but were not simultaneous with larval data. In future research, we plan to track drogued buoys to give better (and synoptic) estimates of divergence. The spatial and temporal scales required to study transport and distribution differ from those needed to study dispersion and mortality (Smith 1981). Analyses such as those here can help define sampling requirements but do not resolve this basic dichotomy.

Acknowledgments

We thank A.W. Kendall, Jr. for providing data on larval walleye pollock. This work is part of the Fisheries Oceanography Coordinated Investigations of NOAA and is contribution number 0057.

References

BAILEY, K. M. 1981. Larval transport and recruitment of Pacific hake. Mar. Ecol. Prog. Ser. 6: 1-9.

BOWDEN, K. F. 1983. Physical oceanography of coastal waters. Ellis Horwood, Chichester, England. 302 p.

DAHLBERG, L. M. 1979. A review of survival rates of fish eggs and larvae in relation to impact assessments. Mar. Fish. Rev. 41: 1-12.

HARYU, T. 1980. Larval distributions of walleye pollock, *Theragra chalcogramma*, in the eastern Bering Sea, with special reference to morphological changes. Bull. Fac. Fish. Hokkaido Univ. 31: 121-136.

HESS, S. L. 1959. An introduction to theoretical meteorology. Holt, Rinehart, and Winston, New York, NY. 355 p.

HOUDE, E. D. 1987. Fish early life dynamics and recruitment variability. Am. Fish. Soc. Symp. 2: 17-29.

INCZE, L. S., A. W. KENDALL, JR., J. D. SCHUMACHER, AND R. K. REED. 1989. Interactions of a mesoscale patch of larval fish (*Theragra chalcogramma*) with the Alaska Coastal Current. Con. Shelf Res. 9: 269-284.

JAMES, R. W. 1966. Ocean thermal structure forecasting. Spec. Publ. 105, U.S. Navy Oceanographic Office, Washington, DC. 217 p.

KENDALL, A. W., JR., M. E. CLARKE, M. M. YAKLOVICH, AND G. W. BOEHLERT. 1987. Distribution, feeding, and growth of larval walleye pollock, *Theragra chalcogramma*, from Shelikof Strait, Gulf of Alaska. Fish. Bull. 85: 499-521.

KIM, S. 1987. Spawning behavior and early life history of walleye pollock, *Theragra chalcogramma*, in Shelikof Strait, Gulf of Alaska, in relation to oceanographic factors. Ph.D. dissert. Univ. Washington, Seattle, WA. 220 p.

LUKAS, R. 1987. Horizontal Reynolds stresses in the central equatorial Pacific. J. Geophys. Res. 92: 9453-9463.

MCGURK, M. D. 1986. Natural mortality of marine pelagic eggs and larvae: role of spatial patchiness. Mar. Ecol. Prog. Ser. 34: 227-242.

MOLINARI, R., AND A.D. KIRWAN, JR. 1975. Calculations of differential kinematic properties from Lagrangian observations in the western Caribbean Sea. J. Phys. Oceanogr. 5: 483-491.

NELSON, M. O., AND E. P. NUNNALLEE. 1986. Results of acoustic midwater trawl surveys for walleye pollock in Shelikof Strait, 1985, p. 23-49. *In* Condition of groundfish resources of the Gulf of Alaska region as assessed in 1985. NOAA Tech. Memo. NMFS F/NWC-106: 309 p.

NORCROSS, B. L., AND R. F. SHAW. 1984. Oceanic and estuarine transport of fish eggs and larvae: A review. Trans. Am. Fish. Soc. 113: 153-165.

OFFICER, C. B. 1977. Longitudinal circulation and mixing relations in estuaries, p. 13-21. *In* Studies in Geophysics: estuaries, geophysics, and the environment. National Academy of Sciences, Washington, D.C.

OKUBO, A. 1980. Diffusion and ecological problems: mathematical models. Springer-Verlag, Berlin, 254 p.

OLSON, D. B., AND R. H. BACKUS. 1985 The concentrating of organisms at fronts: A cold-water fish and a warm-core Gulf Stream ring. J. Mar. Res. 43: 113-137.

PARRISH, R. H., C. S. NELSON, AND A. BAKUN. 1981. Transport mechanisms and reproductive success of fishes in the California Current. Biol. Oceanogr. 1: 175-203.

PEARSON, C. A., J. D. SCHUMACHER, AND R. D. MUENCH. 1981. Effects of wave-induced mooring noise on tidal and low-frequency current observations. Deep-Sea Res. 28A: 1223-1229.

POSGAY, J. A., AND R. R. MARAK. 1980. The MARMAP bongo zooplankton sampler. J. Northwest Atl. Fish. Sci. 1: 91-99.

REED, R. K., J. D. SCHUMACHER, AND L. S. INCZE. 1987a. Circulation in Shelikof Strait, Alaska. J. Phys. Oceanogr. 17: 1546-1554.

1987b. Water properties and circulation in Shelikof Strait, Alaska during 1985. NOAA Tech. Memo. ERL PMEL-68: 35 p.

ROYER, T. C. 1981. Baroclinic transport in the Gulf of Alaska. Part II: A fresh water driven coastal current. J. Mar. Res. 39: 251-266.

SCHUMACHER, J. D., AND R. K. REED. 1980. Coastal flow in the northwest Gulf of Alaska: the Kenai Current. J. Geophys. Res. 85: 6680-6688.

1986. On the Alaska Coastal Current in the western Gulf of Alaska. J. Geophys. Res. 91: 9655-9661.

SMITH, P. E. 1981. Fisheries on pelagic schooling fish, p. 2-31. *In* R. Lasker [ed.] Marine fish larvae: morphology, ecology and relation to fisheries. Univ. Washington Press, Seattle, WA.

TAGGART, C. T., AND W. C. LEGGETT. 1987. Wind-forced hydrodynamics and their interaction with larval fish and plankton abundance: A time-series analysis of physical-biological data. Can. J. Fish. Aquat. Sci. 44: 438-451.

WEBSTER, F. 1965. Measurements of eddy fluxes of momentum in the surface layer of the Gulf Stream. Tellus 27: 239-245.

A Numerical Model for the Variability of the Northeast Pacific Ocean

William W. Hsieh and Warren G. Lee

Department of Oceanography, University of British Columbia, Vancouver, B.C. V6T 1W5

Abstract

HSIEH, W. W., AND W. G. LEE. 1989. A numerical model for the variability of the northeast Pacific Ocean, p. 247–254. *In* R. J. Beamish and G. A. McFarlane [ed.] Effects of ocean variability on recruitment and an evaluation of parameters used in stock assessment models. Can. Spec. Publ. Fish. Aquat. Sci. 108.

To understand the connection between the interannual variability of the northeast Pacific atmosphere-ocean system and the interannual variability in the return migration routes of the Fraser River sockeye salmon (*Oncorhynchus nerka*), we are developing a numerical ocean model to simulate the interannual variability of the northeast Pacific Ocean. The seasonal cycle of the model has been tested and is presented in this symposium. Extending from 16°N to 60°N, the model was forced by the climatological monthly windstress and surface heat flux. The resulting sea surface temperature variation in the model was small, being 2–3°C too warm in winter and 1–2°C too cool in summer in the northeast Pacific.

While the subtropical gyre displayed relatively minor seasonal variation in the barotropic (i.e. depth-integrated) transport, the subarctic gyre (composed of the Alaskan gyre to the east and the Oyashio gyre to the west) showed strong seasonal variation. The barotropic transport in the Gulf of Alaska varied from a low of 3 Sv in July to a high of 17 Sv in November. An explanation as to why strong barotropic response was found in the subarctic gyre but not in the subtropical gyre was given in terms of Rossby wave dynamics. The lack of accurate bottom topography in the model may be a cause for the large seasonal barotropic response. How this model can be used in the future to predict the return route of the Fraser River sockeye salmon is discussed.

Résumé

HSIEH, W. W., AND W. G. LEE. 1989. A numerical model for the variability of the northeast Pacific Ocean, p. 247–254. *In* R. J. Beamish and G. A. McFarlane [ed.] Effects of ocean variability on recruitment and an evaluation of parameters used in stock assessment models. Can. Spec. Publ. Fish. Aquat. Sci. 108.

Dans le but de comprendre la relation existant entre la variabilité inter-annuelle du système atmosphère-océan du nord-est du Pacifique et la variabilité inter-annuelle des voies migratoires qu'emprunte le saumon rouge du fleuve Fraser (*Oncorhynchus nerka*) lors de sa remontée, nous sommes en train de créer un modèle numérique de l'océan permettant de simuler la variabilité inter-annuelle du nors-est de l'océan Pacifique. Le cycle saisonnier de ce modèle a été établi et nous profitons de ce symposium pour le présenter. Entre les lattitudes 16°N et 60°N, notre modèle était tributaire des variations climatiques mensuelles de l'action du vent et du flux de chaleur à la surface de l'eau. L'erreur de notre modèle en ce qui a trait à la variation de la température de l'eau à la surface de la mer était faible : 2–3°C trop chaud durant l'hiver et 1–2°C trop froid durant l'été dans le nord-est du Pacifique.

Tandis que le tourbillon océanique subtropical a montré des variations saisonnières relativement peu importantes en ce qui a trait au transport barotropique (c.-à-d. en profondeur), le tourbillon subarctique (composé du tourbillon d'Alaska à l'est et du tourbillon d'Oyashio à l'ouest) a montré des variations saisonnières importantes. Le transport barotropique dans le golfe d'Alaska a varié entre 3 Sv, en juillet et 17 Sv, en novembre. Nous nous sommes servis de la dynamique ondulatoire de Rossby pour expliquer le fait que la réponse barotropique s'est montrée forte dans le cas du tourbillon subarctique et faible dans le cas du tourbillon subtropical. Le manque de données précises relatives à la topographie du fond marin pourrait expliquer les variations barotropiques saisonnières importantes que nous avons obtenues. Enfin, la question de l'utilisation future de ce modèle pour prédire les voies migratoires empruntées par les saumons rouges du fleuve Fraser lors de leur remontée est examinée.

1. Introduction

In recent years, the study of ocean–atmosphere interannual variability has been focussed primarily in the tropical region due to the spectacular *El Niño*–southern oscillation (ENSO) phenomenon and its significant biological consequences (Ramage 1986). At higher latitudes, the interannual variability is still important (Mysak 1986). For instance, during the major 1982–83 *El Niño*, the coastal sea surface temperature off the west coast of Vancouver Island was 2°C above normal, while over 80% of the Fraser River sockeye salmon (*Oncorhynchus nerka*) returned by the northern route via Johnstone Strait in 1983 (Fig. 1), compared to an average value of about 20%. The connection betweem ENSO and higher-latitude variability is however not perfect — for instance, warm sea surface temperature anomalies off Vancouver Island do not always appear in an *El Niño* year, and they sometimes occur in a non *El Niño* year. Clearly other processes besides ENSO are important in generating the interannual variability at higher latitudes.

The intriguing problem of how the Fraser River sockeye migration routes are connected to the interannual variability of the atmosphere–ocean system has been under study since 1984 by a strategic grant to L.A. Mysak, K. Hamilton, and C. Groot from the Natural Sciences and Engineering Research Council of Canada. The various research efforts of this project MOIST (Meteorological and Oceanographic Influences on Sockeye Tracks) are described by Mysak et al. (1986). Here we will only describe some of the numerical modelling under project MOIST.

Despite the impressive advances of numerical ocean models in the last two decades, the application of 3-dimensional numerical ocean models to fishery management has never been attempted. Previous studies to predict the diversion rate of the returning sockeye through Johnstone Strait, Wickett (1977) and Groot and Quinn

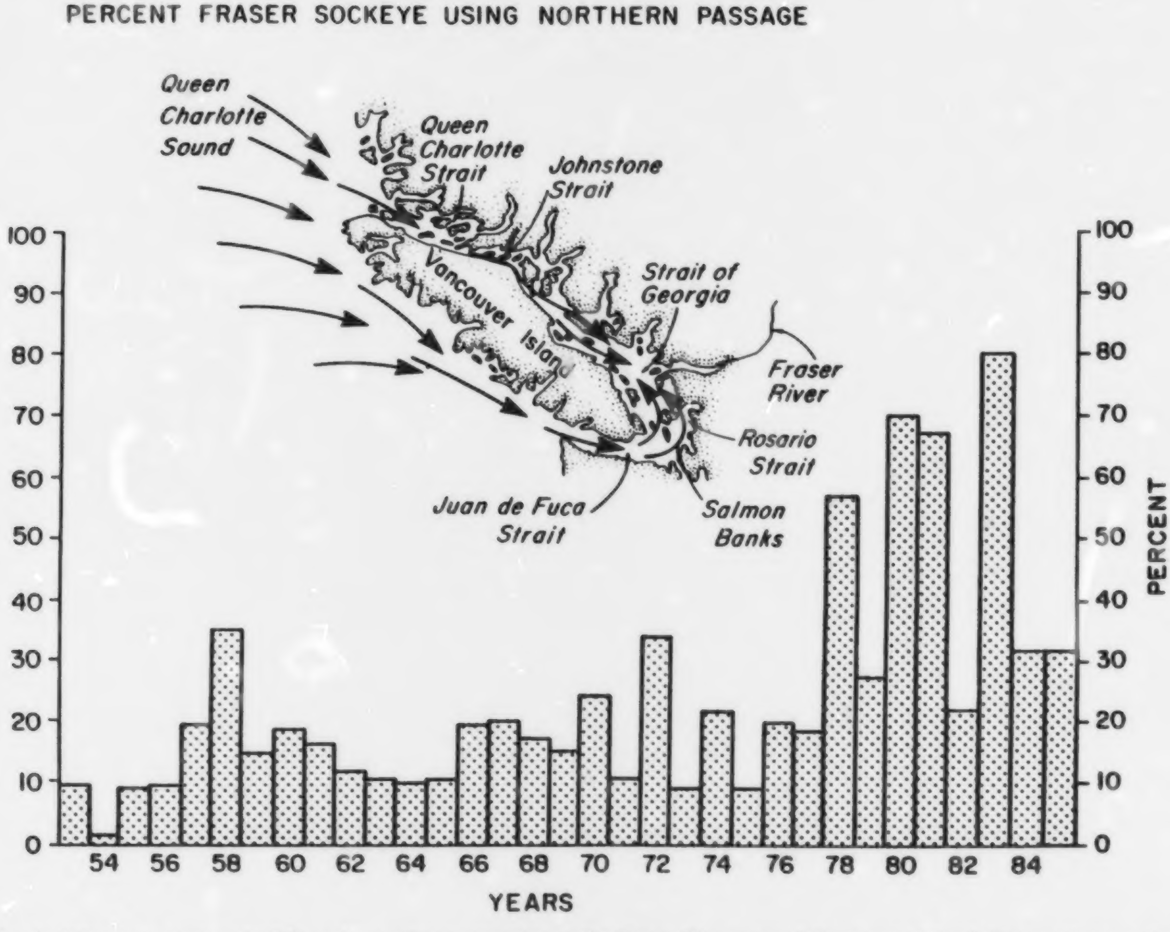

FIG. 1. Migratory routes of adult sockeye salmon returning to the Fraser River around Vancouver Island. The northern route is via Johnstone Strait, while the southern route is via the Juan de Fuca Strait. The bar graph indicates the proportion of the total run that was estimated to have used the northern route. (Reproduced from Groot and Quinn, 1987).

(1987), used multiple regression and correlation between the diversion rate and *coastal* physical variables (river runoff, sea surface temperature and sea level). Recently, Blackbourn (1987) found a correlation between return timing of the sockeye and the sea surface temperature in the Gulf of Alaska — thereby establishing the first solid link between *open ocean* variability and sockeye migration. Unfortunately, the variability in the vast interior of the ocean is in general poorly known. Relevant questions — such as what the strength of the Alaskan gyre was in a particular year, where the gyre was located exactly, what the currents were like and where the upwelling regions were — could neither be answered nor their possible influence on the sockeye migration taken into account. With a numerical ocean model, these effects can be addressed, and upon combining the numerically computed oceanic variability with the observed coastal variability by a statistical method, we may be able to improve the prediction of the salmon return route.

The development of an accurate ocean model is a lengthy process. The model presented here is an improved version of the earlier model by Hsieh (1987). We have modelled the seasonal cycle in the northeast Pacific Ocean as a prelude to modelling the interannual variability, which we hope to present in later publications.

This paper is organized as follows: Section 2 describes the setting up of the model, while Sections 3 to 5 show the model results for the circulation, the temperature and the upwelling fields, respectively. Section 6 discusses how the model can be applied in the future to predict the sockeye return route.

2. The Model

The Cox (1984) version of the GFDL Bryan-Cox 3-dimensional primitive equation ocean model is used. The model extends from 157°E to 124°W, and from 16°N to 60°N (Fig. 2), with solid, no-slip walls all around. There are 5 vertical levels centred at 10, 60, 200, 800, and 3000 m. The horizontal grid spacing is 1° latitude by 1° longitude from 40°N to 60°N. South of 40°N, the north-south grid spacing gradually broadens to 2° latitude at the southern boundary. The east-west extent of the model is not wide enough to allow the model to follow the actual coastline (Fig. 2) in the western and the southeastern parts of the model. This limitation and the coarser resolution in the southern part of the model were adopted for economic reasons and for the fact that we are primarily interested in the higher latitude eastern Pacific region.

The bottom topography was approximated by steps in the Cox (1984) model. In our 5-level model, the depth of the ocean bottom must take on one of the following discrete values: 20, 100, 300, 1300, or 4700 m. This leads to an essentially flat-bottomed ocean except for the continental margins.

Despite the departure of the model coastline from the real eastern boundary south of about 40°N, a continental shelf representative of the area is placed along the eastern boundary of the model south of 40°N to allow the poleward propagation of coastal trapped waves. These waves are nevertheless distorted by the relatively coarse grid resolution (Hsieh et al. 1983).

In our coarse resolution model, we could not accurately represent the small Aleutian Islands and hence the water exchange between the Bering Sea and the North Pacific. As the large depth change between the Pacific and the shallow Bering Sea would permit the propagation of fast topographic waves (Hsieh 1987), filling the Bering Sea with land allowed us to eliminate these fast waves and to significantly increase our timestep to 4320 seconds.

The eddy viscosities in the horizontal and vertical directions are 5 × 10^3 and $10^{-4} m^2 s^{-1}$, respectively, while the eddy diffusivities in the two directions are 2 × 10^3 and $10^{-4} m^2 s^{-1}$, respectively. The horizontal eddy viscosity was chosen satisfying the stability requirement of Bryan et al. (1975, Fig. 1). In the southern part of the ocean, as the north-south grid spacing broadens, the horizontal eddy viscosity is increased linearly with the north-south spacing.

From the COADS data set compiled by the National Center for Atmospheric Research, Boulder, Colorado,

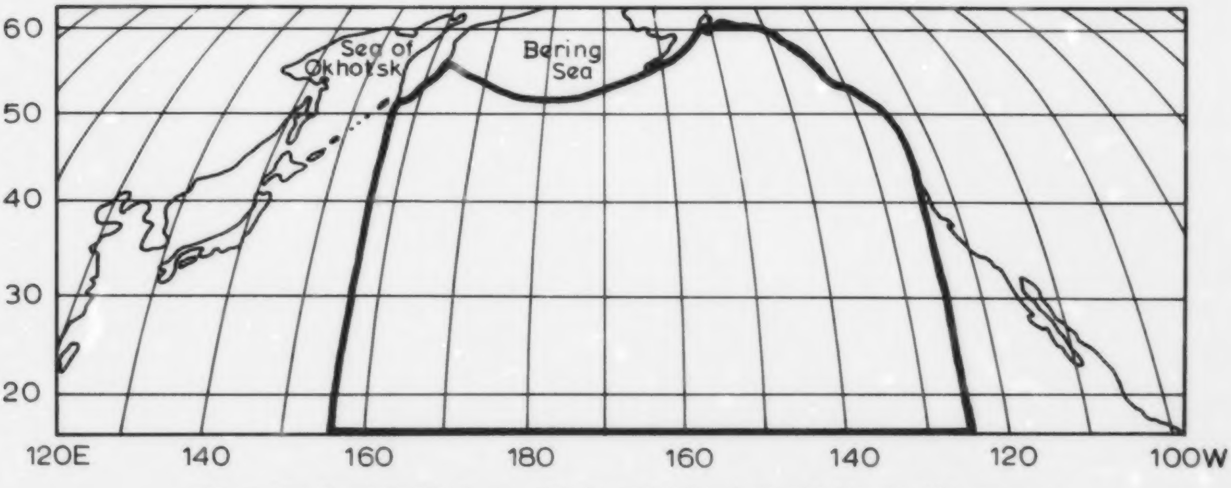

FIG. 2. The North Pacific Ocean, with the model domain bounded by the thick curve.

we computed the climatological monthly windstress using a drag coefficient of 1.2×10^{-3} (Large and Pond 1981), and the climatological monthly air temperature T_{air}. Surface heat flux Q was then imposed by specifying the air temperature and using the Haney (1971, Eq. 34) formula

$$(1) \quad Q = \text{const.}\ (T^{*}_{air} - T_{sea\ surface}),$$

where the "const." is latitude dependent (Haney, Fig. 9), T^{*}_{air} is an apparent air temperature related to T_{air} by Haney (Eq. 35), and in practice, the temperature at level 1 (10 m depth) was used in place of the sea surface temperature $T_{sea\ surface}$.

Observed temperature and salinity data from Emery and Dewar (1982) were used to initialize the model for the five levels. At the deepest level, due to sparse data, a horizontally averaged constant value was used. The model was then spun up from rest with the climatological monthly windstress and surface heat flux forcing. Due to the lack of surface salt flux data, the salinity at the top level was held constant with time. No heat or salt fluxes were allowed through the side boundaries.

3. The Circulation

After 18 years of spin-up, the model has reached quasi-equilibrium. Figure 3 shows the depth-integratred (barotropic) transport streamfunction in February, April, June, August, October, and December of the 19th year. In February (Fig. 3a), the western boundary currents for the subtropical and subarctic gyres have transports of 47 and 28 Sv, respectively (1 Sv = $10^6 m^3/s$). The subarctic gyre is actually composed of the Alaskan gyre to the east and the Oyashio gyre to the west. During spring and summer, the subarctic gyre weakens drastically and recedes northward, so that by July, the Alaskan and Oyashio gyres become separate (Fig. 3d). During autumn (Fig. 3e), the Alaskan gyre builds up first and pushes its way westward, with the western edge of the gyre propagating westward at a speed of 0.45 m/s. It connects with the Oyashio gyre to form a large subarctic gyre by November. From December (Fig. 3f) to February (Fig. 3a), the Oyashio gyre continues to grow and extend southward, while the Alaskan gyre has already begun to weaken. The streamfunction does tend to follow the wind pattern at these latitudes (not shown), which strengthens over the eastern part of the ocean during autumn, then intensifies over the western part during winter, simultaneous with a slow decline over the eastern part.

Figure 4, which gives the velocity fields at level 2 (60 m depth) from 40°N to 60°N for February and August, shows significant decrease in the strength of the currents from winter to summer. The level 1 (10 m depth) currents (not shown) are quite different from those of level 2 due to the Ekman spiralling effect.

An explanation as to why the seasonal variation in the barotropic transport is so large in the subarctic gyre — for instance the transport in the Gulf of Alaska varies from a low of 3 Sv in July to a high of 17 Sv in November — but not in the subtropical gyre can perhaps be given in terms of Rossby wave dynamics. Anderson and Gill (1975) demonstrated the important role of Rossby waves in the ocean's adjustment to a change in the wind forcing. From the familiar Rossby wave dispersion relation on a β-plane (LeBlond and Mysak 1978, p. 154), one can show that for a given frequency and a particular Rossby mode, there is a critical latitude poleward of which free Rossby waves cannot exist. At the annual period, none of the baroclinic (i.e. internal) Rossby modes can exist north of about 40°. Thus, while the barotropic Rossby mode can exist in both the subtropical and the subarctic gyres at the annual period, the baroclinic modes can only exist in the subtropical gyre. This leads to the fundamentally different ways the two gyres respond to the annual period forcing — the subarctic gyre responds predominantly barotropically while the subtropical gyre responds with a much stronger baroclinic component. Hence in Fig. 3, we found large annual variations in the barotropic streamfunction in the subarctic gyre region but not in the subtropical gyre. At lower frequencies, e.g., interannual variation in the model forcing — the subject of our next paper — the baroclinic response in the subarctic gyre may be much stronger.

A second explanation for the strong barotropic response is the weaker stratification at higher latitudes, which can decrease the baroclinic response, as observed in the model of Cox and Bryan (1984). In their steady-state solution to steady wind forcing, the previous mechanism involving Rossby waves does not apply.

Next, we try to compare some of our model values with observed values. Using 1000 m as the reference depth, Tabata (1983, Fig. 3a) estimated from hydrographic data the baroclinic transport across Line P (section between Station P at 50°N, 145°W and the southern coast of British Columbia) to be about 5Sv northward, with most of the data values lying between 3 and 7 Sv. From our model results, we calculated the corresponding baroclinic transport with respect to the 1000 m depth to be 2.6 Sv northward in February and 0.5 Sv northward in August. These values are lower than those from Tabata, presumably due to the fact velocity values in a viscous numerical model are generally lower than those in the real ocean. For comparison, the model barotropic transport across Line P from Fig. 3 varies from 4 Sv southward in August to a peak of 8 Sv northward in November — a variation of 12 Sv which is much larger than the variation of the baroclinic transport, as expected.

4. Temperature

Figure 5a shows the February sea surface temperature from the model (actually at 10 m depth). In the Alaskan gyre region, the model temperature is 2–3°C above the observed SST from the COADS data set (not shown), whereas in the Oyashio gyre region, the discrepancy increases to 3–4°C. In the subtropical gyre, the model SST agrees well with the data in the eastern Pacific, but is again 3–4°C too warm near the western boundary. The poorer performance on the western half is expected, since we have neglected the water exchange with the Bering Sea and the Sea of Okhotsk (Fig. 2), and the western

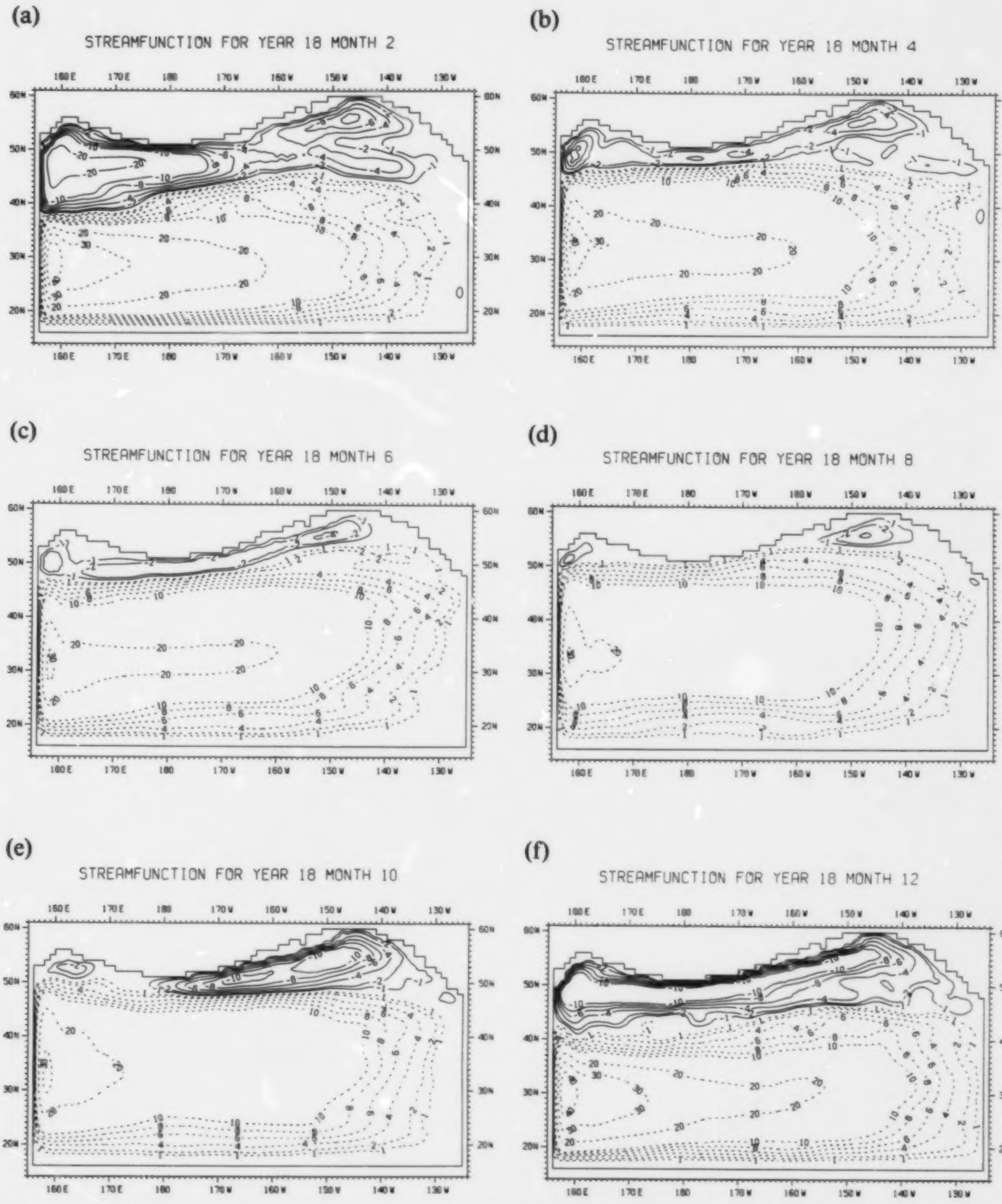
(a)
STREAMFUNCTION FOR YEAR 18 MONTH 2
(b)
STREAMFUNCTION FOR YEAR 18 MONTH 4
(c)
STREAMFUNCTION FOR YEAR 18 MONTH 6
(d)
STREAMFUNCTION FOR YEAR 18 MONTH 8
(e)
STREAMFUNCTION FOR YEAR 18 MONTH 10
(f)
STREAMFUNCTION FOR YEAR 18 MONTH 12
160E
170E
180
170W
160W
150W
140W
130W
60N
50N
40N
30N
20N

FIG. 3. The depth-integrated transport streamfunction, after 18 years of spinup, plotted for (a) February, (b) April, (c) June, (d) August, (e) October and (f) December. Contours in units of Sv ($10^6 m^3/s$).

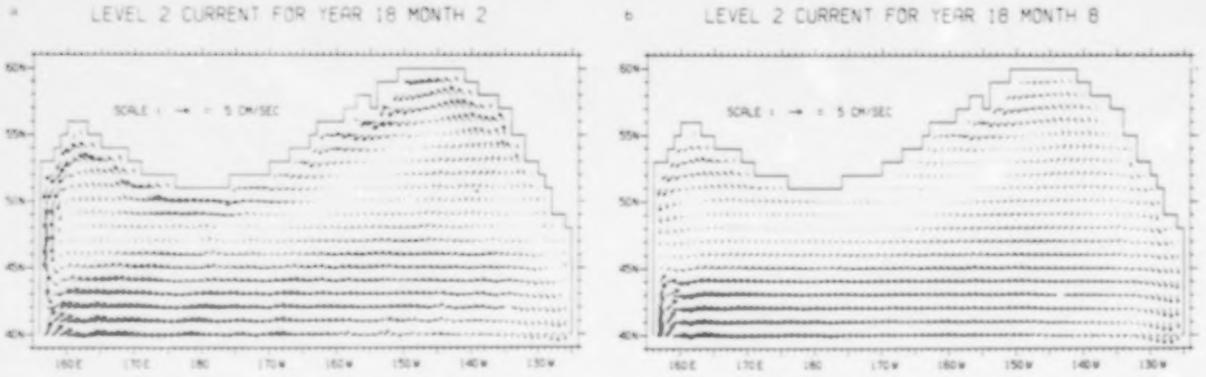

FIG. 4. Horizontal velocity field at level 2 (60 m depth) for (a) February and (b) August. The speed at a location is proportional to the length of the arrow. In places where the velocities exceed 5 cm/s, additional segments are plotted along the stem of the arrows, yielding wider arrows.

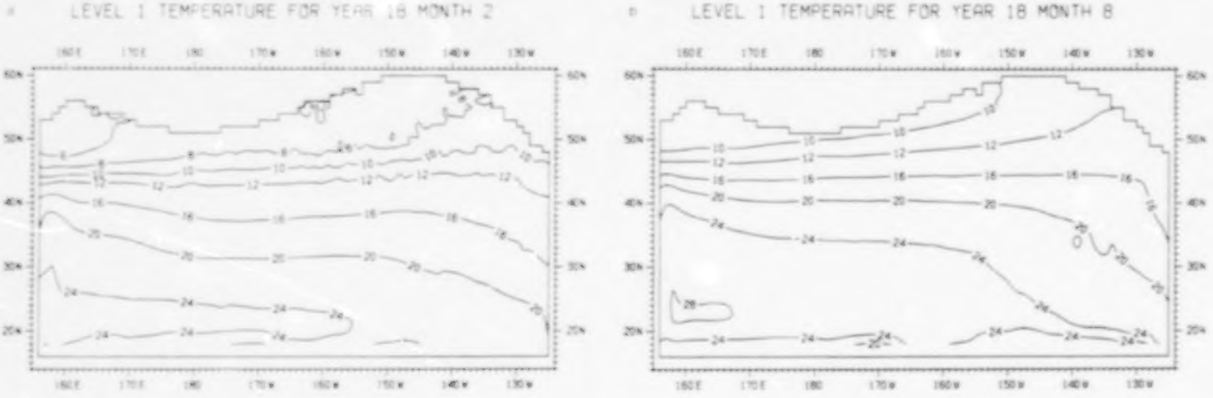

FIG. 5. Model sea surface temperature for (a) February and (b) August. Contours in °C.

boundary has been placed much further east than the real boundary. The artificial southern wall introduces upwelling and cooler temperature near the southern boundary, as seen in Fig. 5a.

Figure 5b illustrates the model SST for the month of August. The subarctic gyre region of the model is generally 1-2°C too cool compared to the observed data. Further south, the model temperature patterns are in agreement with the data except near the artificial southern boundary where unrealistic upwelling is again evident.

5. Upwelling

Figures 6a and b show the vertical velocity component at 20 m depth for the months of February and August, respectively, from the model. In February, there is general upwelling in the subarctic gyre and downwelling in the subtropical gyre, arising from the respective divergence and convergence of the surface Ekman transport in the two gyres. Upwelling near the artificial southern wall is also evident.

In August, the subarctic gyre has receded northward (Fig. 3d) while the corresponding upwelling region has shrunk considerably (Fig. 6b). This northward recession of the upwelling region may cause the northward migration of sockeye salmon during summer as mentioned by Groot and Quinn (1987). The Alaskan Stream flowing along the Aleutian Island Chain remains an upwelling region. Upwelling is also found along the eastern, western and southern boundaries.

6. Summary and Discussion

A numerical model for the northeast Pacific Ocean has been developed to study the seasonal and interannual variability. So far, the seasonal response has been examined, which reveals a large variation in the barotropic transport streamfunction in the subarctic gyre. During spring and summer, the subarctic gyre weakens and recedes northward, with its two components, the Alaskan gyre to the east and the Oyashio gyre to the west, becoming separate. During autumn, the Alaskan gyre begins to strengthen and extend westward, connecting with the Oyashio gyre by November. From December to February, the Oyashio gyre continues to grow while the Alaskan gyre has already begun a slow decline.

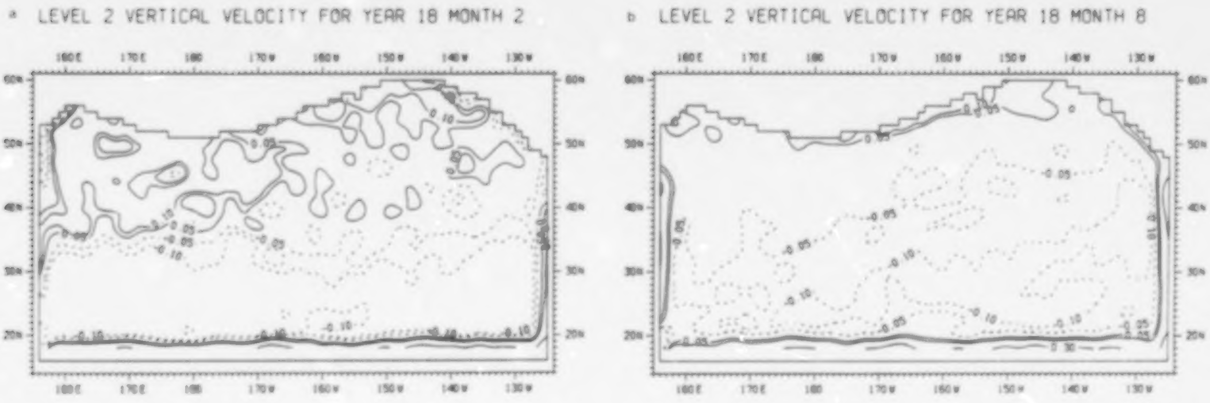
a LEVEL 2 VERTICAL VELOCITY FOR YEAR 18 MONTH 2
b LEVEL 2 VERTICAL VELOCITY FOR YEAR 18 MONTH 8
160E
170E
180
170W
160W
150W
140W
130W
60N
50N
40N
30N
20N
0.10
-0.05
-0.10
0
-0.05
0.05

FIG. 6. Vertical velocity at 20 m depth for (a) February and (b) August, with solid contours for upwelling regions and dashed contours for downwelling. Units in 10^{-3}cm/s. Data have been slightly smoothed.

The large seasonal variation in the barotropic transport may be due to inadequate bottom topography in the model. With only 5 vertical levels, the model ocean has essentially a flat bottom except near the continental margins. P. Cummins (Inst. of Ocean Sciences, Sidney, B.C., Canada V6T 1W5, pers. comm.) tested a 3-layer quasi-geostrophic model with and without bottom topography. He found much bigger variations of the seasonal barotropic transport in the absence of bottom topography.

The seasonal sea surface temperature variation in the model is small, being 2-3°C too warm in winter and 1-2°C too cool in summer. With only 5 vertical levels and without wind mixing, the model was inadequate for properly simulating the mixed-layer.

We have recently finished simulating the interannual variability by driving the model with monthly windstress and surface heat flux data from 1955 to 1979. We then further drove the model with the original climatological seasonal forcing for another ten years to verify that the model had not drifted significantly due to our relatively short spin-up. Though it remains to be seen how successful the model will be in simulating the interannual variability of the Northeast Pacific, it is worthwhile discussing how such a model could be deployed for the prediction of the Fraser River sockeye return routes.

With an accurate model, we have much more information on the ocean behaviour in a given year — where the gyre is located, what the strength of the gyre is, where the upwelling regions are, what the temperature and the currents are in the ocean — factors which may have an influence on the sockeye migration routes but are at present inaccessible. Prediction studies such as Wickett (1977) could only make use of coastal sea level and temperature to predict the return routes. By combining the model output and the observed coastal data from late spring, we may be able to predict with much improved accuracy the Fraser River sockeye return routes in summer with a multiple regression technique.

Acknowledgements

We are indebted to K. Bryan and M.D. Cox for kindly providing us their GFDL ocean model together with many helpful suggestions. We thank Anthony Weaver for producing the computer plots, and L.A. Mysak for his support and comments. This work was supported by the NSERC strategic grant awarded to L.A. Mysak, K. Hamilton, C. Groot, and W. Hsieh, and the NSERC operating grant and the Canadian Fisheries and Oceans subvention to W. Hsieh.

References

ANDERSON, D. L. T. AND A. E. GILL. 1975. Spin-up of a stratified ocean, with applications to upwelling. Deep-Sea Res. 22: 583-596.

BLACKBOURN, D. J. 1987. Sea surface temperature and the pre-season prediction of return timing in Fraser river sockeye salmon (*Oncorhynchus nerka*), p. 296-306. *In* H. D. Smith, L. Margolis, and C. C. Wood [ed.] Sockeye salmon (*Oncorhynchus nerka*) population biology and future management. Canadian Special Pub. Fish. Aquat. Sci. 96.

BRYAN, K., S. MANABE, AND R. C. PACANOWSKI. 1975. A global ocean-atmosphere climate model. Part II. The ocean circulation. J. Phys. Oceanogr. 5: 30-46.

COX, M. D. 1984. A primitive equation 3-dimensional model of the ocean. GFDL Ocean Group Technical Report No. 1, GFDL, Princeton Univervity.

COX, M. D., AND K. BRIAN. 1984. A numerical model of the ventilated thermocline. J. Phys. Oceanogr. 14: 674-687.

EMERY, W. J., AND J. S. DEWAR. 1982. Mean temperature-salinity, salinity-depth and temperature-depth curves for the North Atlantic and the North Pacific. Prog. Oceanog. 11: 219-305.

GROOT, C., AND T. P. QUINN. 1987. Homing migration of sockeye salmon to the Fraser River. Fish. Bull. 85: 455-469.

HANEY, R. L. 1971. Surface thermal boundary condition for ocean circulation models. J. Phys. Oceanogr. 1: 241-248.

HSIEH, W. W. 1987. A numerical study of the seasonal cycle in the northeast Pacific Ocean as driven by the windstress and surface heat flux. Atmos.-Ocean 25: 375-386.

HSIEH, W.W., M. K. DAVEY, AND R. C. WAJSOWICZ. 1983. The free Kelvin wave in finite-difference numerical models. J. Phys. Oceanogr. 13: 1383-1397.

LARGE, W. G., AND S. POND. Open ocean momentum flux measurements in moderate to strong wind. J. Phys. Oceanogr. 11: 324-336.

LEBLOND, P. M., AND L. A. MYSAK. 1978. Waves in the ocean. Elsevier. 602 p.

MYSAK, L. A. 1986. El Niño, interannual variability and fisheries in the northeast Pacific Ocean. Can. J. Fish. Aquat. Sci. 42: 464–497.

MYSAK, L. A., C. GROOT, AND K. HAMILTON. 1986. A study of climate and fisheries: interannual variability of the northeast Pacific Ocean and its influence on homing migration routes of sockeye salmon. Climatol. Bull. 20: 26–35.

RAMAGE, C. S. 1986. El Niño. Sci. Am. 254(6): 76–83.

TABATA, S. 1983. Interannual variability in the abiotic environment of the Bearing Sea and the Gulf of Alaska, p. 139–145. *In* W. S. Wooster [ed.], From Year to Year, Interannual Variatility of the Environment and Fisheries of the Gulf of Alaska and the Eastern Bering Sea, Washington Sea Grant Program, Univ. of Washington, Seattle, WA.

WICKETT, W. P. 1977. Relationship of coastal oceanographic factors to the migration of Fraser River sockeye salmon (*Oncorhynchus nerka*). International Council for the Exploration of the Sea. CM 1977/M 26: 18 p.

Comparisons of Time Scales for Biomass Transfer up the Marine Food Web and Coastal Transport Processes

K. L. Denman, H. J. Freeland, and D. L. Mackas

Department of Fisheries and Oceans, Institute of Ocean Sciences,
P.O. Box 6000, Sidney, B.C. V8L 4B2

Abstract

Denman, K. L., H. J. Freeland, and D. L. Mackas. 1989. Comparisons of time scales for biomass transfer up the marine food web and coastal transport processes, p. 255–264. *In* R. J. Beamish and G. A. McFarlane [ed.] Effects of ocean variability on recruitment and an evaluation of parameters used in stock assessment models. Can. Spec. Publ. Fish. Aquat. Sci. 108.

Oceanic variability can affect commercial fish species either directly (e.g., tolerance to temperature or oxygen anomalies) or by propagation through the food web. For the latter pathway, a simple model based on allometric relationships describes the size distribution of marine organisms and the propagation of disturbances (transient peaks or minima in biomass within a size-class) through the size distribution from small to large organisms. We use the model to obtain time scale estimates for whole ecosystem fluxes (and perturbations), rather than relying on doubling times of individual types of organisms. We calculate time scales for transfer from primary producers to incorporation by small zooplankton (of weeks) and by large zooplankton and fish larvae (of several months). These time scales match the dominant time scale for variability of ocean currents over the continental shelf off British Columbia (10–50 days). Eddy or gyral circulations can retain organisms and extend the periods of contact between predators and their prey, whereas upwelling jets transport and disperse organisms (especially the smaller ones) away from their point of origin. Local (or distant) environmental variability may therefore affect distant (or local) populations of predators. Appropriately averaged long-term temperature data from coastal lighthouses show El Niño and climatic signals, but only some commercial fisheries stocks have comparable data sets.

Résumé

Denman, K. L., H. J. Freeland, and D. L. Mackas. 1989. Comparisons of time scales for biomass transfer up the marine food web and coastal transport processes, p. 255–264. *In* R. J. Beamish and G. A. McFarlane [ed.] Effects of ocean variability on recruitment and an evaluation of parameters used in stock assessment models. Can. Spec. Publ. Fish. Aquat. Sci. 108.

Les espèces commerciales de poissons peuvent subir les effets de la variabilité des océans de façon directe (en ce qui a trait, par exemple, à la tolérance à la température ou à l'apport en oxygène) ou indirectement par la propagation de cette variabilité dans le réseau tropique. Un modèle simple de ces effets indirects fondé sur les relations allométriques décrit la distribution par taille des organismes marins et la propagation des perturbations (sommets et minima transitoires en ce qui a trait à la quantité de biomasse à l'intérieur d'une catégorie de taille donnée) indiquée par la distribution par taille des organismes, distribution allant des petits aux gros organismes. Nous utilisons ce modèle pour obtenir des estimations d'échelles de temps pour l'ensemble des flux (et des perturbations) de l'écosystème, au lieu d'utiliser les temps de doublement de type particulier d'organismes. Nous calculons les échelles de temps relatives à l'incorporation de la biomasse à partir des producteurs primaires jusqu'au petit zooplancton (en termes de semaines), puis par le zooplancton de grande taille et les larves de poissons (en termes de plusieurs mois). Ces échelles de temps correspondent à l'échelle de temps dominante relative à la variabilité des courants marins sur le plateau continental au large de la Colombie-Britannique (10–50 jours). Les mouvements turbulents ou tourbillonnaires des eaux peuvent retenir les organismes et augmenter la durée de la période de contact entre les prédateurs et leurs proies, tandis que les jets de remontée transportent et dispersent les organismes (en particulier les plus petits) loin de leur point d'origine. La variabilité environnementale locale (ou éloignée) peut donc avoir un effet sur les populations éloignées (ou locales) de prédateurs. Des données de températures provenant de phares côtiers prises sur une longue période et dont les moyennes ont été calculées de façon appropriée permettent d'identifier des signaux climatiques et signalent la présence du El Niño, mais seulement certains stocks de pêches commerciaux disposent de données de cette sorte.

Introduction

The evaluation of "Effects of ocean variability on recruitment" presents a major challenge in both its scope and its complexity. Ocean variability encompasses roughly 10 orders of magnitude (decades) in both time (1s to 300 years) and space (1 mm to 10^4 km). Clearly, any study linking ocean variability to recruitment must focus on some range of scales (in time and space) over which variability in certain oceanic processes is transmitted to specific organisms. This statement implicitly assumes the underlying premise of this paper — that fluctuations in the ocean environment are not likely to affect fisheries recruitment unless they operate, either explicitly or in some integrated or average manner, over a sensitive range of time and space scales for the biological process under investigation. For example, a single sunny, calm day would not likely cause a bloom in a red tide organism, but 2 weeks of successive sunny, calm days very well could, if other necessary conditions had been met. We have examined the effects of physical processes on planktonic organisms by matching processes with common scales (Denman and Powell 1984; Mackas et al. 1985). We take a similar approach here but extend the examination to include the scales (in time) of ecosystem transfer from the primary producers to the (large) top predators in the system.

There are numerous examples of fish abundance or catch being correlated with some oceanographic variable, often temperature (e.g., Cushing 1982). Correlations do not confirm cause and effect. In fact commonly used indicators such as temperature may only be "proxy" variables which themselves are correlated with a common causative process, but which are used because they are the only available data (e.g., Southward 1980). Even if we have identified the causative variable, the effect on recruitment could be either *direct*, or *indirect* through a series of predator–prey linkages that form a marine food web. The evidence for direct action by physical variability on the health or survival of adult fishes is not convincing. For example, from 25 years of observations ($n = 3766$) at Ocean Station P, the largest deviation of a single reading in 10 m temperature from the monthly mean was 2.9°C (Tabata and Peart 1985). It is unlikely that even several months of such anomalous temperatures could directly affect the health and subsequent survival of adult fish to produce the large deviations seen in recruitment into the commercial fisheries, although such conditions could affect migration patterns and selection of spawning sites.

Here we will examine one plausible indirect linkage between ocean variability and recruitment: that of a disturbance (or series of disturbances) in primary production, initially forced by oceanic events or processes, which subsequently propagates up the marine food web eventually to harvestable fish (or other large predators). Such a disturbance can either be a variation in biomass amount or (although not considered here) it can be change in phasing or timing of a regular event (e.g., spring bloom) such that the transfer of biomass from prey to predator is significantly altered. First, we will describe an existing mathematical model for the marine food chain based on the biomass distributions of organisms of different sizes. We will use that model to calculate ecosystem (as opposed to organism) time scales for a disturbance in primary production to propagate (through grazing) up to various sizes of predators. We will then consider, qualitatively, the sensitivity of different portions of the biomass size distribution to different time scales and to periodic versus aperiodic environmental fluctuation. Next we will review evidence of variability in physical oceanographic processes on the British Columbia continental shelf. We will focus on advective features that occur over similar time scales to those estimated for ecosystem transfers, and that might be responsible for either retention or dispersal of planktonic organisms over the continental shelf, thereby either favoring or reducing the probability of efficient coupling with the higher predators. Finally, we will show that these event-scale processes can be integrated, both by our data averages and by the organisms, to produce anomalies on the interannual and short climatic time scales.

Time Scales for Ecosystem Mass Transfer

Model of Biomass Size Distribution

Increased use of automatic samplers in the ocean (e.g., particle counters and fluorometers) has stimulated a search for techniques to exploit data of biomass independent of its taxonomic identity. Sheldon et al. (1972, 1973) observed that averaged particle size distributions yielded rather smooth curves, leading them to postulate a flat distribution of organism abundances as a function of geometrically increasing size. Based on these ideas, Kerr (1974) and Sheldon et al. (1977) postulated food chain theories that incorporated size-scaled transfers between trophic levels. Dickie (1972), Fenchel (1974), and Banse (1976) had over the same period presented evidence that various metabolic rates obey allometric laws over a wide range of organism sizes. That is, the specific metabolic rate, $(dw/dt)/w$ follows a power law dependence on organism weight, w. If one can formulate both the trophic fluxes from smaller to larger organisms and the metabolic losses within a given size-class as functions of body weight, then by requiring flux continuity, i.e., conservation of energy transfer, one can produce a model for the abundance of organisms as a function of body weight without reference to trophic level. The model is shown schematically in Fig. 1. Platt and Denman (1977, 1978) developed such a simplified model which produced an exponential dependence for biomass density as a function of organism weight. This functional form yields straight lines when plotted on a log–log scale. Borgmann (1982) has also developed a similar class of models from a different set of assumptions. The model of Platt and Denman was generalized and extended by Silvert and Platt (1978) to include the propagation of a disturbance across the biomass spectrum. Silvert and Platt (1980) considered various nonlinear extensions of the model to include reproduction and explicit grazing on organisms of a given size by organisms of various other sizes. Such terms may have a diffusive effect such that a disturbance

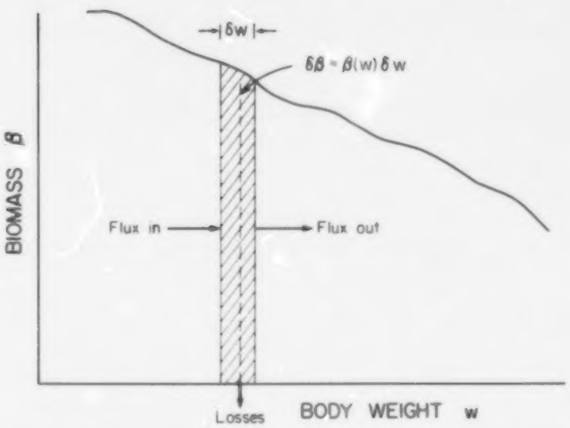

FIG. 1. A schematic showing the model of biomass as a function of body weight w. The biomass in any size interval is the amount such that the flux of biomass from smaller weights due to growth (and implicit grazing) equals the biomass flux to larger weights due to the same processes plus the metabolic loss by organisms within that size-class.

would not pass up the size distribution unchanged but would spread across a number of size-classes as it propagated to generally larger organisms, or they may provide a nonlinear feedback loop whereby a disturbance could grow or change its width and rate of propagation. Finally, the motivation and appropriateness of allometric-based models was reviewed by Platt (1985).

Data consistent with both the shape and slope of the biomass-size curve have been obtained in the pelagic central Pacific Ocean (Beers et al. 1975, 1982; Platt et al. 1984; Rodriguez and Mullin 1986). Data of Davis and Wiebe (1985) from a warm core ring show some seasonality in the size distribution of zooplankton alone. Sprules and Munawar (1986), comparing plankton size distributions from lakes with the data of Rodriguez and Mullin, obtained shallower slopes and more structure in the fitted curves for lakes, where large-scale equilibrium and uniformity are less likely to hold.

Estimate of Biomass Flux Rates and Transfer Time Scales

We apply a simplified model (that of Silvert and Platt 1978) to derive quantitative estimates of the time lag for propagation of a pulse in phytoplankton biomass to organisms (small and large zooplankton, juvenile and adult fish) of larger size. Their model, an extension of that developed by Platt and Denman (1977, 1978), does not explicitly contain many processes known to operate in marine ecosystems (e.g., reproduction and grazing). However, its simplicity allows us to estimate time scales for a disturbance generated in the phytoplankton biomass by ocean events to propagate up to various other sizes of organisms. The time scales obtained pertain to multiple ecosystem transfers rather than to simple turnover or doubling times for individual classes of organisms. We need to know these time scales in order to select from the 10-decade range of physical processes those that operate on time scales similar to those important to the pelagic ecosystem.

We define a biomass $\beta(w)$, normalized such that the total biomass per unit volume in some range of size (weight) classes w_0 to w_f is given as

$$\int_{w_o}^{w_f} \beta(w)dw$$

Then the generalized time dependent equation for conservation of biomass is given as (Silvert and Platt 1978)

$$(1) \qquad \frac{\partial \beta}{\partial t} + \frac{\partial\,(\beta g)}{\partial\, w} + \mu\beta = 0$$

where: $g(w)$ is a generalized growth function "such that energy concentrated in particles of size w at time t will appear in particles of size $w + g(w)dt$ at some later time $t + dt$, as a result both of growth of particles of size w and of predation by larger particles," and $\mu(w)$ is a metabolic energy *loss* rate for particles in the range of w to $w + dw$.

If we define a turnover time $T(w) = 1/g(w)$ and assume the allometric relations (Platt and Denman 1977)

$$(2) \qquad T(w) = Aw^{x-1}$$

and

$$(3) \qquad \mu(w) = \alpha w^{\gamma-1}$$

equation (1) can be solved for the steady state case $d\beta/dt = 0$, giving a solution of the form:

$$(4) \qquad \beta(w) = \beta_0 w^{x-1-\alpha A}$$

where A, x, α, and γ are all constants and the approximation $\gamma + x \approx 1$ has been used. Evidence supporting this approximation is discussed in Platt and Denman (1977, 1978). If the assumption is not made, a polynomial term is added to the function, and curved rather than straight line solutions result when plotted on log scales (Denman, in preparation). The integrations over w to reach (4) result in dimensionally inconsistent solutions, but if we form dimensionless weights w/w_0 and rewrite (2) and (3) with different (numerically) proportionality constants A and α, then dimensional consistency can be preserved (see Appendix in Platt and Denman 1977). However, to keep the familiar notation, we will retain the original equations.

Silvert and Platt (1978) showed that, in the solution to the time-dependent form of equation (1), a fluctuation or disturbance passes to larger organisms unmodified and that the time for it to pass from phytoplankton of weight w_o to be incorporated in another organism size category of weight w_f is

$$(5) \qquad t_f = \int_{w_o}^{w_f} T(w')dw'$$

We can solve this integral (which was not done by Silvert and Platt 1978) by substituting (2) into (5) giving (except in the trivial non-growth case $x = 0$)

$$t_f = \frac{A}{x}(w_f^x - w_o^x) \qquad (6)$$

Usually $w_f \gg w_o$, and we will be able to ignore the term w_o^x relative to w_f^x.

We show in Table 1 the time scales t_f for a pulse in phytoplankton biomass to reach organisms of various relevant weights. (Values for the constants were discussed in Platt and Denman 1977 and 1978, who relied heavily on data from Fenchel 1974). These numbers may seem somewhat large, especially for juvenile salmon (~ 270 d) and a 1 kg adult fish (~ 650 d). However, this time scale is for full assimilation and incorporation of the biomass into animals of that size. It is not the time at which organisms of a given size are first exposed to a fluctuation in their food supply, but rather it is the time after which they themselves present a fluctuation in biomass to their predators. In other words, fish that graze, e.g., adult euphausiids, might be expected to encounter elevated concentrations of euphausiids several months (~ 90 days) after the initial bloom or growth pulse in phytoplankton production.

The organism sizes and corresponding weights in Table 1 are representative of several major components of the ecosystem. This model of the pelagic ecosystem explicitly avoids the concept of tropic levels. Thus, the weight class that we have assigned to adult copepods would also include all other organisms of that weight: fish eggs and especially naupliar stages of euphausiids. Clearly then, a pulse in primary production would reach naupliar stages of euphausiids of the same size as adult copepods before it would reach the (larger) adult euphausiids.

The model used here is extremely simple. However, it has allowed us to calculate time scales for biomass transfer, and for the propagation of environmental disturbance, from the primary producers to larger predators of arbitrary size. Rather than estimating transfer rates from individual turnover or doubling times, equations (5) and (6) provide an ecosystem transfer timescale by integrating over a weight-dependent turnover time from the primary producers to a given predator. In the following section, we discuss ways in which the model could be elaborated to include important nonlinear biological processes and their interaction with environmental variability at various time scales. We believe that such additions would not significantly alter the propagation or transfer timescales, but we caution that nonlinear feedback (e.g., the larger organisms in the leading edge of a pulse grazing the smaller organisms in the trailing edge of a pulse) could generate unexpected behavior that could alter these transfer timescales (Silvert and Platt 1980).

Interaction with Environmental Variability

Sensitivity to Pulse Frequency and Duration

There is a theoretical (Levins 1969; May 1974; Roughgarden 1977) basis for concluding that all organisms have more difficulty exploiting a fluctuating resource than one that is stable in time (although some may gain an advantage over their competitors by being relatively less discomfited). At what time scales do environmental fluctuations have the strongest effect on the organisms? This will vary with organism size, and with both the predictability and the amplitude of the environmental fluctuation. The annual (seasonal) cycle is, in temperate and arctic latitudes, by far the strongest environmental signal. For organisms with short life spans and reproductive time scales (the smallest organisms by our allometric relation), the response to the annual signal is one of consistently positive or negative population growth over several generations. Large changes in population density (up to several orders of magnitude) can and do occur: notably for our purposes the annual spring plankton bloom observed in many regions. But there is not a strong annual peak in total biomass within a fish stock. Why and how does the annual signal get attenuated? First, as noted by Silvert and Platt (1980), nonlinear interactions between and within segments of the biomass size distribution tend to spread a perturbation (across size-classes and in duration) as it progresses up the biomass distribution to larger

TABLE 1. Estimated time for a fluctuation in phytoplankton biomass to propagate to and be incorporated by an organism of a larger size. Equation (6) has been used with the values $x = 0.25$ and $A = 2.5 \times 10^6$s. We assume a phytoplankton weighs 10^{-8}g and all organisms have a wet weight specific density of 1.

Organism	Shape and dimensions	Weight of an individual (g)	Time (d)
Phytoplankton	Equivalent spherical diameter 25 m	10^{-8}	—
Copepod	Cylinder length 3 m diameter 1 mm	2.5×10^{-3}	25
Euphausiid/ fish larva	Cylinder length 2 cm and diameter 0.5 cm	0.4	90
Juvenile salmon	Cylinder length 10 cm and diameter 2 cm	30	270
Small adult fish	Length 50 cm	10^3	650

organisms. "Short" environmental events thereby become more prolonged and gradual changes in the biomass of the larger organisms result. As an example, consider that turnover or doubling times for phytoplankton are typically days (e.g., Eppley 1972; Harris 1986). A wind event of 1–3 days' duration that mixes nutrients into the euphotic zone can be sufficient to trigger a fluctuation in phytoplankton biomass. As the fluctuation propagates up the size distribution, it would spread out among a range of sizes and organisms such that it would have a reduced magnitude in any one size-class and its effect would be spread over a longer time interval. Thus, a series of wind events over a whole season would show up as a single integrated fluctuation in the biomass of larger organisms (as in the example of a year-class of northern anchovy being decimated by a series of storms dispersing the phytoplankton over such a broad layer as to reduce their concentration below levels required for efficient grazing (Lasker 1981; Wroblewski and Richman 1987)).

A perhaps more important mechanism for attenuation of environmental variability results from adaptive biological response (behavioral, or life history) to *predictable* components of environmental variability. The seasonal or annual cycle is large, but it happens every year in more or less similar amplitude and phasing (see Fig. 9, 10), and organisms have had literally geologic time scales over which to evolve strategies that minimize the annually recurrent stress. At least two frequencies of environmental variability (the day–night and seasonal cycles) are so strong and so predictable that even unicells have developed significant adaptive strategies (e.g., circadian physiological rhythms and seasonal resting spore production). An important precondition for these adaptive strategies to be effective is that the component of environmental variability they deal with *must* be predictable, either (or preferably both) in its timing and/or in the presence of detectable environmental precursors. It seems plausible that larger organisms such as fish, which have invested heavily in maintaining their adaptations to the predictable components of variability, may at the same time (and in consequence) be *less* able to deal with aperiodic, unpredictable components of variation such as El Niño events, where the biological response to relatively small amplitude interannual variations can be very large (e.g., fig. 1 in Barber and Chavez 1986). Such an amplification caused by feedback resonance is another possible nonlinear response discussed by Silvert and Platt (1980).

Reproductive Biomass Transfer — Bucking the Flow

When an organism reproduces sexually, it transfers "biomass" to a much smaller body size. This has interesting consequences when viewed from the perspective of propagation of environmental variability to a given species. By careful allocation of reproductive effort, a large organism can seed its offspring into the biomass distribution just ahead (in size) of a predictable peak in resource biomass (the annual biomass peak), and the offspring can "ride" this peak up through the distribution. The benefits of successful timing are obvious, the increased risks of poor timing (effectively the match-mismatch hypothesis of Cushing 1982) perhaps less so. Note that the duration of peak biomass is shorter for smaller body size. This means that the "target" period the parents are aiming for is also smaller. Larvae have relatively little metabolic reserve and a relatively fixed developmental calendar. As individuals (and collectively if spawned en masse), they cannot afford to wait for good times, and their response to near-term environment is either successful growth or die-off.

Dealing with Advective Displacement

Larger marine organisms tend to have considerable capability for directed motion, and hence potentially can avoid or possibly take advantage of fluctuations such as the eddies and jets to be described. Zooplankton are capable to a lesser degree of directed motion, the most obvious being diurnal vertical migration over hundreds of metres in a few hours. Interactions of vertical migration with recurring current patterns in the Oregon upwelling area are thought to be responsible for retention of zooplankton within the geographic area for periods long enough (about 25 days) for eggs to progress to adults capable of reproduction (Peterson et al. 1979; Wroblewski 1982). Rothlisberg et al. (1983) modelled the interaction of vertical migration of planktonic shrimp larvae with wind-forced and tidal currents in the Gulf of Carpentaria. Annually two periods of reproductive activity occur (March and May), but only during the latter period are tidal currents of the correct phase to interact with the vertical migration cycle to effect significant onshore transport allowing the post larvae access to their estuarine nursery grounds. Larger fish have the ability to swim faster than most ocean currents although currents associated with upwelling jets (of order 100 cm s^{-1}) and with tides would play a significant role in affecting fish movement and migration.

To summarize the ideas of this section, we present schematically in Fig. 2 the model curve for a fluctuation in

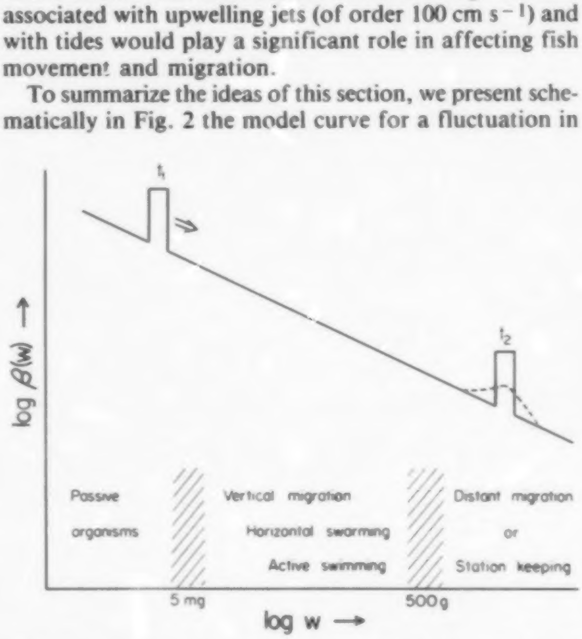

FIG. 2. Solution to the biomass size distribution model for a pulse originating in the phytoplankton (Silvert and Platt 1978). The dashed line shows how the pulse would spread out and decrease in amplitude for time $t_2 > t_1$. Along the bottom we have shown increasing capability for directed motion with increasing body weight.

the size distribution of organisms in the pelagic marine ecosystem along with a qualitative assessment of the boundaries between organisms that are passive, organisms that are potentially motile, and organisms that are active swimmers capable of directed long range migration.

Principal Modes of Variability Along the British Columbia Continental Margin

Coastal Eddies and Upwelling Jets

For a fluctuation in the ocean environment to affect the marine ecosystem via the food web, it (or a series of shorter fluctuations) must first be of sufficient duration to affect the primary production. Second, for a positive local effect on ecosystem production, the oceanic fluctuation should cause a retention of the prey and predators in the same area and at sufficient concentrations for significant biomass transfer to occur. Otherwise, the fluctuation, while producing a positive pulse in phytoplankton biomass, may actually decrease the transfer to larger organisms if it acts to disperse the planktonic organisms. In the same manner that biological processes such as reproduction and grazing spread a fluctuation across size categories and hence time, so also do motility and advection by water motions spread the pulse in space. The more a single fluctuation is dispersed in these three dimensions, as shown schematically in Fig. 3, the smaller will become its magnitude as it propagates to larger organisms.

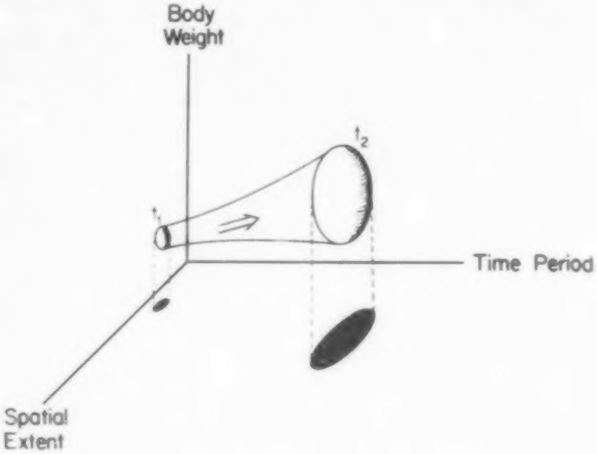

FIG. 3. Schematic showing how a narrow pulse at time t_1 has spread across more size intervals (and hence a larger time duration) by time t_2 due to the effects of grazing and reproduction. Dispersal by advective motions also causes a spread in spatial extent.

To illustrate how oceanic fluctuations can effect either retention or dispersal, we will consider now the time and space scales of the principal sources of advective variability over the continental shelf in light of the time scales for biomass transfer given in Table 1. In particular, we report on a recurring topographic eddy whose presence appears to increase the retention time for planktonic organisms, and on an offshore flowing upwelling jet whose presence removes planktonic organisms from continental shelf waters.

We have become concerned with the retention and dispersal capabilities of eddies and upwelling jets on the continental shelf off southern Vancouver Island because, although elevated primary production and phytoplankton standing stock are apparently sustained for several months each summer by a persistent gyre and upwelling-favorable winds (Denman et al. 1981; Freeland and Denman 1982), the standing stocks of zooplankton are lower than expected given the food availability levels (Mackas et al. unpublished data). Are the zooplankton not grazing the high phytoplankton standing crop, or is there a high zooplankton production rate that is being removed either by currents or by predation on the zooplankton themselves?

The dominant time scales of variability in ocean currents at the shelf edge off Vancouver Island are shown in Fig. 4, a kinetic energy spectrum of horizontal current measured by a current meter maintained at a depth of 50 m for almost 3 years, 1979–81 (Denman and Freeland 1985). The largest peak in the spectrum is, as expected, at the annual cycle. But there is also a broad maximum

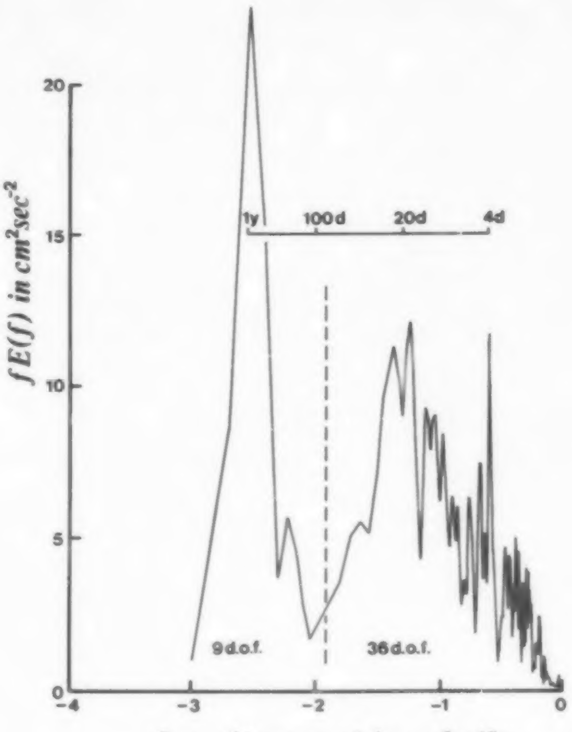

FIG. 4. Power spectrum for current speed at a depth of 50 m for a mooring deployed for almost 3 years off the coast of B.C. In this representation, area under the curve is proportional to kinetic energy at any frequency (from Denman and Freeland 1985).

between periods of about 50 days and 5 days, with a peak near 20 days. Because a power spectrum is based on sinusoids, the duration of energetic events will be of order 10 days (or half a sinusoid). Denman and Abbott (1988) found a similar time scale (about 7 days) for the decorrelation rate of near-surface phytoplankton pigment patterns, determined from cross-spectrum analysis of series of satellite images of ocean colour.

Freeland (1988) has reported on a 106-day time series of the eddy-like motion field from an array of 6 to 7 current meter moorings in the same area off Vancouver Island. In an objectively determined time series of stream function maps, the eddies appear to pass through the sampling area (and evolve in shape) every few days. In Fig. 5 we show maps for 2 days in 1985, one without an eddy and one when an eddy was clearly present. Freeland (1988) used the stream function field to model the motion of particles by seeding a "particle" at the center of the field each day and calculating its simulated trajectory until its range from the center exceeded 20 km. He referred to the time elapsed between seeding and exceeding a 20 km range, as the "exit time". In Fig. 6, we reproduce his plot of exit times as a function of Julian day 1985. Exit times are usually less than 3 days but several episodes show retention of 10 days or more. The shaded areas below the curve indicate days when an eddy was present (i.e., when a maximum or minimum in stream function occurred that day within the 20 km radius). Longer exit (or retention) times result from the presence of an eddy within the observing area. The overall statistics in Table 2 of retention times with and without eddies present also supports the idea that eddies would retain planktonic organisms in the local area. The largest retention times are shorter (by about a factor of 2) than the time estimate for biomass to be incorporated by copepods. However, termination of the simulations at 20 km range precludes the possibility of tracking particles that are retained in an eddy that is being advected horizontally.

The recent development of drifters, drogued to follow the flow in certain depth strata and tracked either by radio from ship or by satellite, is allowing us for the first time to resolve the highly variable near surface flow patterns. In 1986 and 1987 we used drifters to study a recurring upwelling jet. Deployment of the drifters was guided by satellite images of sea surface temperature patterns, which had been transmitted to the ship after preliminary analysis on shore. During northwesterly winds, the jet detaches from the coast at Brooks Peninsula on Vancouver Island (Fig. 7) and flows generally offshore. It contains cold salty nutrient-rich water, develops elevated phytoplankton pigment biomass, and advects properties, particles and passive organisms distances of order 100–200 km in the course of the 5- to 7-day periods that we have tracked it. Furthermore, from Fig. 7 we see that it tends to split, with one branch extending offshore and the other returning inshore and continuing southward along the 200 m depth contour. Currents in the jets are at least 20–50 cm s^{-1} as measured both from the drifter tracks and from the geostrophic current field. These speeds and distances for cohorent advective features are not an isolated case: drifters deployed in 1985 within the

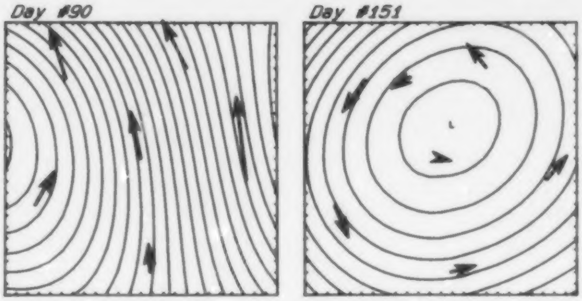

FIG. 5. Current fields in 1985 on Julian days 90 and 151, objectively mapped from time series of current moorings located at bases of the vectors (heavy arrows), off southwestern Vancouver Island. The left-hand panel represents a day when no eddy was present; the right-hand panel, a day when an eddy was present. The box is 24 km on a side.

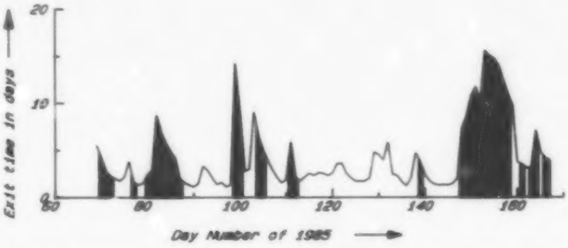

FIG. 6. Exit times for simulated particles to leave a 20 km radius circle centred on the array in Fig. 5. The particles were injected into the centre of the objectively analyzed flow field at noon each day. Shaded portions are for days when an eddy was present. (From Freeland 1988).

TABLE 2. Retention times (days) for simulated particles injected at noon each day in the centre of the objectively mapped current field shown in Fig. 5. The time is measured from injection until particle passes out of a 20 km circle.

Day of injection	Mean retention time (d)	Time for 50% of the particles to leave area (d)
All cases	4.21	2.76
Eddy present	6.88	5.71
No eddy present	2.61	2.16
Ratio of retention times	2.64	2.64

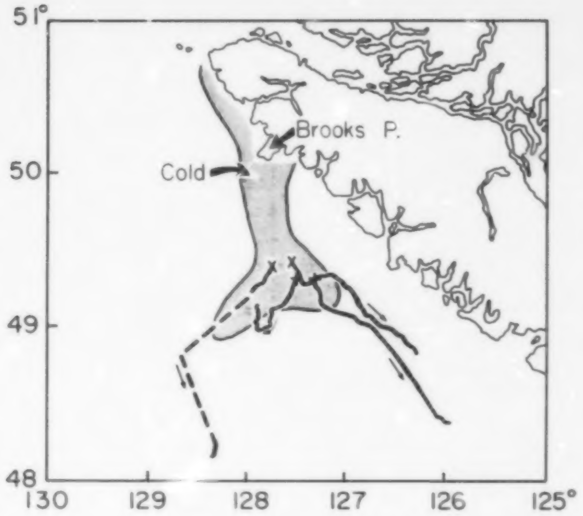

FIG. 7. Tracks of drogued drifters deployed in a cold offshore-flowing upwelling jet in August 1986 (7 days starting from x's) and July 1987 (5 days starting from +'s). Cold water region shown schematically.

array of Freeland (1988) also travelled similar distances at similar speeds (Emery et al. 1986).

Implications for the Pelagic Ecosystem

What can we conclude about the effects of spatially and temporally variable advection on the pelagic marine ecosystem? The current fluctuations on the B.C. continental shelf have time scales of order 10 days. Yet according to Table 1, biomass transfer from the phytoplankton will not have been incorporated by the small zooplankton (of order 1 mg body weight) within that time span. If a physical event is to propagate from the phytoplankton through the food web to the (large) terminal predators, we may have to search for the effect far beyond where the physical disturbance originated, and forward in time according to the estimates in Table 1. Or, conversely, if we are searching for the original causes of a fluctuation in fish biomass, we may have to search both widely in space and backwards in time. The exceptions are of course large scale disturbances, such as ocean climate changes, which are coherent over great distances.

Longer term Lagrangian measurements (following the flow) off B.C. also indicate that, despite mixing and exchange with offshore waters, continental shelf waters may in some sense be retained along the continental margin. In Fig. 8 we show the 90-day track of a drifter deployed in August 1986. It travelled from 49° 25′N down to 40°N and then back to 50° 30′N before grounding, a total distance of about 1000 km. Typical speeds were 10–20 km day^{-1} (10–20 cm s^{-1}). However, after 82 days, it passed within 30 km of its point of deployment. If such current patterns recur annually, then certain organisms may have evolved (or have been selected) to take advantage of a particular pattern or sequence of events. As an example, Cresswell and Golding (1980) observed large eddies off the coast of Western Australia which they hypothesized to be responsible for year-to-year variability in the success of settlement of the puerulus stage of a rock lobster on the inshore reefs. After hatching inshore, larvae of the rock lobster spend 9–11 months at sea before changing to the puerulus stage. Apparently, successful recruitment of a year-class to the inshore reefs requires the presence of large eddies to advect the animals back to the nearshore regions.

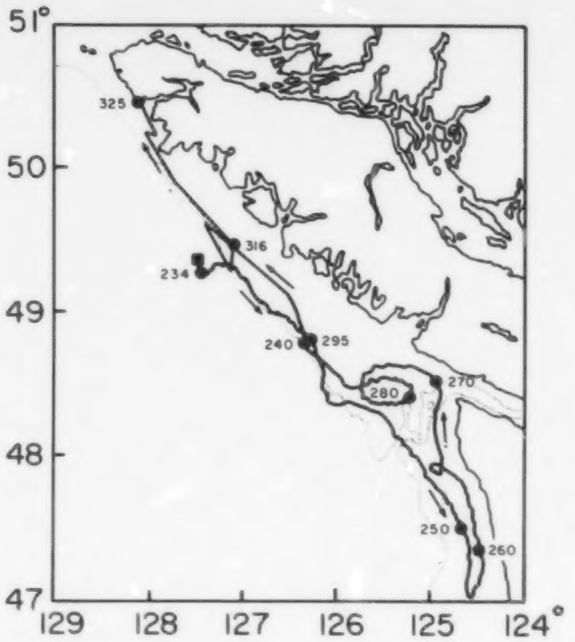

FIG. 8. Track of a drogued drifter for 90 days in 1986. Numbers adjacent to track denote Julian day. Drogue and position data supplied by P. Niiler. Positions were relayed several times a day by satellite.

Interannual and Climatic Variability

Interest in fisheries recruitment usually focuses on interannual to climatic (decades to centuries) time scales (e.g., Cushing 1982). The oceanic events we have presented occur on time scales comparable with time scales of transfer to the smaller zooplankton. We have hypothesized that the ecosystem must integrate or average over a sequence of such events for significant fluctuations on the time scales of the larger fish. However, the integration does not stop at annual time scales. Departures from average conditions (in sea surface temperature or elevation, for example) can persist for years and decades. In Fig. 9 and 10, we show sea surface temperature series derived from daily observations at a lighthouse on the west coast of Vancouver Island (latitude 48° 55′N). In Fig. 9, we have plotted the monthly averages (lower panel) and their departures from the long term mean annual cycle. The arrow shows the start, in about 1977, of a sustained period of warmer temperatures that correlates with other oceanographic variables in regional inshore waters. In Fig. 10, we plot on an expanded time axis the

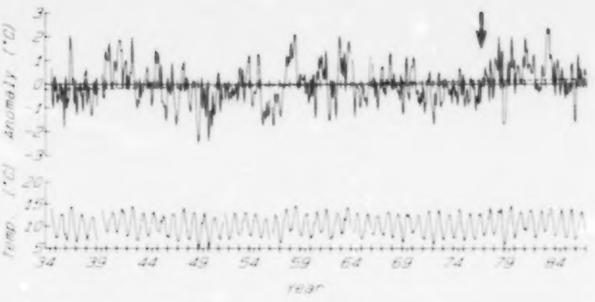

FIG. 9. Time series of monthly average sea surface temperature (lower panel) at Amphitrite Point lighthouse (48° 55′N; 125° 32′W) for the period 1934–86, and of the anomaly from the long-term monthly averages (upper panel). The arrow denotes the start of the recent warm anomaly.

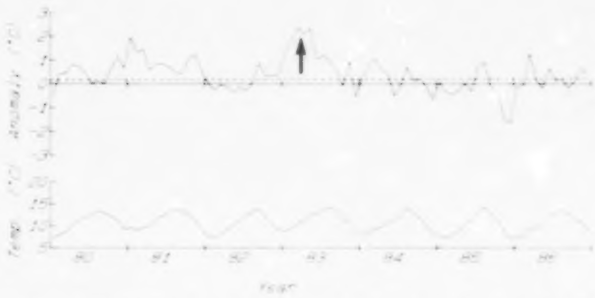

FIG. 10. Same as Fig. 9 but on an expanded scale for 1980–86. The arrow marks the peak anomaly for the 1982–83 El Niño event.

same data for the period 1980–86, showing the large year-long anomaly associated with the 1982–83 El Niño. Despite the striking nature of the eddies and jets described earlier, data that are frequent enough (days to weeks) to resolve these high frequency disturbances, when appropriately averaged, show clearly the interannual to decadal anomalies occurring in the oceanic environment. Unfortunately, although such long data sets do exist for some environmental variables (such as temperature) and for some harvested fishes (e.g., Hollowed et al. 1987), comparable data sets for variables describing the intermediate food web are rare.

Discussion

Our purpose was to examine how, and on what time scales, the interaction between ocean variability and pelagic continental shelf ecosystems is most likely to occur. To obtain time scales appropriate to whole ecosystem mass transfer, from the primary producers to predators of interest, we extended a model that treats biomass only, without attributing it to a species or even to a trophic level. Although the fishery is interested more in a specific type of fish, rather than in biomass, considering all organisms in a given size or weight interval equally is perhaps more analogous to towing a net of a certain mesh size: what is caught is determined (except for net avoidance) by size of organism, not by its taxonomic identity.

The model used here to obtain time scales for ecosystem transfer is obviously too simple to predict year-class strength in fish. However, such models offer an alternative to box models where animals must either shift from box to box, or their box must change its characteristics, as they progress through their life history stages. The challenge then is, through a series of ecosystem models of either type, but of increasing realism, to simulate and predict the passage of the whole spectrum of environmental disturbances through the ecosystem from phytoplankton to harvestable fish stocks. Without development of models based on causal processes, simple correlative predictions are bound to fail, especially when departure from normal conditions is largest and consequently our need for accurate prediction is greatest.

Acknowledgements

We thank P. P. Niiler for providing us with one of his satellite-tracked drifters and allowing us to publish the trajectory. We acknowledge constructive and helpful comments from L. A. Hobson, M. Mullin, T. R. Parsons, and T. Platt.

References

BANSE, K. 1976. Rates of growth, respiration and photosynthesis of unicellular algae as related to cell size — A review. J. Phycol. 12: 135–140.

BARBER, R. T., AND F. P. CHAVEZ. 1986. Ocean variability in relation to living resources during the 1982–83 El Niño. Nature 319: 279–285.

BEERS, J. R., F. M. H. REID, AND G. L. STEWART. 1975. Microplankton of the North Pacific Central Gyre. Population structure abundance, June 1973. Int. Rev. Gesamten Hydrobiol. 60: 607–638.

1982. Seasonal abundance of the microplankton population in the North Pacific Central gyre. Deep-Sea. Res. 29: 227–245.

BORGMANN, U. 1982. Particle-size conversion efficiency and total animal production in pelagic ecosystems. Can. J. Fish. Aquat. Sci. 39: 668–674.

CRESSWELL, G. R., AND T. J. GOLDING. 1980. Observations of a south-flowing current in the southeastern Indian Ocean. Deep-Sea Res. 27: 449–466.

CUSHING, D. T. 1982. Climate and fisheries. Academic Press, New York, N.Y. 373 p.

DAVIS, C.S., AND P. H. WIEBE. 1985. Macrozooplankton biomass in a warm-core Gulf Stream ring: Time series changes in size structure, taxonomic composition, and vertical distribution. J. Geophys. Res. 90: 8871-8884.

DENMAN, K. L., AND M. R. ABBOTT. 1988. Time evolution of surface chlorophyll patterns from cross spectrum analysis of satellite color images. J. Geophys. Res. 93: 6789–6798.

DENMAN, K. L., AND H. J. FREELAND. 1985. Correlation scales, objective mapping and a statistical test of geostrophy over the continental shelf. J. Mar. Res. 43: 517–539.

DENMAN, K. L., AND T. M. POWELL. 1984. Effects of physical processes on planktonic ecosystems in the coastal ocean. Oceanogr. Mar. Biol. Ann. Rev. 22: 125–168.

Denman, K. L., D. L. Mackas, H. J. Freeland, M. J. Austin, and S. H. Hill. 1981. Persistent upwelling and mesoscale zones of high productivity off the west coast of Vancouver Island, Canada. p. 514–521. *In* F. A. Richards [ed.] Coastal upwelling. American Geophysical Union, Washington, D.C.

Dickie, L. M. 1972. Food chains and fish production, p. 201–221. *In* Environmental conditions in the N.W. Atlantic. International Commission for the North West Atlantic Fisheries Spec. Publ. No. 8.

Emery, W. J., A. C. Thomas, M. J. Collins, W. R. Crawford, and D. L. Mackas. 1986. An objective method for computing advective surface velocities from sequential infrared satellite images. J. Geophys. Res. 91: 12865–12878.

Eppley, R. W. 1972. Temperature and phytoplankton growth in the sea. Fish. Bull. U.S. 70: 1063–1085.

Fenchel, T. 1974. Intrinsic rate of natural increase: The relationship with body size. Oecologia 14: 317–326.

Freeland, H. L. 1988. Lagrangian statistics on the Vancouver Island continental shelf. Atmosphere-Ocean 26: 267–281.

Freeland, H. J., and K. L. Denman. 1982. A topographically controlled upwelling center off southern Vancouver Island. J. Mar. Res. 40: 1069–1093.

Harris, G. P. 1986. Phytoplankton ecology. Chapman and Hall, London, 384 p.

Hollowed, A. B., K. M. Bailey, and W. S. Wooster. 1987. Patterns in recruitment of marine fishes in the northeast Pacific Ocean. Biol. Oceanogr. 5: 99–131.

Kerr, S. R. 1974. Theory of size distribution in ecological communities. J. Fish. Res. Board Can. 31: 1859–1862.

Lasker, R. 1981. Factors contributing to variable recruitment of the northern anchovy (*Engraulis mordax*) in the California Current: contrasting years, 1975 through 1978. Rapp. P.-V. Reun. Cons. Int. Explor. Mer 178: 375–388.

Levins, R. 1969. The effects of random variations of different types on population growth. Proc. Nat. Acad. Sci. 62: 1061–1065.

Mackas, D. L., K. L. Denman and M. R. Abbott. 1985. Plankton patchiness: biology in the physical vernacular. Bull. Mar. Sci. 37: 652–674.

May, R. W. 1974. Stability and complexity in model ecosystems. Princeton University Press, Princeton, NJ. 235 p.

Peterson, W.T., C.B. Miller, and A. Hutchinson. 1979. Zonation and maintenance of copepod populations in the Oregon upwelling zone. Deep-Sea Res. 26: 467–494.

Platt, T. 1985. Structure of the marine ecosystem: its allometric basis, p. 55–64. *In* R. E. Ulanowicz and T. Platt [ed.]. Ecosystem theory for biological oceanography. Can. Bull. Fish. Aquat. Sci. 213.

Platt, T., and K. Denman. 1977. Organisation in the pelagic ecosystem. Helgolander wiss. Meeresunters. 30: 575–581.

1978. The structure of pelagic marine ecosystems. Rapp. P.-V. Reun. Cons. Int. Explor. Mer 173: 60–65.

Platt, T., M. Lewis, and R. Geider. 1984. Thermodynamics of the pelagic ecosystem: Elementary closure conditions for biological production in the open ocean, p. 49–84. *In* M. J. R. Fasham [ed.] Flows of energy and materials in marine ecosystems: theory and practice. Plenum Press, London.

Rodriguez, J., and M. M. Mullin. 1986. Relation between biomass and body weight of plankton in a steady state oceanic ecosystem. Limnol. Oceanogr. 31: 361–370.

Roughgarden, J. D. 1977. Patchiness in the spatial distribution of a population caused by stochastic fluctuations in resources. Oikos 28: 52–59.

Rothlisberg, P. C., J. A. Church, and A. M. G. Forbes. 1983. Modelling the advection of vertically migrating shrimp larvae. J. Mar. Res. 41: 511–538.

Sheldon, R. W., A. Prakash, and W. H. Sutcliffe Jr. 1972. The size distribution of particles in the ocean. Limnol. Oceanogr. 17: 327–340.

Sheldon, R. W., W. H. Sutcliffe Jr., and M. A. Paranjape. 1977. Structure of pelagic food chain and relationship between plankton and fish production. J. Fish. Res. Board Can. 34: 2344–2353.

Sheldon, R. W., W. H. Sutcliffe Jr., and A. Prakash. 1973. The production of particles in the surface waters of the ocean with particular reference to the Sargasso Sea. Limnol. Oceanogr. 18: 719–733.

Silvert, W., and T. Platt. 1978. Energy flux in the pelagic ecosystem: A time-dependent equation. Limnol. Oceanogr. 23: 813–816.

1980. Dynamic energy-flow model of the particle size distribution in pelagic ecosystems, p. 754–763. *In* W. Charles Kerfoot [ed.] Evolution and ecology of zooplankton communities. The University Press of New England, New Hampshire.

Southward, A. J. 1980. The Western English Channel — an inconstant ecosystem? Nature 285: 361–366.

Sprules, W. G., and M. Munawar. 1986. Plankton size spectra in relation to ecosystem productivity, size, and perturbation. Can. J. Fish. Aquat. Sci. 43: 1789–1794.

Tabata, S., and J. L. Peart. 1985. Statistics of oceanographic data based on hydrographic/STD casts made at Ocean Station P during August 1956 through June 1981. Can. Data Rep. Hydrogr. Ocean Sci. No. 31.

Wroblewski, J. S. 1982. Interaction of currents and vertical migration in maintaining *Calanus marshallae* in the Oregon upwelling zone — a simulation. Deep-Sea Res. 29: 665–686.

Wroblewski, J. S., and J. G. Richman. 1987. The nonlinear response of plankton to wind mixing events — implications for survival of larval northern anchovy. J. Plankton Res. 9: 103–123.

The Vancouver Island Coastal Current: Fisheries Barrier and Conduit

Richard E. Thomson

Department of Fisheries and Oceans, Institute of Ocean Sciences,
9860 West Saanich Road, Sidney, B.C. V8L 4B2

Barbara M. Hickey

School of Oceanography, University of Washington, Seattle, WA 98195, USA

and Paul H. LeBlond

Department of Oceanography, University of British Columbia
Vancouver, B.C. V6T 1W5

Abstract

THOMSON, R. E., B. M. HICKEY, AND P. H. LEBLOND. 1989. The Vancouver Island coastal current: fisheries barrier and conduit, p. 265–296. *In* R. J. Beamish and G. A. McFarlane [ed.] Effects of ocean variability on recruitment and an evaluation of parameters used in stock assessment models. Can. Spec. Publ. Fish. Aquat. Sci. 108.

Physical oceanographic data collected over the continental margin of Vancouver Island during the last decade reveal the presence of a persistent, poleward flowing coastal current over the inner portion of the continental shelf. Confined landward of the 100 m depth contour, the coastal current is highly baroclinic and is driven by the flux of low density water (runoff) onto the shelf. Maximum near-surface speeds can exceed 0.50 m/s within the core of the current. In summer (April–September), the current is driven primarily by low salinity water emanating from Juan de Fuca Strait and flows counter to the prevailing northwesterly winds along the outer coast. Strong northwesterly winds tend to retard or reverse the flow in the upper 10 to 20 m of the water column so that the core of the coastal current is typically located at depth. In winter (October–March), the current is driven by the combined runoff from Juan de Fuca Strait and streams along the outer coast of Vancouver Island. At this time, the current is further augmented by the prevailing southeasterly winds along the outer coast. The coastal current appears to be poorly organized over the shallow, topographically complex banks at the southernmost end of the continental shelf where the current interacts with the Juan de Fuca Eddy. Meanders and eddies are prominent features of the seaward boundary of the flow throughout its poleward extent. We suggest that the coastal current, in conjunction with other quasi-permanent components of the regional circulation, has a strong impact on a variety of west coast fisheries. In particular, the current acts as an alongshore conduit and cross-shore barrier to the transport of biomass over the continental margin of Vancouver Island.

Résumé

THOMSON, R. E., B. M. HICKEY, AND P. H. LEBLOND. 1989. The Vancouver Island coastal current: fisheries barrier and conduit, p. 265–296. *In* R. J. Beamish and G. A. McFarlane [ed.] Effects of ocean variability on recruitment and an evaluation of parameters used in stock assessment models. Can. Spec. Publ. Fish. Aquat. Sci. 108.

Les données relatives à l'océanographie physique de la marge continentale de l'île Vancouver recueillies durant la dernière décennie révèlent l'existence d'un courant côtier continuel circulant vers le pôle sur la partie de la plate-forme continentale située près de la côte. Ce courant côtier, qui s'étend de la côte jusqu'à l'isobathe de 100 m, est fortement barocline et est déterminé par l'écoulement des eaux de faible densité (eau de ruissellement) vers la plate-forme. Au cœur du courant, la vitesse maximale près de la surface peut être supérieure à 0,50 m/s. Durant l'été (avril–septembre), le courant est déterminé principalement par les eaux de faible salinité provenant du détroit de Juan de Fuca et circule en sens contraire des vents dominants du nord-ouest qui soufflent le long de la côte de l'île située du côté de l'océan. Les vents puissants du nord-ouest ont tendance à ralentir ou à inverser le courant dans la couche supérieure de la colonne d'eau (10 à 20 m) de telle sorte que le cœur du courant côtier est habituellement situé en profondeur. Durant l'hiver (octobre–mars), les eaux de ruissellement provenant du détroit de Juan de Fuca conjugué à celles des cours d'eau situés le long de la côte océanique de l'île Vancouver déterminent le courant. Durant cette période, les vents dominants du sud-est soufflant le long de la côte océanique renforcent le courant. Le courant côtier semble très peu structuré au niveau du banc situé à l'extrémité sud de la plate-forme continentale. C'est au niveau de ce banc peu profond et dont la topographie est complexe que le courant entre en interaction avec le remous de Juan de Fuca. La portion du courant située du côté du pôle est bordée, du côté de la mer, par des méandres et des remous bien visibles. Nous pensons que ce courant côtier, de pair avec d'autres composantes presque permanentes de la circulation des eaux dans cette région, a un impact important sur plusieurs des pêches de la côte ouest. En particulier, ce courant joue un rôle de canalisation et de barrière en ce qui a trait au transport de la biomasse sur la marge continentale de l'île Vancouver.

1. Introduction

The continental margin of Vancouver Island (Fig. 1) supports diverse and highly productive fisheries including commercial stocks of salmon, herring, sablefish, hake, cod and shellfish. As in other areas of the world, recruitment to these fisheries is highly variable and appears to be linked to fluctuations in oceanic water properties and circulation (e.g. Mysak et al. 1982). This link can occur directly through effects on fish movement and physiology or indirectly through effects on food and predator populations. Major oceanic disruptions such as the 1982/83 El Niño-Southern Oscillation (ENSO) event are credited with having a particularly significant impact on fisheries along the west coast of North America (Tabata 1984; Bakun 1986; Mysak 1986).

Among the primary forcing mechanisms affecting the physical oceanographic environment of the outer Vancouver Island coast are winds, tidal currents, and buoyancy fluxes. The oceanography is further modified by interaction of forced motions with the local bottom topography, by frictional effects and by offshore oceanic processes. The net result is a complex and highly variable oceanographic regime that is expected to have con-

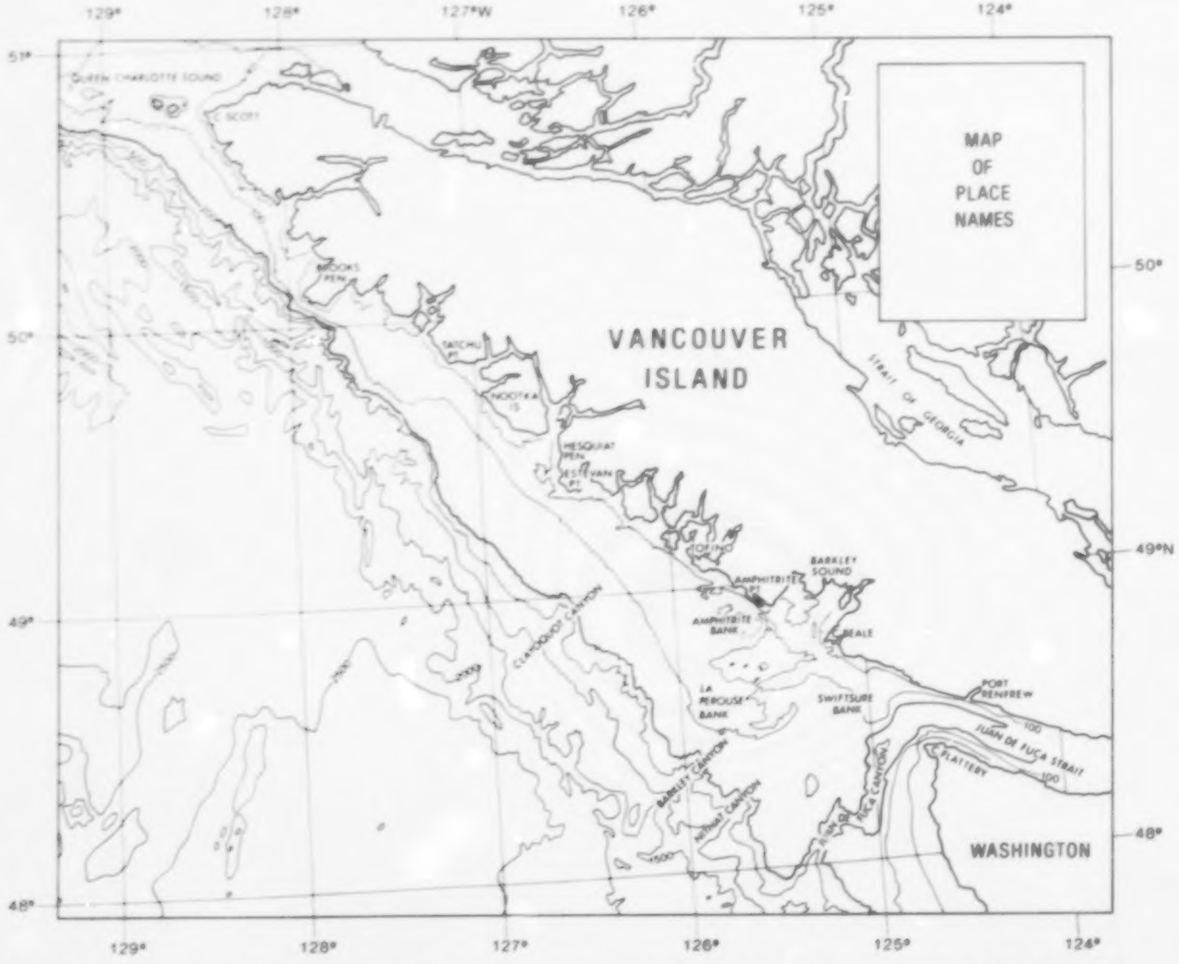
129°
128°
127°W
126°
125°
124°
51°
50°
49°
48°
49°N
QUEEN CHARLOTTE SOUND
C. SCOTT
MAP OF PLACE NAMES
BROOKS PEN
TATCHU PT
VANCOUVER ISLAND
NOOTKA IS
HESQUIAT PEN
ESTEVAN PT
STRAIT OF GEORGIA
TOFINO
AMPHITRITE PT
BARKLEY SOUND
AMPHITRITE BANK
BEALE
CLAYOQUOT CANYON
2000
LA PEROUSE BANK
SWIFTSURE BANK
PORT RENFREW
100
JUAN DE FUCA STRAIT
FLATTERY
BARKLEY CANYON
NITINAT CANYON
JUAN DE FUCA CANYON
1500
WASHINGTON

FIG. 1. The west coast of Vancouver Island (depth in metres). The bold 200 m contour corresponds to the shelf-break.

siderable impact on the recruitment of commercial fish stocks over a wide range of spatial and temporal scales.

Regionally-intensive oceanographic field programs begun in late 1979 indicate that the mesoscale shelf/slope oceanography over the southern continental margin of Vancouver Island is dominated by three quasi-permanent features: (1) The cyclonic (counterclockwise rotating) Juan de Fuca Eddy situated near the head of a major canyon that cuts across the continental slope at the entrance to Juan de Fuca Strait (Freeland and Denman 1982; Denman and Freeland 1985); (2) The reversible summer/winter wind-driven Shelf-Break Current with maximum near-surface speeds centered near the 200 m contour (Thomson 1981; Ware and Thomson 1986); and (3) The narrow, surface-intensified Vancouver Island Coastal Current that flows more than 100 km poleward over the inner portion of the continental shelf from the vicinity of Barkley Sound (Thomson 1981; Freeland et al. 1984: LeBlond et al. 1986a). In addition to these quasi-steady oceanic features, there is evidence for a poleward flowing California Undercurrent Extension over the continental slope (Ingraham 1967; Reed and Halpern 1976; Hickey 1979; Mackas et al. 1987) and for persistent northward flow within the offshore region seaward of the continental margin. Upwelling is a common feature of the shelf-break region in summer (Denman et al. 1981; Freeland and Denman 1982) and non-linear rectification of the strong diurnal and semidiurnal tidal currents can produce intense "residual" flow along the relatively steep sides of the offshore fishing banks. The marked diurnal tidal motions over the shelf have been shown to be dominated by baroclinic shelf waves (Crawford and Thomson 1984; Thomson and Crawford 1982) while the equally strong semidiurnal motions are observed to have a significant baroclinic component associated with the cross-shore propagation of internal tides (Barbee et al. 1975; Torgrimson and Hickey 1979). Low-frequency coastally trapped waves are partly responsible for current variations at periods in the range of days to weeks (Yao et al. 1984). The shelf/slope circulation is also affected by offshore mesoscale eddies formed through the process of baroclinic instability along the slope (Mysak 1977; Ikeda et al. 1984a,b; Thomson 1984).

This paper has a two-fold purpose: (1) To describe the basic physical oceanographic characteristics of the Vancouver Island Coastal Current in the context of prevailing oceanic conditions off the southern coast of British Columbia; and (2) To discuss the possible impact of the coastal current and associated shelf circulation on recruitment to major fisheries. The coastal current is shown to act as both a longshore conduit and a cross-shore barrier to fish movement along the southern continental shelf. Although the paper is written from a physical oceanographic point of view, we endeavour to define mechanisms that might account for variability in stock recruitment along the south-central coast of Vancouver Island. We focus on the coastal current without losing sight of the fact that it is but one component of a complex physical/biological regime that affects the west coast fisheries.

Organization of the paper is as follows. In the next section, we briefly describe the major observational programs that have been conducted on the west coast over the past decade. Section 3 provides an overview of the oceanography of the southern shelf region. Detailed discussion on the spatial and temporal scales of the Vancouver Island Coastal Current is presented in sections 4 and 5 while section 6 presents a brief description of major dynamical aspects of the flow regime. In section 7, we consider the possible relevance of the coastal current and associated shelf circulation to the migration and survival of fish stocks on the west coast of Vancouver Island. A summary and conclusions are presented in section 8.

2. Data Sources

The results presented in this paper are based principally on field programs conducted over the past decade by the Institute of Ocean Sciences in conjunction with university, government and private sector organizations. Data sets include moored current meter observations, CTD/hydro profiles, drifter deployments and satellite imagery. With the noteworthy exception of specific coastal shelf projects initiated by the Pacific Biological Station (Nanaimo, B.C.), spatial separations in data sets collected prior to 1979 are generally too large to delineate the relatively small scale oceanic features that occur near the coast and are therefore not considered in the present description. As noted by Dodimead (1984), ". . . prior to 1979, regular large-scale quasi-synoptic surveys were the major undertakings; whereas considerable effort is now being directed to process-oriented studies . . .confined to relatively small and specific geographic areas. . .".

Coastal Programs Prior to 1979

Early oceanographic information on the Vancouver Island Coastal Current regime is nicely summarized by Dodimead (1984). Of particular relevance are Waldichuk's (1963) analysis of the 1927 and 1931/32 drift bottle studies, which show a difference in flow direction over the inner and outer portions of the southern Vancouver Island shelf, and Lane's (1962, 1963) interpretation of the 1957 to 1962 water bottle data which distinguish between inner and outer shelf water properties. The distinction between inner and outer shelf water is further emphasized in Dodimead's analysis of cruise data collected off the shelf between 1967 and 1971 as part of a fisheries-supported shelf project (Favorite et al. 1976; Dodimead 1984).

Tully (1942) was the first to attempt an interpretation of the circulation off the entrance to Juan de Fuca Strait (a source region for the coastal current) based on dynamics inferred from the observed water property structure. The first direct current measurements in the coastal current regime were obtained from two mooring sites seaward of Tofino from November 1974 to April 1975 (Huyer et al. 1976). Unfortunately, the measurements were taken during the winter circulation regime when the coastal current is not easily distinguished from the prevailing northward wind-forced flow.

Observations of sea surface temperature and salinity from selected offshore locations are also available from the long-term (50-yr) lighthouse program (e.g. Hollister 1964; Giovando 1985). These data are particularly useful for investigation of climatic scale water property changes in the coastal current regime and for monitoring possible anomalous changes in nearshore oceanic conditions (Mysak et al. 1982; Thomson et al. 1984).

Coastal Oceanic Dynamics Experiment

The first major investigation of the circulation and water property variability over the continental margin of Vancouver Island was conducted between May 1979 and September 1980 during the Coastal Oceanic Dynamics Experiment (CODE). An extension of this program involving current meter moorings along the shelf-break was conducted as part of the SuperCODE experiment over the approximate period of June 1981 to September 1982. Details of these experiments are found in Thomson et al. (1986), Freeland (1987) and Huggett et al. (1987). A program (CODE II) dedicated to the spin-up of the Juan de Fuca Eddy was conducted between March and June, 1985. Current observations in this case were obtained from six moorings deployed in a circular array over the Juan de Fuca Canyon.

The positions of the CODE, CODE II and SuperCODE moorings are shown in the experiment composite map of Fig. 2. During CODE, current meter moorings were maintained at 3 to 5 locations along three cross-shelf lines extending seaward from the south, central and northern sectors of Vancouver Island. CTD and hydro surveys were conducted (Thomson et al. 1985) over the region on 7 cruises during the time that the moorings were in place. CODE II moorings were concentrated to the west of Juan de Fuca Strait and detailed CTD surveys were conducted in the region during the time the mooring array was in place. SuperCODE moorings were positioned at the shelf-break (200 m contour) at five locations on the British Columbia coast (Freeland 1987). Two of these sites are relevant to the present study. No CTD surveys were conducted in the region of the moorings.

The CODE current meter observations from the Estevan Point line provide direct verification of a prevailing coastal current along the inner shelf of southern Vancouver Island (Freeland et al. 1984; Thomson et al. 1985; Huggett et al. 1987). These results are supported by the geostrophic currents calculated from dynamic height anomalies derived from the detailed water property surveys. There is also limited evidence for a narrow coastal current off Brooks Peninsula where the shelf width decreases to less than a few kilometres. For the most part, however, the mooring array and water property surveys of CODE were incapable of providing a clear definition of the near-shore flow regime except in the vicinity of Estevan Point. The program also emphasized the difficulty of measuring near-surface currents from moored instrumentation in active fishing zones. Although the CODE II and SuperCODE observations are outside the coastal current regime, we include them to help contrast the differences in flow structure over the inner and outer shelf.

Vancouver Island Coastal Current Experiment

The presence of the relatively intense nearshore poleward flow in the CODE data for the Estevan Point line was the catalyst for a joint field program by the present authors. The Vancouver Island Coastal Current Experiment spanned the period June to November, 1984 and was designed specifically to delineate the spatial and temporal variability of the shelf circulation within the constraints posed by the appreciable fishing activity along the coast. Details of the experiment are found in LeBlond et al. (1986a) and Thomson et al. (1986); positions of the current meter, anemometer and pressure gauge moorings are shown in Fig. 2. In addition to the moorings, water property surveys were conducted over the southern portion of the continental margin during June, July and October 1984. The project also included a satellite-tracked drifter component (jointly sponsored by the Canadian Coast Guard) to measure nearsurface circulation seaward of Vancouver Island during both summer and winter months (Seaconsult Marine Research Ltd. 1984).

Preliminary results from the Coastal Current Experiment have provided considerably more detail on the nearshore structure of the shelf circulation and suggest that both local and remote wind forcing are responsible for variations in the current structure (Hickey et al. 1988). The relation between the strength of the coastal current and integrated runoff into the Strait of Georgia is also being established (LeBlond et al. 1986b; Griffin et al., 1987).

La Perouse Project

The La Perouse Project is a cooperative long-term (10-yr) investigation involving biologists and physical oceanographers within the Department of Fisheries and Oceans (Ware and Thomson 1986, 1988). Formulated in response to the 1982/83 ENSO event along the west coast of British Columbia, the physical oceanographic field component of the La Perouse Project consists of three permanent current moorings and a four-line CTD/hydro grid off the southwest coast of Vancouver Island (Fig. 2). For the past 2 years, the CTD/hydro grid has been completed roughly 12 times per year with observations concentrated in the period April to October. Plankton tows have also been taken on a regular basis at fixed stations imbedded within the CTD grid. Moored instrument data consists of currents, temperatures, salinities and pressure. Since late 1986, transmissivity data has also been collected in the upper portion of the water column.

3. Oceanographic Setting

Bathymetry

The western margin of Vancouver Island is characterized by an extensive shelf, steep slope and broad continental rise (Fig. 1). As delineated by the 200 m depth contour, the continental shelf attains a maximum width in excess of 65 km seaward of Juan de Fuca Strait and narrows poleward to a width of less than 5 km seaward

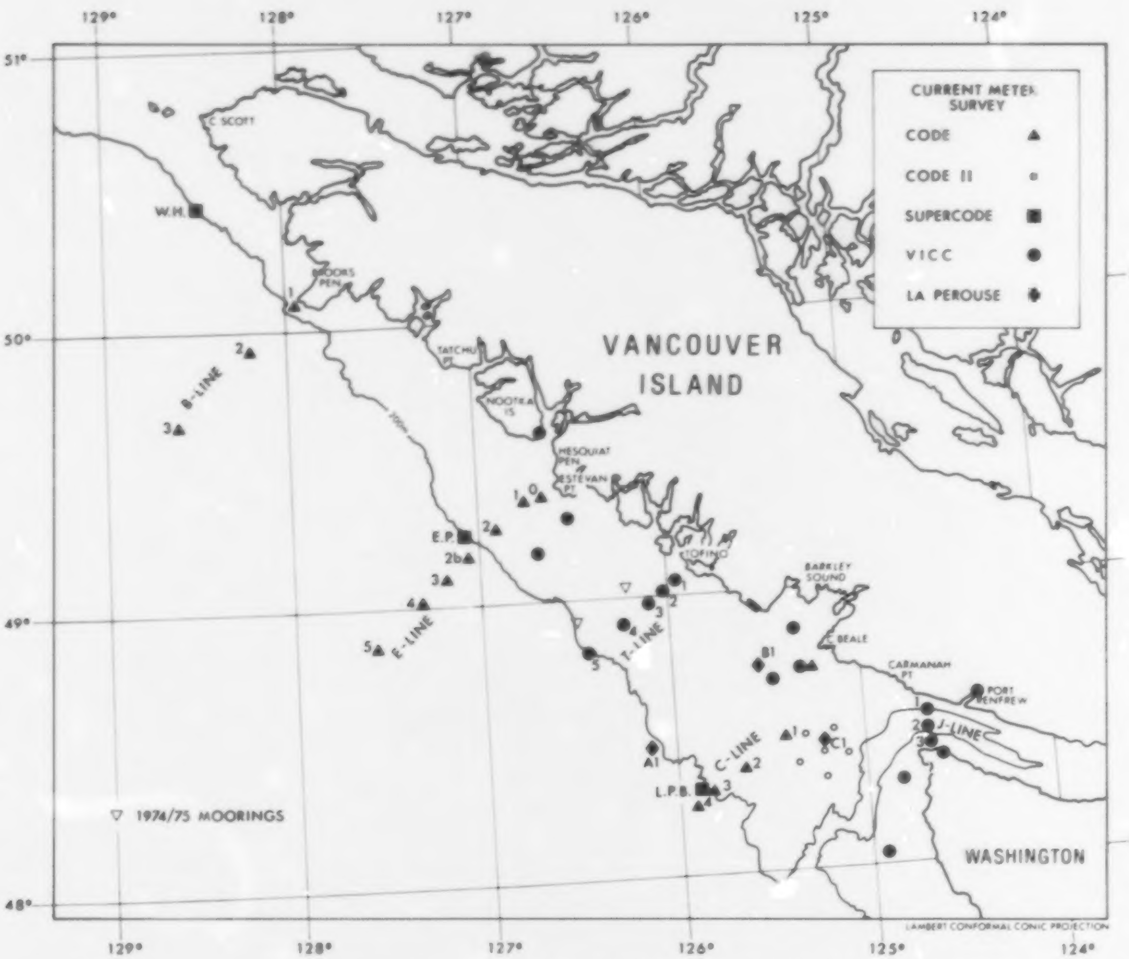
129°
128°
127°
126°
125°
124°
51°
50°
49°
48°
CURRENT METER SURVEY
CODE ▲
CODE II o
SUPERCODE ■
VICC ●
LA PEROUSE ⧫
C. SCOTT
W.H.
BROOKS PEN.
TATCHU PT
B-LINE
VANCOUVER
ISLAND
NOOTKA IS.
HESQUIAT PEN.
ESTEVAN PT.
TOFINO
E.P.
2b
E-LINE
T-LINE
BARKLEY SOUND
BEALE
B1
CARMANAH PT
PORT RENFREW
J-LINE
C-LINE
A1
C1
L.P.B.
▽ 1974/75 MOORINGS
WASHINGTON
LAMBERT CONFORMAL CONIC PROJECTION

FIG. 2. Moored instrument locations for major oceanographic field programs: CODE (▲), CODE II (o), SuperCODE (■), VICC (●) and La Perouse Project (⧫). Also shown are locations of winter 1974/75 moorings ( ).

of Brooks Peninsula near the northern end of the island. Between Barkley Sound and the entrance to the strait, the shelf has a particularly convoluted geometry consisting of numerous shallow banks separated by a series of roughly 100 m deep basins and cut through by a major 400 m deep, approximately 10 km wide canyon (the Juan de Fuca Canyon). To the south of the Juan de Fuca Canyon, the shelf topography is more uniform. Depth contours roughly parallel the coastline except near the shelf edge where the uniformity of the slope is interrupted by numerous canyons.

North of Barkley Sound, the Vancouver Island shelf is divisible into inner and outer oceanic zones separated approximately by the 100 m depth contour. There is also a moderately steep depth gradient centered along the 50 m depth contour approximately 10 km from shore. No extensive fishing banks exist north of Amphitrite Bank (immediately northward of Barkley Sound) and the coastline is highly irregular due to the presence of rugged interconnecting inlets. Major seaward projecting landforms, such as Hesquiat and Brooks peninsulas (Fig. 1), are thought to have a significant effect on the water properties and circulation of the local inner shelf (Thomson and Ware 1988). In addition, the adjoining slope is cut by numerous small-to-intermediate scale canyons that are expected to effect cross-slope exchange processes at the edge of the continental margin. Nitinat and Barkley canyons appear to be prime candidates for future investigations of up-slope transfer of water properties.

Regional Circulation

The west coast of Vancouver Island borders the bifurcation zone of the Subarctic Current, an extensive, albeit poorly defined, zonally flowing, cross-Pacific surface current which originates off the coast of northern Asia (Dodimead et al. 1963; Tabata 1975). To the west of the island, the Subarctic Current splits into the poleward flowing Alaska Current and the equatorward flowing California Current (Fig. 3). Direct observation of a persistent northward nearsurface flow seaward of the Vancouver Island coast suggests that the offshore circulation is dominated by the Alaska Current. As with other eastern boundary currents, the Alaska Current consists

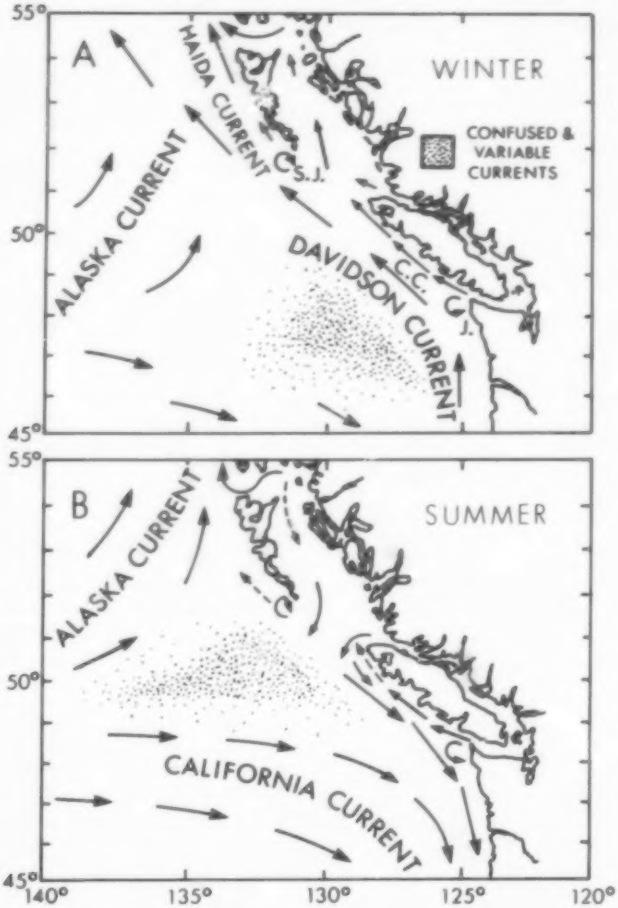

FIG. 3. Regional surface circulation pattern for the northeast Pacific for (*a*) winter and (*b*) summer based on water property surveys and ship drift information (after Thomson 1981). New additions include the Haida Current, the Juan de Fuca Eddy (J), the Vancouver Island Coastal Current (CC) and the Cape St. James Eddy (SJ).

of a comparatively weak, broad and ill-defined drift characterized by intermittent mesoscale eddies and frequent reversals. The current has a characteristic width of order 100 km and typical flow speeds of around 10 cm/s. Documented evidence for eddy activity along the continental margin of the island has been presented by Mysak (1977), Emery and Mysak (1980), Ikeda et al. (1984a, 1984b), Thomson (1984) and Thomson and Gower (1986).

Although it has yet to be fully substantiated, there is evidence for a quasi-permanent, subsurface poleward-flowing California Undercurrent Extension below 200 m along the Vancouver Island continental shelf (Ingraham 1967; Reed and Halpern 1976; Hickey 1979). Current observations obtained from long-term moorings over the slope indicate that the undercurrent undergoes considerable low-frequency variability (periods of weeks to months) and is probably not continuous alongshore at any given moment (Fig. 4). Nevertheless, a water mass analysis by Mackas et al. (1987) suggests that the undercurrent (characterized by relatively high temperatures and low oxygen concentrations) strongly influences the intermediate-depth circulation on the Vancouver Island coast and is the major contributor to upwelled water found over the southern shelf in summer.

In addition to regional variability associated with the major ocean current systems, there is mounting evidence for the longshore propagation of low-frequency coastally trapped waves over the Vancouver Island continental margin (Mysak 1980; Yao et al. 1984; Allen and Denbo 1984; Halliwell and Allen 1984; Hickey 1984; Strub et al. 1987). With time scales of weeks and longshore spatial scales of thousands of kilometres, these propagating current systems are partly responsible for long-term changes in the currents and water property distributions along the coast of Vancouver Island. Moreover, the trapped waves can either be locally or remotely forced by coastal winds. According to Halliwell and Allen (1984), much of the long-wave variability off the British Columbia coast may originate with wind-forced motions off the north-central coast of California. Shorter scale versions of these waves (scales of a few hundred kilometres) have been shown to be responsible for the intense diurnal tidal currents over the southern shelf (Crawford and Thomson 1982, 1984; Thomson and Crawford 1982; Flather 1988).

Prevailing Winds

Coastal winds are an important mechanism influencing the basic circulation over the continental margin. During

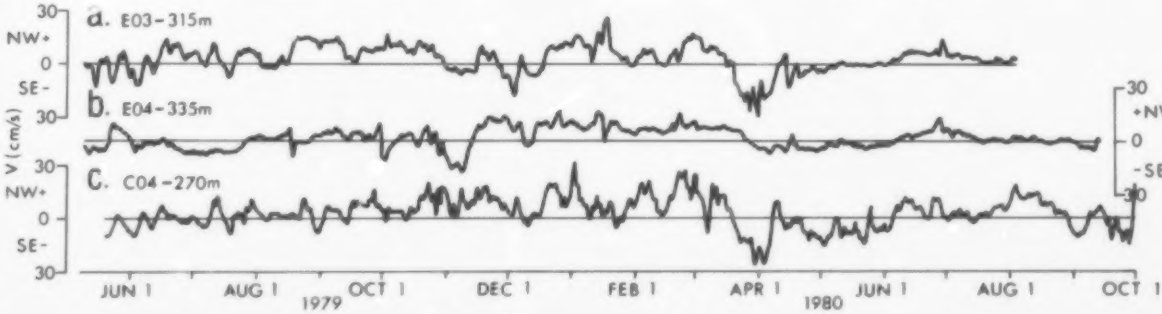

FIG. 4. Longshore components (*V*) of residual (low-pass filtered) intermediate depth currents for the Vancouver Island continental slope (cf. Fig. 2) for the period May 1979 to September 1980. (a) Mooring E03 at 315 m; (b) Mooring E-4 at 335 m; (c) Mooring C-4 at 270 m.

winter, the Aleutian Low dominates the atmospheric pressure distribution in the northeast Pacific so that coastal winds are predominantly from the southeast (Thomson 1981). Especially strong winds occur from October through March and are associated with the passage of extratropical cyclones and accompanying frontal systems. The main departure from these conditions occurs in mid to late winter when cold Arctic air occupies the interior of the province. Seaward flow of relatively dense air from this air mass leads to intense "outflow" winds through coastal channels and to the development of strong offshore winds near the coast.

From April through September, the Aleutian Low weakens and prevailing wind conditions are principally determined by the North Pacific High. As a consequence, winds are predominantly from the northwest along the outer coast. The intensity of westward propagating disturbances diminishes during this period and the mean time interval between low pressure systems increases from 3 days to 10 days (e.g. Fissel 1975).

Figure 5 shows mean monthly winds for the period January 1983 to December 1986 for the location 49°N, 126°W located approximately 10 km seaward of Amphitrite Point. The mean wind vectors are presented in Fig. 5a while the alongshore wind component (oriented at 315°T) is presented in Fig. 5b. Since there are no permanent offshore wind stations along the British Columbia coast, the mean wind vectors have been calculated using 6-hourly pressure-derived geostrophic winds for a 3° × 3° grid covering the northeast Pacific Ocean (Bakun 1973; Andrew Bakun, pers. comm.). These derived winds are representative of the actual winds for wind variations at periods in excess of 2 days (Thomson 1983). As these plots indicate, winds are predominantly from the southern quadrants in winter (October through March) and from the northern quadrants in summer (May through September). Maximum monthly-averaged speeds in winter are in the range of 5 to 10 m/s while in summer maximum speeds are around 5 m/s. As expected, maximum standard deviations in wind speed occur in winter months. The Spring Transition from southerly to northerly winds typically takes place between March and May while the Fall Transition from northerly to southerly winds almost invariably occurs in October. The early reversal of the winter winds in 1983 (c.f. Fig. 5a) is almost certainly linked to the anomalous atmospheric conditions during the 1982/83 El Niño.

Wind-induced summertime upwelling (Fig. 6) occurs on an annual basis over the outer portion of the shelf and appears to be especially pronounced at the edges of

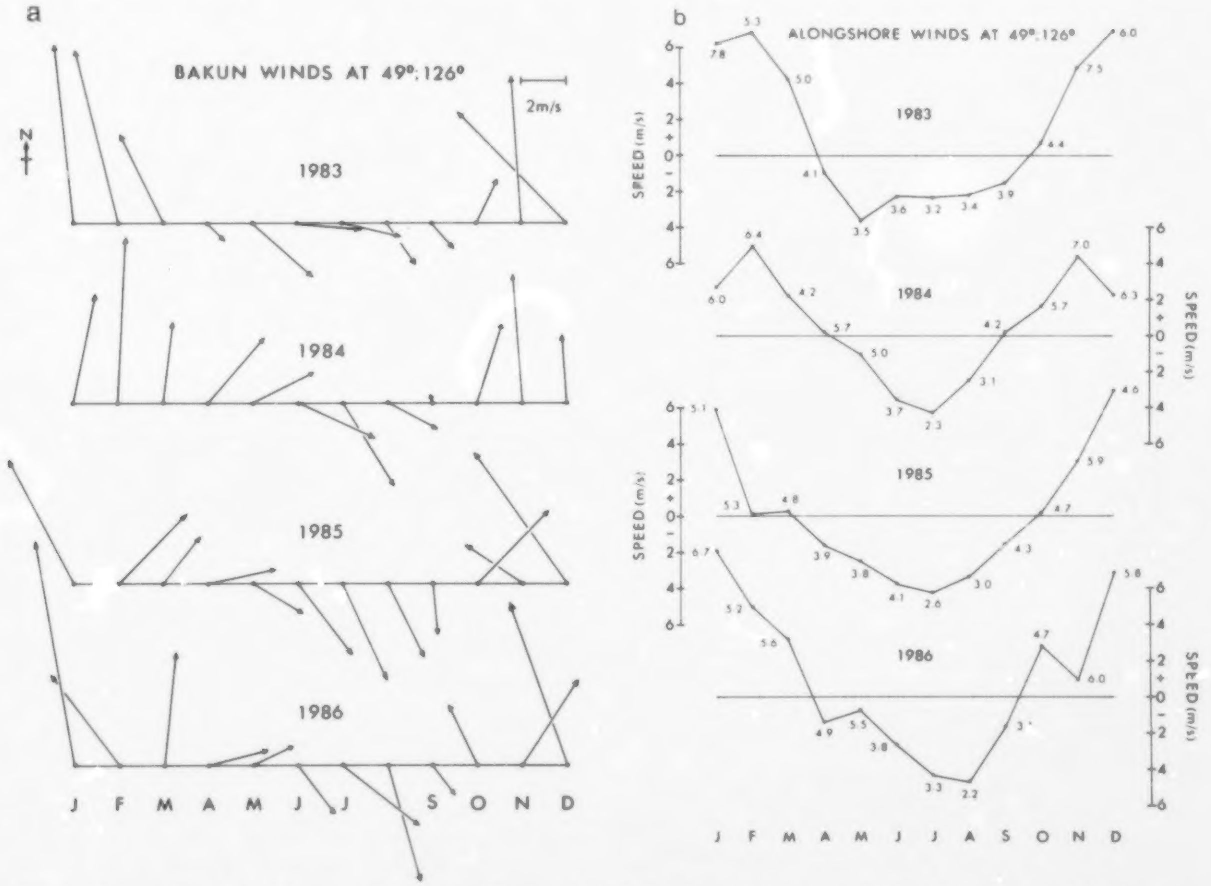

FIG. 5. Time series of monthly mean "Bakun type" coastal winds for the period January 1983 to December 1986 for location 49°N; 126°W. (a) Vectors of monthly mean winds; (b) Longshore component of monthly mean winds (oriented at 315°T) plus standard deviations in m/s (based on original six-hourly records).

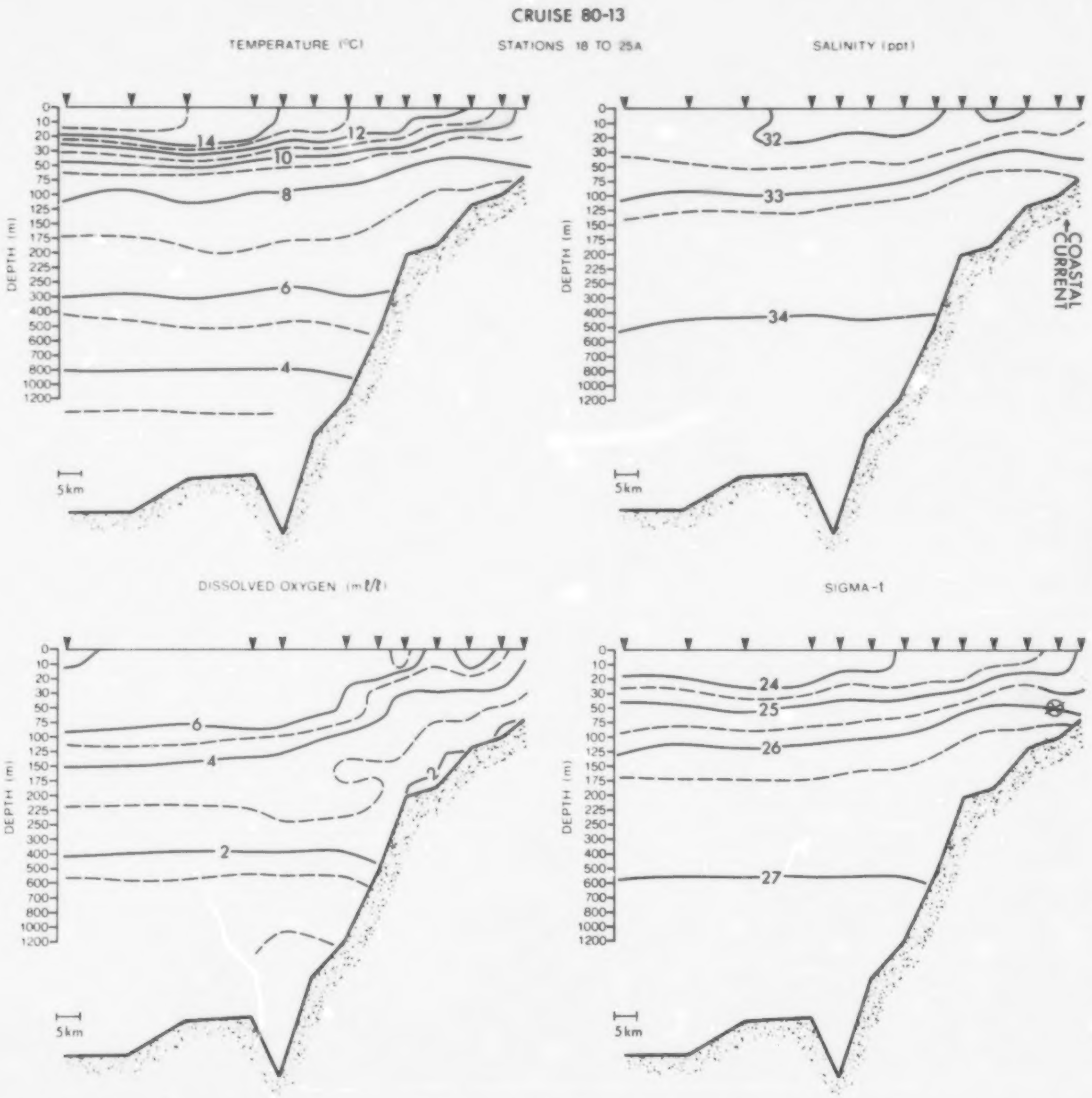

FIG. 6. Cross-shore structure of temperature, salinity, dissolved oxygen and density (sigma-t) seaward of Tatchu Point central coast of Vancouver Island for mid July 1980. Maximum water depth is 2000 m; data extend to roughly 1200 m. Note logarithmic depth scale. Symbol ⊗ in sigma-*t* plot denotes location of the coastal current.

the southern banks owing to the presence of major canyons (Freeland and Denman 1982) or to locally intensified tidally rectified flow. Coastally trapped waves may further modify upwelling patterns and lead to temporal variations that are not well correlated with local wind events (Gill and Schuman 1974). Upwelling structure may be present despite weak or downwelling-favourable winds.

Water Properties

Except near the continental margin, mean water properties in the northeast Pacific tend to be zonally distributed with temperatures and salinities decreasing in the poleward direction. Eastward from the bifurcation region of the Subarctic Current, isopleths gradually become more meridionally distributed until over the continental margin mean water properties are closely aligned with the coastline. Details of the changing spatial structure of water properties over the continental margin of southern Vancouver Island have been presented by Lane (1963). As illustrated by Fig. 7a, winter conditions are characterized by well mixed cold, low salinity coastal current water over the inner shelf (inshore) regime and warmer, more saline, oceanic water over the outer shelf regime.

In summer, a 10 to 20 m layer of relatively warm water typically overlies the southern portion of the shelf

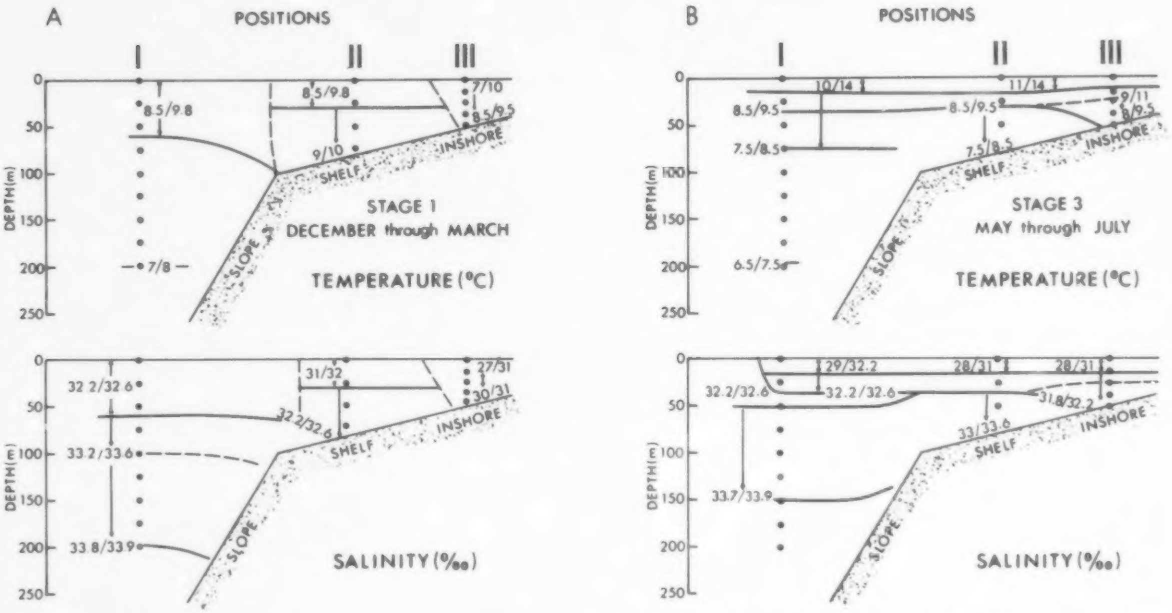
A
POSITIONS
I
II
III
8.5/9.8
8.5/9.8
7/10
8.5/9.5
9/10
INSHORE
SHELF
SLOPE
STAGE 1
DECEMBER through MARCH
7/8
TEMPERATURE (°C)
DEPTH (m)
0
50
100
150
200
250
32.2/32.6
31/32
27/31
30/31
32.2/32.6
33.2/33.6
33.8/33.9
SALINITY (‰)
B
POSITIONS
10/14
11/14
9/11
8.5/9.5
8.5/9.5
8/9.5
7.5/8.5
7.5/8.5
6.5/7.5
STAGE 3
MAY through JULY
29/32.2
28/31
28/31
32.2/32.6
32.2/32.6
31.8/32.2
33/33.6
33.7/33.9

FIG. 7. Stages 1 and 3 (winter and summer) of cross-shore temperature and salinity structure seaward of Amphitrite Point (from Dodimead 1980 after Lane 1963).

(Fig. 7b). This somewhat obscures the coastal current temperature "signature". Only by considering the detailed sub-surface structure of the nearshore zone can the presence of the current be verified. An onshore decrease in salinity over the "inshore" regime appears to be a reliable indication that the coastal current is present at a given section of the coast. To the north of Barkley Sound, the current is more confined to the nearshore region and the presence of the current more readily detected in the upper layer. Observations generally reveal cold low salinity water adjacent to the coast with warmer water offshore.

Coastal Runoff

As discussed later in the paper, coastal buoyancy flux (runoff) is considered to be the primary forcing mechanism for the Vancouver Island Coastal Current. The exact details of the forcing and how it is modified by other factors such as wind and the background shelf circulation are just beginning to be understood (e.g., Hickey et al. 1989).

There are two known sources for the low density water observed along the southwest coast of British Columbia. (1) Runoff is supplied directly to the coast through discharge from precipitaion-fed streams along Vancouver Island. As illustrated in Fig. 8, this discharge is maximal in fall and winter and minimal in summer. (2) Runoff is supplied indirectly to the coast through tidally mixed brackish water flowing seaward from Juan de Fuca Strait. The integrated contribution from rivers entering the Juan de Fuca system are plotted as an overlay in Fig. 8. Most of this water originates as snow-melt and is discharged during the Fraser River freshet which, along with runoff

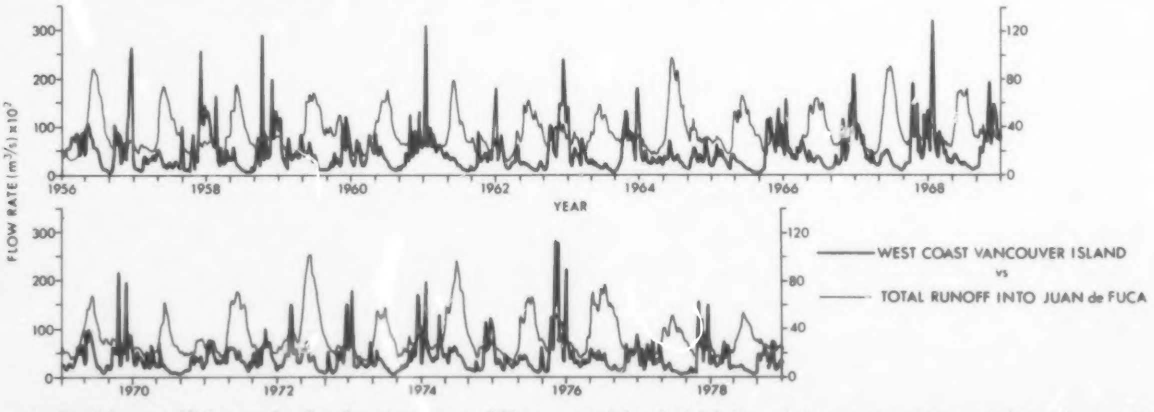

FIG. 8. Weekly runoff time series for the west coast of Vancouver Island (thick line, right scale) and Juan de Fuca Strait (thin line, left scale) for the period 1956 to 1979. (Modified after LeBlond et al. 1983). The west coast series includes all major streams flowing onto the continental margin; the strait series mainly originates with the Fraser River and also includes rivers emptying into Puget Sound.

from other rivers emptying into the Strait of Georgia–Puget Sound system, then works its way seaward as part of the marked estuarine circulation that characterizes the inner coastal waters. In this case, peak discharge takes place in summer while minimal discharge occurs in winter.

As indicated by the above discussion, the two sources differ both in timing and spatial structure. Whereas the coastal streams behave as a "line source" with peak discharge in winter, the brackish discharge from Juan de Fuca Strait behaves as a "point source" with peak discharge in summer (Dodimead 1984; LeBlond et al. 1986a). There is also reason to believe that the summertime runoff through Juan de Fuca Strait is not steady but undergoes fortnightly to monthly "pulses" due to variations in the tidally induced mixing in upstream channels (David Griffin, pers. comm. University of New South Wales, Sydney, N.S.W. Australia). Times of neap tides (weak mixing in the tidal passes) and marked northwesterly winds in the Strait of Georgia are expected to be correlated with pronounced seaward flux of low density water; times of spring tides (strong mixing in the tidal passes) are expected to be correlated with periods of weak seaward flux of low density water.

4. Spatial Structure

Prior to the 1979/81 CODE program, few details were available concerning the nearshore circulation along the outer coast of Vancouver Island. Earlier oceanographic surveys were primarily concerned with the deep-sea or outer shelf regimes and therefore tended to undersample the waters over the inner continental shelf where station spacings of 10 km or less are required to adequately delineate the coastal current features.

The absence of direct current observations does not imply that the existence of the poleward flowing coastal current was completely unknown. Tully (1942) described eddy-like circulation off the mouth of Juan de Fuca Strait which hinted at a poleward flowing nearshore countercurrent to the south of Barkley Sound. An analysis of early drift bottle data by Waldichuk (1963) indicated: (1) A marked northwestward drift within about 40 km of the coast to the north of Barkley Sound; and (2) A southeastward drift toward the Washington coast at distances greater than 40 km offshore. Similarly, Lane (1963) distinguishes between "inshore" and "shelf" waters in the vicinity of Barkley Sound. The inshore domain is characterized by relatively low temperatures and salinities, and is clearly coincident with the region occupied by the Vancouver Island Coastal Current. Modified versions of two of Lane's five temporal stages are reproduced in Fig. 7.

Not all evidence for the coastal current is based on scientific observations. Discussions with fishboat operators prior to the 1979 field-work suggested that commercial fishermen were well aware of a northward longshore summer-time flow over the inner shelf waters north of Barkley Sound. Set and drift operations almost invariably resulted in a northwestward set, counter to the prevailing northwesterly winds along the coast in summer. The "folklore" has since been substantiated by oceanographic observations.

Circulation

Monthly-mean, near-surface current meter observations collected at mooring sites on the continental margin over the past decade are presented in Fig. 9. In preparing this figure, we have used current records from depths <50 m as representative of surface flow. Most observations are from subsurface moorings of Aanderaa RCM4 current meters. Despite the obvious seasonal and interannual variability in the flow and the inability of the limited data to fully delineate the structure of the shelf circulation, the distinction between mean currents over the inner and outer portions of the shelf is clearly evident. This is supported by the drift bottle tracks noted in the previous section and by quasi-Lagrangian surface motions derived via drogued satellite-tracked drifting buoys (Fig. 10). Drogue depths in most cases were 10 to 20 m so that the drifters were close followers of the nearsurface circulation (windage effects on the buoys are assumed to be negligible). Results from the satellite-drifters are corroborated by recent Loran-C tracked drifter studies conducted off the southwest coast of the island (W.S. Huggett, pers. comm. Institute of Ocean Sciences, Sidney, B.C.).

The Vancouver Island Coastal Current is seen as a baroclinic, approximately 15 to 25 km wide, poleward flow with typical speeds in excess of 10 cm/s and an alongshore extent of over 150 km. The current persists throughout the year and can attain prolonged maximum speeds in excess of 50 cm/s. Although the cross-shore current structure is only marginally resolved by current meter observations, it appears that the core of the coastal current is centered adjacent to the weak topographic rise located within the inner portion of the shelf (roughly along the 50 m depth contour) rather than at the coast. Bottom friction and topographic-restoring effects presumably account for seaward displacement of the core. (A similar result is discussed by Thomson and Gower (1986) in connection with wind-forced longshore flow over the Vancouver Island shelf.) Throughout much of its length, the coastal current is separated from a seasonally reversible shelf-break current by an alongshore transition zone of relatively weak and variable flow. The transition zone is especially pronounced in summer and appears to be most extensive over the broad shelf region seaward of Barkley Sound. To the north of the sound, the width of the transition zone decreases poleward toward Estevan Point in concert with a narrowing of the continental shelf. Strong longshore flow is found over the outer shelf with maximum core speeds of roughly 50 cm/s located over the outer edge of the continental shelf-break (cf. Fig. 17a). In contrast to the coastal current, the shelf-break current reverses seasonally in response to the preavailing winds along the outer coast. The flow is predominantly to the southeast in summer and to the northwest in winter.

In addition to the marked cross-shore structure of the shelf circulation, there is a clear distinction between flow structure to the south and north of Barkley Sound. This spatial distinction is particularly obvious in summer when the wind and runoff forcing mechanisms are in opposition. At this time of year, the prevailing circulation in the region between Juan de Fuca Strait and Barkley

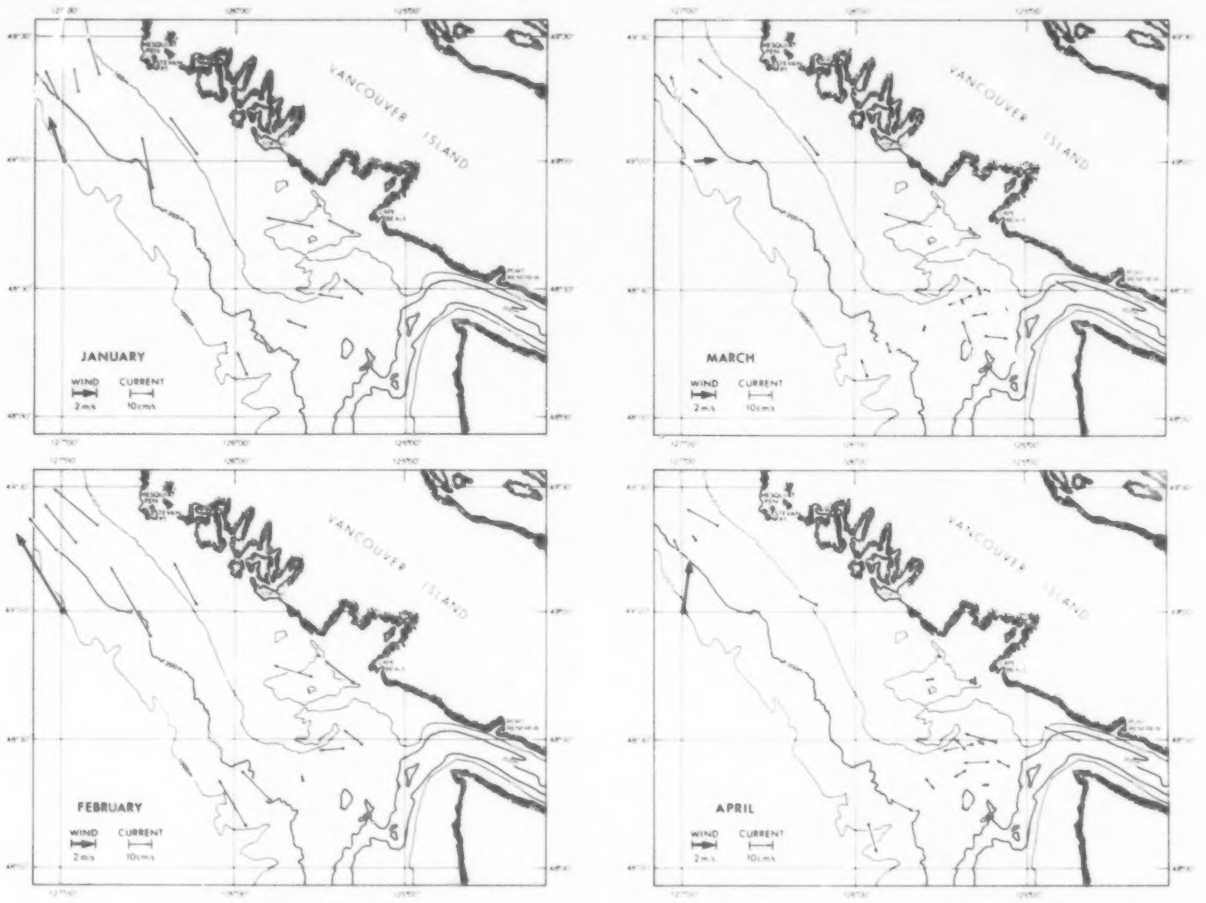

FIG. 9. Monthly mean near-surface current vectors from all available current meter moorings on the south central Vancouver Island continental margin (regardless of year) for the period 1974 to 1987 (cf. Fig. 2). Current meter depths less than 50 m. Dotted arrows are for 5 m depth records from VICC experiment (30 m depth records for VICC experiment are also shown). Thick vector represents the mean monthly Bakun-type geostrophic winds for location 49°N; 126°W for 1980.

Sound is complex and often confused. The transition region is especially pronounced and a branch of the coastal current appears to loop seaward over the La Perouse Bank region (Fig. 11). It is in this region of shallow banks and cross-shelf canyons that the low density water issuing from Juan de Fuca Strait first begins to form into the nearshore buoyancy current. The initial accumulation of low density water near the source region is a common occurrence in coastal areas receiving runoff from a "point" source such as a large river or strait (Beardsley and Hart 1978; Ikeda 1988; LeBlond et al. 1986b).

Because regional depth contours are relatively uniform north of the southern banks region, prevailing currents poleward of Barkley Sound appear to more closely parallel the coastline. This spatial organization may be further aided (through conservation of potential vorticity) by the progressive poleward narrowing of the bottom contours. These contours eventually converge to a narrow (a few kilometres wide) shelf seaward of Brooks Peninsula. The Vancouver Island Coastal Current is particulary well defined along this portion of the coast and is observed to extend at least as far as Tatchu Point and possibly beyond Brooks Peninsula. Present indications are that the flow structure in the vicinity of Brooks Peninsula is quite complicated and variable. Current and drifter studies in the area suggest that a coherent nearshore flow can penetrate beyond the peninsula but that it is fairly common to find a wind-induced shelf-break current sweeping southward past the end of the peninsula (Fig. 12). Brooks Peninsula appears to be a definite barrier to alongshore continuity of the coastal current and could play a significant role in fish migration over the continental shelf.

The three images presented in Fig. 13 illustrate the type of qualitative information on near-surface circulation that is obtainable from satellite AVHRR (Advanced Very High Resolution Radiometer) thermal data. In the summer images, there is a counterclockwise, eddy-like feature to the west of Juan de Fuca Strait, a well-defined coastal current extending poleward over the inner shelf and an extensive filament (or tongue) extending southeastward past Brooks Peninsula from the vicinity of Queen Charlotte Sound. The cold-core Juan de Fuca Eddy curls

FIG. 9. (*Continued*)

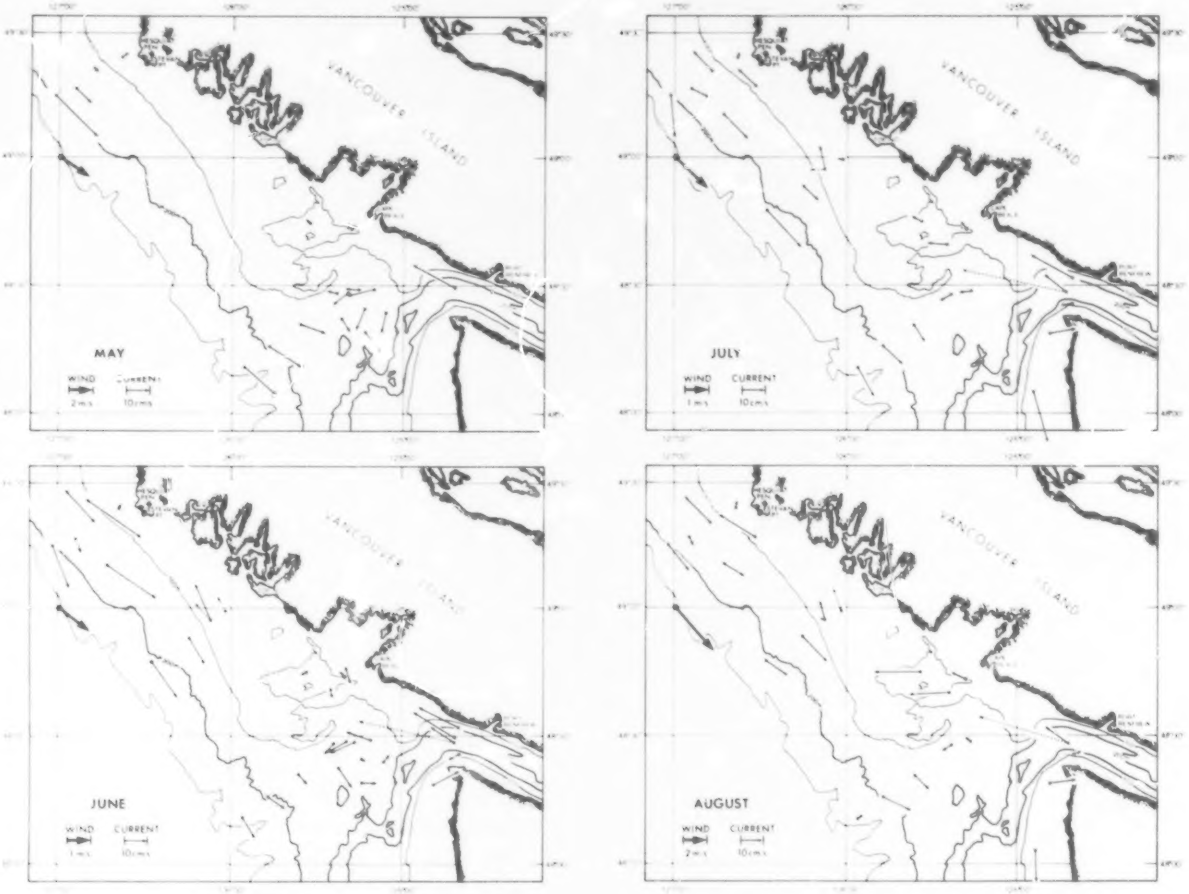

to the southeast and appears to advect surface water toward the Washington coast. A northward branch of the eddy merges with the coastal current regime to the north of Barkley Sound and flows poleward toward Brooks Peninsula. The coastal current is relatively wide over the southern shelf but begins to narrow as the flow continues poleward. Wavelike features are clearly developed along the seaward edge of the current; southeastward flow occurs over the shelf-break. In the October image, the Juan de Fuca Eddy is poorly defined and the flow near Brooks Peninsula is disrupted by a marked mesoscale eddy located to the west of the continental shelf. The coastal current at this time appears to extend poleward of Brooks Peninsula. Other details of the general flow structure are masked by an extensive pattern of baroclinically unstable mesoscale eddies that formed along the Washington–British Columbia coast. The large "hammerhead" structure protruding seaward in Fig. 13c is a good example of such instabilities.

Water Properties

Maps of water properties based on CTD profiles from selected oceanographic surveys are presented in Fig. 14 and 15. Associated maps of geostrophic currents are presented in Fig. 16. In all cases, an objective analysis scheme based on specified spatial correlation scales is used to interpolate the data to a uniform grid prior to contouring. The maps of geostrophic currents are derived from objective maps of dynamic height relative to a specified "depth-of-no-motion". Use of 100 m as the reference depth in Figure 16 enables us to estimate surface geostrophic flow well onto the shelf.

According to Fig. 14 and 15, water properties dome upward over the continental shelf in summer with maximum vertical displacement occurring near mid-shelf. This structure is most pronounced at intermediate water depths (20–100 m) and is presumably related to a combination of wind-forced upwelling (with equatorward flow) and nearshore buoyancy flux (with poleward flow). Comparison of the water property maps with the current maps indicates that the coastal regime occupied by the Vancouver Island Coastal Current typically consists of a narrow band of relatively cool, low salinity, low dissolved oxygen water stretching northward from Barkley Sound. No band-like water property distribution exists in the region of the Juan de Fuca Eddy and bank-deflected circulation over the southern end of the Vancouver Island shelf. The axis of the transition zone coincides with the region of maximum vertical displacement of the water properties (maximum density) and resembles a broad alongshore frontal zone ("barrier")

FIG. 9. (*Concluded.*)

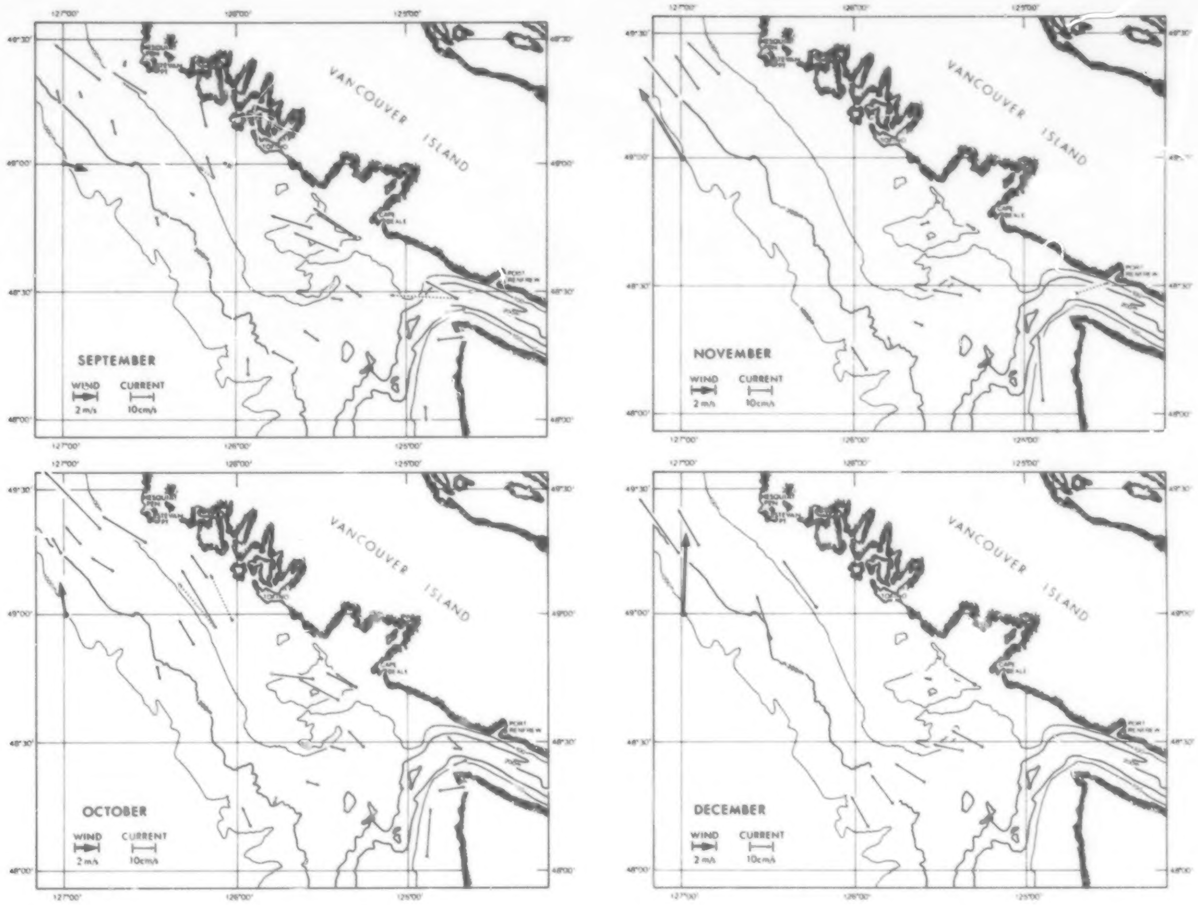

separating the inner shelf waters from the offshore regime. Seaward of the transition zone, isopycnal surfaces slope downward in summer consistent with southeasterly shelf-break flow. Temperatures increase and salinities decrease at fixed depth levels.

In winter, the prevailing currents are poleward over the entire shelf and slope. Accompanying water property surfaces are tilted downward in the onshore direction with an indication of greater downward tilt near the coast, which is presumably coincident with a buoyancy driven nearshore flow along the coast. The spatially integrated winter runoff rate from streams along the Vancouver Island coast is approximately half the summer runoff rate into the Strait of Georgia from the Fraser River during freshet (LeBlond et al. 1986a, 1986b) and therefore is expected to augment the wind-generated component of the nearshore current. The Juan de Fuca Eddy and topographically modified circulation over the shallow banks appear to be obliterated by the predominantly northwesterly flow. It is also in winter when wind-induced flow reversals in the estuarine circulation in Juan de Fuca Strait are most common. Observations reveal that strong (> 10 m/s) southerly winds off the northern Washington coast lead to eastward surges of relatively low-density surface waters as far as 160 km into the strait (Holbrook and Halpern 1982). Such reversals persist for several days and are expected to radically alter the point source contribution to the coastal current provided by the strait.

Depth Dependence

Since the Vancouver Island Coastal Current is primarily buoyancy driven, we expect it to be highly baroclinic (i.e., to have marked vertical shear in the longshore component of flow). This aspect of the current is clearly illustrated by Fig. 17 which shows the cross-shore distribution of mean longshore currents at two different shelf locations. We further expect the flow to be quasi-geostrophic such that the vertical shear is closely related to cross-shore gradients in density structure through the thermal wind equation. The close relationship between vertical shear and cross-shore density structure is seen by comparing Fig. 15 and 17. In the absence of frictional effects, the thermal wind balance reduces to

$$(4.1) \qquad \partial \bar{v}/\partial z = -\, g/f\rho\,\partial\bar{\rho}/\partial x$$

in which $\bar{v}$ is the mean longshore component of velocity, (x,z) are cross-shore and vertical coordinates, $\bar{\rho}$ is the mean density, g the acceleration of gravity and f the local Coriolis paramenter. In general, bottom friction and surface wind stress will also produce significant vertical

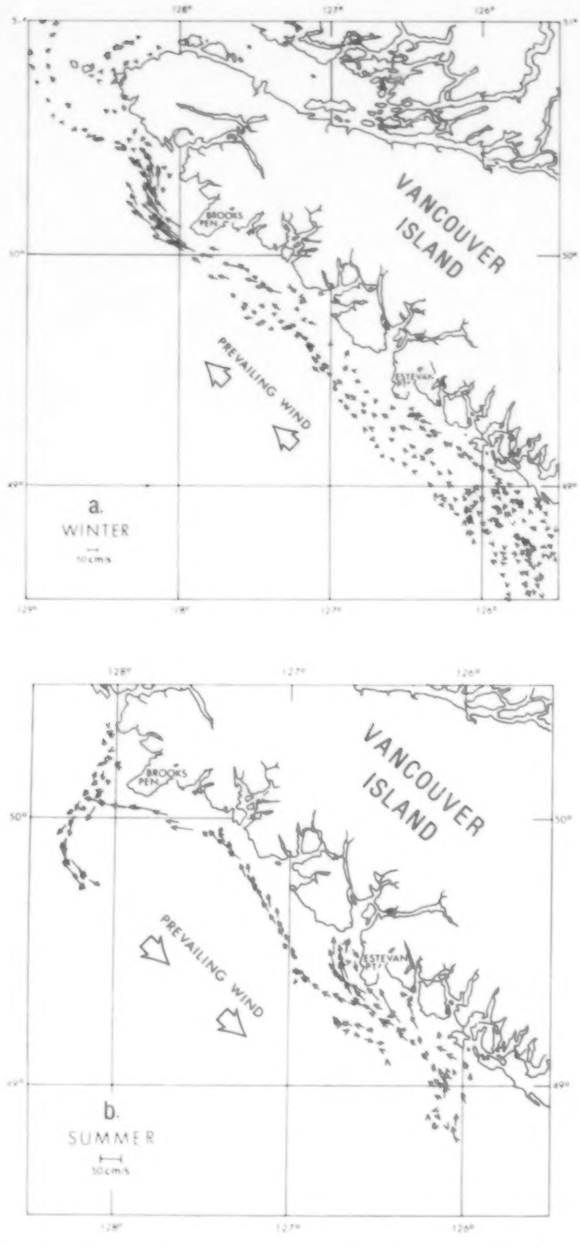

FIG. 10. Spatially averaged (over 5 km intervals) buoy trajectory speeds from the 1984 Canadian Search and Rescue Project (CANSARP) for (a) winter and (b) summer. (Prepared by Seaconsult Marine Research 1984).

shear so that (4.1) is only an approximate balance of terms. Topographic form drag and turbulent friction always reduce the mean flow speed in the lower boundary layer. However, corresponding frictional effects in the upper wind-driven layer increase the near surface flow speed if the buoyancy current and wind are in the same direction and decrease it if the wind and buoyancy flow are in opposing directions. Owing to opposing longshore winds, maximum speeds of the buoyancy current in summer often occur at depths of 10 to 20 m below the surface (cf. Fig. 17b). There will also be a rotation in the principal axis of the horizontal flow with depth due to frictional effects.

5. Temporal Structure

Direct observations reveal that the intensity and spatial structure of the Vancouver Island Coastal Current vary over time scales of days to years. Similar variations are observed for other coastal currents such as the Norwegian Coastal Current along the west coast of Norway (Mysak and Schott 1977; Mork 1981), the Leeuwin Current along western Australia (Cresswell and Golding 1980; Thompson and Veronis 1983), the Gaspé Current along the south shore of the Gulf of St. Lawrence (Tang 1980; Benoit et al. 1985) and the Alaska Coastal Current along the southern coast of mainland Alaska (Schumacher and Reed 1980; Royer 1981a, 1981b). Variations in runoff, wind, regional tidal currents and offshore circulation are among a variety of factors that can effect modifications to coastal current regimes. Shelf circulation can also be influenced by the poleward propagation of remotely forced coastally trapped waves (Allen and Denbo 1984; Hickey et al. 1988) and by local instabilities in which energy is exchanged between the mean and fluctuating components of the flow. Mixed barotropic-baroclinic mesoscale instabilities over the continental slope of the island will also have a marked influence on the spatial continuity of the coastal current (Mysak 1977; Ikeda et al. 1984a; Thomson 1984). Wind-induced topographically controlled eddies are observed to have a strong influence on the shelf-slope exchange processes (Thomson and Gower 1986). Wind mixing and convective overturn will further alter the coastal current structure in winter while surface heating will significantly modify the near surface signature in summer (Lane 1963).

Short-Term Fluctuations

For periods shorter than 2 days, currents over the Vancouver Island continental margin are dominated by diurnal and semidiurnal tidal fluctuations (Crawford and Thomson 1982, 1984). Superimposed on the these high frequency motions are fortnightly and monthly tidal variations plus slowly varying residual (non-tidal) currents with periods in excess of a few days. Tidal currents are generated directly by the astronomical tide-generating force whereas the residual currents are generated through non-tidal forcing mechanisms such as the wind, buoyancy flux or bottom friction. We ignore daily tidal variability in this paper.

Spectra of six-hourly geostrophic ("Bakun") coastal winds and low-pass filtered (tide-removed) near-surface current data from moorings T3, T4 and T5 of the Vancouver Island Coastal Current Experiment are presented in Fig. 18 and 19, respectively. The upper panels in Fig. 19 give the spectral density (left side) and variance preserving spectra (right side) for the cross-shore component of velocity; the lower panels give the corresponding values for the longshore component of velocity. Mooring T3 is within the coastal current regime while mooring T5 is within the shelf-break current regime.

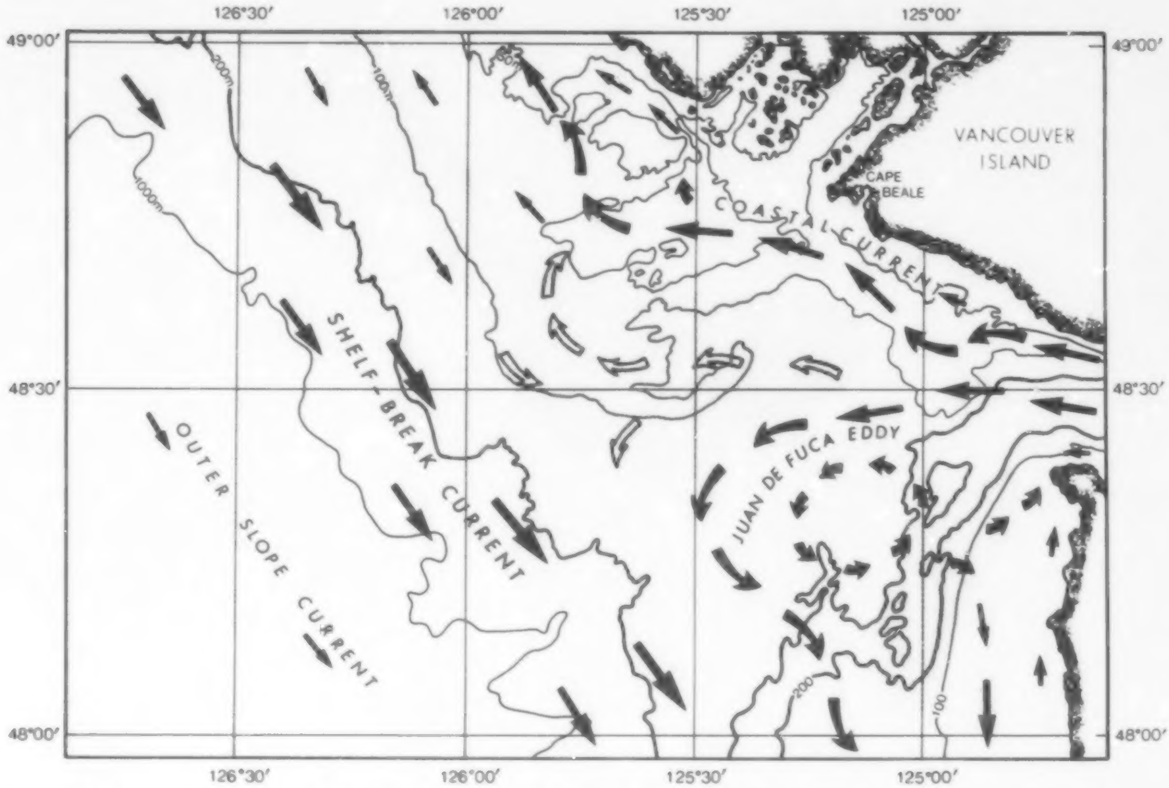

FIG. 16. Schematic plot of residual near-surface circulation over the southern continental margin of Vancouver Island in summer (from Ware and Thomson 1986). Shaded area denotes region of confused and variable flow.

All current spectra show evidence for tidally forced oscillations in the monthly and fortnightly bands and for wind-forced oscillations in the 3 to 10 day band, coincident with the spectral intensification in the wind spectrum (Fig. 18). Wind forced motions are especially prevalent in the upper 10 m of the water column and appear to dominate the cross-shore component at mooring T3. There also appears to be significant low-frequency current variability at periods in excess of a few months that is poorly resolved by the comparatively short 6 month time series. Similar levels of low frequency variability are observed in the salinity and temperature records. Marked fluctuations in the alongshore component of the wind occur at the diurnal period (24 h) associated with daily heating and cooling effects near shore. Verification of longshore diurnal winds has been presented by Thomson (1983) based on directly measured winds from a moored offshore weather station.

In summary, mean current variability in the upper 50 m at periods of days to months is dominated by wind and long-period tidal contributions. Fortnightly and monthly tidal components appear to predominate over the inner shelf (the coastal current regime) and outer shelf (the shelf-break regime) while wind-induced motion prevails over the transition zone (mooring T4) separating the coastal current from the shelf-break region. Wind effects also prevail in the upper 5–10 m of the water column and are responsible for the relatively low near-surface speeds of the coastal current in summer (cf. Fig. 17b). Clearly, northerly summer winds with speeds in excess of 10 m/s are capable of reversing the direction of the top 5 to 10 m of the coastal current. The fact that monthly and fortnightly variations prevail over the inner and outer shelf is presumably related to tidal rectification processes similar to those discussed by Thomson and Wilson (1987) for the southern Queen Charlotte Islands.

Seasonal Variability

The prevailing circulation over the continental margin changes markedly during spring and fall in concert with the annual cycle in the prevailing winds. These Spring and Fall Transitions are not gradual by oceanic standards but take place quite abruptly over periods of a week or so (e.g., Strub et al. 1987). The Spring Transition generally occurs between late February and early May along with a major reversal of the prevailing winds along the coast (Fig. 9). Associated with the wind reversal is a reversal in the current over the shelf-break, a lowering of mean coastal sea level (cf. Tabata et al. 1986), a re-stratification of the shelf/slope waters through increased warming and dilution of the near-surface shelf waters and the onset of upwelling conditions over the outer-shelf. The annual cycle in the shelf-break current is particularly noticeable and, in addition to direct current meter measurements, has been observed in geostrophic transport estimates

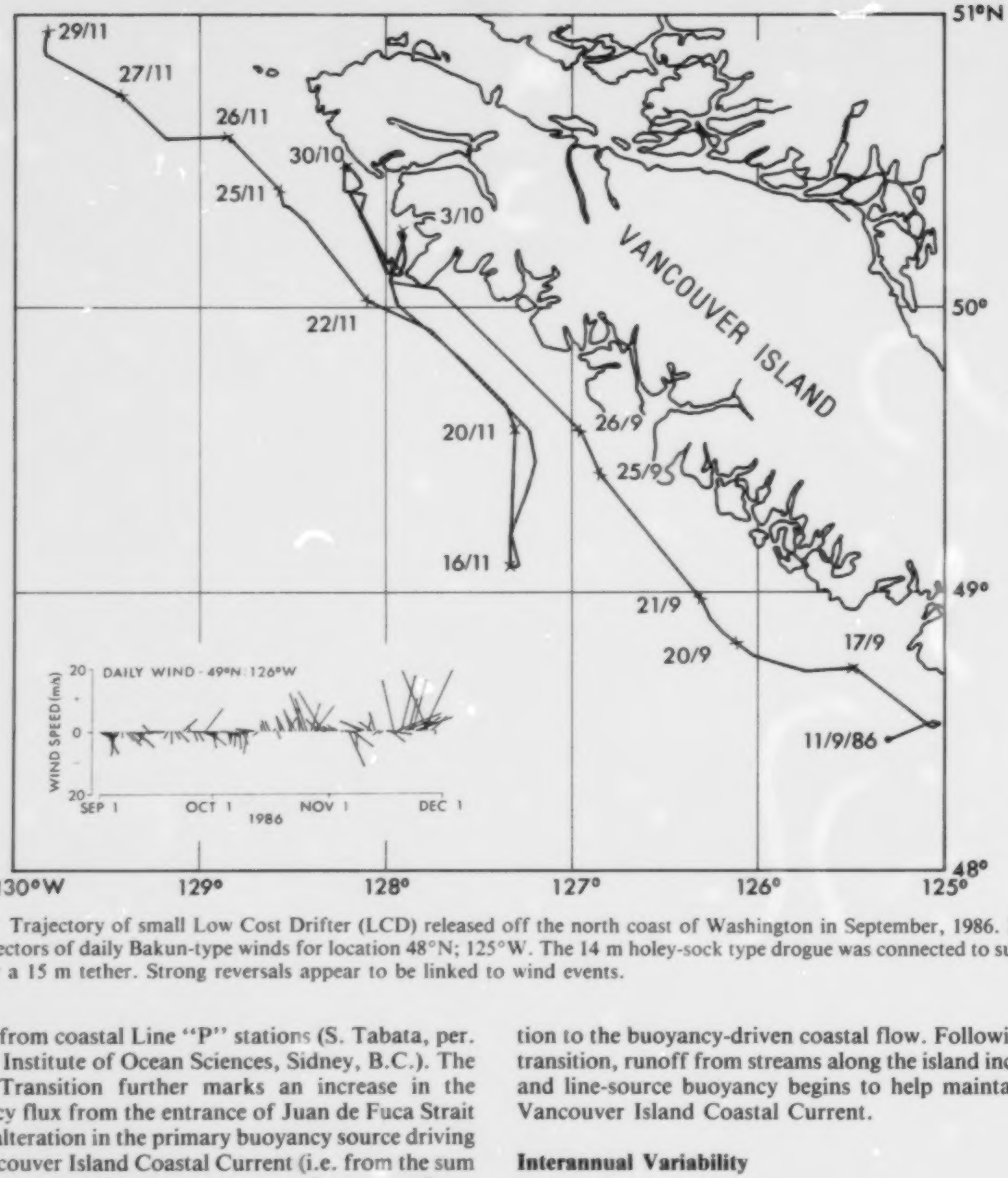

FIG. 12. Trajectory of small Low Cost Drifter (LCD) released off the north coast of Washington in September, 1986. Insert shows vectors of daily Bakun-type winds for location 48°N; 125°W. The 14 m holey-sock type drogue was connected to surface buoy by a 15 m tether. Strong reversals appear to be linked to wind events.

derived from coastal Line "P" stations (S. Tabata, per. comm., Institute of Ocean Sciences, Sidney, B.C.). The Spring Transition further marks an increase in the buoyancy flux from the entrance of Juan de Fuca Strait and an alteration in the primary buoyancy source driving the Vancouver Island Coastal Current (i.e. from the sum of a line source and point source to a point source alone; Fig. 8).

The Fall Transition occurs sometime between mid-September and late October coincident with the first major storm of the season. The reversal to prevailing southeast winds is accompanied by a reversal of the shelf-break flow, a rise in mean coastal sea level, enhanced wind and convective mixing of the surface waters and the cessation of upwelling. At this time, reversals in the estuarine flow near the entrance to Juan de Fuca Strait also become more frequent and more intensified. As illustrated by Fig. 20, the Fall Transition coincides with a marked reversal of the normal pattern of outflow of relatively low density water in the upper layer and inflow of relatively high density water in the lower layer. Such reversals will tend to reduce the point-source contribution to the buoyancy-driven coastal flow. Following the transition, runoff from streams along the island increases and line-source buoyancy begins to help maintain the Vancouver Island Coastal Current.

Interannual Variability

Year-to-year variations in the coastal current are expected to arise through interannual variations in the prevailing winds, coastal runoff and outer shelf/slope circulation. Long-term fluctuations in runoff include changes in total volume as well as spatial variations in the runoff distribution along the coast. Long-term offshore geostrophic wind data is available back to 1945 but the exact nature of the coastal current response to winds is still unknown. Aside from the monitored stream flow data dating back to about 1950 (LeBlond et al. 1983), there is no information on long-term variability of runoff for the British Columbia coast. Again, the response of the coastal current to changes in buoyancy forcing is unknown. Eventually, one would like to demonstrate a correlation between the intensity and

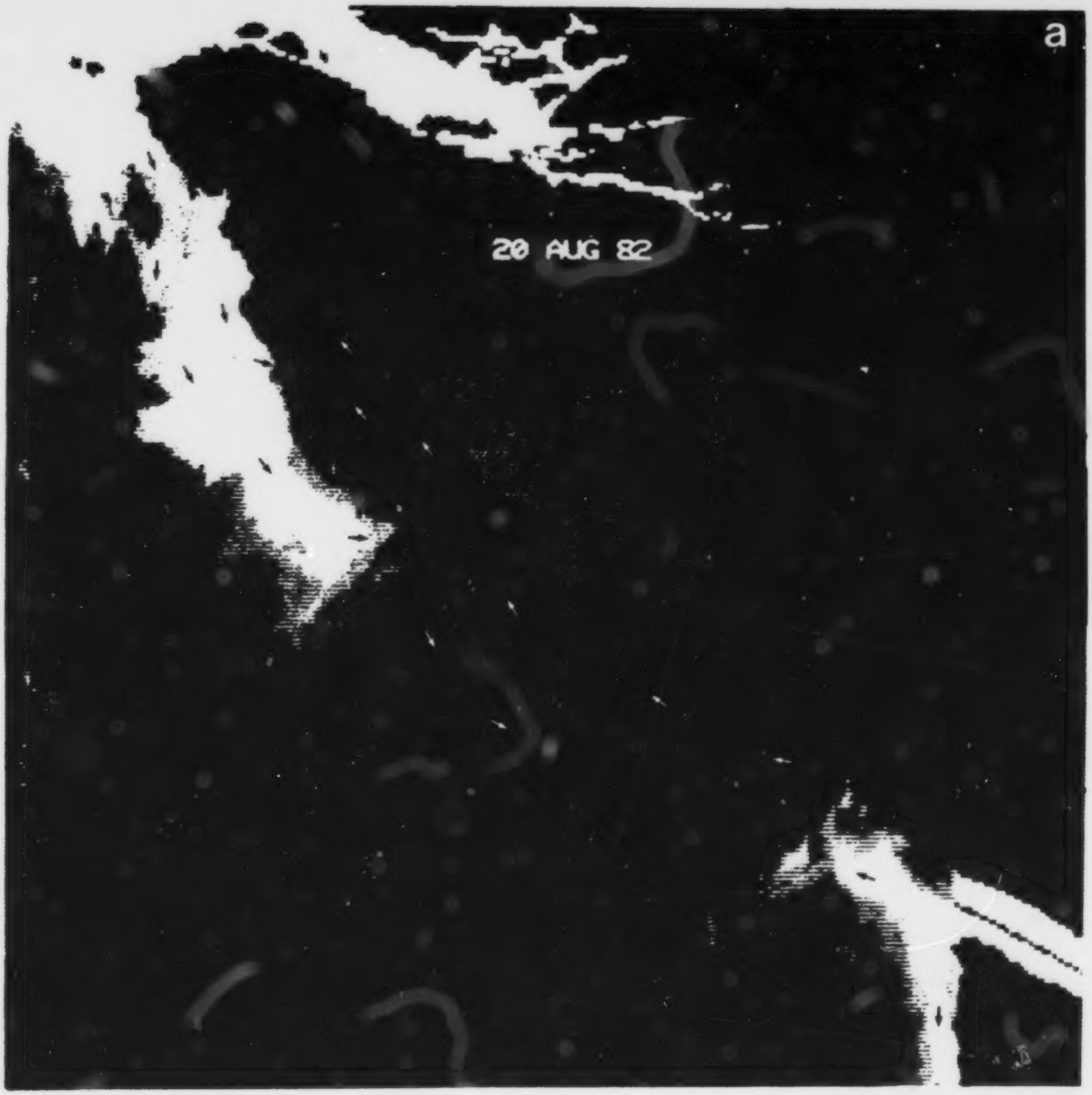

FIG. 13. NOAA satellite thermal images for the west coast of Vancouver Island. (a) 20 August, 1982. Lightest oceanic areas are about 11°C and darkest areas about 15°C; (b) 26 August, 1986. Light = 8°C and dark = 12°C; (c) 12 October, 1986. Light = 7°C and dark = 14°C. Arrows denote direction of flow. The Coastal Current, Juan de Fuca Eddy and wave-like flow perturbations are visible in all images. Relatively cold filaments penetrate southeastward past Brooks Peninsula in summer.

persistence of the coastal current and integrated coastal indices such as the temperatures and salinities obtained from lighthouse stations such as Amphitrite Point. Determination of the interannual scale effects of the shelf/slope region is a formidable problem that will not be readily understood in the next decade. The immediate hope for quantitative long-term information on the coastal current variability lies with data collected during the ongoing La Perouse and MASS (Marine Survival of Salmon) projects. The proposed 10-year program of data collection in the La Perouse Project (Ware and Thomson 1985, 1986) should provide insight into the principal oceanographic processes effecting long-term variability of the coastal current and fish recruitment on the southwest shelf.

6. Flow Dynamics

Except near the entrance to Juan de Fuca Strait, the cross-stream structure of the Vancouver Island Coastal Current represents an approximate geostrophic balance between a runoff-induced cross-shore pressure gradient and the Coriolis force. Low density water entering the coastal regime initially flows from the region of maximum

FIG. 13. (*Continued.*)

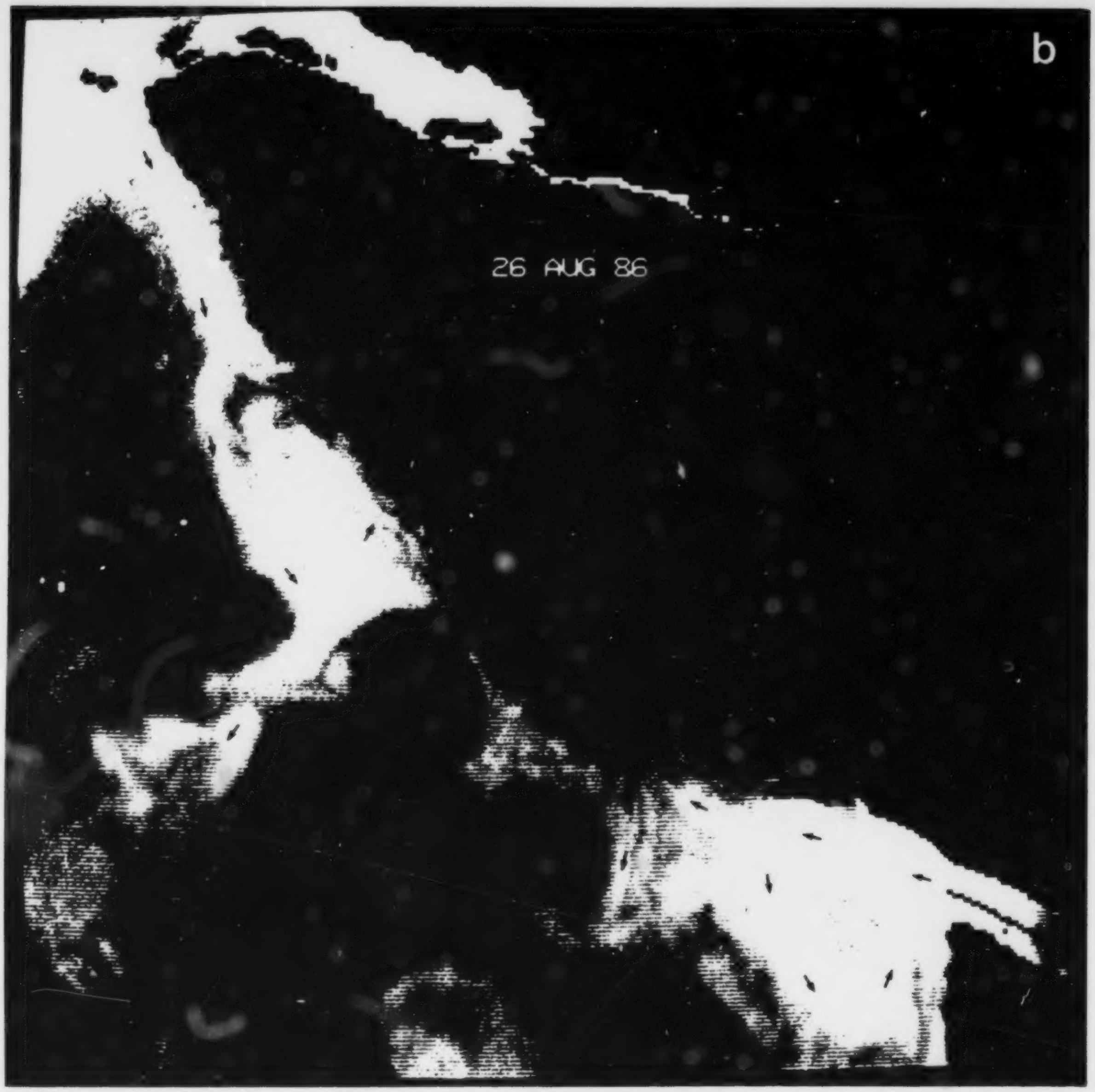

pressure (i.e., the region of maximum runoff accumulation and hydraulic head) toward some offshore region of minimum pressure. The effect of the Coriolis force is to turn the flow to the right (in the northern hemisphere) so that a geostrophically adjusted current moves poleward along the coastal boundary. However, in the absence of other processes, the flow would not remain confined to the coast but would gradually spread seaward and mix with adjoining waters as the flow advanced alongshore. Near the entrance to Juan de Fuca Strait, the flow is further affected by variations in the initial momentum of the outflowing strait water, by bottom friction, and by the complicated bathymetric gradients. Nonlinear tidal rectification also appears to be important over the shallow banks on the southern shelf.

The longshore integrity of the coastal current implies that mechanisms other than those associated with geostrophy also contribute to its existence or that there is a continuous longshore source of freshwater. Although the flow structure is poorly understood, it is clear that coastal winds and buoyancy source distribution can only account for near-shore confinement of the current in winter. In summer, the winds are counter to the coastal current and therefore have a tendency to retard the poleward flow in the near-surface layer and to transport the water offshore as part of a surface Ekman drift. The alongshore continuity of the current in summer must then be due to the topographic restoring influence of the inner shelf topographic gradient, bottom friction or cross-shore pressure gradients associated with coastal upwelling.

FIG. 13. (*Concluded.*)

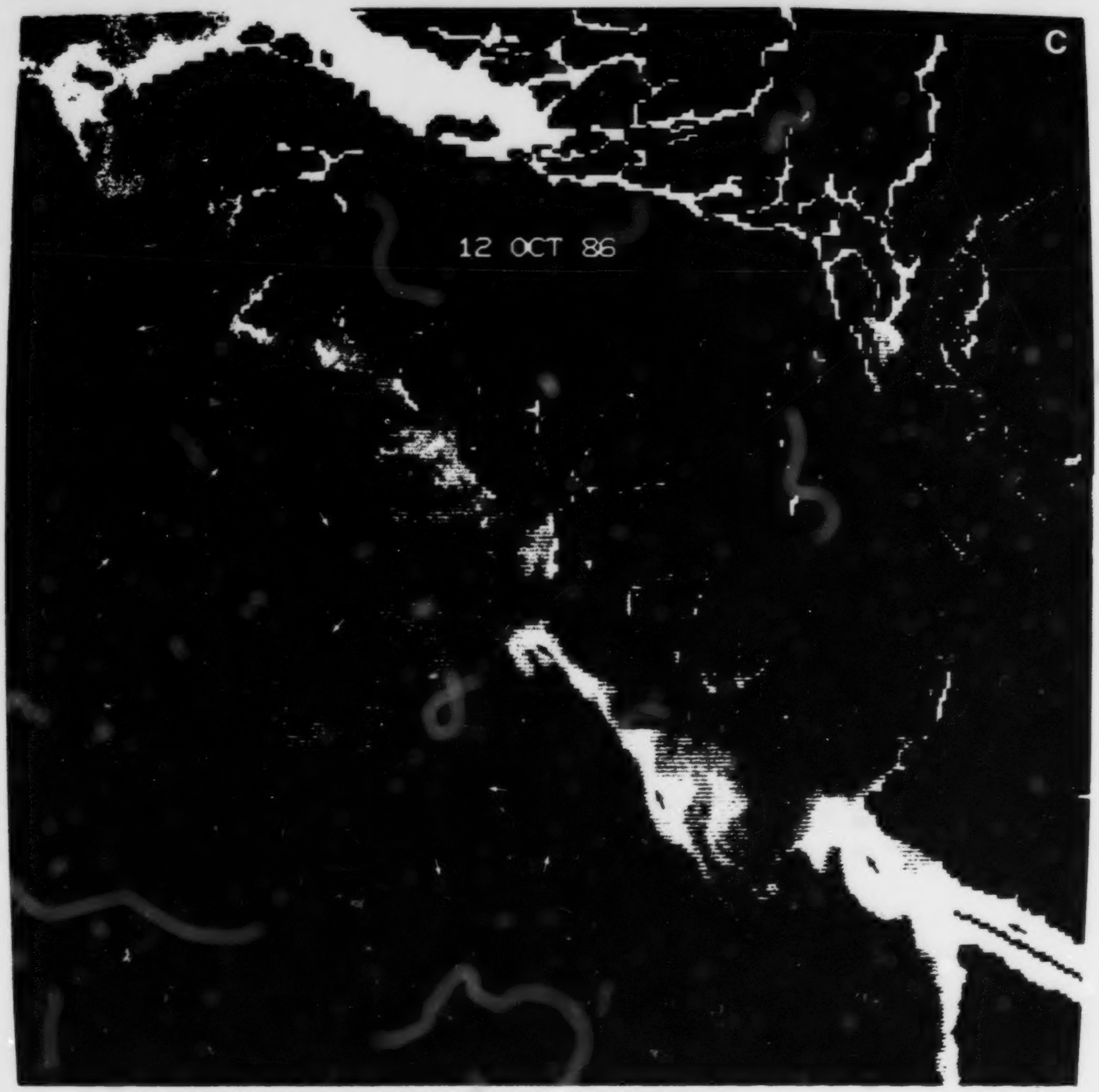

Tidal Rectification

In regions of marked topographic gradients and bottom friction, the non-linear interaction of diurnal and semidiurnal tidal currents can lead to the formation of strong residual ("tidally rectified") currents. Self interaction of the diurnal or semidiurnal currents generates a mean time-independent flow pattern while cross interaction between different tidal constituents (e.g., the M_2 and S_2 tidal current constituents) leads to mean currents with fortnightly and monthly variability. This mechanism is found to be particularly important along the British Columbia coast due the presence of strong and spatially variable tidal streams (Thomson and Wilson 1987; Wilson and Thomson 1989).

Tidal rectification for frictional two-layer flow over the southern Vancouver Island shelf has been described in a recent model developed by Wilson (pers. comm.). Principal time-averaged features in the model are the well defined eddies over the shallow fishing banks and the strong intensified currents over the regions of relatively pronounced seafloor gradients. A strong clockwise eddy occurs over Swiftsure Bank at the entrance to Juan de Fuca Strait and along the western boundary of Juan de Fuca Canyon (Fig. 21). Strong counterclockwise eddies occur to the west of Cape Flattery on the Washington coast and over Amphitrite Point to the north of Barkley Sound. A comparatively intense southeastward flowing current develops along the edge of the La Perouse Bank region and a correspondingly intense northward flow

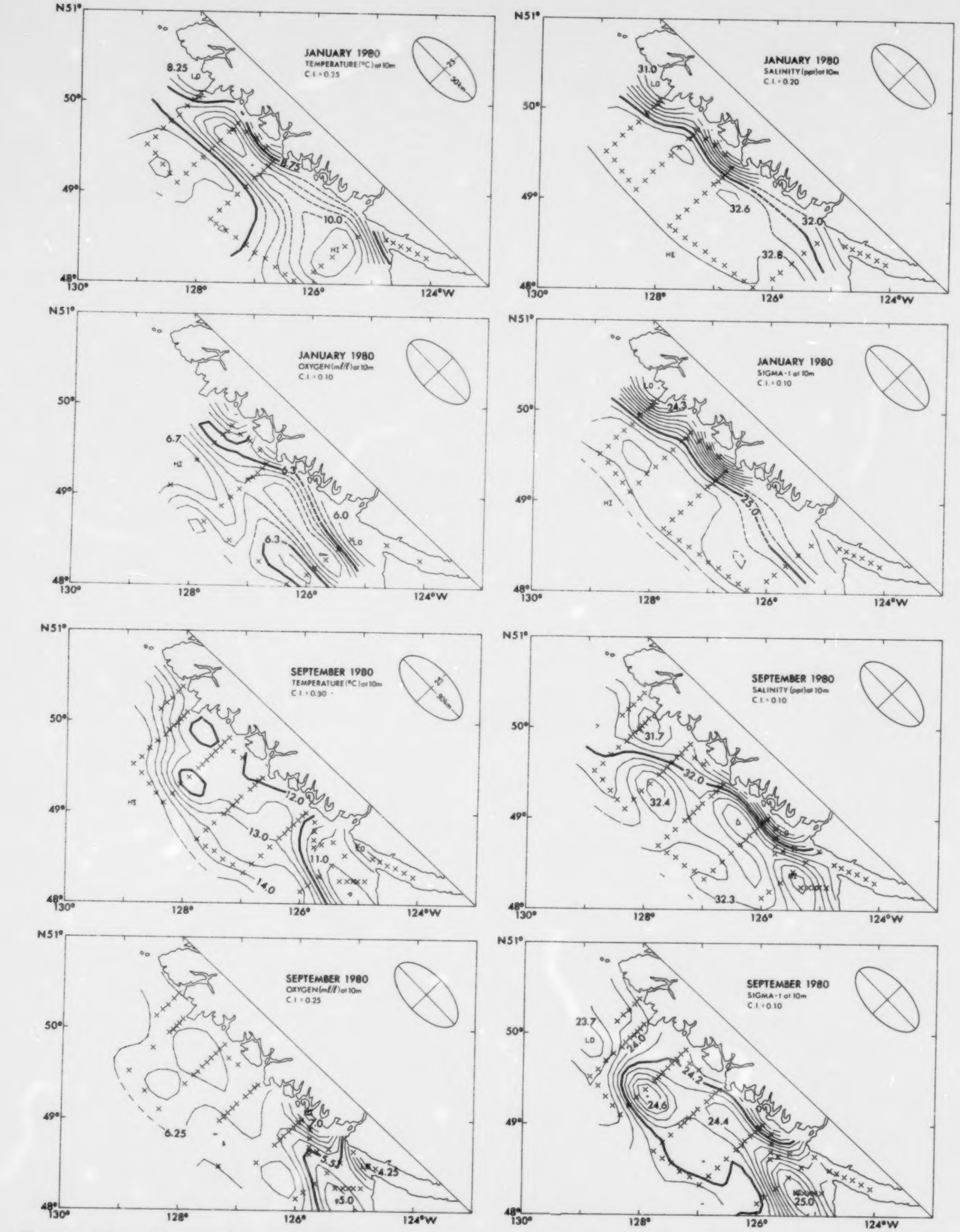
N51°
50°
49°
48°
130°
128°
126°
124°W
JANUARY 1980
TEMPERATURE (°C) at 10m
C.I. = 0.25
25
50km
8.25
LO
8.75
10.0
HI
JANUARY 1980
SALINITY (ppt) at 10m
C.I. = 0.20
31.0
LO
32.6
32.0
32.8
HI
JANUARY 1980
OXYGEN (ml/l) at 10m
C.I. = 0.10
6.7
HI
6.3
6.0
6.3
LO
JANUARY 1980
SIGMA-t at 10m
C.I. = 0.10
LO
24.3
25.0
HI
SEPTEMBER 1980
TEMPERATURE (°C) at 10m
C.I. = 0.50
25
50km
12.0
13.0
11.0
LO
14.0
HI
SEPTEMBER 1980
SALINITY (ppt) at 10m
C.I. = 0.10
31.7
32.0
32.4
32.3
SEPTEMBER 1980
OXYGEN (ml/l) at 10m
C.I. = 0.25
6.25
7.0
5.5
4.25
5.0
SEPTEMBER 1980
SIGMA-t at 10m
C.I. = 0.10
23.7
LO
24.0
24.2
24.6
24.4
25.0

FIG. 14. Objectively smoothed near-surface water property maps. (a) January, 1980; (b) September, 1980; (c) June, 1984; (d) July, 1984. Crosses show actual station locations. Key gives depth of mapped surface (10 m in 1980 and 50 m in 1984), the contour interval (C.I.) and, in the ellipse, the assumed cross-shore and longshore correlations scales of 25 and 50 km, respectively.

FIG. 14. (*Concluded.*)

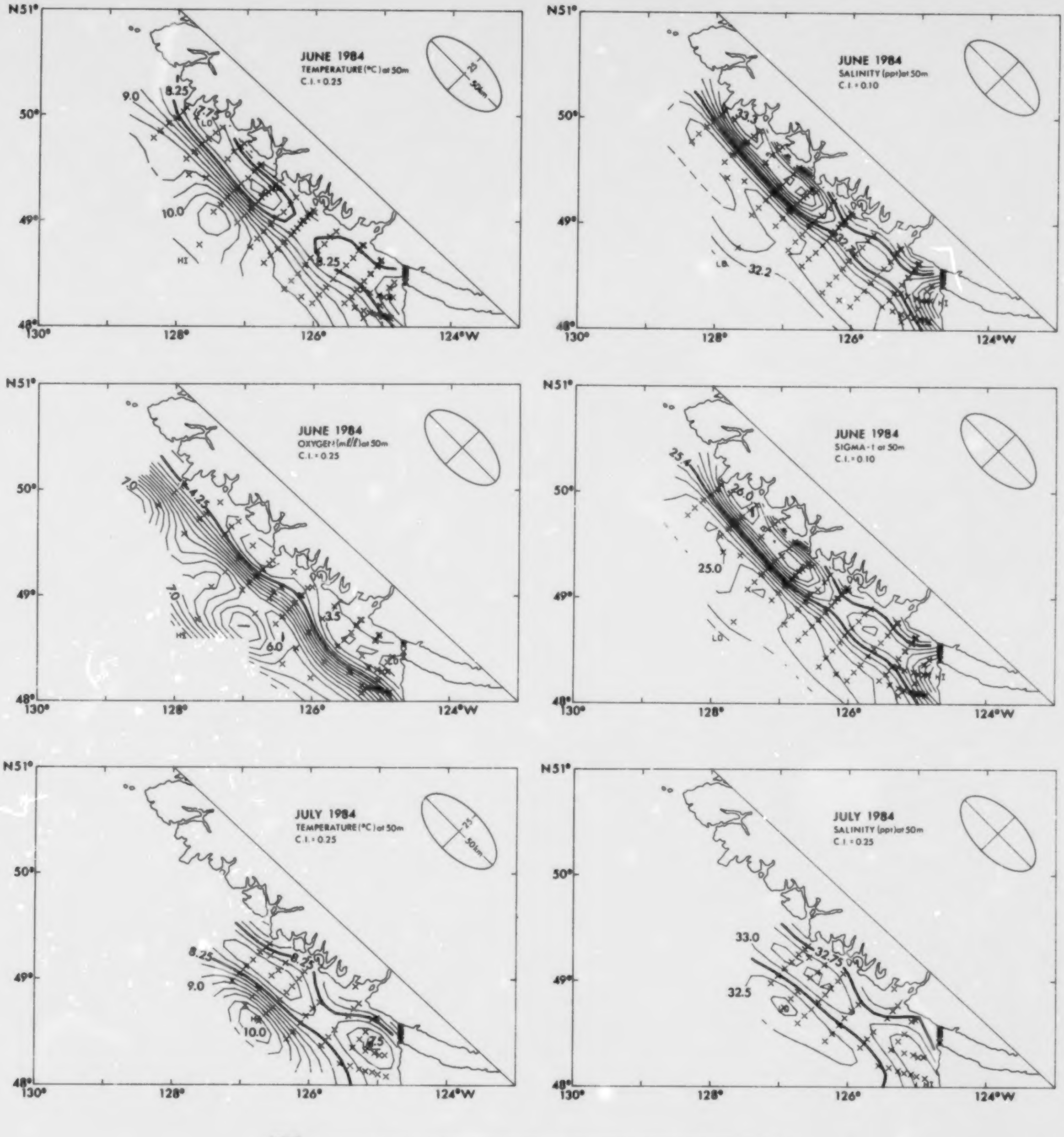
JUNE 1984
TEMPERATURE (°C) at 50m
C.I. = 0.25
9.0
8.25
7.75
LO
10.0
HI
8.25
JUNE 1984
SALINITY (ppt) at 50m
C.I. = 0.10
33.3
32
LO
32.2
HI
JUNE 1984
OXYGEN (ml/l) at 50m
C.I. = 0.25
7.0
4.25
7.0
HI
3.5
6.0
LO
JUNE 1984
SIGMA-t at 50m
C.I. = 0.10
25.4
26.0
25.0
LO
HI
JULY 1984
TEMPERATURE (°C) at 50m
C.I. = 0.25
8.25
8.25
9.0
HI
10.0
7.5
JULY 1984
SALINITY (ppt) at 50m
C.I. = 0.25
33.0
32.75
32.5
HI
JULY 1984
SIGMA-t at 50m
C.I. = 0.25
25.5
25.5
25.0
26.0
25
50km
N51°
50°
49°
48°
130°
128°
126°
124°W

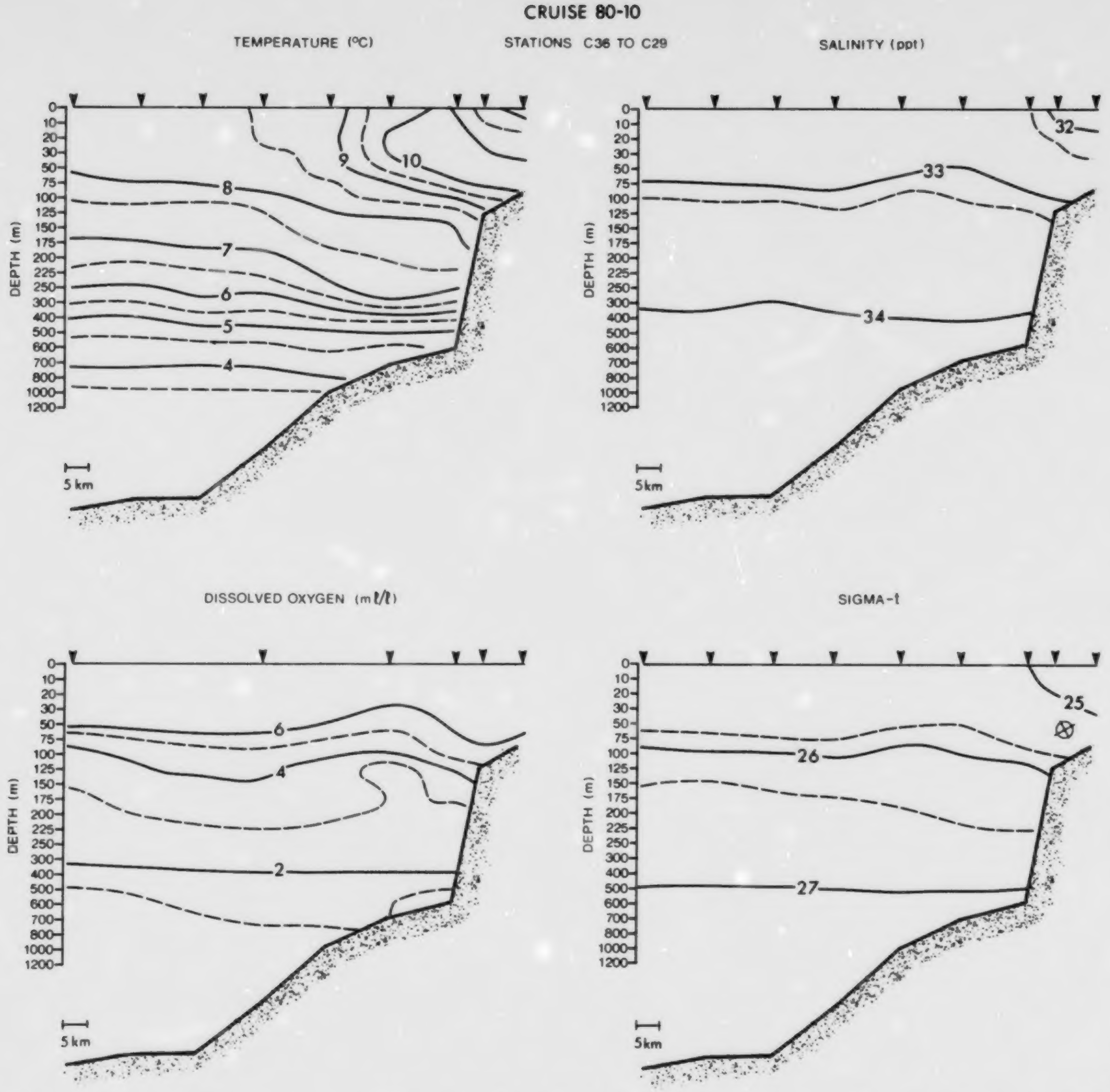

FIG. 15. Objectively smoothed cross-sections of water properties for (a) Tatchu Point line, January 1980; (b) Tatchu Point line, September 1980; (c) Estevan Point line, January 1980; (d) Estevan Point line, September 1980. Approximate maximum water depths 2000 m. The symbol ⊗ in density plot indicates the presence of the coastal current.

develops over the edge of the continental shelf. For the most part, the tidally rectified current is counter to the direction of the Vancouver Island Coastal Current in the near-shore regime. Thus, we can expect the buoyancy-driven component of the flow to be considerably modified by non-linear tidal effects over the southern portion of the shelf.

7. Relevance to Fisheries

The year-round persistence of the Vancouver Island Coastal Current together with its marked intensity, well defined cross-shore structure and considerable longshore extent make it a key factor influencing water properties and circulation over the continental margin. On this basis, we assume that the coastal current will also have a strong influence on the migration and survival of fish and shellfish stocks in the region. In this section, we outline the specific characteristics of the circulation that support this notion and which lead to a distinction between the longshore conduit and cross-shore barrier aspects of the coastal current. Although much of what we have to say is in the realm of speculation, some of the ideas may eventually lead to testable hypotheses.

We identify four distinct temporal stages of the coastal current structure based on runoff and wind conditions: Winter Domain; Spring Transition Domain; Summer Domain; Fall Transition Domain. The four periods coincide (and overlap) with distinct biological time

FIG. 15. (*Continued.*)

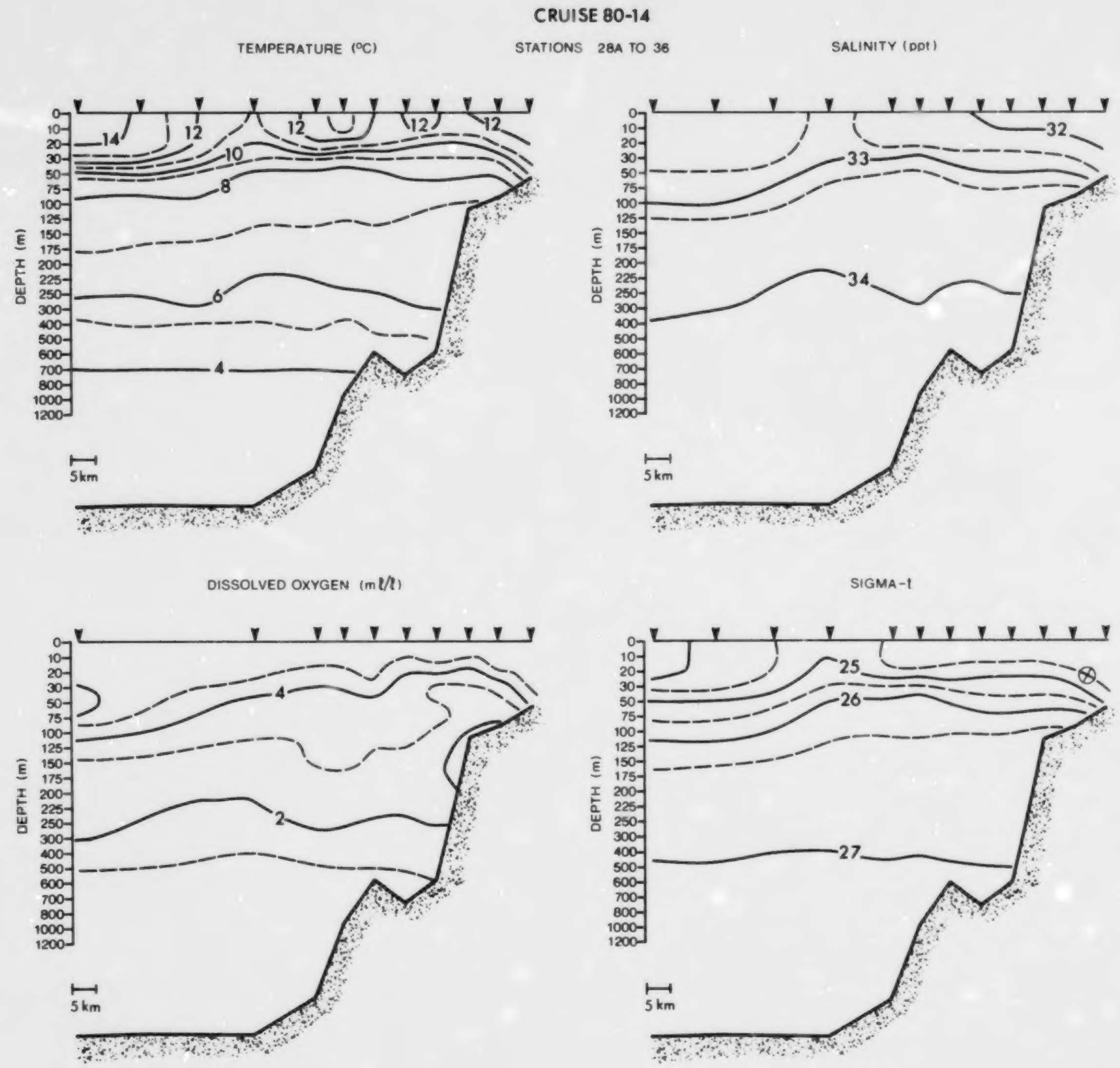
CRUISE 80-14

STATIONS 28A TO 36

periods characterized by differences in ontogeny (egg, larvae and juvenile stages) of various species. Schematic representations of the characteristic flow pattern over the continental margin for the comparatively steady (non-transient) winter and summer periods are presented in Fig. 22a and 22b, respectively.

Winter Domain: October–February

From October through February, the west coast of Vancouver Island is characterized by prevailing southeasterly winds, line-source type buoyancy flux and intense (atmospheric) surface cooling. Augmented by the prevailing winds, the buoyancy-driven coastal current provides a mechanism for poleward advection of eggs, larvae and juvenile fish that occupy (or are swept into) the inner shelf regime. At this time of year, we expect wind-induced onshore convergence of the nearsurface waters and a tendency for the coastal current (defined by a well mixed low salinity/temperature structure) to be confined to the nearshore region (Fig. 22a). Brackish water flowing seaward from the inlets will be advected northward and into southern Queen Charlotte Sound. This, combined with longshore integrity of the coastal current due to the combined input from the winds and local runoff, is expected to provide a broad biomass "conduit" along the entire shelf from the entrance to Juan de Fuca Strait to Queen Charlotte Sound. In contrast to the coastal current regime, poleward wintertime flow within the outer shelf/slope regime will be weaker and less stable, although the coastal current is subject to instability and eddy formation similar to that of other buoyancy-driven flows (e.g., Mork 1981). Mesoscale baroclinic instability processes centered over the continental slope (Mysak 1977; Ikeda et al. 1984a, 1984b) are expected to severely disrupt shelf-break flow

FIG. 15. (*Continued.*)

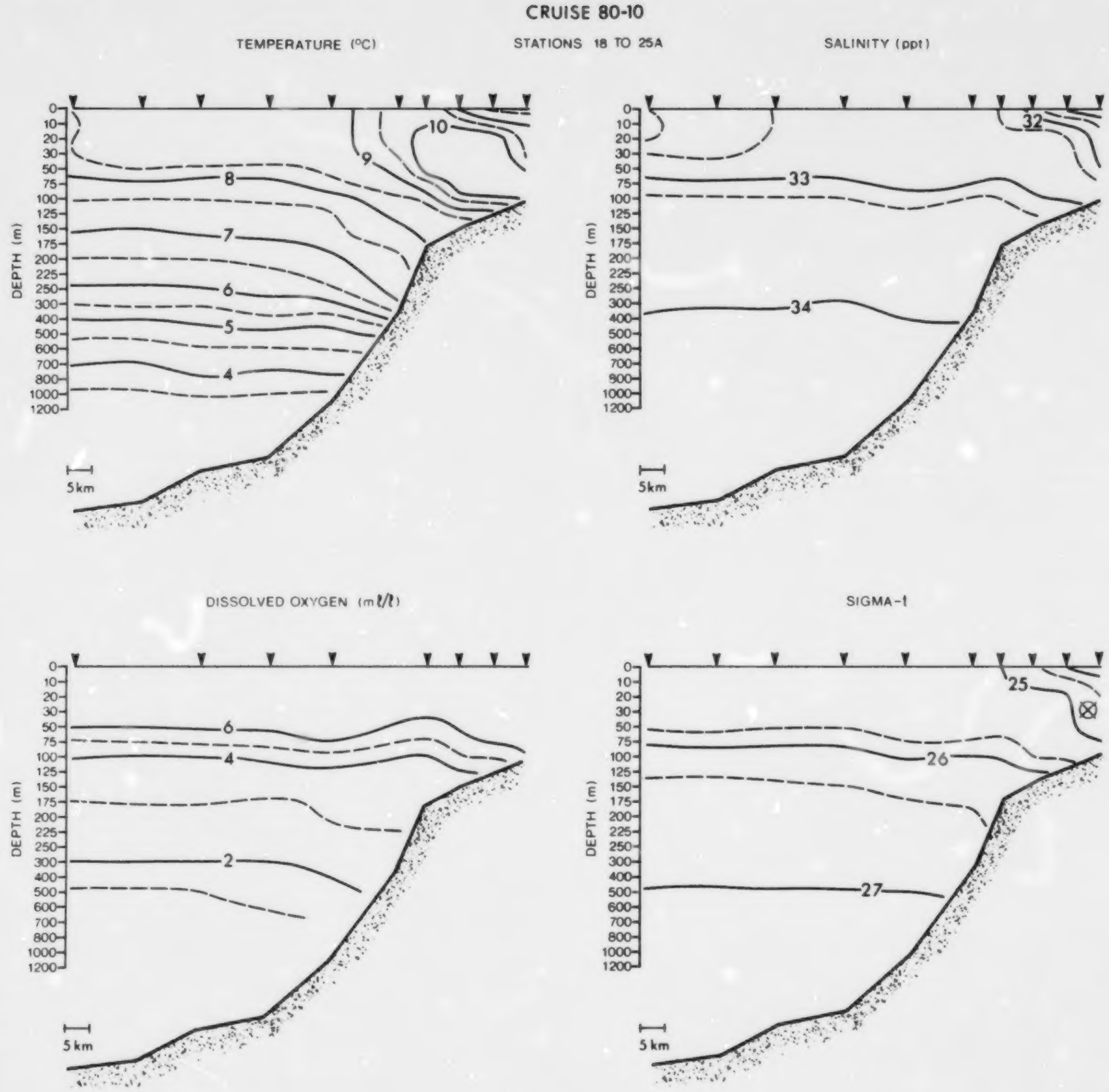

CRUISE 80-10

STATIONS 18 TO 25A

TEMPERATURE (°C)

SALINITY (ppt)

DISSOLVED OXYGEN (mℓ/ℓ)

SIGMA-t

at periods of weeks to months and could have a profound effect on the coastal current over the relatively narrow central and northern sectors of the shelf.

The above pattern will be somewhat modified during extended periods of weak southeasterly winds but continued northerly flow. According to the model of Zhang et al. (1987), geostrophic tilting of the interface between the upper and lower layers under these conditions will cause the surface flow to weaken and spread offshore. Significant accumulation of relatively low density Juan de Fuca Strait water over the La Perouse Bank region can take place.

Interannual variations in winter-time horizontal biomass transport by the coastal current will arise in accordance with corresponding variations in the intensity, cross-shore extent and longshore persistence of the current. The latter will result from year-to-year differences in coastal runoff, prevailing winds and shelf-slope interaction, with differences in coastal runoff affecting both the strength of the buoyancy forcing as well as the stability of the coastal current. Years with considerable eddy-shedding activity are expected to result in anomalously large net cross-shore seaward transport of coastal waters and associated eggs or larvae.

Spring Transition Domain: February–May

The Spring Transition is a relatively abrupt alteration in the physical oceanographic structure that takes place along the west coast of North America in early spring. Long-term wind, sea-level and temperature observations indicate that the transition occurs earliest off northern

FIG. 15. (*Concluded.*)

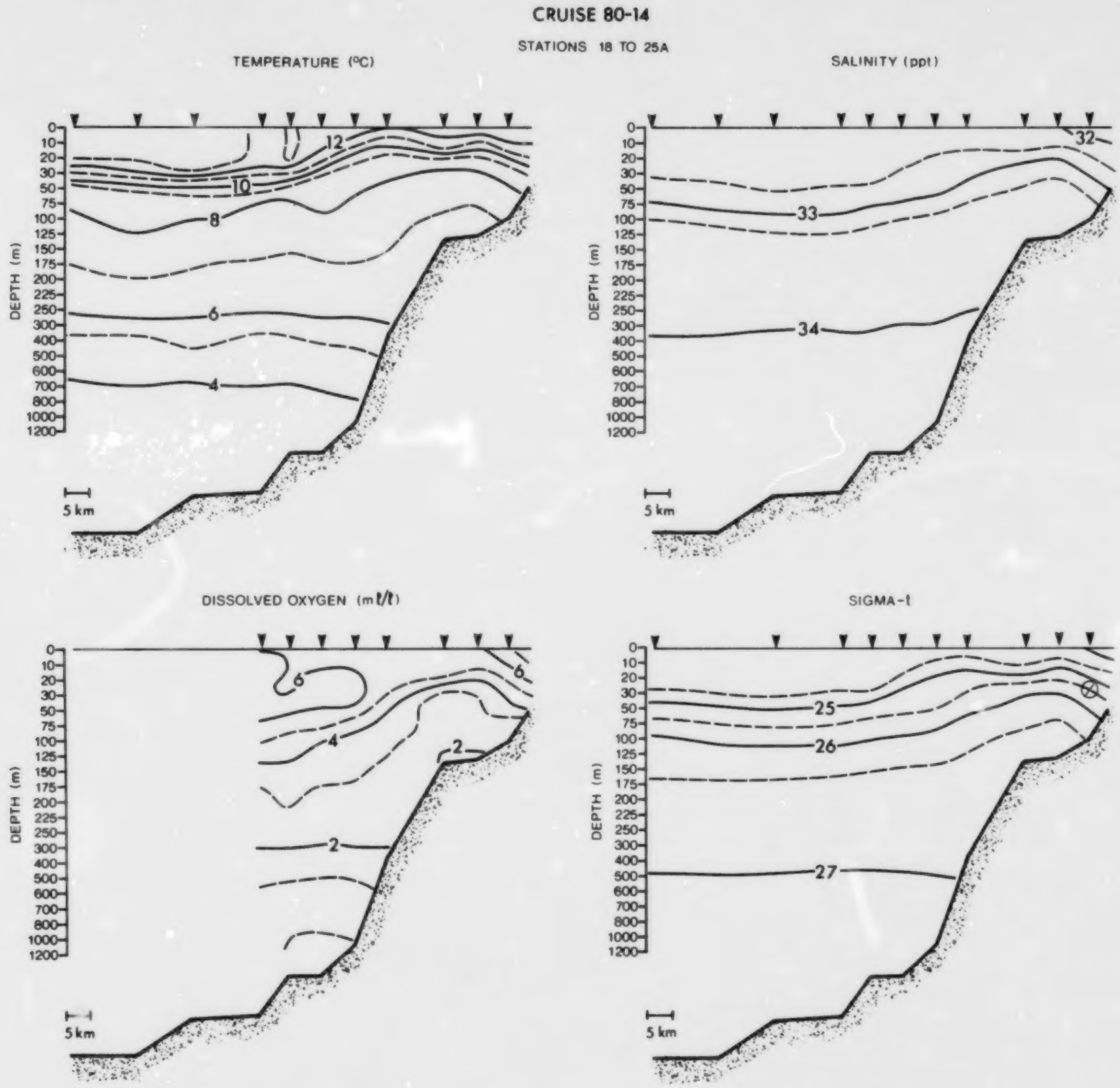

California and moves poleward to the British Columbia coast in a period of about a week. Off the southern British Columbia coast, the transition occurs sometime between early February and late April. At this time there is a transition from southerly to northerly winds, decreased buoyancy flux from coastal precipitation and a reversal of the longshore flow along the outer shelf. The Coastal Current begins to flow "counter" to the prevailing winds and shelf-break currents along the continental margin. Upwelling favourable conditions are simultaneously established along the coast. The transition period is also accompanied by a period of increased biological activity and onshore migration at depths of several hundred metres of certain species of larvae e.g., sablefish (Ware and Thomson 1987).

It is logical to speculate that year-to-year differences in the timing and abruptness of the Spring Transition could have a significant influence on fish stocks on the southern coast. A protracted delay in the reversal of the outer shelf current would mean continued poleward transport of biomass and little opportunity for the establishment of confined circulation and possible associated plankton growth over the southern banks region. Runoff from adjoining inlets would continue to be carried poleward by the coastal current. The coastal current would therefore act as a cross-shore "barrier" to biological exchange processes. An early and abrupt transition, with relatively few minor reversals in winds and currents during the transition period, would encourage growth processes through early establishment of upwelling favourable conditions, longshore advection of nutrients and formation of weak and quasi-confined circulation over the banks. In this case, the weak and confined bank circulation is comprised of an arm of the

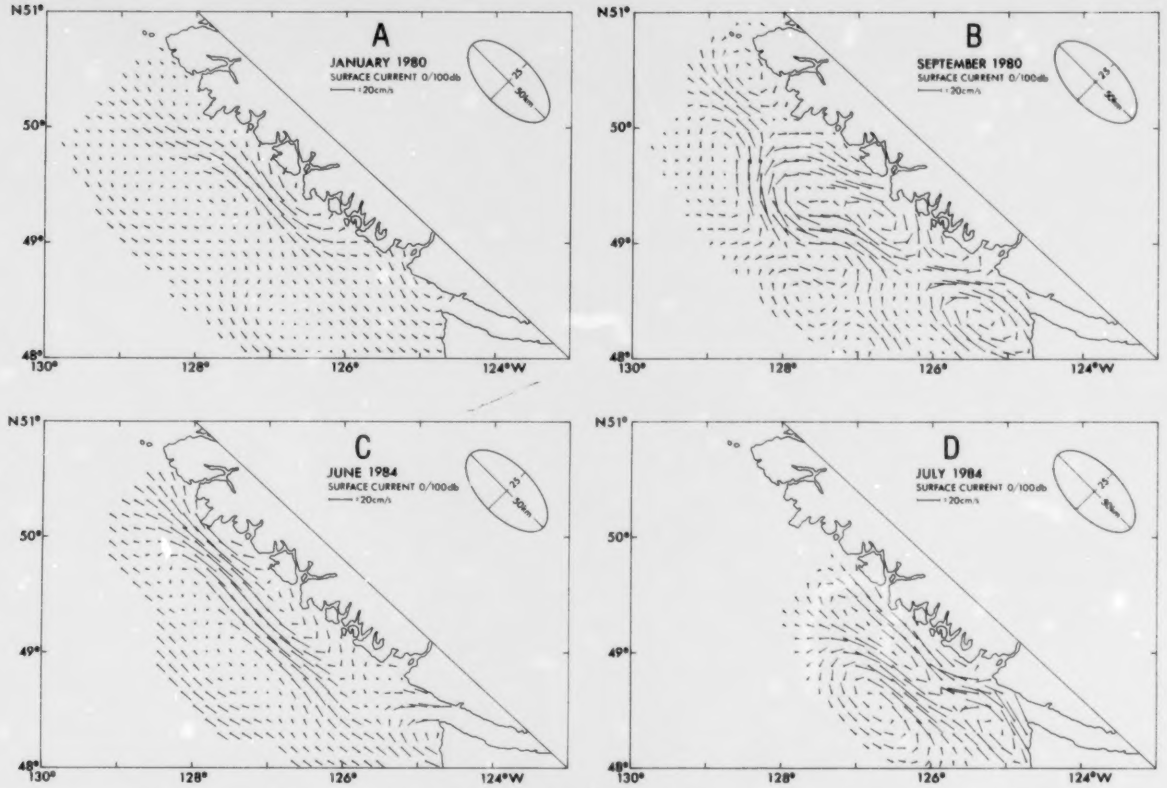

FIG. 16. Geostrophic currents relative to 100 m depth for the survey periods shown in Fig. 14. Derived from objectively smoothed maps of dynamic height topography. Speeds are obtained using given scale. Currents at the boundaries of the domain are dubious.

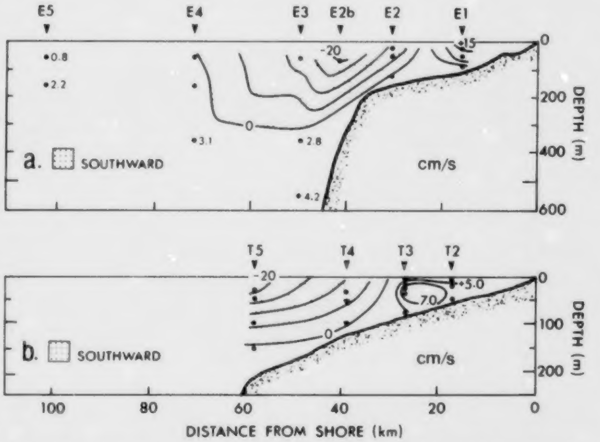

FIG. 17. Cross-sections of directly observed monthly mean longshore component of current velocity. Large dots show positions of current meters. (a) Upper 600 m of the Estevan Point line (CODE) for July 1980; (b) Tofino line (VICC Experiment) for July 1984. Stippled areas denote negative (southeastward) flow. Speeds in cm/s.

coastal current that flows over the banks. Thus, we tentatively link an early and abrupt transition with seaward extension of the coastal current and subsequent growth-favourable conditions over the southern banks; a late or highly variable transition is linked to delayed growth, maturity and survival of susceptible fish stocks over the southern shelf.

Summer Domain: May–September

From approximately May through September, the coastal current is driven primarily through surface outflow from Juan de Fuca Strait. During this period, the coastal current appears to move seaward over the southern portion of the shelf before forming into a narrow inner shelf current to the north of Barkley Sound (Fig. 22b). Outflow from the sound is commonly transported cross-shore and tidal rectification eddies may contribute significantly to the net circulation over the banks. The accumulation of runoff over the banks combined with clockwise rotary motions of the tidally rectified "residual" flow results in an extensive region of weak circulation. Marked upwelling occurs over the shelf-break (Fig. 6) with subsequent onshore transport of deeper slope waters onto the outer shelf. To the north of Barkley Sound, the coastal current again acts as a major "barrier" to cross-shore exchange. The flow in this region is longshore with a mid-shelf doming of density surfaces (Fig. 14) that marks the transition from offshore Ekman transport on the outer shelf to onshore Ekman transport on the inner shelf. This diversion of the surface Ekman flow appears to inhibit movement of animals (such as crab megalopae) from the outer shelf to the inner

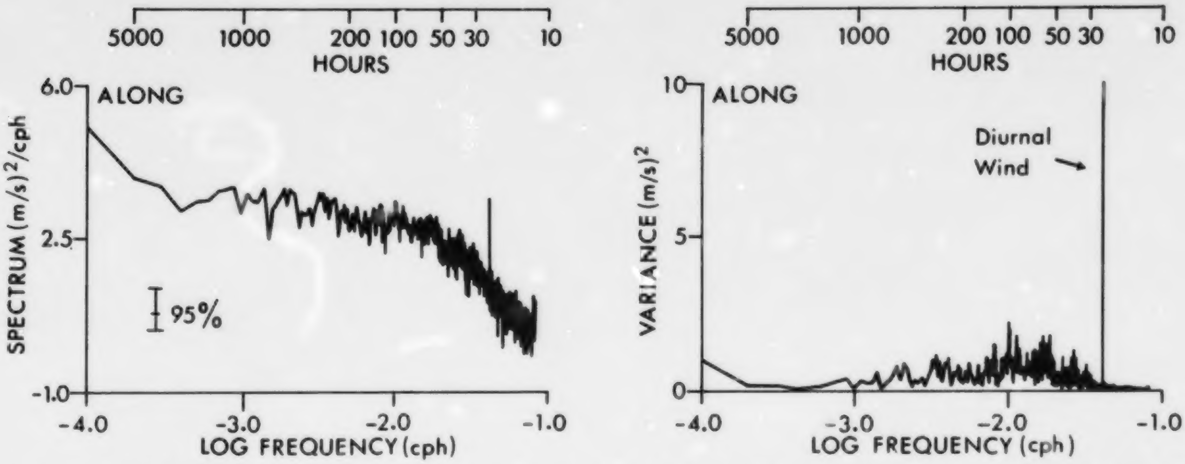

FIG. 18. Spectra of the longshore component (315°T) of the 6-hourly Bakun wind record (location 49°N; 126°W) for the 4-yr period 1 January, 1983 to 31 December, 1986. (a) Spectral density plot; (b) Energy preserving spectral plot (variance spectra). Bandwidth = 10^{-4} cycles per hour (cph).

coastal waters (Glen Jamieson, pers. comm.). At the same time, the coastal current may serve as a "conduit" to the longshore movement of certain nearshore species. In particular, ". . .sockeye smolts may use the northward flowing Vancouver Island Coastal Current as a directing and as a transport mechanism." (Healey 1987).

The coincidence of weak flow combined with relatively warm (surface heated) and fresh stably stratified water over the La Perouse Bank region is conducive to rapid biological growth and the allowance for energy propagation to higher trophic levels. Reversals of the coastal current due to prolonged periods of strong (> 10 m/s) longshore winds is also expected to enhance regional biological activity by contributing to the accumulation of brackish water over the outer banks (cf. Denman et al. 1981). Coincidentally, relaxation of the coastal current leads to a break-down of the barrier to cross-shore transport associated with the doming density ridge centered over mid-shelf and to a diminished longshore transport mechanism. We anticipate that year-to-year variations in primary productivity and recruitment of major fish stocks may be linked to the persistence of the weak circulation over the banks and to the duration of reversal or weak poleward flow of the coastal current in summer. This will be especially true of species such as salmon whose first year survival may be critical to ultimate recruitment to the fisheries.

In addition to longshore flow, the temperature and salinity of the near-surface waters advected by the coastal current affect the biological environment. Years when relatively warm water is carried along the coast from Juan de Fuca Strait may have a significantly different impact on recruitment than years when relatively cold water is carried longshore. As noted in the introduction, this impact may be direct through the fish environment or indirect through levels of planktonic productivity.

The other prominent feature of the summer circulation that may directly affect the west coast fisheries is the southward penetration of large filaments (or "squirts") from the vicinity of Brooks Peninsula (Fig. 12). The extensive 100 km long cold water tongues are most frequently seen in late summer and appear to originate as separated branches of an upwelling-induced shelf-break current that forms in the region south of Cape Scott. Coastal runoff that moves seaward via central Queen Charlotte Sound may also contribute to this current. The filaments surge southward past Brooks Peninsula and cross the continental margin carrying cold low salinity water seaward as far south as 48°N. The presence of these filaments appears to arrest or reverse the Vancouver Island Coastal Current. Water associated with the coastal current can accumulate to the south of the peninsula, be swept southward by the filament, or squeeze past the peninsula. Fish that normally use the coastal current for northward (or homeward) migration could be temporarily disrupted at times of filament formation or blockage of northward coastal current penetration. Thus the timing of arrival of returning adult salmon at the coast may effect the well known interannual variation in salmon diversion through Juan de Fuca versus Johnstone straits (Mysak 1986). We speculate that this disruption may have a profound influence on the eventual survival and year-class strength of the particular species.

Fall Transition Domain: September–October

The first major storm of the season typically occurs between late September and mid-October. This marks a reversal in the prevailing winds and currents over the continental margin and the return of winter oceanographic conditions along the coast. As with the situation in early spring, the Fall Transition is generally fairly abrupt with the alteration in oceanic conditions occurring over a relatively short period of a few weeks.

The effect of the Fall Transition is to accelerate the coastal current and, presumably, to concentrate the buoyancy flux closer to shore. This, combined with a break-down in the comparatively weak circulation over the banks, cessation of coastal upwelling and collapse of the ridge-like oceanic water property structure over the

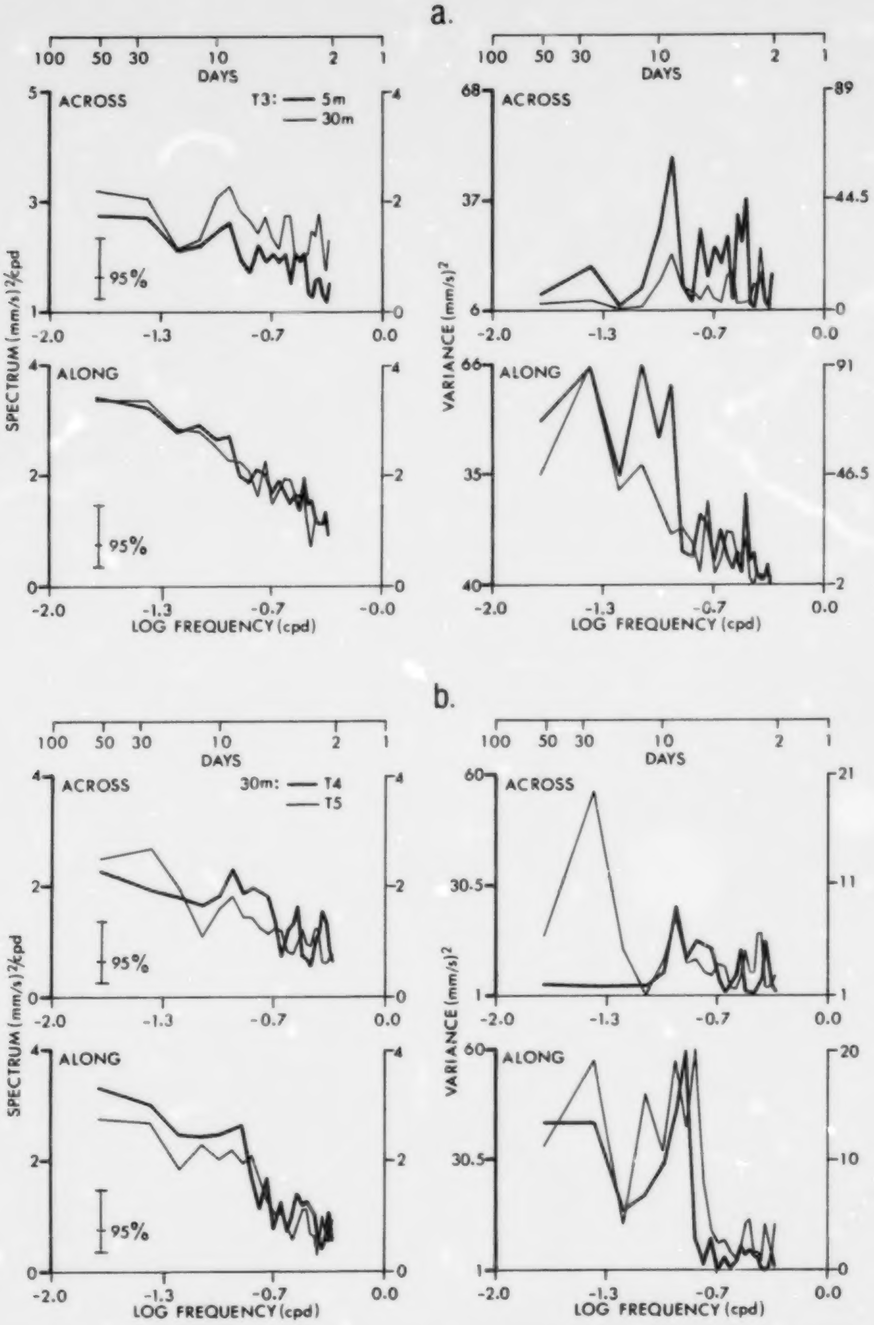

FIG. 19. Spectra of cross-shore and longshore components of hourly records of low-pass filtered current velocity from the Vancouver Island Coastal Current Experiment. (a) Comparison of spectral densities and variance spectra for currents at 5 and 30 m depth at mooring site T3 (cf. Fig. 2). (b) Comparison of spectra for currents measured at 30 m depth at mooring sites T4 and T5. Bandwidth = 0.01 cycles per day (cpd).

banks, is expected to produce a marked alteration in the biology of the shelf region. We further expect that the transition triggers the return equatorward of mature hake and initiates the poleward migration of chinook and coho stocks from the banks region. Other fish stocks may be similarly affected. At present, relatively little is known of this poorly investigated aspect of the coastal environment.

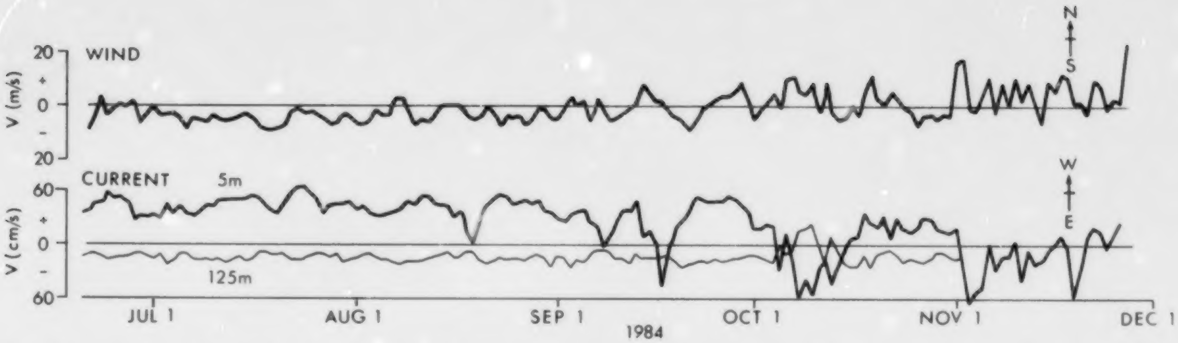

FIG. 20. Reversals of estuarine circulation at the entrance to Juan de Fuca Strait during the period June to December, 1984. Plots show the along-strait component of current at 5 and 125 m depths (positive toward 270°) together with the longshore Bakun wind (0°T) for the location 48°N; 125°W.

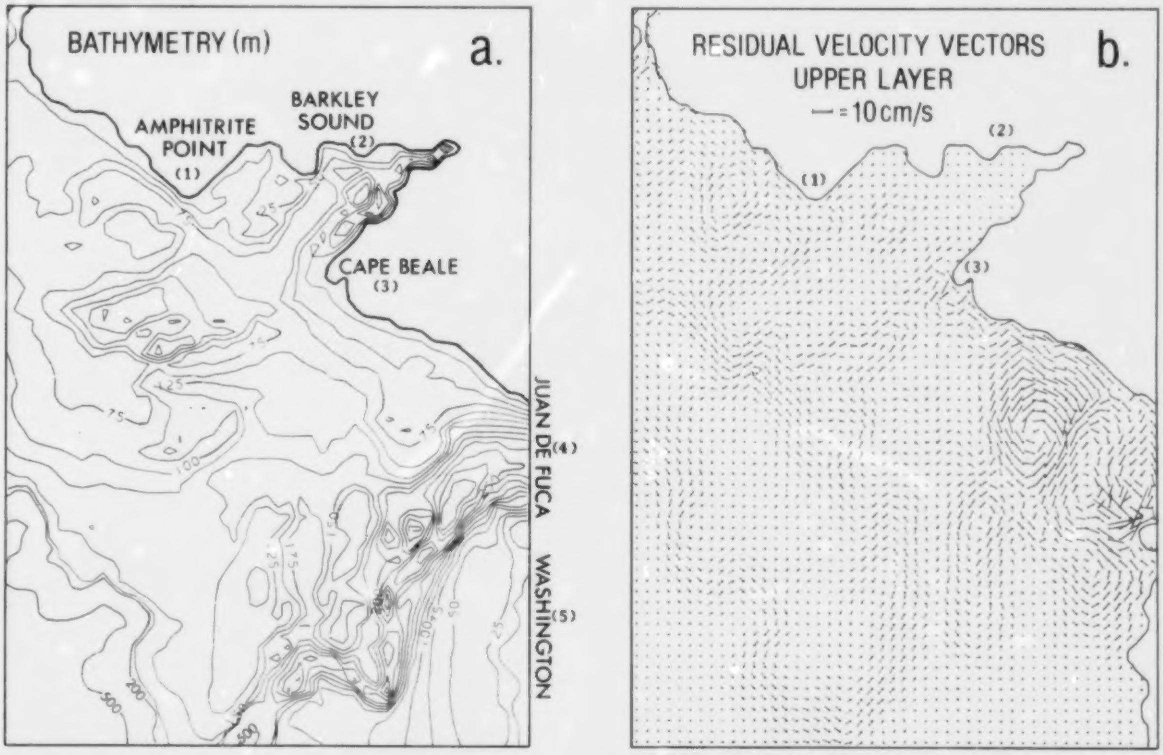

FIG. 21. Preliminary results from the tidal rectification model of R. Wilson (personal communication). (a) Digitized 2 km × 2 km bottom topography for the southern Vancouver Island continental margin; (b) Residual tidally rectified current for the topographic domain of (a) forced at the domain boundaries by the normal component of M_2 tidal velocity. Plot courtesy of R.E. Wilson.

8. Summary and Conclusions

This paper presents a detailed description of the circulation over the southern continental margin of Vancouver Island, with particular emphasis on the Vancouver Island Coastal Current. We attempt to show that spatial and temporal variability in the circulation can have a profound effect on stock recruitment along the British Columbia coast. Specifically, we suggest that the coastal current acts as both a longshore conduit and a cross-shore barrier to biomass movement over the southern continental shelf. Longshore transport of animals and nutrients is aided by the considerable longshore extent and relatively high velocities associated with the current while cross-shore transport of animals and nutrients is hindered by frontal-type water property gradients and suppressed cross-shore circulation. Seasonal and interannual changes in the intensity and spatial structure of the current may, in part, be responsible for variations in stock recruitment either through direct impact on the

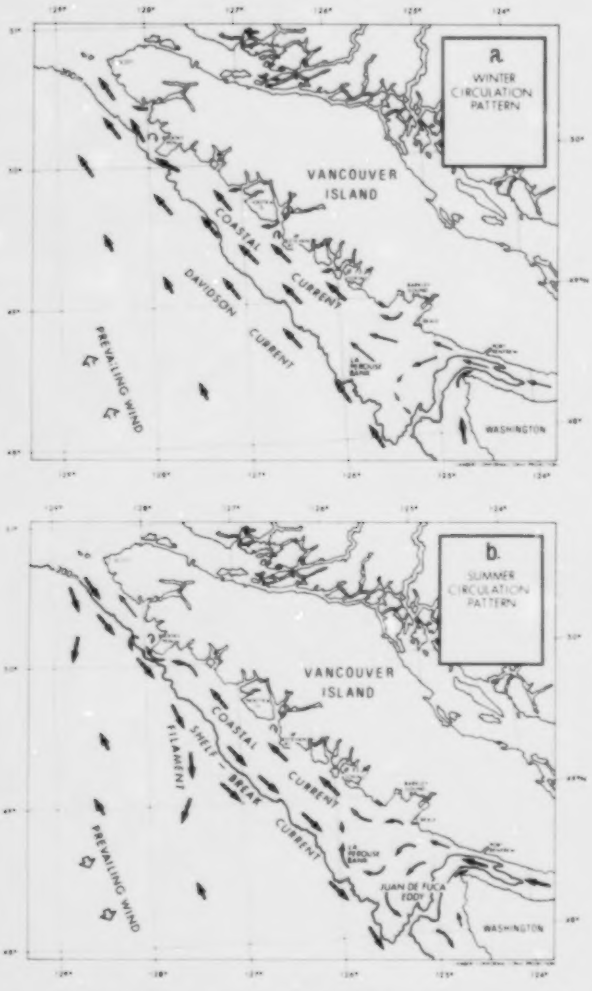

FIG. 22. Schematic interpretation of the prevailing circulation over the Vancouver Island continental margin for (a) winter; and (b) summer.

movement and physiology of the fish or through indirect impact on the food chain and predator populations. We do not claim to have definitive answers for the complex problems that characterize fisheries research on the outer coast. By the same token, we believe there is a tendency to down-play the importance of predominant physical oceanographic features such as the Vancouver Island Coastal Current.

Much of the emphasis in recent years has been on the possible impact of global-scale phenomena such as ENSO events on local physical and biological conditions. Obviously, these have a significant short-term effect on the coastal ocean. Howeer, as this paper attempts to demonstrate, we must also understand the response of local dynamical systems to seasonal and interannual changes. Detailed knowledge of the ambient regional environment is needed if we are to understand the ultimate effects of global scale processes. ENSO-type events may be important in some cases and not in others. Unless we know more about the variability and impact of coastal oceanic phenomena such as the Vancouver Island Coastal Current we will be unable to sort out secular climatic influences from shorter term regional effects. The key lies in understanding of processes on scales and periods pertinent to stages of life history or migration which are decisive for various fish stocks. For example, strong winds or a surge in the buoyancy flux at a particular time of year may modify the coastal current and alter the migration (or survival) of a particular species of fish. How pronounced or persistent these effects need be to disrupt the fish cycle must be determined in context of the regional circulation and timing of the life history. Careful study of coastal ocean response to both local and remote forcing is essential.

Acknowledgements

We thank Joe Linquanti and Dennis Francis for assisting with the data analysis. We are especially grateful to Patricia Kimber for patiently drafting the numerous diagrams. Critical reviews of the manuscript were generously provided by Dan Ware, Mike Healey, Glen Jamieson and Lindy England. We also benefitted from useful discussions with David Griffin. Robert Wilson supplied the plots of tidally rectified current for the southern coast of Vancouver Island and Howard Freeland provided us with mean monthly data from the CODE II and Super CODE programs. We further acknowledge the support of the National Sciences and Engineering Council of Canada (PHL) and United States Office of Naval Research (BMH).

References

ALLEN, J. S., AND D. W. DENBO. 1984. Statistical characteristics of the large-scale response of coastal sea level to atmospheric forcing. J. Phys. Oceanogr. 14: 1079–1094.

BARBEE, W. B., J. G. DWORSKI, J. D. IRISH, L. H. LARSEN, AND M. RATTRAY JR. 1975. Measurement of internal waves of tidal frequency near a continental boundary. J. Geophys. Res. 80: 1965–1974.

BAKUN, A. 1973. Coastal upwelling indices, west coast of North America, 1946–71. NOAA Tech. Rep. NMFS SSRF 671: 103 p.

1986. Definition of environmental variability affecting biological processes in large marine ecosystems, 89–108. *In* K. Sherman and L. Alexander [ed.] Variability and management of large marine ecosystems. AAAS selected Symposium 99.

BEARDSLEY, R. C., AND J. HART. 1978. A simple theoretical model for the flow of an estuary onto a continental shelf. J. Geophys. Res. 83: 873–883.

BENOIT, J., M. I. EL-SABH, AND C. L. TANG. 1985. Structure and seasonal characteristics of the Gaspé Current. J. Geophys. Res. 90: 3225–3235.

CRAWFORD, W. R., AND R. E. THOMSON. 1982. Continental shelf waves of diurnal period along Vancouver Island. J. Geophys. Res. 87: 9516–9522.

1984. Diurnal-period continental shelf waves along Vancouver Island: A comparison of observations with theoretical models. J. Phys. Oceanogr. 14: 1629–1646.

CRESSWELL, G. R., AND T. J. GOLDING. 1980. Observations of a south-flowing current in the southeastern Indian Ocean. Deep-Sea Res. 27A: 449–466.

Denman, K. L., D. L. Mackas, H. J. Freeland, M. J. Austin, and S. H. Hill. 1981. Persistent upwelling and meso-scale zones of high productivity off the west coast of Vancouver Island, Canada, p. 514-521. *In* F. Richards [ed.] Coastal upwelling. American Geophys. Union, Washington, DC.

Denman, K. L., and H. J. Freeland. 1985. Correlation scales, objective mapping, and statistical test of geostrophy over the continental shelf. J. Mar. Res. 43: 517-539.

Dodimead, A. J. 1980. A general review of the oceanography of the Queen Charlotte Sound-Hecate Strait-Dixon Entrance region. Can. MS. Rep. Fish. Aquat. Sci. 1574: 240 p.

1984. A review of some aspects of the physical oceanography of the continental shelf and slope waters off the west coast of Vancouver Island, British Columbia. Can. MS. Rep. Fish. Aquat. Sci. 1773: 309 p.

Dodimead, A. J., F. Favorite, and T. Hirano. 1963. Salmon of the North Pacific Ocean - Part II. Review of oceanography of the subarctic Pacific region. Int. North Pac. Fish. Comm. Bull. 13: 195 p.

Emery, W. J., and L. A. Mysak. 1980 Dynamical interpretation of satellite-sensed thermal features off Vancouver Island. J. Phys. Oceanogr. 10: 961-970.

Favorite, F., A. J. Dodimead, and K. Nasu. 1976. Oceanography of the subarctic Pacific region, 1960-72. Int. North Pac. Fish. Comm. Bull. 33: 187 p.

Fissel, D. B. 1975. A frequency analysis of ten years of surface atmospheric data at Ocean Weathership PAPA (50°N; 145°W) M.Sc. thesis, Univ. British Columbia, Vancouver, B.C. 136 p.

Flather, R. 1987. A numerical model investigation of tides and diurnal period continental shelf waves along Vancouver Island. J. Phys. Oceanogr. 18: 115-139.

Freeland, H. J. 1987. Long time-series of filtered current records for the B.C. Coast, 1979-1982. Can. Data Rep. Hydrogr. Ocean Sci. 52: 75 p.

Freeland, H. J., and K. L. Denman. 1982. A topographically controlled upwelling center off southern Vancouver Island. J. Mar. Res. 40: 1069-1093.

Freeland, H. J., W. R. Crawford, and R. E. Thomson. 1984. Currents along the Pacific coast of Canada. Atmosphere-Ocean 22: 151-172.

Gill, A. E., and E. H. Schumann. 1974. The generation of long waves by the wind. J. Phys. Oceanogr. 4: 83-90.

Giovando, L. F. 1985. Observations of seawater temperature and salinity at British Columbia shore stations, 1984. Can. Data Rep. Hydrogr. Ocean Sci. 41: 102 p.

Griffin, D. A., P. H. LeBlond, R. E. Thomson, and B. M. Hickey. 1987. Estuarine circulation controlled by spring-neap modulated tidal mixing and wind stress. EOS, November.

Halliwell, G. R., Jr., and J. S. Allen. 1984. Large-scale sea level response to atmospheric forcing along the west coast of North America, summer 1973. J. Phys. Oceanogr. 14: 864-886.

Healey, M. 1987. The marine survival of salmon program. Dept. Fish. Oceans Circular. 3 p.

Hickey, B. M. 1979. The California Current system — hypotheses and facts. Prog. Oceanogr. 8: 191-279.

1984. The fluctuating longshore pressure gradient on the Pacific northwest shelf: A dynamic analysis. J. Phys. Oceanogr. 14: 276-293.

Hickey, B. M., R. E. Thomson, H. Yih, and P. H. LeBlond. 1989. A buoyancy-driven coastal current, J. Geophys. Res. (In press)

Holbrook, J. R. and D. Halpern. 1982. Winter-time near-surface currents in the Strait of Juan de Fuca. Atmosphere-Ocean 20: 327-339.

Hollister, H. 1964. Classification of monthly mean sea surface temperatures and salinities at shore stations along the British Columbia and adjacent American coasts, 1915-1962. Fish. Res. Board Can. MS Rep. Ser. (Oceanogr. Limnol.) 177: 123 p.

Huggett, W. S., W. R. Crawford, R. E. Thomson, and M. V. Woodward. 1987. Coastal Ocean Dynamics Experiment (CODE) Part 1. Data record of current observations, Volume XIX. Institute of Ocean Sci., Sidney, B.C. 77 p.

Huyer, A., J. Gagnon, and W. S. Huggett. 1976. Observations from current meters moored over the continental shelf off Vancouver Island, 28 November 1974 to April 8, 1975 and related oceanographic and meteorological data. MEDS Tech. Rep. 4: 54 p.

Ikeda, M. 1988. A model study of wind- and buoyancy-driven coastal circulation. J. Geophys. Res. 93: 5078-5092.

Ikeda, M., L. A. Mysak, and W. J. Emery. 1984a. Observations and modeling of satellite-sensed meanders and eddies off Vancouver Island. J. Phys. Oceanogr. 14: 3-21.

1984b. Seasonal variability in meanders of the California Current System off Vancouver Island. J. Geophys. Res. 89: 3487-3505.

Ingraham, W. J., Jr. 1967. The geostrophic circulation and distribution of water properties off the coasts of Vancouver Island and Washington, spring and fall 1963. U.S. Fish. Wildl. Bull. 66: 223-250.

Lane, R. K. 1962. A review of the temperature and salinity structure in the approaches to Vancouver Island, British Columbia, J. Fish. Res. Board Can. 19: 45-91.

1963. A model of seawater structure near the west coast of Vancouver Island, British Columbia. J. Fish. Res. Board Can. 20: 939-967.

LeBlond, P. H., K. Dyck, K. Perry, and D. Cumming. 1983. Runoff and precipitation time series for the coasts of British Columbia and Washington State. Dep. Oceanogr. Univ. B.C. Rep. No. 39: 133 p.

LeBlond, P. H., B. M. Hickey, and R. E. Thomson. 1986a. Runoff driven coastal flow off British Columbia, p. 309-317. *In* S. Skreslet [ed.] The role of freshwater outflow in coastal marine ecosystems. NATO ASI Series, Vol. G7, Springer-Verlag.

LeBlond, P. H., W. J. Emery, and T. Nicol. 1986b. A climatic model of runoff-driven coastal circulation. Estuarine Coast Shelf Sci. 23: 59-79.

Mackas, D. L., K. L. Denman, and A. F. Bennett. 1987. Least squares multiple tracer analysis of water mass composition. J. Geophys. Res. 92: 2907-2918.

Mork, M. 1981. Circulation phenomena and frontal dynamics of the Norwegian Coastal Current. Phil. Trans. Roy. Soc. Lond. A 302: 635-647.

Mysak, L. A. 1977. On the stability of the California Undercurrent off Vancouver Island. J. Phys. Oceanogr. 7: 904-917.

1980. Recent advances in shelf wave dynamics. Rev. Geophys. Space Phys. 18: 211-241.

1986. El Niño, interannual variability and fisheries in the northeast Pacific Ocean. Can. J. Fish. Aquat. Sci. 43: 464-497.

Mysak, L. A., and F. Schott. 1977. Evidence for baroclinic instability of the Norwegian Current. J. Geophys. Res. 82: 2087-2095.

Mysak, L. A., W. W. Hsieh, and T. R. Parsons. 1982. On the relationship between interannual baroclinic waves and fish population in the northeast Pacific. Biol. Oceanogr. 2: 63-103.

Reed, R. K., and D. Halpern. 1976. Observations of the California Undercurrent off Washington and Vancouver Island. Limnol. Oceanogr. 21: 389-398.

ROYER, T. C. 1981a. Baroclinic transport in the Gulf of Alaska. Part I. Seasonal variations of the Alaska Current. J. Mar. Res. 39: 239–250.

1981b. Baroclinic transport in the Gulf of Alaska. Part II. A fresh water driven coastal current. J. Mar. Res. 39: 251–266.

SCHUMACHER, J. D., AND R. K. REED. 1980. Coastal flow in the northwest Gulf of Alaska: The Kenai Current. J. Geophys. Res. 85: 6680–6688.

SEACONSULT MARINE RESEARCH. 1984. Improved Canadian search and rescue planning (CANSARP) methods for B.C. coastal waters. Contractor Rep. Dep. Fish. Oceans. 193 p.

STRUB, P. T., J. S. ALLEN, A. HUYER, AND R. L. SMITH. 1987. Large-scale structure of the spring transition. J. Geophys. Res. 92: 1527–1544.

TABATA, S. 1975. The general circulation of the Pacific Ocean and a brief account of the oceanographic structure of the North Pacific Ocean. Atmosphere 13: 133–168.

1984. Oceanographic factors influencing the distribution, migration and survival of salmonids in the northeast Pacific Ocean — a review, p. 128–160. *In* W. G. Pearcy [ed.] The influence of ocean conditions on the production of salmonids in the North Pacific, a workshop. Oregon State Univ. Sea Grant College Program ORESU-W-83-001, 327 p.

TABATA, S., B. THOMAS, AND D. RAMSDEN. 1986. Annual and interannual variability of steric sea level along Line P in the northeast Pacific Ocean. J. Phys. Oceanogr. 16: 1378–1398.

TANG, C. L. 1980. Mixing and circulation in the northeastern Gulf of St. Lawrence: A study of a buoyancy driven current system. J. Geophys. Res. 85: 2787–2796.

THOMPSON, R. O. R. Y., AND G. VERONIS. 1983. Poleward boundary current off Western Australia. Aust. J. Freshwater. Res. 34: 173–185.

THOMSON, R. E. 1981. Oceanography of the British Columbia Coast. Can. Spec. Publ. Fish. Aquat. Sci. 56: 291 p.

1983. A comparison between computed and measured winds near the British Columbia coast. J. Geophys. Res. 88: 2675–2683.

1984. A cyclonic eddy over the continental margin of Vancouver Island: Evidence for baroclinic instability. J. Phys. Oceanogr. 14: 1326–1348.

THOMSON, R. E., AND W. R. CRAWFORD. 1982. The generation of diurnal period shelf waves by tidal currents. J. Phys. Oceanogr. 12: 635–643.

THOMSON, R. E., H. J. FREELAND, AND L. F. GIOVANDO. 1984. Long-term sea surface temperature variations along the British Columbia coast. Trop. Ocean-Atmos. Newslett. 26: 9–11.

THOMSON, R. E., W. R. CRAWFORD, AND W. S. HUGGETT. 1985. Water property observations off the west coast of Vancouver Island during CODE: May 1979 to September 1980. Can. Data Rep. Hydrogr. Ocean Sci. 23(1–3): 1039 p.

THOMSON, R. E., AND J. F. R. GOWER. 1986. A wind-induced mesoscale eddy over the Vancouver Island continental slope. J. Geophys. Res. 90: 8981–8993.

THOMSON, R.E., W.R. CRAWFORD, H. J. FREELAND, AND W.S. HUGGETT. 1986. Low-pass filtered current meter records for the west coast of Vancouver Island: Coastal Oceanic Dynamics Experiment, 1979–81. Can. Data Rep. Hydrogr. Ocean Sci. 40: 102 p.

THOMSON, R. E., AND R. E. WILSON. 1987. Coastal countercurrent and mesoscale eddy formation by tidal rectification near an oceanic cape. J. Phys. Oceanogr. 11: 2096–2126.

THOMSON, R. E., AND D. WARE. 1988. Oceanic factors affecting the distribution and recruitment of west coast fisheries. Can. Tech. Rep. Fish. Aquatic Sci. 1626: 29 p.

TORGRIMSON, G. M., AND B. M. HICKEY. 1979. Barotropic and baroclinic tides over the continental slope and shelf off Oregon. J. Phys. Oceanogr. 9: 945–961.

TULLY, J. P. 1942. Surface non-tidal currents in the approaches to Juan de Fuca Strait. J. Fish. Res. Board Can. 5: 398–409.

WALDICHUK, M. 1963. Drift bottle observations in the Strait of Georgia and its contiguous waters, and off the west coast of Vancouver Island. Fish. Res. Board Can. MS Rep. Ser. (Oceanogr. Limnol.) 147: 104 p.

WARE, D., AND R. E. THOMSON. 1986. La Perouse Project: First annual report, 1985. Dep. Fish. Oceans Canada: 25 p.

1987. La Perouse Project: Second annual progress report. 1986. Dep. Fish. Oceans Canada: 31 p.

1988. La Perouse Project: Third annual progress report, 1987. Dep. Fish. Oceans Canada: 64 p.

WILSON, R. E., AND R. E. THOMSON. 1989. Simulations of rectification near an open ocean cape. J. Mar. Res. (submitted)

YAO, T., H. J. FREELAND, AND L. A. MYSAK. 1984. A comparison of low-frequency current observations off British Columbia with coastally-trapped waves. J. Phys. Oceanogr. 14: 22–34.

ZHANG, Q. H., G. S. JANOWITZ, AND L. P. PIETRAFESA. 1987. The interaction of estuarine and shelf waters: A model and applications. J. Phys. Oceanogr. 17: 455–469.

Transportation of Eggs and Larvae of Mackerel, *Scomber japonicus* (Houttuyn), by the Kuroshio Current

Akira Tomosada

Oceanographic Division, Tokai Regional Fisheries Research Laboratory, 5-5-1 Kachidoki, Chuo-ku, Tokyo 104, Japan

Abstract

TOMOSADA, A. 1989. Transportation of eggs and larvae of mackerel, *Scomber japonicus* (Houttuyn), by the Kuroshio Current, p. 297–303. *In* R. J. Beamish and G. A. McFarlane [ed.] Effects of ocean variability on recruitment and an evaluation of parameters used in stock assessment models. Can. Spec. Publ. Fish. Aquat. Sci. 108.

The surroundings of the islands or submarine banks of the Izu Archipelago region are one of the major spawning grounds of Japanese common mackerel, *Scomber japonicus* (Houttuyn). Physical processes producing the movement of the mackerel eggs and larvae into the Kuroshio Current are described from observations over several years and their drift south of the Boso Peninsula is discussed in relation to the equation of motion with the corroboratory evidence provided by closely spaced observations carried out at the Kuroshio frontal region south of Cape Shionomisaki.

Résumé

TOMOSADA, A. 1989. Transportation of eggs and larvae of mackerel, *Scomber japonicus* (Houttuyn), by the Kuroshio Current, p. 297–303. *In* R. J. Beamish and G. A. McFarlane [ed.] Effects of ocean variability on recruitment and an evaluation of parameters used in stock assessment models. Can. Spec. Publ. Fish. Aquat. Sci. 108.

Les environs des îles et des bancs sous-marins de la région de l'archipel d'Izu constituent une des principales frayères du maquereau blanc, *Scomber japonicus* (Houttuyn). Nous décrivons ici les phénomènes physiques responsables du déplacement des oeufs et des larves de maquereau dans le courant de Kuroshio. Cette description repose sur des observations recueillies durant plusieurs années et la dérive des oeufs et des larves au sud de la péninsule de Boso est analysée à l'aide de l'équation de mouvement et des observations rapprochées obtenues dans la région frontale de Kuroshio au sud du cap Shionomisaki, observations qui viennent corroborer cette équation.

Introduction

Submarine banks and island shelves in the Izu Archipelago region (Fig. 1, 2) are one of the major spawning grounds of the Japanese common mackerel, *Scomber japonicus* (Houttuyn). Morphology and ecology of its early-life stages were described in detail by Watanabe (1970). He reported that the eggs are spawned in coastal regions with a weak current, and are drawn into the edge of the Kuroshio. The eggs and larvae drift in the Kuroshio, south of the Boso Peninsula, and some of them are drawn into the Transition Area (Uda 1938), in the coastal region of Kashima-nada.

Hirano et al. (1969) reported that the Kuroshio should be disturbed by the complicated topography in the Izu Archipelago region, because the bottom depth is shallow and very complicated (Fig. 2). However, actual features of these disturbances had not been investigated previously. The author has investigated disturbances in the Izu Archipelago region since 1975.

Physical processes producing the movement of the mackerel eggs and larvae into the Kuroshio Current, and their drift south of the Boso Peninsula will be discussed from the results of investigations and brief equations.

Materials and Methods

Figure 2 shows the bottom topography of the Izu Archipelago region and the station locations of STD, BT and GEK carried out by the R/V *Soyo Maru* (50 m long) in 1975. This survey was conducted in order to observe the disturbances on a smaller scale.

In 1977, the shelf of a small island west of Miyake Island was selected as a model area, and six rounds of XBT casts were completed, at the solid-dot points of W- and E-lines in Fig. 3. And also, sea surface currents were measured at the marginal stations indicated by circles with dots and at the point indicated by a circle with cross (Fig. 3). After completing the six rounds of XBT casts, the research vessel was anchored at the point of the circle marked with cross and lowered an STD to the bottom at 2-h intervals during 4 days from 5 to 8 August 1977. This survey was intended to observe the temporal and spatial scale of eddies generated by the bottom topography.

Multi-spectral scanner (MSS) data were repeatedly taken from an airplane, between Oshima Island and the Boso Peninsula on 31 July 1979 (Fig. 4), when the Kuroshio streamed just south of Oshima Island. Syn-

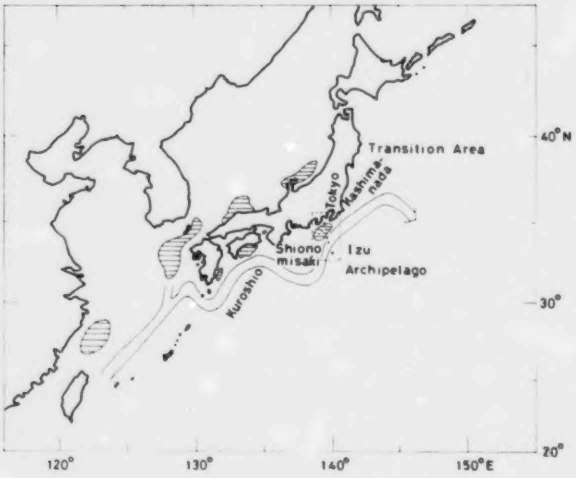
Transition Area
Tokyo
Kashima-nada
Shiono misaki
Izu Archipelago
Kuroshio
40°N
30°
20°
120°
130°
140°
150°E

FIG. 1. Location of dense concentrations of mackerel eggs off Japan. The region enclosed by dashed line is the Izu Archipelago region and its bottom topography is shown in Fig. 2.

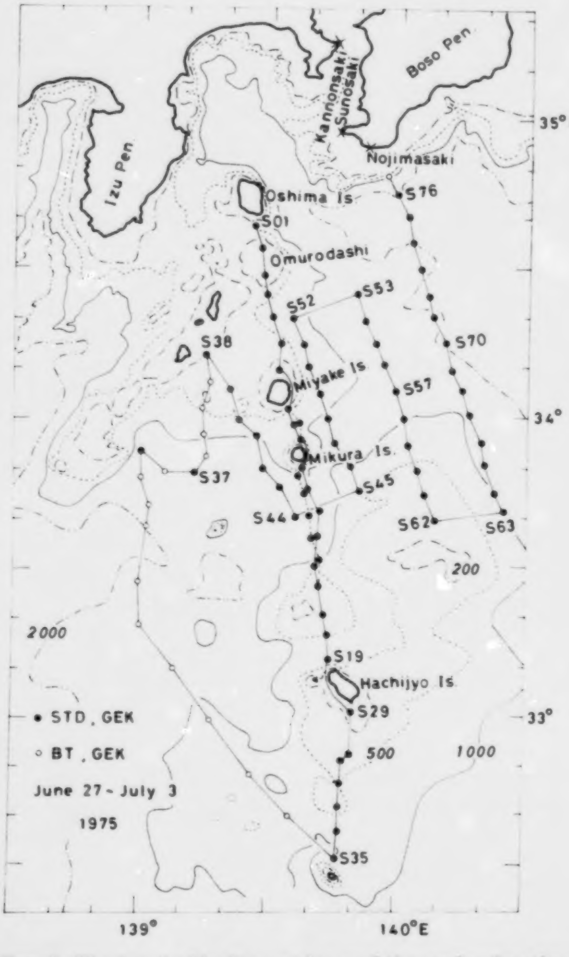
Izu Pen
Kannonsaki
Sunosaki
Boso Pen
Nojimasaki
35°N
Oshima Is
S01
S76
Omurodashi
S52
S53
S38
S70
Miyake Is
S57
34°
Mikura Is
S37
S45
S44
S62
S63
200
2000
S19
Hachijyo Is
S29
33°
• STD, GEK
○ BT, GEK
June 27 - July 3
1975
500
1000
S35
139°
140°E

FIG. 2. The Izu Archipelago region and the station locations of the 28 June–3 July, 1975 survey.

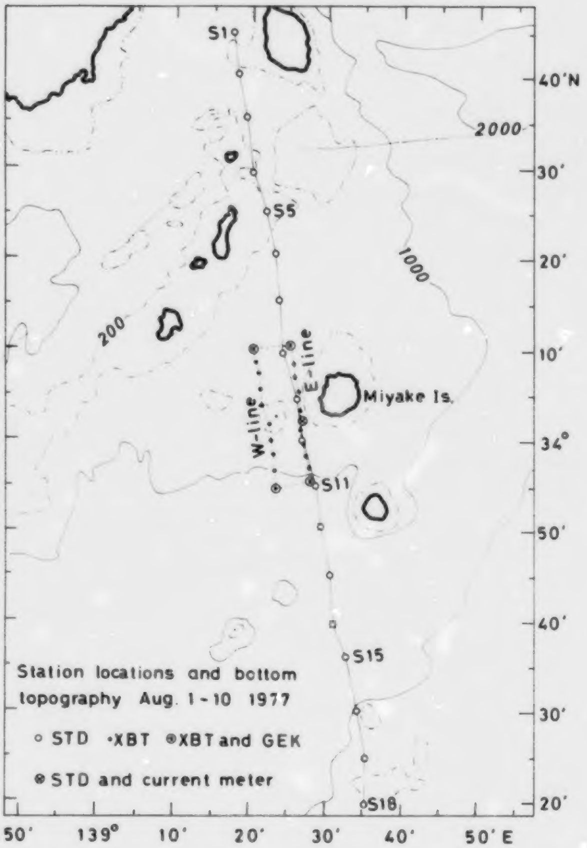
S1
40'N
2000
30'
S5
20'
1000
200
10'
E-line
W-line
Miyake Is
34°
S11
50'
40'
S15
Station locations and bottom topography Aug. 1-10 1977
○ STD •XBT ⊛XBT and GEK
⊛ STD and current meter
30'
S18
20'
50'
139°
10'
20'
30'
40'
50'E

FIG. 3. Hydrographic station locations of 1–10 August 1977. E-line and W-line were traversed six times, launching XBT on 3–4 August 1977.

chronizing with the airplane survey, currents at the sea surface were measured by GEK and temperatures were also measured by XBTs on 31 July to 1 August 1979.

Sea surface temperatures have been monitored from Tokyo to Hachijou Island at intervals of 5 nautical miles by a ship of opportunity since 1978. This data is used for understanding the duration periods of disturbances.

Physical processes producing the movement of the mackerel eggs and larvae into the Kuroshio Current, and their drift south of the Boso Peninsula will be discussed, in relation to the equation of motion. Closely spaced sampling of plankton, and temperature, salinity and velocity measurements were undertaken south of Cape Shionomisaki in 1983 (Fig. 5) to provide corroboratory evidence for the drift along the Kuroshio front.

Results

Absorption of Eggs and Larvae into the Kuroshio

The Kuroshio passed the Izu Archipelago region near Miyake and Mikura islands during the 1975 survey. The survey revealed that eddies were generated around the islands when the Kuroshio passed through the region (Fig. 6).

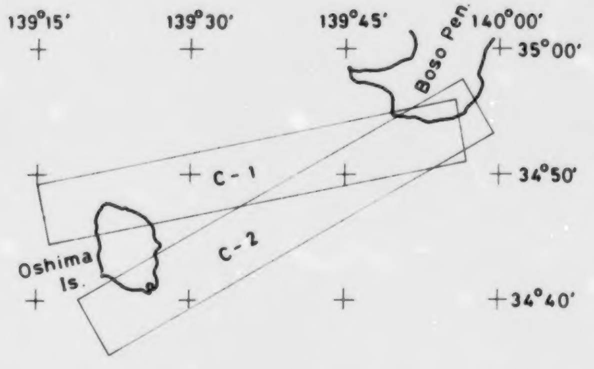
139°15'
139°30'
139°45'
140°00'
35°00'
34°50'
34°40'
Boso Pen.
C-1
C-2
Oshima Is.

FIG. 4. Flight paths and times for aerial surveys of surface temperature "disturbances" between Oshima Island and Boso Peninsula, 31 July 1979. (Altitude = 4500 m)

Course	Time	Course	Time
C-1-1	06:01–06:15	C-2-1	06:17–06:31
C-1-2	10:46–01:01	C-2-2	11:03–01:17
C-1-3	11:50–02:03	C-2-3	12:04–02:16
C-1-4	15:52–06:06	C-2-5	14:58–05:10
		C-2-6	16:07–06:20

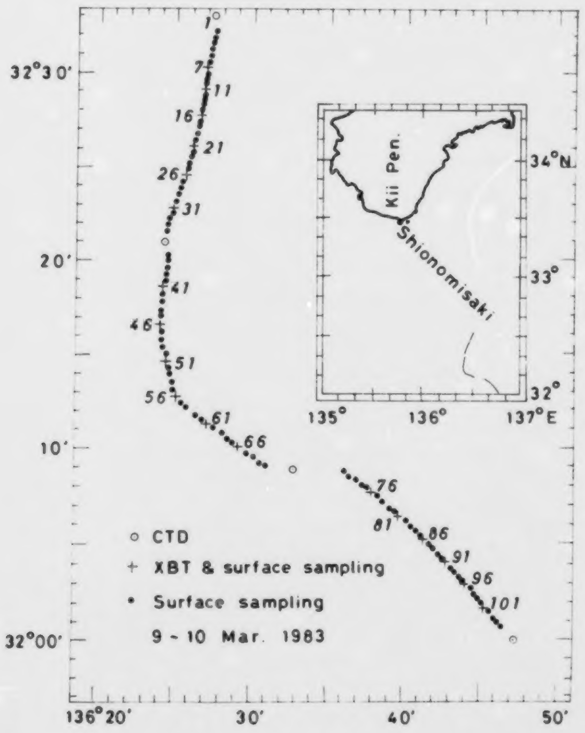
32°30'
20'
10'
32°00'
136°20'
30'
40'
50'
1
7
11
16
21
26
31
41
46
51
56
61
66
76
81
86
91
96
101
○ CTD
+ XBT & surface sampling
• Surface sampling
9 - 10 Mar. 1983
Kii Pen.
Shionomisaki
34°N
33°
32°
135°
136°
137°E

FIG. 5. Locations of the closely spaced stations where sampling was carried out south of Shionomisaki, 9–10 March 1983.

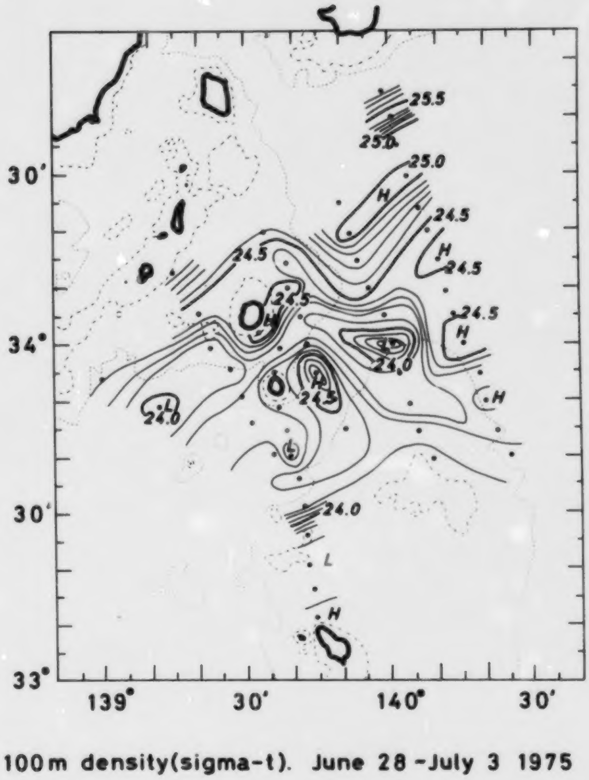
30'
34°
30'
33°
139°
30'
140°
30'
25.5
25.0
24.5
24.0
H
L
100m density(sigma-t). June 28 -July 3 1975

FIG. 6. Sigma-t values at 100 m during the 28 June–3 July, 1975 survey in the Izu Archipelago region.

The Kuroshio streamed the modelled area during the 1977 survey. Figures 7a and 7b show time series of temperature deviations, at 200 m, from the mean of the W-line and E-line, respectively. The temperature is lower than the mean distributed north of 33° 56′N at the first leg, and is lower than the mean distributed through the section in the second leg at W-line (Fig. 7a). As it is estimated the waters with these anomalies were transported by the mean flow of the Kuroshio from west to east, these waters should be observed at E-line with the time lag of transportation. The water with the minus anomaly at W-line which was observed at 00:00 h on 4 August had two cores at 34°05′N and 34°09′N, and the scales of north–south direction are about 3 nautical miles in E-line. Double cores with plus anomaly were also observed at 06:00 h on 4 August. These waters with plus or minus anomalies were observed in E-line 4 h after those in W-line. And the scale of north–south was smaller in E-line than in W-line. This suggests that waters were separated into small scale when they passed around the modelled island. As the distance between W-line and E-line is 4 nautical miles and it took about 4 h for propagation from W-line to E-line, the speed of propagation is 1 knot approximately. This is a reasonable speed for the Kuroshio Current in the Izu Archipelago region (Tomosada 1985). This indicates that small-scale disturbances are generated when the Kuroshio passes an island.

When the thermal pattern was taken between Oshima Island and Boso Peninsula in 1979 (Fig. 4), the Kuroshio passed just south of Oshima Island. On the first flight, along course-2 (Fig. 8a), cold water which flowed along the east coast of Oshima Island joined warm water flowing south of Oshima Island, and made a striped eddy. On the second flight, 5 h later (Fig. 8b), the temperature of this eddy was lower than that of the surrounding water. This indicates that the coastal water is absorbed into the edge of the Kuroshio when an eddy is generated behind an island. The movement of water during the birth stage of an eddy is schematically shown in Fig. 9. Since the eddy was situated at the edge of the Kuroshio, it was intensified by the frictional force of the main current of the Kuroshio. Therefore, the cyclonic shear in the eddy was intensified and upwelling was induced. As a result, the temperature of the eddy became cooler than the surrounding water. XBT and GEK surveys were carried out, synchronized with the airplane survey. Surface velocities by GEK and the estimated stream lines are indicated in Fig. 10. Stream lines converge east of Oshima Island, and over a submarine bank south of it.

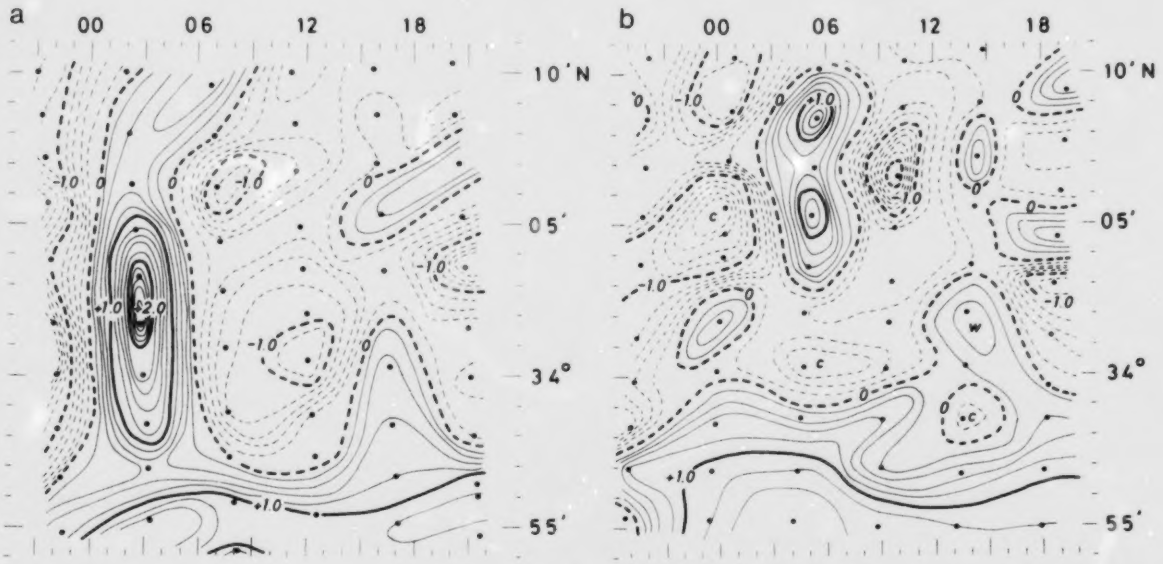

FIG. 7. Time series of temperature anomalies at 200 m, 3–4 August 1977 (Fig. 3). (a) W-line (T = 14.0°C); (b) E-line (T = 14.1°C)

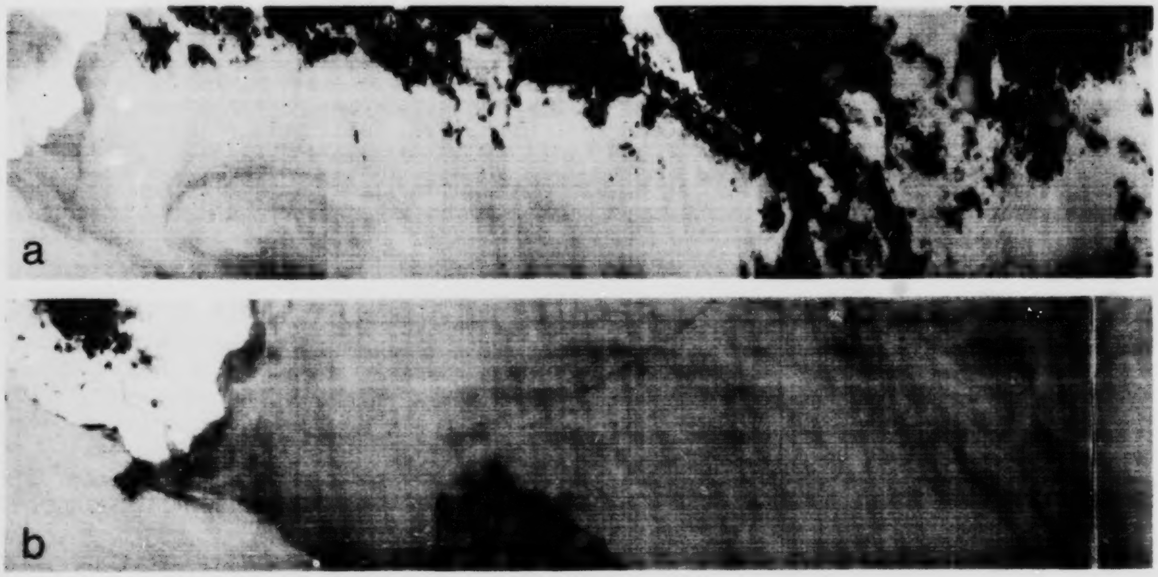

FIG. 8. Thermal patterns observed during the first and second flights along course 2, 31 July 1979. (a) First flight, 06:17–06:31 h; (b) second flight, 11:03–11:17 h.

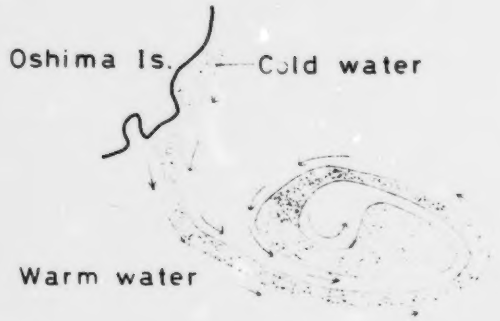
Oshima Is.
Cold water
Warm water

FIG. 9. Schematic portrayal of eddy generation behind Oshima Island.

Figure 11 shows the temperature series from the ship of opportunity for the line between Kannonsaki and Hachijou Island. Topographic eddies are frequently observed along this line. Oshima Island is situated at one third the distance from Nojimasaki to Miyake Island. Reports published biweekly by the Hydrographic Office revealed that the Kuroshio streamed just south of Oshima Island in the latter half of August 1979. The temperature east of Oshima Island cooled repeatedly during the period. When the Kuroshio streams near an island, a temperature colder than the surrounding water is observed for a few days in response to the movement of the Kuroshio Current.

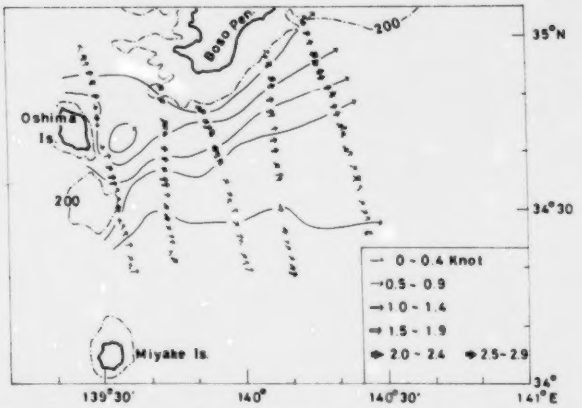
Boso Pen.
200
35°N
Oshima Is.
200
34°30
→ 0 ~ 0.4 Knot
→ 0.5 ~ 0.9
→ 1.0 ~ 1.4
→ 1.5 ~ 1.9
→ 2.0 ~ 2.4
→ 2.5 ~ 2.9
Miyake Is.
139°30'
140°
140°30'
141°E
34°

FIG. 10. Surface velocity by GEK, and estimated stream lines from the research vessel survey, synchronized with the aerial survey, 31 July to 1 August 1979.

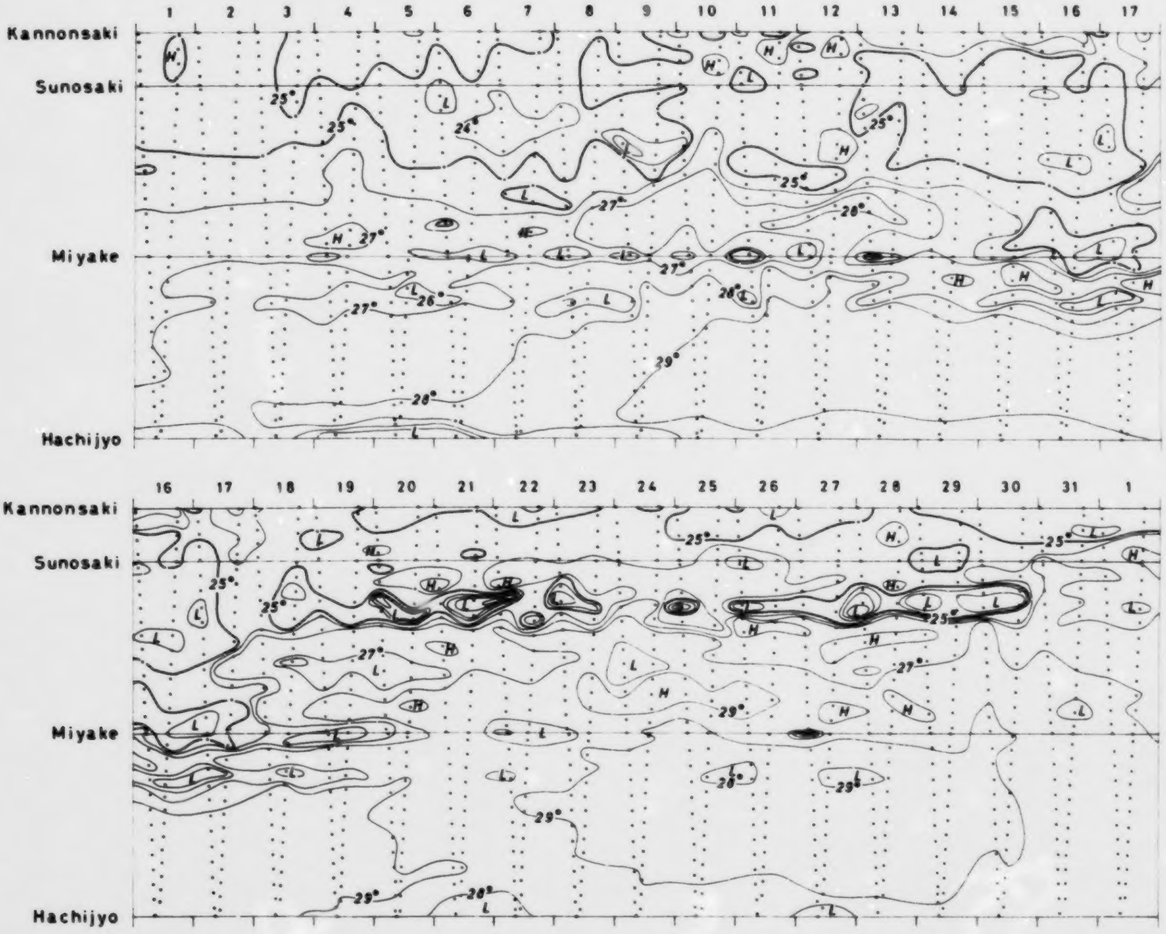

FIG. 11. Time series of daily SSTs collected by the ship of opportunity, from Kannonsaki (mouth of Tokyo Bay) to Hachijou Island, during 1 August through 1 September 1979.

Drifting of Eggs and Larvae South of Boso Peninsula

The velocities across the Kuroshio are schematically shown by the solid line in Fig. 12. The velocity decreases sharply from the maximum to the coastal side, and gradually to the offshore side. The main current induces the north-southward secondary flow perpendicular to the main eastward current owing to the shear effect and induced secondary flow near the surface as indicated by Kawai (1955) as,

$$(1) \qquad V' = [(-A_h)(\partial^2 U_o / \partial y^2)] / [f - (\partial U_o / \partial y)]$$

where, V' = horizontal velocity of secondary flow; A_h = horizontal coefficient of eddy viscosity; U_o = speed of the main current; y = crossing direction (north-south direction) of the main current; and f = Coriolis parameter. The dashed line in Fig. 12 shows the pattern of V'. Assuming the main flow is stationary, the continuity equation is written as

$$(2) \qquad \partial V' / \partial y + \partial W' / \partial z = 0$$

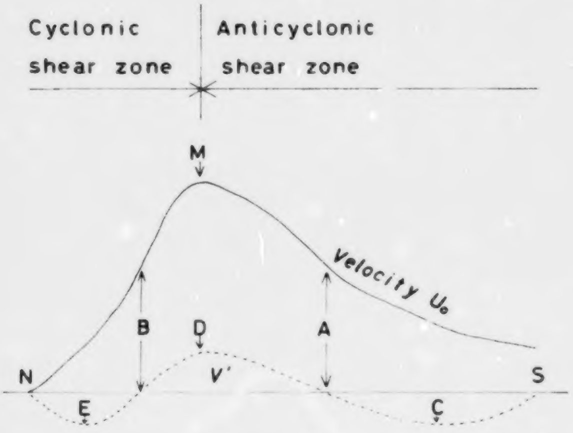

FIG. 12. A schematic velocity pattern across the Kuroshio Current. The solid line indicates the pattern of the main current, and the dashed line indicates the pattern of the horizontal secondary flow.

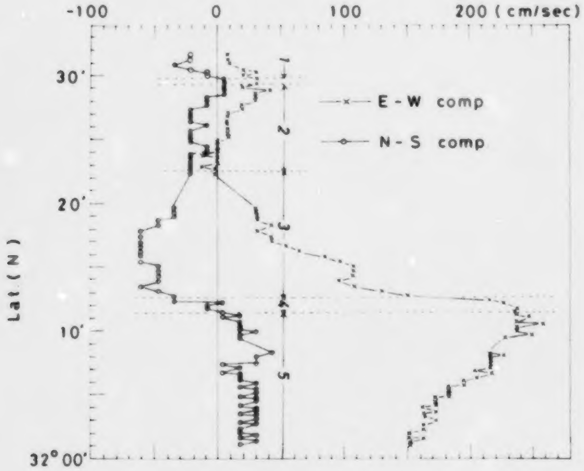

FIG. 13. East-west and north-south components of velocity calculated from the survey off Shionomisaki, 9–10 March 1983 (Fig. 5).

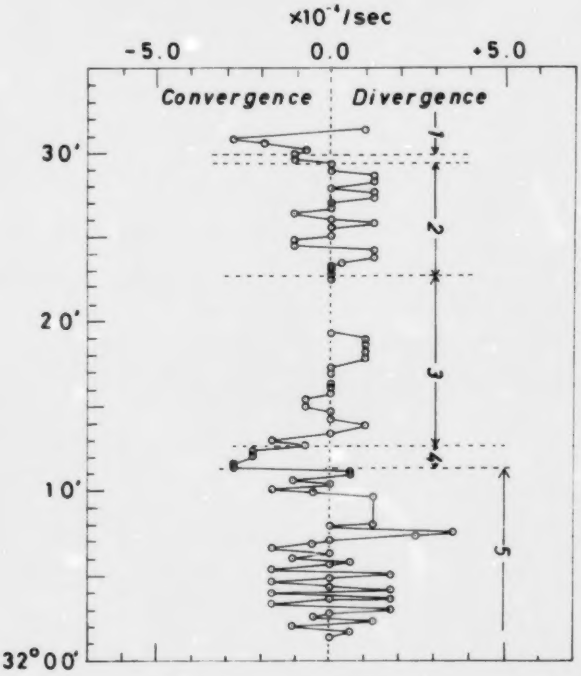

FIG. 14. Divergence and convergence calculated from the velocity patterns of Fig. 13 and the continuity equation (2).

TABLE 1. Estimated convergence and divergence of the surface layer of the Kuroshio.

Region	$\partial V' / \partial y$	$\partial W' / \partial z$	Convergence or divergence
S-C	–	+	Convergence
C-D	+	–	Divergence
D-E	–	+	Convergence
E-N	+	–	Divergence

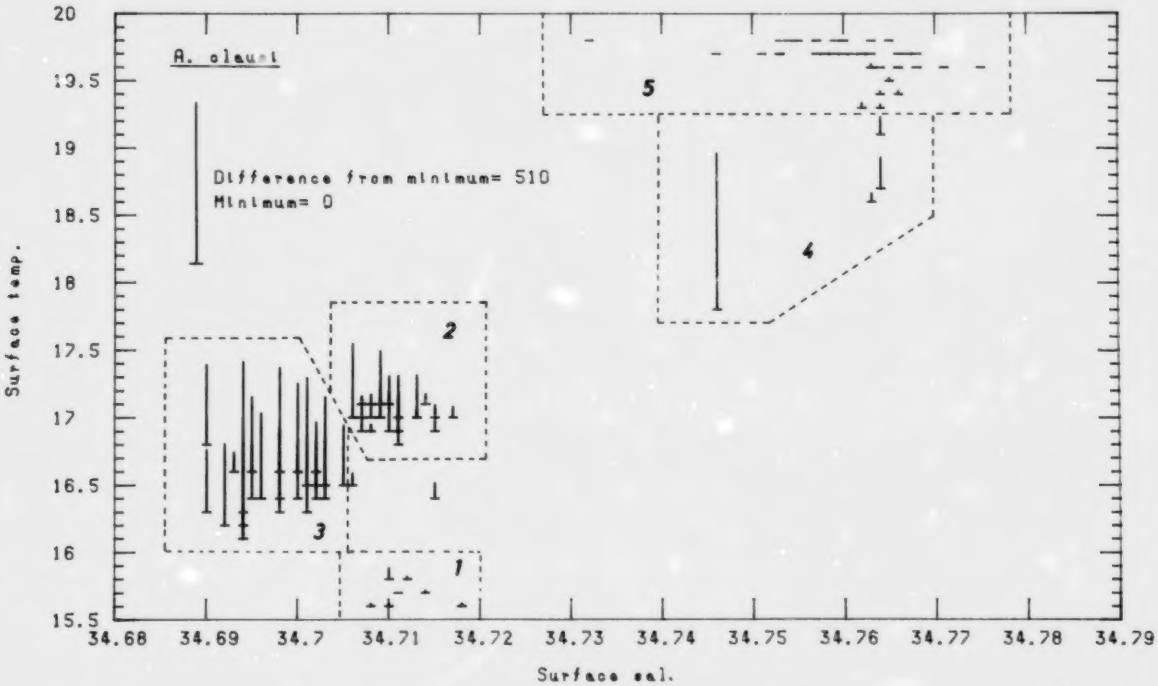

FIG. 15. Distribution of *Acartia clausi* on the temperature, salinity diagram during the Kuroshio frontal region survey off Shionomisaki, 9–10 March 1983.

where, W' = vertical velocity of secondary flow and z = vertical axis. By combining equation (1) with equation (2), convergence and divergence are estimated at the surface layer of the Kuroshio (Table 1). Region D–E (Fig. 12) corresponds to the region of the cyclonic shear zone and horizontal convergence is estimated for this region. Horizontal divergence is estimated in region D–C (Fig. 12) which corresponds to the anticyclonic shear zone. Watanabe (1970) showed that the eggs and larvae of mackerel are densely distributed in region D–E.

Closely spaced sampling of plankton, and measurement of temperature, salinity and velocity were carried out at the Kuroshio frontal region south of Cape Shionomisaki (Fig. 5) as the corroboratory evidence for the convergence and divergence. Velocity profiles of east-west and north-south components are indicated in Fig. 13. Region 4 of Fig. 13 corresponds to the region D–E in Fig. 11. From calculations of convergence and divergence by the continuity equation (2), region 4 was deduced to be a convergence zone (Fig. 14). *Acartia clausi*, one of the coastal species of zooplankton, is densely distributed in region 4 (Fig. 15). The zooplankton concentration provided corroborative evidence of convergence for region 4 which corresponds to the region E–D in Fig. 12.

These results suggest that eggs and larvae of mackerel do not diffuse from the Kuroshio front south of the Boso Peninsula.

Acknowledgements

I wish to thank Dr. T. Hirano and Dr. T. Watanabe for useful discussions regarding the physical and biological aspects of transportation of eggs and larvae. This work was supported by Kuroshio Exploitation and Utilization Research (KER) project, Science and Technology Agency Japan.

References

HIRANO, T., AND M. FUJIMOTO. 1969. Roles of environment and direction of study of environment to the reproduction of fisheries resources. Gyogyo Shingen Kenkyukai Giho 9: 18–33. (In Japanese)

KAWAI, H. 1955. On the polar frontal zone and its fluctuation in the waters to the northeast of Japan (II). Bull. Tohoku Reg. Fish. Res. Lab. 5 : 1–59. (In Japanese with English abstract)

TOMOSADA, A. 1985. Studies on the Kuroshio related to the transportation of mackerel eggs and larvae. Bull. Tokai Reg. Fish. Res. Lab. 117 : 47–119. (In Japanese with English abstract)

UDA, M. 1938. Research on "Siome" or current rip in the seas and oceans. Geophys. Mag. 11 : 307–372.

WATANABE, T. 1970. Morphology and ecology of early stages of life in Japanese common mackerel, *Scomber japonicus* Houttuyn, with special reference to fluctuation of population. Bull. Tokai Reg. Fish. Res. Lab. 62 : 1–283. (In Japanese with English abstract)

Effects of Ocean Variability on the Abundance of Dungeness Crab *(Cancer magister)* Megalopae

G. S. Jamieson, A. C. Phillips, and W. S. Huggett[1]

Department of Fisheries and Oceans, Biological Sciences Branch,
Pacific Biological Station, Nanaimo, B.C. V9R 5K6

Abstract

JAMIESON, G. S., A. C. PHILLIPS, AND W. S. HUGGETT. 1989. Effects of ocean variability on the abundance of Dungeness crab (*Cancer magister*) megalopae, p. 305–325. *In* R. J. Beamish and G. A. McFarlane [ed.] Effects of ocean variability on recruitment and an evaluation of parameters used in stock assessment models. Can. Spec. Publ. Fish. Aquat. Sci. 108.

The longshore and cross-shelf abundance of *Cancer* crab megalopae have been studied off the south coast of Vancouver Island since 1985. Megalopae occur in abundance from about 28 km to at least 170 km offshore, well beyond the general location (70 km offshore) of the continental shelf break (200 m depth). Intermoult staging of megalopae indicates that later stage megalopae are found progressively closer inshore, but in the study area, megalopae may not always reach the coast, which they must do in order to survive as settled juveniles. Since at least 1985, no substantive settlement has occurred in the commercial Dungeness (*C. magister*) fishing areas immediately around Tofino, British Columbia. Since Dungeness crab recruit to the fishery at 3–4 yr of age, a significant decrease in annual landing from this fishery is predicted over the next few years.

Environmental factors influencing the movement of megalopae have been investigated by documenting surface current patterns in the study area by means of drifters, estimating geostrophic flow patterns from STD data, and analyzing meteorological events as contributors to onshore larval movement. Results indicate that the patterns of currents and their relative velocities in the study areas differ on an annual basis. It appears that these current patterns affect where crab megalopae are concentrated in abundance and their subsequent ability to move onshore.

Résumé

JAMIESON, G. S., A. C. PHILLIPS, AND W. S. HUGGETT. 1989. Effects of ocean variability on the abundance of Dungeness crab (*Cancer magister*) megalopae, p. 305–325. *In* R. J. Beamish and G. A. McFarlane [ed.] Effects of ocean variability on recruitment and an evaluation of parameters used in stock assessment models. Can. Spec. Publ. Fish. Aquat. Sci. 108.

La population des mégalopes des crabes du genre *Cancer* le long de la côte et sur la plate-forme continentale au large de la côte sud de l'île Vancouver est étudiée depuis 1955. On retrouve les mégalopes en abondance dans la zone s'étendant de 28 km de la côte à 170 km, bien au-delà de la bordure (autour de 70 km au large) de la plate-forme continentale (d'une profondeur de 200 m). Lors du rassemblement intermue des mégalopes, on observe que les mégalopes, dans leur dernier stade, s'approchent progressivement de la côte, mais dans notre aire d'étude, les mégalopes ne sont pas toujours en mesure d'atteindre la côte, ce qui est indispensable à leur survie et à l'établissement de peuplements de juvéniles. Depuis au moins 1985, il n'y a eu aucun établissement notable de stocks commerciaux de dormeurs du Pacifique (*C. magister*) dans les zones de pêche de la région de Tofino, en Colombie-Britannique. Comme le recrutement du dormeur du Pacifique a lieu quand celui-ci atteint l'âge de 3–4 ans, on prédit une baisse significative des débarquements annuels dans ces eaux pour les quelques années à venir.

Nous avons étudié les facteurs environnementaux ayant un effet sur le déplacement des mégalopes. Pour ce faire, nous avons établi le profil des courants de surface à l'aide de dériveurs dans notre aire d'étude, nous avons estimé les profils d'écoulement géostrophique à l'aide des données CTP et nous avons analysé les phénomènes météorologiques au regard de leurs effets sur le déplacement côtier des larves. Les résultats révèlent que les profils de courants et les vitesses relatives de ces derniers dans les zones étudiées varient avec les années. Il semble que ces profils de courants déterminent les sites de rassemblement des mégalopes et leur capacité subséquente d'atteindre la côte.

---

[1] Department of Fisheries and Oceans, Hydrography Branch, Institute of Ocean Sciences, Sidney, B.C. V8L 4B2.

Introduction

Fisheries for Dungeness crab (*Cancer magister*) occur from Kodiak, Alaska, to central California, with landed value at $CDN 40 million in 1986. Canadian landings are the composite of a number of geographically distinct fisheries (Jamieson 1985), with the major one on the west coast of Vancouver Island near Tofino. Study of factors affecting recruitment to this fishery was initiated in 1985, with focus on megalopal abundance and distribution, juvenile growth and survival after settlement, and adult population dynamics. The seasonal and cross-shelf occurrences of larval Dungeness crab megalopae have been described for 1985 along a transect extending 185 km off Tofino (Jamieson and Phillips 1988) and this study expands those observations by considering long-shelf megalopal occurrence and simultaneous oceanographic monitoring. In 1985, *C. magister* megalopae were abundant from 36–148 km offshore off Tofino, and there was no significant nearshore settlement of *C. magister*.

A number of studies (Lough 1976; Reilly 1983; Jamieson and Phillips 1988) have shown that while *C. magister* larvae are hatched nearshore, some larvae then move a considerable distance offshore. The extent to which these offshore larvae return to nearshore waters is uncertain, and it may be that most nearshore settlement results from those larvae which remained shoreward of as yet undetermined oceanographic boundaries. The degree to which larvae move onshore or offshore may vary with latitude, since current patterns vary considerably over the range of the species. The oceanography off the west coast of Vancouver Island and Washington has been described by a number of recent reports, including Thomson (1981, 1984), Freeland et al. (1984), Leblond et al. (1986), Freeland and Denman (1982), Hickey (1979), Denman et al. (1981), and Ikeda et al. (1984a,b). Of particular interest to this study is the significance of the change that occurs at Cape Flattery. Surface current direction south of Cape Flattery is largely determined by the prevailing wind direction (northwards in winter and southwards in summer). To the north, along the west coast of Vancouver Island, the 30–50 km wide, northward-flowing Vancouver Island Coastal Current hugs the coast and is generally present throughout the year, with the broader Shelf-break Current, a reversing, wind-driven current, extending seaward to at least the continental slope. This latter current is an extension of the continental shelf currents found south of Cape Flattery.

The objectives of this study were to investigate the cross-shelf and long-shelf distributions of *C. magister* megalopae in relation to the strength and direction of surface currents, and to evaluate possible oceanographic and meteorological mechanisms which might influence onshore or offshore movement of megalopae.

Dungeness Crab Larval Biology

Dungeness crab larvae are planktonic and pass through five zoeal stages and one megalopal stage before settling to the bottom. Total larval period is about 110 days (Poole 1966; Lough 1976; Reilly 1983), with about 28 days spent as megalopae (Hatfield 1983). Late stage zoea tend to be found progressively further offshore (Reilly 1983). If significant onshore transport occurs, it seems to be the megalopal stage which returns inshore. Late-intermoult stage megalopae tend to be found progressively closer inshore (Hatfield 1983; Jamieson and Phillips 1988).

Megalopae are the strongest swimming stage (Jacoby 1982), although there is no evidence to date that horizontal navigation occurs. Swimming is rheotropic and megalopae show a pronounced diel vertical migration, being concentrated in the top few metres of the water column at night (Booth et al. 1985). There is relatively little data on their depth preference during daylight hours, and while megalopae have on occasion been found at the surface during daylight (Wickham 1979; Reilly 1983; G. Jamieson, unpubl. data), they are not observed regularly at the surface during the day in abundance comparable to nighttime observations.

Methods and Materials

Biological Sampling

In 1986, megalopal sampling was widespread but was conducted along essentially five transects extending from 10 km offshore to about 120 km offshore, with one of the transects extending to about 170 km offshore (Fig. 1). Individual stations were at about 10 km intervals inshore and at about 30 km intervals furthest offshore. Sampling was conducted from June 9–July 3 on the R/V *Parizeau*.

In 1987, sampling was conducted on two separate cruises, from May 4–15 on the R/V *W. E. Ricker* and from June 15–26 on the R/V *Parizeau*. On each cruise, sampling was carried out in two broad geographical areas, off Tofino on the west coast of Vancouver Island, as in 1985 and 1986, and off Grays Harbor, Washington. In each area, sampling was conducted along 2–4 transects, about 35 km apart, extending from 9–140 km offshore (Fig. 2, 3). The distance between transects in all surveys was arbitrarily established and primarily reflected a compromise between staying within the broadcast range of the drifters and surveying the broadest area possible. While surveying along each transect, the duration of darkness was the limiting factor, and both transect lengths and number of stations sampled were a compromise between the need to complete each transect in a single night and to take as many samples as possible. Individual stations were 10–20 km apart.

Nighttime sampling of megalopal occurrence at each station was done with a neuston sampler, 45 cm on each side, which sampled the top 35 cm of the water column under calm sea conditions (Mason and Phillips 1986). A General Oceanics flowmeter in the mouth of the net was used to establish distance travelled and sea surface area filtered. Tow duration was typically 10 min and sampled 500–600 m^2 of sea surface, but at times of high megalopal abundance (>100 m^{-2}), tow duration was shortened to 5 min. The net was 0.5 mm (1 mm in 1987), black Nitex, and the sampler was towed at 4 kn, parallel to and at a distance of approximately 10 m from the side of the vessel.

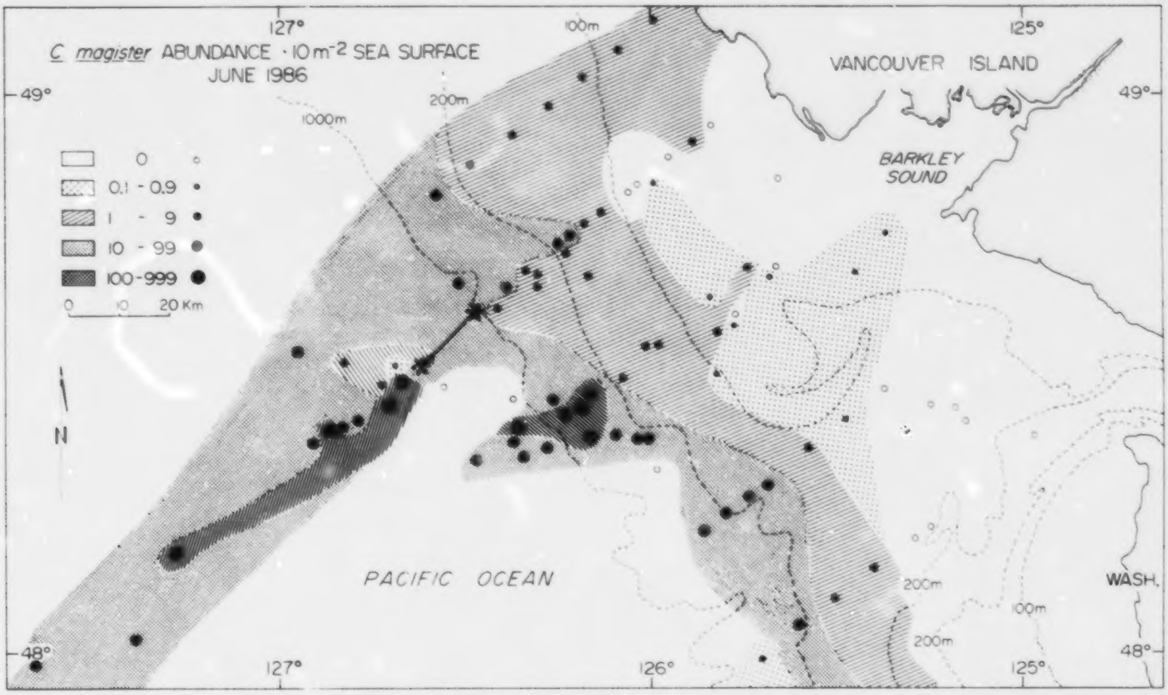
C. magister ABUNDANCE · 10 m⁻² SEA SURFACE
JUNE 1986
0
0.1 - 0.9
1 - 9
10 - 99
100-999
0 10 20 Km
N
127°
125°
49°
48°
126°
100m
200m
1000m
VANCOUVER ISLAND
BARKLEY SOUND
PACIFIC OCEAN
WASH.

FIG. 1. Sample locations (dots) and isopleths of relative megalopal abundance (shaded areas) during June, 1986, off the west coast of Vancouver Island. Stars = location at beginning and end of the 3-day time series of nocturnal neuston sampling.

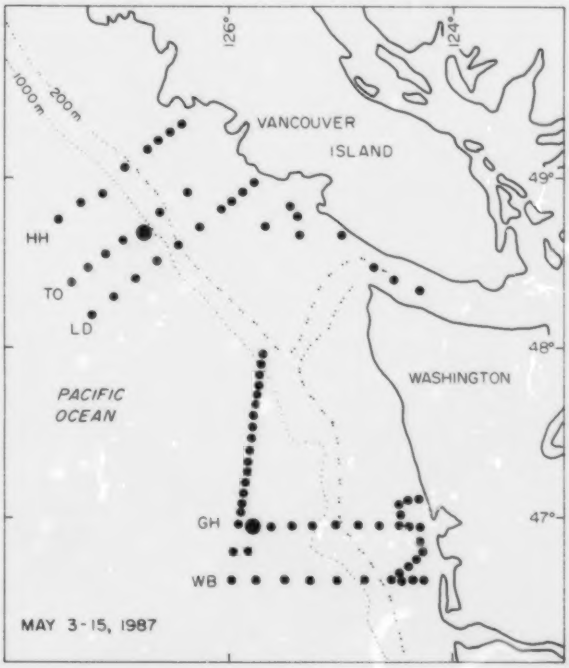
126°
124°
49°
48°
47°
1000m
200m
VANCOUVER
ISLAND
HH
TO
LD
PACIFIC
OCEAN
WASHINGTON
GH
WB
MAY 3-15, 1987

FIG. 2. Sample station locations (dots) during May, 1987, off southern Vancouver Island and Washington. The large dots indicate locations where a concentration of megalopae was monitored continuously through the night. Cross-shelf transects are referred to in later figures by the 2-letter codes indicated.

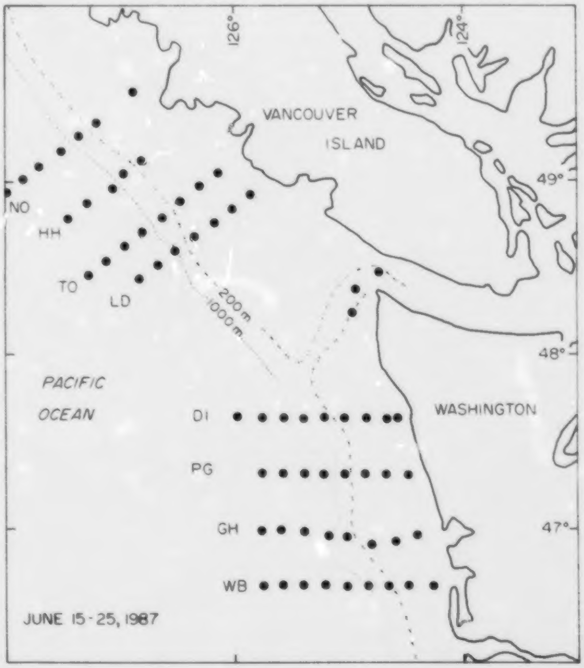
126°
124°
49°
48°
47°
VANCOUVER
ISLAND
NO
HH
TO
LD
200m
1000m
PACIFIC
OCEAN
DI
PG
GH
WB
WASHINGTON
JUNE 15-25, 1987

FIG. 3. Sample station locations (dots) during June, 1987, off southern Vancouver Island and Washington. Cross-shelf transects are referred to in later figures by the 2-letter codes indicated.

During daylight, a Tucker trawl was used in initial studies to ascertain the vertical distribution of megalopae. This 3-serial net trawl had a 1 mm, black Nitex net and a 1 m^2 mouth opening when towed at operational speed (wire angle at 45°, or about 2–3 kn). Tows were of about 20 min duration at 2 kn and sampled 300–900 m^3 per net. Volume of water filtered was used to calculate a haul factor (Mason et al. 1984) which took into account tow depth and allowed expression of the data as the integrated number of organisms beneath 10 m^2 of sea surface.

To establish the hourly abundance of megalopae in the neuston, repetitive neuston tows were taken at the location of maximal megalopal abundance determined during sampling along a cross-shelf transect. During this time, the ship slowly and repetitively circled at 200–300 m distance a deployed drifter whose drogue was centered at a depth of 7.5 m. One drifter was circled for 3 days in June, 1986, and two separate drifters were circled for one night each in May, 1987 (Fig. 1, 2). To establish the long-shore repeatability of observations of megalopal abundance at a specific distance offshore, two 1-night surveys of megalopal long-shore abundance and distribution were conducted in May, 1987 off the Washington coast (Fig. 2), one relatively near shore (9–20 km offshore) and another beyond the shelf break (83–141 km offshore). Both surveys began at dusk and were terminated at dawn the next morning.

Extensive monitoring of the relative abundance of megalopae and newly settled juvenile crab in the inshore waters around Tofino was done through both discussions with local fishermen and the use of a 3-m beam trawl, as described by Gunderson and Ellis (1986) and Jamieson and Phillips (1988). When megalopae are abundant in an area, they are readily visible to fishermen and their presence is reported to us.

All plankton samples were preserved initially in a 4% formaldehyde in saltwater solution. In the laboratory, settled volume was determined and general composition of the plankton noted. Samples were then sieved and *C. magister* larvae, readily identifiable by their larger size (Trask 1970; Lough 1975), picked out, counted, and further preserved in a 2% formaldehyde solution. Intermoult staging used the criteria described by Hatfield (1983), and stages were grouped according to Jamieson and Philips (1988).

Excluding studies establishing the relative hourly abundance of megalopae in the neuston, abundance data was weighted by time of capture at night, with the product reflecting the maximal abundance estimated to be present during the night at that location in that month. Scaling factors ranged from 1.0–20.0, with an upper limit set because accurate value estimation becomes impossible at the times when a majority of megalopae are ascending or descending. In May, data collected between 2100 or 0515 hr was used and the scaling factor used was 1.0, since the linear regression slopes were not significantly different from zero. In June, scaling factors were time specific between 21:30 and 05:00 h, and were determined from the line shown in Fig. 8. A Mann-Whitney test was used to compare the relative abundance levels for different nights and time intervals during the night (Table 1.)

Oceanographic Sampling

Salinity-temperature-depth (STD) profiles of the water column were collected with a Guildline System, and processing of the data to give geostrophic flow values was conducted by Dr. R. Thomson, Institute of Ocean Sciences, Sidney, B.C. Current patterns were determined empirically by the simultaneous deployment of up to 8 Lagrangian drifters at selected distances offshore. Each drifter consisted of a 1.0 m diameter, 0.6 m deep fibreglass buoy containing a Loran C receiver and a radio transmitter with a range of about 90 km (Greisman and Crawford 1985; Crawford and Greisman 1987). Suspended from the buoy was a 1 m diameter, 5 m long, "holey sock" fabric drogue, whose depth was controlled by varying the length of the cable suspending it from the buoy. Most drogues were centered at a depth of 7.5 m, but at selected locations where crab megalopae were particularly abundant, a second drogue was sometimes centered at a depth of 62.5 m. Preliminary sampling offshore (unpub. data) with a Tucker trawl suggested this was a depth range in the study area in which megalopae were abundant during daylight hours, but subsequent sampling (Table 2) suggested that a depth of 25 m would have been more appropriate nearshore in more turbid waters. However, at the locations selected, the 7.5 m and 62.5 m drifters moved in a similar manner, suggesting that there was little difference in current pattern over this depth range. The location (Loran C time differences) of each drifter was transmitted every 30 min, allowing the relative locations of each drifter to be monitored simultaneously from the supporting survey vessel. The drifters were generally allowed to drift for 4–5 days before retrieval and transport to the next study area.

Three distinct geographical deployments of drifters, spread over 3 years and over the months of May and June, are presented. Locations and dates are: in the Juan de Fuca Gyre off the mouth of Juan de Fuca Strait (June, 1985 and 1986), along a cross-shelf transect off Tofino, B.C. (May, 1987, and June, 1986 and 1987), and along another cross-shelf transect off Grays Harbor, Washington (May and June, 1987).

Results

Geostrophic Flow

Mid-June geostrophic surface currents, relative to 100-m depth, determined for mid-June off southern Vancouver Island are presented for the years 1985–87 (Fig. 4a–c), and off Washington for 1987 (Fig. 4c). Currents determined for mid-May, 1987, off both Vancouver Island and Washington are given in Fig. 4d. Boxed areas indicate the outer boundaries of the spatial pattern of STD casts for the specified time period which provided the data used in current determinations.

The basic current pattern shown off Vancouver Island was a counter-clockwise gyre (Juan de Fuca Gyre) off the mouth of Juan de Fuca Strait, a north-flowing current (Vancouver Island Coastal Current) of variable strength centered about 20–30 km offshore from Barkley Sound to Estevan Point, a south-flowing current of again vari-

TABLE 1. A. Linear regression parameters for the relative abundance of megalopae in the neuston against time of night at each location (Fig. 8, 9). B. Observed abundance levels of megalopae at different time intervals at each location. There were significant differences between the means of each date only in 1986. C. Observed abundance levels of megalopae over the 3 nights in June 1986. There was a significant difference between the mean abundance of June 13 and each of the other two nights, and between the means of the time intervals in each of the first two nights. Values in parentheses are standard deviations. Early evening = 21:00–23:30 h; midnight = 23:31–02:30 h; early morning = 02:31–05:30 h.

	1987		1986
	May (Tofino)	May (Grays Hbr.)	June (Tofino)
A. Regression Parameters[a]			
n	17	20	35
Intercept	10.32	13.42	97.16
$p = 0$	0.06	<0.01	<0.01
Slope	0.79	−0.46	−10.18
$p = 0$	0.32	0.17	<0.01
r^2	0.07	0.10	0.30
B. Observed Mean Abundance Levels (N•10 m^{-2} sea surface)			
Early evening	14.8 (4.6)	11.2 (3.9)	65.6 (50.8)
Midnight	15.2 (11.1)	12.1 (4.0)	33.1 (34.7)
Early morning	15.3 (7.9)	8.5 (3.9)	8.7 (6.9)
C. Observed Mean Abundance Levels in June 1986 (N•10 m^{-2} sea surface)			
	June 13/14	June 14/15	June 15/16
n	5	15	15
Early evening	84.4	63.4 (24.7)	64.0 (86.3)
Midnight	3.5 (3.8)	36.6 (8.4)	39.1 (47.0)
Early morning	6.6 (8.6)	15.2 (3.0)	3.3 (3.1)

[a] Time (abscissa): 0 = 19:00 h, 1 = 20:00 h, ... 12 = 07:00 h.

able strength 50–70 km offshore (Shelf-break Current), and furthest offshore, an area of negligible or north-flowing current. The north-flowing Vancouver Island Coastal Current appears to extend seaward over La Perouse Bank, perhaps because of bottom topography, and then moves shoreward until near Estevan Point. Off Washington, there was a broad, south-flowing current (Shelf-break, or California, Current) across the entire shelf, with no particularly strong long-shore currents nearshore. The current pattern seemed to contain ephemeral eddies or gyres. There was little difference between estimated currents at the surface and at 50 m, relative to that at 100 m, off either Vancouver Island or Washington.

Lagrangian Current Measurements (Drifters)

The deployment of drifters across the counter-clockwise Juan de Fuca Gyre is useful in establishing whether crab larvae entrained in the gyre, after drifting south in the southward-flowing Shelf-break Current seaward of the Vancouver Island Coastal Current, are likely to (1) leave the Gyre on its seaward side and continue moving southward, or conversely, (2) circle around in it and leave the Gyre on its shoreward side, to move northwards, closer inshore and entrained in the seaward side of the Vancouver Island Coastal Current. In 1985, all drifters released across the Gyre spun out on the seaward side of the Gyre and moved rapidly southwards at an oblique angle towards the Washington coast (Fig. 5a). In 1986, the opposite occurred, with drifters either circling around within the Gyre or spinning out on its inshore side to move northwards (Fig. 5b). During the periods of observations in both years, winds were consistently light to moderate and primarily from a northerly direction, as would be expected during the month of June. It thus appears that from a transport perspective, dramatically different results can occur between different times during the year or between years, even though the basic geostrophic current pattern appears similar (Fig. 4a, b).

Along the transect off Tofino, drifters were deployed 10–25 km apart, thereby allowing determination of the relative directions and strengths of the currents across and beyond the continental shelf. The basic pattern evident (Fig. 6a – c) was an inshore, northward-flowing current of variable strength (strong in 1986 but weak in 1987), and a southward-flowing current centered slightly seaward of the shelf break (200 m depth). In 1986, the drifter deployed seaward of this latter current (90 km offshore) was essentially stationary while the drifter deployed 100 km offshore moved strongly northwards (Fig. 6a). This outermost, northward-flowing current was not evident in 1987 (Fig. 6b, c).

TABLE 2. Vertical distribution of *C. magister* megalopae from Tucker trawl tows in 1987. Abundance is expressed in number of megalopae per 10 m^2 sea surface over each depth interval sampled, following Mason et al. (1984).

		Tucker trawl (daylight)					Neuston tow (night)[a]
Date	Location	Depth interval (m)	Volume filtered (m^3)	Actual catch	N•10 m^{-2} of sea surface	% by interval	N•10 m^{-2} of sea surface
05 May	111 km off Grays Hbr, WA.	50–0	367	30	40.9	100	10.9[b]
		100–50	383	0	0.0	0	
		25–0	325	21	16.2	91	
		50–25	307	2	1.6	9	
		25–0	576	31	13.5	95	
		50–25	733	2	0.7	5	
		12–0	365	7	2.3	30	
		25–12	590	26	5.7	70	
		12–0	320	2	0.8	13	
		25–12	500	22	5.7	87	
10 May	74 km off Tofino, B.C.	30–0	600	1	0.5	63	14.1[c]
		50–30	600	1	0.3	37	
		13–0	756	13	2.2	83	
		25–13	886	3	0.4	17	
19 June	37 km off coast at Destruction Is., WA.	30–0	675	3	1.3	69	n/a
		50–30	497	1	0.4	31	
		25–0	300	6	5.0	72	
		50–25	900	7	2.8	28	
		25–0	600	7	2.9	57	
		50–25	574	5	2.2	43	
23 June	119 km off Tofino, B.C.	36–0	694	4	2.0	46	n/a
		53–36	586	4	1.2	54	
		20–5	637	5	1.2	83	
		30–20	671	1	0.1	17	

[a] Night tows made with neuston gear at similar locations within 12 h of Tucker trawl tows.

[b] $\bar{x} = 10.9$, $n = 15$ tows, SD = 4.06, range: 2.9-16.4 10 m^{-2} of sea surface.

[c] $\bar{x} = 14.1$, $n = 15$ tows, SD = 7.50, range: 4.2-23.0 10 m^{-2} of sea surface.

The relative stabilities of regions in the observed currents off Tofino were established in June, 1986 (Fig. 6a), when about 30 hr after deploying the drifters in moderate westerly 22 kn winds, wind direction shifted to the southeast, but stayed at similar strength. The two drifters on the coastal side of the Shelf-break Current quickly began moving northwards and obliquely towards the coast, whereas all other drifters continued moving at a similar rate and direction as before the change in weather.

The main features pertinent to movement of larvae either onshore or offshore off Tofino, then, are:

1) the presence of generally stable long-shore surface currents, although moderate-to-large meteorological events may significantly influence current strength and direction in some areas;
2) the occurrence of at least one, and possibly two, relatively stable zones of little long-shore and cross-shelf transport, which appear to be at the boundary between opposing surface currents;
3) significant annual difference, in June at least, in the current velocity of the Vancouver Island Coastal Current;
4) general southeasterly long-shore transport at the surface in the Shelf-break Current, presumably because of the seasonal northwesterly winds prevalent off Vancouver Island (it should be noted there was little evidence of cross-shelf, offshore transport, as would be expected from Ekman theory);
5) periodic onshore cross-shelf transport in surface waters in some regions of the Shelf-break Current with the southerly or southeasterly winds associated with summer storms.

As expected, the current pattern off Grays Harbor, Washington, was significantly different from that

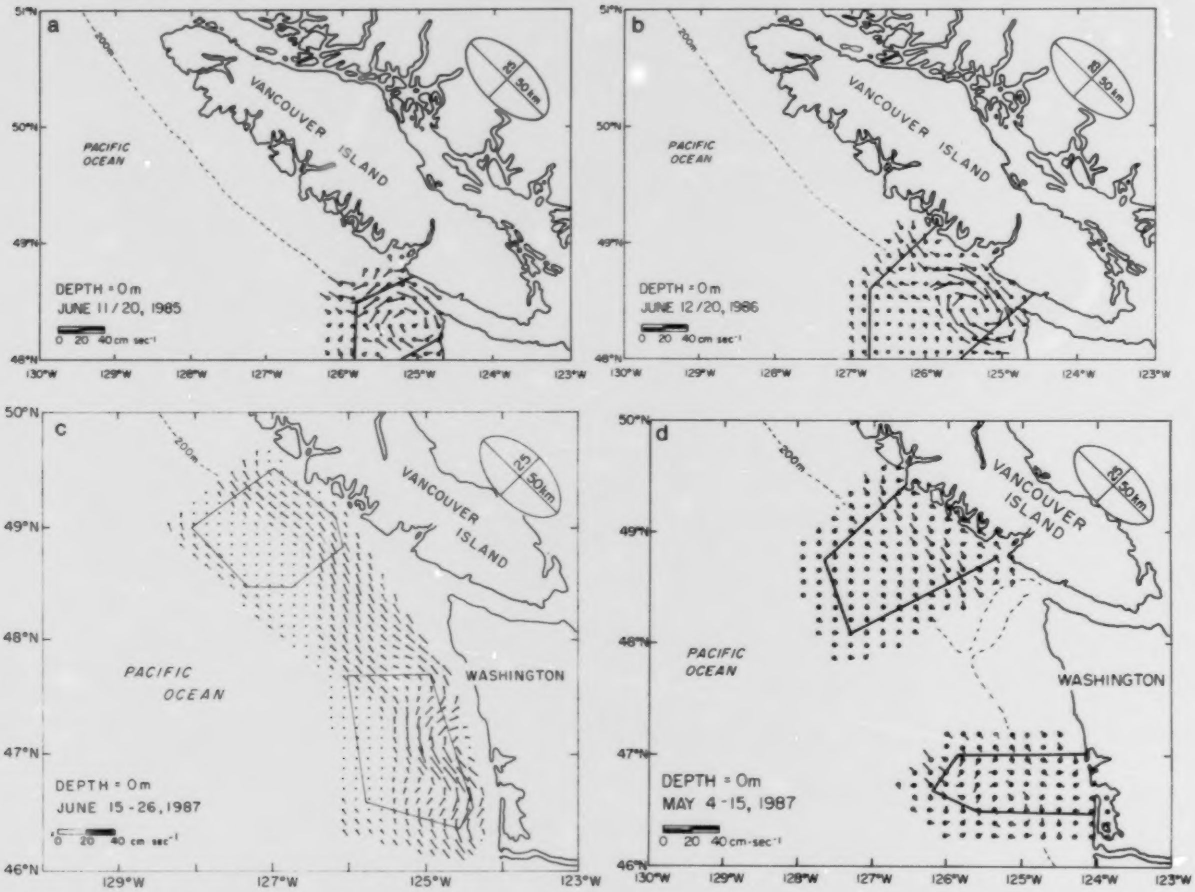

FIG. 4. Objectively smoothed near-surface water property maps of sigma-*t* for a depth of 0 m relative to 100 m. Assumed cross-shore and longshore correlation scales are 25 and 50 km, respectively. a, for June 11–20, 1985; b, for June 12–20, 1986; c, for June 15–26, 1987; d, for May 4–15, 1987.

observed off Vancouver Island. All deployed drifters moved southwards (Fig. 7a, b), regardless of their distance offshore. However, there was variation in longshore current strength across the continental shelf, with maximal velocity (about 15 cm s^{-1}) 50–75 km off the coast. In May, adjacent drifters, deployed about 13 km apart, moved at different speeds, one faster, the next slower, another faster, and so on. This might be explained by an interlocking array of minor eddies, as suggested by the geostrophic flow data (Fig. 4d), which, if so, would probably be an ephemeral event. Just prior to retrieval of the drifters on June 20, wind direction changed for about 6 hr from northerly to southerly and average velocity increased from about 11 to 30 kn. Although the time interval was short, southward transport of the drifters was significantly reduced and there was a pronounced onshore, cross-shelf movement of the drifters (Fig. 7b).

Off Washington, then, zones of little or no long-shore current flow appear less structured and relatively little long-shore variability in current flow and strength existed over most of the survey area during the study period. With northerly winds, all currents were to the south and maximum current strength was just seaward of the shelf break. Current direction and velocity were influenced by moderate wind events which, if from a southerly direction, can result in onshore, cross-shelf transport of surface waters. With the prevalent seasonal northerly winds, southerly long-shore transport of surface water predominated.

Diel Occurrence of Megalopae in Surface Waters

Jamieson and Phillips (1988) described the nocturnal abundance of megalopae in surface waters for one night at a location 9 km off Tofino. However, because relative megalopal abundance was low in comparison to their abundance further offshore, and because the same population of megalopae is not being continuously sampled if geographical location is fixed (currents move it away), relative diel abundance for a specific water mass was determined in this study for both May (1987) and June (1986).

In June, 1986, no megalopae were observed present in surface waters during daylight at the survey site (Fig. 1). Relative abundance of megalopae at this location at night was relatively high, and it subsequently was determined

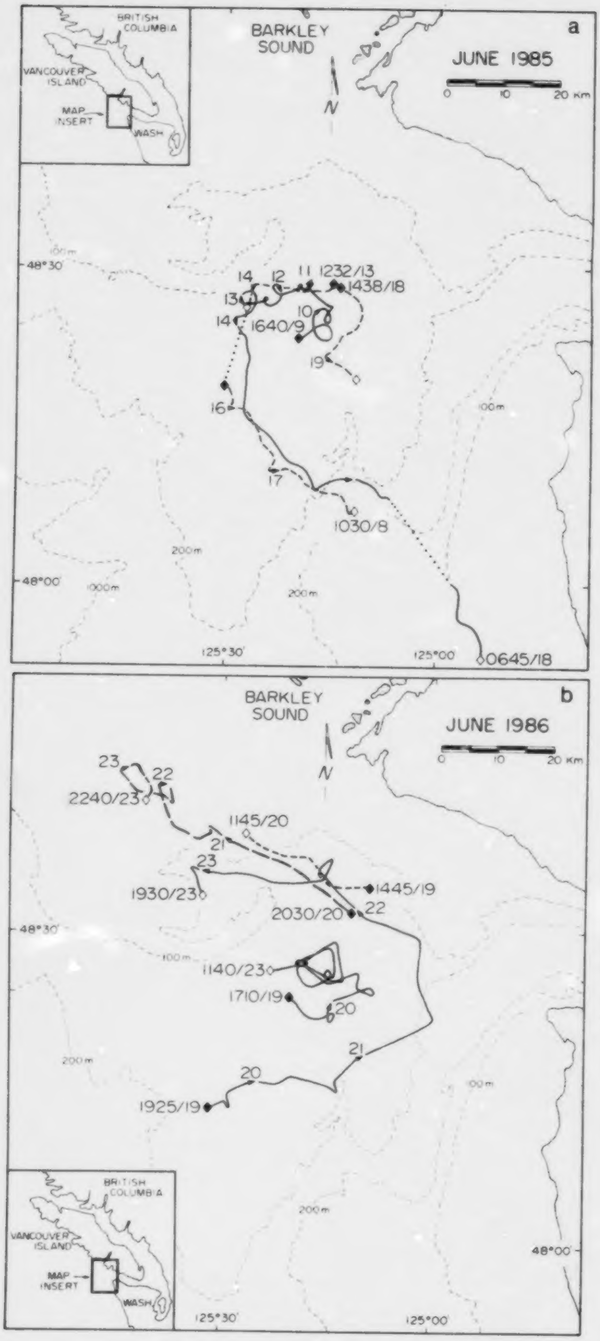
BRITISH COLUMBIA
VANCOUVER ISLAND
MAP INSERT
WASH
BARKLEY SOUND
a
JUNE 1985
0 10 20 Km
N
48°30'
14
12
11
1232/13
1438/18
13
10
14
1640/9
19
16
17
1030/8
200m
100m
48°00'
1000m
125°30'
125°00'
0645/18
BARKLEY SOUND
b
JUNE 1986
0 10 20 Km
N
23
22
2240/23
1145/20
21
23
1445/19
1930/23
2030/20
22
48°30'
100m
1140/23
1710/19
20
21
200m
20
100m
1925/19
200m
48°00'
125°30'
125°00'

FIG. 5. Tracks of drifters deployed across the Juan de Fuca Gyre: a, 3 drifters in June, 1985; b, 4 drifters in June, 1986. Marks along each track indicate the position of each drifter at noon on the day (the adjacent 1 or 2-digit number) indicated. Four-digit numbers refer to the hour the drifter was deployed and/or retrieved.

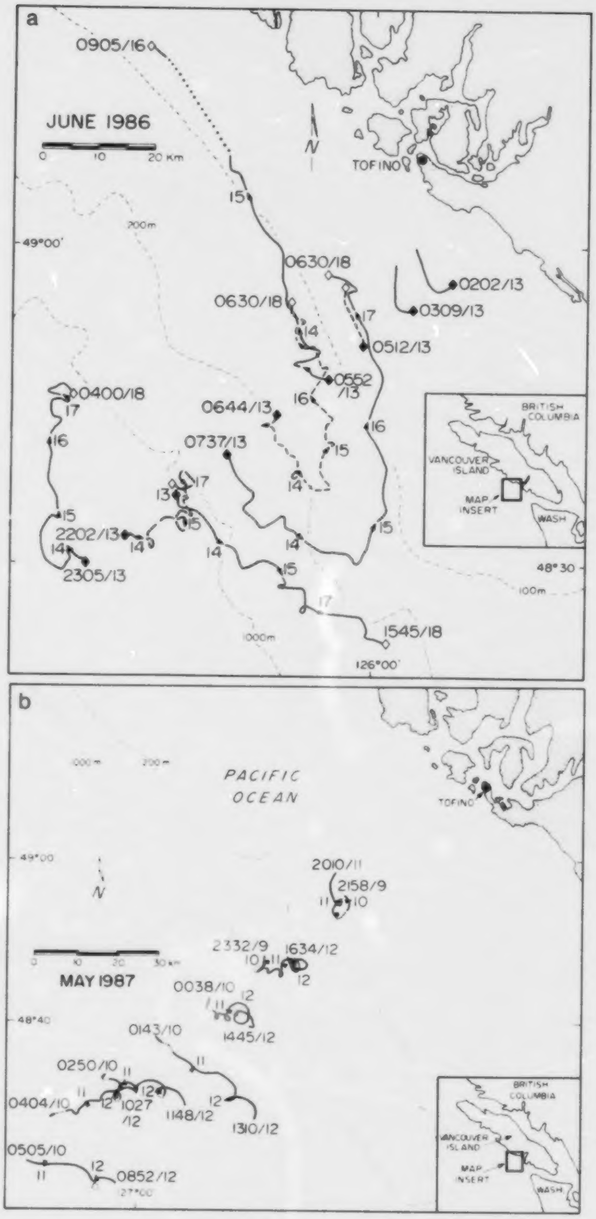
a
0905/16
JUNE 1986
0 10 20 Km
N
TOFINO
15
49°00'
200m
0630/18
0202/13
0309/13
0630/18
17
14
0512/13
0552/13
0400/18
17
16
0644/13
16
16
0737/13
15
15
13
17
14
15
2202/13
14
15
14
14
15
2305/13
17
1545/18
48°30
100m
1000m
126°00'
BRITISH COLUMBIA
VANCOUVER ISLAND
MAP INSERT
WASH
b
PACIFIC OCEAN
TOFINO
1000m
200m
49°00
N
2010/11
2158/9
11
10
2332/9
1634/12
0 10 20 30 km
MAY 1987
0038/10
12
48°40
0143/10
1445/12
11
0250/10
11
12
0404/10
12
1027/12
1148/12
12
1310/12
0505/10
12
11
0852/12
127°00'
BRITISH COLUMBIA
VANCOUVER ISLAND
MAP INSERT
WASH

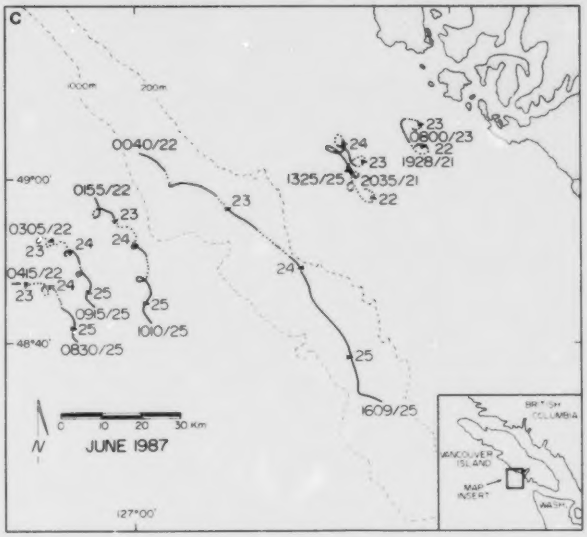
c
1000m
200m
0040/22
49°00'
0155/22
23
0305/22
23
24
0415/22
25
0915/25
0830/25
1010/25
48°40'
1325/25
2035/21
1928/21
0800/23
1609/25
JUNE 1987
0 10 20 30 Km
N
127°00'
BRITISH COLUMBIA
VANCOUVER ISLAND
MAP INSERT
WASH.

FIG. 6. Tracks of drifters deployed along a transect off Tofino, B.C.: a, 9 drifters in June 1986. The second drifter from the left (deployed 22:02 h, June 13) indicates the locations where a concentration of megalopae was monitored for 3 consecutive nights. The 2 drifters closest inshore were retrieved after 8 h since because they were moving northwards so fast, they were approaching the maximum broadcast range of their radio transmitters; b, 7 drifters in May 1987. The third drifter from the right, deployed at 00:38 h, May 9, indicates the location where a concentration of megalopae was continuously monitored all night; c, 6 drifters in June 1987. Marks along each track indicate the position of each drifter at noon on the day (the adjacent 1 or 2-digit number) indicated. Four-digit numbers refer to the hour the drifter was deployed and/or retrieved.

that the drifter being circled remained virtually stationary in long-shore movement (there was a slow inshore drift) throughout the deployment period, regardless of wind direction and velocity. Nocturnal abundance of megalopae in the neuston was similar each night, and the combined data shows that megalopal abundance peaked in the evening at about nautical twilight (sun 12° below the horizon) (Fig. 8). The slope of the regression line of relative abundance versus time of night was significantly negative, although the correlation coefficient was low (Table 1A). Mean megalopal abundance on June 13 was significantly different from that on the other two days, but the overall trend of declining abundance over time was consistent (Table 1C). In May (Fig. 9), regression lines for data from each location were significantly different between each other because of the elevations of the lines. The slopes of neither line were significantly different from zero, although correlation coefficients were again low (Table 1). Because abundance remained effectively constant from civil twilight (sun 6° below the horizon) in the evening to civil twilight in the morning (Fig. 9), results from both locations in May, 1987, differed significantly from those obtained in June, 1986 (Fig. 8). This may indicate a temporal change in vertical distribution behaviour by Dungeness crab megalopae with intermolt stage or over the course of a season.

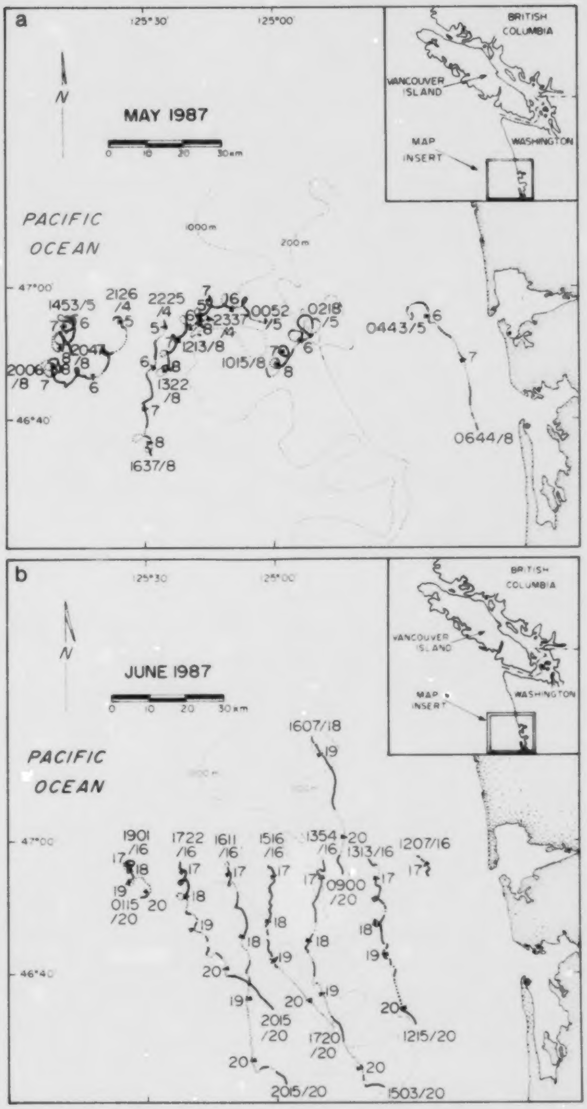
a
125°30'
125°00'
N
MAY 1987
0 10 20 30 km
PACIFIC OCEAN
1000m
200m
47°00'
46°40'
1453/5
2126/4
2225/4
2337/4
0052/5
0218/5
0443/5
1213/8
1015/8
2006/8
1322/8
1637/8
0644/8
BRITISH COLUMBIA
VANCOUVER ISLAND
MAP INSERT
WASHINGTON
b
JUNE 1987
1607/18
1901/16
1722/16
1611/16
1516/16
1354/16
1313/16
1207/16
0115/20
0900/20
2015/20
1720/20
1215/20
2015/20
1503/20

FIG. 7. Tracks of drifters deployed along a transect off Grays Hbr., Washington: a, 7 drifters in May 1987. The end drifter on the left, deployed at 14:53 h, May 5, indicates the location where a concentration of megalopae was continuously monitored all night; b, 7 drifters in June 1987. The end drifter on the right was picked up by a fisherman in the afternoon on June 17, but was recovered and redeployed about 30 km north of the initial deployment at 16:07 h, June 18. Marks along each track indicate the position of each drifter at noon on the day (the adjacent 1 or 2-digit number) indicated. Four-digit numbers refer to the hour the drifter was deployed and/or retrieved.

Preliminary studies on the vertical distribution of megalopae during the day (Table 2) suggest that megalopae are mostly in the top 25 m of the water column nearshore, although data are still limited and diurnal abundance did not always seem to reflect nocturnal abundance at the same location. This may in part reflect the difficulty in comparing data from two gear types.

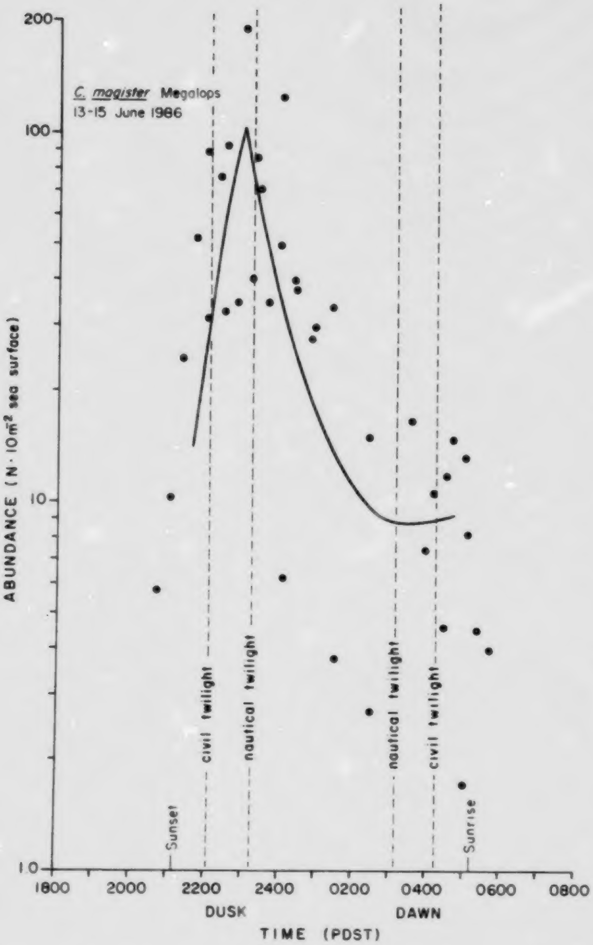

FIG. 8. Abundance of *C. magister* megalopae observed around a drifter over 3 consecutive nights (June 13/14–15/16, 1986). Weighting values to scale abundance by time of capture were derived from the line shown.

Although the volumes of water sampled were comparable, the process of vertically integrating over the depth range sampled means that with a Tucker trawl, a much smaller sea surface area is sampled than occurs with a neuston sampler. The micro-scale patchiness of megalopal distribution is thus more likely to bias the data from a Tucker trawl tow. Preliminary results suggest that the depth to which megalopae descend in daylight is a function of water turbidity, with megalopae closer to the surface in the more turbid waters near the coast (unpub. data).

Megalopal Cross-Shelf Abundance and Distribution

General results (Table 3) obtained in both 1986 and 1987 confirm the observations made in 1985 that crab megalopae were only regularly abundant off the west coast of Vancouver Island in water >40 km offshore, i.e., beyond the probable outer boundary of the Vancouver Island Coastal Current (Fig. 1, 6). Extensive searching in 1985–87 for newly settled juvenile crabs near the coast, using beam trawls and methods described by Jamieson and Phillips (1988), yielded few 0-year-class crabs in each year (Smith 1988; G. Jamieson, unpub. data), supporting the absence of significant megalopal settlement in the Tofino area since 1985. Settlement in 1987 appeared slightly greater than in either 1985 or 1986. Megalopal settlement was apparently substantial as recently as 1983 or 1984, since crabs are considered to largely recruit to the fishery at age 3 (Smith 1988) and landings in 1986 and 1987 in Tofino (Statistical Area 24: 365 and 488 t, respectively) were high (1966–85 average = 160 ± 69 t).

Along the cross-shelf transects sampled off Vancouver Island in both years, maximum megalopal abundance was furthest offshore off southern Vancouver Island but became progressively closer inshore north of Barkley Sound (Fig. 1, 10). Megalopae were caught on the seaward ends of all transects, indicating their distribution extended beyond the maximum distances surveyed offshore (about 140 km on average). In 1986, greatest abundance off Tofino was at about 100 km, nearly twice as far offshore as in 1985 and 1987 (Table 3) and at a location where little longshore drifter movement occurred (Fig. 6a). Megalopal abundance was low at the mouth of Juan de Fuca Strait (Fig. 1). In both 1986 and 1987, maximum megalopal abundance was in the regions indicated by drifter movements to be between major currents moving in opposite directions, with relatively few megalopae (Fig. 10) collected at stations in the Vancouver Island Coastal Current.

Off Washington, the spatial distribution of megalopae (Fig. 11) differed substantially from that observed off Vancouver Island (Fig. 10). While megalopae were again collected along the entire length of each transect, megalopae were on occasion in highest abundance <20 km from shore. North of Grays Harbour in June, 1987, there was a zone of relatively low megalopal abundance near the shelf break, 70–90 km offshore. The presence of megalopae in nearshore waters suggests that relatively greater megalopal settlement was occurring off the central Washington coast than along the west coast of Vancouver Island in both May and June, 1987.

Megalopal Long-Shore Abundance and Distribution

Along the inshore survey 9–20 km off the mouths of both Grays Harbour and Willapa Bay, megalopal density ranged from about 0.1–10/10 m^2 of sea surface (Fig. 12a). Density along the transect 83–141 km offshore ranged from 8–60/10 m^2 of sea surface (Fig. 12b). Considering the latitudinal distances covered (about 56 and 100 km, respectively), average megalopal density was consistently within one order of magnitude at stations along each transect, which is considered to be relatively constant. Patchiness in plankton abundance is expected (e.g., Hardy 1946; Wiebe 1970; Booth et al. 1985), and while megalopal patch sizes were not determined in this study, megalopae were continuously present at all stations.

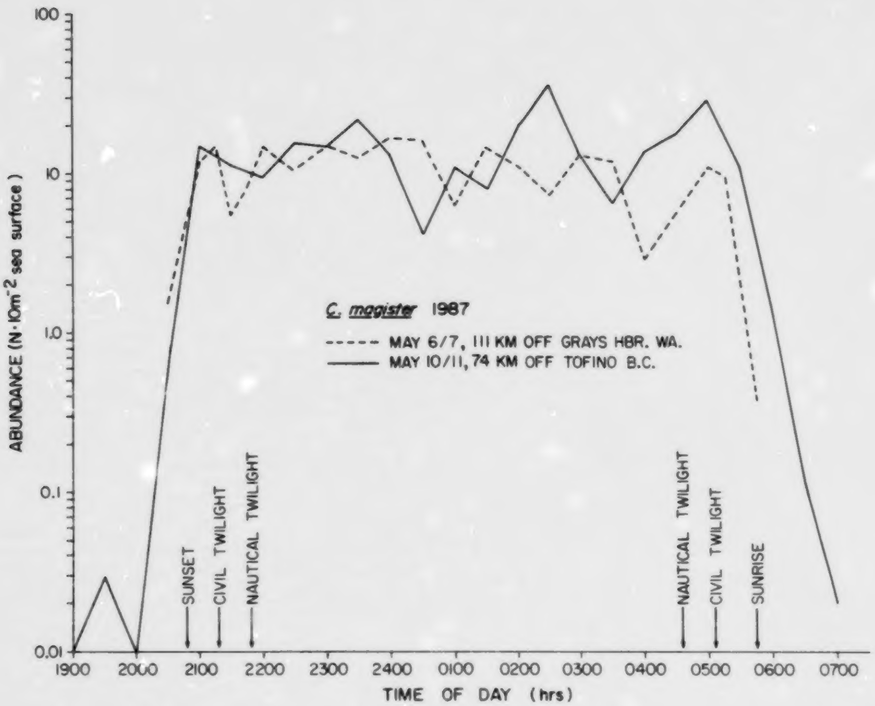

FIG. 9. Average relative abundance of *C. magister* megalopae observed over time on two separate nights between May 6–11, 1987. Specific locations of monitoring are shown in Fig. 6a, 6b and 7a.

Intermoult Stage Distribution

Late intermoult stage megalopae in 1986 were most abundant nearest shore whereas early and mid-intermoult stage megalopae were most abundant further offshore (Fig. 13). However, because total megalopal abundance in both years was relatively low overall close to shore (Table 3), late intermoult stage megalopae comprised a relatively small proportion of the total megalopal population present (Fig. 14), similar to observations in 1985 (Jamieson and Phillips 1988).

Discussion

A problem common to both oceanographic and biological sampling at sea is the compromise between covering a sufficiently large area to develop an understanding of broad-scale events or processes and taking a sufficient number of samples in any specific are to account for microscale patchiness in the parameter being investigated. Until either rapid movement between stations is possible, or inexpensive, deployable, automatic samplers are developed, the only practical approach currently available is the sampling of stations along a grid or transect survey design in as short a time frame as possible coupled with stationary, repetitive sampling at a few locations to try to establish an estimate of local variability. Any compromise is always open to criticism that more samples of either type should have been taken, but the logistic constraints associated with the simultaneous collection of both oceanographic and biological data over the same time period are facts which have to be recognized. Interpretation of our results should be considered in the context of these limitations.

Quantitative sampling of megalopae was primarily conducted with neuston gear because of the relatively large sea surface area sampled in comparison to the integrated area obtained from bongo and Tucker trawl gear. The distribution of plankton is known to be patchy (e.g., Hardy 1946; Wiebe 1970; Booth et al. 1985) and while our ability to establish macroscale (kilometre) variation was limited, as described above, maximizing sea surface area sampled per tow at least tended to minimize microscale (metre) variation. A 10-min neuston tow samples about 500–600 m^2 of sea surface whereas a 20-min Tucker trawl tow to 50-m depth, assuming 2 min down for the first net and 9 min each for the remaining 2 nets coming up over 2, 25-m depth ranges, samples 540 m^3, or 22 m^2 of integrated sea surface area, for each of the last two nets. There is about a 25-fold difference in relative sea surface areas sampled per unit of tow time period in this comparison, and while the ratio decreases by sampling a smaller depth range with the Tucker trawl, the greater awkwardness of using a Tucker trawl relative to neuston gear discourages this for logistical reasons.

However, while sampling with neuston gear at night may be best for rapidly establishing megalopal crab densities, there is some evidence that at different times of the night, crab are not always equally available to this

TABLE 3. Scaling factors (S) used to standardize the actual number of *C. magister* megalopae caught (A) per 10 m^2 of sea surface to the estimated number (E) which would have been caught at the time of peak nocturnal abundance (23:00 h) in June off Tofino, B.C. The shelf-break (200 m depth isopleth) is about 80 km offshore.

Distance offshore (km)	1985			1986			1987		
	S	A	E	S	A	E	S	A	E
0 —									
9 —	3.6	0.1	0.4	1.9	0.3	0.6	—	—	—
19 (15)[a]	1.2	0.1	0.1	2.3	0.5	1.2	12.5	0.0	0.2
28 (30)[a]	1.0	0.2	0.2	3.5	1.4	4.9	13.5	0.2	3.1
37 —	∞	0.1	?[b]	4.2	0.3	1.3	—	—	—
46 (44)[a]	—	—	—	6.8	0.5	3.4	13.3	4.8	63.7
56 (60)[a]	20.0	52.2	1044.0[b]	10.3	3.4	35.0	9.0	5.7	51.6
74	5.2	3.7	19.2	13.7	0.7	9.6	5.0	1.6	7.9
93 (89)[a]	2.4	8.9	21.6	12.9	13.2	170.3	3.4	4.1	13.9
— (103)[a]	—	—	—	—	—	—	1.5	1.6	2.4
111 (118)[a]	1.2	8.4	10.3	12.9	74.4	959.8	9.0	2.1	19.2
148 —	—	—	—	10.3	10.7	110.2	—	—	—
166 —	—	—	—	3.5	5.8	20.3	—	—	—
185 —	—	—	—	3.5	5.8	20.3	—	—	—

[a] Distance offshore for 1987 survey.

[b] Value uncertain because of time of sampling.

gear. The linear regressions calculated to describe the data were significantly different between May and June, but there was considerable variability and the correlation coefficients were low. Because the slope of the regression in June was significantly negative, though, we did weight all the June data presented here for time of capture at night. However, to indicate that this did not alter the basic relative abundance trends observed in the actual data, both the actual and estimated (i.e., weighted) numbers of megalopae present along transects sampled in June from 1985–87 are presented (Tables 3 and 4). In no case did the relative distribution pattern of megalopae change, since megalopae were typically present at either low or very high densities, and weighting was not of sufficient magnitude to alter this. Finally, the long-shore surveys in May, a time when no weighting was justified, support the validity of the observed distribution of megalopae. Even over extensive distances, the relative abundance of megalopae remained within one order of magnitude and was in agreement with our cross-shelf observations. Weighting, then, was used in this study only to allow improved comparison of data, not to justify a different interpretation than would have been suggested by the unweighted data.

Cross-Shelf Movement of Megalopae

Our work over the past 3 yr off the west coast of Vancouver Island suggests that although relatively little crab settlement occurred (most in 1987), Dungeness crab megalopae occur annually in abundance over at least the continental shelf and, for much of the coast, such abundance probably extends many kilometres further offshore. We did not investigate the movement of zoeal stages, which occur earlier in the year, and so the mechanisms whereby larvae from nearshore areas move offshore remain uncertain. Presumably, movement is mostly passive and is affected by Ekman transport, but because the total larval period of *C. magister* is relatively long (about 4 mo) and extends over a time period of major seasonal change in regional oceanography (January–July), estimating long-term movement patterns for any group of larvae is considered impractical with available data. Nichols et al. (1982) had some success attempting this for *C. paguras*, but that species has only a 23–30 d pelagic larval period (Edwards 1979). It was for this reason that our studies have focused on megalopae and on the relatively simpler question of trying to establish which megalopae are potentially able to settle inshore. They must do this

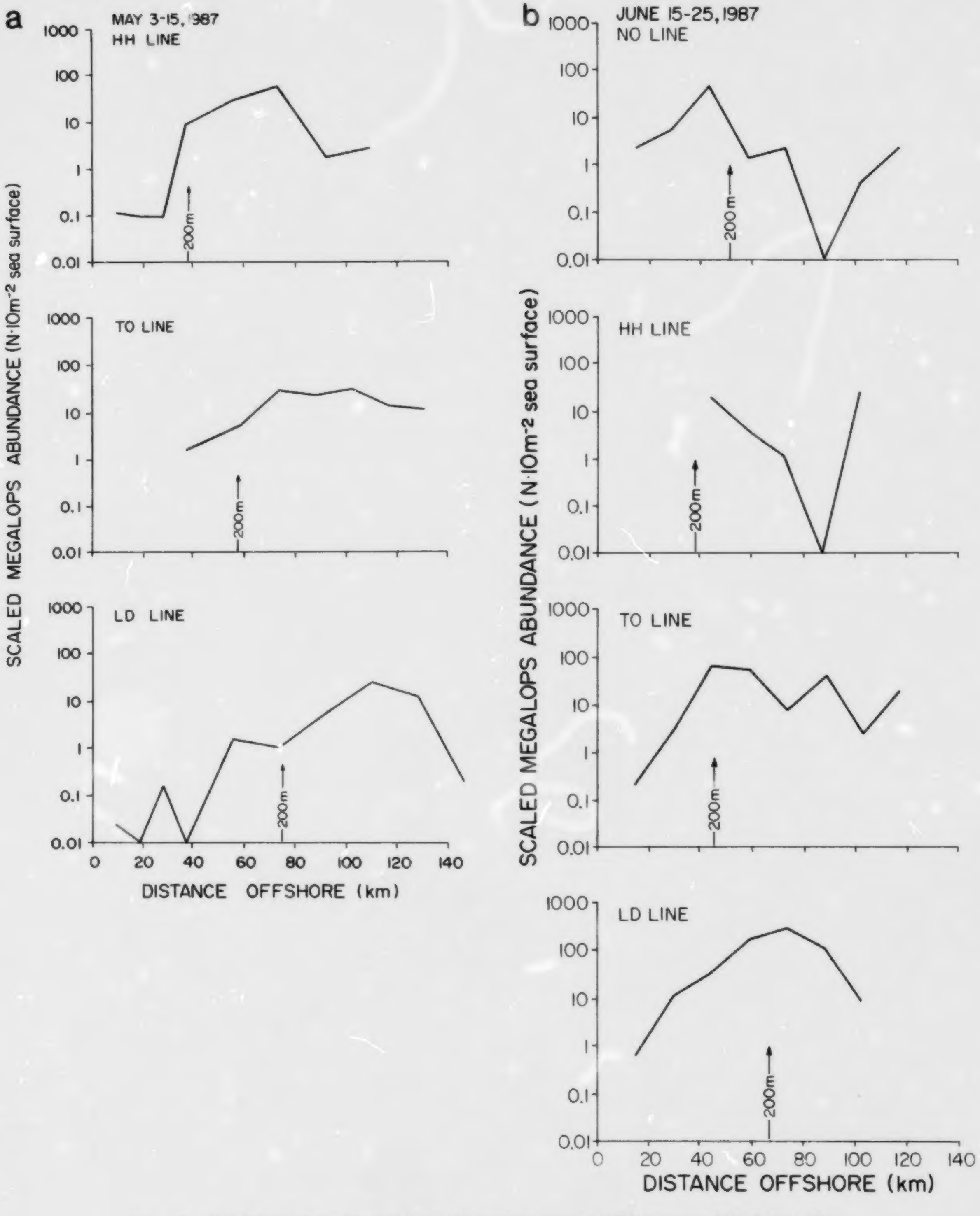

FIG. 10. Abundance of megalopae found along the transects off Vancouver Island in a, May 1987, b, June 1987. The arrow indicates the distance from shore of the shelf break (200 m depth isopleth). Locations of each transect are given in Fig. 2, 3, respectively, referenced by the two-letter codes indicated.

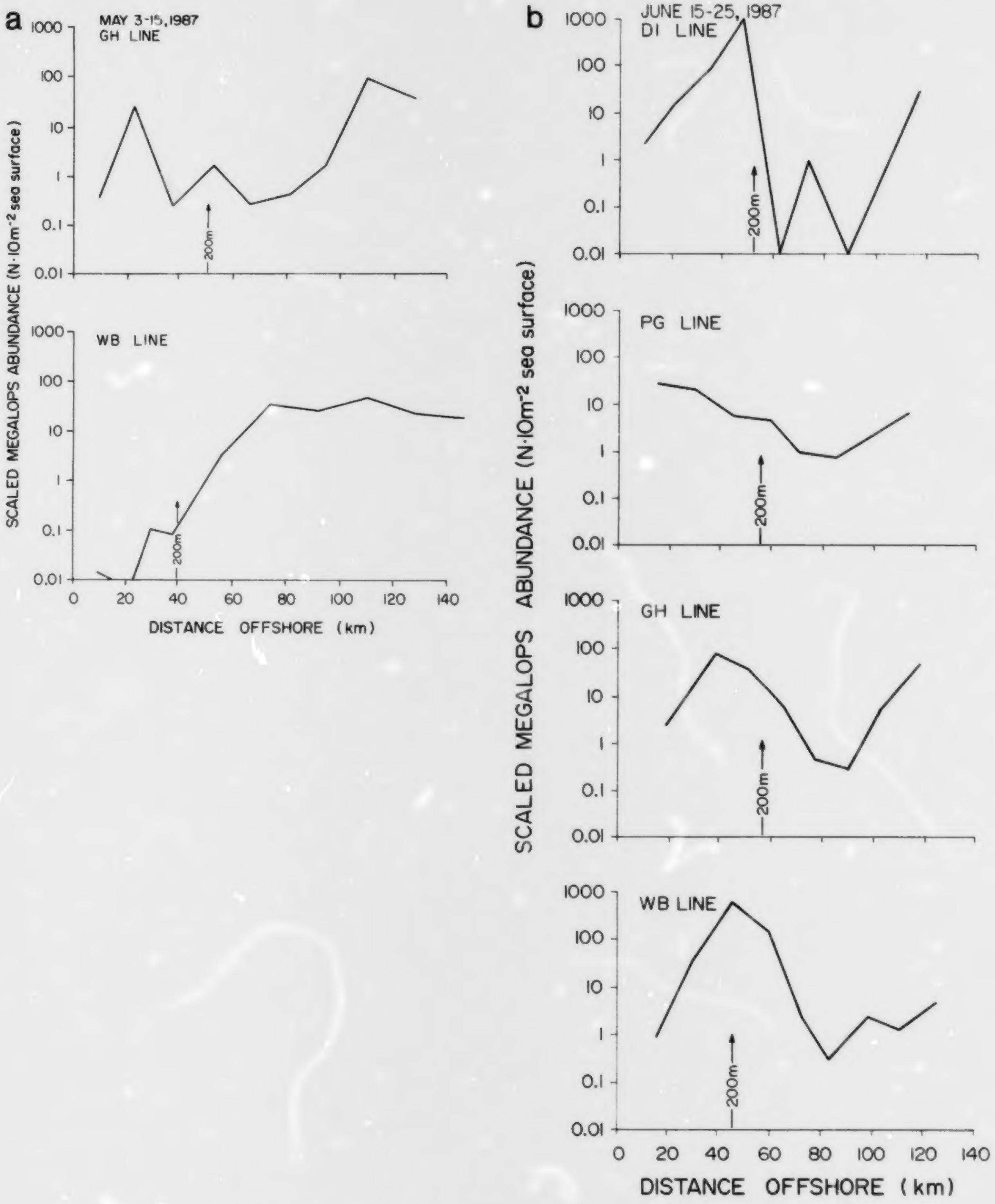

FIG. 11. Abundance of megalopae found along the transects off Washington in a, May 1987, b, June 1987. The arrow indicates the distance from shore of the shelf break (200 m depth isopleth). Locations of each transect are given in Fig. 2, 3, respectively, referenced by the two-letter codes indicated.

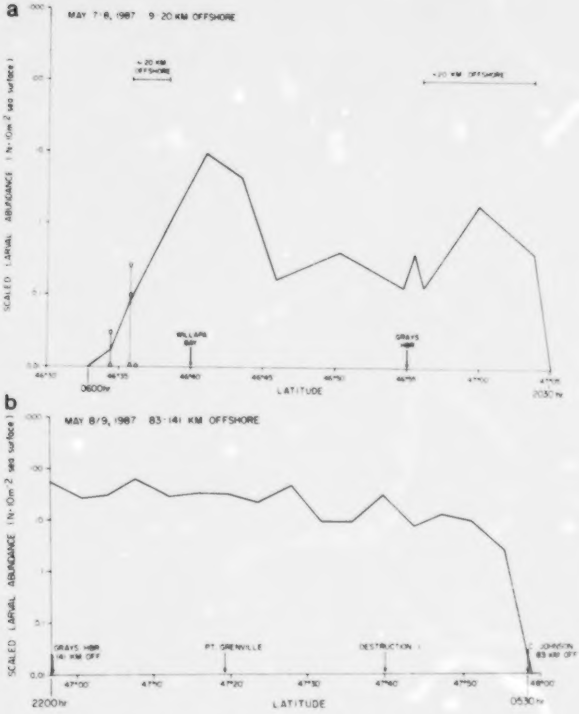

FIG. 12. Abundance of megalopae found along the a. inshore, b. offshore, longshore transects off Washington in May 1987. The arrows indicate the latitudes of significant geographical features, and the times at night that sampling began or terminated are shown. Locations of the transects are given in Fig. 2.

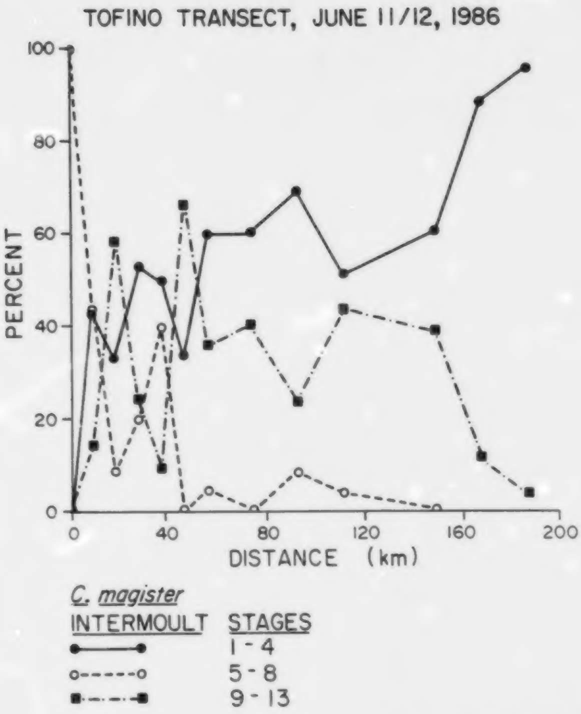

FIG. 13. Percentage of the three *C. magister* megalopal intermoult groups observed at each station on the transect off Tofino, B.C. in June 1986 (Fig. 1). The intermoult stages comprising each group, early (1–4), middle (5–8), and late (9–13), are those of Hatfield (1983).

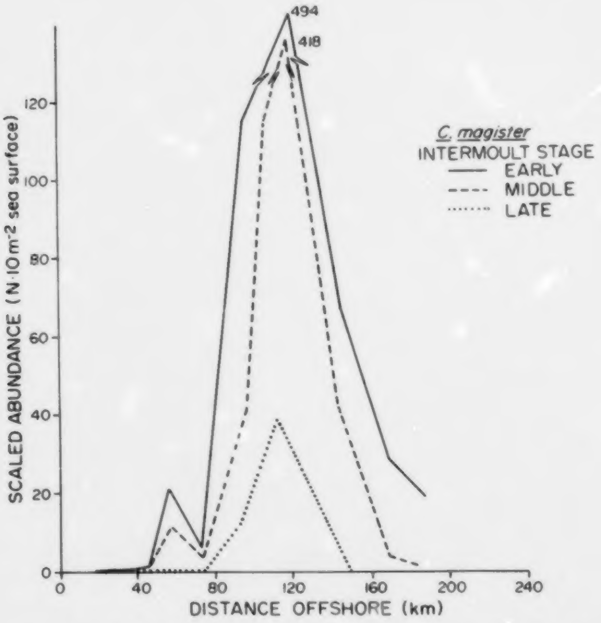

FIG. 14. Scaled abundance of *C. magister* megalopae by intermoult group (see Fig. 13) at each station along the Tofino, B.C., transect in June 1986.

if they are to survive as settled juveniles and, therefore, it is useful to resolve what mechanisms or processes influence their potential onshore movement. Few Dungeness crab juveniles can be found in quantity at depths >64 m (Carrasco et al. 1985) which means that for most of the coast, megalopae must settle within 10–15 km of shore to survive as juveniles.

Evidence for Onshore Movement

Dungeness crab megalopae, along with the megalopae of *C. oregonensis* (Lough 1976; Jamieson and Phillips 1988), another inshore crab species, are often the dominant organisms at the surface at night in the spring in offshore waters (Jamieson and Phillips, unpub. data). Since other *Cancer* species (e.g. *C. productus*) abundant along the coast have larvae which are not abundant in offshore waters, offshore dispersal is apparently neither an essential nor automatic occurrence arising from nearshore hatching of eggs in the spring.

For species indigenous to a region, it would seem likely that a dispersal strategy would evolve which would tend to maximize larval survival to the juvenile stage. It seems unlikely that many, if not most, *C. magister* and *C. oregonensis* larvae would move offshore if there was no mechanism to result in their ultimately returning inshore, at least in most years. Dispersal mortality arising from being in an unfavourable place for survival at settlement

TABLES 4. Actual (A) and scaled (E) numbers of *C. magister* megalopae per 10 m^2 of sea surface in June, 1987, for the transects shown in Fig. 10b and 11b. Transect locations are shown in Fig. 3.

Transect	Data type	Distance offshore (km)							
		15	30	45	59	74	89	103	119
NO Line	A	0.1	0.4	2.7	0.1	0.3	0.0	0.3	1.6
	E	2.3	5.1	36.7	1.4	2.2	0.0	0.8	2.3
HH Line	A	—	—	8.1	0.7	0.1	0.0	1.5	—
	E	—	—	18.5	3.7	1.1	0.0	19.8	—
TO Line	A	0.0	0.2	4.8	5.7	1.6	4.1	1.6	2.1
	E	0.2	3.1	63.7	51.6	7.9	13.9	2.4	19.2
LD Line	A	0.4	3.0	4.3	16.1	24.1	9.1	0.8	—
	E	0.6	11.8	33.8	183.0	330.9	118.8	9.8	—
DI Line	A	0.1	5.9	94.2	0.0	0.2	0.0	0.4	2.8
	E	1.1	80.1	989.0	0.0	0.9	0.0	0.6	27.0
PG Line	A	1.9	1.6	0.6	0.7	0.2	0.4	1.2	0.6
	E	25.5	20.9	6.3	4.6	0.9	0.7	2.3	6.2
GH Line	A	0.1	5.2	2.0	0.6	0.1	0.1	3.6	6.6
	E	2.5	70.0	27.4	5.9	0.5	0.3	4.7	46.5
WB Line	A	0.1	2.9	43.5	14.8	0.3	0.1	1.2	0.6
	E	0.8	38.8	596.0	151.9	2.4	0.3	2.4	6.1

can be termed larval wastage, and although partially unavoidable, the two *Cancer* species are the only inshore crustacean species found regularly in abundance in offshore waters off Washington and Vancouver Island. Some onshore transport process or mechanism thus seems likely to exist.

Onshore movement of megalopae is suggested by the observation that late intermoult stage megalopae tend to be found progressively closer inshore (Hatfield 1983; Jamieson and Phillips 1988; Fig. 13). Megalopae are relatively strong swimmers (Jacoby 1982; J. Booth, 3211 Hammond Bay Rd., Nanaimo, B.C., pers. comm.), yet apart from a nocturnal migration to the water surface, no directed geographical movement has yet been determined. When abundant in surface waters during daylight hours, megalopae were usually found clinging to floating objects (*Velella velella*: Reilly 1983; Wickham 1979; Jamieson and Phillips 1988; dead salps and floating debris: Jamieson, unpub. data). These observations suggest that being at the water surface may be important to the onshore movement of megalopae.

Evidence Against Onshore Movement

Jamieson and Phillips (1988) point out that while earlier studies by Reilly (1983) off northern California and Lough (1976) off Oregon established the occurrence of megalopae in offshore waters, their sampling was primarily during the day with gear not optimal for rapid, accurate estimation of relative areal megalopal abundance. The only other data available are ours off British Columbia (1985–87) and Washington (1987); for the years and locations monitored, no substantial movement of a specific larval concentration was evident and no major Dungeness crab settlement occurred in inshore waters. Substantial crab settlement at any specific location has yet to be correlated with the movement of megalopae from offshore areas to the coast. While it can be argued that monitoring of both settlement and potential transport has been limited, available data nevertheless fail to show that major transport to shore can or does occur. A major settlement apparently occurred at Tofino in 1983 or 1984 (Smith 1988), and major settlements were reported off the Washington coast in 1984 and 1985 (Armstrong et al. 1987, but both in 1986 and 1987, when our studies, which might have detected larval movement through correlation with Lagrangian drifters, were underway, no major crab settlement occurred at these locations (1986: Armstrong et al. 1987; 1987: D. Armstrong, Univ. of Washington, Seattle, Wa., per. comm.). It cannot be proven that earlier annual settlements involved larvae which had left the nearshore environment.

In the absence of data to refute either argument, only additional observations will resolve this issue. *Cancer magister* megalopae are probably always abundant off Washington and southern British Columbia in May and June within about 140 km of shore, and the potential for substantial settlement to occur somewhere along the coast is probably high. Study of factors which prevent major inshore settlement may be more relevant than trying to establish where successful onshore settlement would be permitted. If settlement in the area of a particular fishery is very poor, later recruitment to the fishery will be low, even with high subsequent juvenile survival. Survival of juveniles in the few months immediately after settlement can be quite variable (Armstrong et al. 1987), so a high settlement of megalopae does not necessarily mean high recruitment at a later date.

The probable settlement locations of progeny hatched in a specific region and the degree of intermixing of larvae originating from different coastal regions are issues relevant to both fishermen and managers. Factors affecting both the magnitude of Dungeness crab recruitment and the timing of major fluctuations are still speculative. The cyclical fluctuation in crab abundance is well documented from northern California to Washington (see Botsford 1986) but, to date, no satisfactory explanation has been developed. The Tofino fishery does not fluctuate in a similar cyclical manner, but its fluctuations are nevertheless substantial (Jamieson 1985).

Currents and the Spatial Distribution of Megalopae

The geostrophic method of estimating current flows and patterns utilizes information on the distribution of density in the ocean, and while it ignores the effect of wind, it is easier to obtain density information than it is to measure currents directly over a large survey area. Currents estimated by this method express the balance between the pressure force and the Coriolis force, and give the relative velocity component between two depths, i.e., the velocity shear. It assumes no friction (and hence is less useful close to shore or in shallow water) and assumes that there is no motion at some specified depth level. With all these assumptions, results are perhaps more qualitative than quantitative, but they are nevertheless useful because they do indicate probable current patterns in surface waters when winds are relaxed. However, this is not always the case, particularly in surface waters, and while geostrophic currents may partially indicate a region's currents, only by direct measurement of the movement of water masses can the interplay of all oceanographic and meteorological variables be established. This can only be done for a few locations at any specific time because of resource and logistic constraints, so geostrophic and direct current measurements should be complementary.

Oceanographic events, excluding the effects of wind, account for long-shore movement of megalopae but do not explain offshore or onshore movement in the study area, except in the vicinity of the Juan de Fuca Gyre. The concentration of megalopae at distances offshore which seem to coincide with the boundaries between long-shore currents flowing in opposite directions suggests that while oceanographic processes may not facilitate onshore megalopal movement, they can impede it, and it is perhaps this aspect which is most important to cross-shelf megalopal movement, at least off British Columbia.

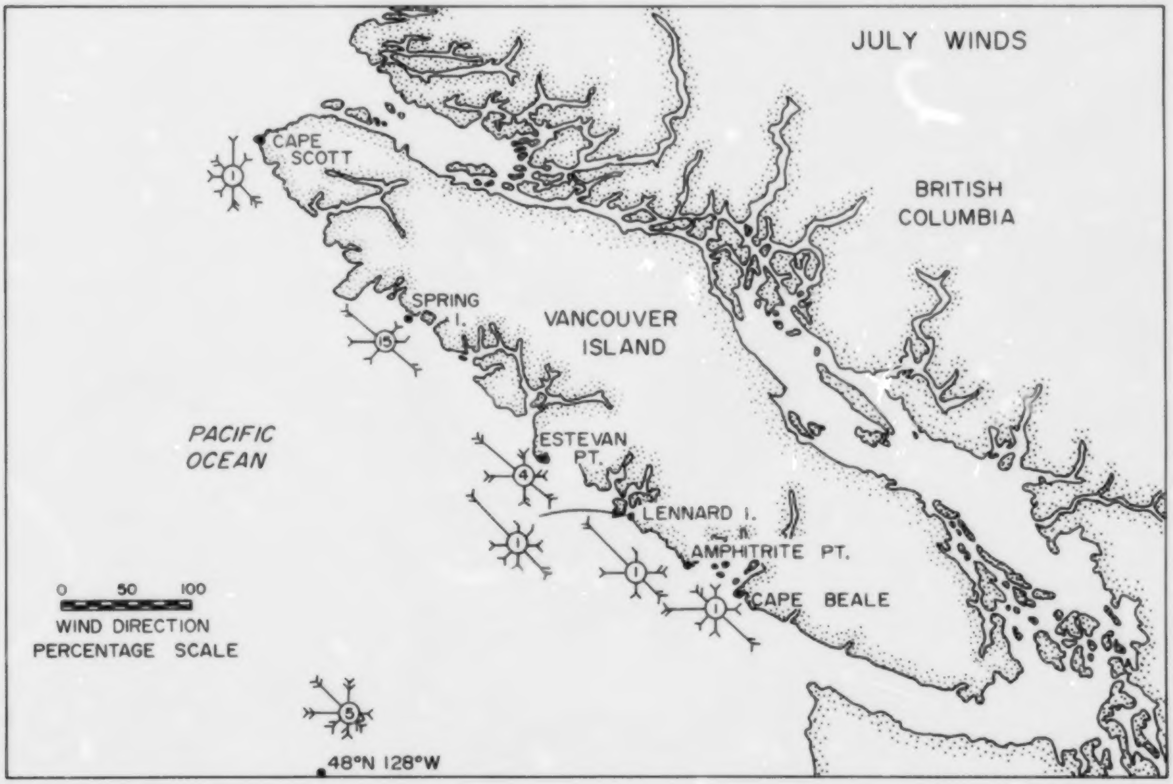

FIG. 15. Geographical locations of Amphitrite and Estevan Points relative to Tofino. The "feathered circles" off each lighthouse on the west coast of Vancouver Island illustrate the average direction (location of arrow), average force (Beaufort scale: number of feathers) and maximum winds observed over the previous 7–10 years. Thus, off Amphitrite Point, NW winds blew 45% of the time (measure the length of the arrow against the scale) at Force 3, with calms 1% of the time (values in circle). [Source: Sailing Directions — British Columbia Coast (South Portion). Vol. 1, 14th ed., 1987, Department of Fisheries and Oceans, Insititute of Ocean Sciences, Sidney, B.C.].

The substantial Lagrangian drifter movement observed supports earlier suggestions (Gaumer 1971; Reilly 1983; Jamieson and Phillips 1988) that over the estimated 4-mo larval period of Dungeness crab, larvae can move considerable distances long-shore.

Meteorological Considerations

The only pronounced onshore movement of drifters observed was in association with meteorological change. This suggests that southerly winds, typically indicative of a passing storm front, may serve as a mechanism to rapidly move megalopae at the surface at specific locations onshore.

The only extensive time series of hourly wind data for the west coast of Vancouver Island are those from lighthouses. It is recognized that wind data from lighthouses are only partially reflective of meteorological conditions which might occur on the continental shelf or beyond, both because of regional variability in wind patterns and because of the influence of land on coastal winds. Nevertheless, these data are presented because while it might be argued that the relative magnitude and direction of winds at any specific time is not representative of conditions somewhere else, the relative frequency of storms, their relative strengths, and the general wind pattern in the region are all considered. These data are not presented here to explain microscale events but are rather used to suggest both the importance of meteorological events and the need to obtain more accurate wind data from moored weather-monitoring buoys located on the continental shelf.

Wind data are presented here for both Amphitrite and Estevan points, which are located 37 km south and 50 km north of Tofino, respectively (Fig. 15). Wind direction was analyzed in terms of its vector orientation to the coast, with positive ordinate values indicating onshore movement and negative ordinate values indicating offshore movement (Fig. 16). Because megalopae are primarily present off Tofino in May and June (Jamieson and Phillips 1988) and the megalopal stage is of about 28 d duration, wind data from April 1–July 31 each year were analyzed.

Preliminary study of megalopae at night with a series of 0.01 m^2 Miller nets suspended at 1 m intervals over a depth range of 0–4 m indicated that in calm sea conditions at least, megalopae were concentrated in the top metre of the water column (in 3, 20 m^3 per depth interval tows, the total number of megalopae caught between 21:00–00:05 h, June 23, 1987, at 0,1, 2, 3 and 4-m depths were 11, 0, 1, 1, and 0, respectively). It was therefore assumed that movement of megalopae by winds was comparable to that of oil slicks, i.e. with a velocity 3% that of the wind and in the direction of the wind. Ekman theory, which suggests surface transport is at a direction 15° to the right of the wind, does not seem to apply to oil slicks (A. Ages, Inst. of Ocean Sciences, Sidney, B.C., pers. comm.), but since megalopae, unlike oil, are not in the top few millimetres of the water column, additional analyses where Ekman transport does occur are also presented. Analyses in both cases are presented with the assumption that megalopae are either continuously, i.e. both day and night, at the water surface or are only present at the surface at night. In the latter case, the change in number of hours of darkness over the course of the season was considered, with night defined as the hours between civil twilight in the evening and morning (rounded to the nearest hour).

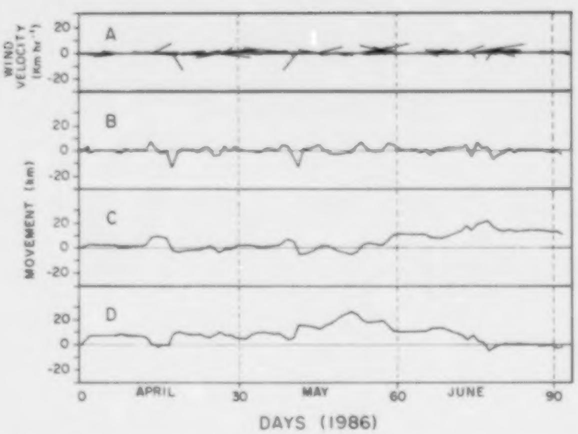

FIG. 16. An example of analysis of the wind data for each year for each of the two lighthouse locations. Data presented is for Amphitrite Point, April 1–June 30, 1986. Vector directions have been rotated by 45° because of the angle of the coast to magnetic north, allowing onshore and offshore movements to be indicated by positive and negative values, respectively. Values are averages for each 6–h time interval, but in this analysis, only wind data between civil twilight in the evening and morning is included. This therefore assumes that megalopal transport is only affected by winds at night. A. Wind strength (km•h^{-1}) and direction. B. Onshore (+) and offshore (−) wind movement (km) at each time interval. C. Relative accumulative positioning onshore or offshore (km) of a particle starting at any specified location, commencing April 1 and ending June 30. Here it is assumed movement is at 3% of the wind speed and at an angle 15° to the right of the wind. D. Maximum onshore movement (km) over the next 28 days (= duration of megalopal stage) for a particle starting at any specified location on each date, assuming movement relative to the wind as in (C).

Finally, onshore-offshore transport was measured in two ways:

1) where, relative to a location on any date, would a megalopae end up 28 days (i.e., the duration of the megalopal stage) later and
2) what were the relative frequencies of days at each site when the maximum net onshore transport over the next 28 days was greater than the following specified distances between April 1 and June 30: 10, 15, 20, and 25 km.

Results indicate that average maximum onshore transport at Estevan Point (31.4 km) is greater than twice that at Amphitrite Point (14.4 km) and that the frequency of days with stronger onshore transport is also greater at Estevan Point (Table 5). Comparison of average onshore transport (Tables 5c, 6) for dates arbitrarily selected as the first 6 yr of each of the 1970s and 1980s, indicated

TABLE 5. Estimated onshore transport of neuston between April 1 and June 30, assuming transport is at a direction of 15° to the right of the wind for 28-day periods commencing during this time frame. A. Average minimum and maximum transport (km) by location over a 15-yr period (1969/70–1986). B. Average number of days (maximum possible is 91) during which onshore transport of neuston exceeded selected distances over a 15-yr period (April–June, 1969/70–1986). C. Average number of days during which onshore transport of neuston exceeded selected distances over two 7-yr periods (April–June). Day = day and night presence in neuston; night = night only presence in neuston.

A.	Average 28-d onshore transport (km): 1969/70–1986			
	Estevan Point		Amphitrite Point	
	Min.	Max.	Min.	Max.
Night $\bar{x}$	−0.5	31.4	−1.5	14.4
SD	6.4	8.8	2.5	7.4
Day $\bar{x}$	−9.6	78.4	−9.9	32.5
SD	13.8	42.2	4.7	25.4

B.	Average number of days (April–June, 1969/70–1986)							
	Estevan Pt. — onshore transport (km)				Amphitrite Pt. — onshore transport (km)			
	>10	>15	>20	>25	>10	>15	>20	>35
Night $\bar{x}$	60.4	41.9	26.6	14.2	20.4	7.3	2.6	0.6
SD	21.5	22.5	19.4	17.7	21.6	15.7	8.5	2.3
Day $\bar{x}$	54.9	50.2	40.1	43.4	37.3	22.9	22.5	17.1
SD	24.7	25.8	27.9	25.1	30.0	28.2	22.7	19.3

C.	Average number of days (April–June)							
	Estevan Pt. — onshore transport (km)				Amphitrite Pt. — onshore transport (km)			
Time period	>10	>15	>20	>25	>10	>15	>20	>35
1970–76	55.9	35.4	29.4	23.3	27.4	13.6	5.4	1.3
1980–86	53.6	37.1	21.3	11.7	9.9	2.4	0.1	0

that for onshore transport >10 km and >20 km at Amphitrite and Estevan points, respectively, onshore transport in the 1980s was considerably lower. Different threshold transport levels are used for the two sites since because average transport is relatively high at Estevan Point, little observed difference in transport between the two time intervals occurred if the Estevan Point data were considered at the >10 km level. This difference between the two time periods may be biased by the presence of a particularly strong El Niño in 1983 (Wooster and Fluharty 1985), but exactly how this might be correlated with meteorological change and might have influenced crab settlement is uncertain. Crab settlement appears to have been high at Tofino in 1983 or 1984 on the basis of recent fishery performance (Smith 1988).

Future direction

On the basis of biological, oceanographic, and meteorological observations to date, some general hypotheses can be established which are capable of being evaluated by monitoring future events:

1) Onshore movement of megalopae is facilitated by diel vertical migration.

Moderate winds from the southeast or south noticeably affect drifter movements and cause them to move shorewards. The timing and magnitude of such events seems important, and transport to a barrier, such as the coast or a frontal zone, should be correlatable with storm event scale and frequency. Location of megalopae at depth during the day may be more to avoid predation than to benefit from transport by subsurface currents.

2) The Vancouver Island Coastal Current is normally an effective barrier to onshore surface movement.

The absence of megalopae in the current in May and June suggests both an absence of megalopae in the current's source, Juan de Fuca Strait, and little entrainment of continental shelf water and megalopae during its progression along the coast.

3) Relaxation of the Vancouver Island Coastal Current allows onshore surface movement to the coast.

Annual variability in Coastal Current strength can be expected to occur because of variation in prevailing winds, coastal runoff and outer shelf/slope circulation

TABLE 6. Number of days between April 1 and June 30 in which net wind transport off Amphitrite Point exceeded four specified distances (10, 15, 20, and 25 km) over the subsequent 28 days. A. Transport is in the direction of the wind. B. Transport is at a direction of 15° to the right of the wind.

	Days of onshore transport > specified distances (km)							
	A. 0° to wind				B. 15° to wind			
Year	10	15	20	25	10	15	20	25
1970	54	20	13	0	83	61	33	9
1971	16	10	2	0	28	9	3	0
1972	7	1	0	0	13	5	0	0
1973	0	0	0	0	23	0	0	0
1974	4	0	0	0	13	0	0	0
1975	11	3	0	0	38	18	2	0
1976	8	1	0	0	24	2	0	0
1977	0	0	0	0	25	0	0	0
1978[a]	—	—	—	—	—	—	—	—
1979[a]	—	—	—	—	—	—	—	—
1980	0	0	0	0	0	0	0	0
1981	0	0	0	0	0	0	0	0
1982	0	0	0	0	0	0	0	0
1983	5	0	0	0	8	0	0	0
1984	24	12	8	3	19	8	1	0
1985	0	0	0	0	32	6	0	0
1986	11	0	0	0	10	0	0	0
Mean	9.3	3.1	1.5	0.2	20.4	7.3	2.6	0.6
SD	14.2	6.0	3.8	0.8	21.6	15.7	8.5	2.3

[a] No wind data available.

(R. Thomson, Institute of Ocean Sciences, Sidney, B.C., pers. comm.). The relation between current strength and onshore movement of megalopae needs to be further investigated.

4) Southeasterly or southerly winds enhance onshore movement of megalopae.

Wind alone in the spring appears insufficient to move neuston particles more than about 30 km onshore on average during a 28-day developmental period (Table 5a). Megalopal behaviour and the significance of the relatively strong swimming ability of megalopae need to be established before the location of offshore concentrations of megalopae can be related to inshore settlement patterns. The relatively strong swimming ability of megalopae may primarily allow megalopae to remain as close to the surface as possible in the turbulent waters associated with storms, and so benefit maximally from wind-induced transport.

In conclusion, while our studies partially explain megalopal crab dynamics and have enabled us to advise both fishermen and managers on why landings in the Tofino Dungeness crab fishery should be relatively low for the next few years, many basic questions relating to the potential movement of larvae over sometimes considerable distances remain to be answered. What has become obvious is that the problem is not a biological one alone, and that collaboration between biologists and oceanographers is essential if answers are to be determined. Both biotic and abiotic factors are involved, and it is the result of this mix that seems largely to determine the magnitude of Dungeness crab movement and, presumably, recruitment.

Acknowledgments

We thank the many students and technicians who assisted in biological data collection and analysis, in particular Glen Brown, Bruce Jeffs, and Dorothy Young. We thank Fred Hermiston for his help in drifter data collection and Joe Linguanti for his patience and assistance in geostrophic flow analysis. Throughout the study, Rick Thomson and Bill Crawford generously provided advice and analytical support. We also thank Jim Boutillier, Loo Botsford and Rick Thomson for their critical reviews of this manuscript, and Don Noakes and Peter Slootweg for their assistance in analysis of the meteorological data.

References

ARMSTRONG, D. A., T. C. WAINWRIGHT, J. ORENSANZ, P. A. DINNEL, AND P. R. DUNBAULD. 1987. Model of dredging impact on Dungeness crab in Grays Harbour, Washington. Final Rep. to Seattle District Corps of Engineers, Univ. of Washington, School of Fish. Rep. Ser. FRI-UW-8702: 167 p.

BOOTH, J., A. C. PHILLIPS, AND G. S. JAMIESON. 1985. Fine scale spatial distribution of *Cancer magister* megalopae and its relevance to sampling methodology. Proceedings of the Symposium on Dungeness Crab Biology and Management. Lowell Wakefield Fish. Symp. Ser. Oct 9-11, 1984. Anchorage, Alaska. Alaska Sea Grant Rep. 85-3: 273-286.

BOTSFORD, L. W. 1986. Effects of environmental forcing on age-structured populations: northern Dungeness crab (*Cancer magister*) as an example. Can. J. Fish. Aquat. Sci. 43: 2345-2352.

CARRASCO, K. R., D. A. ARMSTRONG, D. R. GUNDERSON, AND C. ROGERS. 1985. Abundance and growth of *Cancer magister* young-of-the-year in the nearshore environment. Proceedings of the Symposium on Dungeness Crab Biology and Management. Lowell Wakefield Fish. Symp. Ser. Oct. 9-11, 1984. Anchorage, Alaska. Alaska Sea Grant Rep. 85-3: 171-184.

CRAWFORD, W. R., AND P. GREISMAN. 1987. Investigation of permanent eddies in Dixon Entrance, British Columbia. Cont. Shelf Res. 7: 851-870.

DENMAN, K. L., D. L. MACKAS, H. J. FREELAND, M. J. AUSTIN, AND S. H. HILL. 1981. Persistent upwelling and meso-scale zones of high productivity off the west coast of Vancouver Island, Canada. p. 514-521. *In* F. Richards [ed.] Coastal Upwelling. Am. Geophys. Union, Wash., DC.

EDWARDS, E. 1979. The edible crab and its fishery in British waters. Fishing News Books, Ltd., Farnharn, Surrey, England. 140 p.

FREELAND, H. J., AND K. L. DENMAN. 1982. A topographically controlled upwelling center off southern Vancouver Island. J. Mar. Res. 40: 1069-1093.

FREELAND, H. J., W. R. CRAWFORD, AND R. E. THOMSON. 1984. Currents along the Pacific coast of Canada. Atmosphere-Ocean 22: 151-172.

GAUMER, T. I. 1971. Controlled rearing of Dungeness crab larvae and the influence of envrionmental conditions on their survival. Commer. Fish. Ser. Act. Closing Rep., Nov. 16, 1985 to June 30, 1971. Oreg. Fish Comm. 43 numb. leaves.

GREISMAN, P., AND W. R. CRAWFORD. 1985. First current survey using Loran-C drifting buoys. Marit. Industries 1: 22-23.

GUNDERSON, D. R., AND I. E. ELLIS. 1986. Development of a plumb staff beam trawl for sampling demersal fauna. Fish. Res. 4: 35-41.

HARDY, A. C. 1946. Observations on the uneven distribution of the oceanic plankton. Discovery Rep. 11: 511-538.

HATFIELD, S. E. 1983. Intermolt staging and distribution of Dungeness crab, *Cancer magister*, megalopae, p. 85-96. *In* P. W. Wild and R. N. Tasto [ed.] Life history, environment, and aquaculture studies of the Dungeness crab, *Cancer magister*, with emphasis on the central California fishery resource. Calif. Dep. Fish Game Fish. Bull. 172.

HICKEY, B. M. 1979. The California Current system — hypotheses and facts. Prog. Oceaogr. 8: 191-279.

IKEDA, M., L. A. MYSAK, AND W. J. EMERY. 1984a. Observations and modelling of satellite-sensed meanders and eddies off Vancouver Island. J. Phys. Oceanogr. 14: 3-21.

1984b. Seasonal variability in meanders of the California Current System off Vancouver Island. J. Geophys. Res. 89: 3487-3505.

JACOBY, C. A. 1982. Behavioral responses of the larvae of *Cancer magister* Dana (1852) to light, pressure and gravity. Mar. Behav. Physiol. 8: 267-283.

JAMIESON, G. S. 1985. The Dungeness crab (*Cancer magister*) fisheries of British Columbia. Proceedings of the Symposium on Dungeness Crab Biology and Management. Lowell Wakefield Fish. Symp. Ser. Oct 9-11, 1984. Anchorage, Alaska. Alaska Sea Grant Rep. 85-3: 37-60.

JAMIESON, G. S., AND A. C. PHILLIPS. 1988. Occurrence of *Cancer* crab (*C. magister* and *C. oregonensis*) megalopae off the west coast of Vancouver Island, British Columbia. Fish. Bull. 86(3): 525-542.

LEBLOND, P. H., B. M. HICKEY, AND R. E. THOMSON. 1986. Runoff driven coastal flow off British Columbia, p. 309-317. *In* S. Skreslet [ed.] The role of freshwater outflow in coastal marine ecosystems. NATO ASI Series, Vol. G7, Springer-Verlag.

LOUGH, R. G. 1975. Dynamics of crab larvae (Anomura, Brachyura) off the central Oregon coast, 1969-1971. Ph.D. thesis, Oregon State Univ., Corvallis, OR. 299 p.

1976. Larval dynamics of the Dungeness crab, *Cancer magister*, off the central Oregon coast, 1970-71. Fish. Bull. 74: 353-375.

MASON, J. C., AND A. C. PHILLIPS. 1986. An improved otter surface sampler. Fish. Bull. 84: 480-484.

MASON, J. C., A. C. PHILLIPS, AND O. D. KENNEDY. 1984. Estimating the spawning stocks of Pacific hake (*Merluccius productus*) and walleye pollock (*Theragra chalcogramma*) in the Strait of Georgia, B.C. from their released egg production. Can. Tech. Rep. Fish. Aquat. Sci. 1289: 51 p.

NICHOLS, J. H., B. M. THOMPSON, AND M. CRYER. 1982. Production, drift, and mortality of the planktonic larvae of the edible crab (*Cancer paguras*) off the north-east coast of England. Netherlands J. Sea Res. 16: 173-184.

POOLE, R. L. 1966. A description of laboratory-reared zoea of *Cancer magister* Dana and megalopae taken under natural conditions (Decapoda, Brachyura). Crustaceana 11: 83-97.

REILLY, P. N. 1983. Dynamics of Dungeness crab, *Cancer magister*, larvae off central and northern California, p. 57-84. *In* P. W. Wild and R. N. Tasto [ed.] Life history, environment, and mariculture studies of the Dungeness crab, *Cancer magister*, with emphasis on the central California fishery resource. Calif. Dep. Fish Game Fish. Bull. 172.

SMITH, B. D. 1988. An evaluation of the current minimum legal size limit for the Dungeness crab (*Cancer magister* Dana) fishery near Tofino, British Columbia. Ph.D. thesis, Univ. British Columbia, Vancouver, B.C. 160 p.

THOMSON, R. E. 1981. Oceanography of the British Columbia coast. Can. Spec. Publ. Fish. Aquat. Sci. 56: 291 p.

1984. A cyclonic eddy over the continental margin of Vancouver Island: Evidence for baroclinic instability. J. Phys. Oceanogr. 14: 1326-1348.

TRASK, T. 1970. A description of laboratory-reared larvae of *Cancer productus* Randall (Decapoda, Brachyura) and a comparison of larvae of *Cancer magister* Dana. Crustaceana 18: 133-146.

WICKHAM, D. E. 1979. The relationship between megalopae of the Dungeness crab, *Cancer magister*, and hydroid, *Velella velella*, and its influence on abundance estimates of *C. magister* megalopae. Calif. Fish. Game 65: 184-186.

WIEBE, P. H. 1970. Small-scale spatial distribution in oceanic plankton. Limnol. Oceanogr. 15: 205-218.

WOOSTER, W. S., AND D. L. FLUHARTY [ed.] 1985. El Niño North: Niño effects in the eastern Subarctic Pacific Ocean. Wash. Sea Grant Publ. WSG-WO 85-3: 312 p.

Effects of Temperature and Stock Size on Year-Class Production for Rock Sole (Lepidopsetta bilineata) in Northern Hecate Strait, British Columbia

J. Fargo and S. McKinnell

Department of Fisheries and Oceans, Biological Sciences Branch, Pacific Biological Station, Nanaimo, B.C. V9R 5K6

Abstract

FARGO, J., AND S. MCKINNELL. 1989. Effects of temperature and stock size on year-class production for rock sole (*Lepidopsetta bilineata*) in northern Hecate Strait, British Columbia, p. 327–333. *In* R. J. Beamish and G. A. McFarlane [ed.] Effects of ocean variability on recruitment and an evaluation of parameters used in stock assessment models. Can. Spec. Publ. Fish. Aquat. Sci. 108.

Results of catch-at-age analysis for rock sole in northern Hecate Strait from 1946 to 1969 were analyzed using response surface analysis to examine the effects of ocean surface temperatures at time of spawning and stock size on rock sole year-class production. The relationship described by the response surface between year-class production and temperature was dome-shaped. Temperatures above 7°C and below 5.5°C exerted a negative effect on rock sole year-class production while a temperature of 6.3°C corresponded with optimum year-class production. A stock-recruit relationship was also described by the response surface. Year-class production was low at low stock sizes, rose rapidly as stock size increased, then decreased slightly at high stock sizes.

Résumé

FARGO, J., AND S. MCKINNELL. 1989. Effects of temperature and stock size on year-class production for rock sole (*Lepidopsetta bilineata*) in northern Hecate Strait, British Columbia, p. 327–333. *In* R. J. Beamish and G. A. McFarlane [ed.] Effects of ocean variability on recruitment and an evaluation of parameters used in stock assessment models. Can. Spec. Publ. Fish. Aquat. Sci. 108.

Les résultats de l'analyse des captures en fonction de l'âge de la sole du Pacifique dans la partie nord du détroit d'Hécate de 1946 à 1969 ont été analysés à l'aide d'une surface de réponse pour étudier les effets des températures de surface de l'océan au moment de la fraie de même que l'effet de la taille des stocks sur la production annuelle de sole du Pacifique. La relation entre la production annuelle et la température établie par la surface de réponse donne une courbe en forme de cloche. Les températures supérieures à 7°C et inférieures à 5.5°C ont un effet négatif sur la production annuelle de sole du Pacifique tandis qu'une température de 6.3°C donne une production annuelle optimale. La surface de réponse a aussi permis d'établir une relation entre la taille des stocks et la production de recrues. La production annuelle est faible quand les effectifs sont réduits, puis elle s'accroît rapidement quand les effectifs augmentent pour enfin décroître légèrement quand la taille des stocks est grande.

Introduction

The rock sole (*Lepidopsetta bilineata*) is an important component of the British Columbia trawl fishery in Hecate Strait (Fig. 1). Since the early 1950's, the species has been one of the dominant flatfish in landings in British Columbia with production in International Area 5D varying from 187 t to 1583 t annually (Fig. 2). Fluctuations in landings have coincided with recruitment fluctuations for the species. Recruitment to the commercial fishery in North Hecate Strait has been highly variable (Forrester and Thomson 1969; Stocker 1981; Fargo 1985). Data on stock size and recruitment has fitted conventional stock recruit models poorly (Fig. 3).

The rock sole is characterized by moderate growth ($k = 0.21$) and mortality rates ($M = 0.20$). Beginning about age 3, females grow faster than males and comprise 60–80% of the commercial landings in Hecate Strait by number. Rock sole recruit at age 4 and the majority of fish in the landings are between 4–7 years of age. Results of recent tagging experiments (Fargo and Westrheim 1987) have suggested that a single stock of rock sole exists in International Area 5D. The results also indicate that this stock does not undergo extensive migrations characteristic of other flatfish species in Hecate Strait.

A previous study by Forrester (1964a) has suggested that temperature of surrounding seawater at the time of egg incubation may be an important factor in the rate

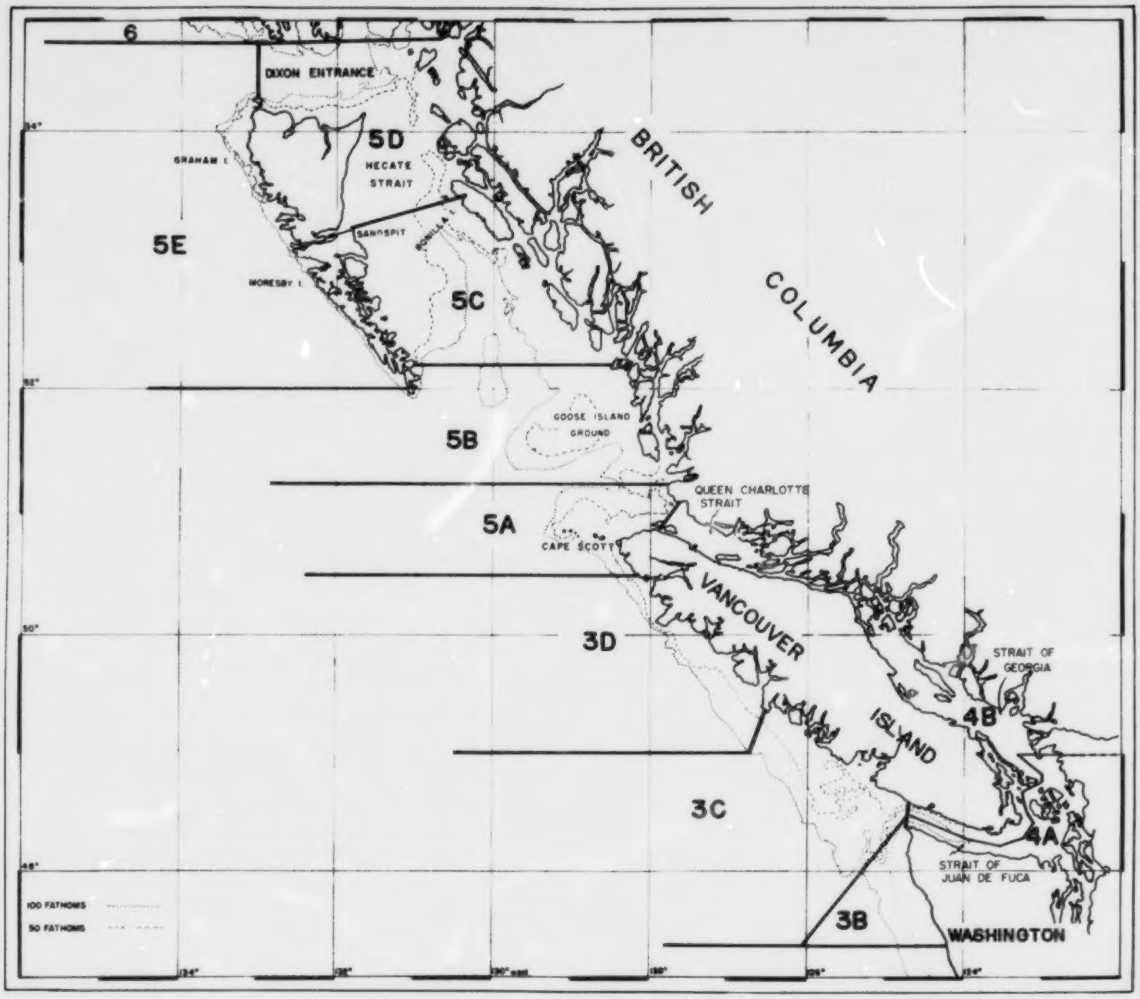
6
DIXON ENTRANCE
54°
5D
HECATE STRAIT
GRAHAM I.
BRITISH COLUMBIA
5E
SANDSPIT
MORESBY I.
5C
52°
GOOSE ISLAND GROUND
5B
QUEEN CHARLOTTE STRAIT
5A
CAPE SCOTT
VANCOUVER ISLAND
50°
3D
STRAIT OF GEORGIA
4B
3C
4A
48°
STRAIT OF JUAN DE FUCA
3B
WASHINGTON
100 FATHOMS
50 FATHOMS
134°
132°
130°
128°
126°
124°

FIG. 1. The British Columbia coast, showing the study area in northern Hecate Strait.

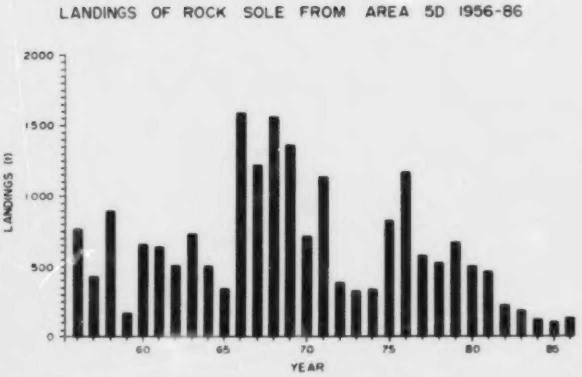

FIG. 2. Landings (t) of rock sole from northern Hecate Strait from 1956–86.

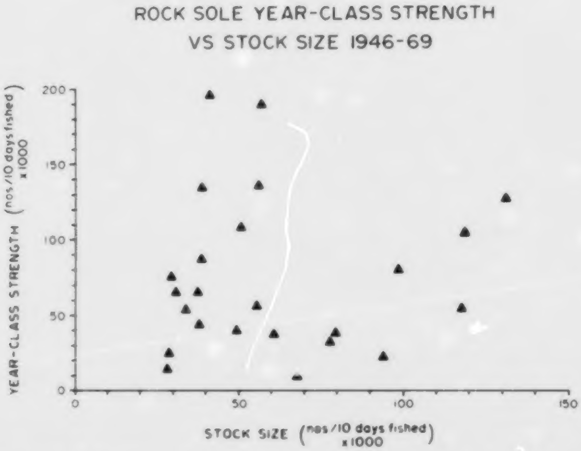

FIG. 3. Scatter plot of rock sole year-class strength vs. stock size from 1946–69.

of development and hatching success of rock sole eggs. Rock sole spawn in the spring of the year, with the peak period in March. Spawning takes place in shallow water (10–30 m) in western Hecate Strait. The eggs for this species are demersal and adhesive (Forrester 1964b), probably an adaption for a species spawning in areas where there are strong ocean currents or tidal effects (Moiseev 1955) as exist in the shallows of Hecate Strait. Oceanographic data collected during the spawning period from this area indicates that the water column is generally isothermal to depths of 50–90 m (Fargo et al. 1985). It would be logical then to investigate the relationship between ocean-surface temperatures collected at B.C. lighthouses and rock sole year-class success assuming that hatching success is at least partly dependent on ocean temperature at the time of spawning (egg incubation). If year-class abundance is fixed at a relatively early stage in the life history, recruitment observed in the commercial fishery should reflect this relationship.

In fact, Wickett (in Ketchen 1980) discussed several environmental effects, including temperature, on production for rock sole in northern Hecate Strait. Using standard linear multivariate regression methods he developed a model explaining 41% of the variation in rock sole year-class production over time. A non-significant independent variable in this analysis was average sea surface temperature at Triple Island lighthouse in March. Although sea surface temperature was eliminated from this analysis, he noted that a definite dome-shaped relationship existed in a plot of rock sole year-class strength vs sea surface temperature at Triple Island (Fig. 4). He did not pursue this further.

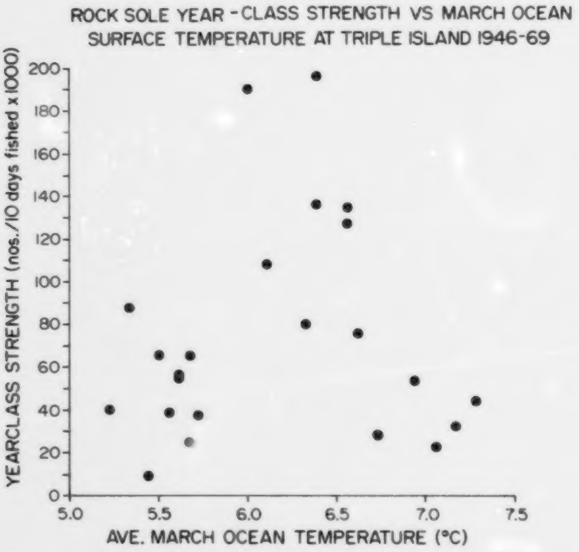

FIG. 4. Scatter plot of rock sole year-class strength vs. ocean temperature.

We examined the effects of temperature and stock size on production of rock sole year-classes in North Hecate Strait using response surface analysis (Schnute and McKinnell 1984). RSA was chosen because second order curve fitting is appropriate for dome-shaped relationships. RSA also provides the opportunity to test alternate models, and the RSA parameters are interpretable. Our purpose was to use RSA as a qualitative tool to investigate recruitment hypotheses for the species. We address the limitations of this analysis in the discussion section of this paper.

Materials and Methods

Data Time-Series

The index of stock size used in this study was derived by Forrester and Thomson (1969) from summed nominal CPUEs (numbers caught/10 days fishing) of age 4–7 female fish in year *j* while the year-class index was derived from summed CPUEs (numbers caught/10 days fishing) of age 4–7 fish in years *j* + 4 to *j* + 7 (Table 1). That is,

$$\text{Stock size } j = \sum_{i=4}^{7} = \text{CPUE}_i \text{ and}$$

$$\text{Year-class } k = \sum_{i=4,\ j=k+4}^{7,k+7} \text{CPUE}_{ij} \text{ where}$$

i = age class

j = year

k = year-class

The majority (80%) of fish in the stock are between ages 4–7, and ageing error is minimal over this range of ages.

Error in the estimates of catch and effort which were used in the computation of recruitment and stock size indices could come from several sources:

1) Increasing vessel efficiency cover the study period would make fishing effort data uncomparable. 2) Fishing effort was recorded for a variable percentage of vessels in each year and effort for the total amount of rock sole landed during the year was assumed to be proportional to those landings for which effort was recorded. If the sample of boats for which effort was recorded was unrepresentative of the fleet, then the total effort figures for the year would be in error. 3) There were no consistent reports of rock sole discards (fish discarded at sea) during the study period, and if significant amounts of fish were discarded at sea, the landings of rock sole may not have reflected the true catch.

The sources of error described in the previous paragraph were dealt with in the following way:

1) Fishing effort (boat days) was standardized by Forrester and Thomson (1969) to account for changes in vessel efficiency which took place over the study period. In fact, the major changes in vessel horsepower and electronic fishing aids, which are major contributors to increasing vessel efficiency, took place after 1970. 2) Between 75% and 90% of the vessel landings for each year of the study period were monitored with regard to fishing effort, and these samples are probably representative of the fleet. 3) Based on periodic reports from fishermen recorded on weekly trip reports, we have no reason to believe that discards were significant at any time during the study period, or that the ratio of discards to

TABLE 1. Rock sole stock size, year-class strength (from Ketchen 1980) and March sea surface temperatures at Triple Island, 1946–69.

Year	Sea surface temperature	Index of stock size No./10 days fishing × 1000 (ages 4–7) females)	Index of year-class No./10 days fishing × 1000
1946	6.62	29.388	75.990
1947	6.39	55.985	136.269
1948	6.11	50.602	108.342
1949	5.33	38.608	87.481
1950	5.50	37.359	65.745
1951	5.56	79.563	38.605
1952	5.72	60.578	37.642
1953	6.56	38.721	134.982
1954	6.39	41.036	196.288
1955	6.00	56.757	190.115
1956	5.67	30.908	65.503
1957	5.67	28.553	25.071
1958	7.17	77.728	32.645
1959	6.33	98.408	80.582
1960	6.56	130.855	127.748
1961	7.56	118.546	104.858
1962	5.61	55.294	56.384
1963	7.28	37.870	44.450
1964	6.94	33.866	53.910
1965	5.61	117.560	55.333
1966	7.06	93.815	23.128
1967	5.44	67.648	9.243
1968	6.61	28.276	14.533
1969	5.22	49.373	40.249

catch was different over the study period. Thus the possibility of bias being incorporated into the data set is probably minimal.

The index of ocean-surface temperatures used in this study was taken from the Triple Island lighthouse station in northern Hecate Strait and error for this data was assumed to be negligible. The variation around the mean monthly temperature for March was low.

The Response Surface Model

Response surface analysis was used to produce models incorporating Forrester and Thomson's CPUE time series of year-class strength, and stock size (1946–69) and sea surface temperatures from Triple Island. The response surface model is summarized in the Appendix. One factor (year-class vs temperature) (year-class vs stock size) and two factor (year-class vs temperature and stock size) models were produced.

To summarize the Schnute-McKinnell parameterization of the response surface model, start with a simple quadratic model:

$$Y = p + q_1 X_1 + r_{11} X_1^2$$

The relationship between Y and X is a symmetric hill top if $r_{11} < 0$ or a symmetric valley if $r_{11} > 0$. As X varies over an appropriate range of values, the response Y will either peak, then decrease (hill top) or descend, then increase again (valley). In either case, both the hill or the valley have symmetric form. Note that the parameters p, q_1, and r_{11} are all linear, and that the model can be fit to the data with linear regression methods.

This simple quadratic model can be made more flexible with the addition of the non-linear parameters α, γ shown in the equation below:

$$Y^{\gamma} = p + q_1 X_1^{\alpha_1} + r_{11} X_1^{2\alpha_1}$$

The addition of the non-linear parameters (α, γ) allow the quadratic model to assume less restrictive shapes. Notice that if $\alpha = 1$ and $\gamma = 1$, the model is the simple quadratic. If $\alpha <> 1$ or $\gamma <> 1$, asymmetrical shapes are possible. In simple terms, the valley or hill can be steeper on one side than the other. As well, the peak or valley can be acute or broad and flat.

The addition of another independent variable requires the addition of more parameters:

$$Y^\gamma = p + q_1 X_1^{\alpha_1} + q_2 X_2^{\alpha_2} + r_{11} X_1^{2\alpha_1} + r_{22} X_2^{2\alpha_2} + r_{12} X_1^{\alpha_1} X_2^{\alpha_2}$$

With the addition of another variable, the model shape becomes a 3 dimensional surface where the response levels are determined by 2 variables. For each additional independent variable, there is a "linear" term added, a "quadratic" term, and one term for each of all possible interactions of the independent variables. The subscripts of the various parameters indicate which variable is involved.

The original data are also transformed (see Appendix) in order to centre and scale the variables. The transformation results in parameters that are independent of one another, have similar magnitudes and as a result, are more easily interpretable.

In summary, the response surface analysis involves estimating the parameters of a non-linear quadratic model of biological data. The magnitude and sign of the various estimated parameters determine the shape of the surface and assist the biologist in describing data observations.

Model Fit

We did not use Schnute and McKinnell's (1984) *B*-statistic to determine significance of the independent variables in the analysis. The major reason for not using this statistic was because our time-series indices of year-class strength and stock size are bound to contain some autocorrelation. Use of the *B*-statistic requires independent data observations.

We used the *A*-statistic (objective function value) as an index of relative fit for different models. Analysis of variance of this data cannot be accomplished using response surface analysis. However, we feel that the *A*-statistic does provide us with a relative measure of the amount of variation in the response variable that is accounted for by the independent variable(s).

Results

The *A*-statistic values for six models using Forrester and Thomson's LPUE data are listed below. Lower values for the *A*-statistic indicate a better fit.

Model	Linear function	Non-linear function
stock size	243365	160512
temperature	201118	152282
temperature & stock size	177715	87185

In the nonlinear models, the residuals were more homogeneous and more normally distributed than in the linear models. Parameter estimates for the different models are listed in Table 2.

The final model, incorporating temperature and stock size effects, resulted in the *A*-statistic decreasing. The response surface for this model is shown in Fig. 5. Parameter estimates for the final model are also listed in Table 2. Parameters in the new model suggest the following relationships: Values for q_1 and q_2 indicate slight positive linear trends in year-class vs temperature and stock size, respectively. Parameters r_{11} and r_{22} indicate a quadratic component with regard to temperature and stock size. The quadratic relationship is dome-shaped because of the negative sign for this parameter, and this relationship is more pronounced for temperature than for stock size. The parameter $r_{12} > 0$ suggests an interaction between temperature and stock size.

TABLE 2. Parameter estimates for the one-factor (temperature) and two-factor (temperature and stock size) response surface models.

	Model		
Parameter	One factor (temperature)	One factor (stock size)	Two factor (temperature & stock size)
α_1	−0.985	3.007	−0.549
α_2	N/A	N/A	−2.779
γ	0.337	0.265	0.311
p	0.243	−0.147	0.661
q_1	0.131	0.300	0.059
q_2	N/A	N/A	0.332
r_{11}	−0.637	0.569	−0.922
r_{12}	N/A	N/A	0.460
r_{22}	N/A	N/A	−0.778

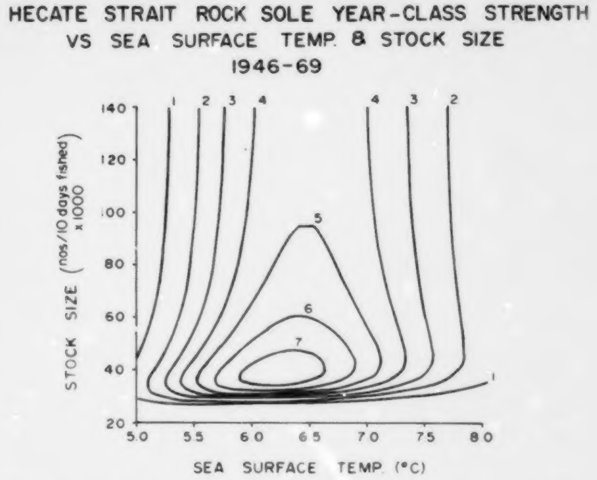

FIG. 5. Isopleth contours of the year-class response surface against stock size and temperature. The contours 1-7 correspond to year-class strengths of 10, 30, 50, 70, 90, 110, and 130 thousand fish per 10 days fishing, respectively.

Time series trends from 1946–69 were produced for rock sole year-class strengths from 1946–69 using the two-factor non-linear model and are shown in Fig. 6. The model consistently estimated smaller year-class sizes than observed in peak years (1954, 1960), and the model fit was best for the early years (1946–57).

In summary, the relationship between temperature and year-class strength was dome-shaped with optimum year-class sizes produced at temperatures near 6.3°C. The relationship between stock size and rock sole year-class strength was also dome-shaped, but more asymmetric with the left hand limb increasing rapidly and the right hand limb decreasing slowly. Year-class production was low at low stock sizes regardless of temperature.

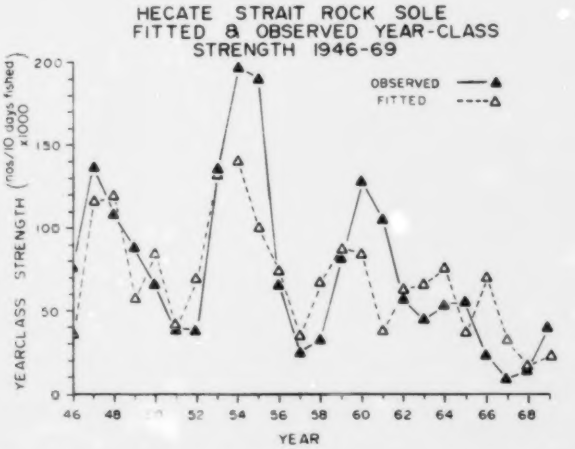

FIG. 6. Fitted and observed indices of year-class strength over the period 1946–69.

Discussion

The response surface in Fig. 5 indicates that year-class strength is more sensitive to low stock levels. As stock size increases above the lowest recorded values, the index of year-class strength increases rapidly to a maximum response, and then decreases slowly. At low stock levels there, presumably, are no density-dependent effects operating to curb production. Also, the rate of reproduction at low stock levels may increase as an adaptation for long-term survival of the species. There would of course be a limit to the size of the spawning stock which could sustain adequate production. This "critical" stock size is also suggested by the response surface. For example, in 1964 and 1968, even with close to optimum temperature conditions, year-class production was low. Stock sizes for these two years were among the lowest recorded for the entire time period. Above critically low stock levels, temperature becomes a major determinant of year-class production.

We found some verification of the relationships described by the response surface in an examination of more recent time series of rock sole data. A cohort analysis of north Hecate Strait rock sole including data for 1970–78 was published in Stocker (1982). These results include indices of stock size and recruitment in absolute numbers, thus they are not directly comparable to Forrester and Thomson's index. This data indicates that recruitment to the fishery from the early through mid-1970's was relatively low (late 1960's–early 1970's year-classes). However, recruitment increased significantly in 1978 (1974 year-class). As anecdotal evidence further corroborating the existence of a strong mid-1970's year-class, fishermen complained of excessive discarding of undersize rock sole in 1978–79, and areas where the reported discarding problem was occurring was closed to trawling in 1980.

Temperature from the late 1960's through the early 1970's was near optimum in only 1 year (1968), however, stock size in this year was very low. Therefore the response surface model would predict that year-classes of the late 1960's–early 1970's would be low, which they were. In 1974, March ocean temperature was close to optimum (6.1°C) and stock size was higher than the late 1960's levels. Therefore the model would predict that the 1974 year-class would be significantly larger than those preceding it and this did occur.

Laboratory studies regarding effects of physical factors on egg production and brood success have produced data sets where observations are independent, error can be quantified and analytical techniques justifiably applied (Alderdice and Forrester 1971, 1974). Results of such studies have been viewed with some skepticism because of the "controlled" nature of these experiments. On the other hand, "real" data sets contain unmeasurable and often times, unknown error. Application of analytical techniques such as RSA for the purpose of analysis of variance and developing predictive models using stock and recruitment time series data is difficult. It is, however, possible to use the response surface from the RSA in a qualitative manner. The response surface presented here describes some biologically meaningful relationships between rock sole year-class production and temperature and stock size.

We are continuing to examine effects of stock size and environmental variables on rock sole recruitment. New work will also examine the effects of autocorrelation in the year-class index on the RSA results. Though there is a need to verify results from the RSA for this situation we suggest that response surface analysis is an appropriate tool for investigating recruitment hypotheses.

Acknowledgments

Comments and suggestions by Dr. A. V. Tyler and two anonymous reviewers improved the final version of this manuscript.

References

ALDERDICE, D. F., AND C. R. FORRESTER. 1971. Effects of salinity and temperature on embryonic development of petrale sole (*Eopsetta jordani*). J. Fish. Res. Board Can. 28: 727–744.

1974. Early development and distribution of the flathead sole (*Hippoglossoides elassodon*). J. Fish. Res. Board Can. 31: 1899–1918.

FARGO, J. 1985. Flatfish. *In* A. V. Tyler and G. A. McFarlane [ed.]. Groundfish stock assessments for the west coast of Canada in 1984 and recommended yield options for 1985. Can. MS Rep. Fish. Aquat. Sci. 1813: 57–115.

FARGO, J., J. R. SELSBY, AND T. SWEETEN. 1985. Trawl survey of juvenile flatfish in Hecate Strait, April 9–26, 1985. Can. Data Rep. Fish. Aquat. Sci. 542: 74 p.

FARGO, J., AND S. J. WESTRHEIM. 1987. Results through 1985, of the rock sole (*Lepidopsetta bilineata*) tagging experiments in Hecate Strait (British Columbia) during April–May 1982 with regard to stock delineation. Can. MS Rep. Fish. Aquat. Sci. 1912: 51 p.

FORRESTER, C. R. 1964a. Rate of development of eggs of rock sole (*Lepidopsetta bilineata* Ayres). J. Fish. Res. Board Can. 21(6): 1533–1534.

1964b. Demersal quality of fertilized eggs of rock sole (*Lepidopsetta bilineata* Ayres). J. Fish. Res. Board Can. 21(6): 1531–1532.

FORRESTER, C. R., AND J. A. THOMSON. 1969. Population studies on the rock sole (*Lepidopsetta bilineata*) of northern Hecate Strait, British Columbia. Fish. Res. Board Can. Circ. 96: 47 p.

KETCHEN, K. S. [ED.]. 1980. Assessment of groundfish stocks off the west coast of Canada. Can. Data Rep. Fish. Aquat. Sci. 185: 213 p.

MOISEEV, P. A. 1955. Influence of oceanologic regimen of the far-eastern seas on commercial fish populations. Proceedings of the UNESCO Symposium on Physical Oceanography, p. 253–259.

SCHNUTE, J., AND S. MCKINNELL. 1984. A biologically meaningful approach to response surface analysis. Can. J. Fish. Aquat. Sci. 41: 936–953.

STOCKER, M. [ED.]. 1982. Groundfish stock assessments off the west coast of Canada in 1981 and recommended total allowable catches for 1982. Can. MS Rep. Fish. Aquat. Sci. 1626: 282 p.

Appendix

The equation used to calculate the predicted values of recruitment, η, was:

$$(1)\ \eta = p + q_1\xi_1 + r_{11}\xi_1^2 + r_{12}\xi_1\xi_2 + q_2\xi_2 + r_{22}\xi_2^2$$

where:

$$(2)\qquad \eta = \frac{2Y^\gamma - V^\gamma - v^\gamma}{V^\gamma - v^\gamma}$$

and:

$$(3)\qquad \xi_i = \frac{2X_i^{\alpha_i} - U_i^{\alpha_i} - u_i^{\alpha_i}}{U_i^{\alpha_i} - u_i^{\alpha_i}}$$

where $i = 1$, or 2 indexes the independent variables.

The procedure for using the equation, for example to calculate a predicted recruitment from a set of the independent variables, is to transform each X_i to ξ_i (eq. 3), calculate η (eq. 1) using the parameters given in the text, then solve for Y (eq. 2).

A Family of Ricker SRR Curves of the Prawn *(Penaeus orientalis)* under Different Environmental Conditions and its Enhancement Potential in the Bohai Sea

Qisheng Tang, Jingyao Deng, and Jinsheng Zhu

Yellow Sea Fisheries Research Institute, Qingdao, China

Abstract

TANG, Q., J. DENG, AND J. ZHU. 1989. A family of Ricker SRR curves of the prawn (*Penaeus orientalis*) under different environmental conditions and its enhancement potential in the Bohai Sea, p. 335–339. *In* R. J. Beamish and G. A. McFarlane [ed.] Effects of ocean variability on recruitment and an evaluation of parameters used in stock assessment models. Can. Spec. Publ. Fish. Aquat. Sci. 108.

A new modification of the Ricker stock recruitment model was developed to account for environmentally induced variation in recruitment. Based on this analysis, fluctuations in recruitment of prawn (*Penaeus orientalis*) in the Bohai Sea are explained with respect to both environmental conditions and spawning-stock size.

Enhancement of this valuable living resource is discussed with respect to potential and strategy.

Résumé

TANG, Q., J. DENG, AND J. ZHU. 1989. A family of Ricker SRR curves of the prawn (*Penaeus orientalis*) under different environmental conditions and its enhancement potential in the Bohai Sea. p. 335–339. *In* R. J. Beamish and G. A. McFarlane [ed.] Effects of ocean variability on recruitment and an evaluation of parameters used in stock assessment models. Can. Spec. Publ. Fish. Aquat. Sci. 108.

Nous avons apporté une nouvelle modification au modèle de recrutement de Ricker de manière à rendre compte des variations du recrutement induites par les conditions environnementales. À partir de cette analyse, nous avons pu expliquer les fluctuations du recrutement de la crevette orientale (*Penaeus orientalis*) dans le golfe de Bohai à partir des conditions environnementales et de la taille du stock du géniteurs.

Le développement de cette ressource naturelle est examiné au regard de son potentiel d'acroissement et des stratégies de gestion.

Introduction

The prawn, *Penaeus orientalis* Kishinouye, is a valuable crustacean that is widely distributed, and found in the Bohai Sea and Yellow (Huanghai) Sea. It is believed that there are two different geographical populations — a small one on the west coast of Korea, and a large one on the coast of China (Mako et al. 1966; Kim 1973; Deng et al. 1983b). The main spawning grounds of the latter lie near the estuaries along the coast of the Bohai Sea (Fig. 1). Principal locations are the estuaries of the Yellow River (Laizhou Bay), Hai and Luan rivers (Bohai Bay), and the Liao River (Liaodong Bay). Life span is about 1 yr. Spawning occurs in late spring, after which most of the adult prawns die. Juvenile prawns grow rapidly and reach commercial size in September. Commercial fishing for this species is most important economically during autumn in the north China Sea. When water temperatures begin to drop significantly in autumn, the prawns migrate out of the Bohai Sea to overwinter in the Yellow Sea Depression. Annual catches from the Bohai Sea ranged from 5 200 to 39 500 t during 1962–85 (Fig. 2). Abundance, based on catch, exhibited large annual fluctuations. Apparent stock abundance has been low in recent years.

The purpose of this paper is to examine the fluctuations in recruitment with respect to a family of Ricker stock-recruitment relationship (SRR) curves, under different environmental conditions. Based on this study, we will also present some tentative ideas on enhancement potential and strategy for the prawn stock in the Bohai Sea.

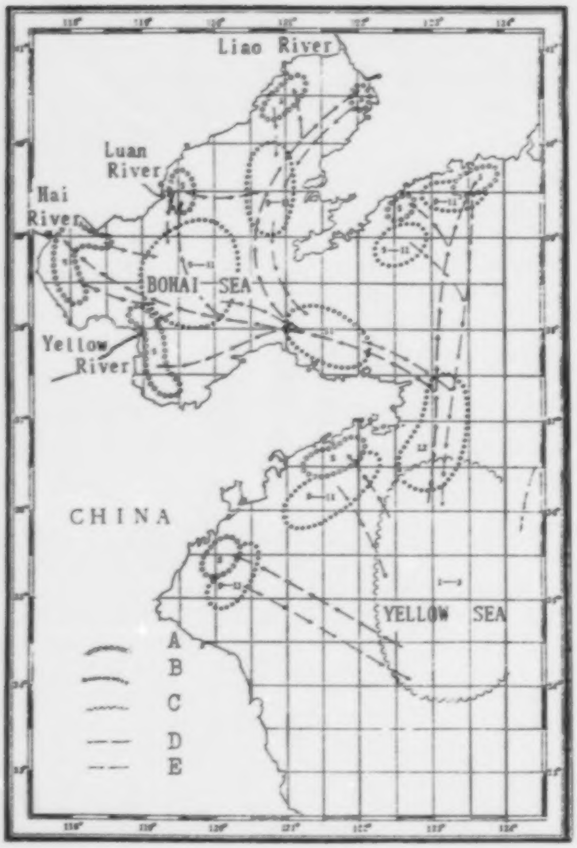

FIG. 1. Migration routes of prawns in the Bohai and Yellow seas (adapted from Anon. 1978).
Key: A — spawning ground; B — feeding ground; C — overwintering ground; D — spawning migration routes; E — feeding and overwintering migration routes.

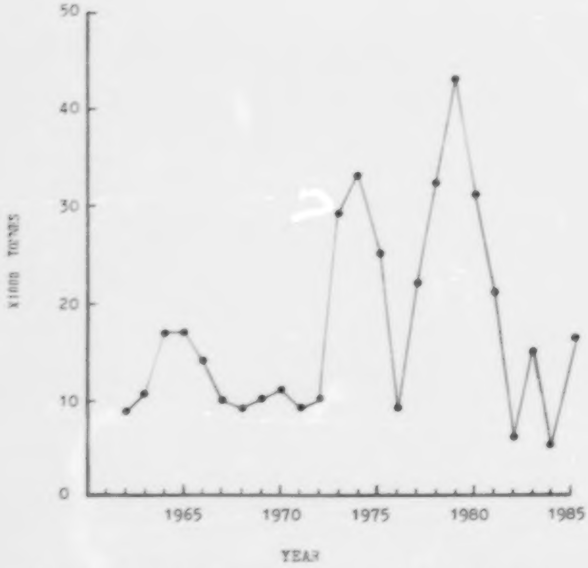

FIG. 2. Catch (t) prawns in the Bohai Sea, 1962–85.

Materials and Methods

Estimation of Recruitment and Spawning Stock

In general, commercial catch reflects the trends in abundance of a well exploited stock, such as the prawns in the Bohai Sea. The term "recruitment" as defined by Gulland (1969) is the process by which young fish enter the exploited area, and can be captured with fishing gear. For Bohai prawns, the numbers caught from September, in year t, through the following April (year $t+1$) were considered as an index of recruitment for year-class t. Thus,

$$R_t = \sum_{m=9}^{12} C_t + \sum_{m=1}^{4} C_{t+1},$$

where R_t = recruitment of year-class t; C_t = numbers caught during September–December in year t; C_{t+1} = numbers caught during January–April in year $t+1$; and m = month.

The spawning migration of Bohai prawns begins in late spring (around April),) and these mature prawns become the spawning stock in May. Thus, numbers caught during the spawning migration in year t were considered to be the index of abundance of the spawning stock for year-class t (Table 1).

TABLE 1. Abundance indices (millions of individuals) for spawning stock (S_t) and resulting recruitment (R_t), by year, of prawns in the Bohai Sea, 1962–83.

Year	S_t	R_t	Year	S_t	R_t
1962	29.26	343.15	1973	23.85	889.80
1963	35.11	372.99	1974	66.49	975.92
1964	29.93	582.27	1975	40.84	691.72
1965	45.81	563.24	1976	17.23	300.99
1966	38.38	447.91	1977	7.87	611.35
1967	27.40	309.68	1978	15.86	793.00
1968	10.85	280.73	1979	17.79	1072.53
1969	16.43	315.00	1980	19.54	804.15
1970	13.02	310.36	1981	9.44	524.17
1971	12.30	245.02	1982	8.24	179.36
1972	7.74	294.45	1983	10.69	359.07

Selection of Environmental Factors

The results, since 1963, of trawl surveys of the eggs, larvae, and juveniles of Bohai prawns indicated that the success of recruitment is apparently related to the environment during the early life history, especially in the larval phase (Deng 1980; Deng et al. 1983a; Deng and Ye 1986; Ma 1986). Therefore, in this study, the major factors affecting the hydrographical conditions of the Bohai Sea during spring and summer were selected as the potential environmental factors affecting recruitment. These factors were: streamflow, rainfall, air temperature, daylight, wind, water temperature, and salinity (Table 2). All environmental variable data used here were taken from Shouguang, Longkou hydrographic and meteorological stations near Laizhou Bay, Tanggu, Huanghua

TABLE 2. The potential environmental factors affecting recruitment in the Bohai Sea.

No.	Factor
X_1	Flow of Yellow River (m^3), Apr.–May
X_2	Flow of Yellow River (m^3), Apr.–June
X_3	Flow of Yellow River (m^3), May–June
X_4	Flow of Yellow River (m^3), Jan.–June
X_5	Flow of Yellow River (m^3), Jan.–June & year t-1
X_6	Flow of Yellow River (m^3), Jan.–June & year t-2
X_7	Rainfall ($mm \cdot d^{-1}$), Apr.–May
X_8	Rainfall ($mm \cdot d^{-1}$), Apr.–June
X_9	Rainfall ($mm \cdot d^{-1}$), year t-1
X_{10}	Rainfall ($mm \cdot d^{-1}$), year t-2
X_{11}	Air temperature (°C), Apr.–June
X_{12}	Air temperature (°C), May–June
X_{13}	Daylight ($h \cdot d^{-1}$), May–June
X_{14}	Daylight ($h \cdot d^{-1}$), May–early June
X_{15}	Wind ($m \cdot s^{-1}$), Apr.–June
X_{16}	Wind ($m \cdot s^{-1}$), May–early June
X_{17}	Surface water temperature (°C), May–June
X_{18}	Surface salinity (‰), May–June

hydrographic and meteorological stations near Bohai Bay, and Jizhou, Qinghuangdao hydrographic and meteorological stations near Liaodong Bay.

Review of Stock Recruitment Models

The spawning stock-recruitment relationship models have been developed by many authors (e.g., Ricker 1954; Beverton and Holt 1957; Cushing 1973; Chapman 1973). Shepherd (1982) showed that each of these models has the same general form,

$$(1) \qquad R = (aS)\,[f(bS)],$$

where R = recruitment; S = spawning stock; a = a parameter related to density-independent mortality and is a scaling factor for the ordinate of a SRR curve; b = a parameter related to density-dependent mortality and specifies the spawning stock size corresponding to maximum recruitment; and $f(bS)$ is some function of bS.

Both "a" and "b" were assumed to be constant in all of these models mentioned above. However, "a" and/or "b" may vary with time. Tang (1985) assumed that "b" could be considered characteristic of a stock, and therefore relatively stable for that stock. Furthermore, deviation from predicted recruitment would be attributed mainly to changes in "a" over time, and thereby to fluctuations in density-independent mortality. Under this assumption, if "a" can be viewed as a variable related to environmental conditions, the Ricker SRR model can be written, where,

$$(2) \qquad R_t = a'_t\, S_t \exp(-b\, S_t),$$

and a'_t can be written as a function of environmental conditions,

$$(3) \qquad a'_t = g\,[X_1(t), X_2(t), \ldots, X_m(t)],$$

where a'_t = an index of environmental conditions affecting density-independent mortality at time t; and $g\,[\;]$ is an arbitrary function of m environment factors $X_i(t)$ at time t. Substituting (3) into (2) gives a modified Ricker SRR model, as follows,

$$(4) \qquad R_t = g\,[X_1(t), X_2(t), \ldots, X_m(t)]\,(S_t) \exp(-b\, S_t).$$

Formula (4) is the basis for the analysis and discussions which follow.

With respect to the estimations of the parameters of equation (4), the method of Tang (1985) was used. In this approach, the estimation procedure is divided into several stages.

Results and Discussion

Ricker SRR Model for Bohai Prawns Under Different Environmental Conditions

A traditional Ricker SRR model for Bohai prawns, based on the data in Table 1, has been fitted as follows:

$$(5) \qquad R = 42.47\, S \exp(-0.024985\, S)$$

where 42.47 corresponds to an average of the a'_t values in equation (2) or (3). Estimates of each a'_t were derived from the following equation,

$$(6) \qquad a'_t = (R_t/S_t) \exp(b\, S_t).$$

Figure 3 displays the good relationship between the index of environmental conditions, a'_t, and the index of recruitment, R_t, for 1962–83. As mentioned in Tang (1985), the functional form of the relationship between a'_t and environmental factors will depend on characteristics of the given stock and environment, and typically will be unknown. For this analysis, the relationship

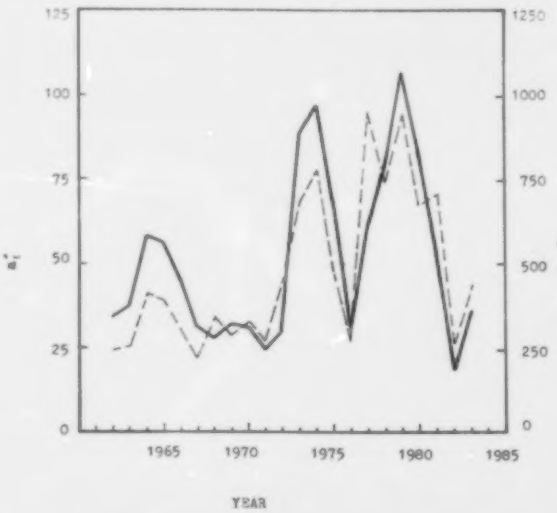

FIG. 3. Indices of environmental conditions (a'_t = ——) and recruitment (R_t = — — —) for prawns in the Bohai Sea, 1962–83.

between a'_t and environmental factors is assumed to be approximately linear. Therefore, step-wise regression was used to select valuable environmental factors from Table 2. Based on the data of 1962–83, streamflow, rainfall, daylight and salinity were selected for inclusion in the index of environmental conditions. The results are shown in the following equation,

$$
\begin{aligned}
(7)\quad a'_t = {} & 141.39 + 1.2754\,X_1 - 1.0124\,X_2 \\
& - 0.4461\,X_4 + 0.0584\,X_5 + 0.3633\,X_8 \\
& + 0.7627\,X_{13} - 1.4356\,X_{14} - 0.2113\,X_{18}
\end{aligned}
$$

Substituting the right side of (7) and $\hat{b} = 0.024985$ of (5) into (4) gives the following modified Ricker SRR model for prawns in the Bohai Sea,

$$
\begin{aligned}
(8)\quad R = {} & (141.39 + 1.2754\,X_1 - 1.0124\,X_2 \\
& - 0.4461\,X_4 + 0.0584\,X_5 \\
& + 0.3633\,X_8 + 0.7627\,X_{13} \\
& - 1.4356\,X_{14} - 0.2113\,X_{18}) \\
& S\exp(-0.024985\,S) \\
& R^2 = 0.745 \qquad P < 0.01
\end{aligned}
$$

A plot of the observed and estimated indices of prawn recruitment during 1962–83 is shown in Fig. 4.

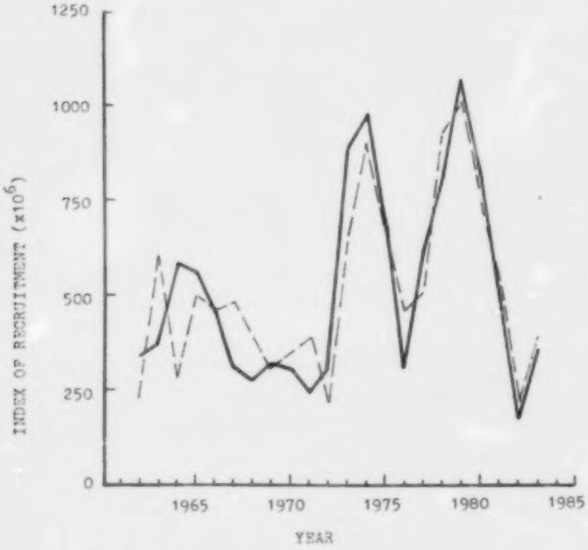

FIG. 4. Observed (______) and estimated (__ __ __) indices of recruitment for prawns in the Bohai Sea, September–April 1962–63 through 1983–84.

Because each a' in equation (2) or (3) results in a level of recruitment, from equation (8), a family or Ricker SRR curves under different environmental conditions have been derived (Fig. 5), where each curve represents the relationship between recruitment and spawning stock for a particular set of environmental conditions. With changing environmental conditions from year to year, Fig. 5 indicates that the relationship between spawning stock and recruitment for Bohai prawns is characterized by multi-curves.

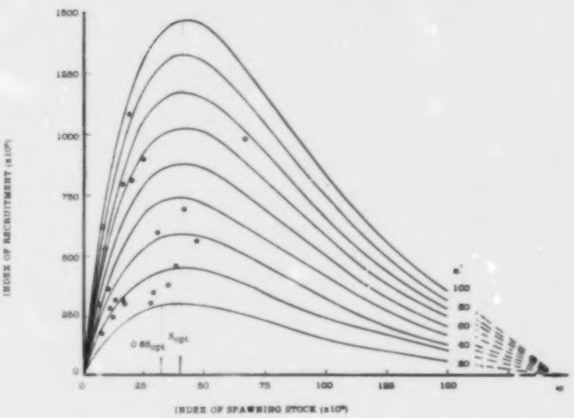

FIG. 5. Spawning stock-recruitment relationship curves for different environmental conditions.

Causes of Fluctuations in Prawn Recruitment

In November 1981, FAO held a workshop on the scientific basis for the management of penaeid shrimp (Gulland and Rothschild 1984). Some of the papers noted that penaeid shrimp were sensitive to the environment, and recruitment was determined largely by environmental factors. Other papers discussed the dependance of recruitment upon spawning stock size.

In this study, we found that both environment and spawning-stock size were related to fluctuations in recruitment of Bohai prawns, and that the relative importance of the two factors varied among years. Examples of the three possible combinations of dominant factors have been noted in the 1962–83 records of the Bohai prawns, viz., environment, spawning stock size, and environment + spawning stock size.

Environmental effects were well delineated for 1979 (high a' value) and 1976 (low a' value) (Fig. 6). In both years the spawning stock was the same small size, but the 1979 year-class produced three times the recruitment of the 1976 year-class.

Spawning stock effects were evident during 1981–83, when low recruitment coincided with the small size of the parent spawning stock.

Favorable environmental conditions plus a suitable large spawning stock resulted in a large recruitment, as in 1973–74 and 1978–80.

From the viewpoint of resource management, it should be pointed out that recently the fishery has aggravated fluctuations in recruitment due to overfishing, and spawning stock has been reduced to a below-normal level. The spawning stock in 1981–83 is only one-third of 0.8–1.0 S_{opt} (see Fig. 5 and Table 1). Thus, it is reasonable to say that implementation of strict regulation measures is essential. The main options could include: (1) reducing fishing effort and limiting the fishing season in autumn, in order to control fishing mortality, (2) intensifying conservation of spawning stock, especially during the overwintering season and during the spawning migration.

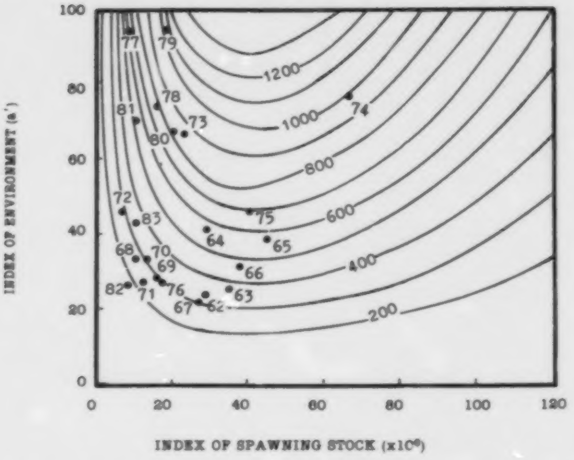

FIG. 6. Calculated recruitment isopleths for prawns in the Bohai Sea, based on observed indices (dots) of environment, spawning stock abundance, and recruitment, 1962–83. (Based on equation [8]).

Enhancement Potential for the Bohai Sea Prawn Stock

In order to rehabilitate and incease the prawn resource, and its fishery, two major measures have been taken into account to date. One is to retain a sufficiently large spawning stock from the fishable stock by effective management, as mentioned above. The other is to develop a re-stocking program.

Since artificial enhancement of prawns in the southern coastal waters of Shandong Peninsula met with success (Wang 1987), the artificial enhancement program for Bohai prawns has been advocated since 1985. Now the question is how many juvenile prawns should be released. In terms of the family of SRR curves previously developed, the following formula provides an estimate for individual years,

$$(9)\ R_r = (R_{\max} - R_t)/S$$

where R_r = number of juvenile prawns released; $R_{\max}$ = maximum recruitment under best environmental conditions (≈1500 million, based on data in Fig. 5 and Table 1); R_t = recruitment in year t (estimated from equation (8)); and S = survival rate of juvenile prawns released.

From this tentative idea, the optimum number of juvenile prawns to be released in the Bohai Sea will be variable. For example, for 1982 (R_t = 180 million), if S is estimated at 0.1, the optimum number released is about 13 billion. On the other hand, for 1979 (R_t = 1072 million), the comparable value is only 4 billion.

References

ANON. 1978. Handbook of fishing ground. Agriculture Publ. House, Beijing. (In Chinese)

BEVERTON, R. J. H., AND S. J. HOLT. 1957. On the dynamics of exploited fish populations. U. K. Min. Agric. Fish., Fish. Invest. (Ser. II) 19: 533 p.

CHAPMAN, D. G. 1973. Spawner-recruit models and estimation of the level of maximum sustainable catch. Rapp. P.-V. Reun. Cons. Int. Explor. Mer 164: 325–332.

CUSHING, D. H. 1973. The dependence of recruitment on parent stock. J. Fish. Res. Board Can. 30: 1965–1976.

DENG, J. 1980. Distribution of eggs and larvae of penaeid shrimp in the Bohai Bay and its relation to natural environment. Mar. Fish. Res. 1: 17–25. (In Chinese, English abstract)

DENG, J., AND C. YE. 1986. The prediction of penaeid shrimp yield in the Bohai Sea in autumn. Chin. J. Oceanol. Limnol. 4: 343–352. (In Chinese, English abstract)

DENG, J., Y. KANG, AND J. ZHU. 1983a. Tagging experiments of the penaeid shrimp in the Bohai Sea and Huanghai Sea in autumn season. Acta Oceanol. Sinica. 2: 308–319. (In Chinese, English abstract)

DENG, J., Y. KANG, Y. JIANG, J. ZHU, AND S. MA. 1983b. A summary of surveys of the penaeid shrimp spawning ground in the Bohai Bay. Mar. Fish. Res. 5: 18–32. (In Chinese, English abstract)

GULLAND, J. A. 1969. Manual of methods for fish stock assessment. Part I. Fish Population Analysis. FAO Manuals in Fish. Sci. No. 4: 154 p. FAO, Rome.

GULLAND, J. A., AND B. J. ROTHSCHILD [Ed.]. Penaeid shrimps, their biology and management. Fishing News Books, Ltd. Farnham, U.K. 308 p.

KIM, B. 1973. Studies on the distribution and migration of Korean shrimp *Penaeus orientalis, KISHINOUYE* in the Yellow Sea. Bull. Fish. Res. Dev. Agency, Busan 11: 7–23. (In Korean, English abstract)

MA, S. 1986. The relationship between the survival of eggs and juveniles of Bohai prawn and its environment. Mar. Fish. Res. Pap. 30: 65–70. (In Chinese)

MAKO, H., K. NAKASHIMA, AND K. TAKAMA. 1966. Variation of length composition of Chinese prawn. Bull. Seikai Reg. Fish. Res. Lab. 34: 1–10. (In Japanese)

RICKER, W. E. 1954. Stock and recruitment. J. Fish. Res. Board Can. 11: 559–623.

SHEPHERD, J. G. 1982. A versatile new stock-recruitment relationship for fisheries, and the construction of sustainable yield curves. J. Cons. Cons. Int. Explor. Mer 40: 67–75.

TANG, Q. 1985. Modification of the Ricker stock recruitment model to account for environmentally induced variation in recruitment with particular reference to the blue crab fishery in Chesapeake Bay. Fish. Res. 3: 13–21.

WANG, S. 1987. Artificial ranching propagation in large area along the coast of the southern part of Shandong. Mar. Fish. 9: 265–267. (In Chinese)

Contributions of Ozernaya River Sockeye Salmon *(Oncorhynchus nerka)* to Ocean Catches with Special Reference to Their Distribution in Space and Time

M. M. Selifonov

Pacific Research Institute of Fisheries and Oceanography (TINRO),
Kamchatka Branch, Petropavlovsk-Kamchatsky, USSR

Abstract

SELIFONOV, M. M. 1989. Contributions of Ozernaya River sockeye salmon (*Oncorhynchus nerka*) to ocean catches with special reference to their distribution in space and time, p. 341–352. *In* R. J. Beamish and G. A. McFarlane [ed.] Effects of ocean variability on recruitment and an evaluation of parameters used in stock assessment models. Can. Spec. Publ. Fish. Aquat. Sci. 108.

Biological markers including scale pattern, age and maturity characteristics together with run timing data were used to estimate the contributions of sockeye salmon (*Oncorhynchus nerka*) originating in the Ozernaya River, Kamchatka, to Japanese ocean driftnet catches during 1962–75. Most mature Ozernaya sockeye were caught during June in the centre of a zone situated between 48–54°N and 160°E–175°W; after July 1, mostly immature fish were caught in this zone. Immature Ozernaya sockeye were also abundant in catches south of 48°N in late May and early June. The ocean fishery tends to selectively harvest the largest Ozernaya sockeye. Most mature Ozernaya sockeye taken by the fishery were female whereas most immature fish were male. Before 1962 the total abundance of Ozernaya sockeye was positively correlated with the proportion of 6-year-old fish (mostly age 5_2+) in ocean catches and negatively correlated with the proportion of 5-year-old fish (mostly age 4_2+). Since 1963, the total abundance of Ozernaya sockeye has been positively correlated with the proportion of 5-year-old fish in ocean catches and there has been a decrease in the mean age of the spawning escapement to the Ozernaya River. The overall contribution of Ozernaya River sockeye to ocean catches during 1962–75 has remained relatively constant. However, the proportion of immature sockeye in the catches more than doubled during 1967–72, and subsequently the total stock of sockeye, including the Ozernaya population, has declined in abundance.

Résumé

SELIFONOV, M. M. 1989. Contributions of Ozernaya River sockeye salmon (*Oncorhynchus nerka*) to ocean catches with special reference to their distribution in space and time, p. 341–352. *In* R. J. Beamish and G. A. McFarlane [ed.] Effects of ocean variability on recruitment and an evaluation of parameters used in stock assessment models. Can. Spec. Publ. Fish. Aquat. Sci. 108.

Des marqueurs biologiques comme les caractéristiques morphologiques des écailles, l'âge et les caractéristiques de la maturité conjugués avec des données portant sur la période de montaison nous ont permis d'estimer les proportions de saumons rouges (*Oncorhynchus nerka*) provenant de la rivière Ozernaya au Kamchatka pêchés dans la mer par les Japonais à l'aide de filets dérivants entre 1962 et 1975. La plupart des saumons matures de l'Ozernaya ont été capturés au mois de juin au centre d'une zone limitée par les lattitudes 48–54°N et les longitudes 160°E–175°O; après le 1er juillet, ce sont surtout des poissons immatures qui ont été capturés dans cette zone. Les saumons immatures de l'Ozernaya ont également été pêchés en grand nombre au sud du 48°N à la fin mai et au début de juin. En mer, les pêcheurs ont tendance à capturer sélectivement les plus gros saumons de la rivière Ozernaya. Parmi les prises, la plupart des saumons matures de l'Ozernaya étaient des femelles tandis que la plupart des poissons immatures étaient des mâles. Avant 1962, la quantité totale de saumons rouges de l'Ozernaya était corrélée positivement avec la proportion des prises de poissons de 6 ans (surtout d'âge 5_2+) dans les captures océaniques et corrélée négativement avec la proportion des prises de poissons de 5 ans (surtout d'âge 4_2+). Depuis 1963, la quantité totale de saumons rouges de l'Ozernaya a été corrélée positivement avec la proportion des prises de poissons de 5 ans dans les captures océaniques et il y a eu une diminution de l'âge moyen des poissons qui réussissent à aller frayer dans la rivière Ozernaya. De 1962 à 1975, la proportion de saumons rouges de l'Ozernaya dans les captures océaniques est restée relativement constante. Cependant, la proportion de saumons rouges immatures capturés a plus que doublé entre 1967 et 1972, d'où la réduction subséquente importante du stock totale de saumons rouges dont fait partie la population de saumons rouges de l'Ozernaya.

Introduction

Juvenile Ozernaya sockeye salmon (*Oncorhynchus nerka*) typically migrate to sea after spending 2 or 3 yr in Lake Kuril. Most spend 2 or 3 yr at sea, but a minority stay in the ocean for 1 or 4 yr. The most numerous age-groups of Ozernaya sockeye at maturity are 4_2+ and 5_2+.[1] The same age-groups occur in the ocean catches, but with somewhat different frequencies.

Sockeye salmon occur throughout a broad region in the northern part of the Pacific Ocean. Most investigators believe that Asian sockeye range from the Kamchatka coast seaward to 175°W. The region of greatest mixing of Asian and American sockeye is between 170°W and 180°W (Konovalov 1971).

The distribution of total catches of sockeye in the northwest Pacific between 1962 and 1975 is shown in Fig. 1. The bulk of both immature and mature sockeye were caught from the Commander and Aleutian islands, south to 46°N. During this period, fishing was conducted in the northern part of the Pacific Ocean, usually beginning in mid- to late May. Catches in the region situated between 48-52°N and 165-170°E were as high as 650 000 individuals in some years. In June and July, fishing expanded into the western Bering Sea, almost to 62°N, but most of the catch was still from the Pacific. Catches in the region between 48-54°N and 165-175°E were typically 800-1400 thousand in June. In July, the main fishing area was closer to Kamchatka, with catches varying from 300 000 to 500 000 and occasionally up to 1.7 million sockeye. Catches also increased in the western Bering Sea in July with about 600 000 being caught near Olyutorka Bay in some years.

Studies of the distribution and migration of Pacific salmon in the northwestern Pacific (Birman 1958), and later the identification of parasites characteristic of particular stocks (Konovalov 1971) have made it possible to distinguish salmon stocks according to their area of origin and to determine their time and route of migration. In this respect, sockeye of the Ozernaya River have been the most thoroughly investigated Asian stock (Birman and Konovalov 1968; Konovalov 1971; Selifonov 1975). In this paper I estimate the number and distribution of immature and mature sockeye originating from the Ozernaya River, that were taken in ocean catches during 1962-75. I also present data on the sex, length, weight, and age composition of Ozernaya sockeye in ocean catches. These data were used to assess the present status of the stock.

Materials and Methods

The following terms require explanation:

Quadrat: Region delineated by a rectangle measuring 2° of latitude by 5° of longitude in the northwestern Pacific Ocean. For example, quadrat 4865 is the region of the Pacific situated between 48-50°N and 165-170°E.

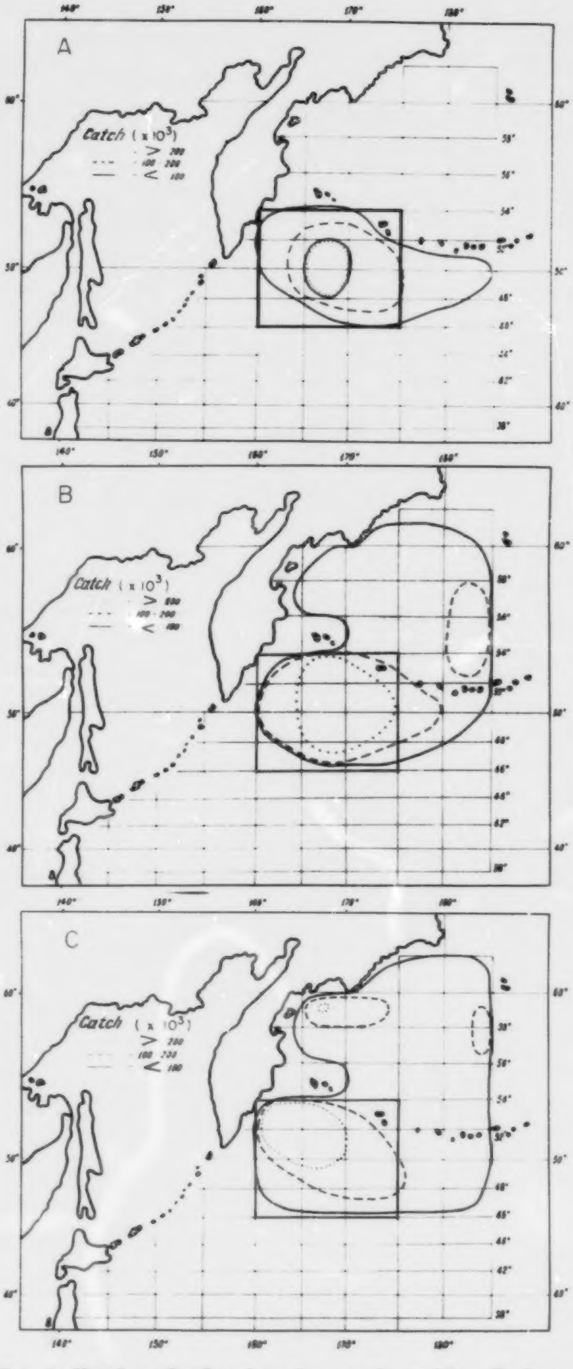

FIG. 1. Total catch of sockeye by month. A. May. B. June. C. July.

Ozernaya Quadrangle (O.Q.): The zone situated between 46-54°N and 160°E-175°W where most Ozernaya sockeye are caught. It comprises quadrats 4660 through 5280.

Sockeye ages: Ages of sockeye caught at sea are designated by a convention commonly employed in the USSR. For example, 4_2+ represents the age of a

---

[1] Note: Russian age convention used throughout (see Materials and Methods).

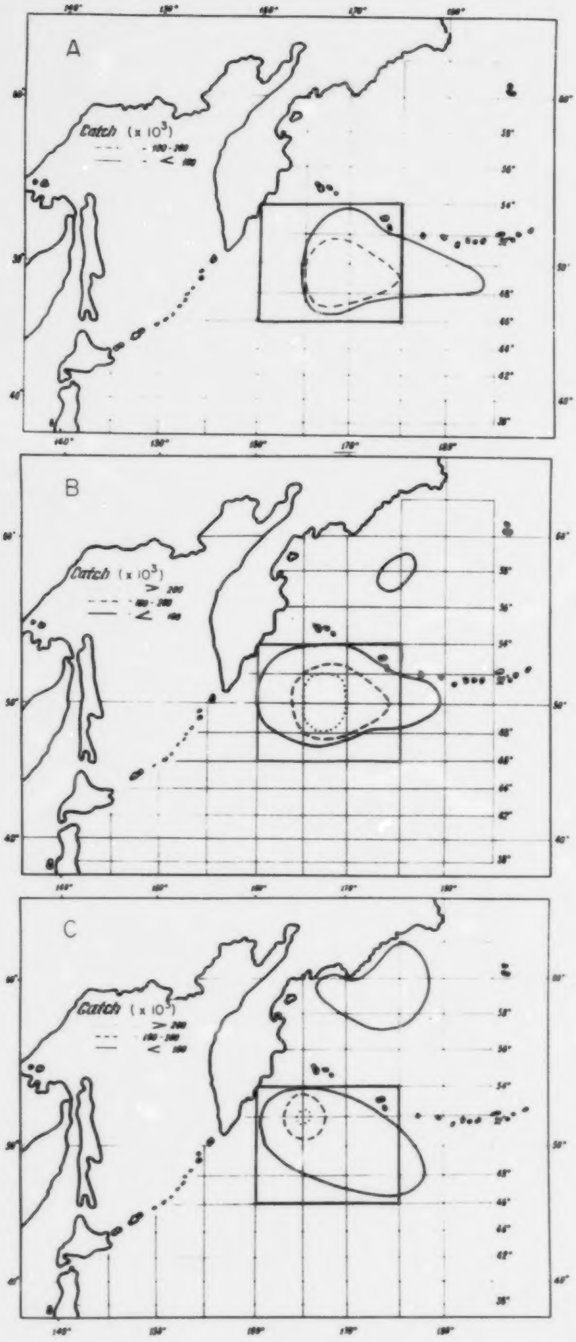
A
Catch (x 10³)
100-200
< 100
B
Catch (x 10³)
> 200
100-200
< 100
C
Catch (x 10³)
> 200
100-200
< 100
140°
150°
160°
170°
180°

FIG. 2. Catch of mature Ozernaya sockeye by month. A. May. B. June. C. July.

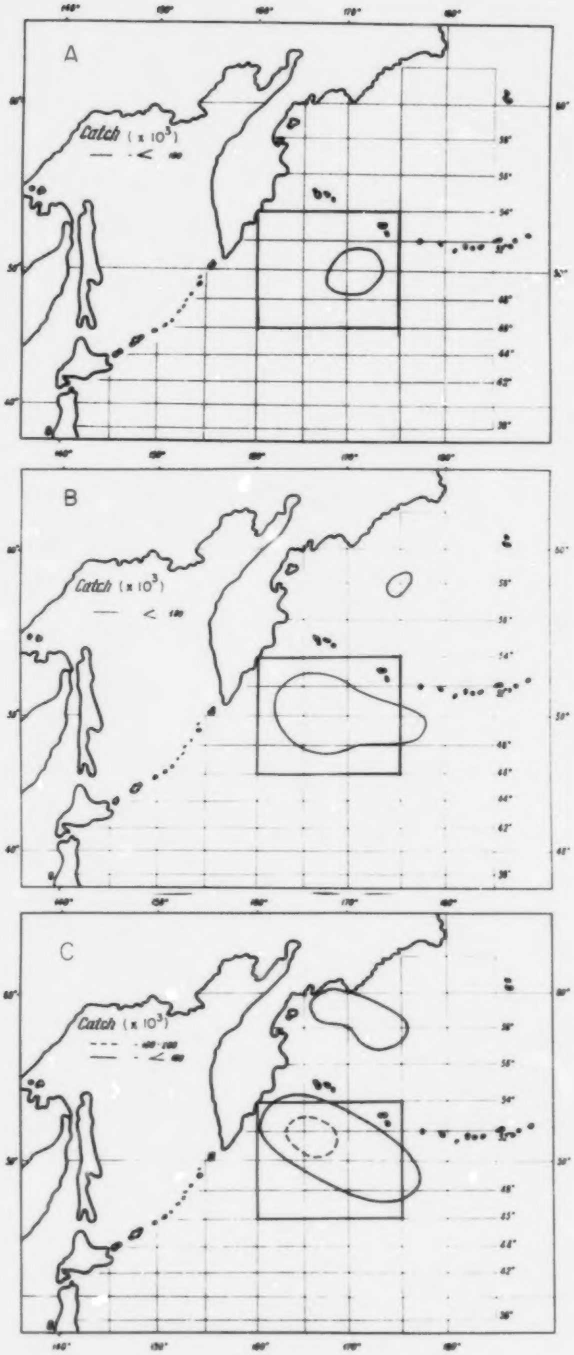
A
Catch (x 10³)
< 100
B
Catch (x 10³)
< 100
C
Catch (x 10³)
100-200
< 100
140°
150°
160°
170°
180°

FIG. 3. Catch of immature Ozernaya sockeye by month. A. May. B. June. C. July.

fish that had 2 complete years of freshwater growth (two freshwater annuli) and is in its third year of ocean growth, approaching 5 years in all. The same fish would be 5_3 in the Gilbert convention.

To estimate the proportion of Ozernaya sockeye in ocean catches, I used criteria developed by Krogius (1967) involving analysis of age structure, run timing, state of maturity, and scale structure. Following Krogius, I used biostatistical data on catches, by 10-day periods, in the appropriate quadrats of the Pacific Ocean and the Bering Sea during the period 1962–75 for which the best information is available. Immature and mature sockeye of the Ozernaya River were identified in ocean catches. State of maturity was identified using the technique proposed by Evleva (1964).

Results and Discussion

Distribution of Mature Ozernaya Sockeye

Most mature Ozernaya sockeye in ocean catches were encountered south of the Commander and Aleutian islands (Fig. 2). In May, the largest catches (100 000–200 000) were from quadrats 5065, 4865, and 4870. The largest quantities of Ozernaya sockeye during this time are found eastward of 175°E, with monthly catches of 2 000 to 37 000 fish. It should be noted that in this region, Ozernaya sockeye were found in catches only in certain years (1964, 1966, 1967, and 1969). In June, the majority of the catch of Ozernaya sockeye was from the O.Q. The largest catches occurred in quadrats 5065 and 4865 and, in 1962 and 1963, were as high as 600–700 thousand fish. Mature sockeye caught east of 175°E and south of 52°N after the middle of June may all be considered to be from Ozernaya River (Hanamura 1966). Small quantities of Ozernaya sockeye (1 300 in 1964 and 4 000 in 1965) are also caught in the Bering Sea in June. In July, the bulk of mature Ozernaya sockeye are caught close to Kamchatka (200–300 thousand per month).

Distribution of Immature Ozernaya Sockeye

Very few immature Ozernaya sockeye (up to 20 000 in some years) are caught in May. They are caught principally in the eastern O.Q. (Fig. 3). In June, the area where immature sockeye are caught expands throughout the O.Q. east to 180°. The catch of immature Ozernaya sockeye in June was sometimes close to 100 000 fish. In July, catches varied from 100 000 to 200 000 fish in quadrats 5260 and 5065, and toward the end of the fishing season increased in the rest of the O.Q. also.

Analysis of the distribution of catches by the Japanese fleet for a series of years indicates that the greatest total catch of sockeye was in June and July, but in July the by-catch of immature sockeye was higher. Mature Ozernaya sockeye were caught mainly in June in the centre of the O.Q. when the proportion of immature sockeye was not large. In July mostly immature sockeye are caught in this region.

Age and Size Composition of Sockeye in Ocean Catches

Variations in average length of mature Ozernaya sockeye in ocean catches are summarized in Table 1 for the following age groups: 3_2+, 4_3+, 4_2+, 5_3+, 5_2+, 6_3+. As a rule, males were larger than females; this is also true during spawning runs, and is characteristic of Pacific salmon in general. Size increased in all age-groups during the ocean fishing season, from April to August.

Analysis of the variation in length of immature Ozernaya sockeye from 1962 to 1972 suggests that size has varied relatively little over time (Fig. 4). Size differences of fish of the same sex and age-group were not

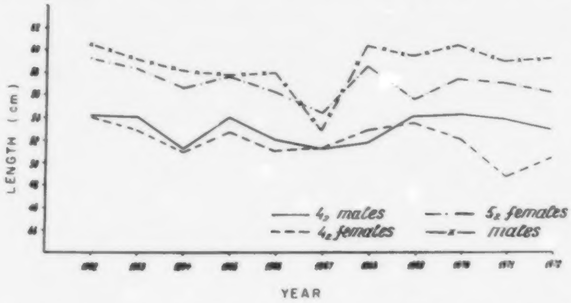

FIG. 4. Mean size of mature Ozernaya sockeye in ocean catches.

TABLE 1. Size of mature Ozernaya sockeye (cm).

Year	Month	3_2+	4_2+		5_2+		4_3+	5_3+		6_3+	
		Male	Male	Female	Male	Female	Male	Male	Female	Male	Female
1970	April		47.0	48.5							57.0
	May		50.9	49.7		53.7		50.1	49.4	53.0	
	June		53.8	51.2	59.6	57.2		53.9	54.2	59.5	57.3
	July	39.0	56.6	58.2	61.0	58.0		57.4	54.6	59.4	55.6
	August	46.5	51.4	54.0		59.0		57.3	53.0	57.0	
	$\overline{X}$ =	44.0	54.4	52.2	60.6	57.5		55.3	53.8	58.4	56.3
1971	May		53.4	53.5	58.9	56.3		53.3	52.6	60.1	56.2
	June	40.0	54.5	47.3	59.1	57.0		54.4	52.3	60.9	58.0
	July		53.2	52.8	60.8	58.9		55.2	53.9	62.6	59.1
	August	41.6	57.6	53.9	58.4	59.1	40.0	57.3			61.4
	$\overline{X}$ =	41.1	54.0	49.8	59.2	57.2	40.0	54.3	52.5	60.9	57.9
1972	April		52.1	48.6	56.2	53.6		49.8	49.5		54.9
	May		51.7	47.6	58.0	55.6		50.7	50.3	59.2	56.4
	June	46.0	54.2	51.5	59.9	56.8		52.8	51.4	59.0	56.9
	July	41.0	56.2	54.3	62.5	59.2	41.8	51.5	54.7	63.8	59.0
	$\overline{X}$ =	41.7	53.1	50.6	59.4	56.4	41.8	51.2	51.6	59.7	56.3

TABLE 2. Weight of mature Ozernaya sockeye (kg).

Year	Month	3_2+ Male	4_2+ Male	4_2+ Female	5_2+ Male	5_2+ Female	4_3+ Male	5_3+ Male	5_3+ Female	6_3+ Male	6_3+ Female
1970	April		1.30	1.60							2.50
	May		1.63	1.52		2.03		1.57	1.64	1.70	
	June		2.08	1.95	2.72	2.48		2.26	2.13	2.70	2.43
	July	0.80	2.22	2.04	3.22	2.78		2.57	2.26	2.78	2.20
	August	0.90	1.87	2.18		2.85		2.67	2.14	2.60	
	$\overline{X}$ =	0.87	2.06	1.94	3.07	2.63		2.34	2.15	2.62	2.31
1971	May		1.96	1.94	2.75	2.31		2.06	1.81	2.95	2.33
	June	0.80	2.15	1.90	2.81	2.50		2.09	1.86	3.13	2.56
	July		2.16	2.00	3.00	2.73		2.16	1.84	3.40	2.82
	August	0.95	2.43	2.14	2.73	2.82	0.83	2.60			3.10
	$\overline{X}$ =	0.90	2.07	1.93	2.80	2.49	0.83	2.11	1.84	3.09	2.60
1972	April		1.64	1.36	2.18	1.92		1.43	1.40		2.03
	May		1.74	1.53	2.46	2.20		1.62	1.48	2.50	2.24
	June	1.14	2.16	1.79	3.04	2.61		2.05	1.79	2.93	2.59
	July	0.92	2.51	2.27	3.54	2.92	0.93	1.83	2.35	3.80	2.90
	$\overline{X}$ =	0.95	1.96	1.78	2.83	2.43	0.93	1.72	1.76	2.93	2.34

statistically significant in most cases. This was probably a consequence of the selectivity of the driftnets used. Similar patterns are observed in the mean weight of mature Ozernaya sockeye caught at sea: males were larger than females, the greatest mean weights occurred late in the fishing season and weight increased across the various age-groups in the same order as for length (Table 2).

In spite of the broader range of variations of mean weight from year to year as compared with length, differences in mean weight between consecutive years are not large (except for 5_2+ in 1966–68) (Fig. 5). Also, no relationship was observed between mean weight and the abundance of either the mature stock as a whole, or of individual age-groups. It is likely that the lack of correlation between length or weight and the abundance of mature sockeye also reflects the selectivity of the driftnets.

The two most numerous age groups of sockeye are 4_2+ and 5_3+ and immature fish of these ages were examined for variations in mean weight and length. Mean length of immatures varies little from year to year (Table 3), particularly in age-group 4_2+ (Fig. 6). Immature sockeye of age 4_2+ and 5_3+ were similar in mean length throughout the fishing season.

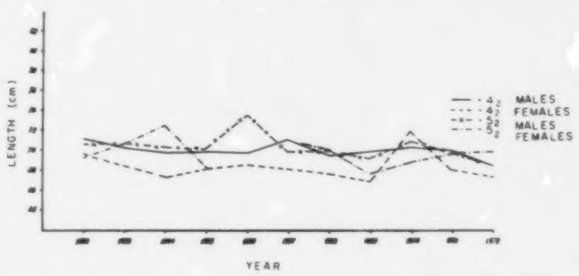

FIG. 6. Mean size of immature Ozernaya sockeye in ocean catches.

Weight of immature Ozernaya sockeye also varied only slightly between years (Fig. 7). No seasonal differences in weight were observed in the most numerous age-groups. However, the weight of males exceeded that of females somewhat (Table 4). Thus, fishing mortality on immature Ozernaya sockeye occurred with a narrow range of length and weight and was probably most severe on the largest individuals.

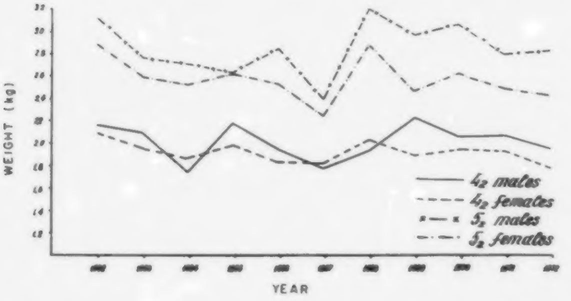

FIG. 5. Mean weight of mature Ozernaya sockeye in ocean catches.

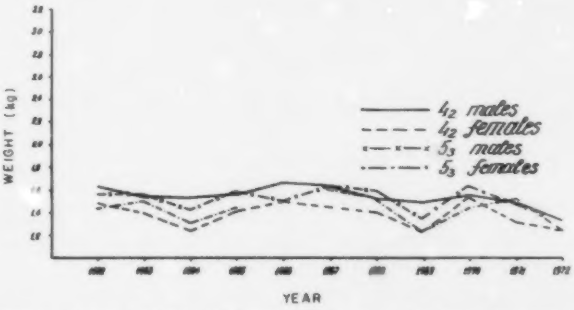

FIG. 7. Mean weight of immature Ozernaya sockeye in ocean catches.

TABLE 3. Size of immature Ozernaya sockeye (cm).

Year	Month	Age									
		3_2+		4_2+		5_2+		4_3+		5_3+	
		Male	Female	Male	Female	Male	Female	Male	Female	Male	Female
	April			45.0	46.7					49.0	47.0
	May			51.3	48.0		47.0			49.7	—
	June			50.0	48.3	51.3				51.6	50.0
1970	July			50.2	53.6	55.0	53.0			51.1	48.2
	August	38.5	32.0	51.1	49.5	57.0				49.7	50.0
	September	38.9	38.8	50.0	48.0			40.0			
	$\bar{X}$ =	38.8	37.7	50.3	52.0	54.3	51.5	40.0		50.9	48.8
	May			48.4	48.5	55.3	54.5			48.7	50.0
	June			50.0	47.3	52.6	48.5			49.7	48.3
1971	July			50.4	48.4	52.7				49.8	50.8
	August			50.5	51.2	53.8	45.2			52.3	48.4
	$\bar{X}$ =			50.0	48.0	53.2	49.0			49.8	49.7
	April			46.2	45.9	50.0				47.6	46.6
	May			47.6	47.0		50.3	35.2		49.0	48.5
1972	June			47.7	46.3	53.4	53.3	39.4		48.2	46.4
	July			49.9	48.1			41.4	39.0	48.9	54.7
	$\bar{X}$ =			48.5	47.3	52.3	51.6	40.1	39.0	48.5	49.8
	April		33.4	47.7	46.0					46.3	46.9
	May			47.6	47.2	56.4	47.6	40.4		48.3	47.0
1973	June		47.6	48.9	46.9	54.5	52.3			48.8	47.6
	July			49.8	47.9	59.7	61.0			51.7	48.7
	$\bar{X}$ =		40.5	48.6	47.3	57.0	52.1	40.4		48.8	47.6
	April			47.6	48.1	51.4	48.4			47.7	48.6
	May	41.2		47.7	47.4	53.2	48.9			48.2	46.3
1974	June	37.9		48.0	46.6	50.7	55.9			48.4	47.4
	July	38.2		50.2	48.2	50.3	50.3	40.8	38.4	50.9	48.4
	$\bar{X}$ =	39.1		48.5	47.6	51.6	51.0	40.8	38.4	48.9	47.4
	April			47.7	47.2		49.1			47.1	47.2
	May			48.3	48.2	53.0	47.2	42.8		46.6	48.4
1975	June	34.5		48.3	46.5	53.8	53.6	38.1		48.4	48.0
	July			49.1	47.6	54.5	49.6	42.6		49.5	47.1
	$\bar{X}$ =	34.5		48.4	47.3	53.4	51.1	39.6		48.2	47.8

Sex Composition of Ozernaya Sockeye in the Ocean

The sex composition of Ozernaya sockeye caught at sea is another index of stock status as is length or weight. Mature males of age 3_2+ and 4_3+ occurred as an insignificant component of ocean catches (Table 5). These age-groups were caught in June and July. Note that among mature fish in the youngest dominant age-group (4_2+), mature females usually predominated only early in the season, although for many years the whole season catch was also predominantly female; among mature fish in age-group 5_2+, females predominated throughout the season. No obvious trends in sex composition were noted in the small catches of other mature age-groups.

A different picture is presented by the catches of immature Ozernaya sockeye (Table 6). These included a small component of ages 3_2+ and 4_3+. As a rule, the other age-groups included mostly males. This was probably related to the larger size of immature males, which made them more vulnerable to fishing gear permitted under existing regulations.

Overall, most mature fish in ocean catches were female whereas most immature fish were male. This has resulted in an approximately equal sex ratio among spawners which escaped the fishery. Excesses of males, or of females, observed in certain years, were probably related to differences in the impact of the fishery on the immature versus the mature part of the population. Similarly, Ivankov (1968) concluded that the sex ratios in spawning escapements of South Kuril pink salmon (*O. gorbuscha*) shifted in favour of males (137–204 males to 100 females), and the number of the large females (with the greatest fecundity) decreased, owing to removals by the ocean driftnet fishery during the period 1956-64. Thus, the driftnet fishery appears to affect the structure of the mature part of far-eastern salmon stocks, acting to decrease the length and weight of those that escape to spawn and to decrease the number of females in older age-groups.

TABLE 4. Weight of mature Ozernaya sockeye (kg).

Year	Month	Age									
		3_2+		4_2+		5_2+		4_3+		5_3+	
		Male	Female	Male	Female	Male	Female	Male	Female	Male	Female
1971	May			1.38	1.37	1.96	2.00			1.48	1.60
	June			1.48	1.25	1.63	1.43			1.47	1.32
	July			1.57	1.35	1.68				1.45	1.67
	August			1.56	1.66	1.98	1.20			1.62	1.34
	$\bar{X}$ =			1.50	1.32	1.73	1.48			1.48	1.52
1972	April			1.10	1.13	1.36				1.18	1.14
	May			1.22	1.19		1.50	0.52		1.36	1.32
	June			1.27	1.14	2.05	1.72	0.60		1.32	1.17
	July			1.48	1.35			0.78	0.70	1.16	1.31
	$\bar{X}$ =			1.34	1.25	1.79	1.61	0.70	0.70	1.32	1.24
1973	April		0.39	1.22	1.09					1.14	1.09
	May			1.21	1.18	2.28	1.24	0.67		1.25	1.20
	June		1.20	1.32	1.20	1.95	1.82			1.34	1.24
	July			1.39	1.25	2.10	3.10			1.55	1.33
	$\bar{X}$ =		0.80	1.29	1.21	2.08	1.84	0.67		1.32	1.24
1974	April			1.23	1.19	1.50	1.36			1.16	1.39
	May	0.82		1.24	1.37	1.95	1.52			1.31	1.15
	June	0.72		1.24	1.15	1.55	1.92			1.25	1.16
	July	0.66		1.53	1.35	1.49	1.48	0.70	0.67	1.61	1.30
	$\bar{X}$ =	0.73		1.33	1.28	1.67	1.61	0.70	0.67	1.35	1.23
1975	April			1.20	1.20		1.51			1.14	1.18
	May			1.28	1.28	1.73	1.30	0.95		1.14	1.28
	June	0.43		1.25	1.13	1.86	1.88	0.56		1.20	1.25
	July			1.41	1.27	1.64	1.56	1.04		1.48	1.22
	$\bar{X}$ =	0.43		1.29	1.21	1.75	1.67	0.70		1.27	1.24

TABLE 5. Age and sex composition (%) of mature sockeye in ocean catches in the Northwest Pacific.

Year	Month	Age													
		3_2+	4_2+		5_2+		6_2+		4_3+	5_3+		6_3+		Total	
		Male	Male	Female	Male	Female	Male	Female	Male	Male	Female	Male	Female	Male	Female
1970	May		51.48	29.40							12.14	6.38		58.46	41.54
	June		32.57	32.51	3.44	6.88				9.15	11.76	1.50	2.25	46.60	53.40
	July	0.54	28.44	32.62	3.99	6.53			0.21	8.97	15.52	1.98	1.20	44.13	55.87
	$\bar{X}$ =	0.34	30.62	32.46	3.66	6.42			0.14	8.70	14.15	2.00	1.57	45.46	54.54
1971	May		26.72	21.09	13.33	18.82				8.41	7.35	1.22	3.06	49.68	50.32
	June	0.09	24.44	28.97	8.08	25.25				4.73	6.08		2.36	37.34	62.66
	July		17.46	27.96	11.68	19.48				5.23			18.19	34.37	65.63
	$\bar{X}$ =	0.05	24.76	26.04	10.25	22.49				6.10	6.10	0.44	3.77	41.60	58.40
1972	May		20.20	14.98	20.47	30.17				4.88	4.88	2.21	2.21	47.76	52.24
	June		15.34	19.72	13.67	33.64				4.76	7.13	2.87	2.87	36.64	63.36
	July	2.59	18.08	19.87	18.18	20.79			0.79	5.87	10.29	1.77	1.77	47.28	52.72
	$\bar{X}$ =	0.44	17.81	17.80	17.22	30.03			0.13	5.00	6.74	2.41	2.42	43.01	56.99
1973	May		24.70	18.82	13.53	25.30		0.59		4.71	7.06	1.76	3.53	44.70	55.30
	June	1.32	15.57	13.46	13.46	22.16	0.26			11.34	10.29	3.17	8.97	45.12	54.88
	July	3.13	7.81	14.06	7.81	31.25			1.56	14.06	6.25	4.69	9.38	39.06	60.94
	$\bar{X}$ =	0.43	21.78	17.20	13.41	24.50	0.07	0.41	0.03	6.77	7.98	2.22	5.20	44.71	55.29
1974	May		13.29	15.19	20.89	36.71				4.43	6.96	1.90	0.63	40.57	59.49
	June	1.15	7.47	8.04	31.61	39.66				1.15	2.87	3.45	4.60	44.83	55.17
	July	6.72	10.09	10.93	15.13	35.29		0.84		2.52	7.56	3.36	7.56	37.82	62.18
	$\bar{X}$ =	0.89	12.22	13.78	21.78	36.89		0.01		4.00	6.67	2.22	1.55	41.11	58.89
1975	May		25.21	38.66	7.28	14.85		0.28		3.08	5.32	1.12	4.20	36.69	63.31
	June	0.64	30.67	37.06	3.83	12.46			0.64	4.79	3.20	1.28	5.43	41.85	58.15
	July		29.19	41.62	7.03	8.12		0.54	1.08	5.94	3.24	1.62	1.62	44.86	55.14
	$\bar{X}$ =	0.07	25.77	38.63	6.94	14.50		0.27	0.07	3.30	5.09	1.10	4.26	37.25	62.75

TABLE 6. Age and sex composition (%) of mature Ozernaya sockeye in ocean catches in the Northwest Pacific.

Year	Month	Age										
		3_2+	4_2+		5_2+		4_3+		5_3+		Total	
		Male	Male	Female	Male	Female	Male	Female	Male	Female	Male	Female
1970	May		81.82						18.18		100.00	
	June		33.32	33.32	8.03				21.10	4.23	62.45	37.55
	July		36.27	38.80	1.42	1.07			14.59	7.85	52.28	47.72
	$\overline{X}$ =		36.88	37.64	1.92	0.97			15.17	7.42	53.97	46.03
1971	May		19.52	37.32	23.57					26.59	36.09	63.91
	June		53.12	18.88	3.98	5.29			13.48	5.25	70.58	29.42
	July		49.48	20.61	7.82				8.82	13.27	66.12	33.88
	$\overline{X}$ =		50.76	19.96	5.41	4.32			12.22	7.33	68.39	31.61
1972	May		40.84	40.84					18.32		59.16	40.84
	June		49.36	16.91	4.46	2.24	2.36		13.07	11.60	69.25	30.75
	July		41.82	31.98			1.47		11.91	12.82	55.20	44.80
	$\overline{X}$ =		41.51	27.00	1.63	0.82	1.70		12.70	11.64	60.54	39.46
1973	May		45.79	23.83	0.47	0.93	0.47		15.42	13.09	62.15	37.85
	June	0.44	50.00	17.54	0.88	1.76			21.05	8.33	72.37	27.63
	July		40.54	38.51	1.35	0.68			7.43	11.49	49.32	50.68
	$\overline{X}$ =	0.06	46.22	23.64	0.54	1.07	0.36		15.90	12.21	63.08	36.92
1974	May	2.82	50.70	16.90	7.04	7.04			11.27	4.23	71.83	28.17
	June	3.07	41.54	26.15	4.62	4.62			13.85	6.15	63.08	36.92
	July	2.60	41.56	33.76	3.90	2.60	1.30	2.60	9.08	2.60	58.44	41.56
	$\overline{X}$ =	2.80	48.91	18.94	6.52	6.37	0.01	0.01	11.80	4.66	70.03	29.97
1975	May		52.71	30.23	3.10	0.78	0.78		5.43	6.97	62.02	37.98
	June	1.83	46.95	32.31	1.22	1.83	2.44		9.15	4.27	61.59	38.41
	July		43.85	33.33	0.88	0.88	0.88		14.16	7.02	58.77	41.23
	$\overline{X}$ =	0.20	52.21	30.43	2.84	0.88	0.88		5.89	6.67	62.02	37.98

Trends in the Relative Abundance of Different Age-Groups in Catches

The age composition of Ozernaya sockeye in ocean catches was analyzed separately for mature and for immature fish in two fishing areas: the convention fishing area north of 48°N (the "Northern Zone"), and the zone of fishing by medium tonnage drifters south of 48°N (the "Southern Zone").

Most fish caught in the Northern Zone were mature and 81% were either age 4_2+ or 5_2+ (Table 7). The frequency of other age-groups decreased progressively in the sequence 5_3+, 6_3+, 3_2+, 4_3+. The proportion of ages 4_2+ and 5_2+ varied, with each group predominating in different areas. The ratio of these age-groups in ocean catches has reflected a pattern that is typical for Ozernaya sockeye: age 5_2+ fish were predominant during times of high population abundance and age 4_2+ fish during low abundance (Selifonov 1975). Thus the age composition of mature sockeye caught at sea reflects quite adequately the general abundance of the population.

Until now, no efforts have been made to analyze the age composition of immature Ozernaya sockeye caught by the fishery. Most immature fish in ocean catches (66.66%) were in their 5th year (Table 8); immature fish in their 6th year (ages 5_2+ and 5_3+) were only half as numerous, but of these, age 5_3+ fish were most common. When the proportion of fish in their 5th year increased in catches, that of fish in their 6th year decreased; overall, the catch of older fish decreased when the total catch decreased.

The Japanese fleet began active fishing for sockeye in the Southern Zone in 1967. Many immature sockeye were caught in this area (Selifonov 1975). More than 71% of the commercial, mature stock in this region were fish in their 5th year and contributions by fish in their 6th year were low (Table 9). The proportion of age 4_2+ fish in catches of immatures has continued to increase (Table 10), while that of age 5_2+ was little more than 2%. Thus, it may be supposed that mainly the younger age groups migrate to the regtion south of 48°N; presumably, older sockeye migrate from their wintering areas to more northerly latitudes along the Kamchatka coast.

The mature stock of Ozernaya sockeye decreased most rapidly after 1961 (Fig. 8). Of course, the numbers of individuals within each age-group also decreased, but the decrease in numbers of age 5_2+ fish caught after 1961 was especially pronounced compared to that of fish caught in their 5th year. Birman (1951) showed that the growth rate of autumn Amur River chum salmon (*O. keta*) decreased and the number of older fish increased as abundance increased. A similar phenomenon was observed earlier among Ozernaya sockeye (Egorova at al. 1961). Recognizing that the ratio of older to younger

TABLE 7. Age composition of mature Ozernaya sockeye in ocean catches north of 48°N.

Year	Catch		Age													
	Total	Mature	3_2+	4_2+	5_2+	6_2+	4_3+	5_3+	6_3+	3_2+	4_2+	5_2+	6_2+	4_3+	5_3+	6_3+
	(× 10^3)		(× 10^3)							(%)						
1962	5041	4426		1276	2225	16		740	169		28.82	50.28	0.36		16.71	3.83
1963	4255	3529		960	1617	24		178	750		27.20	45.82	0.67		5.04	21.27
1964	1704	1370		633	506			174	57		46.22	36.92			12.72	4.14
1965	2530	2034		1026	552			315	141		50.44	27.16			15.46	6.94
1966	3417	2954		1079	1411			44	420		36.54	47.75			1.48	14.23
1967	4400	3217		1907	1027			283			59.28	31.93			8.97	
1968	3813	3000		941	1421	34		412	192		31.37	47.37	1.12		13.73	6.41
1969	2346	2188		223	1700	+	19	100	146		10.20	77.72	0.01	0.86	4.55	6.66
1970	2368	1370	5	864	138		2	313	48	0.34	63.08	10.08		0.14	22.85	3.51
1971	1552	1188	1	603	380			145	50	0.05	50.80	32.74			12.20	4.21
1972	1151	895	4	319	423		1	105	43	0.44	35.61	47.25		0.13	11.74	4.83
1973	1113	695	3	109	364	1	+	111	107	0.42	15.71	52.40	0.10	0.04	15.96	15.33
1974	661	578	8	76	426	2		25	41	1.47	13.69	73.62	0.40		4.30	7.02
1975	647	550	1	301	162	2	+	39	45	0.20	54.70	29.40	0.44	0.08	7.05	8.13
$\overline{X}$	2500	2000	2	736	883	6	2	213	158	0.10	36.80	44.15	0.30	0.10	10.65	7.90

NOTE: "+" indicates sample size less than a thousand.

TABLE 8. Age composition of immature Ozernaya sockeye in ocean catches north of 48°N.

Year	Catch		Age									
	Total (× 10^3)	Mature (× 10^3)	3_2+	4_2+	5_2+	4_3+	5_3+	3_2+	4_2+	5_2+	4_3+	5_3+
			(× 10^3)					(%)				
1962	5041	615		347	14		254		56.39	2.35		41.26
1963	4255	726		488	115		123		67.26	15.82		16.92
1964	1704	334		195	87		52		58.41	26.15		15.44
1965	2530	496		267	88		141		53.84	17.75		28.41
1966	3417	463		278	113		72		60.12	24.34		15.54
1967	4400	1186		853	186		147		71.92	15.65		12.43
1968	3813	813		563	53		197		69.31	6.42		24.27
1969	2346	158		61	86		11		38.50	54.80		6.70
1970	2368	998		744	29		225		74.52	2.89		22.59
1971	1552	364		257	36		71		70.72	9.73		19.55
1972	1157	256		183	6	4	63		71.50	2.45	1.71	24.34
1973	1113	418		306	18		94		73.29	4.30		22.41
1974	661	83	2	48	24		10	1.60	57.66	28.93		11.81
1975	647	97		80	7		10		82.09	7.51		10.40
$\overline{X}$	2500	501	+	334	62	+	105	+	66.66	12.38	+	20.96

NOTE: "+" indicates sample size less than a thousand or percentage less than 0.01%.

ages in spawning stocks of salmon may not always be a reliable index of the state of the stocks (Krykhtin and Smirnov 1962), and that both biotic and abiotic factors influence age composition, I concluded, nevertheless, that the decrease in mean age of Ozernaya sockeye was related to the considerable decrease in their abundance. One peculiarity of Ozernaya sockeye should be noted: the abundance of the mature stock was positively correlated with the abundance of age 5_2+ fish, which are part of this stock, but negatively correlated with the number of age 4_2+ fish, at least until 1962. Since 1963, the abundance of the mature stock has been positively correlated with the abundance of age 4_2+ fish.

Abundance in Ocean Catches

The number of Ozernaya sockeye caught (both mature and immature) has been estimated on the basis of scale pattern and biostatistical data from samples. Sampling data were available for about 50% of the total catch in the Northern Zone but the catch of Ozernaya sockeye was estimated using the weight of the entire catch (Table 11). It is clear that the catch of sockeye in this area has been decreasing at a higher rate for the mature stock than for the immature stock. However, the ratio of immature to mature stock in the total catch has varied only within a narrow range.

TABLE 9. Age composition of mature Ozernaya sockeye in ocean catches south of 48°N.

Year	Catch		Age													
	Total (× 10^3)	Mature (× 10^3)	3_2+	4_2+	5_2+	6_2+	4_3+	5_3+	6_3+	3_2+	4_2+	5_2+	6_2+	4_3+	5_3+	6_3+
			(× 10^3)							(%)						
1967	1273	849		660	117			64	8		77.74	13.80			7.49	0.97
1968	902	386		295	27			64			76.41	6.88			16.71	
1969	1020	624		232	338			35	19		37.13	54.24			5.66	2.97
1970	777	371		320	19			31	1		86.28	5.08			8.34	0.30
1971	669	284		196	22		46	19	1		68.92	7.75		16.29	6.56	0.48
1972	1512	456	3	376	21			56		0.76	82.49	4.46			12.29	
1973	2103	434	2	321	21			90		0.58	73.98	4.76			20.68	
1974	1172	309		189	28			92	+		61.21	8.90			29.87	0.02
1975	2051	1089		855	91			113	30		78.47	8.35			10.37	2.81
$\overline{X}$	1275	534	1	383	76		5	63	6	0.19	71.72	14.23		0.94	11.80	1.12

NOTE: "+" indicates sample size less than a thousand.

TABLE 10. Age composition of immature Ozernaya sockeye in ocean catches south of 48°N.

Year	Catch		Age									
	Total (× 10^3)	Immature (× 10^3)	3_2+	4_2+	5_2+	4_3+	5_3+	3_2+	4_2+	5_2+	4_3+	5_3+
			(× 10^3)					(%)				
1967	1273	424		330	12		82		77.80	2.79		19.41
1968	902	516		428	+		88		82.96	+		17.04
1969	1020	396		329	15		52		82.99	3.81		13.20
1970	777	406	3	354	3		46	0.83	87.08	0.83		11.26
1971	669	385	46	330	+		9	11.84	85.82	0.02		2.32
1972	1512	1056	2	763	12		279	0.14	72.29	1.14		26.43
1973	2103	1669	3	1189	10	3	464	0.15	71.25	0.62	0.16	27.82
1974	1172	863	27	655	62		119	3.18	75.87	7.15		13.80
1975	2051	962	14	760	35	23	130	1.44	79.00	3.62	2.42	13.52
$\overline{X}$	1275	742	11	571	16	3	141	1.48	76.96	2.16	0.40	19.00

NOTE: "+" indicates sample size less than a thousand or percentage less than 0.01%.

TABLE 11. Catch of sockeye north of 48°N.

Year	Total catch (× 10^3)	Mature			Immature			Ozernaya sockeye	
		Total (× 10^3)	Ozernaya sockeye		Total (× 10^3)	Ozernaya sockeye		Total (× 10^3)	As a % of total catch
			(× 10^3)	As a % of mature		(× 10^3)	As a % of immature		
1962	10500	9800	4426	45.16	1790	615	34.36	5041	47.60
1963	8902	6550	3529	53.88	2352	726	30.87	4255	47.79
1964	7097	4677	1370	29.29	2420	334	13.80	1704	24.01
1965	12038	10176	2034	19.99	1862	496	26.64	2530	21.02
1966	7254	5854	2954	50.46	1400	463	33.07	3417	47.10
1967	8087	6422	3217	50.09	1665	1186	71.23	4403	54.44
1968	6373	4942	3000	60.70	1431	813	56.82	3813	59.83
1969	5935	4208	2188	52.00	1727	158	9.15	2346	39.53
1970	6944	4958	1370	27.63	1986	998	50.25	2368	34.10
1971	3554	2144	1188	55.41	1410	364	25.82	1552	43.69
1972	3184	1796	895	49.83	1388	256	18.44	1151	36.15
1973	2613	1800	695	38.61	813	418	51.42	1113	42.60
1974	2282	1880	578	30.74	402	83	20.65	661	28.97
1975	2171	1357	550	40.53	814	97	11.09	647	29.80

TABLE 12. Catch of sockeye south of 48°N.

Year	Total catch (× 10³)	Mature			Immature			Ozernaya sockeye	
		Total (× 10³)	Ozernaya sockeye		Total (× 10³)	Ozernaya sockeye		Total (× 10³)	As a % of total catch
			(× 10³)	As a % of mature		(× 10³)	As a % of immature		
1967	2492	1322	849	64.22	1170	424	36.24	1273	51.08
1968	2788	809	386	47.71	1979	516	26.07	902	32.35
1969	2467	1265	624	49.33	1202	396	32.95	1020	41.34
1970	2929	1288	371	28.80	1641	406	24.74	777	26.53
1971	2996	1482	284	19.16	1514	385	25.43	669	22.33
1972	3711	955	456	47.75	2756	1056	38.32	1512	40.74
1973	3308	877	434	49.49	2431	1669	68.65	2103	63.57
1974	3155	1140	309	27.11	2015	863	42.83	1172	37.15
1975	2969	1251	1089	87.05	1718	962	56.00	2051	69.08

TABLE 13. Catch of sockeye north of 48°N.

Year	Total catch (× 10³)	Ozernaya sockeye									
		Mature				Immature					
		Catch in area north of 48°N (× 10³)	Catch in area south of 48°N (× 10³)	Total (× 10³)	As a % of total catch	Catch in area north of 48°N (× 10³)	Catch in area south of 48°N (× 10³)	Total (× 10³)	As a % of Ozernaya catch	As a % of total catch	% of total catch
1962	10590	4426		4426	41.79	615		615	12.20	5.81	47.60
1963	8902	3529		3529	39.64	726		726	17.06	8.15	47.79
1964	7097	1370		1370	19.31	334		334	19.60	4.70	24.01
1965	12038	2034		2034	16.90	496		496	19.60	4.12	21.02
1966	7254	2954		2954	40.72	463		463	13.55	6.38	47.10
1967	10579	3217	849	4066	38.43	1186	424	1610	28.36	15.22	53.65
1968	9161	3000	386	3386	36.96	813	516	1329	28.19	14.51	51.47
1969	8402	2188	624	2812	33.47	158	396	554	16.46	6.59	40.06
1970	9873	1370	371	1741	17.63	998	406	1404	44.64	14.22	31.85
1971	6550	1188	284	1472	22.47	364	385	749	33.72	11.44	33.91
1972	6895	895	456	1351	19.59	256	1056	1312	49.27	19.03	38.62
1973	5921	695	434	1129	19.07	418	1669	2087	64.89	35.25	54.32
1974	5437	578	309	887	16.31	83	863	946	51.61	17.40	33.71
1975	5140	550	1089	1639	31.89	97	962	1059	39.25	20.60	52.49
$\overline{X}$ (1962-66)	9176	2863		2863	31.20	527		527	15.55	5.74	36.94
$\overline{X}$ (1967-75)	7551	1520	534	2054	27.20	486	742	1228	37.42	16.26	26.57

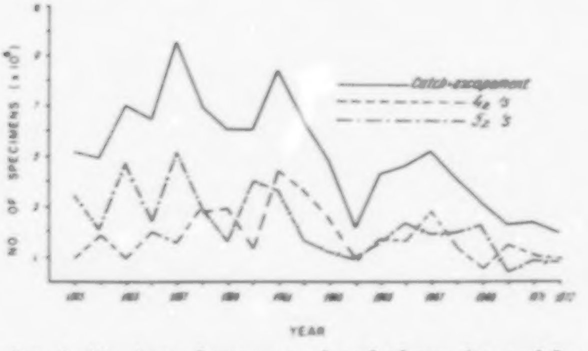

FIG. 8. Numbers of mature stock and of ages 4_2+ and 5_2+ in various years.

It has been more difficult to identify mature and immature sockeye from catches in the Southern Zone. Biostatistical data for May and June are more or less complete for only three quadrats (4460, 4465, and 4470). However, analysis of the data available revealed that all Ozernaya sockeye caught in the Southern Zone were taken within these quadrats. The ratio of mature to immature Ozernaya sockeye in the catch from this area was estimated by quadrats and by months using the few scale samples that were available (Table 12). The total catch of sockeye in the Southern Zone has gradually increased, and so has the proportion of Ozernaya sockeye in the total catch. This trend has resulted in increased catches of immature fish.

The contribution of Ozernaya sockeye to the total ocean catch of the species during 1962–75 varied from 21.02 to 54.32% (Table 13), and it decreased somewhat during 1967–75. The proportion of immature fish has increased significantly since 1967, especially between 1970 and 1975.

The fact that the proportion of Ozernaya sockeye in the total ocean catch has deviated only a little from its long-term average value does not imply that the abundance of this stock has remained constant. Since 1971 there has been a steadily decreasing trend in total sockeye catch as a consequence of severe fishing mortality on immature fish. There has also been a corresponding decrease in the abundance of Ozernaya sockeye.

References

BIRMAN, L. B. 1951. Qualitative indices of stocks and dynamics of abundance of the autumn chum in the Amur River. Izv. TINRO 35: 17–31. (In Russian)

1958. Features of distribution of the Pacific salmon species in the sea and the influence of the environmental factors on their abundance, p. 17–35. *In* Lososevye khozyaistvo Dal'nego Vostoka. Nauka, Moskva. (In Russian)

BIRMAN, L. B., AND S. M. KONOVALOV. 1968. Marine distribution and migrations of the local stock of sockeye, *Oncorhynchus nerka* (Walbaum) from Lake Kurilskoe. Vopr. Ikhtiol. 8(4): 728–736. (In Russian)

EGOROVA, T.V., F. V. KROGIUS, I. I. KURENKOV, AND R. S. SEMKO. 1961. Reasons for the abundance fluctuations of the sockeye in the Ozernaya River. Vopr. Ikhtiol. 1(3): 439–447. (In Russian)

EVLEVA, M. YA. 1964. Histological structure of the gonad of salmon during the period of their marine migration, p. 127–141. *In* Lososevye khozyaistvo Dal'nego Vostoka. Nauka, Moskva. (In Russian)

HANAMURA, N. 1966. Sockeye salmon in the Far East, p. 1–27. *In* Salmon of the North Pacific Ocean. Part III: A review of the life history of North Pacific salmon. Int. North Pac. Fish. Comm. Bull. 18.

IVANKOV, V. N. 1968. Impact of the marine driftnet fishery on the structure of the spawning populations of pink salmon. Izv. TINRO 65: 263–265. (In Russian)

KONOVALOV, S. M. 1971. Differentiation of local stocks of sockeye salmon. Izd. Nauka, Leningrad. 229 p. (In Russian)

KROGIUS, F. V. 1967. Methods of determining abundance of sockeye, p. 71–77. *In* T. F. Dement'eva and K. A. Zemskoi [ed.] Metodi Otsenki zapasov i prognozipovaniia ulovov ryb. Tr. VNIRO 62. (In Russian)

KRYKHTIN, M. L., AND A. I. SMIRNOV. 1962. On the interrelationship between abundance and qualitative indices of spawning stocks of salmon in the Amur River. Vopr. Ikhtiol. 2(1): 29–41. (In Russian)

SELIFONOV, M. M. 1975. Reproduction of, and fishery for, sockeye in the basin of the Ozernaya River. Avtor, diss., Vladivostok. 23 p. (In Russian)

The Role of Environmental Factors in Fluctuations of Stocks of Walleye Pollock *(Theragra chalcogramma)* in the Eastern Bering Sea

O. A. Bulatov

Pacific Research Institute of Fisheries and Oceanography (TINRO), Vladivostok, 690600, USSR

Abstract

BULATOV, O. A. 1989. The role of environmental factors in fluctuations of stocks of walleye pollock (*Theragra chalcogramma)*) in the eastern Bering Sea, p. 353-357. *In* R. J. Beamish and G. A. McFarlane [ed.] Effects of ocean variability on recruitment and an evaluation of parameters used in stock assessment models. Can. Spec. Publ. Fish. Aquat. Sci. 108.

Two periods of high abundance of walleye pollock have been observed between 1964–86: one in 1966–69, and another in 1983–85. Analysis of water temperature and solar activity patterns in the period after spawning indicated that the most abundant year-classes appeared during the first years of warm periods, at the start of the ascending limb of the solar activity pattern. There was no relation between recruitment and abundance of spawners. It is anticipated that unfavourable environmental factors will result in a continual decline in pollock abundance from 1990 onward. Abundant year-classes will likely not occur until 2005 at the earliest.

Résumé

BULATOV, O. A. 1989. The role of environmental factors in fluctuations of stocks of walleye pollock (*Theragra chalcogramma)*) in the eastern Bering Sea, p. 353-357. *In* R. J. Beamish and G. A. McFarlane [ed.] Effects of ocean variability on recruitment and an evaluation of parameters used in stock assessment models. Can. Spec. Publ. Fish. Aquat. Sci. 108.

Les stocks de morue du Pacifique occidental ont été abondants à deux reprises de 1964 à 1986 : entre 1966 et 1969, puis entre 1983 et 1985. L'analyse des profils de la température de l'eau et de l'activité solaire dans la période suivant la fraie a révélé que les classes d'âge les plus abondantes sont apparues durant les premières années des périodes chaudes, au commencement de la montée de l'activité solaire. Nous n'avons observé aucune relation entre le recrutement et l'abondance des géniteurs. Nous nous attendons à ce que des facteurs environnementaux défavorables entraînent une diminution continuelle de la population de morue à partir de 1990. L'apparition de classes d'âge abondantes ne devrait pas survenir avant l'an 2005 au plus tôt.

Introduction

The expansion of world fisheries has resulted in a predominance, in the catch of many different commercial fishes. In different years the most numerous commercial species, such as the Peruvian anchoveta, the sardine and the Chilean jack mackerel, the walleye pollock (*Theragra chalcogramma*) and the Atlantic cod (*Gadus morhua*) the Cape hake or stockfish, the capelin, and the west Pacific sardine, have made up half of the total catch of marine fish (Moiseyev 1985). However, the fluctuations in abundance of individual species have been catastrophic for the industries involved in these fisheries. For example, landings of west Pacific sardine in 1940–41 crashed to 5 000 t, only 1/600 of their peak, while Peruvian anchoveta fell from 14 million t in 1972 to 0.8 million t in 1980.

Recently, special attention has been given to studying the fluctuations in abundance of the walleye pollock. In recent years it has been an important species in the world fishery with catch exceeding 6 million t in 1984. Fishing for walleye pollock in the eastern Bering Sea began on a massive scale in the late 1960's and was at its peak in 1972–74, with average annual landings of 1.5 million t (Bakkala and Wespestad 1983). Since the introduction of the United States 200-mile economic zone, the catch of pollock has been strictly controlled and has not exceeded 1.0 million t. The history of the fishery and comparative analysis of the intensity of spawning (Bulatov 1987) show that the eastern Bering Sea contains one of the most abundant populations of pollock in the North Pacific.

A number of Soviet reports (Fadeyev 1980; Kachina and Sergeyeva 1981; Gavrilov and Bezlyudnyi 1983, 1986; Vasil'kov and Glebova 1984; Bulatov and Khen 1984; Sokolovskii and Glebova 1986) discuss the population dynamics of pollock in the northern part of the Pacific Ocean. These studies show that the appearance of strong year-classes of pollock is related to periods of positive anomalies of water temperature. However, all these studies use relative indices of abundance, expressed in arbitrary units, that makes it extremely difficult to assess the state of the stocks or to use the resulting data to forecast catches. In the present work, I have tried to use different methods to evaluate year-class strengths.

Materials and Methods

Materials were collected during Soviet research cruises in 1980–86. Standard bottom trawl surveys were carried out during this period using the grid of stations proposed by scientists of the United States Northwest Fishery Center in Seattle (Pereyra et al. 1976). Surveys were carried out during daylight hours at depths from 12 to 500 m. Altogether about 2 200 trawl hauls were made in 7 surveys.

Biomass of pollock was estimated using the technique of Aksyutina (1968):

$$P = \sum_{i=1}^{n} \left(\frac{Q_i \bullet X_i}{q \bullet k}\right)$$

where P is the biomass of a population, in metric tonnes;

Q_i is the area of the i^{th} catch, in square kilometres;

X_i is the mean actual catch in zone (i), in tonnes per hour;

q is the area harvested in 1 hour, in square kilometres;

k is the fishing efficiency index (arbitrarily chosen to be 1.0, for compatibility between United States and Soviet data); and

n is the number of zones.

The catches obtained were mapped and contours of equal catch were drawn. The following intervals were used (tonnes per hour): 0.001–0.005, 0.005–0.10, 0.10–1.00, 1.00–5.00, 5.00–10.00, and above 10.00.

United States scientists estimate stocks using mean weighted catches for each statistical area. We compared walleye pollock biomass estimates obtained both from equal catch contours and from mean weighted catches, for 1985. The former estimate was 6 375 000 t; the latter was 6 478 000 t (1.6% more). Thus, the estimation techniques used in USSR and USA tend to yield almost identical results.

Stocks of bottom fishes have been monitored by U.S. scientists since 1975, and Soviet scientists since 1980. The mean of the biomass estimates of both countries was used when both were available. The situation is more complicated for the period 1964–74, when an intensive fishery was in progress and no annual surveys were carried out.

Fisheries statistics obtained by various authors (Alton and Fredin 1974; Low and Ikeda 1980; Okada et al. 1982; Bakkala and Wespestad 1983) in 1964-82 have been used to reconstruct biomass values. For years when direct surveys were available the mean biomass values were indexed to the mean commercial catches to produce a transfer key. Using the transfer key calculated from the data for 1975-82, biomass values were reconstructed for 1964-74. Biomass was determined as a ratio of the commercial catch to research biomass estimates. In cases when 2 or 3 values were available, their arithmetic mean was used.

Because only short series of observations were at our disposal, I did not consider it possible to use cross-spectral analysis; therefore, the regression analysis methodology was used. The following analyses were carried out: linear regression, regression by stages, and multiple regression. The results of the latter two analyses were no better than the linear regression analysis, so only the former is reported here.

Age composition of pollock was obtained from data of Serobaba (1979) and Moiseyev (1983).

Discussion

It has been generally believed (Bulatov and Khen 1984; Sokolovskii and Glebova 1986) that water temperature is the most important factor among the complex of factors that determine year-class strength of the walleye pollock stock of the eastern Bering Sea. Warm years were observed to be more favourable for formation of abundant year-classes. However, indices of relative abundance based on age structure have commonly been used to analyze year-class abundance. This may provide misleading results because average-sized year-classes may wrongly be determined to be strong. Having obtained the mean body weight of 5-yr-olds (which predominate in the commercial stock) from biological data, and their representation in the population each year (Serobaba 1979; Moiseyev 1983), it is possible to estimate year-class abundance in absolute figures.

Oceanographic studies in the eastern Bering Sea were fragmentary until 1966; only since that period have reliable data become available concerning the temperature regime in the 0–100-m layer (data from TINRO scientist G. Khen). Therefore, data for 1966–84 were used in analyzing the impact of temperature conditions on the production of abundant year-classes. Analysis of year-to-year variability in solar activity, as one of the factors influencing temperature patterns in the Bering Sea, has shown that the highest values of positive water temperature anomalies, observed in 1978–82, corresponded to the maximum of the 21st cycle of solar activity. The 20th cycle was accompanied by a less significant increase in temperature. According to the relationship formulated by Soviet scientist A. I. Ohl (Kupetskii 1984), the odd and even 11-yr sun-spot cycles form a 22-yr physically-coupled cycle. From 1966 to 1981 strong year-classes appeared in the first years of the warming (Fig. 1); that is, on the ascending limb of the solar activity cycle. During the even-numbered solar cycle there appeared two strong year-classes (1966 and 1967), and during the odd cycle there were four (1977–80). Note that the strong pollock year-classes of 1977–80 appeared during a period when the spawning stock consisted of the weak year-classes spawned in 1972–75. Thus, the appearance of these strong pollock year-classes does not appear to be a result of an abundance of spawners.

During the period 1964 to 1986, two periods with high abundance of pollock were identified (Table 1). The first was in 1966 to 1969 when the estimated biomass was 6.3-7.2 million t. In this period intensive harvesting of pollock began with catches increasing from 262 000 to 863 000 t. Further increases in the catches were accompanied by decreasing catch per unit effort (Bakkala and Wespestad 1983). Thus, the greatest biomass was

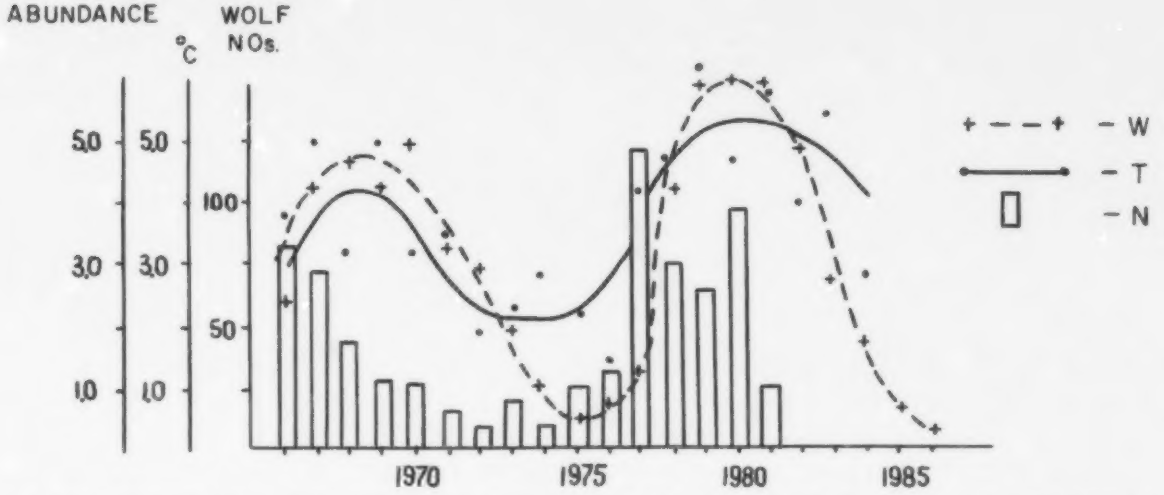

FIG. 1. Interannual variability of solar activity, water temperature and abundance of pollock year-classes: 1 — Wolf number (*W*); 2 — average July water temperature (°C) in a 0-100-m layer (*T*); 3 — abundance of year-classes, 10^9 individuals (*N*).

TABLE 1. Relative abundance indices and estimated biomass for walleye pollock in 1964-86.

Year	USA[a] (t/10^3hp)	Japan[b] (t/h)	INPFC[c] (% of 1975)	USA[d] Research vessels (kg/ha)	Estimated biomass USA[e] (10^6 t)	USSR (10^6 t)	Reconstructed (10^6 t)
1964	9.5						2.9
1965	18.3						5.7
1966	23.6						7.2
1967	21.3						6.5
1968	23.8		194				6.4
1969	31.5		154				6.9
1970	18.7		175				5.2
1971	14.2		172				4.5
1972	14.2		189				4.8
1973	8.6	13.7	166				3.6
1974	10.4	10.4	118				3.1
1975	9.3	9.8	100	66.0	2.426		2.6
1976	9.4	9.8	103				2.6
1977	8.6	9.2	98				2.6
1978	9.4	9.7	105				2.7
1979	9.4	9.8	110	63.5	3.552		3.0
1980	6.7	9.3	88	31.2	1.509	2.941	
						*	2.3
1981	8.4	9.6	88	57.6	2.544	7.400	
						*	2.6
1982		10.9	92	58.7	2.667	3.180	3.0
1983				133.0	6.051	5.270	
1984					4.585	4.883	
1985					4.517	6.478	
1986						4.426	

NOTE: * — survey carried out later than optimum period.

[a] Alton and Fredin (1974); [b] Okada et al. (1982); [c] International North Pacific Fisheries Commission; [d] Low and Ikeda (1980); [e] Anon. 1985. Northwest and Alaska Fisheries Center Quarterly Report, July-September 1985. U.S. Dep. Commerce, NOAA Tech. Rep. 50 p.

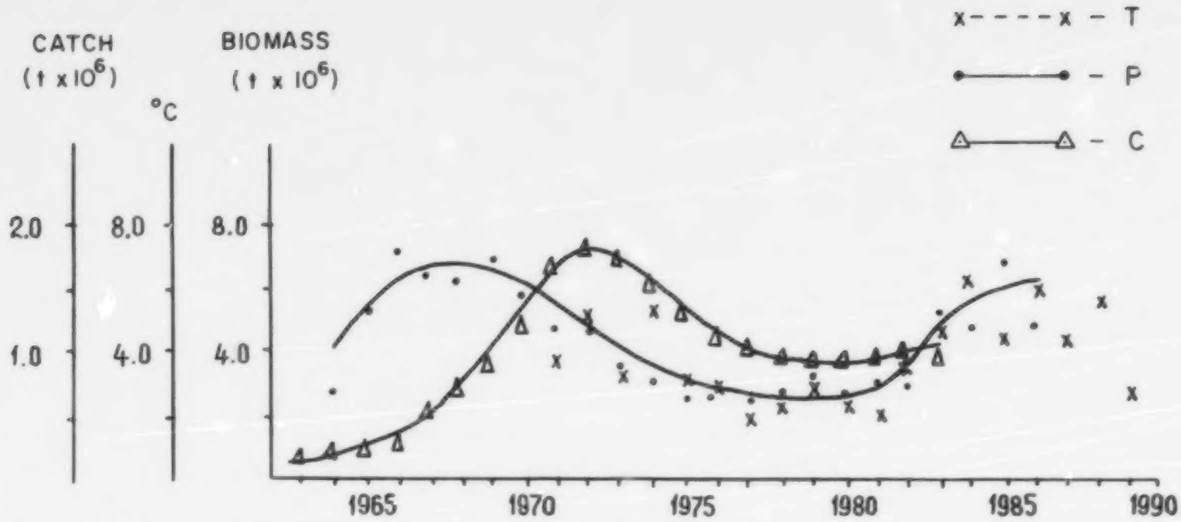

FIG. 2. Variation of pollock biomass by bottom trawl surveys, water temperature and volume of pollock catch: 1 — average July water temperature (°C) in 0–100-m layer (T) lagged by 5 yr; 2 — pollock biomass (P), t × 10^6; 3 — pollock catch (C), t × 10^6.

observed 4–5 years before the peak of the harvest (Fig. 2). The period of low abundance observed in 1974–82 was related to the recruitment into the fishery of the weak year-classes of 1971–76, that were hatched during the descending limb of the sun-spot cycle, when solar activity was at its lowest (Fig. 1).

The second upsurge in abundance began in 1983 (Fig. 2). According to Fig. 1, the increase in stock is related to the strong year-classes of the late 1970's.

The relationship of pollock year-class abundance to Wolf number and water temperature was analysed for 1966 through 1981 (Fig. 1). In the limits of the linear model

$$N_i = b_o + b_1 \bullet T_i + b_2 \bullet W_i \tag{1}$$

the following regression coefficients were determined:

$$b_o = 0.02, \quad b_1 = 0.81, \quad b_2 = -0.01.$$

As a whole, the equation was statistically significant ($P < 0.05$) as the variance ratio exceeded the critical level $F_{0.05\,(2,12)} = 3.89$ with a multiple correlation coefficient $R = 0.65$. But this equation cannot be used for forecasting, because it has a statistical error:

$$\frac{S_o}{\overline{N}} \bullet 100\% = \frac{1.049}{2.033} \bullet 100\% = 51.6\%$$

where S_o is the estimated statistical error and $\overline{N}$ [illegible] e average pollock abundance of 1966–81 year-cl [illegible]

The relation of the 1971–86 pollock biomass (p) to water temperature (T) in the post-spawning period (1966–81) was checked using similar calculations. The two series are offset by 5 yr, because the main population biomass usually consists of 5-yr-old pollock. The linear model is as follows:

$$p_i = 1.36 + 0\,63T_{i\text{-}5} \tag{2}$$

This equation is statistically significant at $P < 0.05$, as the variance ratio exceeds the critical level ($15.5 > 4.5$). The mean statistical error and relatively high correlation coefficient ($r = 0.71$) make it possible to use equation (2) in forecasting. But in some years (1969, 1979) this relation has had a much weaker expression.

The comparison of variations in observed biomass of pollock with the temperature conditions 5 years earlier indicated that they are related. This relationship is particularly evident during periods of low abundance, while during periods of high abundance (1983–85) the relationship was not as strong.

The coincidence of the trends in pollock biomass and of temperature conditions during the post-spawning period suggests that there will be a marked decrease in stock starting in 1990. The period of the "quiet sun" (Kupetskii 1984) is expected to end in 1988–89; however, a significant increase of pollock stocks is not expected in 1994–95, because the next solar cycle (No. 22) should have a lower peak than the previous even-numbered (20th) cycle. Therefore, restoration of the pollock stock in the eastern Bering Sea to the level of the 1980's is not to be expected earlier than the year 2005.

Acknowledgements

The author wishes to acknowledge the contribution made by TINRO applied mathematics laboratory scientists O. Frolov and S. Pak in the statistical processing and data interpretation.

References

AKSYUTINA, Z. M. 1968. The elements of mathematical assessment of the results of observations in biological and fisheries investigations. Pischevaya promyshlennost, Moskva. 288 p. (In Russian)

ALTON, M. S., AND R. A. FREDIN. 1974. Status of Alaska pollock in the eastern Bering Sea. Document submitted to the annual meeting of the Int. N. Pac. Fish. Comm., Oct. 1974. Northwest and Alaska Fish. Cent., Natl. Mar. Fish. Serv., NOAA, Seattle, WA 98112. 10 p.

Bakkala, R. G., and V. G. Wespestad. 1983. Walleye pollock, p. 1-28. *In* R. G. Bakkala amd L. L. Low [ed.] Condition of groundfish resources of the eastern Bering Sea and Aleutian Islands region in 1982. NOAA Tech. Memo. NMFS F/NWC-42.

Bulatov, O. A. 1987. Distribution of eggs and larvae of Alaska pollock in the eastern Bering Sea, p. 100–114. *In* N. S. Fadeyev [ed.] Populatsionnaya structura, dinamika chislennosti, ekologiya mintaya. TINRO, Vladivostok. (In Russian)

Bulatov, O. A., and G. V. Khen. 1984. Factors determining year-class strength of the walleye pollock and yellowfin sole in the eastern Bering Sea, p. 68–69. *In* O. A. Skarlato [ed.] Prirodnaya sreda i biologicheskiye resursy morei i okeanov. Nauka, Leningrad. (In Russian)

Fadeyev, N. S. 1980. Was there a "flash" of the pollock in the North Pacific? Biologiya morya 1980(5): 66–71. (In Russian)

Gavrilov, G. M., and A. M. Bezlyudnyi. 1983. Dynamics of catches of walleye pollock in the southwestern Sea of Japan. Rybn. Khoz. 1983(7): 38. (In Russian)

1986. Dynamics of abundance of pollock in the southwestern Sea of Japan, p. 5–38. *In* N. S. Fadeyev [ed.] Treskovye dal'nevostochnykh morei. TINRO, Vladivostok. (In Russian)

Kachina, T. F., and N. P. Sergeyeva. 1981. Dynamics of abundance of the eastern Okhotsk walleye pollock, p. 19–27. *In* N. S. Fadeyev [ed.] Ecologiya, zapasy i promysel mintaya. Vladivostok. (In Russian)

Kupetskii, V. N. 1984. Forecasting and sunspot activity, p. 139-140. Chelovek I Stikhiya. Gidrometeoizdat, Leningrad. (In Russian)

Low, L. L., and L. Ikeda. 1980. Average density index for walleye pollock (*Theragra chalcogramma*) in the Bering Sea. NOAA Tech. Rep. NMFS SSRF-734, 11 p.

Moiseyev, E. I. 1983. Age composition and growth rate of the eastern Bering Sea walleye pollock (*Theragra chalcogramma* Pallas). Izv. TINRO 107: 94–101. (In Russian)

Moiseyev, P. A. 1985. The high abundance species of fishes of the world fisheries, p. 175–181. *In* L. S. Berdichevskii, T. F. Dement'eva, D.S. Pavlov and M. I. Shatunovskii [ed.] Teoriya formirovaniya chislennosti i ratsionalnogo ispolzovaniya stad promyslovykh ryb. Nauka, Moskva. (In Russian)

Okada, K., H. Yamaguchi, T. Sasaki, and K. Wakabayashi. 1982. Trends of groundfish stocks in the Bering Sea and the Northeastern Pacific based on additional preliminary statistical data in 1981. Unpubl. manuscr., Jpn. Fish. Agency, Far Seas Fish. Lab., 1000 Orido, Shimizu, 424, Japan, 80 p.

Pereyra, W. T., J. E. Reeves, and R. Q. Bakkala. 1976. Demersal fish and shellfish resources of the eastern Bering Sea in the baseline year 1975. Processed Rep., Northwest and Alaska Fish. Cent., Natl. Mar. Fish. Serv., NOAA, Seattle, WA. 619 p.

Serobaba, I. I. 1979. The reproductive capability of the walleye pollock *Theragra chalcogramma* (Pallas) from the eastern part of the Bering Sea in relation its abundance. Biologiya morya 1979(3): 74–77. (In Russian)

Sokolovskii, A. S., and S. E. Glebova. 1986. Long-term fluctuations of walleye pollock abundance in the Bering Sea. Izv. TINRO 110: 38–42. (In Russian)

Vasil'kov, V. V., and L. Yu. Glebova. 1984. Factors determining year-class strength of the walleye pollock, *Theragra chalcogramma* (Gadidae), of western Kamchatka. Vopr. Ikhtiol. 24(4): 561–570. (In Russian)

Fisheries Production Domains in the Northeast Pacific Ocean

D. M. Ware and G. A. McFarlane

Department of Fisheries and Oceans, Biological Sciences Branch,
Pacific Biological Station, Nanaimo, B.C. V9R 5K6

Abstract

Ware, D. M., and G. A. McFarlane. 1989. Fisheries production domains in the Northeast Pacific Ocean, p. 359–379. *In* R. J. Beamish and G. A. McFarlane [ed.] Effects of ocean variability on recruitment and an evaluation of parameters used in stock assessment models. Can. Spec. Publ. Fish. Aquat. Sci. 108.

Examination of the large-scale circulation features and distribution of commercial quantities of marine fishes indicates that there are three major production domains in the northeast Pacific Ocean: the Central Subarctic Domain, the Coastal Upwelling Domain, and the Coastal Downwelling Domain. The Subarctic Current and Alaska Gyre are the prominent physical features in the Central Subarctic Domain, which is dominated by sockeye, chum and pink salmon. We estimate there are 482 thousand tonnes(t) of salmon in this domain, which produce an average annual fisheries catch of 159 thousand t. This represents a yield of 0.05 t•km^{-2}•yr^{-1}, and an average catch/biomass (C/B) ratio of 0.33. The Coastal Upwelling Domain extends from Baja California (25°N) to the northern tip of Vancouver Island (50.5°N). The prominent circulation features in this domain are the equatorward flowing shelf-break current, generated by longshore winds, and the equatorward flowing branch of the Subarctic current, called the California Current. The average yield of the dominant pelagic fish in the Coastal Upwelling Domain (Pacific hake, Pacific sardine, northern anchovy and Pacific mackerel) is 2.7 t•km^{-2}•yr^{-1} which represents an average C/B ratio of 0.24. The Coastal Downwelling Domain extends from Queen Charlotte Sound to the Aleutian Islands (170°W); the prominent circulation features in this region are the poleward flowing Alaska Current, and Alaska Coastal Current. The dominant species in this domain (walleye pollock, Pacific cod, Pacific halibut, sablefish and Pacific herring) seem to be influenced by events that affect production in the Central Subarctic domain, and along the western boundary of the Gulf of Alaska. Thus the Coastal Downwelling Domain may be linked to the Central Subarctic Domain, by the Alaska current, in much the same way as the Coastal Upwelling Domain is linked to the Central Subarctic by the California current. The average yield of commercial fish in the Coastal Downwelling Domain is 1.4 t•km^{-2}•yr^{-1}, which represents a C/B ratio of 0.13. Possible reasons for the difference in C/B ratios, and recruitment variability in the dominant species in each domain, are discussed.

Résumé

Ware, D. M., and G. A. McFarlane. 1989. Fisheries production domains in the Northeast Pacific Ocean, p. 359–379. *In* R. J. Beamish and G. A. McFarlane [ed.] Effects of ocean variability on recruitment and an evaluation of parameters used in stock assessment models. Can. Spec. Publ. Fish. Aquat. Sci. 108.

L'examen des caractéristiques de la circulation à grande échelle des eaux et de la répartition des stocks de poissons marins montre qu'il existe trois domaines principaux de production dans le nord-est de l'océan Pacifique : le domaine central subarctique, le domaine côtier de la remontée, et le domaine côtier de la plongée des eaux. Le courant subarctique et le courant gyratoire d'Alaska sont les caractéristiques physiques dominantes dans le domaine central subarctique, lequel renferme surtout du saumon rouge, kéta et rose. D'après nos estimations, ce domaine, dont les captures annuelles moyennes totalisent 159 000 tonnes, renferme 482 000 t de saumons. Cela représente un rendement de 0.05 t•km^{-2}•année^{-1}, et un rapport moyen capture/biomasse (C/B) de 0.33. Le domaine côtier de la remontée s'étend de la Basse Californie (25°N) à l'extrémité nord de l'île Vancouver (50.5°N). Les caractéristiques dominantes de la circulation dans ce domaine sont le courant de la bordure de la plate-forme généré par les vents côtiers et circulant vers l'équateur de même que la portion du courant subarctique qui circule vers l'équateur, baptisée courant de Californie. Le rendement moyen des poissons pélagiques dominants dans le domaine côtier de la remontée (merlu du Pacifique, sardine du Pacifique et maquereau blanc) est de 2.7 t•km^{-2}•année^{-1}, ce qui représente un rapport moyen C/B de 0.24. Le domaine côtier de la plongée des eaux s'étend du détroit de la Reine-Charlotte aux îles Aléoutiennes (170°W); les caractéristiques dominantes de la circulation dans cette région sont le courant d'Alaska circulant vers le pôle, et le courant côtier d'Alaska. Les espèces dominantes dans ce domaine (c'est-à-dire la morue du Pacifique occidental, la morue du Pacifique, le flétan du Pacifique, la morue charbonnière et le hareng du Pacifique) semblent subir les effets de phénomènes qui ont un effet sur la production dans le domaine central subarctique, et le long de la limite ouest du golfe d'Alaska. Ainsi, le domaine côtier de la plongée peut être relié au domaine central subarctique par le courant d'Alaska d'une manière assez analogue au cas du domaine côtier de la remontée qui est relié au domaine central subarctique par le courant de Californie. Le rendement moyen des captures dans le domaine côtier de la plongée est de 1.4 t•km^{-2}•année^{-1}, ce qui représente un rapport C/B de 0.13. Les raisons permettant d'expliquer la différence entre les rapports C/B, et la variabilité du recrutement chez les espèces dominantes dans chaque domaine sont examinées.

Introduction

Physical oceanographers have identified specific domains in the upper zone of the northeast Pacific Ocean where the water properties are influenced predominantly by seasonal heating and cooling, precipitation, evaporation and wind mixing. Dodimead et al. (1963) described four principal domains: (1) the Central Subarctic Domain which is dominated by the Alaskan gyre, (2) the Transitional Domain which is a zonal (east–west) Region, just north of the Subarctic Boundary with currents that bifurcate into northward and southward flowing branches near the North American coast, (3) the Coastal Domain, which encompasses the waters near the coast and which differs markedly from one area to another due to local variations in runoff, winds, heating and cooling, tides and currents, and (4) the Alaskan Stream Domain which is associated with the relatively dilute, warm water flowing out of the Gulf of Alaska, along the south side of the Aleutian Islands east of Kodiak island where the flow narrows and accelerates. Thomson (1981) and other workers modified this scheme and recognized: (1) the Coastal Upwelling Domain, which lies adjacent to the coast from Baja California to southern British Columbia, (2) the Dilute Domain, (3) the Transitional Domain, and (4) the Ridge Domain. The last three domains correspond roughly to the Coastal, Transitional and Central Subarctic Domains in the scheme suggested by Dodimead et al. (1963).

The question we posed was: do these physical domains also define discrete fisheries production zones in the northeast Pacific Ocean? The coastal upwelling system off California and Oregon has long been recognized as a productive region which is dominated by a unique assemblage of pelagic species. The Central Subarctic region also contains a distinct array of fish species, namely Pacific Salmon, which have evolved some unique life history traits that enable them to sustain high growth rates in a region characterized by low primary and secondary production. Although there has been no formal distinction made between the fish production assemblages on the Continental Shelf seas from Washington State to Alaska to date, there is an acknowledged region of high productivity in Alaska along the continental shelf west of Kodiak Island which supports a significant walleye pollock fishery.

After reviewing some of the key physical oceanographic, biological, and fisheries data we conclude that there are three fish production domains in the northeast Pacific Ocean, and we define their approximate boundaries. Information on the biomass and historical yields of the dominant species in each domain is presented; we also compare their catch/biomass ratios, and respective recruitment variability. In what follows, we have taken an overview to reduce the complexity of how to deal with the dominant physical and biological features of a region as vast as the northeast Pacific Ocean. We acknowledge that we can not capture the details of each region but, instead, attempt to use the details to uncover the boundaries and key production characteristics of each domain.

Physical Oceanography

Although it is recognized that there are distinct oceanographic domains in the Subarctic Pacific region, there is no agreement on a conventional set of names. We therefore decided to modify the list suggested by Dodimead et al. (1963) and Thomson (1981) so the names describe where the domains are located and relate something about their prominent features. Hence we suggest that the northeast Pacific Ocean contains three principal oceanographic regions: (1) the Coastal Upwelling Domain, (2) the Coastal Downwelling Domain, and (3) the Central Subarctic Domain (Fig. 1). The Transitional Domain is

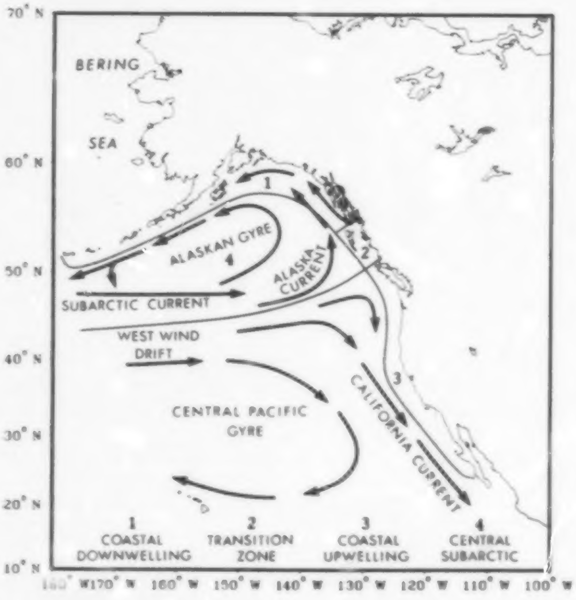

FIG. 1. Approximate areas of oceanic domains and prevailing current directions in the Northeast Pacific Ocean (modified after Favorite et al. 1976, and Thomson 1981).

the fourth region but is not dealt with here because it occurs to the south, and seaward, of the area of interest. Similarly, the Bering Sea is another domain which is beyond the scope of this study.

Coastal Upwelling Domain

The Coastal Upwelling domain lies adjacent to the coast from Baja California to the south coast of British Columbia. As its name implies this domain is defined physically by the normal summer pattern of wind stress curl and Ekman divergence, or upwelling (Parrish et al. 1981). Upwelling is driven predominantly from May to Sept. by northwest winds which cause intermediate depth, cold water to rise onto the continental margin. The large scale circulation off California is dominated by an offshore, equatorward flow called the California Current, and a nearshore, poleward subsurface flow called the California undercurrent. The California Current originates near the coast of North America where a divergence in the prevailing wind pattern causes the Subarctic current to divide into two branches: a northern branch, or Alaska Current, which curves to the northeast and a southern branch which turns to the southeast as the California Current. The formation of these branches is not abrupt, but occurs in a rather confused manner between 45 and 50°N and 130–150°W (Thomson 1981). Drift bottle studies by Thompson and van Cleve (1936) suggested that the division occurs near 50°N in August and somewhat further south in winter. The nearshore undercurrent flows poleward from Baja California to Vancouver Island throughout the year. In winter (Nov.–Feb.) the undercurrent is particularly strong off Pt. Conception (about 35°N) where it reaches the surface, and is called the Davidson Current (McLain and Thomas 1983). Southerly winds dominate the Coastal Upwelling Domain during winter causing onshore transport combined with downwelling and poleward transport of surface waters (Dewees and Strange 1984). During summer, persistent winds from the northwest occur along the entire west coast of North America from Vancouver Island to California and blow the surface water equatorward, over the undercurrent which continues to flow poleward at depths of 200–500 m (McLain and Thomas 1983).

The annual transition between the predominantly downwelling and upwelling seasons occurs in the spring (Mar.–Apr.) and in the fall (Sept.–Oct.), with the seasonal reversal in the prevailing alongshore winds and currents (Thomson et al. 1988). In contrast, upwelling favourable winds occur year round off Baja California where maximum upwelling takes place from March to June (Bakun and Nelson 1977). Interannually, warming in the upper layer occurs along the California coast when the cool California Current weakens, when upwelling weakens, or when the poleward flowing alongshore currents intensify (McLain and Thomas 1983). All of these processes may force significant interannual changes in production in the southern part of the Coastal Upwelling Domain.

Coastal Downwelling Domain

The Coastal Downwelling Domain extends from Queen Charlotte Sound in British Columbia, northward along the coast of southeast Alaska to Prince William Sound, and then westward along the Aleutian Islands. The dominant feature, the Alaska Current, flows adjacent to the coast of North America and sweeps poleward, seaward of the continental margin, at a speed of roughly 25 cm/s in summer, and 35 cm/s in winter. This current is forced primarily by a wind stress curl, augmented by freshwater addition and an alongshore wind-induced sea level gradient. Along most of the Gulf of Alaska these mechanisms are additive, yielding a counterclockwise flow (Schumacher and Reed 1983). Freshwater runoff in northern B.C. and southeast Alaska causes a poleward driven coastal current which extends out some 40 km from the coast and flows at an average speed of about 20 km/d. This prominent coastal current originates in northern B.C. and flows around the eastern Gulf of Alaska as far as Unimak Pass on the Alaskan peninsula. There is a weak spring transition in the prevailing coastal winds; however, due to the general behaviour of the cyclonic meteorological systems in the region, the wind stress tends to augment the baroclinic component of the coastal circulation by confining it to the shore. For this reason, downwelling generally persists in the Alaska Coastal Current regime from Cape St. James to Kodiak Island except for a few months in the summer. Somewhere near Kodiak Island a transition occurs and the wind stress tends to favour weak upwelling between April and December (Schumacher and Reed 1983).

In the fall, the Aleutian Low begins to intensify and increases the circulation around the Alaska Gyre. This, combined with a coastward shift of the axis of the Alaska Current leads to stronger nearshore currents in winter than in summer (Thomson 1981). Once they attain the northernmost reaches of the Gulf of Alaska both the Alaska Current and the Alaska Coastal Current are constrained to turn southwestward along the coast of the Alaskan Peninsula and Aleutian Islands where they form a strong boundary current known as the Alaskan Stream. This current flows at a mean speed in excess of 100 cm/s (Thomson 1981).

For simplicity, we include the continental shelf and coastal waters bounded by the Alaska Current in this domain because the coastal area is affected by changes in the continuity and stability of this flow, as well as by the nearshore Alaska Coastal Current. The southern boundary of this domain is not sharply defined from a strictly oceanographic standpoint.

Central Subarctic Domain

The Central Subarctic Domain is bounded by the Subarctic Current to the south, the Alaska Current to the east, and the Alaska Stream to the north. The dominant feature within this zone is the Alaska Gyre. It is linked to the positive wind stress curl which causes it to rotate in a counterclockwise, or cyclonic, direction (Fig. 1).

Upwelling occurs in the core of the gyre because the wind stress curl causes the upper oceanic layer to diverge, and hence the density to dome upward (Thomson 1981). The climatological winter pattern in atmospheric pressure is dominated by the Aleutian Low which stretches from Kamchatka to the Alaskan Peninsula. The prevailing geostrophic surface winds are directed northeastward from the subtropical Pacific Ocean into the Gulf of Alaska (Emery and Hamilton 1985). During the period of peak barotropic flow (December–March) deeper water may be drawn up across the shelf (Schumacher and Reed 1983). In spring, the Aleutian Low begins to weaken and is shifted to the northwest by the subtropital anti-cyclone (North Pacific High) to the south, which has strengthened and expanded westward. In summer, the North Pacific High builds northward, pushing the Aleutian Low into the Arctic.

Namias (1985) found a relationship between El Niño-Southern Oscillation (ENSO) episodes off Peru and atmospheric circulation in the North Pacific. During ENSO episodes both the Aleutian Low and the westerlies at mid-latitudes are stronger, particularly around 50°N. This appears to lead to a stronger than normal poleward advection of warm water along the west coast of North America. Emery and Hamilton (1985) confirmed that almost all warm equatorial winters coincided with an anomalously strong Aleutian Low, while cold years generally coincided with a weak Aleutian Low. They also present evidence showing that winter and spring temperatures along the B.C. coast are highly correlated (positively) with the winter mean North Pacific atmospheric pressure index, suggesting that seasonal sea surface temperature anomalies are maintained largely by anomalous wind-driven advection in the surface layer of the ocean.

Primary and Secondary Production

These physical oceanographic domains correspond broadly to one of the three generic biological production systems: oceanic (Central Subarctic Domain), continental shelf (Coastal Downwelling Domain) and upwelling (Coastal Upwelling Domain). The major distinction between these systems is the general level of productivity and the size of the dominant phytoplankton species (Parsons et al. 1984). Oceanic systems tend to have the lowest levels of primary production, typically around 50–100 g $C{\bullet}m^{-2}{\bullet}yr^{-1}$, and are dominated by small phytoplankton species, called nannoplankton. Continental shelf systems are more productive, averaging 100–300 g $C{\bullet}m^{-2}yr^{-1}$, and are dominated by large diatoms and dinoflagellates that typically fit into the microphytoplankton size range. Finally, upwelling food chains are characterized by high levels of primary production, about 300 g $C{\bullet}m^{-2}{\bullet}yr^{-1}$, and tend to be dominated by macrophytoplankton (large diatoms and dinoflagellates, including chain forming species). These three production systems differ significantly in the number of trophic steps involved in transferring energy from phytoplankton to commercially sized fish species. Ryther (1969) suggested that oceanic systems have 5 trophic levels, continental shelf systems 3 levels and upwelling systems roughly 1.5 levels. More recent information however, indicates that there are roughly 4 trophic steps between phytoplankton, and salmon and pomfret (the dominant fish species in the Central Subarctic Domain) which means that the food-chain in this oceanic production system is about 1 step longer than a typical continental shelf system (W. G. Pearcy, Oregon State Univ., pers. comm.).

Coastal Upwelling Domain

The marine climate off California consists of three fairly well defined seasons, which are modulated by shifts in the prevailing winds. During the upwelling season (Feb.–Sept.) surface water is driven south and offshore, by the prevailing northwesterly wind, and is replaced by intermediate depth, nutrient rich, water. Upwelling is strongest south of 30°N from March to June. Inshore, the net plankton, largely colonial diatoms, develop above a shallow pynocline and are abundant throughout the upwelling season, while the smaller nannoplankton stocks decline (Garrison 1976). Further offshore, diatoms only dominate the phytoplankton community during periods of strong upwelling. The oceanic season (Sept.–Oct.) is preceded by a decline in wind stress, and is strictly a coastal phenomenon since it prevails in a relatively narrow band where upwelling occurred in summer. When upwelling ceases during the oceanic period, the cold coastal water sinks and a thin layer of warm surface water flows in from the north to take its place (Bolin and Abbott 1963). The net plankton remain associated with the sinking pynocline and, although they do not encounter limiting nutrient concentrations, light levels are potentially limiting a short distance below the surface. This decreases the primary production rate and causes the netplankton:nannoplankton ratio to fall. The oceanic period is followed by the Davidson Current period (Nov.–Feb.) which is characterized by a shift to southerly winds and a strong inflow of oceanic water into the coastal region from the south (Bolin and Abbott 1963). A similar seasonal shift in the prevailing wind field also occurs in the northern part of the Coastal Upwelling Domain. Between 33°N to 49°N latitude the fall transition from predominantly northwest to southeast winds occurs in October, while the spring transition from predominately southeast to northwest winds, which characterize the upwelling season, occurs in March–April (Strub et al. 1987).

Data collected by Garrison (1976) indicate that the annual primary production rate near the coast of California is about 195 g $C{\bullet}m^{-2}{\bullet}yr^{-1}$, (range 142-248 g $C{\bullet}m^{-2}{\bullet}yr^{-1}$), making it comparable to the estimate of 152 g $C{\bullet}m^{-2}{\bullet}yr^{-1}$ obtained by Anderson (1964) for the upwelling zone off the Washington and Oregon coasts. *Chaetocerous deblis* tends to be the most abundant diatom during the upwelling season, whereas *Rizosolenia* spp. tend to be the dominant diatom during the downwelling, or Davidson Current period. Dinoflagellates tend to be much rarer than diatoms in coastal waters, but are more predominant in warm years.

Zooplankton in upwelling regions are characterized by a low species diversity, a high abundance of herbivorous copepods and euphausiids, and a high biomass per unit volume. Longhurst (1967) concluded that the diversity of zooplankton in the upwelling region off Baja California (25°N) resembles that of higher latitudes in its low diversity, dominance by a few species of filter feeding herbivores and a small number of carnivorous species. The biomass of zooplankton in the southern part of the Coastal Upwelling Domain averages between 200–500 mg/m^3 during spring and summer (Bernal and McGowan 1981). In the early 1960's, Reid (1962) recognized that a significant part of the high zooplankton standing stock in the northern part of California was transported there from the Central Subarctic Domain by the California Current. Zooplankton volumes tend to decline rapidly with distance south of Pt. Conception (35°N) and there is a striking transition from more northerly species to more southerly forms near the southern tip of Baja California. Wickett's (1967) analysis supported Reid's suggestion that significant quantities of zooplankton are transported southward out of the Central Subarctic Domain by Ekman transport and appear off California roughly 1 year later, and 2224 km downstream from their point of origin.

Recently a more detailed analysis of a much longer-time series corroborates that the production system off the Californias responds to both large-scale wind driven advection from the north, and to local upwelling. After analyzing the 30-yr CalCOFI time series, Chelton et al. (1982) concluded that zooplankton abundance off California is primarily influenced by large-scale variations in the flow of the California Current. Increased zooplankton biomass is associated with a decrease in water temperature and increased equatorward flow, while decreased zooplankton abundance is associated with an increase in water temperature and weak equatorward flow. Local coastal upwelling, driven by the alongshore component of the wind stress, is uncorrelated with the observed variations in water flow and zooplankton biomass. Chelton et al. (1982) speculated that these variations in secondary production may reflect increased primary productivity in response to nutrients either advected downstream from high latitudes or brought to the surface by the vertical advection associated with geostrophic tilting of isopycnals due to variations in the flow. The causes of these large-scale interannual variations have not been fully resolved. They appear to be strongly related to ENSO episodes, but the relationship sometimes breaks down.

As a rule zooplankton biomass is highest in cool years off California presumably when there is a greater influx of subarctic water. Reid (1962) observed that in cool years high concentrations of zooplankton extend far to the south (25°N) and retreat far to the north (37°N) during ENSO episodes, such as 1957/58. Fulton and LeBrasseur (1985) found some indication that the subarctic boundary may also advance and retreat along its climatological mean north–south axis in response to fluctuations in the southerly transport of subarctic water in the California Current.

Coastal Downwelling Domain

Primary production estimates for the oceanic and continental shelf regions of the Coastal Downwelling Domain are spotty and there are no rigorous estimates of secondary production. What little information there is suggests that production in the oceanic regions is about 72–100 g $C \cdot m^{-2} \cdot yr^{-1}$ (Sambrotto and Lorenzen 1987). Comparable estimates for shelf waters in this domain range between 185–330 g $C \cdot m^{-2} \cdot yr^{-1}$. Zooplankton production rates are suspected to be in the order of 10-30g $C \cdot m^{-2} \cdot yr^{-1}$ in the oceanic region and 30-50 g $C \cdot m^{-2} \cdot yr^{-1}$ on the shelf and protected inside waters (Cooney 1986).

A mixed assemblage of oceanic and neritic zooplankton species inhabit the shelf and coastal zone regions of this domain. Seasonally the community shifts from oceanic species domination in late winter to early spring, to domination by neritic species in summer and fall (Cooney 1986). Two oceanic *Neocalanus* species are the dominant forms which are advected onto the continental shelf and inshore waters by the seasonally persistent onshore Ekman transport which lasts for roughly 8 months (Sept.–April). During the summer when this onshore transport weakens the zooplankton assemblage is dominated by small neritic copepods such as: *Pseudocalanus* spp., *Centropages acartia*, and *Centropages* spp. These organisms increase in abundance after the spring plankton bloom. *Calanus marshallae* is a medium sized copepod which is abundant in summer. Cooney (1984) observed that since the oceanic *Neocalanus* copepods are seasonally dominant members of the shelf plankton community, the Central Subarctic Domain is probably an important source of organic matter for the Coastal Downwelling Domain. He estimated that as much as 5 times the annual secondary production along the shelf and coastal regions of this domain may be advected shoreward from the Central Subarctic region and eventually flows around the eastern margin of the Gulf of Alaska. Therefore it is not surprising that the assemblage of zooplankton in the northern and western portions of the gulf are similar to the zooplankton community at Ocean Station P. As a result of this advective flow, coupled with cross-shelf mixing processes, there is also an oceanic influence on the composition of the community in coastal waters.

Plankton concentrations vary seasonally and spatially between the continental shelf region and protected inside waters. In the vicinity of Kodiak Island zooplankton concentrations are highest in summer, averaging about 31 g/m^2 compared to 6 g/m^2 in winter, and are also higher on the continental shelf than they are nearshore. In inside waters, such as Prince William Sound, zooplankton concentrations can be high, averaging between 320–770 g/m^2 in the fall–early winter. Most of this biomass, however, consists of large herbivorous copepods which overwinter at depths below 300–400 m, and therefore are not available to planktivorous fish species during this period. According to Reid (1962) and Parsons et al. (1966) some of the highest surface concentrations of copepods in the northeast Pacific Ocean can be found within the Subarctic and Coastal Downwelling systems.

Central Subarctic Domain

The standidng stock of phytoplankton in the Central Subarctic is virtually the same year-round and is dominated by very small forms. McAllister (1972) concluded that the primary production at Ocean Station P (50°N 145°W) varied between 45–72 $\mathrm{g\ C \cdot m^{-2} \cdot yr^{-1}}$. A more recent estimate using nutrient mass balance methods yields a figure of 100 $\mathrm{g\ C \cdot m^{-2} \cdot yr^{-1}}$ (Sambrotto and Lorenzen, 1987). Phytoplankton production is believed to be controlled by grazing, primarily by two very large herbivorous copepods: *Neocalanus plumchrus* and *Neocalanus cristatus*, which account for about 75% of the zooplankton biomass. Both of these species have special adaptations that enable them to feed on small phytoplankton; they also have an unusual reproductive pattern, since they reproduce at depth in late winter when the primary production cycle is still light-limited (Miller et al. 1984). By reproducing before the phytoplankton growth cycle begins, *Neocalanus* is closely coupled to the primary production cycle and virtually eliminates the lag period observed in the subarctic Atlantic which is dominated by *Calanus finmarchicus*. Two species of euphausiids, both predominantly herbivores, are also present in substantial quantities: *Euphausia pacifica* and *Thysanoessa longipes*.

Zooplankton biomass in the Central Subarctic during April through June (the time period encompassing the seasonal zooplankton peak) averages 147 $\mathrm{mg/m^3}$ (Fulton and LeBrasseur 1985). There is some indication that zooplankton concentrations may be lower in the center of the Alaska Gyre. Reid (1962) suggested that nutrient levels there may be able to sustain a larger biomass of zooplankton than the divergence of the surface waters in this region will allow to accumulate. Distributional information summarized by Wickett (1967) and Fulton and LeBrasseur (1985) indicates that the biomass of zooplankton tends to be more densely concentrated around the edges of the Alaska Gyre, which supports Reid's hypothesis.

Fisheries Production

Coastal Upwelling Domain

Northern boundary

The paleontologic sediment record establishes that the southern part of the Coastal Upwelling Domain has been dominated, for the past 1600 years, by four pelagic species: Northern anchovy, Pacific hake, Pacific sardine and Pacific mackerel (Soutar and Isaacs 1969). With the exception of anchovy, the adults of these species undergo an extensive annual migration (between 15–20 degrees of latitude) to summer feeding grounds off southern British Columbia. They complete a return migration in the fall to southern and Baja California where they spawn the following winter and early spring (Table 1).

The limits of these annual migrations provide strong evidence that the average position of the northern boundary of the coastal upwelling domain lies between 50–51°N (Fig. 2). First, commercial concentrations of hake normally extend as far north as 49°N in summer, occasionally as far as 50°N, and rarely beyond 51°N (Bailey et al. 1982; Beamish and McFarlane 1985). Second, Hart (1973) noted that commercial concentrations of Pacific sardine in the summer, during the 1930's and 1940's, were found south of Brooks Peninsula (50°N), less frequently in Quatsino Sound (50.5°N), and infrequently off the central coast of B.C. (51°N). More specifically, Hart (1943) mentions that "the supply of pilchards north of Esperanza Inlet (49.7°N) was too uncertain to support a profitable industry". Third, Pacific mackerel tend to be abundant off the west coast of Vancouver Island during periods when the migratory stock is large as it was in the 1930's and 1940's, and recently in the early 1980's.

The distribution of Northern anchovy also supports our belief that the northern boundary of the Coastal Upwelling Domain is around 50°N lat. Three major subpopulations of anchovy are currently recognized (Fig. 2). The southern population occurs off Baja California (25–28°N); the central population occupies the southern California bight (30–34°N); and the northern population is dispersed from roughly 40–50°N. Most of the northern population spawns in the Columbia River plume (44–46°N) in summer (Richardson 1981), but some components of this subpopulation spawn in Canadian waters off the west coast of Vancouver Island (WCVI). The presence of small anchovies in B.C. indicates that successful reproduction occurs there and is sufficiently reliable to sustain small resident stocks, most notably in Barkley and Nootka sounds (50°N). Historically, anchovy have been more plentiful along the west coast of Vancouver Island than they are currently (Hart 1973).

There is some evidence that changes in oceanic conditions and in the biomass and distribution of Pacific hake have a significant impact on the survival of pre-recruit herring in southern B.C. waters (Ware and McFarlane 1986). From this we reasoned that the recruitment time series for the seven major herring stocks (Fig. 3) should be highly correlated if they spend the offshore phase of their life cycles in the same production domain and, conversely, should be less well correlated if the stocks live in different production domains. The results of a correlation analysis of the recruitment time series (Fig. 4) suggest 3 major groupings which are statistically significant at the 1% level (the shaded areas in Fig. 4). These statistical groupings are consistent with the idea that the lower WCVI herring stock inhabits a different production zone namely, the Coastal Upwelling Domain. Similarly, the data suggest that the upper WCVI, upper Strait of Georgia, Central Coast, and Queen Charlotte Island stocks occupy a transitional zone, since they all show strong affinities with more than one stock. These stocks spend the summer feeding off the upper west coast of Vancouver Island and in Queen Charlotte Sound, and are undoubtedly sensitive to oceanic influences originating in both the Coastal Downwelling and Upwelling

TABLE 1. Dominant species, some key life history parameters, and recruitment coefficient of variation for each production domain. The von Bertalanffy growth equation parameters L_{max} and K are listed where known. The recruitment variability estimates are averages for 10 or more years of data, the sources are indicated. The remaining life history information comes from Hart (1973). The abbreviations "P" and "D" indicate pelagic and demersal eggs, respectively.

	Age (years)		Growth		Spawning			Population dynamics
Species	Maturity	Max.	L_{max} (cm)	K	Season	Egg	Location	Recruitment C.V. (%)
A. COASTAL UPWELLING DOMAIN								
Northern anchovy	1	7	21	0.45	W-Sp	P	S. and Baja Calif.	75[a]
Pacific sardine	2	13	29	0.45	A,W,Sp	P	Baja Calif.	84[b]
Pacific hake	4	20	53	0.28	W-Sp	P	S. Calif.	117[c]
Pacific mackerel	2	10	41	0.22	Sp-S	P	Baja Calif.	94[d]
Jack mackerel	1	35	60	0.09	W-Sp	P	Baja Calif/Oceanic	67[e]
Pacific herring	3	15	29	0.45	Sp	D	Coastal bays	66[f]
Sablefish	5	50	74	0.27	W	P	Shelf/slope	52[g]
B. COASTAL DOWNWELLING DOMAIN								
Walleye pollock	3	20	54	0.32	Sp	P	Shelf	82[h]
Pacific cod	2–3	8	108	0.20	W	D	Shelf/slope	76[i]
Sablefish	5	50	74	0.27	W	P	Slope	44[j]
Pacific herring	3	15	29	0.45	Sp	D	Coastal bays	93[f]
Pacific halibut	12	33	184	0.14	W	P	Slope	40[k]
Chinook salmon	3–5	8	147	—	All	D	Rivers	—
Coho salmon	3	5	98	—	A	D	Freshwater	—
C. CENTRAL SUBARCTIC DOMAIN								
Chum salmon	2–3	3	102	—	A	D	Rivers	54[l]
Pink salmon	2	2	76	—	A	D	Streams	57[l]
Sockeye salmon	4–5	5	84	—	A	D	Rivers/lakes	55[l]
Coho salmon	3	5	98	—	A	D	Rivers	46[j]
Chinook salmon	3–5	8	147	—	All	D	Rivers	—

Data sources: [a] Methot (1988); [b] MacCall (1979); [c] Francis et al. (1984); [d] Parrish and MacCall (1978); [e] MacCall and Stauffer (1983); [f] Haist et al. (1987); [g] McFarlane and Beamish (1983); [h] Megrey and Alton (1986); [i] Thompson et al. (1986); [j] McFarlane and Beamish (1986); [k] Quinn et al. (1985); [l] This paper (Table 4).

Domains. The recruitment data also support the idea that the North Coast stock inhabits a coastal oceanographic region in Hecate Strait that is weakly linked to the west coast of Vancouver Island, and more strongly linked to the Central Coast and Queen Charlotte Island stocks.

Evidence for Pacific cod, halibut, sablefish and Oregon coho also suggests that the stocks to the north and south of the northern tip of Vancouver Island live in different production domains. The biomass of adult cod off the west coast of Vancouver Island follows a different trend than the stocks in Queen Charlotte Sound and in Hecate Strait, which tend to show similar behaviour (Walters et al. 1986). The commercial catch of halibut also shows a striking drop below the northern tip of Vancouver Island (Int. Pac. Hal. Comm. Rept. 16, 1978). Commercial halibut fisheries occur throughout the entire Coastal Downwelling Domain, but it seems significant that there are no major commercial halibut fisheries in the Coastal Upwelling Domain. Recent studies also show differences in resident and dispersal behaviour of adult sablefish to the north and south of the northern tip of Vancouver Island (Beamish and McFarlane 1988). Tag returns from coho salmon born in Oregon show that their poleward movements rarely extend beyond the northern tip of Vancouver Island, demonstrating that these stocks spend the entire oceanic phase of their life cycle in the Coastal Upwelling Domain (W. G. Pearcy and J. P. Fisher 1988). The same conclusion may apply to the coho stocks scattered along the southwest coast of Vancouver Island, and California stocks found off southern Oregon.

Taking the average positions of the southern and northern boundaries of the Coastal Upwelling Domain at 25°N and 50.5°N, respectively, we estimate that the surface area of the biologically productive region of this domain is 480 thousand km^2. Sixty-four percent of this area is off Baja and southern California: between 25°N and 35°N it extends about 220 km offshore (Bernal and McGowan 1981); the surface area of this region is about 309 thousand km^2. The surface area in the productive zone between central California and Southern B.C. is about 171 thousand km^2: between 35°N to 42°N, and 49°N to 50°N the productive area appears to be largely within a 40 to 55 km band along the coast, so we assumed that the width of the domain in this region was defined by the 200 m isobath; between 42°N to 49°N the most productive area extends 170 km offshore (Richardson 1981).

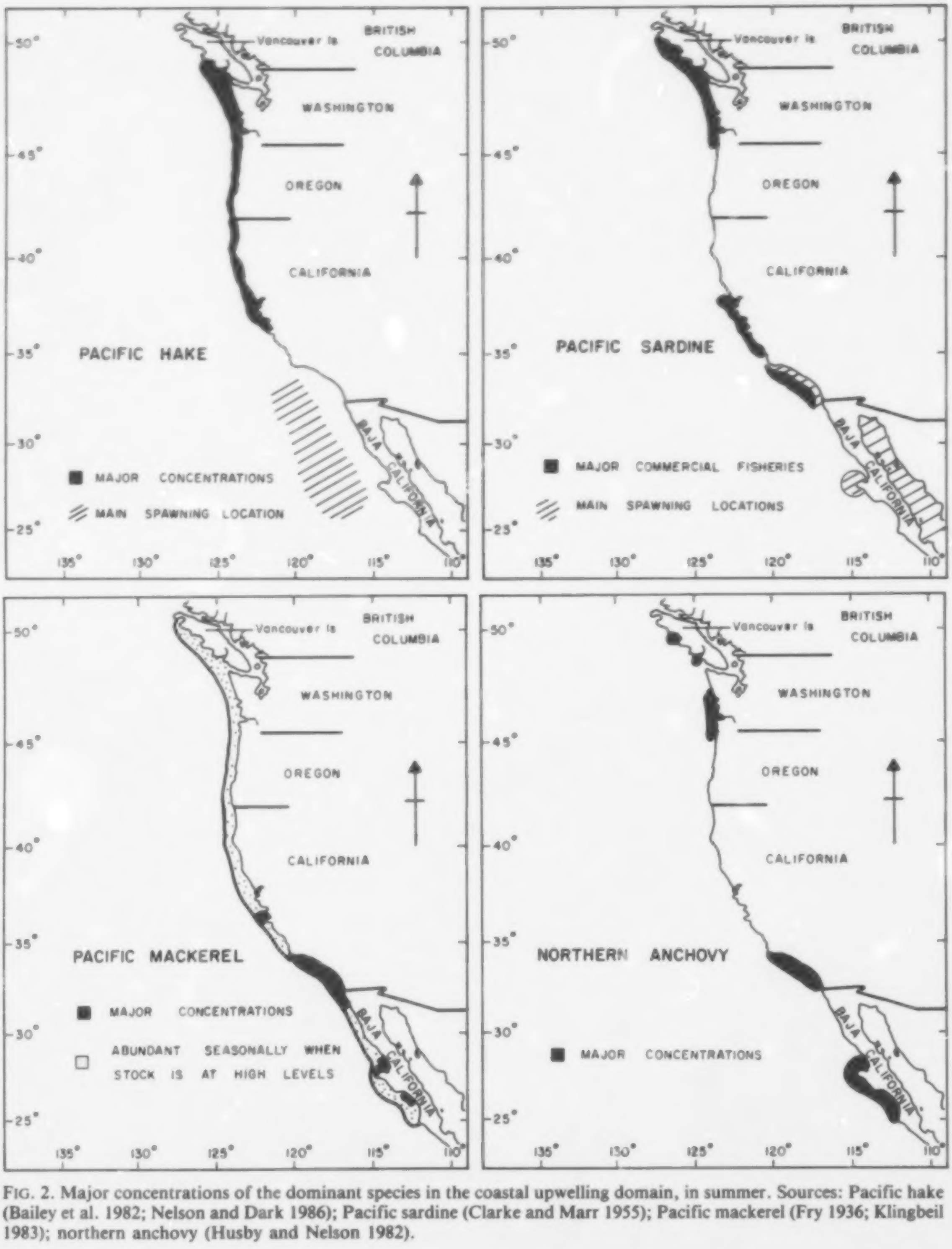
PACIFIC HAKE
MAJOR CONCENTRATIONS
MAIN SPAWNING LOCATION
PACIFIC SARDINE
MAJOR COMMERCIAL FISHERIES
MAIN SPAWNING LOCATIONS
PACIFIC MACKEREL
MAJOR CONCENTRATIONS
ABUNDANT SEASONALLY WHEN STOCK IS AT HIGH LEVELS
NORTHERN ANCHOVY
MAJOR CONCENTRATIONS
Vancouver Is
BRITISH COLUMBIA
WASHINGTON
OREGON
CALIFORNIA
BAJA CALIFORNIA
50°
45°
40°
35°
30°
25°
135°
130°
125°
120°
115°
110°

FIG. 2. Major concentrations of the dominant species in the coastal upwelling domain, in summer. Sources: Pacific hake (Bailey et al. 1982; Nelson and Dark 1986); Pacific sardine (Clarke and Marr 1955); Pacific mackerel (Fry 1936; Klingbeil 1983); northern anchovy (Husby and Nelson 1982).

Species Characteristics and Interactions

Table 1 summarizes the vital statistics on maturity, longetivity, growth, spawning time, and recruitment variability for the dominant species in the Coastal Upwelling Domain. All but sablefish have characteristically small to medium body sizes, low ages at maturity (Fig. 5), high recruitment variability and, with the exception of anchovy, sablefish and herring, undergo long-range migrations each year. As a rule, sardine migrate at a speed

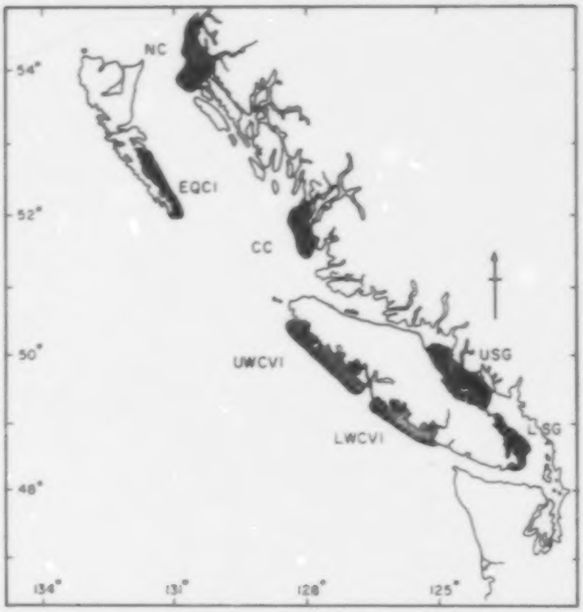

FIG. 3. Locations of the major spawning stocks of migratory herring in British Columbia: NC = North coast; EQCI = East coast Queen Charlotte Islands; CC = Central coast; USG = Upper Strait of Georgia; LSG = Lower Strait of Georgia, UWCVI = Upper west coast Vancouver Island; LWCVI = Lower west coast Vancouver Island.

	LWCVI	UWCVI	LSG	USG	CC	EQCI
UWCVI	+0.466					
LSG	−0.032	+0.546				
USG	+0.212	+0.463	+0.646			
CC	+0.234	+0.456	+0.421	+0.370		
EQCI	+0.277	+0.290	+0.288	+0.379	+0.831	
NC	+0.130	+0.261	+0.327	+0.214	+0.526	+0.421

FIG. 4. Recruitment time series correlations for the major spawning stocks of British Columbia herring between 1950–85. Stock abbreviations are defined in Fig. 3. Data source: Haist et al, 1987. For $N = 36$, the correlation coefficient (r) has to exceed ±0.418 and ±0.325 to be significant at the 1% and 5% level, respectively. The shaded areas indicate where r exceeds the 1% level of significance.

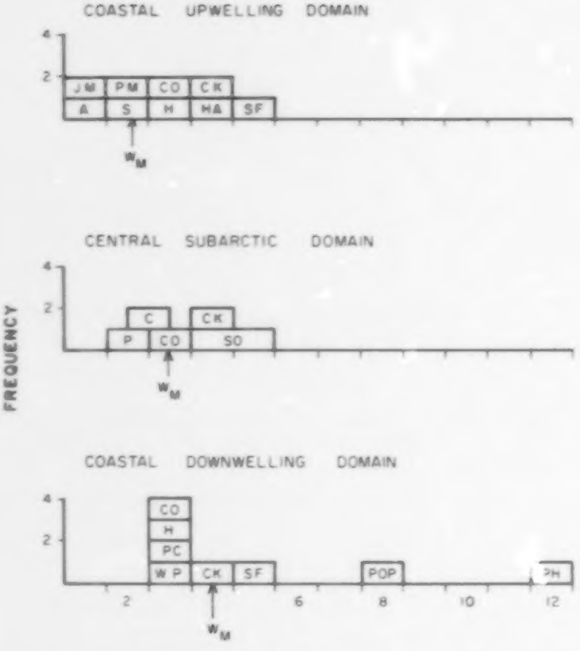

FIG. 5. Average age at maturity of the dominant species in each domain. The arrow labelled WM indicates the average age at maturity in each domain, weighted by the average biomass of the dominant species.

of about 10–12 km/day (Hart 1945). At this rate Pacific sardine would take 275 d to complete their annual north-south migration, leaving roughly 90 d (July–Sept.) for intensive feeding near the northern extremity of the Coastal Upwelling Domain. This timing is consistent with Hart (1943) who noted that "the main bodies of pilchards usually appear off the Canadian coast between the middle of June to the end of July and remain until some time between the middle of June and middle of October." By comparison, Pacific hake spawn off southern California (31°N) in Jan–Feb. then migrate northward. They appear off San Francisco (37° N) in early March, and off the lower west coast of Vancouver Island (49°N) by mid-June. These sightings indicate that the stock migrates at an average speed of about 16–18 km/d. The larger fish move into the Canadian zone where they feed primarily on euphausiids from mid-June to late October (roughly 126 d), when they begin returning south to spawn. In completing their annual migration, hake cover an extraordinary distance of 4224 km in 239 d.

The appearance of large numbers of hake in the northern region of the Coastal Upwelling Domain may have a significant impact on the local herring stocks. Ware and McFarlane (1986) found a negative correlation between herring year-class strength and the estimated food ration consumed by hake in the Canadian zone in summer. They estimated that the hake population consumes about 21–34% of the adult biomass of the lower west coast of Vancouver Island herring stock each year, on average, with some indication that the impact may be higher in warm summers.

The sediment record indicates that the biomass of sardines expands intermittently in the Coastal Upwelling Domain, and that they are currently at a low point in their abundance cycle (Soutar and Isaacs 1969). Over the past 1850 years there have been 12 main occurrences of sardines which last between 20–150 yr. The average period between occurrences is 80 yr, with a range of 20 to 200 yr. During the last period of high abundance, the supply of sardines off southern B.C. supported a dependable summer fishery for 20 yr (1926–46), which yielded an average annual catch of 46 thousand t. The sardine population has not produced a really strong year-class since 1939. It is relevant to ask if this migratory stock might have had an impact on herring off the lower west coast of Vancouver Island. An analysis of the catches of these two species in B.C. between 1917–47 reveals a negative correlation. This may indicate a biological interaction between sardine and herring on the summer feeding grounds, or it may be caused by some fluctuating, reciprocal demand for the two species in the marketplace. However, the fact that the coefficient of variation of the sardine (91%), and herring catch (61%) during this period is almost identical to the respective recruitment variabilities of these two species (Table 1) suggests that catches in B.C. reflect real changes in abundance. Cross-correlation analysis reveals that peak sardine catches tend to lead the lowest herring catches by 1 yr ($r = -0.51$); the zero yr lag correlation was also significant ($r = -0.47$). These findings suggest that high levels of sardine may adversely affect herring survival, during the summer off the lower west coast of Vancouver Island, resulting in poorer herring catches the following fishing season.

Whether or not there is a biological interaction between sardine and hake on the summer feeding grounds in B.C. is an unknown, but interesting possibility. Did these stocks fluctuate in- or out-of-phase when sardine were abundant during the late 1920's and early 1930's? Although this question is difficult to answer there may be some anecdotal clues in old research documents and cruise reports. An analysis of scales in sediment cores from suitable locations in the northern part of the Coastal Upwelling Domain might also provide an answer. The evidence supporting a biological interaction of the dominant pelagic species in the sediment record off California is equivocal. The following pairs of species: (1) Northern anchovy and Pacific sardine, and (2) Pacific hake and northern anchovy were negatively correlated in the Soledad Basin core from Baja California, but were positively correlated in the Santa Barbara core from California (Soutar and Isaacs 1974).

With respect to the general level of productivity, the sediment record from Santa Barbara points to a sharp decline in pelagic fish production in the Coastal Upwelling Domain which began in 1925 and continues unabated to date. Northern anchovy were 3–4 times more abundant 1100 yr ago (Soutar and Isaacs 1969) and, even as recently as 1897 were considered to be an "abounding potential commercial species" in B.C. (Hart 1973).

Recruitment Variability

Chelton et al.'s (1982) conclusion that zooplankton volumes in the southern part of the Coastal Upwelling Domain are being forced mainly by advection from the Central Subarctic Domain prompted us to compare the interannual variability of the zooplankton with the variability in recruitment of the dominant species. An inspection of Table 2 indicates that the recruitment variability of hake, sardine and Pacific mackerel is of the same order as the 21 yr coefficient of variation in zooplankton volumes (83–129%) in the areas off southern and Baja California where these species spawn and their young develop (Bernal 1979). Jack mackerel is a transient member of the Coastal Upwelling Domain. It spawns offshore (over 180 km) from March–June (MacCall and Stauffer 1983), in an oceanic regime characterized by low zooplankton biomass (Bernal and McGowan 1981) and presumably low variability. Thus recruitment fluctuations in this species may be relatively small because the egg and early larval stages are dispersed over a large area, during a protracted spawning season, where the interannual variability in zooplankton biomass is also low. Although the CALCOFI plankton grid does not extend far enough offshore into the main spawning area of jack mackerel, Bernal's (1979) analysis indicates that zooplankton variability was lower in the offshore stations. In contrast, hake larvae can be found from the coast to over 130 km offshore. The larvae tend to be distributed offshore and most concentrated in southern California (Bernal's statistical areas II and III) where the variability in zooplankton volumes is highest (Table 2). Perhaps it is not coincidental

TABLE 2. Comparison between recruitment coefficient of variation of different species and the zooplankton volume coefficient of variation (CV) in the main spawning and rearing areas in the southern portion of the coastal upwelling domain. The center of distribution of the fish larvae was estimated from Moser et al. 1987 (Table 3); recruitment CV comes from Table 1; and zooplankton CV from Bernal (1979). The geographical areas used by Bernal are shown in Roman numericals. Percent of larvae in inshore waters comes from Moser et al. (1987).

Species	Centre of distribution	% Larvae inshore	Coefficient of variation (%)	
			Recruitment	Zooplankton
Pacific hake	SCAL (offshore)	38	117	118–129 (III–II)
Pacific mackerel	CBCAL (inshore)	82	94	83–118 (IV–III)
Pacific sardine	CBCAL (inshore)	79	84	83 (IV)
Northern anchovy	SCAL (inshore)	79	75	?

Abbreviations: SCAL = Southern California.
CNCAL = Central Baja California (see Moser et al. 1987).

that hake also have the highest recruitment variability. Pacific sardine and mackerel spawn from the coast out to 81 km offshore; their eggs are most concentrated inshore, and off central Baja California. The long-term coefficient of variation of zooplankton volumes in these areas is strikingly similar to the coefficient of variation in sardine and mackerel recruitment[1]. This apparent link between the variances in zooplankton volume and recruitment in the main spawning and rearing areas off California (Table 2) does not tell us anything about the mechanisms that might be involved, but it suggests that events which force variations in the zooplankton may also be forcing recruitment in the dominant pelagic species, either directly or indirectly, with very little damping or amplification.

Identifying the factors that determine interannual variations in year-class success is a complex problem that is beyond the scope of this paper. We suggest, however, that variations in large zooplankton predators and in the food supply during the egg and early larval stages may be as, or more, important than advection in determining year-class success. Bailey and Francis (1986), and Sinclair et al. (1985) observed that hake and Pacific mackerel produce poor year-classes in cool years, and generally better year-classes in warm years. In cool years the California Current is strong, and transports the zooplankton of subarctic origin further south than usual along the coast of southern and Baja California (Reid 1962). This phenomenon may have three adverse impacts on hake and mackerel: (1) it may, as Bailey and Francis (1986) and Sinclair et al. (1985) have suggested, transport a significant proportion of eggs and larvae out of the area with disastrous consequences; however, (2) the eggs and larvae might also experience a higher predation rate due to the rise in abundance of large subarctic euphausiids, ctenophores and amphipods in the area; and (3) this abnormal influx of subarctic water and associated fauna may not provide as suitable a food supply for hake and mackerel larvae and juveniles as the normal assemblage of plankton.

Thus all three factors: advection, predators and food probably change in a complicated and interrelated fashion off southern California in cool years, and may affect recruitment and production of the dominant pelagic species in the region in different ways. In cool years, when the California Current and local upwelling are strong, anchovy tend to produce good year-classes because feeding conditions may be more favourable near the coast (Douglas 1980), and the subarctic zooplankton may not have a strong negative impact on the more southern, nearshore spawning areas of the anchovy. In contrast, in warm years the California Current is weaker, coastal upwelling is reduced, and there is a greater volume of oceanic water near the coast. Consequently, primary production declines, zooplankton volumes are lower (Reid 1962), and anchovy experience poor recruitment success in the coastal region (Douglas 1980). In contrast, these factors seem to enhance the survival of young-of-the-year hake and Pacific mackerel.

Any mechanism that purports to explain recruitment variability in the dominant pelagic species in the Coastal Upwelling Domain must account for why hake and Pacific mackerel do well in warm years, while anchovy do better in cool years. The fact that two of the three species in this complex are out of phase seems significant, particularly since anchovy have an average biomass of 1.9 million t, while hake and mackerel have a combined average biomass of 1.6 million t (Table 3). Thus half the pelagic biomass appears to be sensitive to cool conditions, while the remaining half is sensitive to warm conditions. This 'balanced' response may provide a damping mechanism that makes the total biomass of pelagic fish in the region less variable than the sum of the variability of the individual species. Within these groups, however, there have been trade-offs in biomass, such as the most recent decline of the sardine and the increase in anchovy in the late 1960's. The last decade has been anomalously warm which has tended to favour an increase in hake and Pacific mackerel production.

Coastal Downwelling Domain

Fish Distributions and Boundaries

The distribution of commercial concentrations of Pacific halibut, Pacific cod and walleye pollock defines the northern and southern boundaries of the Coastal Downwelling Domain (Fig. 6). According to these distributions, this domain stretches around the Gulf of Alaska from Queen Charlotte Sound (51°N 130°W) to the Aleutian Islands (52°N 170°W). Taking the edge of the continental shelf as the seaward limit, the total surface area of the coastal downwelling domain is about 348 thousand km². Later we note that it is important to distinguish between the eastern and western boundaries of the Gulf. The eastern boundary region extends from Queen Charlotte Sound to Prince William Sound and has a surface area of roughly 144 thousand km²; the western boundary encompasses the rest of the domain and has a surface area of 204 thousand km².

Pacific herring are abundant only along the eastern boundary of the Coastal Downwelling Domain. As noted earlier, 4 of the 7 herring stocks in B.C. spend the summer feeding in a transitional zone near the southern boundary of this domain. Although this boundary fluctuates seasonally and interannually in response to changes in oceanic conditions, we assume that these transitional zone stocks and the north coast herring stock normally inhabit the Coastal Downwelling Domain. Thus we suggest that British Columbia herring stocks live in two different production domains and we assigned the mean catches to each area, accordingly (Table 3).

Sablefish is one of the most widely dispersed groundfish species in the Northeast Pacific ocean. Fishable concentrations occur from the Aleutian Islands to California. Recently about 50% of the commercial catch has come from the Coastal Upwelling Domain and the remaining half from the Coastal Downwelling Domain.

---

[1] A similar comparison can't be made for anchovy, because the central stock spawns primarily inshore off southern California (Bernal's Area II). Bernal didn't estimate the variability in the inshore component of the plankton in Area II.

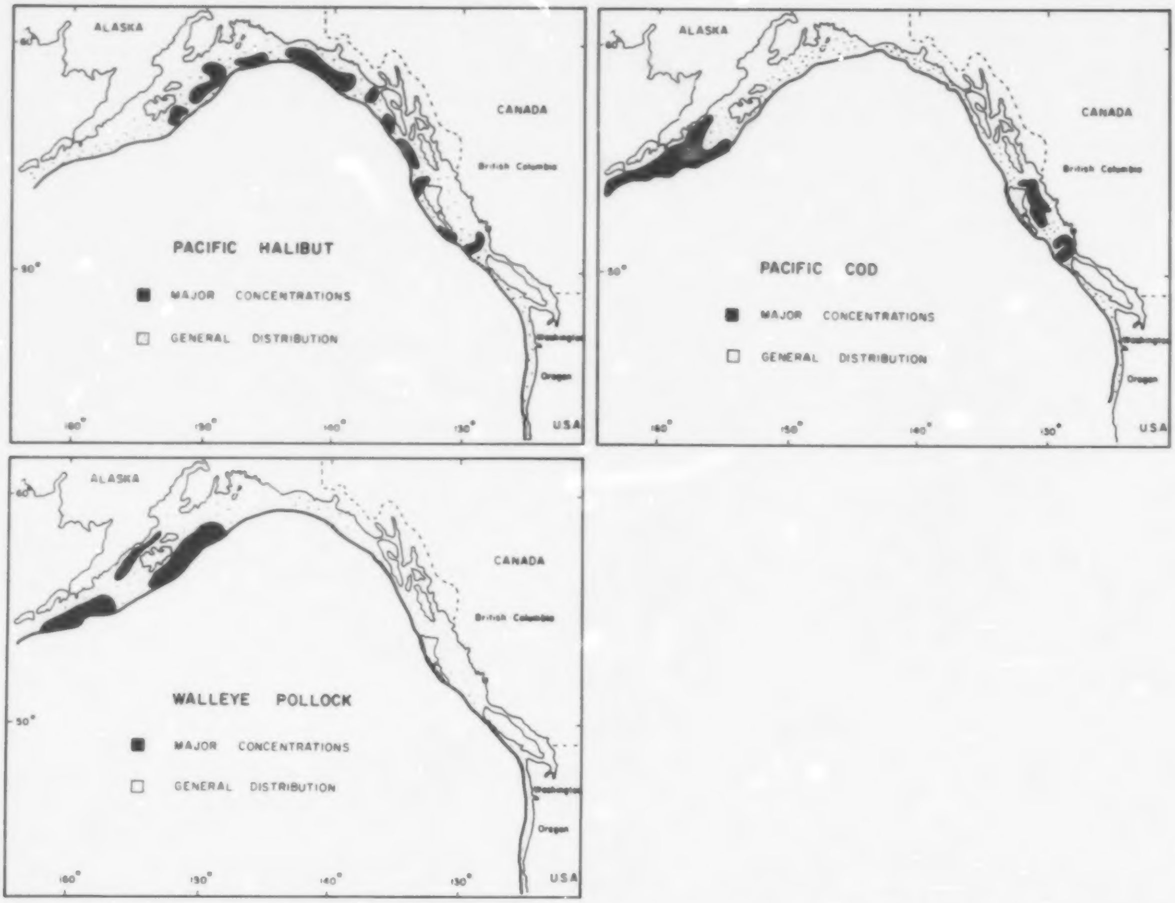

FIG. 6. Major concentrations of the dominant species in the Coastal Downwelling domain. Sources: Halibut (St. Pierre 1984); cod (Bakkala et al. 1984); pollock (Bakkala et al. 1986).

Historically, the relative importance of these two domains in supporting sablefish catches has fluctuated back and forth.

Species Characteristics and Interactions

The Coastal Downwelling Domain is dominated by a mixture of pelagic and demersal fishes. The dominant pelagic species: pollock, herring, chinook, and coho salmon, make up 50% of the estimated long-term average fishable biomass (Table 3). Over the last 2 decades the dominant demersal species: cod, Pacific ocean perch, halibut, sablefish, and a variety of less abundant species, have accounted for the remaining biomass. One reason why demersal species are more important in this domain is because the continental shelf is twice as wide (90 km) as it is in the Coastal Upwelling Domain (38 km, on average). Along the western boundary of the Coastal Downwelling Domain the width of the continental shelf averages 140 km.

With respect to oceanographic conditions and fish production, the eastern and western boundary regions of the Gulf of Alaska are strikingly different. The western boundary is a productive region dominated by pollock and cod. These species have high turnover rates characterized by low ages at maturity (Fig. 5), high natural mortality rates, relatively short life-spans, and high fecundity per unit of body weight. These characteristics enable pollock and cod to respond quickly to changes in the production capacity of the environment. In this sense, the dominant planktivore, pollock, plays the same role in the Coastal Downwelling Domain as anchovy does in the Coastal Upwelling Domain. In contrast, the eastern boundary of the Gulf is predominantly a convergent region dominated by herring, halibut, sablefish, coho and chinook salmon, and seasonally by large numbers of northward migrating juvenile salmon from U.S. and Canadian stocks (Hartt and Dell 1986). Collectively, these species (excluding juvenile salmon) make up 22% of the biomass in the Coastal Downwelling Domain. Pacific herring is the dominant pelagic species along the eastern boundary; it is slow growing, matures at an early age, has a high natural mortality rate ($M = 0.45$), and an annual reproductive output equivalent to 25% of the body weight (Ware 1985). By comparison chinook and coho are fast growing (primarily because their principal foods consist of squid and fishes such as herring and sand lance), and mature at 3-5 yr of age.

TABLE 3. Surface area of biologically productive zone, long-term average estimates of stock biomass, the average catch (between 1974–83), estimated catch/biomass ratio (C/B), and mean weight of the dominant species in each domain. The numbers in parentheses indicate the potential catch of underexploited species.

Species/stock	Mean biomass	Mean catch	Mean wt	C/B
	(thousands of tonnes)		(g)	
A. COASTAL UPWELLING DOMAIN (480 × 10^3km^2)				
Northern anchovy				
— Southern stock	500[a]	(200)[c]	—	—
— Central stock	774[b]	172 (310)[c]	15[b]	(0.22)[t]
— Northern stock	600[a]	— (240)[c]	—	—
Total anchovy	1874	172 (750)		
Pacific hake[d]	1500	131 (200)	1000	0.13
Pacific sardine[e]	<20 (1250)	0 (297)	138	0.24
Groundfish	520[s]	78	—	—
Jack mackerel[f]	970	22 (195)	—	0.20
Pacific herring				
— California	43	5	—	—[g]
— Washington	15	4	—	0.26
— B.C., LWCVI[m]	56	12	—	0.21
— B.C., LSG[m]	15	4	120	0.26–0.34
Total herring	129	25		
Pacific mackerel[h]	123	22	317	0.21–0.29
Sablefish	115	15	3100	0.13
Coho salmon				
— Cal/Ore/Wash	17[s]	7	3400	—
— B.C., WCVI	10[s]	4	3400	—
Total coho	27	11[r]		
Chinook salmon				
— Cal/Ore/Wash	46[s]	10	6500	—
— B.C., WCVI	21[s]	4	6500	—
Total chinook	67	14[r]		
Total:	5345 (6575)	490 (1607)		
B. COASTAL DOWNWELLING DOMAIN (348 × 10^3km^2)				
Walleye pollock[i]	1500	204	1000	0.14
Pacific cod[j]	536	30 (100)	2500	(0.05)[t]
POP complex[u]	275[s] (1300)[v]	20	1000	(0.07)
Misc. groundfish	533[s]	80	—	—
Sablefish[k]	250	17	3100	(0.07)[l]
Pacific herring				
B.C., USG[m]	37	8	123	0.22
B.C., UWCVI[m]	19	5	123	0.26
B.C., CC and EQCI[m]	113	14	—	(0.11)[t]
B.C., North Coast[m]	44	4	—	(0.09)[t]
SE Alaska	73[s]	18	—	—
Total herring	286	49		
Pacific halibut[n]	215[q]	18 (23)[q]	13500	0.10
Chinook salmon	22[s]	5	6500	—
Coho salmon	10[s]	4	3400	—
TOTAL	3627	427 (502)		

C. CENTRAL SUBARCTIC DOMAIN ($3140 \times 10^3 km^2$)

Chum salmon[o]	167	46[r]	4200	0.27
Pink salmon[o]	150	62[r]	1700	0.41
Sockeye salmon[p]	136	40[r]	2600	0.29
Coho salmon	27[s]	11	3400	(0.41)
Chinook salmon	2[s]	0.4	6500	(0.21)
TOTAL	482	159		

Notes and Data Sources: [a] Richardson (1981); [b] Methot (1988); [c] Northern anchovy are currently underexploited; this is the potential catch assuming a C/B ratio of 0.4 (see Fig. 7); [d] Pacific hake are currently underexploited, there is general agreement that the stock could support a catch of 200 000 t (Francis et al. 1984); [e] Between 1916–51, the sardine stock averaged 1 250 thousand t and produced an average annual catch of 297 thousand t (MacCall 1979); [f] MacCall and Stauffer (1983); [g] The California fishery is controlled by a catch quota, which explains the low C/B ratio; [h] Parrish and MacCall (1978); [i] Alton et al. (1986); [j] Zenger and Blackburn (1986); this stock could support a potential yield of 100 thousand t; [k] Fujioka (1985); [l] This estimate seems low; the stock biomass may be overestimated; [m] Haist et al. (1987); [n] Hoag and McNaughton (1978); [o] This paper; [p] Peterman and Wong (1984); [q] Long-term mean biomass and catch (1935–84). The total biomass figure shown here for age 8–20 halibut is equivalent to roughly twice the exploitable biomass figures calculated by the INPHC (S. Hoag, pers. comm); [r] Average catch between 1956–72; sockeye biomass increased by a factor of 2.2 between 1978–83 largely due to an increase in the Bristol Bay stock complex; during the same period pink biomass increased by a factor of 1.6 and chum a factor of 1.5, largely due to an increase in the biomass of natural and enhanced stocks (Rogers 1987). Chinook and coho increased by a factor of 1.1; [s] Estimated from assumed C/B ratio; [t] Estimate is low, stock was probably underexploited; [u] "Pacific ocean perch" complex consists of five species: *Sebastes alutus, S. polyspinis, S. aleutianus, S. borealis, S. zacentrus;* [v] Estimated biomass of POP complex in early 1960's (Alton et al. 1986). The estimated biomass for the period (1974–83) is not well determined so the C/B ratio is approximate.

In contrast to the dominant pelagic species, sablefish and halibut have evolved a different life history pattern which operates over a much longer time scale. These species mature later, have a lower natural mortality rate and are much longer-lived. They spread their biomass and production over the entire Coastal Downwelling Domain and some individuals undergo extensive north-westward migrations (or advections) as juveniles in the prevailing direction of the Alaska Current, and as adults make a slow return migration over several years, particularly along the eastern boundary of the Gulf of Alaska. In view of the fact that halibut biomass has fluctuated in roughly a 30-yr cycle since 1935, whereas the sablefish biomass has fluctuated in a 10–15-yr cycle, as a result of periodic strong year-classes (McFarlane and Beamish, 1983), there does not appear to be any striking interaction between these species that leads to a trade-off in stock biomass.

Historically, there have been some remarkable changes in the biomass and production of the dominant species inhabiting the western boundary of the Coastal Downwelling Domain. In the early 1960's the biomass of the Pacific ocean perch complex was about 1.1 million t. An intensive fishery reduced the biomass by 70% by 1970. Coincidentally, the pollock biomass increased sharply reaching 1 million t in the early 1970's; in the early 1980's it expanded again to about 2 million t. Alton et al. (1986) suggested that pollock may have replaced Pacific ocean perch in the early 1970's, because they eat similar prey (namely euphausiids and other nekton) and have overlapping distributions; however, they could not explain why the pollock biomass increased again in the late 1970's. In view of the lack of reliable estimates of fish biomass from this area in the 1960's, the events and mechanisms leading to the expansion of pollock are not clear. However, it is important to note that even in the early 1960's pollock were considered to be "one of the most widely distributed and most abundant fish species in the whole north Pacific" (Kasahara 1961).

Juvenile salmon are transient members of the Coastal Downwelling Domain. All five species enter the coastal seas along the eastern and western boundaries of the Gulf of Alaska by late June. Individuals from stocks south of the northern Gulf (Yakutat region) migrate northward within a narrow coastal belt less than 36 km wide (by comparison the width of the continental shelf in this region averages 60 km). In the northern Gulf where the shelf is wider (100 km), juvenile salmon migrate westward toward the Aleutian Islands and are dispersed over the entire shelf (Hartt and Dell 1986). During their first summer juvenile salmon feed extensively on euphausiids, larval fish, pteropods, copepods and amphipods. Hartt and Dell (1986) noted that this nearshore migration pattern minimizes overlap with large oceanic predators such as albacore, pomfret, and jack mackerel which move northward into the Central Subarctic Domain in August and September. Another potential benefit associated with the coastal migration route is that there is a low standing stock of potential, resident, finfish predators on the continental shelf along the eastern boundary of the Gulf of Alaska (Table 5). By late November, pink, chum, and sockeye juveniles begin moving out of the Coastal Downwelling Domain into the Central Subarctic Domain. Some coho and chinook also move offshore, but many remain in coastal, or nearby, oceanic waters for their entire lives.

Recruitment Variability

Recruitment variability in pollock, herring and Pacific cod stocks in the Coastal Downwelling Domain is twice as high (CV = 70–80%; Table 1) as it is for the much longer-lived sablefish and halibut stocks (CV = 40–44%). The reasons for this are undoubtedly complex and are not well understood. Wind mixing is an important variable in this domain, because a higher than average frequency of storms during May–July enhances primary production and may increase the flux of organic matter to the benthos and large herbivorous copepods such as *Neocalanus plumchrus* (Sambrotto and Goering 1983). Conversely, *Pseudocalanus* may be enhanced under calm conditions; this species seems to play an important role in determining interannual variation in pollock year-classes (Bailey et al. 1986). An alternative view is that the biomass of pollock, like anchovy in the Coastal Upwelling Domain, may rise and fall in response to the general level of productivity along the western boundary. Thus over the long run one might expect a positive correlation between primary production and pollock biomass. Advection and food have been implicated as important sources of recruitment variability in cod. Tyler and Westrheim (1986) found a negative correlation between cod year-class strength and water transport in northern B.C. when the larvae were in the water column. In this part of the Coastal Downwelling Domain, cod and herring biomasses are inversely correlated and possibly linked in a classical predator-prey interaction (Walters et al. 1986). Herring year-class strength also seems to be affected by oceanic conditions during the first year of life. Recruitment of southeast Alaska herring (Rounsefell 1930; Favorite and McLain 1973) and north coast of B.C. herring (Stocker 1986) is positively correlated with temperature. In contrast, Ware and McFarlane (1986) found a negative correlation for the west coast of Vancouver Island herring stocks. Perhaps this change in the sign of the correlation can be explained by fluctuations in the flow of the Alaska Current. In warm winters, the strength of the Alaska current may be increased by an intensification of the Aleutian Low. The resulting convergence of oceanic water near the coast may increase the supply of nutrients and zooplankton, and possibly change the predator community in some way that is favourable for herring survival along the eastern boundary of the Coastal Downwelling Domain.

Cooney (1984) suggested that the Alaska Current transports significant amounts of oceanic zooplankton to the outer edge of the Alaska Coastal Current during the spring, prior to the appearance of juvenile salmon in the Alaska Coastal Current, and in the fall before they move offshore. In view of the lack of data on zooplankton variability in the Alaska coastal current, and the limited time series from Ocean Station P (OSP) which lies in the Central Subarctic Domain, it is difficult to test Cooney's suggestion that variations in the flow of the Alaska Current may affect the marine survival of juvenile salmon. We did, however, compute the coefficient of variation in the maximum summer biomass of zooplankton at OSP over the 20-yr time series (Fulton 1983), and compared it with the coefficient of variation in returning run size for sockeye, pink, chum and coho salmon from various stocks (here, run size is equivalent to recruitment as the estimates were obtained by adding catch and escapement data). Table 4 shows that the variability in recruitment in Pacific salmon (46–63%) is of the same order as the variability in zooplankton biomass at OSP (53%). This table does not tell us anything about the possible mechanism: it may reflect the amount of plankton available to juvenile salmon during their first year at sea, and consequently their growth, physiological condition and survival; or it may reflect the abundance of marine fish predators which, in turn, may be sensitive to variations in the amount of plankton; or, most likely, it is some complex variation on the food and predator themes. Whatever the explanation, Table 4 suggests that the Coastal Downwelling Domain may be linked to the Central Subarctic Domain, by the Alaska Current, in much the same way as the Central Subarctic Domain is linked to the Coastal Upwelling Domain by the California Current; and that this connection is an important factor forcing recruitment in some of the dominant species in each domain. This hypothesis is consistent with what is known about the Alaska Current, the seasonal appearance of oceanic plankton in the Coastal Downwelling Domain, and the nearshore migration route of juvenile salmon.

Central Subarctic Domain

Boundaries

There are no obvious geographical boundaries to the Central Subarctic Domain, it is broadly defined by the margin of the continental shelf to the east and to the

TABLE 4. Coefficient of variation of maximum zooplankton biomass at Ocean Station "P", and run size in various Pacific salmon stocks. *N* indicates the number of years in the time series. Data sources: zooplankton (Fulton 1983); sockeye run size (Foerster 1968, Int. Pacific Salmon Fish. Comm. reports); Fraser River pink and chum run size (Int. Pacific Salmon Fish. Comm, reports); Carnation Creek coho (B. Holtby, Pacific Biological station, pers. comm.).

Variable	*N*	Coefficient of variation (%)
Zooplankton biomass (Ocean Station P)	20	53
Sockeye run size		55
Fraser River	33	63
Karluk Lake	28	52
Naknek-Kvichak	28	49
Columbia River	19	58
Pink run size (Fraser River)	12	57
Chum run size (Fraser River)	22	54
Coho run size (Carnation Creek)	54	46

north, and to the west by the Aleutian islands. We placed the oceanic boundary at 170°W because this is close to the western edge of the Alaska Gyre, and it approximates the western limit of distribution of North American salmon stocks inhabiting the Gulf of Alaska (Hart 1973). The southern boundary is more problematical because its position fluctuates seasonally: the average position of the Subarctic current is near 50°N in summer and 45°N in winter. We chose the latter boundary because it marks the southern limit of distribution of North American salmon stocks. The total surface surface area in the Central Subarctic Domain is about 3.1 million km^2.

Species Characteristics and Biomass Estimates

The large nekton in this region is dominataed by pink, chum and sockeye salmon and seasonally (in summer) by pomfret, Pacific saury, albacore tuna and jack mackerel. During the oceanic phase of their life cycle, sockeye, pink and chum are mainly in the upper 15–20 m of water during the day and night. These species forage opportunistically with pink and chum being more planktivorous, while sockeye consistently eat more oceanic squid and fish (LeBrasseur 1972). Euphausiids and amphipods are staple items in the diet of sockeye salmon, but squid tend to be the most important item in the southern portion of the Central Subarctic Domain. Fish tend to dominate their diet in the central and western portions of the Gulf of Alaska (Foerster 1968). The relative importance of these items, however, can change from year-to-year. Ito (1964) found that fish and squid were paramount in the diets of sockeye in even years; and euphausiids, amphipods and copepods in odd years. Immature sockeye aggregate in summer and fall in areas where there are consistently high concentrations of large zooplankton (French et al. 1976). Seasonal changes in major concentrations of immature chum salmon also seem to coincide with shifts in the abundance of zooplankton in the central and western Pacific (Neave et al. 1976).

Estimates of the abundance of salmon in the Gulf of Alaska are not readily available, except for the stock reconstruction analysis by Peterman and Wong (1984) for Bristol Bay and B.C. sockeye stocks. We used their estimates of abundance of age 2–6 fish, adjusted for an annual survival rate of 85%, and multiplied them by the mean body weight of each age-group. We obtained an average biomass of 145 thousand t. This figure was raised to 181 thousand t, because the stocks Peterman and Wong considered comprised 80% of the North American catch; this figure was then multiplied by 0.75 because about 25% of the distributional area of Alaska sockeye is in the Bering Sea. Hence, we estimate that the biomass of sockeye in the Central Subarctic Domain averaged 136 thousand t between 1956–72. The corresponding biomass of chum and pinks in this domain was calculated from the proportions of these species, relative to sockeye, in: (1) the total high seas salmon catch in numbers, and (2) the catch east of 170°E (Manzer et al. 1965, Table 47). The resulting abundance estimates, multiplied by the mean body weight in the high seas catch, produced the following estimates (for 1955–60):

Species	Average biomass (thousands of tonnes)	
	1.	2.
Chum	155	180
Pink	150	47
Coho	28	26
Chinook	2	2

The mean value in each case was chosen as the best estimate, with the exception of pink salmon, where the second figure was excluded because it is clearly too low (Table 3C).

The average production of salmon removed by North American commercial fisheries (i.e. the catch) that originated in the Central Subarctic Domain was estimated from distribution maps for sockeye, pink and chum compiled by Hart (1973). For these three species, 100% of the Canadian catch and 75% of the USA catch was assumed to come from the Central Subarctic Domain (the remaining 25% of the USA catch originates in the Bering Sea). In addition to this, we estimated that 10% of the Japanese pink catch and 33% of their chum catch was produced in the Central Subarctic Domain. The resulting catch estimates are summarized in Table 3C.

Since coho and chinook tend to be more concentrated along the eastern boundary of the Gulf of Alaska (Hart 1973), the estimated biomass of these species in the Central Subarctic Domain only represents a small fraction of the total biomass. The remaining biomass of these species in the Coastal Upwelling and Downwelling Domains was estimated from a catch/biomass ratio. These ratios were extrapolated from a regression of the C/B ratio for sockeye, pink and chum relative to their mean growth and mortality rates in their last year at sea (Ricker 1976). Coho have a very high growth/mortality ratio like pink, and hence probably have a correspondingly high C/B ratio (= 0.41). By contrast, chinook have the lowest growth/mortality ratio of the five salmon species and therefore probably have a low C/B ratio (about 0.21). The coho and chinook catch in each domain was estimated by subtracting the catch originating from the biomass of these species in the Central Subarctic Domain from the total North American catch, and allocating the remaining catch in proportion to the amount taken in each domain. The resulting biomasses were calculated by dividing the catch by the C/B ratio (Tables 3A and B).

Catch/Biomass Relationships

This section considers the potential yield in each domain, and the catch/biomass ratio of some of the dominant species. Between 1974–83 the average annual catch removed by commercial fisheries in the Coastal Upwelling Domain was 490 thousand t (Table 3). The average yield could have been about 1300 thousand t if the market demand for anchovy, hake and jack mackerel wasn't limited. In a historical context, the Coastal Upwelling Domain sardine fishery produced an average annual catch of 297 thousand t. Assuming the other species in this domain (including anchovy) retained their average production potential during this period, the potential yield was 1600 thousand t (Table 3). This represents a catch/biomass (C/B) ratio of 0.24 and an average yield of 3.3 t•km^{-2}•yr^{-1}. Coincident with the warming trend in the Northeast Pacific in the last decade, the sardine stock is at a low level of abundance, while the hake stock has increased to roughly 2 million t. The potential yield in the Coastal Upwelling Domain, therefore, currently averages about 2.7 t•km^{-2}•yr^{-1} (Table 5).

TABLE 5. Average biomass and potential yield per unit area of the dominant species in each domain.

Domain	Biomass (t • km^{-2})	Yield (t • km^{-2} • yr^{-1})	C/B
Coastal upwelling[a]	11.1 (13.7)	2.7 (3.3)	0.24
Coastal downwelling	10.4	1.4	0.13
Eastern boundary	6.9	0.9	
Western boundary	13.8	1.8	
Central subarctic[b]	0.15	0.05	0.33

[a] Figures including Pacific sardine are in parentheses.

[b] Figures do not include pomfret, Pacific saury, jack mackerel, and albacore tuna which account for a significant biomass and potential yield.

The Coastal Downwelling Domain supports some very productive pelagic and demersal fisheries, particularly along the western boundary of the Gulf of Alaska. During the last decade, U.S. and foreign fleets removed an average annual catch of some 427 thousand t (Table 3). The potential yield in this domain is about 500 thousand t: Pacific cod are currently under-exploited and could support a catch of 100 thousand t. This represents an average C/B ratio of 0.13, and an area-averaged yield of 1.4 t•km^{-2}•yr^{-1}. On a regional basis, however, this figure is misleading because the yield along the western boundary of the Gulf of Alaska is twice the rate along the eastern boundary (Table 5). By comparison, the average finfish landings per unit area from the continental shelf seas in the Northwest Atlantic are slightly higher, varying between 1.9–4.0 t•km^{-2}•yr^{-1} (the exceptionally productive Georges Bank has averaged 8 t•km^{-2}•yr^{-1}); in the Northwest Pacific, landings from the Japan Sea average 1.5 t•km^{-2}•yr^{-1}. One reason why the western boundary fisheries in the Coastal Downwelling Domain are more productive is probably because upwelling, albeit weak, occurs there fairly continuously from June-September (Schumacher and Wilson 1986). Accordingly, the production of benthic organisms potentially available to demersal fishes in the western region (180 g •m^{-2}•yr^{-1}) is significantly higher than it is along the eastern boundary (23–64 g•m^{-2}•yr^{-1}; Cooney 1986).

Our estimates of the salmon catch from the Central Subarctic Domain, suggest that this region produces a yield of 0.05 t of salmon•km^{-2}•yr^{-1}, assuming the effective surface area of this domain is 3.1 million km^2. This represents an average C/B ratio of 0.33 (Table 5). These figures do not include the potential yield of other seasonally important members of the nekton such as pomfret, Pacific saury and jack mackerel, which we have not attempted to estimate.

A plot of the average yield of the dominant species in each domain with respect to their mean size in the catch reveals that the catch/biomass ratio is a decreasing function of the size of the organism (Fig. 7). In general, there appear to be two distinct stanzas: one describing the continental shelf species, and one describing salmon, which we will consider below. Amongst the first group, the data indicate that small-bodied planktivores have C/B ratios between 0.2 to 0.3. Larger forms that feed on a mixed diet of plankton, large nekton, and fish have C/B ratios between 0.1 to 0.2.

Pacific Ocean perch falls below the regression line in Fig. 7; we suspect this estimate is conservative because it is uncertain what the biomass of the stock was between 1973–83. In the early 1960's when the P.O.P. stock was

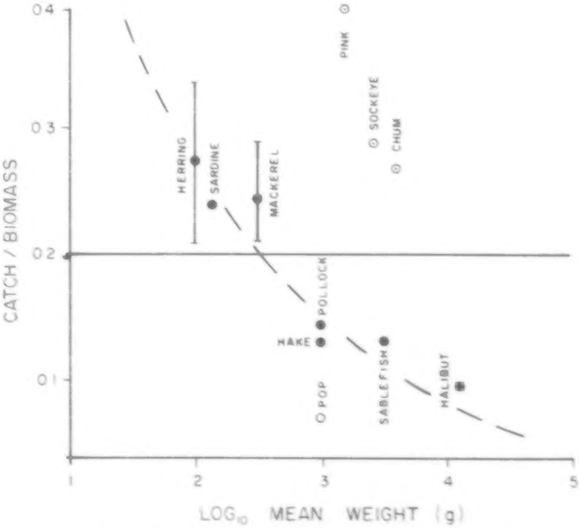

FIG. 7. Catch/biomass ratios with respect to body weight. The estimated ratios are only shown for the species where long-term estimates of average biomass and yield available (see Table 3). The dashed line shown here would be straight on a log-log plot and can be described by: $C/B = 0.74\ W^{-0.22}$ ($N = 7$; $r = -0.94$).

about 1.3 million t the catch averaged 242 thousand t (C/B = 0.19). At this rate of exploitation the stock responded with a sharp decrease in biomass, which is not surprising because this slow growing, long-lived species probably has a maximum sustainable C/B ratio around 0.1. Northern anchovy were not included in Fig. 7 because this species is clearly underexploited. According to the regression line in Fig. 7, if the mean weight of the fish in the commercial catch is 20 g then anchovy can support, in theory, a C/B ratio of 0.4.

In a recent study, Boudreau and Dickie (pers. comm.) collated production data from 14 fish populations and found that the production/biomass ratio was size-dependent: $P/B = 2.88\ w^{-0.33}$, where w is the weight of the species at maturity (expressed in k calories). After converting calories to grams and allowing for the fact that the average weight of fish in the catch is about 40% larger than the weight at first maturity the corresponding proportionality constant in Boudreau and Dickie's P/B relationship is 2.81.

Assuming this relationship applies to the species in Figure 7, excluding salmon, the ratio of Boudreau and Dickie's P/B relationship to our C/B relationship indicates the maximum sustainable proportion of the total production that can be removed by the fishery. The result suggests the catch/production ratio is about 0.44 for small pelagic species such as herring, and 0.56 for larger species such as Pacific hake; the remaining production in each case is removed by predators and other natural causes, and is invested in reproduction and somatic growth to rebuild the stock biomass.

Pacific salmon have significantly higher C/B ratios than similar sized species inhabiting the continental shelf. An analysis of the catch and biomass of specific stocks indicates that Pacific salmon C/B ratios are indeed as high as we estimate for the total stock complex (D. Blackbourn, pers. comm.). Salmon are able to sustain such remarkably high C/B ratios because: (1) they are semelparous — until they are caught all their surplus energy has been used to increase their body size, none has been "lost" as reproductive products; and (2) they have a high growth/natural mortality ratio during their ocean residence (Ricker 1976).

Concluding Remarks

Our review of some of the key oceanographic, biological and fisheries data highlights the fact that there are three major fisheries production domains in the northeast Pacific Ocean. The boundary between the two coastal domains lies in central British Columbia, which is significant because it means the fish stocks off the southwest coast of Vancouver Island live in a different production domain than the stocks in northern B.C. This conclusion has important management implications and provides a conceptual basis for understanding why the recruitment patterns of northern B.C. herring stocks differ from the southern stocks; it has parallel implications for Pacific cod, sablefish, and some salmon stocks.

Our estimates of the biomass of salmon in the Central Subarctic Domain are clearly approximations, and would have been very difficult to derive without Peterman and Wong's (1984) study. We estimate that between 1956–72 the biomass of salmon in this domain averaged 480 thousand t. In the 1970's the biomass of sockeye, pink and chum salmon increased sharply, primarily due to an increase in the productivity of natural and enhanced stocks (Rogers 1987). Between 1973-84 the resulting biomass of salmon in the Central Subarctic may have reached 820 thousand t, an increase of 70% over what it had been in the two previous decades. It is tempting to speculate that the Aleutian low may have strengthened in the 1970's, increasing the amount of upwelling in the Alaska Gyre and productivity in the Central Subarctic Domain. This may explain, in part, why the productivity of the 3 oceanic species (sockeye, pink and chum) rose, while the average run size of the 2 coastal sea species (coho and chinook) showed a much weaker response (Rogers 1987).

It has been recognized for some time that the Central Subarctic Domain is linked to the coastal domains by the Alaska Current in the north and the California Current in the south. There is increasing evidence that variations in the flow of the Alaska Current may affect the plankton biomass and may be forcing a significant amount of the recruitment variability in some of the dominant species in the Coastal Downwelling Domain, in much the same way as variations in the flow of the California Current may affect the recruitment of some of the dominant species in the Coastal Upwelling Domain. The mechanisms, however, have not been clarified.

Our analysis of the fish catch in the coastal seas indicates that the potential yield in the Coastal Upwelling and Downwelling Domains averages between 1.5 to 3 $t \bullet km^{-2} \bullet yr^{-1}$, which is comparable to other temperate, continental shelf regions with primary production rates in the order of 150–300 $g\ C \bullet m^{-2} \bullet yr^{-1}$. On a longer time-scale it is important to remember that the Coastal Upwelling Domain has not been particularly productive for some time. It was 5 times more productive between 1830–1925 (Soutar and Issacs 1974), presumably in response to an intensification of coastal upwelling, or the California Current.

Acknowledgements

We thank Rick Thomson, Bob Francis and Richard Brodeur for critically reviewing the manuscript. Our thanks also to Dave Blackbourn, Chris Wood, and Bill Pearcy for supplying helpful references and information about salmon; and Paul Boudreau and Lloyd Dickie for sharing the results of their P/B analysis.

References

ALTON, M. S., M. O. NELSEN, AND B. A. MEGREY. 1986. Changes in abundance and distribution of pollock (*Theragra chalcogramma*) in the western Gulf of Alaska (1961–1984). *In* M. S. Alton [ed.] Workshop on comparative biology, assessment and management of gadoids from the North Pacific and Atlantic oceans. Northwest and Alaska Fisheries Center, Seattle, WA.

ANDERSON, G. C. 1964. The seasonal and geographic distribution of primary productivity off the Washington and Oregon Coasts. Limnol. Oceanogr. 9: 288.

Bailey, K. M., and R. C. Francis. 1986. Environment and population dynamics of Pacific whiting (*Merluccius productus*). Int. North Pac. Fish. Comm. Bull. 45: 317-333.

Bailey, K., R. Francis, and J. Schumacher. 1986. Recent information on the causes of variability in recruitment of Alaska pollock in the eastern Bering Sea: Physical conditions and biological interactions. Int. North Pac. Fish. Comm. Bull. 47: 155-165.

Bailey, K. M., R. C. Francis, and P. R. Stevens. 1982. The life history and fishery of Pacific whiting, *Merluccius productus*. Calif. Coop. Fish. Invest. rep. 23: 81-98.

Bakkala, R., T. Maedan, and G. McFarlane. 1986. Distribution and stock structure of pollock (*Theragra chalcogramma*) in the North Pacific Ocean. Int. North Pac. Fish. Comm. Bull. 45: 3-20.

Bakkala, R., S. Westrheim, S. Mishima, C. Zhang, and E. Brown. 1984. Distribution of Pacific cod (*Gadus macrocephalus*) in the North Pacific Ocean. Int. North Pac. Fish. Comm. Bull. 42: 111-115.

Bakun, A., and C. S. Nelson. 1977. Climatology of upwelling related processes off Baja California. Calif. Coop. Oceanic Fish. Invest. Rep. 19: 107-127.

Beamish, R. J., and G. A. McFarlane. 1985. Pacific hake stocks off the west coast of Vancouver Island. Mar. Fish. Rev. 47(2): 75-78.

1988. Resident and dispersal behaviour of sablefish in the slope waters off Canada's west coast. Can. J. Fish. Aquat. Sci. 45: 152-164.

Bernal, P. A. 1979. Large-scale biological events in the California current. CALCOFI Rep. Vol. 20: 89-101.

Bernal, P. A., and J. A. McGowan. 1981. Advection and upwelling in the California current. *In* F. A. Richards [ed.]. American Geophysical Union, Wash. D.C.: 381-399.

Bolin, R. L., and D. P. Abbott. 1963. Studies on the marine climate and phytoplankton of the central coastal area of California 1954-1960. Calif. Coop. Oceanic Fish. Invest. Rep. 9: 23-45.

Chelton, D. B., P. A. Bernal, and J. A. McGowan. 1982. Large-scale interannual physical and biological interaction in the California current. J. Mar. Res. 40: 1095-1125.

Clark, F. N., and J. C. Marr. 1955. Population dynamics of Pacific sardine. Calif. Coop. Oceanic Fish. Invest., Prog. Rep. July 1, 1953-March 31, 1955: 11-48.

Cooney, R. T. 1984. Some thoughts on the Alaska coastal current as a feeding habitat for juvenile salmon, p. 256-268. *In* W. G. Pearcy [ed.] The influence of ocean conditions on the production of salmonids in the North Pacific. Oregon State University.

1986. Biological oceanography of the Northeast Pacific, p. 41-68. *In* M. Alton [ed.]. A workshop on comparative biology, assessment and management of gadoids from the North Pacific and Atlantic oceans. Northwest and Alaska Fisheries Center, Seattle, WA.

Dewees, C. M., and E. M. Strange. 1984. Drift bottle observations of the nearshore surface circulation off California, 1977-1983. Calif. Coop. Oceanic. Fish. Invest. Rep. 25: 68-73.

Dodimead, A. J., F. Favorite, and T. Hirano. 1963. Salmon of the North Pacific Ocean — Part II. Review of oceanography of the subarctic Pacific region. Int. North Pac. Fish. Comm. Bull. 13: 195 p.

Douglas, A. V. 1980. Geophysical estimates of sea-surface temperatures off western North America since 1671. Calif. Coop. Oceanic. Fish. Invest. 21: 102-112.

Emery, W. J., and K. Hamilton. 1985. Atmospheric forcing of interannual variability in the Northeast Pacific Ocean: connections with El Niño. J. Geophys. Res. 90: 857-868.

Favorite, F., A. J. Dodimead, and K. Nasu. 1976. Oceanography of the subarctic Pacific region, 1960-71. Int. North Pac. Fish. Comm. Bull. 33: 187 p.

Favorite, F., and D. R. McLain. 1973. Coherence in trans-Pacific movements of positive and negative anomalies of sea surface temperature, 1953-60. Nature 244: 139-143.

Foerster, R. E. 1968. The sockeye salmon (*O. nerka*). Bull. Fish. Res. Board Can. 162: 422 p.

Francis, R. C., G. A. McFarlane, A. B. Hallowed, G. I. Swartzman, and W. M. Getz. 1984. Status and management of the Pacific hake (*Merluccius productus*). Resource and fishery off the west coast of the United States and Canada. Natl. Mar. Fish. Service NWAFC Processed Rept. 84-18.

French, R., H. Bilton, M. Osako, and A. Hartt. 1976. Distribution and origin of sockeye salmon (*Oncorhynchus nerka*) in offshore waters of the North Pacific ocean. Int. N. Pac. Fish. Comm. Bull. 34: 113 p.

Fry, D. H., Jr. 1936. A preliminary summary of the life history of the Pacific mackerel. Calif. Fish and Game 22: 30-39.

Fujioka, J. 1985. Sablefish. *In* R. Major [ed.]. Condition of groundfish resources in the Gulf of Alaska region as assessed in 1985. 429 p. (Document submitted to the annual meeting of the Int. North Pac. Fish. Comm., Tokyo, Japan, October 1985.) U.S. Dept. Comm. NOAA, NMFS, NAFC, Seattle, WA.

Fulton, J. D. 1983. Seasonal and annual variations of net zooplankton at Ocean Station "P", 1956-1980. Can. Data Rep. Fish. Aquat. Sci. 374: 65 p.

Fulton, J. D., and R. J. LeBrasseur. 1985. Interannual shifting of the subarctic boundary and some of the biotic effects on juvenile salmonids. *In* W. S. Wooster and D. L. Fluharty [ed.]. El Niño North: 237-247. Washington Sea Grant Publication.

Garrison, D. L. 1976. Contribution of the net plankton and nannoplankton to the standing stocks and primary productivity in Monterey Bay, California, during the upwelling season. Fish. Bull. 74: 183-194.

Haist, V., J. F. Schweigert, and D. Fournier. 1987. Stock assessments for British Columbia herring in 1986 and forecasts of the potential catch in 1987. Can. MS Rep. Fish. Aquat. Sci. 1929: 63 p.

Hart, J. L. 1943. The pilchard *Sardinops caerulea* on Canadian fishing grounds with special reference to an unusual abundance of young fish. Trans. Roy. Soc. Can., Ser. 3, 37: 55-73.

1973. Pacific fishes of Canada. Fish. Res. Bd. Can. Bull. 180: 740 p.

Hartt, A. C., and M. B. Dell. 1986. Early oceanic migrations and growth of juvenile Pacific salmon and steelhead trout. int. North Pac. Fish. Comm. Bull. 46: 105 p.

Hoag, S. H., and R. J. McNaughton. 1978. Abundance and fishing mortality of Pacific halibut, cohort analysis, 1935-1976. Int. Pac. Halibut Comm. Sci. Rep. No. 65: 45 p.

Husby, D. M., and C. S. Nelson. 1982. Turbulence and vertical stability in the California current. Calif. Coop. Oceanic. Fish. Invest. 23: 113-129.

Ito, J. 1964. Food and feeding habits of Pacific salmon (genus *Oncorhynchus*) in their oceanic life. Bull. Hokkaido Reg. Fish. Res. Lab. 29: 85-97.

Kasahara, H. 1961. Fisheries resources of the North Pacific Ocean. H. R. MacMillan lectures in fisheries. The University of British Columbia, Vancouver, B.C. 135 p.

Klingbeil, R. A. 1983. Pacific mackerel: A resurgent resource and fishery of the California current. Calif. Coop. Fish. Invest. Rep. 24: 35-45.

LeBrasseur, R. J. 1972. Utilization of herbivore zooplankton by maturing salmon, p. 581–588. *In* A. Y. Takenouti [ed.]. Biological oceanography of the northern North Pacific Ocean. Idemitsu Snoten, Tokyo, Japan.

Longhurst, A. R. 1967. Diversity and trophic structure of zooplankton communities in the California currents. Deep-Sea Res. 14: 393–408.

MacCall, A. D. 1979. Population estimates for the waning years of the Pacific sardine fishery. Calif. Coop. Oceanic Fish. Invest. Rep. 20: 72–82.

MacCall, A. D., and G. D. Stauffer. 1983. Biology and fishery potential of jack mackerel (*Trachurus symmetricus*). Calif. Coop. Oceanic Fish. Invest. Rep. 24: 46–56.

Manzer, J. I., T. Ishida, and M. G. Hanavan. 1965. Salmon of the North Pacific Ocean — Part V. Offshore distribution of salmon. Int. North Pac. Fish. Comm. Bull. 15. 452 p.

Megrey, B. A., and M. S. Alton. 1986. Condition of the walleye pollock resource of the Gulf of Alaska as estimated in 1986. *In* R. L. Major [ed.]. Condition of groundfish resources in the Gulf of Alaska region as assessed in 1986. (Document submitted to the annual meeting of the Int. North Pacific Fish. Comm., Anchorage, Alaska, October 1986.) Natl. Mar. Fish. Ser., Northwest and Alaska Fisheries Center, Seattle, WA.

McAllister, C. D. 1972. Estimates of the transfer of primary production to secondary production at Ocean Station P, p. 575–579. *In* A. Y. Takenouti [ed.] Biological oceanography of the northern North Pacific Ocean. Idemitsu Shoten, Tokyo.

McFarlane, G. A., and R. J. Beamish. 1986. Production of strong year-classes of sablefish (*Anoploma fimbria*) off the west coast of Canada. Int. North Pac. Fish. Comm. Bull. No. 47: 191–202.

McFarlane, G. A., W. Shaw, and A. V. Tyler. 1985. Sablefish–coastwide stock assessments, p. 163–186. *In* A. V. Tyler and G. A. McFarlane [ed.] Groundfish stock assessments off the west coast of Canada in 1984 and recommended yield options for 1985. Can. MS Rep. Fish. Aquat. Sci. 1813: 353 p.

McLain, D. R., and D. H. Thomas. 1983. Year-to-year fluctuations of the California countercurrent and effects on marine organisms. Calif. Coop. Oceanic Fish. Invest. Rep. 24: 165–181.

Miller, C. B., B. W. Frost, H. P. Batchelder, M. J. Clemons, and R. E. Conway. 1984. Life histories of large grazing copepods in a subarctic ocean gyre: *Neocalanus plumchrus*, *Neocalanus cristatus* and *Eucalanus bungii* in the Northeast Pacific. Prog. Oceanogr. 13: 201–243.

Moser, H. G., P. E. Smith, and L. E. Eber. 1987. Larval fish assemblages in the California current region, 1954–1960, a period of dynamic environmental change. Calif. Coop. Oceanic Fish. Invest. Rep. 28: 97–127.

Namias, J. 1985. New evidence for relationships between North Pacific atmospheric circulation and El Niño. Trop. Ocean-atmos. Newsletter. March 1985.

Neave, F., T. Yonemori, and R. G. Bakkala. 1976. Distribution and origin of chum salmon in offshore waters of the North Pacific Ocean. Int. North Pac. Fish. Comm. Bull. 35: 79 p.

Nelson, M. O., and T. A. Dark. 1986. The distribution, abundance, and biological features of the Pacific whiting resource based on 1977 and 1980 research vessel surveys. Int. North Pac. Fish. Comm. Bull. 45: 334–364.

Parrish, R., and A. D. MacCall. Climatic variation and exploitation in the Pacific mackerel fishery. Cal. Dept. Fish and Game, Fish Bulletin 167: 1–110.

Parrish, R. H., C. S. Nelson, and A. Bakun. 1981. Transport mechanisms and reproductive success of fishes in the California current. Biolog. Oceanog. 1(2): 175–203.

Parsons, T. R., L. F. Giovando, and R. J. LeBrasseur. 1966. The advent of the spring bloom in the eastern subarctic Pacific Ocean. J. Fish. Res. Board Canada 23: 539–546.

Parsons, T. R., M. Takahashi, and B. Hargrave. 1984. Biological oceanographic Processes. Pergamon Press. New York. 330 p.

Pearcy, W. G., and J. P. Fisher. 1988. Migrations of coho salmon, *Oncorhynchus kisutch*, during their first summer in the ocean. Fish. Bull. 86: 173–195.

Peterman, R. M., M. J. Bradford, N. C. H. Lo, and R. D. Methot. 1988. Contribution of early life stages to interannual variability in recruitment of northern anchovy, *Engraulis mordax*. Can. J. Fish. Aquat. Sci. 45: 8–16.

Peterman, R. M., and F. Y. L. Wong. 1984. Cross correlations between reconstructed ocean abundances of Bristol Bay and British Columbia sockeye salmon (*Oncorhynchus nerka*). Can. J. Fish. Aquat. Sci. 41: 1814–1824.

Quinn, T. J. II, R. R. Deriso, and S. H. Hoag. 1985. Methods of population assessment of Pacific halibut. Int. Pac. Halibut Comm. Sci. Rep. No. 72: 52 p.

Reid J. 1962. On circulation, phosphate-phosphorus content, and zooplankton volumes in the upper part of the Pacific Ocean. Limnol. Oceanor. 7: 287–306.

Richardson, S. L. 1981. Spawning biomass and early life of northern anchovy, *Engraulis mordax*, in the northern subpopulation off Oregon and Washington. Fish. Bull. 78: 855–876.

Ricker, W. E. 1976. Review of the rate of growth and mortality of Pacific salmon in salt water, and noncatch mortality caused by fishing. J. Fish. Res. Board Can. 33: 1483–1524.

Rodgers, D. E. 1987. Pacific salmon, p. 461–476. *In* D. W. Hood and S. T. Zimmerman [ed.] The Gulf of Alaska: physical environment and biological resources. Alaska Office Ocean Assessment Division, NOAA, Wash., DC.

Rounsefell, G. A. 1930. Contribution to the biology of the Pacific herring, *Clupea pallasii*, and the condition of the fishery in Alaska. Bull. U.S. Bur. Fish. 45: 227–320.

Royer, T. C. 1983. Interannual variability in the abiotic environment of the Bering Sea and the Gulf of Alaska. *In* W. S. Wooster [ed.]. From Year to Year. Washington Sea Grant publication: 134–138.

Ryther, J. H. 1969. Photosynthesis and fish production in the sea. Science 166 72–76.

St. Pierre, G. 1984. Spawning locations and season for Pacific halibut. Int. Pacific Halibut. Comm. Sci. Rep. No. 70: 46 p.

Sambrotto, R. N., and J. J. Goering. 1983. Interannual variability of phytoplankton and zooplankton production on the southeast Bering Sea shelf. *In* W. S. Wooster [ed.] From Year to Year: Washington Sea Grant Publication: 161–177.

Sambrotto, R. N., and C. J. Lorenzen 1987. Phytoplankton and primary production. *In* D. W. Hood and S. T. Zimmerman [ed.] The Gulf of Alaska: Physical environment and biological resources. U.S. Dep. Commerce. Springfield: 249–282.

Schumacher, J. D., and R. K. Reed. 1983. Interannual variability in the abiotic environment of the Bering Sea and Gulf of Alaska. *In* W. S. Wooster [ed.] From Year to Year. Washington Sea Grant Publication: 111–133.

Schumacher, J. D., and J. G. Wilson. 1986. On the atmospheric and oceanic environment of the Gulf of Alaska. *In* M. Alton [ed.] A workshop on comparative biology, assessment and management of gadoids from the North Pacific and Atlantic oceans. Northwest and Alaska Fisheries Center, Seattle: 135–178.

Sinclair, M., M. J. Tremblay, and P. Bernal. 1985. El Niño events and variability in a Pacific mackerel (*Scomber japonicus*) survival index: support for Hjort's second hypothesis. Can. J. Fish. Aquat. Sci. 42: 602–608.

Soutar, A., and J. D. Isaacs. 1969. History of fish populations inferred from fish scales in anaerobic sediments off California. Calif. Coop. Oceanic Fish. Invest. Rep. 13: 63–70.

1974. Abundance of pelagic fish during the 19th and 20th centuries as recorded in anaerobic sediment off the Californias. Fish. Bull. 72(2): 257–273.

Stocker, M. 1986. Environmental-dependent Ricker stock-recruitment models for Pacific herring. *In* C. W. Haegele [ed.]. Can. MS Rep. Fish. Aquat. Sci. 1871: 119–125.

Strub, J. S. Allen, A. Huyer, and R. L. Smith. 1987. Large-scale structure of the spring transition in the coastal ocean off Western North America. J. Georphys. Res. 92: 1527–1544.

Thompson, W. F., and R. van Cleve. 1936. Life history of the Pacific halibut. 2. Distribution and early life history. Int. Pac. Hal. Comm. Rep. 9: 184 p.

Thompson, G. G., D. H. Ito, and J. W. Balsiger. 1986. A management-oriented model of the population dynamics of Pacific cod (*Gadus macrocephalus*) in the Eastern Bering Sea, P. 1245–1268. *In* M. Alton [ed.]. A workshop on comparative biology, assessment and management of gadoids from the North Pacific and Atlantic oceans. Northwest and Alaska Fisheries Center, Seattle, WA.

Thomson, R. E. 1981. Oceanography of the British Columbia coast. Can. Spec. Publ. Fish. Aquat. Sci. 56: 291 p.

Thomson, R. E., B. M. Hickey, and P. LeBlond. 1988. The Vancouver Island coastal current: Fisheries barrier and conduit. Can. J. Fish. Aquat. Sci. 45:

Tyler, A. V., and S. J. Westrheim. 1986. Effects of transport, temperature and stock size on recruitment of Pacific cod (*Gadus macrocephalus*). Int. Pac. Fish. Comm. Bull. 47: 175–190.

Walters, C., M. Stocker, A. V. Tyler, and S. J. Westrheim. 1986. Interactions between Pacific cod (*Gadus macrocephalus*) and herring (*Clupea harengus pallasi*) in the Hecate Strait, British Columbia. Can. J. Fish. Aquat. Sci. 43: 830–837.

Ware, D. M. 1985. Life history characteristics, reproductive value, and resilience of Pacific herring (*Clupea harengus pallasi*). Can. J. Fish. Aquat. Sci. 42 (Suppl. 1): 127–137.

Ware, D. M., and G. A. McFarlane. 1986. Relative impact of Pacific hake, sablefish and Pacific cod on west coast of Vancouver Island herring stocks. Int. North Pac. Fish. Comm. Bull. No. 47: 67–78.

Wickett, W. P. 1967. Ekman transport and zooplankton concentrations in the North Pacific Ocean. J. Fish. Res. Board Can. 24: 581–594.

Zenger, H. H., and J. E. Blackburn. 1986. Pacific cod. *In* R. L. Major [ed.] Condition of groundfish resources in the Gulf of Alaska Region as assessed in 1986. (Doc. submitted to the annual meeting of the International North Pacific Fisheries Commission, Anchorage, Alaska, Oct. 1986). U.S. Dep. Comm., Natl. Oceanic Atmospheric Adm., Natl. Mar. Fish. Ser., NW and Alaska Fish. Center, Seattle, WA 90115: 35–66.